14th International Conference on Sustainable Energy Technologies

25th to 27th August 2015, Nottingham, UK

SUSTAINABLE ENERGY FOR A RESILIENT FUTURE

Conference Proceedings
Volume III

Sustainable Energy for a Resilient Future

Volume III

Edited by

Lucelia Rodrigues

SET 2015 Co-Chair and Chair of the Scientific Committee
Architecture, Energy & Environment Research Group
Department of Architecture and Built Environment
Faculty of Engineering, University of Nottingham

Reference to a conference paper:

To cite a paper published in these conference proceedings, please substitute the highlighted sections of the reference below with the details of the article you are referring to:

Author(s) Surname, Author(s) Initial(s), 2016. 'Title of paper'. In: Rodrigues, L. ed*., Sustainable Energy for a Resilient Future: Proceedings of the 14th International Conference on Sustainable Energy Technologies*, 25-27 August 2015, Nottingham, UK. University of Nottingham: Architecture, Energy & Environment Research Group. Volume X, pp XX-XX. Available from: eprints.nottingham.ac.uk [Last access date].

FOREWORD

Dear Reader,

I am delighted to present you with the volume III of the 14th International Conference on Sustainable Energy Technologies - SET 2015 proceedings, focused on the research stream 'Sustainable Cities & Environment'.

Sustainability and resilience in cities have become buzzwords in recent years. Sustainability refers to the capacity of an entity to efficiently sustain its current levels of activity, e.g. a sustainable city should be able to manage its resources in a way that guarantees welfare of current and future generations. Resilience refers to the ability to adapt and recover from changes; e.g. a resilient city should be capable of absorbing shocks and stresses to its infrastructure as well as social, economic, and technical systems whilst maintaining its functions, structures and identity.

The paradigms of sustainability and resilience, associated with the pressures of climate change, have had significant impacts on both research and practice in the built environment. At SET 2015 we saw fascinating examples of this reflected in world-class research. Keynote Speaker Professor Matheos Santamouris spoke about the risks and consequences of heat island effect in cities in his talk "Urban Warming: Evidence, Impacts and Mitigation". He discussed the negative impact on health and wellbeing and discussed how research may help mitigate some of the issues observed. Keynote Speaker Professor Edward NG delivered an incredibly stimulating and interesting talk entitled "Sustainable Living in Compact Urban and Built Environment in the Tropics" where he showed examples of how research can impact on practice and help deliver a more comfortable and energy efficient built environment.

Apart from the keynote speeches, the conference has also gathered a large number of authors delivering exceptional papers on various issues that impact the sustainability and resilience of cities. It was refreshing to see new approaches to known problems, innovative technologies and processes, new thinking and changing perspectives. It was also great to experience so much dedication and passion and to share those days with leading authors in the field. In these pages, you will find some of the best recent work in topics including sustainable urban planning, collaborative planning, social resilience, energy demand and use optimization, energy efficiency in buildings, urban sprawl, heat island effect, comfort within others.

In addition to disseminating the original research presented at SET 2015, I hope I have also managed to capture in these conference proceedings some of the wonderful atmosphere of collegiality, originality, commitment and friendship we experienced at SET 2015.

Dear Reader, I hope you enjoy the proceedings as much as I enjoyed writing it.

Dear SET family, thank you for your contribution and I see you in SET 2016!

Dr Lucelia Rodrigues
Associate Professor and Sustainable and Resilient Cities Research Leader
SET 2015 Co-Chair

CONFERENCE PROCEEDINGS STRUCTURE

Volume I

Energy Technologies & Renewables

Keynote Speaker Professor Chi-Hwa Wang: "Challenges on the Co-gasification of Woody Biomass and Solid Waste: A Singapore Story on Waste Minimization and Energy"

Session 1: Biofuels & Biomass

Session 5: Building Energy Systems

Session 9: Low-carbon/ Low-energy Technologies

Session 13: Biomass Systems

Session 16: Solar Energy

Session 17: Biomass & Biofuels

Session 20: Solar Energy

Session 21: Solar Energy

Session 22: Solar Energy

Session 25: Building Energy Technologies

Session 26: Solar Energy

Session 29: Low-carbon/ Low-energy Technologies

Session 32: Heat Pumps

Session 33: Low-carbon/ Low-energy Technologies

Session 36: Low-carbon/ Low-energy Technologies

Poster Session A

Poster Session B

Poster Session C

Poster Session E

Volume II

Energy Storage & Conversion

Keynote Speaker Professor Tianshou Zhao: "Innovating Energy Storage Technologies for a Sustainable Energy Future"

Session 2: Heating and Cooling Systems

Session 6: Heating and Cooling Systems

Session 10: Ventilation and Air Conditioning

Session 14: Smart and Responsive Buildings

Session 18: Phase Change Materials

Session 23: Smart and Responsive Buildings

Session 30: Heating and Cooling System

Session 34: Carbon Sequestration

Poster Session A

Poster Session C

Poster Session D

Policies & Management

Keynote Speaker Chris Twinn: "The goalposts are changing – are we ready for the new direction?"

Session 4: Environmental Issues and the Public

Session 8: Energy and Environment Security

Session 12: Energy and Environment Policies

Poster Session A

Poster Session D

Volume III

Sustainable Cities & Environment

Keynote Speaker Professor Matheos Santamouris: "Urban Warming: Evidence, Impacts and Mitigation"

Keynote Speaker Professor Edward NG: "Sustainable Living in Compact Urban and Built Environment in the Tropics"

Session 3: Sustainable and Resilient Cities

Session 7: Energy Demand and Use Optimization

Session 11: Energy Efficiency in Buildings

Session 15: Green and Sustainable Buildings

Session 19: Green Buildings and Materials

Session 24: Energy Efficiency in Buildings

Session 27: Energy Efficiency in Buildings

Session 28: Energy Efficiency in Buildings

Session 31: Energy Efficiency in Buildings

Session 35: Energy Efficiency in Buildings

Poster Session A

Poster Session D

Poster Session E

CONTENTS

SUSTAINABLE CITIES & ENVIRONMENT

Keynote Speaker Professor Matheos Santamouris: "Urban Warming: Evidence, Impacts and Mitigation"

Mat Santamouris is Professor of Energy Physics at the University of Athens and visiting professor at the Cyprus Institute, Metropolitan University of London, Tokyo Polytechnic University, Bolzano University, Brunel University and National University of Singapore. He is also the Director of the Laboratory of Building Energy Research, at the University of Athens.

Prof Santamouris is the Editor in Chief of the Energy and Buildings, Past Editor in Chief of the Journal of Advances Building Energy Research, Associate Editor of the Solar Energy Journal and Member of the Editorial Board of the International Journal of Solar Energy, Journal of Buildings and Environment, Journal of Sustainable Energy, Journal of Low Carbon Technologies, Journal of Open Construction and Building Technology, Sustainable Cities and Society and of the Journal of Ventilation.

He was also the editor of the Series of Book on Buildings, Energy and Solar Technologies published by Earthscan Science Publishers in London, and the editor and author of 12 international books on topics related to heat island, solar energy and energy conservation in buildings published by Earthscan in London.

He is the coordinator of many international research programs and author of almost 210 scientific papers published in peer review international scientific journals, as well as the guest editor of twelve special issues of various scientific journals.Reviewer of research projects in 14 countries including USA, UK, France, Germany, Canada, Sweden, etc.

Keynote Speaker Professor Edward NG: "Sustainable Living in Compact Urban and Built Environment in the Tropics"

Professor NG Yan Yung Edward is Professor of Architecture in the School of Architecture of The Chinese University of Hong Kong (CUHK). He is the first incumbent of the Yao Ling Sun Endowed Chair in Architecture. He obtained his doctoral degree from the University of Cambridge. He worked as an architect before becoming a professor. He specializes in Green Building, Environmental and Sustainable Design, and Urban Climatology for City Planning. At CUHK, Professor Ng is also the Director of the Master of Science of Sustainable and Environmental Design Programme, the Associate Director of the Institute of Future Cities (IOFC), and the Team Leader of Urban Sustainability and Public Health in the Institute of Energy, Environment and Sustainability (IEES). As an environmental consultant to the Government of the Hong Kong Special Administrative Region, Professor Ng developed the performance-based daylight design practice note, the Air Ventilation Assessment Technical Guidelines and the Urban Climatic Maps for City Planning. He is now working with the governments and agencies in Singapore and Macau, as well as a number of Chinese cities, on Urban Climatic Maps. Among many of his research interests, he is collaborating with public health colleagues to investigate the impact of city design and climate change on urban living.

In 2005, Professor Ng pioneered the idea of "Wu Zhi Qiao" (Bridge to China) and successfully built the first bridge in Gansu in China together with students from CUHK and other universities and professionals. Later, in 2007, he founded the "Wu Zhi Qiao (Bridge to China) Charitable Foundation" and held the founding chairmanship until 2013. In 2006, while still building bridges, Professor Ng initiated "A School To Learn" campaign and led his architecture students to build school facilities and start an education assistance programme in Guangxi in South West China. In early 2014, noting the

cultural and socio-economical needs of remote villagers in South West China, Professor Ng established the "One University One Village Project Initiative" to continue his humanitarian work with his students. He believes that knowledge creates the future, and it is the responsibility of academia to chart this future.

Professor Ng has published over 400 papers and 3 books. He has twice received the International Award from the Royal Institute of British Architects (RIBA). He has also twice been honoured by the UNESCO Asia Pacific Heritage Jury Commendation for Innovation Award. He was the recipient of the 2010 Red Cross Humanitarian Award and was named as one of the "Asian of the Year" by Reader's Digest in 2011.

SESSION 3: SUSTAINABLE AND RESILIENT CITIES

156: A simplified 3D urban unit representation for urban microclimate simulations

A case study in China's 'Hot Summer and Cold Winter' climate zone

Leonidas Bourikas[1], Patrick A.B. James[1], Abubakr S. Bahaj[1], Mark F. Jentsch[2], Tianfeng Shen[3] , David H.C. Chow[4], Jo Darkwa[5],

1 Energy & Climate Change Division, Sustainable Energy Research Group (SERG), Faculty of Engineering and the Environment, University of Southampton, Southampton SO17 1BJ, UK
2 Urban Energy Systems, Bauhaus-Universität Weimar, Weimar, Germany
3 Centre for Sustainable Energy Technologies (CSET), University of Nottingham Ningbo, P.R. China
4 School of Architecture, Faculty of Humanities and Social Sciences, University of Liverpool, UK
5 Faculty of Engineering, University of Nottingham, UK

Urban and building energy simulation models are usually initiated with typical meteorological year weather data. However, the locations where these historical datasets were collected (usually airports) do not represent the local, site specific micro-climates that cities develop. An idealised "urban unit model" (250m radius) has been developed for use with simulation modelling as a method for adapting commonly available weather data files to the local micro-climate. The idealised "urban unit model" presented in this work is based on the main thermal and morphological characteristics of nine sites with residential / institutional (university) use in Hangzhou, China. The size of the urban unit was investigated in relation to the source area footprint of the air temperature signal at the centre of the unit, where air temperature and relative humidity measurements were collected. This newly introduced idealised "urban unit model" was implemented into micro-climatic simulations using a Computational Fluid Dynamics – Surface Energy Balance analysis tool (ENVI-met, Version 4). Following model validation, two scenarios were developed, one for assessing the impact of vegetated surface's location on air temperature in relation to the air temperature measurement point (3.5m above ground) and a second one for analysing the effect of the vegetated surface area on the average urban unit (250m radius) air and surface temperature. The performance of the "urban unit model" was deemed satisfactory considering the assumptions integrated into the simulation initialisation process and the simulation itself. The performance evaluation indices were comparable to previously published work (RMSE: 1.3; MAPE: 3.1%). The results of Scenario 1 (spatial distribution of green space in the urban unit) showed that the location of the vegetated surface had only marginal impact on the air temperature at the middle grid cell of the urban unit. As would be expected, the air temperature was lower for the case where the vegetation was at the centre of the model. Scenario 2 (changing the green space percentage in the urban unit) revealed that large vegetated surface areas can reduce the day-time maximum air temperature. Specifically, the increase of green space resulted in an increase in the occurrence frequency of air temperatures towards the cooler end of the temperature distribution. This study concluded that in places with a humid subtropical climate such as Hangzhou, for successive hot, dry summer days, the reduction in soil water content can negate, to a large extent, the cooling benefits of added vegetation. This work presents a methodology that addresses the implications of urban morphology representation for micro-climate modelling. The method developed is appropriate for investigating the urban and building energy use and the implications for cities.

Keywords: idealised urban model, micro-climate simulations, vegetation, urban air temperature, cities

1. INTRODUCTION

Urban and building energy simulation models are usually initiated with hourly weather datasets for a 'typical' year (8,760 hours) (Crawley, 1998: page 1). Common typical weather year formats have the form of a synthetic year with months representative of the climatic conditions for the site of interest (Hacker et al., 2009: page 4). One important consideration for the use of these typical year weather time series in energy simulations is the representativeness of the location where the source data were collected. Many of these locations are at airports nearby large cities. However, locations within the city develop local, site specific micro-climates that cannot always be represented by these historical datasets (Mylona, 2012: page 59). This work aims to provide a more comprehensive methodology that delivers a more appropriate and relevant analysis of urban micro-climates.

This paper introduces an idealised "urban unit model" (on a 250m radius) that represents the main thermal and morphological characteristics of urban sites at the neighbourhood scale. This model can be used with simulations as a method for adapting commonly available weather data files to the local micro-climate. A case study was developed for the assessment of (1) the impact of vegetated surface's location on air temperature in relation to the air temperature measurement point (3.5m above ground) and (2) the effect of the vegetated surface area on the average urban unit (250m radius) air and surface temperature in places with a humid subtropical climate such as the case study city Hangzhou, China.

2. METHODOLOGY

A small size neighbourhood was selected as the scale of interest. Therefore, the size of an "urban unit" has been defined as a disk with a radius of 250m around a temperature and relative humidity sensor with a data logger. Air temperature and relative humidity were collected at 26 urban sites in Hangzhou (30˚15'N 120˚10'E) in Zhejiang Province, China (Bourikas et al., 2013: page 8; Shen et al., 2014: page 4). The sensors were installed on lampposts at a level 3m to 5m above ground. They measured and logged air temperature at 11-Bit (0.0625˚C) resolution and relative humidity at 12-Bit (0.04%) resolution (Maxim Integrated, 2013). The manufacturer stated air temperature accuracy is +/-0.5 °C and the RH accuracy is +/- 5% (Maxim Integrated, 2013). For calibration purposes air temperature (°C) and RH (%) readings within 1 minute intervals were compared to the readings of two separate thermocouples in an environmental chamber at ambient air temperatures of -10 °C, 0 °C, 10 °C and 40 °C (Shen et al., 2013: page 4). The results showed that all the sensors operated within the reported accuracy margin and fitted well to the thermocouple measurements (Shen et al., 2013: page 4).

Air temperature and relative humidity observations in the surface layer can be expected to be representative of an area ranging from 100m to several hundred meters in a direction upwind and around each sensor (Oke, 2006: page 8). However, most of the sensors were collecting measurements in the roughness sub-layer and not in the surface layer (Cheng & Castro, 2002: page 231) (Figure 1). The location of the measurement sites was carefully selected to have as homogeneous characteristics as possible for a large city and the sensors were installed with a reasonable distance to points of noticeable surface type change (Bourikas et al., 2013: page 8).

The impact of the urban unit's size was analysed by assessing the vegetation cover's influence on air temperature. Twelve urban sites were selected across the city centre in Hangzhou (Northern part above Qiantang River, Figure 2) in order to examine the urban unit borders' extent. Each sensor was considered to be the centre of concentric circles at radii of 10m, 25m, 50 m, 100m, 150m, 200m, 300m, 400m and 500m. Then the footprint of the vegetated surface was estimated and apportioned to these annuli areas (Figure 3).

The analysis was carried out for 14 weeks of hourly data collected during summer 2013. The air temperature (T_{air}) shown in Figure 3 is the mean air temperature departure from the mean temperature of the twelve sensors in this group. The vertical shaded reference line marks the 250 m radius from the centre (sensor). The legend shows the mean summer air temperature departure from the group's mean and the goodness of fit of the non-linear regression line in parentheses (Figure 3).

General siting conditions of the sensors (blue bullet point)	Circle of influence on the sensor's signals

Sensor on a lamppost close to a tall building	Sensor on a lamppost next to a road
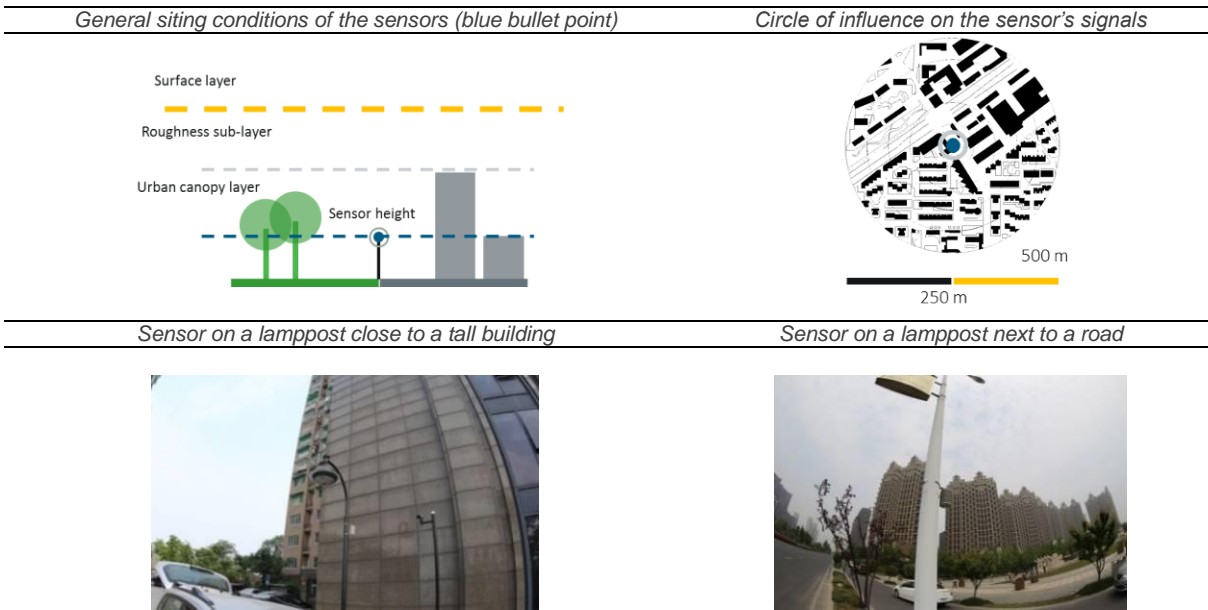
Figure 1: Siting of selected sensors in Hangzhou and representation of the size of the" urban unit" (Top Right).

Figure 2: Location of the12 sites for the urban unit size assessment (Left) and a typical fisheye image used for estimating the Sky View Factor in Hangzhou (Right). (Note: The colour scheme of the bullet points in the map is consistent with Figure 3.)

$$\text{\% green area } (r) = y_0 + a\, e^{-br}$$
$$\text{or } = y_0 + a\, e^{(-0.5\,((r-x_0)/b)^2)}$$

| Tair: -1.4 (R^2=0.71) |
| Tair: -0.4 (R^2=0.91) |
| Tair: -1.0 (R^2=0.73) |
| Tair: +0.2 (R^2=0.90) |
| Tair: +0.5 (R^2=0.96) |
| Tair: +0.2 (R^2=0.78) |
| Tair: +0.2 (R^2=0.96) |
| Tair: +0.6 (R^2=0.92) |
| Tair: +0.2 (R^2=0.48) |
| Tair: +0.4 (R^2=0.81) |
| Tair: -0.2 (R^2=0.96) |
| Tair: +0.4 (R^2=0.85) |
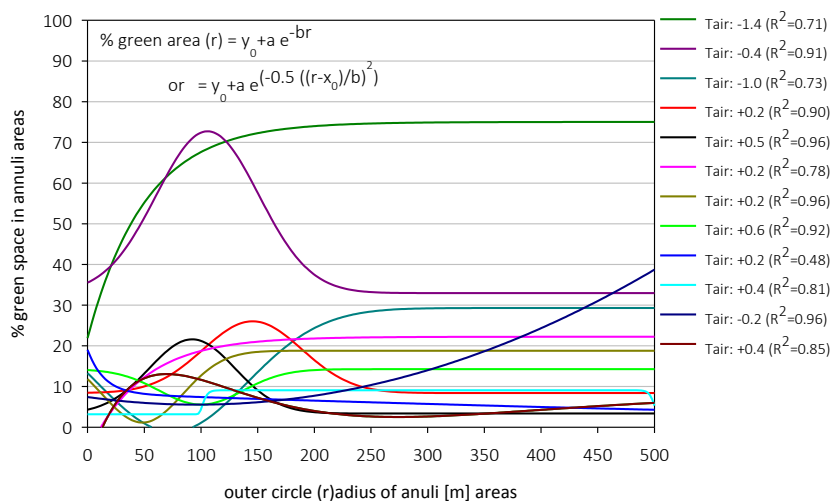
Figure 3: Regression lines of the percentage vegetated area in each annulus area on the distance from the centre (sensor).

It would be expected that the influence of green space is larger when closer to the sensor and diminishes if it is more towards to the outer annuli areas. The strong influence of vegetated areas is evident from the first peak of vegetated surface area in comparison to the general trend in the group of sensors. The

locations of sensors 3 (dark green; -1.4 °C) and 10 (purple; -0.4 °C) have a lower than the group average air temperature and their vegetated surface area is large with an early peak within the first 100 meters from the sensor (Figure 3). Interestingly, sensor 12 (dark cyan; -1.0 °C) which also shows a negative temperature departure from the group mean has a small vegetated area in the first 150 meters away from the sensor, comparable with those at locations with higher than the group average temperature. Its negative trend seems to be explained with the steep rise in vegetated surface area at the annuli area from 150 to 200 meters, showing that the influence of vegetation remains strong at this distance (Figure 3). Further evidence comes from the comparison between sensor 1 (black, +0.5 °C) and sensors 2, 5 and 9 (pink, red, gold; +0.2 °C). The regression trend lines indicate that the location where sensor 1 resides is warmer than the locations of sensors 2, 5 and 9 despite the larger vegetated surface within a 0 to 100m radial distance from the sensor. In the case of sensors 2, 5 and 9 the vegetated surface area peaks occur later at distances from 100 to 150 meters showing the persistent impact of the green space area. In addition, site 5 (red; +0.2 °C) has a similar vegetated surface area to site 1 (black; +0.5 °C) with the only difference being a delay of the peak, that is seen at distances 50 to 100 m farther outwards. Sensor 11 (dark blue, -0.2 °C) has a lower air temperature than the group average but the green space percentage peak occurs after the 250m radius border. However, in this case the low air temperature is mainly attributed to the site's proximity to a large wetland (i.e. Xixi). Based on these results a conservative estimate is therefore made for a representative circular "urban unit" with a 250m radius. It is expected that the total area of 196,350m^2 (250m radius) surrounding the sensor will be the representative part of the source area for the air temperature and relative humidity signal. The size of the proposed urban unit agrees with other authors' studies for the sufficient windward distance from a point of roughness or thermal change (~200-500m) and the internal boundary layer extent in zones within local climate classification schemes (r ~ 200-500m) (Stewart & Oke, 2012: page 1889).

2.1 Land cover analysis and urban classification

This study adopts a combination between a local urban classification scheme and the simulation of the local specific weather development for urban unit layouts with a typical residential / institutional (university, college) use in the case study region. Micro climatic simulation modelling is used to assess the influence of the pervious surface ratio (P_r) on the local, street level air temperature. The main advantage of using a surface classification scheme is that it provides generic input data for the simulation modelling (Stewart & Oke, 2012: 1893) and the simulation results can be attributed back to typical urban morphology characteristics.

A visual inspection of aerial and eye view images was considered to suit well to the scale and scope of the analysis. Step 1 - Each sensor was set at the centre of a circular area (i.e. disk) of a 250m radius (Figure 4). Step 2 - A selection of metadata (e.g high resolution images taken on site) was used to draw polygons for the vegetation (green colour), water (blue colour) and buildings' (black colour) surfaces (Figure 4). The residual was designated as other impermeable surface (white colour) and it included street and pavement surfaces. A set of morphological parameters was then calculated for each site including: the mean building height $\bar{H}$, the roughness length z_0, the height to width aspect ratio, the frontal area ratio λ_f, the building surface fraction F_r, the impervious surface fraction I_r and the pervious surface fraction P_r.

Each urban unit was classified according to the land cover analysis into a "Local Climate Zone" following an urban classification scheme developed by Stewart and Oke (2012). Each zone (i.e. thermally homogenous regions of uniform surface characteristics) in the scheme exhibits a distinctive diurnal temperature development profile at "screen" height (~1.5 to 3m) at the local scale (Stewart & Oke, 2012: page 1884). The resulting Local Climate Zones (LCZs) describe 17 generic environments consisting of 10 zones for built (e.g. open high-rise) and 7 for non-urban land cover types (e.g. scattered trees) (Stewart & Oke, 2012: page 1886). Each zone is represented by a set of ten morphological parameters and a descriptive definition of the typical location and use of the urban sites classified into a zone.

Nine urban units out of a total of 26 investigated areas in Hangzhou were classified as "Local Climate Zone 5" (LCZ5) (Figure 5). Three additional sites were removed from the study because of their proximity to large water bodies and large inhomogeneities in their surface characteristics. This study will focus on the nine sites classified as "LCZ5".
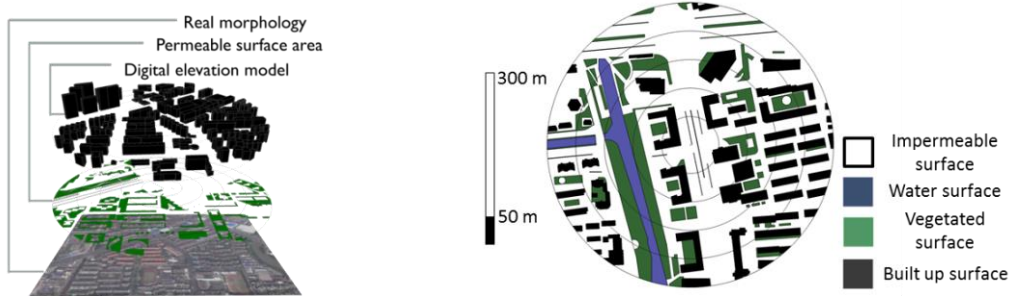
Figure 4: The digital elevation model and the land cover are built based on the metadata (Left). Four land surface types have been identified and their surface area is estimated by the model. The sensor is located at the centre of a disk of 250m radius (Right).

Figure 5: The nine studied urban units classified into LCZ 5 (locations, marked with blue bullets) in Hangzhou (Left).(Note: The Mantou Mountain, National Principle Weather station's location (reference, typical meteorological year file source) is marked as NP). Example of the land cover analysis for Site 2 (Right). Buildings are marked with black and vegetation with green.

2.2 A simplified model for urban micro-climatic simulations

In idealised models building geometry is usually substituted with arrays of cubes. Typical methods use cubes in staggered or aligned arrays (e.g. Cheng & Castro, 2002; Xie & Castro, 2006; Santiago et al., 2007; Kanda & Moriizumi, 2009; Millward-Hopkins et al., 2013). Cubes in regular arrays are spaced in repeated intervals equal at all directions to the cube's edge length (i.e. aspect ratio = 1) (Figure 6).

Idealised models used to represent urban morphology		
(1) Uniform height and aspect ratio	(2) Variable height and aspect ratio	(3) Variable height, aspect ratio and shape of blocks plus water (blue) and vegetation (green) surfaces.
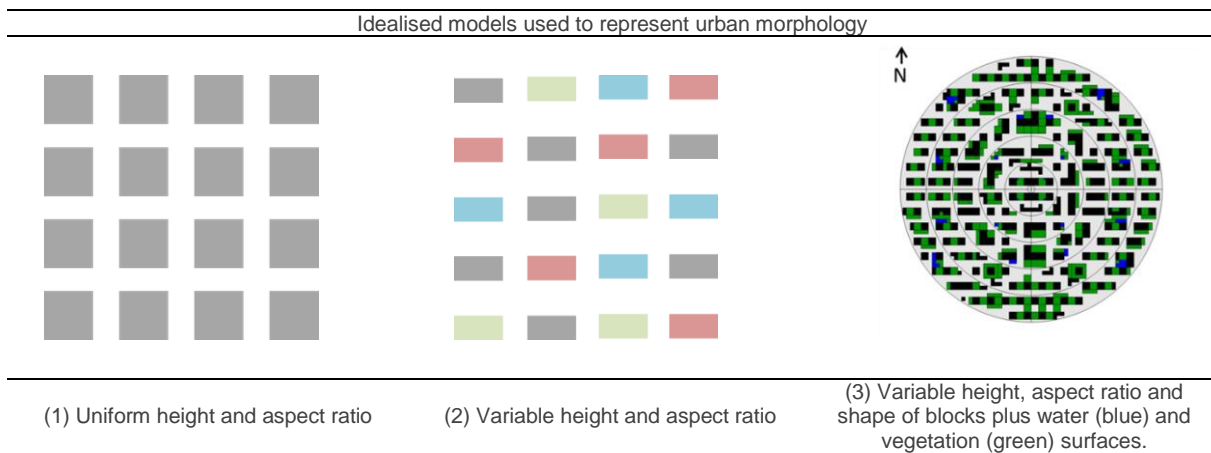
Figure 6: Typical urban morphology representations with idealised models (Left & middle) and the idealised "urban unit model" in this study (Right). (1) and (2) in figure were adapted from Millward-Hopkins et al. (2013) page: 449.

In this study, the generic "urban unit model" comprises of square based boxes (i.e. blocks) with a non-uniform height in a staggered irregular array (Figure 6, right). The staggered block array has a North-South orientation. Each block has a base of 3m x 3m (9 m^2). Blocks can be combined on the horizontal (not in height) at any possible number and shape. Each block can represent a building (black), vegetated surface (green, grass or tree) or water surface (blue, zero height). The residual space between the

blocks represents the impervious surface (grey, e.g. roads, paved) (Figure 6, right). The generic, idealised "urban unit model" has a similar planar area ratio and mean weighted (footprint) building height to the nine studied sites. The individual surface energy balances are represented in the model by the pervious, impervious and building footprint surface area ratios. The centre of the urban unit is always surrounded by an "empty" disk with a periphery at a radius equal to the computational grid resolution. Empty means that the surface of the central disk can either be pervious surface (e.g. vegetation) or impervious surface (e.g. road) but not a building.

Table 1: Overview of the median and the (range) for 80% of the key morphological parameter observations from the nine investigated sites. (R-r refers to the inner and outer radius of the annuli borders)

Annulus R-r (m)	$\overline{H}$ (m)	P_r (%)	I_r (%)	λ_f (%)	F_r (%)	d (m)	z_0 (m)
0-50	20 (15–22)	7 (0-15)	72 (50-85)	17 (7-25)	21 (7-30)	6.7 (3.6-11.1)	1.8 (1.3-4)
50-100	18 (13-25)	11 (0-17)	61 (54-70)	15 (6-20)	27 (8-40)	8.9 (3.6-12.9)	1.4 (0.5-3)
100-150	20 (13-24)	15 (0-25)	65 (56-70)	13 (6-20)	23 (4-30)	7.6 (2.0-10.6)	1.8 (0.5-3)
150-200	17 (12-20)	15 (5-25)	60 (50-66)	14 (10-17)	24 (19-28)	8.6 (5.5-9.7)	1.2 (0.7-2)
200-250	19 (16-24)	15 (12-25)	56 (54-66)	13 (10-20)	23 (16-27)	8.3 (5.8-11.3)	1.8 (0.7-3)

The morphology characteristics of each annulus area were based on the median value observations from the statistical analysis for the nine LCZ5 urban units (Table 1). The median was preferred over the mean because it is not affected by extremely low or high values and the calculated distributions were rather skewed than normal. The pervious surface area ratios increase with the increase of the distance from the centre of the urban unit (Table 1). This positive correlation (Spearman's $r_s(43)=0.503 > 0.294$ (p=0.05)) is specific to Hangzhou but it is meaningful for the wider study of temperature development in relation to green space in the context of Hangzhou. The distance between the blocks in each annulus area is random and the number of blocks was defined by the F_r ratio observations. The distribution of the blocks in each annulus area is similar in all notional quarter annuli. The changes to the packing density and distance between the blocks had produced a randomly dispersed layout that is expected to fit better to the high spatial inhomogeneity of real cities than a regular staggered cube array.

3. URBAN MORPHOLOGY SCENARIOS

Two scenarios have been investigated for assessing the sensitivity of the model to the area covered by vegetation and its impact on the air temperature development. The first scenario (Scenario 1) compared the air temperature at 3.5m height above ground ($T_{3.5m}$) in Case 1, where the vegetation was distributed according to the statistical results, with Case 2, where all the vegetation surface area was moved to the centre of the urban unit and Case 3 where the vegetated area was moved towards the outer annuli (Figure 7). The pervious surface area ratio (0.15) remained the same for the urban unit at all cases.

Scenario 2 compared the air temperature ($T_{3.5m}$) from Case 1 with 5 additional Cases (4 to 8) that had increasing ratios of pervious surface area that was distributed evenly (same percentage) in each annulus area (Figure 8). Each case had 5%-points more vegetated surface area (i.e. in the form of grass) than the previous one up to a maximum of $P_r = 0.4$ which represents the upper limit for the "Local Climate Zone 5" classification.

The air temperature development in the idealised "urban unit" for both scenarios was simulated with ENVI-met (Version 4) for August 10, 2013 which represented a sunny hot day in Hangzhou. On the 10th of August 2013 the mean ambient temperature was 36 °C. The average RH was 44% and the wind was blowing from a South – South West direction with an average speed of about 2 m/s (The Weather Underground, 2014). The sky was clear. The previous four days had been dry with 41 °C maximum air temperature and similar weather conditions as the day of the simulations. The analysis was conducted for 24 hours from 00:00 China Standard Time (CST) to 23:00 CST. To validate the simulation results obtained with the idealised "urban unit", the average air temperature ($T_{3.5m}$) simulation results (average across all the disk area of the urban unit excluding buildings) were compared against the average air temperature observations from the nine studied sites in Hangzhou (Figure 9).
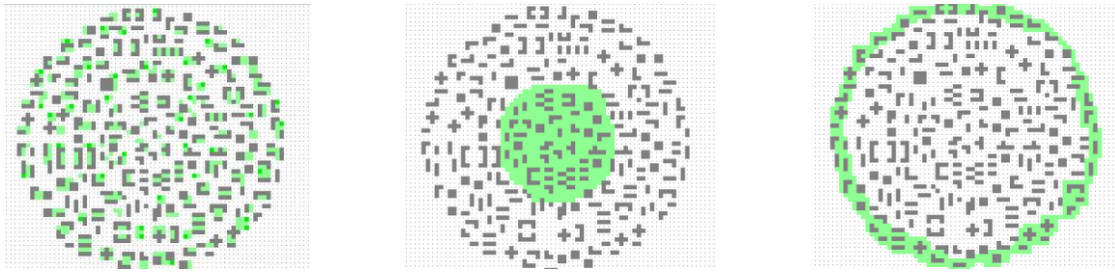
Case 1. Vegetation distribution according to annuli areas' statistics	Case 2. Vegetated surface moved into the central annuli areas (centric)	Case 3. Vegetated surface moved out to the outer annuli areas (outer)

Figure 7: Different distribution of the vegetated surface area in the urban unit for the cases considered in Scenario 1.

Scenario 2	pervious surface fraction P_r		
Case 1	15%		
Case 4	20%		
Case 5	25%		
Case 6	30%		
Case 7	35%		
Case 8	40%	Case 4. $P_r = 0.2$	Case 8. $P_r = 0.4$

Figure 8: The different percentages of vegetated surface area in the "urban unit" for the cases in Scenario 2. Top plan view of the computational domain (Right) for the cases with $P_r = 0.2$ and $P_r = 0.4$.

Table 2: Main input parameters for the simulation

Input parameter	August 10, 2013	Source
Specific humidity 2,500 m (750 mbar) *gr w/kg dry air*	13	NCEP/NCAR US (2000)
Prevalent wind direction (N = 0 clockwise)	210	The Weather Underground (2014)
Wind speed 10m ab. gr. *m/s*	2	The Weather Underground (2014)
Roughness length z_0	0.1	Stewart and Oke (2012: page 1890)
Mean wall albedo	0.23	Yang et al. (2013: page 97)
Mean roof albedo	0.50	Yang et al. (2013: page 97)
Wall heat transmittance *W. m⁻². K⁻¹*	1.4	
Roof heat transmittance *W. m⁻². K⁻¹*	0.9	
Underground soil temperature (Upper-Middle-Deep layer) *K*	304	NCEP/NCAR US (2000)
	298	"
	292	"
Underground soil humidity (Upper-Middle-Deep layer)	25 %	NCEP/NCAR US (2000)
	29 %	"
	33 %	"
Timesteps (solar angle < 35 deg)	2 sec	
35 deg. < solar angle< 55 deg	2 sec	
55 deg. < solar angle	1 sec	

3.1 Micro-climatic simulations

ENVI-met is a three dimensional non-hydrostatic numerical micro-climate model that couples an atmospheric, a soil and a one-dimensional (1-D) vegetation model and the surface energy balance. The atmospheric model is based on the incompressible Reynolds averaged Navier Stokes (RANS) equations (Bruse & Fleer, 1998: page 374). The boundary layer is reproduced with a 1-D model that extends up to 2500 m and provides the inflow (i.e. only in the case of forced boundary conditions at the inflow) and top boundary conditions to the 3-D domain (Bruse & Fleer, 1998: page 374). The boundary layer model is usually initiated with regional weather conditions (i.e. measured data from a nearby airport weather station). Wind speed and direction remain constant during the simulation while the effect of the surrounding urban environment can be modelled with the use of cyclic (periodic) lateral and outflow boundary conditions (i.e. turbulence from last grid cells at outflow boundary are copied to the first grid cell at the inflow boundary) (Bruse & Fleer, 1998: page 375). Temperature and relative humidity at the inflow boundary are forced by the boundary layer model according to a 24 hourly input. The turbulence field is updated every 15 minutes; solar radiation is modelled with a dynamic time step (i.e. smaller when

solar radiation is at peak (1 sec) and larger during morning and afternoon (2 sec)); the internal temperature of buildings (free running) is calculated according to the heat transfer through walls and roofs, where all walls and roofs have the same heat transmittance and albedo respectively. The spin-up period was set to 46 hours (starting at 02:00 two days before the simulated day). The main simulation parameters and the input sources are shown in Table 2.

The computational domain in ENVI-met comprises an equidistant grid that can be compressed / stretched to the vertical (z, height) dimension by using an expansion ratio but there is no option for the local refinement of the horizontal computational grid. The starting grid cell (i.e. in contact with the ground surface) height was set to 0.5m and the grid remained equidistant below the height of 2.25m with a grid cell spacing equal to dz=0.5m. The combination of a 0.5m starting grid cell height with a 18% grid height expansion ratio resulted in a vertical grid with 16 grid cells at the lower part of the domain (i.e. the lower 20m within the roughness sub-layer). The "urban unit's" 250m radius resulted in 3D computational grids of 72 x 72 x 28 with a resolution of 8m. A sensitivity analysis of the simulation results showed that an increase of the resolution to 6m delivered no significant change in model output.

4. RESULTS AND DISCUSSION

The evaluation of the model's performance showed that urban micro-climate simulations using the newly introduced idealised "urban unit" adequately capture the main characteristics of the diurnal air temperature development (Figure 9). Under a Case 1 set-up, the modelled air temperature at 3.5m above ground ($T_{3.5m}$) peaks at 15:00, an hour earlier than the observed peak in the averaged measured data, but in agreement with some of the sites (background colour lines in Figure 9). However, daytime air temperatures are underestimated with the model failing to predict the maximum temperature. Nevertheless, the simulation results fit well to the observed data at night time, in early morning and afternoon. This could be a result of inaccurate representation of thermal mass and heat storage in the model (Middel et al., 2014: page 21). The prediction of the expected urban heat island during night ($\Delta T_{Case - NP\ reference}$) is an indication that this level of inaccuracy is not detrimental to the overall function of the model.

In general, the accuracy of the model can be viewed as satisfactory in relation to its purpose, considering the uncertainties involved in the initialisation of the model and the simulation itself. The model performance evaluation indices' scores (**Error! Reference source not found.**) are similar to other published work (Yang et al., 2013: page 103; Middel et al., 2014: page 20). The index of agreement d takes values in the range {0, 1} with a value of 1 indicating a perfect match between the model prediction and the observations (Willmote, 1982: page 1310; Middel et al., 2014: page 19). The systematic component of the root mean square error (RMSEs) represents the error attributed to the simulation and the error integrated into the initialisation estimates, it should approach 0 (Middel et al., 2014: page 19). The unsystematic component should approach the value of RMSE (Willmote, 1982: page 1311).

Scenario 1 (Cases 1-3) investigated the impact of vegetation's location in relation to the air temperature development ($T_{3.5m}$) at the middle of the idealised urban unit. Case 2 that describes the condition where all the vegetation was allocated at the centre of the urban unit returned lower temperatures at the middle grid cell for the largest part of the day (Figure 10, Top). The marginal difference between the cases in Scenario 1 shows that the air temperature development at the middle grid cell captures well the effect of the larger area surrounding it and that it is not only sensitive to the ground surface material of the grid cell itself. Figure 10 depicts the urban heat island intensity at night time and the existence of an urban cool island at day-time that can be attributed to the low aspect ratio (building height to street width ratio) within the urban unit and the high thermal capacity of the built surfaces (Johansson, 2006: page 1332; Erell et al., 2011: page 77). In Scenario 2, the percentage of vegetated surface in the urban unit was increased from 15% in Case 1 to 40% in Case 8 with a step increment of 5% per case. A 40% permeable surface area is the upper limit for the Local Climate Zone 5 classification. The results indicate a very small change in the average $T_{3.5m}$ between the cases, while Case 8 had the lowest temperature for most of the time (Figure 10, Bottom). This is also seen in the frequency of the air temperature occurrences where there is a shift of $T_{3.5m}$ towards lower air temperatures following the increase in vegetated ground surface (Figure 11). High vegetation rates lead to higher frequency of occurrence of lower air temperature values towards the 38 °C end of the histogram. The small change of air temperature in the different vegetated surface ratios is consistent with the Local Climate Zone classification of the sites and it demonstrates the representativeness of the LCZ5 for a distinctive and typical local climate (Stewart et al., 2014: page 11).

In addition, the simulation was run for hot, dry weather that was preceded by 2 days with similar weather conditions. After the spin-up period (46 hrs) the relative soil wetness at 1.5 cm depth was below 10%. It is argued that most of the soil water content evaporated during the spin-up period, significantly reducing the evapotranspiration cooling potential of the vegetation. Lastly, it is to be noted that all the vegetation added in the cases was in the form of grass and the shading effect of vegetation was not taken into account. The impact of vegetation is more evident on the surface temperatures (T_{surf}). The average surface temperature over the urban unit shows a negative correlation with the percentage of permeable ground surface (Figure 10, Bottom). It can also be seen that surface temperatures peak closer in time to the solar noon. The similarity of the surface temperatures during the day-time in the different cases supports the initial argument that evapotranspiration was reduced due to limited water availability. In essence, the absorbed solar radiation led to a surface temperature increase (Erell et al., 2011: page 183) that negated, to a large extent, the effect from any planted surface area added to the urban unit.

5. CONCLUSION

The micro-climate simulations using the newly introduced idealised "urban unit model" showed that the performance of the model was good and that the simulation results displayed a satisfactory accuracy (RMSE: 1.34), comparable to that of previous micro-climate simulation studies (e.g. Yang et al., 2013; Middel et al., 2014). This reveals that there is a potential for the simplification of urban site modelling and for the wider application of the introduced method as a tool for the adaptation of typical meteorological weather data files to the neighbourhood scale urban environment.

The assessment of the impact of the vegetation's location on the air temperature development in the urban canopy revealed that the proximity to "green" – vegetated space can lower the urban heat island intensity during night time and the maximum day-time air temperature. The marginal difference between the cases with a central allocation of the vegetated surface area with those were the vegetation was positioned at the outer border of the urban unit is an indication that the distance to a vegetated area is not enough to alone produce large cooling benefits during the day and attenuate the night time urban heat island intensity. The distance to vegetation must be examined in conjunction with other parameters that can directly affect the urban energy balance, such as the type of vegetation, urban density, wind penetration, soil water content and nearby surface materials' properties. In Scenario 2, an increase to the urban unit's permeable surface area showed a small decrease in the average air temperature across the urban unit. The case with the largest vegetated surface area had the lowest daily air temperatures. A shift was noted in the air temperature distribution towards a higher occurrence frequency of temperatures at the cooler end. The differences between the cases were more evident in the average surface temperatures. The results suggested that high percentages of vegetated space can reduce the surface temperatures within the cities. There were, however, also strong indications that in places with a humid subtropical climate such as Hangzhou, in the case of successive hot, dry summer days, a reduction in soil water content will negate, to a large extent, the cooling benefits of the added vegetation.

6. ACKNOWLEDGEMENTS
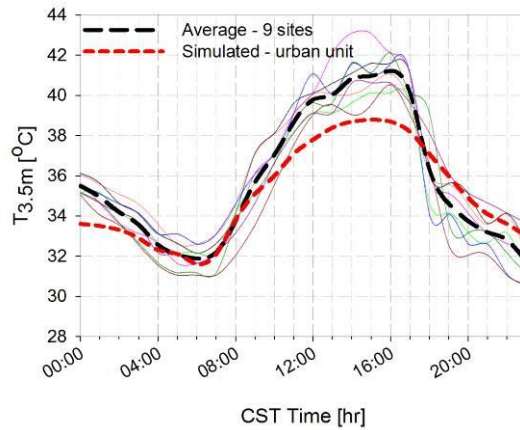
Figure 9: Comparison of the observed and modeled air temperature at 3.5m above ground (T3.5m) for August 10, 2013 in Hangzhou. Time in China Standard Time – (CST : GMT+8).
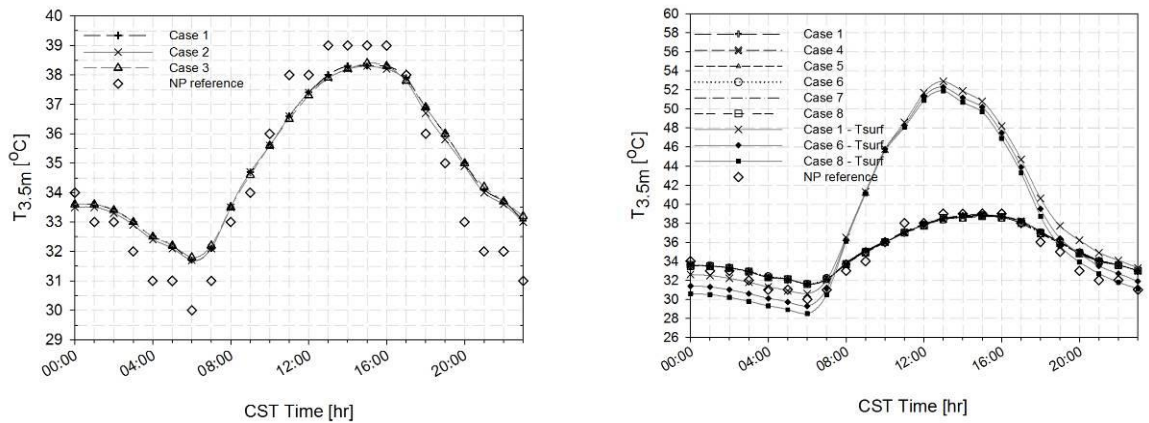
Figure 10: Scenario 1 : Impact of the vegetation's location on the air temperature development ($T_{3.5m}$) at the middle of the "urban unit model" (Top). Scenario 2 : Comparison of the modeled $T_{3.5m}$ and T_{surf} for cases in Scenario 2 (Bottom). Note: NP reference shows the referencemeteorological data from Mantou Mountain weather station.
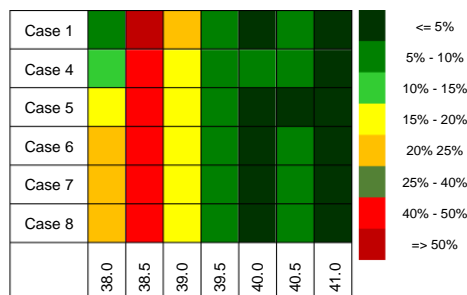
Figure 11: Frequency of occurrence of air temperature (rounded to 0.5 ^{o}C) for each Case (1 to 8) in Scenario 2 (rows). Note: Case 2 and 3 are identical to Case 1 in terms of vegetated percentage and not shown. Image adapted from Middel et al., 2014: page 25

7. REFERENCES

BOURIKAS L., Shen T., James P.a.B., Chow D.H.C., Jentsch M.F., Darkwa J. and Bahaj A.S. (2013) Addressing the challenge of interpreting microclimatic weather data from urban sites Journal of Power and Energy Engineering, vol. 1, p.p. 7-15

BRUSE M. and Fleer H. (1998) Simulating surface–plant–air interactions inside urban environments with a three dimensional numerical model. Environmental Modelling & Software, vol. 13 (3–4), p.p. 373-384

CHENG H. and Castro I.P. (2002) Near wall flow over urban-like roughness. Boundary-Layer Meteorology, vol. 104 (2), p.p. 229-259

CRAWLEY D.B. (1998) Which weather data should you use for energy simulations of commercial buildings? ASHRAE Transactions 104 Part 2: p.p. 498-515 Atlanta, USA: ASHRAE.

ERELL E., Pearlmutter D. and Williamson T. (2011) Urban microclimate: designing the spaces between buildings. (1st Edition) London: Earthscan

HACKER J., Capon R. and Mylona A. (2009) Use of climate change scenarios for building simulation: the CIBSE future weather years. London, UK: The Chartered Institution of Building Services Engineers

JOHANSSON E. (2006) Influence of urban geometry on outdoor thermal comfort in a hot dry climate: A study in Fez, Morocco. Building and Environment, vol. 41 (10), p.p. 1326-1338

KANDA M. and Moriizumi T. (2009) Momentum and Heat Transfer over Urban-like Surfaces. Boundary-Layer Meteorology, vol. 131 (3), p.p. 385-401

Maxim Integrated (2013) iButton Temperature / Humidity logger with 8 kb data logger memory. Available from: http://www.maximintegrated.com/products/ibutton/data-logging/

MIDDEL A., Häb K., Brazel A.J., Martin C.A. and Guhathakurta S. (2014) Impact of urban form and design on mid-afternoon microclimate in Phoenix Local Climate Zones. Landscape and Urban Planning, vol. 122 (0), p.p. 16-28

MILLWARD-HOPKINS J.T., Tomlin A.S., Ma L., Ingham D.B. and Pourkashanian M. (2013) Aerodynamic Parameters of a UK City Derived from Morphological Data. Boundary-Layer Meteorology, vol. 146 (3), p.p. 447-468

MYLONA A. (2012) The use of UKCP09 to produce weather files for building simulation. Building Services Engineering Research and Technology, vol. 33 (1), p.p. 51-62

Ncep/Ncar Us (2000) National Centers for Environmental Prediction (NCEP)/National Weather Service/NOAA/U.S. Department of Commerce. NCEP Final Operational Model Global Tropospheric Analyses, continuing from July 1999. Research Data Archive at the National Center for Atmospheric Research, Computational and Information Systems Laboratory. Boulder CO.,: National Center for Atmospheric Research,

OKE T.R. (2006) Initial guidance to obtain representative meteorological observations at urban sites. Instruments and observing methods 2006 (WMO/TD-No. 1250):47 Available from: http://www.wmo.int/pages/prog/www/IMOP/publications/IOM-81/IOM-81-UrbanMetObs.pdf

SANTIAGO J., Martilli A. and Martín F. (2007) CFD simulation of airflow over a regular array of cubes. Part I: Three-dimensional simulation of the flow and validation with wind-tunnel measurements. Boundary-Layer Meteorology, vol. 122 (3), p.p. 609-634

SHEN T., Chow D.H.C., Cui T. and Darkwa J. (2013) Generating a modified weather data file for urban building design and sustainable urban planning accounting for the Urban Heat Island (UHI) effect. Paper presented at 12th International Conference on Sustainable Energy Technologies. Hong Kong Polytechnic University

SHEN T., Chow D.H.C., Darkwa J. and Yao R. (2014) Impact of Urban Heat Island on Building Cooling Energy Consumption in Hangzhou. Paper presented at 13th International Conference on Sustainable Energy Technologies. 25-28 August 2014, Geneva, Switzerland

STEWART I.D. and Oke T.R. (2012) Local Climate Zones for Urban Temperature Studies. Bulletin of the American Meteorological Society, vol. 93 (12), p.p. 1879-1900

STEWART I.D., Oke T.R. and Scott Krayenhoff E. (2014) Evaluation of the 'local climate zone' scheme using temperature observations and model simulations. International Journal of Climatology, vol. 34, p.p. 1062-1080

The Weather Underground (2014) Hangzhou weather data from Mantou mountain's National Principle WMO-listed weather station

WILLMOTE C.J. (1982) Some comments on the evaluation of model performance. Bulletin of the American Meteorological Society, vol. 63 (11), p.p. 1309-1313

XIE Z. and Castro I.P. (2006) Large-eddy simulation for urban micro-meteorology. Journal of Hydrodynamics, Ser. B, vol. 18 (3, Supplement), p.p. 259-264

YANG X., Zhao L., Bruse M. and Meng Q. (2013) Evaluation of a microclimate model for predicting the thermal behavior of different ground surfaces. Building and Environment, vol. 60, p.p. 93-104

347: Public spaces for resilient cities

A design proposal to address climate variability and changes

LUCA MARICCHIOLO

PhD candidate in Architecture - Theories and Project at Sapienza University of Rome, via A. Gramsci 53 - 00197 Rome - Italy, e-mail: luca.maricchiolo@libero.it

This work is based on the belief that sustainability and resources management problems are not only referred to ecological systems, but are strictly linked with human activities, and concern socio -ecological systems of cities as a whole. Therefore, the study addresses the question of the balance between people and environment. Cities resilience depends on the stability of this balance in its projection in time, assuming the concept of resilience not just as the ability of the system to maintain a stable equilibrium condition, but, according with "resilient thinking" theories, as the ability to generate new stability landscapes that keep similar performances, identity and structure.

This research investigates socio-ecological urban systems resilience, and it focuses on urban environment and specifically on city public spaces. The base hypothesis is that resilience of urban systems as a whole it is mainly determined by the balance of his social substratum, and that this is possible through a combination of strength and fragility in urban development. Public domain is the base structure of the city, where it comes, and it develops over time, the sense of citizenship on which depends the cooperation between people and its balance with environment. Hence, this is the field where this study investigates the concepts of persistence and change, and where it identifies stability frames and adapting elements.

The first goal of this study is to demonstrate the relevance of public domain in keeping general resilience of the city. Then, it will investigate how public spaces could be designed based on the balance of persistence and change, which are the frames in public spaces that shouldn't change over time, to keep urban quality and collective identity, and, conversely, which elements should adapt to absorb stresses and to ensure general resilience. This will be verified through the comparison of recent studies and case studies, and a design of the author.

Keywords: urban resilience, public space, sustainability

1. INTRODUCTION

Many advances in operational possibilities of the concept of resilience have been done from the acknowledgement by ecological theories about the intimate link between ecological and biological systems with social and anthropological ones. This theoretically opened the field of study of the concept of resilience to urban systems as an operational methodology of analysis. The acceleration of human activity and its relevance on natural balances forced to consider the two systems as a whole, and to investigate sustainability integrating social and ecological points of view.

This allows using the concept of ecosystem resilience, as related with concepts of adaptability and transformability, to hypothesize an application to urban areas, considering the city as a complex adaptive system, made up of elements and relationships between them, and assuming that relationships represent the true nature of the city. Starting from this parallel, public space is identified as a preferential field to investigate and design urban systems resilience, and to define its control variables.

In the article, therefore, it is proposed an application hypothesis of these concepts, illustrating how urban design could integrate the instruments to address climate variations and changes, with the construction of a persistent identity in its public spaces.

2. RESILIENCE OF URBAN SYSTEMS

The recent evolution of urban systems and the emergence of ever-increasing environmental issues, related to energy consumption and to climate change, have rekindled the attention on their causes; this unfolded the applicability of the principles of sustainability not only to ecological systems in itself, but to the socio-ecological systems as a whole, given the importance of human activities in the entire balance of the biosphere. Its stability depends on the mutual relations between anthropic and ecological systems, and particularly on dynamics between man and nature, as these emerge through the qualities of resilience, adaptability and transformability (WALKER, HOLLING, CARPENTER, et al., 2004). From this assumption it is possible to apply the same methods of investigation to human systems, and to socio-ecological systems that mainly affects territories and environment: cities. As in natural sciences, since seventies, was introduced and consolidated the concept of ecosystem resilience, a similar conceptual tool is conceivable applicable to urban systems, which could be called eco-urban resilience. In 1973, Crawford Stanley Holling distinguishes the concept of ecosystem resilience from engineering resilience: in engineering, resilience is the property of a material to restore the initial condition after a disturbance, whereas definition of ecosystem resilience provides the conceptual shift from the notion of restoring previous condition unchanged, to the ability of the system to change, keeping the same relationships within the system, and to persist absorbing state variables, driving variables and parameters changes. (HOLLING, 1973: page 17). Literature later developed, through the experiences of Resilience Alliance researchers, pointed out the components of the ecosystem resilience and functioning mechanisms, which will be recalled here to be applied to urban design.

2.1 Adaptability, Transformability and Resilience for Urban Systems

Social changes are intimately linked to equilibrium of ecosystems, so the assessment of global resilience of these depends on adaptive capacity of human activities; therefore it will be discussed resilience according to theories on social-ecological systems interdependence, to be intended as an interpretation and design tool for urban systems.

Resilience is the capacity of a system to reorganize and absorb disturbance, keeping the qualities of its behavior within critical thresholds that marks the limit basin of attraction of its stability domain. The basin of attraction is given by the region around an equilibrium point of the system, and the set of points of attraction makes the stability domain. The capacity of absorbing perturbations depends on the ability of the systems to adapt to changes. Adaptability, therefore, is the way how the system reorganizes itself to absorb disturbance, keeping within its basin of attraction. This capacity refers to experience, inertia and knowledge of a place to modulate the response to change due to external pressure. Hence, the adaptive capacity of a social system, allocated in a place, is the capacity of the actors in the system, or of the system itself, to influence resilience, and to drive changes within the current stability domain or basin of attraction (FOLKE, CARPENTER, WALKER, et al., 2010: pages 2-3).

Historically, in urban systems, adaptability represents the continuous process of adjustments of their character to territorial qualities and conditions, through trials and errors guided by inhabitants, which the *genius loci* is made of. This is the layered image of the resilience of a city during time, driven by mutations in the surrounding area (ORLANDO, 2009). For urban systems, the equilibrium points are the fulfillment of performances offered by the city, which will be described here by four benchmarks. However, it's infrequent that all these performances can be simultaneously fulfilled, thus the equilibrium point is mainly the limit the city should tend toward.

Transformability has been defined as the capacity to create a new system when the ecological, social or economic structures of the system make this untenable, or the system has entered into a basin of attraction that is not desired. In these cases the actors in the system need to build a new stability domain, defined by new state variables (WALKER, HOLLING, CARPENTER, et al., 2004: page 5). Urban planning and designing are deliberated transformations, since they outline new stability landscapes; their objective should be to build more elastic threshold for state variables of the system, so that it will not require new transformations to absorb undesired changes. Hence, the goal of the design for a system, to pursue its resilience, is to avoid the need of new transformative changes, managing it to remain within the stability domain through adaptive processes.

Resilience, therefore, "is the capacity of a system to absorb disturbance and reorganize, while undergoing change, so as to still retain essentially the same function, structure, identity and feedbacks" (WALKER, HOLLING, CARPENTER, et al., 2004: page 2).

Extending the use of the categories of Holling's ecosystem resilience to social systems, it opens a field of research about planning and designing capacity of adaptive systems. This goes beyond the knowledge of the inner workings of the systems, in order to investigate the external drivers, such as identity, habits, cultural values, that influence adaptability, and to understand how to design dynamic landscapes. Cities have a relevant role in conditioning of human behavior, evolving and transforming with inhabitants, through planned and spontaneous processes. Cities are dynamic but homeostatic systems, reorganizing continuously along their transformations. Hence, the research on city resilience is the investigation about the role it plays, facilitation or restraint, for the adaptation of its socio-ecological systems in presence of physical transformations. Or whether if its reorganization keeps or to diverges from equilibrium (FABBRICATTI, 2013).

3. THE ROLE OF PUBLIC SPACE IN KEEPING URBAN RESILIENCE

The investigation of cities in a systemic way shift the focus of the analysis from the elements composing the system to the field of the relationships existing among them. The component that keeps alive and prosperous urban systems isn't the sum of their elements, but their inner vitality, the unstable equilibrium that is established between them, and that evolve naturally and spontaneously to be continuously self-organized. The failure of many theories and plans on city depends, in fact, just from having neglected this aspect (BATTY, BARROS, JUNIOR, 2006). Indeed, the assessment of the transformation of the city must be focused on the space where these relationships are activated, they unfold their quality for the operation of the system, and keep themselves remain, even in variation of some elements that compose it. The systemic reading of the city leads, therefore, to analyze the operating performance through linking users behavior to the quality of space, identifying the measurement of its resilience in the variation within satisfactory performance threshold of its public space (FABBRICATTI, 2013).

This is, in fact, the place to express value for urban users, to sense identity, for reasons that refer both to the perceptual and cultural sphere, and to the systemic and functional one. The system of the voids of the city, in fact, plays a central role in morphology and performance, constituting simultaneously the field where urban identity unveils itself, and the channel that hosts the inner relations within the city. This happens in the ordinary public space, articulated through the city, and not localized in specialized public facilities: the structure of the urban system, the spatial rules that holds together the elements of the city, is the urban fabric public space, the space of everyday life distributed into voids defined by architectures, and differentiated to fruition and activities.

Urban space, then, is the heart of the significance of the city, of its identity and its function. It is the path in which it the city is organized as adaptive system, which hosts structure, identity, function and feedback relations between elements, and in which dysfunctions occur due to changes of environmental, social, or structural external conditions. The growth of a part of the city, the modification of its fabrics, the new

function of its facilities, have a repercussion on the consistency of the image and the performance of public space, and on the quality of relationships that ensure the system functioning. It is therefore in public space that the adaptive capacity of the city can be read, as well as its ability to change over time keeping the quality of relationships among its physical, social and ecological systems.

The relationship between persistence and change, between elements that need to be maintained over time, and elements subject to change, is the focus of assessing the role of public space in keeping the general resilience of the city. The city may change in its physical form, the elements of the system can modify its quality or quantity, as well as the channels through which relations take place, but in order to have the socio-ecological system persist over time, even in conditions of instability and in presence of not deliberated transformations, urban performances are mandatory to persist. Therefore, the permanent features of the city are public spaces performances, belonging to the categories of perception and enjoyment of the city.

3.1 Urban Morphology and Sense

From the point of view of the sense of the city, the void is the field in which urban landscape manifests itself, where it is possible to read and relate the components that constitute it, and to check the consistency of its evolution. The landscape, in fact, "means an area, as perceived by people, whose character is the result of the action and interaction of natural and/or human factors" (EUROPEAN LANDSCAPE CONVENTION, 2000: art. 1). The air volume that surrounds the observer makes possible the perception of the city, the reading of its aesthetic text, which builds sense of citizenship and urbanity and that make people feel belonging to a place. Public space distributed along urban fabrics and main architectures makes readable the territorial and spatial structure that links the elements of the system, through which are manifested the visual relationships and it's possible to perceive its images in a dynamic way. This is the place where the figurative identity of the city shows up. Hence, investigating the city in its dynamic evolution, and the changes of its identity when its technical organization varies, means investigating the value of the city through the persistence of the sense and the consistency of the empty space surrounding the observer to perceive light, and defined by borders.

Sense is given by the identity of the place, the image of space as well as it is perceived through the five senses, and the clearness of the formal structure of the city, as to facilitating mind maps creation (LYNCH, 1981: pages 131-134). In presence of an adaptation, public space should therefore maintain its sense, by avoiding obsolescence or the inconsistency of its spatial structure because of the coming up disruption, becoming no more readable and adjustable by the user.

Consistency, or fit, is the ratio between the shape of the space and the activities that take place inside. It represents the figurative and morphological attitude of the public space to host relationships between elements. An area poorly configured, or fragile, that loses its completeness at the variation of only one of the elements which make it up, quickly becomes unsuitable for urban life and produces a negative feedback to the system. Consistency, therefore, ensures the stability of behavior in places and their relationships. Adaptability of space and system close affects its consistency: in fact the more space will be designed to fit in, the more it will maintain consistency; on the contrary, a strict space which does not provide the possibility of physical change and it is not prepared for diverse activities, loses his adequacy at the first manipulation or change in use and form (LYNCH, 1981: pages 151-158).

3.1. Performances of Public Space

Public space is the channel of relations, where the city exists as an adaptive system. Here, relations by purpose or unintended between users or between users and the city take place. Its operation and performance, therefore, depend on the ability to ensure the persistence of livability, health and safety of these relations and the possibility for everyone to have access to them.

The primary relationships between users and the city, the proximity between place of accommodation and facilities, are substantiated in the urban space. In the same way the relationships between persons occur: meetings, economic and cultural exchanges, and casual relationships, that gather people without intimate knowledge required to meet in one place, and produce the size of sociability and vitality. These conditions are maintained by the diversity of public spaces, due to coexistence of diverse functions, plot and business set up, producing the attendance of space by various interest groups, and a spontaneous social equilibrium (JACOBS, 1961). Vitality is function of life quality and of harmony among public space

and the biological structure of man, in terms of scale and comfort. Vitality is given therefore by the control of wellness of public space, maintaining adequacy for attendance by persons under varying climatic conditions, and risk protection (LYNCH, 1981: page 121).

The public nature of the space is embodied by permitting its use to everybody, by the absence of organizational structures that could exclude part of the population, and by allowing access to city facilities, raising the standard of life quality. Ordinary space in the city hosts the character of the civic life of the community, becomes the path of the formation of public awareness of individuals, the place to trust other than intimate, accessible to all in need because of an organization, and through this, training the sense of citizenship (ROGERS, 1997). Access performance is then the guarantee of access to goods and functions, activities, places, resources and information to all. The accessibility, consists of the possibility to move within the city, and of the quality and feasibility of movements. Hence, it represents the tool to ensure equal rights to all inhabitants, and it is the foundation of the democratic construction of cities.

3.2 Adaptability of Public Space

The desirable response of public space is to be able to adapt in order to increase the resilience of the system of the city. This consists of fixed elements, like architectures, infrastructures, service buildings and green spaces, and of a system of actions: within these elements actors move, perform actions, meet themselves, have the use of facilities and image of the city.

Referring to the definitions of resilience of socio-ecological systems, it is possible to compare variable needed to keep their quality in absorbing disturbance: structure of the system consists of the type of mutual relations between elements; function is the ability to fulfill need of people moving and performing actions in the public domain; identity is given by the qualification of processes, the way people experience the space in-between, conformed by architecture and orographic elements; feedback is the combination of stimuli that the system gives in response: a system with negative feedback tends towards stability, but stops growing, whereas, on the contrary, a positive feedback stimulates the growth and diversification of the system, but make it continuous changing (ORLANDO, 2009).

An adaptive public space allows the maintenance of these four parameters. It allows the social system to persists in its operating mechanism, in presence of external perturbations which would tend to curb, slow down or impede the activities. To make this happen, the space should change its configuration, and switch to another that allows the same mode of use.

Public space will be much more adaptable as it can change uses modality without altering its nature. On a morphological point of view, it is necessary that the variation of some components of the city nevertheless retains unaltered the level of readability of the spatial structure and the consistency of its form. Thus, the urban identity is still perceived as a recognizable landscape. Performances, as vitality and accessibility, need to be maintained even under changing conditions: it is not important the stability of means, nor the communication channel, nor the modalities, but that such relations persist and serve the same function. As for the conditions of vitality, the external perturbations are often related to climatic conditions and energy, so design regards the compatibility of the project with environment, and the way it ensures well-being compared to the external conditions.

Adaptability and resilience should be pursued through new generation of public spaces, not configured in static mode as in the traditional city, but designed as complex systems themselves, able to change, to take different forms and materials, retaining similar functionality in their performance. By this way the space, while not being infinitely malleable, can address the adaptation of social systems, and constitutes the trajectory on which changes happen.

4. A DESIGN PROPOSAL: PUBLIC SPACES ADAPTABILITY TO ADDRESS CLIMATE VARIABILITY AND CHANGES

A design hypothesis of the concepts of adaptability for public spaces is herewith presented, making use of an urban project that the Author of this article, with a group of architects, submitted to the Europan competition in 2013: Hammarö water_sc[r]ape (CIRESI, DE SIMONE, GUERRIERI, MARICCHIOLO, ROMA, 2013). This is a conceptual and qualitative hypothesis, a concept of urban design, therefore it is not dimensioned in a quantitative way.

The project concerns the construction of a satellite community to the town of Hammarö in Sweden, able to work independently, with a clear imprint of ecological and social sustainability. Hammarö is a small city near Skoghall, born in the early years of the XX century for industrial activities. Skoghall has therefore developed as an industrial city, to host people who worked in factories in Hammarö. With the post-industrial transition in the seventies, the village of Hammarö was converted to residential and service functions, and began to grow in population, reaching today almost 15,000 inhabitants. The project site is located on an island of the archipelago in the north of Lake Vänern, on the delta of river Klarälven, and it includes a former nursing home. The surrounding area is characterized by a marked fragmentation of the coast, and by a high presence of water. Next to the project site, on the island, the small lake Sättersviken is surrounded by wetlands with massive presence of reeds, and connected to the Lake Vänern.

The regime of the waters around the river Klarälven is uneven. The main river has a steady state, as well as the main channels of the delta into the lake Vanern, which includes also some minor courses next to the project. In addition, the orography of the project site is characterized by torrential or temporary channels, which level varies in the short term, relating to the seasons, to the rainfall and melting snow. Another variation is conceivable in the long term: the phenomenon of progressive melting ice due to climate change will increase the volume of water that will flow the flat land, exacerbating the problems for human settlements due to irregularity of the waters system.

In order to envisage an independent and completely environmentally and socially sustainable settlement, the project interprets the change of environmental characteristics of the place as a guiding principle for urban design. The goal is to fit symbiotically into the environmental context, interpreting both characters of static territorial identity, of land fragmentation related to water, and its dynamic characters, such as the variability of landscape over time.

The hypothesis outlined by the project is that the natural form and the uneven regime of water become the rule of the urban structure. The goal is to make the technological components of environmental sustainability coexisting with urban morphology. Hence, water constitutes the matter that structures the city, representing at the same time the tool to shape identity, and to meet climate adaptation needs on different temporal orders: heating mitigation along seasons, absorption of hydrographic regime irregularity due to meteoritic phenomena and climate change.

4.1 Urban Structure

The urban structure proposed for the new settlement is based on public space, on relational space thought as nodal place for the development of a complex system, and as a tool to ensure an high level of resilience. It takes the concept of porosity as a metaphor to build up a spatial model based on empty spaces, to create a network of places for relationships, as porosity represents, from an architectural standpoint, a morphological model shaped by cavities. In the metaphor, the fluid that occupies voids represents urban community, that, as water, doesn't have his own shape, assuming the container's one (SECCHI, VIGANO', 2011). The same concept of porosity is also used for a further conceptual leap in the relationship between city and water, between solid and liquid matter: water is conceived as a tool to shape the form, using the liquid material as a urban rule. Water and its dynamics are therefore morphogenetic element of urban design, in both static, to define the structure, and dynamic ways, in defining changes of urban landscape.

Different kinds of water have been identified in the territory: each of them plays different role in the structure of public space, and achieves different goals. The project defines three qualities of water, as shown in figure 1. First one is artificial, is the founding act of the designed city and it is the instrument to historicize the existing assets and to propose those as heritage. It is an artificial canal that surrounds the present settlement, to be identified as an historical center for the new satellite, making it perceptible from faraway and making it the persistent centerpiece of urban identity. This channel will be always full of water, because artificially fed. The second type of water is the natural affluent of the lake, with low variability, which constitutes the main axe of the city, and provides connections with the basins of the territory on a larger scale. The water level may vary, but not so much to dry up. The third quality of water is the collection of rainwater and snow melt, which structures the minute public spaces of districts, and has an high variability, adapting public performances according to different conditions. This system, according to the rule of the plan, could be theoretically expandable and repeatable as to provide environmental or urban expansion needs.

1. **Scraping begins**
   activating main canal connecting
   digging artificial ring around existing city
   permanent flooding
   ▬ natural water paths and lake
   ▬ artificial water paths

2. **Scraping creates urban fabric**
   creating canals and basins for rain
   water and melted ice collection
   variable flooding
   ▬ rainwater paths

3. **Landscape conservation**
   ▬ wetland
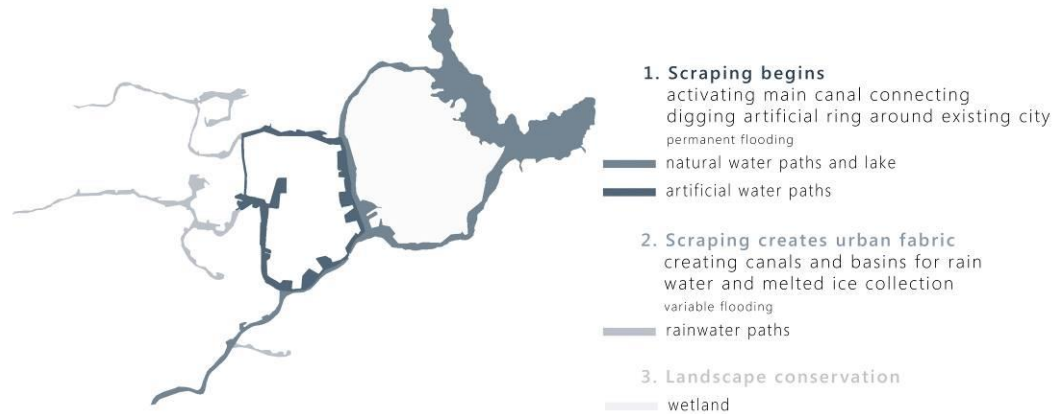
Figure 12: Hammarö water_sc[r]ape: water qualities and phases of urban growth

According to this principle, the grid of urban fabric is constituted by a network of grooves, filled by water, that traces the present hydrographic structure, and gives the main identity of the project, as shown in figure 2; so, the name water_sc[r]ape plays with the meanings of water landscape and water scratch. The grooves are around 5-8 meters lower compared to the natural ground level. The public space of the city is articulated alongside these paths shaped by the water itself; it makes a continuous and articulated network, shaped on a human scale, and located in a protected position from cold winter winds.

Through the thickness of the grooves buildings are hosted, directly facing public space, so as to be peopled and diversified in uses and functions. Residential buildings are on the north side of the grooves, to catch sunlight from the south and ground heating from the north. The southern border hosts public facilities and services in a semi underground position, designed to shelter from cold winds and exploit the thermal inertia of the ground as a temperature controller. Public spaces comfort is ensured by this design strategy, providing healthiness and distinction by driving paths that run over the ground level.

Public spaces within the urban fabric, along the canals, are shaped according to different profiles at different levels. This produces a dynamic configuration, showed by figure 3, making water level variation changing urban landscape: the different forms of public space, the range of activities that can take place, the different reflections of the city in the water, comply with natural variations. In summer, urban space will be dry and practicable, to be gradually filled by water at environmental changes, according to silhouette and geometries pre-defined by the project, always maintaining public space and city functionality.

Figure 13: Hammarö water_sc[r]ape masterplan
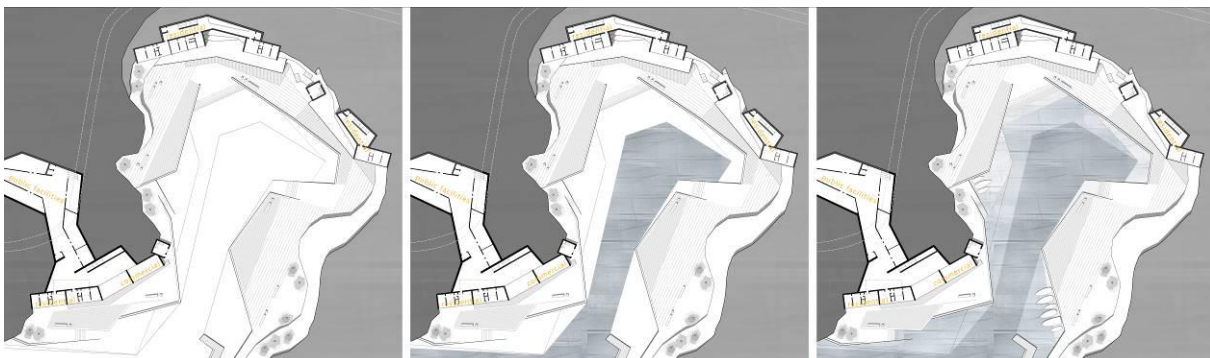
Figure 14: Hammarö water_sc[r]ape: plans of an urban fabric, showing variations of public spaces due to different water levels.

4.2 Adaptabilities

It is necessary to point out the difference between general resilience and specific resilience. The first defines the resilience of the entire system to any perturbation, while the latter is the resilience of a part of the system to a specific perturbation (FOLKE, CARPENTER, WALKER, et al., 2010: page 4). Adaptability and resilience can therefore be described and measured only by specifying which is the system under consideration - resilience *of* what - and which are the perturbations - resilience *to* what. Compared to this, there will be fast variables of the system, showing the dynamics of changing, due to perturbation, and slow variables, which keep adaptation within thresholds and ensure the functionality of the system (CARPENTER, WALKER, ANDERIES, et al., 2001: pages 777-778).

The Hammarö project concerns adaptability of public space to temperature and water level changes, as they happen in several temporal orders: seasonal heating and raining variations, mid-term variations during settlement development, and long-term variations due to climate change. The project's goal is not to achieve an adaptable configuration to these environmental changes through technological systems, but through urban form: hence, the structure and the morphology of the space are the slow variable of adaptation, that keep structure, identity, function and feedback of the system. Moreover, a

series of *abilities* of the public space have been conceived for its dynamic variations related to occurring perturbations, that represent the fast variables of adaptation, and overall constitute its adapt*ability*.

Suitability

Suitability is the consistency of the new settlement with the characters of his territory. This allows imagining a good place to live even in difficult climate conditions, adapting housing to climate. The section in figure 4, through a typical public inner space, in between houses and local public facilities, shows the position of houses, built in grooves on the north side, catching sunlight by south façade. This exploits earth heating and sunlight to increase indoor comfort. Local facilities are on the south border of the groove, providing a widespread availability and public spaces screened from the wind. Water itself mitigates climate, thanks to its thermal inertia.
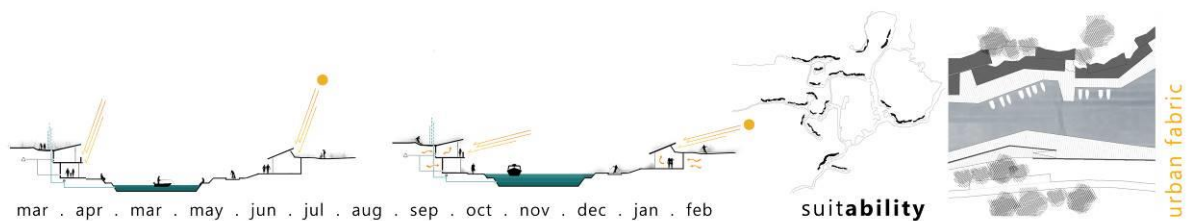
Figure 15: Hammarö water_sc[r]ape suitability: sections through urban space showing adaptation to climate variability during year, plan of residential buildings distribution, and sample plan of urban fabric.

Sociability

Sociability is the ability to provide social life of the city even in unfavorable climate conditions. This can happen through designing adaptive sociable spaces, protected by winter climate rigidity and maximizing earth heating. This is obtained through paths built in earth, with a removable cover, providing attractive and viable public spaces adapting seasonally, ensuring easy and comfortable access to local facilities and shopping spaces. Such spaces exploit earth heating and sunlight during winter and are being transformed from winter indoor spaces into alleys during summer, as it is showed in figure 5.
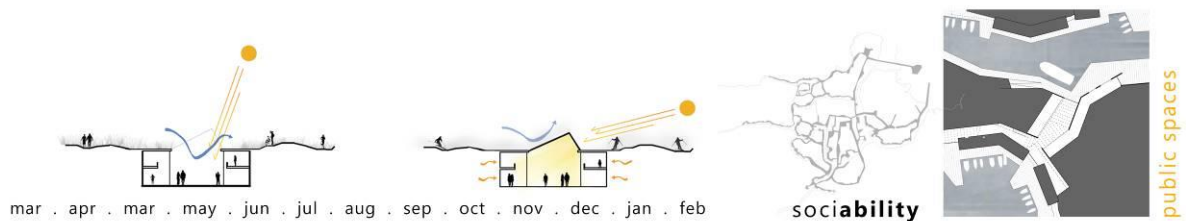
Figure 16: Hammarö water_sc[r]ape sociability: sections through public sociable space showing adaptation to climate variability during year, plan of public spaces grid, and sample plan of public spaces.

Durability

Durability means the ability of city and its image, to preserve quality and identity over time. It indicates a process of historicizing, as in small medieval town ability of integrating landscape, recognizability and dense civic life during long times. It outlines a design strategy to improve the image of the existing buildings, to propose it as a cultural heritage. Figure 6 shows the land engraving around existing village to make the main channel of the new settlement surround it, as to structure its perception from long distances and to project it in a timeless dimension compared to change around. This allows improving central village identity, keeping present value and attractiveness in time, and recognizing existing buildings as a heritage for the future.
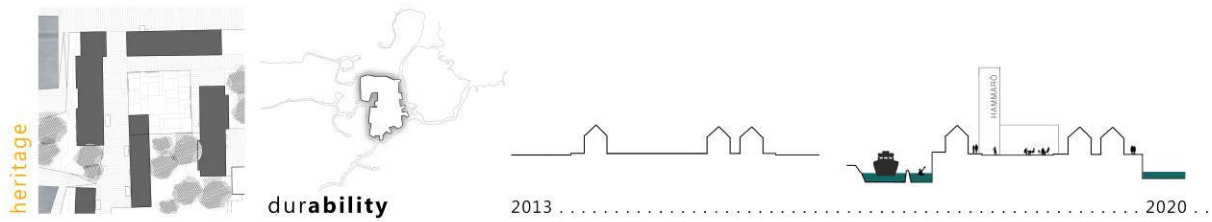
Figure 17: Hammarö water_sc[r]ape durability: plan of main square of the city, plan of existing village to be recognize as heritage, sections through existing village, showing historicizing process in mid-term period.

Connectability

Restructuring the natural channels of the water flow allows them to be navigated, catalyzing development from the whole region trough new transportation systems. This creates new public routes by boat, public paths along canals provided by urban and environmental quality that express territorial identity. Connectability is, hence, adapting natural paths to cross-country transportations routes, on a mid-term period, as in figure 7, and adapting themselves seasonally to driving, shipping, pedestrian, cycling and skiing paths, keeping same performances during time.
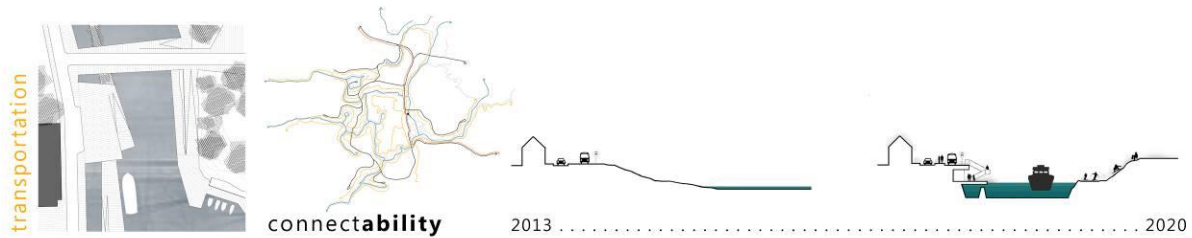
Figure 18: Hammarö water_sc[r]ape connectability: plan of a transportation hub, plan of main urban connections by canals (blue) and by streets (orange), section showing natural canals restructuration in mid-term period.

Sustainability

Sustainability is, finally, the ability of human works and social systems to create progressive equilibrium states with natural changes and ecological systems. Resilience, hence, is the way to sustainability intended in a dynamic thinking, due to adaptability of cities and landscape to climate change in a long lasting period. Natural landscape and environmental protection are pursued through the canal and wetland systems across the city, as a device able to set the level of the water coming from rainfalls and melted ice, as in figure 8. Wetlands implies reopening of the canal between Lake Sättersviken and Lake Vänern for a better circulation of water, and giving back lake Sättersviken to the city, not as a reed-land but as a public park and a new marina.
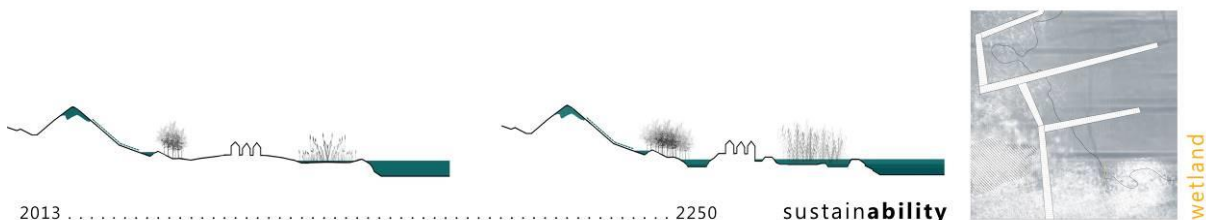
Figure 19: Hammarö water_sc[r]ape sustainability: territorial section showing adaptation to climate change in long-term period, and plan of the wetland with the marina.

5. CONCLUSIONS

In the frame of the conceptual model of resilience, as it was initially defined by Holling, urban design can have a strong role in influencing adaptability and resilience of socio-ecological systems that interact with it; this role is mainly a spatial issue, not just a technical or technological one, referred to urban

morphology and image. Space, and particularly urban space, is the channel where social systems take place as adaptive systems, and represents the slow variable of his adaptive capacity, as here all the relationships between people takes place, and between people and the built environment and natural environment. For this reason, it is necessary that the space is properly designed, so that the socio-ecological system of the city is resilient, suitable to change dynamically, still preserving its behavior,

According to this framework, the project presented as a case study, assumes the principle of adaptability as founding element, and addresses its aesthetic-morphological implications. Resilient strategies have been outlined in a qualitative way to emphasize the spatial component of adaptive urban devices. Hence, the principle of adaptability, taken as a design rule, affects the spatial structure, organization and morphology of the city. This is to demonstrate the relevance of architectural design of urban space in adaptability issues concerning the general resilience of the city: sustainability of urban development is mainly an aesthetic-morphological issue that can lead to a shift in the conception of the idea ofthe city.

6. REFERENCES

BATTY, Michael, Barros, Joana, and Junior, Sinesio Alves, 2006. Cities: continuity, transformation and emergence. In: Garnsey, Elizabeth, Mcglade, James (Editors). Complexity and co-evolution: continuity and change in socio-economic systems. Cheltenham (UK): Edward Elgar Publishing, pp. 61-76.

CARPENTER, Stephen R., Walker, Brian, Anderies, J. Marty, Abel, Nick, 2001. From metaphor to measurement: resilience of what to what?. Ecosystems, 4, 765-781.

CIRESI, Francesco, de Simone, Irene, Guerrieri, Alessia, Maricchiolo, Luca, Roma, Chiara, 2013. Europan 12: The Adaptable City, Inserting Urban Rhytms: Hammarö.

COLUCCI, Angela, 2012. Le città resilienti: approcci e strategie. Pavia (Italy): Jean Monnet centre of Pavia.

EUROPEAN LANDSCAPE CONVENTION, 2000. Firenze (Italy): Council of Europe.

FABBRICATTI, Katia, 2013. Le sfide della città interculturale: la teoria della resilienza per il governo dei cambiamenti. Milano (Italy): FrancoAngeli.

FOLKE, Carl, Carpenter, Stephen R., Walker, Brian, Scheffer, Marten, Chapin, Terry, and Rockstrom, Johan, 2010. Resilience thinking: integrating resilience, adaptability and transformability. Ecology and Society, 15 (4), 20.

HOLLING, Crawford Stanley, 1973. Resilience and stability of ecological systems. Annual Review of Ecology and Systematics, 4, 1-23.

JACOBS, Jane, 1961. The death and life of great American cities. New York (NY, USA): Random House.

LYNCH, Kevin, 1981. A theory of good city form. Cambridge (MA, USA): The MIT Press.

ORLANDO, Giuseppe, 2009. Disastri e territorio: un modello per l'analisi della resilienza nei sistemi urbani. Bari (Italy): PhD thesis in urban planning at Politecnico di Bari.

ROGERS, Richard, 1997. Cities for a small planet. London (UK): Faber & Faber.

SECCHI, Bernardo, Vigano', Paola, 2011. La ville poreuse: un projet pour le Grand Paris et la métropole de l'après-Kyoto. Genève (CH): MétisPresses.

WALKER, Brian, Holling, Crawford Stanley, Carpenter, Stephen R., and Kinzig Ann, 2004. Resilience, adaptability and transformability in social-ecological systems. Ecology and society, 9 (2), 5.

389: Developing indicators framework to evaluate the sustainability of urban infrastructure systems in middle eastern cities

MUSTAFA AL-ALWANI[1], SUAD ALFATLAWI[2]

1University of Babylon, Hilla, Babel, Iraq, E-mail: mustafalwani@yahoo.com
2University of Babylon, Hilla, Babel, Iraq,E-mail:suadalfatlawi@yahoo.com

Presently, cities face problems in the implementation of sustainable urban infrastructure systems. Sustainable infrastructure systems are essential to achieving sustainable cities because the lack of adequate services affects every aspect of daily life of the community. This research aims to develop indicators framework to evaluate the sustainability of urban infrastructure systems (wastewater treatment, energy, transportation and water resources) taking the city of Hilla, Iraq (as one of the Middle Eastern cities) as a case study. Exploration of an extensive and wide array of literature, interviews and personal communications with stakeholders and experts were conducted to acquire the information necessary for obtaining indicators framework. Moreover, that will identify and examine various issues in urban infrastructure systems and assist formulation, and selection of indicators framework which can then guide the evaluation of urban infrastructure systems' sustainability in Middle Eastern cities. The framework developed in this research succeeded and could be considered applicable, capable and effective in constructing a set of indicators which consist of 10 water resources indicators, 8 wastewater treatment indicators, 14 transportation indicators and 18 energy indicators. These indicators will reflect most of the issues regarding sustainability of urban infrastructure systems and can guide the promotion of the development of sustainable urban infrastructure systems in Middle Eastern cities.

Keywords: framework, indicators, sustainability, urban infrastructure systems, middle eastern cities

1. INTRODUCTION

There has been less attention paid to the sustainability of urban infrastructure systems yet (Huang and Yeh, 2008). Sustainable development had been defined as "development that meets the needs of the present without compromising the ability of future generations to meet their own needs" (WCED, 1987, p. 54). Infrastructure is sustainable when the system is capable to manage for changing conditions and working well without increasing resource consumption and without impacting well-being as well as people's health (Upadhyaya, 2012). In other words, sustainable infrastructure is the infrastructure that capable to operate in a manner that not adversely affects the system's ability to work in the future. Moreover, it is essential to the infrastructure not only to be working, but to be resilient in order that it is capable to serve for a long time. Various research studies (Sahely et al., 2005; Lim and Yang, 2006; Ugwu and Haupt, 2005) identified the scope of sustainable infrastructure and relevant indicators. However, while sustainable infrastructure focuses on construction processes and buildings, there is a real need to advance sustainability and consistence of the principles of urban sustainability when making decisions, evaluating and design of new or optimization of existing infrastructure (UofT, 2001). Generally, many cities in the world (including those in the Middle East) do not have systematic assessment of urban problems. The current tools for urban policy in Middle East countries is insufficient to provide an overall image about the city and how it works. Moreover, a serious problem of urban policy makers in Middle Eastern cities is the lack of suitable information on some infrastructure systems and rarely information gathered in a consistent framework. Therefore, cities need methods and tools for evaluating infrastructure systems sustainability. It is important for decision makers to achieve an understanding of sustainability indicators for infrastructure systems decision-making. Sustainability indicators are an important factor in the overall assessment of progress towards sustainability. They are helpful for measuring and monitoring the environment state by considering a manageable number of variables (McLaren and Simonovic 1999). Moreover, indicators are important tools to communicate information to decision-makers because information in its raw form is not easy to judge and to act upon. Furthermore, indicators quantify information and provide a simple form of information. They also simplify information about complex phenomena, in order to improve communication. Urban infrastructure systems sustainability has received little attention by governments of Middle East countries but there are many factors that make it an important issue for future growth strategies in some Middle East countries, especially in the Gulf, which faces energy shortages owing to plentiful gas consumption (Smeets and Bayar, 2012). Therefore, there are major challenges to overcome to prevent a decline of the urban infrastructure systems. These challenges need to be addressed by developing a framework which guides the creation of sustainable urban infrastructure systems for future generations. This research proposes an evaluation tool (framework) for sustainability assessment of urban infrastructure systems that cover wastewater, energy, water resource, transportation infrastructure. This framework, which will assist in developing sustainability indicators, should be clear, understandable and easy to use.

2. METHODOLOGY

The methodology adopted for this research was conducted using a combination of structured interviews with stakeholders, case study infrastructure systems data, literature review on sustainability research, and workshop with experts for indicator formulation, selection and validation. Generally, the understanding of the infrastructure system is important to obtain, because the familiarity of the system is critical in sustainability assessment. Therefore, a comprehensive approach to develop the methodology had been taken. The main goal of this research was to develop a sustainability assessment indicators framework for urban infrastructure systems that can cover long term and changing issues. The important tasks which had been carried out to achieve the aim are as follows:

2.1 Identify the Existing Urban Infrastructure Systems

An observation occurred aiming to pick up detailed information about the urban infrastructure systems. This observation included site visits to the major organizations. Moreover, this observation consisted of personal communications with stakeholders in the field. Past personal experiences were also gathered to build an inclusive idea about the infrastructure systems.

2.2 Identify the Existing Frameworks of Sustainability Assessment

Analysis of the scientific literature had been conducted to examine whether the existing frameworks could be utilized in evaluating the sustainability of infrastructure systems. As had been seen from the literature review there were found to be numerous frameworks for sustainability assessment previously developed that could provide guidelines for planning and management of infrastructure systems. However, there was no single framework used so far to improve sustainability would be totally sufficient when new issues were emerging. Current sustainability frameworks do not consider the changing conditions that influence the infrastructure system performance in the decision making. Furthermore, most of the sustainability assessment frameworks do not consider the importance of system dynamics, and in addition to not consider the dynamic of sustainability. Instead, this research developed an indicators framework to evaluate the infrastructure systems sustainability from stakeholders' perspective towards sustainability.

2.3 Develop an Appropriate Indicators Framework

Most excellent practice recommends that indicators should be developed through logical structures, called frameworks (Pintér et al., 2005). In fact, there is a real need for the development of a systematic process (frameworks) for the formulation and selection of indicators to assess sustainability of urban infrastructure systems. The most important advantages of indicators frameworks are that they can be used as a tool for classifying indicators to verify which issues have been covered and which have been disregarded. On the other hand, frameworks encourage interpretation and make the indicators more effective. Furthermore, they explain and highlight what to measure, what can be expected from measurement and which indicators can be applied (Pintér et al., 2005). For the above reasons, this research developed a suitable framework that can cover broader and long term issues in the future as well as current issues.

2.4 Applying the Framework to a Case Study

Case studies are an appropriate research strategy when there is focus on contemporary events, when the researcher has little control over events, when a holistic, in-depth investigation is needed and when evaluating and testing the theory or framework in a natural situation is needed. The case study is a reliable methodology when implemented carefully and knowledgeably. Therefore, the authors of this research decided to apply the proposed framework to a case study to demonstrate how the sustainability evaluation indicators of urban infrastructure systems could be selected and formulated.

3. URBAN INFRASTRUCTURE SYSTEMS SUSTAINABILITY EVALUATION FRAMEWORK

It is necessary to develop indicator sets to evaluate progress towards sustainable urban infrastructure systems which are useful for decision-makers and for policy monitoring and evaluation. Developing indicators should be an open communication rather than a purely scientific process (Valentin and Spangenberg, 2000). To achieve this broad principle, suitable steps should be applied to propose a set of indicators. In this research, building a framework for finding appropriate indicators to evaluate sustainability of urban infrastructure systems in the Middle Eastern context involves a number of steps. These steps are as follow:

3.1 Identify a Variety of Issues and Needs

In each infrastructure system, a variety of issues and needs would be identified and efforts would be made to deal with these issues and needs. This happened by developing an interview with stakeholders working in the wastewater treatment, energy, transportation and water resources sector to achieve understanding of the infrastructure systems related issues. Moreover, interview was developed to gain insight about the issues, challenges, data and information availability. In addition to incorporate the feedback from people involved in infrastructure systems management, and their opinion was incorporated into the overall framework development.

3.2 Review of the Literature

Review of the literature to find which indicators had been used in the past to assess the urban infrastructure systems.

3.3 Selection of Initial Set of Indicators

This occurred by selecting an indicators set from existing indicators via literature and desktop research. The set of indicators which would be selected were, as far as possible, relevant to different infrastructure systems, quantifiable, reliable, meaningful and capable to refer to progress towards sustainability or away from it. Existing indicators would be selected, as much as possible, because they had already been tested and implemented. On the other hand, new indicators were proposed through a workshop with a team of expert when no of the existing indicators represent essentially the performance measures that we intended to measure.

3.4 Workshop with a Team of Experts

The user needs and issues associated with urban infrastructure systems are so important to guide the development of indicators. The user needs assessment, together with the appraisal of existing Indicators, would form the basis for participatory development of urban indicators. New indicators were also proposed wherever necessary. Workshop with a team of experts was proposed to hold in order to demonstrate the previously identified infrastructure systems issues and attach their new indicators. Furthermore, this step was also aimed to identify indicators deemed irrelevant and choose of a short list of previously selected indicators, which was applicable, by a team of experts. The indicators set should critically review to ensure that it reflects the infrastructure systems issues and a wide array of conceptions of what infrastructure sustainability may require. Certain parameters were taken into consideration in developing the new indicators, these included: importance (indicators should be relevant to policies), priority (indicators should be recognized based on priority), understood (easy, simple and reliable), cost effective (information to be gathered in a cost effective manner), measurable (show the magnitude of the problem) and sensitive (flexible enough to accept changes).

4. CASE STUDY

Case studies are the ideal strategy when: the study is about a contemporary phenomenon within some real-life context; the researcher has slight control over events (Yin 1994). Punter (1986) supports adopting a case study approach when there is a need for testing the formulation of a framework which can be accomplished by outlining, commenting on and linking it to a case study. This view is consistent with the opinion of Soy (1997) who stated that a case study is suitable for validating a framework developed earlier. Stake (1998) also promoted the dependence of the case study approach because it permits researchers to study contemporary events and the naturalness of phenomena. Moreover, Yin (1994) explained that case studies offer the scope to study real life situations by means of multiple sources of data. Based on the views that had been mentioned above and the fact that the issue of urban sustainability arises in the real world along with an understanding that the challenges of sustainability are best approached through case study based investigations, a case study was considered to be the appropriate and accurate research methodology for this research which aimed to test the formulated framework. The city of Hilla, Iraq is one of the Middle East cities with a total population of 484,007 people. It is located on both sides of the Hilla river which is a branch of the Euphrates river in the position of the intersection of longitude (44.26) east and with latitude (32.29) north (Al Khatib, 1972). The city of Hilla, Iraq had been selected as the single case study, because Iraq has characteristics typical of many other countries in the Middle Eastern area, especially as an oil rich country which has suffered from several conflicts, in addition to having similar cultural backgrounds and sustainability problems. Therefore, the city of Hilla relates to different Middle Eastern cities. There is a unique opportunity for the city of Hilla because of its location close to the site of the ancient city of Babylon, which has given the city a significant importance in terms of development opportunities. For applying the framework, there were four steps as follows:

4.1 Identify a Variety of Issues and Needs

The first step aimed to explore the major issues, needs and problems of infrastructure systems within the city of Hilla, Iraq. Books, newspapers, journal articles, government records, unpublished reports,

non-government reports, academic reports, local historical records, maps and other sources relevant to the case study used to collect the issues of the infrastructure systems. Moreover, semi structured interview involved open-ended questions with Stakeholders to investigate the most important issues and needs of infrastructure systems within the city of Hilla. Stakeholders were selected for participation in the interview by recommendation resulting in a total of 40 participants.

4.2 Review of the literature

Generally, the literature review focused on infrastructure system issues and sustainability. A number of assessment models and techniques was published such as Deakin and Curwell, 2004; Berger et al., 2007; Kashem and Halfiz, 2006; Weng and Yang, 2003; O'Regan et al., 2002; Quental et al., 2004; Sahely et al., 2005. Moreover, they had suggested several sustainability indicators. Daniel et al., 2005; O'Regan et al., 2002; Sahely et. al, 2005; Kashem and Hafiz, 2006; Stokes and Horvath, 2006; Weng and Yang, 2003, proposed lists of sustainability indicators. Through a review and analysis of existing types of sustainability indicator frameworks, there were many weaknesses and disadvantage points. Moreover, there was a real need for development and applied of a systematic process for the formulation and selection of indicators to assess sustainability of urban infrastructure systems in Middle Eastern cities.

4.3 Selection of Initial Set of Indicators

As much as possible, quantifiable, reliable, capable, relevant and meaningful indicators had been selected to build up the first set of potential indicators. The first set of potential indicators was then analysed, revised and selected through a workshop with a team of experts (academics and practitioners) from various fields.

4.4 Workshop with a Team of Experts

After the selection process, the indicators were evaluated, analysed and revised by a team of experts through workshop concerning their suitability for the sustainability measurement of infrastructure systems and to ensure that no relevant indicators were missing. A workshop was held with experts from the City of Hilla and approximately 20 experts (10 academics and 10 practitioners) were attended. There were multiple purposes of the workshop, but the discussion focused on demonstrate the previously identified infrastructure systems issues and attached their new indicators and selected of a short list of previously developed indicators that was applicable. Furthermore the workshop focused on the appropriateness of the indicators and to review, evaluate, analyse and revise these Indicators. At the end of the workshop, issues were reviewed and formulation of indicators was done. This resulted in the production of 50 indicators. This application illustrated the applicability, capabilities, and practicality of the indicator framework (Table 1 shows the final set of infrastructure systems sustainability indicators for the case study).

5. RESULTS

The final set of indicators consisted of 10 water resources indicators, 8 wastewater treatment indicators, 14 transportation indicators and 18 energy indicators. So these 50 indicators are suggested to be the indicators for measuring the urban infrastructure systems sustainability of the city of Hilla and other Middle Eastern cities (Table 1).

6. CONCLUSIONS AND RECOMMENDATION

This research set out to develop an indicators framework to evaluate the sustainability of infrastructure systems that would cover long-term, broader, and changing issues. The results of this research were achieved through the methodology adopted. Interviews were used as a tool for an understanding of the infrastructure systems, common issues, and how such issues are managed. The survey provided an important basis for developing the framework. Such framework was built from a literature review. The framework is flexible, can be applied in infrastructure systems such as water, wastewater, transportation, and energy.

A case study approach is suitable and it is a widely used method in sustainability research because multiple issues are at play and there is limited control over the system variables.

The framework developed in this research succeeded and could be considered applicable and, capable in constructing a set of indicators which consist of 10 water resources indicators, 8 wastewater treatment indicators, 14 transportation indicators and 18 energy indicators. As a result, these 50 indicators were suggested to be the indicators for measuring sustainability of the urban infrastructure systems of the city of Hilla and other Middle Eastern cities. On the other hand, this indicators framework will reflect the majority of the issues concerning urban infrastructure systems sustainability and can guide the development and create better and healthier infrastructure systems to support the society in Middle Eastern cities.

Finally, the following recommendations were suggested to assist applicability of this sustainability evaluation framework, in addition to improve the framework itself:

- Increase the number of stakeholders interviewed for future surveys
- Increase the data collection by using an effective monitoring plan, such as modelling approaches and tools together data for indicators
- Develop staffs working on infrastructure systems to deal with new and emerging issues.

Table 3: Final set of indicators suggested for measuring the urban infrastructure systems sustainability of the Middle Eastern cities

Water Systems Indicators	Wastewater Indicators	Transportation indicators	Energy Indicators
Water intake by municipal services	Population served by Sewage system	Expenditure on roads, parking, public transit, ports, etc.	Service/commercial energy strengths
Borne diseases through the water	Municipal revenues, from wastewater management	Per capita congestion	Domestic energy intensities
Connections of water and sewer	Municipal costs of wastewater management	Proportion of portion of trips by non-motorized modes	Agricultural energy strengths
The possibility of affected of Groundwater	Population served by wastewater treatment plants	Crash deaths and injuries	End-use energy costs by fuel and by sector
Population served by water supply systems	Expenditure per 1000 inhabitants on wastewater management	Quality of walking, cycling, public transit, driving, taxi, etc./	External prices of energy use
Total water intake	Rate of Wastewater produced	Quality of accessibility for people with disabilities	Efficiency of energy transformation and supply
Total water treated	Rate of wastewater treatment	Land devoted to transport facilities	Domestic energy use for each income group and equivalent fuel mix
Total public water consumption	Wastewater treatment in wastewater treatment plant	Total vehicle emissions	Joined heat and power generation
Water losses		Proportion of emissions from facility construction	Annual energy consumption, total and by main user group
Leakage of water		Economic costs of traffic collisions	Reserves-to-manufacture ratio
		Proportion of people exposed to traffic noise	Industrialized energy intensities
		Affordable housing accessibility	Transport energy strengths
		Using a method of investment in transport infrastructure	Fuel shares in energy and power
		Modal divided of passenger transport	Renewable energy share in energy and power
			Net energy import need
			Pollutant discharges in liquid effluents from energy systems
			Ratio of solid waste generation of units of energy produced
			Air pollutant emissions from energy systems
			Reserves-to-manufacture ratio

7. REFERENCES

AL KHATIB, S.M., 1972. City of Hilla, the major function and regional relations. Thesis (Msc.) Baghdad University.

BERGER, T., Birner, R., Diaz, J., Mccarthy, N. and Wittmer, H., 2007. Capturing the complexity of water uses and water users within a multi-agent framework, Water Resources Management, 21, pp. 129-148.

DANIELL, K., Sommerville, H., Foley, B., Maier, H., Malovka, D., and Kingsborough, A., 2005. Integrated urban system modelling: methodology and case study using multi-agent systems. In International Congress on Modelling and Simulation. 16th: 2005: Melbourne, Victoria.

DEAKIN, M., and Curwell, S., 2004. The BEQUEST framework: the vision and methodology of a collaborative platform for sustainable urban development. In18th International Conference Informatics for Environmental Protection, Geneva, 23, 91-104.

HUANG R.Y. and Yeh C.H., 2008. Development of an assessment framework for green highway construction. Journal of the Chinese Institute of Engineers, 31(4): 573–585.

KASHEM, S. B., and Hafiz, R., 2006. Sustainability Appraisal of development trends in the urban fringe: an MCA approach. In 42nd IsoCaRP Congress, İstanbul.

LIM S.K. and Yang, J., 2006. Understanding the need of project stakeholders for improving sustainability outcomes in infrastructure projects. Proceedings of Joint CIB Conference: Performance and Knowledge Management, Australia, 333–343.

O'REGAN, B., Moles, R., Kelly, R., Ravetz, J. and Mcevoy, D., 2002. Developing indicators for the estimation of sustainable settlement size in Ireland. Environmental Management and Health, 13(5), 450-466.

PINTÉR, L., Peter, H. and Peter, B., 2005. Sustainable Development Indicators, proposals for a way forward, Prepared for the United Nations Division for Sustainable Development. International Institute for Sustainable Development, New York: United Nations Division for Sustainable Development

PUNTER, J.V., 1986. Aesthetic Control within the Development Process: A Case Study. Land Development Studies, 3, 197-212.

QUENTAL, N., Lourenço, J., and Silva, F. N., 2006. Um modelo integrado de desenvolvimento sustentável às escalas global e urbana. In II Congresso Luso-Brasileiro para o Planeamento Urbano, Regional, Integrado e Sustentável, PLURIS, 27-29.

SAHELY, H.R., Kennedy, C.A. and Adams, B.J., 2005. Developing sustainability criteria for urban infrastructure systems. Canadian Journal of Civil Engineering, 32, pp.72-85.

SMEETS, B and Bayar, A., 2012, Sustainability of economic growth in Abu Dhabi - a Dynamic CGE Approach. Topics in Middle Eastern and African Economies, Vol. 14.

SOY, S. K., 1997. The case study as a research method. Unpublished paper, University of Texas, Austin.

STAKE, R. E., 1998. Case Studies. In Denzin, N. K., & Lincoln, Y. S. (Eds.). 2008. Strategies of qualitative inquiry. 2, Sage.

STOKES, J. and Horvath, A., 2006.Life cycle energy assessment of alternative water supply systems. International Journal of Life Cycle Assessment, 11(5), pp. 335-343.

UGWU O.O. and Haupt T.C., 2005. Key performance indicators and assessment methods for infrastructure sustainability – a South African construction industry perspective. Building and Environment 42(2): 665–680.

UNIVERSITY OF TORONTO, 2001. Sustainable Infrastructure Engineering Definition, University of Toronto, Available from: http://www.civ.utoronto.ca/sir/default.htm [Accessed 3 May 2015].

VALENTIN, A. and Spangenberg, J., 2000. A guide to community sustainability indicators. Environmental Impact Assessment Review, 20, 381–92.

WCED, Our Common Future ("The Brundtland Report"), The World Commission on Environmental and Development for the General Assembly of the United Nations, 2007 Available from: www.are.admin.ch/themen/nachhaltig/00266/00540/00542/ index. html? lan=en, [Accessed1 May 2015].

WENG, Q. and Yang, S., 2003 An approach to evaluation of sustainability for Guangzhou's urban ecosystem. International Journal of Sustainable Development and World Ecology, 10, 69-81.

YIN, R. K., 1994. Case Study Research: Design and Methods. London: Sage Publications.

SESSION 7: ENERGY DEMAND AND USE OPTIMIZATION

193: Towards an integrated computational method to optimise design strategies for the built environment

POLYTIMI SOFOTASIOU[1], JOHN K. CALAUTIT[2], BEN R. HUGHES [3], DOMINIC O'CONNOR [4]

1 University of Sheffield, Western Bank Arts Tower, psofotasiou1@sheffield.ac.uk
2 University of Sheffield, Western Bank Arts Tower, j.calautit@sheffield.ac.uk
3 University of Sheffield, Western Bank Arts Tower, b.hughes@sheffield.ac.uk
4 University of Sheffield, Western Bank Arts Tower, dboconnor1@sheffield.ac.uk

The distinctly need for developing energy efficient and functional structural designs, demands the adoption of multidisciplinary techniques that will guarantee constructions' integrity. Towards this objective, engineers and scientists employ Computational Fluid Dynamic (CFD) tools and optimisation techniques, in order to first predict the physical phenomena occurring in the built environment and in sequence to find optimum solutions that will assist the conceptual design phase. In the current study, a methodology to conduct design optimisation studies is demonstrated, using coupled CFD and Response Surface Methodology (RSM) meta-model based optimisation techniques. Regarding the assessment of the natural ventilation performance of a cross ventilated building, the design optimisation of the window openings was performed. The results revealed the ability to obtain locally optimal solutions, along with a further insight on the influential role of the design parameters in design's response. The methodology was validated with wind tunnel experiments and the optimisation results were verified, confirming the competence for conducting similar design optimisation studies.

Keywords: Computational Fluid Dynamics, Response Surface Methodology, optimisation, natural ventilation

1. INTRODUCTION

Optimality in design spaces is a rising concept in the studies of built environment, necessary to meet functional requirements and high quality occupational standards. Therefore, scientists and engineers employ simulation-assisted optimisation strategies to evaluate buildings' behaviour at the early design stages. However, the complexity of the built environment and the numerous parameters that are involved, allow defining specific individual or limited number of design objectives at a time (Evis, 2013). Depending on the research purpose and the achievable goals, computational optimisation techniques are used in buildings' performance evaluation, including energy consumption requirements (Wang et al., 2005), building retrofit scenarios (Asadi et al., 2014), performance assessment of building services (Huang et al., 2009) and ventilation performance (Stavrakakis et al., 2012).

Response Surface Methodology (RSM) has been proven an accurate technique on the investigation of multivariable design solutions that satisfy a pre-defined set of conditions, in substantially less computational cost. It has been widely adopted to perform parametric studies that enable to understand the behaviour of several parameters and quantify their impact on design solutions (Myers et al., 2009). By employing statistical and mathematical methods, approximation models are constructed, based on physical or computer experiments (Montgomery, 2000). The technique relies on Design of Experiments (DoE) studies that enable the generation of a dimensional space, within which the exploration of design optimality occurs.

In building design, the RSM technique is mainly used for the study of the internal micro-environmental improvement, regarding the ventilation efficiency provided by several structural configuration systems. Shen et al. (2012) studied different DoE methods to assess the ventilation performance of a natural ventilated building under variable wind speed and direction, validating the obtained results with Computational Fluid Dynamics (CFD) simulations. In a latest study (Shen et al., 2013), they assessed the performance of different DoE methods for developing response surface models to evaluate the ventilation rate in naturally ventilated buildings, based on CFD simulations studies. Khan et al. (2012) employed simulation based optimisation tools to investigate the optimum ventilation system design to control pathogen dispersion and comfort in a two-dimensional patient room, by developing a methodology based on coupled RSM method and genetic algorithm (GA).

When RSM methodologies are combined with computer simulation software, the advantages offered are particular impressive in terms of robustness and computational time (Myers et al., 2009). In the current study a coupled CFD-RSM metamodel-based optimisation methodology is presented using a commercial simulation software. Based on a deterministic simulation model of a cross ventilated building, the ventilation performance is evaluated regarding the optimisation of the window opening configuration.

2. METHODOLOGY

The current work is based on simulation-driven design optimisation, using ANSYS software; a user friendly simulation interface integrated with RSM-based design optimisation algorithms. The proposed methodology can be described in five main steps, which are also depicted in the flowchart in Figure 20. In the first step, the initial design case is created. This includes the generation of model's geometry and computational mesh, along with the simulation setup and the collection of the CFD results. In the second step, the Design of Experiments (DoE) technique is employed. In this part the design variables (input parameters), their ranges (design space) and the design responses (output parameters) are defined. The required number of the design points for the problem investigation is thereafter generated. The step three concerns a feedback system, according to which the simulation runs for the design points are performed and the obtained data are collected. The generated results will compose the design space of responses, known as response surface. In step four the objective function is defined and an optimisation method is employed, for the identification of the optimal design solution. Finally, step five includes the verification of the results and the evaluation of model uncertainties.
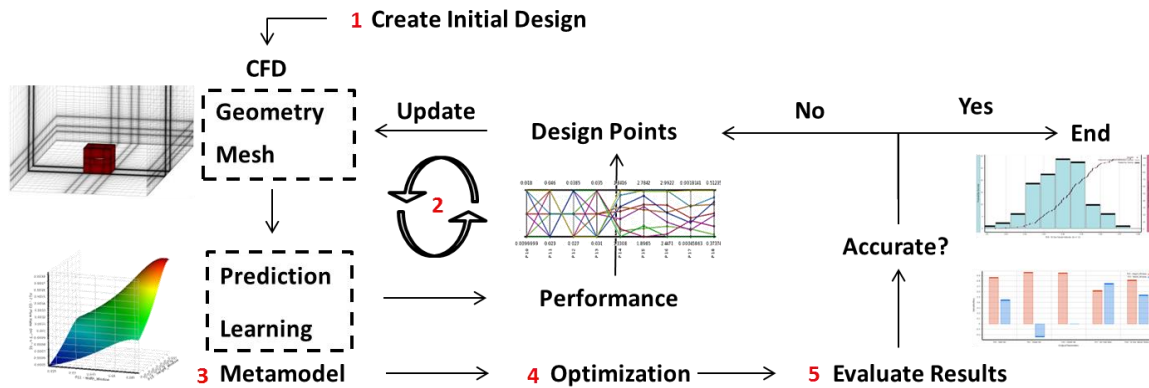
Figure 20: Proposed methodology for the design optimisation study

3. INITIAL CASE STUDY DESCRIPTION

For application of the proposed methodology, a simple cross-ventilated cubic structure was created in Design Modeller of ANSYS 15.0. The building model of 0.1 x 0.1 x 0.08 m^3 (L x W x H) and wall thickness 0.002 m consisted of two window openings of 0.018 x 0.046 m^2 (H x W), placed on the opposite sides at the centres of the walls to promote natural airflow with the least resistance (Figure 21).

3.1 Geometry and mesh generation

The dimensions of the computational domain were set according to the wind tunnel's working section dimensions that would be used in sequence for a full scale validation study (Calautit et al., 2014). As illustrated in Figure 2, the domain is 1.0 m long, 0.5 m wide and 0.5 m high, allowing a blockage ratio (Area$_{model}$/Area$_{tunnel}$ x 100%) of 2.8%, which lies within the recommended values for accurate simulation studies of air flow around buildings (Joerg, 2006) (Figure 21).
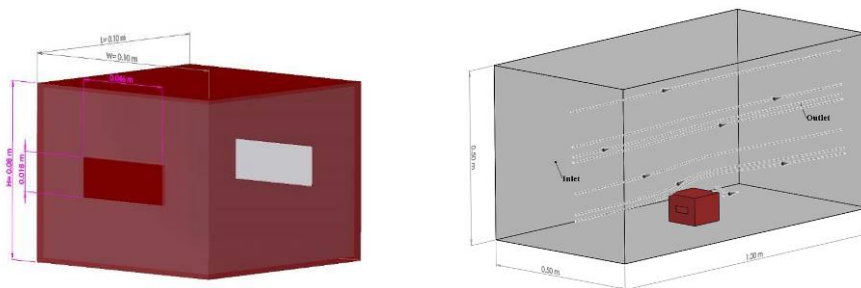
Figure 21: Dimensional characteristics of the studied building model (left) and the computational domain (right)

Grid independency

The generation of the mesh resulted to 1,071,790 high quality structured hexahedral cells. As illustrated in Figure 22, in the areas of interest (window openings and building edges) grid refinements have been made to allow for computational resolution. A grid independency study was also performed regarding the comparison of average velocity values on the two window openings. The results are presented in

Table 4, indicating that the initially generated mesh shows a good performance in velocity prediction with the selected RANS turbulence model.
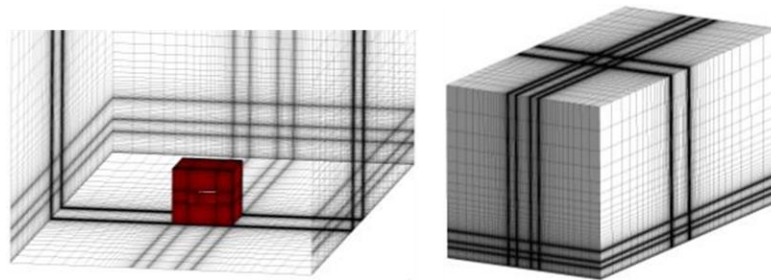
Figure 22: Mesh generation of the computational domain.

Table 4: Mesh independency study and error estimation

Computational Grid Size	Average Velocity (m/s)	$\varepsilon = (f_2-f_1)/f_1*100\%$
Coarse: 647,542	1.79	4.5 %
Middle: 1,071,790	1.88	-
Fine: 1,236,636	1.92	2.1 %

3.2 CFD simulation set up

The calculations for the prediction of the flow distribution patterns were performed using Fluent 15.0. The description of the boundary conditions is presented in Table 5. The standard k-ε turbulence model was used with standard wall functions, proven for its good performance on wind flow predictions around bluff bodies (Blocken, 2014). Further settings included the selection of Semi-Implicit-Method for Pressure Linked Equations (SIMPLE) scheme and second-order spatial discretization of the momentum and the turbulence transport equations.

Table 5: Boundary conditions for the CFD simulation

Inlet	Constant velocity U = 3m/s
Outlet	Zero pressure
Side, top and ground walls	k_s=0.001 m and C_s=0.5
Building walls	k_s=0.001 m and C_s=0.5

3.2 CFD methodology validation

A full scale experimental study was carried out for the validation of the airflow distribution patterns resulting from the steady RANS CFD simulation. The closed-loop subsonic wind tunnel that was used, enabled the generation of a uniform velocity profile of 3m/s, measured prior the positioning of the model at the centre of the working section (Figure 23a). The performance assessment was based on velocity measurements in five different locations. Three points were equally distributed at the interior of the block and two points were sited at the exact proximity of the window openings, as illustrated in Figure 23b. The speed measurements were conducted with a hot wire probe (Testo 425), considering an error of uncertainty equal to ± 1.0% rdg. for the specified velocity speed. The results, presented in Table 6, were in good agreement with the CFD values, reproducing accurately the wind velocity that confirms the followed methodology. However, a maximum error of 14.5% at Point 5, located at the leeward underpressure region of the block, may be explained due to the expected locally-induced turbulence.
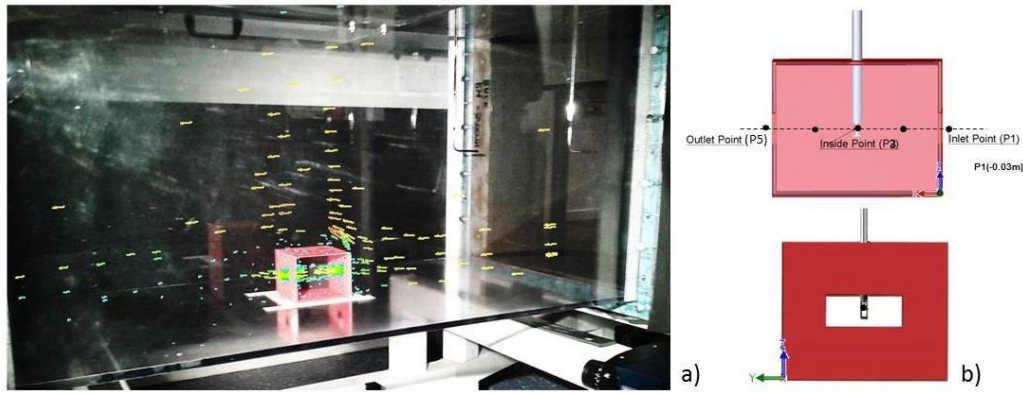
Figure 23: Wind tunnel validation model (a) and velocity measurement points (b)

Table 6: Wind tunnel validation measurements of velocity in five building locations

Measurement Point	P1	P2	P3	P4	P5
WT. Velocity	1.95 m/s	2.66 m/s	2.67 m/s	2.36 m/s	2.54 m/s
CFD Velocity	1.84 m/s	2.87 m/s	2.76 m/s	2.59 m/s	2.97 m/s
Error	5.9%	7.3%	3.0%	8.8%	14.5%

4. DESIGN OF EXPERIMENTS

Design of experiments (DoE) is a data collection strategy that enables the investigation of relationships between the design independent parameters and the dependent response variables. It is the tool for the RSM to generate the exploration region of responses, based on the adequate number of simulation data.

The implementation of the DoE study requires three main attributes, including the following (Shen et al., 2012):

- the identification of the performance measures (output) that need to be optimised and the parameters (inputs) that are considered to influence more their performance;
- the delimitation of the design space (constrains) within the input parameters will vary and,
- the generation of the design points and their responses.

4.1 Assignment of design parameters

In case of cross-ventilated buildings, the attainment of comfortable indoor environments is an important design attribute, mainly counted in terms of air volume induced in the occupied space, to provide sufficient ventilation, and in terms of homogeneity, to equally distribute the flow within the areas of interest. The parameters that have been found to play a decisive role are the window opening configuration and the window positioning (Stavrakakis et al., 2012; Bangalee et al., 2013). Thereby, regarding the initial simulation results, the input and output parameters decided for evaluation are shown in Table 7, along with the rationally selected design constraints set.

Table 7: Definition of input and output parameters, their design space and design constraints.

Parameters	Name	Description	Design space/ Constraints	Initial case value
Inputs	P1_Window Height	-	$0.01\ m \le P1 \le 0.018\ m$	0.018 m
	P2_Window Width	-	$0.023\ m \le P2 \le 0.046\ m$	0.046 m
	P3_Centralised Wind.Height	-	(0.08-P1)/2	*/keeps window design always at wall centre
	P4_Centralised Wind.Width	-	(0.1-P2)/2	
Outputs	P5_Flow Rate_Q	$Q = \dfrac{\dot{m}}{\rho}$	Maximise	1.814×10^{-3} m³/s

P6_St_Velocity_Deviation	$SD = \sqrt{\dfrac{\sum(U_i - \overline{U})^2}{n}}$	Minimise	0.5123 m/s

where: Q is the flow rate at the windward window (m³/s), $\dot{m}$ the mass flow rate (kg/s), ρ is the air density (kg/m³), SD is the standard deviation (m/s), n is the number of computational cells at the interior of the model, U_i is the velocity at interior location i (m/s) and $\overline{U}$ is the mean velocity at the interior of the model (m/s).

4.2 Generation of design points

After having defined the number of input parameters and the variable design space within they will be evaluated, the Auto-defined Central Composite Design (CCD) scheme was adopted for the generation of the design points. The CCD consists of one central point, 2N star (or axial) points and a two-level full factorial design (2^N factorial points). The number of the design points can then be determined based on the Equation 1:

Equation 1: Number of design points based on CCD scheme.
$$DP = 1 + 2N + 2^N$$

Where:

- N = the number of factors/ input parameters

For the current case study, eight rotatable and symmetrical designs were created, in addition to the initial one. The calculation of their responses was the most time consuming part, since sequential simulation runs were performed, allowing the analysis to reach convergence. The results are shown in Table 8 below:

Table 8: Design points generated based on CCD scheme and their responses

Design Point	P1_Window_Height (m)	P2_Window_Width (m)	P5_Flow_Rate_Q (m³/s)	P6_St_Vel_Deviation (m/s)
DP 0	0.018	0.046	1.703 x 10⁻³	0.511
DP 1	0.01	0.023	0.446 x 10⁻³	0.419
DP 2	0.01	0.0345	0.71 x 10⁻³	0.406
DP 3	0.01	0.046	0.955 x 10⁻³	0.419
DP 4	0.014	0.023	0.626 x 10⁻³	0.469
DP 5	0.014	0.0345	1.013 x 10⁻³	0.473
DP 6	0.014	0.046	1.364 x 10⁻³	0.484
DP 7	0.018	0.023	0.809 x 10⁻³	0.492
DP 8	0.018	0.0345	1.279 x 10⁻³	0.501

5. RESPONSE SURFACE METHODOLOGY

RSM is used to study the unknown functional relationships between independent variables (x) and a response variable yield (y). A general equation that describes that relationship is given in Equation 2:

Equation 2: Relationship between a response variable and independent variables
$$y = f(x, \theta) + \varepsilon$$

Where:

- ε = is treated as a statistical error

By employing mathematical and statistical methods, first-order and second-order approximation models are constructed, based on physical or computer experiments. However, second-order models are commonly used for optimisation processes, due to their flexible nature and ability to perform better in complex problems (Myers et al., 2009). The general mathematical formula describing second-order response surface models is presented in Equation 3:

Equation 3: Second-order response surface model $y = \beta_0 + \sum_{i=1}^{k} \beta_i x_i + \sum_{i=1}^{k} \beta_{ii} x_i{}^2 + \sum \sum_{i<j=2}^{k} \beta_{ij} x_i x_j + \epsilon$

Where:

- β_0 = parameter that fixes the intercept of the plane
- $\beta_{i,j}$ = regression coefficients
- i, j = 1, 2,…, k,   describe the dimensional space of the regressor variables

The Response Surface Methods calculate approximate values for the regression coefficients, based on the evaluation of the simulation results generated for the design points. Once the best fitted approximation function is found, several design combinations can be examined, without the need of conducting deterministic response analysis that require significant computational time.

6. RESULTS AND DISCUSSION

6.1 RSM results

As mentioned earlier, the aim of this study was to improve the ventilation performance of a cross-ventilated building, by investigating the optimum window dimensional configuration. The response surface results were generated using regression analysis, based on the Standard Response Surface-Full Second Order Polynomial modelling algorithm. Figure 24 shows the obtained 3D graphical exploration of the response surfaces. Every surface represents a response output and its variation according to the dimensionally defined inputs. Based on the observed fitted surfaces, both the flow rate and the standard deviation of velocities increase, as the window openings increase in height and width.
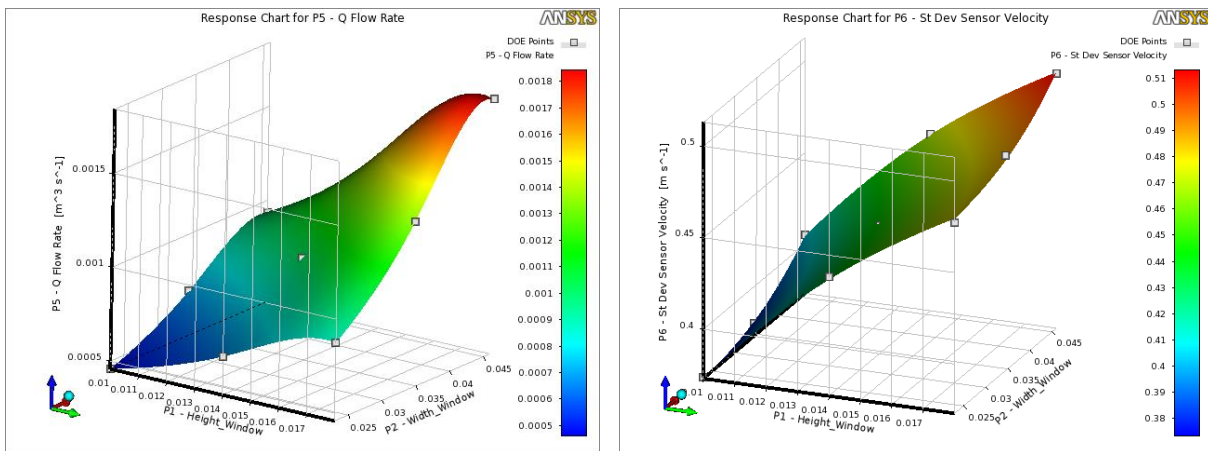
Figure 24: Response surfaces for P5_Flow_Rate_Q (left) and P6_St_Vel_Deviation (right)

Design sensitivity information were also generated. Figure 25 presents the local sensitivity charts that show the influential role of each input parameter on the output responses. The values were calculated considering the variance of one input parameter at a time and its impact on the change of the design outputs. It was observed that for every design alternative the window width was more significant parameter on the flow rate values, as opposed to the window height, which had greater influence on the standard deviation of velocities.
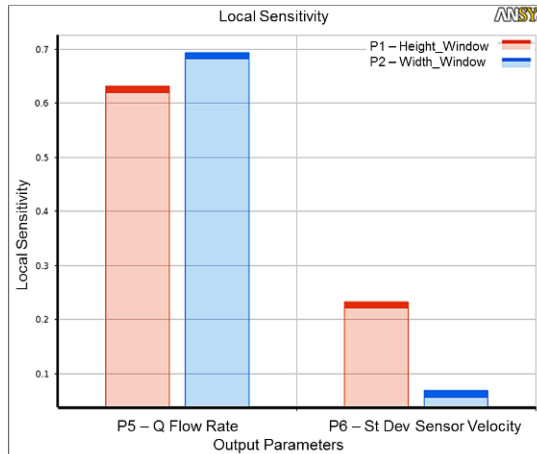
Figure 25: Chart of input parameter sensitivities on the output values

6.2 Optimisation results

The optimization goal was the improvement of the ventilation performance, by increasing the flow rate and decreasing the standard deviation of velocities. The employment of the Screening optimisation method allowed the generation of 1,000 window design samples that were evaluated against the objectives set. Tradeoff charts (Figure 26) were created allowing the exploration of the best (blue), worst (red) and feasible (green) design points. Three candidate design points that show the best behaviour regarding the established objectives and constraints were generated. As shown in Table 9, the multi-objective optimization revealed that the point that satisfies the established objectives for maximizing the flow rate and minimizing the standard deviation is DP 22. The dimensions of the optimum window opening are 0.01 m height and 0.0418 m width. The values of the output parameters deviate -49% and -18% for the flow rate and the standard deviation respectively, compared to the initial design. It is worth highlighting that the flow rate was not maximized, but minimized in order to achieve local optimality, after superimposing the two Pareto fronts.
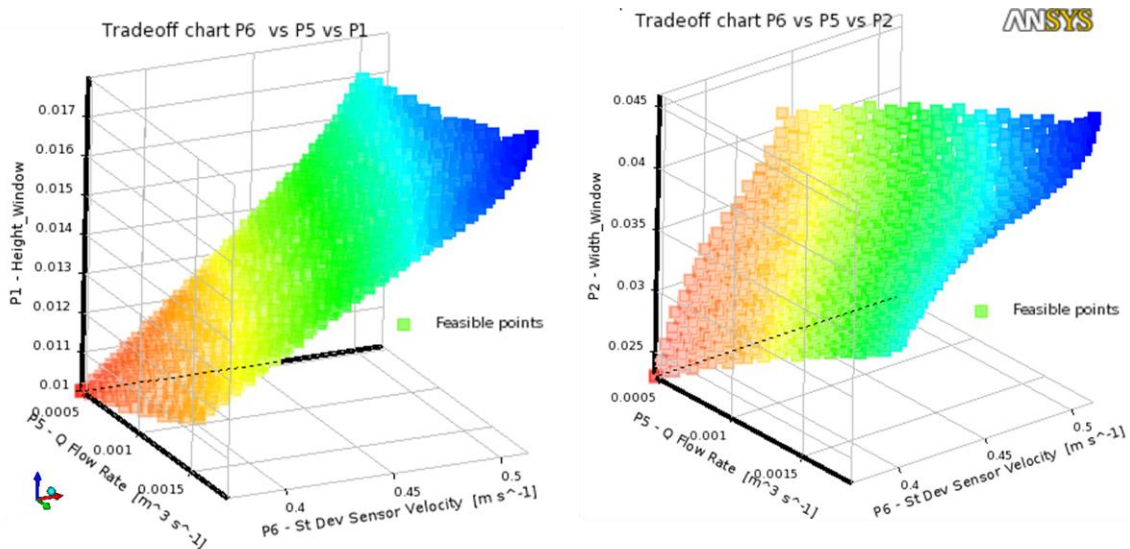
Figure 26: Pareto fronts created from the screening-generated samples; P1_Window Height (left) and P2_Window Width (right)

Table 9: Candidate points generated from screening optimisation method

Candidate Points	P1_Window Height (m)	P2_Window Width (m)	P5_Flow Rate (m3/s)	P6_St Vel Deviation (m/s)
Candidate Point 1 (DP 22)	10.00×10^{-3}	41.80×10^{-3}	0.871×10^{-3}	0.417
Candidate Point 2 (DP 23)	10.12×10^{-3}	45.09×10^{-3}	0.902×10^{-3}	0.421
Candidate Point 3 (DP 24)	10.01×10^{-3}	34.79×10^{-3}	0.714×10^{-3}	0.414

6.3 Six Sigma Analysis

Further insight on the parameters' correlation was given by the Six Sigma Analysis. Figure 27 shows the global sensitivity values that were generated out of 100 design samples. Opposing to the local sensitivities, these are statistical sensitivities that enable the correlation of the output parameters with respect to the input parameters. The calculated sensitivity correlation coefficients (R^2) highlighted the window width to affect most the flow rate with a value of 75.57% and the window height to maintain the highest impact role on the Standard Deviation response, with a correlation coefficient equal to 82.06%.
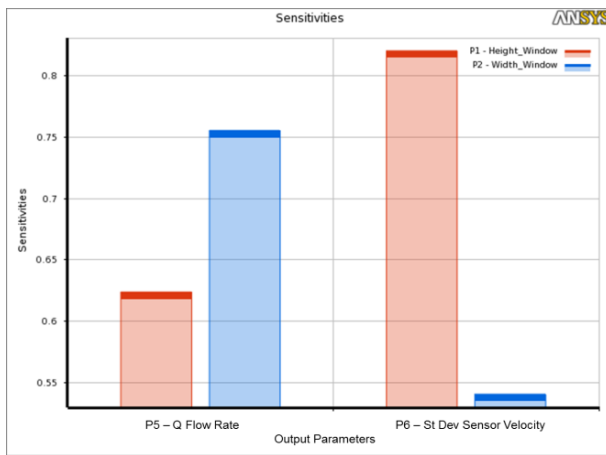
Correlation	R^2
P1 – P5	62.39%
P2 – P5	75.57%
P1 – P6	82.06%
P2 – P6	54.04%

P1 = Window_Height
P2 = Window_Width
P5 = Flow Rate (Q)
P6 = St_Dev_Sensor_Vel (SD)

Figure 27: Global sensitivities of parameters obtained by Six Sigma Analysis

6.4 Verification of results

Direct CFD simulation runs were carried out to verify the three candidate points. The results, shown in Figure 28, were in good agreement, to prove the accuracy of the method to obtain optimal solutions. The error for the flow rate was between 0.47% to 5.1% and 0.17% to 1.63% for the standard deviation of velocities. The verification results confirmed the local optimality of the DP22 design, showing the best behaviour over the other two design points.

Error	0.47%	5.1%	0.51%	1.63%	0.17%	1.23%
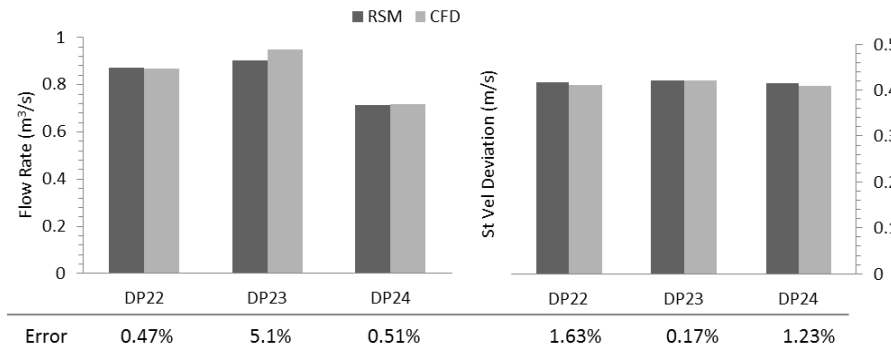
Figure 28 Comparison of RSM and CFD-generated results for the candidate points

7. CONCLUSION

A methodology coupling CFD-RSM meta-model-based optimization techniques using the ANSYS commercial platform was presented. The application of the method was tested on the improvement of the ventilation performance of a simple cross ventilated building. The CFD solution was validated with wind tunnel experiments and the RSM-obtained optimal solution was verified. Improved ventilation performance was achieved by a smaller window opening that resulted to 49% reduction in flow rate and 18% reduction in standard deviation of velocities. The main advantages and disadvantages of the method are summarised below:

- The method requires substantial less computational time, compared to the conventional deterministic studies.
- The investigation of the most influential parameters is permitted, and thus decision making process is enabled at the early design stages.
- The DoE study, within a certain design space, bounded by dimensional constraints, can only conclude to improved design solutions, or local optimal, which sometimes may abstain from the global optimal solution.
- The verification of the estimated optimal solution is deemed necessary for the conclusion to the final design decision.
- The final solution may reach design optimality in one aspect, but may be far from optimal regarding other criteria or even impractical for other responses.

8. REFERENCES

ASADI, E., Da Silva, M., Antunes, C., Dias, L. and Glicksman, L., 2014. Multi-objective optimization for building retrofit: A model using genetic algorithm and artificial neural network and an application. Energy and Buildings, 81, pp.444-456.

BANHALEE, M., Miau, J., Lin, S. and Yang, J., 2013. Flow visualization, PIV measurement and CFD calculation for fluid-driven natural cross-ventilation in a scale model. Energy and Buildings, 66, pp.306-314.

BLOCKEN, B., 2014. 50 years of Computational Wind Engineering: Past, present and future. Journal of Wind Engineering and Industrial Aerodynamics, 129, pp.69-102.

CALAUTIT, J., Chaudry, H., Hughes, B. and Sim, L., 2014. A validated design methodology for a closed-loop subsonic wind tunnel. Journal of Wind Engineering and Industrial Aerodynamics, 125, pp.180-194.

EVINS, R. (2013). A review of computational optimisation methods applied to sustainable building design. Renewable and Sustainable Energy Reviews, 22, pp.230-245.

HUANG, H., Ooka, R., Chen, H. and Kato, S., 2009. Optimum design for smoke-control system in buildings considering robustness using CFD and Genetic Algorithms. Building and Environment, 44(11), pp.2218-2227.

JOERG, F., 2006. Recommendations of the COST action C14 on the use of CFD in predicting 524 pedestrian wind environment. Fourth International Symposium on Computational Wind Engineering, pp. 529–532.

KHAN, M., Noakes, C. and Toropov, V.. 2012. Development of a numerical optimization approach to ventilation system design to control airborne contaminant dispersion and occupant comfort. Building Simulation, 5(1), pp.39-50.

MYERS, R., Montgomery, D. and Anderson-Cook, C. 2009. Response surface methodology. Hoboken, N.J.: Wiley. 3rd Edition.

MONTGOMERY, D. C., 2000. Design and Analysis of Experiments, Wiley, New York. 5th Edition.

SHEN, X., Zhang, G. and Bjerg, B., 2012. Investigation of response surface methodology for modelling ventilation rate of a naturally ventilated building. Building and Environment, 54, pp.174-185.

SHEN, X., Zhang, G. and Bjerg, B.. 2013. Assessments of experimental designs in response surface modelling process: Estimating ventilation rate in naturally ventilated livestock buildings. Energy and Buildings, 62, pp.570-580.

STAVRAKAKIS, G., Zervas, P., Sarimveis, H. and Markatos, N., 2012. Optimization of window-openings design for thermal comfort in naturally ventilated buildings. Applied Mathematical Modelling, 36(1), pp.193-211.

WANG, W., Zmeureanu, R. and Rivard, H., 2005. Applying multi-objective genetic algorithms in green building design optimization. Building and Environment, 40(11), pp.1512-1525.

369: Model predictive control algorithm for multilevel inverter in high performance load

ALI ALMAKTOOF[1], ATANDA RAJI[2], MTE KAHN[3]

1Cape Peninsula University of Technology, Bellville Campus, 7535, South Africa, 213301091@mycput.ac.za
2Cape Peninsula University of Technology (CPUT), Bellville Campus, 7535, South Africa, rajia@cput.ac.za
3Cape Peninsula University of Technology (CPUT), Bellville Campus, 7535, South Africa, Khant@cput.ac.za

In the applications of high voltage renewable energy systems such as wind and solar farm the use of model predictive control (MPC) in the power conversion stage is very advantageous. The strict requirements of utility or transmission operators or high performance loads for standalone need a very sophisticated and robust control strategy. A three-phase, flying capacitor multilevel converter is considered in this research work for high performance standalone load modelled as a simple resistive-inductive load (RL-load).

Two primary control objectives employed in this work are reference current tracking and flying capacitor voltage balancing, both of which are done concurrently by means of a multivariable control algorithm. A hysteresis-based algorithm is presented to balance the flying capacitor voltage in a complimentary way with the finite state-model predictive current control (FS-MPCC) algorithm. In the implementation stage of FS-MPCC for the control of a three-phase, three-level flying capacitor converter (FCC) for RL-load, the estimation step, predictive step and optimization step are performed. The performance of the proposed control is assessed by parameter mismatching between the model and the actual system parameters. Because of in nearly all systems, the parameters can change or are, to a degree, indeterminate. To evaluate the parameter sensitivity of the proposed control algorithm, different values for the load resistor and inductor are used. These values are estimated in order to determine how robustly the system could track the reference signal, balance the flying capacitor voltage, and the extent of the total harmonic distortion (THD). Co-simulation is effected by means of MATLAB/Simulink with PSIM software.

Keywords: Flying capacitor converter; finite state-model predictive current control; hysteresis-based algorithm; resistive-inductive load; total harmonic distortion

1   INTRODUCTION

The increase in the use of power from renewable energy systems, has led to the need for research on both new control strategies and better topologies for high-power converters; this is necessary to provide in the dual demand for performance and efficiency. In the last couple of decades, the multitude of applications of multilevel converters found in most industrial domains, have been intensively researched. By reflecting upon the increasing worldwide energy needs and the requirements for improved power quality and better efficiency, it is clear that control and power conversion by means of power electronics are becoming increasingly vital issues in renewable energy system applications in the present. The flying capacitor multilevel converter was presented by Meynard and Foch in the early 1990s as an alternative to diode-clamped inverters (Meynard & Foch 1992). The advantages of the FCC topology over other multilevel topologies such as diode-clamped converters and cascaded converters (Fazel et al. 2007; Lai & Peng 2002; Nami et al. 2008), has of late featured prominently in the literature (Defay et al. 2010; Escalante et al. 2002; Fazel et al. 2007; Feng et al. 2007; Hotait et al. 2010; Lai & Peng 2002; Lezana et al. 2009; McGrath & Holmes 2008; Meynard et al. 1997; Thielemans et al. 2010).

Many studies have been concluded in which an FS-MPCC scheme for three-phase multilevel inverters and drive applications has successfully been incorporated (Almaktoof et al. 2014; Li et al. 2009; Rodríguez & Cortés 2012; Vargas et al. 2007; Yaramasu et al. 2013). For renewable energy systems applications, the robustness and power of the FS-MPCC technique for a multilevel inverter, has been assessed when subjected to variable DC-link voltages, and variations in specific model parameters (Almaktoof et al. 2014(a)). The results indicated that FS-MPCC gives excellent performance under these conditions. For MPC with a flying capacitor multilevel inverter, the two foremost control objectives are reference current tracking and balancing the voltages of the flying capacitor. These objectives are achieved concurrently by the multivariable control scheme. The MPC algorithm inputs are the measured currents and flying capacitor voltages, as well as the reference currents. The algorithm output corresponds to one of the switch states of the converter, without the application of a modulation scheme. A flying capacitor voltage algorithm based on predictive control, is presented to balance the flying capacitor voltage, because the natural balancing of the capacitor voltages of FCCs fails in certain circumstances, as in the case with PWM (Defay et al. 2010; Feng et al. 2007; Hotait et al. 2010; Khazraei et al. 2012).

This paper presents a predictive current control technique for an FCC inverter (section 2). The control scheme used to control the load current and flying capacitor voltages of the model of the power converter is developed in section 3 and section 4. Results and discussions of the performance of the algorithm are presented by considering the RL-load in section 5. The last section contains the conclusion.

2   SYSTEM MODEL

A three-level flying capacitor inverter as depicted in Figure 1 with only one flying capacitor per phase, this is one of the less complicated converters, and it is for this reason that it was chosen for the analysis of the MPC; it was not expected to add any complications. The three-level FCC uses two pairs of complementary controlled switches, (S_1, S'_1) and (S_2, S'_2). These switches facilitate the connection of the flying capacitors, C_{1x} $(x = a, b, c)$, in a series with the RL-load. In Table 1, a summary of the different switch states and their corresponding output voltage is presented.

Because the maximum voltage stress occurs at $v_{DC}/2$, this requirement provides an optimal voltage rating for the switches. The transitional output voltage is generated by the two conditions of each phase; this allows a correction of the voltage of the capacitor for every possible direction, and it furthermore presents a way of controlling the capacitor voltage.
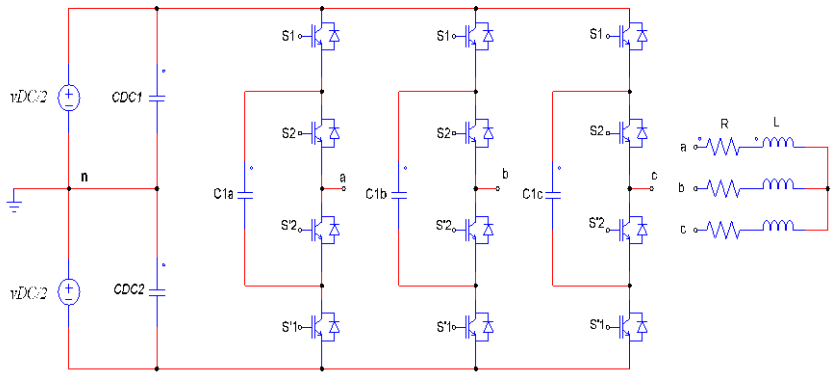
Figure 1: Three phase, three-level FCC inverter with RL-load

Table 10: Switching states in one leg of the three-level FCC

Voltage Level	complementary pair no. 1		complementary pair no. 2		Leg voltage (v_{an})
	S_1	S'_1	S_2	S'_2	
1	1	0	1	0	$v_{DC}/2$
2	1	0	1	0	0
	0	1	0	1	
3	0	1	0	1	$-v_{DC}/2$

3 CONTROL TASK OF FLYING CAPACITOR MULTILEVEL INVERTER

A block diagram of the complete control algorithm of an FCC inverter with RL-load is depicted in Figure 2. The switching state minimizing the cost function is identified and selected from information obtained by considering the error between the reference and predicted values. The switching signals of the state selected, S are thereafter applied to the converter. The effort of calculation increases exponentially with prediction horizon if the optimum inverter switching state is determined directly with a model predictive control algorithm. To decrease the required computational effort arising from the switching possibilities, voltage vectors generated by a three-level converter is used, the switching state that delivers the best voltage vector among 19 voltage vectors, is determined. A three-phase, three-level FCC can only deliver 64 possible switching states, of which 45 are redundant; this leaves 19 different voltage vectors. Some switching states are redundant, generating the same voltage vector; for example, the innermost voltage vector, V_0, can be generated by three different switching states: (+, +, +), (0, 0, 0) and (−, −, −). With this redundancy, a finite state-model predictive control with greater than one prediction step can be implemented.

In this paper, the selection of the most suitable voltage vector of the 19 delivered, was done with a prediction horizon of one prediction step. This facilitates a marked decrease in the amount of calculation required, as compared to carrying out the calculations for all 64 switching possibilities in one prediction step. Hence, the task is split in two different control algorithms based on MPC. For these algorithms, a single cost function was used. In the implementation stage of FS-MPCC of a three-phase, three-level FCC for RL-Load, an estimation step, a predictive step and an optimization step were performed.
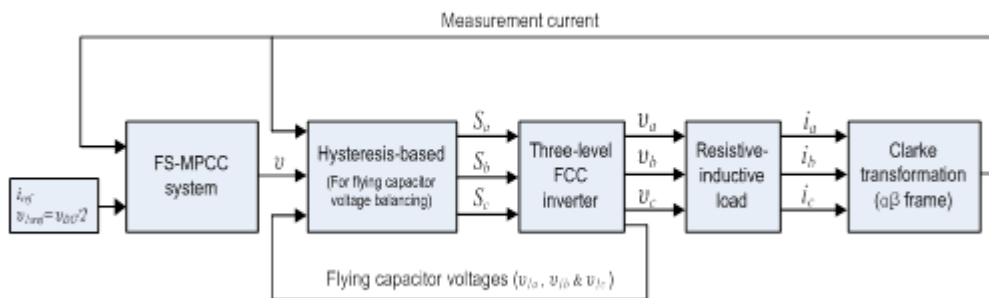
Figure 2: Block diagram of the proposed control algorithm of an FCC inverter

3,1 Estimation and predictive step

The measurements of the phase currents, $i_x(k)$, and the flying capacitor voltage, $v_{1x}(k)$ with $x = a, b, c$, are taken at time k. These measurements in combination with the applied switch states, $S_{ix}(k)$, are used as inputs for the system model, so as to obtain an estimation of the state variables at $(k + 1)$. The switch states, $S_{ix}(k)$, remain unaltered throughout the update period, and any change in the capacitor voltage is taken to be sufficiently small for it to be neglected when the output voltage is calculated. With the aforementioned assumptions, the equations below have been derived for the voltage, v_{xn}:

$$v_{xn}(k + 1) = \left(S_{2x}(k) - \frac{1}{2}\right) v_{DC} - \left(S_{2x}(k) - S_{1x}(k)\right) v_{1x}(k) \qquad (1)$$

where: the DC-link voltage, v_{DC}, is obtained by measurement. The load phase voltage, v_{xo}, (between the output pole and the neutral point), is determined from:

$$v_{on}(k + 1) = \frac{v_{an}(k+1) + v_{bn}(k+1) + v_{cn}(k+1)}{3} \qquad (2)$$

and

$$v_{xo}(k + 1) = v_{xn}(k + 1) + v_{on}(k + 1) \qquad (3)$$

where: v_{on} is the star-point voltage. The flying capacitor voltages and output currents at time $(k + 1)$ have to be estimated.

From Equations 2 and 3 it is apparent that in the system model the phase output voltages of all phases determine the phase voltage of the load. The outcome is a set of equations that are convincingly linked. The results of all the switch state combinations are determined and applied in the optimization step; this is similar to the prediction phase where all the control actions have to be evaluated.

Estimation and predictive of the output current:

At time $(k + 1)$ the expression for the current can be determined by means of the Euler forward method, which yields a discrete-time equation that can be used to find the future load current. To derive the continuous-time, state-space equations for the load of each phase, consider the differential equation of the load current:

$$v_{DC}(t) = R.i(t) + L\frac{di}{dt} \qquad (4)$$

With the Clarke transformation applied to the load model, the load currents can be stated in relation to a simplified coordinate system having linearly independent axes, α and β. After applying the transformation, the continuous-time, state-space equation of the load takes on the following form:

$$\begin{bmatrix} i_\alpha \\ i_\beta \end{bmatrix} = \begin{bmatrix} -\frac{R}{L} & 0 \\ 0 & -\frac{R}{L} \end{bmatrix} \begin{bmatrix} i_\alpha \\ i_\beta \end{bmatrix} + \begin{bmatrix} \frac{1}{L} & 0 \\ 0 & \frac{1}{L} \end{bmatrix} \begin{bmatrix} v_\alpha \\ v_\beta \end{bmatrix} \qquad (5)$$

The Euler forward equation (see Equation 6) is used to derive a discrete-time equation system representation for the future load current, which is required to obtain a discrete-time system representation. The derived approximation is given by:

$$\dot{x} \approx \frac{x(k+1) - x(k)}{T_S} \qquad (6)$$

where: T_S is the sampling time; k is the current sampling instant; and x is the state variable.

The equation of the discrete-time load model is then expressed by

$$\begin{bmatrix} i_\alpha(k+1) \\ i_\beta(k+1) \end{bmatrix} = \begin{bmatrix} 1 - T_S \frac{R}{L} & 0 \\ 0 & 1 - T_S \frac{R}{L} \end{bmatrix} \begin{bmatrix} i_\alpha(k) \\ i_\beta(k) \end{bmatrix} + \begin{bmatrix} \frac{T_S}{L} & 0 \\ 0 & \frac{T_S}{L} \end{bmatrix} \begin{bmatrix} v_\alpha(k) \\ v_\beta(k) \end{bmatrix} \qquad (7)$$

Estimation and predictive of the flying capacitor voltage:

At the end of the time $(k+1)$, the flying capacitor voltages have to be estimated. The switch state determines whether, and in which sense the load current passes through the capacitors; this is given by $(S_{2x}(k) - S_{1x}(k))$ in Equation 8

$$v_{1x}(k+1) = v_{1x}(k) - \frac{T_S}{2C}\big(i_x(k) + i_x(k+1)\big)(S_{2x}(k) - S_{1x}(k)) \qquad (8)$$

where: C is the capacitor values of the flying capacitor; and x is a, b, c.

Equations 7 and 8 are used to predict the load current and flying capacitor voltage for each switching likelihood. For determining the subsequent values of the load currents and flying capacitor voltages, the cost function, g, is calculated for every one of the 19 possible voltage vectors produced by the inverter. The voltage vector that results in a minimum cost function is chosen and implemented during the sampling instance that follows. This is because the current and flying capacitor voltage will always be on or outside the hysteresis band. The switching state will therefore constantly be changed.

3.2 Optimization step

By assessing a cost function, g, the best sequence can be chosen; however, this can only happen after the paths of the state variables for all possible control sequences have been computed. The sequence with the minimum cost is chosen, the first switch state is initiated by the controller at time $(k+1)$, and the algorithm is re-started, producing what is called a receding horizon. The cost function assigns a cost to a deviation of state variables from their desired values, which are the reference values. In general, the cost is defined by the difference between the predicted variables and their reference. When adding all the cost functions for each predicted future state, the total cost function is obtained. For a three-phase, three-level FCC inverter, a straightforward cost function can be expressed as an absolute value term with a single prediction step, as given in the following equation:

$$g = \big|i_{refx}(k+1) - i_x(k+1)\big| + \lambda_{DC}\big|v_{1xref}(k+1) - v_{1x}(k+1)\big| \qquad (9)$$

The respective reference values are i_{refx} and v_{1xref} for the phase current and the voltage of capacitor C_{1x} respectively, with the weighting factor λ_{DC}, expressing the relative importance of an error in the flying capacitor voltage compared to an error in the output current. To simplify calculations in this study, the following approximation is taken into account: the current reference is considered to remain constant when the prediction horizon has a short sampling time, T_S; this is shown in the following equation.

$$i_{ref}(k+N) \approx i_{ref}(k) \qquad (11)$$

4   HYSTERESIS-BASED FOR FLYING CAPACITOR VOLTAGES

To balance the flying capacitor voltages in a complimentary way when using the FS-MPCC scheme, a hysteresis algorithm, based on predictive control, is presented. It must be noted that to enable the inverter to switch zero voltages, the flying capacitors, C_1, C_2 and C_3, have to be charged to a voltage of $v_{DC}/2$ If in a phase, one of the zero switching states is selected, it will cause the corresponding flying capacitor voltage to either increase, or decrease. The voltage change—increase or decrease—will be established by the direction of the current in the phase being considered, and by the possibility that the voltage selected will be zero. Therefore, regardless of the switching states selected, the flying capacitor voltages must at all times remain balanced. After determination of the most suitable voltage vector for the sampling cycle to follow, the corresponding optimum switching state generating this voltage vector, must be identified. The voltage of each of the three flying capacitors, has to remain within the tolerance set by a hysteresis band which straddles the reference voltage, $v_{DC}/2$. For the control algorithm

presented, natural voltage balancing effects are insufficient for maintaining the flying capacitor voltages within the specified proximity to their reference values, making it necessary for an additional voltage balancing algorithm to be incorporated (Defay et al. 2010; Feng et al. 2007; Khazraei et al. 2012; Hotait et al. 2010; Wilkinson et al. 2006). This algorithm selects the switching state which gives the derived optimum voltage vector and maintains the flying capacitor voltages inside their hysteresis bands. Provided that the flying capacitor voltage remains within its limits, either of the switching state combinations leading to a voltage of zero are allowed for this situation, and the switching state corresponding to zero that can be assigned with the lowest number of transitions is chosen. However, the flying capacitor voltage does drift outside the boundaries of the hysteresis band straddling the reference voltage, only the switching state which forces the voltage back into the limits of that band, is allowed. The selection of the zero switching state to be used, is made taking the direction of the current in that phase, into consideration. The width of the hysteresis band is the result of selecting a tolerance of 0.1% of the v_{DC} value in this study. This allows a finite state-model predictive control with a prediction step greater than one, to be implemented. If an FCC is controlled directly, the switching states can only be changed at the beginning of a sampling cycle, which is different to conventional PWM. As a result, the flying capacitors have to be dimensioned with care as a zero voltage will be applied for a whole sampling cycle; this is in contrast to modulator-controlled inverters. A worst-case estimation of the necessary capacitor size can be done easily (see Equation 12) on the assumption that the maximum allowed current per phase, i_{max}, is drawn for the whole sampling cycle, T$_S$, and that the maximum flying capacitor voltage ripple, ΔV is defined as:

$$C_f = \frac{i_{max}\text{T}_\text{S}}{\Delta V} \qquad (12)$$

5   RESULTS AND DISCUSSION

In nearly all systems, the parameters can change or are, to a degree, indeterminate. For example, the stator and rotor resistances of an induction machine can be change due to temperature changes. For that, a mismatch between selected model parameters and the corresponding system parameters was considered. To evaluate the parameter sensitivity of the proposed control algorithm, different values for the load resistor and inductor were used. These values were estimated in order to determine how robustly the system could track the reference signal, balance the flying capacitor voltage, and the extent of the THD. The FS-MPCC strategy for a three-phase, three-level FCC was co-simulated with MATLAB/Simulink together with PSIM. Table 2 shows the parameters and their values, as used for the co-simulations.

Table 2: Parameters used for the co-simulations

Parameter	Value
Load resistor, R	15 Ω
Load inductor, L	10 mH
Flying capacitor	560 µF
DC-link voltage, v_{DC}	400 V
Amplitude of the reference current, i_{ref}	14A
Sampling time, Ts	25 and 100 µs
Weighting factor, λ_{DC}	0.02

5.1 Inductance Sensitivity

The actual inductance was estimated both 50% higher and 50% lower, than the parameter used in the model, with sampling times, T$_S$= 25 µs and T$_S$= 100 µs. In another case, the inductance was increased to 100%, with T$_S$= 25 µs and T$_S$= 100 µs.

As indicated in Figure 3(a), when the load inductance was estimated at +50% with T$_S$=25 µs (THD = 0.63%), the control algorithm showed excellent reference tracking behaviour. However, when T$_S$ was increased to 100 µs, the current ripple on the load current increased (THD = 2.43%) as depicted in Figure 3(b). Comparatively, when the load inductance was estimated +100% for T$_S$= 25 µs (THD = 1.97%), the control algorithm demonstrated excellent reference tracking behaviour as shown in Figure 3(c). The effect of increasing the sampling time to   100 µs, on the current ripple of the load current (THD = 2.16%), is shown in Figure 3(d).
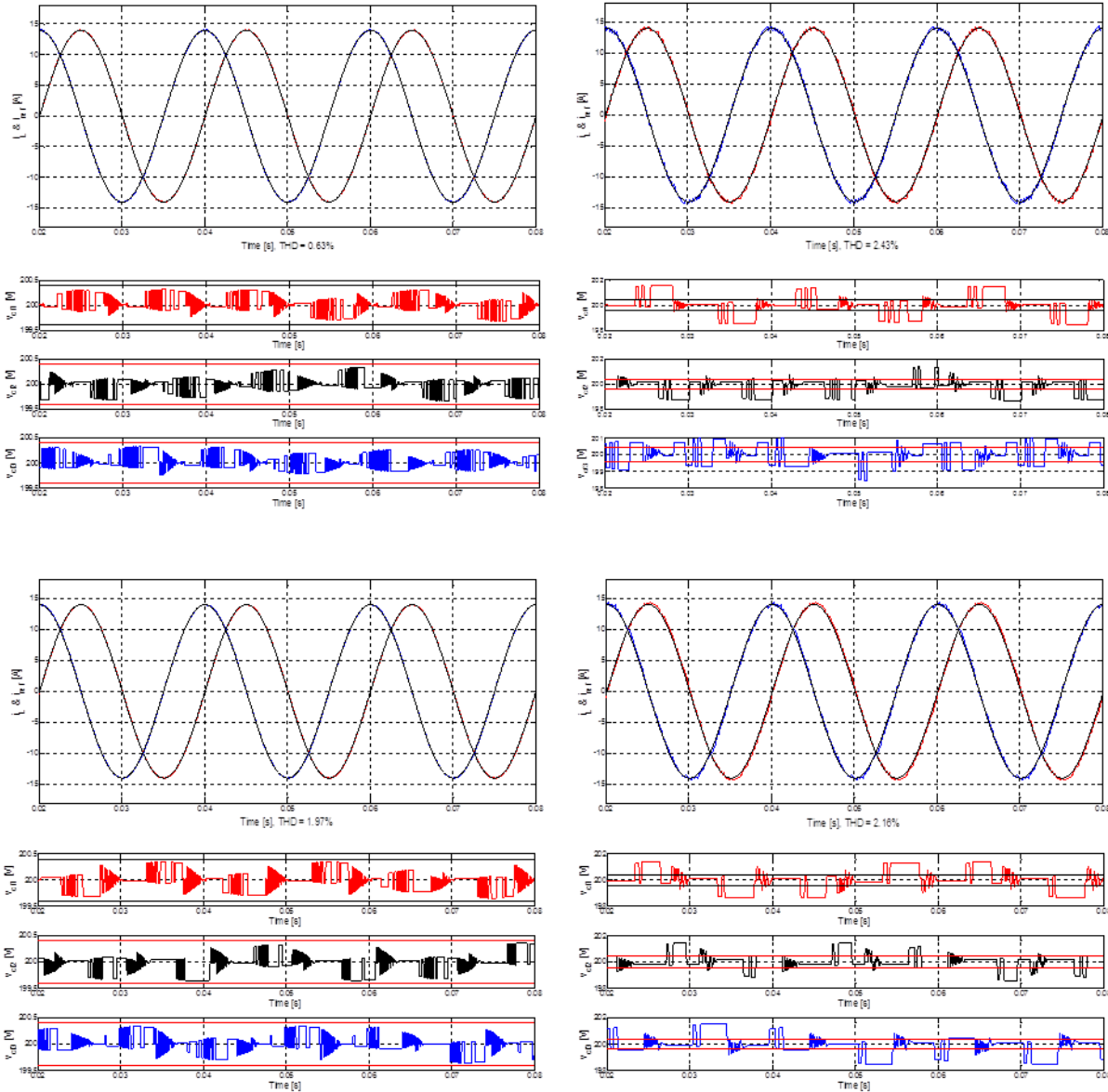
Figure 3: Inductance sensitivity for load current and flying capacitor voltage

If, however, the inductance was estimated at 50% lower than the parameter used in the model, and with T_S= 25 µs, the load current ripple increased marginally, compared to the model inductance value (THD = 2.36%). Whereas, with T_S=100 µs, the current ripple increased substantially (THD = 10.23%), as seen in Figure 4. On other hand, the hysteresis-based algorithm has kept the flying capacitor voltages in all inductor values around their desired voltage at $v_{DC}/2$ as shown in Figures 3 and 4.
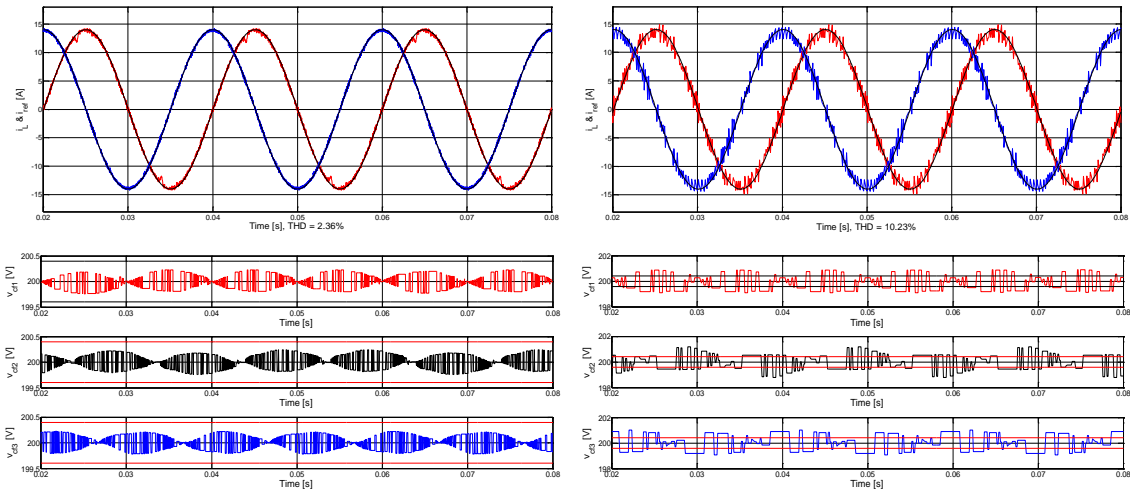
(a) -50% for 25 μs   (b) -50% for 100 μs

Figure 4: Inductance sensitivity for load current and flying capacitor voltage

5.2 Resistance Sensitivity

Figures 5 and 6 show the simulation results when: the actual resistance was estimated at 40% lower than the parameter used in the model with T_S=25 μs, and T_S=100 μs; and at 40% higher than the parameter used in the model with T_S=25 μs, and T_S=100; respectively. In both situations where the load resistance was estimated at -40%, the load currents are higher than their reference value with THD = 0.82% when T_S = 25 μs (see Figure 5(a)), and TDH = 3.14% when T_S = 100 μs (see Figure 5(b)).

(a) -40% for T_S = 25 μs   (b) -40% for T_S = 100 μs

With the actual resistance estimated at +40% higher, T_S=25 μs (see Figure 6(a)), the predictive control method produced a better result with regard to tracking the load current references and in balancing the flying capacitor voltages, than, T_S=100 μs (see Figure 6(b)). With the estimated the load resistance at +40% however the load currents were lower than their reference value, and with THD = 1.73% when T_S= 25 μs, and THD = 3.09% for T_S= 100 μs. In the case where the actual resistance was estimated at -40% with T_S= 25 μs (see Figure 5(a)), the predictive control method performed better, both in tracking the load current references and flying capacitor voltage balancing, than when the actual resistance was estimated at +40% with T_S= 25 μs (see Figure 6(a)).

(a) -
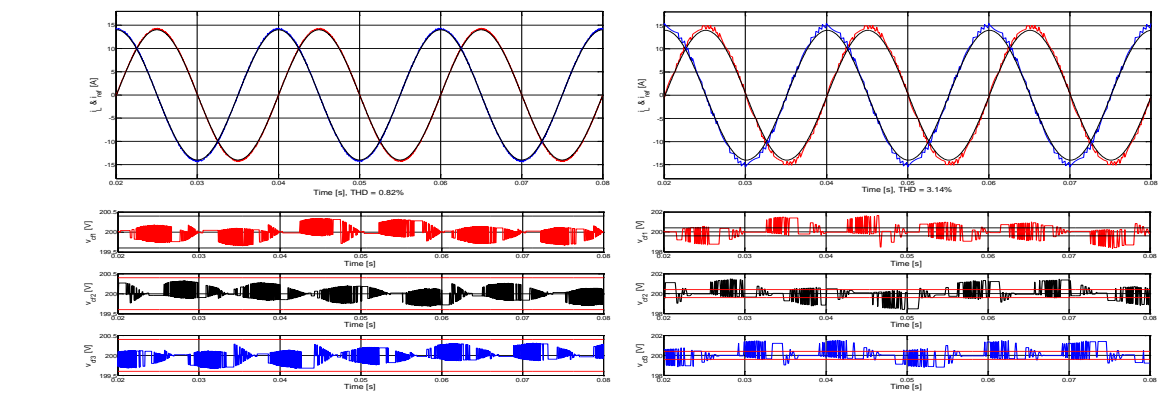
40% for T_S = 25 μs   (b) -40% for T_S = 100 μs

Figure 5: Resistance sensitivity for load current and flying capacitor voltage

(a) +40% for $T_S = 25$ μs   (b) +40% for $T_S = 100$ μs
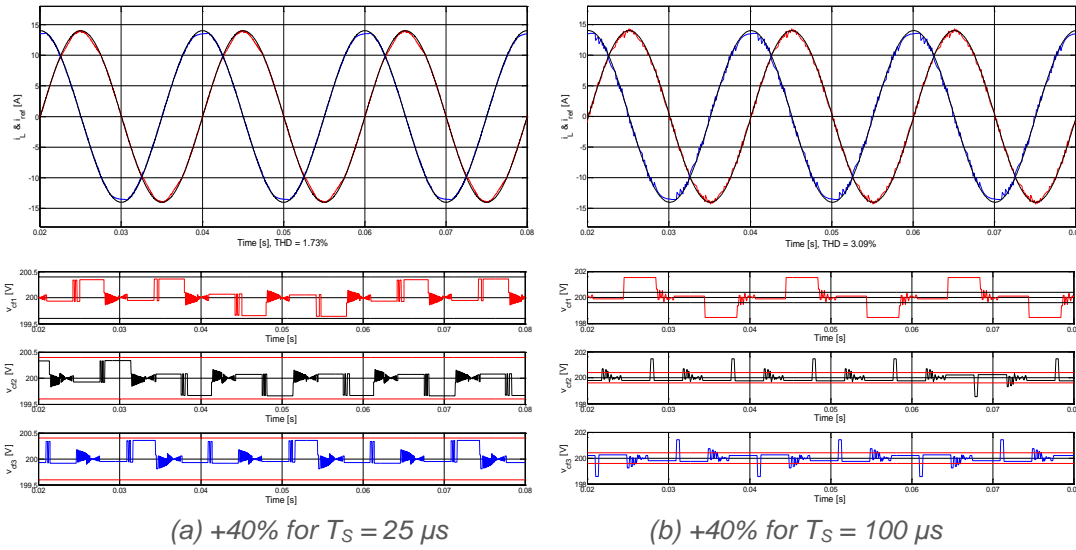
The results obtained in a mismatching between the model and the actual system parameters are tabulated in Table 3 in terms of fundamental output current, THD and sampling period.

Table 3: A mismatching between the model and the actual system parameters

Sampling time TS, [μs]	Inductance, L		Resistance, R		Output current at 50 Hz, [A]	THD [%]
	%	Value[mH]	%	Value [Ω]		
25	+50	15	-	-	14.02	0.63
25	+100	20	-	-	13.96	1.97
100	+50	15	-	-	14.12	2.43
100	+100	20	-	-	14.13	2.16
25	-50	5	-	-	13.9	2.36
100	-50	5	-	-	13.65	10.23
25	-	-	+40	21	13.73	1.73
25	-	-	-40	9	14.21	0.82
100	-	-	-40	9	14.83	3.14
100	-	-	+40	21	13.75	3.09

5   CONCLUSION

The FS-MPCC strategy with one-step prediction time was presented, to control the three-level FCC. The best 19 unique voltage vectors out of a possible 64, were selected and applied to the inverter. The minimization of the current and capacitor voltage errors by using a cost function provides a fast dynamic response for load current control and guarantees balanced flying capacitor voltages. The proposed control strategy does not require a linear controller, or the application of a modulation technique. Additionally it affords the designer the freedom to adjust the weighting factor λ_{DC} in order to fulfil the requirements in terms of reference current tracking and flying capacitor voltage balance. The hysteresis-based voltage balancing algorithm presented, has the ability to keep the flying capacitor voltages within the required proximity of their reference values.

The FS-MPCC algorithm was evaluated, subject to different conditions, in terms of reference current tracking and flying capacitor voltage balance; this evaluation by processing the results obtained through co-simulation. The performance of the proposed control was assessed by creating a mismatch between the model parameter and the actual, corresponding system parameter. These results indicated that the

FS-MPCC approach gives excellent results under these conditions. In general, when the sampling time was increased, the load current ripple increased, while the flying capacitor voltages at some points exceeded the hysteresis boundaries for a longer time due to the control algorithm, but this situation was remedied by the operation of the control algorithm which brought the voltage back within the confines of the hysteresis band. FS-MPCC concept can be extended to any power converter system, and the developed hysteresis-based voltage balancing algorithm will be able to keep the flying capacitor voltages within the bounds of their reference values.

6 REFERENCES

ALMAKTOOF A. M., Raji A. K., & Kahn M. T. 2014. Finite-Set Model Predictive Control and DC-Link Capacitor Voltages Balancing for Three-Level NPC Inverters, Proceeding of the 16th International Power Electronics and Motion Control Conference and Exposition (PEMC 2014), pp. 305–310, on 21–24 September, 2014, Antalya-Turkey.

ALMAKTOOF, A. M., Raji, A. K. Kahn, M. T. E. 2014(a). Finite Set-Model Predictive Current control of three-phase voltage source inverter for Renewable Energy Systems (RES) applications, Journal of Energy and Power Engineering, USA, 8 (2014), pp. 748–755.

DEFAY F., Llor A. M., & Fadel M. 2010. Direct Control Strategy for a Four-Level Three-Phase Flying-Capacitor Inverter, Industrial Electronics, IEEE Transactions on, vol. 57, no. 7, pp. 2240–2248.

ESCALANTE M. F., Vannier J. C., & Arzande A. 2002. Flying capacitor multilevel inverters and DTC motor drive applications, Industrial Electronics, IEEE Transactions on, vol. 49, no. 4, pp. 809–815.

FAZEL S. S., Bernet S., Krug D., & Jalili K. 2007. Design and comparison of 4-kV neutral-point-clamped, flying capacitor, and series-connected H-bridge multilevel converters, Industry Applications, IEEE Transactions on, vol. 43, no. 4, pp. 1032–1040.

FENG, C. Liang, J. and Agelidis, V. G. 2007. Modified Phase-Shifted PWM Control for Flying Capacitor Multilevel Converters. IEEE Transactions on Power Electronics, 22(1), pp. 178–185.

HOTAIT H. A., Massoud A. M., Finney S. J., & Williams B. W. 2010. Capacitor voltage balancing using redundant states of space vector modulation for five-level diode clamped inverters, Power Electronics, IET, vol. 3, no. 2, pp. 292–313.

KHAZRAEI, M., Sepahvand, H., Corzine, K.A. & Ferdowsi. M. 2012. Active Capacitor Voltage Balancing in Single-Phase Flying-Capacitor Multilevel Power Converters. IEEE Transactions on Industrial Electronics, 59(2), pp. 769–778.

LAI J. S. & Peng F. Z. 2002. Multilevel converters-a new breed of power converters, Industry Applications, IEEE Transactions on, vol. 32, no. 3, pp. 509–517.

LEZANA, P., Aguilera R., & Quevedo D. E. 2009. Model predictive control of an asymmetric flying capacitor converter, Industrial Electronics, IEEE Transactions on, vol. 56, no. 6, pp. 1839–1846.

LI, J., Zhuo, F., Wang, X., Wang, L., & Ni, S. 2009. A grid-connected PV system with power quality improvement based on boost + dual-level fourleg inverter, in Proc. IEEE Int. Power Electron. and Motion Control Conf., Wuhan, China, pp. 436–440.

MCGRATH B. P. & Holmes D. G. 2008. Analytical modelling of voltage balance dynamics for a flying capacitor multilevel converter, Power Electronics, IEEE Transactions on, vol. 23, no. 2, pp. 543–550.

MEYNARD, T., Fadel M., & Aouda N. 1997. Modeling of multilevel converters, Industrial Electronics, IEEE Transactions on, vol. 44, no. 3, pp. 356–364.

MEYNARD, T.A. & Foch, H. 1992. Multilevel conversion: High voltage choppers and voltage source inverters, in IEEE PESC Conf. Rec., 397–403.

NAMI, A., Zare, F., Ledwich, G., Ghosh, A. & Blaabjerg, F. 2008. Comparison between Symmetrical and Asymmetrical Single Phase Multilevel Inverter with Diode-Clamped Topology. Proceeding in 39th IEEE Power Electronics Specialists Conference (PESC08), June 2008, pp. 2921–2926. Rhodes, Greece.

RODRÍGUEZ, J. & Cortés, C. 2012. Predictive control of Power Converters and Electrical Drives, (UK: A Johan Wiley & Sons, Ltd., 2012).

THIELEMANS S., Ruderman A., Reznikov B. & Melkebeek J. A. A. 2010. Self-precharge for single-leg odd-level multilevel converter, in Power Electronics, Machines and Drives (PEMD 2010), 5th IET International Conference on. IET, 2010, pp. 1–6.

VARGAS, R., Cortés, P., Ammann, U., Rodríguez, J. & Pontt, J. 2007. Predictive control of a three-phase neutral-point-clamped inverter, in IEEE Transactions on Industrial Electronics, vol. 54, no. 5, Oct. 2007, pp. 2697-2705.

WILKINSON, R. H., Meynard, T. A. & Mouton, H. 2006. Natural balance of multicell converters: The general case, IEEE Transactions on Power Electronics, vol. 21, pp. 1658–1666.

YARAMASU, V. Wu, B. Rivera, M. and Rodríguez, J. 2013. Predictive current control and DC-link capacitor voltages balancing for four-leg NPC inverters, Industrial Electronics (ISIE), 2013 IEEE International Symposium on, Tehran, pp.1–6.

453: Are batteries the PV energy self-consumption optimisation solution for homes?

Techno-economic comparison of battery and hot water tank storage technologies in the UK

DAVID PARRA[1],A, GAVIN S. WALKER[2], MARK GILLOTT[3]

1 University of Nottingham, Energy Technologies Research Institute, Faculty of Engineering, University of Nottingham, University Park, Nottingham NG7 2RD, UK,
2 University of Nottingham, Energy Technologies Research Institute, Faculty of Engineering, University of Nottingham, University Park, Nottingham NG7 2RD, UK, gavin.walker@nottingham.ac.uk
3 University of Nottingham, Energy Technologies Research Institute, Faculty of Engineering, University of Nottingham, University Park, Nottingham NG7 2RD, UK, mark.gillott@nottingham.ac.uk
A Moved to University of Geneva and current email address is david.parra@unige.ch

Growing support to decarbonise energy systems together with increasing retail energy prices are converting self-generation into a more attractive energy supply option. At the consumption level, solar PV is the most widespread generation technology due to declining capital costs, modularity and easy maintenance. The intrinsic dependence of solar energy generation on weather patterns and conditions affects the performance, final supply to the local demand load (i.e. local self-consumption) and final revenue. Energy storage is an available technological option to increase the value of local PV generation by increasing the self-consumption of PV-generated electricity. Therefore, understanding the performance, cost, value and optimum energy storage technology for managing PV generation is key for current and new customers with rooftop PV installations. In this study, energy storage for single homes is optimised by quantifying the performance, levelised cost, levelised value and profitability of hot water tanks (supplying domestic hot water), lead-acid batteries and lithium-ion batteries (supplying electricity). Although the assumed storage medium cost for Li-ion batteries (350 £/kWh) was 2.5 times higher than that of PbA batteries (140 £/kWh), Li-ion technology's greater round trip efficiency and cycling capability resulted in lower levelised cost (0.37 £/kWh) and higher levelised value (0.15 £/kWh) than PbA technology. The best economic case was for hot water tanks with a size ranging between 100 l and 200 l which were able to achieve internal rate of return values higher than the assumed discount factor (4%), especially when the property already had a hot water tank and domestic hot water was previously met by using retail electricity.

Keywords: PV, battery, hot water tank, levelised cost, internal rate of return

1. INTRODUCTION

Renewable energy (RE) technologies are a key alternative to reduce carbon dioxide emissions. However, they do not offer the same level of dispatchability as fossil generators do. Energy storage (ES) is a flexible option to increase the penetration and value of RE technologies and there are different technologies available in the market depending on the application scale and discharge duration (Brunet, 2013). The implementation of PV-coupled battery systems at single homes has been identified as one of the key potential ES business opportunities taking place in the next 10 years. Battery systems allow end users to increase the amount of local PV generation used on-site, the value of PV self-consumption being higher than the value of PV export due to higher retail prices than wholesale prices. The German residential battery storage subsidy of 30% of the initial investment has already been a success and 4000 new batteries were installed based on it by May 2014 after the first year (Pv-speicher, Kairies, Magnor, & Sauer, 2014).

As a consequence, previous research has analysed the power and seasonal energy flows from/to the battery (Braun, Büdenbender, Magnor, & Jossen, 2009; Parra, Walker, & Gillott, 2013). The voltage characteristics of different battery technologies available in the market were also compared by N. Nair et al. using simulation modelling and experimental research in a different study (Nair & Garimella, 2010). Using only the chemistry cost, this research concluded that Li-ion technology offers the most stable voltage plateau and this technology will be the most cost competitive when the capital cost of Li-ion batteries comes down to four times higher than that for PbA batteries. However, most previous studies focused on calculating the optimum battery system for single homes according to different RE generation and demand profiles. The same optimization method based on discrete time-series was utilised in all the cases (Braun et al., 2009; Jenkins, Fletcher, & Kane, 2008; Mulder et al., 2013). The optimum battery capacity was defined as the one which maximised the ratio between the self-consumption (kWh) and the battery capacity (kWh) (Jenkins et al., 2008) or the one which maximises the profitability (Braun et al., 2009; Mulder et al., 2013).   Mulder et al. concluded that batteries will quickly become attractive, even without government subsides, with an electricity price annual growth rate of 4% (Mulder et al., 2013).

Regarding battery models utilised in previous research, those studies which focused on the economic benefits assumed constant values for key performance parameters such as round trip efficiency and life (Hoppmann, Volland, Schmidt, & Hoffmann, 2014; Santos, Moura, & Almeida, 2014). Only two studies including economic considerations did not assume constant battery characteristics: Braun et al. focused on a specific Li-ion battery model for a battery manufactured by Saft to calculate the internal rate of return (IRR) (Braun et al., 2009) and D. Parra et al. calculated the revenue without including it into a more comprehensive techno-economic assessment (Parra et al., 2013). None of these studies compared PbA and lithium batteries although both technological options are available in the market for single home solutions.

From the literature review above, there are still two important research questions which should be answered: (i) what is the performance, cost, value, profitability and optimum system for PbA and Li-ion battery storage performing PV energy time-shift in a single home and (ii) how these indicators compare with other ES technologies suitable for single home installation, specifically hot water tanks due to their wide availability.

2. METHODOLOGY

This section provides an overview of the methodology followed in this study including the definition of the ES application, presentation of PV generation, demand data and energy prices utilised for the assessment.

2.1 PV Energy Time-Shift

PV energy time-shift consists of storing surplus PV energy and using it on-site later to meet the local demand.   PV generation mismatch to the domestic daily and seasonally demand loads are shown in Figure 1. PV energy time-shift allows end users to manage their own PV electricity, reduce their energy bills and potentially secure their energy supply against network failures. From a distributor network operator perspective, PV energy time-shift can contribute to reduce the maximum peak demand load and defer or avoid distribution capital investment, mitigate possible voltage problems, reduce the losses

(and the related power regulation needs) and increase the reliability of the distribution system (Paatero & Lund, 2007).
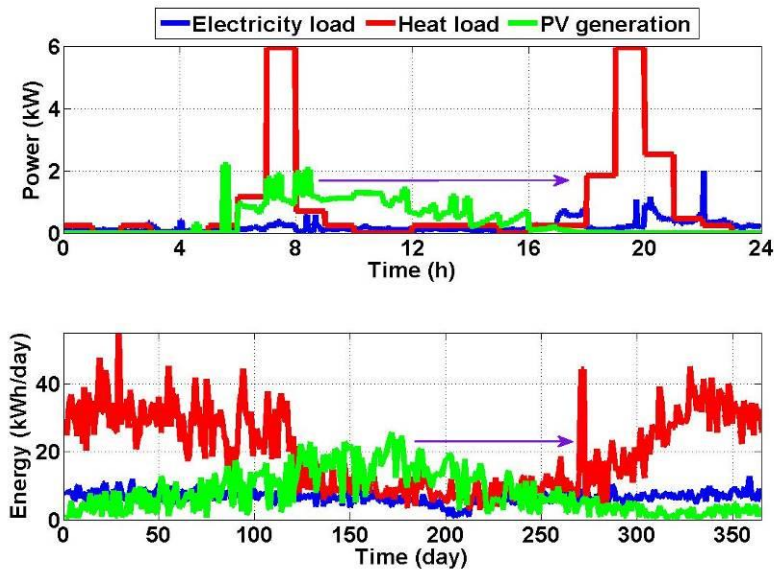
Figure 29: Daily and seasonal mismatch between PV generation and different demand loads in a single house with a 3 kWp array.

2.2 Demand Data and PV Generation

Electrical and domestic hot water demand data were monitored in 130 dwellings at the north of London (UK) (UKERC, 1990). A house with annual demand values which are representative for the UK was selected for this study from this large domestic data set. Specifically, the electrical and domestic hot water (DHW) annual demand data were equal to 3.1 MWh/year and 3.2 MWh/year respectively, the consumption of an average house in the UK being equal to 3.0 MWh/year for both energy demands according to J. I. Utley et al. (Utley & Shorrock, 2008).

Regarding PV generation, environmental variables including solar irradiance and temperature were also monitored together with the demand data set. These environmental variables were utilised as input data to model the PV generation of a 3 kWp rooftop array tilted at 30°. The PV system nominal power and the inclination were chosen according to the average domestic PV installation in the UK concluded by a research report created by the UKERC (Infield, 2007). A single diode PV panel model including a maximum power point tracker system was utilised for this purpose based on the work developed by Villalva et al. (Villalva, Gazoli, & others, 2009). Besides, the global horizontal irradiance data monitored in the community was transformed into irradiance tilted at 30° using a sky model presented by J. A Duffie et al. (Duffie & Beckman, 2013). The demand data and the PV generation utilised for this study have a temporal resolution of 1 minute. The performance and economic benefits of ES technologies depend on the mismatch between PV generation and demand, the peaks in the demand load and PV generation profiles therefore this temporal resolution allowed an appropriate quantification of them (Parra, 2014).

2.3 Energy Prices

Equation 1 is used to calculate the revenue created by an ES system performing PV energy time-shift. According to it, energy prices and their evolution are key to understand the potential business case. Import prices refer to the retail energy prices, i.e. electricity price and natural gas price. Since retail prices vary depending on the utility, the average price reported by the British Government for 2014 was utilised in this study, specifically 14.7 p/kWh and 5.6 p/kWh for electricity and natural gas respectively (HM Government, 2014). Additionally, the valley electricity price from the tariff Economy 7 was also included in the hot water tank analysis, the value in 2014 being equal to 7.1 p/kWh. Electricity and natural gas retail prices increased by 20% and 24% respectively between 2011 and 2014 (equivalent to 5% p.a. and 6% p.a. respectively). In this case, a conservative approach was considered due to the long investment horizon time (up to 20 years) and retail prices were assumed to increase by 2% p.a.

Regarding the export price or feed-in tariff, the value in 2014 in the UK was equal to 4.85 p/kWh and it was assumed to remain constant until 2020 in agreement with wholesale latest projections from the European Energy Exchange (SPOT, 2014)

Equation 4: PV energy time-shift revenue
$$\mathrm{Re}\,v_{PVts} = \mathrm{E}_{dis} \cdot P_i - E_{char} \cdot P_{ex} = E_{char} \cdot P_i \cdot \left(\eta - \frac{P_{ex}}{P_i} \right)$$

Where:

- Rev_{PVts} = PV energy time-shift revenue (£)
- E_{dis}= annual discharge of the ES system (kWh)
- E_{char}= annual PV charge of the ES system (kWh)
- P_i= import price (£/kWh)
- P_{ex}= export price (£/kWh)
- η= round trip efficiency

2.4 Energy Storage Technologies

Three different ES technologies are compared in this paper: PbA batteries, Li-ion batteries and hot water tanks. PbA technology was selected because it is the most mature battery technology and is also being offered for single homes applications. Li-ion technology was also incorporated in this study because is the most attractive battery technology for short-term ES from a technical point of view although its capital cost is around twice or more that of PbA batteries (Divya & Østergaard, 2009). Hot water tanks are used in this paper as baseline ES technology since there are 19.3 milion hot water tanks in the UK (most of them deployed in the 1970s before the development of "combi" natural gas boilers). In order to perform a techno-economic assessment of these three ES technologies, a comprehensive ES modelling approach including technical performance, durability and economic performance was followed. The performance submodels for PbA (Copetti & Chenlo, 1994), Li-ion (Beltran, Swierczynski, Luna, Vazquez, & Belenguer, 2011) and hot water tank technologies (Parra, Gillott, & Walker, 2014) were selected from the literature but also technical data from different manufacturers including Hitachi, Solom and Grant respectively were incorporated where appropriate. The two battery models are based on the equivalent circuit of PbA and Li-ion batteries including an open source voltage and the equivalent impedance in series. Uniform temperature across the hot water tank (perfect mixed) was assumed for this ES technology.

Table 11: comparison of the technical input data for the three different ES technologies.

Parameter	PbA	Li-ion
State-of-charge range	0.5	0.8
Maximum state-of-charge	0.9	0.9
Minimum state-of-charge	0.4	0.1
Maximum charge current (A)	$0.2 \cdot C_{nom}$	$3 \cdot C_{nom}$
Minimum discharge current (A)	$0.4 \cdot C_{nom}$	$3 \cdot C_{nom}$
Storage medium cost (£/kWh)	140	350
3 kW inverter cost (£)	1100	
Balance-of-plant cost	60	
Maintenance cost	6.5	
Maximum cycle life (EFC)	1500	4000
Cycle loses (%/EFC)	0.02	0.0075
Calendar losses (%/month)	0.12	0.07

Additionally, some electronics is required in order to deliver and absorb the PV electricity. In the case of battery storage, a bidirectional inverter is connected in series with the battery and performs the DC/AC and the AC/DC conversion for the charge and discharge respectively. State-of-art technology from the company SMA Solar Technology AG for this purpose (Technology, 2014). Alternatively, A PV controller

system should be installed in order to divert any surplus PV generation into the immersion heater placed in the tank.

The performance of the ES system is characterised by the annual round trip efficiency considering the inverter efficiency in the case of battery technologies. The impact of the ES technology system in the single home was quantified by two different indicators: the PV ratio defined as the ratio between the amount of annual PV generation supplied to the ES system and the annual PV generation as defined in Equation 2; the demand ratio, defined in Equation 3, which quantifies the fraction of the annual demand (electricity and DHW for battery and how water tank respectively) met by the ES system

Equation 2: PV ratio

$$PV_{ES} = \frac{E_{char}}{E_{PV}}$$

Where:

- PV$_{ES}$ = PV ratio (relative to the ES system)
- E$_{PVES}$= annual PV generation supplied to the ES system (kWh)

Equation 3: Demand ratio

$$D_{ES} = \frac{E_{dis}}{E_d}$$

Where:

- D$_{ES}$ = Demand ratio (relative to the ES system)
- E$_d$= annual demand (kWh)

The durability submodel quantifies the ageing of different ES technologies. It includes both calendar and cycle losses for both battery chemistries, these losses reducing the battery capacity according to the battery performance and stand-by operation respectively. It was assumed that the battery life finishes when the battery capacity reaches 70% of the nominal battery capacity (Parra, Gillott, Norman, & Walker, 2014). The durability of PbA and Li-ion batteries was quantified by means of the number of equivalent full cycles (EFC) defined in Equation 4 as the ratio between the discharge of the battery system (including the inverter efficiency) throughout the battery lifetime divided by the battery nominal capacity. Modelling the degradation of domestic hot water tanks was not necessary since it was considered that how water tanks last 20 years or more when properly utilised and maintained after consulting two different manufacturers, Mcdonald Engineers and Grant. Finally, 20 years was used as input datum for the techno-economic analysis, also for the PV controller since is manufactured using similar components to those found in inverters and other electronic devices. The different durability input data for both battery technologies are reported in Table 1.

Equation 4: Equivalent full cycles

$$EFC = \frac{E_{dis} \cdot Life}{C_{nom}}$$

Where:

- EFC = number of equivalent full cycles of the battery system (cycles)
- Life= number of operational years of the battery system (years)
- C$_{nom}$= nominal battery capacity (kWh)

The capital investment and maintenance costs for both battery technologies is also shown Table 1. In the case of hot water tanks, the two companies contacted for the durability (Mcdonald Engineers and

Grant) also supplied initial cost data. Specifically, the cost of cooper unvented cylinders was supplied as a function of the capacity, ranging from £670 to £5000 for a 100 l and a 1000 l hot water tank. These cost data are not representative for the majority of hot water tanks previously installed in the UK which are made of cooper and vented and cheaper as a consequence. Additionally, a PV controller is necessary to divert surplus PV generation into the immersion heater placed in the tank and it cost was £500 based on the current cost of a product in the market, the ImmerSUN®. Three different economic indicators are calculated in this study to quantify the economic benefits of ES systems performing PV energy time-shift in a single home. The levelised cost is the net cost of the energy system (including CAPEX and OPEX) divided by the life-time energy output and it is defined in Equation 4; the levelised value is the net revenue of the ES system through its lifetime divided by the life-time energy output and it is defined in Equation 5; and the internal rate of return which is a profitability indicator defined in Equation 6. A discount factor equal to 4% was utilised in agreement with other previous studies in ES for single homes (Hoppmann et al., 2014; Mulder et al., 2013). Table 1 shows the different technical data including durability and cost utilised as input data for the model depending on the ES technology.

Equation 4: Levelised cost of ES

$$LCOES = \frac{TLC}{\sum_{k=0}^{Life} \frac{E_{dis}}{(1+r)^k}}$$

Where:

  - LCOES = levelised cost of energy storage (£/kWh)
  - TLC= total levelised cost (£)
  - r= discount factor

Equation 5: Levelised value of ES

$$LVOES = \frac{\sum_{k=1}^{Life} \frac{Rev_{PVts}}{(1+r)^k}}{\sum_{k=0}^{Life} \frac{E_{dis}}{(1+r)^k}}$$

Where:

  - LVOES = levelised value of energy storage (£/kWh)

Equation 6: Internal rate of return

$$0 = \sum_{k=0}^{Life} \frac{CF_k}{(1+IRR)^k}$$

Where:

  - IRR = internal rate of return (%)
  - CF= cash flow (£)

3   RESULTS

Results are presented as a function of the ES capacity i.e. battery capacity (kWh) for battery systems in Figure 2 and volume (l) for hot water tanks in Figure 3. Ten different capacities are tested for any ES technology. In the case of battery technology, the largest capacity (20 kWh) correspond to the day of the year in which more surplus PV energy was available to be stored i.e. the maximum ES demand for PV energy time-shift. Then, the smallest battery size and the resolution of the capacity discretisation were chosen to be a tenth of the maximum size i.e., 2 kWh. This rationale was also utilised for hot water

tank technology although the capacity range was based on the range of available models in the market for single home ranging from 100 l to 1000 l.

3.1 Performance Results

Figure 3 shows the number of equivalent full cycles, round trip efficiency, PV ratio and demand ratio for PbA and Li-ion batteries in a single home. The round trip efficiency, PV ratio and demand ratio followed a similar positive logarithmic trend with the capacity but this trend reduced with the capacity, especially in the case of the round trip efficiency of Li-ion technology. A 20 kWh Li-ion battery was able to absorb the 45% of the annual PV generation (D_{ES}=0.45) and meet the 34% of the annual electrical demand (D_{ES}=0.34) as seen in Table 2. In the case of the number of equivalent full cycles, PbA and Li-ion batteries followed different patterns. In both cases, the battery system with a capacity of 4 kWh was able to achieve the highest number of cycles, specifically 932 EFC and 2511 EFC for PbA and Li-ion technology respectively. Beyond this capacity, the number of equivalent full cycles decreased, especially for Li-ion battery systems. Li-ion batteries achieved better performance results for any of the parameters as summarised in Table 2.
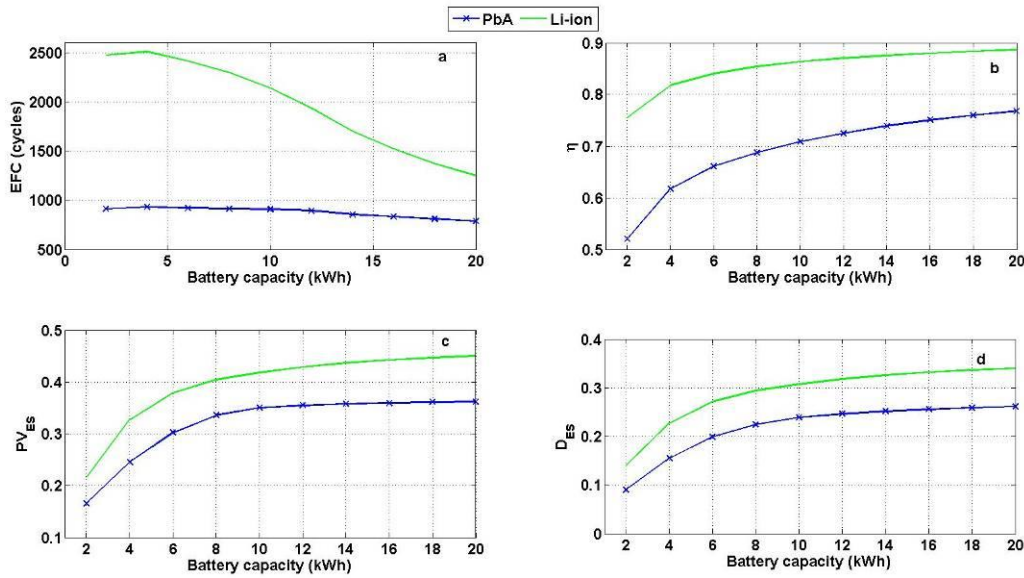
Figure 30: Performance results of PbA and Li-ion batteries performing PV energy time-shift as a function of the battery capacity: (a) number of equivalent full cycles, (b) round trip efficiency, (c) PV ratio and (d) demand ratio.

As seen in Figure 4, the efficiency of hot water tanks decreased with the tank capacity because the water was stored for longer periods despite the ratio between the external area of the tank and the tank volume reduces with the capacity (the external area of the 100 l and 1000 l water tank is 1.59 m^2 and 6.1 m^2 respectively). The PV ratio followed a logarithmic pattern similar to the one followed by battery systems and grew with the capacity of the tank up to 0.69. Similarly, the demand ratio grew faster for small capacities but it reached a maximum of 0.45 for a hot water tank capacity equal to 500 l. Beyond this capacity, the efficiency was lower than 0.7 and this affected the final DHW met by hot water tank using PV generation. In other words, the self-discharge of the water tank became important and reduced the demand ratio.
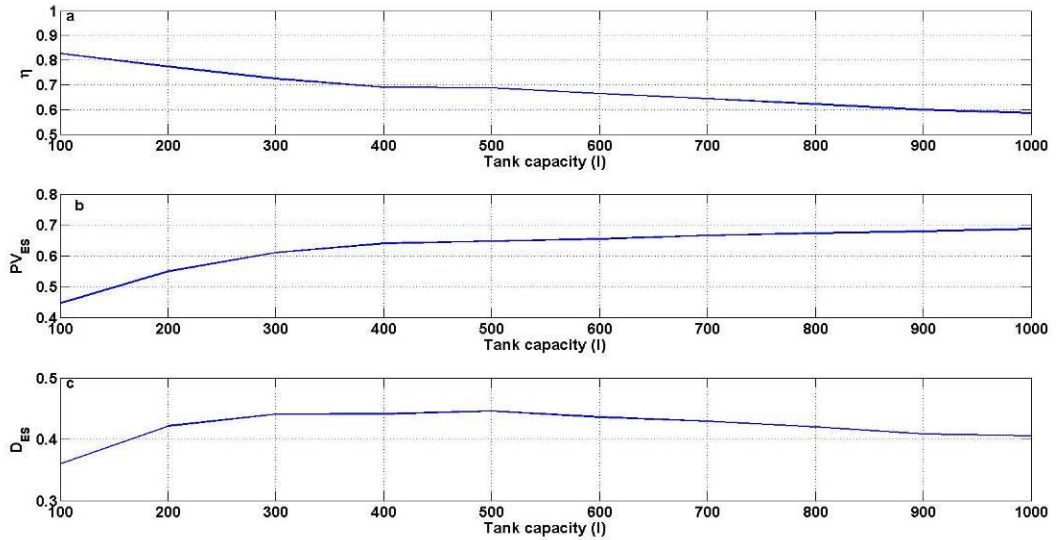
Figure 31: Performance results of hot water tanks performing PV energy time-shift as a function of the tank capacity: (a) tank efficiency, (b) PV ratio and (c) demand ratio.

Table 12: performance indicators optimised for PbA, Li-ion and hot water tank technologies performing PV energy time-shift. The capacity of the battery (kWh) and the hot water tank (l) which achieved the optimum values is shown in brackets.

Technology	EFC	η	PV_{ES}	D_{ES}
PbA	932 (4 kWh)	0.85 (20 kWh)	0.45 (20 kWh)	0.26 (20 kWh)
Li-ion	2511 (4 kWh)	0.89 (20 kWh)	0.36 (20 kWh)	0.36 (20 kWh)
Hot water tank		0.83 (100 l)	0.69 (1000 l)	0.45 (500 l)

3.2 Economic Results

Based on the performance results, Figure 4 shows the *LCOES*, *IRR* and *LVOES* for the three ES technologies in a single home. For both battery technologies, there was an optimum battery capacity which minimised the LCOES of performing PV energy time-shift. This result was related with the maximum number of equivalent full cycles discussed above but also the round trip efficiency played a role. While the battery capacity which maximised the maximum number of equivalent full cycles was 4 kWh for both battery technologies, the battery capacities which minimised the *LCOES* were 12 kWh and 8 kWh for PbA and Li-ion battery systems respectively as shown in Table 3. The minimum LCOES values were 0.41 £/kWh and 0.37 £/kWh for PbA and Li-ion technologies respectively.

The *LVOES* increased with the battery capacity because the durability was proportional to the battery capacity and this allowed battery systems to perform more efficiently as shown in Figure 4 (as suggested by Equation 1, the revenue obtained by performing PV energy time-shift i.e. the *LVOES* is proportional to the round trip efficiency) and to profit from higher retail prices (according to the 2% increase p.a. assumed in Section 2.3). Only, increasing the battery capacity beyond 12 kWh did not have any positive effect for Li-ion battery systems because the maximum durability was restricted by the calendar life. This means that Li-ion batteries achieved higher *LVOES* than PbA batteries up to 0.15 £/kWh. The maximum *IRR* was equal to -6.3% and -3.9% for a 20 kWh PbA and 10 kWh Li-ion battery system, these values being a balance between those explained for the *LCOES* and *LVOES*.
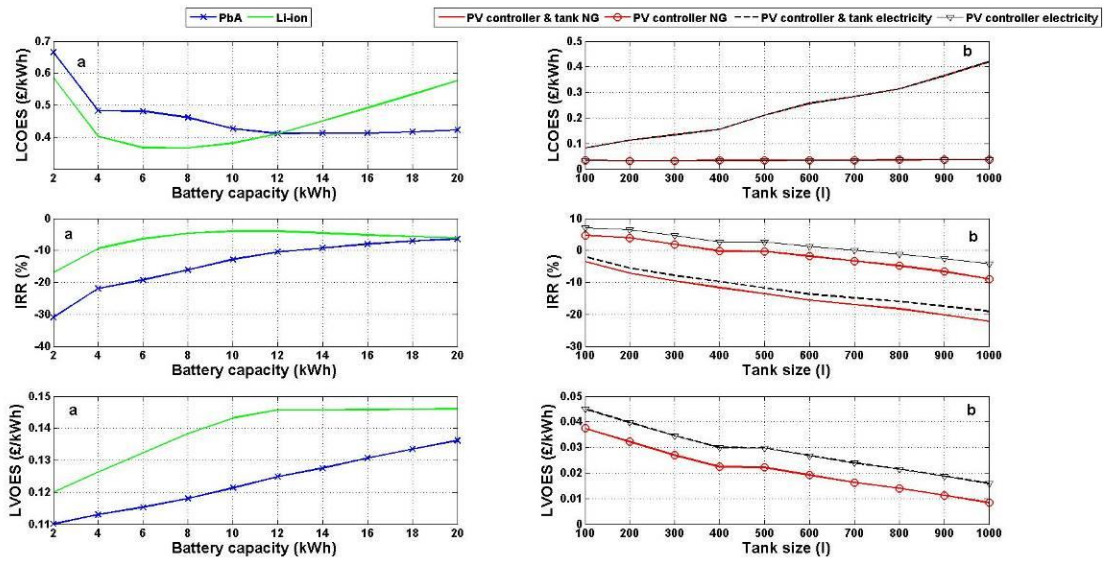
Figure 32: LCOES, IRR and LVOES for (a) PbA and Li-ion battery systems as a function of the battery capacity and for (b) hot water tanks as a function of the tank size for different scenarios when performing PV energy time-shift.

Four different scenarios were considered for evaluating the economic results of hot water tanks depending on the initial investment (the initial cost of the installation only includes the PV controller necessary to divert the surplus PV generation or the initial cost also considers the hot water tank) and what energy source was used previously to meet the DHW demand (natural gas or electricity assuming Economy 7). The *LVOES* of using PV generation to replace natural gas was lower (up to 0.04 £/kWh) than the *LVOES* of using it to replace electrical heat (up to 0.05 £/kWh). Additionally, the *IRR* was less negative or even positive when the hot water tank was not part of the investment. For example, the LCOES of installing a PV controller in a house which already had a 200-l water tank was equal to 0.03 £/kWh while the *IRR* value was equal to 3.9% and 6.4% depending on what type of energy source was previously used to generate DHW i.e., natural gas and electricity respectively.

Table 13: Economic parameters optimised for PbA, Li-ion and hot water tank technologies using PV energy time-shift. The capacity of the battery (kWh) and the hot water tank (l) which achieved the optimum values is shown in brackets. If the hot water tank already exits, only a PV controller is installed to divert the surplus PV generation

Technology	LCOES (£/kWh)	IRR (%)	LVOES (£/kWh)
PbA	0.41 (12 kWh)	-6.4 (10 kWh)	0.14 (20 kWh)
Li-ion	0.37 (8 kWh)	-3.9 (20 kWh)	0.15 (20 kWh)
Tank & PV controller (natural gas)	0.08 (100 l)	-3.5 (100 l)	0.04 (100 l)
PV controller (natural gas)	0.03 (200 l)	4.8 (100 l)	0.04 (100 l)
Tank & PV controller (electricity)	0.08 (100 l)	-2.0 (100 l)	0.05 (100 l)
PV controller (natural gas)	0.03 (200 l)	7.0 (100 l)	0.05 (100 l)

4 CONCLUSION

The combination of a hot water tank and a PV controller is the best ES system for performing PV energy time-shift from an economic point of view in the UK, especially when the domestic property already has a water tank. In this case, IRR values were always higher than the assumed discount rate (4%) for standard hot water tank sizes, e.g., 200 l. This result was more emphasised when electricity was used by end users to supply DHW (Economy 7 was assumed for this purpose in the UK) since retail electricity price is higher than the price of retail natural gas.

A 10 kWh Li-ion battery system achieved an *IRR* value equal to -4.3%, the highest amongst all capacities tested including PbA technology. Although the assumed storage medium cost for Li-ion batteries (350 £/kWh) was 2.5 times higher than that of PbA batteries (140 £/kWh), the higher round trip efficiency and cycling capability of Li-ion battery capacities resulted in lower levelised cost (the minimum value equal to 0.37 £/kWh) and higher levelised value (the maximum value equal to 0.15 £/kWh) than PbA batteries, mainly for battery systems which a capacity between 4 kWh and 10 kWh.

Despite being the most profitable option, governments and customers should understand that shifting PV generation to meet the DHW using hot water tanks means that the electrical and heat demand loads are not met by local RE generation. Governments, in collaboration with utility companies and energy services companies   should therefore legislate and propose ES value propositions which account for several service and strategic benefits in the case of battery technology. Only in this case, battery storage in single homes would have a stronger economic case (in comparison with hot water tanks) and a wider impact as an enabling technology in the wider energy system.

5   ACKNOWLEDGEMNTS

6   REFERENCES

BELTRAN, H., Swierczynski, M., Luna, A., Vazquez, G., & Belenguer, E. (2011). Photovoltaic plants generation improvement using Li-ion batteries as energy buffer. In *Industrial Electronics (ISIE), 2011 IEEE International Symposium on* (pp. 2063–2069).

BRAUN, M., Büdenbender, K., Magnor, D., & Jossen, A. (2009). Photovoltaic self-consumption in Germany using Lithium-ion storage to increase self-consumed photovoltaic energy. *ISET, Kassel.*

BRUNET, Y. (2013). *Energy storage*. Wiley. com.

COPETTI, J. B., & Chenlo, F. (1994). Lead/acid batteries for photovoltaic applications. Test results and modeling. *Journal of Power Sources*, *47*(1), 109–118.

DIVYA, K. C., & Østergaard, J. (2009). Battery energy storage technology for power system. An overview. *Electric Power Systems Research*, *79*(4), 511–520.

DUFFIE, J. A., & Beckman, W. A. (2013). *Solar engineering of thermal processes*. John Wiley & Sons.

HM Government, D. of E. (2014). *Consumer prices index: fuel components*. Retrieved from https://www.gov.uk/government/statistical-data-sets/annual-domestic-energy-price-statistics

HOPPMANN, J., Volland, J., Schmidt, T. S., & Hoffmann, V. H. (2014). The economic viability of battery storage for residential solar photovoltaic systems--A review and a simulation model. *Renewable and Sustainable Energy Reviews*, *39*, 1101–1118.

INFIELD, D. (2007). A Road Map for Photovoltaics Research in the UK. *UK Energy Research Centre (UKERC) Research Report, REF UKERC/RR/FSE/2007/001.*

JENKINS, D. P., Fletcher, J., & Kane, D. (2008). Lifetime prediction and sizing of lead-acid batteries for microgeneration storage applications. *Renewable Power Generation, IET*, *2*(3), 191–200.

MULDER, G., Six, D., Claessens, B., Broes, T., Omar, N., & Mierlo, J. Van. (2013). The dimensioning of PV-battery systems depending on the incentive and selling price conditions. *Applied Energy*, *111*, 1126–1135.

NAIR, N.-K. C., & Garimella, N. (2010). Battery energy storage systems: Assessment for small-scale renewable energy integration. *Energy and Buildings*, *42*(11), 2124–2130.

PAATERO, J. V, & Lund, P. D. (2007). Impacts of energy storage in distribution grids with high penetration of photovoltaic power. *International Journal of Distributed Energy Resources*, *3*(1), 31–45.

PARRA, D. (2014). *Optimum community energy storage for end user applications*. University of Nottingham.

PARRA, D., Gillott, M., Norman, S. A., & Walker, G. S. (2014). Optimum community energy storage system for PV energy time-shift. *Applied Energy*.

PARRA, D., Gillott, M., & Walker, G. S. (2014). The role of hydrogen in achieving the decarbonization targets for the UK domestic sector. *International Journal of Hydrogen Energy*, *39*(9), 4158–4169.

PARRA, D., Walker, G. S., & Gillott, M. (2013). Modeling of PV generation, battery and hydrogen storage to investigate the benefits of energy storage for single dwelling. *Sustainable Cities and Society*.

PV-SPEICHER, W., Kairies, K., Magnor, D., & Sauer, D. U. (2014). Scientific Measuring and Evaluation Program for Photovoltaic Battery Systems. In *4th Solar Integration Workshop*.

SANTOS, J. M., Moura, P. S., & Almeida, A. T. de. (2014). Technical and economic impact of residential electricity storage at local and grid level for Portugal. *Applied Energy*, *128*, 254–264.

SPOT, E. P. E. E. (2014). EPEXSPOT. European Power Exchange [online]. Retrieved from http://www.epexspot.com/en/

Technology, S. S. (2014). SMA Solar Technology AG. *Unknown Journal*. Retrieved from http://www.sma.de/en/products/battery-inverters.html

UKERC. (1990). Milton Keynes Energy Park Dwellings. *Unknown Journal*. http://data.ukedc.rl.ac.uk/cgi-bin/dataset_catalogue/view.cgi.py?id=9.

UTLEY, J. I., & Shorrock, L. D. (2008). Domestic energy fact file 2008. *Department of Energy and Climate Change, BRE, Watford*.

VILLALVA, M. G., Gazoli, J. R., & others. (2009). Comprehensive approach to modeling and simulation of photovoltaic arrays. *Power Electronics, IEEE Transactions on*, *24*(5), 1198–1208.

169: Sensitivity analysis for minimization of input data for urban scale heat demand forecasting

ANETA STRZALKA[1], DIRK MONIEN[2], ATHANASIOS KOUKOFIKIS[3], URSULA EICKER[4]

1 Stuttgart University of Applied Sciences, Schellingstr. 24, 71174 Stuttgart, aneta.strzalka @hft-stuttgart-de
2 Stuttgart University of Applied Sciences, Schellingstr. 24, 71174 Stuttgart, dirk.monien @hft-stuttgart-de
3 Stuttgart University of Applied Sciences, Schellingstr. 24, 71174 Stuttgart, athanasios.koukofikis @hft-stuttgart.de
4 Stuttgart University of Applied Sciences, Schellingstr. 24, 71174 Stuttgart, ursula.eicker @hft-stuttgart.de

In the paper a methodology based on 3D building and city models is presented to calculate urban heat demand for different refurbishment scenarios. This methodology is validated on six case study buildings of the City of Essen in Germany.

The influences of the availability and quality of data input regarding the geometrical and physical parameters on the accuracy of simulation models are analysed. Different CityGML Levels of Details (LoDs) of the building models as well as different sources of the physical parameters are tested in order to investigate the uncertainty of the methods used.

In the first step, a semi-automated method with data pre-processing (FME software,) as well as simulation of the heat demand (INSEL8 software) is used. The results are compared with a fully-automated method implemented in the urban simulation platform SimStadt, whose development is ongoing in the project with the same name (www.simstadt.eu). This platform has a special module integrated, which allows an automatic data pre-processing. Both methods calculate heat demand based on monthly energy balance (standardised in Germany with the DIN V 18599, or in Europe with the ISO 13790).

The calculation of the heat demand with different accuracy of the data input enables to make a statement about which parameters have the most influence on the results. Considering the difficulties in obtaining data available at a city scale this information is very useful for future reductions of the effort of data capturing. For example, the analysis showed that the geometrical Level of Detail can give up to 12% of error depending which of the LoDs are available for the analysed building.

In the next stage, the methods tested first on the six case study buildings can be extrapolated for the whole City of Essen. This methodology could be even extended to other cities on condition that they have 3D city models available.

Keywords: heat demand simulation, 3D building model, varied Levels of Detail, SimStadt-platform

1. INTRODUCTION

The building sector has the largest potential in the EU-economy for achieving energy efficiency gains and CO_2-reductions and is thus a priority area for achievement of the ambitious climate and energy targets for 2020 and 2050. In order to reach the 2% energy refurbishment rate promoted by the European Union and at long-term climate neutral communities, a change of rhythm and of scale is highly required. The building energy evaluation tools available today are only able to effectively analyse individual buildings and require a high amount of input data. Therefore, there is a strong need in order to develop a 3D GIS-based tool to precisely and easily perform the forecast of heat demand at the urban district level. The fundamental research challenge is to move from the analysis of individual buildings to integrated analysis of the built environment at a district or even municipal level.

There are many different methods and models for the analysis of energy use in buildings and cities available. RABL, 1988: page 1 intends that no single one method is universally the best, but the choice in a given situation, which depends on what one wants to calculate and what input data are available is important. The virtual city models, which stores geometrical and semantic data of whole cities occurred to be a good solution in order to perform urban energy analyses, like e.g. in Karlsruhe and Ludwigsburg realised by NOUVEL ET AL., 2013 or in Berlin, CARRION, 2010 and CARRION ET AL., 2010.

The data quality of the city models is very variable, depending on the available public databases and the information data collected on-site, NOUVEL ET AL., 2014. Therefore NOUVEL ET AL., 2014 presents a methodology of urban heat demand analysis that enables the investigation of the uncertainty of the model, analysing the influence of the building information data (geometrical and semantical) on the simulated heat demand. The work of CARRION, 2010 showed an average error of 19% between the calculated and measured data of heat demand/consumption. KADEN, R., KOLBE, T.H., 2013 recognised that these errors are mainly caused by the fact, that in the most available methods the actual building rehabilitation state is generally not citywide known, so that the estimates mostly based on energy characteristic values or heat transfer coefficients (U-values) of the year of construction. Therefore, in this paper, two standard refurbishment scenarios will be analysed and the influence on the result on heat demand calculation will be shown.

Previous works of STRZALKA ET AL., 2010, 2011 analysed the deviations between measured and calculated values for a low energy city quarter of Scharnhauser Park (SHP), in which the buildings had a high energy performance and therefore the rehabilitation state could not have an influence on these deviations. The analysis done in SHP showed a reasonable correlation for many buildings, but there were also many buildings with extreme deviations greater than 100%, what led to an average deviation between 30-40%. These high deviations were mainly caused by the lack of detailed geometrical information. This fact encouraged the author for further analysis of these uncertainties within this paper; different CityGML Levels of Detail (LoD1, LoD2 and LoD3) will be tested in order to recognize the error they can cause. Not only the geometrical parameters but also the influence of each physical parameter used in the heat demand simulation will be analysed. This should help to recognize, which of the parameters has the most influence on the result of the heat demand calculation and which of them does not play a crucial role and can be assumed or taken from the standards. Considering the difficulties in obtaining data availability at a city scale, this analysis will be very useful for future reductions of the effort of data capturing.

2. CASE STUDY BUILDINGS

The analysis is based on six case study buildings of the City of Essen, representing different building categories; years of construction and refurbishment states, see Table 1.

Table 14: List of reference buildings

Building No	Building type	Year of Construction
1	Multi-family house (MFH)	1907
2	Multi-family house (MFH)	1954
3	Multi-family house (MFH)	1910
4	Multi-family house (MFH)	1955
5	High tower (HH)	1974
6	Single-family house (EFH)	2004

3. METHODS

Two methods have been tested in order to simulate the heat demand of six reference buildings of the City of Essen. The results can be then extrapolated for the whole City of Essen or even extended to other cities on condition that they have 3D city models available. The first method is a semi-automated one, which uses a FME-software as well as INSEL building simulation model. The second one is a fully-automated method implemented in the urban simulation platform SimStadt. Both methods requires the same data input and the calculation algorithm is based on monthly energy balance (standardised in Germany with the DIN V 18599, or in Europe with the ISO 13790).

3.1 Data availability

U-values

The building physics properties like heat transfer coefficients (U-values) of the building elements are assessed from the IWU building typology library (IWU, 2015a) developed in the TABULA (IWU, 2015b) project. Here buildings are classified as to their type (e.g. multi-family house, single-family house or high tower) and building age class.

Weather data

The meteorological data used for the simulation are TRY weather data for the City of Essen, which are available in monthly as well as hourly time resolution.

3.2 Semi-automated method

Data pre-processing with FME-Tool

Feature Manipulation Engine (FME) is a software application developed by Safe Software, Inc. Among other capabilities, FME is used for converting, transforming, integrating and validating spatial/non-spatial data. The graphical authoring environment controls the conversion flow via elements called transformers. The transformation of the content of the data is realized by generating new attributes or altering attributes exposed by the FME input types. A complete workflow project can be created, saved and edited using the FME Workbench application.

The case study input building files are all in DXF/DWG format (Figure 33). Although the Drawing Exchange Format is for general purpose modelling, semantic information can be exposed by the concept of grouping building entities into layers. All geometry parts that belong to the wall surface of a building need to be separated by orientation criteria. Polygons that have the same (or similar) direction are grouped in the same layer (Figure 34).
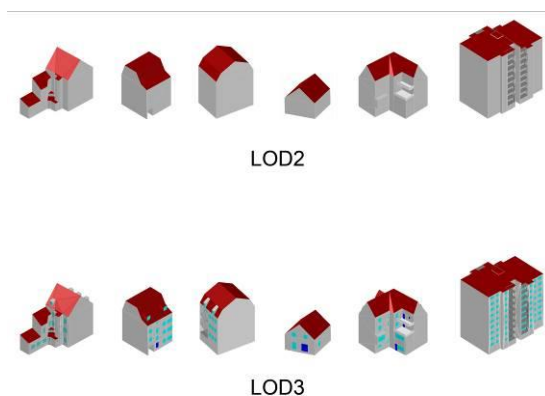
Figure 33: Case study buildings in Level of Detail 2 & 3   Figure 34: Geometry definition with DraftSight
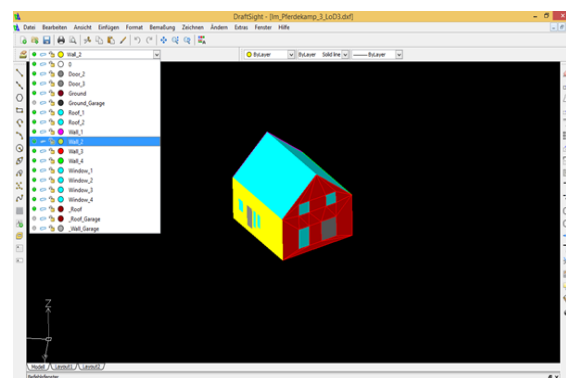
In FME, two workbench implementations, one for each level of detail, convert the DXF files to CityGML. The workbench that converts to LoD2 is the base workflow that is partially extended by the workbench

that converts to LoD3. Initially the polygons with the normal vector pointing inwards the building shell are reversed to point outwards in order to restore the actual face orientation. Additionally, every polygon is appended a number of CityGML-specific attributes to define the level of detail (citygml_level_of_detail), the geometry type (citygml_lod_name), the role (citygml_feature_role), and the feature hierarchy (gml_parent_id and a gml_id). The geometry of the LoD2 output is modelled as MultiSurface.

The workbench that converts to LoD3 extracts additional layers from the DXF file that contain the building doors and windows. Next, this workbench specifies the parent-child relationship between the boundary surfaces and the openings (doors, windows). This step is required to define the openings that belong to a single wall.

Each building is geo-referenced to the DHDN/Gauss-Kruger zone 2 Coordinate Reference System. The reference system is available in a list of predefined coordinate systems in FME. In order to apply the false easting of DHDN/3GK2, all buildings are translated by an affine transformation. Since the buildings reside in the 2nd zone, in the settings of the "3DAffiner" transformer we set the value of 2000 km in the X translation.

The conversion from LoD2 to LoD1 (see Figure 35) utilizes the basic methodology for deriving LoD1 building shells: the building footprint is extruded to the average height of the roof. The semantics exposed by the LoD2 buildings allow an effortless conversion to LoD1. Each boundary surface becomes an FME input feature type. The Z values are extracted from the vertices of the RoofSurface and sent to the "StatisticsCalculator" transformer where the average elevation is calculated. The average elevation is transformed to the building height by subtracting the average GroundSurface elevation. Next, the GroundSurface is extruded to the building height and exported as CityGML LoD1 solid.
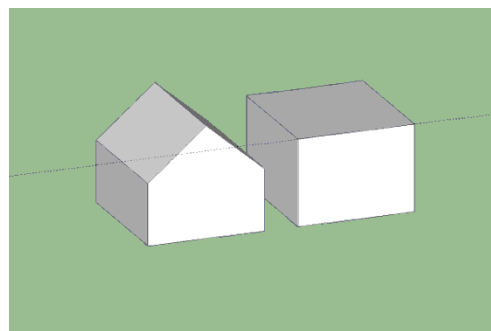
Figure 35: Creating LoD1 from LoD2
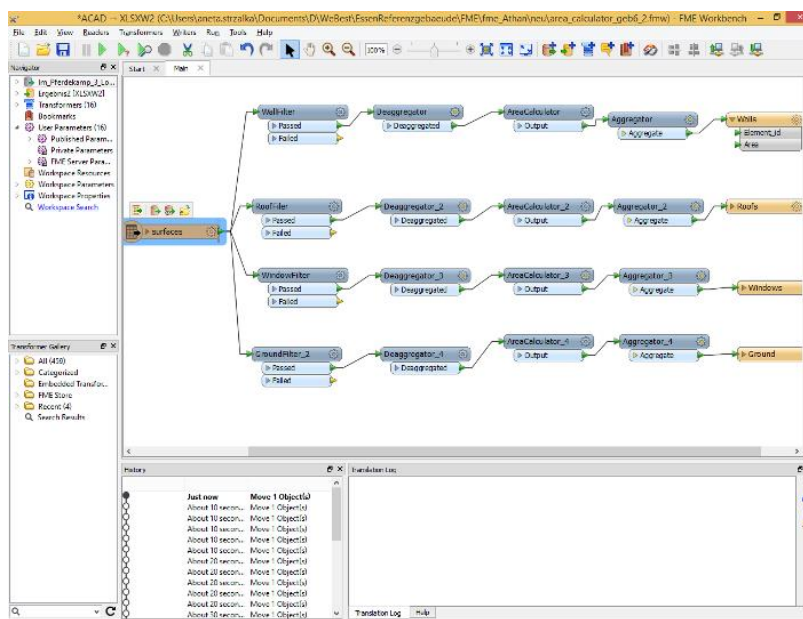
Figure 36: Extraction of building dimensions within FME-Workbench

The Figure 36 shows an FME-Workbench, which was used to extract the building dimensions used in the INSEL simulation.

INSEL-Simulation

The geometries extracted in the previous step (Figure 36), which include building dimensions, were then entered into the INSEL building simulation model (www.insel.eu). The model considers the entire energy balance with transmission and ventilation losses as well as solar and internal gains following the well-established energy balance method described in German Standard DIN V 18599, DIN e.V., 2010. In the model, assumptions regarding the user behaviour parameters have been firstly done in order to analyse only the variations of geometrical and physical parameters. These assumptions are as follows: heating set-point temperature of 20°C, air exchange rate of 0,5 1/h and internal heat gains of 3,8 W/m².
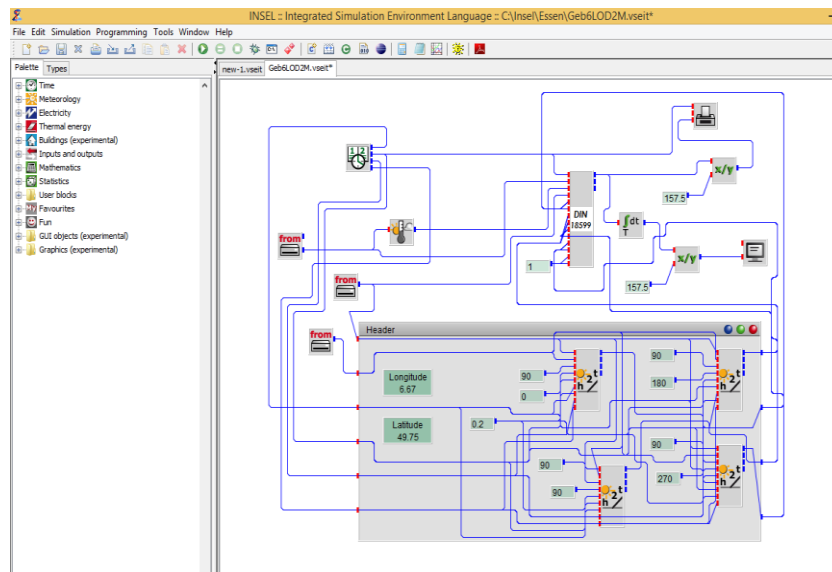
Figure 37: Graphic editor VSEit of the software INSEL

Figure 37 shows the graphic editor VSEit of the software INSEL in which the simulation model for the calculation of heat demand has been created from existing blocks, like e.g. solar radiation blocks, read blocks, etc. Only for the energy balance model described in German Standard DIN V 18599, DIN e.V., 2010 a new block called ENERBA has been created using a special INSEL programming interface.

3.3 Fully-automated SimStadt-Platform

The second method used for the calculation of the heat demand is a fully-automated method, which an urban simulation platform is called SimStadt, whose development is ongoing in the project with the same name (SimStadt, 2014). This urban simulation platform has been chosen in order to consider the heat demand calculation at city scale, as the most available building simulation models, tools are only limited to separate buildings.
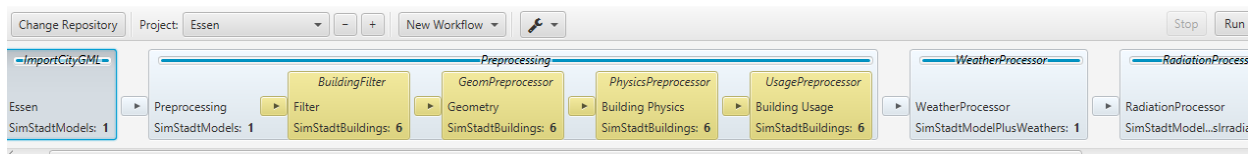
Figure 38: Workflow of the Urban Simulation Platform SimStadt

Figure 38 shows the data processing steps within the SimStadt user interface. The first step of importing the 3D city model(s) is followed by several pre-processing steps where the corresponding building physics and building usage libraries are assigned. After the further steps of weather and radiation

processing the workflow ends up with the calculation of heat demand calculation on the basis of DIN V 18599.

3.4 Parametric study

The parametric study is firstly done to analyse different Levels of Detail (LoD1 to LoD3) regarding the geometries by using the SimStadt platform. This platform is also used to test two different refurbishment scenarios, like a "medium" and an "advanced" one.

The INSEL method is mainly used to precisely perform the parametric study regarding the physical parameters, but also some of the user behaviour parameters. Hereby different U-values of building elements, window types as well as set point temperature, internal heat gains and air exchange rate are tested separately in order to give an information, which of the parameters changes the value of annual heat demand most of all.

4   RESULTS

4.1 Parametric Study – Geometrical Parameters

The SimStadt platform was firstly used to compare the results for different Levels of Detail (from LoD1 to LoD3) regarding the geometries. Figure 39 shows the comparison between LoD1, LoD2 and LoD3 for all case study buildings. LoD3 is in this case restricted to consider only the real window areas. Neither the real positioning of window areas nor overhangs and dormers have been taken into account in this study.
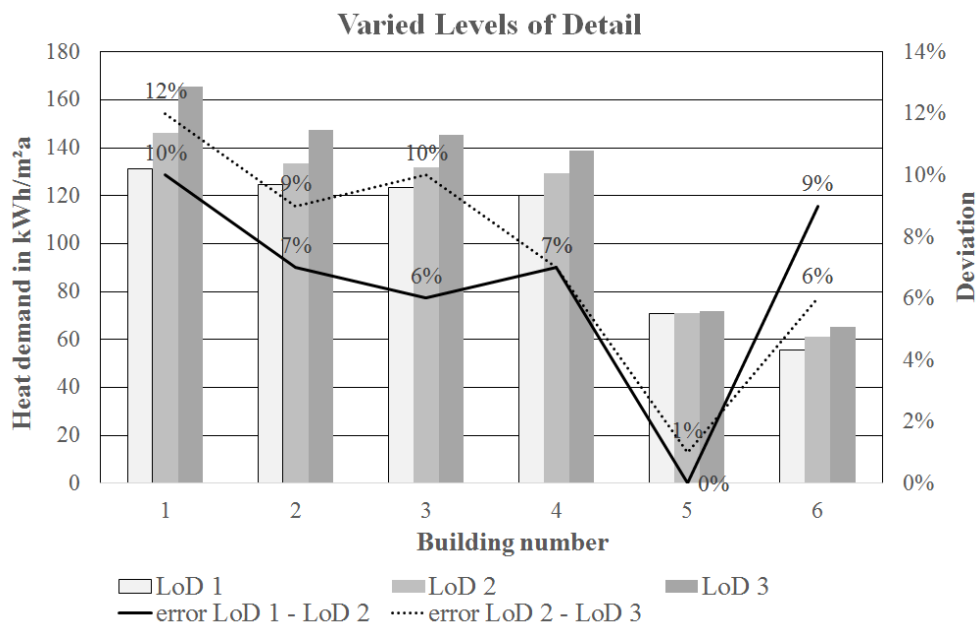
Figure 39: Errors in demand calculation as function of Level of Detail regarding the geometry

The deviation between LoD1 and LoD2 is smaller or equal to 10%; in case of building 5 there is no difference, as this building has a flat roof. The comparison between LoD2 and LoD3 is smaller than 12% for all buildings.

Finally, two different refurbishment states have been chosen in order to analyse their impact on the result of the heat demand calculation. The analysis was done for all buildings, and the results are shown in Figure 40.
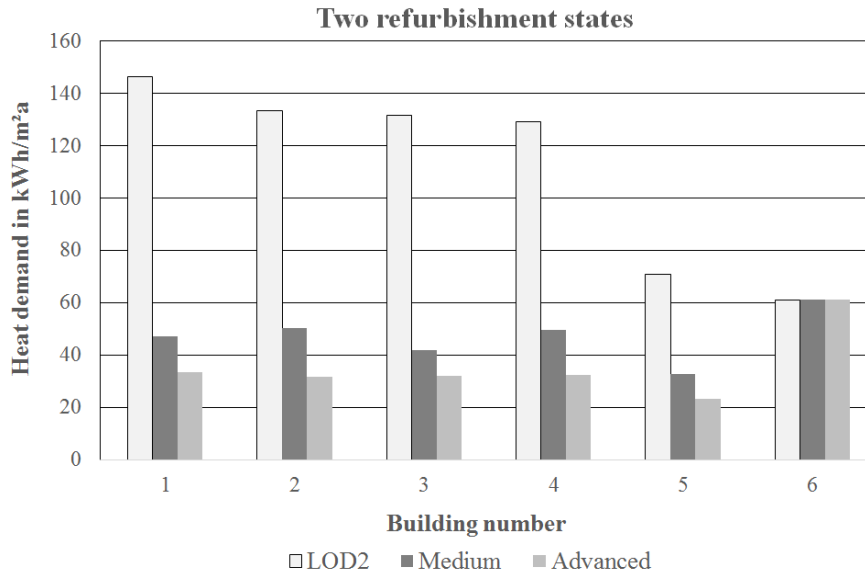
Figure 40: Errors in demand calculation for two different refurbishment states

The "Medium" scenario here corresponds to the practical implementation of refurbishment measures to achieve the minimum requirements of the German EnEV 2014. The "Advanced" scenario is oriented towards what is technically feasible today and complies with the insulation standards of passive houses. In both scenarios an individual set of measures per building type such as insulation of the ceiling, façade roofs or replacement of the windows was modelled after the recommended measures of the IWU. For building 6 no refurbishment scenarios could be calculated as the IWU did not develop any refurbishment measures for single-family-houses built after 1994. On this account the SimStadt platform does not consider any refurbishment for building 6 either.

Comparison of both methods

Building 6 was used to compare the results between both mentioned methods, which are the fully-automated SimStadt and the semi-automated INSEL methods. The settings, like physical parameters, user behaviour etc. were put as the same in order to make these both calculations comparably. The comparison shows a very good agreement; for LoD2 both methods calculate the heat demand of 61 kWh/m²a.

4.2 Parametric Study – Physical Parameters

Variation of window to wall ratio and window type

The parametric study of the physical parameters has been done for Building 6 regarding the window to wall ratio, window type and the U-values of its building elements, like outside wall, roof and ground floor. Firstly, different window to wall ratios and different window types have been varied in order to estimate an error they can cause in case there is no information on it, see Figure 41.

The SimStadt platform estimates automatically the window to wall ratio as standard values for each of the building type, e.g. for single-family houses 20% of outer wall and 10% of the roof. In real, the window to wall ratio for the outside wall is of almost 8% and there are no windows in the roof.

As it is in Figure 41 shown, in case the real window to wall ratio is known, the error regarding the choice of the window type does not exceed 25%. In case of the Simstadt window to wall ratio this error can increase to almost 70%.
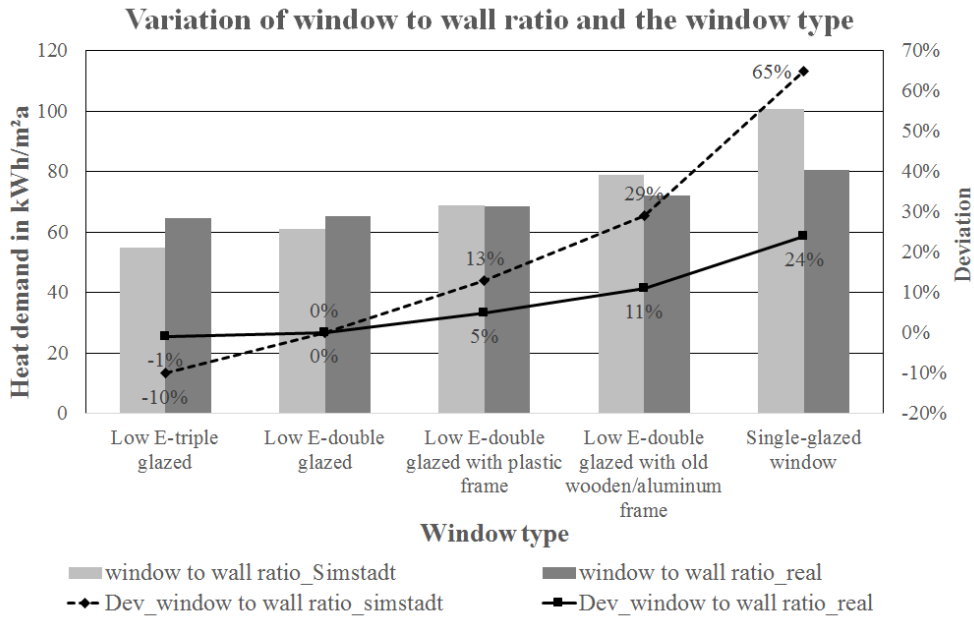
Figure 41: Variations of the window to wall ratio and the window type

Variation of U-Values

In the second step, different variations of U-values for each of the building element was analysed. The results are shown in Figure 42:
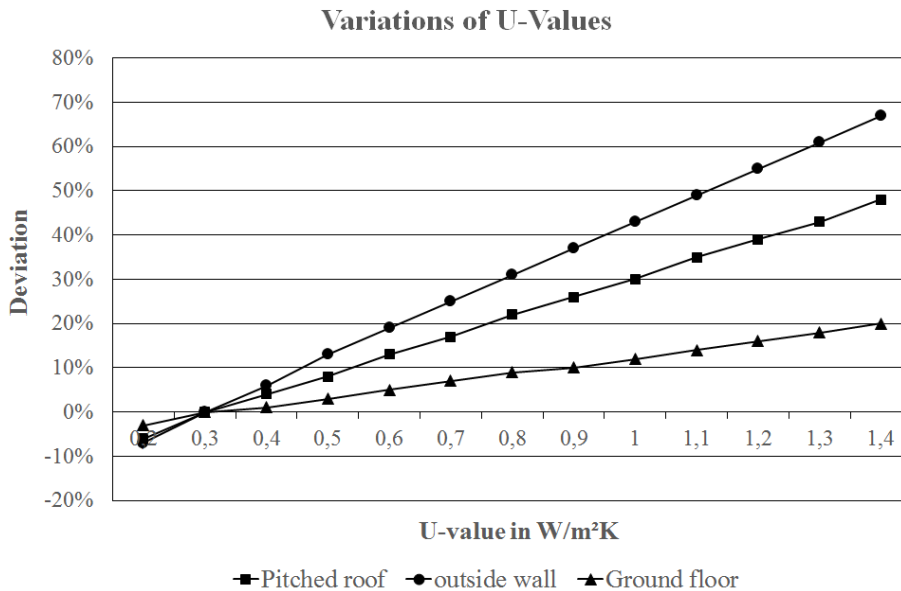
Figure 42: Variations of U-values for different building elements – %-deviation in heat demand from the starting point, which is the U-Value of 0,3 W/(m²K)

This analysis shows that the U-value of the outside wall has the greatest influence on the heat demand calculation, followed by the U-value of the roof. The U-value of the ground floor gives the smallest error.

Table 15 consists of the area values for all building elements, which are taken into account by the calculation of the errors shown in Figure 42.

Table 15: Building elements areas in m²

Wall	Wall area (incl. window area)
Wall NE	55,8 m²
Wall NW	44,9 m²
Wall SW	55,8 m²
Wall SE	44,9 m²
Pitched Roof	113,2 m²
Ground Floor	86,9 m²

Variation of user behaviour parameters

The main important user behaviour parameters considered in the INSEL-Simulation are the set-point temperature, air exchange rate and the internal heat gains. The variations of the set-point temperature are shown in Figure 43; deviations up to 40% are possible.
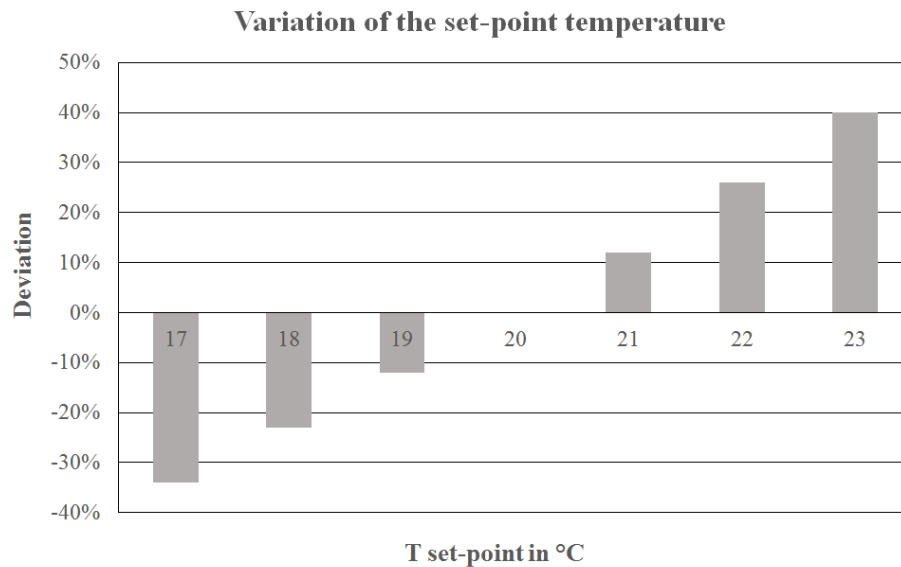
Figure 43: Variation of the set-point temperature; deviations in percentage from the standard set-point temperature of 20°C

The variations of the internal heat gains as well as air exchange rate are shown in the Table 16.

As Table 3 shows, the air exchange rate has a higher impact on the heat demand result as the internal heat gains. However, the most influence of all analysed user behaviour parameters has the set-point temperature. Therefore, the knowledge of the real temperature set-points would give more reliable results of the heat demand calculation.

Table 16: Variations of the internal heat gains and air exchange rate; deviations in % from the standard values (Qin = 3,8 W/m², n = 0,5 1/h)

Internal heat gains	Heat demand [kWh/m²a]	Deviation [%]
3,4 W/m²	63 kWh/m²a	3%
3,8 W/m²	**61** kWh/m²a	**0**
4,2 W/m²	59 kWh/m²a	-3%
4,6 W/m²	57 kWh/m²a	-6%
5,0 W/m²	55 kWh/m²a	-10%
5,4 W/m²	53 kWh/m²a	-12%
5,8 W/m²	52 kWh/m²a	-15%
6,2 W/m²	50 kWh/m²a	-18%
6,6 W/m²	48 kWh/m²a	-21%
Air exchange rate		
0,3 1/h	51 kWh/m²a	-16%
0,4 1/h	56 kWh/m²a	-8%
0,5 1/h	**61** kWh/m²a	**0**
0,6 1/h	66 kWh/m²a	8%
0,7 1/h	70 kWh/m²a	15%
0,8 1/h	75 kWh/m²a	22%
0,9 1/h	79 kWh/m²a	30%
1,0 1/h	84 kWh/m²a	37%
1,1 1/h	88 kWh/m²a	44%

5   CONCLUSION

This paper presents two methods of heat demand forecast. One of them is a semi-automated method and the second one is an automatic urban simulation platform using an integrated process. One goal was to test how effectively a 3D model can estimate the heat energy use. But the primary goal was to test, which of the both analysed methods is faster and requires the less data input possible, but is still enough precise in order to perform the heat demand simulation. Therefore, a parametric study has been done in order to show, which of the parameters have the most influence on the result and which of them could be assumed or taken from default values as they have a rather low impact on the calculation of the heat demand.

The presented approach shows that 3D models are useful for heat demand simulations. Depending on the data availability and therefore assumptions, which have to be made errors up to 80% considering the physical parameters and up to 40% for the user behaviour parameters could be estimated. The geometrical Level of Detail gives deviations between LoD1 → LoD2 up to 10% and LoD2 → LoD3 lower or equal to 12%.

The analysis showed that both of the tested methods were suitable for the heat demand forecast based on 3D models. The SimStadt-method would be the one to choose in a direct comparison. It efforts less because of its automatic manner and can therefore be used very effectively at the district or city scale.

6   REFERENCES

CARRION, D., 2010. Estimation of the energetic rehabilitation state of the buildings for the city of Berlin using a 3D city model represented in CityGML. Master Thesis. Technical University of Berlin. Germany.

CARRION, D., Lorenz, A., Kolbe, T.H., 2010. 5th International Conference on 3D Geo-Information 2010 in Berlin. The International Archives of the Photogrammetry, Remote Sensing and Spatial Information Sciences, XXXVIII-4/W15/ Estimation of the energetic rehabilitation state of the buildings for the city of Berlin using a 3D City Model represented in CityGML. Berlin, pages 31-36.

DIN e.V., 2010. DIN V 18599 – Energy efficiency of buildings – Calculations of the net, final and primary energy demand for heating, cooling and ventilation, domestic hot water and lighting – Supplement 1: Balancing of demand and consumption.

IWU, 2015a. German Building Typology.

IWU, 2015b. http://www.iwu.de/1/forschung/energie/completed-projects/tablua/

KADEN, R., Kolbe, T.H., 2013, ISPRS Annals of the Photogrammetry, Remote Sensing and Spatial Information Sciences, Vol II-2/W1, SPRS 8th 3DGeoInfo Conference & WG II/2 Workshop, Nov 2013, Istanbul, Turkey

NOUVEL, Romain, Schulte, Claudia, Eicker, Ursula, Pietruschka, Dirk, 2013, IBSA World 2013/CityGML-based 3D City Model for energy diagnostics and urban energy policy support. Place: Publisher.

NOUVEL, Romain, Zirak, M., Dastageeri, H., Coors, V., Eicker, U., 2014. BauSIM 5th German-Austrian IBPSA Conference/Urban energy analysis based on 3D city model for national scale applications. RWTH Aachen University.

RABL, A., 1988. Methods for Dynamic Analysis of Measured Energy Use. *Journal of Solar Energy Engineering*, Vol. 110, page numbers.

SimStadt PROJECT, Heat demand simulation of city quarters. 2012-2014. Website (June 2014): www.simstadt.eu

STRZALKA ET AL., 2010, Modelling Energy Demand for Heating at City Scale/4th National Conference of IBPSA-USA, August 11-13, New York, USA

STRZALKA ET AL., 2011, 3D City modelling for urban scale heating energy demand forecasting. *Journal HVAC&R Research,* Vol. 17/4, pages 526-539.

SESSION 11: ENERGY EFFICIENCY IN BUILDINGS

251: Harnessing post occupancy evaluation to understand student use of indoor environmental controls in a modern halls of residence

[1]Rucha AMIN, Despoina TELI, Patrick JAMES, Leonidas BOURIKAS

[1]Sustainable Energy Research Group, Energy & Climate Change Division, University of Southampton, University Road, Southampton, S017 1BJ, R.Amin@soton.ac.uk

User behaviour is increasingly being seen as the major determinant of 'performance gap' in buildings. This study is using a modern University hall of residence building occupied by a highly heterogeneous student population; here, we would expect to see user behaviour driven performance gap to appear.

The case study building is a newly built, £70 million student hall of residence building complex in Southampton, UK; the complex consists of three individual buildings of varying size that together provide 1104 rooms. A post occupancy evaluation (POE) was undertaken in the building which included an online questionnaire survey and environmental monitoring. The questionnaire, carried out at month 5 of their 9 month stay, asked occupants about the environmental conditions in their room and the use of controls to change their indoor environment. A total of 223 responses were gathered of which approximately 26% were non-UK students. The environmental monitoring was undertaken in 80 student rooms and involved measurements of air temperature and relative humidity for this period.

This paper analyses students' reported use of indoor environmental controls regarding window opening and indoor space heating, and compares their responses to the environmental measurements. The results highlight the diversity in the reported use of the available environmental controls within rooms with similar typological characteristics. The potential reasons for the different levels of user control (as reported) such as climate history and gender are explored. The paper provides insights into the impact of occupant behaviour on the energy performance of the newly built halls of residence.

Keywords: post occupancy evaluation, occupant behaviour, thermal comfort, performance gap

1. INTRODUCTION

Post occupancy evaluation (POE) studies are increasingly being seen as integral to meeting the building design process (Loftness et al. 2011; Menezes et al. 2012; Bordass & Leaman 2005; Meir et al. 2009) by creating a feedback loop based on system performance and user satisfaction and by providing information on how to address the so-called performance gap; the difference between expected and actual energy use. At present, POE studies are not compulsory in the UK and there are no formalised requirements to complete one however in general, the tools employed in such studies include indoor environment monitoring, indoor air quality assessment, plan analysis, walk through surveys, user satisfaction questionnaire, focus group discussions and interview (Meir et al. 2009; Bordass & Leaman 2005).

Broadly speaking, the performance gap can be attributed to three factors; (i) design assumptions and modelling, (ii) construction and build quality and (iii) users (including management) (Menezes et al. 2012). POE studies can provide useful insights not only into which technologies are most effective but how users interact with systems and how this affects functionality and energy use. As Grandclément et al. (2014) indicate, energy use in buildings is socio-technical whereby users take a more active role than merely being passive receivers of design strategies. Given this, it becomes necessary to understand how users interact with the indoor environment and furthermore to address diversity in these interactions and the relevant influencing factors.

1.1 Characteristics impacting indoor temperature preference

At present there are few conclusive results on personal characteristics or traits that significantly impact indoor thermal preference, studies generally suggest that the differences in temperature preference between men and women is marginal and often due to choice of clothing there is some evidence that women display a narrower band of thermal comfort (Karjalainen 2007). That is to say that they feel uncomfortably cold or warm at higher or lower temperatures respectively than their male counterparts (Karjalainen 2007). Further to this, Karjalainen (2007) found that in a residential setting, male participants used thermostats more often than women. While this study alone is not enough to confirm a general difference in temperature preference between genders it indicates that this may be a significant characteristic in understanding individuals' indoor environment preferences.

1.2 Thermal adaptation

A key driving force for user behaviour in the indoor environment is to achieve comfort. Adaptive thermal comfort theory states that people take actions to restore their thermal comfort such that they are able to compensate for changes in their thermal environment (Nicol et al. 2012). The theory also appreciates that neutral temperatures are likely to be influenced by recently experienced climate conditions and that occupants are more likely to achieve comfort when they have control over their local environment. Based on adaptive comfort, thermal sensation depends on outdoor climate and the expectations it creates about the indoor environment (Humphreys 1978). The thermal adaptive mechanisms can be distinguished into three categories (de Dear & Brager 1998):

a) *Behavioural* – Behavioural adjustments include actions that aim to improve the indoor climate or the thermal state of the body and can be personal (e.g. clothing and posture changes, activity, moving to different locations), technological (e.g. opening/closing windows or blinds, controlling fans or HVAC systems) or cultural (e.g. schedule adjustments or dress code).
b) *Physiological* – Physiological adaptation includes all the physiological changes that result from the exposure to climate and that lead to greater tolerance towards the climatic conditions.
c) *Psychological* – Psychological adaptation refers to changed perception due to past experience. Having lower indoor climate expectations results in occupants having greater tolerance to temperature fluctuations.

It is clear that past experiences and exposure to a specific climate can impact occupant behaviour. Students in the UK come from various locations around the world having experienced very different climatic conditions. Their diverse thermal and cultural history could have an impact on their adaptive behaviour when they move into UK halls of residence.

This study aims to examine the level of diversity in use of indoor environmental controls and subsequent impact on use of energy for heating and to explore factors which may be influencing this, namely gender and climate history. This will be done using a case study building; Southampton University's newly built Mayflower halls of residence complex, which was completed in the summer of 2014 and first occupied in September of the same year.

1.3 Mayflower Halls of Residence case study

The complex is comprised of 3 separate buildings providing a total of 1104 rooms; Figure 44 shows a general plan of the three buildings and their orientation on the left and Figure 45 shows a thermal image of the south east façade taken in March 2015. The majority of rooms are single, ensuite rooms with shared kitchen/living room area where the number of rooms per flat varies; a small number of accommodation rooms are studio flats. The complex is naturally ventilated with individual heating controls in each room (1 to 5 dial on radiator) and top opening tilt-windows. As part of the planning conditions, this building is required to undertake a POE within one year of occupation; some of the results from the POE are used in this study.

Figure 45 shows a thermal image of the south east facade, as indicated in Figure 44, taken in March 2015. The image was taken before sunrise so as to eliminate the influence of solar radiation on the results. The ambient temperature at the time the image was taken was 5°C. As can be seen in the figure, there is significant heat loss from the open windows with rooms displaying varying degrees of window opening; some close, some fully open and some partially open. This shows a variable use of indoor environmental controls, in this case window use pattern which as various authors have indicated (Gill et al. 2010; Bonte et al. 2014) can have implications for buildings energy performance. This paper further investigates the variability in window opening and heater use behaviour of students through questionnaires and indoor environmental measurements.
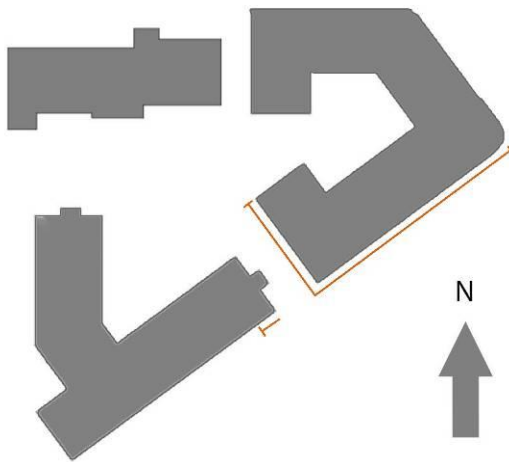
Figure 44 Schematic diagram of the layout of Mayflower halls of residence complex. The orange lines highlight the south east façade shown in Figure 45.
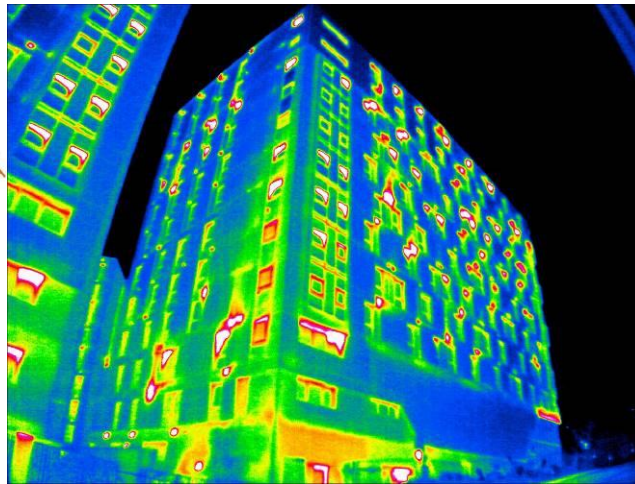
Figure 45 Thermal image of south east facade of Mayflower halls of residence as highlighted in Figure 44

The following two sections of this paper (Methodology and Results) will be divided into two sections where Part 1 uses the results from an online POE questionnaire to understand diversity in use of indoor environmental controls and Part 2 considers monitoring of temperature and humidity in conjunction with the same questionnaire to investigate in more detail and with a smaller sample, indoor air temperature and factors which may determine this.

2. METHODOLOGY

2.1 Part 1

An online post occupancy evaluation questionnaire was sent by email to 955 (out of a total 1029) residents of Mayflower Halls of Residence in March 2015 using the University of Southampton's iSurvey software. The online survey, approved by the local ethics review committee, consisted of questions relating to the occupants level of satisfaction with the building in general, their opinion on the indoor environmental conditions in their bedroom, use of indoor environmental controls such as heating, window opening, curtains and artificial lighting and some details about them. This resulted in 223 complete questionnaires returned representing a response rate of 22%.

2.2 Part 2

Temperature and relative humidity data loggers (MadgeTech RHTemp101A) were placed in 78 rooms in Mayflower Halls in November 2014; these 78 participants were not included in the online POE survey outlined in Section 2.1. Rooms were selected based on position in the building complex so as to provide a representative sample taking account of floor level and orientation in all 3 buildings of the complex and were placed with the permission of the occupant. These 78 rooms were then contacted in May 2015 in order to carry out a questionnaire and to arrange collection of the data loggers; this questionnaire was largely identical to the online POE survey outlined in the previous section (Section 2.1). The data loggers were programmed to record measurements of temperature and relative humidity every 5 minutes and were placed in one of two positions in each room depending on layout of the room and ease of access. The locations were chosen such that they remain out of direct solar radiation and to cause as little disruption to the occupants as possible. Of the 78 rooms with data loggers, 30 residents responded and took part in the questionnaire resulting in 30 complete questionnaires with corresponding temperature and humidity data for the 5 previous months.

3 RESULTS & DISCUSSION

3.1 Part 1

Of the 223 respondents to the online survey, 123 (55%) were female, 96 (43%) were male and 4 (2%) unknown. The age of respondents ranged from 18 to 52 with 139 (62%) being 18-19, 61 (27%) being 20- 24 and 21 (9%) being 25 or over; 2 respondents' (1%) ages are unknown. The number of hours reportedly spent in the bedroom (i.e. their private space) including sleeping time on a typical weekday and typical weekend day are shown in Figure 46. This indicates a highly irregular occupancy profile by comparison to office buildings or households with some respondents reporting spending less than 5 hours in their bedroom and others reporting 23 hours; this represents a standard deviation (σ) of 3.1. It is possible that some of the very low responses were due to a misunderstanding of the question on the part of the participants such that sleeping time was not included in their response despite the question stating that it should be. Greater variation in number of hours spent in the bedroom is evident on a typical weekend day with responses varying from 0 to 24 and a standard deviation (σ) of 4.6. Observing such variation in number of occupancy hours indicates clearly how unique this type of building is where it would be unrealistic to hold it to any of the existing occupancy profiles for residential buildings where occupancy hours are taken to be in the region of 13 hours for a working couple or 20 hours for a retired couple (Martinaitis et al. 2015) as shown in Figure 46. This in part may be due to the mixed use of such buildings where bedrooms serve also as studies and social spaces and where students' lecture schedules vary greatly.
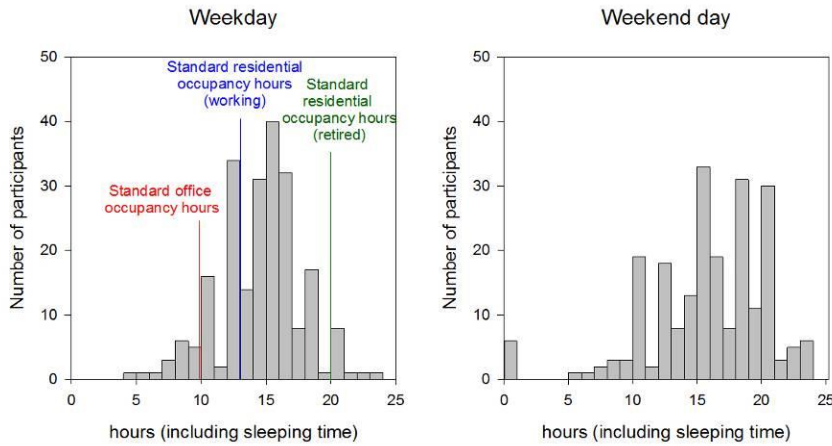
Figure 46 Histogram showing reported number of hours spent in the bedroom (including sleeping time) by residents of Mayflower halls of residence complex. Also shown are some typical values for number of occupancy hours (CIBSE 1998) for office buildings (red) and for two typical residential scenarios, working (blue) and retired occupants (green) (Martinaitis et al. 2015)

Responses to questions on the use of indoor environmental controls, specifically use of heater, window opening and use of curtains show diversity in the behaviour of occupants. Use of the heater shows a relatively even spread across the categories with a majority reporting using the heating controls less than once per month ("never"); this does not, however, specify whether the heating is left on or off for most of the time. Respondents demonstrated a high rate of window opening and curtain use with 76% and 77% respectively reporting using these controls either daily ("often") or more than once a day ("frequently"). As with use of heating controls it is not specified whether those reporting opening windows or curtains less than once per month have these controls open or closed for the majority of the time.

When the use of controls are considered by gender, male participants reported using both windows and curtains more than once a day ("frequently") significantly more than female respondents. In the case of curtain use, this was 47% for males and 33% for females and for windows, 50% for males and 37% for females. In both cases, females have a higher representation for the next category representing use of these control daily ("often"). By contrast, male respondents report using their heating controls less than once per month ("never") more than female respondents (40% and 25% respectively) with female respondents carrying a higher percentage in categories representing more frequent use of heating controls. However, these differences, shown in Figure 47, are small and could imply that factors other than gender play a more significant role in determining behaviour with respect to indoor environmental controls e.g. familiarity with type of heating system or control regime in previous residence.

Figure 47 Occupants' reported use of indoor environmental controls for heating, window opening and curtains classified by gender where "never" is less than once per month, "rarely" is once per week, "sometimes" is 1-2 times per week, "often" is daily and "frequently" is more than once per day

Finally, the use of controls were examined with respect to previously experienced climate; in this instance, participants were asked which city they had mostly been living in for the two years prior to moving into the case study building. These responses were then broadly grouped into "cool/cold" (Category A) or "warm/hot" (Category B) climates based on the Köppen- Geiger climate classification

system (Kottek et al. 2006) where Category A climates were taken to be any warm temperate, snow or polar climates with corresponding cool, cold or polar temperature classification based on winter temperatures. All others were considered to be Category B climates. In all cases the category was decided based primarily on the average winter temperatures. The aim of this system of classification is to group participants into those who have regularly experienced winter as cold as or colder than the average UK winter and those who have not. Use of indoor environmental controls were then considered with respect to this parameter; since there were significantly more responses from Category B climates (174) than Category A climates (46), the use of indoor environmental controls are considered by percentage rather than absolute number (Figure 48). It is observed that those from Category A climates report higher use of curtains and windows with higher percentages reporting both daily and more than once a day and lower use of heating controls.
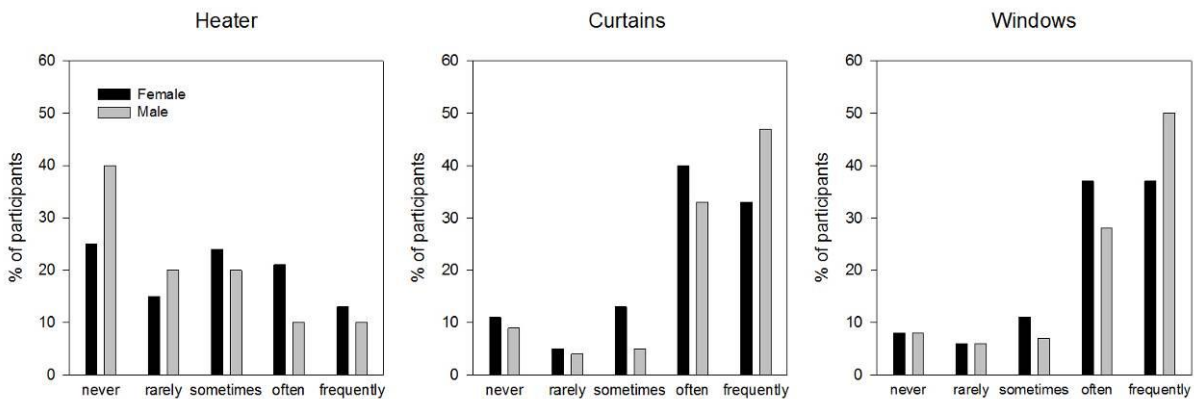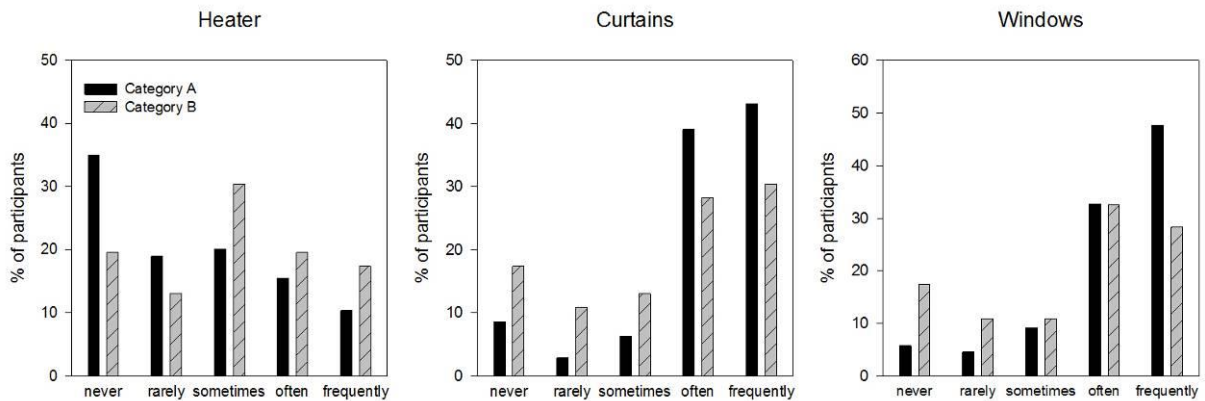

Figure 48 Occupants' reported use of indoor environmental controls for heating, window opening and curtains classified by climate prior to moving to the case study building where "never" is less than once per month, "rarely" is once per week, "sometimes" is 1-2 times per week, "often" is daily and "frequently" is more than once per day. Category A refers to "cool/cold" climates and Category B to "warm/hot" climates.

In order to understand in greater detail how use of indoor environmental controls affects overall satisfaction the indoor environment the use of controls is shown along with answers to one of the online POE questions regarding how occupants would describe the temperature in their rooms during the winter. It can be observed first that majority (56%) of the residents feel that the temperature is satisfactory or ok and there are more residents reported being too warm (8%) than too cold (2%). Responses indicating slightly too warm or too cold are similar in number at 18% and 15% respectively. Considering heater use, it is interesting to note that those who report being satisfied with the indoor temperature in their bedroom show a relatively even spread across all categories of heater use which implies the importance of being able to control the indoor environment for satisfaction and comfort. Furthermore, those that report feeling too warm or a bit too warm are strongly represented in the category of never using the heater and frequently using the windows which implies adaptive comfort behaviours despite not being entirely satisfied with the temperature conditions. However it is unclear at this stage whether or not these adaptations can be said to be effective since the circumstances under which each type of action is taken is not stated.
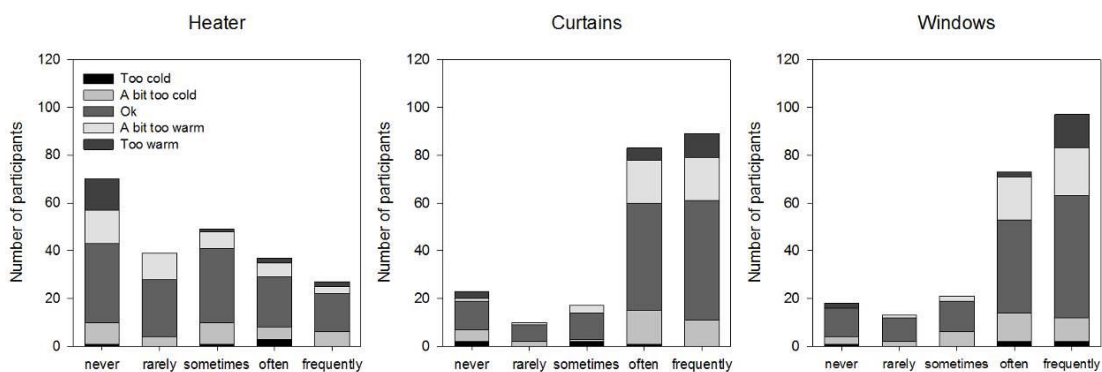
Figure 49 Stacked bar chart showing occupant's reported use of indoor environmental controls categorised by occupants' general description of indoor temperature during the winter

3.2 Part 2

Monitored data of temperature and relative humidity at 5 minute intervals was collected from December 2014 to May 2015 in 30 rooms of Mayflower Halls alongside the same questionnaire used in Section 3.1 relating to use of indoor environmental controls. The results showed average indoor temperatures varying from 19°C to 29°C, with minimum and maximum temperatures reaching 12.4°C and 32.9°C respectively. Since a certain degree of variation is expected over the year due to seasonal weather changes, a shorter period of time, the month of February 2015, was considered. This month was chosen since it is in the heating season and during academic term time so the student residents would be occupying the buildings. It was observed that mean indoor temperature ranged from 19°C to 32°C where the standard deviation (σ) of these means is 2.4. Figure 50 shows the air temperature distribution of these 30 rooms for February 2015 where the box plots represent the 10th, 25th, 75th 90th percentiles and median, the red line represent the mean and the outliers are shown by the grey circles. It can be seen that while the majority of the samples presented here have mean values that lie within the recommended indoor temperature range for heating, taken from EN 15251 (BSI 2007), they all have values outside this range as depicted by the grey dots. This has implications for the design process since it is likely that mean values of indoor temperature are used in energy models and it is evident that these may not lead to acceptable indoor temperatures at all times which could lead to negative feedback at the POE stage. Interestingly, as seen in Figure 49, students' general feedback on their room's temperature is positive, which means that the range of room temperatures for this diverse population is acceptable overall.
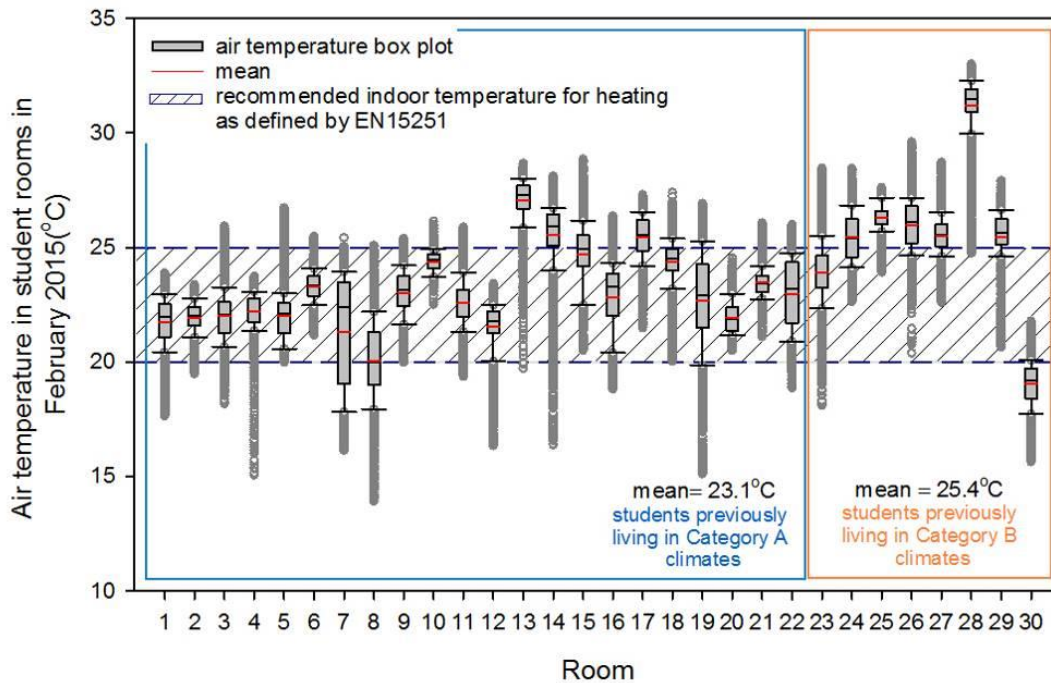
Figure 50 Boxplot of air temperature in 30 monitored rooms of Mayflower Halls of residence for February 2014 where the 10th, 25th, 75th, 90th percentiles and median are shown in the boxplot. The red line represented the mean and outliers are showing by the grey circles; students previously living in Category A (cool/cold) climates are shown in the blue box and Category B (warm/hot) climates are shown in the orange box. The shaded area represents the recommended indoor temperature for energy calculations taken from BS EN 15251:2007 (BSI 2007)

Also highlighted in Figure 50 are the participants in the sample who, for the two years prior to moving to the case study building, have been living in Category A (cool/cold climates) and those who have been living in (warm/hot) climates, as defined in Section 3.1. It can be seen that the meant air temperature between the two groups differs by over 2°C where those from Category B climates have a mean of 25.4°C compared to 23.1°C for those previously living in Category A climates. This difference is significant in the climate of Southern England, where the case study is situated, since the typical annual temperature is 10°C compared to the typical heating set point of 21°C meaning that a 1°C temperature difference can represent approximately 10% of the annual heating load. It is also observed that 7 of the 8 (88%) participants from Category B climates had mean indoor temperatures outside the recommended range for heating compared to 14% of the participants from Category A climates. Additionally, the participants were asked to rank their overall perception of the temperature conditions in their bedroom

during the winter where the response options were: Too cold (-2), A bit too cold (-1), Ok (0), A bit too warm (1) or Too warm (2). It is interesting to note that the average for the participants from Category A climates was 0.2, indicating that on average, these residents feel slightly warm and for the Category B participants, the average was -0.4 which implies that despite having a higher average indoor temperature, residents from warmer climates still report feeling slightly cool in the building. These responses are plotted against mean indoor temperature in Figure 51.

Considering then the cases where the mean value lies above the recommended range, it is interesting that only one participant (Room 26) answered "Too hot" when asked to describe the indoor temperature during the winter. Perhaps more notable however, is that 3 of the 7 Category B participants (Rooms 27, 28 and 29) whose mean temperature is outside the recommended range all reported being either too cold or a bit too cold despite having average temperatures over 25°C with one (Room 28) having an extremely high average of 31°C. By contrast, the three participants from Category A climates whose mean values were above the recommended range all responded 'Ok' when asked about the temperature conditions in their rooms. This implies that while on paper, these indoor temperature would be considered unacceptably high, in this instance, they are satisfactory for the occupant. This is further highlighted by Figure 51 where there is a cluster of Category B points in the bottom left indicating higher temperatures but with participants describing their thermal environment as cool. Conversely, there is a cluster of Category B points in the top left indicating residents from cooler climates feeling warmer at lower temperatures. Thus, it seems that the diversity in temperature preference may not be sufficiently well catered for given that many residents have expectations and adaptations that are significantly different than those catered for in the relevant building standards; this could affect the buildings energy performance thereby demonstrating user driven performance gap.
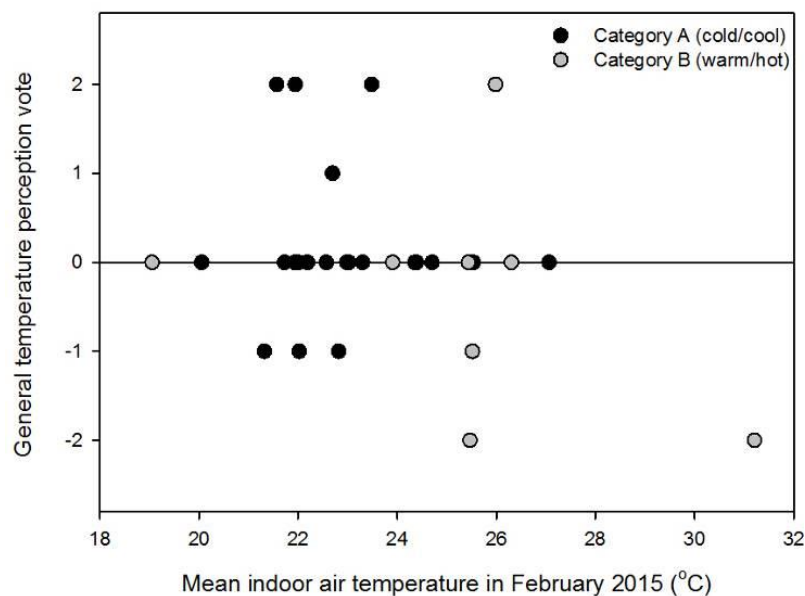
Figure 51 Plot of overall temperature preference vote for the winter against mean indoor temperature for February 2015 where -2 is Too cold, -1 is A bit too cold, 0 is ok, 1 is A bit too warm and 2 is Too warm on the y axis

4 CONCLUSION

In this paper, results from on an online POE study of a newly built halls of residence complex were used to examine the level of diversity in how occupants of a relatively uniform building complex use the indoor environmental controls available to them. While it is likely that some of this variation is due to differences in the conditions in the rooms due to orientation and floor level it is possible that there are other influencing factors at play. Some of these, like level of proactivity in addressing thermal discomfort which is largely a personality trait, are hard to address and impossible to predict. However, differences observed in use of controls by occupants from Category B climates indicate that there are factors relating to long term thermal history, previous experience of indoor environments and perhaps cultural practices that are driving behaviour. While this initial study does not draw any generalisations, should it be more fully understood, this type of parameter has the potential to be included, in some capacity in the design process either as an input at the design stage or as part of a post occupancy, 'soft-landings' approach.

The second part of this study used monitored air temperature measurements for February 2015 along with questionnaire results to investigate variation in indoor temperatures in 30 rooms of the case study building complex. Mean temperatures ranged from 19°C to 31°C with a standard deviation (σ) of 2.4. While indoor temperatures cannot be expected to be uniform throughout a building like this where there are many influencing factors both in building design and occupant preferences, this large range is striking. The mean values of temperature are also noteworthy when considered with respect to the recommended indoor temperature range (20°C -25°C) where it was found that almost all the mean values that lay above this range were of rooms where the occupant had, for the two years prior to living in the case study building had been living in a warm or hot climate and furthermore, that some of these occupants reported finding the temperature in their room generally too cold (or a bit too cold). . While the sample sizes presented here are too small to form generalisations this presents an interesting question of whether or not buildings designed for UK standards are able to meet the comfort needs of international residents and moreover how this can be addressed in the future. It is also expected that over time, residents from differing climates are likely to adapt to the thermal conditions in their new environment however since this study has only considered one month in the year (February 2015) and the residents would have moved in four months prior (October 2014), it is not possible to say how much (if at all) of this adaptation has taken place. Further work will need to be done in the earlier months of residents' occupancy in order to investigate this lag in adaptation time. This is of particular interest in this case due to the unique nature of the building where, for the most part, there is a new set of occupants each year and thus this time lag could have significant implications for overall energy performance.

Further research is necessary to understand how best to address the issues of varying preferences and behaviour based on climate history however it raises some interesting questions on how best to develop inclusive management and design strategies to account for significantly different indoor temperature preferences. Perhaps, for example, in situations where it is expected that there will be residents with diverse climate histories (like the case study used in this paper) it may be possible to design specifically for multiple indoor climates such that the entire building is not designed for a homogenous population. Alternatively, in cases of existing buildings it may be possible to place occupants who are likely to have higher temperature preferences in parts of the buildings where there is high solar gain and perhaps is known to overheat by UK standards thereby optimising the characteristics to the building to suit the specific needs of the occupants.

5. REFERENCES

BONTE, M., Thellier, F. & Lartigue, B., 2014. Impact of occupant's actions on energy building performance and thermal sensation. Energy and Buildings, 76, pp.219–227.

BORDASS, B. & Leaman, A., 2005. Making feedback and post-occupancy evaluation routine 1: A portfolio of feedback techniques. Building Research & Information, 33(4), pp.347–352.

BSI, 2007. Indoor environmental input parameters for design and assessment of energy performance of buildings addressing indoor air quality, thermal environment, lighting and acoustics,

CIBSE, 1998. Building energy and environmental modelling, Applications Manual AM11.

DE DEAr, R. & Brager, G.S., 1998. Developing an adaptive model of thermal comfort and preference. Center for the Built Environment.

GILL, Z.M. et al., 2010. Low-energy dwellings: the contribution of behaviours to actual performance. Building Research & Information, 38(5), pp.491–508.

GRANDCLÉMENT, C., Karvonen, A. & Guy, S., 2014. Negotiating comfort in low energy housing: The politics of intermediation. Energy Policy.

HUMPHREYS, M.A., 1978. Outdoor temperatures and comfort indoors. Batiment International, Building Research and Practice, 6(2), p.92.

KARJALAINEN, S., 2007. Gender differences in thermal comfort and use of thermostats in everyday thermal environments. Building and Environment, 42(4), pp.1594–1603.

KOTTEK, M. et al., 2006. World Map of the Köppen-Geiger climate classification updated. Meteorologische Zeitschrift, 15(3), pp.259–263.

LOFTNESS, V. et al., 2011. The value of post-occupancy evaluation for building occupants and facility managers. Intelligent Buildings International.

MARTINAITIS, V. et al., 2015. Importance of occupancy information when simulating energy demand of energy efficient house: A Case study. Energy and Buildings, 101, pp.64–75.

MEIR, I.A. et al., 2009. Post-Occupancy Evaluation: An Inevitable Step Toward Sustainability. Advances in Building Energy Research, 3(1), pp.189–219.

MENEZES, A.C. et al., 2012. Predicted vs. actual energy performance of non-domestic buildings: Using post-occupancy evaluation data to reduce the performance gap. Applied Energy, 97, pp.355–364.

NICOL, F., Humphreys, M. & Roaf, S., 2012. Adaptive Thermal Comfort, Routledge.

115: A post-occupancy case study on the relationship between domestic energy use and occupancy profiles

SOPHIE NAYLOR[1], MARK GILLOTT[1], EDWARD COOPER[1]

Department of Architecture and Built Environment, Faculty of Engineering, University of Nottingham,
1Corresponding author - laxsjn@nottingham.ac.uk

This study covers the analysis of occupancy and energy use data collected from a live housing project in Nottingham, UK. Post occupancy evaluation/monitoring in buildings has been established to be of great importance, but implementation levels are generally low. Broader uptake of monitoring systems will increase understanding of buildings in use, allowing improved responsive building controls and future design feedback.

The analysis covered assesses: how closely domestic energy uses currently relate to inferred occupancy, whether wasteful energy behaviours can be identified between occupants in similar buildings, how these wastes might be addressed and how effectively occupancy/behaviour can be quantified using a simple and non-intrusive sensor system. Data was gathered from an existing energy platform recording space heating, water use and circuit-level electrical use in 8 high-environmental-performance houses. Occupancy was detected via two motion sensors present in each house, one per major floor. Two houses were equipped with CO_2 sensors, allowing for more detailed analysis on a limited subset of the data. Data fidelity issues caused by backup at the data logger necessitated processing of the data prior to further analysis.

The results of the study show high variation in sensor response to occupancy despite the similarity between tested buildings. True occupancy levels and behaviours thus cannot be reliably inferred from simple sensor data alone, highlighting the need for a greater depth of information gathering in order to fully sense building context for the purpose of control or detailed analysis. While the relationship between domestic electrical energy use and occupancy rates is confirmed, it is difficult to prove from the data gathered whether all energy used provides utility to the occupant. Heating behaviours across unoccupied houses show approx. 14kWh per day difference, suggesting the significant impact of occupant control and behaviour in the home.

Keywords: occupancy, energy profiles, monitoring, performance, domestic

1. INTRODUCTION

Post occupancy evaluation/monitoring in buildings has widely been established to be of great importance to understanding and improvement of the built environment. However, uptake of data collection in working buildings is typically low, leading to a significant lack of information sources in this field (Lowe and Oreszczyn, 2008). In particular, the influence of building occupancy and user behaviour on energy usage has been identified as a source of uncertainty in current understanding of operational buildings (Menezes et al., 2012) and yet is rarely directly monitored. Broader uptake of monitoring systems will increase understanding of buildings in use, leading to improved responsive building controls and future design feedback.

In the context of finding affordable, useful monitoring solutions, this study addressed the following key questions:

- How well can domestic occupancy be quantified using motion sensor and CO_2 data when no further context is available?
- How well does domestic energy use relate to occupancy; which energy uses have the closest correlation?
- Can any energy uses consistently be used to add reliability to simple occupancy sensor data?
- Does the behaviour of occupants in different houses cause quantifiable energy waste relative to other houses?

2. DATA SOURCE

2.1 Green Street Project Background

The Green Street housing project is a group of low-energy design residences based in Nottingham, UK. Real-time energy use and basic occupancy data is available from eight houses, labelled A-H for anonymity. The data sources available for the eight houses are shown in Table 0-1. It should be noted that the houses take one of two designs, with A,B,C,D from 'Phase 1' and E,F,G,H from 'Phases 2 & 3'.

Data is collected via wireless sensor nodes, detected by a centralised hub and sent to a central storage point. This allows web access to the data in CSV format and was maintained by a contracted company during the study. However, the nature of the centralised wireless detection caused some issues with data fidelity, discussed below.

Table 0-1 - Occupancy and Energy Data available from the Green Street Project

Information Type	Data Name	Description	Measured Units	Houses Available
Occupancy	Footfall – Downstairs	Number of times the downstairs hallway PIR motion sensor was triggered	Count (whole numbers)	All
	Footfall – Upstairs	Number of times the downstairs hallway PIR motion sensor was triggered	Count (whole numbers)	All
	CO_2	CO_2 concentration in living room	ppm (parts per million)	C, G
Electrical Energy	Main Electric Import	Total electricity imported to house on top of any generated electricity	kWh	All
	Main Electric Export	Total electricity exported from house from generated electricity	kWh	All
	Extraction System/Heat Recovery	Electrical energy used by the house ventilation system	kWh	All
	Hob/Cooker	Electrical energy used by the cooker	kWh	All
	Sockets Downstairs	Phase 1 - 1st Floor and Kitchen, Phase 2&3 – Ground Floor	kWh	All
	Sockets Upstairs	Phase 1 – 2nd Floor, Phase 2&3 – 1st and 2nd Floor	kWh	All
Heating Energy (Gas boiler)	Heating	Energy used in heating the house	m^3 for A, C, D and kWh for B, E-H	All
	Main Gas	Gas used by the boiler for heating and hot water	m^3	All
Water Use	Hot Water	Hot water use in the house	m^3 for A, C, D and kWh for B, E-H	All
	Mains Water	Total water use in the house	m^3	All

2.2 Data Fidelity

Initial visualisation of the data showed several issues with data fidelity, including sensor noise, nonzero readings where zero is expected and extended periods of sensor dropout followed by spikes several orders of magnitude higher than average. The sensor dropout periods were found to be caused by issues with the data logging central hub, meaning all sensors were affected at once. This pattern made it possible to write a script to identify these periods.

The identification script was run on data from House C (all sensors on 5 minute period, CO_2 data also available). A total of 183 dropouts were identified during the period 15/05/2013-06/07/2014. 18 randomly sampled dropouts were manually verified and were found to be correctly identified. It was therefore assumed that the algorithm can detect sensor dropouts accurately.

The shortest dropout periods (one or two 5-minute slots) can be neglected for most analysis. Longer dropouts that delay readings to the next day, week or month can significantly affect observable trends in the data. Gaps larger than five minutes and their peaks were deleted from the data, to ensure that only valid measured data was used for analysis.

3. INFERRAL OF BUILDING OCCUPANCY

Occupancy rates in buildings can be inferred in a large number of ways, including through motion/PIR sensors (Bruckner and Velik, 2010), local CO_2 level, occupant tagging (Li et al., 2012) etc. PIR alone does not provide a perfect estimation of occupancy, both for absence/presence and number of people (Naghiyev et al., 2014). Combining multiple sensor types to improve accuracy and reliability is a common route (Dong et al., 2010; Ebadat et al., 2013; Lam et al., 2009; Yang et al., 2012), but requires some verified 'ground truth' data, often manually collected through physical observation, in order to train a model of how the sensor readings combine in relation to different occupancy states. In this study, it was investigated whether CO_2 could be used to provide any further context to the Green Street data in the absence of ground truth data.

3.1 CO_2-PIR Correlation

The first stage of analysis was to examine any patterns occurring in the PIR and CO_2 data over time. Figure 3-1, lower graph, shows a sample week for House C. The correlation between CO_2 and PIR readings in House C follows a visible pattern: the greatest daily peak in PIR readings corresponds to the greatest daily peak in CO_2, with a delay of 0-2 hours. The delay in response time of CO_2 sensors is possibly due to the time required for CO_2 to circulate to the house's single CO_2 sensor. This may explain why the delay is much longer than the 10-20 minutes demonstrated with room-level CO_2 sensing (Naghiyev et al., 2014). The pattern correlation between CO_2 and motion sensor data for House G (Figure 3-2, lower) is less obviously defined, with greater daily variation and the highest motion values not corresponding to the highest CO_2 levels. This may be due to the higher variation in daily cycle of occupancy in this house, with occupants having no particular peak to daily activity levels.

Without some ground truth data to provide context, it is impossible to accurately tell how many people are present from limited PIR and CO_2 data. It may be possible to use the CO_2 to strengthen the PIR's reliability and infer occupancy levels, although this cannot be reliably verified without known accurate occupancy measurement for at least some period of time in order to train a model.

3.2 Binary Occupancy

Given the difficulties found in inferring the number of people, the next stage of investigation covered using PIR and CO_2 data to infer binary occupancy – simply whether occupants are present or not at any given time. Once again, it is not possible to verify without true occupancy data, but an estimate of effectiveness can be made by visual inspection and comparison of different methods' correlation to energy use. Various assumptions were applied to allow binary occupancy to be estimated by varying PIR and CO_2 levels:

The assumptions for PIR were:

- Non-zero or non-background values of motion sensor count for upstairs or downstairs denotes house occupancy;
- Zero/background motion sensor values for both upstairs and downstairs denote occupant absence.

The assumptions for three methods of classifying binary occupancy through CO_2:

1. Occupancy is assumed when CO_2 is above a certain threshold – in this case above the mean value over the observed period (519ppm for House C and 597ppm for G).
2. Occupancy is assumed when current CO_2 is higher than the mean over the previous 30 minutes.
3. Occupancy is assumed when the mean CO_2 over the last 10 minutes is higher than the mean over the previous 1 hour – this should reduce the effect of minor variations caused by noise.

Figure 3-1 and Figure 3-2 (upper) show binary occupancy assumed either when both sensors indicate occupancy ('AND' rule), or when either sensor indicates occupancy ('OR' rule). Use of 'AND' increases certainty that the presence reading is true, but is more likely to miss occupants (false negative readings). 'OR' ensures occupants are missed less often, but may be more likely to indicate occupancy even when people are not present (false positive readings). Depending on the application, either of these systems could be more beneficial. For example, when applied to controls, the 'AND' rule will save more energy, while the 'OR' rule will ensure more consistent occupant comfort.

It can be seen in Figure 3-1 that binary occupancy assumption in House C shows significant noise, and does not produce clearly defined patterns. This may be due to the influence of standing background noise on the PIR sensor, despite efforts to reduce noise in calculation. House G (Figure 3-2) shows more clearly defined patterns. Both houses, however, show a somewhat consistent pattern of 'non-occupancy' centred around midnight. Here it is important to note that occupants are likely actually in the house, but not picked up due to their lack of motion and CO_2 in the living spaces while sleeping in the bedrooms. CO_2 sensors placed in each room may allow for sleeping periods to be defined from true absences.
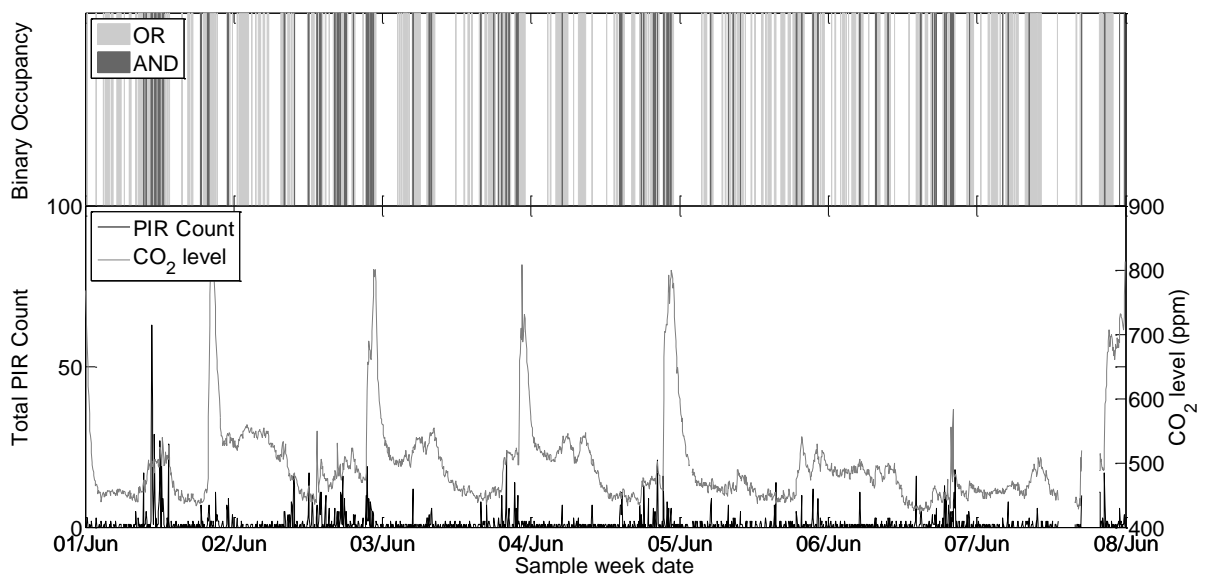
Figure 3-1 - House C. Raw data vs. Binary Occupancy Assumption
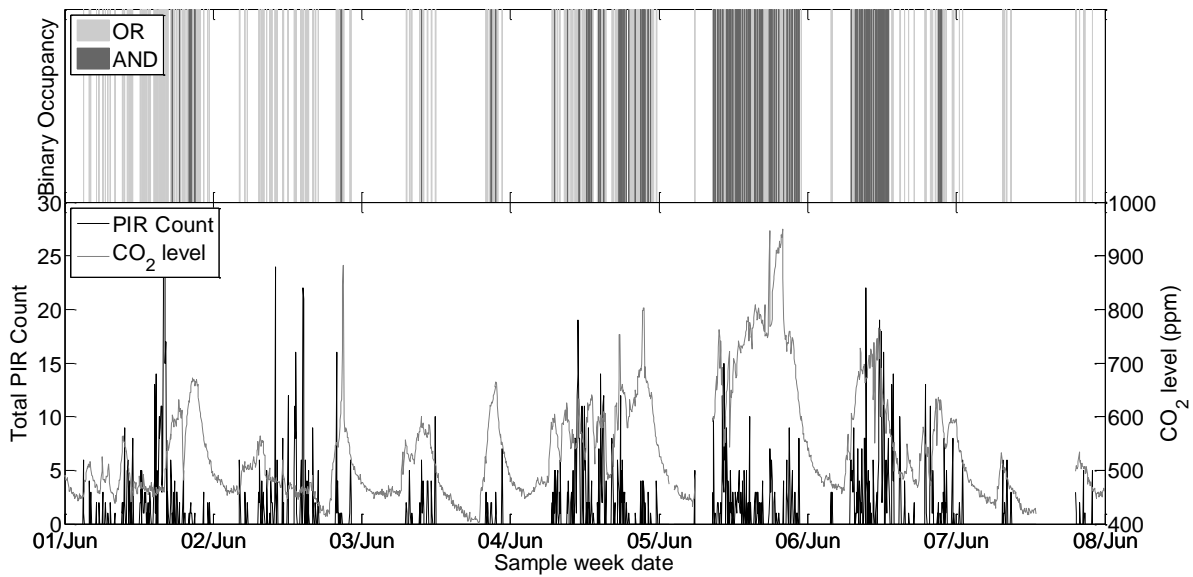
Figure 3-2 - House G. Raw data vs. Binary Occupancy Assumption

4   CORRELATION OF OCCUPANCY AND ENERGY

4.1 CO$_2$/PIR Magnitude and Energy

This section investigates whether greater levels of occupancy/activity consistently relate to greater energy use, which allows estimation of where energy is being used directly by the occupants (stronger correlation) and identification of potential energy wastes (weaker correlation) for further exploration.

From

Figure 4-1 it can be seen that on a daily level, a positive correlation between detected occupancy and electricity demand exists: higher demands occur on days with higher total motion counts. On an hourly and 5-minute scale, this correlation becomes less distinct. No correlation at shorter time scales can be observed with other energy uses and has several possible reasons and implications:

- Given that motion and CO$_2$ sensors were centrally located, if the occupant was out of sensor range inside a room and using energy, their presence was not logged until they left the space – this creates a disconnect between short-term occupancy measurement and energy use.
- An occupant does not use all forms of energy in a house at any given time s/he is present, but over a full day is more likely to interact with more forms of energy use.
- Potential energy waste, if true occupant presence is not related to short-term energy use, this implies that energy consumed is not always providing benefit to the occupants.
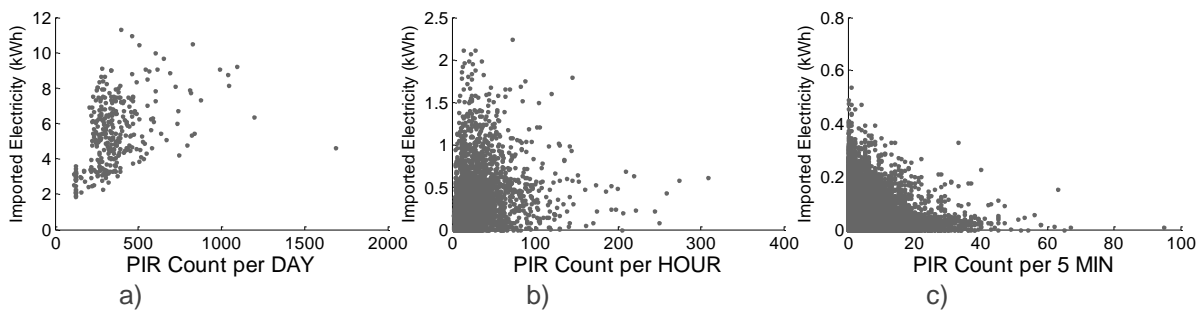
Figure 4-1 - House C. Correlation between Energy and Daily, Hourly and 5 Minute Occupancy measurements

As daily values alone show a defined correlation, these were used to compare the relative relationship of various domestic energy uses to motion count and CO_2 in houses C and G. This was explored both graphically and numerically, although only numerical is included in this paper for brevity.

The graphical analysis showed that the strongest trends in correlating occupancy/energy were linear, allowing a correlation coefficient to be calculated. This is a numerical measure of how closely correlated two variables are: a value close to zero implies no correlation, while a value closer to -1 or 1 implies a strong negative or positive correlation, respectively. In Table 4-1, the coefficients are weighted using the p-value, which helps to eliminate false correlations caused by high variance or statistical outliers. A high p-value implies there is a high probability of the correlation coefficient occurring when no relationship actually exists between the variables, meaning that that correlation coefficient is not reliable and should be weighted towards zero. It should be noted that, in this application, a perfect correlation is not expected for any variables. There will be a high number of zero-energy use readings for all levels of occupancy. This is because an occupant does not use all forms of energy in a house all the time s/he is present, and because most energy uses can depend on other factors, e.g. heating on outside temperatures.

Table 4-1 and Table 4-2 show that the strongest correlations of energy with occupancy are seen for water, hot water, downstairs sockets and electrical import, all of which show an approximately linear positive trend. This has two potential implications:

- Electrical and water consumption depend on the number of people present;
- Electrical and water consumption depend on the length of time the house is occupied during the day.

Without explicit knowledge of the number of people in the house at a given time, it is difficult to confirm which of these implications has the strongest influence.

The weakest correlation in House C is seen in the extractor and upstairs sockets, both of which appear to be independent of occupancy levels. In the case of upstairs sockets, it appears that the building occupants have a small, constant electrical load, but do not often use much more electrical energy upstairs. The correlation with CO_2 and motion was significantly different for the gas and heating use. The reason for this will be further explored in later sections.

All other energy uses show a weak positive relationship with occupancy, suggesting a combination of:

- Dependence on other factors - for example, the energy used by the heating system will heavily depend on outside temperature and so is difficult to relate only to occupancy;
- Energy use without full benefit to the occupant, resulting in wasted energy.

In House G, the average CO_2 level correlates more strongly than the motion count for several energy measurements including electrical import, downstairs socket and cooker use. This house's CO_2 sensor is placed on the same storey as both the kitchen and living room (high electrical and water load), whereas in House C the kitchen is located on a lower storey to the CO_2 sensor. This may explain some of the discrepancy.

Table 4-1 - House C. P-value adjusted Correlation Coefficient between Daily Sensor Measurements

	Cooker	Extract	Gas	Heating	Elec Export	Elec Import	Sockets D	Sockets U	Water	Hot Water
CO_2	0.27	-0.16	0.35	0.29	0.01	0.53	0.45	0.04	0.66	0.54
Total PIR	0.29	-0.01	0.14	0.07	0.12	0.43	0.59	0.01	0.71	0.64
PIR Downstairs	0.31	0.00	0.18	0.11	0.14	0.45	0.59	0.02	0.70	0.67
PIR Upstairs	0.25	-0.01	0.10	0.03	0.09	0.38	0.53	0.01	0.64	0.55

Table 4-2 - House G. P-value adjusted Correlation Coefficient between Daily Sensor Measurements

	Cooker	Extract	Gas	Heating	Elec Export	Elec Import	Sockets D	Sockets U	Water	Hot Water
CO_2	0.41	-0.14	0.47	0.43	-0.24	0.76	0.64	0.09	0.55	0.54

Total PIR	0.09	0.31	0.00	-0.02	0.16	0.37	0.07	0.34	0.70	0.59
PIR Downstairs	0.06	0.23	0.03	0.00	0.13	0.39	0.14	0.25	0.65	0.54
PIR Upstairs	0.10	0.36	-0.03	-0.09	0.16	0.29	0.00	0.40	0.64	0.54

4.2 Simplified Binary

The estimation of binary occupancy set out in section 3.2 was assessed by taking the difference between average energy use when unoccupied and occupied: a greater difference implies a greater correlation of the assumed occupancy to the energy use type. Assumptions made in this assessment included:

- Downstairs sockets are reliant on downstairs PIR only, and upstairs with upstairs PIR.
- The cooker is reliant on downstairs PIR only, assuming that the occupant must be in or near the kitchen to be cooking.

The percentage difference for all occupancy estimation methods is summarised in Figure 4-2 and Figure 4-3. It can be seen that no single method of assuming occupancy consistently correlates best with all forms of energy use. PIR was generally better correlated to water and cooker use, while CO_2 was better correlated to heating. This implies that either:

- The relative location of the motion and CO_2 sensors allows each to detect some activities better than the other. For example, both houses have PIR sensors directly outside the main bathroom and kitchen, meaning that when an occupant travels to this room to use water, the PIR is more likely to sense their presence than the living-room-based CO_2 sensor.
- Outside factors can bias the effectiveness of PIR or CO_2 in certain situations – for example, CO_2 is correlated to heating use much more strongly than PIR. This may be because occupants are more likely to keep windows closed during winter when heating is most required, so conserving high CO_2 levels.

The most consistent strong correlation across methods was found with hot water and cooker use – this is logical as most domestic systems do not allow for these to be operated when the occupant is not directly controlling them.

The least correlation with estimated presence was found with the extractor and upstairs sockets. In particular, the extraction system shows no correlation at all with occupancy. This potentially means that energy is being wasted while the house is not occupied. It should be noted that slow-response systems such as heating/ventilation may need to run when occupants are not there to achieve comfort, but it is unlikely that they are required to run constantly.

The analysis also confirmed that neither PIR or CO_2, nor a combination of both, can be used to perfectly estimate whether occupants are present or away. The 'unoccupied' mean for water and cooker use is not zero, despite the assumption that occupants will not use either if not present in the building. These are 'false negative' occupancy estimations - reading zero occupancy when in reality there are occupants present. As there are only two PIR sensors and one CO_2 sensor per house, this can be explained by people being out of range of the sensors but still present in the house. A possible explanation for this is that both water use and cooking occur in specific rooms, meaning that the occupant might not always trigger the centrally-placed PIR/CO_2 as they are located in a room further away from the sensors.

With the information available it is impossible to prove with this analysis if 'false positives' (reading occupancy when nobody is present) occur, as it might be that occupants are present in the house without actively using any energy.

It should also be noted that the performance of the various binary occupancy measures appears to vary dramatically between houses. It was found that hourly-based-CO2 estimation provided the highest correlation for House C, while instantaneous CO2 was best for House G. This informed the choice of which CO2 estimation was used for the AND/OR combinations. The graphs show that neither AND/OR

provide a greater relationship to energy uses on an individual basis, although the performance of AND/OR over all energy uses is less varied than the individual sensor readings alone, particularly in House G.

The fact that the same sensor setup can have such different successes in two highly similar houses shows how the significant influence user behaviours can have on understanding buildings in use and the robustness of a sensing system. This makes a case for more diverse or physically extensive sensing systems when occupancy is to be fully accounted for in post-occupancy evaluation.
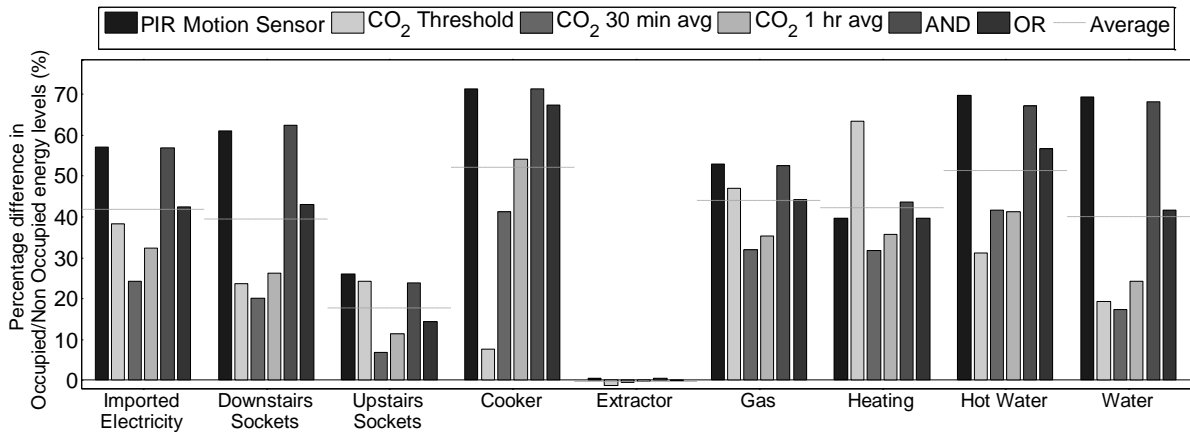
Figure 4-2 - Percentage Increase in Energy Use when Occupied, Comparison of various Occupancy Estimation Methods for House C
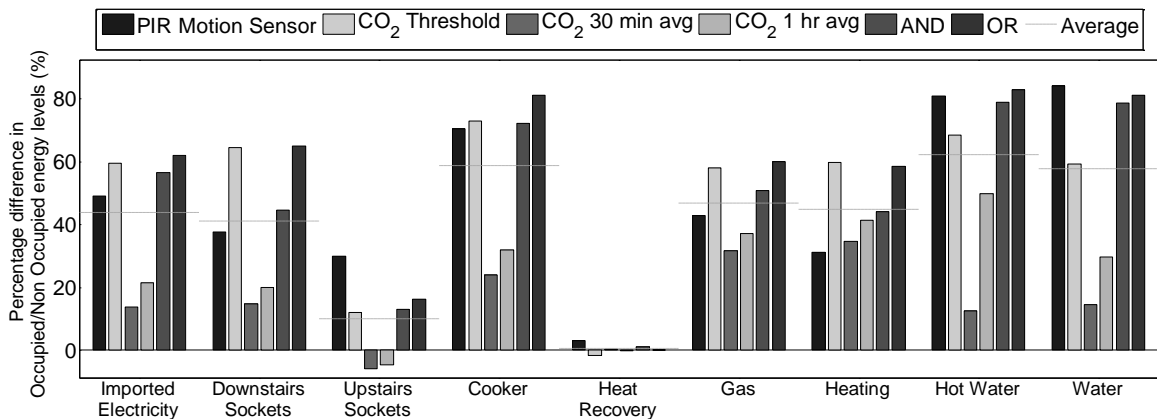
Figure 4-3 - Percentage Increase in Energy Use when Occupied, Comparison of various Occupancy Estimation Methods for House G

5   COMPLEMENTING OCCUPANCY SENSOR DATA

As mentioned above, the highest energy-occupancy correlations found were with water and some small power electrical use. Intuitive analysis shows this to be logical; however, the relationship is not proportional as occupants are not guaranteed to use water or electricity all the time, and the degree of correlation can be variable between houses. These energy uses can thus help to reduce false negatives in occupancy estimation, but cannot guarantee that false positives are caught.

6   BEHAVIOURAL ENERGY WASTES

One instance in which it can be confidently said that the house is not occupied is during extended periods of absence: when the occupants are on holiday, for example.

It must be carefully considered which combinations of parameters denote low or zero occupancy. Given the results discussed in Section 5 of this study, it is assumed that:

- Typical domestic water outlets denote occupant presence;
- If all sensors and meters read zero, the cause is likely dropout and not occupant absence.

Water consumption is therefore used to verify the motion sensor readings denoting extended periods of occupant absence. Two examples of absence during the heating period (October to April) have been identified in houses C and D: 22/12/2013-03/01/2014 for House C and 04/01/2014-12/01/2014 for house D. Thus the impact of different heating behaviours can be investigated.

Figure 6-1and Figure 6-2 show various energy uses over the two identified periods of absence. For each house, the consistent drop in both water/electric use confirms absence over the period, as detailed above. In House C, the motion sensor registered a consistent 1-2 readings throughout the period, suggesting that it can pick up outside movement from its location or is otherwise too sensitive. The extractor is in near-constant operation over the whole absence period – it is not affected by occupancy level, presumaby supplying the same amount of fresh air to house despite the fact that no occupants are present. This strengthens the conclusions made in Section 4. A point of interest in Figure 6-1 is that heating has apparently been turned off during the occupants' absence. This is not an automated behaviour and so must have been manually chosen by the occupants. A slight peak in heating demand can be seen after the off-period, corresponding to the need to heat the house from a lower than typical temperature upon returning.

In House D, a shorter absence period can be seen & verified by water/electricity use. The motion sensor count is zero during absence, unlike House C. The extractor is once again apparently unaffected by whether occupants are inside the house or not.

Heating is also consistent over the absence and the following week: the same amount of energy was used for heating when the occupants are not in the house. In total, $12.92m^3$ of natural gas was used 04/01-12/01 inclusive. Assuming the energy from natural gas is $10.75kWh/m^3$ ("Natural Gas," n.d.) and boiler efficiency 90% (Ebbs, 2011), the heating energy delivered over the 9 day period was 125kWh – nearly 14kWh per day. However, it should be noted that keeping heating on can be beneficial, to keep pipes from freezing, ensure the house is comfortable as soon as the occupants return and eliminate a spike in heating demand when occupants return home.
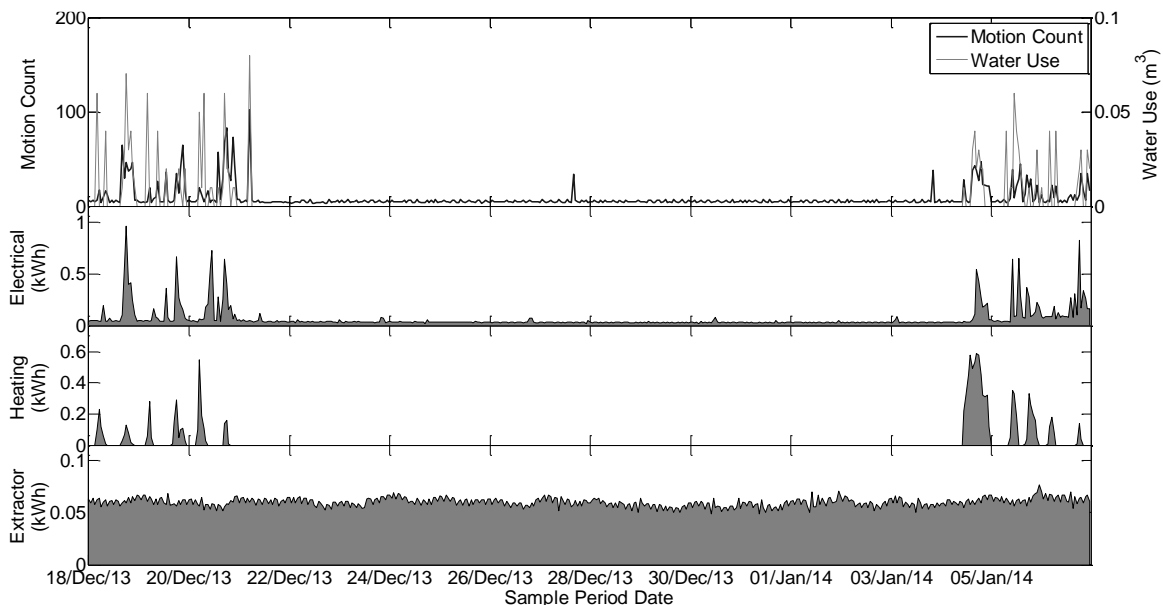
Figure 6-1 - House C, Energy Uses During Occupant Absence
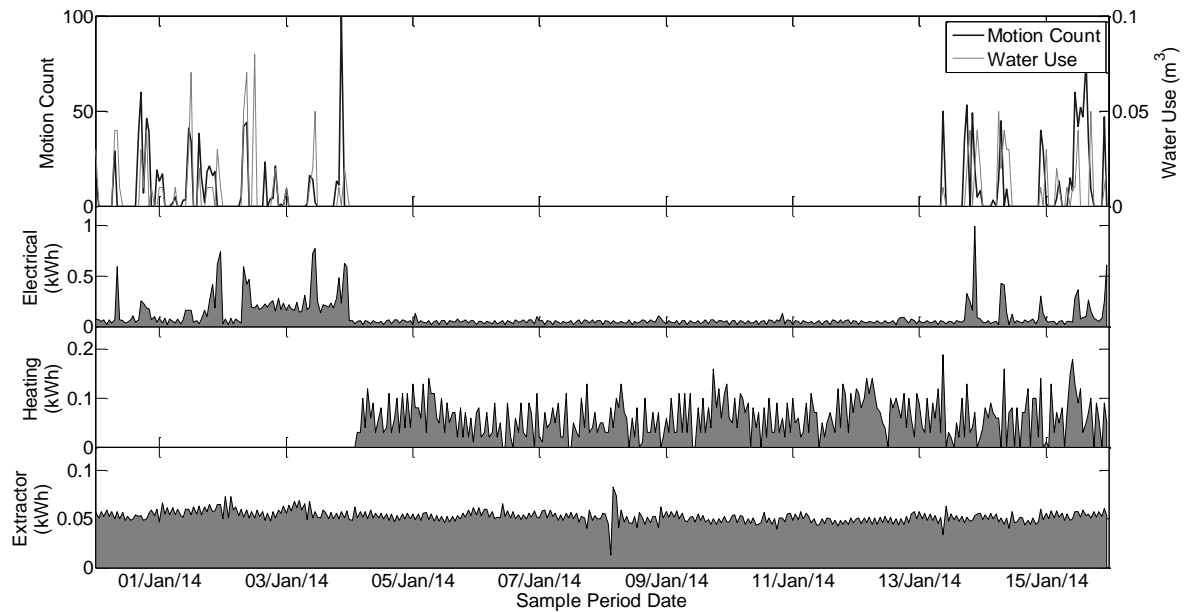
Figure 6-2 - House D, Energy Uses During Occupant Absence

7 CONCLUSIONS

One of the major conclusions to draw from the study of Green Street data is that gaining meaningful, reliable information can be extremely difficult given limited data sources. The PIR and CO_2 data showed some similar trends, but did not agree closely enough to confidently estimate occupancy at a given time. It is also impossible to relate the magnitude of sensor reading to a physical number of people without prior training with known true occupancy rates.

Whole-house occupancy is difficult to relate directly to energy, as presence in the house does not imply that any particular activity must be taking place. It is also impossible to prove that energy being consumed is actually providing utility to the user without context on where the user is at a given time. This makes it difficult to highlight energy waste at any time other than extended periods of absence.

It was found that some measured variables could be used to verify periods of occupant absence over the longer term: a lack of water use over a whole day implies the occupant is not at home. However, this cannot be extended to shorter timescales as it is possible for the occupant to be present for short periods without using water.

It was proven that an occupant's behaviour towards heating control can have a significant impact on the energy used while away for a period of several days. In a study between two Green Street houses, it was shown that approximately 14kWh more energy per day was used on heating an empty home depending on whether the occupants turned off their heating prior to an extended absence during winter 2013/2014.

The study also highlighted that data quality issues can affect what conclusions can be drawn from data analysis. For example, the frequent sensor dropouts can look similar to periods of occupant absence, making it difficult to reliably draw conclusions on changing energy use with occupancy. Issues such as this will be common to many sensing applications, meaning analysis should be designed to be as robust as possible to sensor dropouts, interference etc. It was also found that similar sensor setups had significantly different strengths and weaknesses in similar houses, depending on the different behavioural habits of the occupants. This highlights the need for more high-resolution, context-aware sensing when occupancy is to be fully accounted for in post-occupancy evaluation. It is essential in order to effectively and reliably use building occupancy and energy data to inform building management/controls or future design feedback.

8 ACKNOWLEDGEMENTS

9 REFERENCES

BRUCKNER, D., Velik, R., 2010. Behavior Learning in Dwelling Environments With Hidden Markov Models. IEEE Trans. Ind. Electron. 57, 3653–3660. doi:10.1109/TIE.2010.2045992

DONG, B., Andrews, B., Lam, K.P., Höynck, M., Zhang, R., Chiou, Y.-S., Benitez, D., 2010. An information technology enabled sustainability test-bed (ITEST) for occupancy detection through an environmental sensing network. Energy Build. 42, 1038–1046. doi:10.1016/j.enbuild.2010.01.016

EBADAT, A., Bottegal, G., Varagnolo, D., Wahlberg, B., Johansson, K.H., 2013. Estimation of building occupancy levels through environmental signals deconvolution. ACM Press, pp. 1–8. doi:10.1145/2528282.2528290

EBBS, N., 2011. Environmental Design in Architecture: Delivery of Sustainable Development -- Challenges and Opportunities. Green Street in the Meadows and Nottingham Waterside (Trent Basin).

LAM, K.P., Hoynck, M., Zhang, R., Andrews, B., Chiou, Y.-S., Dong, B., Benitez, D., 2009. Information-theoretic environmental features selection for occupancy detection in open offices, in: Eleventh International IBPSA Conference, Edited by PA Strachan, NJ Kelly and M Kummert. pp. 1460–1467.

LI, N., Calis, G., Becerik-Gerber, B., 2012. Measuring and monitoring occupancy with an RFID based system for demand-driven HVAC operations. Autom. Constr. 24, 89–99. doi:10.1016/j.autcon.2012.02.013

LOWE, R., Oreszczyn, T., 2008. Regulatory standards and barriers to improved performance for housing. Energy Policy 36, 4475–4481. doi:10.1016/j.enpol.2008.09.024

MENEZES, A.C., Cripps, A., Bouchlaghem, D., Buswell, R., 2012. Predicted vs. actual energy performance of non-domestic buildings: Using post-occupancy evaluation data to reduce the performance gap. Appl. Energy 97, 355–364. doi:10.1016/j.apenergy.2011.11.075

NAGHIYEV, E., Gillott, M., Wilson, R., 2014. Three unobtrusive domestic occupancy measurement technologies under qualitative review. Energy Build. 69, 507–514. doi:10.1016/j.enbuild.2013.11.033

Natural Gas [WWW Document], n.d. URL http://www.natural-gas.com.au/about/references.html (accessed 9.17.14).

YANG, Z., Li, N., Becerik-Gerber, B., Orosz, M., 2012. A multi-sensor based occupancy estimation model for supporting demand driven HVAC operations, in: Proceedings of the 2012 Symposium on Simulation for Architecture and Urban Design. p. 2.

475: Investigating the energy performance and indoor environmental quality of a social housing building

AFRODITI SYNNEFA[1], ROSA FRANCESCA DE MASI[2], KONSTANTINA VASSILAKOPOULOU[1], ELENA MASTRAPOSTOLI[1], THEONI KARLESS'[1], MAT SANTAMOURIS[1]

1 National and Kapodistrian University of Athens, Building of Physics - 5, University Campus, 157 84 Athens, Greece, Email: asynnefa@phys.uoa.gr
2 University of Naples Federico II Piazzale Tecchio, 80, 80125 Napoli, Italy

In the framework of the FP7 project HERB: Holistic energy-efficient retrofitting of residential buildings project a 7 story social housing apartment building located in Athens, Greece is being renovated following a holistic energy efficient retrofit process. The retrofit plan includes commercially available technologies like insulation and energy efficient windows, innovative technologies like energy efficient lighting and smart coatings as well as passive techniques like night ventilation, aiming to achieve a reduction in the energy consumption and CO2 emissions by 80% and significant improvement of thermal comfort conditions in the apartments. An experimental campaign is under execution in order to measure and validate the energy savings and indoor comfort conditions before and after the retrofit. In this paper the results of the monitoring prior to the retrofit are reported and analyzed. Measurements include air leakage and thermal imaging for determining leakage rate and heat loss through the fabric of a building, smart meters to record energy consumption and indoor and outdoor environmental measurements (temperature, humidity, light levels, ventilation rate, ambient air temperature and solar radiation levels). Measurement results will be combined with the results of the holistic analysis that has been carried out using dynamic energy modeling in order to determine the optimum retrofit plan.

Keywords: energy efficiency, retrofitting, energy monitoring, building envelope, indoor environmental quality

1. INTRODUCTION

The building industry is a large contributor to CO_2 emissions, with buildings accounting for 40% of the total European energy consumption and 36% of CO_2 emissions in the EU. In order to address climate change the European Commission has set specific targets to be achieved by 2020, known as the 20/20 targets. These targets are to reduce energy consumption by 20%, reduce CO2 emissions by 20% and provide 20% of the total energy share with renewable energy. While new buildings generally need less than three to five litres of heating oil per square meter per year, older buildings consume about 25 litres on average. Some buildings even require up to 60 litres. Currently, about 35% of the EU's buildings are over 50 years old (European Commission, 2015).

Developments in sustainable energy technologies and building management systems have enabled new buildings to meet the European Directive on Energy Performance of Buildings. However, at least 75% of the building stock that will be present in the next 20 to 30 years is already in existence and of this 70-80% is residential. As residential buildings dominate building stock with respect to living space, and have an unfavourable ratio of building envelope compared to the floor area, this type of building has a high specific heating/cooling energy demand, and a significant contribution to greenhouse gas emissions. Therefore, retrofitting of residential buildings represents a major challenge and a holistic solution for retrofitting has the highest potential to transform existing and occupied buildings into energy-efficient buildings, presenting major opportunities for cost-effective investments in efficiency.

In this framework, the FP7 project called "HERB: Holistic energy-efficient retrofitting of residential buildings" aims at the creation of a framework of development, demonstration and dissemination of very innovative and cost-effective energy efficiency technologies for the achievement of very low energy residential buildings through a holistic retrofit process. Technologies envisaged for envelope retrofitting include various types of insulation materials such as Aerobel/aerogel, vacuum insulated panels, smart windows, surface coatings, multi-functional lightweight materials integrated with phase change material for thermal storage and integrated heat recovery panels. Energy efficient solutions will also be deployed including energy efficient lighting using LED and light pipes, energy efficient HVAC, passive heating/cooling, heat pumps integrated with heat recovery and thermal storage, and renewable energy systems based on solar thermal and photovoltaics. The holistic approach and the technologies developed within the HERB project will be applied for the retrofit of different types of residential buildings at seven countries (UK, Italy, Portugal, Greece, Switzerland, Spain and Netherlands). Performance monitoring of the buildings will take place before and after the retrofit and the impact of the retrofit in terms of energy and CO_2 savings, environmental quality and socioeconomic impact will be evaluated. The technologies and buildings retrofitted will be demonstrated to the public.

This paper focuses on the on the work carried out for the Greek retrofit case. More specifically, a 7 story social housing apartment building located in Athens is being renovated following the HERB holistic energy efficient retrofit process. An experimental campaign is under execution in order to measure and validate the energy savings and indoor comfort conditions before and after the retrofit. Measurements include air leakage and thermal imaging for determining leakage rate and heat loss through the fabric of a building, smart meters to record energy consumption and indoor and outdoor environmental measurements (temperature, humidity, light levels, ventilation rate, ambient air temperature and solar radiation levels). The methodology and results of the monitoring prior to the retrofit are analysed. The retrofit plan that resulted from the holistic analysis that has been carried out using dynamic energy modelling is reported and validated by the findings of the experimental investigation.

2. BUILDING DESCRIPTION

The Greek demonstration building is located in Athens at the Municipality of Peristeri, a densely built urban area, approximately 4.5 km from the centre of Athens. It is the 4th largest municipality in Greece with medium low income population and high rates of unemployment. The strong urbanization and the lack of free/green spaces have caused strong UHI effect.

The building consists of two identical semi-detached, 7 story apartment buildings, one of which has been selected for retrofit in the framework of the HERB project. The building has a rectangular shape and the main façade is on north-east exposition. The total building area is around 1'160 m2 with 15 apartments, each of which belongs to a different owner. Each apartment has an area of about 69 m2 and consists

of four main rooms. The bedrooms have windows on the south-west façade, while the kitchen and living room have a window and a glass-door respectively, facing north-east.

The apartment building is made of reinforced concrete and brick walls, without any insulating material and a concrete roof and ceiling. Table 3 describes the representative characteristics of the construction elements and the openings in the majority of the apartments. The maximum U-values according to the Greek Regulation of Energy Performance of Buildings (KENAK, 2010), is 0.50 [W/m2 K] for walls, 0.45 [W/m2 K] for roof an floor and 3.00 [W/m2 K] for windows. Considering these limits, it is clear that all the elements have poor performance and great heat losses due to transmission are expected. The apartments initially had old type windows with wooden frames and single glazing. Most owners have replaced some or all of the windows with aluminium frame with single glazing and one of them with double glazing.
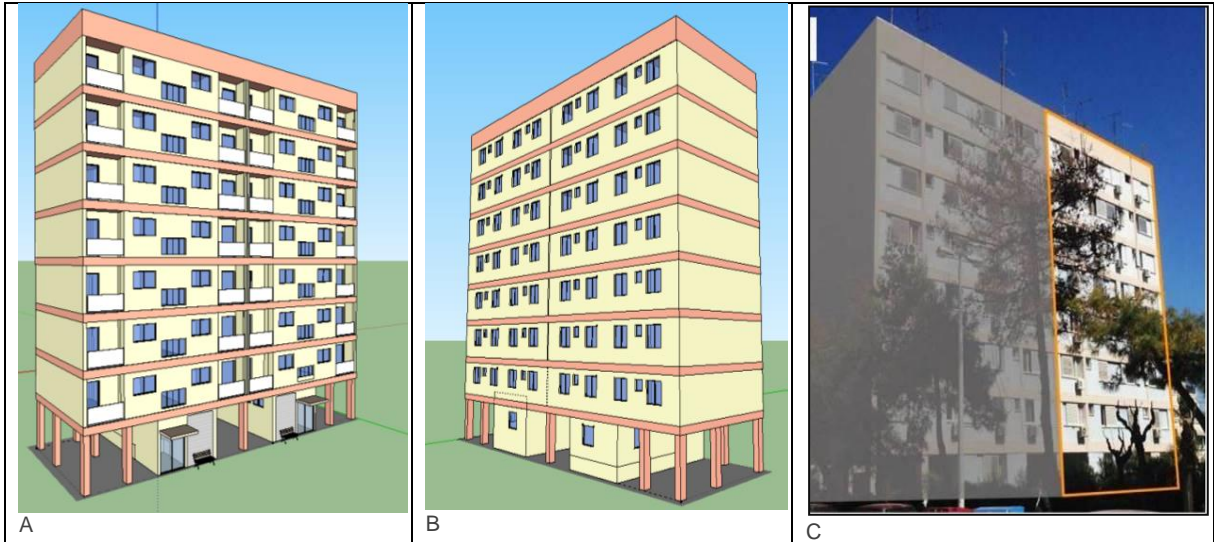
Figure 3: Three dimensional model for architectural front (A) and rear (B) views on SketchUp and rear part of the building SW elevation (C)

Table 4: Thermal characteristics of the building envelope and openings

	External wall	Internal wall	Roof	Floor	Glazing	Frame
Type	reinforced concrete and brick	reinforced concrete and brick	concrete	concrete	Single	Wood/Aluminium
Thickness (mm)	200	150	250	150	6	-
U – value (W/m^2 K)	1.90	2.36	2.45	3.41	5.8	3.633

The apartments are heated by a central oil boiler, without having the opportunity to adjust the interior temperature to the desired levels by an individual control. Since 2013, the central heating has not been used due to the lack of financial resources of the residents. The interventions that some of the owners or tenants have implemented include the installation of air-conditioning units or other heating devices (e.g. portable electric radiators), solar water heaters. Most apartments are lit by domestic type luminaires, housing incandescent or compact fluorescent lamps with a mean power between 4-13 W/m2.

3. EXPERIMENTAL INVESTIGATION

This section describes the methodology and instrumentation used to carry out the monitoring activities in the Greek building. The monitoring is still ongoing. Measurements refer to the period prior to the retrofit.

3.1 Infrared Thermography

The infra-red thermography has been used in order to detect potential problems on the building envelopw (i.e., missing or damaged thermal insulation, thermal bridges, air leakages and vapor condensation). The measurements have been performed during several days representing cold, warm and temperate weather conditions. The temperature difference (indoor-outdoor) was around 5-10°C and

the measurement conditions have been considered almost optimal. The instrumentation used is a Dual View Thermal Imaging Camera IR32 DS.

3.2 Air-Tightness & Ventilation Rates Testing

In order to determine the air tightness, air leakage and ventilation rates of the building three apartments were chosen as they were representative of the conditions prevailing in the building a)one representing low air tightness, with old type wooden frames and single glazing b) one representing medium air tightness, Mixed situation: some old type wooden frames and single glazing and some aluminium frames and double glazing and c) one representing good air tightness with new type aluminium frames and double glazing. Air tightness and ventilation rate measurements have been conducted twice during the experimental period: On the 3rd of July 2014 and on the 15th of September 2014. Air leakage testing has been performed on the 3rd of July 2014.

More specifically, the blower door method was used to estimate the air tightness of the building in accordance with EN 13829 (2001). Air leakage measurements have been performed in collaboration with the University of Nottingham using a novel pulse leakage tester. This is a novel technique is developed at the University of Nottingham which accurately relates a known volume pulse to flow through the building envelope at pressures typically found in infiltration, hence significantly improving on the current steady technique.

To evaluate the indoor air quality under conditions of natural ventilation, the air change rate has been determined through standard tracer gas measurement during the 3rd of July and the 15th of September 2014. The instrumentation used for this measurement consists of the INNOVA 1312 Photoacoustic Multigas Monitor (LumaSense Technologies) connected to the INNOVA 1303 multipoint sampler and doser controlled by a PC on which the INNOVA7620 software is installed. The tracer gas decay method has been used according to ISO12569(2012). The tracer decay method was performed using the following three steps:
1. All possible openings were carefully closed and a quantity of gas was injected into the different rooms in the apartment;
2. A fan was used for creating homogeneity;
3. After restoring the ventilation conditions by opening the windows, the concentration decay was measured.

Moreover, three ventilation scenarios representative of the actual habits of the tenants during both winter and summer have been investigated:
- 1st scenario (SC1): No ventilation: all windows and doors are closed;
- 2nd scenario (SC2): Medium ventilation conditions: some window/s and /or balcony doors are open (usually in one side of the apartment)
- 3rd scenario (SC3): High ventilation conditions: many window/s and /or balcony doors are open (cross ventilation conditions)

3.3 Energy Use

Smart meters have been installed in almost all the apartments. Energy Management Modules (EMM by Ether) have been used; these are electronic devices that record the energy consumption (electricity) and max power of electric energy and the indoor temperature. These gather the data in a portal for remote access in which the monitored values can be elaborated with intervals of 15 minutes, each hour or with monthly or annual frequency.

3.4 Building Environmental Parameters (Including Thermal Comfort and IAQ Conditions)

In order to assess the thermal comfort conditions inside the apartments, the following parameters have been monitored: air temperature, relative humidity, mean radiant temperature and air velocity. More specifically, the TinyTag TGP-4500 temperature and relative humidity data loggers have been placed at a height of about 1.50 m from the floor level in at least 2 rooms in each flat in order to represent different thermal zones (bedroom and kitchen or living room, and hallway). Measurements have been taken every 15minutes on a continuous basis during the experimental period. The mean radiant temperature has been measured using a black-globe thermometer (Delta Ohm) and air velocity has been measured using an air velocity meter by Dantec (54N50 Low velocity flow analyser). These measurements have been done on selected dates representing hot, cold and temperate conditions during the pre-retrofitting

experimental period and in several apartments. Measurements were conducted in at least 2 different rooms, mainly the bedroom and the living room at a height of about 1-1.5m.

Moreover, the indoor air quality has been assessed inside the apartments by measuring the concentration of CO_2, VOCs and PMx. Concentration levels of volatile organic compounds (VOC) and carbon dioxide (CO_2) have been surveyed with an IAQ stations - F2000TSM-VOC-L series which record values every 15min. Furthermore, the concentration of PM10, PM5, PM2.5, PM1, PM0.5, was conducted by a portable instrument Handheld3016 IAQ (Lighthouse Worldwide solutions) which has been calibrated according to ISO 21501-4 (2007) using polystyrene latex spheres. Measurements were conducted for 10minutes in each apartment with a 20s step. The concentration outside the apartment was also measured.

3.5 Meteorological Parameters

A meteorological station measuring air temperature and relative humidity with a Tiny Tag sensor on a continuous basis has been installed outside the 2nd floor of the building. In addition the following meteorological parameters have been recorded from nearby station of the National Observatory of Athens, on an hourly basis: Air temperature (C), Relative humidity (%), Wind direction and wind speed (m/s), Precipitation (mm), Diffuse and total solar radiation (W/m2), Air pressure (hPa).

3.6 Lighting Measurements

The objectives of the monitoring of the lighting conditions in the apartments of the demonstration house, are:
1. To assess the daylight availability in the apartments,
2. To record the artificial lighting conditions in the apartments,
3. To record the users' opinions on the existing lighting conditions,
4. To propose measures for the improvement of the lighting conditions in the property
The lighting parameters that have been recorded in indicative apartments of the Greek demonstration house are the Interior horizontal illuminance (lux) and the Exterior horizontal illuminance (lux). The equipment used for the illuminance measurements in the apartments includes two TES 1335 digital illuminance meters. The natural lighting conditions were measured in all the rooms of three representative apartments and on the upper flight of stairs, below the position where the light pipe is going to be installed during the retrofit, as shown in the following pictures.

4. RESULTS

The monitoring campaign of the Greek 7 story apartment building has been conducted during the period of August 2013 and March 2015 and is still ongoing. The results and analysis reported in this document focus mainly on measurements referring to the whole year of 2014. The main findings are summarized in this section.

4.1 Building Envelope

Different building inspection techniques including infrared thermography, air tightness, ventilation measurements have been used to assess the condition of the building envelope which is directly related to its energy performance and the thermal comfort of the occupants. Using infrared thermography several problems of the building envelope have been identified with most prominent being the important heat losses in winter and heat gains in summer because of the lack of insulation and the thermal bridges. Surface temperatures of the roof slab exceeding 50°C have been recorded during summer indicating the overheating of the building. In addition, the infrared inspection around the window's frame evidenced also air leakages and infiltrations which have been verified by the air tightness measurements and also the occupant surveys.
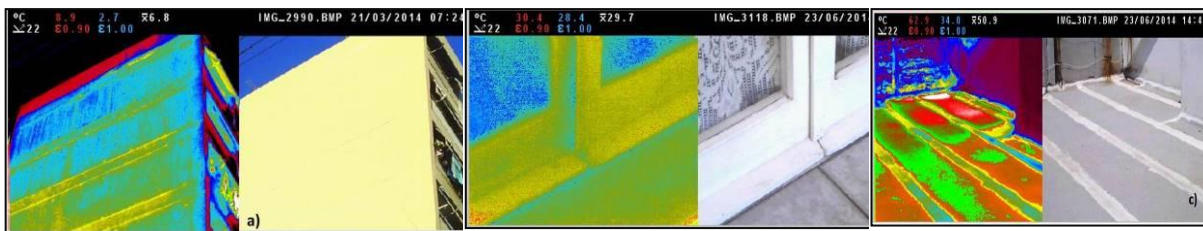
Figure 4: : Thermal Images: a)missing thermal insulation, b) Air leaks from the window and c) high surface temperature of the roof slab

Air tightness measurements were conducted using different techniques (blower door, novel pulse air leakage, ventilation measurements) in three representative apartments characterized each by: a) old type wooden frames and single glazing (2nd floor flat) b) new type aluminium frames and double glazing (3rd floor flat) and c) Mixed situation: some old type wooden frames and single glazing and some aluminium frames and double glazing (7th floor flat).

Table 2: Air flow coefficient, and air flow exponent, air leakage rate, the air change rate (results from blower door test)

	C_L	n	$\dot{V}_{50}$[m^3/h]	n_{50}[h^{-1}]
2nd floor -flat	134	0.5	947	5.20
3rd floor - flat	52.0	0.6	546	3.00
7th floor -flat	137	0.5	969	5.33

The measurement results showed that the apartments in which the windows aren't replaced or only in part, have a medium level for the envelope tightness; meanwhile the flat of 3rd floor has high quality. Comparing however the values measured with the corresponding values of energy efficient buildings with the flats under investigation have a very poor efficiency.

4.2 Energy Performance

Energy consumption (electricity) has been measured on a continuous basis using smart energy meters. The central heating system is not operated by the occupants due to financial restraints. Heating and cooling in the apartments is provided by AC units and/ or other devices like electric radiators, ventilators etc. Although the energy consumption of the building is not very high due to the lack of heating and cooling systems the analysis shows that when the outside temperature drops in winter to e.g. 10°C the energy consumption doubles and the same applies for summer conditions. It should be noted that the energy demand of the last floor is higher than the energy demand of the rest of the floors due mainly to heat losses and gains from the uninsulated roof slab. The results indicate very low energy efficiency of the building and high levels of thermal discomfort.

4.3 Thermal Comfort

The measurement results indicate increased thermal discomfort during both summer and winter especially taking into consideration that 2014 was characterized by mild winter and summer conditions. More specifically, the mean monthly indoor temperatures range around 17 -20°C during the winter but in several days the indoor temperature can reach values below 16°C (temperatures as low as 13°C have been recorded). During the summer months the indoor temperature exceeds always 28°C with maximum values going over 32°C (temperatures as high as 36°C have been recorded). In addition, the percentage of hours in comfort range have been calculated and it was found that for the winter period the temperature is below than the comfort value about in 70-80% of the hours while for the summer period there are very unsatisfactory results in almost all thermal zones. In general, the indoor temperature values and the relative humidity values do not meet the national requirements as set by the Technical Guideline of the Technical Chamber of Greece (TOTEE 20701-1/2010) in all the apartments.
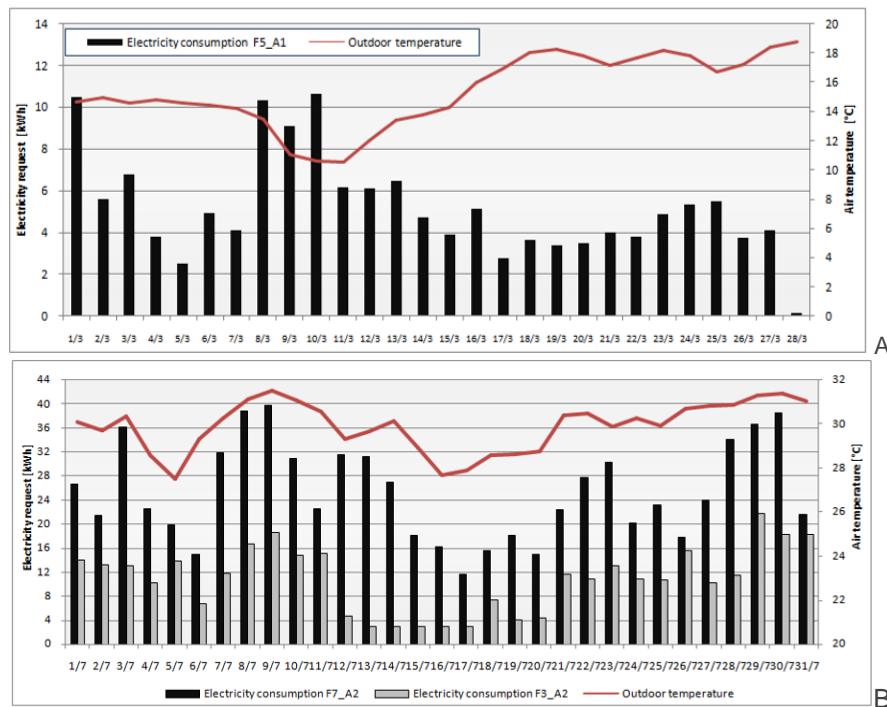
Figure 5: Daily electricity consumption and outdoor temperature during March 2014 (A) and during July2014 (B) for selected apartments

4.4 Indoor Air Quality

In order to assess the indoor air quality conditions in the building the following parameters have been measured: CO_2, VOCs and PMx in selected apartments. The results indicate poor indoor air quality inside most of the apartments. More specifically:

- For all of apartments where measurements were conducted the values for the concentration of PM10 exceed the recommended limits of 50µg/m3 while the concentration of PM2.5 exceeds the recommended limit only in some apartments.
- Regarding CO2 concentration, in the majority of the apartments, the air quality is characterized as "bad" as it exceeds the limit of 600ppm. In most apartments the CO2 concentration exceeds the limit of 1000 ppm in the 16% of the values recorded.
- Concerning the VOCs concentration, it was found that in the majority of the apartments it can lead to possible irritation or discomfort. In several apartments the concentration values recorded are in the discomfort range with more severe symptoms

4.5 Lighting

Generally, the illuminance values measured in the apartments are considered to be moderate for domestic environments. Regarding the measurements on the stairs leading to the roof, because of the lack of natural lighting sources, the illuminances are almost zero under any exterior lighting conditions. The building users rely on the use of artificial lighting sources to be able to ascend to the roof. Under these circumstances, it is considered that the light pipe installation during the energy retrofit will provide significant energy savings and visual comfort to the building users.

4.6 Meteorological Conditions

The meteorological conditions recorded for 2014 indicate that this was a mild year both during summer and winter with average monthly temperatures ranging from 12.3°C in January and February to 28.7°C in August and relative humidity ranges from 48% in August to 81% in January. No extreme cold or hot conditions have been recorded. Wind directions for the case study area are fairly consistent with the dominant wind direction being from the North-East reaching an average wind speed of 3m/s. Precipitation levels are quite low, especially during the summer.

5   THE RETROFIT PLAN

This section summarizes the methodology involving a holistic analysis that was followed within the HERB project in order to determine the optimum retrofit scenario for the Greek building. The estimated results of the retrofit are reported in terms of energy and CO2 savings, indoor environmental quality and financial impact.

5.1 Holistic Analysis

In order to design an optimal solution for the retrofit a holistic analysis has been performed that includes:
- Dynamic energy modelling (TRNSYS)
- Comfort modelling (PMV-PPD) (TRNSYS)
- Carbon emissions savings calculations
- Application of economic calculation theory to analyse the financial feasibility of the solutions.
- Other analyses for assessing HERB innovative technologies (e.g. PV modelling (PVGIS), custom model for energy efficient lighting)

Following the Integrated energy design process, an iterative process and taking into account the Greek & HERB project's specific requirements the Existing Case (current building situation) was analysed and compared to several other retrofit scenarios including innovative "HERB" technologies like energy efficient lighting, smart coatings and PVs, state of the art commercially available technologies like insulation and energy efficient windows as well as passive techniques like night ventilation.

Figure 6: The HERB design methodology

6   RESULTS

The results of the holistic analysis showed that energy efficiency technologies were the most effective in relation to retrofit approach (roof & wall insulation, replacement of single glazed windows with double glazing) followed by the application of passive and low cost measures (night ventilation, ceiling fans, shading, smart coating). Although useful, renewable technologies were less effective with respect to impact (PVs on SE facade).

The results for the optimum retrofit scenario:
- Annual energy savings of 80.3% against building performance before retrofit
- Reduction of CO2 emissions of 80.3%
- A global energy consumption (excluding appliances) in primary energy of 30.5 kWh/m²/year while reducing peak loads against the values measured before retrofit
- An energy saving for lighting of 85.7% over the average consumption of the installed base
- A significant improvement of indoor thermal comfort based on calculations according to ISO 7730
- A payback period of 9 years compared to the existing case
- All relevant national regulations are fulfilled.

It is estimated that after the retrofit the annual saved energy costs for the residents will amount to €11,344.72.

Scenario	Description
Existing case	As built
Case A	As built+insulation
Case B	Case A + energy efficient windows
Case C	Case B + ceiling fans
Case D	Case C + night ventilation
Case E	Case D + smart coating
Case F	Case E + shading
Retrofit case	Case F + PVs
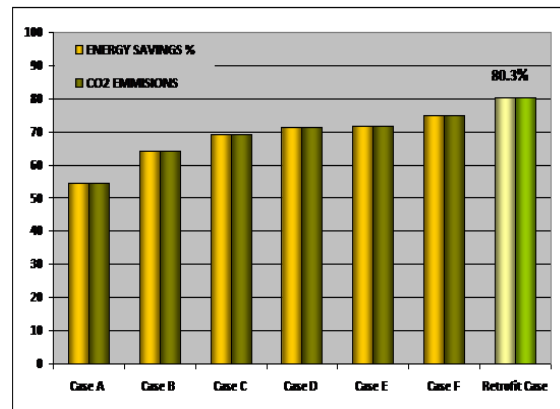
Figure 7: Retrofit scenarios & energy and carbon savings

7   CONCLUSIONS

An experimental campaign has been carried out in order to determine the energy performance and indoor environmental quality of a 7 story social housing apartment building that is going to undergo an energy efficient retrofit. The results indicate that it is a building with low energy efficiency and poor indoor environmental conditions. The design methodology that was followed in order to determine an optimum retrofit scenario in terms of energy, carbon, thermal comfort and socioeconomic performance involving solutions like Insulation of the building fabric, energy efficient windows, ceiling fans and night ventilation, external shading, replacement of the incandescent lamps and installation of integrated light pipe and led system and   smart photocatalytic coatings for the building envelope with improved anti pollutant, self-cleaning and cool (increased solar reflectance) characteristics. PV panels will be installed on the SE façade. The results show annual energy and carbon savings of 80% and improved indoor environmental quality. The saved energy costs for the residents amount to €11,344.72. The results of the monitoring have verified that the retrofit measures that have been adopted for the Greek building are appropriate and will greatly improve the energy and environmental performance of the building as well as the indoor environmental conditions of the occupants.

8   ACKNOWLEDGMENT

9   REFERENCES

EN 13829 (2001), Thermal performance of buildings. Determination of air permeability of buildings. Fan pressurization method. ISBN 0 580 36935 8.

EUROPEAN COMMISSION (2015), Energy efficiency, Buildings [online]. Available at: https://ec.europa.eu/energy/en/topics/energy-efficiency/buildings [Accessed 10 July 2015]

HERB (2015), HERB project website [online]. Available at: http://www.euroretrofit.com/ [Accessed 10 July 2015]

ISO 12569 (2012), Thermal performance of buildings and materials -- Determination of specific airflow rate in buildings -- Tracer gas dilution method

ISO 21501-4(2007), Determination of particle size distribution -- Single particle light interaction methods -- Part 4: Light scattering airborne particle counter for clean spaces

KENAK (2010), Greek Regulation for the Energy Efficiency of Buildings: Ministerial Decision Δ6/B/οικ.5825/30-03-2010, ΦΕΚΒ΄407 [online]. Available at: http://www.ypeka.gr/LinkClick.aspx?fileticket=aiS4GyKxx04%3d&tabid=525&language=el-GR [Accessed 10 July 2015]

TOTEE 20701-1 (2010), Technical Guideline of the Technical Chamber of Greece: Technical Guidelines on Buildings' Energy Performance, Technical Chamber of Greece, Athens, Greece.

183: Appraisal of a zero energy solar house model via reduction of the ghg emission and improvement of energy efficiency

CLAUDIA OLIVEIRA[1], FERNANDA ANTONIO[2], MIGUEL UDAETA[3]

University of São Paulo - FAU, Rua do Lago No. 876 – São Paulo - SP - Brasil, ctao@ups.br
[2] University of São Paulo - FAU, Rua do Lago No. 876 – São Paulo - SP – Brasil, f.antonio@ups.br
[3] University of São Paulo – GEPEA, Av. Prof. Luciano Gualberto Trav. 3 No. 158 – São Paulo - SP – Brasil, udaeta@pea.usp.br

This study aims to demonstrate the modelling and architecture of a Zero Energy Solar House towards sustainable development, based in first instance on global greenhouse gases emissions mitigation. The methodology is based on multiple criteria accounting for aspects such as electricity conservation, power generation and greenhouse gases emissions reduction. The potential and limitations of photovoltaic systems, as well as the residential sector electricity consumption are studied. The guidelines and strategies of a Zero Energy Solar House are defined, focusing on the use of the sun in architecture, solar heating and photovoltaic system. These studies are carried out through a zero energy house model (considering the annual consumption of a residence connected to the grid) that incorporates the guidelines and strategies of a Solar House. The bioclimatic strategies and solar systems are analysed considering its application in the city of São Paulo. The evaluation of passive strategies for thermal conditioning demonstrates a potential to increase by 70% the hours of comfort in the year. On the other hand, the adoption of more efficient technologies for lighting shows energy conservation potential around 12.5%, within the defined parameters and considering the average residential consumption. The use of solar system for water heating indicates a potential to save up to 16.3% of energy compared to a business-as-usual scenario (traditional house). The electricity generation by photovoltaic systems combined with the adoption of energy efficiency measures demonstrates a potential to achieve, at least, zero net annual energy balance relatively to the business-as-usual residential consumption of the grid. Thus, it is estimated a potential to avoid up to 1.66 t CO2 per year for each housing unit.

Keywords: Zero energy home; Solar energy; Architecture; Energy conservation; Sustainable development

4. INTRODUCTION

The current economic development model considers the environment as an endless reservoir of natural resources with unlimited capacity to receive waste generated by human activity, embracing inefficiency and wasteful use of natural resources, especially energy, which is one of the essential supplies for the basic conditions of human life. Such model and the unbalanced operation and use of environment are the vectors of environmental problems.

Brazil is a developing country and as so, the tendency is that energy demand will increase along with the economy, implying the construction of new hydroelectric and thermoelectric plants, causing significant environmental, social and economic impacts. In Brazil, 44% of the generated energy is consumed in buildings (BRAZIL, 2011), in which the occupancy phase is the most representative in energy consumption considering the whole life cycle of buildings (UNEP, 2007). The residential sector consumes 26% of total Brazilian electricity and the increase in purchasing power, particularly of the low-income population, leads to an increase in energy consumption by this sector. This highlights the need to adopt energy efficiency measures and alternative and renewable energy sources, so that people can have access to consumer goods and improve their quality of life in an efficient way.

In the National Interconnected System (SIN), 67% of energy comes from hydropower, what makes the Brazilian electricity matrix to be considered clean. Nevertheless, increasing concern with environmental and social impacts of the construction of new plants has been noticed. On the other hand, studies show the enormous potential for the exploitation of solar energy in the country, due to favourable levels of solar radiation throughout the year and photovoltaic systems for distributed generation are approaching an economic feasibility (EPE, 2012). Therefore, it is argued that solar energy has demonstrated potential to contribute to supply this growing demand.

Given this scenario, this study aims to determine the contribution of a Zero Energy Solar House (ZESH) to the sustainable development through energy efficiency and the use of solar energy, allowing the reduction of greenhouse gases (GHG) emissions associated to energy consumption by residential sector in Brazil. To verify the potential of these actions on a larger scale, is taken as geographical boundaries the city of São Paulo, considering the replacement of a percentage of single-family houses by units (or systems) along the lines of the ZESH. Methodologically this study adopts "Ekó House", a solar-house prototype that verifies the ZESH. Thus, it is possible to predict the effective reduction of GHG emissions associated with energy use by Brazilian residential sector.

A ZESH follows the Zero Energy Building (ZEB) concept. According to Torcellini et al. (2006), ZEB is defined as a building that produces, through local sources, the energy it consumes, considering an annual review (here understood as sustainable energy residence). The ZEB can be connected to the public network and integrate a system of distributed generation of electricity. Preferably, the energy comes from renewable sources and is produced, for example, through the building of integrated water heaters by solar irradiation, small-scale facilities for the production of wind energy, photovoltaic panels among others. In this study, authors adopt the term Solar House, which defines a housing unit that uses solar energy in architecture and energy generation, regardless of achieving a zero balance (ANTONIO, 2015).

The Ekó House prototype was developed by Team Brazil, a partnership between University of São Paulo and Federal University of Santa Catarina to participate on Solar Decathlon Europe in 2012. This prototype is adopted because it meets the requirements of a ZESH.

2. ELECTRICITY GENERATION IN BRAZIL

The National Interconnected System (SIN) is a large hydrothermal system, with a strong predominance of hydroelectric plants. Only 3.4% of the country's capacity of electricity production is out of SIN, in small isolated systems located mainly in Amazon region (ONS, 2013). Hydroelectric plants correspond to 67% of energy generation, such participation enables to consider the Brazilian electricity matrix a clean matrix. Nevertheless, with the need to build new power plants to meet growing demand for electricity, more pressure comes from society and NGOs because of environmental and social impacts caused by the implementation of such new plants. To meet the growing demand for electricity it is planned to count on new thermoelectric systems, including one more nuclear power plant (Angra III), and coal-fired plants as a complement and rational diversification of usable hydropower potential naturally limited (BRASIL,

2007). It is also important to note that the losses in transmission and distribution stages reach 16.9% in SIN (BRASIL, 2012). The graph in Figure 1 discriminates participation by source in SIN.
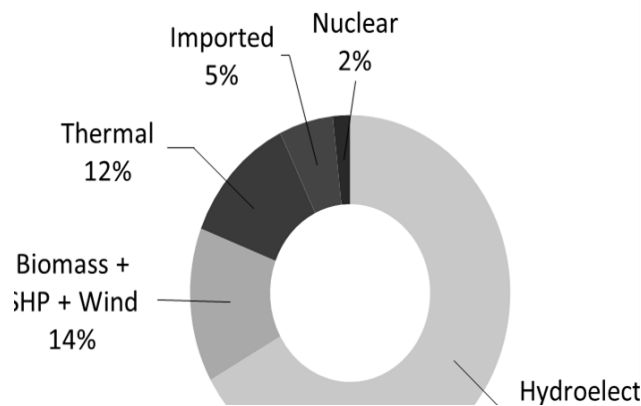
Figure 1:   Participation by source in SIN. (EPE, 2012)

Another condition that highlights the need to explore other energy sources is the fact that most of the hydric resources in Southern and South-eastern are already exploited, and most of the remaining reserves are in the Amazon, away from industrial and population centres (OECD, 2001). It is important to note the potential for solar energy exploitation due to favourable annual irradiation levels in the country, ranging on average from 1.260 to 1.420kWh/m²/year (EPE, 2012). Further, the National Electrical Energy Agency (ANEEL) approved in 2012 a resolution that allows installing grid-connected PV micro-generation in dwellings.

On the other side of the equation is the electricity consumption. The residential sector accounts for 26% of total electricity consumption in the country, and it is expected that this participation will remain for the next 10 years, with an estimated increase of 48.3% by 2021 (BRASIL, 2012). This amount considers energy efficiency measures due to use of more efficient equipment in Brazilian dwellings.

It is important to notice that peak demand in Brazil usually occurs by the end of the day, from 6:00 p.m. to 9:00 p.m. and is associated to use of artificial lighting, home appliances and electric shower. However, in 2014 during the summer, new records in peak consumption were registered in South-eastern/Midwest and South SIN subsystems, as shown on Figure 2 graphics. Such shift on peak time is associated to constant high temperature and thermal discomfort index in these regions, at the higher insolation period, which increased the use of HVAC systems and consequently the electricity consumption (ONS, 2014).
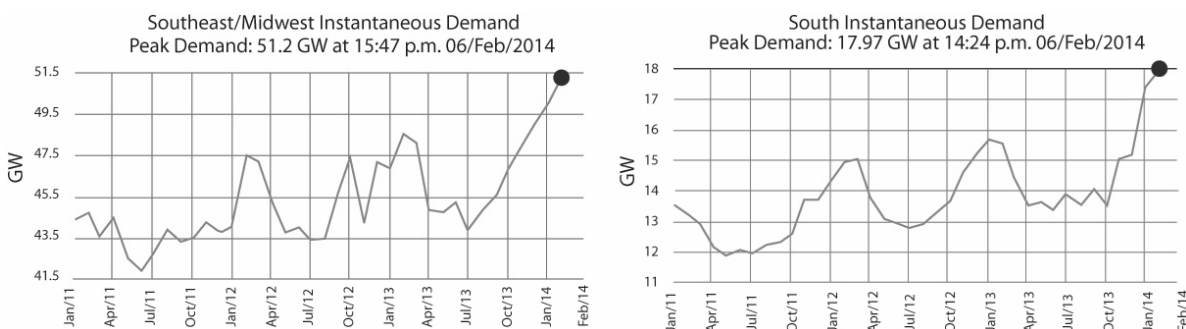
Figure 2:   Instantaneous peak demand in SIN subsystems. (ONS, 2014; ANTONIO, 2015)

The episodes of peak consumption associated with high temperatures demonstrate the inefficiency of buildings, which often are constructed without considering the local climate and therefore require high amounts of energy for the maintenance of environmental comfort conditions for the occupants. In addition to this inefficiency is highlighted the fact that the year 2014 was recorded as the warmest since 1880 (NOAA, 2015).

2.1 GHG emissions by SIN generation

As already pointed, it is estimated that participation in electricity consumption by the residential sector will continue in the coming years, with an increase in energy consumption and, consequently, in associated GHG emissions, which must pass from 18 Mt CO_2-eq in 2011 to 23 Mt CO_2-eq in 2021 (BRASIL, 2012).

To estimate GHG emissions associated with electricity generation in the SIN, data provided by the Ministry of Science and Technology are adopted, which indicate that GHG emissions were 0.5931 t CO_2/MWh in 2013. These values are calculated based on specific methodologies for small-scale CDM projects (UNFCCC, 2013).

Also with respect to emissions associated with electricity generation, SIN operation analysis in recent years allows us to identify an increase in the emission factor operating margin, associated with a more intensive use of conventional thermoelectric plants (ANTONIO, 2015), as shown in Figure 3. The increase in thermoelectric actuation is associated with low precipitation and an increase in electricity consumption, which points to the need to increase the efficiency of buildings and count on alternative sources for electricity generation in Brazil.
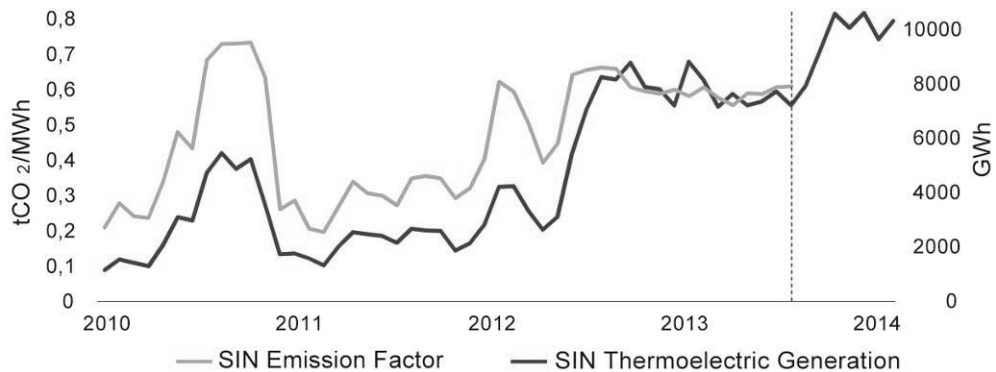
Figure 3: Emission Factor and thermoelectric generation in SIN. (ANTONIO, 2015)

2.2 Insertion of the PV systems in the Brazilian energy matrix

Despite the favourable geographical conditions for the exploitation of solar source in Brazil, the laws that support the incorporation of these systems to buildings and measures that promote the economic viability thereof are very recent. In this context, ANEEL passed the Resolution No. 482 of 17 April 2012 laying down rules for micro (up to 100 kW) and mini-generation (between 100 kW and 1 MW) in the country (ANEEL, 2012). The goal is to enable the installation by consumers of solar panels connected to the grid in dwelling, business or industry buildings, so that the output from these devices can generate credits through a clearing system.

Projections to the year 2050 indicate that the SFV for the residential sector must have a reduction of around 70% in costs, and by the year 2022 should achieve rate parity in almost the entire country (EPE, 2014). Scenarios considering discount on income tax, tax exemption of photovoltaic modules, the non-taxation of compensation, and the implementation of virtual net metering system can significantly contribute to the increase in the market in the residential sector. The most optimistic scenario, which includes all these mechanisms to reduce PV costs, it is estimated that by 2023 the country could count on 1.033 million households with PV systems (KONZEN, 2014). A wider dissemination of ZEB and the environmental awareness by the Brazilian consumers are also factors that can impact positively on increasing adoption of these systems (EPE, 2014).

3. ELECTRICITY CONSUMPTION BY THE BRAZILIAN RESIDENTIAL SECTOR

Regarding the specific consumption by appliance and equipment, a research on "equipment checkout and use habits" (PROCEL, 2007) indicates the participation of different appliances in energy consumption by the Brazilian residential sector, as shows the graph on Figure 4. In South-eastern Brazil

the average electricity consumption is around 165 kWh/month for each dwelling (EPE, 2014). This indicates that there is room for increasing electricity consumption by this sector.

Such data regarding electricity generation in Brazil and specific consumption by the residential sector are applied to assess the benefits of a ZESH, regarding the adoption of energy efficiency measures and the PV generation by reducing energy consumption and avoiding GHG emissions.

From the perspective of energy efficiency it is assumed that the quality of energy services will increase faster than the equipment power to generate such service (EPE, 2014). Thus, in some cases, a service can be obtained with a low expenditure of energy. However, changes in ownership of equipment and usage habits, also associated to the reduction of pent-up demand in the country, should contribute to an increase in energy consumption by the sector. It is observed, therefore, a considerable upward trend in energy consumption by the residential sector by 2050. However, it is estimated that energy efficiency measures can contribute to energy conservation of about 19.5% compared to a scenario without conservation, in the horizon of the study. The graph in Figure 5 illustrates these projections.
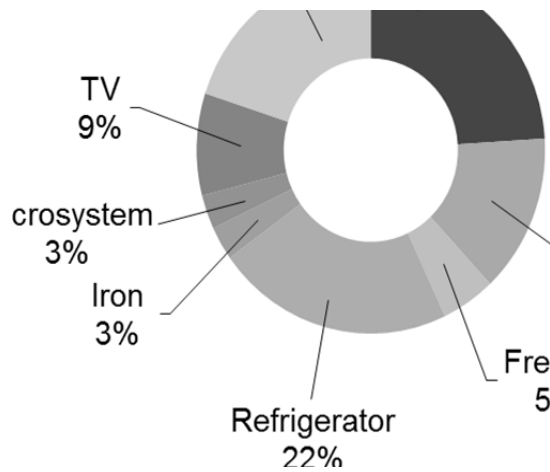
Figura 4:   Share of appliances consumption in Brazilian dwellings. (PROCEL, 2007)

	Air Conditioning	Entertainment	Cooking	Water Heating	Refrigerator	Other Uses	Lighting	Saved Energy
2020	42,427	28,929	1,84	21,288	38,561	14,111	17,754	13,726
2050	123,302	97,792	5,672	20,455	62,939	8,354	8,354	84,289
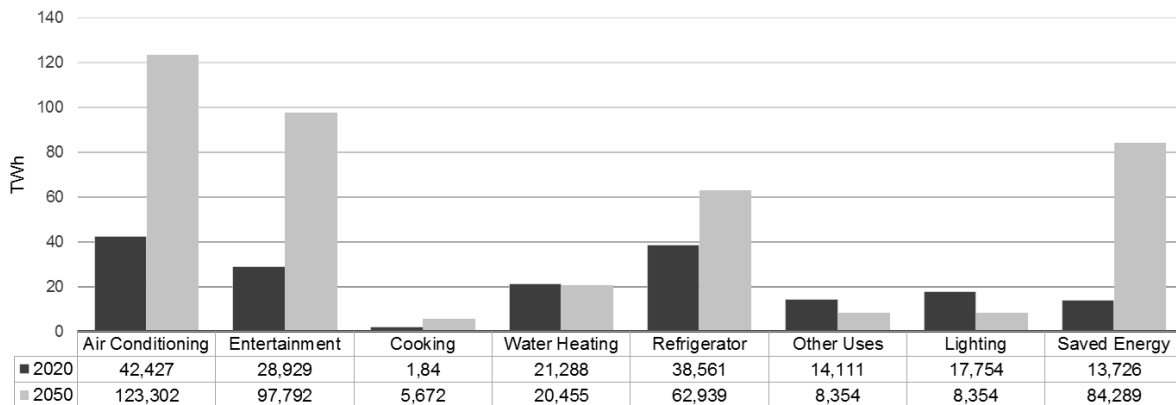
Figure 5: Electricity consumption by use and energy saved for the Brazilian residential sector in 2020 and 2050. (EPE, 2014; ANTONIO, 2015)

We observe an increasing trend in the consumption of electricity in the Brazilian households resulting from the increase and better distribution of income of the population and the search for satisfactory levels of comfort, reducing the pent-up demand in Brazil. This scenario demonstrates the importance of architectural design and construction features for energy efficiency, as well as the incorporation of solar systems for power generation in single-family housing units in Brazil.

5. SOLAR HOUSE MODEL AIMING TO REDUCE GHG EMISSIONS

Solar energy in an active or passive way, has great potential to be harnessed in buildings (IEA, 2012), and can meet the different demands for energy in a Solar House. The water heating may be provided by a system of solar collectors; electricity can be generated by photovoltaic modules; the internal heating can be obtained by direct solar gains and also for solar water heating system; natural lighting can be harnessed effectively, the cooling indoors can be facilitated by natural ventilation, and shading elements can prevent overheating inside passively.

Thus, the prototype Ekó House exemplifies and summarizes the application of different strategies for harnessing the sun in architecture. The prototype envelope is the result of a study of solar geometry. From this study, considering the deployment in Madrid, south orientation was considered the most favorable to benefit from the sun throughout the year. Therefore, the geometry is more elongated in the east-west axis and the largest area of openings is located on the south side of the prototype. The cover, which is the surface that receives a higher incidence of solar radiation throughout the year, was chosen for installation of the solar systems. The diagram in Figure 6 illustrates these strategies.

1	PV Modules
2	Solar Collectors
3	Automated external blinds
4	Bamboo frames / Verandas
5	Support for Solar Systems
6	South facade windows
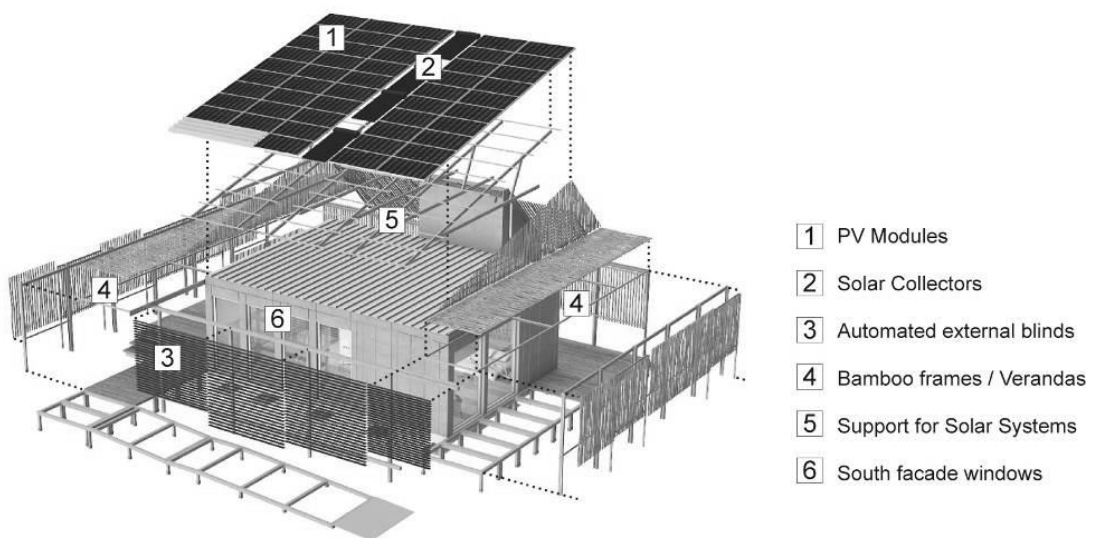
Figure 6: Ekó House prototype strategies and systems. (Projeto Ekó House, 2012)

The prototype also has shading devices to control the incidence of solar radiation throughout the year for both thermal conditioning and for the use of natural lighting. In the southern facade was installed a system of automated external blinds. The east and west facades are protected by verandas with bamboo frames. Internally translucent blinds are used. The prototype adopts floor, walls and roof components with high levels of thermal insulation. The openings are sealed and double-glazed with a low-e coating. With these solutions is possible to achieve thermal comfort passively and reach daylight autonomy of 60% for the prototype, which saves the energy for environmental conditioning. The artificial lighting is designed to complement the use of natural light, and uses LED technology, which ensures greater efficiency compared to the other technologies.

The prototype has a DHW solar system with vacuum pipe technology, which ensures a solar fraction of about 90%, including the use of hot water to feed radiators for space heating. The PV system has 48 modules with a 18.5% efficiency, accounting for an installed capacity of 11.04 kWp. A home automation system integrated to the use of equipment and the general prototype operation contributes to a more efficient operation. This system can be programmed to guide the occupant, informing about energy generation and consumption and to control lighting and temperature, activating equipment and systems based on pre-established comfort ranges or person presence indoor. Strategies for sun use together with solar systems ensure the prototype a positive energy balance throughout the year, as shown in the graph in Figure 7.
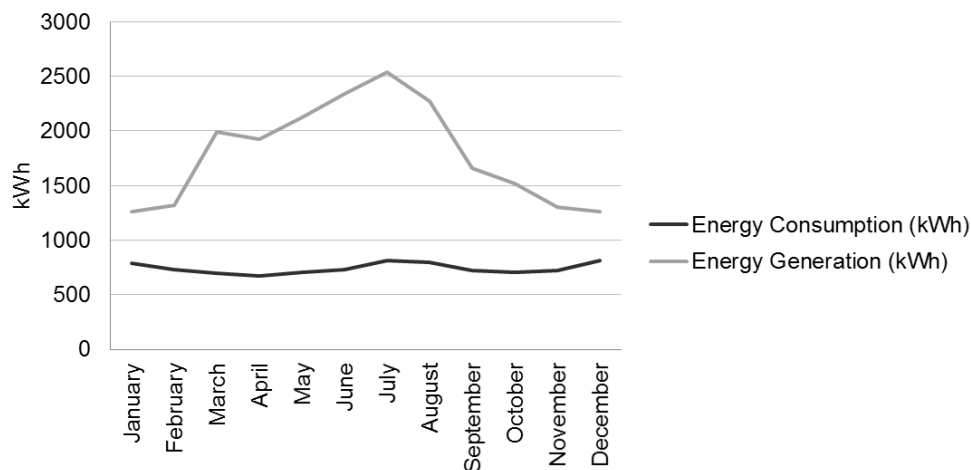
Figure 7: Balanço energético anual do protótipo Ekó House. (PROJETO EKÓ HOUSE, 2012; ANTONIO, 2015)

The Ekó House prototype exemplifies a Solar House model, which is premised on the harnessing of sun. A housing unit can be considered the most elementary version of Solar House when designed considering a proper study of solar geometry and solar orientation. Other strategies and systems can be incorporated by using different combinations of these solutions, improving the performance and efficiency of the unit.

6. SOLAR HOUSE MODEL APPLIED IN THE CITY OF SÃO PAULO

In this paper we analyse the impact of adopting three solutions for energy efficiency and energy generation: artificial lighting systems more efficient and the adoption of solar systems for DHW and electricity generation. Projections of the impact of adopting such solutions on large-scale are made taking as a backdrop the city of São Paulo, the most populous in Brazil and one of the largest cities on the planet. In a city of this scale, rational use of resources is a focal point for the welfare and satisfaction of the basic needs of the population. In addition, from 3.5 million housing units, about 80% are single-family units (IBGE, 2010), typology considered the most favourable for the adoption of solar systems. The analyses are based on an average electricity consumption of 165 kWh per month for Brazilian households (EPE, 2014).

To estimate the gains obtained by the adoption of measures to reduce energy consumption, it was considered the replacement of artificial lighting systems with more efficient technologies (comparing incandescent, compact fluorescent lamps – CFL, and lighting emitting diode – LED) and also the adoption of solar collectors for water heating as an alternative to electric shower. For DHW systems it was considered a solar fraction close of the minimum allowed in specific legislation for the city of São Paulo (PREFEITURA DA CIDADE DE SÃO PAULO, 2008), 43% (DHW A), and also a system with solar fraction of 68% (DHW B), close to the value considered optimal for DHW systems solar (IEA, 2012). The graph in Figure 7 represents the gains achieved in terms of energy conservation through these strategies, based on the participation of end uses in Brazilian households presented in the graph in Figure 8.

Regarding electricity generation, two PV systems were set based on indications of installed capacity by consumer group in the Brazilian scene. For an average consumption of 165 kWh/month, it is indicated a PV system from 1.0 to 1.5 kWp. From this point, two scenarios were defined, with the less and more favourable strategies combinations in terms of energy conservation and power generation. In the first scenario (C1) were accounted the smallest gain in energy conservation by replacing artificial lighting system, the DHW system with solar fraction of 43% and the PV system with 1.0 kWp of installed capacity. The second (C2), is the combination of more favourable strategies. Table 1 summarizes the data concerning the electricity conservation and generation for each strategy separately and for the two defined scenarios.

Sequentially, emissions that would be avoided for each strategy or combination of strategies were accounted, in comparison to a baseline or business as usual scenario where these strategies would not be adopted. The baseline scenario is defined by a residence with a 165 kWh/month average

consumption, powered by SIN electricity, where the emission factor is 0.59 g CO_2/kWh. Therefore, the emissions associated with the average electricity consumption in a household in Brazil are 97.3 kg CO_2/month. The graph in Figure 9 represents the avoided emissions for each strategy considering the adoption of measures for electricity conservation and generation.
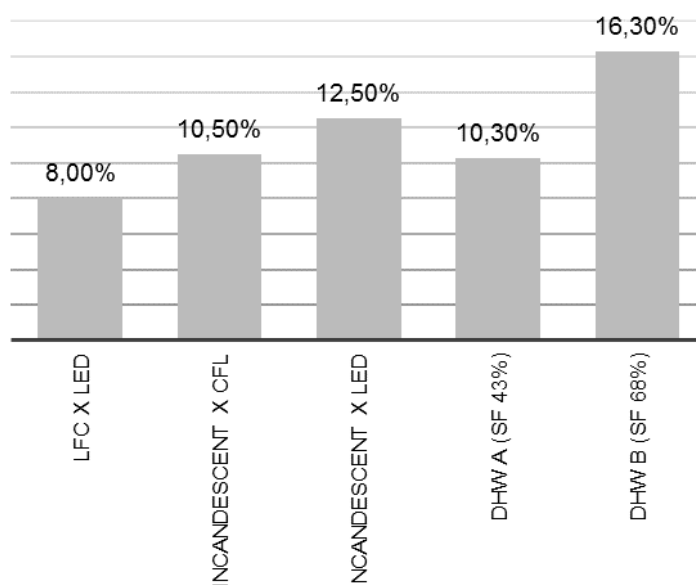
Figure 8: Reduction in total energy consumption in a household by adopting different electricity conservation strategies. (DOE, 2012; ANTONIO, 2015).

Table 1: Energy conservation, energy generation and energy balance. (ANTONIO, 2015)

	Strategies	Energy Saving (%)	Energy Saving (kWh/mês)	Total Consumption (Withou conservation) (kWh)	Balance PV 1 kWp (129 kWh/mês)	Balance PV 1,5 kWp (187 kWh/mês)
Base	-	0	0	165	-165	
PV System		-	-	165	-36	+22,8
L1	CFL X LED	8	13,2	151,8	-22,8	+35,2
L2	Incandescent X CFL	10,5	17,3	147,7	-18,7	+39,3
L3	Incandescent X LED	12,5	20,4	144,6	-15,6	+42,4
DHW A	SF 43%	10,3	17	148	-20	+39
DHW B	SF 68%	16,3	26,8	138,2	-9,2	+48,8
C1	CFL X LED + DHW A	18,3	30,2	134,8	-5,8	+52,2
C2	Incandescent X LED + DHW	29	47,8	117,2	+11,8	+69,8
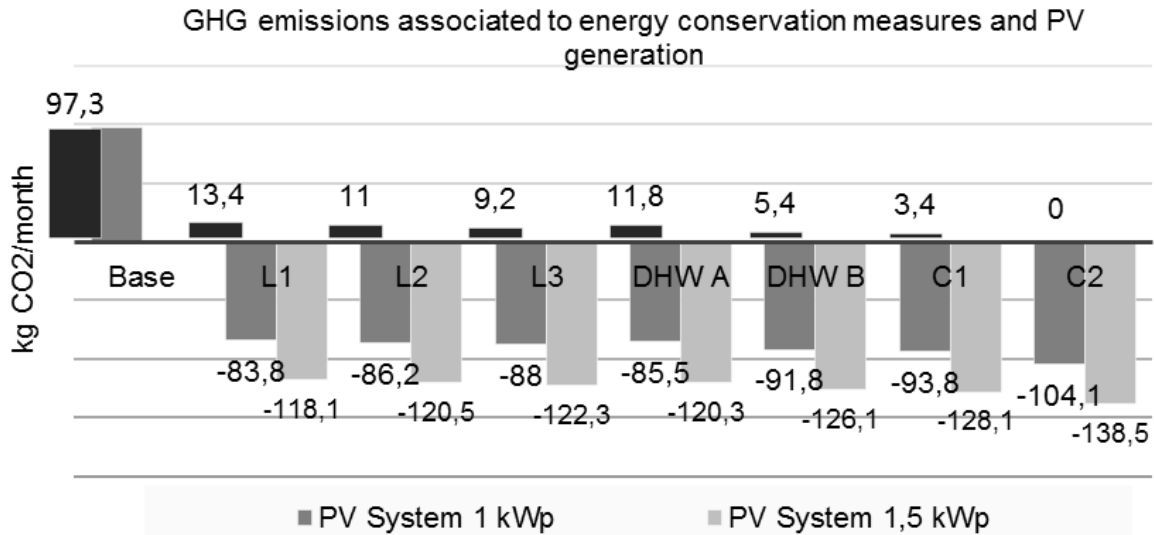
Figure 9: Emissões de GEE associadas às estratégias de conservação e geração de energia. (ANTONIO, 2015)

5.1 Projection of GHG emission reduction potential in large-scale

From the data presented in Figure 8 it is possible to project the impacts that could be achieved in terms of GHG emission reduction if strategies for energy conservation in lighting and solar systems were adopted on a large scale. Therefore, the city of São Paulo is taken as a backdrop, with about 2.8 million single-family housing units.

For projections related to gains in energy conservation for more efficient artificial lighting systems, it was considered that all single-family housing units replace their systems by more efficient technologies, as it is a technological replacement that occurs naturally. On the adoption of solar systems for water heating and SFV, specific projections of penetration of these systems in the Brazilian market were considered. For the DHW solar system, projections indicate that by the year 2050 about 20% of households will have adopted these systems (EPE, 2014). Regarding PV systems, it is estimated that in 2023 about 1.5% of Brazilian households will count on PV for electricity generation (KONZEN, 2014; ANTONIO, 2015). It is estimated a potential to reduce up to 1.66 t CO_2/year for each unit in the best scenario in terms of electricity conservation and power generation. The graphs in Figure 10 illustrate the GHG emission reduction potential in the scale of a housing unit, and projections for large-scale adoption of these strategies.
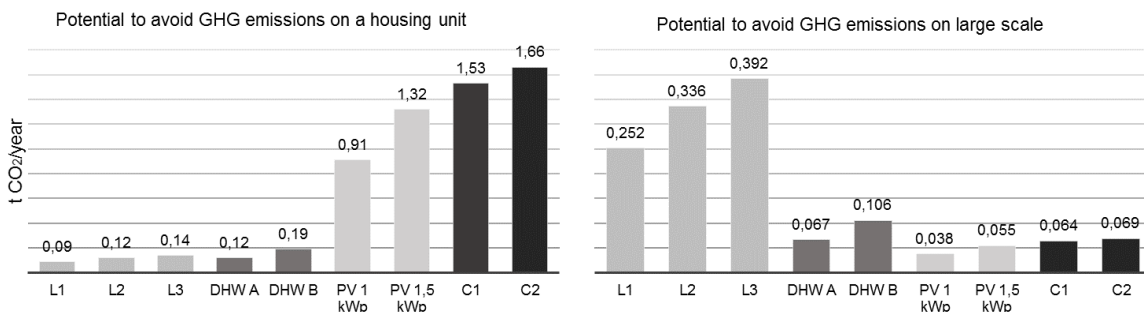
Figure 10: Potencial de redução de emissões de GEE por unidade e pela adoção das estratégias para conservação e geração de eletricidade em larga escala. (ANTONIO, 2015)

The potential to avoid GHG emissions observed in the specific case of artificial lighting technologies for a wide-scale, clearly demonstrates the effectiveness of creating legislation to regulate the energy efficiency products commercialized in the country The withdrawal of incandescent bulbs from the market results in a GHG emission reduction between 0.336 and 0.392 Mt CO_2-eq considering this substitution only in single-family housing units in São Paulo. This represents between 1.8% and 2.17% of total GHG emissions associated with the generation and use of electricity by the Brazilian residential sector in 2011, which was 18 Mt $CO_{2\text{-eq}}$. Solar systems have an even higher potential to reduce GHG emissions per housing unit, so its adoption in large scale could bring significant benefits in electricity conservation and generation and, consequently, in GHG emission reduction associated with the energy use by the Brazilian residential sector.

7. CONCLUSION

Based on the parameters defined for this study, quantitative analysis shows a potential energy conservation between 8% and 12.5% for artificial lighting through the adoption of more efficient technologies. It is demonstrated a potential to save between 10.3% and 16.3% of energy for water heating by the adoption of DHW solar system. The combination of these strategies results in a potential to save between 18.3% and 29% of the total electricity consumed per month in a household. In this case, for an average consumption of 165 kWh/month, conservation could vary between 30.2 kWh/month and 47.8 kWh/month.

For a housing unit with average Brazilian consumption avoided emissions can vary between 0.09 t CO_2 / year and 1.51 t CO_2 / year, according to the defined parameters and different situations analysed for the conservation and generation of electricity.

In short, from these analyses and results the authors conclude that housing units along the lines of a Solar House can contribute to the energy conservation in residential sector, to increase the share of renewable sources in the Brazilian energy matrix, and in the mitigation global warming through the greenhouse gas emissions reduction. These solutions are essential to the sustainable development of the country and highlight the potential of Brazilian residential sector to contribute in energy efficiency and also in the generation of energy by a renewable source, in this case, the solar energy.

8. REFERENCES

ANEEL, 2012. Resolução Normativa ANEEL n. 482, de 17 de abril de 2012. Brasil: Agência Nacional de Energia Elétrica.

ANTONIO, Fernanda, 2015. Premissas e estratégias para uma casa solar visando à redução de emissões de gases de efeito estufa por meio da conservação e geração de energia. Dissertação (Mestrado em Tecnologia da Arquitetura). São Paulo: FAU/USP.

BRASIL, 2012. Ministério de Minas e Energia, Empresa de Pesquisa Energética. Plano Decenal de Expansão de Energia 2021 – PDE 2021. Brasília: EPE.

BRASIL. Ministério de Minas e Energia, Empresa de Pesquisa Energética, 2011. Plano nacional de eficiência energética: premissas e diretrizes básicas. Brasília: MME.

DOE, 2012. Life-Cycle Assessment of Energy and Environmental Impacts of LED Lighting Products Part I: Review of the Life-Cycle Energy Consumption of Incandescent, Compact Fluorescent, and LED Lamps. U. S. Department of Energy. United States: DOE.

EPE, 2014. Demanda de energia 2050. Estudos da demanda de energia, Nota técnica DEA 13/14. Rio de Janeiro: Empresa de Pesquisa Energética.

EPE. 2012. Nota Técnica: análise da inserção da geração solar na matriz elétrica brasileira. Empresa de Pesquisa Energética. Rio de Janeiro: EPE.

IBGE, 2010. Censo Demográfico 2010. Brasil: Instituto Brasileiro de Geografia e Estatística.

IEA, 2012. Solar energy system s in architecture: Integration criteria and guidelines. IEA Solar Heating and Cooling Programme: Task 41. Solar Energy & Architecture. International Energy Agency.

KONZEN, Gabriel, 2014. Difusão de sistemas fotovoltaicos residenciais conectados à rede no Brasil: uma simulação via modelo de Bass. Dissertação (Mestrado em Ciências). São Paulo: IEE/USP.

NOAA, 2015. State of the Climate: Global Analysis for December 2014. National Climatic Data Center. Washington: NOAA.

OECD, 2001. OECD economic surveys: Brazil. Organization for Economic Co-Operation and Development. Paris: OECD.

ONS, 2014. Boletim de Carga Especial de 07/02/2014. Brasil: Operador Nacional do sistema Elétrico.

PREFEITURA DA CIDADE DE SÃO PAULO, 2008. Decreto nº 49.148, de 21 de Janeiro de 2008. São Paulo: Prefeitura da cidade de São Paulo.

PROCEL, 2007. Pesquisa de posse de equipamentos e hábitos de usos: Setor residencial. Programa Nacional de Conservação de Energia Elétrica. Rio de Janeiro: PROCEL.

PROJETO EKÓ HOUSE, 2012. Project Manual. São Paulo: Team Brasil.

TORCELLINI, Paul, Pless, Shanti, Deru, Michael, 2006. Zero energy buildings: a critical look at the definition. ACEEE Summer Study Pacific Grove. Proceedings. California: NREL.

UNEP, 2007. Buildings and climate change: Status, challenges and opportunities. United Nations Environment Programme. UNEP.

UNFCCC, 2013. Methodological tool: Tool to calculate the emission factor for an electricity system. Tool 07, Version 04.0, Clean Development Mechanism. United Nations Framework Convention on Climate Change.

SESSION 15: GREEN AND SUSTAINABLE BUILDINGS

63: A brief discussion on current vertical greenery systems in Hong Kong: the way forward

K.W.D.K.C. DAHANAYAKE [1], NADIA C.L. CHOW [2]

1 Department of Architecture and Civil Engineering, City University of Hong Kong, Hong Kong, China,
kkiramawe2-c @my.cityu.edu.hk
2 Department of Architecture and Civil Engineering, City University of Hong Kong, Hong Kong, China,
cheuchow @cityu.edu.hk

Fast growing cities consume natural resources in vast quantities resulting adverse effects to both human and natural environment. Integrating sustainable initiatives to development projects cannot be overlooked. Thus, vertical greening is gaining popularity throughout the world as a viable option of integrating greenery into urban inhabitants. Vertical greenery systems offer wide range of environment, economic and social benefits. Vertical greenery is merely use of vegetation on facades of the building. Growing climbers on building walls is not a novel perception; it has been a practice from ancient time. However, vertical greenery systems are being developing with new technologies allowing more design flexibility.

In Hong Kong, vertical greenery is gaining popularity among all sectors including commercial, institutional, government and residential. This initiative is a good answer for severe air pollution and heat island effect in Hong Kong. This paper discusses on environmental, economic and social benefits from vertical greenery systems, different classifications of vertical greenery systems, vertical greenery applications in Hong Kong, plant species used in vertical greenery in Hong Kong and codes and standards that can be adopted for vertical greenery systems. In Hong Kong, vertical greenery is still at its infancy stage which is yet to explore to maximize the benefits and to uplift the quality of built environment.

Keywords: Vertical Greenery, Green Facades, Living Walls, Hong Kong

1. INTRODUCTION

Rapid urbanization and development of industrial activities have led to increased greenhouse gas emissions and heat island effect. In large modern cities buildings, infrastructures and materials impact on the local climate of urban spaces and cause a significant rise of temperature especially in city centers which is known as the heat island effect (Alexandri and Jones, 2008). This unstoppable force of urbanization results in extensive replacement of natural vegetation with concrete buildings (Wong, Tan, Chen et al., 2010a). These have created a negative impact on the natural environment in cities. The challenge is to develop cities with minimal environmental pollution and minimal use of energy. Sustainable measures should be taken to protect the environment against global warming and environmental pollution (Safikhani, Abdullah and Ossen, 2014). Urban greenery is a good solution for environmental issues arising from high concentration of buildings in cities (Wong, Chen, Ong et al, 2003). Thus, in many urban cities there is a growing trend to integrate nature into buildings and infrastructures (Jaafar, Said and Ras, 2011). Vertical greenery systems are becoming an emerging solution for integrating greenery into concrete jungles. Vertical greenery is new phenomenon which provides an ecological solution to urban areas. However, historical evidences show that the concept of green walls is not merely an innovative technology.

Plants grown on vertical surfaces can be simply called a vertical greenery system (Safikhani et al., 2014). Many decades ago building facades were decorated with the use of self-climbing plants and vines growing upward or cascading down which rooted on the floor, containers, or rooted on coarse of building surface (Greenscreen, 2012a). In addition, there were instances of using twining plants supported by trellis and pergolas or use of individual plants on vertical surfaces such as stacked rocks (Jaafar et al, 2011). In present, vertical greenery systems use traditional architectural features along with advanced materials and advanced technology to enhance design flexibility and to promote sustainable building functions (Kohler, 2008). Apart from using of building facade as growing or supporting media for vegetation, separate structural systems are also attached to the building facade with plants grown on it which is called a living wall (Loh, 2008). As green wall technology is still at its infancy stage it requires proper maintenance a special consideration in terms of irrigation, drainage and supply of nutrients. It is challenging to maintain regular plant substance for a long time span over large vertical surfaces (Greenscreen, 2012a).

2 BENEFITS OF VERTICAL GREENERY SYSTEMS

Integration of greenery into buildings grants an extensive range of environmental, economic and social benefits. Vertical greenery systems are gaining popularity as a new building technology mainly due to its wide range of positive benefits (Loh, 2008).

2.1 Environmental Benefits

Green facades improve environmental benefits by basically enhancing the potential area for greenery in urban settings (Kohler, 2008). Green walls contribute to reduce heat island effect by lowering the temperature of building envelope by "shading, reducing reflected heat, and evapotranspiration" (Green Roofs for Healthy Cities, 2008: p. 14). Green facades found to be the most viable solution for reflection of heat from hard surfaces, which known as the main causes for heat island effect in cities and for the deficiency of greenery in crowded urban environments (Loh, 2008). The increased thermal performance of buildings further contribute to minimize greenhouse gas emissions by reducing the energy consumption of air conditioning system a building (Loh, 2008). A study showed that in Hong Kong, "canyon air temperature decrease reaches 8.4^0C maximum and 6.9^0C daytime average in the green-all case while for the green-wall case these numbers become 3.9^0C and 2.5^0C, respectively" (Alexandri and Jones, 2008, p. 486). "When both walls and roofs are covered with vegetation, reaching up to 8.4^0C maximum temperature decrease for humid Hong Kong" (Alexandri and Jones, 2008: p. 493).

According to Sheweka and Magdy (2011) vertical greenery systems also provide environmental benefits by enabling control of water runoff from the building roofs and minimizing the sound pollution in the urban areas by acting as a sound barrier. Environmental benefits of the vertical greenery systems further extends to air quality improvement by reducing the concentration of airborne particles and absorbing gaseous pollutants (Sheweka and Magdy, 2011). Green facades facilitate tolerable substitute environment for urban vegetation and inhabitant wildlife (Sheweka and Magdy, 2011). Some of other

possible benefits that that be gained from green walls include enhancement of urban biodiversity and urban food production (Loh, 2008).

2.2 Economic Benefits

Vertical greenery systems vastly contribute to reduce energy cost of heating or cooling of a building by acting as effective shading to the building facade (Sheweka and Magdy, 2011; Loh, 2008). The degree of the economic benefit depends on number of factors including climatic conditions, distance from sides of buildings, characteristics of the building envelope and configuration of the greenery cover (Green Roofs for Healthy Cities, 2008). Effective use of vertical greenery systems can contribute to significant reduction in building cooling load. According to Wong et al. (2010a) in tropical climates maximum reduction of 11.58^0C of wall surface temperature can be obtained, which will greatly impact on reduction of building energy consumption.

Vertical greenery systems also help to reduce the extent of the use of storm water drainage infrastructure of the building (Sheweka and Magdy, 2011). In addition, vertical greenery systems "protects exterior facade finishes from UV radiation, the elements, and temperature fluctuations that wear down materials" (Green Roofs for Healthy Cities, 2008, p: 16) which will result in reduced cost on the painting materials and other finishes (Sheweka and Magdy, 2011). Vertical greenery systems can be further used as a green marketing tool which will provide indirect economic benefits (Green Roofs for Healthy Cities, 2008).

2.3 Social Benefits

Enhancing the visual richness of the environment with plants can be considered as social benefits as greenery effect on human psychology and enable stress releasing which result in health benefits (Sheweka and Magdy, 2011; Loh, 2008). "Plants can generate restorative effects leading to decreased stress; improve patient recovery rate and higher resistance to illness" (Sheweka and Magdy, 2011: p. 596). Thus, visual and physical contacts that can be created by vertical greenery systems can result in direct social benefits of the occupants in the building as well as the general public.

In summary, vertical greenery systems can be considered as an upcoming conception of incorporating greenery into built environment mainly in urban settings in which its applications, benefits and technical information are yet to be fully explored and exploited to gain optimum benefits (Wong, Tan, Tan et al., 2010b; Loh, 2008).

3   CLASSIFICATIONS OF VERTICAL GREENERY SYSTEMS

Vertical greenery systems are designed and developed in many different configurations based on its field aspects and system requirements. Thus, vertical greenery systems different from each other based on their formations and arrangements. Many researchers have proposed classifications considering fundamental design criteria of these systems. This section provides explanation on different classifications proposed by researchers.

Most of the researchers have classified vertical greenery systems into two main sections namely; green facades and living walls (Dunnett and Kingsbury, 2004) (Perez, Rincon, Vila et al., 2011) (Green Roofs for Healthy Cities, 2008) (Perini, Ottele, Fraaij et al., 2011) (Perini and Rosasco, 2013) (Jaafar et al., 2011). In green facades plants are rooted on the floor whereas in living walls plants are rooted on a vertical base which is attached to the building facade (Dunnett and Kingsbury, 2004). Francis and Lorimer (2011) introduced bio walls as category of vertical greenery systems in addition to green facades and living walls. Chen, Li, and Xiaohu (2013) have also proposed the same classification in their study. According to that bio wall can be a green facade or a living wall but which is constructed on an indoor wall of a building (Chen et al., 2013).

Perez et al. (2011) have classified green facades into three different systems namely; traditional green facades, double skin green facade or green curtain and perimeter flowerpots. Vertical greenery systems with "climbing plants or hanging port shrubs are developed using special support structures, mainly in a directed way, to cover the desired area considered as traditional green facades" (Perez et al., 2011; p. 4855). The systems that use modular trellises, wired, and mesh structures provides vertical support to

plantations are categorized under double skin green facades (Perez et al., 2011). According to Green Roofs for Healthy Cities (2008) green facades are classified into modular trellis panels which use a rigid wire panel to support plants and cable and wire-rope net which use either cables and/or a wire-net.

Dunnett and Kingsbury (2004) have classified living wall systems into three sections namely; hydroponic systems, vegetation mats and living fences. Hydroponic method is based on growing plants on a nutrient based solution without using soil. Vegetation mat is a new development of living wall systems which has no direct link between plants and underlying soil and most of vegetation mats consists with drought resistant sedums. Living fences use effect of sandwich of substrate between vegetation layers with a supporting structure (Dunnett and Kingsbury, 2004). According to Green Roofs for Healthy Cities (2008) living walls are categorized into modular living walls, vegetated mat wall, bio filtration walls and landscape walls. In modular systems growing media is hold by panels attached to the vertical surface. In vegetated mat wall system growing media and plant support is made with "layers of synthetic fabric with pockets" (Green Roofs for Healthy Cities, 2008, p. 12). Bio filtration walls are designed with the purpose thermal regulation by bio-filtering the indoor air. Landscape walls are basically designed for noise reduction and slope stabilization which made by loading up material made of plastic or concrete (Green Roofs for Healthy Cities, 2008).

Loh (2008, p.10) pointed out a definition given by The Centre for Subtropical Design at Queensland University of Technology. According to that "designed, built and maintained vegetation elements associated with a building" will be considered as a living wall. Loh (2008) has classified living walls into basically four categories namely; panel system, felt system, container and/or trellis system and interior living walls. Pre-planted panels which are fixed to the facades are called panel system. In felt system growing medium consists with felt pockets along with waterproofed backing where vegetation can be fitted into it. If plants are grown in containers and climb onto trellises those systems are called container and/or trellis system. Any type of living wall system which is built inside a building is called interior living wall.

According to the classification developed by Ottele (2011) vertical greenery systems are basically categorized under two main groups based on the plants rooted into the ground or rooted into artificial substrate or potting soil. In each category direct greening is refers to the systems which use facade as the guide to grow upwards. Indirect greening refers to the use of use a supporting system for climbers to grow and climb up such as planter boxes, foams, laminar layer felt sheets and mineral wool, thus it has an air space between the facade and greening system (Ottele, 2011).

Sheweka and Magdy (2011) have classified vertical greenery systems in a different aspect which is namely; wall climbing, hanging down and module type. Wall climbing refers to the climbers planted on ground or plant box which requires minimal supporting structure. Hanging down refers to the plants with hanging down stem and need to plant in each floor and Module type refers to the latest concept of vertical greenery system. It uses short plants with a supporting structure on the facade to accommodate modules (Sheweka and Magdy, 2011).

It is clear that many researchers have classified vertical greenery systems in different ways. There are some contradictions between classifications. This is mainly due to vertical greenery systems share some similar characteristics, thus it make difficult to distinct them separately. In all classifications of vertical greenery systems growing media is a basic concern. If the roots of the plants are located on the ground and the plants are grown vertically, it is called a green facade. If the growing media stands vertically along with the building facade it is called a living wall system. The other main concern in most classification is use of vertical support system. If there is no vertical support system for the plants to climb it is called a direct system and if there is a vertical support it is called an indirect system. Living wall system is a modern technique which provides flexibility to use variety of plants. Cost for producing a living wall is much higher than cost of producing a green facade. Moreover, living walls require careful ongoing maintenance and operation compared to green facades (Greenscreen, 2012a). Selection of suitable vertical greenery system depends on the purpose of installation, climatic conditions, availability of facilities, budget limits and many other factors.

By considering the different classifications given by researchers a more detailed classification is suggested as shown in figure 01. This classification is used in this study to identify types of vertical greenery classifications in Hong Kong. This classification is developed based on the features of the growing medium and the vertical support system.

4   APPLICATIONS IN HONG KONG

Vertical greening systems are gaining popularity in Hong Kong in recent years. Population density of the Hong Kong is 6,480 persons/ km², which is a very high value of population density. Cities are filled with concrete structures of buildings and infrastructures to cater the high urban population. Therefore, Hong Kong is affected by urban heat island and lack of greenery space (Hui, 2013). Vertical greening is gaining popularity in Hong Kong as a green initiative to maximize greening effect in cities (Hui, 2013). Architectural Services Department of the Hong Kong is looking forward and exploring opportunities to integrate vertical greening systems for government buildings in Hong Kong. Moreover, Architectural Services Department is working together with related organisations and professional institutes to promote the effect of greening (Architectural Services Department, 2014). Greening, Landscape and Tree Management Section in the Development Bureau of Hong Kong is also working towards urban greenery together with Greening Master Plans (GMPs) (Development Bureau, 2014). In this paper vertical greening applications in Hong Kong are discussed under commercial applications, institutional applications, residential applications and applications in government buildings. A summary is shown in Table 2.

4.1 Commercial Applications

Citywalk 1 and Citywalk 2 Shopping Mall– Tsuen Wan

This is pioneering green project in Hong Kong jointly developed with government Urban Renewal Authority. It has become the first and largest green mall in Hong Kong. This project integrates concepts in horticulture, geotechnical, irrigation, structural engineering and create a wonderful harmony among nature and shopping. The vertical garden consist with three main components namely a frame structure, an automatic irrigation system and green panels with plant materials. The vertical greenery system is located at Citywalk 1 is 15m above from the ground level and spreads over an area of 700m². Vertical greenery system at Citywalk 2 is integrated to an interior wall in order to provide a visually pleasing and environmentally friendly atmosphere. These vertical greenery systems contribute to control ambient temperature and improve indoor air quality while acting as an insulation layer. This project won the Skyrise Greenery Gold Award in 2012 and under Hong Kong Building Environment Assessment Method Society this was rated Platinum (HK – BEAM Society) for its idiosyncratic green characteristics and designs (Greening, Landscape and Tree Management Section, 2012) (Citywalk, 2015).

18 Kowloon East Building - Kowloon Bay

This is a 28 story commercial building serving various spaces including offices, residential spaces, retail spaces and a car park. Extensive vegetation has been introduced into exterior and interior facades of the ground floor and outer edge of the car park from 1/F to 8/F floors which positioned at the lower segment of the tower, which provides environmentally sustainable feature into to an industrial area. In here vertical greenery system is integrated with the aluminium and stone cladding to create a seamless combination of prefabricated units. It was made up with planting panels with low maintenance plant materials and automatic irrigation system. The project expectation is to create a visually pleasing environment in order to improve the quality of life of occupants as well as the pedestrians on the street level by contributing a greening effect to the building surrounding. In addition, the greenery cover reduces the suspended particulates in the car park and improves the air quality of the environment (Greening, Landscape and Tree Management Section, 2012).

The Hennessy - Wan Chai

The Hennessy is a 29 storied building which cater varies functions including commercial, retail and dining. The vertical greening system is located at two different areas, each facing the busy streets on both sides one facing Hennessy Road and the other Johnston Road. The vertical greenery system covers a total area about 150m² which is developed from 15m above ground level. The system consists with a variety of plant materials facilitated by an automatic irrigation system on a base structural frame attached to the building shell. Pre-fabricated planting troughs enable flexibility of use of different shrubs and ground covers. The vertical greening facing Hennessy Road consist with three planter boxers within the green wall system to allow for planting of small trees. These trees give volume to the design and create a sculptural quality to the green wall. At Johnston Road, green wall is smaller in scale, but more

variety in colours and textures which is designed to greet visitors of the building (Greening, Landscape and Tree Management Section, 2012).

4.2 Institutional Applications

Teaching Hotel Complex, The Hong Kong Polytechnic University - Tsim Sha Tsui East

This project consists with a hotel, a school (the School of Hotel and Tourism Management) and staff quarters. Hotel lobby consist with a three story high interior vertical green wall which adopted by hilly topography of Hong Kong inspired by an organic design. This is one of the largest interior green walls in Asia with 15 m height and 30 m long. In order to create an ideal environment for the green wall natural light setting and integrated irrigation system is provided. Variety of plants including tropical and sub-tropical plants are selected and vertically installed according to their natural habitat. For instance, herbaceous epiphytes (Anthurium, Philodendron) and shrubby epithytes (Medinilla and Scheffl era) are installed at the top. Plants growing near forest streams (Spathiphyllum, Aglaonema and Ludisia), including the rheophytic Phyllanthus myrtifolius grown in the streams of Sri Lanka, are installed in the lowest parts. Many hanging plants like Rhipsalis, Hoya, Dischidia and Aeschynanthus, which are growing in the wild on tree branches, are also installed (Greening, Landscape and Tree Management Section, 2012).

Ng Yuk Secondary School

This project consists with an extensive green roof and a simple vertical greening system. The main feature in these greening systems was use of recycle materials for construction. Green roof and vertical greening system both provided with automatic irrigation system and solar panel system (Development Bureau, 2014).

4.3 Residential Applications

The Hermitage, Kowloon

External facade of the building is integrated with hanging greenery to enhance the aesthetic appearance of the building. Vertically built planters are surrounded with decorative metal frame attached to the green facade which fit into the facade arches creates a classical architectural beauty to the building (Greening, Landscape and Tree Management Section, 2012).

Avignon - Tuen Mun

In this project vertical greening is integrated in several locations including external wall near tower 1 and 2, enclosed wall at banquet room, enclosed wall at banquet room, enclosed wall along the corridor of clubhouse, external wall near the entrance to the house area, external wall of the lift machine room at the roof of clubhouse, and climbers planted on the roof of clubhouse with the aim of maximising the green areas. Automatic irrigation system is installed for easy maintenance of vegetated spaces (Greening, Landscape and Tree Management Section, 2012).

4.4 Government Building Applications

Electrical and Mechanical Services Department Headquarters, Kowloon Bay

This is a redevelopment project which was completed in 2004. Some parts of the existing building were demolished and the main elevations of the external walls were converted into environmental facades. In this living walls G.M.S. structural frames fix the pre-vegetated panels into the structural wall. The design theme of the building was sustainable use of energy and space. This project experiments on effect of impact of green architectural features on spatial quality and energy efficiency. The panels are 1500mm / 2000mm long and 500mm high and are inserted into the G.M.S. structural frame. The system consists of 2 sets of solar powered irrigation system with 4 solenoid valves (Architectural Services Department, 2014) (Greening, Landscape and Tree Management Section, 2012).

Fire Station-cum-Ambulance Facility - Cheung Yip Street, Kowloon Bay

This project consists with a six-storey building and a single-storey building within the area of 2,250 m2 to support urban search and rescue operation. In this project greenery system is well integrated to the fore station. Up to 43% of site is covered with green roofs and green walls (Architectural Services Department, 2014).

Many government authorities in Hong Kong are looking forward to encourage building developers to integrate vertical greenery systems by adopting more sustainable building practices. It is clear that modular living wall systems have become more popular in Hong Kong. This is mainly due to its design flexibility of modular living walls to use at different heights, flexibility in integrating into existing structures and flexibility in using variety of plants. Vertical greenery applications in Hong Kong shows the emerging interest of integrating vertical greenery systems into all types of facilities including commercial, institutional, residential and government sectors.

5   SELECTION OF PLANTS

Proper selection of plants is a critical success factor of vertical greenery systems. Selection of suitable plant species depend upon many factors such as climatic condition, orientation, wind effect, type of the soil, characteristics of the container, requirement of water and nutrient, neighbouring plant materials and preferred visual effect. Native plants should be given priority in selecting plant species as they are well adapted to local weather condition. Use of mixture of plant species provides diversity and seasonality (Greenscreen, 2012a). Plants can be selected to cater the functional requirements of building, for instance a vine screen or ivy screen can be used as an effective sunscreen (Hoyano, 1988). Regular maintenance should be carried out appropriately to maintain desired visual effect of the green facade (Greenscreen, 2012b).

Ivy (Hedera helix) covered walls are a common application in Hong Kong, especially in sub-tropical regions of China. Ivy cover on building walls can reduce the surface temperature by enhanced evaporation. It also protects the external walls from direct solar radiation. As ivies just naturally climb upward on the facade additional sustaining arrangements are not required to hold ivies. Thus, ivy-covered walls have a simple configuration with the ivy canopy (leaves) and the root grid as major components of the system (Zaiyi and Niu, 1999).

Low maintenance requirement and suitable for thin growing medium were the major considerations of selection of plant species for Ng Yuk Secondary School project. In order to accommodate limited structural loading ability, light weight (approximate 100 mm thick) growing substrate on detachable planters was used. Major plant species used in this project included Chlorophytum comosum, Sansevieria trifasciata 'Hahnii' and Tradescantia zebrine (Development Bureau, 2014).

A research study carried out in Sha Tin Sewage Treatment tanks, found showed that Quisqualis indica as the best growing plant and it had reached to the upper edge of the tank during few months. Antigonon leptopus and Wisteria sinensis found as other fast growing species. However, they are tending to deciduous lost some of its foliage in winter warmth and rainfall in summer the leaf cover will resume. In addition, colourful designs can be combined to vertical greenery designs by integrating plants such as Pseudocalymma alliaceum, Pyrostegia venusta and Podranea ricasoliana (The HKIE Civil Division, 2011).

At Electrical and Mechanical Services Department Headquarters - Kowloon Bay living walls was composed using pre-vegetated panels using G.M.S. structural frame to fix into the wall. "Modular panels are comprised of HDPE containers, irrigation device, growing medium and vegetation" (Greening, Landscape and Tree Management Section, 2012, p. 37). Species used in the living wall includes Tradescantia spathacea (Compacta), Peperomia obtusifolia, Asparagus densiflorus (Sprengeri), Schefflera arboricola (Variegata) and Chlorophytum comosum (Variegatum) (Greening, Landscape and Tree Management Section, 2012).

According to the Geotechnical Engineering Office most commonly used climbers in Hong Kong include Bougainvillea spectabilis (Beautiful Bougainvillea), Duranta erecta (Golden Dewdrops), Embelia ribes (White-flowered Embelia), Ficus pumila (Creeping Fig), Parthenocissus dalzielii (Diverse-leaved Creeper), Smilax glabra (Glabrous Greenbrier) (Geotechnical Engineering Office, 2011).

6   CODES AND STANDARDS

As vertical greenery concept is relatively new there are no standard technical guideline established yet. "System selection, design, plant selection, maintenance and client/owner education" should be properly performed in order to attain a successful green wall (Greenscreen, 2012a, p. 21). Number of design considerations and technical requirements has been identified in 'Advanced Green Facade Design: White Paper version' (Greenscreen, 2012a). According to that a designer should be well aware on opportunities and the limitations of the project.

In addition to the above factors scopes of contractors, contractor qualifications and training and experience on similar projects contribute to successful implementation. Designers and contractors should be carefully selected whom are well-known with the mechanism of vertical greenery systems. Linear project management is also becoming compulsory to run the project smoothly and for successful completion. Having proper written maintenance specifications and procedures is vital for successful operation of the vertical greenery system (Greenscreen, 2012a).

Even though proper standards and guideline are not established yet, there are number of standards for green roofing systems which can be successfully adapted to vertical greenery systems as both systems share some similar characteristics. According to the ASTM E2777-14, Standard Guide for Vegetative (Green) Roof Systems, green roofs should fulfil many technical requirements for successful application (ASTM International, 2014). The principle requirements from ASTM E2777-14 are shown in Table 1, which are applicable to vertical greenery systems.

Approval Standard for Vegetative Roof Systems, Class Number 4477 evaluates the performance of vegetative roof systems in relate to fire, structural deck, foot traffic and water leakage. Combustibility from above the roof deck will be assessed by performing the fire test of the roof covering using the spread of flame test. Combustibility from below the roof deck will be also assessed for acceptance of the construction material calorimeter test. Water leakage resistance test will be conducted to determine the water migration resistance through roof membrane (FM Approvals LLC, 2010). These tests can be successfully adopted with minor modifications as standard tests for vertical greenery systems to enhance the performance and structural stability of vertical greenery systems.

7   CONCLUSION

Hong Kong is facing heat island effect and air quality issues as it is very much congested with concrete structures. Maximization of the greenery coverage especially in city centers is a necessity. Government sector as well as private sector is looking forward to integrate greenery into their new projects and also for existing projects. In present, many vertical greenery projects can be found throughout Hong Kong in different scales in commercial, institutional, residential and government buildings. The target of many projects is to contribute to greening effect to uplift the quality of living environment, to gain air quality improvement in congested city centers, to control ambient temperature, to gain energy benefits by enhancing thermal performance of the building and decorative purposes. Plant selection should be done carefully in accordance with the environmental conditions and desired visual effect as it is a main success factor of vertical greenery systems. Even though proper codes and standards are not established yet some existing codes and standards can be successfully adopted to align with vertical greenery systems. Some technical requirements on systems selection and minimum requirements that need to be taken into account can be obtained from 'Advanced Green Facade Design: White Paper version'. Furthermore, 'ASTM E2777-14, Standard Guide for Vegetative (Green) Roof Systems can be modified to cater for vertical greenery systems to ensure its proper application. More research should is required in vertical greenery in terms of Hong Kong to explore ways to maximize benefits and to ensure successful implementation vertical greenery systems.

8   ACKNOWLEDGEMENT

9 REFERENCES

AGNES, L. Y. (2012). Feasibility study of green noise barriers in Hong Kong (Masters Thesis). Hong Kong: The University of Hong Kong.

ALEXANDRI, E., and Jones, P. (2008). Temperature decreases in an urban canyon due to green walls and green roofs in diverse climates. Building and Environment, 43: pp. 480–493.

Architectural Services Department. (2011). Greening and landscaping [online]. Available at: http://www.archsd.gov.hk/archsd/html/report2011/en/greening.html [Accessed 05 January 2015]

Architectural Services Department. (2014). Low carbon building design [online]. Available at: http://www.archsd.gov.hk/archsd/html/report2013/en/low-carbon-building-design.html [Accessed 20January 2015]

Architectural Services Department. (2014). Skyrise greenery award [online]. Available at: http://www.archsd.gov.hk/en/exhibition/exhibition-list.aspx?id=1799andname=Project%20Award [Accessed 05 November 2015]

ASTM International. (2014). ASTM E2777-14, Standard Guide for Vegetative (Green) Roof Systems, PA (2014). West Conshohocken.

CHEN, Q., Li, B., and Xiaohu, L. (2013). An experimental evaluation of the living wall system in hot and humid climate. Energy and Buildings, 61: pp. 298–307

Citywalk. (2015). About Citywalk [online]. Available at http://www.citywalk.com.hk/site/about [Accessed 05 January 2015]

Development Bureau. (2014). Skyrise greenery [online]. Available at http://www.greening.gov.hk [Accessed 05 January 2015]

Development Bureau, The Government of the Hong Kong Special Administrative Region. (2012). SkyriseGreenery Awards 2012 [online]. Available at http://www.greening.gov.hk/en/people_tree_harmony/doc/SGA2012%20 Awards%20with%20images.pdf [Accessed 05 January 2015]

DEWOLF, C. (2010, January 26). Green experiments in public housing [online]. Available at http://www.urbanphoto.net /blog/2010/01/ [Accessed 20 January 2015]

Drainage Services Department. (2014, September 25). Drainage and sewerage facilities [online]. Available at: http://www.dsd.gov.hk [Accessed 20 January 2015]

DUNNETT, N., and Kingsbury, N. (2004). Planting Green Roofs and Living Walls. Portland: Timber press Inc.

FM Approvals LLC. (2010). Approval Standard for Vegetative Roof Systems, Class Number 4477, June (2010).

FRANCIS, R. A., and Lorimer, J. (2011). Urban reconciliation ecology: The potential of living roofs and walls. Journal of Environmental Management, 92: pp. 1429-1437

Geotechnical Engineering Office. (2011). Technical guidelines on landscape treatment for slopes [online]. Available at: http://www.cedd.gov.hk/eng/publications/geo/doc/ep1_2011.pdf [Accessed 20 March 2015]

Green Roofs for Healthy Cities. (2008). Introduction to green walls technology, benefits and design [online]. Available at:www.greenroofs.org [Accessed 20 March 2015]

Greening, Landscape and Tree Management Section. (2012). Skyrise greenery awards 2012. Hong Kong: Development Bureau.

Greenscreen. (2012a, September). Considerations for Advanced Green Facade Design: White Paper version [online]. Available at: www.greenscreen.com/direct/Considerations/AdvancedGreenFacadeDesign_Fall12.pdf [Accessed 20 March 2015]

Greenscreen. (2012b). Recommended Plant List by Hardiness Zone [online]. Available at: http://www.greenscreen.com/greenscreenPlantList_v1.pdf [Accessed 25 Fenruary 2015]

Hong Kong Housing Authority. (2014). Kwai Chung Estate, Kwai Tsing, New Territories West [online]. Available at:http://www.housingauthority.gov.hk/en/global-elements/estate-locator/detail.html?propertyType=1andid=2826 [Accessed 05 November 2015]

Hoyano, A. (1988). Climatological uses of plants for solar control and the effects on the thermal environment of a BUILDING. Energy and Buildings, 11: pp.181 - 199.

HUI, S. C. (2013). Benefits and potential of vertical greening systems. A lecture at the CIBSE Hong Kong Branch Annual General Meeting held on 5 March 2013.

JAAFAR, B., Said, I., and Ras, M. H. (2011). Evaluating the Impact of Vertical Greenery System on Cooling Effect on High Rise Buildings and Surroundings: A Review. 12th International seminar on Environment and Architecture (p. 8pp). Indonesia: University of Brawijaya.

KOHLER, M. (2008). Green facades—a view back and some visions. Urban Ecosyst, 11: pp. 423–436.

Leisure and Cultural Services Department. (2014, October). Hong Kong Ornamental Plants [online]. Available at:http://www.lcsd.gov.hk/en/green/greeningknowledge/plantphoto/shrub_passage/shrub_28.html [Accessed 05 January 2015]

LOH, S. (2008). Living Walls – A Way to Green the Built Environment. BEDP Environment Design Guide, 1(TEC 26), 1-7. Retrieved from http://www.environmentdesignguide.com.au/

LOH, S., and Stav, Y. (2008). b. Subtropical Cities 2008 Conference : From Fault-lines to Sight-lines : Subtropical Urbanism in 20-20 (pp. 1-10). Brisbane,Queensland: State Library of Queensland.

OTTELE, M. (2011). The green building envilop: Vertical greening (Doctoral Thesis). Netherland: SiecaRepro.

PEREZ, G., Rincon, L., Vila, A., Gonzalez, J. M., and Cabeza, L. F. (2011). Green vertical systems for buildings as passive systems for energy savings. Applied Energy 88: pp. 4854–4859.

PERINI, K., and Rosasco, P. (2013). Cost benefit analysis for green façades and living wall systems. Building and Environment, 70: pp. 110-121.

PERINI, K., Ottele, M., Fraaij, A. L., Haas, E. M., and Raiteri, R. (2011). Vertical greening systems and the effect on air flow and temperature on the building envelope. Building and Environment, 46: pp. 2287-2294.

SAFIKHANI, T., Abdullah, A. M., and Ossen, D. R. (2014). A review of energy characteristic of vertical greenery systems. Renewable and Sustainable Energy Reviews, 40: pp. 450–462.

SHEWEKA, S., and Magdy, N. (2011). The living walls as an approach for a healthy urban environment. Energy Procedia, 6: pp. 592–599.

The HKIE Civil Division. (2011). 3+1 Approach for Greening Works at Sha Tin Sewage Treatment Works [online]. Available at: http://www.dsd.gov.hk/EN/Files/DOC/215.pdf. [Accessed 05 January 2015]

WONG, N. H., Chen, Y., Ong, C. L., and Sia, A. (2003). Investigation of thermal benefits of rooftop garden. Building and Environment, 38: pp. 261 – 270.

WONG, N. H., Tan, A. Y., Chen, Y., Sekar, K., Tan, P. Y., Chan, D., Chiang, K., Wong, N. C. (2010a). Thermal evaluation of vertical greenery systems for building walls. Building and Environment, 45: pp. 663–672.

WONG, N. H., Tan, A. Y., Tan, P. Y., Sia, A., and Wong, N. C. (2010b). Perception Studies of Vertical Greenery Systems in Singapore. Journal of Urban Planning and Development, 04: pp.330–338.

ZAIYI, L., and Niu, J. L. (1999). Study on thermal function of Ivy-covered walls. Building Simulation'99. Japan: Kyoto University.

10 ANNEXURE

*Table 1: Principal requirements of vertical greenery systems from ASTM E2777-14. **Source: (ASTM International, 2014)***

Design Considerations	
Maintenance	Detailed written maintenance procedures manual should include instructions for • Operation of irrigation systems • Directions for proper weeding and fertilization • Methods for recognizing and dealing with commonly encountered problems
Performance	Shall convey to the owner a written description of the system showing specified performance characteristics
Longevity	• Degradation or loss of function of components of the vegetative • Premature failure
Structural Loads	• Effect on the live, dead and seismic loads
Access	• Maintenance and other personnel shall be provided with a safe means of access • Safe access to that equipment
Wind Resistance	• Damage by wind

Table 2: Summary of applications of VGSs in Hong Kong

Project	Aspects of vertical greenery cover	Vertical greenery system characteristics	Classified type
Commercial Applications			
Citywalk 1 and Citywalk 2 Shopping Mall– Tsuen Wan	Citywalk 1 - 15m above from the ground level, covering area of 700m², approximately 90% of the exterior facade of the top floor Citywalk 2 – Interior wall of a building	- Structural frame - Automatic irrigation system - Green panels with plant materials	Modular living wall
18 Kowloon East Building	Covering divisions of exterior and interior facades of the ground floor and 1/F to 8/F outer edge of the floor slab	- Prefabricated units of Aluminum and stone cladding -Planting panels with low maintenance materials - Automatic irrigation system	Modular living walls
The Hennessy	Located 15m above from the ground level covering area of 150m²	- Structural frame attached to the envelope of the building - Pre-fabricated planting troughs - Automatic irrigation system - Consist with three planter boxers within the green wall	Modular living walls
Institutional Applications			
Teaching Hotel Complex, Hong Kong Polytechnic University	Consist with a 15m high and 30m long interior green wall covering approximately covering 50% of the interior facade	- Structural frame - Initrated irrigation system - Green panels with plant materials - Natural light setting	Modular living walls
Ng Yuk Secondary School	Located at the ground floor exterior facade of the building	- Structural frame - Green panels with plant materials using recycle materials - Automatic irrigation system - Solar panel system	Modular living walls
Residential Applications			
The Hermitage	Located at the upper floor exterior facade of the building, integrated with hanging greenery covering approximately 8% of the interior facade	- Structural frame - Automatic irrigation system - Vertically built planters surrounded with decorative metal frame - Hanging down greenery	Modular living walls and Traditional green facades
Avignon	Vertical greening is integrated in several locations and climbers planted on the roof	- Structural frame - Green panels with plant materials - Automatic irrigation system - Climbers planted on the roof	Modular living walls and Traditional green facades
Government Building Applications			
Electrical and Mechanical Services Department Headquarters	Covering approximately 50% of the exterior facade including five sections of green walls	- Pre-vegetated panels that are affixed to a structural wall with G.M.S. structural frame - Solar powered irrigation system with 4 solenoid valves	Modular living walls

Project	Aspects of vertical greenery cover	Vertical greenery system characteristics	Classified type
Fire Station-Cum-Ambulance Facility	Vertical greening is integrated in several locations and up to 43% of site is covered with green roofs and green walls	- Structural frame - Automatic irrigation system - Green panels with plant materials - Self climbing plants	Modular living walls and Traditional green facades

Figure 1: Proposed classification of vertical greenery systems

Vertical Greenery Systems

Green Facades

Traditional green facades

Self-climbing plants or hanging port shrubs developed directly on the facade without any supporting system

Double skin green facade (Green curtain)

Systems that use modular trellises, wired, and mesh structures provides vertical support to plantations

Living Walls

Modular living walls

Growing media is hold by panels attached to the vertical surface

Hydroponic systems

Based on growing plants on a nutrient based solution without using soil

Vegetation mats

No direct link between plants and underlying soil and most of vegetation mats consists with drought resistant sedums
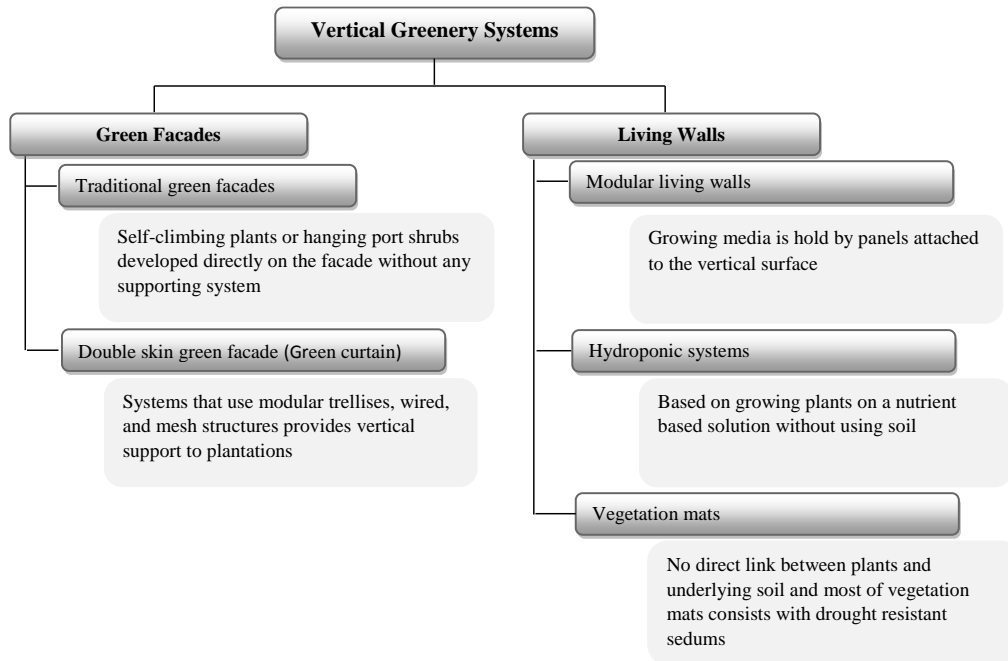
Figure 1: Proposed classification of vertical greenery systems

58: The investigation of practice on green residential buildings in Shenzhen, China

LIQING ZHANG[1]; LIBEN JIANG[2]

1. University of Central Lancashire, Preston, PR1 2HE, UK. Email: lqzhang@uclan.ac.uk
2. University of Central Lancashire, Preston, PR1 2HE, UK. Email: ljiang2@uclan.ac.uk

Construction industry throughout the world has been one of the biggest contributors to the energy consumption and CO2 emission, while the world is facing serious energy resources shortage. Sustainable development of construction has been seen in the past years to reduce the negative impacts on the environment but at the same time to assure the function of buildings was properly delivered. Current literature showed that majority of studies focused on the commercial and public green buildings, while for the residential buildings, research was mainly focused in developed countries such as Great Britain, America and Australia. There were generally few studies on the specific high-rise residential buildings which are common in the big cities with high-density population in the developing countries. This paper will investigate the practice of green buildings for residents in Shenzhen, China, which is one of the six Tier 1 cities with urban population of more than 10 million and GDP of more than USD 24,000 per head. The study will investigate the attitude of potential customers and the satisfaction of existing customers towards them, and will identify the opportunities and challenges of green residential construction in Shenzhen from the point of view of developers and managers. The results will show some inside views of green residential buildings from driving forces (consumers), and provide additional suggestion for the developers and local governmental agency in the future development.

Keywords:

1. INTRODUCTION

The energy demand for constructing and operating those buildings is inevitably posing threats to our environment in terms of natural recourse consumption and CO2 emission associated with those activities (Yudelson & Meryer, 2012, P.3; Allen & Thallon, 2011, P. 10). The construction activities could also have great impact on people's health (Nahmens, 2009) since they resulted in a large amount of pollution and waste from the time when houses are being built to the time when they are used (Horvath, 2004; UNEP, 2007; Wu & Low, 2010). Out of the concern for environment and for the well-being of humans, it is quite necessary to make the whole process of residential construction environmentally friendly.

Previous studies on green residential construction mainly discussed its development and practice in developed countries such as Great Britain, America and Australia. However, there were not many studies which have set out to explore the practice of green residential construction in developing countries, such as China. Many of them adopted a theoretical perspective instead of a practical one. Therefore, there is a gap to fill in. As we all know, China is a developing country with largest population. The economic booming in the past twenty years saw more houses needed than those in any other countries and thus created a higher pressure on our Earth by building a much larger number of houses. It is therefore especially important to understand how green residential construction has been practiced in China.

Yet, we know that China is a large country geographically and it is almost impossible to collect data in every city to show the general condition of green residential construction in the whole country. The scope of the study was therefore narrowed down to focus on a specific city of China, the city of Shenzhen, which is one of the six Tier 1 cities with urban population of more than 10 million and GDP of more than USD 24,000 per head. Shenzhen is a newly developed city since 1980 as a Special Economic Zone and its population has increased dramatically in the short period of a few decades. Starting with 30,000 in 1980, the population living in the city increased to 4 million in 1994. Ten years later, the number doubled and exceeded 8 million. By 2012, the population was more than 10 million (SZTJ, 2013). The sharp increase and the large population lead to a high demand for houses and a huge increase in the construction activities. According to the statistics of the city, the floor space of buildings under construction by the end of 2008 was about 54 million square meters while the figure had increased to be more than 97 million square meters by the end of 2012(SZTJ, 2013). Such large-scale construction activities in the city of Shenzhen showed that it urgently needs green residential construction to ease the heavy dependence on natural resources and energy.

This paper, therefore, aims to investigate how green residential construction has been practiced in the city of Shenzhen, China. Questionnaires and face-to-face interviews were taken place to investigate (1) to what extent the green residential construction has been practiced and their specific aspects in practice; (2) the attitude of potential & existing consumers toward green residential construction; (3) the opportunities & challenges for green residential construction in the city.

2. METHODOLOGY

As for the research methods, the study combined questionnaires and interviews. Questionnaires were developed and sent by email to 30 housing developers that have housing projects in the city of Shenzhen. The questionnaires mainly asked the housing companies about the situation that they practiced green residential construction. If they gave positive answers, they were also invited to share why and through what specific actions they did so. As a result, 10 housing developers filled in the questionnaire and sent them back with their opinions.

Interview was conducted in person to obtain information about what the potential customers considered to buy houses with green construction practices. The questions were all open-ended ones. Another set of interview was conducted within the existing residents of green houses, who came from three different green communities in different districts of the city. 30 interviewees were contacted as potential and existing customers respectively.

Telephone interviews were finally conducted with 3 managers in the industry to investigate the opportunities and obstacles for green house construction. Two of them were project managers who have been responsible for green projects; while one was the executive manager of a construction company. All three managers had at least 5 years of working experience in the housing industry.

3. RESULTS AND DISCUSSION
a. Case 1: Questionnaires from Developers

The development of green residential project in the city of Shenzhen was questioned among the 10 bosses (owners) of selected construction companies. Results showed that 5 companies(50%) have developed green residential projects, and 3 companies(30%) are not currently developing but planning to develop green residential projects in the future, while the remaining 2 companies(20%) are not developing and do not plan to develop green residential projects. Within the 8 companies planning to develop or having developed green residential projects, 5 companies (62.5%) stated that they did so because of the requirement from government; while 3 companies (37.5%) said that they did so mainly because of positive market prospects. In other words, they believed developing green residential projects would help them to make profits. Meanwhile, no companies are driven to develop green residential projects because of "green" belief or environmental protection awareness.

Identifying the "Green" characteristics was included in the questionnaires. 5 companies have included the characteristics of conserving land resources and providing good exterior facilities but they failed to incorporate other green characteristics such as saving water and conducting operation management to reduce the negative effects on the environment and people living near the construction site. For example, noise, dust and construction waste were commonly brought by construction

House decoration is one of the important factors which will directly affect the customers' choice, and this was questioned as well. The responses of the 5 companies that have developed green projects indicated that 4 out of 5 companies (80%) would like to give customers their own choice to decorate their houses at their wills, while the remaining 1 company (20%) has tried to decorate the houses using environment-friendly material, as they believed that decorating houses collectively and using environment-friendly materials can be beneficial to the environment. Even though, the percentage of decorated houses was 30%, while the remaining 70% houses were undecorated.

Incentives play very important roles in promoting green housing projects, and developers were asked their availability in the city. Feedback showed that majority of the contacted companies (4 out of 5) did not receive any incentives from either local or central government. The only lucky one received subsidy from local government because of the application of using renewable energy in buildings, i.e. solar thermal energy.

The concept of green residential projects was tested within the dynamic housing market. Only 40% of the companies admitted that the green projects were more appealing to customs than the traditional ones, while another 60% were not sure about its marketing. The confidence level directly affected their further investment in green residential projects and their corresponding response for that was in line with the marketing results. Interestingly, no companies gave definite answers that they will not develop green house in the future. The results also showed that there were some general reasons for the companies to go forward with green residential projects, i.e., they believe that being green and environment-friendly will be a trend and will be more and more popular in the future. The confidence on the market demands requires them to continue developing. There were also obvious reasons for the companies not to be involved further. First, they believed that the current acceptance of customers toward green residential projects is low and a majority of consumers have no idea about them or would not purchase them because of higher prices. Also with low attraction to customers, it is hard for developers to turn the high cost into profits in the short period of time.

b. Case 2: Interviews with Potential Customers

The interview took place with potential customers as they would be driving force for the future green residential houses. The result showed that about 87% of the respondents replied that they did not know exactly about the idea and felt that the housing project with green construction would have higher rate of green coverage in the community or is good for the environment. In other words, they only got a general idea, but failed to know what kind of specific actions it should incorporate. The understanding of customers toward green residential construction is still superficial and needs to be improved in order to further promote green construction in the housing industry, for example, via dissemination and/or education.

The interview result also indicated the attraction of potential customers to green houses is not obvious. Only 40% of the respondents said that they would be willing to choose green houses in their purchasing decision. By contrast, the remaining 60 % of the respondents are not willing to do so, because they believed that green

houses would generally cost more than traditional house per square meters. The lack of understanding can also account for the low attraction of green houses.

c. Case 3: Interviews with Existing Residents in Green Houses

The feedback from existing residents in the so called "green residential housed" is vital and they were considered as piloting customers for the new style of living. The interviews with the existing residents show that 73% of the existing residents replied that they were satisfied with the living conditions of the green houses. The specific aspects they are satisfied with included: (1) good indoor environment provided by good ventilation and designs to ensure appropriate lighting levels; (2) good air quality enhanced by the high rate of green coverage in the neighbourhood; (3) providing convenient much-needed facilities around, i.e., schools, hospitals/clinics, shopping malls, supermarkets, and public transportation.

Additionally, there was still room for improvement. The respondents surveyed pointed out the following aspects to be improved: (1) the noise level can be further controlled. This, to some extent, complied with the result of the questionnaire that only 60% of housing developers surveyed used specialized building materials to reduce the level of noise; (2) the waste created by the residents in the neighbourhood was also advised to be classified more carefully and collected separately so that some can be recycled. Overall, the existing residents surveyed gave positive comments on the green houses.

d. Case 4: Telephone Interviews with Managers in the Green Housing Industry

The interviews with three managers showed the following opportunities: (1) More and more customers will choose green houses in the future, which means the market prospect for green residential construction will become better sooner or later. The interview with the potential customers showed that only 40% of the consumers are willing to buy green houses. Yet, the managers interviewed believed that this percentage will increase in the future. The underlying reason they gave was that along with the increase of their income, they would naturally want to live a life with higher-quality, part of which can be met by living in green houses. In addition, when the society continues to develop, people's awareness to protect the environment will also increase, which accordingly fuel the development of green residential construction. (2) Considering that China has a big duty to reduce CO_2 emission under international agreements, Chinese central and local governments will put more efforts in the development of green construction in housing industry. They have also realized the environmental problems caused by the boom of housing construction and have issued some regulations to relieve the environmental stress. They will continue to enhance the implementation of related rules and regulations in the future.

The interviews with three managers also found the following obstacles: (1) the cost of certain types of environmentally friendly material serves as the financial barriers to green residential construction. The green residential houses usually have to be built in different ways with different materials at some aspects. For instance, in order to conserve energy and use renewable energy like solar energy, certain equipment has to be installed and extra cost is inevitable. Such higher cost will turn into the higher price of the built house, which hinders some consumers from buying it although there will be some financial benefits in the later operation stage. (2) Currently consumers failed to have adequate understanding of the concept of green residential houses. They don't know clearly what construction practices or characteristics green residential houses must incorporate, neither their advantages over traditional houses. (3) The current financial incentives from the central and local government are not enough. Currently, there is some subsidy for green efforts to conserve energy. Yet, there is no subsidy for other green attempts such as conserve water and improve good indoor environment.

4. CONCLUSIONS

To sum up, it can be seen that green residential construction has actually been practiced in the city of Shenzhen, China, but on a relatively small scale. Its market is not mature yet due to the following reasons

- Its perception among potential customers is still low and not many people understand green residential houses and their advantages clearly.
- The incentives from governments are still limited and currently incentives will only be awarded towards the application of renewable energy technologies.
- The development of green construction is still hindered by higher financial cost.

However, it can also be concluded that people who have been living in green houses mostly enjoyed the living experiences and believed that living in green houses have clear advantages. Under such situation, the joint efforts of housing developers and government will make the future of green residential construction even more prospective, with the promotion on the public awareness and more incentives and rigorous enforcement of its regulations for green residential construction.

5. REFERENCES

ALLEN, E.& Thallon, R. (2011). *Fundamentals of Residential Construction*, 3rd Edition. New York: John Wiley& Sons.

NAHMENS, I. (2009). From lean to green construction: a natural extension. PhD thesis, Louisiana State University, Baton Rouge, LA.

SZTJ. (2013). Households, Population, Birth, Death and Natural Growth(1979-2012). The Bureau of Statistics of Shenzhen. Available at: http://www.sztj.gov.cn/nj2013/indexce.htm

SZTJ. (2013). Households, Population, Birth, Death and Natural Growth(1979-2012). The Bureau of Statistics of Shenzhen. Available at: http://www.sztj.gov.cn/nj2013/indexce.htm

SZTJ. (2013). Main Economic Indicators on Construction Enterprises（2008-2012. The Bureau of Statistics of Shenzhen. Available at:http://www.sztj.gov.cn/nj2013/indexce.htm

WU, P. & Low, S.P. (2010). Project management and green buildings: lessons from the rating Systems. *Journal of Professional Issues in Engineering Education and Practice* , Vol. 132No. 2, pp. 64-70.

YUDELSON, J. &Meryer,U. (2012). *The World's Greenest Buildings*. London: Routledge.

123: Climate-responsive design in contemporary Australian housing

The poetics and pragmatics in the Ball-Eastaway and Marika-Alderton houses by Glenn Murcutt

MAURICIO LECARO[1], BENSON LAU[2]

1The University of Nottingham, Department of Architecture and Built Environment,
mauricio.lecaro @alumni.nottingham.ac.uk
2The University of Nottingham, Department of Architecture and Built Environment,
Benson.Lau @nottingham.ac.uk

Glenn Murcutt is nowadays recognized as one of the most influential environmental architects of the century. His design philosophy, environmental awareness and in-depth understanding of the Australian context and vernacular architecture, have led him to become one of the leaders of critical regionalism worldwide. His buildings aim not only to provide shelter, but to lower their environmental impacts through simple, yet innovative design solutions.

Murcutt's buildings are well documented and published, nevertheless, they have not received much academic attention and limited evidence based research and publications are available to assist holistic understanding of his work. Through a critical review of two of his most celebrated projects (i.e. the Ball-Eastaway and Marika-Alderton house), the authors aimed to fill this research gap.

Although the selected houses share a similar building typology, their location, orientation, materiality and environmental requirements greatly differ. While the Ball-Eastaway was conceived as a relaxing habitat, embedded in a secluded bush land in NSW and the main design concept was to exploit the local landscape and views, the Marika-Alderton house was designed as a climate responsive shelter for an aboriginal family on the seaside of Eastern Arnhem, NT.

By conducting theoretical qualitative and quantitative analysis, the close connection between the spatial quality, environmental design strategies and performance of the two houses were thoroughly studied. Through this study, the effect of these elements on Murcutt's unique way of materialising environmentally conscious buildings was revealed. The research outcomes indicate that even though both buildings experienced occasional visual and thermal discomfort, they performed well for most of the time as intended free-running buildings, proving that their constant connection with the exterior greatly affects their internal comfort conditions.

Through his environmental design principles, Murcutt's buildings are sensibly designed to be adaptable, spatially delightful and to have a low carbon footprint, while having a continuous dialogue with nature. The significance of Murcutt's work lies precisely in this delicate liaison between his romanticism and practicality.

Keywords: Critical regionalism, environmental design, responsive architecture, free-running buildings, comfort.

1. INTRODUCTION

The significance of Murcutt's work derived from the accumulation of lifelong experimentation and experiences in designing and building climate responsive architecture. While the influence of modern architecture is irrefutable as Fromonot (2003) described, the combination of Thoreau's life principles, of living a modest life in permanent contact with nature and Murcutt's environmental awareness and profound knowledge of the Australian context and vernacular architecture, shaped his work. It is in this theoretical and physical context that Murcutt convincingly designed responsive buildings, whose elements are assembled 'responsibly to the land', as stated by Beck and Copper (2002), while harmonizing and merging with the Australian landscape.

Considering Murcutt's extensive oeuvre, this study focused on assessing two of his most renowned projects, the Ball-Eastaway house in New South Wales and the Marika-Alderton house in the Northern Territories. These houses were selected based on their similar building typology and distinctively different sites, aiming to holistically assess the relation between Murcutt's environmental design practice and their effect on the buildings' spatial delight and performance.

Initially, a qualitative analysis for both houses explored their location's climate, (based on weather data from NatHERS in Richmond, NSW and Darwin, NT) orientation, spatial arrangement and materiality aiming to understand Murcutt's design principles and how they respond to specific contexts; then, a quantitative analysis was done by computer aided modelling (in Autodesk's Ecotect and EDSL TAS), to comprehend the luminous and thermal environments of key spaces (i.e. living rooms and bedrooms).

2. SPATIAL DELIGHT IN THE BALL-EASTAWAY HOUSE

The Ball-Eastaway house is located in a remote bush land in Glenorie, NSW (33.6° S) and it was designed as a retreat for its owners. Murcutt intentionally positioned the house over a sandstone bed, and varied his distinctive north orientation to exploit the site's views (Figure 8) to create a more peaceful atmosphere.

Figure 8. Left: Exterior view by Max Dupain. Source: El Croquis (2013). Right: Plan and spatial arrangement. By Authors

The house's configuration as suggested by Farrelly (2012), responds to the sandstone's bed shape, which offered Murcutt the opportunity to lift the house off the ground on steel stilts (Figure 8), protecting the building from wildfires while providing a less invasive building process; the interior spaces were clearly defined between served spaces (i.e. bedrooms), positioned to the SW and serving spaces (i.e. living space) to the NE, intending to position the main spaces in contact with the exterior.

The section derived from a thoughtful site analysis; when the site's high rainfall and surrounding trees were considered, Murcutt recognised that conventional gutters and pipes would block, therefore a vaulted, corrugated iron roof with broad gutters (Figure 9) was his response. Additionally, he favoured for a light-weighted steel structure, (minimizing the use of timber) and corrugated iron exteriors, contrasting with the natural setting and the softer and warmer interior.

According to NatHERS (2014), the site experiences a seasonal climate having a temperature range between 39,5°C (January) and 0°C (August) and a monthly mean rainfall ranging from 122 mm (February), to 28,5 mm (July); therefore the building's orientation and envelope are essential to cope with the site's climatic conditions.

When the building's orientation is analysed in relation with the sunpath, Murcutt's intention of favouring the site's views over a valuable north orientation was shown. As Figure 9 shows, the house's orientation exposed public areas to partial daylight access during mornings, while underexposed the private ones. According to NatHERS (2014), the optimum orientation would convey in better solar access (and heat gains) during winter, while providing a better opportunity to exploit the site's prevailing winds during summer.
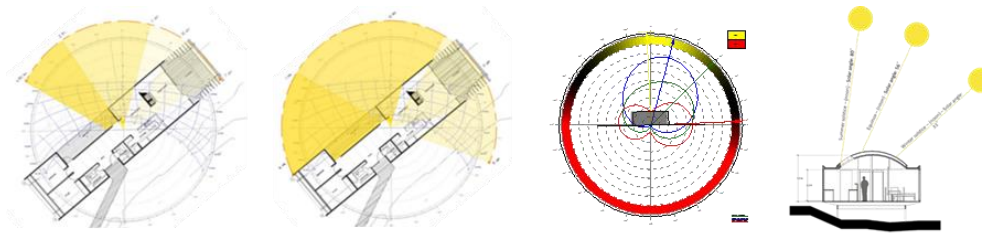
Figure 9. Left: Ball-Eastaway's orientation vs. sunpath during winter and summer solstice and optimum orientation. Source: NatHERS (2014) Right: Section vs. solar access at noon during summer solstice, equinox and winter solstice. Source: Authors

When the house's section is overlapped with the solar angles during equinox and solstices at noon, it is clear that the roof was not intended to respond to the sun as Figure 9 shows, reinforcing the argument that orientation was not a priority; nevertheless, the roofing still provides shelter from the summer's noon sunlight and heat gains, while admitting partial solar access during winter. As a free-running building, the house was designed to be cooled by natural ventilation, hence Murcutt raised it off the ground intending to improve cross-ventilation and reduce interior temperatures during summertime.

3. DAYLIGHT ASSESSMENT OF THE BALL-EASTAWAY HOUSE

Visual performance under overcast sky conditions

To assess the daylight performance of the house's main spaces, (i.e. living room and bedroom) and to ensure that the spaces were correctly day-lit, a target daylight factor of 2%, based on BSI (2008) standard guidelines, was chosen to analyse their visual performance under overcast sky conditions. As shown in Figure 10, the average daylight factor in the main spaces was above 5%, indicating that all spaces are well-day lit and no supplementary lighting from artificial sources is needed as CIBSE (1994) established.
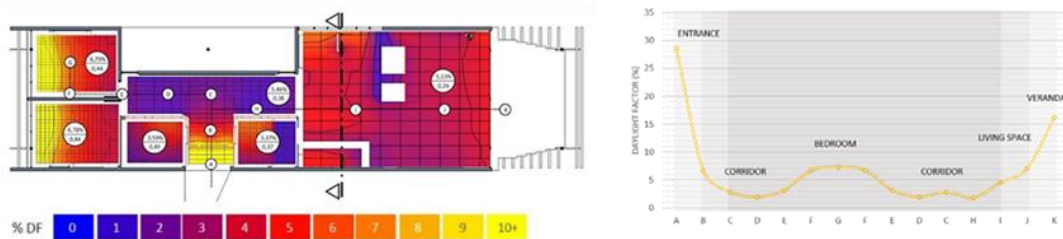

Figure 10. Daylight factor plot and section, uniformity ratios and light journey in the Ball-Eastaway house. Source: Authors

The uniformity ratios and light journey achieved (Figure 10) in the internal spaces, showed that Murcutt designed and positioned the openings intentionally to create a dynamic, yet relaxing atmosphere. Despite the house's orientation is not optimum, Murcutt was able to make a clear transition between the living space and the bedrooms; as shown, the most dramatic variation can be perceived in the main entrance, where the DF drastically lowered providing visual adaptation to the inhabitant through the corridor.

Visual performance and comfort under sunny and overcast sky conditions

To assess the illuminance distribution within the house's most occupied space (i.e. living room), illuminance was assessed at noon under sunny sky (Equinox) and overcast skies conditions, to have a broader understanding of its performance. The results were compared to CIBSE (1994) 300 lux recommendation.

As Table 5 illustrates, the high illumination levels (+680 lux average) present during sunny sky conditions in Equinox, indicates that while the space is well day-lit, a stressful atmosphere or visual fatigue might be conveyed; in overcast sky conditions, the illuminance levels significantly decreased to 280 lux average, indicating a correct daylighting that offers some visual sharpness; nevertheless, in both cases, the high illuminance levels achieved towards the opening, indicate that in order to improve the ambiance, the use of blinds or operable shading devices is desirable.

To assess the luminous intensity, the brightness contrast ratio (Hopkinson, 1966) was used to evaluate whether the house conveyed visual comfort for its occupants in the living room. Although the sky conditions on site are mostly overcast, the luminance mapping was performed under both, sunny (Equinox) and overcast skies conditions, so that a more realistic luminous environment could be evaluated.

Table 5. Illuminance (lux) plots at noon under sunny sky (Equinox) and overcast sky conditions. Source: Authors

Table 6. Luminance (cd/m2) assessment at noon under sunny sky (Equinox) and overcast sky conditions. Source: Authors
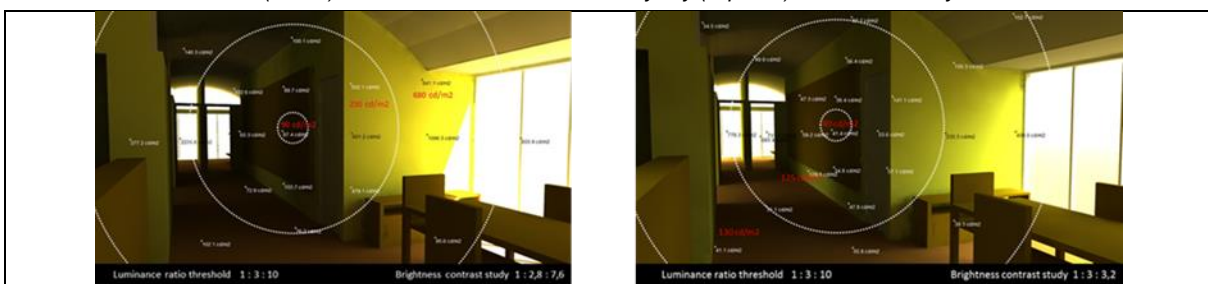
Murcutt designed the corridor as an exposition area for paintings, representing the best target to assess luminance. As Table 6 shows, the target considered yields no major visual discomfort; nevertheless and as the results demonstrate, if the target is shifted towards the dining room, the results might have significantly varied, implying that under these skies conditions the inhabitants may suffer from glare discomfort; if blinds or other external architectural features were included, a more visually comfortable space would be provided.

4. THERMAL PERFORMANCE AND SPATIAL DELIGHT IN THE BALL-EASTAWAY HOUSE

Evaluating the thermal environment of the house was essential to have a full understanding of the building's performance and its impact on comfort, especially when Murcutt's projects are designed as free-running buildings, with operable envelopes designed to adapt and as Kallenbach (2002) echoed Murcutt's words '[just as] we layer our clothing…our buildings should equally respond to their climates.'

The house's orientation and spatial arrangement pointed to an unlikely positive thermal performance, hence a model of the house was built in EDSL TAS, distributing each space as a separate thermal zone (Figure 11); simulations were performed aiming to have an overall idea of the annual performance in key spaces, nevertheless, analysing winter's performance was essential and the chimney's heat transfers were considered.

Case	Description
Case 1	Shell with 0.5 infiltration rate, no ventilation or internal heat gains considered.
Case 2	Shell with 0.5 infiltration rate + natural ventilation* (1.5 ach) with 30% aperture when resultant temperature reaches 19°C + internal heat gains.
Case 3	Shell with 0.5 infiltration rate + natural ventilation* (1.5 ach) with 90% aperture when resultant temperature reaches 19°C + internal heat gains + chimney heat gains **

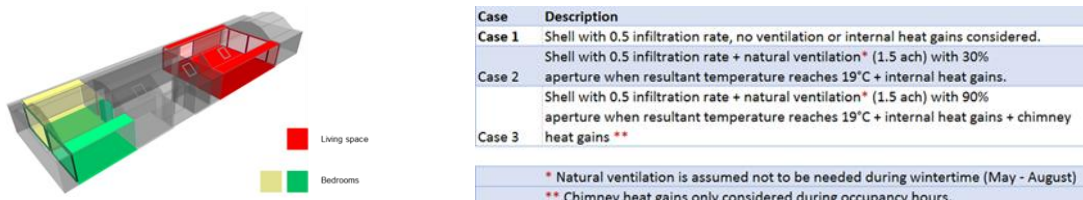|	
* Natural ventilation is assumed not to be needed during wintertime (May - August)	
** Chimney heat gains only considered during occupancy hours.	

Figure 11. Left: Thermal assessment and zoning of key spaces in the Ball-Eastaway house. Thermal assessment in EDSL Tas. Right: Summary of thermal cases examined. From: Authors

The assessment considered three possible cases (Figure 11), all having a constant natural infiltration rate of 0,50, shading as designed and varying in the levels of internal heat gains and natural ventilation rates. Case 1 was set up as a base example; Case 2 as summer's scenario with natural ventilation and heat gains; Case 3 represented winters' scenario, were all internal heat gains were included and natural ventilation was set to

occur only if the resultant temperatures surpassed the established comfortable temperature range. Aperture variation in openings was considered to recognise the influence of natural ventilation on thermal comfort.

In order to define a comfort zone, monthly average temperatures were used as a base to calculate the optimal temperature for comfort (i.e. T_{comf}) in Richmond, NSW, based on the Adaptive Model by Nicol, Humphreys and Roaf (2012).

The following assumptions were considered for the simulations:

- Weather: Energy Plus weather data for Richmond, New South Wales.
- Comfort range: winter between 19°C to 23°C, and 22°C to 27°C during summertime.
- Calendar: Annual
- Internal Gains:
    o Occupancy: two adults with heat gains assumed to be of 180W (sensible) and 100W (latent).
    o The occupancy schedule was set for 24 hours.
- Lighting: compact low-energy florescent bulbs with a total load of 2,5 W/m^2
- Equipment gains: hob, a washing machine, a dishwasher and a fridge, all with a total load of 25 W/m^2.
- Chimney sensible gains of with a total load of 40 W/m^2.
- Ventilation: during occupancy periods all openings had the same opening pattern; starting to open when the temperature reached 19°C and fully opened at 27°C.

Thermal Assessment Results

Thermal analysis outcomes were compared between both thermal zones, comparing seasonal thermal performance vs. average resultant temperatures to examine any correlations. Results were shown as a percentage of time when the resultant interior temperature ranged between 19°C to 23°C in winter, and 22°C to 27°C in summer. As

7 shows, both spaces share a similar thermal performance; nevertheless, during winter the living room's performance improved while the bedroom's plunged. The following conclusions were drawn from this analysis:

- Case 1: Annually, the spaces perform an average of 20% of the time, (except during winter when performance falls to 15%) inferring heat gains are essential to improve the thermal performance.
- Case 2: The thermal comfort in the internal spaces is within the comfort range for 25% of the time; despite heat gains improved the percentage of time within the comport range, resultant temperature was 17°C (below comfort); in summer, natural ventilation can help improve the thermal environment as the predicted resultant temperature reached 22°C.
- Case 3: represented the best scenario during winter for the living room, while unexpectedly the worst for the bedrooms; the chimney's heat gains seem to have a significant impact on the living room's thermal performance, but seemingly the envelope's airtightness is not enough, as heat gains from the chimney seemingly do not reach the bedrooms. During summer there was no perceptible improvement, signifying that natural ventilation by itself is not enough to dissipate the interior's heat. Annually both spaces performed an average of 30% of the time.

7. Seasonal thermal performance of main spaces vs. average exterior and resultant temperatures. Source: Authors

Zone	Frequency (%) of hours in comfort zone vs. seasonal average resultant temperatures.
Living space	
Bedroom	
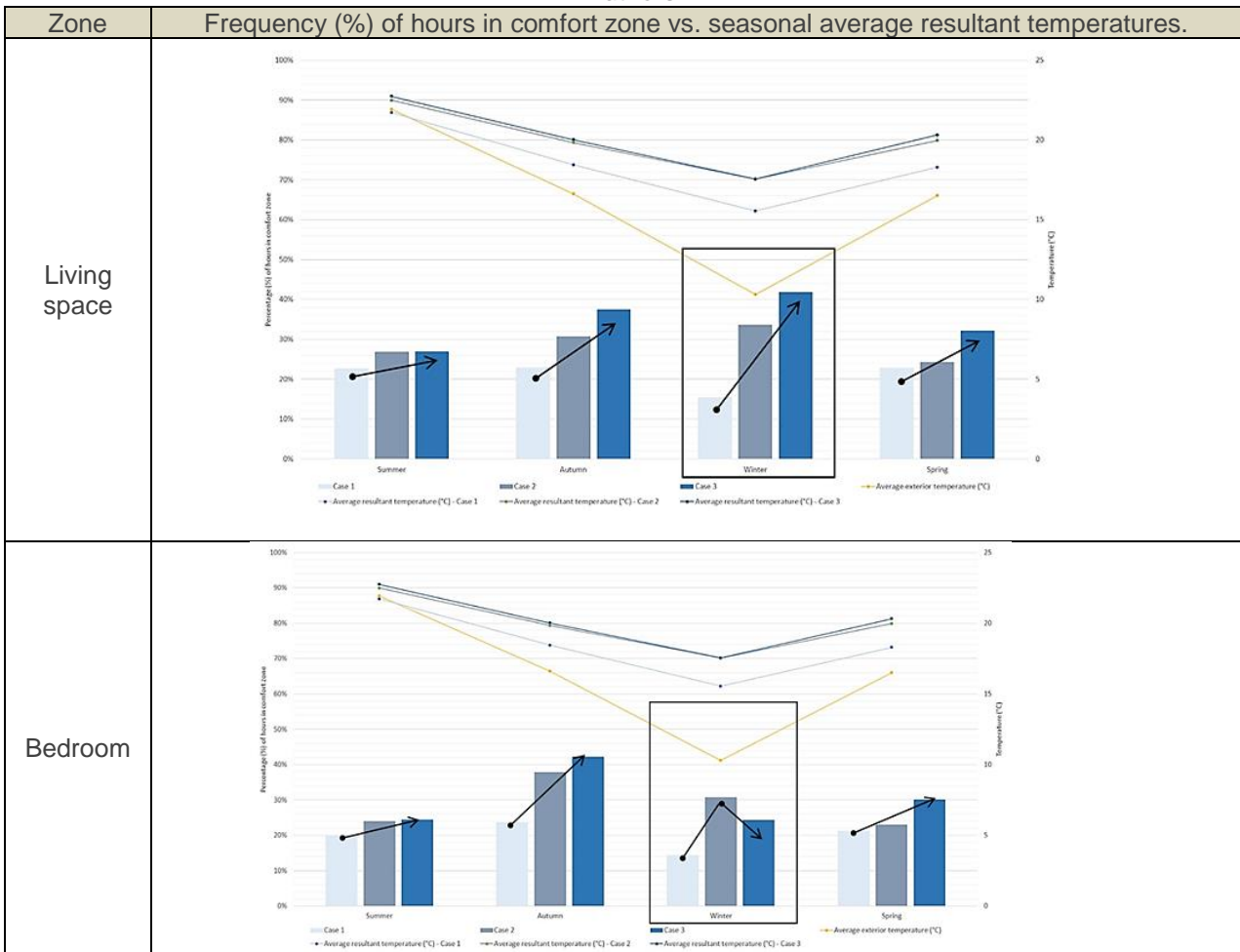
5. SPATIAL DELIGHT IN THE MARIKA-ALDERTON HOUSE

The Marika-Alderton house is positioned by the seaside in Eastern Arnhem, NT (12.5° S). According to Beck and Copper (2002), the house was designed for an aboriginal family intending to create a dwelling that followed native traditions, while providing shelter from climate. Murcutt oriented the house facing north (Figure 12), while arranging the spaces responding to aboriginal tradition, were the adult's room is positioned to the West, where the sun sets and dies, while the children's bedrooms are located to the East, where the sun rises symbolizing new life. In this project, Murcutt converged and materialized his life learnings on Thoreau's (2012) philosophies, with the lessons learnt from vernacular architecture and aboriginal way of life.

Figure 12. Left: Marika-Alderton house. Photography by: Reiner Blunck. Source: El Croquis (2013). Right: Spatial arrangement and section vs. solar angles. By Authors

The house's section was conceived to fully respond to the site's tropical climate, (i.e. harsh sunlight, high temperatures, humidity levels and occasional cyclones) while providing visual contact with the exterior; Murcutt conceived a slim, symmetrical section (Figure 12) raised off the ground on steel pillars to improve the effect of natural ventilation, while the roof's long overhangs protect the interior from sun and rain. An operable and

permeable envelope, (composed by slatted shutters, doors, tilting plywood panels and sun breakers) ensures a constant inflow of fresh air, while the sun breakers provide shading to all bedrooms from low-angled southern sunlight.

When the envelope and structure's materiality is observed, the pragmatic and unpretentious intentions of Murcutt surface; through modest building materials such as steel, timber, plywood and corrugated iron, it is possible to orchestrate a space that adapts accordingly to climate.

According to BOM (2014), the site experiences constant high temperatures (18°C to 35°C), humidity, rainfall, solar radiation levels and occasional cyclonic winds, thus while encouraging natural ventilation, blocking undesired sunlight is required. As Figure 13 shows, the house's orientation as designed is very close to the optimum.

Murcutt merged the outside and inside pursuing to cool down the interior through natural ventilation and shading; nevertheless, its permanent contact with the exterior makes the building dependent on exterior temperatures to achieve comfort, hence an increase in wind speed is necessary; conscious of this, Murcutt included in the roof several Windworkers designed to increase air flow within the house, encouraging natural ventilation and the extraction of heat trapped in the roof (Figure 13).
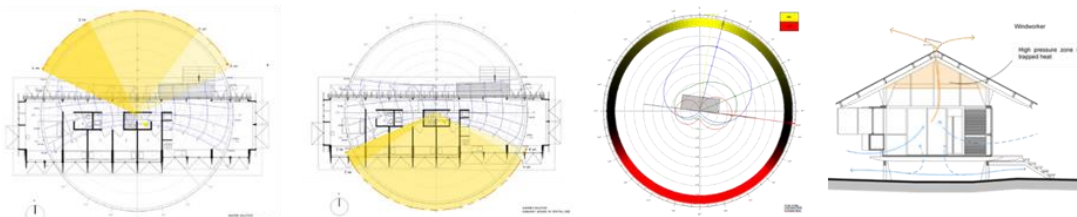

Figure 13. Left: Spatial arrangement and sunpath during winter and summer solstice; Optimum orientation. Source: NatHERS and Ecotect's weather tool (2014). Right: air movement and cross-ventilation produced by Windworkers. Source: Authors

6. DAYLIGHT ASSESSMENT OF THE MARIKA-ALDERTON HOUSE

Visual performance under overcast sky conditions

Following the methodology described in Section 3, the daylight performance of the house's main spaces, was studied to ensure a correct daylighting under overcast sky conditions. As (Figure 14) shows, the average daylight factor in the main spaces ranged from 3% to 5%, indicating that all spaces are naturally well-day lit and no artificial lighting is required. Additionally, the light journey shown indicates a continuous variation in daylight, ranging from a vivid atmosphere in serving spaces, to a calmer one in the bedrooms.
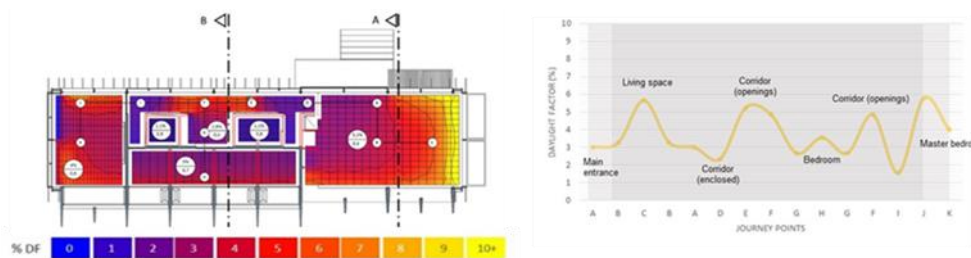

Figure 14. Daylight factor plot and section, uniformity ratios and light journey in the Marika-Alderton house. Source: Authors

Visual performance and comfort under sunny and overcast sky conditions

The illuminance was assessed in the living space, at noon under sunny sky (Equinox) and overcast skies conditions; results were compared to CIBSE (1994) 300 lux recommendation.

As illustrated in Table 8, in sunny sky conditions during Equinox, shading elements completely protect surfaces from direct exposure to sunlight, yet the high lux levels (+600 lux average) indicate that even if the space is

well day-lit, visual fatigue may be experienced, suggesting that if the operable openings were closed, this condition might considerably improve; under overcast skies, the illuminance levels achieved (ranging between 250 – 300 lux average) convey a correct daylighting, offering some visual acuity.

Table 8. Illuminance (lux) plots at noon under sunny sky (Equinox) and overcast sky conditions. Source: Authors
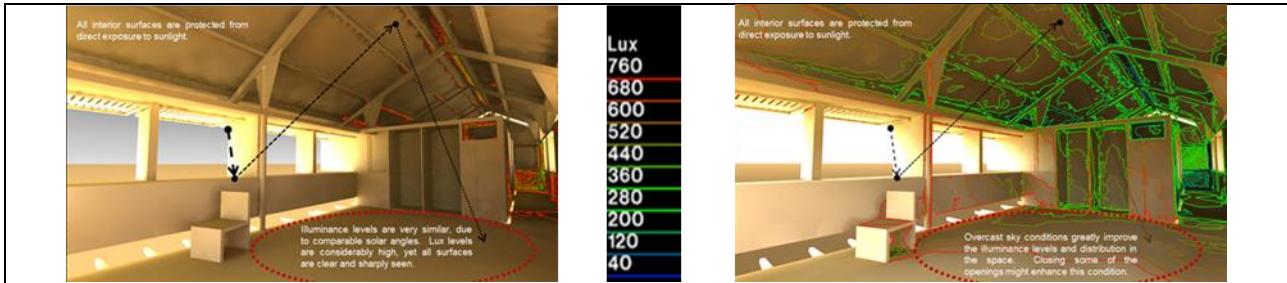
According to the results of the brightness contrast analysis (Table 9), the relationship between the visual targets and their surroundings proved that experiencing visual discomfort is unlikely to occur. The clever selection of building materials with low reflectance (i.e. mostly wood in the interior), decreased the chance of experiencing visual discomfort. Nevertheless, this study was performed considering all shutters remained opened (as worst case scenario); if they were lowered the results most probably will improve and further reduce the risk of visual discomfort.

Table 9. Luminance (cd/m2) assessment at noon under sunny sky (Equinox) and overcast sky conditions. Source: Authors


7. THERMAL PERFORMANCE AND SPATIAL DELIGHT IN THE MARIKA-ALDERTON HOUSE

The constant permeable nature of the house was considered, as it is dependent on the exterior air temperatures and wind speeds to cool down the interior. Additionally, the shallow envelope (built on elements with low thermal properties), and warm air been constantly pushed into the house were taken into account.

To assess the thermal conditions, a model of the house was built in EDSL TAS (Figure 15), distributing each space as a separate thermal zone. The simulations were performed aiming to have an overall idea of the annual performance of the main living spaces and to provide evidence on the effect that solar radiation, natural ventilation and internal heat gains had on the resultant temperatures annually. In order to have more realistic results, the Windworkers' 'Venturi' effect was simulated by adding opaque openings to the roof.

The assessment considered three possible cases (Figure 15), all having as constants: shading, natural ventilation (varying accordingly to each case) and infiltration rate 0,50; heat gains were the only variants. Case 1 was set as a base example with partial natural ventilation and no heat gains; case 2 represented the worse scenario, as heat gains were included; case 3 was designed as the best possible scenario, as natural ventilation was increased to have a stronger perspective on the influence natural ventilation had on thermal comfort.
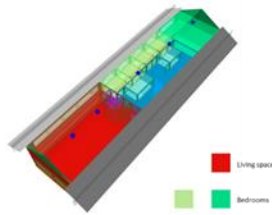
Case	Description
Case 1	Shell with 0.5 infiltration rate + 1 ach (30% natural ventilation*) NO internal heat gains considered.
Case 2	Shell with 0.5 infiltration rate + 1.5 ach (30% natural ventilation*) + internal heat gains considered.
Case 3	Shell with 0.5 infiltration rate + 2.5 ach (90% natural ventilation*) + internal heat gains considered.
	* Natural ventilation is assumed 24 hours, 365 days

Figure 15. Left: Thermal assessment and zoning of key spaces in the Marika-Alderton house. Thermal assessment in EDSL Tas. Right: Summary of thermal cases examined. From: Authors

Setting a comfort zone for this analysis, followed the same principles, equations and guidelines described in Section 4, based on the optimal temperature for comfort (i.e. T_{comf}) in Darwin (NT), and based on the Adaptive Model by Nicol, Humphreys and Roaf (2012).

The following assumptions were considered for these simulations:

- Weather: Energy Plus weather data for Darwin, NT.
- Comfort range: assumed to be between 23°C to 28°C
- Calendar: Annual
- Internal Gains:
    - Occupancy: 2 adults and 4 children; heat gains assumed 450W (sensible) and 250W (latent).
    - The occupancy schedule was set assuming a 24 hours.
- Lighting: compact low-energy florescent bulbs with a total load of 1,5 W/m^2
- Equipment gains: equipment's considered were a hob and a fridge, with a total load of 25 W/m^2.
- Ventilation: opening schedule is based on occupancy, partial natural ventilation is allowed 24 hours a day.

Thermal Assessment Results

Thermal analysis outcomes were compared between both zones, relating seasonal thermal performance vs. average resultant temperatures. Results are shown as a percentage of time when the resultant interior temperature ranged between 23°C to 28°C; yet the consequences of the house being an open space have to be recalled.

As Table 10 shows, both spaces shared a similar thermal performance; annually none reached a 30% of time within the comfort range, having significantly high resultant temperatures fluctuating between 27°C to 35°C. The following conclusions were drawn from the analysis:

- Case 1: 20% of the occupied hours in a year time are within the comfort range (without any heat gains). During winter the thermal performance fell with 16% of the occupied hours falling within the comfort zone.
- Case 2: Presented an insignificant improvement when compared to Case 1; only a 3% increase of the time within the comfort zone was experienced when natural ventilation was introduced; overheating could be experienced and extra cooling is needed.
- Case 3: The comfort range slightly increased to 25% when twice the air flow was introduced, still the building is unable to rapidly exhaust warm air trapped under the roof, leading to overheating.

Table 10. Seasonal thermal performance of main spaces vs. average exterior and resultant temperatures.
Source: Authors

Zone	Frequency (%) of hours in comfort zone vs. seasonal average resultant temperatures.
Living space	
Bedroom	
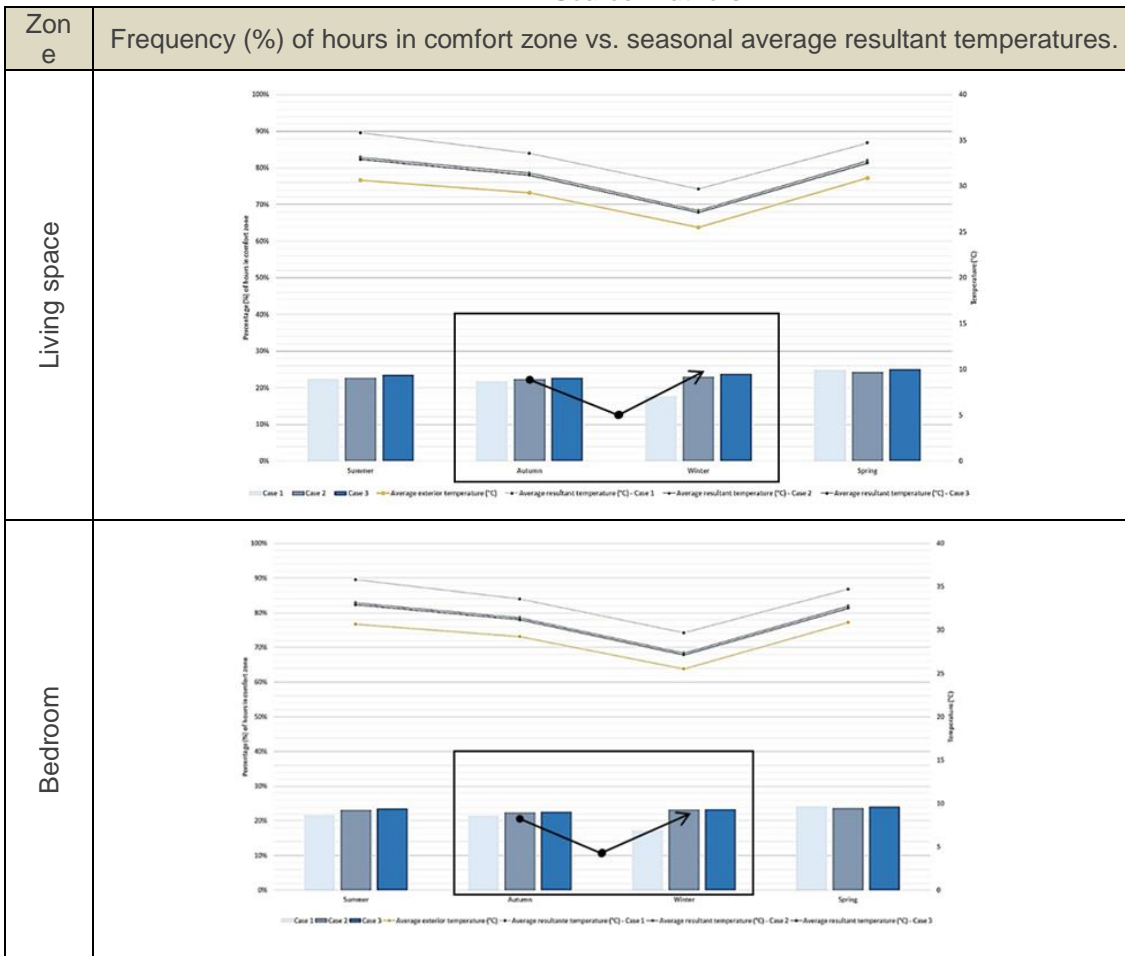
Overall, the thermal performance of both spaces is poor, only 30% of the occupied hours in a year are within the comfort range, demonstrating it potentially needs mechanical cooling; however, the thermal conditions could potentially be improved and moderated by the occupants' control of the building's operable envelope.

8. CONCLUSION

Through an in-depth analysis of both houses, the authors have attained a holistic understanding on the significance of Murcutt's oeuvre, supported by the factual evidence gathered from qualitative and quantitative analysis.

From a qualitative perspective, not only were Murcutt's design intentions revealed, but also, the intrinsic connection he proposed between the manmade space and nature. Through simple forms and humble materials, Murcutt merges his buildings with nature, not implying the superiority of one over the other, but through unity, his architecture constantly reminds us the significance of nature.

Detailed site-specific climate analysis including the solar trajectory, prevailing winds, rainfall and landscape, are Murcutt's essential first step in dealing with a design challenge; when all these factors combine, nature seems to speak and guide him to define forms and spaces which are translated into climate responsive, potentially free-running vernacular inspired architecture. Once this in-depth contextual knowledge is overlaid with his main environmental design principles, (i.e. orientation, narrow plans with climate-responsive sections, natural ventilation, shading and light-weighted operable skins) an architecture that adapts to the local climate and site conditions is born.

When the luminous environments were analysed, they proved to be well-day lit and convey a general sense of well-being and comfort. Additionally, Murcutt's expertise in sculpting daylight, produced subtle light

journeys, which varied in intensity depending on the spatial function and intended atmosphere, ranging from vibrant light in public spaces, to soothing light in private ones.

However, the thermal analysis revealed some occasional thermal discomfort. Considering the houses' envelopes as designed, the results showed that in the Ball-Eastaway house, the performance of the main spaces fell below an annual average of 30% of the time within the comfort range, suggesting that improving the envelope's insulation and airtightness, combined with extra heating (for winter) could potentially enhance the house's thermal comfort. In the Marika-Alderton house, which presented an annual average of 25% of the time within the comfort range, showing that even when the effect of the Windworkers was considered to increase the air movement, the main spaces still experienced overheating, caused mainly by the fact that the building's envelope was designed to be light-weight and the roof is not insulated. However, occupants' active control of the operable building envelopes might potentially help reduce a certain degree of overheating in summer.

The spatial and environmental delight in Murcutt's buildings lie in this delicate relationship between his romanticism and practicality. Through his pragmatism, Murcutt designed buildings responding to particular site conditions and climate, and whose unique architectural orchestration, solely desires to enrapture the inhabitant in an emotive composition of light, wind and textures borrowed from nature. Through this balance between poetics and pragmatics, between man and nature, Murcutt's buildings are vivid, healthy and delightful. Furthermore, he created spaces which continually invite the inhabitant to communicate with the local landscape and live a simple life.

9. REFERENCES

BECK, H., Cooper, J., 2002. Glenn Murcutt: A Singular Architectural Practice. Edition. Images Pub.T

Bureau of Meteorology, BOM, 2014. Climate of New South Wales. Available at: www.bom.gov.au/lam/climate/levelthree/ausclim/ausclimnsw.htm [Accessed 23rd August 2014]

British Standards Institution, BSI, 2008. Lighting for buildings. Code of practice for daylighting. B S I Standards.

Chartered Institution of Building Services Engineers, CIBSE, 1994. Code for interior lighting. London: Chartered Institution of Building Services Engineers.

FARRELLY, E. M., 2002. Three houses: Glenn Murcutt. London: Phaidon.

FROMONOT, F, 2003. Glenn Murcutt: Buildings and Projects 1962-2003, Second Edition. Rev Sub Edition. Thames & Hudson.

HOPKINSON, R. G. Petherbridge, P. & Longmore, J., 1966. Daylighting. London: Heinemann.

KALLENBACH, L, 2002. Architect Profile: Glenn Murcutt. Available at: http://www.motherearthliving.com/green-living/nh-natural-home-journal2.aspx#axzz3BRxfGvyC

LEVENE, R. C., & Márquez, C., 2012. Glenn Murcutt 1980-2012: Plumas de Metal - Feathers of Metal. Madrid. El Croquis.

NICOL, F. Humphreys, M. A. & Roaf, S., 2012. Adaptive thermal comfort: principles and practice. London: Routledge.

SESSION 19: GREEN BUILDINGS AND MATERIALS

76: Study on case analysis and support system development for green remodelling of buildings

JI-YEON PARK[1], CHANG-U CHAE[2]

1 Korea Institute of Civil Engineering and Building Technology, 283 GoyangdaeRo IlsanseoGu GoyangSi GyeonggiDo Republic of Korea, Jypark@kict.re.kr
2 Korea Institute of Civil Engineering and Building Technology, 283 GoyangdaeRo IlsanseoGu GoyangSi GyeonggiDo Republic of Korea, Cuchae@kict.re.kr

In the architectural field, energy reduction of new architectures for reducing emitting CO2 and energy consumption has been recommended since 2000s. By reflecting this, the supporting system and institution weighting on new buildings have been formed.

However, based on 2014, with the era of existing buildings amounting to 6.8 million, the target for energy reduction has been changed from new buildings into existing buildings.

Since the renovation plan or remodelling for energy reduction is executed in the existing buildings, which have been supplied more than new buildings. And also, the rate of CO2 emission came to be higher than the rate of CO2 for new buildings. Therefore, it is necessary to change the support system focusing on new buildings into the support system of existing buildings for activating green remodelling.

In order to activate green remodelling, institutional support of government, technology development related to green remodelling, green remodelling manual development for building owner and residents are required to be established systematically.

In this study, case analysis of technology and institution for activating green remodelling market in domestic and foreign country, plan to secure support system, applying the current situation, will be prepared. For the establishment of green remodelling support system, the activation of green remodelling market is predicted and the energy efficiency improvement and the emission of environmental load are expected.

Keywords: Green Building, Green Remodelling, Energy Efficiency Improvement, Supporting System

1. INTRODUCTION

1.1 Background

In the 2000s, reduction of energy consumption has been recommended for the newly built architectural projects to reduce power demand carbon dioxide emissions, and a support system and institutions reflecting this trend have been established.

However, as the demand for new buildings has decreased and the era of the existing buildings counting up to 6.8 million buildings with the global economic recession, an energy-saving plan focusing more on existing architecture rather than new architecture has been promoted. It implies that reducing energy consumption and carbon dioxide emissions in existing architecture is more efficient than newly built architecture.

Therefore, the green-remodelling market is expanding with the activation of the green-remodelling industry for existing buildings domestically and abroad and it is thought that a system to activate the green remodelling market in Korea is necessary.

1.2 Purpose and Necessity of the Study

It is estimated that the green-remodelling-related activity will account for more than 60% of the whole architectural market after 2030. Also, it is estimated that the buildings, of which the lapse year is more than 15 years among the 6.8 million buildings for 18 years, from 2013 to 2030.

As a result of a survey on annual energy consumption, it can be analysed that the annual energy consumption in 2011 increased 14% compared to 1997, which means that energy consumption is on the rise. As the service life of architecture is increased and buildings deteriorate, it is estimated that the amount of energy consumption of existing buildings is likely to increase.

Therefore, continuous improvements in conditions and functions of existing buildings are required. Plans for reduction of energy consumption and greenhouse gas emissions are required. For the revitalization of the system, the increase in demand for green remodelling is estimated and can lead to the revitalization of relevant industries such as the development of factors related to green remodelling.

In order to settle a system suitable for the domestic market, preparation of plans to establish the policy is required. Also, it is necessary that organized support from government such as technology development related to green remodelling and manual development of green remodelling are required during preparation of the support system to vitalize green remodelling.

In this study, cases of technology and a system for revitalization of domestic and foreign green remodelling are analysed and plans to establish the support system to apply the present conditions are provided.

2. PRESENT CONDITIONS OF GREEN REMODELING

2.1 Definition of Green Remodeling

Words related to renovation/building repair are defined and used differently by different countries.

In Japan, modifying parts of existing buildings is 'renovation.' Modifying only partitions without changing the main structure is 'rearrangement.' Changing only the finishing parts is 'refinishing'.

In the United States, 'remodelling' is a common word. In the United Kingdom and Australia, 'refurbishment' and 'retrofit' are used according to the scope and method of renovation.

In Korea, the term 'remodelling' has been adopted for the repair and maintenance of a building in accordance with the Buildings Act and green remodelling means improvement of energy functions and efficiency to build eco-friendly buildings.

Table 11: Definition of Building Repair

Classification	Definition
Remodelling [1]	It means major repair or additional construction for the control of damage and improvement of function
Retrofit [2]	Re-building of a product to specifications of the original manufactured product using a combination of reused, repaired and new parts.
Remanufacturing [3]	Retrofitting is the process of modifying something after it has been manufactured. For buildings, this means making changes to the systems inside the building or even the structure itself at some point after its initial construction and occupation. Typically this is done with the expectation of improving amenities for the building's occupants and/or improving the performance of the building. The development of new technologies mean that building retrofits can allow for significant reductions in energy and water usage.
Refurbishment [3]	During a refurbishment a building is improved above and beyond its initial condition. Refurbishments are often focused on aesthetics and tenant amenities, but they can also include upgrades to the building's mechanical systems and can potentially have an effect on energy and water efficiency.
Renovation [3]	Renovations are very similar to refurbishments and the terms are sometimes used interchangeably. The major difference is the term renovation applies specifically to buildings, while refurbishment does not. As with refurbishments, renovations are often focused on aesthetics and tenant amenities, but they may also include upgrades to the building's mechanical systems and potentially have an effect on energy and water efficiency.
Tune-up [3]	'Building tune-up' is a generic term that may encompass maintenance on the building's existing systems, or aspects of retrofitting and retro-commissioning as defined above. Many cities around Australia have implemented building tune up programs with the goal of improving energy and water use efficiency.

1) Seoul Metropolitan Government
2) Wikipedia
3) http://www.melbourne.vic.gov.au/

2.2 Market Situation of Domestic Green Remodelling

(A) Present Condition of Policies and Promotion of the Domestic Green Building System

According to the details of promoting policies related to domestic green buildings, there were difficulties in application to existing buildings since the policies and systems were developed focusing on existing buildings.

After that, policies and systems for existing buildings were established and relevant policies related to remodelling for the improvement of the energy efficiency of existing buildings were promoted, putting top priority on the policies related to remodelling for improvement of energy efficiency of existing buildings.

In 2013, a green remodelling creative centre was established in accordance with the green remodelling revitalization plan for reduction of building energy consumption and promotion of the project was supported in connection with business owners, building owners and private finances.

In the public sector, a green remodelling project for public buildings with low performance is promoted, starting with the improvement of building energy efficiency. Also, through the promotion in connection with a green school of green facilities and improvement of energy performance for civil architecture, the project is gradually expanding.

Through government support, the public sector is making an effort to expand the project for the policy and systems related to green remodelling.

So far, it is in the beginning stage and relevant technologies and cases are insufficient, therefore there is a limit in conducting the project in the civil sector.

(B) Policies and Kinds of Systems Related to Domestic Green Remodelling

In domestic policies related to green remodelling, strengthening energy standards of newly built buildings, introducing energy saving by building owners and improving energy efficiency of existing buildings are promoted.

For relevant policies, the energy efficiency rating system in 2001, the green building certification program in 2002 and the Housing Performance Grading Indication System in 2006 were executed and the Renewable Energy Building Certification System in 2011, the Greenhouse Gas/Energy Target Management System in 2012 and the Green Building Fostering Support Act in 2013 were executed in accordance with the execution of 2010's Low Carbon Green Growth Basic Act.

The executed systems related to green remodelling in Korea include the energy conservation plan, energy consumption certificate program, energy consumption quota system, greenhouse gases and energy target management system and energy consumption management.

Table 2: Policies and Kinds of Systems Related to Domestic Green Remodelling

Classification	Energy Conservation Plan	Energy Consumption Certificate Program	Energy Consumption Quota System	Green House Gas and Energy Target Management System	Energy Consumption Management
Purpose	Submit plan to prevent heat loss for efficient control of energy of building	Utilize real estate by issuing certificates of energy information such as energy efficiency ratio	Divide total energy consumption for 1 year by unit area and maintain energy consumption per unit area	Set amount of emission and consumption of greenhouse gases through discussion between companies and government and submit execution plan	In connection with building and energy consumption information, establish integrated management system per building (electricity, gas, heating)
Applicable Acts	Article 14 of Green Building Fostering Support Act / standards of energy saving design of the building etc.	Based on Article 14 of Green Building Fostering Support Act	Based on Article 14 of Green Building Fostering Support Act	Article 42 of Low Carbon Green Growth Act / Instructions on Energy Target Management Operation, etc.	Article 44, Article 45, Article 54 of Low Carbon Green Growth Act and Article 10 of Green Building Fostering Support Act, etc.
Target	Buildings of total floor area more than 500㎡	Apartment buildings of more than 500 households and business facilities of total floor area more than 3,000㎡	Large buildings such as business facilities of total floor area more than 10,000㎡ and expand the target buildings by stages	Large buildings emitting greenhouse gases and consuming energy substantially (designate companies of duty and manage them)	700,000 individual buildings nationwide
Related	Korea Energy Management Corporation, Korea Infrastructure Safety and Technology Corporation	Ministry of Land, Infrastructure and Transportation	Ministry of Land, Infrastructure and Transportation	Ministry of Environment	Ministry of Land, Infrastructure and Transportation, Ministry of Trade, Industry and Energy, energy suppliers

(C) Analysis of Problems in Domestic Green Remodelling Market

The domestic green remodelling market is at the beginning stage so the policies and systems are dispersed, therefore the system is not well established. Since the cases of technology related to green remodelling are insufficient, there is a limit in revitalizing the verification of investment and achievement.

Also, there are problems such as electric power shortage because of an increase in energy consumption considering only the design at the time of remodelling construction.

2.3 Present Conditions of Foreign Green Remodelling Market

For the purpose of improving the energy efficiency rate, the foreign green remodelling markets of the USA, Germany, the UK, Japan, etc. provide various support systems such as offering financial support for the buildings, and the markets are becoming vitalized.

(A) USA

Regarding the energy efficiency of buildings, various government organizations on the federal level, state level and local level offer various types of support.

Subsidy and loan support worth more than USD 100,000 are being promoted. Also, regarding energy efficiency, 266 types of loan support and 56 subsidies are offered. Remodelling guidelines are developed and operated under the REGREEN program.

(B) Germany

As the 10-year basic policy on energy efficiency is promoted, the EnEV such as insulation, heating and cooling has strengthened.

Therefore, the current remodelling market of Germany accounts for 30% of the whole architectural market. With the aid support policies, the government supports a maximum KRW 32 million (maximum 25%) per household from the fund worth of KRW 1.7 trillion through the KfW efficiency index.

In connection with KfW, loan support with an interest rate is promoted and subsidies and private financial loans are offered within 17.5% of the investment (up to KRW 22 million) according to the effect of remodelling improvement (energy-saving rate).

(C) United Kingdom

The remodelling market accounts for 45% of the whole architectural market and remodelling construction is supported through the subsidy systems based on the Construction and Regeneration Act.

The subsidy systems of the United Kingdom are conducted by the DECC.

The Green Deal project is operated to collect investments consumed with energy cost, saved through green remodelling projects. Through the Green Deal, jobs are created in evaluation institutions, consulting companies, developers and construction companies.

(D) Japan

Japan, where remodelling accounts for 30% of the whole architectural market, has the largest index in Asia.

Since there are lots of old houses, the potential of the remodelling market is quite high. Since 2006, policies focusing on newly built buildings have been changed to policies focusing on maintenance and remodelling of existing buildings.

Currently, non-residential buildings and business buildings are leading the remodelling market.

2.4 Comparative Analysis of Project Cost Related to Green Remodelling

About KRW 2 billion is provided as interest support yearly for green remodelling of existing buildings. Maximum KRW 20 million for apartments and KRW 3 billion for non-residential buildings per project are offered by government subsidies and private financial loans.

The government subsidies of the United Kingdom total KRW 220 billion. Subsidies 100 times higher than domestic, are provided and the annual average KRW 2.7 million per project is provided as the total government subsidies.

Although the government subsidies for domestic green remodelling are insufficient compared to other countries, they are expected to increase with the establishment of relevant systems through the revitalization of systems related to green remodelling, considering that the domestic green remodelling policies are in the beginning stage compared to other countries.

3 DEVELOPMENT OF SUPPORT SYSTEM FOR GREEN REMODELLING AND REVITALIZATION PLAN

3.1 Support System for Green Remodeling

(A) Definition and Roles of Relevant Parties

The process of green remodelling is mainly divided into preparation and execution stages. The preparation stage entails a remodelling plan and organizational response. The execution stage sees the establishment of progress direction of the plan, composition of proposal for remodelling, decision of the construction company, progress of construction, completion of construction and delivery.

Parties conducting the progress are classified as members of association, board of directors, expert committee, expert company and construction company.

The members of association consist of apartment owners who propose the requirements for remodelling and receive opinions on selecting construction companies, etc.

The representatives of the members of association consist of the board of directors, conducting public relations to the residents, consignment contract with a specialized company, selection and contract of the construction company, etc.

The specialized committee consists of specialized consultants and submits the remodelling plan, surveys and diagnoses the apartment and conducts a questionnaire and public hearings.

Expert companies consist of apartment management company, company of deterioration diagnosis, and design company.

These specialized companies conduct a report on degradation progress, design of the remodelling drawing, submission of the calculated construction cost, etc.

The construction company executes remodelling construction and delivers after completion of construction.

(B) Mutual Cooperation System per Relevant Parties

For green remodelling, the building owner, design company, construction company and each specialized company cooperate very closely through mutual cooperation.

With the deduction through interrelation, the work of the design companies can be conducted.

The building owner and specialized companies execute the plan and proposal for remodelling with the approval of residents and the design company decides the improvement level through the green remodelling in cooperation with experts on structure, machines, facility, energy diagnosis, and law.

The planned remodelling is executed by the construction company, a supervision company, and a commissioning company with cooperation of developers, and reports the field conditions and executes remodelling.

3.2 Revitalization Plan for Green Remodelling Industry

In order to revitalize the green remodelling industry, relevant technologies and factors are required based on the green remodelling support system.

Firstly, technology development and utilization related to green remodelling is required. For technology development, revitalization of the green remodelling market can be expected through the preparation for revitalization opportunities of green remodelling introduction to market, strengthening of company capacity, and differentiated technological power per company.

Secondly, with the establishment and utilization of an integrated information system related to green remodelling, system manuals can be prepared, considering the convenience of business operators, building owners and system operation, through cooperation among government departments and a place can be prepared for information exchange such as systems, technical support and financial products related to green remodelling.

Also, it is expected that the business cases related to green remodelling such as energy cost saving effects and satisfaction of occupants can be promoted.

Thirdly, various financial systems such as the promotion of low-interest business and energy-saving effects made by green remodelling can be developed through remodelling subsidies and tax support for green remodelling, etc.

Forth, by creating manpower specialized for consulting and evaluating green remodelling, professionals with a knowledge of architecture, environment, energy, etc. can be trained, contributing to job creation.

Lastly, effects of system revitalization and promotion can be expected by preparing awards systems for the best green remodelling cases.

4   CONCLUSION

In the architectural field, it is estimated that the annual energy consumption and greenhouse gas emission of existing buildings will increase, and repair/maintenance or remodelling are executed to respond to this.

Therefore, the green remodelling industry in domestic and foreign construction and institutional systems should be revitalized.

In this study, various advanced cases for green remodelling for existing buildings have been analysed and plans for revitalization of the system for green remodelling have been prepared.

The domestic green remodelling market is insufficient compared to the market in other countries, and with the introduction of the best advanced cases in foreign countries, a basis shall be prepared in order for the domestic green remodelling market to grow in an appropriate direction.

By addressing the problems of the domestic green remodelling market, a system can be established and with technological development and utilization of green remodelling, establishment and utilization of an integrated information system related to green remodelling, green remodelling project subsidies, tax support, financial system, etc, creating manpower specialized in consulting and evaluation of green remodelling and awarding excellent cases of green remodelling, a basis for revitalization of green remodelling is required.

Through this, the revitalization of the green remodelling market is expected. Also, it is expected to contribute to a reduction of environmental effects through energy saving, reduction of greenhouse gas emissions, etc.

However, the present domestic green remodelling market is in the beginning stage. And efforts to establish a systematic basis are required and continuous research is required for revitalization of technological development supplementing all these advantages to respond to climate changes, environmental systems and financial products.

5   REFERENCES

Ministry of Land, Infrastructure and Transport, July 2013, Plan of Revitalization of Green Remodeling for Reducing Demand for Energy of Buildings

McGraw-Hill, 2012, Smart Market Report 2012

McGraw-Hill, 2013, World Green Building Trends

McGraw-Hill, 2012, The Green Residential Building Market

Korea Environmental Industry and Technology Institute, June 2014, Prospect of Green Architectural Industry and Direction of Development

217: Technology research and development boost the development of green buildings in China

QINGQIN WANG [1, 2], SHANGQUN XIE [1, 2]

1. China Academy of Building Research, Beijing 100013, China
2. Beijing International Collaboration Base on Green Building, Beijing 100013, China

By improving the technology innovation vitality and the development of green buildings, Chinese government is promoting the transformation and upgrading of the building industry. This paper, the overall situation of the government support for research and development in the field of green building in China is introduced, the development status of standards, key technologies, products and equipment, and projects of green building summarized, the effect of green building for energy saving and emission reduction analysed, and the development trend and priorities of green buildings in China discussed.

The development of green building has become a strategic choice to change the mode of development of construction industry in China as well as urban and rural construction. It is significant for increasing energy saving and emission reduction in building, improving built environment and promoting sustainable development for economic growth. The competent department of the Chinese government pays a great attention to the work of science and technology in the field of green building. By continuously supporting a set of National Key Science and Technology Research Program and National Key Technologies Research and Development Program, there are a number of significant breakthroughs in key technologies of green building achieved, a number of new products, new materials, new technology and new type of construction equipment of green building developed, the preliminary green building technology standard system in China formulated. By vigorously promoting the large-scale application and demonstration of green building, green building has been developing healthy and rapidly in China. In January 2013, the State Council issued the green building action plan (published by State Council [2013] No.1), which promoted the development of green building as a national development strategy.

1. GREEN BUILDING HAS BEEN LEADING THE URBAN CONSTRUCTION TECHNOLOGY DEVELOPMENT DIRECTION

"National medium and long-term science and technology development plan (2006-2020)" has set the "building energy saving and green building" priority work in the field of "urbanization and urban development", and demanded carrying out the scientific research of "green building design technology, building energy saving technology and equipment, integration of renewable energy devices and application technology, exquisite construction and green building construction technology and equipment, energy-saving materials and green building materials, and building energy-saving standard" etc..

1.1, The government continuously increasing investment in science and technology of green building

During "The 10th Five-Years Plan" period (2001-2005), the research on key technology of green building had been organized and implemented as a National Key Science and Technology Program. Through tackling key problems tackle key problems and making breakthroughs in green building technology, a number of ecological and low energy consumption demonstration models of green buildings had been built.

During "The 11st Five-Years Plan" period (2006-2010), almost 10 National Key Science and Technology Programs had been organized and implemented, such as "research and demonstration on key technologies of Building energy saving ","research and demonstration on key technologies of modern architectural design and construction ","research and development of eco-friendly construction material and product ","research and demonstration on key technologies of energy efficiency retrofitting of existing buildings"," research and demonstration on key technologies and equipment of scientific energy use in hot summer and cold winter zone" and "research on key technologies of improving the residential environment in cities and towns " etc. With the support from aspects of building energy efficiency, the use of renewable energy, eco-friendly building materials, the retrofitting of existing buildings, construction equipment, design and construction and improvement of residential environment, a number of periodical results in green building technology had been achieved, which provided important scientific and technological supports to some key state projects, such as stadiums of the Beijing Olympic Games, the Shanghai's expo and the Guangzhou Asian games.

During "The 12nd Five-Years Plan" period (2006-2010), more than 20 National Key Science and Technology Programs had been organized and implemented, such as "technology research and development on evaluation system and standards for green building", "research on the support system of building energy saving technology"," research and demonstration on key technologies of green building construction "," research and demonstration on key technologies of green transformation of existing buildings ","research and demonstration on a package of application technologies of energy-saving building materials ","research and demonstration on technologies of a new kind of precast concrete frame", "research and demonstration on key technologies of control and improvement of healthy indoor environment " etc.. The comprehensive plans for the development of science and technology was formulated from aspects of evaluation system and standards for green building, basic information database, life-cycle implementation technology, green transformation of existing buildings, a new type of green building materials and products, control device of indoor and outdoor environment, building energy-efficient products and equipment, construction equipment, green building technologies which are suitable for different climatic zones and green town etc., which is significant for accelerating the promotion of ability of green building planning and design, technology integration, engineering implementation, operation and management and enhancing the core competitiveness of construction industry.

1.2 Consistently promoted green building industry as a major national project during The 12th Five-Year Plan period

Since the 12nd Five-Years, China's Ministry of Science and Technology pays more attention to the top-level design and making an overall plan, and takes developing the green building as a breakthrough of scientific and technological work on urbanization and urban development during "The 12nd Five-Years Plan" period. China's Ministry of Science and Technology issued the "special planning of green building technology development for 'The 12nd Five-Years Plan'" (National Science [2012] No.692) in May 2012, and completed the special strategic research on green building special for "the 12nd Five-Years" by the end of the same year. With the full implementation of the green building, the scale development of green building has been promoting, which is taking "the key generic technology system of green building, Green building industry propulsion system, green building technology standards and comprehensive evaluation of service technology system construction" as the three key technical support. While taking the main line as changing the mode of development of the construction industry, upgrading the quality of construction, improving the building environment and reducing resource consumption, we will improve the technology innovation system of green building from five aspects of the technical research and development, standards and norms, materials and equipment, demonstration and popularization and platform construction. With enterprises as the main body, the market as the guidance, we will improve the technology innovation system of green building, integrating with education and research.

1.3 Green building will continue be as China's key research task in The 13rd Five-Year Plan

Since 2013, according to the requirements and the overall plan of deepening the reform of the science and technology systems, China's Ministry of Science and Technology has organized experts to carry out the medium-term assessment, technology prediction and specific research for "The 13rd Five-Years Plan" on urbanization and city development for the "National medium and long-term science and technology development plan (2006-2020)". It has been clarified that the technology research and development of green building would still be a top priority, especially when the Ministry of Science and Technology suggested that "green building and its industrialization" would be the key research task witch is given priority to in the "Notice on carrying out the opinion collection on national key R & D program "(National Science [2015] No. 52).

2. THE TECHNICAL LEVEL OF GREEN BUILDING INDUSTRY HAS BEEN SIGNIFICANTLY ENHANCED

Through the guidance and continuous support of national science and technology projects, the innovation of green building technology from enterprises, universities, and research institutes has been unleashed, a number of breakthroughs have been made in establishing the standard system of green building, completing technical system and the development of new products and new equipment. The systematicness and usability of the technologies and products has been enhanced obviously, which provided technical support for the popularization of the scale green building including residential and public buildings and other types of buildings.

2.1 Technical standard system has been formed preliminarily

Since the "Evaluation standard for green building" (GB/T 50378-2006) was released in 2006 for the first time, the evaluation of green building has been extended to other types of buildings. After the approval and implementation of national standards such as "Evaluation standard for green industrial building" (GB/T 50878-2013)," Evaluation standard for green office building" (GB/T 50908-2013) and the latest revision of "Assessment standard for green building" (GB/T 50378-2014), a standard system of green building at government and industry level has been built, which including standards of specific stage and type, and other subset of specific stages and specialties. There are more than 10 national and industry standards of green building covering the main stages of the lifecycle of green buildings such as design, construction, operation, retrofitting, and covering the main types of building like industrial building, office building, store building and hospital building, so the standard system of green building has been formed preliminarily.

2.2 The core and key technology has made periodic progress

We have initially established the system of pre-assessment and diagnosis framework for green building planning in line with national conditions and the basic architecture and data structure of the planning and design software of green building which is based on the information model of building; and built the remote monitoring system of renewable energy system operation performance, which actualized the energy monitoring and situational analysis of China's buildings; and completed a number of key technology researches

on the intelligent control system of polyurethane foam production in severe cold zone, the application of different heat sources of heating in severe cold zone, the energy distribution of combined heating system, and the optimum load distribution ratio of heating system with multi-energy complementary technology.

2.3 The level of green building products and the assemble of that have been gradually increased

We researched and developed the sea-water-source heat pumps to which the sea water can be directly imported, improved the efficiency and greatly reduced the cost of the system. We have developed the water after treatment and waste water heat pumps in cold zone. We completed the integration and demonstration project of comprehensive utilization technology of solar energy and other kind of energy in the building, and developed new products for solar heating and air conditioning such as medium or high-temperature solar heat collector and heat collecting pipe and multi heat source heating devices.

A series of energy-saving products have been researched and developed, such as functional composite wall plate which is suitable for different climate zones, energy-saving sintered wall material, and ultralight high-efficiency Class-A fireproof cement based thermal insulation material, which can effectively enhance the insulation performance of wall and reduce the building energy load. Some of the products have realized the industrialization and have broad application prospects. At present, the new wall materials production accounts for more than 55% of the total wall application materials, Such as a new type of exterior wall which has completed the technological improvements of insulation performance has an annual production capacity of 3 million square meters, more than 2 million square meters for building applications and annual output value of 600 million yuan.

The newly developed exquisite construction and green building construction technology and equipment have completed automatic examination and analysis, accurate construction and planning and quota-allocation of material, which is significant to reduce the construction dust and increase the utilization efficiency of building materials, such as the no scaffolding installation equipment series can effectively solve the growing problem of construction of large span building structure, improve the construction efficiency, and reduce the load of electricity in construction site.

3   THE SCALE DEVELOPMENT OF GREEN BUILDING HAS BEEN PROMOTING DAY BY DAY AND PROMOTING THE ENERGY-SAVING AND EMISSION REDUCTION IN THE BUILDING INDUSTRY

By the end of December 31, 2014, there are 2538 projects have got the Green Building Label with total floor area of 290 million square meters (see figure 1). Among them, the number of projects that got the Green Building Design Label is 2379, which accounted for 93.7% with the total construction area of 271.118 million square meters; a total of 159 projects have got the Green Building Operation Label, which accounting for 6.3% of the green buildings with construction area of 19.547 million square meters. The average building area of green building projects is 115,000 square meters.

Through the preliminary analysis on 79 of the green building labelling projects with different star levels, the greening rate reaches 38% on average, and the average energy saving rate will reach 58, with the average saving rate above 15.2% and an average 7.7 percent of utilization of recyclable materials.

According to the requirements of "Green Building Action Plan", in "the 12nd Five-Year Plan" period (2011-2015), more than 1 billion square meters of green buildings should be built. By the end of 2015, more than 20% of the new buildings in cities and towns must meet the green building standards. Chin's green buildings will, by then, account for more than half of the world. More importantly, the No.1 document stressed that any government invested or government subsidized schools, hospitals, museums, science and technology museums, gymnasiums and other buildings, including the low-income housing in municipalities, provincial capital cities and cities with independent planning and large public buildings with areas of more than 20000 square meters should fully implement the green building standards from 2014. Green building will play an important role in the countrywide reduction of carbon emissions.
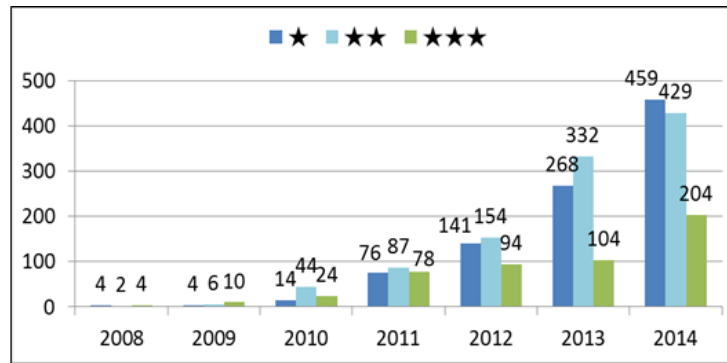
Figue1. The development situation of the number of Green building labelling project in each year from 2008 to 2014

4 THE DEVELOPMENT TRENDS AND PRIORITIES OF GREEN BUILDINGS

4.1 To conduct researches on green building assessment and constantly improve the quality of green buildings

To solve the problem of quality and performance of the green buildings, firstly we should control the quality of green building evaluation. The green building labelling programs have been more than two thousand with the area of over 300 million square meters. Facing the requirements that 20% of new buildings in cities and towns are required to achieve green building standards by the end of 2015, how to ensure the quality of green building labelling projects? Secondly, we should control the performance and quality of the buildings after their completion. How would the actual improvement situation of energy and water saving, cost saving and environmental quality be? Aiming at these problems, there is an urgent need to carry out researches on post evaluation, feedback to the design and construction units, and constantly improve the quality and performance of green buildings.

4.2 Continue to develop green building technologies and products, and improve the level of green building technology

China is a vast landscape, with huge differences in climate, economic and customs and diversification of the type of constructions, so green building technology must be developed in line with the local conditions. At the same time, the development of green buildings has driven the development of a series of new technologies, equipment and products, so it is necessary to solve the problem of technology maturity synchronized with building life. For example, in terms of the green construction integration technology, China is only in the infancy of this field and there is still a big gap compared with developed countries, Although residential industrialization ensure the quality of residential buildings, avoid the safety, energy consumption and emissions, and environmental problems in the construction site.

In the field of green construction, China has made some key achievements on material substitution, resources recycling, new technology, new tools, and new construction technologies. But look from whole, the information level of construction is not high, and the further study and engineering applications are still needed.

4.3 Build green ecological city to help the large-scale development of green building

China's green buildings are gradually developing from monomer constructs to regional architectures, which need the support of city planning and municipal infrastructure. At present some research institutes and universities in China have done a lot of researches on exploring the construction mode of green ecological city, proposed the government - driven mode, industry-driven mode, naturalistic mode and several other suitable construction modes, which promoted the development of green ecological city. In April 2013, China's Ministry of Housing and Urban-Rural Development released the "development planning of green building and green ecological city for 'The 12nd Five-Years Plan'", which clearly put forward implementing the construction of 100 green ecological cities and promoting the scale-development of green building.

4.4 Strength the cultivation of green industry and promote the green industry's upgrading

The rapid development of green building will greatly stimulate the technological requirements of new green building materials and products, new equipment and parts, green construction platform and technology, and matching material, product, equipment, technology, construction technology of building energy-saving and environment. We should accelerate the upgrading of the technology originality of construction industry and real estate industry, promote the application of green building's new technology, new materials and new products, continue to expand and extend the industrial chain, prompt the formation and development of a series of related new industries and enhance the core competitiveness of green-construction-related enterprises.

5 CONCLUSION

As the advancement of "Green Building Technology Development Plan for 'The 12nd Five-Years Plan',", " Development Planning of Green Building and Green Ecological City for 'The 12nd Five-Years Plan'" and "Green Building Action Plan" and the gradual implementation of the tasks, China's green building technology work has entered a stage of rapid development. Combined with the current key tasks, the green building technology work should continue to systematically clear up, summarize and advocate the key achievements of green building development during the period of "The 12nd Five-Years Plan", raise public awareness of green building, promoting the application and industrialization of green building technology through the modelling and leading role.

In December 2014, the State Council issued the "Notice on deepening the management reform plan of central budget for science and technology program (special project, fund, etc.)" (published by state council [2014] No.64), aiming at strengthening the top-level design, breaking the departmental and regional barriers, accelerating the functional division of labour and establishing the target and performance oriented system of management of science and technology programs(special project, fund, etc.) with Chinese characteristics.

Therefore, the development of green building technology needs collaborative innovation of enterprises, research institutes and universities to form the evaluation system and a complete set of techniques of green building with China's indigenous intellectual property and in line with national conditions to realize the sustainable development of the green building, through the construction of demonstration platform and the cultivation of innovation team and new industries.

25: Precast ferrocement hollow core slab /wall panels

WAIL N .AL-RIFAIE[1], AHMED M .A .SAKRAN[2]

1 Professor of Civil Engineering, Philadelphia University, Amman, Jordan, wnrifaie@yahoo.com
2 Research Scholar, College of Engineering, University of Tikrit, Iraq

A total of five full scale ferrocement multi-cell box slab panel were constructed and tested under flexural loads. The main parameters considered in present work were number of wire mesh layers at top and bottom flanges and webs and the positions of the intermediate diaphragms. The behaviour was monitored by reading deflections at mid-span and by observing the crack patterns and mode of failure. From the results obtained, it was found that decreasing number of wire mesh layers at the bottom flanges tend to decrease the load capacity and increase the lateral deflections. It is concluded that the precast ferrocement multi-cell box slab/ wall panels developed in the present work can be used as a building system and comparison of tests results with the standard design loads of buildings showed that the proposed system matches the design loads and can be used in construction of a wide range of buildings.

Keywords: precast, ferrocement, multi-cell box, energy, slab, wall.

1. INTRODUCTION

The growing need for green construction has been the topic of studies for a number of years .Considerable research in this respect is being done all over the world .Although ferrocement has been implemented more than 150 years ago, ferrocement engineering has been developed mainly during the past thirty years and continuously subject to various investigations (ACI Committee , 1993, ACI Committee, 1997). This is mainly because of its potential of wide range of applications .Prefabricated ferrocement panels present a series of possibilities for the solution of construction problem (Al-Rifaie, W .N., and Hassan, A.H.,1994: page115-126, Naaman, A .E. 2000: page 372, Al-Rifaie, W .N .and Alihmedawi, A .N., 2000: page 85-103). The use of ferrocement in pre-fabricated buildings provides many advantages in terms of lightness of weight, ease of handling, low labor cost)skilled and non -skilled (in its production and a durable material requiring little maintenance .Evidently, for these reasons ferrocement has gained advantage over other reinforced concrete and steel structures .Ferrocement is characterized by fine diameter mesh reinforcement (ø), 0.5 ≤ ø ≤1.5mm and mesh size (S), 6 ≤ S ≤ 25mm .The surface area per unit volume of mortar may be as much as ten times that of conventional reinforced concrete .The volume fraction of reinforcement normally lays between 2 ﹪≤ Vf ≤ 8 ﹪for balanced, bidirectional meshes .Regular reinforcing bars in a skeletal form are often added to thin wire meshes in order to achieve a stiff reinforcing cage .Conventional cement mortars and water-cement ratios are used .

Building system must not only cope with strengths and flexibility requirements, but the insulation value is of high importance .In summer heat must be kept outside as much as possible .The structural system for ferrocement construction based on generic services facilities and insulating these structures involves the application of insulation material (Al-Rifaie Wail N., et al., 2014, Al-Rifaie Wail N., et al., 2014, Al-Rifaie Wail N., et al., 2014).

In the present work, the ability of constructing ferrocement multi-cell box (hollow core) slab /wall panels to be used as precast units in building construction are investigated .This aim was achieved by constructing five ferrocement full scale multi-cell box panels 4.20x1.00x0.17m)four-cell section (and tested under flexural loads .By using the unique properties of ferrocement with a relatively low amount of reinforcement, ferrocement slab /wall panels developed in the present investigation can be assembled into an effective multi-purpose panel system .The major advantages of this system over current construction methods are mainly due to the reduction in structural dead load and the use of fewer building elements, which are much easier to handle . The use of the lightweight panels allows maximum unobstructed space by using a standard module having dimensions such that flexibility in design is maintained .In addition, introducing the proposed ferrocement construction based on generic services facilities and insulating these structures involves the application of insulation material by means of accommodating 60mm thick insulation material within the box cells .This insulation material is working as a form work to form top and bottom flanges and webs as well.

It is concluded that the precast ferrocement multi-cell box slab /wall panels can be used as a building system and comparison of tests results with the standard design loads of buildings showed that the proposed system matches the design loads and can be used in construction of a wide range of buildings.

2 SCOPE OF THE WORK AND CONSTRUCTION OF FERROCEMENT OF FOUR-CELL BOX-LIKE PANELS

In order to study the structural behaviour of ferrocement multi-cell box slab panels to be used as a slab /wall unit when subjected to flexure load, a total of five full scale ferrocement multi-cell box slab panels were constructed and tested.

A pilot multi-cell box slab panel was constructed first to gain experience of the use of ferrocement material in constructing multi-cell box slab units, and to establish a method of construction and to assess its suitability for the construction of multi-cell box slab /wall units. Each box beam panel was subjected to a uniformly distributed load along the span by means of sacks of sand (15kg /sack) .All slab panels have been constructed using

sand passing sieve B.S. No. 7 (2.36mm) in the sand -cement mixture .The sand -cement mixture was mixed in the ratio of one part by weight of ordinary Portland cement to two parts of sand .The water -cement ratio used was 0.45 .Square welded steel wire mesh with an average diameter of 1mm has been used with opening of 12.7x12.7mm with mild steel mesh as a skeletal reinforcement having 4mm bar diameter .It is noted that the skeletal reinforcement with 200mm was used for top and bottom flanges and 50mm opening for the webs. Three strands were taken from wire meshes with three samples of mild steel of the skeletal reinforcement and tested in tension to determine the average of yield stress, ultimate strength and modulus of elasticity .(Table 1) gives the average values of the obtained results.

Table 1 Yield stress, Ultimate strength and modulus of elasticity of wire mesh and skeletal reinforcement used in the present investigation.

Type of reinforcement	Diameter mm	Yield stress f_y, MPa	Ultimate strength f_u, MPa	Modulus of elasticity E, MPa
Wire mesh	1	440.7	488.9	66100
Skeletal bar	4	396.0	450.0	189800

*Tests for wire mesh and steel bar of skeletal reinforcement were carried out according to ACI code 549 and ASTM A615/A615M-09 respectively.

Super-plasticizers (Structuro 502) are used for obtaining self compacted mortar during the construction of five multi-box slab units .(Table 2) gives the general specification of this material.

Table 2 Specifications of the super-plasticizers (Structuro 502) used in the present investigation

Appearance	Light brown colored liquid
pH value	6.5
S.G .@ 20oC	1.06 ± 0.02
Chloride content	Nil
Alkali content	Typically less than 1.5 gm Na2O equivalent per liter of admixture

3   SUBSIDIARY TESTS

To establish the cement mortar properties, cube mortar 50mm for measuring the compressive strength f_{cu} and 160x40x40mm prism for measuring the modulus of rupture, *fr*, a number of control specimens were cast and tested accordance with ASTM C109-87 for f_{cu} and ASTM C384 for *fr* .

4   CONSTRUCTION OF FERROCEMENT MULTI-BOX SLAB PANELS

As reinforcement of slab panels considered in the present investigation is given in (Table 3).

Table 3 Detailed reinforcement of slab panels considered in the present investigation.

Slab unit	Reinforcement :No .of wire mesh layers			Skeletal reinforcement	Diaphragms
	Top flange	Bottom flange	Webs		
MC1	4	4	4	4mm dia .with 200mm opening for top & bottom flanges and 50mm opening for webs	at both ends
MC2	4	4	4		at both end + intermediate) ½ - span(
MC3	4	4	4		at both end +3 intermediate) one at ½ span +2 at ¼ span(
MC4	4	2	4		at both ends
MC5	4	2	2		at both ends

All diaphragms, 30mm thick, were constructed and reinforced with four layers of wire mesh and two layers of skeletal reinforcement.

The mesh layers and skeletal reinforcement were cut to an appropriate size .The mesh layers were stretched, straightened and bounded to the skeletal steel cage using mild steel binding wires. After cleaning and oiling the steel mold, the cage was placed on the mold. As it was mentioned earlier that insulation material is working as a form work to form top and bottom flanges and webs as well. It may be noted that the mold was built from steel plate as shown in (Figure 1).
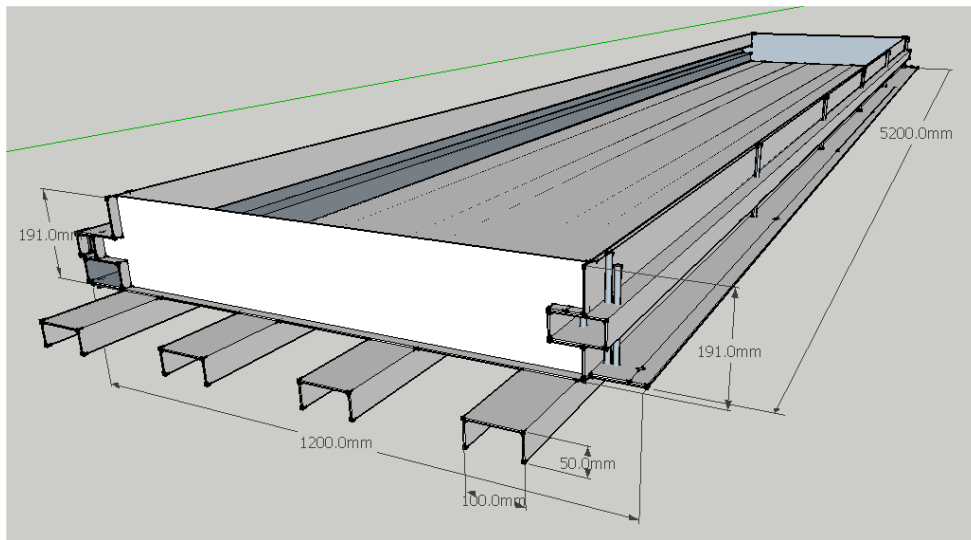
Figure 1 : Details of mold.

A typical cross section of the tested multi-cell box slab panel is shown in Figure)2(and in Figure)3(the positions of diaphragms along the span of the slab panel are shown.

All the materials required were weighed carefully, and then mixed in a mechanical mixer .Sand and cement were first mixed for 1min, then water was added and mixed for 2min .in a mixer with a capacity of 0.07m^3. The mortar was poured into the mesh reinforcement cage with trowels. Mortar control specimens were taken from the same mix.

Detail (B)   Detail (A)
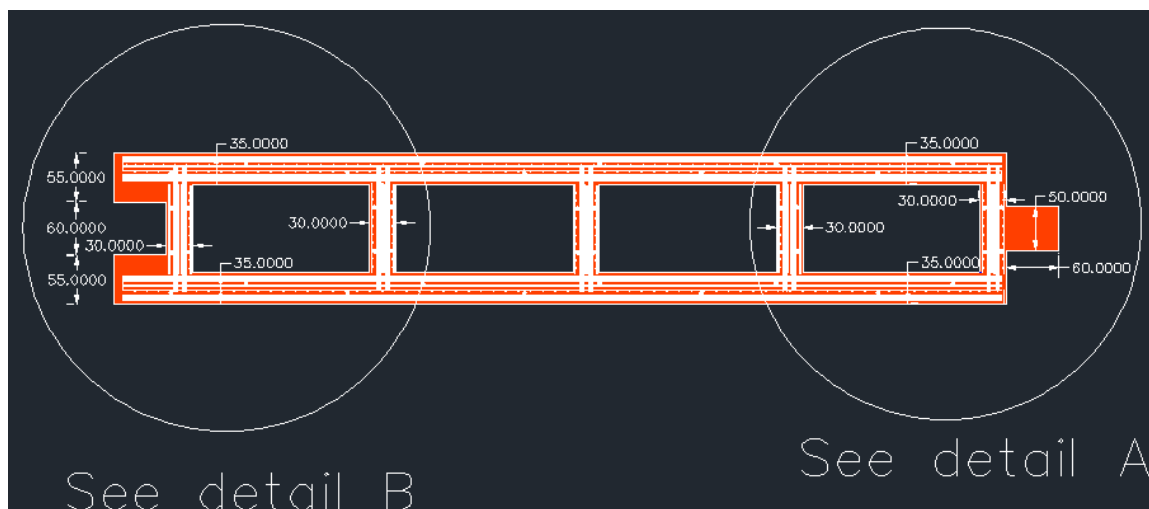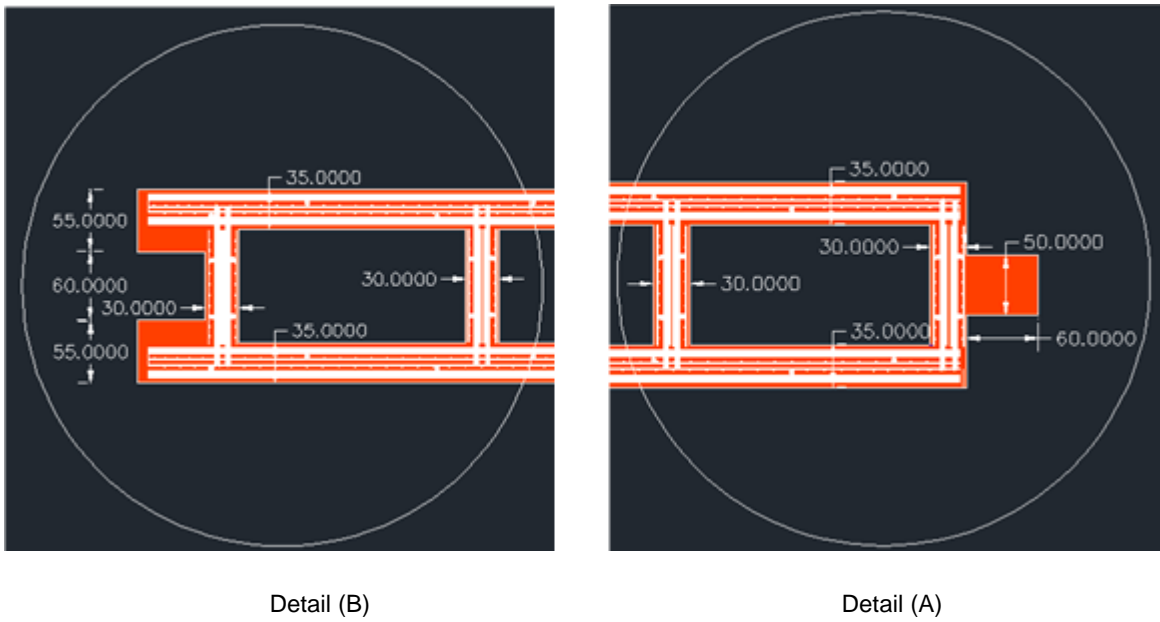
Figure 2: A typical cross section of the constructed multi-cell box slab panel in the present work.
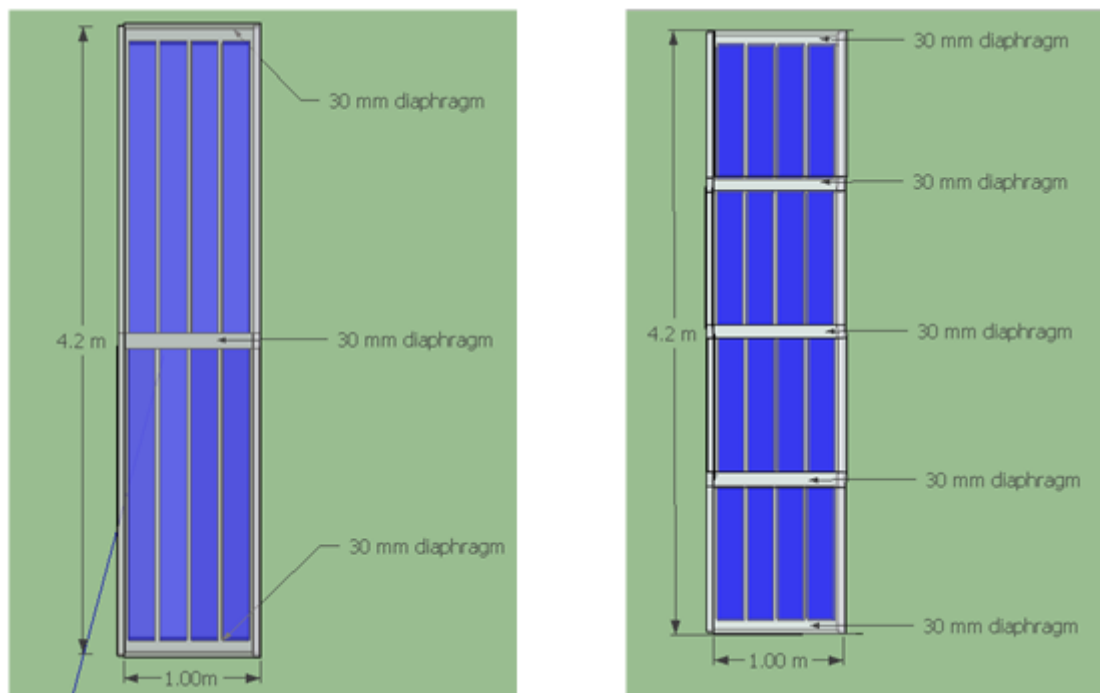
Figure 3: Positions of diaphragms along the span.

5 INSTRUMENTATION

The lateral deflections were measured at ½ -span by using dial gages having a minimum graduation of 0.01mm positioned at the mid-span of both edges of the bottom flange.

6 LOADING TEST PROCEDURE

Having placed and positioned each multi-box slab panel on the special support base, so that the following criteria are satisfied, see (Figure 4)

- To restrain all the end movement of the edge box-beams.
- To restrain the rotation about the longiudinal axis.

– To permit free rotations of the edge beams normal to their plane.
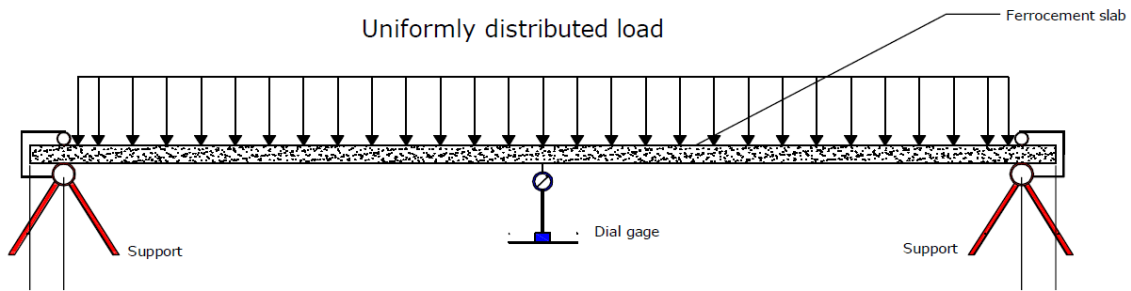
Figure 4: Multi-cell box slab panel under the test.

All slab panels were subjected to uniformly distrbuted load condition applied at the top flange. Having assembled the slab panel with a testing span of 4000mm, the dial gages were fixed at their appropriate locations .The initial readings of dial gages were recorded at the beginning of the test.

As it was mentioned earlier that each box slab unit is subjected to a uniformly distributed load along the span by means of sacks of sand (15kg /sack). The load was applied in stages .Each stage consist of one layer of sacks of sand with a total of 131.25kg/m^2 per layer, each stage lasting about 5 minutes in order to measure the deflections of the slab units. The loading continued until the appearance of first crack.

7 RESULTS

The results of the control specimens are given in (Table 4).

Table 4 Test results of control specimens

Multi-box slab unit	Compression strength, f_{cu} (MPa)	Modulus of rupture, fr (MPa)
Pilot slab unit	67.5	4.82
MC1	63.8	4.58
MC2	64.46	4.67
MC3	62.23	4.02
MC4	63.57	4.54
MC5	62.52	4.53

(Table 5) gives the measured first cracking load, first cracking deflection, and ultimate load .The mid-span deflections for different stages of loading are plotted in (Figures 5).

Table 5: Test results of ferrocement multi-cell box slab panels

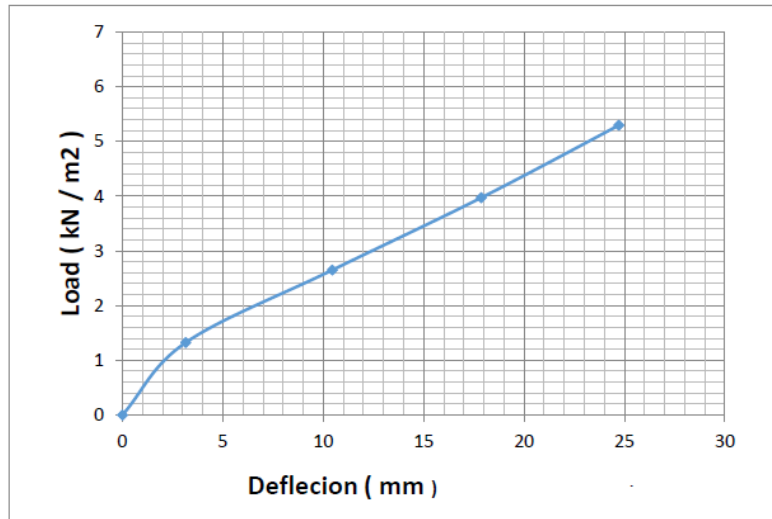| Multi-cell box slab unit	1st .Cracking load kN/m^2	1st .Cracking deflection, mm	Ultimate load kN/m^2	$\dfrac{\text{1st. Cracking load}}{\text{Ultimate load}}$
MC1	5.886	13	13.244	0.4444
MC2	6.511	12	14.237	0.4575
MC3	6.180	12	13.795	0.5086
MC4	3.863	14	8.608	0.4488
MC5	2.720	11	6.033	0.4509
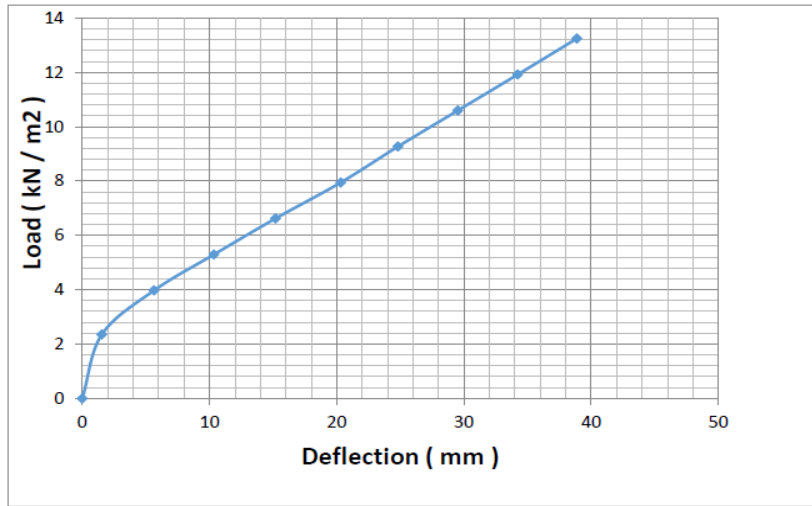
(a) Slab panel MC1
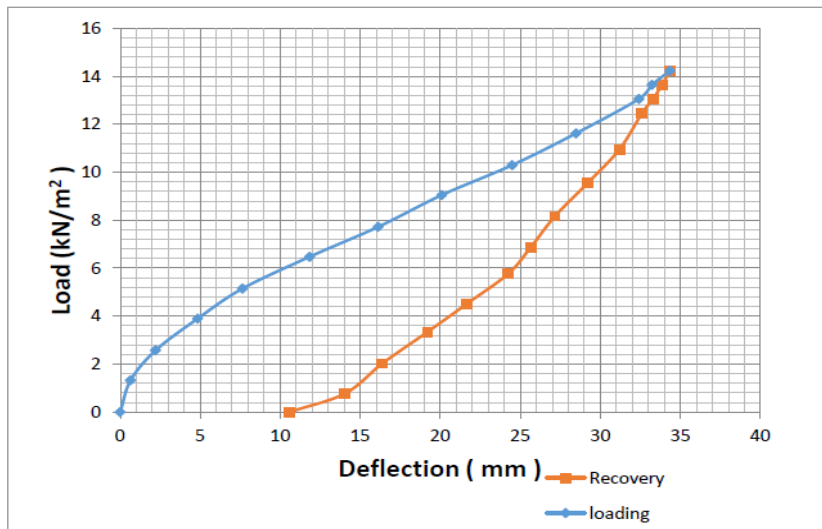
(b) Slab panel MC2
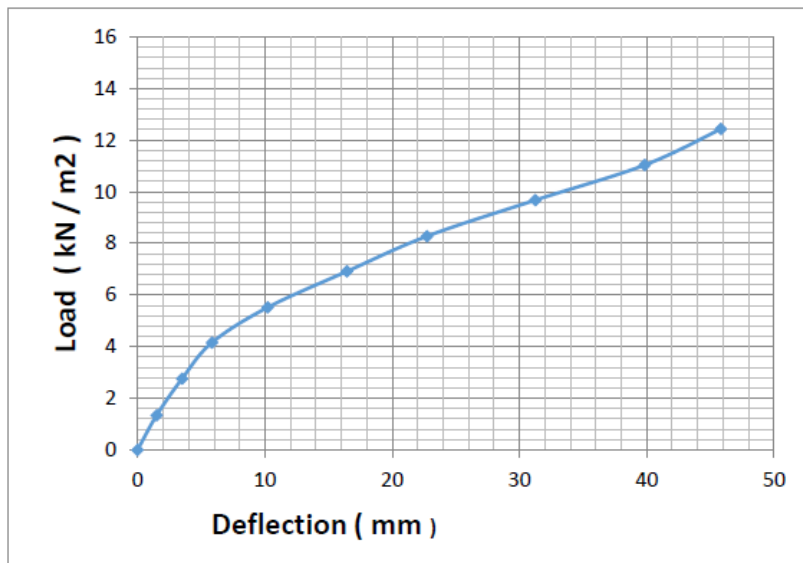
(c) Slab panel MC3
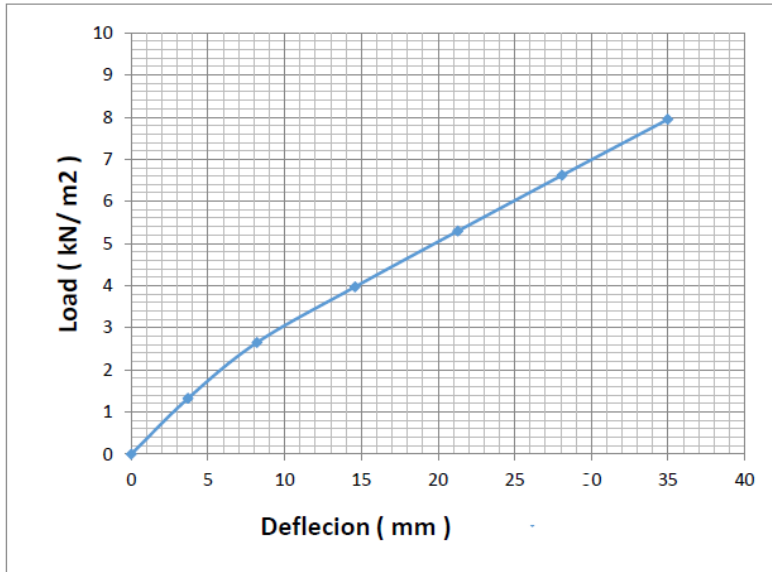
(d) Slab panel MC4

(e) Slab panel MC5

Figure 5: Mid-span load-deflection curve of multi-box slab panels

One of multi-cell slab panel considered during the test in the present work is shown in the following photo.

On the basis of the above results, the effects of number of wire mesh layers at top and bottom flange and at the webs and the positions of the diaphragms may now be discussed:

1 By having an intermediate diaphragm at mid-span, i.e., MC2 tend to increase the first cracking and ultimate loads. It may be noted that the recovery during removing the loads gradually, the load-deflection relationship is not linear and the value of residual deflection was 10.6mm when the all loads are removed.

2 Decreasing number of wire mesh layers at the bottom flange tend to decrease the first cracking and ultimate loads by 34.4 and 35 %respectively.

3 Decreasing number of wire mesh layers at the bottom flange and webs tend to decrease the first cracking and ultimate loads by 53.75 and 57.62 %respectively.

4 It may be noted that the ratio of first cracking load to ultimate load are ranging between 0.45 to 0.5 in all multi-cell box slab units.

8 CONCLUSIONS

On the basis of the experimental investigation carried out in the present work it may concluded that the precast ferrocement hollow core slab /wall panels can be used as a building system and comparison of test results with the standard design loads of buildings showed that the proposed system matches the design loads and can be used in construction of a wide range of buildings .By comparing the weight of the proposed ferrocement multi-cell box slab /wall panel with a solid reinforced concrete slab unit having same dimension, the weight is reduced to 48.%

As stated in references (Al-Rifaie, et al., 2014)(that with thermal insulation installed as part of the construction panels lend to achieving high levels of thermal performance and that the modern method)ferrocement eco-housing system (is able to produce very energy efficient dwellings resulted in a reduction in the emission of CO_2

9 REFERENCES

ACI Committee 549-1R-93, 1993, "Guide for the Design Construction, and Repair of Ferrocement". Farmington Hills, Michigan.

ACI Committee 549-R97:26,1997, "State of the art report on ferrocement in manual of concrete practice", 1997.

AL-RIFAIE, W .N., and HASSAN, A.H., , April 1994, '' Structural Behavior of Thin Ferrocement One-Way Bending Elements '', Journal of Ferrocement, Vol.24, pp.115-126.

AL-RIFAIE, W .N .and Alihmedawi, A .N., January 2000, '' Structural Behavior of Ferrocement Shell Roofs'', Journal of Ferrocement, Vol.30, No .1,.pp.85-103.

AL-RIFAIE Wail N., AHMED Waleed K. , IBRAHEEM Latif E., Al-SAMARRAIE Hashim Y., March 2, 2014. Proceedings of the 3rd "International Conference on Renewable Energy :Generation and Applications ICREGA14 / Thermal Performance of Ferrocement Green Building System, Al Ain, United Arab Emirates,.

AL-RIFAIE Wail N., AHMED Waleed K. , IBRAHEEM Latif E., Al-SAMARRAIE Hashim Y., 2014, "Ferrocement in Eco-Housing System", International Journal of Renewable Energy Research, Vol .4, No .1.

AL-RIFAIE Wail N., HASOON R., and AHMED Waleed K., (25-28th) August, 2014, 13th International Conference on Sustainable Energy technologies (SET2014) / Performance of Ferrocement Eco-Housing System Under Direct Fire, Geneva.

NAAMAN, A .E., 2000, '' Ferrocement & Laminated Cementations Composites'', Techno Press 3000, Michigan, USA, pp 372.

SESSION 24: ENERGY EFFICIENCY IN BUILDINGS

261: Design and optimisation of a novel passive cooling wind tower

John Kaiser CALAUTIT[1], Ben Richard HUGHES[2], Polytimi SOFOTASIOU[3]

[1] *University of Sheffield, Sheffield, UK, j.calautit@sheffield.ac.uk*
[2] *University of Sheffield, Sheffield, UK, ben.hughes@sheffield.ac.uk*
2 *University of Sheffield, Sheffield, UK, psofotasiou1@sheffield.ac.uk*

Buildings are responsible for almost 40% of the world energy usage. Heating Ventilation and Air-Conditioning (HVAC) systems consume more than 60% of the total energy use of buildings. In hot climates, the percentage of energy consumption by air conditioning is significantly larger due to the more extreme conditions of the local climate. Clearly any technology which reduces the HVAC consumption will have a dramatic effect on the energy performance of the building. Natural ventilation offers the opportunity to eliminate the mechanical requirements of HVAC systems by using the natural driving forces of external wind and buoyancy effect. A technology which incorporates both wind and buoyancy driven forces is the wind tower. Wind towers are natural ventilation systems based on the design of traditional architecture. Though the movement of air caused by the wind tower will lead to a cooling sensation for occupants, the high air temperature in hot climates will result in little cooling. In order to maximise the properties of cooling by wind towers, heat transfer devices were incorporated into the design to reduce the supply air temperature.

The aim of this work was to design and optimise a wind tower integrated with heat transfer devices using CFD modelling, validated with wind tunnel and field experiments. Care was taken to generate a high-quality CFD grid and specify boundary conditions. An experimental model was created using 3D printing. Qualitative and quantitative wind tunnel measurements were compared with the CFD data and good correlation was observed. Field testing of the wind tower was carried out to evaluate its performance under real operating conditions. A prototype of the device was produced and installed on top of a test facility in Ras Al Khaimah, UAE. The study highlighted the potential of the wind tower in reducing the temperature by up to 12˚C and supplying the required fresh air rates. The technology presented here is subject to a patent application (PCT/GB2014/052263).

Keywords: buildings; computational fluid dynamics (CFD); heat pipes; natural ventilation; wind tunnel

1. INTRODUCTION

There is a large reliance on electricity to run mechanical systems to provide ventilation and thermal comfort in buildings situated in hot regions. Commercial and residential buildings are responsible for 40 % of the world energy usage as well as 40-50 % of the global carbon emissions (WBCSD, 2009: page 1). Heating Ventilation and Air Conditioning (HVAC) systems consume more than 60 % of the total energy use in buildings (WBCSD, 2009: page 16). This represents a significant opportunity for reducing the energy consumption and greenhouse gas emissions. Natural ventilation devices such as wind catchers are increasingly being employed in building design for increasing fresh air rates and reducing energy consumption (O'CONNOR *et al.*, 2014: page 799). An example of this ventilation device is the Malqaf (Figure 1a), a uni-directional wind catcher which is a shaft projecting on the roof. It has a large opening facing the predominant wind that captures the air from high elevation and directs it downward into the room (HUGHES *et al.*, 2012:page 610). Figure 1b demonstrates the operation of a Malqaf wind catcher as part of a complete ventilation system, which includes an air escape roof that extracts the air out of the building. The system primarily depends on the air movement caused by the pressure differential, although convection produces the stack effect as well.
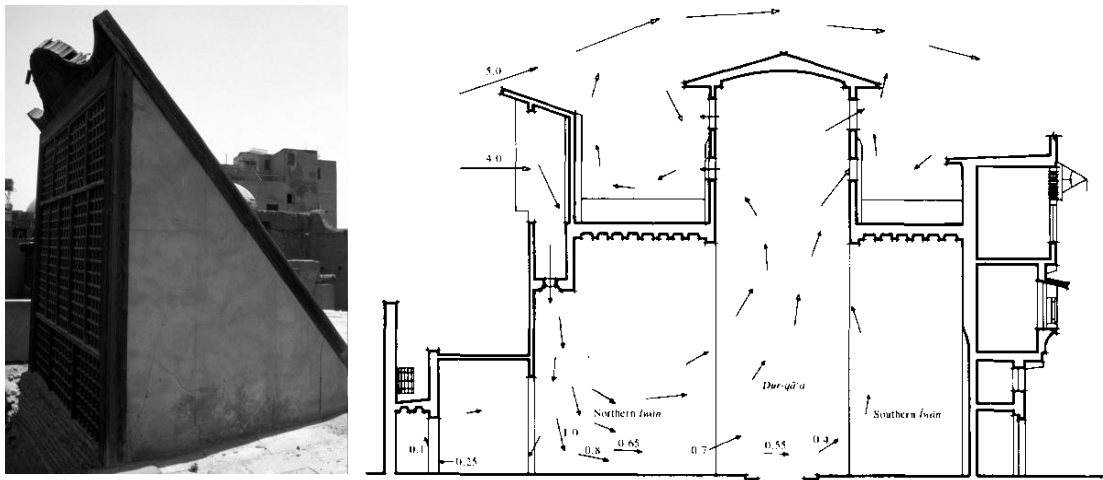
Figure 16: A traditional Malqaf wind catcher (left) airflow through a building with Malqaf (right)(FATHY, 1986).

1.1 Literature Review

A number of works have investigated the performance of wind catchers using numerical and experimental analysis (HUGHES *et al.*, 2014:page 607). Attia and Herde (2009) assessed the ventilation performance of a uni-directional wind catcher used in residential buildings. Wind tunnel and flow visualisation testing were carried out to evaluate the airflow rate and distribution in a room integrated with the wind catcher. The result indicated that a single uni-directional wind catcher was capable of supplying up to 4 ACH. Montazeri and Azizian (2008) evaluated the performance of a similar wind catcher using wind tunnel and smoke testing. A scale model of the ventilation device was mounted to a room which was installed beneath the base of the ventilation device. Results showed that the one-sided wind catcher had the potential to be provide ventilation in urban settings.

Traditional wind catchers were integrated with evaporative cooling devices to increase its thermal performance. Bahadori *et al.* (2008) evaluated the cooling performance of two designs of wind catchers using experimental testing. The two designs were one with wetted columns, equipped with cloth curtains suspended in the channel and one with wetted surfaces was equipped with cooling pads at the entrance. The results indicated that the device with wetted column was more effective during high wind conditions, while the device with wetted surfaces was more effective during low wind conditions. Safari and Hosseinnia (2009) used CFD modelling to investigate the thermal performance of new designs of wind catchers with wetted columns. The numerical results showed that the wetted columns with the height of 10 meters were able to reduce the air temperature by 12 K.

Bouchahm *et al.* (2011) evaluated the ventilation and thermal performance of a wind catcher incorporated to a building using experimental analysis. Clay conduits were mounted inside the shaft of the device to improve the heat transfer and a water pool was situated at the bottom of the device. Kalantar (2009) evaluated the performance of a wind catcher with evaporative cooling spray in the hot region of Yazd using CFD. It was

found that the wind catcher was able to reduce the air temperatures by 10 to 15°C at its optimum performance. Using the same CFD method, Calautit *et al.* (2013a) compared the thermal performance of an evaporative cooling and heat transfer device assisted cooling for traditional wind catchers. The heat transfer device system works on a similar principle of providing cooling but unlike evaporative cooling, which directly evaporates water to the airstream, a heat transfer device is an indirect cooling devices Therefore, there is less increase in humidity compared to evaporative cooling techniques, making it viable for regions with moderate humid conditions. There is also less risk of contamination of the airstream (for example, waterborne bacteria). Furthermore, the study concluded that height was not a factor for the heat transfer device integrated wind catcher, making it viable for commercial devices.

1.2 Objectives

In our previous work (CALAUTIT *et al.*, 2013b, CALAUTIT *et al.*, 2013c, CHAUDHRY *et al.*, 2015), we evaluated the integration of heat transfer devices into traditional and modern wind catchers. The results showed that the system was capable of reducing the temperature and supplying the recommended fresh air rates. Although, the previous analysis were completely CFD-based and assessment by experimental methods was of further interest. This study will use CFD, wind tunnel and field-test analysis to address the gap in the literature.

Figure 2 shows the operation of the proposed wind catcher with heat transfer devices. The hot outdoor air enters the wind catcher through the louvers which are used to deflect the impact of weather, noise, direct sunshine and other small objects from entering the wind catcher. The airflow is driven downwards and passed through a series of heat transfer devices which absorbs the heat from the airflow (evaporator) and transfers it to a parallel cool sink (condenser). The heat transfer device is a simple device of very high thermal conductivity with no moving parts that can transport large quantities of heat efficiently over large distances fundamentally at an invariable temperature without requiring any external electricity input. It is essentially a conserved slender tube containing a wick structure lined on the inner surface and a small amount of fluid such as water at the saturated state. Adjustable dampers are mounted at the bottom of the unit to control the delivery rate of the outdoor air, as fluctuations in external wind speed greatly influence the air movement rate within the occupied space. The cooled air is supplied to the room beneath the channel via the ceiling diffusers.
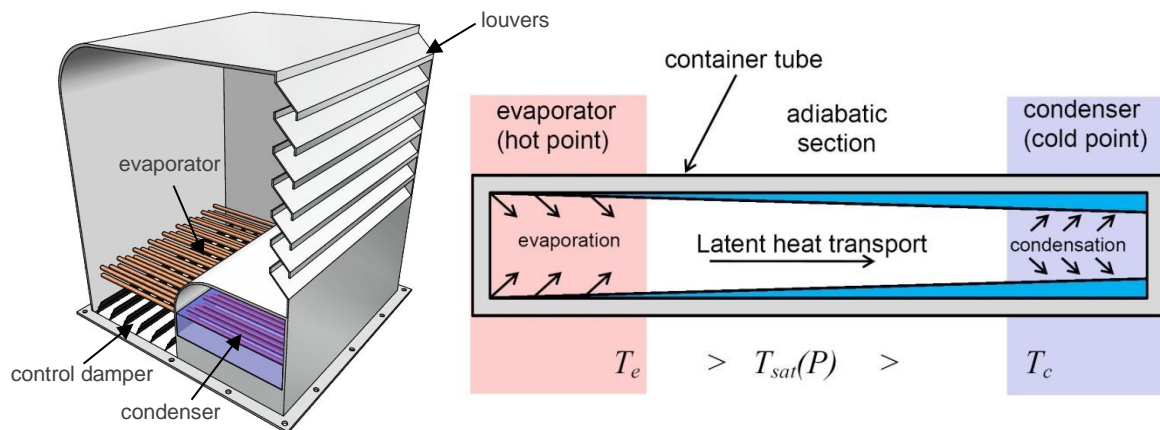

Figure 2: Wind catcher with heat transfer devices (left) heat transfer device operation (right) (ESPCI, 2015).

2   METHODOLOGY

2.1 Numerical Modelling

The basic assumptions for the numerical simulation include a three-dimensional, fully turbulent, and incompressible flow. The internal and external flow was modeled by using the standard *k*–epsilon turbulence model, which is a well-established method in research on natural ventilation (CALAUTIT *et al.*, 2013d). The CFD code was used with the Finite Volume Method (FVM) approach and the Semi-Implicit Method for Pressure-Linked Equations (SIMPLE) velocity-pressure coupling algorithm with the second order upwind discretisation (SOFOTASIOU *et al.*, 2015: page 17). The general governing equations are available in (ANSYS, 2014).

The wind catcher geometry (Figure 3) was created using a commercial CAD software and then imported into ANSYS Geometry (pre-processor) to create a computational model. The solid parts of the wind catcher and test room geometry were created using the CAD software. However, replicating the physical geometry of the wind catcher does not represent a computational domain. To create a computational domain, the fluid volume was extracted from the solid model as shown in Figure 4. The fluid domain was separated into three parts: the macro-climate (outdoor), wind catcher and micro-climate (indoor). The macro-climate was created to simulate the outdoor airflow. The macro-climate consisted of an inlet on one side of the domain, and an outlet on the opposing boundary wall. The macro-climate dimensions was 5 m x 5 m x 10 m (CALAUTIT *et al.*, 2014a). According to the dimensions of the wind catcher (1 m x 1 m x 1 m), the model produced a blockage of 4.8 % (CALAUTIT *et al.*, 2014b). The wind catcher was incorporated to a micro-climate with the dimensions of 3 m x 5 m and 5 m, representing a small room (CALAUTIT *et al.*, 2014c). The wind catcher was modelled with seven louvres angled at 45°. The wind catcher was assumed to be supplying at 100 % (fully open), therefore the volume control dampers was not added to the model. The cylindrical heat transfer devices, each with an outer diameter of 0.02 m, were integrated in to the lower part of the channel as shown in Figure 3. The horizontal distance between each pipe was 0.05 m.
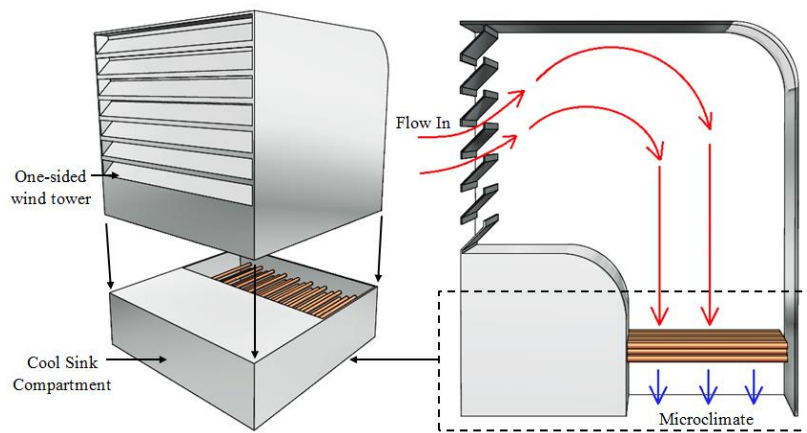
Figure 3: CAD model of the wind catcher with cylindrical heat transfer devices.

Due to the complexity of the model, a non-uniform mesh was applied to volumes of the computational domain (CALAUTIT *et al.*, 2013). The generated computational mesh of the wind catcher and room model are shown in Figure 4. The grid was modified and refined according to the critical areas of interests in the simulation such as the heat transfer devices. The size of the mesh element was extended smoothly to resolve the areas with high gradient mesh and to improve the accuracy of the results. The inflation parameters were set according to the complexity of the geometry face elements, in order to generate a finely resolved mesh normal to the wall and coarse parallel to it [19].
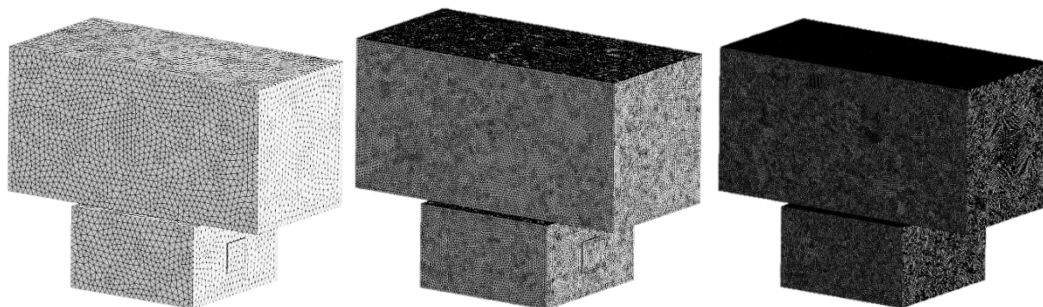

Figure 4: Mesh refinements: 1 million, 2.1 million and 4.9 million cells.

Mesh adaptation was used to verify the computational mesh of the wind catcher and room model. The process increased the number of elements between 1 and 7.2 million. Each stage continued until an acceptable compromise was reached between: number of elements; computational time to solve; and the posterior error indication. At 4.9 million elements the error indication between refinements was at its lowest; coupled with the computational time, made it an acceptable compromise. Figure 4 shows the stages of refinement from 1 million to 4.9 million elements.

The boundary conditions for the CFD model are summarised in Table 1.

Table 12: Summary of the CFD model boundary conditions

Boundary Conditions	Set Value
Discretisation Scheme	Second order upwind
Algorithm	SIMPLE
Time	Steady State
Velocity inlet	1-5 m/s
Pressure outlet	Atmospheric
Gravity	-9.81
External temperature	318 K
Heat transfer device temperature	293 K

2.2 Experimental Wind Tunnel Testing

A 1:10 scale model of the wind catcher was used in the experimental study. The investigation was conducted in a closed-loop wind tunnel detailed in (CALAUTIT *et al.*, 2014d, CALAUTIT *et al.*, 2014e). The wind tunnel had a test section with the dimensions of 0.5, 0.5, and 1 m (Figure 5). According to the dimensions of the 1:10 model and the wind tunnel cross-section, the wind catcher scale model produced a wind tunnel blockage of 4.8%, and no corrections were made to the measurements obtained with these configurations (CALAUTIT *et al.*, 2015a). The creation of an accurate scaled wind tunnel prototype was essential for the experimental study. Therefore, the model of wind tunnel was constructed using 3D printing. Figure 5 shows the 3D printed 1:10 wind catcher scale model design The model of the wind catcher was connected to a 0.5 x 0.5 x 0.3 m room, which was mounted underneath the test section. A single 0.1 x 0.1 m outlet window was located at the leeward side of the room. The test room was made of acrylic perspex sheet to facilitate the flow visualisation of the airflow.

The airflow into the room was measured using a hot-wire anemometer, which was positioned below the channels of the wind catcher. The cross-sectional area of the wind catcher was divided into several portions and the supply rate through the channel was calculated. The hot-wire sensor gave airflow velocity measurements with uncertainty of ±1.0 % rdg. at speeds lower than 8 m/s and uncertainty of ±0.5 %rdg. at higher speeds (8–20 m/s).

Figure 5: Low-speed wind tunnel (left) 3D printed model (right) (CALAUTIT et al., 2015b).

2.3 Experimental Field Testing

Experimental field testing of the wind catcher with heat transfer devices was carried out to evaluate its performance under real operating conditions. A prototype of the wind catcher was produced and mounted on top of a 3 m x 3 m x 3 m test room on an open field site in Ras Al Khaimah, UAE. Figure 6 shows the site location and the test setup. Ras Al Khaimah is located at latitude 25.78°N and longitude 55.95 °E. Its climate can be characterised as a hot-desert climate. High temperatures can be expected from June to September, with a maximum temperature ranging between 312 K and 315 K and a minimum temperature ranging between 297 K and 303 K. The predominant wind angle is between N and N-W direction. Therefore, the opening of the wind catcher was positioned to face the predominant wind. The average wind velocity is between 3 m/s and 4 m/s.

Figure 6: Test site in Ras Al-Khaimah (top) wind catcher mounted on the roof (bottom left) measurement setup (bottom right).

The experimental tests were carried out during the month of September, between 11:00 AM and 4:00 PM (highest outdoor air temperatures). The test room was constructed from insulated studwork (weather-proofed). An opening located on the leeward side of the room was used as an outlet. The prototype was constructed using aluminum plate with a thickness of 3 mm. The overall dimension of the wind catcher was 1 m x 1 m x 1.2 m. A total of 50 cylindrical heat transfer devices (each with an outer diameter of 0.02 m and total length of 0.95 m) and a parallel cold sink (fed by water at approximately 288 K - 293 K) were incorporated into the wind catcher to provide the cooling.

3 RESULTS AND DISCUSSION

3.1 Numerical Simulation Results

Figure 7 illustrates a cross-sectional plot of the velocity contours in the room and wind catcher with heat transfer devices. The right hand side of the plot shows the scale of airflow velocity (m/s). The contour plot in the fluid domain is colour coded and related to the CFD colour map, ranging from 0 to 3.7 m/s. As observed, the airflow passed around the wind catcher, parts of it entered the wind catcher and parts of it exited through the pressure outlet on the right side of the domain. After entering the wind catcher, the airflow was accelerated as it hit the rear wall of the channel and re-directed downward towards the room. Separation zone was observed near the lower edge of the opening, which caused a sharp variation in velocity in this region and reduced the maximum efficiency of the wind catcher. High draft speeds were observed at the centre of the room reaching up to 0.83 m/s. The air stream was circulated inside the structure and exited the opening located on the leeward side of the room. The average air velocity inside the room model was 0.28 m/s.
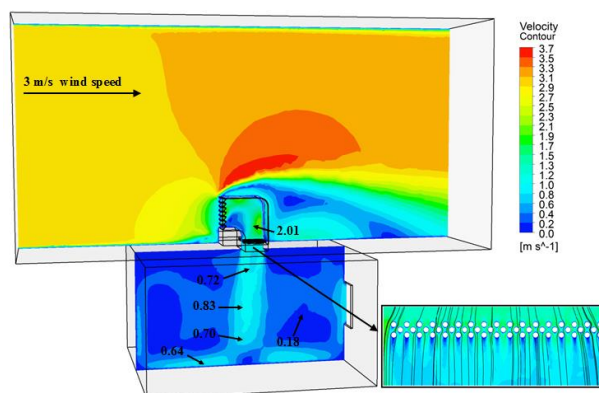
Figure 7: Cross-sectional plot of the velocity contours.

Figure 8 displays a cross-sectional plot of the temperature distribution inside the room with a wind catcher. The right hand side of the contour plot shows the scale of static temperature (K). The contour plot in the fluid domain is colour coded and related to the CFD colour map, ranging from 293 K to 318 K. The average temperature inside the room was 310.4 K when the temperature of the outdoor wind was set at 318 K. The

temperature was reduced further at the immediate downstream of the heat transfer devices with a supply temperature value of 309 K. Figure 9 shows the effect of the variation of wind speed on the thermal performance of the wind catcher system.
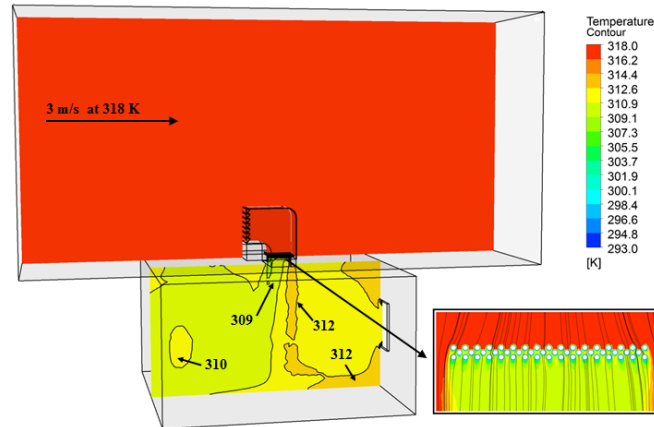

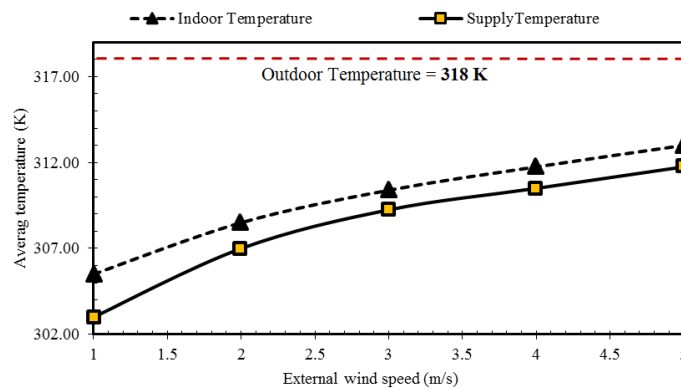Figure 8: Cross-sectional plot of the static temperature contours.

Figure 9: Effect of wind speed on supply and indoor temperature.

3.2 Wind Tunnel Test Results

Figure 10 shows the comparison between the predicted and experimental results for the airflow velocity measurements below the wind catcher channel. An uneven airflow distribution was observed below the supply channel. The airflow speed on the right corner of the channel (Points 1, 4 and 7) was 30 – 60 % higher than the left corner (Points 3, 6 and 9). This was due to the flow separation created by the sudden change in direction (90˚ bend). Good agreement was observed between the CFD results and measurement, with the error below 10 % for all the points except for point 6. The average error across the points was 7.2 %. Figure 11 compares the smoke testing results with the CFD flow visualisation.
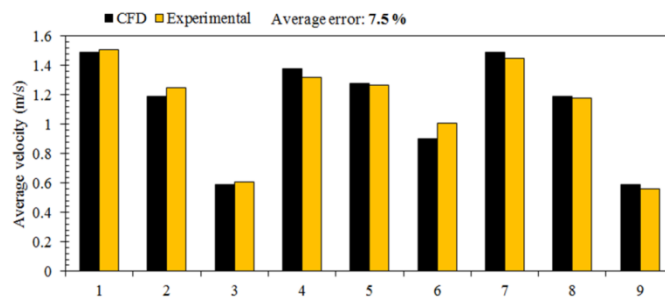
Figure 10: Comparison between the prediction of the CFD and the measurement of the airflow speed at different points.
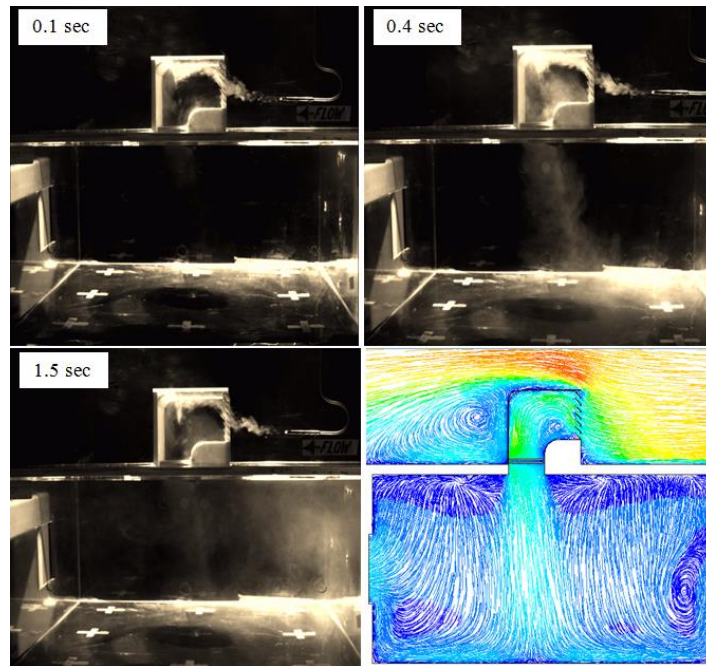
Figure 11: Wind tunnel flow visualisation and CFD streamlines.

3.3 Field Test Results

Figure 12a is an example of the day-time cooling of the wind catcher during a windy and summer day. It shows the external air temperature, heat transfer device surface temperature and the temperature downstream of the heat transfer devices from 11:00 AM to 4:00 PM, September 17, 2014. The cold sink was fed with water every 15 – 20 minutes to maintain the sink temperature at around 293 K. This was initiated when the wind catcher began to deliver airflow inside the room (11:40 AM), although the wind was still mostly out from the W direction at this point. The air temperature decreased by 3 K - 4 K at 12:00 PM when the wind started to flow inside the wind catcher. At 1:00 PM, the wind was blowing more consistently from WNW direction (45˚ approach angle) and the reduction was 4 K - 5 K. From 2:00 to 4:00 PM, the wind was parallel to the opening of the wind catcher and the temperature reduction ranged between 2 K - 7 K.

Figure 12b shows the measured outdoor, supply and heat transfer device surface temperature from 11:00 AM to 4:00 PM, September 18, 2014. The wind catcher began to deliver airflow into the room at 11:30 AM and the temperature reduction ranged between 3 - 4 K. From 1:00 to 4:00 PM, the wind was blowing mostly from NW and NNE direction and the temperature reduction ranged between 3 K – 11.5 K.
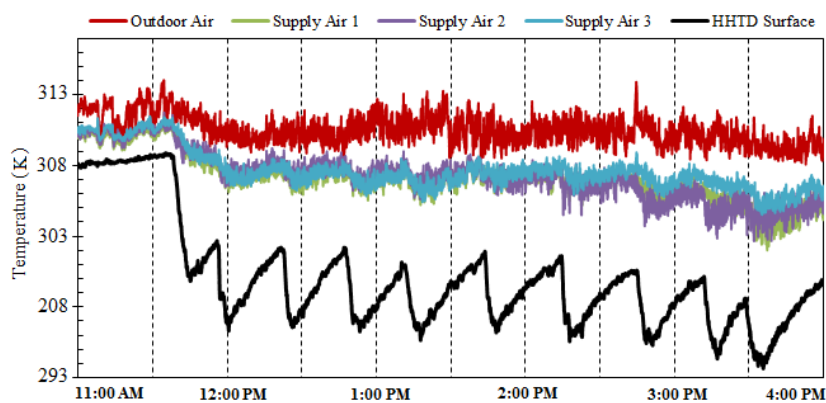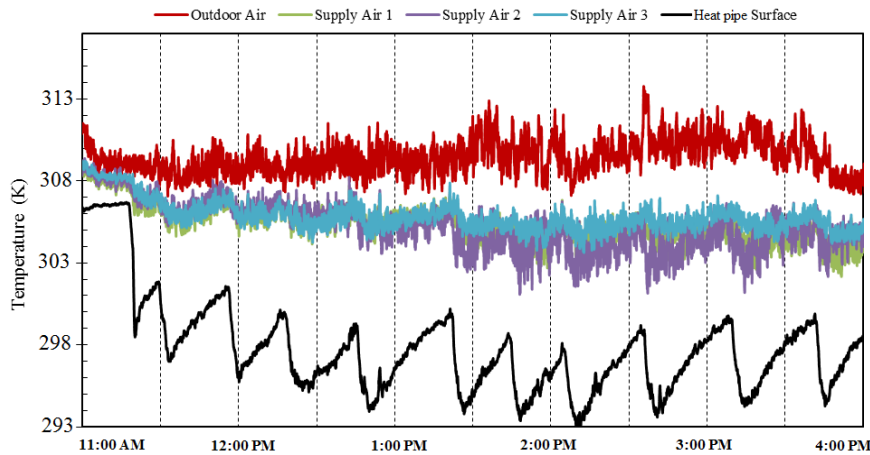
Figure 12: September 17 testing results from 11:00 to 4:00 (top). September 18 testing results from 11:00 to 4:00 (bottom).

4   CONCLUSION

The integration of wind catchers as a low energy alternative to HVAC systems has the potential to improve the thermal comfort of occupants, the indoor air quality and reduce energy consumption and greenhouse gas emissions. In this study, a standard roof-mounted wind catcher was integrated with heat transfer devices to reduce the temperature of the supply airflow. The work used CFD, wind tunnel analysis and field testing to evaluate the performance of the wind catcher with heat transfer devices. The CFD model provided detailed analysis of the airflow and temperature distribution inside the wind catcher and also the indoor space. A cooling potential of up to 12 K was identified in this study. Simulation of various outdoor wind speeds showed that the cooling performance of the heat transfer devices were indirectly proportional to the speed of the outdoor airflow. At 5 m/s outdoor wind speed, the air temperature was only reduced by 5 K - 6 K. While, a higher temperature reduction was observed at lower wind speed, 9.5 K reduction at 2 m/s. The difference between the wind tunnel measurements and CFD results was 10 % on average. Full-scale testing of the wind catcher was carried out to evaluate its performance under real conditions.

5   REFERENCES

ANSYS® Academic Research, 2014. ANSYS FLUENT User's Guide Release 14.0. Available online: https://www.ansys.com.

ATTIA, S, DE HERDE, A, 2009. Designing the Malqaf for summer cooling in low-rise housing, an experimental study, Conference on Passive and Low Energy Architecture, Quebec City, Canada, 22-24.

BAHADORI, M, MAZIDI, M, DEHGHANI, R, 2008. Experimental investigation of new designs of wind towers. *Renewable Energy,* 33, 2273–2281.

BOUCHAHM, Y, BOURBIA, F, BELHAMRI, A, 2011. Performance analysis and improvement of the use of wind tower in hot dry climate. *Renewable Energy*, 36, 898-906.

CALAUTIT, JK, 2013. Integration and Application of Passive Cooling Within a Wind Tower, PhD thesis, University of Leeds.

CALAUTIT, JK, CHAUDHRY, HN, HUGHES, BR, GHANI, SA, 2013a. Comparison between evaporative cooling and heat transfer device assisted thermal loop for a commercial wind tower in hot and dry climatic conditions, *Applied Energy,* 101, 740-755.

CALAUTIT, JK, HUGHES, BR, CHAUDHRY, HN, GHANI, SA, 2013b. CFD analysis of a heat transfer device integrated wind tower system for hot and dry climate. *Applied Energy,* 112, 576-591.

CALAUTIT, JK, HUGHES, BR, GHANI, SA, 2013c. Numerical investigation of the integration of heat transfer devices into wind towers. *Chemical Engineering Transactions,* 34, 43-48.

CALAUTIT, JK, HUGHES, BR, GHANI, SA, 2013d. A Numerical Investigation into the Feasibility of Integrating Green Building Technologies into Row Houses in the Middle East. *Architectural Science Review*, 56, 279-296.

CALAUTIT, JK, O'CONNOR, D, HUGHES, BR, 2014a. Determining the optimum spacing and arrangement for commercial wind towers for ventilation performance. *Building and Environment*, 82, 274-287.

CALAUTIT, JK, HUGHES, BR, 2014b. Measurement and prediction of the indoor airflow in a room ventilated with a commercial wind tower. *Energy and Buildings*, 84, 367-377.

CALAUTIT, JK, HUGHES, BR, 2014c. Wind tunnel and CFD study of the natural ventilation performance of a commercial multi-directional wind tower. *Building and Environment*, 80, 71-83.

CALAUTIT, JK, CHAUDHRY, HN, HUGHES, BR, SIM, LF, 2014d. A validated design methodology for a closed-loop subsonic wind tunnel. *Journal of Wind Engineering and Industrial Aerodynamics*,125, 180-194.

CALAUTIT, JK, HUGHES, BR, 2014e. Integration and application of passive cooling within a wind tower for hot climates. *HVAC&R Research*, 20, 722-730.

CALAUTIT, JK, O'CONNOR, D, SOFOTASIOU, P, HUGHES, BR, 2015a. CFD Simulation and Optimisation of a Low Energy Ventilation and Cooling System. *Computation*, 3, 128-149.

CALAUTIT, JK, HUGHES, BR, SHAHZAD, SS, 2015b. CFD and wind tunnel study of the performance of a uni-directional wind catcher with heat transfer devices. *Renewable Energy*, 83, 85-99.

CALAUTIT, JK, O'CONNOR, D, HUGHES, BR, SHAHZAD, SS, 2015c. Performance Investigation of a Commercial Wind Catcher with Horizontally-arranged Heat Transfer Devices (HHTD). *Proceedings of the 3rd Annual Conference on Architecture and Civil Engineering (ACE 2015)*, 1.

CALAUTIT, JK, HUGHES, BR, O'CONNOR, D, SHAHZAD, SS, 2015d. CFD and Wind Tunnel Study of the Performance of a Multi-Directional Wind Tower with Heat Transfer Devices. *Energy Procedia*.

CHAUDHRY, HN, CALAUTIT, JK, HUGHES, BR, 2015. Computational analysis of a wind tower assisted passive cooling technology for the built environment. *Journal of Building Engineering*, 1, 63-71.

ESPCI, 2015, Modelling of pulsating heat transfer device, available on: http://www.pmmh.espci.fr.

FATHY, H, 1986. Natural energy and vernacular architecture: principles and examples with reference to hot arid climates. The University of Chicago Press Chicago and London.

HUGHES, BR, CALAUTIT, JK, GHANI, SA, 2012. The Development of Commercial Wind Towers for Natural Ventilation: a review. *Applied Energy*, 92, 606-627.

HUGHES, BR, CHAUDHRY, HN, CALAUTIT, JK, 2014. Passive energy recovery from natural ventilation air streams. *Applied Energy,* 113, 127-140.

KALANTAR, V, 2009. Numerical simulation of cooling performance of wind tower (Baud-Geer) in hot and arid region. *Renewable Energy*, 34, 246–254.

MONTAZERI H, AZIZIAN, R, 2008. Experimental study on natural ventilation performance of one-sided wind catcher. *Building and Environment* , 43, 2193–2202.

SAFFARI, H, HOSSEINNIA S, 2009. Two-phase Euler-Lagrange CFD simulation of evaporative cooling in a Wind Tower. *Energy and Buildings*, 41, 991–1000.

SOFOTASIOU, P, HUGHES, BR, CALAUTIT, JK, 2015. Qatar 2022: Facing the FIFA World Cup climatic and legacy challenges. *Sustainable Cities and Society*, 14, 16-30.

O'CONNOR, D, CALAUTIT, JK, HUGHES, BR, 2014. A Study of Passive Ventilation Integrated with Heat Recovery. *Energy and Buildings*, 82, 799-811.

WBCSD, 2009, Energy Efficiency in Buildings – Transforming the Market.

372: Assessing energy efficiency in a newly designed office building

Case study petrojet company new head office building in Cairo, Egypt

Nayera R. Abdallah[1], Ali K. Abdel-Rahman[1],
S. Ookawara[1,2], Essam K. Mahrous[3]

1 Department of Energy Resources Engineering, Egypt- Japan University of Science and Technology E-JUST, New Borg Elarab, Alexandria 21934, Egypt, nayera.abdelhafez@ejust.edu.eg, ali.kamel@ejust.edu.eg
2 Department of Chemical Engineering, Graduate School of Science and Engineering, Tokyo Institute of Technology, Tokyo, Japan, sokawara@chemeng.titech.ac.jp
3 Department of Architectural Engineering, Faculty of Engineering, Assiut University, Assiut, Egypt, dr_essam_mahrous@yahoo.com

Energy use in buildings is closely linked to their design (form, orientation and building materials), operational and space utilization characteristics and the behaviour of their occupants. Due to demand for sustainability, more passive buildings will be built in Egypt. This study evaluates the energy performance in a newly designed office building in Egypt. In this building, energy efficiency aspects were considered during the design. The evaluation is done using two different tools - Portfolio Manager (PM) and Target Finder (TF) - related to ENERGY STAR (ES) using the Energy Use Intensities (EUI). The only difference is that PM needs at least 12 consecutive months of metered utility bills to perform the evaluation calculations, while TF needs an estimated annual energy use for each type of energy consumed in the building. Energy consumption was determined by two ways: simulation and calculation. DesignBuilder (DB) has been used in the current study to simulate the building energy use for a whole year considering building design, building materials, optimization of thermal comfort, lighting, weather data and activity in the case study building. In addition, calculations for annual energy use were done using the data sheets with each energy consuming system utilized in the building based on operating hours of each. The ES scores for both simulation and calculation results were obtained. The main conclusions were that ES can be used to evaluate energy performance of office buildings in Egypt. Moreover, the results showed that the Egyptian office buildings can compete with the USA office buildings in applying energy efficiency strategies. Results of the optimizations showed significant reduction in terms of energy consumption. Finally, the simulation results showed the relative effect of the applied design, shading, orientation and the energy efficient lighting and HVAC systems on the annual energy consumption and ES score.

Keywords: energy efficiency, ENERGY STAR, Simulation

1. INTRODUCTION

A great portion of world energy consumption is related to the built environment. Building sectors are responsible for approximately 42% of the world's total annual energy consumption. Most of this energy is consumed by lighting, heating, ventilation and air conditioning systems (HVAC) and electricity based office appliances (Rahman et al., 2010). The relation between the increased greenhouse gases (GHG) emitted to the atmosphere and the energy use is also a motive to follow a more efficient energy usage and lowering the total energy demand. Among various aspects of energy conscious design, energy performance of the building deserves great attention, especially for office buildings. With rapid economic growth, there have been marked increases in large office building development projects, and there is a growing concern about energy consumption in buildings (especially commercial developments such as office buildings) (Eskin and Türkmen, 2008). A review was provided of the energy saving policies and technologies on double glazing windows, central heating and air conditioning in office buildings. The results showed that among factors that make managers have a more energy saving profile willingness to undertake specific energy efficient measures for heating and cooling are ownership, awareness status, recent establishment of the company, companies dealing with services, companies with a high number of personnel, and companies with high ratios of electricity bill per annual turnover (Tsagarakis et al., 2012).

Energy conservation measures often provide better indoor air quality (IAQ) and enhance occupancies productivity. However, a cost penalty is experienced if poor IAQ is traded for reduced energy consumption (Rahman et al., 2010). Many studies investigated factors affecting energy consumption and cost in a building. Some studies have shown that the building shape can have a significant impact on the energy consumption and costs. Different results obtained depending on climate: rigorous or mild. The shape affected the energy consumption when the climate is cold. If the conception of buildings is expected to be energy efficiency, compactness will be looked for. When the climate is mild, the shape is no longer effective and compactness can no longer be recommended. The shape is no longer relevant in mild and sunny climates (Depecker et al., 2001).

Actual building energy consumption depends on inhabitants' behaviour and will mainly depend on their awareness of the energy saving topic (Depecker et al., 2001). The role of the individual to achieve energy savings in this changing environment is increasing as plug load energy use is usually directly under the control of individuals, and may be reduced through changes in their behaviour. Historically lighting and heating and cooling have been viewed as the large energy consumers whereas plug loads have been viewed as essential to the operation of the organization, a necessary and unavoidable use. Plug-in loads are the fastest growing category of energy use nowadays. While in lighting, HVAC and water heating advanced controls can be applied to achieve savings, by 2030 commercial electricity use will be dominated by fast increase of independent devices, under the immediate control of individuals, many of which it is convenient to leave on "stand-by" (Orland et al., 2014).

Conventional energy saving measures like high-quality windows, solar shading and the installation of additional insulation are simple and well known solutions for achieving better performing buildings. However, it has become common to design either fully or highly glazed office buildings without any considering energy consumption. This results in high heating and cooling needs, high investment costs and often poor solar protection and glare. Optimizing the performance of the envelope, while providing natural lighting and views to the outside, could be seen as one key method of achieving nearly Zero Energy Building by 2021 (Pikas et al., 2014). High-efficiency envelope with shading can improve indoor thermal comfort and productivity. In addition, daylighting dimming when utilized in perimeter area and set illumination is 400 lux can show big energy saving results (Pan et al., 2008). Another study showed that shading can reduce both the cooling load and yearly energy consumption of buildings. However, this study did not incorporate any occupancy schedule or internal loads for the buildings (Dascalaki and Santamouris, 2002). Buildings which have a well-insulated outer envelope and well optimized glazed windows have lower energy consumption, since heating and cooling loses are less (Karabay and Arici, 2012). The importance of fenestration design (window to wall ratio, window orientation, and width to depth ratio) was studied finding that optimal design can decrease building energy consumption in office buildings and achieve energy savings in all climate zones. Better energy savings would be achieved in hot climates. Optimal fenestration design would be least effective in cold climates. The results of this analysis show that conventional energy efficiency technologies such as thermal insulation, low-emissivity windows, window overhangs, and day lighting controls can be used to decrease energy use in new commercial buildings by 20–30% on average and up to over 40% for some building types and locations (Susorova et al., 2013).

The relative total energy use increases with window size independently of the (window to wall ratio) value. In addition, the rate of increase of relative total energy use vs. window area depends on the glazing type. The higher is the SHGC (solar heat gain coefficient) for the glazing, the higher is the rate of increase of total building energy use as a function of window size for cooling dominated climates (Ourghi et al., 2007). Heat losses from windows are the greatest amount of the total heat loss of a building (Kaynakli, 2012). The use of improved energy saving double glazing windows can contribute considerably to the energy efficiency for heating, cooling and lighting of buildings as well as to the improvement of thermal and acoustic comfort conditions in the indoor environment. Double glazed windows only have about half of the heat transfer coefficient of a single one. The potential energy saving by replacement of single glazing with double glazing provides a potential energy saving equal to 39–53% according to an assessment carried out in the commercial building sector in the United Kingdom. Double glazing windows costs 28 $/m^2 (for materials and installation work) and can provide energy savings of up to 35%. For offices heated and cooled with air-conditioning, energy savings can be equivalent to 5.5 $/year for 10 m^2 of windows, and the payback period is estimated at 6.5 years. These typical figures are reported for buildings with 15% openings of their total area (Tsagarakis et al., 2012). In a previous study, it was found that the highest energy consumption of chillers is reduced by 4.9% monthly and it is equivalent to 2.1% of total energy consumption by considering double glazed window of low emittance (e=0.1) (Rahman et al., 2010).

Design of office and public buildings, which involves mechanical ventilation, can lower energy consumption (Siew et al., 2011). Also considerable savings can be achieved if requirement capacity is revisited and have oversized units replaced (Rhodes et al., 2011). At present, nearly, all existing standards require airflow rates, which are based on the assumed odour emissions by the occupants. Outdoor air ventilation is required for all occupied spaces in a building in order to meet indoor air quality. The impact of the ventilation rates on the annual building load is significant. (Eskin and Türkmen, 2008). A reduction in the energy consumed for cooling in office buildings can be achieved by improving the building envelope, using alternative cooling techniques or by using more efficient air-conditioning systems (Kolokotroni et al., 2004). The installation of units with improved design and control air conditioning systems could potentially provide a 20% energy saving (Tsagarakis et al., 2012). Energy saving can also be achieved by effectively adjusting the temperature set point and using optimal control techniques (Chinnakani et al., 2011).

According to a recent review, investing in energy-efficient lighting is one of the most cost-effective ways to reduce CO_2 emissions, and other studies have shown that existing technology could reduce electricity use for lighting by 50% (Dubois and Blomsterberg, 2011). Lighting for a typical office building represents about 40% of the total electrical energy use. There are a variety of simple and inexpensive measures to improve the efficiency of lighting systems. As an alternative to standard lighting, daylighting offers a lighting source that most closely matches human visual response and provides more pleasant and attractive indoor environment. It was found that energy savings of up to 15.6% can be achieved by using more energy efficient lighting and stepped dimming daylighting control strategies (Rahman et al., 2010). However, the current efficiency of LED lighting is similar to that of fluorescent lighting; cool white LED lights have an efficiency of 60–150 lm/W, which is comparable to 50–100 lm/W, the efficiency of linear fluorescent lights (Ahn et al., 2014). Furthermore, as shown in (Table 13) approximately 75≈85% of the light electric power in LED lights is still generated as heat, although heat generation and thermal management technologies are being developed (Bing, 2012).

Table 13: Distribution of heat from lighting (U.S. Department of Energy | Office of Energy Efficiency & Renewable Energy, 2007)

	Incandescent	Fluorescent	LED
Visible light %	8	21	15–25
Convective heat %	92	42	75≈85
Radiant heat %		37	-

During building design stage, architects and engineers face many social, economic, environmental, technical and aesthetic constraints. Despite the fact that a building is a very complex object and almost always unique, energy savings and pollution reduction must remain one of the principles of high environmental quality building conception. When a project sketches are prepared at its early design stage, architects need global and operative knowledge concerning: the setting up on the site (concerning the climate analysis of the site), the shape of the works (concerning morphology), the performance of the walls (concerning materials), the performance of basic thermal systems (concerning the heating, ventilating and cooling systems), the performance of complementary systems (concerning energy savings). The tools used have to be easy, quickly and efficiently evolves towards energetic solutions (Depecker et al., 2001). Studying factors affecting the energy performance of office buildings and the energy characteristics of the building systems is essential for

a better understanding of the energy conserving design principles, and operational strategies. With the help of computer programs for detailed building energy simulation, it is now possible to examine these factors extensively and systematically through the use of a computer modelling technique (Eskin and Türkmen, 2008) (Ourghi et al., 2007).

Until now, energy modelling has generally been done by mechanical engineers or specialized consultants. This practice has led to that integrated design practice increased up-front costs. That is why design teams might reconsider actually carrying out energy simulation by architects. However, more advanced modelling tasks including complex HVAC systems and advanced system integration are likely to be performed by engineers and energy consultants. The potential benefits of this practice are shorter communication paths and more effective design feedback loops leading to shorter design times. The disadvantages are equally clear as this could turn into one more task that the architect must take on without necessarily increasing project budgets (Proceedings and Simulation, 2009). Energy modelling is utilized on buildings more often for two main purposes: modelling for building and HVAC system design and associated design optimization (forward modelling), and modelling energy use of existing buildings for establishing baselines and calculating retrofit savings (data-driven modelling) (ASHRAE Handbook, 2005). Forward modelling of building energy use begins with a physical description of the building system or component of interest. For example, building geometry, geographical location, physical characteristics (e.g., wall material and thickness), type of equipment and operating schedules, type of HVAC system, building operating schedules, plant equipment, etc., are specified. The energy use of such a building can then be predicted or simulated by the forward simulation model. Forward modelling can help designers compare various design options and lead them to energy-efficient designs in manner of cost-effectiveness (Pan et al., 2008). Dynamic simulation of HVAC and lighting energy consumptions in the buildings are of considerable interest for engineers and architects due to its cost effective way of analysing and assessing energy conservation measures before or after the building is built or retrofitted (Rahman et al., 2010).

Benchmarking energy use is a critical energy management activity. It enables organizations to determine whether better energy performance should be expected for a facility, process or piece of equipment and aids them in achieving their energy reduction goal setting and in providing them a way to evaluate the reasonableness of such goals. ENERGY STAR (ES) is a voluntary government/industry partnership Introduced in 1992 by the US Environmental Protection Agency (EPA) that offers information to businesses and consumers on energy-efficient solutions, making it easier to save money and protect the environment for future generation. To aid decision-making that reduces energy use, EPA designed the ES certification mark as a label for products, homes, and facilities that meet or exceed performance guidelines. The ES mark is a recognized symbol of energy efficiency. Selected buildings and facilities can earn the ES if actual energy performance scores in the 75th percentile or higher on the EPA's national energy performance rating system. This rating system enables specific space types to be benchmarked to determine their energy efficiency as compared to a normalized population of actual US facilities (Boyd et al., 2008).

Throughout the survey, it was found that energy consumption in buildings is closely linked to their design (form, orientation and building materials), operational and space utilization characteristics and the behaviour of their occupants. Therefore, this research is studying these factors effect on the energy performance of office buildings.

2 METHODOLOGY AND PROCEDURES

The energy performance in an office building was evaluated using two different tools - Portfolio Manager (PM) and Target Finder (TF) - related to ES using the Energy Use Intensities (EUI). Performance assessment results are obtained by comparing the performance indicators (e.g. EUI or CO_2 emission) against established benchmarks. PM requires a set of data based on a minimum of 50% occupancy, 12 consecutive months of metered utility bills, and basic building and space use characteristics, such as building size and location, operating hours, and number of occupants, to compute performance metrics. PM normalizes for factors including climate, vacancy, and space use. PM does provide the means to prospectively analyse a building via a tool called TF. TF provides an estimate of what PM rating a building might obtain upon completion of 12 months of operation, if managed to achieve the estimated EUI (McCabe and Wang, 2012).

Energy consumption was determined by two methods: calculation and simulation. On one hand, calculations for annual energy use were done using the data sheets with each energy consuming system utilized in the building based on operating hours of each. On the other hand, an appropriate simulation tool is required to efficiently and accurately simulate the performance of building systems. Although, many simulation programs

SUSTAINABLE CITIES & ENVIRONMENT

are available, not all of them do meet these criteria. A new and unique graphic user interface based simulation tool – DesignBuilder (DB) - was used in this study to evaluate the building model simulation. DB's calculation method is based on energy plus simulation engine. DB creates a virtual environment where HVAC and lighting systems of the building are evaluated without compromising thermal comfort (Rahman et al., 2010). DB has been used to predict the building annual energy use considering building design, building materials and optimization of thermal comfort, lighting, weather data and activity in the case study building. Finally, the ES rating tools were used to evaluate energy consumption for both methods.

2.1 Building and System Description

Petrojet Company new head administrative office building shown in (Figure 17) was selected for this case study. The building is located in New Cairo, Egypt at Latitude 30°1'11"N and Longitude 31°24'52"E. It is 5 storeys high above grade, and two storeys below grade. The floor-to-floor height from ground F to 5F and the basement is 3.90 m, and that of lower ground F is 4.5 m. The main function of the buildings is office but housing a library. The building is designed to be mainly open plan offices to allow more workspaces and more occupants. They are part of the energy conservation strategy as only one centralized area is being heated, or cooled, and lighted. Building total gross floor area is 50900 m2, complete air-conditioned floor area of the building is 33665 m2. It is still under construction. Building is operating for 8 hours from 7:30 a.m. to 3:30 p.m. 5 days per week. The expected number of occupants was 1650 and number of computers was 1240.

Figure 17: Petrojet Company new head administrative office building

The office building was designed to utilize multiple energy efficiency strategies to save energy. The building design is a combination of high efficiency building envelope, high-efficiency lighting system and daylighting dimming in perimeter area, and high-efficiency HVAC system. These strategies showed improvements in:
- Building envelope—wall and roof U-factors, glazing performance (double glazed window of low emittance (e=0.1) with blind), and sunshades.
- Lighting—reduction of lighting power density and instalment of compact florescent lighting. The lighting system serving the building is mainly of regular 36 Watt double compact fluorescent lamps.
- Daylighting—installation of daylighting switching/dimming systems in perimeter area.
- HVAC—improved equipment efficiencies, several system enhancements and design options, e.g., Natural gas direct fired absorption chiller, variable speed pumps and variable speed cooling tower. The HVAC systems used in the building is chilled water system with 33 air-handling units (AHUs) and 525 fan-coil units (FCU) serving the different zones of the building. The cooling of the building is provided by chilled water from natural gas direct fired absorption chiller (4 units) on site with total capacity of 6330 kW. All chillers are controlled by the cooling demand of the AHUs and FCU.

2.2 Data Collection

Each zone of the building was investigated with the assistance of the building's designers and construction engineers in order to obtain information and data on the building lighting, equipment and occupancy for the purpose of knowing details of thermal characteristics of building envelope. The building architectural and working drawings were also studied. The equipment used in this building includes personal computers, small printer, and few scanners. Total number of equipment and lighting fixtures of each zone of the building was counted. Information on HVAC systems, AHUs and chillers was collected as per the design data, equipment tags, as well as the information provided by the HVAC system consultant.

2.3 Calculation method

The energy consumed by building systems (HVAC, Lighting, and computers) was determined from information per the design data, equipment tags, as well as the information provided by the HVAC system consultant on HVAC systems, AHUs and chillers, equipment and lighting fixtures and illustrated in (**Error! Reference source not found.**).

Table 14 : Energy consumption by calculation (KWh/month) for the building

	Lighting	HVAC	Computers
Monthly Energy consumption (KWh)	55401.98	179778.72	43648

2.4 Simulation and Base Model Development

The building was modelled and simulated using DB as shown in (Figure 18). DB model was structured in order of site, building, block, zone and surface data. This structure sets up data globally in a building model. Building blocks are basic geometric shapes that are used to assemble a 3D model as similar to the building physical model. In the modelled building, building blocks, which represent the outer shell of the model or part of the model, are composed of building elements such as walls, floor slabs and roofs, and are partitioned internally to form zones. The partition of the space boundaries of the zones were modelled according to the working drawings as shown in (Figure 19). DB comes with extensive data templates for a variety of building simulation inputs such as typical envelope construction assemblies, lighting systems, and occupancy schedules.
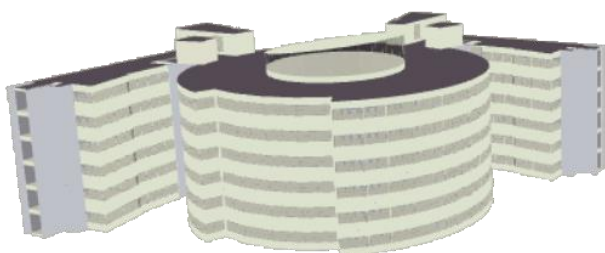
Figure 18 : Model Geometry of the building in DB
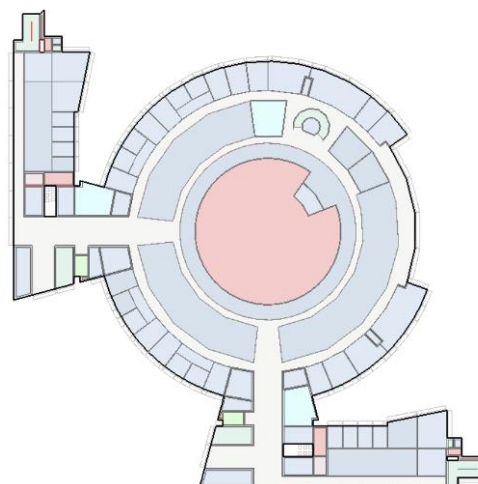
Figure 19 : Repeated floor block partitioned forming zones according to the working drawings

In building model, there are 590 zones, among which 420 are conditioned. Toilets, storage and basement floor are unconditioned spaces. Due to current limitations in the DB, purchased Absorption chiller was not an available option for cooling and instead was modelled as fan coil unit. Supply and return air ducts are located around the perimeter of the building. Temperature set point in offices and lobby is 22 ˚C for cooling and 20 ˚C for heating with dead band. The only spaces in the building with operable windows are some of the offices. In naturally ventilated spaces, natural ventilation was turned on in the model and set to be automatically controlled by DB based on occupancy schedule. The operation schedule of lighting and equipment was simulated according to the typical profiles for weekdays and weekends. The heat gains from the people were calculated according to their activity levels and the indoor design temperature. Equipment use is directly connected to occupancy. Therefore, the equipment schedule was linked with the occupancy schedule. Since the plug-loads in the offices seemed fairly typical, the equipment power density was set to 8 W/m² (Ourghi et al., 2007) and computer power density was set to 15 W/m². Compact florescent lighting was utilized in the building with lighting controls. Lighting depends on the occupancy schedule and the lighting power density was set to 10 W/m² (Pan et al., 2008). The default target illuminances ranged from 100 - 400 lux depending on the space type. Infiltration rate = 0.25 ac/h, ventilation rate = 2.36 l/sec for 1 person = 0.32l/sec for 1 m² (Mendell and Apte, 2014). The properties of the various materials used in this building are summarized in (Table 15).

Table 15 : Properties of the various materials used in building simulation

Element	Construction materials	U-Value (W/m².K)
External Walls	Aluminium cladding on brick	2.033
	Aluminium cladding on reinforced concrete	2.796
	curtain wall (Double clear low emissivity glass with air gap)	1.357
Internal Walls	Brick (ceramic face and painted face)	1.63
	Brick (painted faces)	1.635
	Reinforced concrete (ceramic face and painted face)	2.087
	Reinforced concrete (painted faces)	2.094
	Gypsum board partition	1.906
	aluminium partition	2.273
	Below grade reinforced concrete walls	2.234
Flat roof	Granite with suspended Gypsum board	0.309
	Granite with Aluminium tiles	0.316
	Granite with paint on cement plaster	0.352
Internal Floors (floor and adjacent ceiling)	Carpet with paint on cement plaster	1.257
	Carpet with suspended Gypsum board	0.831
	Granite with paint on cement plaster	1.66
	Granite with suspended Gypsum board	0.985
	Ceramic or porcelain with suspended Aluminium tiles	1.042
	Ceramic or porcelain with suspended Gypsum board	0.961
Window glazing	Double clear low emissivity glass with air gap	1.772

The whole building energy simulation was performed using weather data from the nearest available hourly weather station (Cairo Airport). Using a prepared climate file does not seem to compromise significantly the simulation accuracy. In DB, the benefit of using customized weather data as opposed to a local TMY3 file turned out to be small (Proceedings and Simulation, 2009).

3   RESULTS AND DISCUSSION

The annual energy consumption of the building for both calculation and simulation methods is illustrated in (Figure 20). It is clear that simulation monthly energy consumption is lower than the calculated one all over the year. The total annual energy use for calculation and simulation methods was 3345944.4 KWh and 2599707.8 KWh; respectively. This means that the annual energy use decreased by 22% in the simulation method.
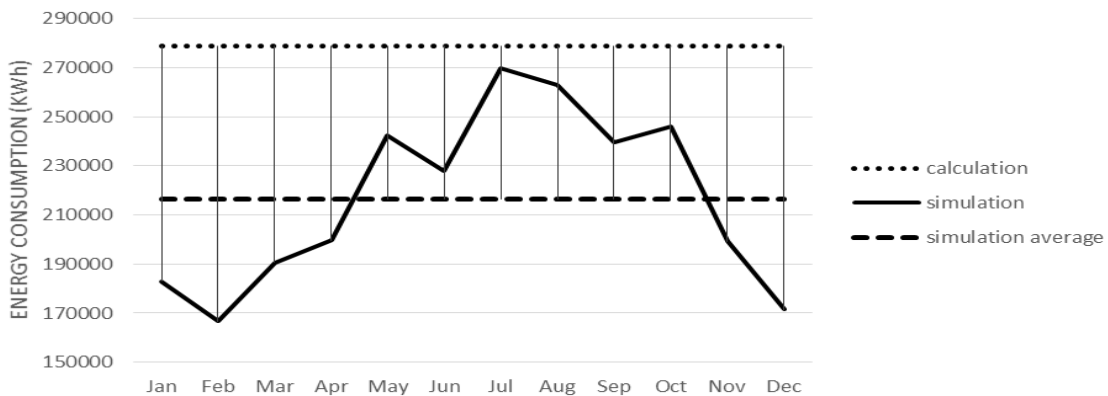
Figure 20: Total monthly energy use in the study case building

Energy consumption breakdown for both methods – calculation and simulation - is illustrated in (Figure 21). It is clear that the energy consumption distribution on different systems is more equilibrium in the simulation method. It is noticed that the percentage of energy consumed by HVAC system decreased 1/3 in the simulation method. This reflects the direct effect of taking into consideration system operating hours which depend on occupancy schedules, temperature setting points and weather data which affects the loads on the system. In addition, partial loads were simulated though applying variable speed pumps and cooling towers in DB. However, it is well noticed that the percentage of energy consumed by equipment was doubled in the simulation method. This is related to that the simulation program takes into consideration during simulation all available equipment in the building including computers, plug-in loads, electric water heaters and printers. Regarding lighting system, its energy consumption percentage is nearly the same in both methods. This reflects that the operation schedule and the electric loads of lighting system are nearly the same in both.

Calculated Consumption

Simulation Consumption

Figure 21: Energy use break down percentage for both methods

Considering lighting system, monthly lighting energy consumption (calculation and simulation results) for the study case building is illustrated in (Figure 22). It was found that the annual energy consumption decreased by 14 % in the simulation method. This reflects the direct effect of taking into consideration system operating hours which depends on occupancy schedules along weekdays and weekends. In addition, lighting control systems were applied in the simulation which is a great factor that can't be taken into consideration in the calculation method. It was noticed that all values ranged between 44000KWh/month and 52000 KWh/month which is a narrow range for this scale of usage. This means that weather profile along the year doesn't have a significant effect on lighting system energy consumption but least consumption rates appeared mainly during February, June and December when there are main holidays during the year. Large Glazing area included in the building design also provided acceptable daylighting which decrease artificial lighting loads.

Figure 22: Monthly lighting energy use in the study case building

Considering HVAC system, monthly HVAC energy consumption (calculation and simulation results) for the study case building is illustrated in (Figure 23). It was found that the annual energy consumption decreased by 47% in the simulation method. This reflects the direct effect of taking into consideration AHUs and FCUs operating hours which depends on occupancy schedules along weekdays and weekends and temperature set point. In addition, this reflects the direct effect of taking into consideration system operating season which depends on weather data along the year for the absorption chiller as it is shut down during winter. It was noticed that maximum energy consumption was during July and the minimum energy consumption was during December with a difference about 90000 KWh. This clears the direct effect of weather data simulation on the operation of HVAC system. Building form and the applied shades affects direct solar radiation reaching the building outer envelope, while the glazing and building materials affects directly amount of heat entering the building.
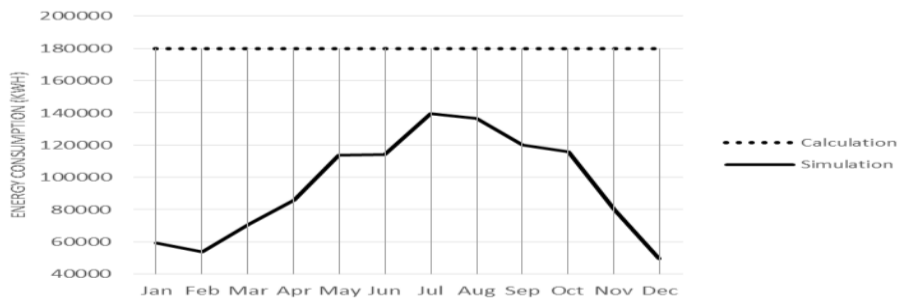
Figure 23: Monthly HVAC energy use in the study case building

Considering equipment, the monthly equipment energy use (calculation and simulation results) for the study case building is illustrated in (Figure 24). It was found that the annual energy consumption increased by 68 % in the simulation method. This reflects the direct effect of taking into consideration all types of equipment including copmuters, plug-ins, electric heaters, printers…etc. following occupancy schedules depending on each zone activity. It was noticed that all values ranged between 68000KWh/month and 78000 KWh/month which is a narrow range for this scale of usage. This means that annual weather profile doesn't have a significant effect on equipment energy consumption.
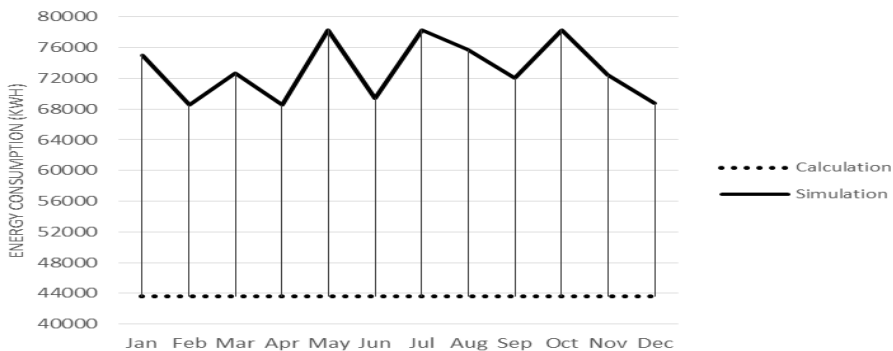
Figure 24: Monthly equipment energy use in the study case building

PM and TF evaluation results are illustrated in (Table 16). The "Property Estimate at Design" results refers to calculation consumption and "Property Measurement in Use" results refers to simulation consumption. The ES score for both is 100. The source and site EUI and total GHG emissions for both are better than the "design target". The source EUI for calculation and simulation method is 0.74 GJ/m² and 0.58 GJ/m² respectively. The site EUI for calculation and simulation method is 0.24 GJ/m² and 0.18 GJ/m² respectively. This means that source and site EUI decreased by 22 % and 25 % respectively for the simulation results. The annual GHG emission as evaluated by ES for calculation method is 1879.5 metric tCO_2e while for the simulation method is 1460.3 metric tCO_2e. This means that annual GHG emissions decreased by 22 % for the simulation results.

Table 16: ENERGY STAR Portfolio Manager results for the new head office building

Metric	Property Estimate at Design	Design Target*	Median Property*	Property Measurement In Use
ENERGY STAR score (1-100)	100	100	50	100
Source EUI (GJ/m²)	0.74	0.81	2.69	0.58
Site EUI (GJ/m²)	0.24	0.26	0.86	0.18
Total GHG Emissions (Metric Tons CO2e)	1879.5	2042.1	6797.9	1460.3

4 CONCLUSION

In this study, the energy performance in Petrojet office building in Cairo, Egypt was evaluated using ES rating tools. After analysing the collected data and applying the assessment tools, the main conclusions are:

1- Building detailed simulation significantly affected building energy consumption as it decreased by 22% annualy. In addition, energy consumption breakdown has widely changed as the percentage of energy consumed by HVAC system decreased 1/3 and the percentage of energy consumed by equipment was

doubled in the simulation method. Annual energy consumption for lighting and HVAC decreased by 14 % and 47% respectively while for equipment increased by 68 % in the simulation method.

2- Systems operating hours depending on occupancy schedules and holidays had a direct effect on energy consumed by HVAC, lighting and equipment. Therefore, schedules for lighting, HVAC and equipment during energy performance analysis seems advisable on every project as it has a noticeable effect on the overall energy consumption. However, in the design phase of a project, the architect may have no enough information available forcing him to lake for the benefits of carefully simulating a building during the design stage.

3- Annual Weather profile accompanied by temperature setting points had a direct effect on energy consumed by the absorption chiller, AHUs and FCUs. They don't have a significant effect on lighting energy consumption.

4- Applying energy efficiency strategies like lighting control systems, temperature setting points, shades and blinds, variable speed pumps and cooling tower, efficient materials and glazing ratio included in the building design showed better way to evaluate building energy performance.

5- Taking into consideration many factors affecting the energy performance of office buildings and the energy characteristics of the building systems (shape, materials, shading, lighting, HVAC and equipment) operational strategies through detailed building simulation significantly affected ES results. PM and TF evaluation results showed that source and site energy use decreased by 22 % and 25 % respectively, while annual GHG emissions decreased by 22 % for the simulation results.

6- Results are limited to one building; therefore, the numbers cannot be readily extracted to another project, but rather gives insight into the effect of degree of available building details during energy performance evaluation process. Presented results offer architects, building managers and HVAC engineers a better understanding of the dynamic interactions between many factors affecting end energy consumption. For new design projects, these simulation assumptions should be carefully reviewed with the building owner.

5   ACKNOWLEDGMENT

6   REFERENCES

AHN, B.L., Jang, C.Y., Leigh, S.B., Yoo, S., Jeong, H., 2014. Effect of LED lighting on the cooling and heating loads in office buildings. Appl. Energy 113, 1484–1489.

ASHRAE Handbook, 2005. Fundamentals, American Society of Heating, Refrigerating and Air Conditioning Engineers, Atlanta.

BING, L.Y., 2012. On Thermal Structure Optimization of a Power LED Lighting. Procedia Eng. 29, 2765–2769.

BOYD, G., Dutrow, E., Tunnessen, W., 2008. The evolution of the ENERGY STAR® energy performance indicator for benchmarking industrial plant manufacturing energy use. J. Clean. Prod. 16, 709–715.

CHINNAKANI, K., Krishnamurthy, A., Moyne, J., Gu, F., 2011. Comparison of energy consumption in HVAC systems using simple ON-OFF, intelligent ON-OFF and optimal controllers. IEEE Power Energy Soc. Gen. Meet. 1–6.

DASCALAKI, E., Santamouris, M., 2002. On the potential of retrofitting scenarios for offices. Build. Environ. 37, 557–567.

DEPECKER, P., Menezo, C., Virgone, J., Lepers, S., 2001. Design of buildings shape and energetic consumption. Build. Environ. 36, 627–635.

DUBOIS, M.C., Blomsterberg, Å., 2011. Energy saving potential and strategies for electric lighting in future north european, low energy office buildings: A literature review. Energy Build. 43, 2572–2582.

ESKIN, N., Türkmen, H., 2008. Analysis of annual heating and cooling energy requirements for office buildings in different climates in Turkey. Energy Build. 40, 763–773.

KARABAY, H., Arici, M., 2012. Multiple pane window applications in various climatic regions of Turkey. Energy Build. 45, 67–71.

KAYNAKLI, O., 2012. A review of the economical and optimum thermal insulation thickness for building applications. Renew. Sustain. Energy Rev. 16, 415–425.

KOLOKOTRONI, M., Robinson-Gayle, S., Tanno, S., Cripps, A., 2004. Environmental impact analysis for typical office facades. Build. Res. Inf. 32, 2–16.

MCCABE, M., Wang, N., 2012. Commercial Building Energy Asset Rating Program: Market Research.

MENDELL, M.J., Apte, M.G., 2014. Balancing energy conservation and occupant needs in ventilation rate standards for " Big Box " stores and other commercial buildings in California : Issues related to the ASHRAE 62 . 1 Indoor Air Quality Procedure.

ORLAND, B., Ram, N., Lang, D., Houser, K., Kling, N., Coccia, M., 2014. Saving energy in an office environment: A serious game intervention. Energy Build. 74, 43–52.

OURGHI, R., Al-Anzi, A., Krarti, M., 2007. A simplified analysis method to predict the impact of shape on annual energy use for office buildings. Energy Convers. Manag. 48, 300–305.

PAN, Y., Yin, R., Huang, Z., 2008. Energy modeling of two office buildings with data center for green building design. Energy Build. 40, 1145–1152.

PIKAS, E., Thalfeldt, M., Kurnitski, J., 2014. Cost optimal and nearly zero energy building solutions for office buildings. Energy Build. 74, 30–42.

Proceedings, C., Simulation, B., 2009. MODELLING AN EXISTING BUILDING IN DESIGNBUILDER / E + : CUSTOM VERSUS DEFAULT INPUTS Holly Wasilowski and Christoph Reinhart.

RAHMAN, M.M., Rasul, M.G., Khan, M.M.K., 2010. Energy conservation measures in an institutional building in sub-tropical climate in Australia. Appl. Energy 87, 2994–3004.

RHODES, J.D., Stephens, B., Webber, M.E., 2011. Using energy audits to investigate the impacts of common air-conditioning design and installation issues on peak power demand and energy consumption in Austin, Texas. Energy Build. 43, 3271–3278.

SIEW, C.C., Che-Ani, a. I., Tawil, N.M., Abdullah, N. a G., Mohd-Tahir, M., 2011. Classification of natural ventilation strategies in optimizing energy consumption in Malaysian office buildings. Procedia Eng. 20, 363–371.

SUSOROVA, I., Tabibzadeh, M., Rahman, A., Clack, H.L., Elnimeiri, M., 2013. The effect of geometry factors on fenestration energy performance and energy savings in office buildings. Energy Build. 57, 6–13.

TSAGARAKIS, K.P., Karyotakis, K., Zografakis, N., 2012. Implementation conditions for energy saving technologies and practices in office buildings: Part 2. Double glazing windows, heating and air-conditioning. Renew. Sustain. Energy Rev. 16, 3986–3998.

U.S. Department of Energy | Office of Energy Efficiency & Renewable Energy, 2007. Thermal Management of White LEDs.

200: Thermal performance assessment of new type structure applied in a tent

JUN WANG[1], FENG XIONG[2,] SIQIANG LV[3], MING QU[4]

1 College of Architecture and Environment, Sichuan University, No. 24, First loop south first section, Chengdu City, Sichuan Province, China, wangjunhvac@163.com
2 College of Architecture and Environment, Sichuan University, No. 24, First loop south first section, Chengdu City, Sichuan Province, China, fxiong@scu.edu.cn
3 College of Architecture and Environment, Sichuan University, No. 24, First loop south first section, Chengdu City, Sichuan Province, China, Lusiqiang@scu.edu.cn
4 Sichuan Provincial Architectural Design and Research Institute, No. 688, Tianfu road middle section, Chengdu City, Sichuan Province, China, 306322159@qq.com

A tent can be regarded as one kind of special building or man-made space, which is widely used for the wild living, nomadic living and disaster relief. The envelop enclosure of tent is formed by fabric layer, which has very thin thickness of 0.5-2 mm and high air permeability and thermal radiation adsorption. Accordingly, its indoor thermal environment is very poor in most cases, as a result of low thermal inertia and resistance of tent envelope. For improving thermal environment of tent, new type structure was proposed and applied in tent, including outer fabric layer, phase material (PCM) layer and inner fabric layer. Meanwhile, theoretical model depicting heat transfer of this new type structure used in tent was established and verified. Moreover, for the climatic conditions of Chengdu city in China, the thermal performance of composite three layers structure of tent were evaluated with the aid of numerical simulation under the influence of different PCM thermo-physical properties, containing PCM thermal conductivity coefficient, latent heat, specific heat capacity and phase-transition temperature. Low PCM thermal conductivity coefficient and phase-transition temperature, high phase change latent heat and specific heat capacity are needed to achieve the excellent thermal performance of new type structure.

Keywords: tent; new type structure; phase change material; numerical simulation

1. INTRODUCTION

The envelop enclosure of tent is formed by fabric layer, which has very thin thickness of 0.5-2 mm and high air permeability and thermal radiation adsorption. Accordingly, its indoor thermal environment is very poor in most cases, as a result of low thermal inertia and resistance of tent envelope. Therefore, it's very necessary to build composite structure of tent envelope for improving its thermal performance, e.g. combination of fabrics and other materials. Phase change material (PCM) may be one possible choice as a result of its multiple advantages (WAQAS, 2013: page 612). According to the findings in previous studies, the PCM can provide free cooling and heat release under high and low air temperature environment, respectively, which is benefit for refining envelope thermal performance. CHWIEDUK (2013: page 305) carried out the analysis on dynamic thermal performance of a wall with external PCM composite panel, which can substitute standard heavy mass walls comprised of insulation and brick (or concrete or other standard high thermal mass structure). ALQALLAF (2013: page 78) performed the thermal analysis of building concrete roof with vertical cylindrical holes filled with PCM. The results indicated that the heat flux at the indoor surface of roof was reduced between 9% and 17.26%, depending on the selected PCM, working hours and operating month. ZHU (2013: page 511) proposed and validated one simplified dynamic model of double layers shape-stabilized phase change materials wallboards. The results showed that the simplified dynamic model can represent light weight walls and median weight walls integrated with double layers shape-stabilized PCM with good accuracy. ZWANZIG (2013: page 33) examined a PCM composite wallboard incorporated into the walls and roof of typical residential building across various climate zones and numerically studied the potential of PCM on energy saving for residential homes. MANDILARAS (2013: page 98) experimentally studied one wall system with multiple layers of insulation materials and gypsum plasterboard panels containing PCM for thermal energy storage purposes, the thermal mass of which was enhanced during late spring, early summer and autumn, due to the PCM implementation. According to the above findings, it may be certain that favourable effect has been achieved for PCM applied in the envelope of traditional building. However, the effectiveness of PCM applied in tent is unknown and needed to be determined. Especially, it is necessary to judge the influence of different PCM thermo-physical properties on thermal performance of tent envelope. Therefore, the purpose of this study is to propose one new type tent envelope with composited three layers structure, establish its heat transfer model. Meanwhile, the influence of PCM thermo-physical properties on the thermal performance of this new type tent envelope is determined for outdoor climate in Chengdu city of China.

3 HEAT TRANSFER MODEL

Composite three layers structure of tent proposed in this study include outer fabric layer (δ_1), phase change material layer (δ_2) and inner fabric layer (δ_3). Energy conservation of tent envelope is taken into consideration, which is shown in Figure 1.
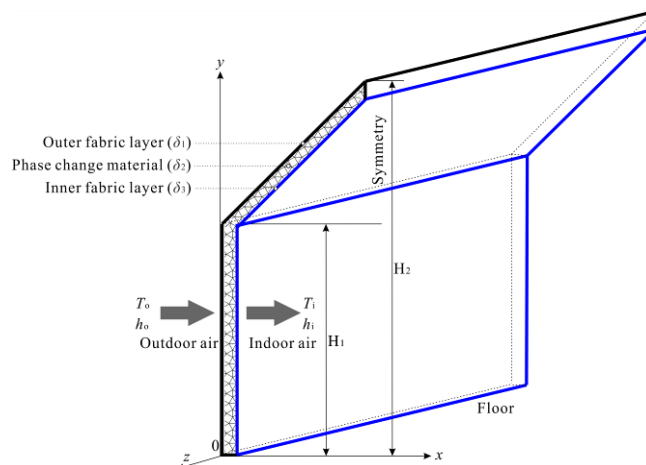

Figure 25: The heat transfer of tent envelope

Meanwhile, it is assumed that the heat transfer through each layer is three dimensional and time dependent. Therefore, the heat transfer model of tent envelope is as the following equation:

Equation 1: Temperature distribution in tent envelop

$$\frac{\partial}{\partial t}(\rho T_{\mathrm{f}}) = \mathrm{div}(\lambda_{\mathrm{ef}}\,\mathrm{grad}T_{\mathrm{f}})$$

Where:

- ρ = the tent envelope material density (kgm^{-3})
- t = the time of transfer process (s)
- λ_{ef} = the heat conductivity coefficient of fabric layer (Wm^{-1}K^{-1})
- T_{f} = the temperature of tent envelope material (K)

On the other hand, as there is difference between the heat transfer mechanism of PCM layer and that of fabric layer, mathematical models for describing their heat transfer are needed to be provided, respectively. One enthalpy model (LIN, 2006: page 53) is chosen to describe the heat transfer of PCM layer, so as to simplify the solution of PCM heat transfer and not to explicitly track the solid–liquid interface, which is depicted as:

Equation 2: Heat transfer of PCM layer

$$\rho_{\mathrm{p}}\frac{\partial H_{\mathrm{p}}}{\partial t} = \lambda_{\mathrm{p}}(\frac{\partial^2 T_{\mathrm{p}}}{\partial x^2} + \frac{\partial^2 T_{\mathrm{p}}}{\partial y^2} + \frac{\partial^2 T_{\mathrm{p}}}{\partial z^2})$$

Where:

- ρ_{p} = the PCM density (kgm^{-3})
- λ_{p} = the PCM heat conductivity coefficient (Wm^{-1}K^{-1})
- H_{p} = the PCM enthalpy (kJkg^{-1})
- T_{p} = the PCM temperature (K)

In addition, the heat flux can be regard as conservation at the interface between fabric layer and PCM layer:

Equation 3: Energy conservation between two layers

$$-\lambda_{\mathrm{ef}}(\frac{\partial T_{\mathrm{f}}}{\partial x} + \frac{\partial T_{\mathrm{f}}}{\partial y} + \frac{\partial T_{\mathrm{f}}}{\partial z}) = -\lambda_{\mathrm{p}}(\frac{\partial T_{\mathrm{p}}}{\partial x} + \frac{\partial T_{\mathrm{p}}}{\partial y} + \frac{\partial T_{\mathrm{p}}}{\partial z})$$

For the thermal boundary conditions at the outer side of composite three layers structure:

Equation 4: Boundary at the outer side

$$-\lambda_{\mathrm{ef}}\frac{\partial T_{\mathrm{f}}}{\partial \mathrm{n}}\Big|_{(x,y,z)_{\mathrm{out}}} = h_{\mathrm{o}}(T_{\mathrm{o}} - T_{\mathrm{f,out}}) + \alpha I$$

Where:

- h_{o} = the outer side convective heat-transfer coefficient (Wm^{-2}K^{-1})
- T_{o} = the outdoor air temperature (K)
- I = the solar radiation intensity (W/m^2)
- α = the absorption coefficient of solar radiation

For the thermal boundary conditions at the inner side of composite three layers structure:

Equation 5: Boundary at the inner side

$$-\lambda_{\text{ef}} \frac{\partial T_{\text{f}}}{\partial \mathbf{n}}\bigg|_{(x,y,z)_{\text{in}}} = h_{\text{i}}(T_{\text{i}} - T_{\text{f,in}})$$

Where:

- h_{i} = the inner side convective heat-transfer coefficient (Wm^{-2}K^{-1})
- T_{i} = the indoor air temperature (K)

For the thermal boundary condition at the bottom of composite three layers structure:

Equation 6: Boundary at the bottom

$$\left.\begin{aligned} -\lambda_{\text{ef}} \frac{\partial T_{\text{f}}}{\partial y}\bigg|_{y=0,z=0} = 0 \\ -\lambda_{\text{p}} \frac{\partial T_{\text{p}}}{\partial y}\bigg|_{y=0,z=0} = 0 \end{aligned}\right\}$$

The initial conditions are:

Equation 7: Initial condition

$$\left.\begin{aligned} T_{\text{f}}(x,y,z,t)\big|_{t=0} = T_{\text{f}}(x,y,z,0) \\ T_{\text{p}}(x,y,z,t)\big|_{t=0} = T_{\text{p}}(x,y,z,0) \end{aligned}\right\}$$

4   THERMAL PERFORMANCE ASSESSMENT

One typical tent with composite three layers structure is chosen for calculation and analysis, which has shoulder height of 1.70 m, roof height of 2.80 m, roof length of 2.73 m, fabric layer thickness of 1 mm and PCM layer thickness of 20 mm, shown in Figure 2(a). Convection thermal boundary is fed to the outer surface of composite three layers structure and h_{o} = 23.25 Wm^{-2}K^{-1}. The solar radiation absorption coefficient of outer fabric layer is 0.7. The outdoor air temperature and solar radiation intensity are derived from the climate of Chengdu city in China, provided in Figure 3. The bottom surface of composite three layers structure adopts adiabatic boundary condition. The initial temperature of each layer is 17 ℃. In addition, the density of PCM is 1300 kgm^{-3}. In order to obtain the impacts of different phase-transition temperature, its three levels are selected, containing from 14 ℃ to 22 ℃, from 18 ℃ to 26 ℃ and from 22 ℃ to 30 ℃. The final total quantity of meshes is 37281, shown in Figure 2(b).
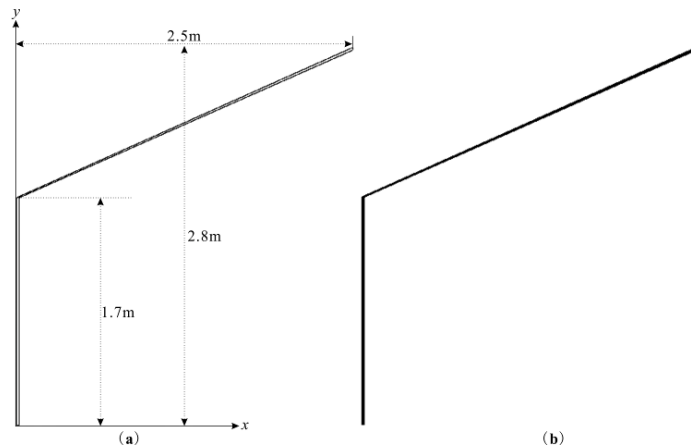
Figure 2: One typical tent with composite three layers structure: (a) geometry size and (b) grid division
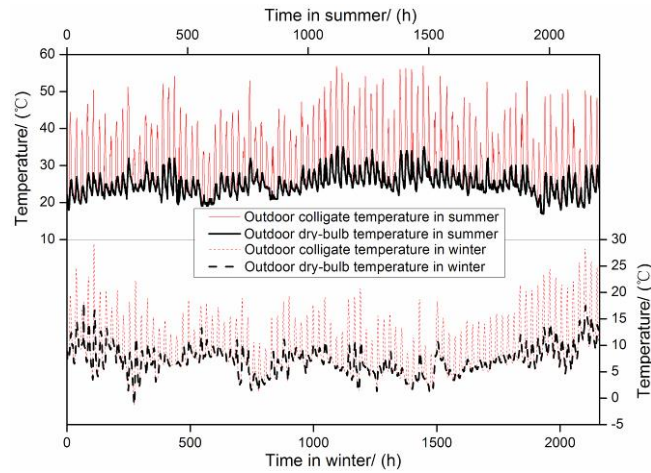
Figure 3: Outdoor air temperature and solar radiation intensity of Chengdu city in summer and winter

As to the specific heat capacity of PCM is 1785 Jkg^{-1}K^{-1} and its latent heat is 178.5 kJkg^{-1}, Figure 4 presents the variation of inner surface temperature with time in summer for high and low PCM thermal conductivity coefficients, which are equal to 0.75 Wm^{-1}K^{-1} and 0.05 Wm^{-1}K^{-1} at solid and liquid states, 0.375 Wm^{-1}K^{-1} and 0.025 Wm^{-1}K^{-1} in phase transition process, respectively. It can be found that, owing to that the indoor air temperature is higher than the initial temperature of inner surface; the inner surface temperature rises with time from the start moment, which makes their difference become narrow. Meanwhile, when the PCM thermal conductivity coefficient is high, the small thermal resistance of PCM layer induces the heat transfer to be strengthened. Correspondingly, the obvious fluctuation of inner surface temperature emerges under the influence of thermal disturbance caused by outdoor colligate temperature. In addition, the difference among results derived from three level phase-transition temperature ranges is very small, the peak value of which is less than 3.7%. In fact, this phenomenon can be attributed to the full phase transition of PCM layer induced by high outdoor colligate temperature in summer. Moreover, this result indicates that the PCM thermal conductivity coefficient may produce more obvious impact on the thermal performance of composite three layers structure than its phase-transition temperature, when the PCM thermal conductivity coefficient is high. On the other hand, as the PCM thermal conductivity coefficient is low, the influence of outdoor colligate temperature becomes weakened. Accordingly, the fluctuation of inner surface temperature is significantly reduced. Namely, the composite three layers structure has well heat preservation performance. Moreover, the decline of phase-transition temperature is benefit for the dropping of inner surface temperature as a result of the greater degree of phase transition. In addition, compared with the result for phase-transition temperature range from 22 ℃ to 30 ℃, the inner surface temperature descends by 3.8% for phase-transition temperature range from 18 ℃ to 26 ℃ and by 4.3% for phase-transition temperature range from 14 ℃ to 22 ℃. Therefore, it can be confirmed that the influence of phase-transition temperature becomes more obvious for low PCM thermal conductivity coefficient.
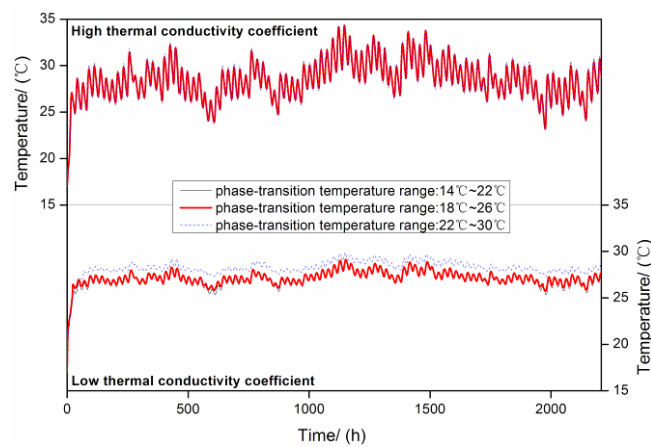

Figure 4: Variation of inner surface temperature with time in summer for high and low PCM thermal conductivity coefficients

Secondly, the variation of inner surface temperature with time in winter for high and low PCM thermal conductivity coefficients is given in Figure 5.
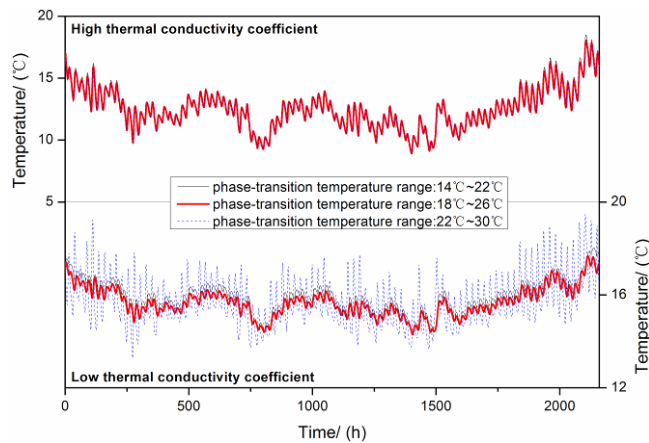

Figure 5: Variation of inner surface temperature with time in winter for high and low PCM thermal conductivity coefficients

For high PCM thermal conductivity coefficient, scarce occurrence of phase transition under low outdoor colligate temperature makes the main role of PCM layer just be to raise the thermal resistance of composite three layers structure and not to absorb the transfer heat by phase transition. Consequently, owing to the thermal disturbance derived from outdoor colligate temperature variation, very obvious fluctuation of the inner surface temperature with time appears. Meanwhile, as lacking the phase transition, the impact of phase-transition temperature on the inner surface temperature may be ignored. However, when the PCM thermal conductivity coefficient is low, thermal resistance rise of the PCM layer brings greater impact on the inner surface temperature originated from indoor air temperature and not from outdoor colligate temperature. Moreover, the heat exchange between indoor air and inner surface can induce phase transition for low phase-transition temperature, which further weakens the influence of outdoor colligate temperature and the fluctuation of inner surface temperature. Especially, this phenomenon becomes more obvious for the phase-transition temperature range from 14 ℃ to 22 ℃ than that under the phase-transition temperature range from 18 ℃ to 26 ℃. Namely, the composite three layers structure under the former case behaves better thermal insulation performance. But when the phase-transition temperature is high, e.g. range from 22 ℃ to 30 ℃, the heat exchange is not enough to cause phase transition and then the greater fluctuation of inner surface temperature emerges. Therefore, according to above results, low PCM thermal conductivity coefficient and phase-transition temperature are needed for obtaining preeminent heat-insulating performance in summer and heat-retaining performance in winter of composite three layers structure.

When the PCM specific heat capacity is 1785 Jkg^{-1}K^{-1} and its thermal conductivity coefficients are 0.5 Wm^{-1}K^{-1} at solid and liquid states and 0.25 Wm^{-1}K^{-1} in phase transition process, the variation of inner surface temperature with time in summer for high and low phase change latent heat is provided in Figure 6.
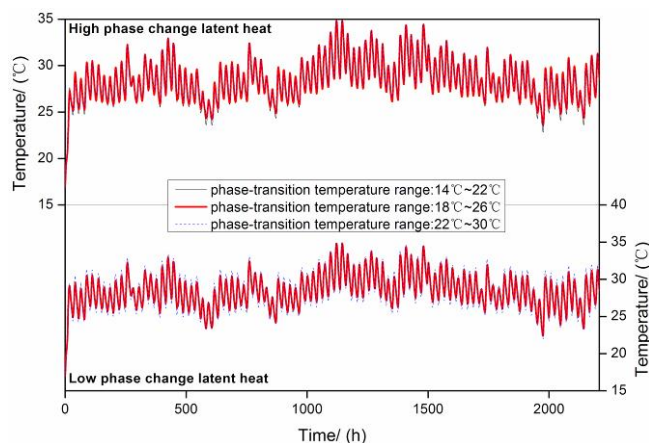

Figure 6: Variation of inner surface temperature with time in summer for high and low phase change latent heat

As the initial inner surface temperature is less than indoor air temperature, the inner surface temperature increases with time in the initial phase. Then ups and downs change is observed for the inner surface temperature under the action of outdoor colligate temperature. Moreover, the fluctuations emerging in the result of low phase change latent is more substantial than that derived from high phase change latent heat. Next, for the high phase change latent heat, due to the high degree of phase change and the large quantity of heat adsorption happen under the joint impact of outdoor colligate temperature and indoor air temperature, the inner surface temperature acquired with the phase-transition temperature range from 14 ℃ to 22 ℃ is smaller than that obtained by the high phase-transition temperature, e.g. range from 18 ℃ to 26 ℃ or from 22 ℃ to 30 ℃. Namely, great heat preservation performance can be observed for the former case. Meanwhile, the difference between the inner surfaces temperature calculated with high phase-transition temperature become very little as a result of the decline of phase change degree. Thirdly, as the phase change latent heat is low, the lacking of full phase change at high phase-transition temperature leads the fluctuation of inner surface temperature to grow up and then its maximum peak and valley values appear. In addition, according to the comprehensive result of inner surface temperature in summer, its variation at the low phase-transition temperature range from 14 ℃ to 22 ℃ has the best acceptability.

On the other hand, Figure 7 depicts the variations of inner surface temperature with time in winter for high and low phase change latent heat.
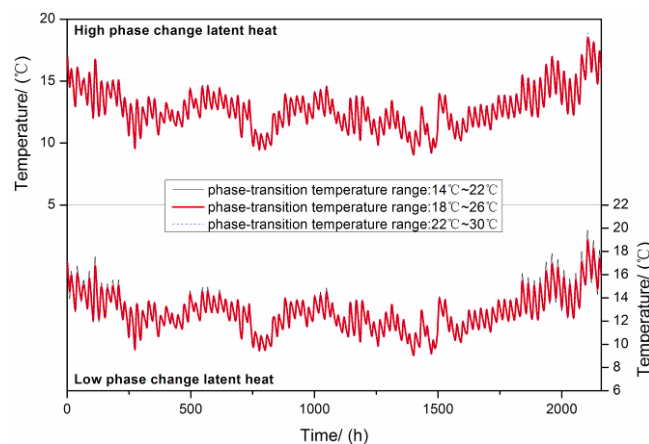
Figure 7: Variation of inner surface temperature with time in winter for high and low phase change latent heat

Owing to the outdoor colligate temperature is low, occurrence of phase change is only found for the low phase-transition temperature, e.g. range from 14 ℃ to 22 ℃. Accordingly, the inner surface temperature obtained from the low phase-transition temperature is more than those derived from the high phase-transition temperature, e.g. range from 18 ℃ to 26 ℃ or from 22 ℃ to 30 ℃. Namely, the composite three layers structure has well thermal insulation performance for the low phase-transition temperature. Meanwhile, there is not any difference between the inner surfaces temperature acquired from the high phase-transition temperature, as a result of lacking phase change. In addition, for the condition of phase change occurring, the high phase change latent heat is benefit for improving this performance further and the corresponding inner surface temperature rises. The above behaviour of inner surface temperature variation with time in summer and winter indicates that it is necessary to apply PCM layer with high phase change latent heat and low phase-transition temperature in the composite three layers structure, so as to improve its thermal performance.

For the PCM latent heat is 178.5 kJkg^{-1} and its thermal conductivity coefficients are 0.5 Wm^{-1}K^{-1} at solid and liquid states and 0.25 Wm^{-1}K^{-1} in phase transition process, Figure 8 shows the variation of inner surface temperature with time in summer for high and low PCM specific heat capacities.
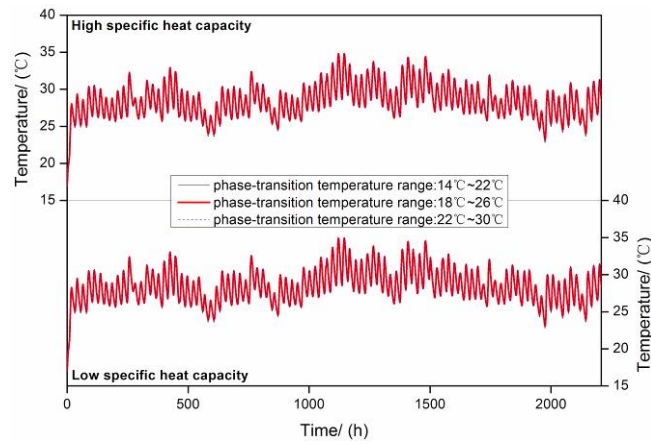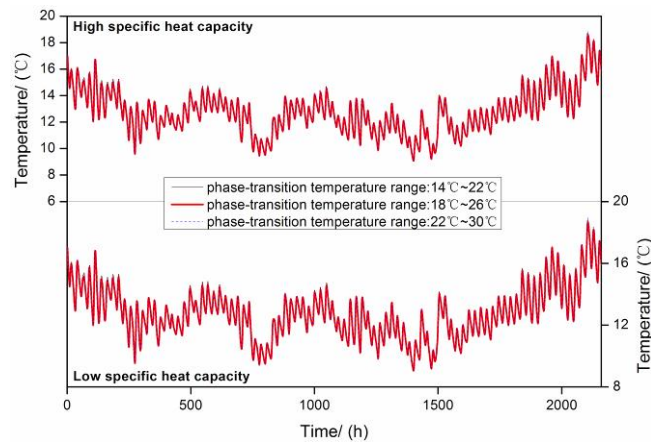
Figure 8: Variation of inner surface temperature with time in summer for high and low PCM specific heat capacities

It can be observed that the inner surface temperature increases firstly and then becomes to fluctuate with time. The initial variation is induced by the difference between indoor air temperature and inner surface temperature and the follow-up change is caused by the thermal disturbance of outdoor colligate temperature. Meanwhile, with regard to the same phase-transition temperature, the inner surface temperature calculated with high PCM specific heat capacity is slightly less than that under the low PCM specific heat capacity, as a result of large quantity heat adsorption. Moreover, compared with the results acquired by phase-transition temperature range from 18 ℃ to 26 ℃ or from 22 ℃ to 30 ℃, the lowest inner surface temperature emerges both for high and low PCM specific heat capacities under the action of phase-transition temperature range from 14 ℃ to 22 ℃. However, the difference among the inner surface temperature obtained from these three kinds of phase-transition temperature becomes very narrow, when the PCM specific heat capacity is low. In fact, the high PCM specific heat capacity may lead deep phase change to happen only for the low phase-transition temperature, but obvious phase change may appear both for the low and high phase-transition temperature as the PCM specific heat capacity becomes small.

Figure 9: Variation of inner surface temperature with time in winter for high and low PCM specific heat capacities

Next, the variation of inner surface temperature with time in winter for high and low PCM specific heat capacities is given in Figure 9. As to the same phase-transition temperature, the small quantity heat adsorption under low PCM specific heat capacity makes the corresponding inner surface temperature be slightly more than that for high PCM specific heat capacity. Of course, their difference is very minor. In addition, with the influence of phase change and PCM layer thermal resistance rising under low outdoor colligate temperature, the PCM layer with low phase-transition temperature range from 14 ℃ to 22 ℃ is benefit for the rising of inner surface temperature, which is more than that obtained by high phase-transition temperature. Therefore, according to the variation characteristics of inner surface temperature with time in summer and winter, the thermal performance of composite three layers structure can be improved by using the PCM layer with high specific heat capacity and low phase-transition temperature.

5   CONCLUSION

As to the tent envelope, its new type that composite three layers structure is proposed in this study. The thermal performance of this structure is evaluated and determined for different PCM thermo-physical properties under the climatic conditions of Chengdu city in China, based on one established and verified heat transfer model and numerical simulation. Low PCM thermal conductivity coefficient and phase-transition temperature, high phase change latent heat and specific heat capacity are needed to achieve the excellent thermal performance of composite three layers structure. This research gives one feasible method and some meaningful guides for application of PCM in the tent envelope.

6   ACKNOWLEDGEMENTS

7   REFERENCES

ALQALLAF H.J., Alawadhi E.M., 2013. Concrete roof with cylindrical holes containing PCM to reduce the heat gain. Energy and Buildings, 61, 73-80.

CHWIEDUK D.A., 2013. Dynamics of external wall structures with a PCM (phase change materials) in high latitude countries. Energy, 59, 301-313.

LIN K., 2006. Study of the application principles and effects for PCM building envelope components. Ph.D. Dissertation, Tsinghua University, Beijing.

MANDILARAS I., Stamatiadou M., Katsourinis D., Zannis G., Founti M., 2013. Experimental thermal characterization of a Mediterranean residential building with PCM gypsum board walls. Building and Environment, 61, 93-103.

WAQAS A., Din Z.U., 2013. Phase change material (PCM) storage for free cooling of buildings—A review. Renewable and Sustainable Energy Reviews, 18, 607-625.

ZHU N., Hu P.F., Xu L.H., 2013. A simplified dynamic model of double layers shape-stabilized phase change materials wallboards. Energy and Buildings, 67, 508-516.

ZWANZIG S.D., Lian Y.S., Brehob E.G., 2013. Numerical simulation of phase change material composite wallboard in a multi-layered building envelope. Energy Conversion and Management, 60, 27-40.

18: A Study on the application of simulation-based simplified PMV regression model in office buildings

SUNG-JUN YUN[1], JUNG-HO HUH[2]

1 Parsons Brinckerhoff Korea, 741 Yoeongdong-daero, Seoul, Republic of Korea,
yun.sungjun@pbworld.com
2 University of Seoul, 90 Jeonnong-dong, Seoul 130-743, Republic of Korea, huhj0715@uos.ac.kr

Recently, the Korean Government enacted a new law aimed at reducing energy losses in buildings throughout Seoul. According to the regulation, buildings over a certain size must keep the indoor temperature above 26 ℃ during the summer season and below 20 ℃ in the winter season. However, these energy-savings were accompanied by thermal discomfort for occupants who work indoors, thus leading to reduced work efficiency. In order to address these problems, several recently published studies have investigated thermal comfort controls that can reduce air-conditioning energy use while also satisfying the thermal comfort needs of occupants. However, thermal comfort controls can prove more difficult to monitor than temperature controls due to the way the existing regulation is written, with far more variables involved in the former. This creates additional costs for multiple measuring sensors, additional time required for monitoring, and an overall greater likelihood for errors.

Thus, this study used EnergyPlus, a program with high accuracy for thermal comfort control prediction, to model an actual office building. A PMV regression analysis was conducted for this model based on a database of PMV variables. PMV regression model simplification was completed through sensitivity analysis, and the Energy Management System (EMS) in EnergyPlus was used to establish a simplified PMV regression analysis-based thermal comfort control.

Keywords: EnergyPlus, PMV, regression analysis, simplification, thermal comfort control

1. INTRODUCTION

1.1 Background and purpose of research

The Korean Government enacted a new law aimed at reducing energy use while maintaining appropriate indoor temperatures. Although the regulation for indoor temperature reduces heating and cooling energy usage, occupants often became dissatisfied with thermal comfort at the same time. As a result, the following research was conducted for thermal comfort controls, based on the Fanger PMV model and study about occupant satisfaction with indoor temperatures. Many variables must be considered in this process, thus, when thermal comfort controls are applied to an actual building, it is important to utilize a number of sensors and monitor over an extended period.

The goal of this study is to solve the issues about thermal comfort based on the Fanger PMV, and compare it with the effects of thermal comfort controls based on that model and a simulated simplified PMV model.

1.2 Research method

The research has been conducted in a manner that simplifies physical parameters in thermal comfort control, based on the Fanger PMV model. This method is illustrated in Figure 1. A database of PMV values was utilized for the simulation model at an actual office building. Acceptable calibration tolerances under the M&V Guidelines were used to establish a calibrated simulation model. The established database for multiple regression analyses suggested the use of a PMV regression model, which is verified by F-test and K-fold cross validation statistical methods. The Energy Management System (EMS) in EnergyPlus is used to establish thermal comfort control based on the simplified PMV regression model.
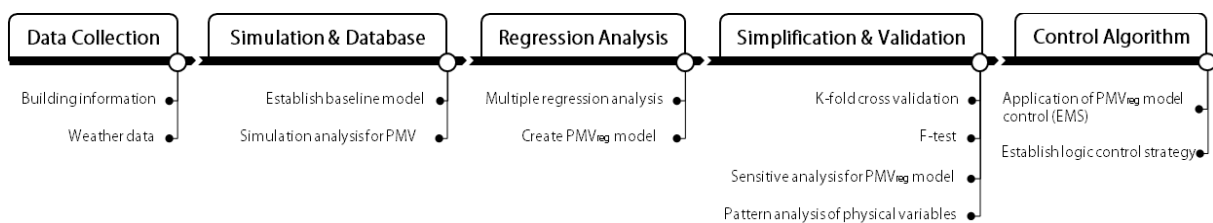
Figure 26: Schematic diagram of simplified PMV regression model development process

2. PMV REGRESSION MODEL

2.1 Database construction

The building for the PMV regression model has nineteen floors above ground and two underground. The envelope is composed of drywall (Drywall) and double glazing. Additional information about the structure is provided in Table 1. OpenStudio plug-in for SketchUp as a third party software of EnergyPlus was used for building envelope modelling. EnergyPlus 7.0 was used to model all other elements besides building envelope. The Federal Energy Management Program (FEMP) M&V Guidelines were used to establish a calibrated simulation model. The verification results of calibrated simulation model are illustrated in Table 2. MBE and Cv(RMSE) were obtained from the following three equations:

Equation 5: Mean Bias Error (MBE)

$$MBE \ [\%] \ = \frac{\sum_{Period} (S-M)_{Interval}}{\sum_{Period} M_{Interval}} \times 100$$

Equation 6: Root Mean Square Error

$$RMSE_{Period} = \sqrt{\frac{\sum (S - M)^2_{Interval}}{N_{Interval}}}$$

Equation 7: Coefficient of Variation of the Root Mean Square Error

$$Cv(RMSE_{Period}) = \frac{RMSE_{Period}}{A_{Period}} \times 100$$

Where:

- S = the simulated kWh or fuel consumption during the same time interval
- M = the measured kWh or fuel consumption during the time interval
- $N_{Interval}$ = the number of time intervals in the monitoring period
- A_{Period} = the mean of the measured data for the period

The calibrated model was confirmed within acceptable calibration tolerances. A database was constructed by setting PMV as the dependent variable, and by setting physical parameters of room air temperature, MRT and relative humidity as the independent variables. However, the air velocity, because it is set to the input values during simulation run, has a maximum value for static air velocity. It is illustrated in Table 3 as a single value. The database of PMV variables was built in accordance with interior and perimeter of direction, with 1,480 data points in summer, and 2,160 data points in winter.

Table 17: Brief descriptions of target building

Classification		Contents
Location		Seoul, Korea
Floor Area		32,488 m^2
Construction	Windows	U-value = 3.7 W/m^2·K
	External Wall	U-value = 0.45 W/m^2·K
	Floor	U-value = 0.32 W/m^2·K
Internal Gains	People	2500 Persons
	Lighting	11 W/m^2
	Equipment	15 W/m^2
HVAC System	Type	CAV
	Set-point Temp.	25℃ (Summer) 22℃ (Winter)
Operating Time	Mon. to Fri.	08:00 - 16:00

Table 18: Verification result of simulated model

Classification	Elec	Gas	Chiller	Error Tolerance
MBE	-0.6%	1.6%	4.4%	±5%
Cv(RMSE)	5.5%	9.0%	11.4%	15%

Table 19: Input value condition for single value setting

Classification	Contents
Metabolic Rate (met)	1.2 (70W/m^2)
Clothing (clo)	0.5 (Summer)
	1.0 (Winter)
Air Velocity (m/s)	0.1

Table 20: PMV regression model coefficient and F-value during the summer season

Classification		Regression Coefficient				r^2	F-Value	$F \geq F_{(3, 1476, 0.05)}$
		c_0	c_1	c_2	c_3			
Perimeter Zone	North	-8.69	0.162	0.160	0.0132	99.8	473,628	O
	South	-8.65	0.161	0.162	0.0131	99.7	452,631	O
	East	-8.68	0.162	0.160	0.0130	99.7	455.384	O
	West	-8.66	0.160	0.163	0.0132	99.3	213,214	O
Interior Zone		-8.54	0.159	0.161	0.0116	99.4	360,527	O

Table 21: PMV regression model coefficient and F-value during the winter season

Classification		Regression Coefficient				r^2	F-Value	$F \geq F_{(3, 1476, 0.05)}$
		c_0	c_1	c_2	c_3			
Perimeter Zone	North	-4.74	0.129	0.084	0.0027	99.7	1,050,721	O
	South	-4.82	0.113	0.101	0.0043	99.2	779,956	O
	East	-4.84	0.110	0.105	0.0041	99.9	1,544,801	O
	West	-4.81	0.121	0.094	0.0036	99.8	1,348,723	O
Interior Zone		-4.83	0.119	0.097	0.0041	99.8	1,325,347	O

2.2 Development and verification of PMV regression model

To create a PMV regression model, multiple regression analysis was performed using the statistical software Minitab-16. The result of this analysis was derived from the database for summer and winter values, and is shown in Table 4 and Table 5, respectively. Also, the F-test of the derived regression model was found to be significant because the entire regression model is larger than the F-value of the confidence interval of 95%. Since the coefficient of determination (r^2) is 90% or more, PMV regression model is possible to explain 90 or more data of 100 data from the 95% confidence interval, indicating high correlation.

The 10-fold cross validation was performed in order to confirm whether simulation data were equally used or not in the process of deriving the PMV regression model. The result of that validation indicated that the average and variation value of Mean Absolute Error (MAE) and Root Mean Square Error (RMSE) is less than 0.01. Therefore, it is judged that the result of PMV regression model obtained in this study is unlikely to change by a specific value. For the perimeter zone, the South was set to be a representative orientation because there is no big difference among the regression coefficients of orientations.

Table 22: Physical variables for sensitivity analysis coverage

Classification			Coverage
Physical Parameter	Air Temperature [℃]	Summer	18℃ ~ 35℃
		Winter	10℃ ~ 28℃
	Mean Radiant Temperature [℃]	Summer	20℃ ~ 36℃
		Winter	11℃ ~ 29℃
	Relative Humidity [%]		20% ~ 100%

Table 23: Comparison between Fanger PMV and simplified PMV regression model

	Classification	MAE	RMSE	r^2
Summer	Perimeter Zone	0.01	0.0014	0.989
	Interior Zone	0.084	0.0027	0.97
Winter	Perimeter Zone	0.021	0.0017	0.982
	Interior Zone	0.128	0.0031	0.988

Equation 8: Equation of simplified PMV regression model
$$PMV_{S,Perimeter} = 0.161\,T_z + 0.162\,T_r - 7.79\;(summer)$$

Equation 9: Equation of simplified PMV regression model
$$PMV_{S,Interior} = 0.271\,T_z + 0.0116\,RH - 6.17\;(summer)$$

Equation 10: Equation of simplified PMV regression model
$$PMV_{S,Perimeter} = 0.113\,T_z + 0.101\,T_r - 4.54\;(winter)$$

Equation 11: Equation of simplified PMV regression model
$$PMV_{S,Interior} = 0.199\,T_z + 0.0041\,RH - 4.35\;(winter)$$

Where:

- T_z = Zone indoor air temperature (°C)
- T_r = Zone mean radiant temperature (°C)
- RH = Zone Relative Humidity (%)
- PMV = Predicted mean vote

2.3 Simplification of PMV regression model

PMV regression model simplification was carried out as follows. That is, physical parameters of indoor air temperature, mean radiant temperature and relative humidity were fixed as single values through sensitivity analysis showing their small impact on the thermal comfort. Similar data were determined as single values by database analysis. Table 6 shows a significant range of physical parameters through sensitivity analysis. In both interior and perimeter zones, the sensitivity of indoor air temperature and MRT is similarly high and relative humidity is relatively low, as shown in Figure 2. PMV variation range of the relative humidity in summer and in winter is ± 0.2 resulting in the amount of change of 0.4. Thus, the relative humidity of a relatively small influence on the perimeter zone PMV was set to 65% of the average value of the significant range. The variables database indicated that, in case of the interior zone, exposure to solar radiation is less than a twentieth part of perimeter zone level. As anticipated, it was found that the amount of transmitted solar radiation though the window is less than the perimeter zone directly affected by transmitted solar radiation.

As a result, the PMV regression model was simplified by replacing the mean radiant temperature of the interior zone with indoor air temperature. This allowed for a simple regression analysis to be conducted for indoor air temperature and mean radiant temperature. Comparative results of the simplified PMV regression model and Fanger PMV model are shown in Table 7. The results of this comparison showed that the simplified PMV regression model was able to replace the Fanger PMV model. The equations for this analysis are shown in example equations 4, 5, 6 and 7.
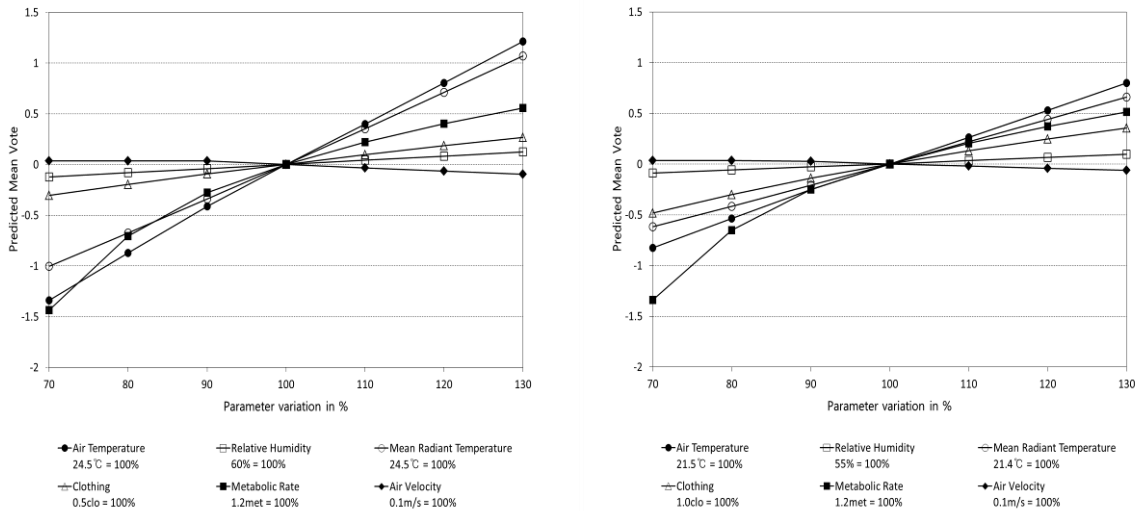
Figure 27: Result of sensitivity analysis during the summer season (Left) and winter season (Right)

3. APPLICATION OF SIMPLIFIED PMV REGRESSION MODEL CONTROL

3.1 Control algorithms for simplified PMV regression model

The simplified PMV regression model using thermal comfort control set controllable indoor air temperatures in the dependent variable, which was converted to the equation for deriving the set-point temperature for satisfying the simplified PMV value. The set-point temperature calculation that reflects the thermal comfort of occupants is shown in example equations 8, 9, 10 and 11.

Equation 8: Equation for set-point temperature calculation

$$T_{Set,Perimeter} = PMV_{Set} + 7.79 - 0.162 \ T_r \ / \ 0.161 \ (summer)$$

Equation 9: Equation for set-point temperature calculation

$$T_{Set,Interior} = PMV_{Set} + 6.17 - 0.0116 \ RH \ / \ 0.271 \ (summer)$$

Equation 10: Equation for set-point temperature calculation

$$T_{Set,Perimeter} = PMV_{Set} + 4.54 - 0.101 \ T_r \ / \ 0.113 \ (winter)$$

Equation 11: Equation for set-point temperature calculation

$$T_{Set,Interior} = PMV_{Set} + 4.35 - 0.0041 \ RH \ / \ 0.199 \ (winter)$$

Where:

- $T_{Set,\ Perimeter}$ = Set-point temperature at perimeter zone (°C)
- $T_{Set,\ Interior}$ = Set-point temperature at interior zone (°C)
- PMV_{Set} = Set-point PMV value

PMV control conditions have taken the deviation of simplified PMV regression model and Fanger PMV model into account. The set-point PMV value of perimeter zone and interior zone was set at 0.2 in the summer season and -0.2 in winter. The building operation times are generally targeted as being 8 a.m. to 5 p.m. The control algorithm for the simplified PMV regression model is shown in Figure 3.
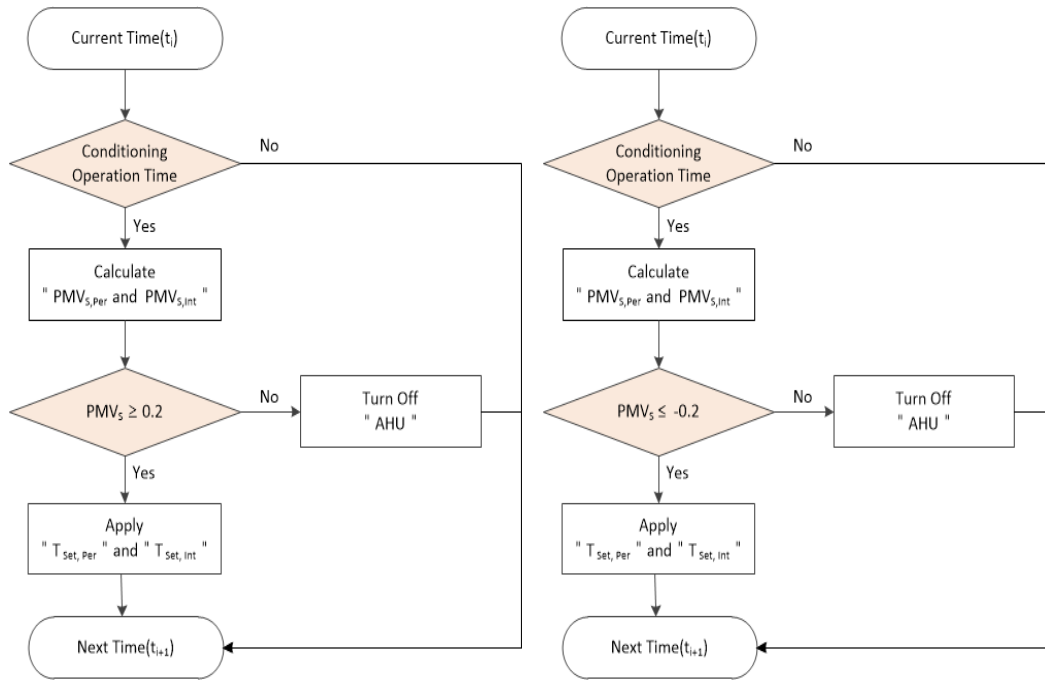
Figure 28: Control algorithm for simplified PMV regression model during the summer season (Left) and winter season (Right)

3.2 Comparative analysis of simplified PMV regression model control

Comparative results of the simplified PMV regression model control and Fanger PMV model control illustrated that PMV values in the perimeter and interior zones had a difference of less than 0.1, as is demonstrated in Figures 4 and 5. At that time, the simplified PMV regression model control showed that it was controlled via the set-point temperature, and had PMV values equal to the Fanger PMV control. When the thermal comfort control is based on the Fanger PMV model, and the simplified PMV model applies, the set-point temperature during the summer and winter season averages 24℃ and 20℃, respectively. The application of thermal comfort controls during the summer and winter seasons are indicated in the frequency of occurrence of thermal comfort range by set-point temperatures, as is shown in Tables 8 and 9. The results of the analysis show that the simplified PMV regression model control consumes an additional 2.4% (6,849 kWh) of cooling energy and 2.7% (3,221m³) of heating energy when compared with the Fanger PMV model control. It is important to consider that the set-point temperature is caused by deviation Fanger PMV model control and a control based on the simplified PMV model.

Table 24: Frequency of occurrence of thermal comfort range during the summer season

Range	Simplified PMV Control [h]		Fanger PMV Control [h]	
	Interior	Perimeter	Interior	Perimeter
~22.0	15	19	12	15
22.0~23.0	78	77	78	77
23.0~24.0	75	74	94	96
24.0~25.0	72	79	89	90
25.0~26.0	61	59	66	67
26.0~27.0	44	41	55	46
27.0~	31	33	4	1
Set-point Temp. [℃] (Average)	24.0	24.2	24.2	24.3

Table 25: Frequency of occurrence of thermal comfort range during the winter season

Range	Simplified PMV Control [h]		Fanger PMV Control [h]	
	Interior	Perimeter	Interior	Perimeter
~18.0	3	11	17	4
18.0~19.0	18	38	36	87
19.0~20.0	177	213	145	178
20.0~21.0	273	316	356	378
21.0~22.0	139	115	115	67
22.0~23.0	86	41	55	46
23.0~24.0	34	19	8	1
24.0~	38	15	36	8
Set-point Temp. [°C] (Average)	20.3	20.6	20.0	20.2
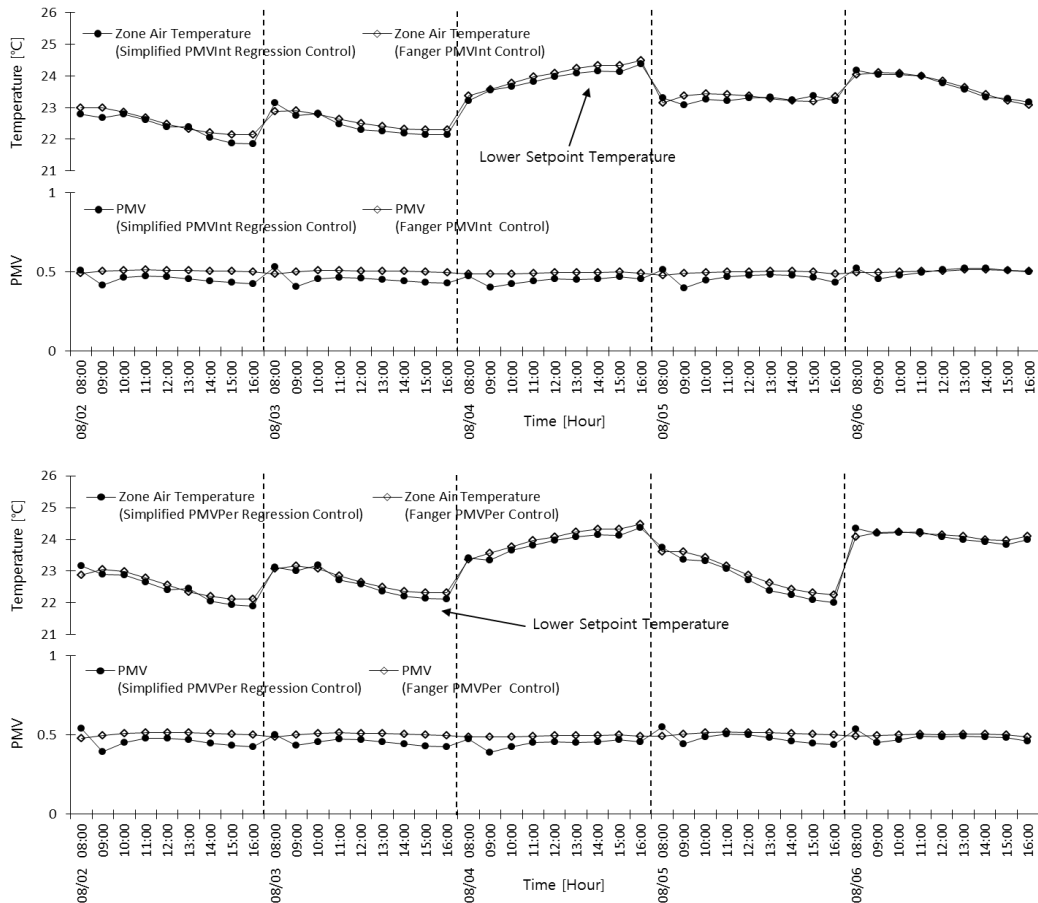
Figure 29: Comparison of thermal comfort controls at interior zone (Upper) and perimeter zone (Bottom) during the summer
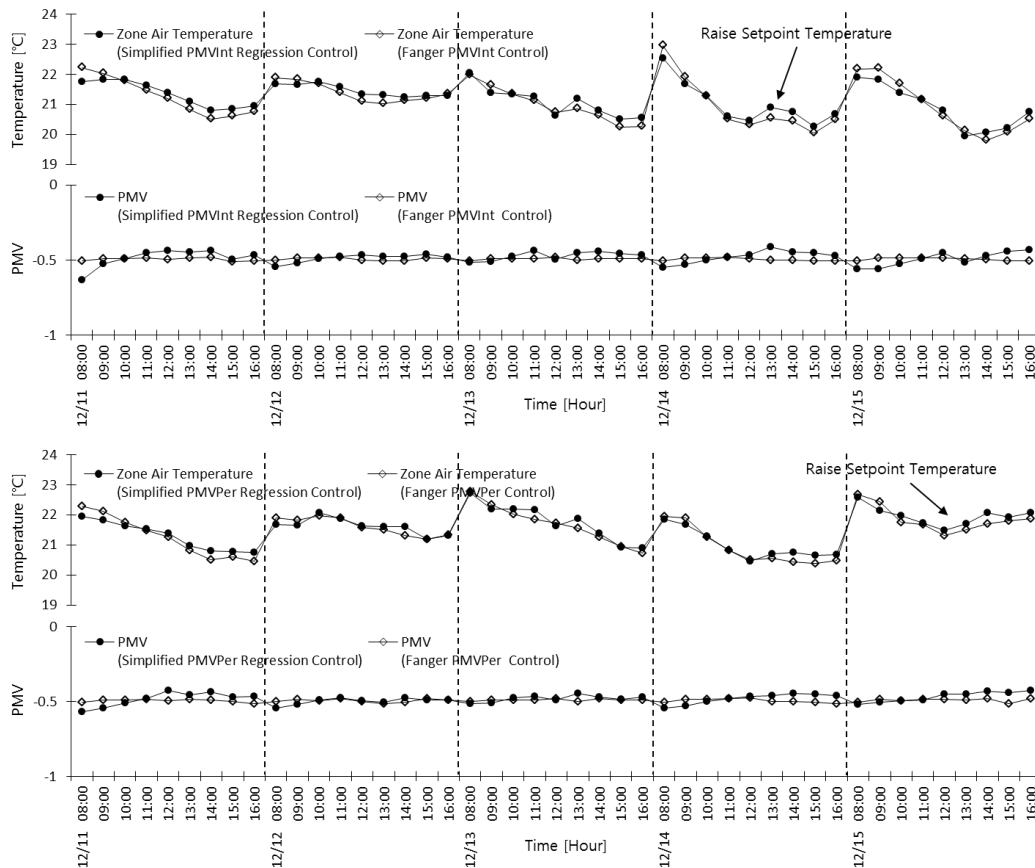
Figure 30: Comparison of thermal comfort controls at interior zone (Upper) and perimeter zone (Bottom) during the winter
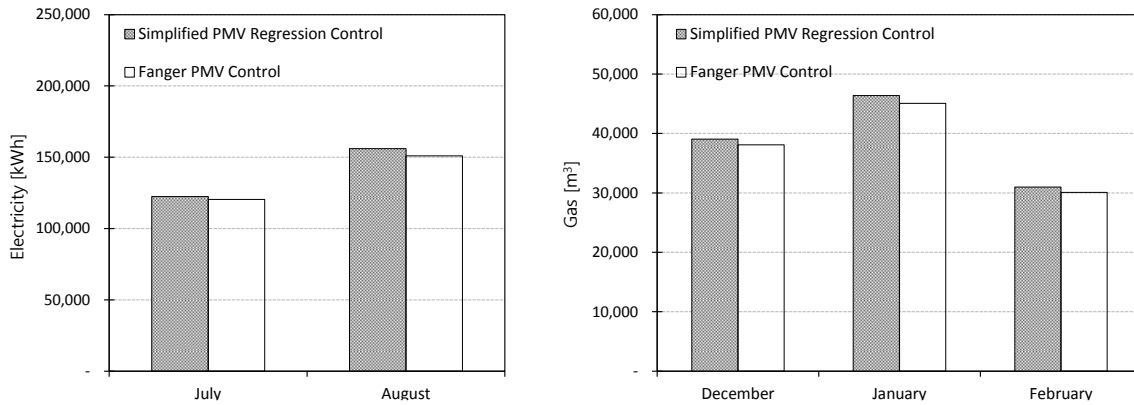
Figure 31: Comparison of energy consumption during the summer season (Left) and winter season (Right)

4. CONCLUSION

PMV simple regression model based on reducing the physical parameters and Fanger PMV model were simulated and compared in terms of thermal comfort and energy consumption. The actual office building utilizing the EnergyPlus simulation was modelled and the result has shown the effectiveness of model.

(1) The sensitivity of the perimeter PMV regression model shows that the relative humidity of the perimeter is fixed at 65%, which is considered the average value of significance range, and indoor is simplified by substituting mean radiant temperature to indoor air temperature based on analysis of additional data. Study shows that the Fanger PMV model can be substituted with a simplified PMV regression model.

(2) The simplified PMV regression model control consumes an additional 2.4% of cooling energy and 2.7% of heating energy, as compared with the Fanger PMV model control. These numbers are considered as predicted deviation between the simplified PMV regression model control and Fanger PMV model.

(3) When applying thermal comfort controls, the average set-point temperature is approximately 24℃ during the summer season, and 20℃ during the winter season, respectively. Thus, the regulation on set-point temperature is considered to not accounting for the thermal comfort of office building occupants.

5. REFERENCES

[1] ATTHAJARIYAKUL, S. and Leephakpreedaz, T., 2005, Neural computing thermal comfort index for HVAC systems, Energy Conversion and Management, Vol. 46, Issues 15-16, pp. 2553-2565.

[2] HUMPHREYS, M. A. and Nicol, J. F., 2002, The validity of ISO-PMV for predicting comfort votes in every-day thermal environments, Energy and Buildings, Vol. 34, Issue 6, pp.667-684

[3] BURATTI, C., Ricciardi, P. and Vergoni, M., 2013, HVAC systems testing and check: A simplified model to predict thermal comfort conditions in moderate environments, Applied Energy, Vol. 104, pp. 117-127.

[4] KOSONEN, R. and Tan, F., 2004, Assessment of productivity loss in air-condition buildings using PMV index, Energy and Buildings, Vol. 36, Issue 10, pp. 987-993.

[5] FANGER, P. O., 1982, Thermal Comfort Analysis and Application in Environmental Engineering, McGraw-Hill Book Company.

[6] ISO, 1994, ISO 7730:1994 Moderate thermal environmental-Determination of the PMV and PPD Indices and Specification of the conditions for Thermal Comfort, International Organization for Standardization.

[7] U. S. Department of Energy Federal Energy Management Program, 2008, M&V Guide lines: Measurement and verification for federal Energy Projects Version 3.0

252: A novel approach on measuring solar transmittance of glazings

GEORGE GORGOLIS, NIKOLAOS SKANDALOS, DIMITRIS KARAMANIS

University of Patras, G.Seferi str. Agrinio, ggorgolis@upatras.gr
nskandalos@upatras.gr
dkaraman@upatras.gr

Due to the increased interest of reducing building energy demand, innovative glazings are being developed and tested worldwide. Among other properties, solar transmittance should be carefully measured in order to be used in the building thermal simulation studies. Currently, the standard measuring procedure relies on the application of the ASTM E424-71 method by the use of a spectrophotometer and artificial light sources or a pyranometer and the sun. In this work, an alternative method was developed based on an in-house designed and built wind tunnel of controllable conditions of air RH, temperature and wind flow, simulated solar radiation by a 1000 W Xe source and a pyranometer of class A. The system was calibrated by an electrochromic glazing of 10x10 cm2 that was biased at different time intervals in order to scan all the transmittance range. Prior to the solar simulator measurements, electrochromic transmittance values were determined by an UV/VIS/NIR spectrophotometer with an 150mm integrated sphere. The method was applied in the solar transmittance measurement of innovative glazings like semi-transparent PV and insulating aerogels. The results of solar transmittance that were produced from this proposed method were very close to the corresponding produced results after the reduction of the observed transmittance spectrum with the ASTM G173 spectrum. Also, the results were in good agreement with the values of solar transmittance that were observed using the method of measuring the ratio of solar radiation with and without a glazing material. So, the method can be used as a fast and accurate procedure for solar transmittance measurement, while in the same measurements, the reflected radiation can be monitored.

Keywords: glazings, solar spectrum, materials, thermal behaviour

1. INTRODUCTION

Glazings are used in buildings for the controlled penetration of both solar light and solar heat energy in their interior. Most of the solar energy that enters a building has wavelengths between 300 and 2500 nm. Because of the fact that the visible part is small compared to the entire solar spectrum, segregation between the solar transmittance and the luminous transmittance of glazing materials should be performed. Solar transmittance is an important property for the performance of windows and fenestrations.

Transmittance can be divided into specular, diffuse and total, depending on which direction or if all directions are considered, while the spectral transmittance, t_λ (where λ denotes wavelength), of a glazing material equals to the transmitted part of the incident solar radiation to this incident radiation. The solar transmittance is defined as the ratio of the transmitted solar radiation to the incident solar radiation and depends on the measurement method, the spectral composition of the incident radiation, the incidence angle and the solid angles of the incident and transmitted radiation. Solar transmittance can be written as

Equation 12: Solar transmittance

$$t = \frac{\int_0^\infty t(\lambda) \cdot \Phi_{\lambda_i} \cdot d\lambda}{\int_0^\infty \Phi_{\lambda_i} \cdot d\lambda}$$

where:

- t = solar transmittance (%)
- λ = wavelength (nm)
- t(λ) = spectral transmittance observed from spectrophotometer (%)
- Φ_{λ_i} = the incident spectral flux (W)

It is noticeable that the integration is not over wavelength. It can also be written as

Equation 2: Solar transmittance

$$t = \frac{\int_0^\infty \int_\Omega L_{\lambda_i} \cdot d\Omega_t \cdot d\lambda}{\int_0^\infty \int_\Omega L_{\lambda_i} \cdot d\Omega_i \cdot d\lambda}$$

where:

- L_{λ_i} = spectral radiance that incidents from direction (θ$_i$, φ$_i$, θ and φ are angles)
- L_{λ_t} = spectral radiance which is transmitted in direction(θ$_t$, φ$_t$)
- dΩ = the solid angle equal to sinθcosθdθdφ.

The g-value or the total solar energy transmittance is the sum of the solar direct transmittance t_e and the secondary heat transfer towards the inner part of a building, q_i. The secondary heat transfer is a result of convection and longwave IR radiation of the part that has been absorbed in the glazing (CHOW, LI, LIN, 2010):

Equation 3: g-value

$$g = t_e + q_i$$

where:

- g = total solar energy transmittance (%)
- t$_e$ = solar direct transmittance (%)

- q_i = secondary heat transfer factor (%)

The solar direct transmittance of a glazing can be calculated with:

Equation 4: Solar direct transmittance.

$$t_e = \frac{\sum_{\lambda=300\,nm}^{2500\,nm} t(\lambda) \cdot S_\lambda \cdot \Delta\lambda}{\sum_{\lambda=300\,nm}^{2500\,nm} S_\lambda \cdot \Delta\lambda}$$

where S_λ is the relative spectral distribution of the solar radiation.

The secondary heat transfer factor expressed with the assistance of the heat transfer coefficients towards the inside and outside, depends mainly on the glazing position, the temperatures inside and outside the glazing, the temperatures of the two glazing surfaces and wind velocity, and can be written as:

Equation 5: Secondary heat transfe

$$q_i = a_e \cdot \frac{h_i}{h_e + h_i}$$

where:

- a_e = solar direct absorbance (%)
- h_i = heat transfer coefficient towards the inside (W/m²·K)
- h_e = heat transfer coefficient towards the outside (W/m²·K)

The different methods for the g-value measurement under steady-state laboratory conditions have been described analytically (KUHN, 2014) and measured g-values for transparent and translucent building materials as well as building-integrated PV systems (BIPV) have been reported.

ASTM methods

In order to find the solar transmittance, the spectral transmittance data between wavelengths of the visible part of the spectrum which has been obtained by the spectrophotometer measurements is multiplied with the relative spectral distribution of the solar radiation given by Standard Tables of ASTM E891, S_λ, and with the photopic spectral luminous efficiency function, V_{λ_i} (ASTM E971 – 88). This product is integrated over the visible part (from 400 to 700 nm) and a summation helps to calculate the integral. This procedure is repeated for the product of the solar energy spectral distribution and the photopic spectral luminous efficiency. The solar luminous transmittance (400-700 nm) of a sample is defined as the ratio of the two integrals. The same reasoning can be extended for the UV part (280-400 nm) and the NIR part (700-2500 nm):

Equation 6: Solar luminous transmittance.

$$t_v = \sum_{i=1}^{N} t(\lambda_i) \cdot S_\lambda \cdot V_{\lambda_i} \cdot \Delta_{\lambda_i} / \sum_{i=1}^{N} S_\lambda \cdot V_{\lambda_i}$$

where:

- N = the number of wavelengths for which S_λ is known for the 400-700 nm part
- $\Delta\lambda_i$ = the difference between adjacent wavelengths (nm)
- V_{λ_i} = photopic spectral luminous efficiency

This method can measure the solar luminous transmittance of glazing materials, but only for samples without large corrugations and inhomogeneities.

The ASTM E972-96 test method is used for measuring solar luminous transmittance of materials in sheet form and exploits sun as light source, and an illuminance meter in an enclosure. This method was especially developed for sheet materials that contain inhomogeneities and is appropriate for transparent and translucent samples as well as for samples with altered transmittance like patterned, corrugated or with incorporated fibers. A similar procedure is described in ASTM E1084-86, with the only difference that a pyranometer is used as an illuminance meter. Additionally, the method includes solar transmittance measurements at several angles. The transmittance is obtained as the ratio of the measured flux with the sample inside the enclosure to the measured flux without the sample. This method also, is suitable for glazing materials with reduced transmittance (using reflective films usually) and measures transmittance at angles up to 60° off normal incidence. The last two mentioned methods, though, have some drawbacks too. They are not easy methods, since they can be conducted only during sunny days (cloudy sky and haze will produce incorrect measurements) and during particular hours (close to solar noon), they have some limitations like that no building or vegetation should be close to the pyranometer's field and concerning the latter method, an alignment of the device must be performed at least every 15 min, while it is not precise for large incidence angles. According to the ASTM E1175-87 method, the solar transmittance of semi-transparent, patterned or inhomogeneous materials can be measured with a device consisted of a visual-response photometric detector and a solar simulator or sun as light source. In the ASTM E903-82 method, transmittance data of the material are collected by a spectrophotometer with an integrating sphere. In order to find the solar transmittance, the data are weighted by the relative spectral distribution of the solar radiation and integrated, as in ASTM E971-88 method. The method can be applied to materials with both diffuse and specular optical properties but not to those of patterned surface.

In this study, a novel method for the determination of the solar transmittance is proposed. The method combines data from spectrophotometer measurements (ASTM E903-82) with transmitted radiation measurements by an in-house designed and built wind tunnel of controllable conditions of air RH, temperature and wind flow, simulated solar radiation by a 1000 W Xe source and a pyranometer of class A. An electrochromic glazing of 10x10cm^2 was used for the calibration of the system and different colouring times were used in order to cover the transmittance region as much as possible. This method has several advantages over the previously reported methods as it can be conducted easily inside the laboratory, is fast, has been found accurate and it is independent on weather conditions and time of measurement.

2   EXPERIMENTAL PROCEDURE

2.1 Materials

The glazing materials were two electrochromic samples, coded W14 and W16, two amorphous silicon (a-Si) semi-transparent photovoltaic samples, a laminated coded a-Si and an unlaminated with a code name PV-glazing, with thicknesses 8.5 cm and 4 cm respectively, and finally a sample of commercial granular insulating silica aerogel.

The granular silica aerogel was inserted between two glass panes of a handmade construction. The dimensions of the panes were 10 cm x 10 cm, the thickness for each one was 0.4 cm, while the distance between the panes was 0.6 cm. The aperture on the upper part of the construction was sealed with an aluminum tape. Both electrochromic and photovoltaic samples had the same dimensions with the aerogel sample, 10 cm x 10 cm. For the W16 sample, only the intensity of the bleached state was measured, while for the W14 sample, both bleached and colored states were utilized. The colorization of the sample W14 was sequential and three measurements were conducted.

2.2 Experimental Setup

Prior to measurements with the "wind tunnel", the transmittance of the samples was measured with a PerkinElmer UV/VIS/NIR spectrophotometer (Lambda 950, with a 150 mm diameter InGaAs integrating sphere that measures both specular and diffuse radiation) covering the whole solar spectrum (250-2500 nm) with an interval of 2 nm. The calibration of the instrument was performed with a set of Lab sphere certified standards, while the normalization of the data was conducted using the ASTM G173-08 spectrum.

In our method, a "wind tunnel" of controllable environmental conditions (KRIMPALIS, KARAMANIS, 2015) has a key role. Starting from the left, the tunnel consists of an aramid honey comb chamber, a contraction zone while about in the middle, there is the space that hosts the sample's holder and the tested material. After that, there is a diffuser and lastly a fan housing with which the wind speed or air flow of each experimental run

can be controlled (Figure 1). Temperature and relative humidity can be constantly measured with a sensor that is located inside the diffuser and the air flow is recorded through a flow meter. The test samples are mounted in a way that are in contact with the air flow and perpendicular to the light radiation, and at the same time, two or three thermocouples can be adjusted to show the sample's temperature for different depths. All these measurements are collected by a CR1000 data logger.

Exactly above the sample, a solar simulator which reproduces the solar spectrum as Class B in a uniform collimated beam of 80 mm diameter (LOT Oriel) was adjusted (Figure 1). The used lamp is an ozone-free 1000 W Xe, with a 90° beam turner incorporated for perpendicular direction of the beam towards the sample. The lamp's height is changed desirably, while the voltage and the current of the power supplier have been set to provide a light intensity of about 1000 W/m^2 on the samples surface, very close to the respective average sunlight intensity on the earth's surface. The distance between the sample and the solar simulator was kept constant at 16.6 cm.

Figure 1: The "wind tunnel" of controllable environmental conditions (Krimpalis and Karamanis. 2015).

The pyranometer (Figure 2b) was mounted in the middle of two empty squared holders from expanded polystyrene in order to be thermally insulated and was confirmed that the measurement was not disturbed by surrounding elements. A third supportive layer from expanded polystyrene was also introduced (Figure 2d). The device was located on the level of the wind flow without disturbing it and reaching the appropriate distance from the light source. Also, before starting the procedure, the intensity of the radiation from the solar simulator was measured by the pyranometer and found to be 946.87 W/m^2. The light direction was perpendicular to the pyranometer. For calibration reasons, four extra measurements were taken for the perimeter of the starting point and they were equal to 938.76, 936.05, 941 and 936.05 W/m^2.

Then, the experimental procedure was the following: At first, all the samples were examined in the spectrophotometer and afterwards, they were inserted in the tunnel on a position exactly above the pyranometer, each one separately. The solar simulator was irradiating the sample perpendicularly and a black mask around the device was used (Figure 2a). The intensity of the transmitted solar radiation was monitored by the class A pyranometer and it was being recorded at the data logger. Each measurement was lasted for 2-3 min.

3   RESULTS AND DISCUSSION

3.1   Determination of solar transmittance with ASTM E971 – 88, E903-82 methods

The determination of the solar transmittance for the electrochromic materials resulted from the procedure which was described in the introduction, through equation 6. The transmittance spectra of the electrochromics (Figure 3) were observed by the spectrophotometer measurements. Then, the solar transmittance for the entire spectrum but also for each region separately, was calculated computationally. The calculations include a reduction of the observed transmittance spectrum with the ASTM G173 spectrum, the summations and then the weighting of each partial transmittance (UV, VIS, and NIR) to the total summed transmittance. In Table 1, the values of the total solar transmittance as well as the corresponding values shown by the pyranometer for the electrochromics are shown. For the W14 electrochromic, a great reduction of the solar transmittance is observed and accompanied with the reduction of the transmitted radiation intensity. This is a sequence of the intense colorization that was imposed in order to scan as best as possible the solar transmittance values. The electrochromic phenomenon can be shown also from the spectrophotometer measurements in Figure 4, where colored W14 starts from a visible transmittance of about 70% and drops to 15% for its third measurement (the induced voltage in this case was higher than the other two colored measurements as well as the applying time). It can be also shown that the aerogel sample and the bleached W14 exhibit a high visible transmittance, while the electrochromic W16 and the two photovoltaics do not show comparable visible transmittance. In Table 2, the solar transmittance measurements of all the tested samples are shown separately for each main region of solar spectrum.
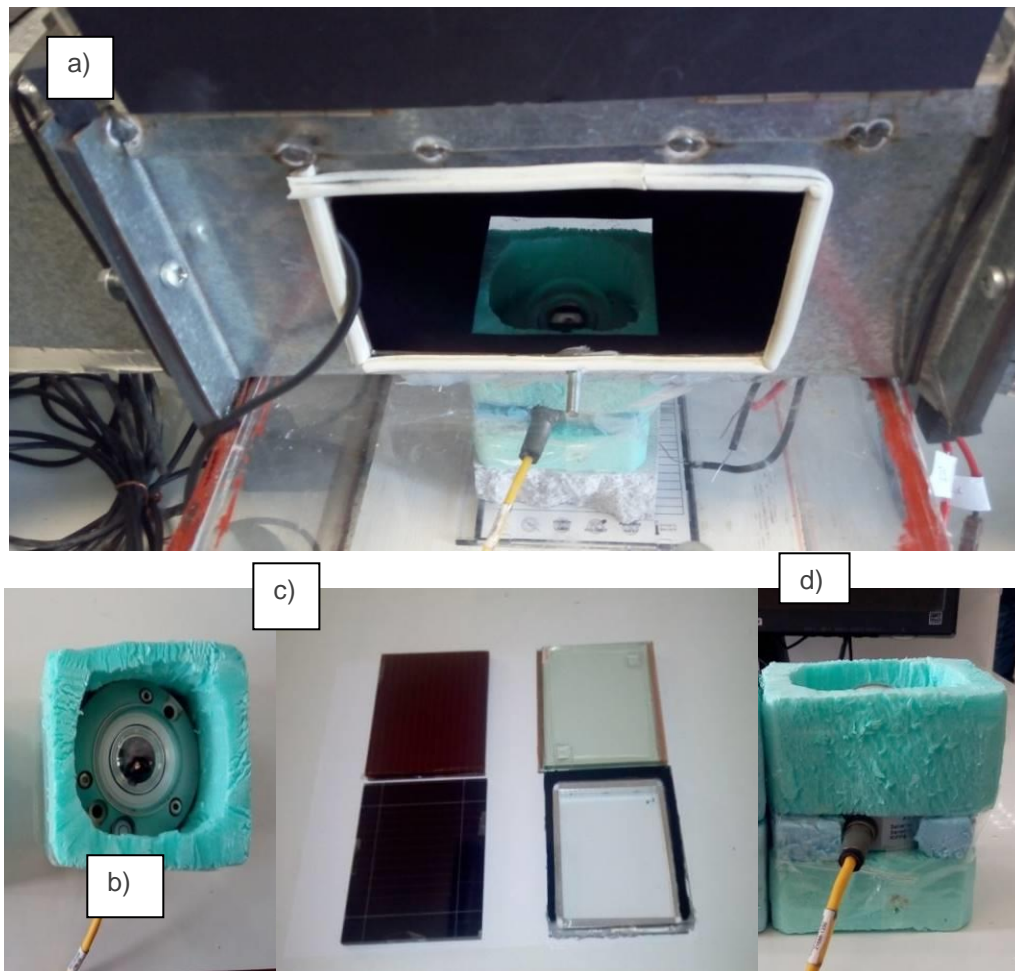
Figure 2: a) the device located inside the test sample area of the tunnel, b) a top view of the pyranometer, c) some of the tested glazing materials and d) a side view of the pyranometer.

Table 1: Solar transmittance of the electrochromic materials

Material	Reflectance	Transmittance	Absorbance	Transmitted radiation intensity
Electrochromic W16 (bleached state)	7.268 %	21.051 %	71.681 %	170.38 W/m^2
Electrochromic W14 (bleached state)	10.984 %	56.378 %	32.380 %	492.37 W/m^2
Electrochromic W14 1st measurement (colored state)	10.087 %	50.891 %	38.944 %	432.71 W/m^2
Electrochromic W14 2nd measurement (colored state)	7.992 %	33.600 %	58.401 %	275.85 W/m^2
Electrochromic W14 3rd measurement (colored state)	6.637 %	9.305 %	84.051 %	70.31 W/m^2

Table 2: Solar transmittance for the three regions of the solar spectrum

Material	UV solar transmittance	VIS solar transmittance	NIR solar transmittance	Total
Electrochromic W16 (bleached state)	10.2 %	70 %	19.8 %	100 %
Electrochromic W14 (bleached state)	5 %	54.9 %	40 %	99.9 %
Electrochromic W14 1st measurement (colored state)	5.6 %	57.3 %	37.1 %	100%
Electrochromic W14 2nd measurement (colored state)	8 %	63.9 %	28.1 %	100%
Electrochromic W14 3rd measurement (colored state)	19.6 %	70.2 %	10.2 %	100 %
Aerogel luminar	6.8 %	47.8 %	45.4%	100%
PV-Glazing	0.1 %	8 %	91.9%	100 %
a-Si PV	0.1%	21.3 %	78.6 %	100 %

3.1 Our proposed combining method

A calibration curve, which is illustrated at the Figure 4, correlates the calculated solar transmittance of the electrochromic materials with the measurements of the transmitted radiation intensity by the pyranometer. There is also the linear fit of these data. An almost straight line is observed and this is reasonable, because higher transmittance means more transmitted radiation through the glazing material, and consequently, higher recorded values from the pyranometer. Additionally, the fact that the solar simulator was facing perpendicularly each glazing material and there were no angle-dependent losses contributed to these results. A proportion between transmittance and radiation intensity is nearly observed and it can be deduced that the largest part of solar energy from the simulator is utilized in an increase of the material's absorbance, as shown in Table 1. Table 3 shows the data of the linear fit. The straight line of the linear fit is found to be:
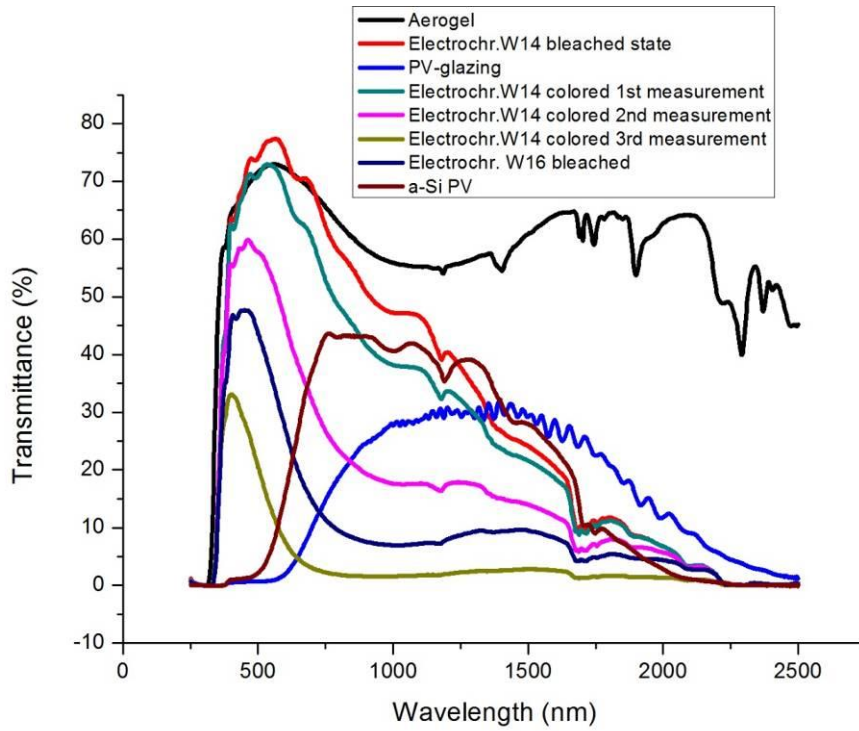
SUSTAINABLE CITIES & ENVIRONMENT

Figure 3: Transmittance spectra over the solar spectrum.

Equation 7: Linear fit of observed points from Figure 4. $$y = 8.90401 \cdot x - 16.59386$$

where:

- − y = intensity of transmitted radiation (W/m^2)
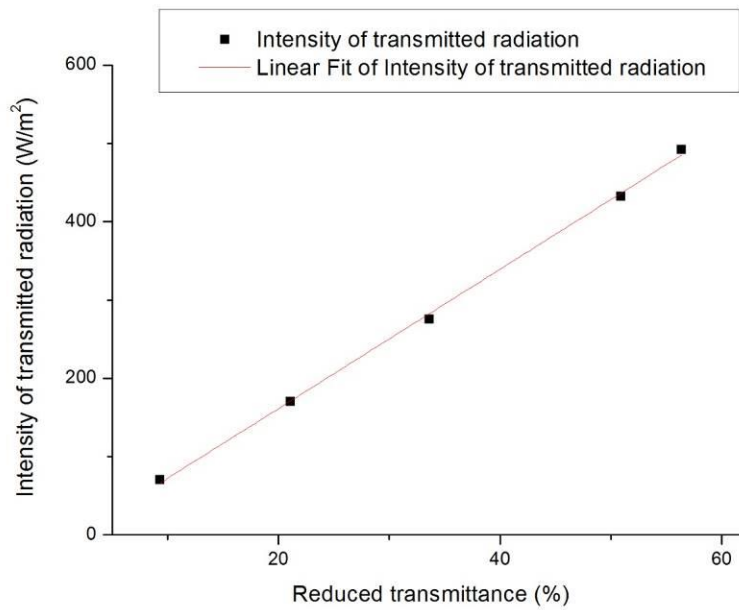- − x = reduced transmittance (%)

Figure 4: Calibration curve with Linear Fit of the electrochromic materials. In the x-axis, transmittance after reduction with the ASTM G173 spectrum, is used.

Therefore, the linearity of the measurements for the spectrophotometric calibrated samples points out the validity of the developed setup for glazing transmittance measurements.

Table 3: Linear fit parameters to the experimental data of Fig. 4

	Value	Standard error
Intercept point	-16.3 W/m^2	6.3 W/m^2
Slope	8.9 $(\frac{W}{m^2} \frac{1}{\%})$	0.2 $(\frac{W}{m^2} \frac{1}{\%})$

In Table 4, a summarizing table of all the tested glazing materials, except electrochromics, is presented. In the first two columns, results similar to the Table 1 are shown. Namely, for the three materials, their reduced solar transmittance was calculated with the previously described procedure for the electrochromics. Afterwards, the solar transmittance of the two photovoltaics and the aerogel was found exploiting the linear fit of the calibration curve of the Figure 4. The corresponding differences and errors are also shown in Table 4, while additionally, the solar transmittance as the ratio of the incident solar radiation with glazing material to the solar radiation without a glazing material is displayed. It is obvious that solar transmittance values observed with our method are very close to the corresponding reduced solar transmittance values and the errors are in a reasonable range. Especially for the aerogel and the a-Si photovoltaic, the errors are very small, 2.63% and 3.22% respectively. Our proposed method limits the errors of the direct measurements (spectrophotometer measurements and radiation ratio with and without glazing material) because it includes much more measurements for determining the corresponding equation. Based on our findings, the developed method is an efficient method for the determination of the solar transmittance for façade or glazing materials and building integrated photovoltaics (BIPVs) and can lead to accurate measurements.

Table 4: Summarizing table of other glazing materials

Material	Calculated reduced Solar Transmittance	Solar Transmittance as the ratio of solar radiation with and without glazing material	Solar Transmittance calculated with our method	Transmitted radiation intensity	Difference of our method Solar Transmittance from reduced Solar Transmittance	Error
Aerogel luminar	63.288 %	62.835 %	64.956 %	594.97 W/m^2	1.668 %	2.63 %
Photovoltaic a-Si	23.509 %	24.571 %	24.266 %	232.66 W/m^2	0.757 %	3.22 %
Photovoltaic PV-Glazing	12.210 %	14.569 %	13.629 %	137.95 W/m^2	1.419 %	11.62 %

4   CONCLUSION

A novel, fast and efficient method of measuring the solar transmittance of building materials is presented. The method combines spectral transmittance measurements for the entire solar spectrum with a wind tunnel of controllable conditions of air RH, temperature and wind flow, simulated solar radiation by a 1000 W Xe source and a pyranometer of class A. The solar transmittance of some electrochromic materials was the basis of a linear fitted calibration curve for the intensity of the transmitted radiation as a function of solar transmittance. This method is more fast than the ASTM method since with the proposed combining method, time-consuming calculations and reductions are not necessary and the sole measurement that has to be taken is the intensity of the transmitted radiation. Then, someone has to use this measurement inside Equation 7 and find solar transmittance of each glazing material. The saved time cannot be quantified but we believe it is worth reporting. Calculations of solar transmittance with the proposed method for an insulating aerogel and two semi-

transparent photovoltaics led to very good result agreement with the spectrophotometric measurements. Moreover, additional processes can be monitored like reflected radiation in the same measurement.

5   ACKNOWLEDGEMENTS

6   REFERENCES

CHOW, Tin-tai, LI, Chunying, LIN, Zhang, 2010. Innovative solar windows for cooling-demand climate. Solar Energy Materials and Solar Cells, 94 (2), 212-220.

KRIMPALIS, Spiros, karamanis, Dimitris. 2015. A novel approach to measuring the solar reflectance of conventional and innovative building components, Energy and Buildings, 97 (0), 137-145.

KUHN, Tilmann, 2014. Calorimetric determination of the solar heat gain coefficient g with steady-state laboratory measurements, Energy and Buildings, 84 (0), 388-402.

331: The investigation of the luminous environment in ETFE structures

DAWA MASIH[1], BENSON LAU[2]

1 Koya Univesity, Koya, Kurdistan Region, Iraq , KOY45, Email: dawa.azad@koyauniversity.org
2 University of Nottingham, Nottingham, UK, NG7 2RD, Email: Benson.Lau@nottingham.ac.uk

ETFE (ethylene tetra fluoro ethylene) is a lightweight material that is increasingly used in building applications. Typical ETFE cushions can provide a degree of thermal insulation with reduced initial cost investments and fewer supports compared with a glazed roof. However, there is limited research regarding the luminous environment inside the ETFE cushion or panel covered structures and limited availability of information on its optical properties, which necessitated the current study. This paper presents a qualitative and quantitative study to assess the lighting performance of an encapsulated ETFE panel structure. Through on-site monitoring and the physical modelling, this research project aims to: understand the existing luminous environment and the current lighting problems identified inside this ETFE structure; develop and test the design alternatives to deal with glare, visual comfort, three-dimensional modelling; and develop workable solutions to improve the normally dull and uniform lighting conditions inside ETFE enclosures. This study concluded that by careful manipulation of the opacity and transparency of the ETFE structure, the luminous environment can be significantly improved or enhanced.

Keywords: ETFE structures, Luminous environment, Daylighting performance, ratio, Field Studies, Experimental Testing

1. INTRODUCTION

Ethylene Tetra Fluro Ethylene (ETFE) is a modified copolymer of ethylene and fluoroethylene. It is used for a range of applications including building cladding, such as glazing in transparent roofing and curtain wall systems. This partly crystalline plastic has inspired changes in the way buildings are designed, and rarely has a new construction material had such an impact on the design and performance of buildings. The increasingly use of this relatively new lightweight material in buildings is mainly due to its lightweight properties, its high daylight transmittance and associated potential for energy savings as well as its reduced weight in comparison with standard solutions that use glass.

ETFE can be extruded into large thin sheets, referred to as foils or films, which can be used in single or multi-layer cladding applications. Films currently in production range in thickness from 50µm to 300µm. A major attraction of ETFE is the considerable savings it offers for materials required to support cladding. ETFE polymer is 1% the weight of glass, expands to three times its normal length without losing elasticity, and it offers shade and insulation control (Barbian, 2008). This saving translates into a more efficient building structure and low maintenance cladding system. When used for cladding, sheets of ETFE are usually assembled into cushions, which are inflated (for structural reasons) by means of compressors. The system consists of two or more sheets of foil laid on top of each other and joined at the edges to form the cladding equivalent of an inflatable cushion. As stated, ETFE cushions can provide thermal insulation, with reduced initial cost investments and fewer supports compared to a glazed roof (Robinson, 2005).

ETFE has 95% light transmission of all frequencies but does not offer the clear visibility of glass (Robinson, 2005). ETFE films can be printed or fritted with intelligent patterns of varied transmittance properties that can be used to reduce solar gain without sacrificing its transparency to light. Nowadays, multi-layered cushions are manufactured with a combination of fritting, in which either the top or top and middle layers are fritted with patterns so that the shading coefficient can be altered. In some cases the middle layer can be adjusted to rise and fall by means of air pressure, thus achieving better solar control. In today's context (i.e. the pursuit of sustainable construction and building), ETFE is also a green material that is completely recyclable and also requires reduced energy for transporting and installation.

Previous ETFE studies have focused mainly on structural properties and related issues, while little research has been carried out in order to determine properties and characteristics of luminous environment inside the ETFE covered structures. This is also due to the lack of information on the material properties and luminous environment, making it difficult for designers to deliver energy efficient and environmentally comfortable designs. Additionally, since ETFE is not opaque to long-wave radiation, treating it as a glass layer can lead to errors when evaluating its performance. Therefore, it is essential to gain knowledge and develop methods to model this material it order to maximize performance (and minimize functional and financial risk).

1.1. Research objective

The first aim of this research is to understand the existing luminous environment inside ETFE structures and the current problems inside such buildings. Another aim of this research is to develop an envelope for these structures that can help to improve the luminous environment by changing the typical fully clear building envelope, in which the designers could benefit from it at early stage of design while using this type of envelopes. The aim of this study is also to evolve a methodology that helps us to analyse and understand the visual and luminous environment inside the ETFE structures.

1.2. Research Significance

The paucity of research pertaining to ETFE in building applications and the limited availability of information on its material properties justify the need for the present study. As mentioned earlier, ETFE is a popular emerging replacement for glass structures, but a more in-depth understanding of its nature, properties and performance study is needed to have a clearer picture. This study not only investigates the internal luminous environment of ETFE envelopes, but also develops an envelope for these structures that can help to improve and enhance the visual appearance and visual interest.

1.3. Research Methodology

This research aims to investigate and enhance the luminance performance of the ETFE panel structure as previously mentioned. Seeking to achieve the research objective described above, the following methodology was adopted. From the literature review, information was gathered regarding the application of ETFE in the building industry as an alternative material. It also covers the fundamental information of ETFE in terms of its properties, luminous behaviour and visual environment inside ETFE buildings. This was important to develop an inclusive understanding of the ETFE in buildings and its response to light.

Therefore, for the purpose of investigation of luminous environment performance of ETFE, three main steps have been adopted. Firstly, onsite monitoring was performed for two ETFE covered buildings, namely the ETFE Test Structure at Grantham and the Engineering and Science Learning Centre (ESLC) at Nottingham. Secondly, a scaled physical model of ETFE building was made as a base case, using the existing dimensions on one of the visited buildings, on which lab tests were conducted. Thirdly, different envelope patterns were added to the base case building envelope to investigate the differences in luminous environment.

The amount of daylight reaching a building is proportional to its relationship with its location and the sun path. At The first part of the site microclimate analysis was carried out and it was followed by the analysis of the luminous environment. The second step adopted was the physical model testing. This was carried out by building a scale physical model similar to the ETFE live test structure. A sample of ETFE film was obtained from the site to build the physical model, and testing was done under lab conditions on artificial sky and heliodon testing, using the measurement tools of DL5X2(S) digital light-meter for daylighting performance analysis and 'iPhotoLux' for luminance mapping to evaluate the visual environment and luminance distribution ratio. The third method was by taking the same physical model into a lab to do similar testing on it, but this time a different envelope arrangement was used, which led to creating ten cases. Each case was considered to be an exhibition and work space, thus appropriate objects were placed inside them. Furthermore, in order to evaluate the luminous environment in these cases, the following steps were undertaken.

Initially, the luminance mapping was created for all of the ten cases under overcast sky conditions by means of artificial sky, in order to specify the cases with the best visual environment in terms of the luminance distribution patterns, overall perception, and 3-D modelling. Then, daylighting performance analysis was conducted under artificial sky for the best selected cases and the base case, which is the fully transparent envelope. In this calculation no objects or furniture were put inside the space in order to show only the effect of the different envelope pattern of the selected cases on the light distribution. In this part three cases were evaluated. Finally, after the daylighting performance analysis, the best case was selected and compared with the base case. Therefore, the selected cases were reduced to two cases, the base case and the best case (i.e. the best building envelope). Furthermore, each case was separated to art space and work space by introducing the relevant furniture and objects into the spaces. In this stage, further luminance analysis was done both for sunny sky condition using heliodon and overcast sky condition with use of artificial sky. The luminance analysis in this part of the research was more detailed compared with the previous parts by considering more aspects of the luminance environment.

The results from the above studies reveal what the luminous environment of ETFE panel test structure is, and how it has been investigated. This enables improvement of its luminous environment by changing it from fully transparent to semi-transparent-opaque envelope.

2. ONSITE MONITORING (ETFE TEST STRUCTURE AT GRANTHAM)

Primarily, the process of onsite monitoring was conducted under overcast sky conditions, which is typical in the UK throughout the year. The purpose of this step is to evaluate the luminous environment of ETFE envelopes in real-time conditions, as well as to understand the quality of the space and its thresholds. The more comprehensive the analysis, the more satisfactory the performance conclusion will be. After visiting the site, luminance measurements was taken by means of digital instruments such as Luminance Meter and PhotoLux for measuring the internal and external luminance levels and distribution patterns at certain defined points.

Figure 32: images of the interior and outside of the ETFE Test Structure (source: author)
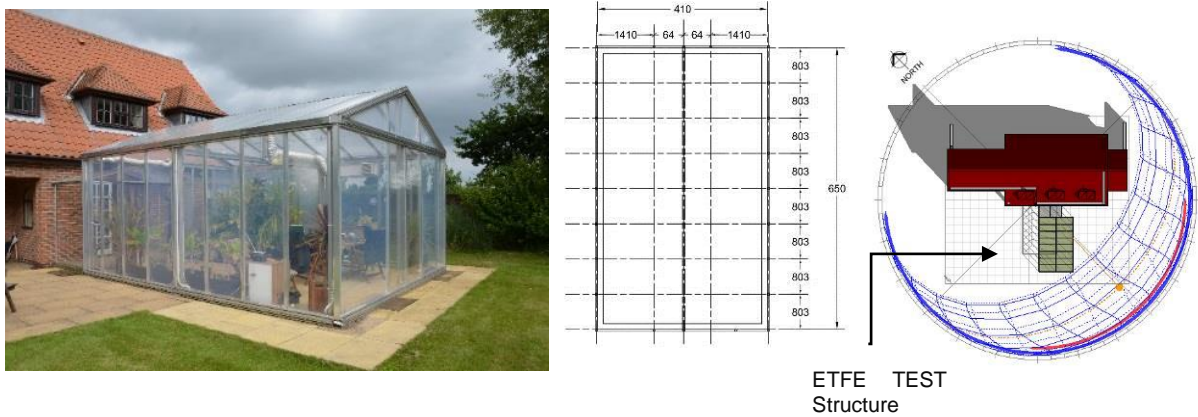

ETFE TEST
Structure

Figure 33: Images of elevations of ETFE Test Structure (source: author), Site Plan with Sun Path Diagram and position of Test Structure to the Pinfold House, and Structural plan of ETFE TEST Structure.

Source: Digital model from (Eyas, 2012), edited by author.

The structure is 6500mm in length by 4100mm in width by plan. The longer axis of the test structure is oriented towards Northeast & Southwest and the shorter axis towards Southeast & Northwest. It consists of aluminium frames filled with different types of ETFE foil. Different ETFE foils are installed in each frame, which vary from ETFE cushions to ETFE panels.

2.1. Onsite Monitoring data

The visit was carried out on the 7th of July 2014. The illuminance readings were taken in the late afternoon, from 5.30 to 6.00 pm, of overcast sky condition. The average exterior illuminance was 1631.3 lx.

2.2. Daylighting Performance Assessment

A defined grid was plotted to carry out reading at each point 1 metre height above the ground to examine the luminous environment of the test structure. An illuminance analysis was then adopted and the daylight factor of the space was calculated. Daylight factor results indicate the quantity and distribution of light under overcast sky condition.

From Figure 3, it was observed that the maximum illuminance value under the test structure is 1171 lx and the minimum value is found to be 478.67 lx. The average illuminance level inside the structure was found to be 919.5 lx, with average daylighting factor of 56.4%. The daylighting factor was found to be very high, as it reflects the predominant use of ETFE as a construction material for covering this free-standing test structure.
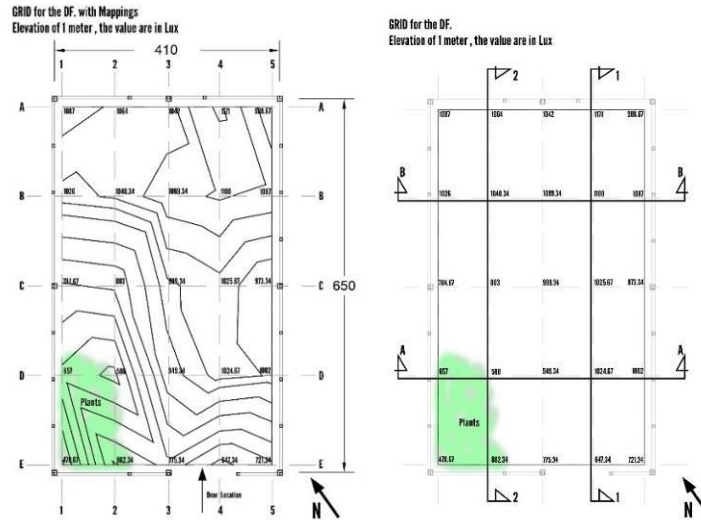
Figure 34: Images showing the illuminance level inside the ETFE test structure under overcasting sky condition

2.3. Uniformity Ratio

To evaluate more precisely the distribution of light over the space, a uniformity ratio calculation was carried out. By calculating the uniformity ratio from the above statement, which is a minimum value of daylight factor divided with the average daylight factor of the room, the ratio was found under the test structure to be 0.9, which is higher than the optimum value recommended by CIBSE guide.
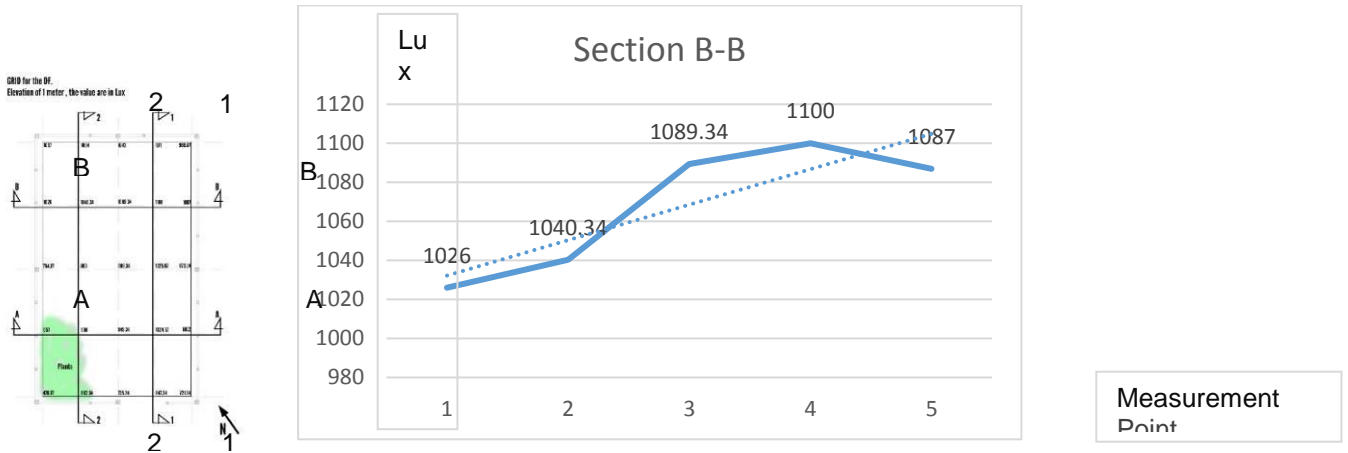
Figure 35: Illuminance distribution value along section B-B

(Average lux level: 1068.54, Uniformity Ratio: 0.96)

2.4. Visual Environment

Luminous mapping was used to evaluate the test structure in terms of the luminance distribution ratio, brightness contrast and visual performance so as to figure out the impact of the envelope on the perception of spaces and internal objects (since light penetrates through it). The recommended ratio of task luminance to immediate surround to far surround ought to be of the sequence of 10:3:1 (task: immediate surround: far surround), according to the CIBSE Code for Interior Lighting (1994) and in Daylighting by Hopkinson, et al (1966).

The summary shows that the task-to-immediate surround and task-to-general surround luminance ratios are in a reversed order or they have a close value to each other, which caused by the excessively uniform lighting field distribution, meaning the background is always brighter than the task, or they have similar brightness. This reversed luminance ratio makes the details of tasks become less visible. The equally valued luminance ratio also makes it very difficult to see the task details clearly. However, the results show it has not exceeded

a maximum acceptable ratio of brightest to dimmest light for good vision (in the order of 1:10). This similar luminance would not help the visual task with more clarity and would cause visual distraction.
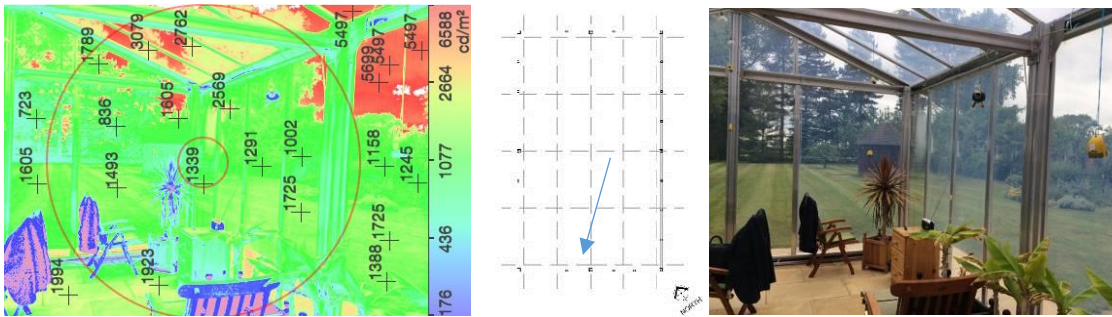

Figure 36: (Viewpoint A) Focus: Immediate Surround: Far Surround= 1: 1.36: 2.17
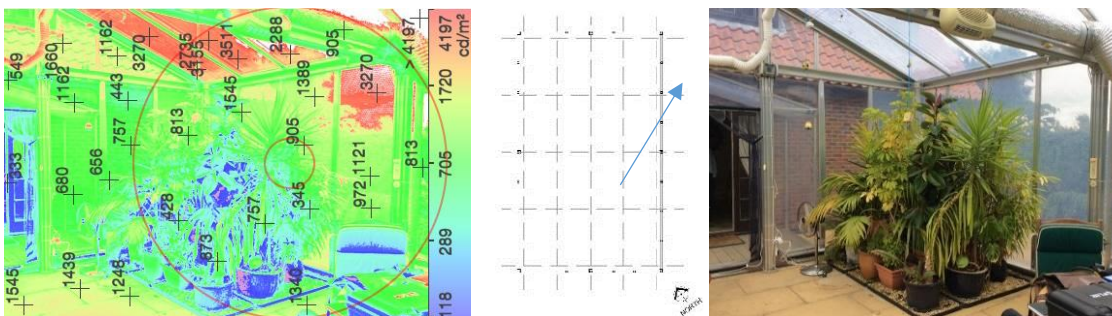

Figure 37: (Viewpoint B) Focus: Immediate Surround: Far Surround= 1: 1.5: 1.76

Table 26: task: immediate surround: far surround

	The task-to-immediate surround	task-to-far surround
Viewpoint A	1: 1.36	1: 2.17
Viewpoint B	1: 1.5	1: 1.76

2.5. Analyzing the 3-D Vision

In the test structure which is covered by transparent ETFE panels the visual appearance of the internal objects are adequately revealed, but the 3-D modelling is rather dull.
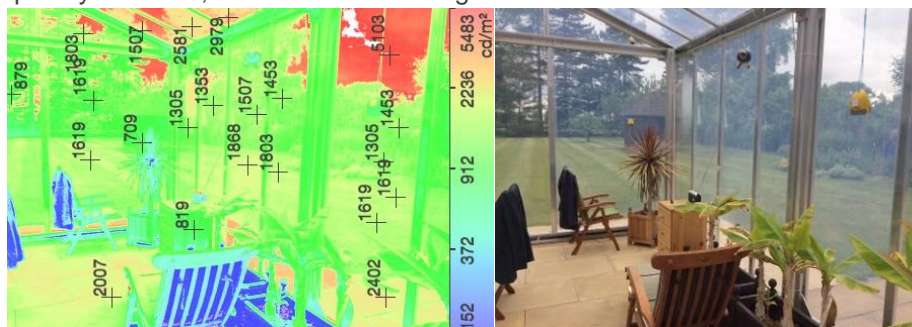
Figure 38: luminance distribution

It can be seen from figure 7 that luminous values on the surface of the ETFE structure mostly depend on their other side (exterior) background, based on transparency. The luminance values can vary, but if they have same background the values are the same or close to each other. As shown in the picture those, for panels with grass in their background the value is (1619 cd/m²). It is very hard to separate different objects inside the space or even one side of the object with a different side. For example, there is a slight difference in the luminance value of the table and the plant in the corner of the space, similar to the sides of the table, whose value is about (800 cd/m²). This is because the field of view is uniformly lit and the eye receives a uniform image, so that there is little differentiation between objects and planes. Thus the perception of object

orientations and spatial positions is likely to be poor in a space fully enclosed by a uniformly diffusing membrane skin.

3. PHYSICAL MODEL TESTS

This part of research was carried out by testing a 1:20 scale model, with the same dimensions of the existing ETFE Test Structure, under overcast sky condition as well as sunny sky condition. The model was covered with different envelope patterns, each one representing a case, in order to get the most satisfactory results in terms of luminance and illuminance environment, represented with artificial sky and heliodon.

Ten cases were considered to perform the tests:
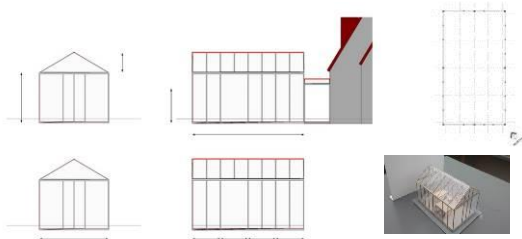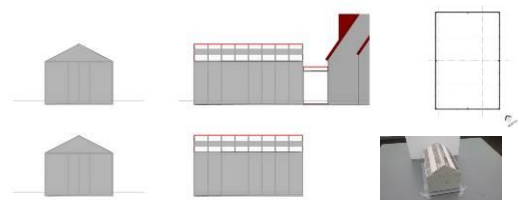

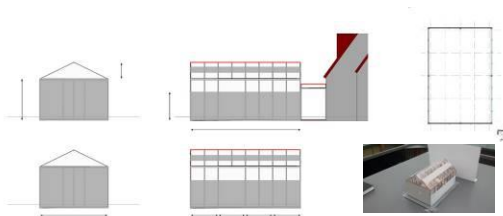*Figure 8: Case 1*
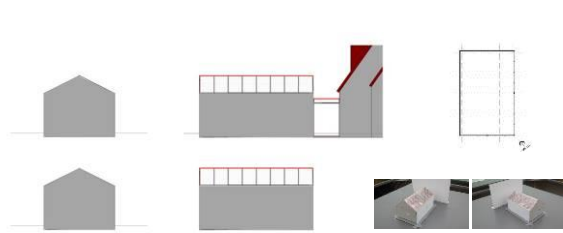
Figure 9: Case 2
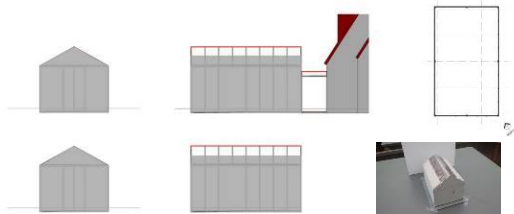
Figure 10: Case 3
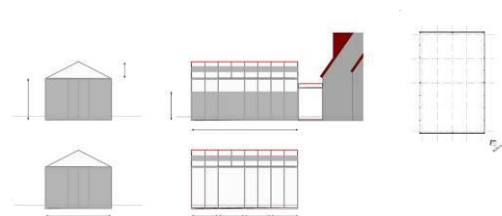
Figure 11: Case 4
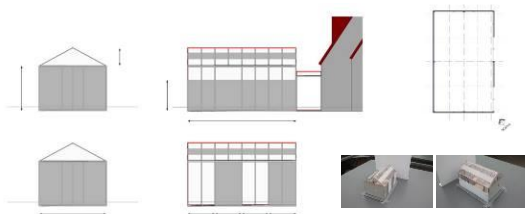

Figure 12: Case 5

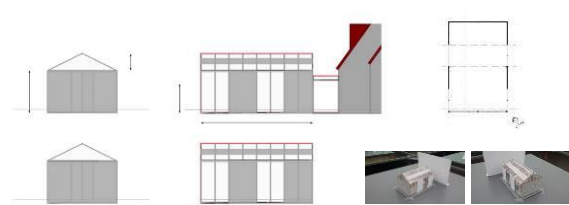*Figure 13: Case 6*

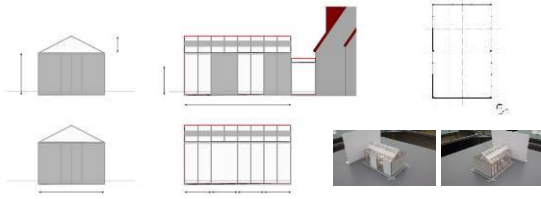*Figure 14: Case 7*

Figure 15: Case 8
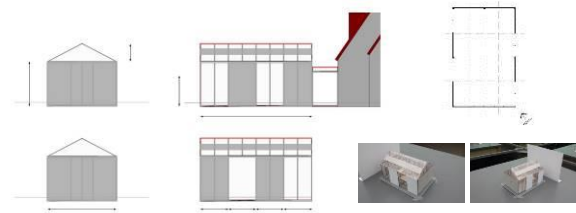
Figure 16: Case 9   Figure 17: Case 10

Photo-lux has been used for the purpose of understanding luminous environment and visual comfort study. Tests were conducted from equinox, summer solstice and winter solstice at 9:00 am, 12:00 am, 15:00pm and 18:00 respectively. This is also readings on the illuminance environment of both inside and outside of the model has been recorded using DL5X2(S) digital light-meter considering the base case, seventh and eighth case.

3.1. Assumptions

Since we want to evaluate the daylight and sunlight for ETFE building envelopes, it is appropriate to conduct daylight studies with generic models. The first case was tested using a physical model, to give an idea about the luminous and illuminous environment in more controlled conditions compared to the existing Test Structure. The second case was to determine the same model with light penetration only in the roof as a skylight, in order to ascertain the light effectiveness of the transparent roof on the space. The third and fourth cases are to identify the effect of different roof patterns on light inside the space. The fifth to tenth cases show the impact of the sides and roof by using different patterns on all of them in order to get the best luminous and illuminous environment.

3.2. Testing Procedure

The physical model testing procedure was conducted using the 1:20 scale model both in the artificial sky and on the heliodon. Considering more than one type of envelope as described with the cases and two different types of space activities, the process continued.

Within the artificial sky, the luminous mappings of all the cases was undertaken in terms of art and work space. The luminous mappings (unit Cd/m^2) were created by firstly taking pictures with fisheye lens of the objects inside the space, and then giving the value of each intended point within the picture. In consideration of work space, luminous mapping of all ten cases was carried out, whereas for the art space the choice was more selective, with only the best cases being used, namely case 1, 6, 7, 9 and 10, in order to get more comparative results.

After that, the DF was similarly measured within the artificial sky, for two of best selected cases with the base case. The measurements has been made under the artificial sky. Initially a grid of 55x55cm was considered, resulting in 104 defined points. Readings on the illuminance value of each point inside the space and outside of it were recorded using DL5X2(S) digital light-meter (figure 18) by placing the light sensor on each point of the grid. In this process only the base case, seventh case and eighth case were considered to achieve understanding of the outcomes and solutions.

Furthermore, the heliodon testing with photo-lux was used for the purpose of understanding luminous environment under sunny sky and visual comfort study. With consideration to the art space and work space, seven cases (1, 2, 3, 4, 5, 7 and 9) were used for this part of physical model testing. For the base case and the fifth case, tests were conducted on the equinox, summer solstice and winter solstice at 9:00 am, 12:00 am, 15:00 pm and 18:00 pm. For the second, third, fourth, seventh and ninth cases the test took place only at noon of the equinox, summer solstice and winter solstice. The reason for selecting fewer cases related to sun-lighting study is that a generic understanding of the issue is sought, with recognition and evaluation of the case that gives least glare compared to the other selected cases, not to solve the particular phenomena inside these spaces by designing specific envelopes for them.

Thus three groups of tests were carried out for different purposes. In the first group, by creating luminous mappings, the effect of the building envelopes on the luminance environment inside these building was

examined. Measurements were then taken under standard overcast sky conditions, by making use of artificial sky. Cases 1, 2, 3, 4, 5, 7, 8, 9 and 10 for work space as well as case 1, 6, 7, 9, and 10 intended for work space were used for these tests.

In the second group of tests, the effect on daylight level inside ETFE Test Structure and outside spaces with three different arrangements of envelopes was examined. Cases one, seven and eight were used for these tests and the following experiments were conducted. In the third group of tests, by creating luminous mappings the effect of different brightness and contrast and visual environment for a sunny sky condition via heliodon inside these building enclosures was examined. Cases 1, 2, 3, 4 and 5 were used in these tests.
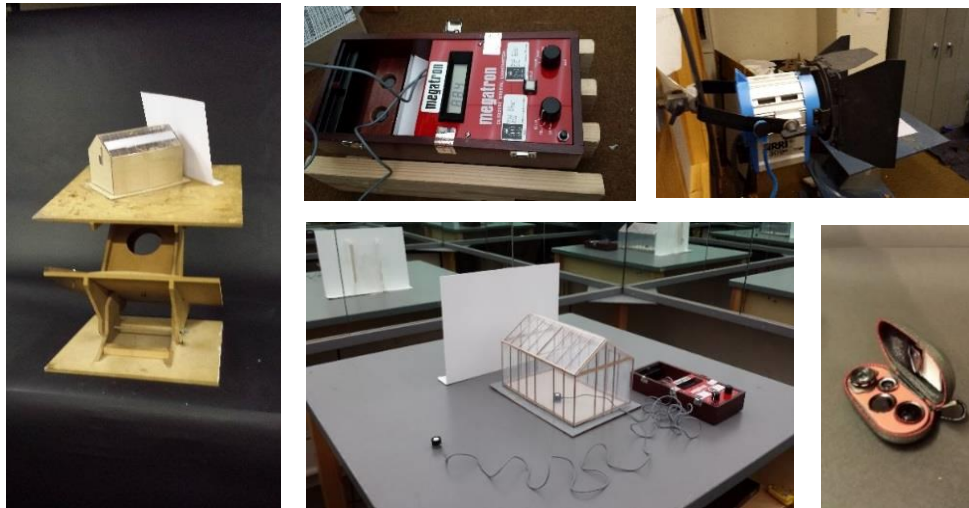

Figure 18: a) Use of model in conjunction with a heliodon. b) Use of model in artificial sky at the department of architecture and built environment university of Nottingham. c) DL5X2(S) digital light-meter. d) Camera lenses.

3.3. Internal environment

Illuminance measures the amount of light incident on a surface (in other words, the amount of light illuminating the surface). Illuminance is the density of photons falling within a given surface area. It is measured in lux, or foot-candle (fc). Illuminance can be measured with a lux meter. For a given light source, the closer to a light source the illuminated area is, the higher the Illuminance value.

3.4. Daylighting Performance Analysis

With the intention to determine the luminous environment of the "ETFE Test Structure" an illuminance assessment was performed and also daylight factor (DF) was calculated for the space, as described previously. The result of the DF gives indications with regard to the quantity and light distribution under overcast-sky conditions, as does AV. DF indicated average daylight factor derived from the illuminance reading taken from the 104 measurements for three cases, as indicated in figure 15 (a, b and c).
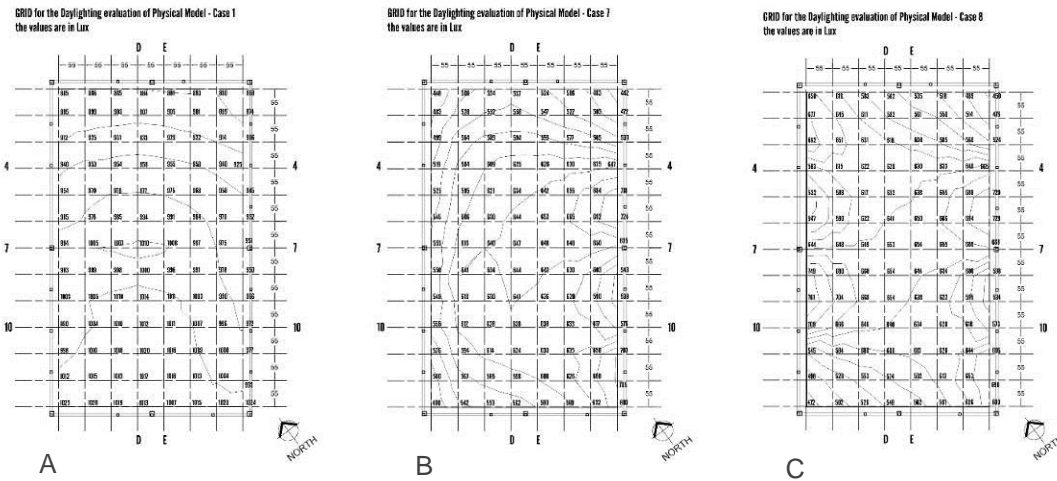
Figure 39 : Daylighting distribution with the installed grid for case 1, 7, and 8 (a, b, c)

From the above graphic, it can be seen that the first case had the maximum illuminance value of 1028 lx, which is the highest illuminance at any point of the working plane, under the physical model; the lowest illuminance value on the working plane (and the minimum illuminance value) was 800 lx. The average illuminance level inside the model was 970 lx. The average daylight factor inside the ETFE test structure was calculated to be 73.5%. Due to the fact it is a free-standing test structure predominantly composed of ETFE in the form of the construction material, the daylight factor appears to be excessive, as the recommended lux values of the CIBSE Code for Interior Lighting (1994) are shown to be 300-500 lm/m^2; museums and art galleries are recommended 150-300 lx. Hence this level of light under overcast sky condition is very high, and will cause too much light penetration when the sun appears, consequently this may effect heat gain in the hot days and energy consumption may occur for the purpose of reducing the temperature.

While performing the same tests on the seventh and eighth case there is a noticeable decease in the highest value of illuminance, whereby the envelope pattern contains more opaque parts compared to the 1st case, which is found to be 724 lx for the seventh case and 761 lx for the eighth. There is also a similar decrease in the minimum value of 442 and 450 lx for the seventh and eighth cases, respectively. The recommended daylighting factor is around 3-6% according to CIBSE Code for Interior Lighting (1994). The calculation result of average daylight factor inside the space found to be 45% for the seventh case, with 46.5% for the eighth, in comparison to 73.5% of the fully transparent envelope of first case. Through these results the evidence and evaluation are identifiable: the seventh case of the ETFE Test structure envelope was found to be better in terms of the luminosity of the space.

Table 27: Daylighting Performance Summary

	Case 1	Case 7	Case 8
AV. DF (%)	73.5	45	46.5
Uniformaty ratio - UR	0.9	0.74	0.73
Average interior (Lux)	970	595	615
Average exterior (Lux)	1321	1321	1321

3.5. Uniformity Ratio:

To evaluate more precisely the distribution of light over the space, a uniformity ratio calculation was carried out. The uniformity ratio is defined in the CIBSE *Lighting Handbook* as the minimum value of daylight factor that is measured on a relevant working plane, divided by the average daylight factor of the room. According to the recommendations, the optimum value in a room should not be less than 0.7 in order to achieve even distribution light. By calculating the uniformity ratio from the above statement, the ratio found under the test structure was 0.9, which is higher than the recommended range. However the uniformity ratio of both cases seven and eight are 0.74 and 0.73, which is closer to the recommended value of CIBSE design guide.

From the illuminance distribution graphs (table 2, Case 1) it can be observed that during overcast sky condition the illuminance is high. It is found from the shoebox test model that 93% of visible light is transmitted through a single-layer ETFE film. Since the physical model is made with two layers of ETFE, similar to the live structure, the light transmittance is reduced when compared to single layer. The illuminance level inside the test structure is relatively even at all points. For more detailed analysis, if we look at the cases one by one, we notice that in Case 1, the illuminance level along sections (4-4, 7-7 and 10-10), which cuts through the middle of the structure, is between 925 to 1010 lux, and UR is (0.97, 0.95 and 0.97) respectively. On the other hand, this value decreases while looking at the seventh and eighth cases, considering the same sections of (4-4, 7-7 and 10-10). In case 7 the value varies between 519-650 lux, with uniformity ratio of (0.85- section 4-4, 0.88- section 7-7 and 0.91- section 10-10). In case 8 the lux value varies from a minimum of 573 to 709 within these sections. The uniformity ratios are (0.93 of section 4-4, 098 of section 7-7 and 0.89 of section 10-10).

We can summarise from the above data that in case 7, because of having different cover for both side walls, the illuminance level changes more from one side to the other, rendering the object to more visible based on the fact that it can reflect different luminance levels on its surface. Considering the sections (D-D and E-E), which are longer, generally for all the cases the values decreases as we go closer to the existing building because of the protection it affords. Firstly, the base case illuminance value of sections (D-D and E-E) varies from 880 to 1010 lux, with a uniformity ratio of (0.9) for both sections. Secondly, in case 7 the lux values range from (525-650 lux) and the uniformity ratio of section D-D is 0.87 and E-E is 0.85. Finally, in case 8 illuminance values vary between 535 to 655 lux, whereas is section D-D the range is more significant and UR is 0.87, and the UR of section E-E is 0.89.

3.6. Luminance Mapping (Visual Appearance Analysis)

As mention before number of cases (envelope patterns) has been investigated and used for the ETFE test structure model in order to select the best performed cases regarding the luminance performance under overcast sky condition by means of artificial sky. For this purpose initially the first case is been evaluated as shown in fig14. After taking into consideration the objects (cube, sphere and cylinder) individually. It can be seen that in terms of 3D modelling visual appearance, the cylinder seems like it has a plain surface, because there is no barrier for light to enter to all around the space. The values on the cylinder surface is (110 to100 cd/m2) by ratio of (1.1: 1). On the other hand, if we look at the cube it can be clearly seen and differentiate all of the 3 surfaces that is visible in the picture, and the values demonstrates this fact. The luminance on each surface are (205, 125, and 95 cd/m2) with ratio of (2: 1.3: 1). Similar to the cube, the sphere has good 3d modelling visibility, as its surface luminance value are as follow (200 to 100 cd/m2) with ratio of (2:1). Nevertheless, due to the fully transparent envelope that first case presents, the significant solar radiant or daylight penetrates into the space that could cause glare and heat gain especially in the sunny day. This is also the illuminance value of the space as tested is very high compared to the recommended values. The need of covering the space is crucial to avoid these issues.
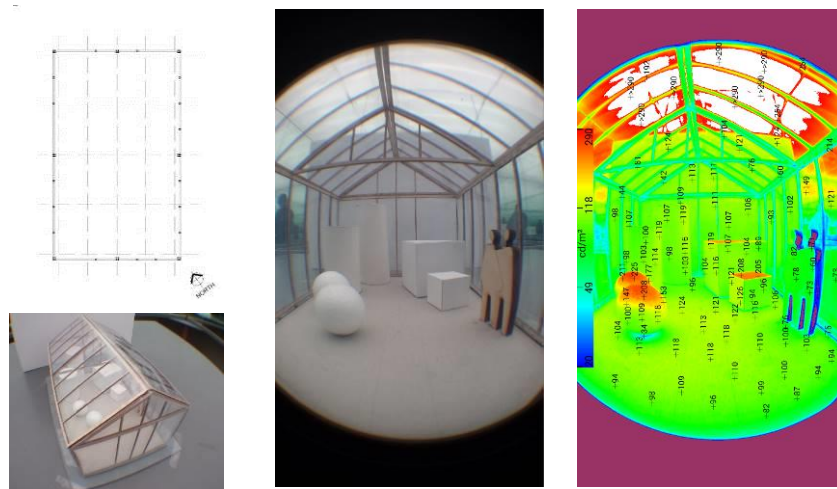

Figure 20: luminance mapping of case 1

In the seventh case as shown in fig21. It seems that the added covers helped to create more controlled environment for the space.

For instance the 3D modelling visual appearance of the cylinder has improved. On the cylinder surface the values are lower than the 1st case and become more distinct, as it differs between (75 and 50 cd/m²) by ratio of (1.5: 1). This is also considering the cube, Although the values are not as different as the 1st case, the 3d modelling effect is still good and all of the 3 surfaces are differentiated , which is clear in the picture, and the values demonstrates this fact. The luminance on each surface are (130, 70, and 50 cd/m²) with ratio of (2.6: 1.4: 1). When it comes to the sphere, the luminance value on the object has divided to three parts which helped the 3d modelling visibility. The sphere surface luminance values of the parts are as follow (130, 90 and 60 cd/m²) with ratio of (2.1: 1.5: 1). This envelope can decrease solar radiant or daylight penetration into the space comparing to the 1st case. Since the luminance values that are reflected from the space is less, also the illuminance values are smaller as daylight calculation has been adopted for this case. Consequently the glare and heat gain issues will be less.
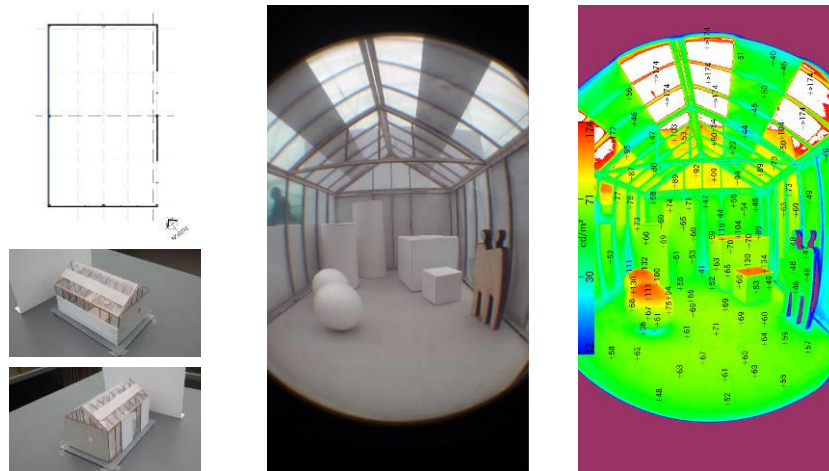

Figure 21: luminance mapping of case 7

4. CONCLUSIONS

This study aimed to understand the luminous environment in ETFE structures. This was undertaken through two interlinked research objectives:

- To understand the existing luminous environment inside the ETFE envelopes, and consider some of the present issues in such constructions.
- To enhance the luminance environment by generating an envelope for the ETFE structures.

The preceding analysis chapter reflected upon whether the aim and objectives had been realized, whereas this chapter presents the key findings, evaluates the methodological approach, provides recommendations for policy and practice, and identifies areas for future research. The common aspect between the three methodologies is that they investigate the luminous environment. Since ETFE has high transmittance and a free-standing structure exposed to direct solar radiation, at almost all times of the year the illuminance level inside the test structure is high. In general, the uniform light distribution and visual comfort was observed using all three methods, but the quantity of light transmitted is very high.

4.1. Key Findings Related to Onsite Monitoring

In general, the average daylighting factor is very high inside all of the ETFE buildings. The key findings of the onsite monitoring for the two buildings visited are:

Firstly, Since ETFE is a free-standing structure exposed to direct solar radiation throughout the year, it has high transmittance, and the illuminance level inside the test structure is correspondingly high. From daylighting performance analysis, it can be seen that the daylight distribution is uniform for ETFE Test Structure. However, the luminance distribution pattern inside the ETFE Test Structure, which is covered by transparent ETFE panels, has adequate revelation of the visual appearance of the internal objects, but the 3-D modelling is rather dull and the quantity of light transmitted is very high. Furthermore, there is no abrupt change of brightness inside its fully transparent covered space, and there is no glare issue under the overcast sky condition.

Secondly, as regards to ESLC building atria, although the average daylighting factor is high, the daylight is unevenly distributed. In other words, the uniformity ratio is low, which is caused by the adjacent walls of the atria. On the other hand, the luminance distribution pattern is uneven, with abrupt change of brightness, which causes a high luminance contrast ratio. The visual appearance of the internal environment is uninteresting, and the overall perception of the atrium space is rather dull. Overall, the 3-D modelling of the building details of the internal objects is poor, while in the top floor some objects near the existing double-height side of glazing are affected by a side light, and the 3-D modelling of them is much more apparent.

4.2. Key Findings Related to Physical Model Tests

It was discovered that by using combination of opaque with clear ETFE envelopes, satisfying space could be achieved with respect to the luminous environment. Using the same scaled physical model of the ETFE Test Structure for all types of envelope combination helped explore the luminous environment. Additionally, by looking at the comparative analysis between the best-case with the base-case, the comparative results showed that a solution could be found.

The calculation result of average daylight factor inside the best case was found to be approximately one-third lower in comparison with the case one. This means that the luminous level is very high inside the fully clear envelope, but it can be decreased by adding opaque surfaces to the envelope. Looking at the daylight distribution inside the first case, it was found to be uniform compared with the best case, which has lower illuminance value inside the interior space. This indicated the effect of the transmittance properties of ETFE panel for light penetration.

In terms of space perception evaluation, case 7 was found to be the best-case envelop resulting from navigating different experimental envelope patterns on the ETFE test structure. The external configuration can create scenes with intended lighting distributions and luminance contrasts through considerate manipulation of the external combination, which can enrich the spatial experience inside the space. Luminance differences within an area influence the considered length as often as they effect the luminance contrast between the focus along with the background.

5. REFERENCES

ARAJI, M (2008). Balancing Human Visual Comfort and Psychological Wellbeing in Private Offices. Doctor of Philosophy in Architecture, University of Illinois.

BEHLING, S et al. (2010). Innovative Design and Construction. Germany: Detail.

CHILTON et al., (2004). European Design Guide for Surface Tensile Structures – Internal Environment. Brussels: TensiNet. pp. 97-146.

CIBSE Code for Interior Lighting (1994). CIBSE.

CIBSE Lighting Guide 10: Daylighting and window design, Year: 1999, ISBN 0-900953-98-5, Publisher: CIBSE

LANDRELL, A. n.d. ETFE Design Guidance.

LANDRELL, A. (2011). ETFE: An Economical Alternative to Glass. Articles, [Online]. 9th April, 1. Available at: http://www.architen.com/articles/etfe-foil/ [Accessed 16 August 2014].

LAU, B., & Chilton, J. (No date). Chapter 9 (unpublished book chapter). In: Llorens, J. Fabric structures in architecture. Polytechnic University of Catalonia, Spain (e-mail: ignasi.llorens@upc.edu): Woodhead Publishing.

LECUYER, A. (2008). ETFE - Technology and Design. Basel: Birkhäuser Verlag AG.

ROBINSON, L (2004). Structural Opportunities of ETFE (ethylene tera fluoro ethylene). Masters in Engineering, Massachusetts Institute of Technology.

ROBINSON-GAYLE S., et al. (2001). ETFE foil cushions in roofs and atria. Journal of Construction and Building Materials 15, p 323-327.

TAI NC and Inanici M. "Space Perception and Luminance Contrast: Investigation and Design Applications through Perceptually based Simulations," Spring Simulation Multi-conference, Symposium on Simulation for Architecture and Urban Design (SimAUD2010), Orlando, FL, April 12-15, 2010.

327: Performance assessment of sageglass electronically tintable glazing

DAN JESTICO

Hilson Moran, Shackleton House, 4 Battlebridge Lane, London SE1 2HP,djestico@hilsonmoran.com

SAGE Electrochromics have developed a glass coating which can be controlled electronically to be clear or tinted, reducing solar heat gain and glare in buildings whilst remaining transparent and therefore not blocking views out. The glazing can be controlled in a variety of ways, including integration into the building management system (BMS).

The potential benefits of installing SageGlass electrochromic glazing in office facades for four different European climate zones have been assessed, comparing the performance of SageGlass against a number of typical façade systems for each climate zone. Performance metrics such as energy consumption, CO2 emissions, utility costs, chiller sizing, chiller cost, lettable area impact and façade cost were assessed.

In order to analyse the performance of SageGlass, a control methodology had to be developed and implemented into the DTM software to allow for dynamic switching of the façade states. This algorithm was assumed to be implemented via a BMS to minimise unwanted solar gain during summer, whilst ensuring sufficient daylight was admitted to reduce artificial lighting energy consumption.

Results showed that SageGlass was able to provide performance benefits in the following areas:

- Reduced annual energy consumption, and therefore lower CO2 emissions and utilities costs.

- Optimised daylight penetration through the façade, and control of glare, whilst maintaining thermal comfort conditions and outside views for occupants.

- Removing the need to add external shading devices to control solar gain with no impact on net lettable area.

- Reduced peak cooling demand with similar or lower costs than comparable façade systems.

These benefits were found to be enhanced in warmer climate zones.

Keywords: Facades, smart buildings, solar control, glazing, demand optimisation

1. INTRODUCTION

1.1 Technology

SAGE Electrochromics Inc. have developed a coating which is applied to a single piece of glass that can then be fabricated into a double or triple glazed unit for use in architectural façade systems. The coating is controlled electronically to be clear or tinted, reducing solar heat gain and glare in buildings whilst remaining transparent and therefore not blocking views out. The glazing can be controlled in a variety of ways, including integration into the building management system (BMS). This paper investigates a potential algorithm that could be used to control the glazing states and quantifies the a number of performance benefits from using the glazing in office facades.

By incorporating SageGlass in an architectural double or triple glazed unit, the heat and light transmission of the glass can be controlled to;

- Maintain occupant thermal comfort during periods of high solar gain
- Minimise glare without the need for internal blinds
- Minimise unwanted solar gain, reducing the energy consumed by mechanical cooling systems
- Optimise views out for building occupants

The glass can be tinted to a number of intermediate states and can be controlled either manually or by the BMS. The full table of double and triple glazed unit properties assumed for this study are shown in Table 28.

Table 28: Properties of SageGlass in various tint states

Glass State	Double Glazed Unit (DGU)			Triple Glazed Unit (TGU)		
	Visible Light Transmission (%)	Solar Factor (g-value)	U-value (W/m²K)	Visible Light Transmission (%)	Solar Factor (g-value)	U-value (W/m²K)
Fully tinted	1.1	0.05	1.1	1.0	0.03	0.8
Intermediate #1	6.6	0.07		5.9	0.06	
Intermediate #2	20.0	0.13		18.7	0.12	
Intermediate #3	40.0	0.23		40.0	0.26	
Clear	59.4	0.38		53.5	0.35	

1.2 Methodology

This manuscript presents an analysis of the performance of SageGlass electrochromic coatings applied to the facades of office buildings in four different European climate zones.

- UK and northern Europe (London)
- Central Europe (Frankfurt)
- Southern Europe (Madrid)
- Scandinavia (Copenhagen)

The construction and operation of modern office buildings represents a significant capital expenditure and ongoing operational expenditure. In addition, the CO2 emissions resulting from the operation of buildings is being driven downwards by a combination of building regulations, planning policies and corporate social responsibility policies of occupiers. Design teams are therefore under pressure to reduce operational emissions and operating costs, whilst maximising returns through lettable area without increasing construction costs. The analysis compared the performance of SageGlass against a number of typical façade systems for each climate zone, investigating the effect of utilising SageGlass on;

- The building energy consumption over the course of a year, simulated using dynamic thermal modelling (DTM)
- The CO_2 emissions resulting from the above energy consumption
- The annual cost of utilities related to energy consumption
- The peak cooling demand, used to determine the size of cooling equipment required to condition the building

- The approximate chiller cost
- The available net internal area (NIA) for lettable space, given a basic building footprint and accounting for external shading devices
- The façade cost, based on data provided by SAGE Electrochromics Inc (2013).

DTM has been utilised to assess the different façade options in each of the four climate zones. DTM software dynamically models transient heat gains from conduction, convection and radiation based on external weather conditions. The models consider variation of external conditions on an hour-by-hour basis.

Building element constructions and internal heat gains are used to assess thermal comfort, energy usage and plant sizing.

For this analysis, the DTM software used was Tas, from EDSL. Tas was selected due to the fact that it allows the dynamic switching of building element constructions, essential for investigating the potential for electrochromic glazing. It is also accredited by the UK Government for conducting energy assessment calculations, required by UK Building Regulations.

The DTM software was set up to mimic the behaviour of SageGlass given a typical control algorithm, switching the glass based a on a number of control factors, described in more detail below.

1.3 Model Setup

The building energy model developed for this investigation was based on a consistent office specification across all climate zones. The site footprint measured 30.0m east to west and 60.0m north to south. The office was assumed to be open plan with a net:gross efficiency of 80%, across eight floors, with the core centrally located, giving a total net internal floor area (discounting building core) of 11,520m² (gross area = 14,400m², including building core). Perimeter zones were assumed to be 4.5m deep, with a floor to floor height of 4.0m. The floor to ceiling height was assumed to 3.0m. Facades were modelled as fully glazed with 10% frame giving a total glass area of 3,865 m² and a window to wall ratio of 67%. This configuration represents a typical office design in the climate zones studied. U-values for non-glazed elements are given in Table 29 below.

Table 29: Reference U-values for opaque elements

Element	U-value (W/m²K)
Roof	0.25
Ground floor	0.25
Window frame	3.6
Spandrel	1.1

Internal heat gains were based on those defined by the Building Research Establishment (2013) as follows:

- Lighting: 12 W/m² (400 lux) with daylight dimming and presence detection – 8am – 7pm
- Occupancy: 1 person per 9m² - 8am – 7pm
- Equipment: 12 W/m² - 8am – 7pm

All office spaces were heated to 22°C and cooled to 24°C between the hours of 6am – 7pm, with a setback minimum temperature of 12°C during unoccupied hours, as per the Building Research Establishment (2013) calculation methodology.

For each of the models simulated, automated, BMS controlled daylight dimming was employed for the perimeter office zones, aiming to maintain a minimum internal illuminance level of 400 lux. Artificial lighting levels were varied linearly, depending on the internal illuminance provided by daylight to meet the 400 lux target level. Thus, with daylight providing an internal illuminance of 400 lux the artificial lighting load will be 0.0 W/m² and with daylight providing zero internal illuminance the artificial lighting load will be 12.0 W/m².

In order to convert the heating, cooling and ventilation demand figures to energy consumption metrics, building systems scenarios were assumed that are typical to each of the climate zones. These are given below in Table 30 with system efficiencies provided in

Table 31.

Table 30: System types, and heating and cooling sources

Climate Zone	Space Conditioning	Heating Source	Cooling Source
London	4 pipe fan coil unit	Gas fired boiler	Electric chiller
Frankfurt	Chilled beam	Gas fired boiler	Electric chiller
Madrid	4 pipe fan coil unit	Gas fired boiler	Electric chiller
Copenhagen	Chilled beam	District heating	Electric chiller

Table 31: Mechanical system efficiencies

Climate Zone	Fresh Air Fan SFP (W/l/s)	Extract Fan SFP (W/l/s)	Terminal Fan SFP (W/l/s)	Air-to-Air Heat Exchanger Efficiency	Heating Efficiency	Cooling CoP
London	1.4	0.8	0.3	70%	90%	5.0
Frankfurt	1.4	0.8	n/a	70%	90%	5.0
Madrid	1.4	0.8	0.3	70%	90%	5.0
Copenhagen	1.4	0.8	n/a	70%	100% (at building)	5.0

For each climate zone, the performance of dynamic SageGlass was compared against three alternative façade systems, simulating SageGlass in either a double or triple glazed configuration as appropriate. The reference façade systems were chosen as they represent typical façades selected for high specification office buildings, relevant to each of the climate zones analysed. In some climate zones, solar protection is prioritised to mitigate solar heat gain during summer months. In other zones, reducing heat through the building fabric during winter months will be the priority. Good façade design will address both these factors to minimise year-round energy consumption. A summary of the glass types used for each climate zone is given below in Table 32.

Table 32: Facade types tested for each climate zone

Climate Zone	Glass Type (LT = Light Transmission, g = g-value)				
	DGU, LT = 40%, g = 0.24	DGU, LT = 60%, g = 0.28 + External Shading	Externally Ventilated Facade	TGU, LT = 53%, g = 0.24 + External Shading*	DGU, LT = 17%, g = 0.2 + External Shading
London	✓	✓	✓	✗	✗
Frankfurt	✗	✓	✓	✓	✗
Madrid	✗	✓	✓	✗	✓
Copenhagen	✗	✓	✓	✓	✗

In each case, to ensure that the façade systems were being compared on an equal basis, the thermal comfort performance of the office spaces were assessed using the BS EN ISO 7730:2005 standard (BSI, 2006) to calculate thermal comfort indices of Predicted Mean Vote (PMV) and Percentage People Dissatisfied (PPD). Compliance with this standard was used to determine the type and extent of external shading devices for the relevant reference glazing cases. In each case, the results from the DTM simulations were interrogated to ensure that the PMV was between -0.5 and +0.5 (relating to no more than 10% PPD).

For all reference glazing cases excluding the externally ventilated façade, manually controlled blinds were assumed to be fitted in order to control the impact on occupant glare. The impact of these blinds on building energy consumption was determined by taking the average energy consumption of DTM simulations with all blinds down and all blinds up. This therefore represents a condition where blinds will be in use for 50% of the occupied hours for each of the relevant reference cases. The use of blinds will mitigate some of the solar gain entering the building, reducing cooling energy consumption, but will also significantly reduce the natural daylight penetration through the façade, increasing the energy consumed by artificial lighting. For the externally ventilated façade models, automated cavity blinds were assumed to be in use to both mitigate glare and control solar gain. These were assumed to be controlled in a similar manner to the SageGlass switching methodology, outlined below.

2   CONTROL ALGORITHM

The control algorithm for the SageGlass was assumed to be implemented via a BMS to minimise unwanted solar gain during summer, whilst ensuring sufficient daylight was admitted to reduce artificial lighting energy consumption. During heating seasons, the use of passive solar gain to offset heating energy consumption was also maximised. Again, models were checked according to BS EN ISO 7730:2005 (BSI, 2006) to ensure thermal comfort was maintained for all climate zones. The 1.5m x 3.0m façade module was assumed to be split vertically into three 1.5m x 1.0m panels, each panel individually addressable by the BMS. Typically, the three adjustable zones are accommodated on a single piece of glass.

Although each façade was assumed to be treated identically, the modulation of the panels follows the same algorithm, dependent on the following factors:

- Heating/cooling season
- Solar azimuth
- Solar altitude
- Solar intensity
- External illuminance
- Building occupancy
- Internal illuminance

These factors were addressed using the control algorithm described below to determine whether the glazing is in Glare or Daylight mode. Glare mode is intended to minimise unwanted solar gain, maintain occupant thermal comfort, control glare and minimise cooling energy consumption. Daylight mode aims to optimise the daylight admitted through the façade to reduce artificial lighting consumption, without admitting excessive amounts of solar gain. A flow chart describing the control algorithm is shown in Figure 40.
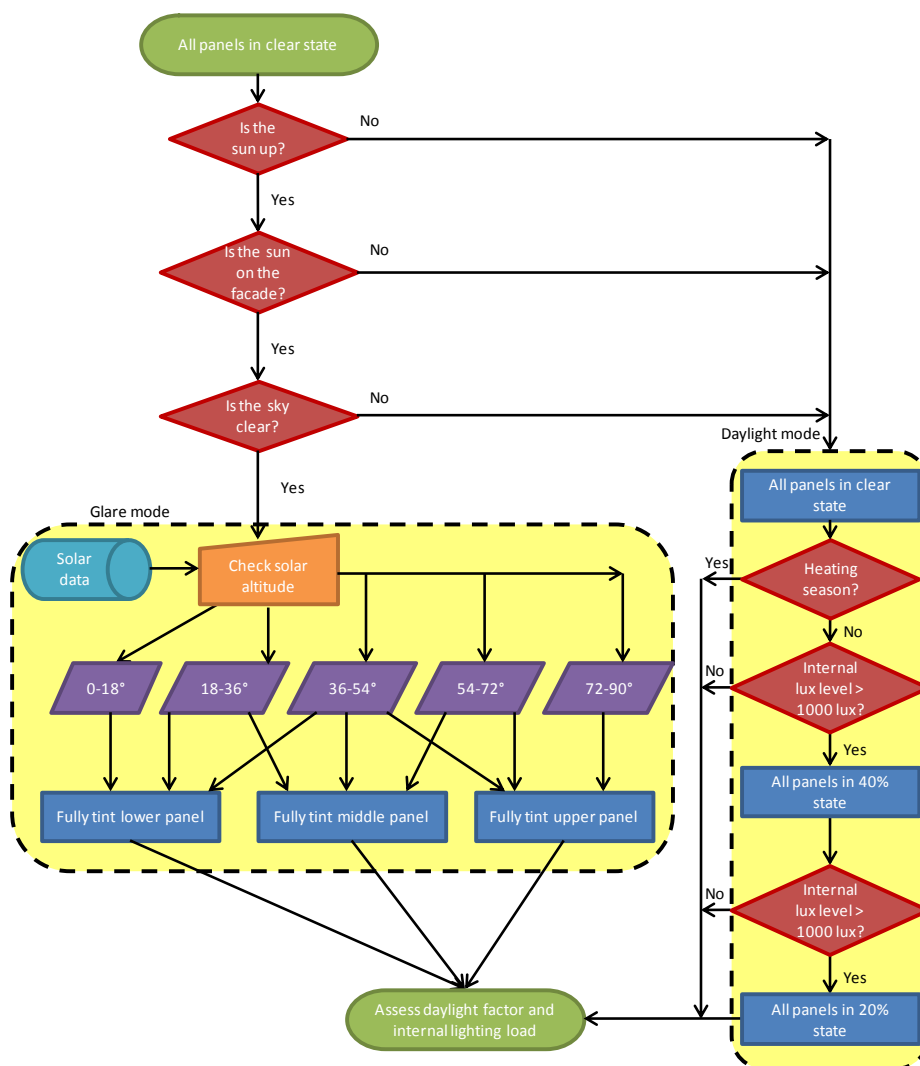

Figure 40: SageGlass control algorithm

This flow chart can be explained as follows:

- The algorithm checks the solar altitude to see if the sun is above the horizon. If not, the panels will be in a clear state to maximise views out.
- The algorithm checks the solar azimuth and cloud cover to see if the sun is shining on the building façade. If not, the panels are in Daylight mode.

SUSTAINABLE CITIES & ENVIRONMENT

- If the panels are in Daylight mode, the algorithm checks to see if the building is in heating mode. The heating season will be different for each climate zone and will need adaptation and refinement of the control algorithm to select suitable times of the year and day. If the building is in heating mode, all panels are set to a clear state to benefit from passive solar heat gain.
- If the panels are in daylight mode and the building is not in heating mode, they will be modulated to be as clear as possible to allow daylight into the building, without admitting excessive amounts of solar gain. If the internal illuminance from daylight is above 1,000 lux, all panels are switched from the clear state to a semi-tinted state, with a light transmission of 40%. The internal illuminance is then reassessed with the new glazing light transmission. If it is still greater than 1,000 lux, the panels are further tinted to a state with 20% light transmission. Analysis showed that tinting the glazing to states with a light transmission of less than 20% was likely to provide low levels of daylight and would hence require additional artificial lighting.
- If the sun is up and is shining on the building façade, the façade will be in Glare mode. Individual panels will then be fully tinted, depending on the height of the sun, to protect occupants against glare, whilst providing some daylight penetration to reduce artificial lighting levels. Again, the full Glare mode control strategy may be climate zone and façade design dependent, and may require further optimisation based on individual building design.
- Once the façade panel states have been determined in either Glare or Daylight mode, the algorithm then determines the overall façade light transmission figure and related internal lighting load required to meet the target internal illuminance of 400 lux.

3   RESULTS

As stated above, dynamic thermal models were simulated for SageGlass and the reference glazing cases for each climate zone. The results from these models were processed to obtain energy consumption figures using efficiencies for the typical mechanical systems in Table 30. Results were generated for the main contributors to building energy consumption affected by facade design;

- Heating
- Cooling
- Auxiliary (fans & pumps)
- Lighting

The energy consumption data has been converted into carbon dioxide emissions using conversion factors obtained from the UK Department of Energy and Climate Change (2012), International Energy Agency (2012) and Danish Energy Agency (2010). The conversion factors are listed in Table 33.

Table 33: Carbon dioxide conversion factors

Climate Zone	Heating (kgCO$_2$/kWh)	Cooling (kgCO$_2$/kWh)	Auxiliary (kgCO$_2$/kWh)	Lighting (kgCO$_2$/kWh)
London	0.204 (Natural gas)	0.457 (Electricity)	0.457 (Electricity)	0.457 (Electricity)
Frankfurt	0.204 (Natural gas)	0.461 (Electricity)	0.461 (Electricity)	0.461 (Electricity)
Madrid	0.204 (Natural gas)	0.238 (Electricity)	0.238 (Electricity)	0.238 (Electricity)
Copenhagen	0.122 (District heating)	0.360 (Electricity)	0.360 (Electricity)	0.360 (Electricity)

Energy consumption figures have also been converted into annual utilities costs by applying prices from Eurostat (2014) and HOFOR (2015) (Table 34), excluding VAT and other recoverable taxes and levies.

Table 34: Energy cost data

Climate Zone	Heating (€/kWh)	Electricity (€/kWh)
London	0.028	0.104
Frankfurt	0.050	0.124
Madrid	0.033	0.116
Copenhagen	0.060	0.093

In addition, the peak cooling loads were calculated to compare the size of cooling equipment required in each case. These have been converted into approximate chiller capital cost using the Aecom (2013) cost data factor of £235 per kW of cooling capacity (€279.65 per kW). This cost covers a high efficiency air cooled R134a refrigerant chiller including control panel, anti-vibration mountings, plantroom pipework, valves, insulation, pumps and pressurisation units. This cost also includes installation and commissioning costs. Costs related to terminal units and associated distribution systems outside of the building plant room have not been included.

Calculations were also undertaken to determine the effect of the glazing modelled on the net internal area (NIA) of the building, given an identical site footprint in each case. Buildings requiring high levels of external shading would therefore detract from the amount of potential lettable NIA offered by the site, assuming the external shading was not permitted to oversail the site boundary.

Using the external area of the façade and the costs provided by SAGE Electrochromics Inc (2013) and (2015) (Table 35), the total façade costs for each of the cases modelled has been calculated and compared. Façade costs include installation and the additional cost of internal blinds in cases without glare protection. Maintenance and cleaning costs have not been included.

Table 35: Facade cost data

Climate Zone	SageGlass DGU	SageGlass TGU	DGU, LT = 40%, g = 0.24	DGU, LT = 60%, g = 0.28 + External Shading	Externally Ventilated Facade	TGU, LT = 53%, g = 0.24 + External Shading*	DGU, LT = 17%, g = 0.2 + External Shading
London	€614.04	n/a	€470.05	€678.30	€1,190.00	n/a	n/a
Frankfurt	€614.04	€733.04	n/a	€678.30	€1,190.00	€761.60	n/a
Madrid	€614.04	n/a	n/a	€708.05	€1,190.00	n/a	€690.20
Copenhagen	€614.04	€733.04	n/a	€678.30	€1,190.00	€761.60	n/a

Table 36 below compares the annual energy consumption results for heating, cooling auxiliary and lighting across climate zones and facade types.

Table 36: Annual energy consumption comparison

	Annual Energy Consumption (kWh/m²)											
	SageGlass DGU	DGU, LT = 40%, g = 0.24	DGU Delta (%)	DGU, LT = 60%, g = 0.28 + external shading	DGU Delta (%)	DGU, LT = 17%, g = 0.2 + external shading	DGU Delta (%)	Externally ventilated facade	DGU Delta (%)	SageGlass TGU	TGU, LT = 53%, g = 0.24 + external shading	TGU Delta (%)
London	49.57	58.34	18%	56.27	14%			52.19	5%			
Frankfurt	66.75			70.03	5%			70.58	6%	59.37	63.17	6%
Madrid	57.85			64.33	11%	68.26	18%	62.47	8%			
Copenhagen	65.56			68.52	5%			69.73	6%	59.27	64.80	9%

Table 37 below compares the annual carbon dioxide emissions resulting from the consumption data given in Table 36 across climate zones and facade types.

Table 37: Annual carbon dioxide emissions comparison

	Annual Carbon Dioxide Emissions (kgCO$_2$/m²)											
	SageGlass DGU	DGU, LT = 40%, g = 0.24	DGU Delta (%)	DGU, LT = 60%, g = 0.28 + external shading	DGU Delta (%)	DGU, LT = 17%, g = 0.2 + external shading	DGU Delta (%)	Externally ventilated facade	DGU Delta (%)	SageGlass TGU	TGU, LT = 53%, g = 0.24 + external shading	TGU Delta (%)
London	19.90	23.84	20%	23.10	16%			21.18	6%			
Frankfurt	22.77			25.11	10%			24.25	7%	21.34	23.68	11%
Madrid	13.44			15.01	12%	15.88	18%	14.54	8%			
Copenhagen	16.47			18.38	12%			17.69	7%	15.77	17.90	14%

Table 38 below compares the annual utilities costs resulting from the consumption data given in Table 36 across climate zones and facade types.

Table 38: Annual utilities cost comparison

	Annual Utilities Cost (€/m²)										
	Sage Glass DGU	DGU, LT = 40%, g = 0.24	DGU Delta (%)	DGU, LT = 60%, g = 0.28 + external shading	DGU Delta (%)	DGU, LT = 17%, g = 0.2 + external shading	DGU Delta (%)	Externally ventilated facade	DGU Delta (%)	Sage Glass TGU	TGU, LT = 53%, g = 0.24 + external shading	TGU Delta (%)
London	49,290	59,438	21%	57,696	17%			52,681	7%			
Frankfurt	68,033			75,370	11%			72,513	7%	64,073	71,381	11%
Madrid	67,360			76,588	14%	80,022	19%	73,487	9%			
Copenhagen	58,184			62,647	8%			62,156	7%	53,985	60,060	11%

Table 39 below compares the peak cooling demand used to size chillers across climate zones and facade types.

Table 39: Peak cooling demand comparison

	Peak Cooling Demand (kW)										
	SageGlass DGU	DGU, LT = 40%, g = 0.24	DGU Delta (%)	DGU, LT = 60%, g = 0.28 + external shading	DGU Delta (%)	DGU, LT = 17%, g = 0.2 + external shading	DGU Delta (%)	Externally ventilated facade	DGU Delta (%)	SageGlass TGU	TGU, LT = 53%, g = 0.24 + external shading	TGU Delta (%)
London	399.5	470.1	18%	453.5	14%			436.8	9%			
Frankfurt	424.3			463.4	9%			466.9	10%	419.7	461.1	10%
Madrid	527.9			537.6	2%	555.2	5%	586.1	11%			
Copenhagen	374.0			427.5	14%			426.7	14%	351.9	430.8	22%

Table 40 below compares the cost of chillers and associated equipment resulting from the chiller sizes calculated in Table 39 across climate zones and facade types.

Table 40: Chiller cost comparison

	Chiller Cost (€)										
	Sage Glass DGU	DGU, LT = 40%, g = 0.24	DGU Delta (%)	DGU, LT = 60%, g = 0.28 + external shading	DGU Delta (%)	DGU, LT = 17%, g = 0.2 + external shading	DGU Delta (%)	Externally ventilated facade	DGU Delta (%)	Sage Glass TGU	TGU, LT = 53%, g = 0.24 + external shading	TGU Delta (%)
London	111,729	131,464	18%	126,814	14%			122,140	9%			
Frankfurt	118,649			129,582	9%			130,579	10%	117,358	128,961	10%
Madrid	147,623			150,339	2%	155,265	5%	163,904	11%			
Copenhagen	104,586			119,564	14%			119,334	14%	98,401	120,472	22%

Table 41 below compares the building net internal area across climate zones and facade types.

Table 41: Net internal area comparison

	Net Internal Area (m²)										
	Sage Glass DGU	DGU, LT = 40%, g = 0.24	DGU Delta (%)	DGU, LT = 60%, g = 0.28 +	DGU Delta (%)	DGU, LT = 17%, g = 0.2 +	DGU Delta (%)	Externally ventilated facade	DGU Delta (%)	Sage Glass TGU	TGU, LT = 53%, g = 0.24 +	TGU Delta (%)

				external shading		external shading						external shading	
London	11,520	11,520	0%	10,666	-7%			10,950	-5%				
Frankfurt	11,520			10,666	-7%			10,950	-5%	11,520	10,856	-6%	
Madrid	11,520			11,329	-2%	11,329	-2%	10,950	-5%				
Copenhagen	11,520			10,967	-5%			10,950	-5%	11,520	10,967	-5%	

Table 42 below compares the building facade cost across climate zones and facade types.

Table 42: Facade cost comparison

Net Internal Area (m²)											
	Sage Glass DGU	DGU, LT = 40%, g = 0.24	DGU Delta (%)	DGU, LT = 60%, g = 0.28 + external shading	DGU Delta (%)	DGU, LT = 17%, g = 0.2 + external shading	DGU Delta (%)	Externally ventilated facade	DGU Delta (%)	Sage Glass TGU	TGU, LT = 53%, g = 0.24 + external shading	TGU Delta (%)
London	2,373,265	1,816,743	-23%	2,621,630	10%			4,599,350	94%			
Frankfurt	2,373,265			2,621,630	10%			4,599,350	94%	2,833,200	2,943,584	4%
Madrid	2,373,265			2,736,613	15%	2,667,623	12%	4,599,350	94%			
Copenhagen	2,373,265			2,621,630	10%			4,599,350	94%	2,833,200	2,943,584	4%

4 CONCLUSIONS

The results presented above show that SageGlass is able to offer significant performance benefits in a number of areas. Across all climate zones investigated, the analysis demonstrates the following:

- SageGlass has been shown to be able to reduce lighting and cooling energy consumption by the use of dynamic switching of façade states. This optimises daylight penetration through the façade without admitting unwanted solar gain in summer, whilst making use of passive solar gain in winter.
- SageGlass is therefore able to offer reduced annual energy consumption, and therefore lower CO_2 emissions and utilities costs. This will provide benefits in terms of regulatory compliance and improved ratings in certification schemes such as BREEAM and LEED. The comparable facade systems analysed above showed up to 18% higher consumption for the tested variables of heating, cooling, auxiliary and lighting energy. When translated into CO_2 emissions and utilities costs, traditional facade systems were found to be up to 20% and 21% higher than the comparable SageGlass system respectively.
- The dynamic switching is able to control glare, eliminating the need and subsequent cost of internal blinds, whilst maintaining thermal comfort conditions for occupants.
- This also maintains outside views for building occupants.
- The use of SageGlass removes the need to add external shading devices to control solar gain which can impact the architectural intent of a building, as well as reduce the amount of valuable floor space available for occupants. Depending on the facade system selected, utilising external shading systems can give up to 7% less net lettable area which will significantly impact a developer's financial returns.
- By employing SageGlass, the peak cooling demand can be reduced. This leads on to smaller cooling plant requirements, taking up less space and reducing the capital expenditure on mechanical systems. Peak cooling demand (and hence chiller capital cost) can be up to 22% higher for traditional facade systems.
- Although the cost of SageGlass is higher than the equivalent solar control glass, once internal blinds have been added for glare control and external shading added to meet thermal comfort limits, the cost of the typical facade systems increase to a figure 10-15% higher than the SageGlass system for DGUs and 4% higher for TGUs. The costs of externally ventilated façade systems have been shown to be nearly twice as high as SageGlass, for similar levels of energy performance.
- SageGlass façade systems have been shown to provide performance benefits in all climate zones analysed. However, in warmer climates, where cooling and lighting energy form the majority of the building energy usage profile, these benefits are even more significant. For the externally ventilated facade reference case, tested for all climate zones, the externally ventilated facade showed an 8% increase in energy consumption over the SageGlass DGU for the Madrid climate zone, compared with only 6% for the Copenhagen climate zone.

SUSTAINABLE CITIES & ENVIRONMENT

5   REFERENCES

Building Research Establishment (2013) National Calculation Method [online]. Available at: http://www.ncm.bre.co.uk/ [Accessed 27 May 2015]

British Standards Institute (BSI) (2006) BS EN ISO 7730:2005. Ergonomics of the thermal environment. Analytical determination and interpretation of thermal comfort using calculation of the PMV and PPD indices and local thermal comfort criteria. London: BSI.

Department for Energy and Climate Change (2012) 2012 Guidelines to Defra / DECC's GHG Conversion Factors for Company Reporting [online]. Available at: https://www.gov.uk/government/uploads/system/uploads/attachment_data/file/69554/pb13773-ghg-conversion-factors-2012.pdf [Accessed 27 May 2015]

International Energy Agency (IEA) (2012) CO2 Emissions From Fuel Combustion Highlights [online]. Available at: http://www.iea.org/publications/freepublications/publication/CO2emissionfromfuelcombustionHIGHLIGHTS.pdf [Accessed 27 May 2015]

Danish Energy Agency (2010) Danish Key Figures [online]. Available at http://www.ens.dk/en/info/facts-figures/key-figures/danish-key-figures [Accessed 27 May 2015]

Eurostat (2014) Energy Price Statistics [online]. Available at http://ec.europa.eu/eurostat/statistics-explained/index.php/Energy_price_statistics [Accessed June 2013]

HOFOR (2015) Prisen på fjernvarme 2015 [online]. Available at http://www.hofor.dk/fjernvarme/prisen-paa-fjernvarme-2015/ [Accessed June 2013]

Aecom (2013) SPONS 2013 Mechanical and Electrical Services Price Book. London: CRC Press

SAGE Electrochromics Inc. (2013) Private communication

SAGE Electrochromics Inc. (2015) Private communication

SUSTAINABLE CITIES & ENVIRONMENT

5   REFERENCES

135: High capacity energy efficiency solar glass

CHIN-HUAI YOUNG[1], SAFFA RIFFAT[2], ERDEM CUCE[3]

1 Marie Curie Fellow, University of Nottingham, chin-huai.young@nottingham.ac.uk
2 Professor, University of Nottingham, saffa.riffat@nottingham.ac.uk
3   Research fellow, University of Nottingham, laxec5@nottingham.ac.uk

A kind of high capacity energy efficiency solar glass developed for zero energy buildings is introduced in this paper. The glass called Heat Insulation Solar Glass (HISG) can generate solar power as well as decrease energy consumption to reach a target of highest energy efficiency capacity. According to a real testing of glass house, the HISG can generate high solar power and save energy consumption of cooling and heating system. All the solar power generation from HISG can supply all the energy consumption of cooling and heating system all year and still have remaining power to supply another energy consumption of a building. Compared with all the other energy efficiency glass, the HISG is a kind of highest energy efficiency solar glass in the world for the application on the zero energy buildings and low carbon buildings

Keywords: solar glass, insulation, energy efficiency, zero energy buildings, low carbon buildings

1. INTRODUCTION

Zero Energy Buildings (ZEB) is a kind of highest ideal for energy efficiency buildings due to no extra power is needed from grid to supply the energy consumption inside the buildings. It requires both reducing the energy consumption and supplying enough renewable energy. A kind of Heat Insulation Solar Glass (HISG) is introduced here to help reach the target of ZEB due to it can both generate high solar power and reduce the energy consumption of cooling and heating system. According to a real testing of glass house, the HISG glass house generated 686 kWh of solar power and only consumed 317 kWh of cooling and heating system and remained 369 kWh power to supply other electric facilities during 265 days. A simulation for the energy efficiency of a large area HISG skylight was performed to show it capacity on energy efficiency on a real building.

4 MECHANISM OF HISG

Fig. 1 shows the structure of the HISG. It indicates that the reflection layer at the back of solar thin film can reflect back the IR to increase the solar power up to 10% and reduce the IR penetration to obtain a good heat insulation during the summer time. In additions, two air spaces on both sides of reflection layer can reduce the U value to save heating consumption during the winter time.
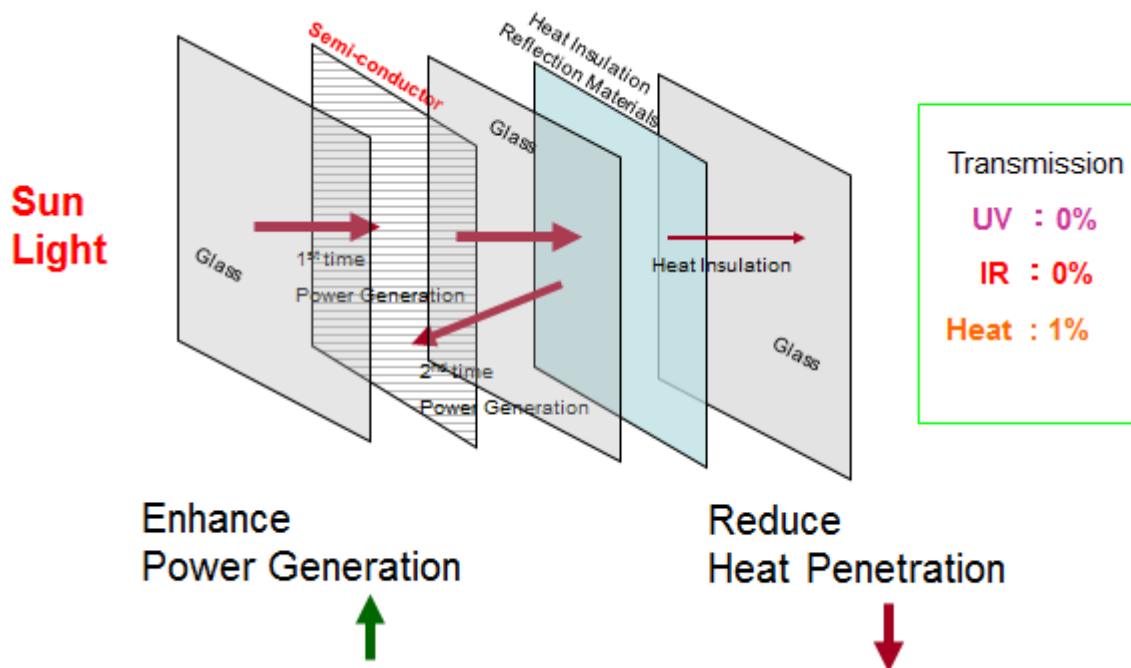

Figure 1: Structure of HISG

5 GLASS HOUSE TESTING

Two glass houses testing was performed in National Taiwan University of Science & Technology to monitor the energy efficiency difference between normal glass house and HISG glass house as shown in Fig.2. Twenty pieces of glass of 110 cm x 140 cm size was built up on each glass house with a dimension of W2.5m x D3 m x H3m. Solar power generation on roof, east, west, south and north vertical sides on HISG glass house was recorded automatically to compare the solar power generation on each directions. As well, the energy consumption on cooling and heating system was also recorded automatically under a setting of 26 ℃ for cooling system and 20 ℃ for heating system. The cooling system turned on automatically while the room temperature was above 26℃ and the heating system turned on automatically while the room temperature was below 20℃.

Figure 2: Glass house testing

6 TESTING RESULT AND DISCUSSION

4.1 Insulation test of glass

A testing of the insulation properties of both glass was shown in Table 1. The HISG possesses lower SC and U value. It indicates HISG can achieve better heat insulation both during summer and winter time.

Table 43: Insulation testing of ordinary glass and HISG

Glass types	SC	U (W / m²k)
HISG	0.155	1.757
Ordinary glass (10 mm)	0.929	5.935

3.3 Energy efficiency of glass house

Fig. 3 shows the ordinary glass house consumed 587 kWh on cooling and heating system during 265 days testing. Meanwhile, the HISG glass house generated 686 kWh of solar power and only consumed 317 kWh of cooling and heating system and then remained 369 kWh power to supply other electric facilities. The test indicated an exciting result to encourage a hope to reach the target of zero energy buildings if the HISG could be applied on the buildings as a construction material due to it can generate enough solar power and save more energy consumption on the cooling and heating system.
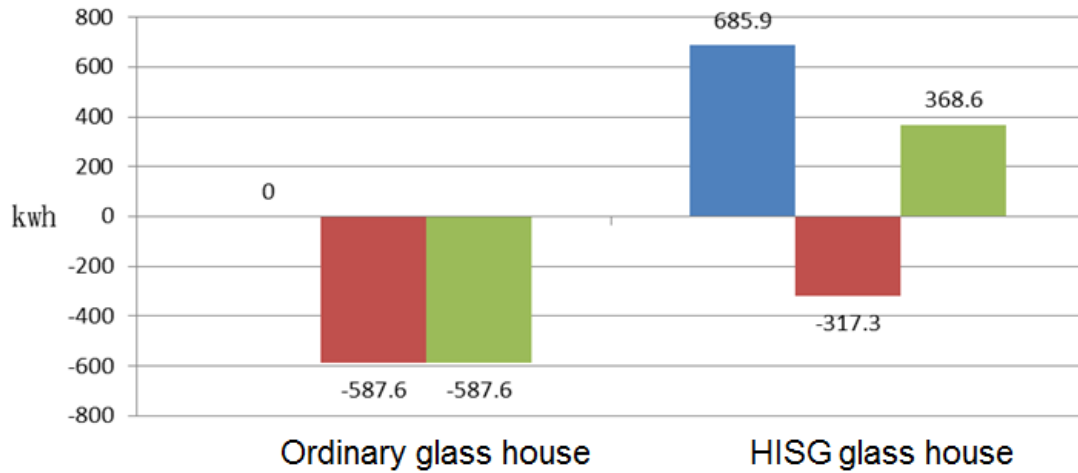
Figure 3: Energy efficiency of glass house

3.4 Shading effect

The indoor shading effect of these two glass houses was also taken into consideration in this test. Fig. 4 shows the indoor visible light comparison of these two glass house. It indicated the HISG house possessed a more comfortable indoors visible light while the ordinary glass house with a too high visible light. Fig.5 shows the HISG house performed a zero UV penetration all day to prevent the damage to human and furniture.
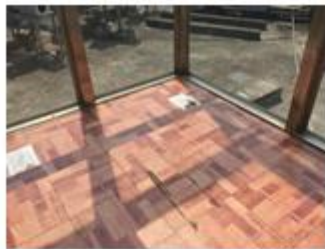
Ordinary glass house indoors
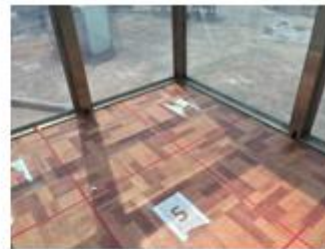
HISG glass house indoors

Figure 4: Indoors visible light comparison

Time	9:00	10:00	11:00	12:00	13:00	14:00	15:00	16:00	17:00	18:00
Outdoors	895	2870	4480	5270	5090	3460	2020	976	446	83
Normal glass indoors	394	1161	1453	1363	1346	630	352	195	112	14
PV insulation glazing indoors	0	0	0	0	0	0	0	0	0	0

Ordinary glass house indoors   HISG glass house indoors

Figure 5: Indoors UV light comparison

4   ENERGY EFFICIENCY SIMULATION FOR REAL APPLICATION

In order to realize the energy efficiency of HISG applied on a real building of skylight with area of 660 square meters and 5 meter high as shown in Fig.6 , a simulation of solar power generation and energy consumption was performed based on the testing result of glass house and insulation parameters. Fig. 7 shows the simulation result of EUI among ordinary glass, Low-e glass and HISG in Tainan Taiwan. The definition of EUI (Energy Usage Intensity) is the energy needed from grid by kWh per square meter in one year. It indicated the EUI were 460, 219 and 69 respectively. The EUI of HISG skylight was only 1/6 of ordinary glass due to it can generate solar power and reduce the energy consumption of cooling and heating system.

Figure 6: Energy efficiency simulation of skylight
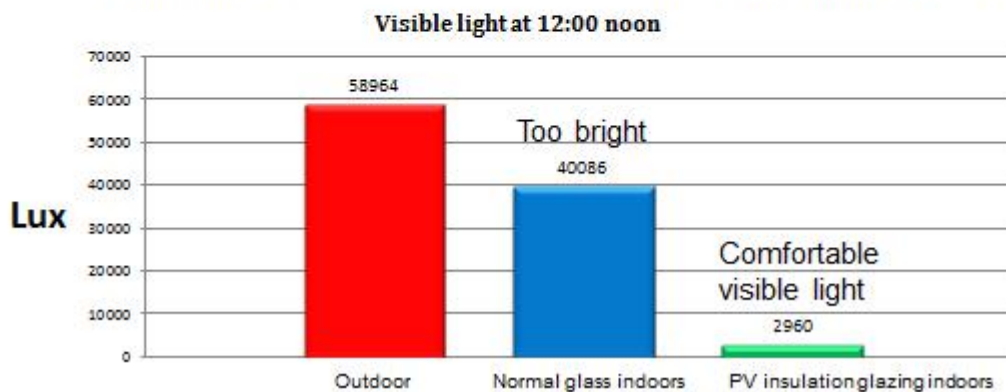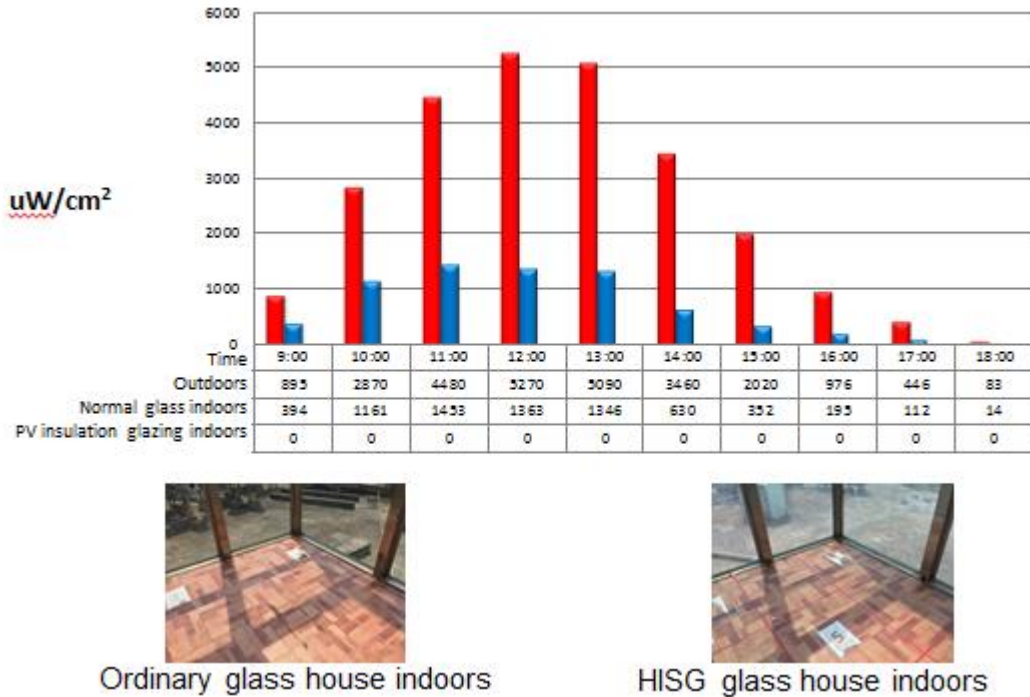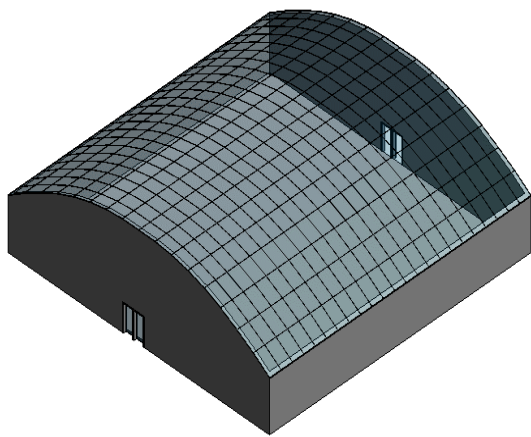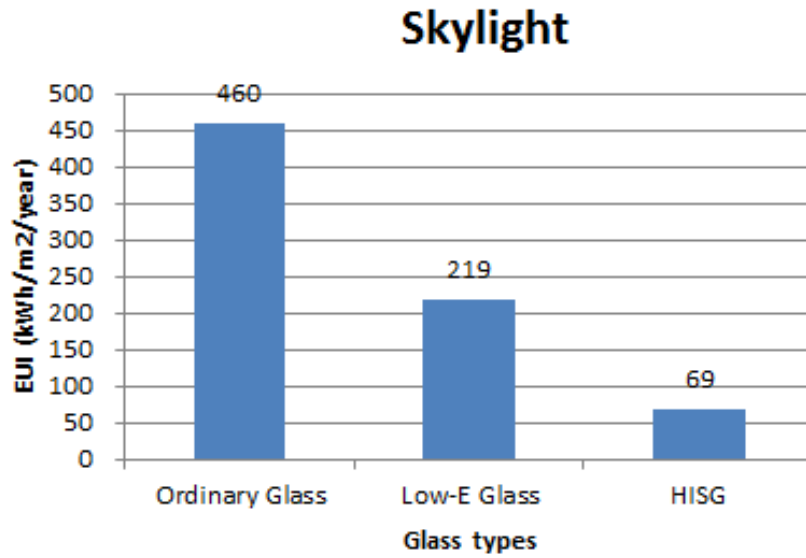
Figure 7: Energy efficiency simulation result of skylight

5   CONCLUSION

The HISG can both generate higher solar power and reduce the energy consumption of cooling and heating system. It can be applied on designing zero energy buildings. In additions, the HISG also possesses a comfortable indoor visible light environment and zero UV penetration.

6   REFERENCES

YOUNG, Chin-Huai, Chen Yi-Lin and Chen, Po-Chun, 2014 "Heat Insulation Solar Glass and Application on Energy Efficiency Buildings", Energy and Buildings, Vol. 78, pp. 66-78.

CUCE, Erdem, Young Chin-Huai, Riffat Saffa B. 2014Performance investigation of heat insulation solar glass for low carbon buildings. Energy Conversion and Management, Vol. 88, pp.834-841.

CUCE, Erdem, Young Chin-Huai, Riffat Saffa B., 2015 "Thermal performance investigation of heat insulation solar glass: A comparative experimental study", Energy and Buildings, Vol. 86, ,pp.595-600.

SESSION 28: ENERGY EFFICIENCY IN BUILDINGS

48: Simulation and parametric analysis of an office building energy performance under Danish conditions

MUHYIDDINE JRADI[1*], ANE ZORROZUA GAMBOA[1], AND CHRISTIAN VEJE[1]

1 Center for Energy Informatics, The Maersk Mc-Kinney Moller Institute, University of Southern Denmark, 5230 Odense M, Denmark
* Corresponding author: Email: mjr@mmmi.sdu.dk

Buildings in Denmark contribute to a large portion of the total energy consumption in the form of heating, ventilation and lighting. Therefore, improving the efficiency of the energy production and supply systems and enhancing the energy performance of buildings is indispensable to meet the ambitious Danish energy objectives. The current study provides an overall analysis of the energy performance of the Maersk office building located at the Odense Campus of the University of Southern Denmark, aiming to reduce the energy consumption and improve the overall energy performance. Energy Plus was employed to model the building and simulate the overall energy performance under the Danish conditions taking into account the construction topology, building envelope properties, HVAC systems, weather conditions and occupants behaviour. The 3D model of the building is created with Google Sketchup including 110 thermal zones, and Open Studio tool was used to establish the link between the 3D model and the Energy Plus simulation engine.

Using the developed holistic energy model, an overall energy simulation for the Maersk office building was performed showing that the heating energy accounts for about 50% of the overall consumption while the other half is used in the form of electricity mostly for lighting, electric equipment and ventilation. A parametric study was carried out to assess the effect of various factors on the building overall energy consumption including the construction material, insulation, windows design and lighting, and various suggestions were provided. It was shown that replacing halogen lights in the corridors with LED lights would bring an energy saving of 144 GJ per year. In addition, using triple pane windows instead of the current double pane windows would save 60 GJ on district heating. In addition, various building envelope configurations were suggested so that the building envelope would comply with the Danish BR 10 regulation for existing buildings.

Keywords: Energy Simulation, Parametric Analysis, Office Building, Energy Plus, Danish Building Regulation

1. INTRODUCTION

The breakdown of the global final energy consumption by sector is depicted in Figure 1, showing that the Buildings sector is the leading sector contributing to about 35% of the overall final energy use and it is expected that the energy consumption in the buildings sector will increase by 50% by 2050 (Houssin & LaFrance, 2013). At the EU level, buildings contribute to about 40% of the overall energy consumption and 36% of the CO_2 emissions (Williams, 2011). Based on the EU numbers, 5% to 6% reduction on the energy consumption in the EU countries could be achieved by improving the energy efficiency of buildings in addition to lowering the CO_2 emissions by about 5%. Thus special consideration has been given to improving the overall energy performance of buildings through enhancing energy efficiency of various systems, increase the share of renewable and alternative energy resources and improve the control and optimization strategies (Broin et al., 2013; Ignjatović, Popović, & Kavran, 2015; Wong et al., 2015; Curtis & Pentecost, 2015). In this context, the 2010 Energy Performance of Buildings Directive has indicated that all new buildings in the EU countries must be nearly zero energy buildings by December 2020 (European Commission 2010), where the 2012 Energy Efficiency Directive stressed that EU countries must make energy efficient renovations to at least 3% of buildings owned and occupied by central government (European Commission 2012). This adds to the European Council ambitious energy and climate change plan to reduce greenhouse gas emissions by 20% by 2020 giving special attention to the role of buildings energy performance to achieve this goal (European Commission 2011).
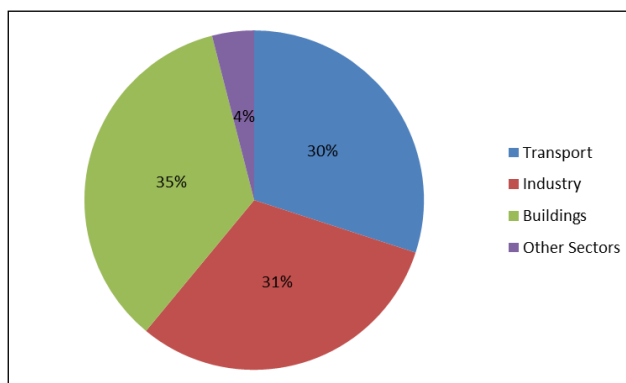

Figure 41: Breakdown of the global final energy consumption by sector (Houssin & LaFrance 2013)

Denmark is one of the most active countries in the EU in terms of improving energy efficiency in Buildings and integrating renewable energy resources in the overall energy production scheme (Lund & Mathiesen, 2009; Kwon & Østergaard, 2012). Denmark's long-term energy goal is to become completely independent of fossil fuel by 2050 (IEA 2011), using 100% renewable energy in the energy and transport sectors. In addition, the Danish building-directive aims at a 75% reduction in energy consumption for new buildings in 2020 relative to 2006 levels (Danish Building & Property Agency, 2011). Regarding the Building standards, the Danish Building Regulations BR10 came into action on 1 January 2011 (PAROC), providing an improvement of 25%, compared to BR08, on the overall building energy performance and insulation requirements for components and building elements. In addition, a low energy building class is included in the BR10 regulation called 'class 2015', and an additional more strict building class 2020 was introduced demanding additional requirements related to documentation. A building is considered to fulfil the requirements of BR10 regulation if the annual overall energy demand, in KWh/m^2 heated floor area, covering heat loss, ventilation, cooling, domestic hot water and lighting does not exceed the numbers in Table 1.

Table 44: Danish Building Energy Regulations (PAROC)

Energy performance framework (kWh/m2 floor area per year)	Dwellings	Other buildings
BR10	52,5 + 1650/A	71,3 + 1650/A
Lavenergiklasse 2015	30 + 1000/A	41 + 1000/A
Bygningsklasse 2020	20	25

With the importance of the energy performance of new and existing buildings in achieving the ambitious Danish energy goals and taking into account the Danish building regulations, the current study presents an overall

analysis of the energy performance of an office building case study in Denmark aiming to decrease the energy consumption and improve the overall energy performance. A holistic energy model for the building will be developed taking into account the construction topology, thermal properties, building systems, weather conditions and occupant behaviour. Using the energy model, the overall energy performance of the considered building case study will be carried out and a parametric study will be conducted to investigate the effect of different model parameters aiming to optimize the building energy performance. This work will serve as a preliminary phase aiding the decision to retrofit the existing office buildings.

2 MODELING AND SIMULATION METHODOLOGY

In the last few decades, several tools were developed to model and simulate the overall energy performance of buildings. Woloszyn & Rode (2008) have provided a detailed description of the major energy simulation tools developed recently comparing their characteristics and specifications. TRNSYS, EnergyPlus, Clim2000 and SimPARK are only a few examples of these simulation tools. In order to run a complete and accurate simulation of the building energy performance, a detailed energy model should be developed providing accurate information about the building including but not limited to: location and orientation, building geometry, envelope properties, climatic conditions, rooms type, HVAC systems, building services and equipment, schedules and occupants behaviour.

In this work, EnergyPlus was used to develop the detailed building model and simulate the overall energy performance of the building. EnergyPlus is a building performance simulation tool combining the best features of BLAST and DOE-2, adding some innovative simulation features and a modular structure for input and output data. EnergyPlus uses the nodal approach to solve the energy conservation equation employing simplified heat resistors and capacitors and assuming that each zone of the building has a homogeneous volume characterized by uniform state variables. EnergyPlus is free, easy to be downloaded, has powerful and validated modelling and simulation engine with a modular structure allowing friendly interface employing other sub-tools. Some drawbacks of EnergyPlus include the limitation of only 4-sided thermal zones and limited flexibility in changing the state variables for the room major parameters including temperatures.

In overall, modelling and simulation of the office building will be carried out using EnergyPlus aided by two supporting tools listed below:

- **Sketchup Pro:** It is a 3D modelling software that can be used to create 3D models of buildings. It was used in the research to create the 3D model of the building providing accurate description of the building geometry and orientation including the detailed rooms, spaces and zones.
- **OpenStudio:** It is an EnergyPlus plug-in for Google Sketchup. Compared to the actual EnergyPlus interface, OpenStudio provides a more friendly and flexible interface allowing the detailed development of the building energy model and the accurate definition of different parameters and inputs.

The block diagram presented in Figure 2 summarizes the modelling and simulation process adopted in this work spread over three main phases.

The modelling and simulation process comprises the following steps:

- **Study of the building:** Information about the weather conditions, building location, orientation and geometry, construction characteristics, zones and spaces of the building will be described in this section.
- **3D model design:** Using the building general characteristics and specifications provided in the previous step, the 3D model of the building will be developed using Google Sketchup.
- **Definition of characteristics:** Different parameters and characteristics of the energy model are defined using OpenStudio including room types, thermal zones, construction materials, building envelope, HVAC system specifications, loads, equipment and schedules.
- **Simulation results:** Using the detailed building energy model developed in OpenStudio, a complete simulation will be carried out using the EnergyPlus engine. The simulation results obtained are documented and analysed.
- **Improvements and suggestions:** Based on the energy performance simulation results obtained, possible improvements are suggested to enhance the overall building energy performance.
- **New 3D model:** Modifications of the 3D model will be considered in Google Sketchup based on the improvements suggested,
- **New Characteristics:** Changes and modifications in the model characteristics are implemented in OpenStudio.

- **Updated improvement results:** The new model will be simulated in EnergyPlus and the results will be analysed and discussed.
- **Comparison of the results obtained:** In this last step, results obtained based on the various improvements are compared with the simulation results of the basic model to optimize the overall energy performance of the building and to decide on the best techniques and measures to be implemented.
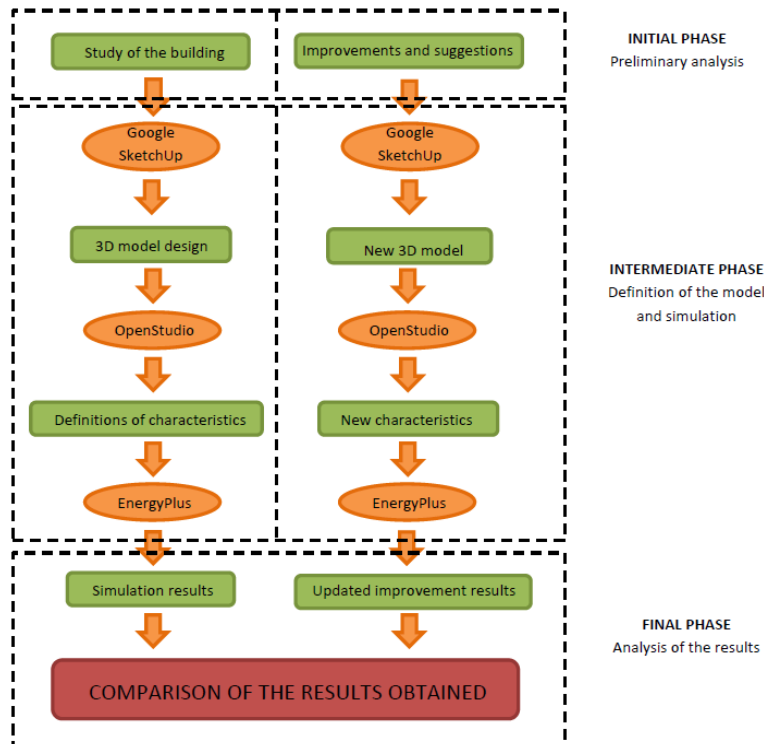

Figure 2: Modelling and simulation process block diagram

3   CASE STUDY: MAERSK OFFICE BUILDING

A case study of an office building in Denmark is considered in this work and the modelling and simulation methodology illustrated in the previous section will be implemented to develop a holistic energy model for the building and carry on a complete analysis of the energy performance aiming to reduce the consumption and improve the building energy efficiency. The building considered is the Maersk Office Building located at the Odense Campus of the University of Southern Denmark, shown in the Figure 3. The 2560 m^2 building is a two floor building with a small basement for the HVAC installations. Most of the rooms in the building are offices but there are also laboratories, meeting rooms and seminar rooms.

Odense has a continental weather conditions similar to Copenhagen. Therefore, the weather data for Copenhagen will be used in this study, as it is available and provided by the US Department of Energy. The 3D model of the building was created with Google Sketchup as shown in Figure 4, having 110 thermal zones, and OpenStudio tool was used to establish the link between the 3D model and the Energy Plus simulation engine taking into account the building various characteristics and parameters.

The building envelope characteristics are listed in Table 2 below with the construction materials specifications. Regarding the energy systems in the building, district heating is used for heating, while electricity is used for other applications including lighting, equipment and ventilation. A snapshot of the building characteristics definition in OpenStudio is shown in Figure 5. As there is no accurate or monitored data regarding the schedules in the building, a pre-defined standard medium office schedules were employed throughout the simulation process.

Figure 3: Maersk Office Building
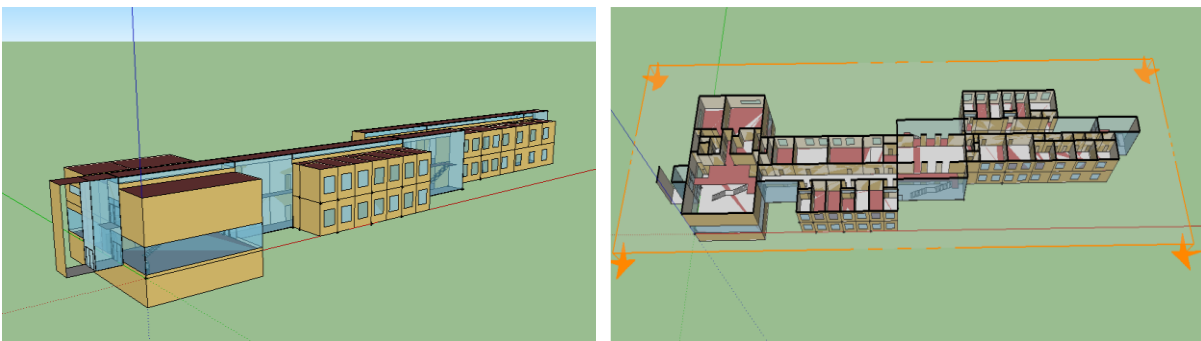
Figure 4: Maersk building 3D Sketchup model, (a) southwest view, (b) floor 1 top view

Table 2: Building envelope characteristics

	MATERIALS AND LAYERS (Outside to inside)		
	LAYER 1	LAYER 2	LAYER 3
Exterior walls	Insulation board 0,1m	Concrete 0,3m	
Interior walls	Concrete 0,1m		
Semiwalls eating room	Concrete 0,42m		
Floor corridor (floor 1)	Wood 0,05m	Steel 0,1m	
Roof	Bitumen 0,1m	Insulation board 0,1m	Concrete 0,3m
Interior floor/ceiling	Concrete 0,2m		
Windows (rooms)	Glass 0,003m	Air 0,013m	Glass 0,003m

Figure 5: Snapshot of the building envelope characteristics definition in OpenStudio

4   BUILDING ENERGY PERFORMANCE ANALYSIS

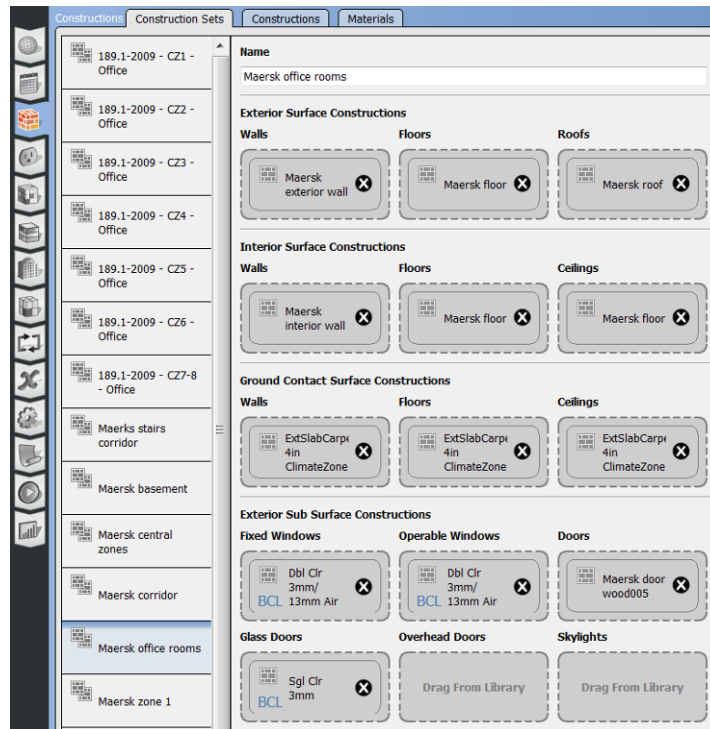The detailed building energy model developed in OpenStudio was used to simulate the overall energy performance of the building throughout the year using the simulation engine of EnergyPlus. It was found that the Maersk Building consumes around 1890 GJ of energy per year, 940 GJ for electricity and 950 GJ as district heating. The overall energy consumption per building conditioned area is around 1.202 GJ/m^2 as shown in Table 3.

Table 3: Maersk building overall energy consumption

Total building area (m^2)	2562.92
Net conditioned building area (m^2)	1572.43
Electricity consumption (GJ)	940.07
District heating energy consumption (GJ)	951.31
Total energy consumption (GJ)	1891.38
Total energy consumption per building area (GJ/m^2)	0.737978556
Total energy consumption per conditioned area (GJ/m^2)	1.202838918

Figure 6 shows the breakdown of the final energy use in the building by application. It is shown that half of the overall energy consumption in the building is used to provide the heating demand where the equipment and lighting contribute to about 41% of the building total energy consumption. It is worth mentioning that ventilation consumes a minimal 7% of the total energy consumed per year.
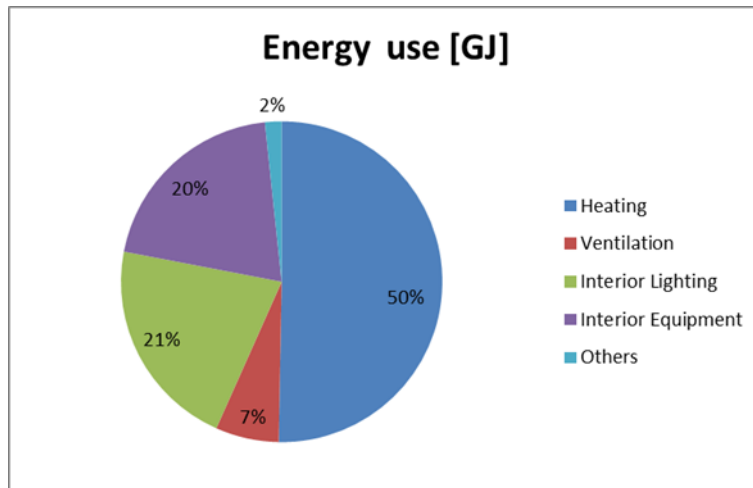
Figure 6: Breakdown of the final energy use in the building by application

Apart from the annual energy consumption, it is relevant as well to analyze the monthly energy consumption to identify the variation in the electricity and heating consumption profile over the year. Figure 7 shows the predicted Maersk building monthly electricity and district heating consumption. It is shown that January is the month with the highest consumption of district heating followed closely by December with less than 1 GJ of difference.

With respect to electricity, the largest amount of electricity is consumed in summer, with August the month with the highest consumption with a bit more than 100 GJ. The electricity is mainly consumed for interior lighting, equipment and ventilation. As shown in Figure 8, the electricity consumption for interior lighting and equipment is considerably uniform, whereas the amount of electricity used for ventilation varies significantly depending on the month. Ventilation consumes very few energy during cold months, but it becomes important in hot months, contributing to almost one third of the total electricity consumption in August.

For the Maersk office building to comply with the BR10 regulation energy standards, the overall energy consumption of the building covering heat loss, ventilation, cooling, domestic hot water and lighting should not exceed 72.5 kWh/m^2. However, the actual building energy consumption based on the overall energy simulation carried out is found to be about 266 kWh/m^2, showing that there is a large room for improvement on the overall energy performance of the building in order to comply with the regulation standards, or at least to reduce the total energy consumption.
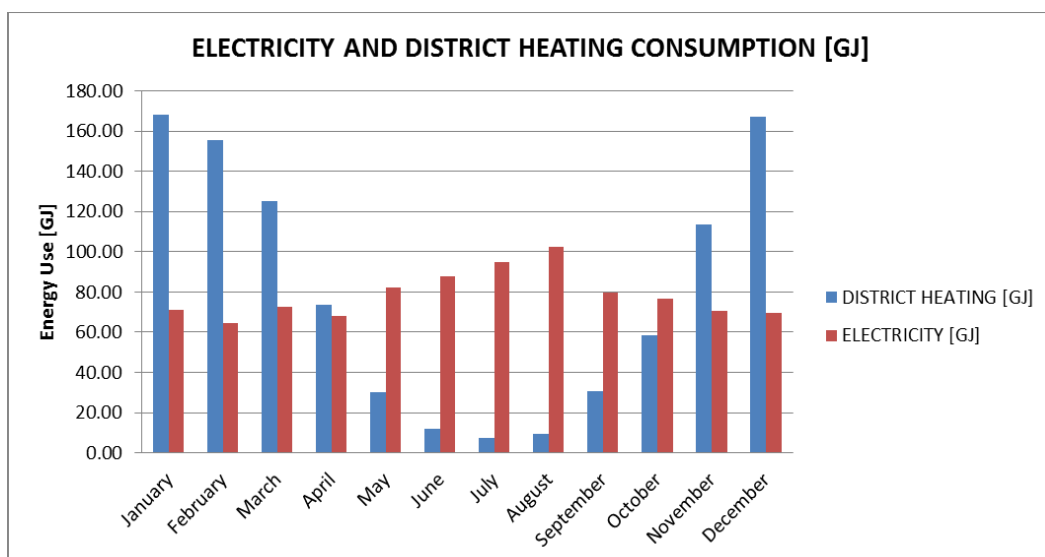

Figure 7: Maersk building monthly electricity and district heating consumption
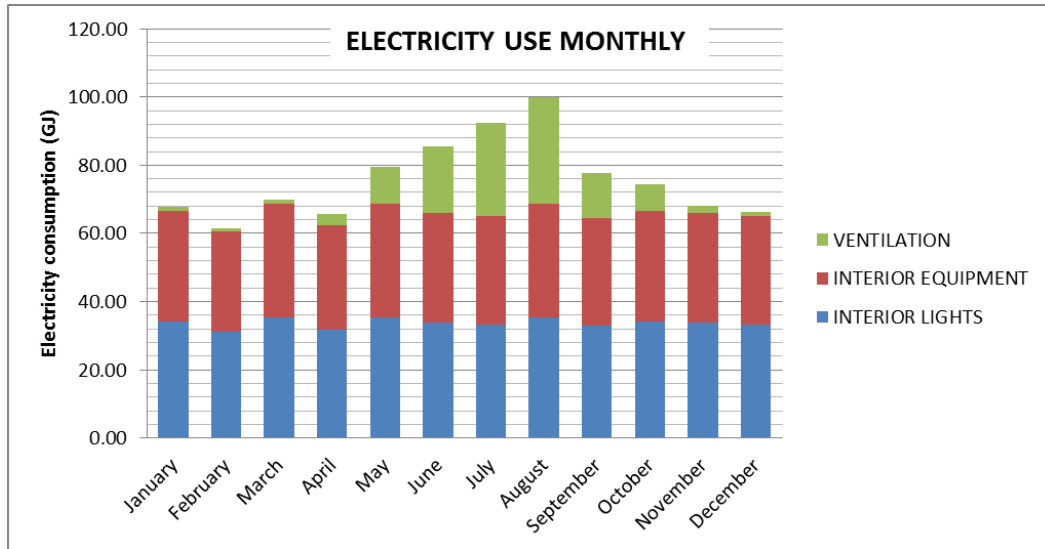
Figure 8: Electricity use in the Maersk building by application

5 PARAMETRIC STUDY AND IMPROVEMENTS SUGGESTIONS

The detailed full scale dynamic simulation of the energy performance of the Maersk building shows that the building doesn't comply with the BR10 regulation standards, consuming a large amount of energy mainly in the form of heat and electricity. Therefore a parametric study will be carried out to examine the effect of various factors on the building total energy consumption including the construction materials, insulation, windows design and lighting, and various suggestions will be provided to enhance the building overall energy performance.

5.1 Replacing Halogen Lights with LED

Halogen lights are located mainly in the building corridors and in the halls. Each of these small lights has a power rating of 100W resulting into high electricity consumption. LED lights have several advantages compared to the conventional lights including low energy consumption, longer life time and the absence of mercury which could have negative impact on the environment. Thus, the energy performance of the building was simulated replacing halogen lights with LED. Table 4 compares the energy consumption of the proposed case using LED with the building base case. It was shown that replacing halogen lights in the corridors and halls with LED lights would bring an annual saving of 204 GJ on the electricity consumption with an increase of 61 GJ on the heating demand. In total, the overall energy consumption of the building will be reduced by about 144 GJ per year.

Table 4: Comparison of energy performance using LED with the building base case model

	Electricity [GJ]	District Heating [GJ]	Total Energy [GJ]
Base Case	940.08	951.3	1891.38
Proposed Case with LED	735.41	1012.59	1748.01
Energy Saving	204.67	-61.29	143.37

5.2 Replacing the Windows with Triple Pane Windows

Windows are one of the major causes of heat addition and heat removal in the building. Thus, changing the type and characteristics of windows could help reducing the heat addition in summer and the heat removal in winter, improving the overall energy performance of the office building. The actual exterior windows in the Maersk building are double pane windows. The energy performance of the building was simulated replacing double pane windows all around the building with triple pane windows. Figure 9 shows the annual energy savings on district heating and electricity in the case of using triple pane windows on the North face and the South face. Generally, it is shown that replacing double glazed windows with triple glazed ones has a minimal

effect on the electricity consumption but will contribute to about 29.9 GJ and 28.7 savings on the district heating if it is applied on the building North side and South side respectively.
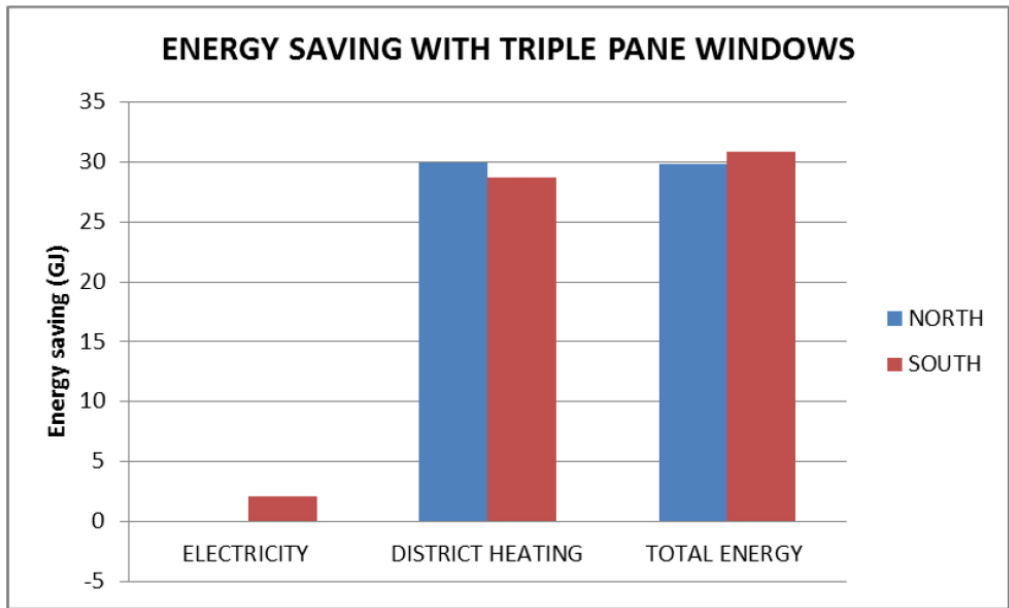
Figure 9: Energy savings using triple glazed windows on the North and South faces

5.3 Increasing the External Walls and Roof Insulation Thickness

Based on the full scale dynamic simulation carried out for the whole office building, it was shown that the opaque surfaces contribute to about 33% of the heat removal in the Maersk building. Therefore, modifying the building envelope and the construction materials characteristics could lead to substantial energy savings mainly in the district heating demand, enhancing the overall energy performance of the building. In this section, the effect of increasing the external walls insulation thickness will be investigated by employing additional insulation on the North side, South side and the Building Roof. The actual insulation thickness used in the building base case is 100 mm. Figure 10 shows the total energy savings through employing insulation thicknesses ranging from 150 mm to 300 mm on the North side, South side and the Roof. As shown in the figure, an insulation thickness of 300 mm could lead to a respective total energy savings of 31.2 GJ, 31 GJ and 44.5 GJ if it is applied on the North face, South face and Building Roof.

Figure 10: Energy savings employing different insulation thicknesses on the North side, South side and the Roof

5.4 Employing an Energy Performance Improvement Pack

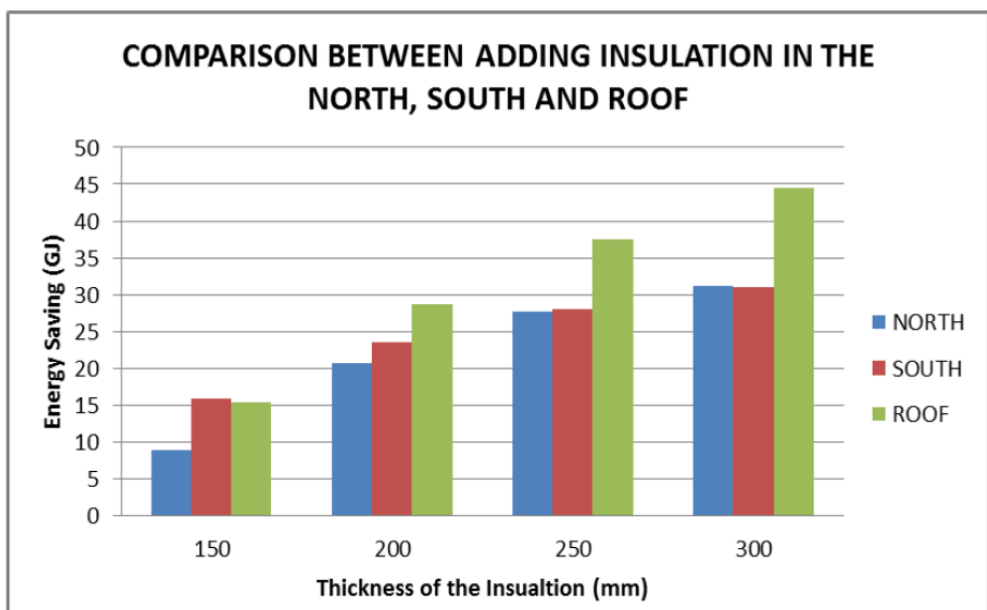Based on the parametric study presented above, an investigation on the effect of an improvement pack on the overall building energy performance is carried out consisting of: replacing halogen lights with LED, replacing double glazed windows with triple glazed ones on the North and South faces and employing 250 mm of insulation on the North face, South face and Building Roof. An overall dynamic simulation of the building energy performance is performed employing the suggested improvement pack. Table 5 summarizes the energy performance of the Maersk building with the improvement pack compared to the base case. It is shown that energy savings of 210.8 GJ and 101.3 GJ on the electricity and the district heating could be attained through implementing the suggested measures.

Table 5: Comparison of energy performance using the improvement pack with the building base case model

	Electricity [GJ]	District Heating [GJ]	Total Energy [GJ]
Base Case	940.08	951.3	1891.38
Proposed Case with the improvement pack	729.25	849.98	1579.24
Energy Saving	210.83	101.32	312.14

6 CONCLUSION AND FUTURE WORK

To attain its ambitious energy objective to become a fossil fuel-independent country by 2050 relying solely on renewable resources in the energy and transport sectors, Denmark has set short term goals to achieve 7.6% reduction on the gross energy consumption by 2020 compared to 2010 numbers with a reduction in the greenhouse emissions by 34% compared to 1990. With their large contribution in the overall energy consumption, new and existing buildings are identified as a major player in improving the energy sector with a targeted energy savings of 70-75% by 2050. In this work, a case study, the Maersk Office Building in Odense, Denmark was considered aiming to reduce the building energy consumption and improve the overall energy performance. A modelling and simulation methodology was set, employing the simulation engine of EnergyPlus aided by Google Sketchup and OpenStudio, and a holistic building energy model was developed taking into account various building characteristics and specifications and weather conditions. Using the developed detailed model, a dynamic full scale simulation for the Maersk building energy performance was carried out showing that about 50% of the building overall energy consumption is used for district heating, where electricity for lighting and equipment contributes to about 40%. It was shown that the building in its current situation is very far from complying with the BR10 Danish building regulations regarding the energy performance. Thus, a parametric study was performed to investigate various solutions and measures to reduce the energy demand and improve the building energy performance. An improvement energy pack is suggested, employing LED lights, triple glazed windows and insulation on exterior walls and roof, and respective energy savings of 210.8 GJ and 101.3 GJ on electricity and district heating were reported. Based on the simulation results obtained, it is concluded that to comply with the BR10 Danish regulations, the building will need an energy optimization and control strategy in addition to applying energy efficient measures and techniques. Therefore the next phase of the research will concentrate on establishing a framework to integrate the holistic building energy model with the building management system to attain a better control and optimization of the overall energy performance.

7 ACKNOWLEDGEMENT

8 REFERENCES

BROIN, E.O., Mata, E., Göransson, A., Johnsson, F., 2013. The effect of improved efficiency on energy savings in EU-27 buildings. *Energy*, 57, pp. 134-148.

CURTIS, J., Pentecost, A., 2015. Household fuel expenditure and residential building energy efficiency ratings in Ireland. *Energy Policy*, 76, pp. 57-65.

Danish Building & Property Agency, 2011. Background Report on building class in 2020, Available from: http://www.ens.dk/sites/ens.dk/files/forbrug-besparelser/byggeriets-energiforbrug/lavenergiklasser/analyser-bygningsklasse-2020/baggrundsnotat_for_tyvetyve.pdf

European Commission, 2010. Directive 2010/31/EU of the European Parliament on the energy performance of buildings, Available from: http://eur-lex.europa.eu/legal-content/EN/ALL/;ELX_SESSIONID=FZMjThLLzfxmmMCQGp2Y1s2d3TjwtD8QS3pqdkhXZbwqGwlgY9KN!2064651424?uri=CELEX:32010L0031

European Commission, 2011. A Roadmap for moving to a competitive low carbon economy in 2050, Available from: http://eur-lex.europa.eu/legal-content/EN/TXT/?uri=CELEX:52011DC0112.

European Commission, 2012. Directive 2012/27/EU of the European Parliament and of the Council of 25 October 2012 on energy efficiency, Available from: http://ec.europa.eu/energy/efficiency/eed/eed_en.htm

HOUSSIN, D., LaFrance, M., 2013. Transition to Sustainable Buildings, Clean Energy Solutions Center IEA Buildings Book Launch, International Energy Agency IEA 2013.

IGNJATOVIĆ, D., Popović, M.J., Kavran, J., 2015. Application of sunspaces in fostering energy efficiency and economical viability of residential buildings in Serbia. *Energy and Buildings*, 98, pp. 3-9.

International Energy Agency (IEA), 2011. Energy Policies of IEA Countries – Denmark 2011Review, Available from: http://www.ens.dk/sites/ens.dk/files/politik/dansk-klima-energipolitik/denmark2011_unsecured-3.pdf

KWON, P.S., Østergaard, P.A., 2012. Comparison of future energy scenarios for Denmark: IDA 2050, CEESA (Coherent Energy and Environmental System Analysis), and Climate Commission 2050. *Energy*, 46(1), pp. 275-282.

LUND, H., Mathiesen, B.V., 2009. Energy system analysis of 100% renewable energy systems-The case of Denmark in years 2030 and 2050. *Energy*, 34(5), pp. 524-531.

PAROC, Danish Building Regulations, Available from: http://www.paroc.dk/Knowhow/Building-regulations/Danish-Building-regulations-in-accordance-to-BR-10?sc_lang=en

WILLIAMS, J., 2011. Zero Carbon Homes - A Road Map. 1st ed. London: Earthscan and Routledge Press.

WOLOSZYN, M., Rode, C., 2008. Tools for Performance Simulation of Heat, Air and Moisture Conditions of Whole Building. *Building Simulation*, 1, pp. 5-24.

WONG, P.S.P, Lindsay, A., Crameri, L., Holdsworth, S., 2015. Can energy efficiency rating and carbon accounting foster greener building design decision? An empirical study. *Building and Environment*, 87, pp. 255-264.

15: A comparison of energy usage between a radiant ceiling system, an active beam system and a fan coil system compared to a VAV system

PETER SIMMONDS[1] , AND JASON KIRCHHOFF[2]

1Principal, Building and Systems Analytics LLC, Marina Del Rey and Hong Kong
2Technical Director, Energize Analytics, Delray Beach, Florida

In a quest to reduce the energy consumption in buildings there has been and introduction of different alternative conditioning systems, namely a Radiant Ceiling System and an Active Beam system which can be used to condition spaces. This paper will attempt to identify any energy and cost savings of these different systems, as well as occupant comfort conditions. As base case, we have used a traditional overhead Variable Air Volume system, a traditional Fan Coils system has also been included in this comparison. The building used for the simulation comparison is 200,000 ft2, 8 story building situated in both New York and Los Angeles. The base case model and the three alternatives have all been constructed in the simulation model in accordance with ASHRAE 90.1 -2013.

1. INTRODUCTION

It was decided to investigate the energy consumption and cost comparison between several HVAC systems to investigate if there are benefits to using radiant ceilings or active beams on projects. This report will show the results of an energy consumption comparison between the following:

- An ASHRAE 90.1 overhead VAV system
- A radiant ceiling system
- An Active Beam system
- A Fan coil system

2 THE STANDARD DESIGN

The Standard Design is generated automatically by the program based on the characteristics of the Proposed Design. The Standard Design:

- Has exactly the same physical size and shape as the Proposed Design;
- Has the same occupancy schedules and zoning as the Proposed Design;
- Has the prescriptive assembly U-Factors and prescriptive glazing U-Factors and solar heat gain coefficients, based on climate zone;
- Has the prescriptive lighting allotment based on occupancy or task requirements;
- Has the mandatory ventilation rates by occupancy;
- Has a mechanical system appropriate for the type installed in the proposed design; and,
- Has a system size which is appropriate for the design heating and cooling loads of the Standard Design.

Full details on the assumptions used to generate the Standard Design building are contained in the state's Alternative Calculation Method (ACM) Manual on the 1995 Nonresidential Standards. Because the Standard Design is based upon many of the characteristics of the Proposed Design, the energy budget always changes when any change is made to the proposed building design.

3 INPUT DATA USED TO OBTAIN RESULTS

3.1 Location

There are two locations being used for this comparison:

- Los Angeles
- New York

3.2 Los Angeles climate

The Los Angeles climate has very low heating requirement during the winter, some 311 hours. There are also 9 hours of cooling and dehumidification, but 2088 hours of internal gains.

Los Angeles is in Climate Zone 3B

HDD 65 = 1458

CDD 50 = 4770

Summer 81 DB/ 64WB

Winter 46.4 DB
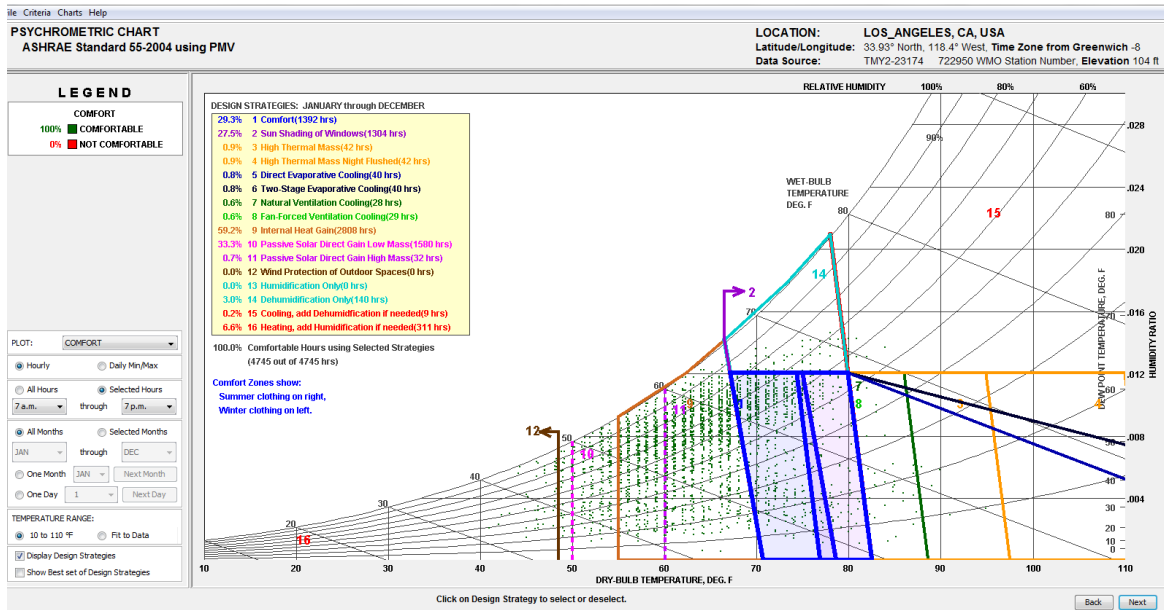
Figure 0-42 shows the Los Angeles climate

3.3 New York Climate

Figure 0-43 shows the New York climate

The New York climate is very different than the Los Angeles climate, it has a distinct heating requirement during the winter, some 1871 hours. There are also 239 hours of cooling and dehumidification and 1017 hours of internal gains.

New York is in Climate Zone 4A

HDD 65 = 4805

CDD 50 = 3634

Summer 82.1 DB/ 74.1WB

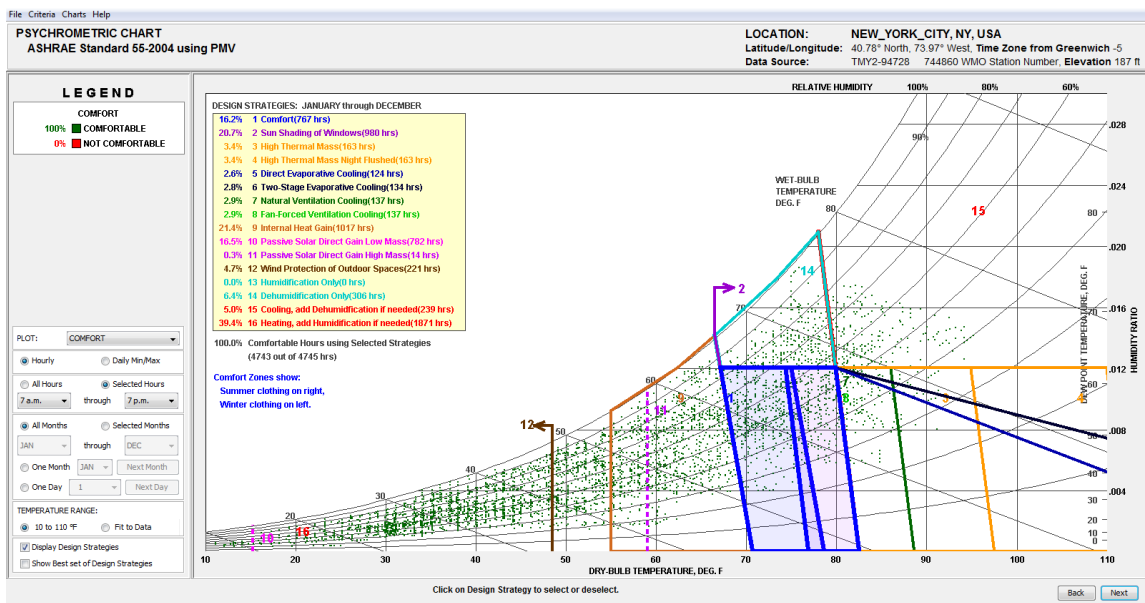Winter 13.6 DB

4   ASSUMPTIONS USED IN THE SIMULATION
4.1 Fan Power

For the VAV system we assumed a pressure drop of 1" WC

For the Fan Coil System we assumed a pressure drop of 0.5" WC

The Radiant ceiling system didn't have any additional pressure resistances and the 100% air system calculation included the pressure drop for the air handling unit and distribution system.

For the active Beam system we included 0.3" WC for the active beam unit.

The fan power for the different alternatives have been calculated as follows:

4.2 New York

					Variable Volume	
	PD	A	bhp	Motor Eff	ASHRAE 90.1 kW	
Base Case VAV	1	43.20247	275.3812	0.88	234.78	0.001315
					Constant Volume	
	PD	A	bhp	Motor Eff	ASHRAE 90.1 kW	
Fan Coil	0.5	0.501693	4.400813	0.875	3.75	0.000905
Radiant Ceiling	0	0	3.89912	0.88	3.32	0.000801
Active Beams	0.3	0.250847	4.149967	0.875	3.54	0.000853

Figure 0-44 shows the calculation of fan power for the New York different alternatives

4.3 Los Angeles

					Variable Volume	
	PD	A	bhp	Motor Eff	ASHRAE 90.1 kW	
Base Case VAV	1	38.92743	248.1312	0.88	211.55	0.001315
					Constant Volume	
	PD	A	bhp	Motor Eff	ASHRAE 90.1 kW	
Fan Coil	0.5	0.501693	4.400813	0.875	3.75	0.000905
Radiant Ceiling	0	0	3.89912	0.88	3.32	0.000801
Active Beams	0.25	0.250847	4.149967	0.875	3.54	0.000853

Figure 0-45 shows the calculation of fan power for the Los Angeles different alternatives

4.4 Boiler system

The base case boiler plant consists of two gas fired boilers each having a minimum efficiency of 82% (combustion efficiency).

Hot water minimum supply temperature set to 150F (66C)

Reset in detailed mode to 50F (10C)

Hot-water design supply temperature shall be modeled as 180°F (82C) and design return temperature as 130°F (54C). Hot-water supply temperature shall be reset based on outdoor dry-bulb temperature using the following schedule: 180°F (82C) at 20°F and below, 150°F (66C) at 50°F and above, and ramped linearly between 180°F (82C) and 150°F (66C) at temperatures between 20°F and 50°F.

The baseline building design hot-water pump power shall be 19 W/gpm (300W/l/s). The pump pumping system shall be modeled as primary-only with continuous variable flow. The hot-water systems shall be modeled with variable-speed drives.

4.5 Chiller plant

The base line chilled water plant will consist of two rotary screw compressors. Required efficiency is 6.10 COP which is 0.577 kW/ton.

Chilled-water design supply temperature shall be modeled at 44°F (6.7C) and return water temperature at 56°F (13.3C).

Chilled-water supply temperature shall be reset based on outdoor dry-bulb temperature using the following schedule: 44°F (6.7C) at 80°F (26.7C) and above, 54°F (12.2C). at 60°F(15.6C) and below, and ramped linearly between 44°F (6.7C) and 54°F (12.2C).at temperatures between 80°F (26.7C) and 60°F (15.6C).

The baseline building design pump power shall be 22 W/ gpm (350W/l/s). Chilled-water systems with a cooling capacity of 300 tons or more shall be modeled as primary/secondary systems with variable-speed drives on the secondary pumping loop.

The water cooled condenser has a two speed fan

The temperature is set to a fixed 70F (21C) per the requirements of the standard.

The heat rejection device shall be an axial fan open circuit cooling tower with variable-speed fan control and shall meet the performance requirements of Table 6.8.1-7. Condenser water design supply temperature shall be calculated using the cooling tower approach to the 0.4% evaporation design wet-bulb temperature as generated by the formula below, with a design temperature rise of 10°F (5.6C).

Approach10°F Range = 25.72 – (0.24 × WB)

Where WB is the 0.4% evaporation design wet-bulb temperature in °F; valid for wet bulbs from 55°F (12.8 C) to 90°F (32.2C).

The tower shall be controlled to maintain a 70°F (21.1C) leaving water temperature where weather permits, floating up to leaving water temperature at design conditions. The baseline building design condenser-water pump power shall be 19 W/gpm. (300W/l/s).

4.6 Air handling units

The fans will be direct drive and provided with variable frequency drives. The air-handling unit shall supply outside air recirculated air through a draw-through arrangement. Sound attenuators will be provided in the supply and return air ducts. Air handling units will consist of the following components:

Supply Fan with VSD

MERV 7 Pre and MERV 14 Final Filters

Cooling Coil

Heating Coil

Economizer Mixing Box

Air is supplied to open plan areas via a pressurized ceiling plenum with perforated face.

5   ALTERNATIVES

The following alternatives were pursued:

- Base case, Overhead VAV
- Alternative 1, Fan Coils
- Alternative 2, Radiant Ceiling
- Alternative 3 , Active Beams

5.1 Overhead VAV

Air handling units will consist of the following components:

Supply Fan with VSD

MERV 7 Pre and MERV 14 Final Filters

Cooling Coil

Heating Coil

Economizer Mixing Box

The fans will be direct drive and provided with variable frequency drives. The air-handling unit shall supply outside air and recirculated air through a draw-through arrangement. Sound attenuators will be provided in the supply and return air ducts. Air is supplied to open plan areas via a pressurized ceiling plenum with perforated face.

The system airflow is varied dependent on the duct static pressure, thus as less air is required by the zones the dampers close increasing the pressure in the duct. The pressure sensor signals the supply fan to slow in order to reduce supply air volume. The system therefore only supplies and conditions air necessary to satisfy demand, thus saving energy. System static pressure will be reset based on polled damper position to further reduce fan energy.

Each modulating damper will be controlled via the set point of a zone thermostat. Each modulating damper will be provided with a minimum turndown, usually 20 percent of airflow for cooling and 50 percent airflow for heating, to ensure that outside ventilation airflow is provided during periods that the building is occupied. The perimeter will be zoned separately from the interior.

5.2 Fan Coil units

Multiple fan coil units with outside air connection filters, hot water heating and chilled water cooling coils will be provided to meet the space heating and cooling demands on the perimeter zone, typically the exterior 15 ft. (4.6m) deep zone in each building. The interior zones will be served by 2-pipe units. The cooling coil in the FCU will have 68F (20C) and 70F(21C) as the chilled water supply and return temperatures and 110F and 100F for the heating coil water supply and return temperatures.

5.3 Active Beams

An active chilled beam is an air diffusion device which introduces conditioned air to the space for the purposes of temperature and latent control. Primary air is delivered through a series of nozzles, creating induction of room air through a unit mounted chilled water coil which conditions it prior to its reintroduction to the space. Depending on the nozzle size and configuration, active beams typically induce 2 to 5 parts of room air for every part of primary air they deliver to the space. Sensible heat removal by the beam's integral cooling coil complements the cooling effect of the primary air supply.

Heat extraction or addition by the coil allows for significant reduction in primary air flow requirements over all-air ducted systems. Energy to transport cooling and/or heating media is reduced due to the high specific heat and density of water. As a result, active beam systems require less space for the mechanical services, due to smaller duct work and air handling unit sizes. As a consequence of the reduction in mechanical service space requirements,

Active beam systems are typically operated with a constant (minimal) volume supply air flow to the space. Constant volume systems offer the benefit of enhanced thermal comfort due to consistent room air movement, and an improved acoustic environment.

Active chilled beam supply water temperatures should be maintained at or above the room dew point temperature in order to prevent condensation on the coil and its supply water piping. Passive chilled beam water supply temperatures should be maintained slightly (2F – 1K) above the room dew point temperature. In both cases, the chilled water supply piping must be adequately insulated to prevent condensation on the pipe work itself. In cases where adequate control of space humidity levels cannot be assured, higher supply water temperatures and/or condensation controls should be considered.

The hot water servicing the coil within the active beam must be chosen to limit the discharge air temperature to less than 20F above the room design set point. Additionally, to ensure proper room air distribution, the discharge velocity should be selected in accordance with ASHRAE standard 55 requirements.

5.4 Radiant Panels

With radiant cooling, heat exchange from the room to the ceiling happens mainly via radiation and convection. Radiation of energy takes place between objects with different surface temperatures. In all cases, the warmer object radiates heat to the cooler object. Just as the hot sun radiates to the cooler earth, in a radiant cooled environment, computers, people, and other sources of heat radiate that heat to the cooler surface of the ceiling. As an added benefit, humans perceive heat transfer via radiation as particularly comfortable. Convection occurs when the room air is cooled as it flows beneath the cooling panels. The cooler air is heavier than the warmer air rising from the heat sources, which creates natural, high volume, low-velocity air currents.

The human body gives off heat to its surroundings as a result of normal activity. The human body can lose the heat three ways:

- By transmitting the heat through the skin and radiating to the cooler surroundings.
- By having cooler air pass over the skin and cooling by convection.
- By evaporation of moisture through breathing and perspiration processes.

Obviously, for human comfort, it is desirable to minimize perspiration and draft as much as possible.

The cool surface of a radiant cooling ceiling is an ideal radiation partner for the skin. The capacity for the quiet, very comfortable heat exchange process that occurs via radiation is almost doubled with the use of radiant cooling. The rate of convection and, especially, evaporation are reduced, and air drafts in the room are reduced to a minimum.

The energy needed to cool depends directly on the heat loads in the room. An important influence factor is the desired room temperature. It is clear that cooling a room to 76-77F (26C) instead of 74F (24C) uses less energy. A radiant chilled ceiling and the human perception of comfort complement each other favorably. Because the human body radiates heat energy to surrounding cooler surfaces, the human brain perceives a higher level of comfort with radiant cooling than it does when a forced air-cooling system is used.

Carbon Dioxide sensors located in the space shall allow for reduction in minimum outside air volume whenever levels are below a preset limit and energy savings would result. Carbon dioxide sensors shall not override the economizer cycle.

The radiant circuit is provided with a dedicated pump and mixing valves to raise the supply temperature of the incoming water under a cooling condition.

6   RESULTS
6.1 New York

Annual Electric Energy by End Use		Annual Energy	Source	Annual Energy	Site	Lighting	HVAC Energy			Peak	
		total	EUI	Electric	Nat Gas	Electric	Electric	Nat Gas	total	Electric	Cooling
Annual Energy Use (kWh)		Mbtu	kBtu/sf/yr	kWh	Therms	kWh	kWh	Therms	Mbtu	kW	tons
0	Base Design - VAV	29,992	167	2,594,809	34,236	599,160	711,876	8,412	3,271	1,025	456
1	0+Fan Coils	31,795	177	2,814,940	29,727	599,160	932,006	3,924	3,573	1,031	513
2	0+Radiant Ceiling	27,349	152	2,336,119	34,295	599,160	453,185	8,482	2,395	862	426
3	0+Active Beams	27,564	153	2,356,092	34,400	599,160	473,158	8,585	2,473	873	461

Figure 0-46 shows the annual electric energy by end use for the alternatives studied for the New York location

The results in table 6-1 show that the radiant ceiling system is 27% lower in energy usage (total MBTU) than the VAV system base case and the active beam system is 24% lower. The electrical usage of the radiant ceiling system is 16% lower than the VAV system and the active beam system consumes 15% less than the VAV alternative. The peak cooling load is reduced by 15% for the radiant ceiling system compared to the VAV base design (426 tons to 456 tons). The active beam system consumes 1% more peak cooling than the VAV base design.

		Electric	Electric	Electric	Nat Gas	Total
Annual Cost		kWh($)	kW($)	Total ($)	Total ($)	($)
0	Base Design - VAV	$347,341	$308,826	$ 657,339	$ 47,770	$ 705,109
1	0+Fan Coils	$376,808	$327,487	$ 705,467	$ 41,972	$ 747,439
2	0+Radiant Ceiling	$312,713	$272,926	$ 586,811	$ 47,830	$ 634,641
3	0+Active Beams	$315,387	$275,031	$ 591,589	$ 47,965	$ 639,554

Figure 0-47 shows the annual energy costs for the alternatives studied for the New York location

The annual costs shown in table 6-2 for New York show the radiant system would reduce utility costs by $70,468.00 per year, but the active beam system would reduce costs by $65,555.00 per year. Most of the savings are due to the reduction in fan power for the alternatives.

If expressed over a 10 year period then the radiant ceiling alternative would cost $704,680.00 less than a VAV alternative and the active beam alternative would cost $655,550.00 less than the VAV alternative.

Annual Electric Energy by Enduse		Ambient	Task	Misc.	Space	Space	Heat	Pumps	Vent	Domestic	Exterior	
Annual Energy Use (kWh)		Lights	lights	Equipment	Heating	Cooling	Rejection	& Aux	Fans	Hot water	Usage	total
0	Base Design - VAV	599,160	0	1,283,781	0	259,885	16,945	49,116	385,930	0	0	2,594,809
1	0+Fan Coils	599,160	0	1,283,781	0	317,032	20,349	54,221	540,404	0	0	2,814,940

2	0+Radiant Ceiling	599,160	0	1,283,781	0	263,042	18,036	86,279	85,828	0	0	2,336,119
3	0+Active Beams	599,160	0	1,283,781	0	270,348	17,754	93,656	91,400	0	0	2,356,092

Figure 0-48 shows the annual electric energy by end uses for the alternatives studied for the New York location

Table 6-3 shows the radiant ceiling system reduces the electric energy end use by 10% and the active beam system reduces the electric energy end use by 9% compared to the VAV base case. The difference between the two is due to the slightly higher fan power required by the active beam system

6.2 Los Angeles

Los Angeles										
Annual Electric Energy by End Use										
		Annual Source Energy		**Annual Site Energy**		**Lighting**	**HVAC Energy**			**Peak**	
		total	EUI	Electric	Nat Gas	Electric	Electric	Nat Gas	total	Electric	Cooling
	Annual Energy Use (kWh)	Mbtu	kBtu/sf/yr	kWh	Therms	kWh	kWh	Therms	Mbtu	kW	tons
0	Base Design - VAV	29,779	165	2,679,658	23,422	599,160	796,725	124	2,732	938	391
1	0+Fan Coils	31,813	177	2,879,748	23,276	599,160	996,816	7	3,403	948	389
2	0+Radiant Ceiling	26,668	148	2,376,977	23,301	599,160	494,044	35	1,690	795	330
3	0+Active Beams	26,824	149	2,392,191	23,309	599,160	509,257	37	1,742	818	346

Figure 0-49 shows the annual electric energy by enduses for the Los Angeles location

The results in table 6-4 shows the total energy usage is reduced by the Radiant Ceiling system by 38% lower than the VAV system base design and the Active Beam system is 36% lower. The peak electrical usage is reduced by 15% for the Radiant Ceiling system compared to the Base Design VAV system and the Active Beam system reduces the peak electrical load by 13%. The Radiant Ceiling system reduces the peak cooling load by 16% (330 tons to 391tons) and the Active Beam alternative reduces the peak cooling load by 11% compared to the Base Design VAV system (346 tons to 391 tons).

		Electric	Electric	Electric	Nat Gas	Total
Annual Cost		kWh($)	kW($)	Total ($)	Total ($)	($)
0	Base Design - VAV	$306,510	$74,173	$384,877	$13,943	398,820
1	0+Fan Coils	$327,816	$75,797	$407,806	$13,859	421,665
2	0+Radiant Ceiling	$270,216	$63,602	$338,011	$13,873	351,884
3	0+Active Beams	$271,631	$64,141	$339,965	$13,878	353,843

Figure 0-50 shows the annual energy costs for the alternatives studied for the Los Angeles location

The annual costs shown in table 6-5 for Los Angeles show the radiant system would reduce utility costs by $46,866.00 per year, but the active beam system would only reduce costs by $44,912.00 per year. Most of the savings are due to the reduction in fan power for the alternatives. If expressed over a 10 year period then the radiant ceiling alternative would cost $468,660.00 less than a VAV alternative and the active beam alternative would cost $449,120.00 less than the VAV alternative.

Figure 0-51 shows the PPD results when conditioning the space with a VAV system during the winter in New York

Figure 6-6 shows the PPD results to be lower than 10% during the occupied period

Figure 0-52 shows the PPD results when conditioning the space with a Radiant Ceiling during the winter in New York

Figure 6-7 shows the PPD results to be mostly lower than 10% during the occupied period

Figure 0-53 shows the PPD results when conditioning the space with a VAV system during the summer in New York

Figure 6-8 shows the PPD results to be lower than the 10% maximum compliance on the warmest summer day

Figure 0-54 shows the PPD results when conditioning the space with a Radiant Ceiling during the summer in New York

Figure 6-9 shows the PPD results to be well lower than the 10% maximum compliance on the warmest summer day
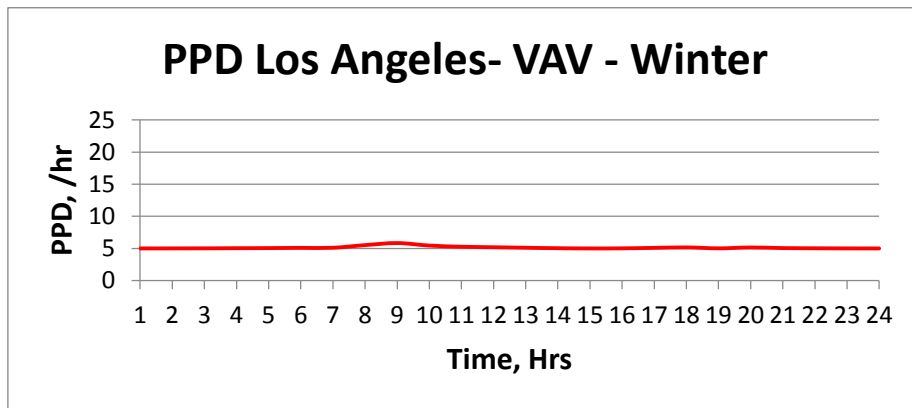
Figure 0-55 shows the PPD results when conditioning the space with a VAV system during the winter in Los Angeles

Figure 6-10 shows the PPD results to be well lower than the 10% maximum compliance on the warmest summer day
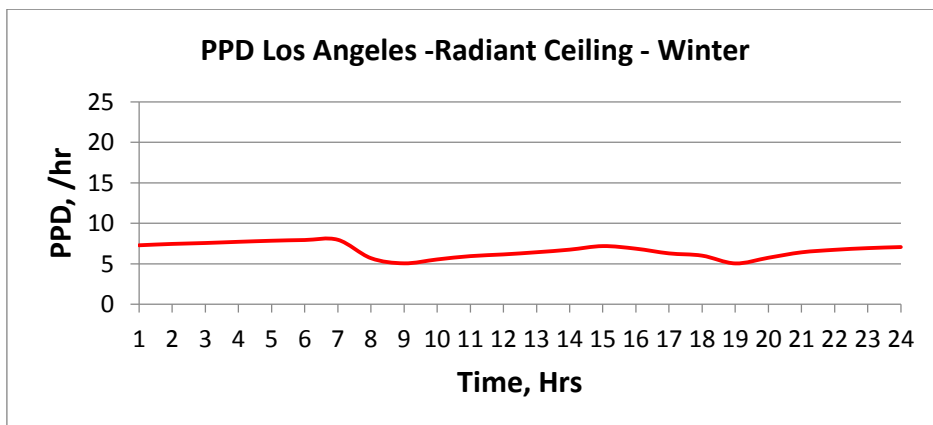
Figure 0-56 shows the PPD results when conditioning the space with a radiant ceiling during the winter in Los Angeles

Figure 6-11 shows the PPD results to be well lower than the 10% maximum compliance on the winter day
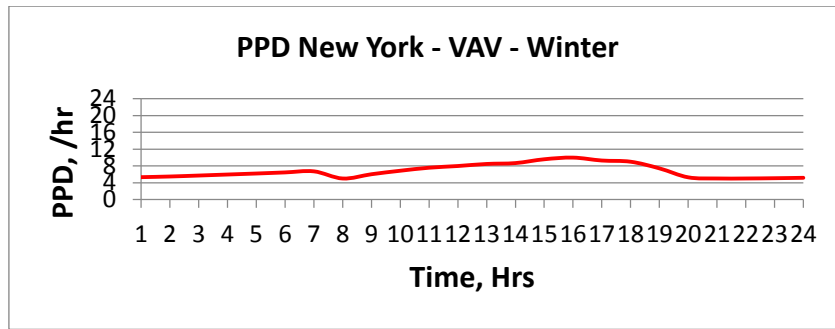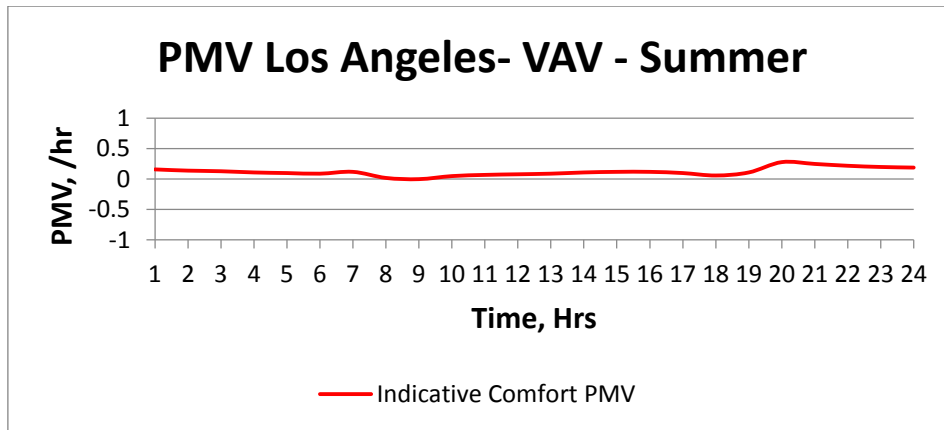
Figure 0-57 shows the PPD results when conditioning the space with a VAV system during the summer in Los Angeles

Figure 6-12 shows the PPD results to be well lower than the 10% maximum compliance on the warmest summer day
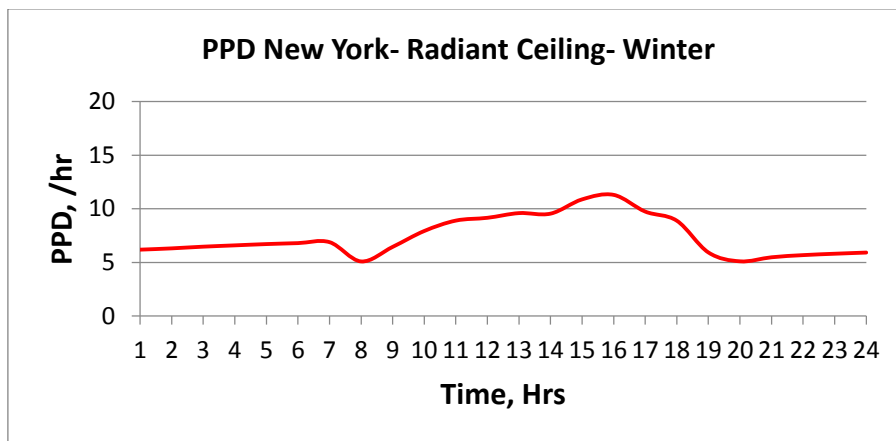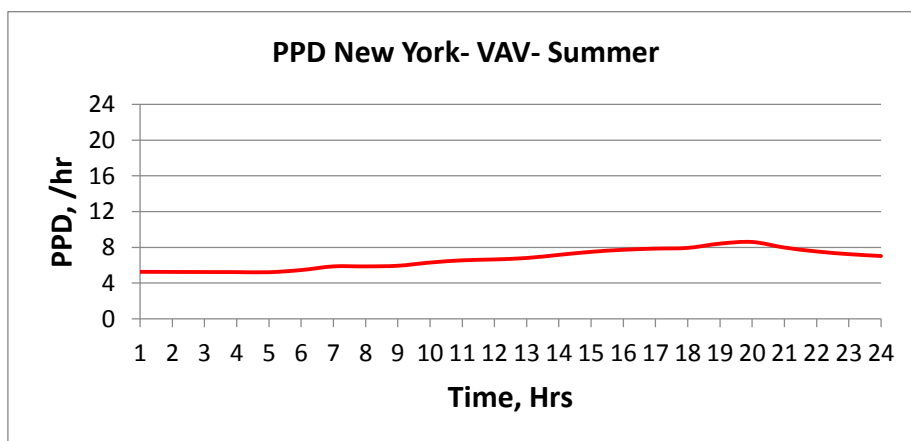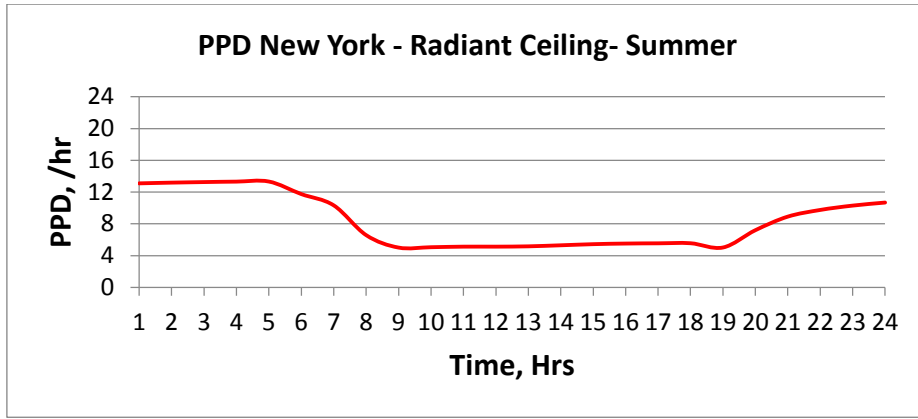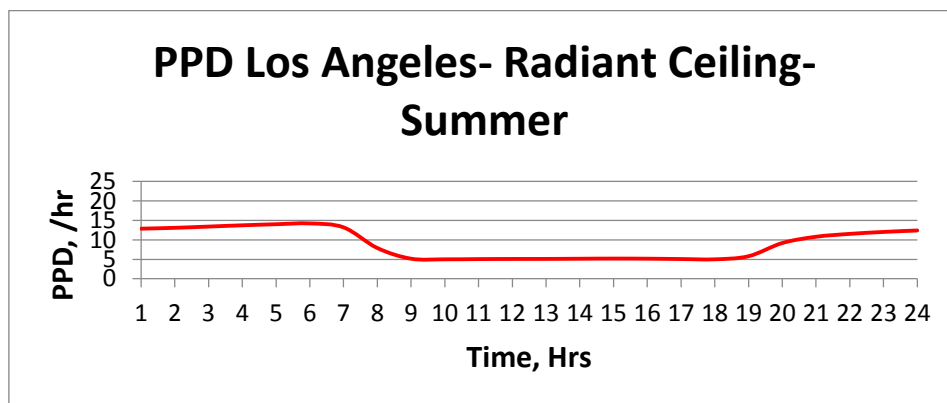

Figure 0-58 shows the PPD results when conditioning the space with a radiant ceiling during the summer in Los Angeles

Figure 6-13 shows the PPD results to be well lower than the 10% maximum compliance on the warmest summer day

7   CONCLUSIONS

There is a very clear difference between the operation of the building in Los Angeles and New York. There are two main reasons:

- The difference in Climate
- The difference in Utility cost

7.1 Energy Usage

The total energy usage in New York is reduced by 27% by the Radiant Ceiling system and reduced by 24% for the Active Beam system compared to the Base Design.

The peak cooling load in New York is 426 tons for the Radiant Ceiling alternative (7% lower than Base Design) and 461 tons for the Active Beam alternative (1% higher than the Base Design). For New York the savings in annual electric end use for the radiant ceiling system compared to the VAV base case is 10% and 9% for the active beam alternative.

The total energy usage in Los Angeles is reduced by 38% by the Radiant Ceiling system and reduced by 36% for the Active Beam system compared to the Base Design.

The peak cooling load in Los Angeles is 330 tons for the Radiant Ceiling alternative (16% lower than the Base Design) and 346 tons for the active beam alternative (11% lower than the Base Design).

For Los Angeles the savings in annual electric end use for the radiant ceiling system compared to the VAV base case is 11% and 11% for the active beam alternative.

For New York the savings in annual electric end use for the radiant ceiling system compared to the VAV base case is 10% and 9% for the active beam alternative.

The total energy usage in Los Angeles is reduced by 38% by the Radiant Ceiling system and reduced by 36% for the Active Beam system compared to the Base Design.

The peak cooling load in Los Angeles is 330 tons for the Radiant Ceiling alternative (16% lower than the Base Design) and 346 tons for the active beam alternative (11% lower than the Base Design).

For Los Angeles the savings in annual electric end use for the radiant ceiling system compared to the VAV base case is 11% and 11% for the active beam alternative.

7.2 Free Cooling

First of all, all alternatives include free cooling in the simulation model. So the results include any possible savings as a result of free cooling)

Typically in VAV systems it is possible to utilize free cooling, especially in the Los Angeles climate. Free cooling can also be utilized for Radiant Ceiling and Active Beam systems. The percentage of energy reduction for the air handling systems is the same for all alternatives. The cost savings must be seriously studied as the savings for a VAV system are higher for peak cooling and heating and zero for a free cooling period, but as the total heating and cooling load is also dependent on the air volume being conditioned, the Radiant Ceiling and Active Beam alternatives consume less energy as the primary air volume is about one third of a traditional VAV system. Explanation: the VAV system requires 178,000 cfm for New York and 160,000 cfm for Los Angeles, so during free cooling the savings are for 178,000 and 160,000 cfm, but the heating for 178,000 and 160,000 cfm and the cooling required for 178,000 and 160,000 outweigh the savings. The percentage savings for the RC and AB alternative are the same but as the CFM is lower only 33,000. The actual cost savings are much smaller.

7.3 Thermal Comfort

The results show that a Radiant Ceiling system provides improved occupant comfort as the radiant heat exchange in a space can be controlled by the radiant ceiling, usually by controlling the supply and return water temperature in the panels which in turn varies the panel surface temperature, which can then control and/or balance the radiant energy exchange in a space. During winter for instance the warm surface area of the radiant ceiling panels will compensate for cold surfaces of windows. During summer, the cool surfaces of the radiant ceiling panels will compensate for warm surface temperatures of the windows.

The following is from Appendix G of ASHRAE Standard 90.1-2013 *"1. Setpoints and schedules for HVAC systems that automatically provide occupant thermal comfort via means other than directly controlling the air dry-bulb and wet-bulb temperature may be allowed to differ, provided that equivalent levels of occupant thermal comfort are demonstrated via the methodology in Section 5.2.3 of ASHRAE Standard 55, "Elevated Air Speed," or Appendix D of Standard 55, "Computer Program for Calculation of PMV-PPD."*

The results shown in this report show space operating temperatures for a Radiant Ceiling system are in the order of 76-78F and still maintain comfort conditions of 10% PPD. The peak cooling load for the New York location is reduced by 35 tons, about 7% due to the setpoint adjustment for Radiant Ceiling. The peak cooling load for the Los Angeles location is reduced by 16 tons, about 4% due to the setpoint adjustment for Radiant Ceiling.

The other three alternatives are pure sensible heating and cooling systems that can be operated to maintain comfort conditions. However, space dry bulb temperatures in the winter are higher to compensate for cool surfaces of windows and are lower in the summer to compensate for warm surface temperatures of windows.

7.4 Cost savings

From the breakdown of installations costs it would appear there is little or no difference between the installation cost for the base case VAV system and the radiant ceiling system at $7,300,000.00

The installation cost for the active beam system would be about $1,600,000.00 lower than the base case system cost

The utility cost savings in New York compared to the VAV base case are $70,468.00 for the radiant ceiling alternative and $65,555.00 for the active beam alternative. If expressed over a 10 year period then the radiant ceiling alternative would cost $704,680.00 less than a VAV alternative and the active beam alternative would cost $655,550.00 less than the VAV alternative.

For Los Angeles the utility cost savings are$46,936.00 for the radiant ceiling alternative and $44,977.00 for the active beam alternative. If expressed over a 10 year period then the radiant ceiling alternative would cost $468,660.00 less than a VAV alternative and the active beam alternative would cost $449,120.00 less than the VAV alternative.

8   REFERENCES

2013 Building owners share experiences with Hydronic radiant cooling systems coupled with DOAS: what works and what doesn't? Annual Conference Co-Author

2012 Designing for net zero energy usage using Radiant-based heating and cooling

Systems, ASHRAE Annual meeting, San Antonio, Author

2012 Radiant Cooling: The Bangkok Airport ASHRAE Annual Conference San Antonio, Author

2011 Modeling Occupant Comfort Control in Larger Non Traditional Spaces ASHRAE Annual Meeting, Montreal, Canada, Author

2011 Hydronic System Concepts and Design Considerations for Radiant High Temperature Cooling and Low Temperature Heating, ASHRAE Annual Meeting, Montreal, Canada, Author

2011 Thermal Comfort Standards: US Developments ASHRAE Winter Meeting, Las Vegas, NV, Author

2011 Do Active Beams Save Energy and Provide Occupant Comfort? ASHRAE Winter Meeting, Las Vegas, NV, Author

2010 Controlling and Operating Active Chilled Beam Systems ASHRAE Annual Conference,

2010, ASHRAE annual meeting, Controlling and Operating Active Chilled Beam Systems, Albuquerque

2010, ASHRAE winter meeting, 30% below Standard 90.1, Its Easy Use Radiant, Orlando, 2010

2009, ASHRAE winter meeting, The Integration of Radiant Components to Maintain Occupant in a Multifunctional Space, Chicago, 2009

2008, ASHRAE winter meeting, Making Green Look Easy: Use Radiant, author

2006, Using Standard 55 PMV scale: Radiant and Variables Control, ASHRAE annual meeting Quebec City, author

2005, How to Design Building and HVAC Systems Based on Standard 55-2004, ASHRAE winter meeting, Orlando, author

2003, Using the PMV to Control the Indoor Environment, ASHRAE/CIBSE conference, Edinburgh, author

2003, Applied Radiant Cooling, ASHRAE winter meeting, Anaheim, author

2003, Can the PPD/PMV Be Used to Control the Indoor Environment?, ASHRAE/CIBSE conference, Edinburgh, author

1994, Radiant Heating and Cooling Systems ASHRAE, summer meeting, Orlando, author

1994, Control Strategies for a Combined Heating and Cooling Radiant System, CIBSE National Conference, Brighton, England, author

1993, Dynamic Comfort Control, CIBSE National Conference, Manchester, England, author

1993, Designing Comfortable Office Climates, ASHRAE Building Design Technology and Occupant Well-being in Temperate Climates, Brussels, Belgium, February 1993, author

1993, Thermal Comfort and Optimal Energy Use, ASHRAE Transactions 1993 V99, Pt 1, author

Building Design Technology and Occupant Well-Being in Temperate Climates, Brussels, Belgium, February, author

1992, The Design, Stimulation and Operation of a Comfortable Indoor Climate for a Standard Office, ASHRAE/DOE/BTEC conference, Clearwater Beach, FL, author

95: Analysis and design optimization of a photovoltaic airflow window for winter heating seasons

ABDULLAH HAREDY[1], GUOHUI GAN[2]

1 Department of Architecture and Built Environment, University of Nottingham, University Park, Nottingham NG7 2RD, UK, evxah3@nottingham.ac.uk
2 Department of Architecture and Built Environment, University of Nottingham, University Park, Nottingham NG7 2RD, UK, guohui.gan@nottingham.ac.uk

Computational Fluid Dynamics (CFD) and ECOTECT have been employed to model the mechanical and natural ventilation of a semi-transparent photovoltaics integrated airflow window and the daylighting impact of various PV transparent degrees (0.15, 0.2, 0.25, 0.3 and 0.35) on the interior space, respectively, for winter conditions noon time in London. This paper presents results of modelling of the airflow window system integrated with an office room for energy efficiency and adequate level of thermal and optical comfort. Results have revealed that buoyancy induced flow spreads the heat internally warming the space to be thermally acceptable during the heating seasons. The thermal and visual comfort was compared for different PV airflow window transparent levels to determine the optimum PV transparency for the office space. It has been found that a PV transparency of about 0.2 and 0.25 are optimal for the indoor comfort.

Keywords: CFD, mechanical ventilation, daylighting, natural ventilation, STBIPV/T.

1. INTRODUCTION

Buildings are accountable for a large portion of consumption of resources and energy in addition to production of a substantial amount of environmental pollutants. Building envelope is a major component that is responsible for transmitting heat between the environment outside and inside a space, therefore, it is essential to carefully balance heat loss and gain during the design process and accurately identify its properties. Fluid flow and heat transfer are the most critical phenomena that need to be analysed for the airflow windows in order to achieve design optimization. Thus, a technique is required for performing these purposes. Computational Fluid Dynamic (CFD) is suited to numerically analyse systems that transfer heat, circulate fluid and involved associated phenomena such as chemical reactions by computer algorithm simulation. This simulation is based fundamentally on replacing the differential equations governing the fluid flow and heat transfer from the principles of conservation of mass, momentum and energy (Patankar 1980; Versteeg and Malalasekera 2007; ANSYS 2009). Different numerical methods are applicable to obtain approximate solutions for governing equations such as the Finite Difference Method (FDM), Finite Element Method (FEM) and the Finite Volume Method (FVM) where the latter is the most employed code (Patankar 1980; Versteeg and Malalasekera 2007; ANSYS 2009).

This study intends to perform a numerical analysis of semi-transparent building-integrated photovoltaic thermal (STBIPV/T) airflow window system, that combines a standard double-pane unit on the inside and an outer PV glass pane separated by an intrusive air cavity where air is driven by pressure differential from outside to the inside through upper and bottom openings as seen in Figure 59, for cold climate conditions as determined by various influencing factors. A CFD analysis for the airflow window system under the effect of mechanical force only, buoyancy force only, and the combination of both forces considering the winter weather conditions for the city of London at noon time for the 29th of January and a solar irradiance of 707.36W/m2 and ambient air temperature of 5.9°C. Furthermore, daylighting studies are included for various PV transparent degrees. Generally, the paper offers a comprehensive optimization of the system and design for energy efficiency consumption and adequate level of thermal and optical comfort when applied to an office building.

The optical characteristics of the PV panel are represented with its transparency ratios where the proportion of daylight is shared comfortably in the interior lighting level providing natural light and mitigating the energy consumption of artificial lights. There are only few references in the literature where the PV transparency levels and its effect on thermal and visual comfort have been numerically investigated (Vartiainen, Peippo et al. 2000; De Boer and van Helden 2001; Miyazaki, Akisawa et al. 2005; Chow, Fong et al. 2007; Chow, Pei et al. 2009; Han, Lu et al. 2009; Chen, Chiang et al. 2012; Lu and Law 2013). Most of these studies discussed the ratio in the range of 10-60 per cent. De Boer and van Helden (2001) assigned the transparency of 25 per cent as a threshold and found that the 15 per cent is the optimum transparent level, though, Chen, Chiang et al. (2012) revealed that 26.9 per cent is the PV transparent ratio that can optimally achieve energy saving and daylighting comfort inside the space. In contrary, the investigation of (Chow, Fong et al. 2007) indicated that the range of 45-55 per cent PV transmittance can do justice to the electricity saving and visual comfort. The same was true with 40 per cent PV transmittance level from (Miyazaki, Akisawa et al. 2005). Thus, visual and thermal analyses will be performed under the effect of the PV transparencies of 0.15, 0.2, 0.25, 0.3, and 0.35 to find the optimal transparent level for the PV window unit during the summer and winter. The transparency will be limited to that range due to the fact that higher transparent values can excessively increase the direct solar contribution, and simultaneously decrease the indirect contribution through the absorption of solar radiation by the PV cells (De Boer and van Helden 2001).
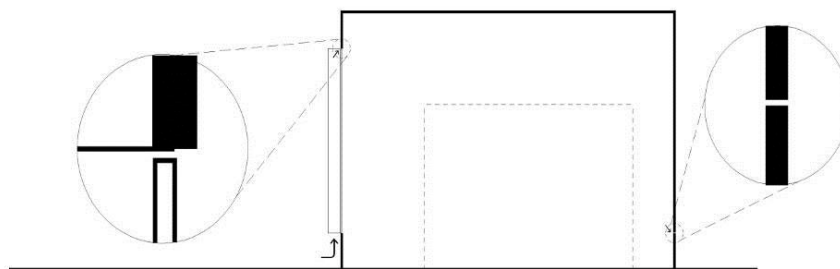

Figure 59: The airflow window system and the openings when designed for winter climate.

2   CALCULATION OF THE HEAT FLUX

The heat flux through the airflow window system can be calculated for the PV panel, glass panes, and the floor primarily based on the thermal properties of the system using the following equations (CIBSE 2006):

Equation 13: $Q_P = (G * \alpha_P) * (R_{se}/R_{si} + R_{se})$
Equation 14: $Q_{ge} = [(G * \tau_P) * \alpha_{ge}]/2$
Equation 15: $Q_{gi} = [(G * \tau_P) * (\alpha_{ge})] * \alpha_{gi}/2$
Equation 16: $Q_f = (G * \tau_P * \tau_{ge} * \tau_{gi} * A_w)/A_f$

Where:

$- Q_P$ is the PV panel heat flux (W/m²)
$- G$ is the solar irradiance (W/m²)
$- \alpha_P$ is the PV panel absorptivity
$- R_{se}$ is the external surface resistance (K.W^{-1})
$- R_{si}$ is the internal surface resistance (K.W^{-1})
$- Q_{ge}$ is the outer glass heat flux (W/m²)
$- \alpha_{ge}$ is the outer glass absorptivity
$- Q_{gi}$ is the inner glass heat flux (W/m²)
$- \alpha_{gi}$ is the inner glass absorptivity
$- Q_f$ is the floor heat flux (W/m²)
$- \tau_{ge}$ is the outer glass transmissivity
$- \tau_{gi}$ is the inner glass transmissivity
$- A_w$ is the window area (m²)
$- A_f$ is the floor area (m²).

3   CALCULATION OF AIR VELOCITY

For the winter condition, the air velocity passing through the airflow window into the inside space to the outlet can be calculated by using the mass balance equation which is as follows:

Equation 17: $q = \dot{m} * C_P * \Delta T$

where:

- q is the heat transfer rate (W)
- $\dot{m}$ is the mass flow rate (kg/s)
- C_P is the specific heat capacity (J/ (kg k))
- ΔT is the difference between the inlet and the outlet temperature (k)

An assumed air velocity of 0.35 m/s was considered to run an initial simulation to find out what type of temperature performance can produce. Then, it revealed that the difference between the inlet temperature and the outlet temperature was 11, therefore, the temperature needs to be increased 3 degrees to achieve the thermal comfort level. Thus, the above mentioned equation reveals that the air velocity of 0.25m/s can achieve the required temperature difference based on q = 90W. If the heat gains are much less, a minimum ventilation rate (e.g 10L/s-person) will be used for simulation.

4   RESULTS AND DISCUSSION

Three attempts of simulation have been carried out first for mechanical ventilation only, second for buoyancy ventilation only, and then for combined mechanical and buoyancy force to identify the effect of the buoyant flow on the performance of the airflow window when providing thermal comfort and adequate ventilation rate. For the mechanical force and combined forces simulations, a fan speed of 0.25 m/s was used as a base air velocity for airflow window at a window height of 2 m and width of 0.15 m.

4.2 Mechanical Ventilation Only

Under fan-driven mechanical ventilation, cool ambient air flowed into the office space from the opening of the airflow window at the bottom flowed across the top opening through the inside space to the outside the space through the outlet aperture at the back of the room as seen from Figure 60. The flow direction of incoming air can maintain the space properly ventilated where air is circulating widely over the inside environment. Even though, the incoming air jet is slightly attached to the room surface due to the Conada effect, the air velocity is relatively high inside the space more specifically inside the area of the occupied zone that is dominated with 3m/s air velocity which considered as uncomfortable. The force rather has elevated the velocity at the outlet to 5.15m/s with a mass flow rate of 66kg/s. Figure 61 shows the predicted temperature distribution inside the office room under fan-induced mechanical ventilation. The cool ambient air flowed from the window openings picking up the accumulated heat between the cavities into the inside space providing the indoor environment with air that maintains it thermally comfortable with a predominated temperature of 22 ^{0}C and 20^{0}C at the outlet.
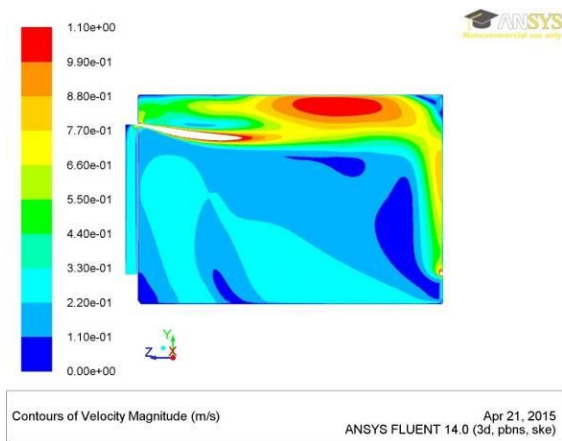
Figure 60: Air flow pattern
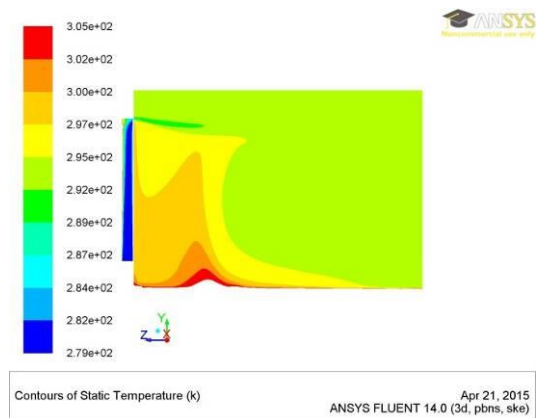
Figure 61: Temperature distribution
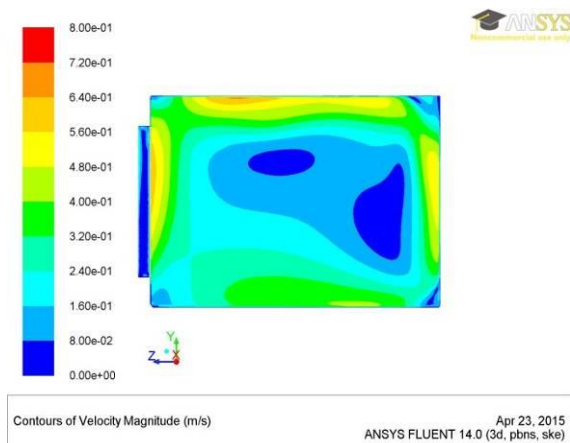
Figure 62: Air flow pattern
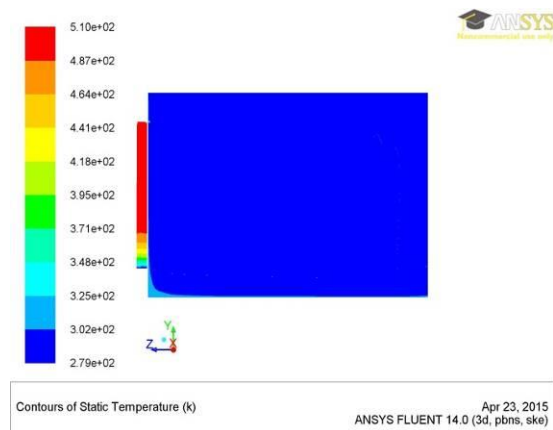
Figure 63: Temperature distribution

a. Buoyancy Ventilation Only

The changing pattern of air velocity behaviour under buoyancy-driven ventilation is shown in Figure 62. Due to the buoyancy effect only, cool ambient air flowed into the office space from the opening of the airflow window at the bottom flowed across the top opening through the inside space to the outside the space through the outlet aperture at the back of the room. Incoming air jets were formed and attached to the floor, roof, and walls with an air velocity ranging between 0.3 and 0.6m/s. Thus, the air movement around the inside space is relatively poor with predomination air velocity ranging between 0 and 0.2m/s which the latter represents the velocity at the outlet. The air flow rate with the buoyancy force rather decreased to a stagnant state of 0 L/s. Figure 63 presents the variation of temperature performance inside the office space due to buoyancy-induced ventilation. It can be noticed that, the accumulated heat between the cavities is impeded from being supplied to the inside environment causing overheating for the PV panel, with quite unrealistic temperature degree,

which in turns disturb the PV panel completely from functioning and leaving the room with thermally unaccepted condition with an average temperature of 28^0C.

b. Combined Mechanical and Buoyancy Ventilation Effects

The air flow patterns in the office space under both fan speed and buoyancy forces are shown in Figure 64. It can be noticed that the air movement is circulating slightly faster inside the space than it flowed under the mechanical force only due to the buoyancy force of cool incoming air which spread the indoor air refreshing the office room before it flows to the outdoor environment along the surface with the assistance of the mechanical force, though, the dominated air velocity varies between 1 and 3m/s with a mass flow rate at the outlet of 66kg/s. The predicted temperature distribution under the combined forces of mechanical and buoyancy is given in Figure 65. It can be seen that the addition of the buoyancy force to the fan speed force made negligible difference in distributing heat throughout the indoor environment where the heat in the left bottom of the space was cooled down slightly as a function of the opposite effect of the buoyancy that dropped the air on the floor vertically along the back (cool) glass pane to circulate more heat than it moved in the case of mechanical force only, however, the predominated indoor air temperature is still thermally comfortable with 22^0C.
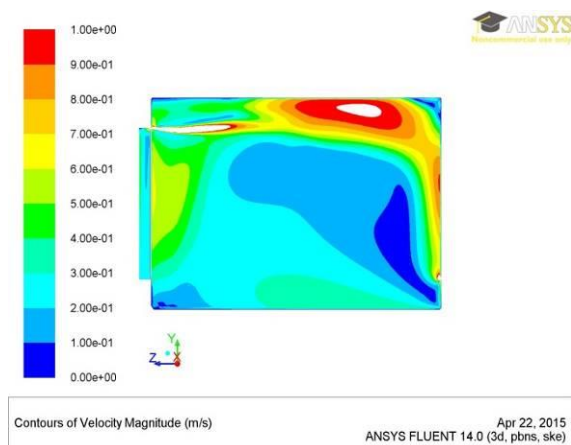
Figure 64: Air flow pattern
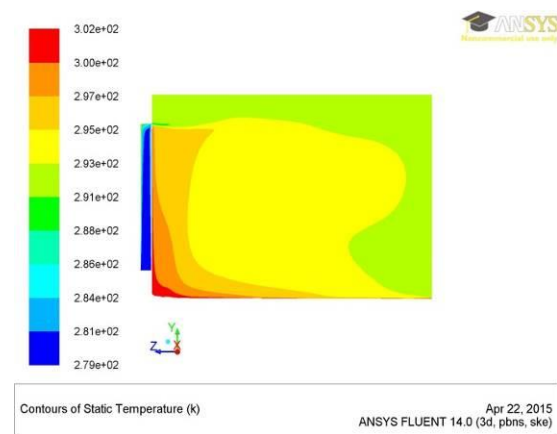
Figure 65: Temperature distribution

5. CONCLUSION

Predicting air flow and temperature distribution inside an office space, for two occupants, equipped with an airflow window due to the mechanical- and buoyancy-driven ventilation has confirmed that the addition of the buoyancy force would contribute in slight increase in air flow to spread the heat around the indoor space warming it to be thermally accepted. Indeed, the buoyancy force can assist the mechanical force for adequate indoor environment during the heating seasons as its force can be an opposing force for venting the air from the bottom of a room. Though, different PV transparency levels must be investigated to achieve the most optimal thermal level from the most suitable driving flow.

6. OCCUPIED ZONES WITH DIFFERENT PV TRANSPARENCY LEVELS

Since the combined forces for driving the flow is appropriate as revealed in the conclusion above, an occupied zone was considered for the model for more accurate analysis to reach the adequate thermally accepted zone under different PV transparency levels. The occupied zone was specified as 0.5m from any wall and 1m from the window with a height of 1.8m where normally the occupants reside the volume of air is confined by specific horizontal and vertical planes (Institution 2014). The zone is represented by two horizontal and three vertical planes where the formers are the head and foot planes and the latter are the front wall, back wall, and the side wall planes. Under each PV transparency the temperature was calculated for each plane and the average temperature of the zone. Each plane was assigned a rake to identify its temperature. Figure 66 illustrates the occupied zone within the model and the rake position of each plane in the zone. The variations of the predicted temperatures inside the occupied zone under the effect of the heat passing through PV panel with different transparencies of 0.15, 0.2, 0.25, 0.3, and 0.35 was plotted for each plane of the zone.
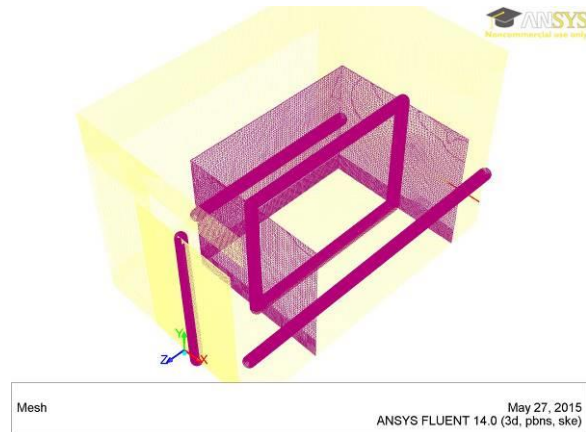
Figure 66: The occupied zone within the model space and the rake of each plane

6.1 PV Transparency Level of 0.15

Figure 67 shows the temperature distribution for the back and front planes vertically along the space height. It can be observed that the temperature of the front plane is slightly higher than the back one due to its direct exposure of the window with a highest temperature approximately of 33.37^0C and the lowest temperature of 20.42^0C while the peak temperature of the back plane is approximately 28.98^0C and the minimum is 19.88^0C. Thus, the temperature of vertical depth of the space is ranging from 19.88-33.37^0C which is thermally unaccepted level for the occupants. Figure 68 shows the temperature distribution for the head and foot planes horizontally along the model width. The temperature of the foot plane is higher than the head plane since the former is directly absorbing the heat from the floor with a highest temperature around 33.37^0C and the lowest temperature of 28.98^0C while the maximum temperature of the head plane is approximately 20.51^0C and the minimum is 20.26^0C. Thus, the temperature of horizontal depth of the room is ranging from 20.26-33.37^0C and that considered as an overheated area for the occupants.

Figure 67: Front and back plane temperatures under 0.15 PV transparency level
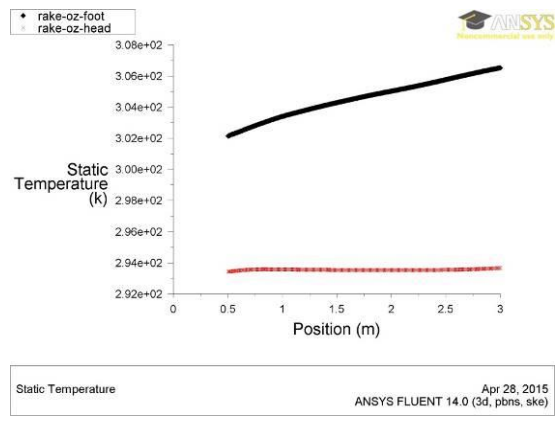
Figure 68: Head and foot plane temperatures under 0.15 PV transparency level

6.2 PV Transparency Level of 0.2

The results given in Figure 69 represent the temperature distribution for the back and front planes vertically as a function of the space height. For the lowest point of the occupied zone, the temperature of the front plane is relatively higher than the temperature of the back one since it receives direct solar radiation from the window with an approximate temperature of 24.55^0C and 17.98^0C for the highest point of the zone while the peak temperature of the back plane is approximately 21.52^0C and the minimum is 17.55^0C. Figure 70 shows the temperature distribution for the head and foot planes horizontally as a function of the zone width. The temperature of the foot plane is in its highest at the nearest point to the window an approximate temperature of 24.55^0C and the lowest temperature of 21.52^0C at the farthest point from the window while the maximum temperature of the head plane is approximately 18.1^0C and the minimum is 17.98^0C. Thus, the temperature of horizontal and vertical depth of the room can bring the space into a thermally adequate level for the occupants.
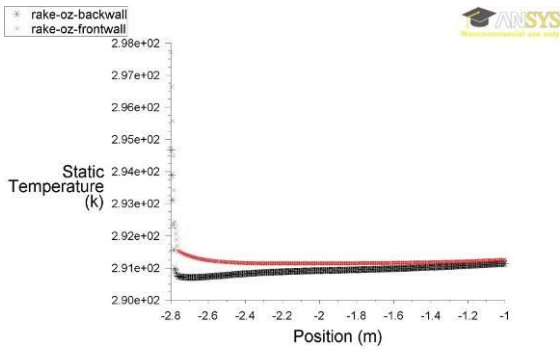
Figure 69: Front and back plane temperatures under 0.2 PV transparency level

Figure 70: head and foot plane temperatures under 0.2 PV transparency leve

6.3 PV Transparency Level of 0.25
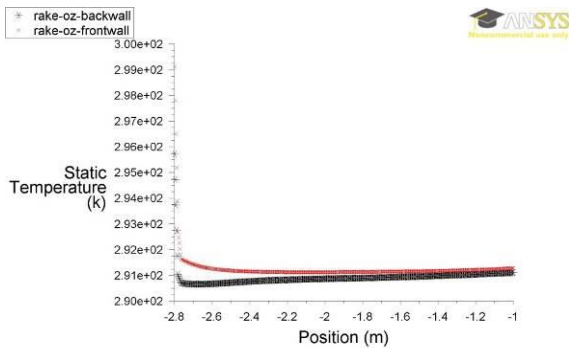
Figure 71: Front and back plane temperatures under 0.25 PV transparency level
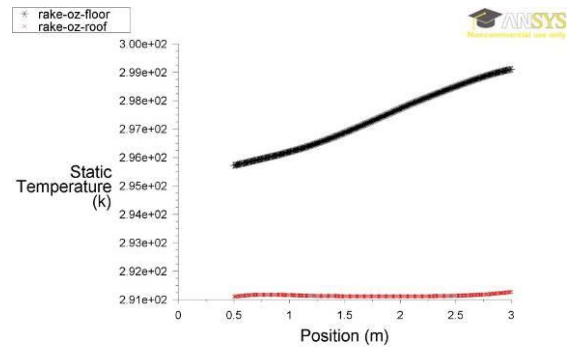
Figure 72: head and foot plane temperatures under 0.25 PV transparency level

The temperature distribution for the back and front planes vertically along the space height is presented in Figure 71. Being close to the window, the temperature of the front plane is slightly higher than the back one. However, the temperatures of both planes are thermally adequate that falls into the range between 17.5-25.95^{0}C with a highest temperature approximately of 25.95^{0}C and the minimum temperature of 17.97^{0}C for the front plane and the highest of 22.56^{0}C and the minimum is 17.5^{0}C for the back plane. The temperature distribution for the head and foot planes horizontally along the room depth is shown in Figure 72. The temperature of the foot plane is higher than the head plane with a maximum temperature of 25.95^{0}C and the minimum temperature of 22.56^{0}C while the highest temperature of the head plane is approximately 18.12^{0}C and the minimum is 17.94^{0}C. Thus, the occupied zone planes achieve the required thermal comfort inside the space.

6.4 PV Transparency Level of 0.3

Figure 73 compares the temperature predictions of the front and the back planes of the occupied zone vertically from their bottom to their top. A slight deviation between the two temperatures can be noticed since the front plane is being close to the window which allows excessive solar radiation to be received. However, the temperatures of the back plane are thermally adequate as they fall into the range between 17.45-23.58^{0}C while they do into the range of 17.98-27.26 for the front plane which consider as overheated. Figure 74 compares the temperature performance for the head and foot planes horizontally from the back offset to the window offset that represents the occupied zone. It can be seen that the temperatures of the foot plane relatively deviate from the head temperatures with a difference of 9^{0}C. This can be explained by the fact that foot plane is absorbing most of the incident solar radiation coming from the window causing the plane to be excessively heated with temperatures range of 23.58-27.26^{0}C. Though, the head plane is still left cold with temperatures ranging in 17.96-18.14^{0}C.
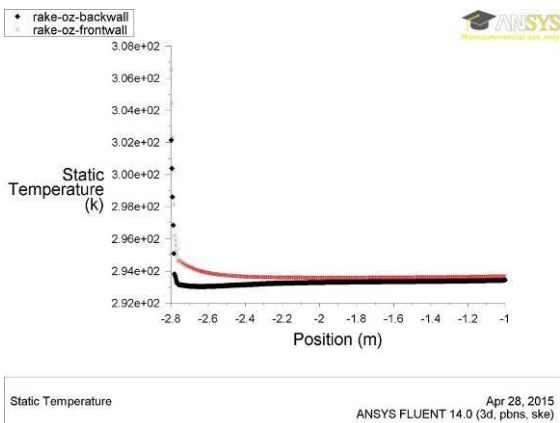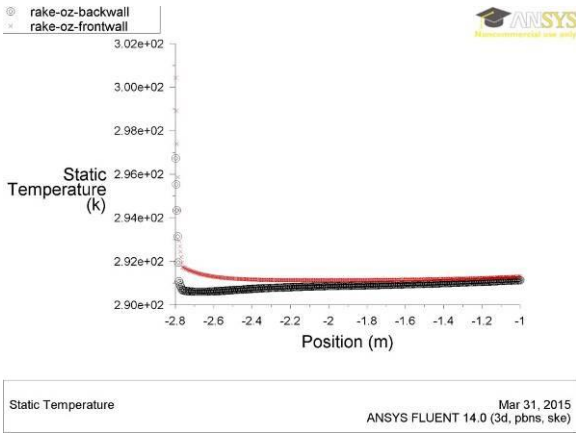
Figure 73: Front and back plane temperatures
under 0.3 PV transparency level

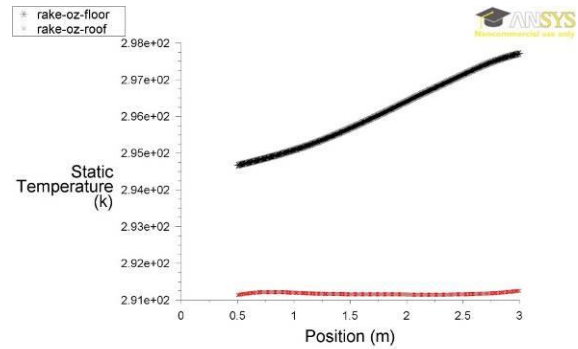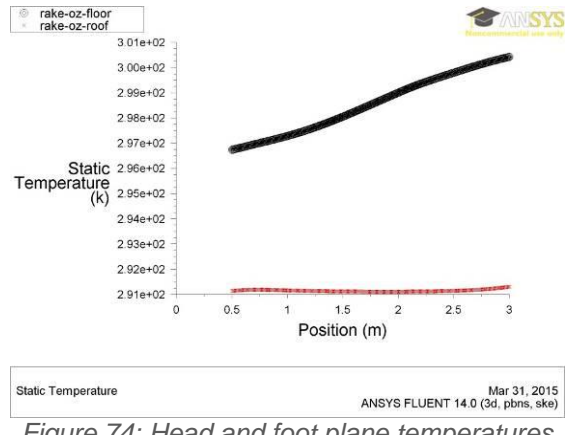Figure 74: Head and foot plane temperatures
under 0.3 PV transparency level

6.5 PV Transparency Level of 0.35
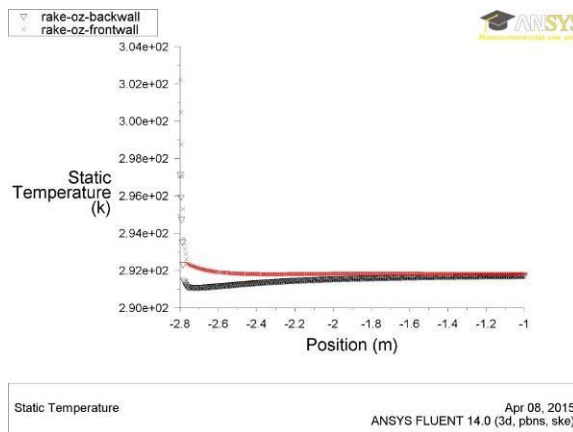
Figure 75: Front and back plane temperatures under 0.35 PV transparency level
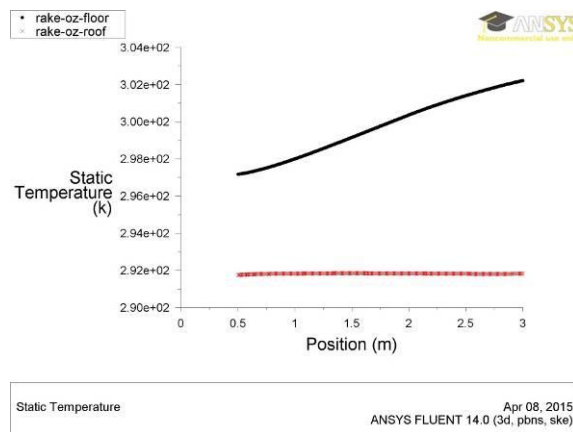
Figure 76: Head and foot plane temperatures under 0.35 PV transparency level

The temperature distribution for the back and front planes vertically along the space height is presented in **Error! Reference source not found.**. The direct expose to the window and the high level of PV transparency has increased the temperature of the front and the back planes where the front plane temperature is relatively higher than the back plane as both temperature magnitudes range between 17.97-29.06^{0}C with a highest temperature approximately of 29.06^{0}C and the lowest temperature of 18.65^{0}C for the front plane and the maximum of 24.01^{0}C and the minimum is 17.97^{0}C for the back plane. The same is true for the temperature distribution of the head and foot planes horizontally along the room depth shown in Figure 76 where the

temperature of the foot plane is higher than the temperatures of the head plane with a maximum temperature of 29.06^0C and the minimum temperature of 24.01^0C while the highest temperature of the head plane is approximately 18.69^0C and the minimum is 18.59^0C due to the buoyancy effect on the floor and the insulation of the head. However, the temperature of horizontal width of the room is ranging from $18.59\text{-}29.06^0$C and it is regarded for occupants as thermally uncomfortable

7   CONCLUSION

An occupied zone was defined within the model interior to attain optimized results for the collective buoyancy and mechanical driving forces employing variable PV transparencies to carefully ensure a thermally accepted area for the occupants. From what has been illustrated above, each PV transparency supplied the interior space with different amount of heat that kept the occupied zone either thermally suitable or overheated. The PV transparency of 0.2 was the only degree that satisfied the required level of thermal comfort; yet, the 0.25 transmittance has attained similar thermal performance with one temperature degree above the thermal standard. However, overheating was prominent with the rest of the transmittance values inside the space. Thus, daylighting analyses essentially needs to be performed for the PV panel with each transparent value to identify the most suitable transparent degree for the room interior that combines thermal and visual comfort.

8   PV Panel Daylighting Analysis

The necessity for the daylighting analysis has urged to utilize a computer tool that can demonstrate each transparent value implications on the PV panel and the interior space. ECOTECT was applied to estimate the indoor illuminanace levels and daylight factors and capture the impact of each transparent degree of the PV panel when equipped with the airflow window for the office space. The daylight factors were predicted, using ECOTECT, as an initial design parameter under each transparency (0.15, 0.2, 0.25, 0.3, and 0.35) for points that aligned with the centre of the window along the space width. The average daylight factor required for general office space is 2 per cent as minimum value (CIBSE 2006), however, the average daylight factor can also be calculated as follows:

Equation 18: D = 0.1 x P

where:

- D = Daylight factor
- P = Percentage glazing to floor area

As such, the average daylight factor for the interior space of the office model can be estimated as follows: $D = 0.1 \text{ x } (5.6 \div 20) \text{ x } (100 \div 1) = 2.8\%$

8.1 PV Panel Transparencies Daylighting Effect
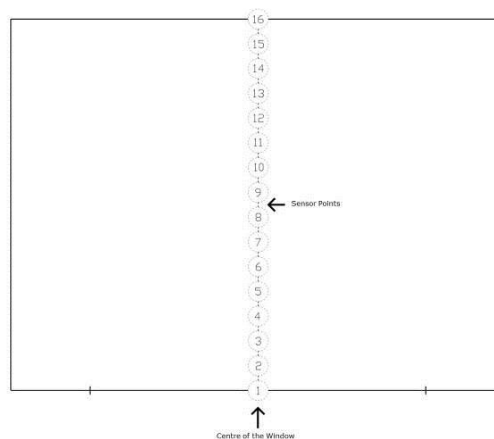
Figure 77: Sensor points along the depth of the room aligned with the centre of the window
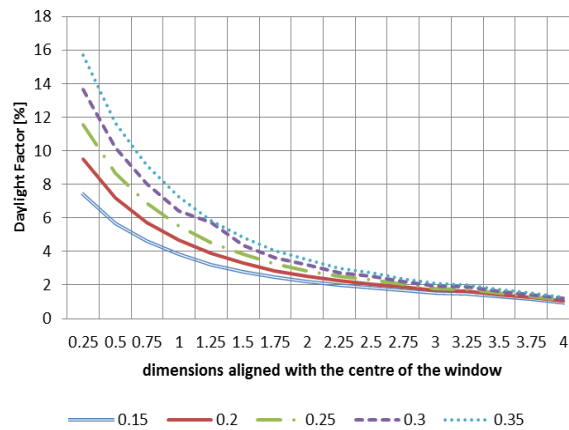
Figure 78: Comparison of the daylight Factors for different transparencies

*The sensor points were defined along the depth of
the room and aligned with the centre of the window
with an interval of 0.25m, presented in*

Figure 77, in order to read the daylight factors of the interior space under the effect of each transparent level. The behaviour of the daylight factors of each transparent degree is shown in Figure 78. It appears that similar trends of daylight factors of each transparency are produced demonstrating a maximum value from the nearest point to the window, where the solar incidence is transferred, with a gradual decrease to the far end of the room. However, the daylight factors of each value are different where the higher transparent value is applied; the higher daylight factors are attained. The most suitable transparent degree is the one that meets the minimum required daylight factor for the space. The average daylight factor for the values 0.15, 0.2, 0.25, 0.3, and 0.35 are 1.96 per cent, 2.29 per cent, 2.62 per cent, 2.92 per cent, and 3.28 per cent respectively.

As a consequence, all of the transmittances are in compliance with the required average daylight factors since they produced more than the minimum required value except the 0.15 degree which its performance is below the standard; yet, the 0.2 and 0.25 degrees are the most suited levels because they combine both comfortable optical and thermal aspects.

9   CONCLUSION

Optical and thermal analyses were performed for the PV panel under the effect of five different degrees of transparencies: 0.15, 0.2, 0.25, 0.3, and 0.35 in order to distinguish the transmittance that achieves the optimum comfort of visual and thermal level for the interior space and maintain the PV sheet in a moderate temperature for an efficient performance. The previous discussion reveals that each level of transparency can be either thermally comfortable or uncomfortable to the room occupants providing the interior with different temperature degrees that reach up to 29^0C. Though, the PV cells can function effectively with each transparent value since they reach up to 29^0C with the lower transparent degree of 0.15 and decrease gradually with higher levels. However, the transparent levels of 0.2 and 0.25 are distinguished with maintaining the inside environment visually and thermally convenient for the occupants as they achieve more than the minimum requirements of the daylight factors for the office room, two per cent while the 0.15 transparent value leaves the interior not adequately lit. Thus, for the time of simulation (noon time) the degrees of 0.2 and 0.25 transparency are the most appropriate transparent level to be specified for the PV panel that encompasses the features of optimizing the PV performance, and guaranteeing the space occupants optical and thermal comfort.

10 REFERENCES

ANSYS, F. T. S. (2009). ANSYS Fluent 14.0 Theory Guide. Lebanon, NH, USA, ANSYS Inc.

CHEN, H. J., C. M. Chiang, et al. (2012). "Thermal and optical properties of semi-transparent amorphous silicon BIPV for building application." Advanced Materials Research **343**: 199-204.

CHOW, T., K. Fong, et al. (2007). "Performance evaluation of a PV ventilated window applying to office building of Hong Kong." Energy and Buildings **39**(6): 643-650.

CHOW, T. T., G. Pei, et al. (2009). "A comparative study of PV glazing performance in warm climate." Indoor and Built Environment **18**(1): 32-40.

CIBSE, G. A. (2006). "Environmental design." The Chartered Institution of Building Services Engineers, London.

DE BOER, B. and W. van Helden (2001). PV MOBI, PV Modules Optimised for Building Integration, Netherlands Energy Research Foundation ECN.

HAN, J., L. Lu, et al. (2009). "Thermal behavior of a novel type see-through glazing system with integrated PV cells." Building and Environment **44**(10): 2129-2136.

Institution, B. S. (2014). Ventilation for non-residential buildings. Performance requirements for ventilation and room-conditioning systems. London, BSI. **BS EN 13779:2004:** 56.

LU, L. and K. M. Law (2013). "Overall energy performance of semi-transparent single-glazed photovoltaic (PV) window for a typical office in Hong Kong." Renewable Energy **49**: 250-254.

MIYAZAKI, T., A. Akisawa, et al. (2005). "Energy savings of office buildings by the use of semi-transparent solar cells for windows." Renewable Energy **30**(3): 281-304.

PATANKAR, S. V. (1980). Numerical heat transfer and fluid flow, Taylor & Francis Group.

VARTIAINEN, E., K. Peippo, et al. (2000). "Daylight optimization of multifunctional solar facades." Solar Energy **68**(3): 223-235.

VERSTEEG, H. K. and W. Malalasekera (2007). An introduction to computational fluid dynamics: the finite volume method, Prentice Hall.

323: The potential of external shading devices for comfort extension and energy savings in Kenya

LORNA KIAMBA[1], LUCELIA RODRIGUES[2], BENSON LAU[3]

1 University of Nottingham, NG7 2RD, Nottingham, UK. Email: laxlk2 @nottingham.ac.uk
2 University of Nottingham, NG7 2RD, Nottingham, UK. Email: Lucelia.Rodrigues @nottingham.ac.uk
3 University of Nottingham, NG7 2RD, Nottingham, UK. Email:Benson.Lau @nottingham.ac.uk

The use of shading systems for climate control in tropical climates is well documented. Previous research has indicated that if shading devices are installed on the exterior of the building, they are able to block solar radiation effectively before it passes through glazing and in so doing reduce the overheating potential. A review of contemporary office buildings in the warm humid city of Mombasa, Kenya reveals the predominance of highly glazed buildings which often rely on active air conditioning systems for cooling purposes. Following an initial study of suitable design strategies for warm-humid climates, the authors found that responsive sun shading could be used to significantly improve indoor thermal comfort conditions and in so doing reduce the need for electricity for cooling. In this paper, using results obtained from the dynamic simulations of a typical office building in Mombasa, the authors focus on quantifying the effect of external shading devices on indoor thermal comfort and energy use. First, the performance of horizontal, vertical and egg crate sun shading devices was investigated. The results indicated that the egg crate shading has the most significant impact in decreasing discomfort hours by up to 50% more than horizontal or vertical shading. Next, solar heat gain coefficients were derived for various shading types (horizontal, vertical and egg crate) and their impact on indoor thermal comfort and energy savings calculated. The solar heat gain coefficients (as a result of external shading) and curve fit equations/graphs suitable for use with various projection factor ratios (a simple ratio used to define the relationship between the shading element depth and window size) were derived for the four cardinal compass orientations. Using these equations and graphs, it was possible to estimate the potential annual energy savings (of up to 120kWh/m^2 or 74.68% improvement) with building information of the glazing area, orientation of the window and the PF ratio. It was suggested that these solar heat gain coefficients, equations and graphs show potential for use by local building practitioners in deriving the potential comfort and energy savings during early design stages of similar type buildings.

Keywords: external shading devices, solar gain, PF ratio, warm humid climate

1. INTRODUCTION

In warm humid regions, the main thermal comfort challenge in buildings arises from relatively high temperatures coupled with high relative humidity. Specifically, in Mombasa, the annual temperature averages range between 27°C to 32°C during the daytime and 21°C to 27°C during the night-time while humidity levels have an annual average of 75%. In a growing number of cases, the effect of these climatic conditions and poor building design can often result in overheating. More often than not, this leads to poor indoor thermal comfort conditions which necessitate the introduction of active air conditioning systems that tend to be costly and unsustainable. In Kenya, latest available figures indicate that electricity usage in non-domestic buildings is responsible for 30% of the total annual consumption. Further, annual growth in electricity demand is forecasted to be 8%, compared to an annual increase of electricity supply capacity of 3 to 4% (KPLC, 2013, p.115-120). In the midst of growing electricity demand and a potential deficit in supply, the influx of poorly designed buildings has intensified the need to ensure that local buildings embrace climate-responsive solutions that can extend occupant comfort thereby reducing the need for electricity intensive environmental control systems.

In general, design strategies for warm humid regions should aim to restrict heat gain and encourage the removal of excess heat that imposes a cooling load within buildings. In a previous case study review, the authors examined the suitability of design strategies for warm-humid climates and identified potentially appropriate design strategies including orientation, shading, daytime and night time ventilation and thermal mass (Kiamba et al., 2014). Further studies stemming from this work have indicated that shading plays a significant role in extending indoor thermal comfort due to the mitigation of solar gain (Kiamba et al., 2015). Indeed, a significant number of researchers have indicated that external shading devices should be integrated in buildings in warm humid regions so as to reduce the impact of solar gain indoors (Koenigsberger et al., 1974, Givoni, 1994, Szokolay, 2008). For purposes of this study, the authors focused on quantifying the effect of external shading on extending indoor thermal comfort for occupants and reducing the need for active air conditioning. With this in mind, solar heat gain coefficients for horizontal and vertical shading elements and a combination of both for various orientations were derived. These solar heat gain coefficients (SHGC) were used to define the impact of using various configurations of shading elements and the resultant effect on indoor thermal comfort and energy use outlined. Guided by the results of this study, estimates were given of the anticipated energy savings that could be achieved by designers depending on the shading type provided. It was suggested that the results of this exercise could serve as a reference for other building practitioners who seek to know the impact of the proposed external shading (as defined by the SHGC) on overall cooling energy reduction.

2. METHODOLOGY

Using dynamic thermal simulations, a series of parametric studies were conducted to investigate the effect of various shading configurations on indoor thermal comfort and energy use. To facilitate this process, a simplified model of a typical office building in Mombasa, the Mombasa Uni Plaza was built and generated using TAS. The full building model was constructed as is shown in Figure 79. However, to reduce modelling complexity and closely exemplify the base case in the case study low-rise office building, selected zones of various orientations on the 3rd floor formed the focus of the study. Guided by the results of the initial simulations, the next stage involved the derivation of the solar heat gain coefficients as a result of external shading (Shading $_{external}$). Firstly, simulations were run for the selected case study building under the existing orientation (the existing orientation is offset by approximately 20° along the North-South axis). Next, to allow for the interpretation of results for similar buildings of different orientations, simulations were run for a 'true' North-South orientation and estimates of energy savings due to a reduction of the SHGC and the results calculated.

Figure 79: Perspective (left), front elevation (middle) and 3rd floor plan(right) of the base case model.

2.1 Assumptions

General assumptions for the base case model are presented in Table 45. Fixed parameters remained the same for all the simulations undertaken (as indicated). Similarly, although they varied in the individual simulation cases, the variations to the shading configurations were the same for all the cases investigated.

Table 45: General assumptions for the base case model

Fixed Parameters
• Weather data: Calibrated EnergyPlus (.epw file) for Mombasa, Mombasa-Moi 638200 (SWERA)
• Location: Latitude -4.03, Longitude: +39.62
• Calendar: Simulations were run for the full year and results extracted for occupancy periods - weekdays, working hours (0800-1800hrs)
• Thermal comfort: Adaptive comfort limits were derived as a function of outdoor temperature (Nicol and Humphreys, 2002) giving a comfort range of 27.5 to 31.5°C for free-running buildings.
• Ventilation: 5ach (National Planning and Building Authority - Kenya, 2009, NN10.9)
• Infiltration: 1 air change per hour (ach)
• Internal Gains: Occupancy + Equipment (21W/m^2)
• Glazing and frame types:10mm Suncool Classic 25/34 Bronze glazing, (Y-value: 5.56W/m^{2}K) in aluminium frame
• Floor Slab/ Ceiling: 150mm Lightweight Hollow Pot (HP) Concrete Slab (Y-value: 4.33 W/m^{2}K)
• External Walls: External: 200mm Lightweight concrete(Y-value: 3.55 W/m2K). Internal: Chipboard on studs (Y-value: 2.67 W/m2K)
• Roof: Concrete Tiles with lightweight concrete slab with attic ventilation (Y-value: 3.95 W/m2K)
• Individual Room/Zone Window Size: 4.5m^2 (1.5m height x 3m width)
Varied Parameters

• Shading:
     a) No shading
     b) Horizontal shading (Various depths of 0.3, 0.6, 0.9, 1.2, 1.5, 1.8 metres)
     c) Vertical shading (Various depths of 0.3, 0.6, 0.9, 1.2 metres)
     d) Egg crate shading (Various depths of 0.1, 0.15, 0.3, 0.45, 0.6, 0.9 metres)

The simulations were run for four varying ventilation conditions for all the zones at the rate of 5ach with 1ach infiltration as is recommended for office buildings in the national regulation requirements (National Planning and Building Authority - Kenya, 2009, NN10.9). These conditions were defined as follows. Condition A: No ventilation (ZV) during weekdays. Condition B: Daytime ventilation (DTV) during weekdays from 0800hrs to 1800hrs (usual office working hours), with a minimum of 33% effective opening window area. Condition C: Night time ventilation (NTV) during weekdays from 1800hrs to 0800hrs, with a minimum of 33% effective opening window area. Condition D: All day ventilation (ADV) during weekdays with ventilation for twenty four hour periods, with a minimum of 33% effective opening window area. On weekends, only infiltration at the rate of 1ach was factored in. Additionally, for all conditions, except ZV, windows were closed if outdoor temperature exceeded indoor temperature.

2.2 Simulation Breakdown

To begin with, dynamic simulations were run for a variety of shading types and depths in a quest to test their efficacy (simulation plan A). The effect of shading devices was investigated and the percentage number of hours that the indoor air temperature recorded annually (for occupancy hours, 0800-1800hrs only) that were predicted to be above the upper comfort limits in Mombasa (31.5°C - as calculated using the adaptive comfort model defined in ASHRAE 55-2010) were derived. For these simulations, the following shading configurations were considered as illustrated in Figure 80.
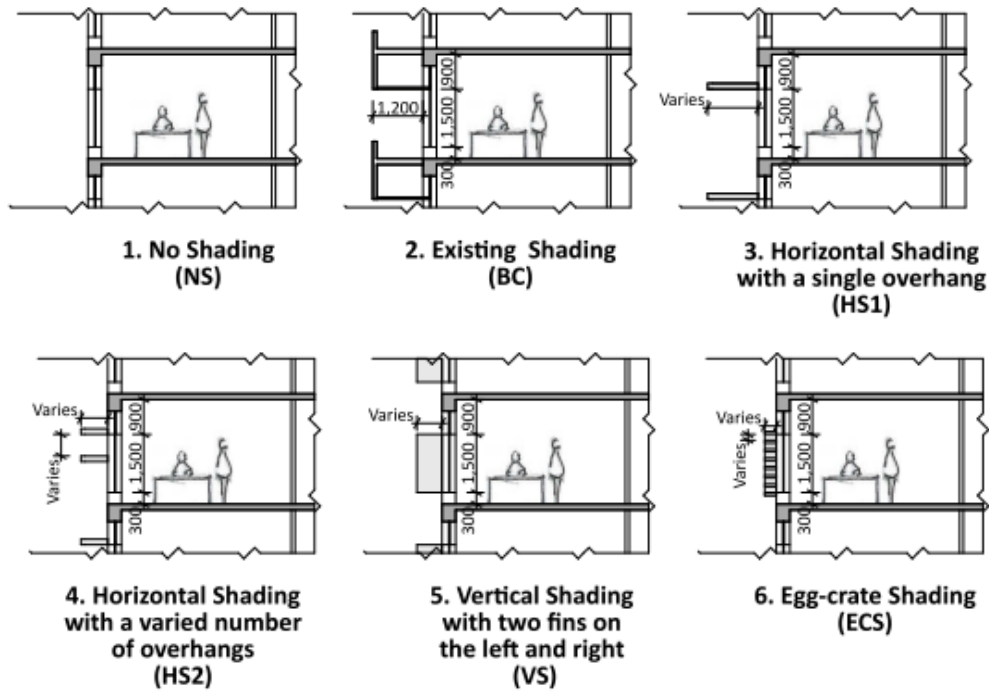
Figure 80: Simulation shading configurations

Next, the authors derived the solar heat gain coefficients for various external shading devices (simulation plan B). These simulations accounted for the reduction of solar heat gain (G-value) due to direct and diffuse shading on a window surface. The G-Value (W/m^2) is the total amount of solar heat that passes through glazing (Szokolay, 2008). The lower the G-value, then the lower the amount of solar heat transferred into the building. Solar heat gain coefficient (SHGC) is a non-dimensional term that refers to the ratio between the solar heat transmitted and the solar irradiance of the window surface (Szokolay, 2008). Using SHGC, one can derive the total solar heat gain (Q_s) using the following equation:

Equation 19: Total solar heat gain (Szokolay, 2008, p. 40) $Q_s = A \; x \; G \; x \; SHGC$

Where:

- A = area of the window
- G = total amount of solar heat that passes through glazing
- SHGC = solar heat gain coefficient

Due to relatively high solar exposure in warm humid regions, it is practical to design for a low SHGC to reduce the risk of overheating. The total solar heat gain coefficient ($SHGC_{total}$) of any fenestration system can be estimated using the following equation:

Equation 20: Total solar heat gain (Building Sector Energy Efficiency Project - BSEEP, 2013, p.114) $SHGC_{total} = SHGC_{external} \; x \; SHGC_{glazing} \; x \; SHGC_{internal}$

Where:

- $SHGC_{external}$ = solar heat gain coefficient of external shading devices (1, if no external shading device is used)
- $SHGC_{glazing}$ = solar heat gain coefficient of the glazing
- $SHGC_{internal}$ = solar heat gain coefficient of internal shading devices (1, if no internal shading device is used)

For purposes of this study, the SGHC $_{glazing}$ of the base case glazing was set at 0.353 as was obtained from TAS for 10mm 'Suncool Classic 25/34 Bronze' glazing as per manufacturer properties. Although some of the occupants in the case study building used internal blinds, their impact was not factored for purposes of this analysis. From these simulations, the SHGC $_{external}$ due to the presence of external shading devices as overhangs, side fins or egg crates, was defined as the ratio of the global solar radiation (direct, diffuse, reflected) received inside the building in the presence of shading devices to the global solar radiation which would be received inside the building without them. The extent to which this is possible was derived from the above simulations for all four orientations of the case study building (North-20°, East-110°, South-200° and West-290°). To allow for the clearer interpretation of results, various shading configurations were categorised in terms of a 'projection factor' as defined by ASHRAE (2013). The projection factor (PF) is defined as the ratio of the horizontal depth (distance between outside edge of shading to the outside surface of the glass) of the external shading projection (A) divided by the sum of the height of the fenestration plus the distance from the top of the fenestration to the bottom of the farthest point of the external shading projection (B), in consistent units. Figure 81 illustrates the PF for horizontal and vertical shading. Egg crate shading considers a combination of the two.
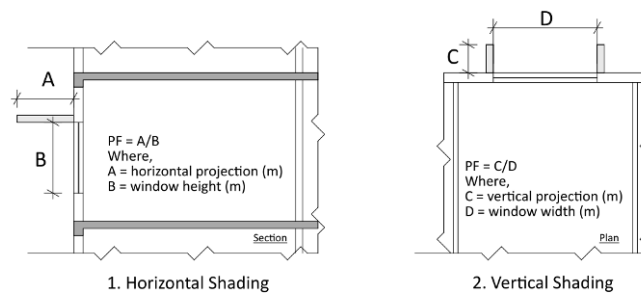
Figure 81: Projection factor ratio for horizontal and vertical shades.

The next set of simulations (simulation plan C) involved the derivation of the SHGC $_{external}$ for the case study building under 'true' North-South orientation (North-0/360°, East-90°, South-180° and West-270°). Further to this, estimates of the energy reduction resulting from the use of external shading devices were derived for various orientations.

3   RESULTS AND DISCUSSION

The results of the various simulations were outlined in separate sections for clarity purposes.

3.1 Simulation Plan A

First, to compare the impact of the existing shading devices (horizontal shading of 1.2m depth) on indoor comfort, dynamic simulations were run for two cases, with and without existing shading, and the results compared. The results revealed that the existing shading significantly decreases discomfort hours indoors during working hours (0800-1800hrs). A comparison of NS and BC under ZV ventilation strategy found that the existing shading reduced the number of discomfort hours by 33%. This figure reduces when comparing NS and BC under other ventilation strategies. This indicates that the ventilation strategy also plays a significant role in improving comfort indoors. Further comparison of discomfort hours under varying ventilation strategies reveals significantly higher differences. The worst performing condition (NS under ZV) was found to have 77.93% more discomfort hours that the best performing condition (BC under ADV). In general, it was found that ADV performed better than all other ventilation strategies for all shading types and all locations whereas ZV gives the worst indoor conditions. Additionally, DTV performed better than NTV and ZV but worse than ADV. In terms of orientation, the zone exposed to the West was found to experience the highest levels of discomfort. Similarly, this zone was worst affected by the lack of sun shading. This performance was anticipated given previous local climate analysis (Kiamba et al., 2015) that found the Western orientation to be the most critical in terms of solar gain. Further, the East orientated zone performed worse than the North and South, respectively. It was also determined that the existing horizontal shading was more effective in the North and South orientated zones and less effective in the West and East. This is suggested to be due to the low angle sun experienced in the West and East orientated zones.

Next, the horizontal depth of existing canopy was varied at incremental intervals of 300mm (with a maximum of 1800mm). The results revealed that the addition of horizontal shading depth significantly decreases

discomfort hours indoors during working hours (0800-1800hrs). An increase in the depth of the horizontal shading element resulted in a significant reduction of discomfort hours of up to 38.97%, 7.62% and 6.32% for simulations run under ZV, DTV and ADV, respectively. The rate of the reduction in discomfort hours reduced significantly after the horizontal depth exceeded 1500mm. As with previous simulations, the zone orientated in the West showed the greatest reduction in discomfort hours with an increase in depth of the horizontal shading element. Similarly, it was noted that an increase in the depth of the horizontal shading element was more effective in reducing the overall number of discomfort hours in the zones orientated to the North and South. Subsequently, the horizontal shade depth was broken down into an increased number of shading elements to reduce the significant depth of 1800mm. These results were compared with single horizontal elements of the total depth of all the horizontal elements. Horizontal elements of 300mm and 600mm deep were selected to reduce the use of overly deep elements. The results revealed that the shading significantly decreases discomfort hours indoors during working hours (0800-1800hrs). An increase in the depth of the horizontal shading element resulted in a significant reduction of discomfort hours of up to 39.01%, 7.62% and 6.36% for simulations run under ZV, DTV and ADV, respectively. These results indicated that it was possible to reduce the overall depth of individual horizontal shading elements and get the same reduction in discomfort hours by using multiple horizontal elements of shorter depth. Further, it was revealed that this action ensured that performance of the shading elements was kept within ±1% of that of the full length elements. As with the previous two simulations, the zones orientated to the North and South showed the lowest number of discomfort hours.

The impact of vertical shading on the increase or decrease of discomfort hours indoors during working hours (0800-1800hrs) was reviewed independently of any other shading. The dynamic simulation results revealed that the shading significantly decreases discomfort hours indoors during working hours (0800-1800hrs). The introduction of vertical shading elements resulted in a significant reduction of discomfort hours of up to 34.06%, 5.1% and 2.99% for simulations run under ZV, DTV and ADV, respectively. Zones orientated to the West and the East showed the highest reduction in percentage discomfort hours of up to 26.36%. Unlike the previous simulations examining the effect of horizontal shading, it was noted that vertical shading had more of an impact on zones orientated to the West and the East. It is suggested that the vertical shading elements work better to reduce the amount of solar heat gain as a result of high angle sun in the mornings (East) and the afternoons (West). Additionally, it was noted that vertical shading has less of an impact in the reduction of discomfort hours for all orientations when compared to horizontal shading elements.

Following the results obtained from horizontal and vertical shades, a combination of both horizontal and vertical shading solutions (egg crate shading) were tested for all the selected zones of varying orientations. The use of egg crate shading resulted in a significant reduction of discomfort hours indoors during working hours (0800-1800hrs). Results indicate that the number of discomfort hours can be almost halved when compared to the performance of horizontal or vertical elements. These results indicate their high shading efficiency, suggested to be as a result of the complex shading patterns that they provide. Further, it was found that an increase in the depth of the egg crate shading to more than 100mm did not significantly increase the number of comfort hours. Additionally, as with the previous simulations, the West and East orientated rooms did not perform as well as the North and South orientated zones. Nonetheless, the use of egg crate shading was found to significantly narrow down the gap in the percentage of discomfort hours for all orientations.

3.2 Simulation Plan B

Shading devices were shown to have a significant impact on improving internal thermal conditions and as a result, extending comfort conditions. Horizontal shades have the greatest impact on the North, South, West, and East orientated zones, respectively. On the other hand, vertical shades have the greatest impact on the West and East facades, respectively. Further, it was found that egg crate devices had the greatest impact in decreasing the number of discomfort hours because of their configuration (combination of overhangs and fin devices), which avoid solar radiation from varied sun angles. Following this, the SGHC $_{external}$ of using horizontal shades in the selected case study building for the four main orientations was calculated and outlined in Table 46. It was observed that difference in the SGHC values from the use of horizontal external shades is relatively small for different shade orientations. This could be explained by the prevalence of significantly higher diffuse solar radiation experienced in the region compared to direct solar radiation (previous climate analysis reveals this to be a common factor in humid regions).

Table 46: SHGC of horizontal shades based on PF ratio.

PF (Horizontal)	0	0.2	0.4	0.6	0.8	1	1.2
SHGC North (20°)	1.00	0.84	0.72	0.63	0.56	0.51	0.47
SHGC East (110°)	1.00	0.84	0.72	0.62	0.55	0.50	0.46
SHGC West(290°)	1.00	0.85	0.73	0.63	0.56	0.51	0.47
SHGC South (200°)	1.00	0.84	0.72	0.64	0.57	0.52	0.48

Further, Table 47 and

Figure 82 present the curve fit equations and graphs for various PF ratios for different orientations. Given the highly positive correlation factors, this information provides very close estimates of the SHGC $_{external}$ value for the outlined PF values for horizontal shading applied to the case study building. The SHGC $_{external}$ can be estimated from these graphs with information of the glazing area, window orientation and the PF ratio. Figure 83 shows the indoor comfort improvement for each orientation of the case study building due to the introduction of horizontal shading elements under various ventilation strategies. It was noted that although the SHGC for various orientations showed little variation, the comfort improvement is significantly higher on the West façade, followed by the East, North and South, respectively.

Table 47: SGHC Curve Fit Equation, where 'x' is the RF ratio and 'y' is the SGHC

Orientation	SGHC Curve Fit Equation	R²
North (20°)	y = 0.3035x2 - 0.7892x + 0.9922	0.9983
East (110°)	y = 0.2898x2 - 0.7919x + 0.9943	0.9992
South (200°)	y = 0.294x2 - 0.7729x + 0.9922	0.9984
West (290°)	y = 0.2747x2 - 0.7665x + 0.9954	0.9993
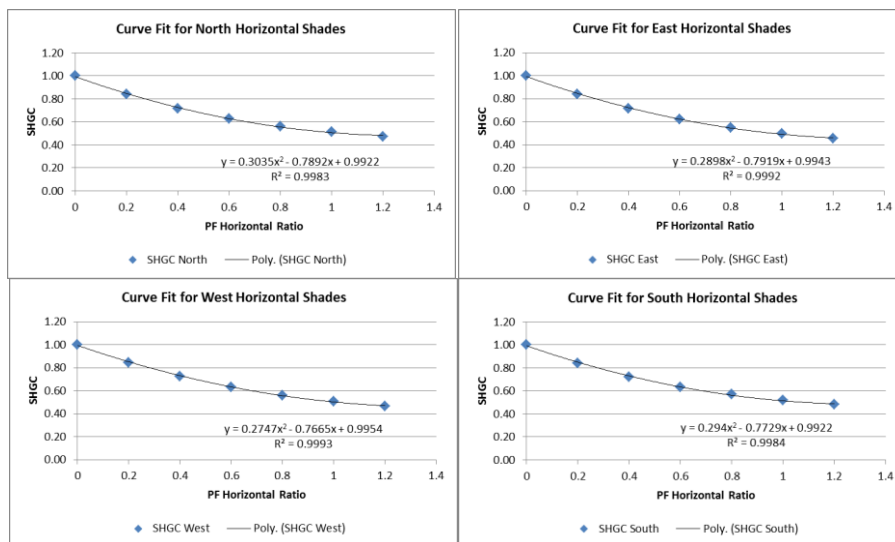
Figure 82: SHGC Curve Fits for horizontal shades for North, East, West and South orientations.

Figure 83: Comfort extension due to provision of horizontal shading

The SGHC $_{external}$ of using vertical shades in the selected case study building for the four main orientations was calculated and outlined in Table 48. Unlike the results obtained from the horizontal shades analysis, more variation is observed in the SHGC values for different orientations. The SHGC values are highest in

the Western orientation and lowest in the Northern orientation. The higher SHGC on the west façade indicates that a higher PF ratio is required to counter the effect of solar radiation.

Table 48: SHGC of vertical shades based on PF ratio.

PF (Vertical)	0	0.1	0.2	0.3	0.4
SHGC North (20°)	1.00	0.70	0.50	0.38	0.30
SHGC East (110°)	1.00	0.74	0.56	0.44	0.36
SHGC West(290°)	1.00	0.85	0.73	0.63	0.56
SHGC South (200°)	1.00	0.84	0.72	0.64	0.57

Further, Table 49 and Figure 84 present the curve fit equations and graphs for various PF ratios for different orientations. Given the highly positive correlation factors, this information provides very close estimates of the SGHC value for the outlined PF values for vertical shading applied to the case study building. As with the horizontal shading, the SGHC can be estimated from these graphs with information of the glazing area, window orientation and the PF ratio. Figure 85 shows the indoor comfort improvement for each orientation of the case study building due to the introduction of vertical shading elements under various ventilation strategies. It was noted that the comfort improvement is significantly higher on the West façade, followed by the East, North and South, respectively.

Table 49: SGHC Curve Fit Equation, where 'x' is the RF ratio and 'y' is the SGHC.

| Orientation	SGHC Curve Fit Equation	R²
North (20°)	$y = 3.706x^2 - 3.2028x + 0.994$	0.9989
East (110°)	$y = 3.0227x^2 - 2.7833x + 0.9961$	0.9994
South (200°)	$y = 1.3487x^2 - 1.6281x + 0.9994$	1
West (290°)	$y = 1.5643x^2 - 1.6916x + 0.9982$	0.9997

Figure 84 SHGC Curve Fits for vertical shades for North, East, West and South orientations.
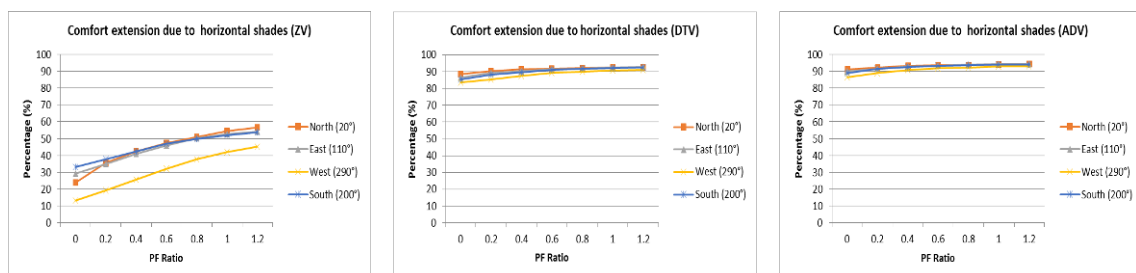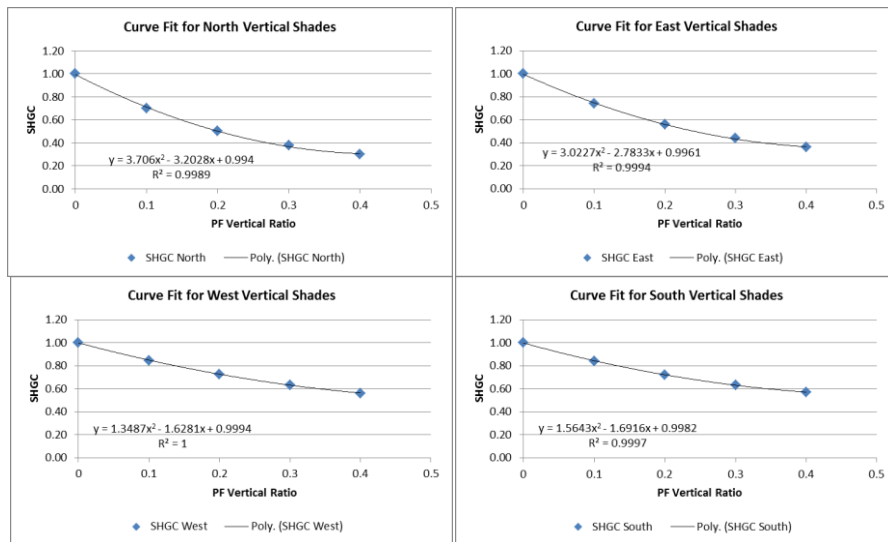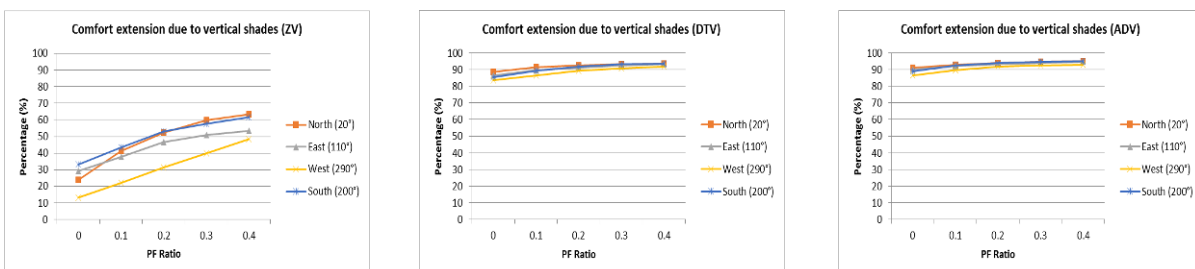
Figure 85: Comfort extension due to provision of vertical shading

The SGHC $_{external}$ of using egg crate shades in the selected case study building for the four main orientations is provided in Table 50 as derived from the simulation studies. As with the results obtained from the horizontal shades analysis, little variation is observed in the SHGC values for different orientations. Additionally, it was noted that the SGHC values are significantly low. This indicates that the combination of the horizontal and vertical PF ratios provide significantly higher protection from solar radiation. Although the SHGC are fairly similar for the different orientations, it was noted that the SHGC values are highest in the Western orientation and lowest in the Southern orientation.

Table 50: SHGC of egg crate shades based on PF ratio.

PF (Horizontal)	0.00	0.07	0.10	0.20	0.30	0.40	0.60
PF (Vertical)	0.00	0.03	0.05	0.10	0.15	0.20	0.30
SHGC North (20°)	1.00	0.23	0.23	0.23	0.23	0.23	0.23
SHGC East (110°)	1.00	0.24	0.24	0.24	0.24	0.24	0.24
SHGC West(290°)	1.00	0.25	0.25	0.25	0.25	0.25	0.25
SHGC South (200°)	1.00	0.22	0.22	0.22	0.22	0.22	0.22

Further, Table 51 presents the curve fit equations for various PF ratios for different orientations. Given the highly positive correlation factors, this information provides very close estimates of the SGHC value for the outlined PF values for egg crate shading applied to the case study building.

Table 51: SGHC Curve Fit Equation, where 'x' is the RF ratio and 'y' is the SGHC.

Orientation		SGHC Curve Fit Equation	R²
Horizontal Shades	North (20°)	$y = 4.8292x2 - 4.0565x + 0.9614$	0.9333
	East (110°)	$y = 4.761x2 - 3.9993x + 0.9619$	0.9333
	South (200°)	$y = 4.8774x2 - 4.097x + 0.961$	0.9333
	West (290°)	$y = 4.6715x2 - 3.9241x + 0.9626$	0.9333
Vertical Shades	North (20°)	$y = 19.317x2 - 8.1131x + 0.9614$	0.9333
	East (110°)	$y = 19.044x2 - 7.9985x + 0.9619$	0.9333
	South (200°)	$y = 19.51x2 - 8.1941x + 0.961$	0.9333
	West (290°)	$y = 18.686x2 - 7.8482x + 0.9626$	0.9333

In terms of indoor thermal comfort improvement, it was noted that the comfort improvement is significantly higher on the West façade, followed by the East, North and South, respectively. Unlike the previous shading system, little variation in comfort improvement was recorded outside of PF (horizontal) 0.03 and PF (vertical) 0.07.

3.3 Simulation Plan C

Following the derivation of the SHGC $_{external}$ for the case study building, the next step involved the derivation of the SHGC $_{external}$ for the case study building under 'true' North-South orientation. Previously, it was noted that the case study building is offset from a 'true' North-South orientation by approximately 20°. Further to this, estimates of the energy reduction resulting from the use of external shading devices were derived for various orientations. It was suggested that the results of this exercise could serve as a reference for other building practitioners who sought to know the impact of the SHGC external on overall cooling energy reduction.

The SGHC $_{external}$ of using horizontal shades in the selected case study building for the four main orientations was calculated and presented in Table 52. As with the previous analysis, it was observed that difference in the SGHC values from the use of horizontal external shades is relatively small for different shade orientations explained to be possibly due to high levels of diffuse radiation. Further, Table 53 presents the curve fit equations for various PF ratios for different orientations. The highly positive correlation factors indicates that this information provides very close estimates of the SGHC value for the outlined PF values for horizontal shading applied to the case study building under a 'true' North-South orientation.

Table 52: SHGC of horizontal shades based on PF ratio.

PF (Horizontal)	0	0.2	0.4	0.6	0.8	1	1.2
SHGC North (0/360°)	1.00	0.84	0.71	0.62	0.55	0.51	0.47

SHGC East (90°)	1.00	0.84	0.72	0.62	0.55	0.50	0.45
SHGC West (270°)	1.00	0.85	0.73	0.64	0.57	0.51	0.47
SHGC South (180°)	1.00	0.84	0.72	0.63	0.57	0.52	0.49

Table 53: SGHC Curve Fit Equation, where 'x' is the RF ratio and 'y' is the SGHC.

	SGHC Curve Fit Equation	R²
North (0°)		
East (90°)	$y = 4.2774x^2 - 3.4459x + 0.9898$	0.9969
South (180°)	$y = 2.8076x^2 - 2.703x + 0.9955$	0.9992
West (270°)	$y = 4.0966x^2 - 3.3392x + 0.9896$	0.9968
North (0°)	$y = 2.5114x^2 - 2.5112x + 0.9961$	0.9994

The SGHC $_{external}$ of using vertical shades in the selected case study building for the four main orientations was calculated and highlighted in

Table 54. Unlike the results obtained from the horizontal shades analysis, more variation is observed in the SHGC values for different orientations. The SHGC values are highest in the Western orientation and lowest in the Northern orientation. Table 55 presents the curve fit equations for various PF ratios for different orientations. Given the highly positive correlation factors, this information provides very close estimates of the SGHC value for the outlined PF values for vertical shading applied to the case study building under a 'true' North-South orientation.

Table 54: SHGC of vertical shades based on PF ratio.

PF (Vertical)	0	0.1	0.2	0.3	0.4
SHGC North (0/360°)	1.00	0.67	0.47	0.36	0.29
SHGC East (90°)	1.00	0.74	0.57	0.45	0.36
SHGC West (270°)	1.00	0.76	0.59	0.48	0.39
SHGC South (180°)	1.00	0.67	0.49	0.37	0.30

Table 55: SGHC Curve Fit Equation, where 'x' is the RF ratio and 'y' is the SGHC.

Orientation	SGHC Curve Fit Equation	R^2
North (0°)	$y = 4.2774x^2 - 3.4459x + 0.9898$	0.9969
East (90°)	$y = 2.8076x^2 - 2.703x + 0.9955$	0.9992
South (180°)	$y = 4.0966x^2 - 3.3392x + 0.9896$	0.9968
West (270°)	$y = 2.5114x^2 - 2.5112x + 0.9961$	0.9994

The SGHC $_{external}$ of using egg crate shades in the selected case study building for the four main orientations is provided in Table 56. As with the results obtained from the horizontal shades analysis, little variation is observed in the SHGC values for different orientations. The SHGC values are highest in the Western orientation and lowest in the Southern orientation. Further, Table 57 presents the curve fit equations for various PF ratios for different orientations. Given the highly positive correlation factors, this information provides very close estimates of the SGHC $_{external}$ value for the outlined PF values for egg crate shading applied to the case study building.

Table 56: SHGC of egg crate shades based on PF ratio.

PF (Horizontal)	0.00	0.20	0.40	0.60
PF (Vertical)	0.00	0.10	0.20	0.30
SHGC North (0/360°)	1.00	0.22	0.22	0.22
SHGC East (90°)	1.00	0.24	0.24	0.24
SHGC West (270°)	1.00	0.26	0.26	0.26
SHGC South (180°)	1.00	0.23	0.23	0.23

Table 57: SGHC Curve Fit Equation, where 'x' is the RF ratio and 'y' is the SGHC.

	Orientation	SGHC Curve Fit Equation	R^2
Horizontal Shades	North (0°)	$y = 4.8885x^2 - 4.1064x + 0.9609$	0.9333
	East (90°)	$y = 4.7682x^2 - 4.0053x + 0.9619$	0.9333
	South (180°)	$y = 4.614x^2 - 3.8758x + 0.9631$	0.9333
	West (270°)	$y = 4.7907x^2 - 4.0242x + 0.9617$	0.9333
Vertical Shades	North (0°)	$y = 19.554x^2 - 8.2128x + 0.9609$	0.9333
	East (90°)	$y = 19.073x^2 - 8.0106x + 0.9619$	0.9333
	South (180°)	$y = 18.456x^2 - 7.7515x + 0.9631$	0.9333
	West (270°)	$y = 19.163x^2 - 8.0484x + 0.9617$	0.9333

3.4 Energy Savings

Further simulations were undertaken to estimate the energy savings due to a reduction of the SHGC $_{external}$ and the results presented in Figure 86. It was found that the data derived from these simulations offers a fairly good estimate of energy saved due to the reduction of SHGC $_{external}$. This energy reduction can be estimated from these graphs with information of the glazing area, orientation of the window and the PF ratio. It was noted that the upper thermal comfort range for these energy use simulations was adjusted to 26.7°C as was derived using the PMV (Predicted Mean Vote) comfort model as defined in ASHRAE Standard 55 (ASHRAE, 2013).

For the horizontal shading devices, it was noted that although the SHGC $_{external}$ for the various orientations was found to be similar for the different PF ratios, the energy reduction was found to be significantly higher in the West, East, North and South façades, respectively. For the vertical shading devices, energy reduction is significantly higher in the West façade. Also, although the SHGC values were lower on the north/south

facades in comparison to the east/west, little variation was noted in the energy reduction of the north, south and east facades unlike when horizontal shading is used. As with the significantly better comfort performance of all the shading elements, egg crate shading had greater energy savings of up to 120kWh/m^2 for relatively lower PF ratios in comparison to values of up to 93.4kWh/m^2 and 92.4kWh/m^2 for horizontal and vertical PF ratios, respectively. This translates into maximum annual energy savings of up to 74.68%, 51.6%and 50.7% for horizontal, vertical and egg crate shading used in Western zones. An estimate of energy savings for other orientations is derivable from Figure 86.
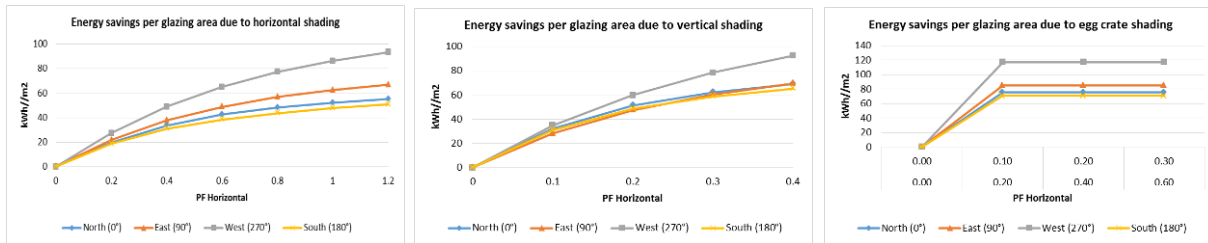
Figure 86 Energy savings per glazing area due to the provision of horizontal, vertical and egg crate shading devices.

4 CONCLUSION

Forming part of a larger study examining the optimization of design strategies to improve thermal performance in office buildings in the warm humid region of Kenya, this study was focused on the impact of external shading devices on improving indoor thermal comfort and increasing energy savings. The main objective of the study was to determine the effect of external shading devices in reducing the impact of solar radiation on glazed surfaces and the consequent reduction of the risk of overheating which substantially contributes to energy consumption. The study found that external shading plays a significant role in the improvement of indoor comfort conditions. Of the shading types investigated, egg crate shading was found to perform significantly better than individual external horizontal and vertical shading elements. In addition, solar data derived from dynamic simulations was used to derive solar heat gain coefficients that were used to specify the required shading control of a façade required to avoid unnecessarily large solar gains through glazing surfaces. By categorising the impact of external shading into coefficients, the derivation of the effect of external shading on indoor thermal comfort and energy use irrespective of shading type was simplified. Further to this, curve fit equations and graphs were derived for the four cardinal compass orientations which may be used by local building practitioners to define the solar heat gain coefficients for various types of external shading devices in similar type buildings.

5 REFERENCES

ASHRAE 2013. 2013 ASHRAE Handbook - Fundamentals (SI Edition). American Society of Heating, Refrigerating and Air-Conditioning Engineers, Inc.

BUILDING SECTOR ENERGY EFFICIENCY PROJECT - BSEEP 2013. Building Energy Efficiency Technical Guideline for Passive Design.

GIVONI, B. 1994. Building design principles for hot humid regions. *Renewable Energy,* 5**,** 908-916.

KIAMBA, L. N., Rodrigues, L. & Lau, B. 2014. Climate-responsive Vernacular Swahili Housing. *PLEA 2014: Sustainable Habitat for Developing Societies.* Ahmedabad, India.

KIAMBA, L. N., Rodrigues, L. & Lau, B. 2015. The Application of Vernacular Swahili Architecture Strategies to Contemporary Office Buildings in Kenya *PLEA 2015: Architecture in (R)Evolution.* Bologna, Italy.

KOENIGSBERGER, O. H., Ingersoll, T. G., Mayhew, A. & Szokolay, S. V. 1974. *Manual of Tropical Housing and Building: Climatic design*, Longman.

KPLC 2013. The Kenya Power and Lighting Company Limited Annual Report and Financial Statements 2012/2013. The Kenya Power and Lighting Company Limited.

NATIONAL PLANNING AND BUILDING AUTHORITY - KENYA 2009. National Building Regulations. *In:* HOUSING, M. O. (ed.). National Planning and Building Authority - Ministry of Housing.

NICOL, J. F. & Humphreys, M. A. 2002. Adaptive thermal comfort and sustainable thermal standards for buildings. *Energy and Buildings,* 34**,** 563-572.

SZOKOLAY, S. V. 2008. *Introduction to Architectural Science: The Basis of Sustainable Design*, Taylor & Francis Group.

SESSION 31: ENERGY EFFICIENCY IN BUILDINGS

90: Photovoltaic ventilated façade as an energy efficient measure for building retrofitting

ISABEL SANCHEZ[1], ELENA RICO[2], DAVID MARTIN[3], TEODOSIO DEL CAÑO[4]

[1] Onyx Solar Energy S.L., Río Cea 1 05004 Ávila (Spain), isanchez@onyxsolar.com
[2] Onyx Solar Energy S.L., Río Cea 1 05004 Ávila (Spain), erico@onyxsolar.com
[3] Onyx Solar Energy S.L., Río Cea 1 05004 Ávila (Spain), dmartin@onyxsolar.com
[4] Onyx Solar Energy S.L., Río Cea 1 05004 Ávila (Spain), tdc@onyxsolar.com

The expected relevant role, within the new energy paradigm of photovoltaic (PV) solar energy, is mainly based on the rapid research and development advances in the PV field. In this sense, the current state of the art of these innovative technologies has allowed reaching the integration of PV glass products in buildings in an attractive and efficient manner. This approach is known as Building Integrated Photovoltaic (BIPV) Solutions which insertion ensures an enormous future for the distributed energy approaches as an energy-efficient measure for retrofitting applications.

In this respect, Onyx Solar participates as a partner of HERB Project (Holistic Energy-Efficient Retrofitting of Residential Buildings) within the funding of the European Commission through its 7th Frame Programme. The HERB Project aim is to implement active and passive energy efficient properties in residential buildings already existing and located in several countries around Europe. Therefore, BIPV solutions are one of the technologies developed.

As a first step, the PV ventilated façade was evaluated by means of computational modelling and façade prototype testing through a prototype in a Paslink test cell. This analysis is very useful for obtaining critical information concerning temperatures in the different layers of the wall, characterization of the air behaviour, heat generated within the façade air chamber and electrical production.

Then, Onyx Solar has coordinated a family house retrofit in Gotarrendura, a village of Ávila (Spain). Among the wide range of retrofitting solutions used, it has been included the integration of a PV ventilated façade using opaque and semi-transparent glass based on a-Si active layer.

This paper summarizes relevant results and conclusions of the research studies, testing carried out and the real case study mentioned whose combination demonstrates the potential of these measures in the field of energy-efficient retrofitting.

Keywords: Building Integrated Photovoltaics, Retrofitting, Energy

1. INTRODUCTION

Buildings are responsible for approximately 40% of the world's energy consumption, according to the United Nations Environment Programme (UNEP). Commercial and residential buildings use about 60% of global of electricity demand. Furthermore, the existing electricity generation system lost approximately 15% of the energy in distribution, due to the great distances from the places of consumption. Therefore, renovation of existing buildings is increasingly important as a strategy in energy demand reduction and the commitment of different governments and supranational organizations are establishing pre-agreements to promote energy efficient projects and clean energies to guaranty on a long term basis the sustainability of earth resources.

In this respect, the use of constructive solutions with photovoltaic materials on retrofitting projects is highly recommended because it improves the energy efficiency of the obsolete buildings that did not follow the modernized patterns of sustainability.

Building integrated photovoltaic solutions (BIPV) are capable of fully replacing conventional construction materials for the building envelope such as skylights, façades, windows, curtain walls, roofs, balcony railings and floors. These multifunctional bioclimatic solutions (Figure 87) combine both active and passive properties, providing greater acoustic and thermal insulation and at the same time producing clean energy on site.
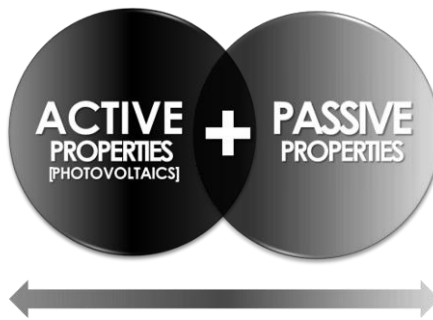
Figure 87: Multifunctional concept of BIPV

In this regard, Onyx Solar participates as a partner of the HERB Project (Holistic Energy-Efficient Retrofitting of Residential Buildings) co-funded by the European Commission through its 7th Framework Programme (G.A. No. 314283), in a consortium managed by the University of Nottingham.

The HERB Project aim is to implement active and passive energy efficient properties in residential buildings already existing and located in several countries around Europe. Onyx Solar main role is to develop BIPV solutions focused on retrofitting residential buildings and to coordinate a family house retrofit project in Gotarrendura, a village of Ávila (Spain)

Setting the general target of the HERB Project on the development and demonstration of energy efficient technologies and solutions for retrofitting applications, several general goals have been established in the DOW, document of work (University of Nottingham, 2011):

- Cumulative annual energy savings of at least 80% measured against building performance before retrofit.
- At least a 60% reduction of CO2 emissions.
- Global energy consumption (excluding appliances) of 50 kWh/m²year while reducing peak loads against the values measured before retrofit.
- At least 80% energy saving for lighting over the average consumption of the installed base.
- User acceptability and long term continued efficient operation.
- A pay-back period of between two and five years compared to current state of the art, depending on the type of technology and solution.

The authors describe in the current paper the retrofit project of the Spanish house, focusing on the photovoltaic ventilated facade system and its properties.

2. PHOTOVOLTAIC VENTILATED FAÇADE SYSTEM

Ventilated facades are very interesting solutions for retrofitting buildings, because they are easy to install and improve thermal and acoustic insulation. In addition, the system could generate electricity and thermal energy without major changes in the constructive scheme.

Thanks to the ventilated air chamber and the application of insulating material, this system increases the acoustic absorption and reduces the amount of heat that buildings absorb in hot weather conditions. The difference between the density of hot and cold air within the air space creates natural ventilation through a chimney effect. This helps in eliminating heat and moisture, enhancing the comfort level of the occupants. In addition, the hot air can be used to reduce the heat demand of the building (HVAC or DHW systems) enhancing the energy efficiency of the buildings.

2.1. PASLINK Test Description

To analyse the passive behaviour of the PV ventilated façade system, PASLINK test cell was utilized with an existing methodology for testing the energetic properties of building envelopes. The main objective of this approach is to measure accurately the heat fluxes through the walls, as well as the evolution of associated surface temperatures and ambient temperatures. All external meteorological parameters were also logged. Basically, the test cell is an accurate calorimeter that quantifies energy transfers between interior and exterior, where the differences correspond with energetic fluxes through the sample.

Following a clear methodology, a laboratory model has been tested under real climate conditions during a limited period, obtaining data about the façade behavior. Extrapolating this information in a simulation analysis, it is possible to obtain information about the performance of the solution during one year period in different climates. It is a useful data to be used to evaluate the real possibilities of this photovoltaic ventilated façade system under different climate conditions.

1- Plasterboard (1,5cm)

2- Solid flat slab (15,6cm)

3- Mortar (1,5cm)

4- Rock wool (5cm)

5- Ventilated air chamber (10cm)

6- PV Opaque amorphous silicon Panels (1,5cm)
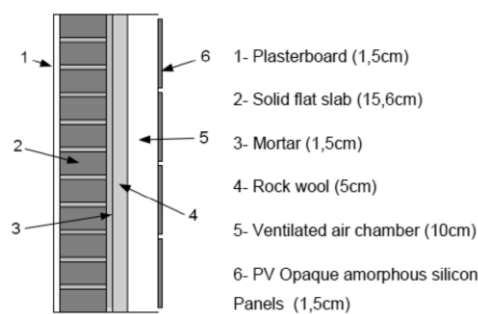
Figure 88: Photovoltaic ventilated facade description

Two façade systems were compared under Madrid (Spain) climate condition: a base wall BW (plaster + concrete blocks + cement mortar) and a photovoltaic ventilated facade, Figure 88, PVF (base wall + thermal insulation+ air chamber+ opaque a-Si photovoltaic glass).

2.2. PASLINK Test Results

Figure 89 shows exchanged energy, both gains and losses, between the controlled indoor and outdoor environment with thermal transmittance values.

The results show the advantages of the photovoltaic façade system in which thermal heat losses and gains are reduced in the cold months and warm months, respectively. Final results showed an important decrease in heat gain during summer. Thermal losses did not decrease as expected. A possible reason to explain this result could be due to the gaps between glasses. In this sense, a better winter performance could be obtained for closed façades.

In an ideal situation, the inner and outer temperatures of a wall would remain constant. This thermal transmittance characteristic is accurately measured by the U-value. In contrast to the ideal condition, the

indoor and outdoor temperatures are not so steady. Therefore, there is a need of defining a dynamic thermal transmittance equivalent, Udin, characterizing the dynamic behaviour of the wall. It is important to underline that the dynamic thermal transmittance values obtained are lower than the constant U value.

	Base Wall (A_{Gv}= 0,83)	Base Wall + PVF
Thermal Resistance (m^2K/W)	0,29	1,56
Thermal Transmittance (W/m^2K)	2,21	0,55
Thermal Capacity (kJ/m^3K)	184	231
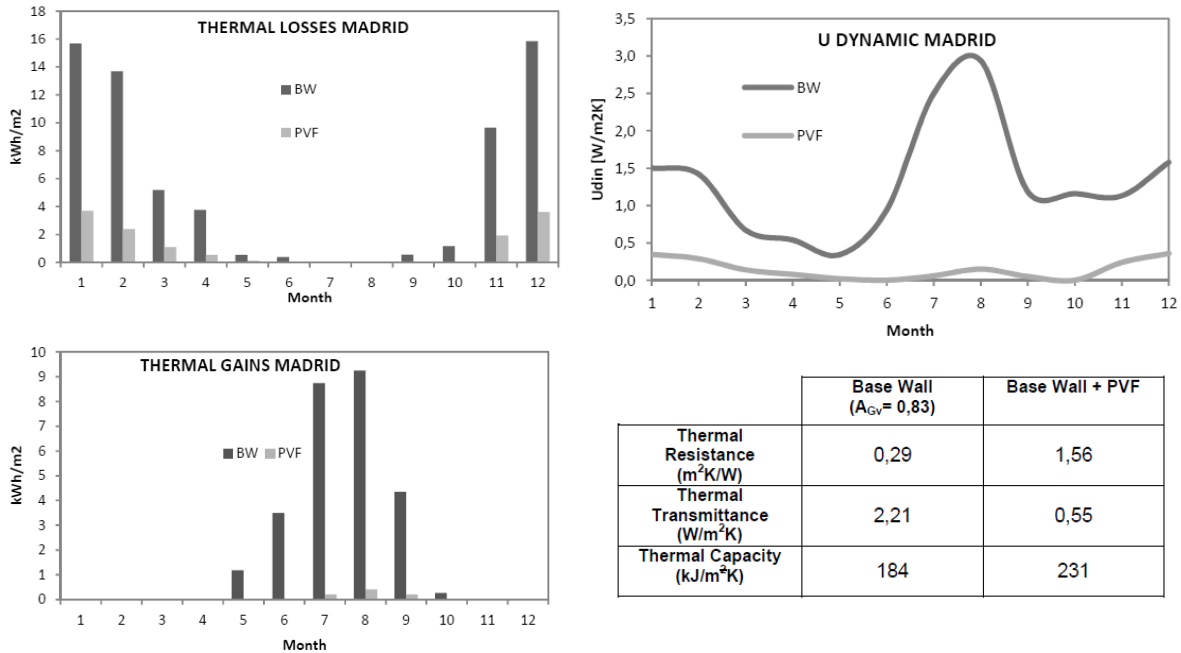
Figure 89: Paslink test thermal exchanges results (passive properties)

Therefore, photovoltaic ventilated façade systems improve thermal behaviour of facades and at the same time produce electricity thanks to the sun. Furthermore, it is possible to recover the heat produced in the air chamber of the system, and to use it inside buildings reducing the consumption of heating systems in cold seasons.

Figure 90 shows the estimated electrical energy production of the photovoltaic glass cladding system and the heat absorbed in the air chamber. Maximum values of heat generation correspond to August when external temperatures are high.

Regarding the electrical generation, the chart shows the kWh obtained per square meter of photovoltaic glass facing to south, in each month of a whole year. Solar radiation is higher in summer months in the Northern Hemisphere than in winter months, but facades are in vertical position. Because of this, even if facing south, the irradiation on the photovoltaic units reach maximum values in spring and autumn seasons. The difference existing in February can be explained by the fact that February has only 28 days and the electricity obtained corresponds to completed months. That is the reason why there is a descent of electricity production in this month.
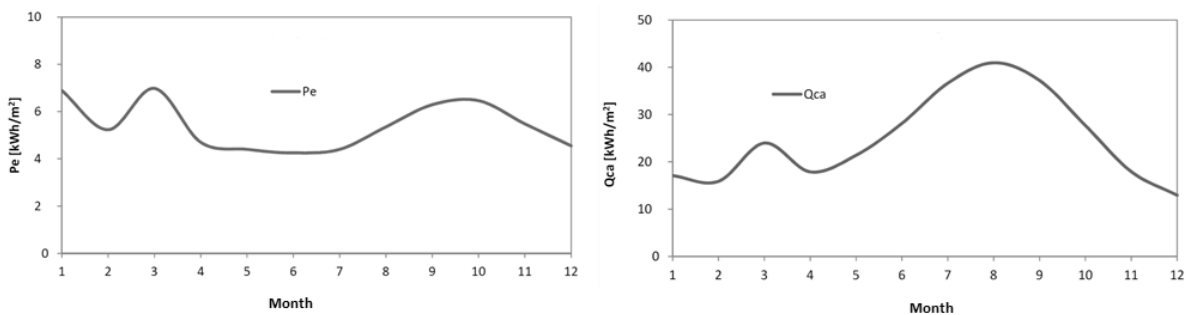
Figure 90: Paslink test energy production results (active properties)

3. ENERGY-EFFICIENT RETROFITTING OF A HOUSE IN SPAIN

The main goal of HERB Project is to develop and demonstrate energy efficient new and innovative technologies and solutions for retrofitting and energy performance of 12 typical residential buildings located in several countries of EU. However, this retrofitting has to be applied from holistic point of view taking into account the HERB project structure.

In the following sections the applied methodology will be exposed, as well as the retrofit project developed for the Spanish house, where a photovoltaic ventilated façade system and a photovoltaic gallery contribute to achieve the objectives of the HERB project.

3.1. The Holistic Analysis. Modelling Methodology

Onyx Solar as main responsible of Spain house retrofitting has defined a modelling methodology based on holistic approach able to achieve the goals of HERB project in terms of cumulative energy savings, efficient lighting, reduction of CO_2 emissions and reduction of global energy demand. Therefore, the modelling methodology consisted of three steps perfectly enclosed and defined. The following schematic diagram, Figure 91, shows this approach suggested:
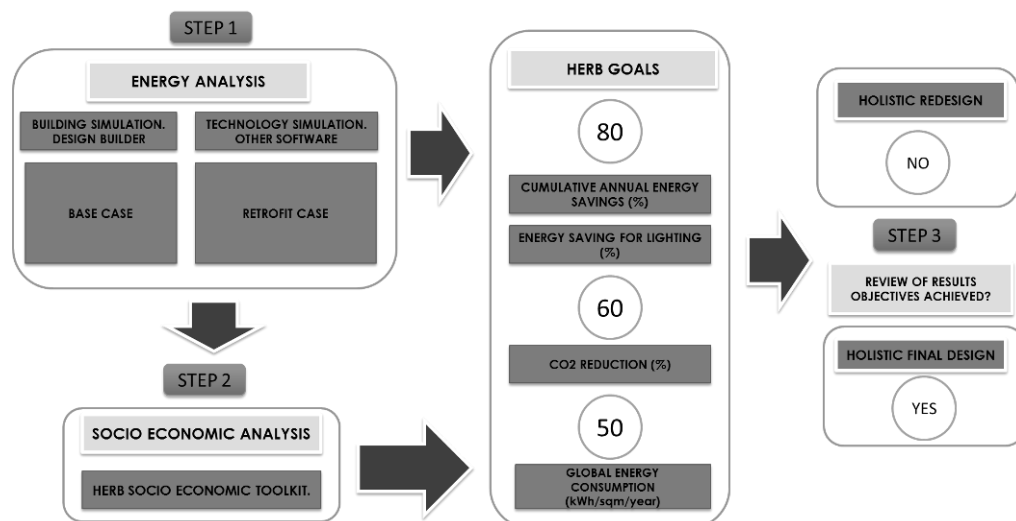
Figure 91: Schematic graph of modelling methodology for Spain house

The first step was "Energy analysis". At this stage, Onyx Solar has carried out several simulations with the aim of comparing the variation of building behavior in terms of energy consumption between two scenarios:

- BASE CASE. The base case was defined taking into account the initial condition of the building through simulations by Design Builder Software, the analysis of the historic energy consumptions by existing invoices and the information collected at survey phase.
- RETROFIT CASE. The retrofit case was defined through simulations combining Design Builder Software, models developed by the technology providers and other commercial softwares.

The outputs of step 1 were able to provide the information required to compare with the HERB goals mentioned in the previous section.

This evaluation/comparison was carried out at step 3 and a final decision agreed according to the review of the results. As a result, the approach of holistic design was validated or no. If it was accepted, the design was considered as a "Holistic Final Design". In the other case, the design was considered unacceptable ("Holistic Redesign") and it was needed to carry out the appropriate modifications and restart the modelling approach from the beginning. Finally, the socio economic analysis corresponding to step 2 has been carried out using the socio-economic modelling and analysis developed in the HERB project.

3.2. Pre-retrofit House Conditions

Spanish building is a private family house located in a small village in Ávila Region named Gotarrendura, located approximately in the geographical centre of Spain. Gotarrendura village is located 664 meters above sea level and the climate is classified as temperate with dry or temperate summer (Csb) according to Köppen classification, which is one of the most common climates in the Spanish Peninsula.

The house represents a typical two-storey rural construction with the two main facades facing north-south. The total area is 206 m². The building dates from 1963 and over the years, the house was refurbished as punctual manner through minor maintenance and operations. However, none of works seemed to have direct significant impact on the thermal behaviour showing a considerable high energy demand (180 kWh/m²year) inferring in an important limitation of use in terms of energy efficiency and O&M economic costs. On the other hand, the housing consumption is directly linked to the users. In this case, the house is inhabited by a four-members-family. This situation is to above Spanish Average in terms of occupation rates in houses.

The house is composed of ground floor and first floor. The main living room, an auxiliary room, a bedroom, the bathroom and the kitchen are located in the ground floor; other four bedrooms and a storage room are located in the first floor. Both façades of the house (south and north) are in contact with open spaces (street and courtyard) so it is partly exposed to the prevailing winds.

The opaque vertical walls were made using adobe bricks partially coated inward by a trim and plaster, and outward by a layer of mortar; the roof has a wooden framing structure with ceramic tiles. Openings were solved using single glazing and frames of different materials (wood and aluminium), most of them old and with artisan style. Only two of them had been renovated.

The house was provided with old convective baseboard heaters fed with grid electricity. For domestic hot water production (DHW) there was a butane boiler fed with individual domestic bottles which meet kitchen and bathroom needs. In the kitchen there were also four butane stoves for cooking and an electric oven. As usual on this region and type of buildings, the house was not provided with any cooling system since just few hours in summer temperature surpasses comfort levels.

Finally, the house had some few electric appliances in the living rooms, kitchen and bedrooms, although the quantity was far from the actual standards for a single family dwelling. All in all, the case-study house was fairly representative of typical old rural house in central region of Spain.

In order to know the energy behaviour of the house, a Design Builder model simulation of the pre-retrofit phase has been developed. This simulation has established an energy consumption of the house of 37,526 kWh/year. Figure 92 shows the annual energy consumption of the house before the retrofit in comparison with average consumption of a Spanish house with the same characteristics, and the energy consumption distribution of the house before the retrofit works.
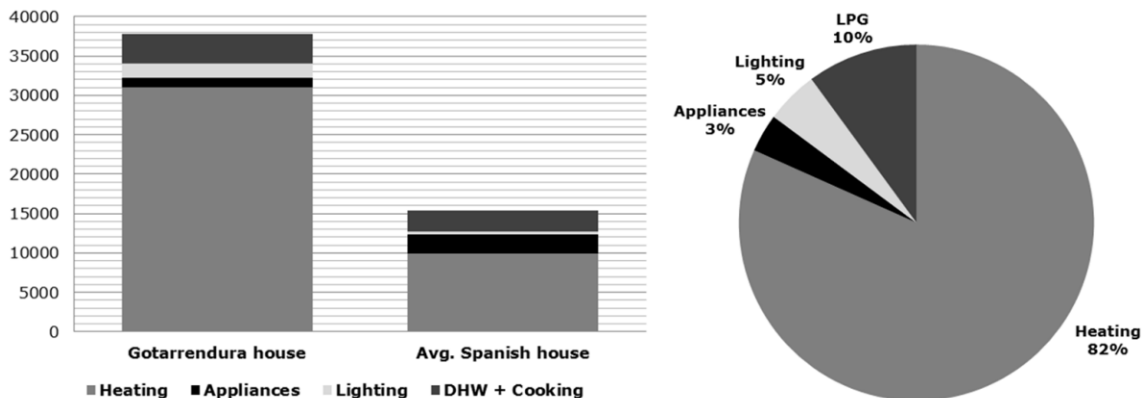
Figure 92: Total energy consumption of Gotarrendura House

Finally, taking into account the HERB project guidelines where appliances have not been considered in the retrofit's global energy consumption goals, the starting point for the energy consumption in the base-case is 36,220 kWh/year (excluding appliances) as it is shown in the Figure 93.
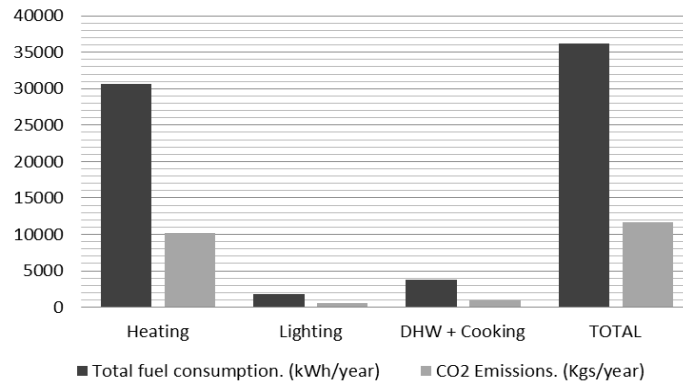
Figure 93: Base-case house: Fuel consumption and CO2 emissions per year

3.3. Summary of Energy Efficient Measures

Taking into account the existing conditions of Spain house in terms of energy consumption, the retrofit plan has been defined. Figure 94 shows the schematic diagram of the "Retrofit strategy".
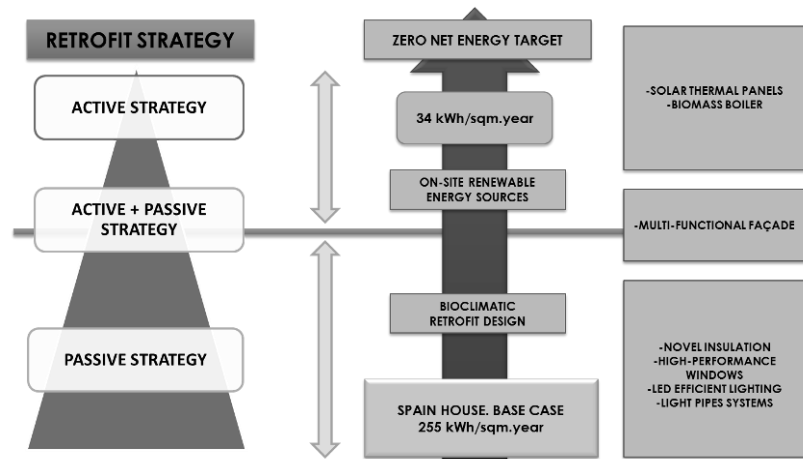
Figure 94: Retrofit Strategy

From the point of view of the passive strategy, several technologies have been involved. Novel insulation materials mainly supplied for HERB partners have been preselected and simulated for validating the improvement of U-value parameter. Furthermore, the single-glazed windows have been replaced by high performance windows due to the results of simulation have identified significant energy losses coming from fenestration elements of the house. Likewise, LED efficient lighting and natural light pipes system have completed the "Passive Strategy" contributing to the reduction of electric consumption and facilitating natural daylight entrance inside the house.

In the same way, the integration of smart multifunctional solutions able to combine active and passive properties provides an added value to the "Retrofit Strategy" allowing on-site RES energy production and thermal envelope benefits. Thus, the multifunctional façade developed by Onyx Solar complies perfectly with the properties recently described. The electricity generated by the multifunctional PV façade will be enough for fulfilling electric demand associated to lighting consumption.

In this respect, the retrofit plan includes the installation of a photovoltaic gallery: glazed buffer zone/sunspace on the south façade which aims to provide both electricity and thermal energy for space heating for better use of solar energy. This hybrid system consists of a semi-transparent PV technology (10% see-trough amorphous silicon) system integrated within a passive solar heating system. The

operation of thermal system differs depending on the season. In winter the gallery windows should be closed to allow air heating due to solar gains. Thus, when buffer internal temperature surpasses bedrooms air temperature heat will flow towards the house. In contrast, windows should be always open in hot conditions to induct ventilation by the stack effect generated on account of space solar gains. In addition to heat generation, PV glass produces electricity at the same time and its performance might be enhanced by thermal system operation. Namely, PV cell efficiencies grows at low temperatures, hence constant air flow in summer conditions due to stack effect potentially increases PV performance. The system can produce up 638.60 kWh/year. Figure 95 shows the photovoltaic gallery installed.

Figure 95: Photovoltaic gallery of the Gotarrendura house

Furthermore, a photovoltaic ventilated façade system has been installed on the other facade, as can be seen in the Figure 96. Opaque amorphous silicon photovoltaic technology offers the best aesthetic solution when combined with other claddings or construction materials due to its plain characteristics. This solution provides thermal and acoustic insulation, and an estimated energy production of 243.98 kWh/year.

Figure 96: Photovoltaic ventilated facade of the Gotarrendura house

Active solutions were selected for generating energy required for the working of heating/cooling equipment and electricity devices (lighting and appliances). Specifically, a biomass boiler system and solar thermal installation will be responsible for satisfying the thermal demand.

3.4. Energy consumption analysis

The holistic energy analysis has been realized through the combination of several simulation tools already existing in the market and other models developed under the umbrella of HERB Project. Figure 97 shows yearly energy saving and CO2 emissions reduction in Gotarrendura house in 7 different retrofit scenarios in comparison with base case. In six first scenarios just one strategy is implemented at a time, whereas last

scenario (right) gathers all strategies plus a solar thermal system for DHW production. At first glance, it can be seen that heating electricity represents by far the largest fraction of total annual consumption in every case.

Overall, it can be seen that the least energy-efficient measure is improving lighting system, which lead only to 1.3% total fuel saving and CO2 emissions reduction. Then, PV/T solar systems (North and South) accounts for 7.6% and 6.0% of total fuel saving and 7.9% and 6.2% CO2 emissions reduction respectively including PV electricity generation. Increasing envelope insulation seems to be the most energy-efficient measure by far with 64.7% of total energy saving and 66.9% of CO2 emissions reduction. In contrast, fenestration upgrade strategy only accounts for 12.7% energy demand reduction and 13.1% CO2 emissions reduction. High efficient biomass boiler leads almost 22% of energy saving and 88% of CO2 associated emission. It seems that the most effective way to reduce house carbon footprint is to replace heating and DHW fuel. Finally, overall fuel consumption in full retrofit scenario decreases 86.7% considering PV and solar thermal on-site energy generation and CO2 emissions decreases 94.9% in comparison with base-case scenario.
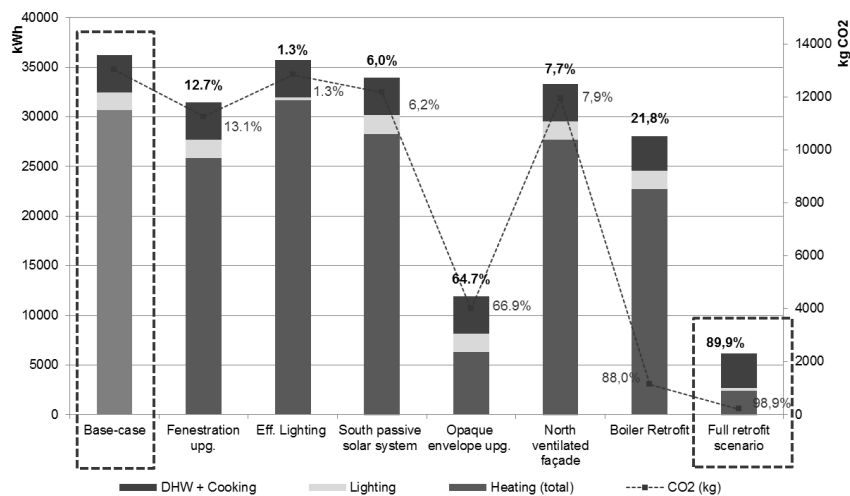
Figure 97: Yearly energy consumption and CO2 emissions in different retrofit scenarios.

Therefore, we can state that proposed holistic energy-efficient retrofit strategy reduces considerably energy consumption in current house configuration and fulfils HERB objectives. In particular, it achieves 86.7% of energy consumption reduction and decreases associated CO2 emissions in 94.9%, which leads to total consumption of 34 kWh/ m2 year (excluding appliances).

Besides, it can be concluded from simulations results that the impact of a holistic energy-efficient retrofit strategy which involves simultaneous different measures is not equal to the sum of their effects measured individually.

4. CONCLUSION

BIPV solutions are valuable energy efficient measures that improve the energetic behaviour of buildings in a sustainable and aesthetic way, not only in new constructions, also in building renovation cases. BIPV systems are energy efficiency measures that can replace conventional materials in the building envelope and produce energy from the sun avoiding CO_2 emissions to the atmosphere.

The PV ventilated façade system is one of the better solutions for retrofitting projects, as it can implemented over the original façade, incorporating a ventilated air chamber and insulating material that increase the acoustic absorption and reduce the amount of heat absorbed by buildings. In this respect, the ventilated façade plays a crucial role as solar shading system because it absorbs and reflects a good part of the incident solar energy, reducing the amount of transmitted energy towards the building: results of testing shows that thermal heat losses and gains are reduced in the cold months and warm months, respectively.

Furthermore, it is possible to recover the heat produced in the air chamber of the system, and to use it inside buildings reducing the consumption of heating systems in cold seasons. Maximum values of heat generation correspond to August when external temperatures are high. Finally, the electricity generation

on-site ensures an enormous future for the distributed energy approaches as an energy-efficient measure for retrofitting applications.

A PV ventilated façade and a PV gallery included in the proposed holistic energy-efficient retrofit strategy for Spanish house help to reduces energy consumption and fulfil HERB objectives. The impact of a holistic energy-efficient retrofit strategy which involves simultaneous different measures is not equal to the sum of their effects measured individually. In particular, it achieves 86.7% of energy consumption reduction and decreases associated CO_2 emissions in 94.9%, which leads to total consumption of 34 kWh/ m2 year (excluding appliances).

5. REFERENCES

INSTITUTO PARA LA DIVERSIFICACIÓN Y AHORRO DE LA ENERGÍA (IDAE), Secretaría General Departamento de Planificación y Estudios, 2011. Análisis del consumo energético del sector residencial en España. Proyecto SECH_SPAHOUSEC. Spain.

INSTITUTO PARA LA DIVERSIFICACIÓN Y AHORRO DE LA ENERGÍA (IDAE), 2012. Factores de conversión energía final-energía primaria y factores de emisión de CO2. Spain.

UNITED NATIONS ENVIRONMENT PROGRAMME (UNEP). http://www.unep.org/

UNIVERSITY OF NOTTINGHAM, 2011. DOW of HERB Project. United Kingdom.

US DEPARTMENT OF ENERGY (DOE), 2005. Design Builder Software. USA

US DEPARTMENT OF ENERGY (DOE), 2009. Statistics for Esp_Avila.082100_swec, 2009. Spain.

VAN DICK AND Tellez, 1995. F. COMPASS Measurement and data analysis procedures. Brussel, Belgium.

VAN DICK AND van der Linden, 1995. PASLINK Calibration and component test procedures. TNO Delft, Netherlands.

146: Study on the diagnosis index system and procedure for green retrofitting of existing buildings

SUZHEN MA[1], JINJIN SUN[2]

[1]China Academy of Building Research, Room D2, 12th Floor Haili Mansion,
No. 88 Dapu Road, Shanghai,
Email: masuzhen@cabr-sh.com
[2]China Academy of Building Research, Room D2, 12th Floor Haili Mansion,
No. 88 Dapu Road, Shanghaii
Email: sunjinjin@cabr-sh.com

It is well known that green retrofitting of existing buildings is key supporting research of China's "Twelfth Five-Year Plan". To undertake and promote retrofitting of existing buildings, especially green retrofitting in China, the primary problem needed to be solved is diagnosis for existing buildings. Just through diagnosis, the present situation of existing buildings can be completely mastered so that the subsequent green retrofitting can become more targeted. In this paper, study for the index system of diagnosis of green retrofitting of existing buildings is discussed. This paper also illustrates the principle of the establishment of the index system of diagnosis. In the meantime, the whole index system of diagnosis, the whole diagnosis framework, procedure and method are also given. All these give a guidance for the diagnosis of green transformation of existing buildings which is significant for technology research of green retrofitting of existing buildings in China.

Keywords: Existing building; Green retrofitting; Diagnosis; Index system

1. INTRODUCTION

In China, there are large quantities of low energy-efficient buildings. By the end of 2014, China's existing buildings area has reached 56 billion square meters, including about 30 billion square meters of urban area, but the proportion of the energy saving buildings in urban area is only about 30%. Considering building's construction age and construction standard, most existing buildings have low level of security, high energy consumption, poor using function, etc. As a result, a large number of existing buildings has been demolished. According to statistics, every year in China, dismantled existing building area lives up to about 400 million square meters. However, the demolition of the existing buildings used just for short time, not only directly causes ecological environment destruction, but also is a great waste of energy resources. Therefore, to the existing non-energy-efficient buildings (especially buildings built before 2005), the implementation of energy-saving transformation and green transformation, on the one hand, can improve the performance of existing buildings. On the other hand, it has great significance for the country's energy conservation and emission reduction.

The definition of green transformation is given in Green Transformation Assessment Standard for Existing Buildings (the draft for approval). In this definition, the goal of green transformation is to save energy resources, improve the living environment, and promote the using function through the existing building maintenance, updating, reinforcement and other measures. According to the standard, transformed buildings fulfilling the green building performance requirements usually can be called green retrofitting project. Since 2010, in China many cities gradually start existing buildings' green retrofitting work. By the end of 2012, there have been 21 projects with a total construction area of 918000 square meters, which met Chinese green building assessment level through transformation. Although the amount of green retrofitting projects of existing buildings is small, these projects provide valuable experience for the transformation of existing buildings in the future.

However, although retrofitting existing buildings in China has made certain achievements, green transformation of existing buildings is still in its infancy, and the related technology system and incentive system are not sound enough. Therefore, more concerted efforts are needed to promote Chinese existing buildings' green retrofitting work.

Green retrofitting of existing buildings contains green retrofitting diagnosis, green retrofitting plan, design, construction, operation, management and other aspects. As the first step of green transformation, green transformation diagnosis is also the most important step. The concept of green transformation diagnosis is that through field investigation, detection and identification, diagnosis of building performance and the status quo of the use function, the energy-saving potential for existing building is analysed to provide basis for green transformation of existing buildings. Though making accurate and effective diagnosis for existing buildings, many problems can be determined, such as performance level of existing buildings, scale of the problem and the influence degree, and economic cost of investment needed. Besides, formulating a series of retrofitting scheme needs to base on the results of the diagnosis. With this regard the discussion about green transformation diagnosis is mainly proposed in this study.

In Green Transformation Assessment Standard for Existing Building (the draft for approval), the green performance of existing buildings is evaluated from six parts including planning and architecture, structure and materials, HVAC, water supply and drainage, electrical and construction management. However, from the perspective of diagnosis, more attention needs to be paid to the green performance of existing buildings, such as energy conservation, water saving, indoor and outdoor environment. Hence, in this paper, the emphasis of diagnosis content is focused on building's environment, enclosure structure, HVAC system, water supply and drainage system, electrical and automatic control system, as well as operation and management. At the same time, as for the diagnosis method of green retrofitting of existing buildings, it is required more comprehensive, more efficient. Moreover, in addition to meeting the existing building energy efficiency diagnosis, the diagnosis method should also meet the water-saving diagnosis, and diagnosis requirements of building environment.

5   PRINCIPLES OF GREEN TRANSFORMATION DIAGNOSIS

Existing buildings green retrofitting involves building environment, enclosure structure, HVAC system, water supply and drainage system electrical and automatic control system and operation and management. Therefore, the reasonable diagnostic scheme and measures formulated should be based on the characteristics of the diagnosed building system and the existing diagnosis conditions. In the concrete implementation process, the following principles should be followed.

2.1 Systemic principle

Green transformation diagnosis should adopt comprehensive green building indexes, such as energy consumption index, water consumption index, indoor comfort index, etc. Through comprehensive indexes it is easy to find the problems existing in the building systems, and then based on these questions, deep analysis can be made to eventually identify the cause of the problems.

2.2 Quantifiable principle

Diagnosis contents of existing buildings should be as quantifiable as possible. With testing, simulation methods, quantitative results of green transformation diagnosis can be obtained, so as to make scientific decision. And unquantifiable indexes should avoid to be used or used less, in order to reduce unnecessary workload.

2.3 Economy principle

Considering the initial cost, field investigation and diagnosis of existing buildings green retrofitting should use diagnostic measures as convenient as possible, and extracting reasonable samples complete the relevant diagnostic work, so as to reduce the cost of diagnostic work.

The ecological construction in our country is still at the exploration stage, therefore there are a lot of problems in the harmonious coexistence process of social economic development and ecological environment protection. The main misconceptions and problems are as follows:

3 CONTENTS OF GREEN TRANSFORMATION DIAGNOSIS

Based on the running status of existing buildings and green transformation goal, the main contents of green transformation diagnosis include building environment, palisade structure, HVAC system, water supply and drainage system, electrical and automatic control system and operation and management. For each aspect, this paper combed the diagnosis contents and indexes of existing buildings green retrofitting, considering Green Transformation Assessment Standard for Existing Building (the draft for approval).

3.1 Building Environment

Building environment includes sound environment, wind environment, light environment, thermal environment and landscape environment. Concrete contents and specific diagnosis indexes of building environment are shown in Table 1.

Table 1: Diagnosis index system of Building physical environment

Diagnosis content category	Classification	Specific diagnosis indexes	
Building environment	Sound environment	Indoor background noise	
		Field environmental noise level	
		Palisade structure sound insulation performance	Air sound insulation performance of wall, door, and window
			Floor knocking sound insulation performance
	Wind environment	wind speed of reference surface with 1.5 m height in outdoor pedestrian area	
	Light environment	Indoor daylight factor	
		Sunshine duration	
		Light pollution	
	Thermal environment	Indoor temperature and humidity	
		Heat island intensity	
	Landscape environment	Green space ratio	
		Stratified greening form	

3.2 Building envelope

Diagnosis of building envelope is mainly about building envelope thermal performance, shown in Table 2.

Table 2: Diagnosis index system of building envelope thermal performance

Diagnosis content category	Classification	Specific diagnosis indexes
palisade structure envelope thermal performance	Building facade	Thermodynamic disfigurement
	External wall, and roof	Heat transfer coefficient
	East and west external walls, and roof	Heat insulation performance(the highest temperature of palisade structure inside surface in summer)
	Thermal bridge site	The temperature of palisade structure inside surface in winter
	External window, and curtain wall	Heat transfer coefficient
		Air tightness level
		Visible light transmittance
	Outside shading device	Shading coefficient
		rationality

3.3 Building structure and material

The evaluation contents of building structure and material involve structure safety, utilization of recycled materials, utilization of high strength materials, and using of flexible partition, etc. Concrete contents and specific diagnosis indexes of building structure and material are shown in Table 3.

Table 3: Diagnosis index system of Building Structure and Material

Diagnosis content category	Classification	Specific diagnosis indexes
Building structure and material	Building structure	Building structure strength
	Building material	Weight ratio of recycled materials
		Utilization ratio of high strength concrete
		Utilization ratio of high strength steel
		Using ratio of flexible partition

3.4 HVAC system

HVAC system is vital to improve the indoor heat and humidity environment (LI,2004,2nd Edition). It includes cold and heat source system, distribution system, and terminal system. They are an organic whole and the problem of any part will influence the running effect of air conditioning system as a whole (XU,2006:13-16;YOU,2005). In addition, the energy consumption ratio of HVAC system is larger than other system in the total energy consumption of building (LI,2004). So to promote the implementation of existing buildings green retrofitting work and building energy conservation work, reducing building energy consumption of air conditioning is very important. As a result, the diagnosis of HVAC system involves energy consumption of HVAC system, and the indoor thermal comfort effect. Concrete contents and specific diagnosis indexes of HVAC system are shown in Table 4.

Table 4: Diagnosis index system of HVAC system

Diagnosis content category	Classification		Specific diagnosis indexes
HVAC system	System energy saving	Air conditioning energy consumption	Air conditioning energy consumption per unit area(XUE,2007)
		Energy efficiency of cold and heat source	COP of water chiller refrigeration
			Thermal efficiency of boiler
		Energy efficiency of distribution system	Unit volume power consumption of fan
			Transmission efficiency ratio of chilled water
			Transmission efficiency ratio of cool water
		Energy efficiency of air terminal	Transmission efficiency ratio of air terminal
	Indoor environment quality control	Indoor heat and humidity environment	Temperature, humidity and wind speed
		Air conditioning water system	Hydraulic balance
		Air conditioning wind system	Air volume balance
		Indoor environment quality	The concentration of CO_2
			New air volume
			Monitoring of CO_2

3.5 Water supply and drainage system

Water supply and drainage system is responsible for building water supply and drainage, and it includes water supply and drainage system, hot water, non-traditional water resources and water saving irrigation. Concrete *contents and specific diagnosis indexes of water supply and drainage system are shown in Table 5.*

Table 5: Diagnosis index system of Water Supply and drainage system

Diagnosis content category	Classification		Specific diagnosis indexes
Water Supply and drainage system	Water supply system		Water consumption per unit area or water consumption per capita
			Water supply pressure
			Pipeline leakage quantity
			Water appliance efficiency
			Itemized metering measures
	Irrigation form		water saving irrigation
	Heat water system	Conventional hot water system	Water outlet temperature
			Efficiency of heat resource (thermal efficiency of boiler, energy efficiency of air resource pump)
		Solar water heating system	Water outlet temperature
			Collection efficiency
	Non-traditional water utilization		Water/rainwater utilization ratio
			Water quality

3.6 Lighting and electrical system

The diagnosis of lighting and electrical system mainly involves power supply equipment, lighting system and control system, etc. Concrete contents and specific diagnosis indexes of lighting and electrical system are shown in Table 6.

Table 6: Diagnosis index system of lighting and electrical system

Diagnosis content category	Classification	Specific diagnosis indexes
Lighting and electrical system	Electrical system energy saving	
	Power supply and distribution	Transformer energy efficiency level
		Transformer load rate
		Itemized metering electricity
	Illumination	Energy efficiency of lamp and rectifier
		lighting power density(LPD)
	BAS system	Rationality of control strategy
	Electrical system quality	
	Quality of power supply and distribution system	Deviation of the power supply voltage
		Three-phase voltage imbalance degree
		Harmonic voltage and current
		Power factor
	Illumination quality	Illuminance
		Colour rendering index
		Unified glare rating(UGR)

3.7 Operation and Management

That building operation is good or bad depends on whether the operation management is in place. The most important three aspects of operation management are management team(WANG,2000), management regulation, and technical management. Concrete contents and specific diagnosis indexes of operation and management are shown in Table 7.

Table 7: Diagnosis index system of Operation and Management

Diagnosis content category	Classification	Specific diagnosis indexes
Operation and Management	Energy management team	Established status of management team
		Technical level of management staff
	Management regulation	Established status of Energy saving, water saving, material saving and greening management
		Established status of equipment desk book
		Equipment work instruction
		Management regulation of equipment operation records
	Technical management	Equipment operation strategy
		Equipment maintenance
		Equipment running records

4   DIAGNOSTIC METHODS AND MEASURES
4.1 Diagnostic methods

According to the green transformation goal, green transformation should be diagnosed and analyzed comprehensively from seven aspects, including building environment, palisade structure, HVAC system, water supply and drainage system, lighting and electrical system, and operation and management. Through these diagnosis and analysis, the existing problems and improvement space can be found, so as to provide the basis for subsequent reconstruction project implementation.

The performance diagnosis of existing buildings should adopt the diagnostic method based on logic of "from problem or phenomenon to reason", and "from entirety to part to reason", shown in Figure 1. In other words, on the one hand, according to the actual situation of diagnosed building, the diagnosis can start from the existing problems or phenomenon of existing buildings, and then troubleshoot the possible causes of this problem or phenomenon with the progressive method form the outside to the inside. Finally, the real cause

of the problem can be determined. On the other hand, considering the lack of related problem or phenomenon, the overall performance indexes of existing buildings can be regarded as the starting point of diagnosis, such as energy consumption index, water consumption index and indoor environment index. By these indexes, the existing problems and associated systems can be quickly judged. And then troubleshoot the associated systems with the progressive method form the outside to the inside. Finally, the real cause of the problem can be determined. In a word, the retrofitting potential of existing buildings can be rapidly found by these two kinds of methods.
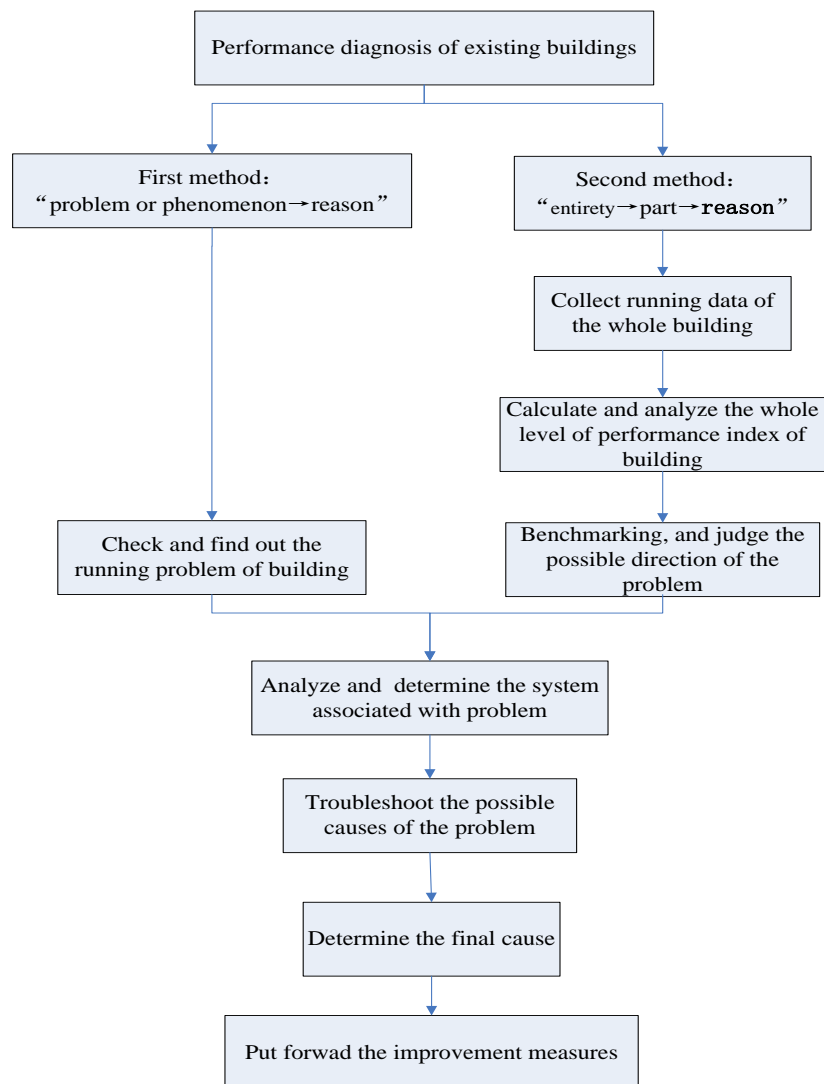
Figure 1: Diagnosis flow diagram

4.2 Diagnostic measures

In the process of implementation of existing buildings green transformation, according to the present situation of existing buildings, based on diagnostic index characteristics and the existing diagnosis conditions, using the method of the combination of long-time data monitoring and short-time data monitoring, the efficiency and quality of diagnosis can be largely improved. The specific diagnosis methods are as followed.

(1) Detection

Detection refers to using of the instrumentation and equipment, such as temperature and humidity meter, watt-hour meter and flow meter, etc. The evaluated objects are directly or indirectly tested in order to get their performance dates. For index parameters which have a clear quantitative data and detection method, such as environmental noise, heat transfer coefficient of enclosure structure, indoor illuminance, etc., diagnosis methods provided by the existing national or industry testing standard can be used. The number

of sampling does not have to be completely carried out in accordance with the standard requirements only if the diagnosis aim can be achieved. For index parameters without available country or industry standard, the detection should be carried out in accordance with the homemade work instructions or testing detailed rules.

(2) Verification

Verification refers to check of technical information and check between data and physical. Verification includes content completeness of technical data, content correctness of technical data, and consistency check of other related data, check of documentation classification and preservation, check and confirm of technical parameters between the corresponding materials, components, equipment or product in the technical data and physicals. For index parameters which are hard to quantify by using measure instrument and equipment, such as the barrier-free facilities, parking space settings and so on, the diagnosis way of verification should be adopted. For contents needing field check, work instructions should be made with detailed verification technology points, including the number of sampling, inspection methods and verification steps, in order to regulate verification diagnosis work, and improve the quality of diagnosis.

(3) Monitoring

Monitoring refers to using instruments and equipment to keep monitoring diagnosed object for a period of time for its running performance data. During the process of existing buildings green diagnosis, if some diagnosis indexes have large changes over time, using short-time site inspection or verification will not meet diagnostic purposes, such as field wind environment, HVAC energy consumption per unit area. For such diagnosis indexes, to obtain running performance data needs to keep monitoring diagnosed object for a period of time with the anemometer, watt-hour meter, heat meter. And then based on these running performance data, the final diagnosis analysis can be given.

5   CASE OF GREEN TRANSFORMATION DIAGNOSIS

Now, this paper uses diagnosis of sound environment as an example to show the specific diagnosis methods. And the specific diagnostic process is shown in Figure 2.
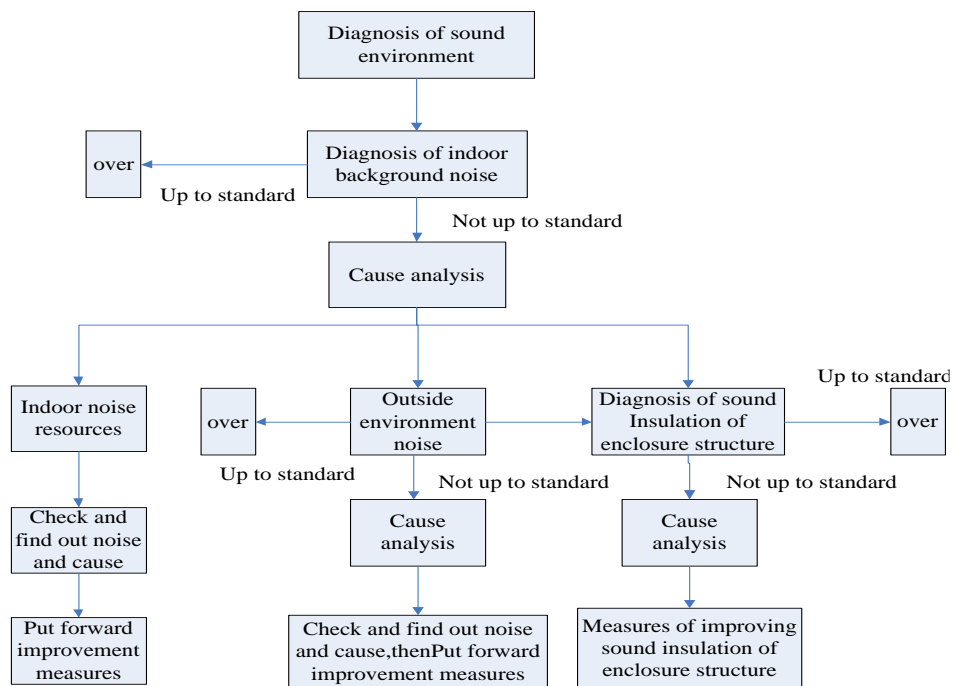

Figure 2: Diagnosis flow diagram of sound environment

Now, with specific cases illustrate diagnosis process:

Phenomenon: a certain office building is located in economic development zone of a certain northern city. And the workers in this building reflect that indoor noise is bigger, especially in places close to the west and south side of the office.

Diagnosis flow is as followed,

First step: according to the feedback of workers, judgment can be given that it is possible for indoor noise not to meet standard. So firstly test the indoor background noise, on the basis of the method provided by appendix A in Code for Design of Sound Insulation of Civil Buildings (GB50118-2010). If the testing results meet the noise limit requirement of the corresponding function room, it shows that the indoor sound environment meet the requirement of standard, and vice versa.

When windows of building are closed, the indoor background noise is detected in the south and west of office, and the results are shown in Table 8.

Table 8: Indoor background noise test results

index	Testing point	Noise value(dB)	Standard value(dB)
Indoor background noise	1 # (close to the western window)	41.6	≤45
	2 # (close to the southern window)	43.1	≤45

From Table 8, the indoor background noise of this case complies with above standard.

Second step: according to detection and analysis of first step, the problem office workers reflect may be caused by outside noise. After investigation and consult, it is known that the workers close to window often open windows, in order to avoid office stuffiness. Therefore, diagnosis workers make preliminary judgment that the outside environment noise is not up to standard, which opening windows cause. Based on this, the outside environment noise is tested by diagnosis workers with reference to article 4.7 of Green Building Detection Technology Standard (CSUS/GBC 05-2014). And the corresponding testing results are shown in Table 9.

Table 9: Diagnosis index system of Operation and Management

index	Testing point	Noise value(dB)	Standard value(dB)
Outdoor background noise	1 # (south)	63.1	≤60
	2 # (west)	59.7	≤60
	3 # (north)	58.5	≤60
	4 # (east)	59.2	≤60

From Table 9, it shows that outdoor background noise in the south is beyond standard value. This is because the south of this project is near four weft road, which have big traffic. So the main noise resource is traffic noise. To the east, the north, and west of this project it is all undeveloped land, and there is no related noise resource.

Through the above two steps, basically the cause of this building indoor noise is determined that in the south of this building traffic noise is bigger, and that leads to that environmental noise value is beyond standard value. Meanwhile, that the indoor office staffs open the windows further lead to indoor so noisy.

For this office building, we put forward the following Suggestions: in building south to grow tall trees green belts or noise barriers, reduce the effects of traffic noise on the site

In above case, the cause the indoor sound environment is worse is that the value of outside environment noise is beyond standard value. In other cases, another situation is that although the value of outside environment noise live up to standard value, the value of indoor environment noise is beyond standard value. To this situation, the diagnosis can be undertaken from the following two aspects.

(1) Check and determination of indoor noise resource: the indoor noise resources mainly include the indoor machine noise of air conditioning, draught noise, and the noise of other household electrical equipment. As

to these noise resources, sound level meter can be used to test equipment, in order to judge whether the noise values of these equipment are up to standard values. For instance, use sound level meter to directly test draught noise values. And if the testing results don't meet the standard values, then the cause that indoor noise value can be determined. But if the testing results meet the standard values, then other equipment needs to be diagnosed one by one.

(2) Sound insulation performance diagnosis of enclosure structure: Even if environmental noise meets standard, bad sound insulation performance of enclosure structure can also lead to that indoor background noise is not up to standard. Sound insulation performance of enclosure structure can be identified by two ways. One is that on the basis of the methods given by "Acoustics-measurement of sound insulation in buildings and of building elements-Part 4: Field measurements of airborne sound insulation between rooms (GB/T18889.4-2005)" and "Acoustics-measurement of sound insulation in buildings and of building elements-Part 7: Field measurements of impact sound insulation of floors (GB/T18889.7-2005)", separately test airborne sound insulation of building elements and impact sound insulation, then according to test results determine whether the sound insulation performance of enclosure structure meets the limit of current standard, "Code for Design of Sound Insulation of Civil Buildings (GB50118-2010)".

The second method is to collect construction drawings of building enclosure structure, and then according to forms of concrete structure of the external wall, window, and floor, determine sound insulation performance of theirs. In the meantime, the ranges of sound insulation of all kinds of palisade structure can be seen appendix A of Code for Design of Sound Insulation of Civil Buildings (GB50118-2010). Finally, if sound insulation performance of enclosure structure does not meet the requirements, the retrofitting of enclosure structure should be considered to raise its sound insulation performance. But if sound insulation performance of enclosure structure meets the requirements, outdoor sound barrier of enclosure structure should be considered.

6   CONCLUSION

At present, Chinese government is actively promoting existing buildings green transformation; and existing buildings diagnosis, as important basic work of existing buildings greening transformation, is an important reference for subsequent transformation plan formulation. Based on both the target of existing buildings green transformation and the content of Green Transformation Assessment Standard for Existing Building (the draft for approval), in this paper, the diagnosis principle of existing buildings green transformation is discussed, the diagnosis content and index system are determined, and the diagnostic methods and measures are put forward. All these provide the direction and reference for the future existing buildings green transformation. In the subsequent actual engineering practice, the diagnosis index system and method in this study will be further implemented and applied to verify its applicability and find improvement direction, in order to finally establish a series of diagnosis technology system of existing buildings green transformation. And thus the realization of green retrofitting of existing buildings can be promoted in China.

7   REFERENCES

LI, E'fei, 2004. HVAC design and common fault analysis [M]. The 2nd Edition. Beijing: China architecture and building press.

LI, Xianrui, 2004. Operation management, energy saving, diagnostic technique guide of Heating and air conditioning system [M].Beijing: China electric power press.

WANG, Qinglan, 2000. Property management and operation guide [M]. Beijing: China architecture and building press.

XU, Xinhua, 2006. Research and development in HVAC system diagnosis [J]. Building science, 49(6A): 13-16.

XUE, Zhifeng, 2007. Energy conservation diagnosis and retrofitting of existing building [M]. Beijing: China architecture and building press.

YOU, Li'ke, 2005. Trouble shooting and energy-saving operation system of central air-conditioning [D]. Chongqing: Chongqing University.

179: A case for application of vacuum insulated panels (VIPs) in high-income area solid wall buildings

Expensive technology for expensive areas

DAVID TETLOW[1], LIA DE SIMON, SAFFA RIFFAT

[1] University of Nottingham, NG7 2RD, Nottingham, UK, Email: david.tetlow@nottingham.ac.uk

The UK is a large producer of carbon emissions releasing over 580 million tonnes of CO_2 equivalent in 2012. One quarter of this (~145 million tonnes) was accounted for by emissions derived from the residential sector. Compared to the 1990 baseline, emission levels in this sector have reduced 14% with this being achieved mainly through a mixture of UK government incentives and imposed energy legislation. However in order for the UK to meet its energy reduction obligations by 2050, significantly higher reductions are required.

According to reviewed UK studies progress in reducing domestic building energy consumption in the past 20 years has been achieved via interventions including: loft and cavity wall insulation, boiler replacements, and installation of double glazing. The majority of these having been targeted in low-income areas, where installation companies can gain access to government sponsored funding schemes such as CERT, CESP, and the ECO. However, these have not extending to enable access to the solutions in middle- and high-income areas, and minor improvements have been made to certain parts of the country, most notably in its city centres that have high-densities of solid wall housing. Recent schemes have been launched to resolve this issue (i.e. the Green Deal); however these have fallen short because of a number of reasons.

This paper addresses two of the main problems: Unsuitability of existing technology, and non-financial feasibility of current innovative solutions. A case study in a Nottingham based end-terrace house is presented for upgrade in which current solid wall insulation solutions are not feasible. A hybrid external-internal solid wall vacuum insulated panel solution was installed in this property and an economic analysis was undertaken based on house prices, rental income, and internal floor area. This was used to analyse the feasibility of this solution for this given case, which was then compared against other similar houses in medium and high income areas of the country. With the installation cost being relatively fixed, the feasibility of this solution became favourable as the value of housing and associated rental increased.

Keywords: Domestic Retrofit, Vacuum Insulated Panels (VIPS), Energy Efficiency, Cost efficiency

1. INTRODUCTION

The demand for solid wall insulation systems in the UK has become relatively stagnant in recent years in the domestic housing sector. Limited growth in demand indicates that UK governmental schemes are proving ineffective at stimulating any kind of growth and the industry is still largely subsidy dependant. One of the likely causes contributing to this factor is that current commercial systems are inadequate in provided a viable retrofit solution for many UK homes, even in those where building owners are actively pursuing a way to save money and reduce their carbon emissions. A solution to this issue is the use of super-insulation based systems, although due to their inherent high price, these are currently marginalised to niche applications. This paper presents the implications of the existing retrofit market to the UK as a whole and the potential drivers for change that are likely to start having impact in the next 10-15 years in the retrofit market. A case study in UK city of Nottingham is then given where a VIP system is to be used with the associated costs and considerations for its investment quality being discussed. Application of this system in comparable buildings in wealthier UK cities is then presented to emphasize the potential impacts that upcoming legislation changes will have in the UK rental market.

2. CLIMATE CHANGE AND THE UK RESIDENTIAL SECTOR
2.1. UK carbon emissions

The impact of climate change is widely recognised as one of the greatest challenges faced by the current generation, with science confirming within a 95% certainty that anthropogenic activities are the leading cause. The recent IPCC document *Climate Change 2013: Physical Science Basis* reported average global land and ocean surface temperature increases ranging between 0.7-0.9°C. This has led to a range of impacts including: diminishing snow and ice, raising sea levels, and erosions of top soils; all of which cause unfavourable global conditions for future generations (IPCC 2013). The *Kyoto protocol* was an international treaty directed at addressing this issue; it was signed by the leading developed world economies in 1997 (*Annex B*), coming into force 2005 (UNFCC 1997). In its first period from 2008-2012, countries directly involved were committed to reducing equivalent CO_2 emissions of leading greenhouse gases (*Annex A*) by at least 5% on assigned 1990 baseline levels (UNFCC 1997; UNFCC 2008). Post completion of this period the protocol was extended through the *Doha amendment* to incorporate the period of 2013-2020, where Annex B countries are committed to reduce emissions by at least 18% of the 1990 baseline (UNFCC 2012).

The United Kingdom ratified the protocol in 2002 and in 2006 published it was committed to reducing its emissions by an ambitious 12.5% on the 1990 baseline (779 MtCO$_2$e) in the first Kyoto period 2008-2012 (DEFRA 2006); this was subsequently followed by the adaptation of legislation through the establishment of the *Climate Change Act* (CCA) in 2008, making it law (Government 2008). According to the recent *Doha amendment* of the protocol, the European Union (and by extension the UK) is committed to reducing GHG emissions by at least 20% on the 1990 baseline in the second Kyoto period 2013-2020; the UK has yet to officially ratify the amendment, however, this will be achieved through its national commitment to reduce emissions by 26% by 2020 as stated in the *Climate Change Act* (CCA) (Government 2008; UNFCC 2012).

In February 2014 the UK Department of Energy and Climate Change (DECC) published the *2012 UK Greenhouse Gas Emissions, Final Figures* report showing the level emissions were reduced in each sector (Energy, Transport, Business, Residential, etc) from 1990 to 2012 ((DECC) 2014). Figures in this document were based on commitments to both *Kyoto protocol* coverage and *UK Carbon Budgets* (CCA), and showed average carbon reductions, on the 1990 base year, ranging from 22.5% - 24.5% (the value dependant on which commitment was considered, i.e. Kyoto or CCA), and if emissions trading was taken into account. These figures demonstrated the UK's commitment to mitigation of climate change; however the savings observed were generally isolated to specific sectors. For example, a 36% carbon reduction in the energy supply sector was observed through the closure of 30% (~15 Mtoe) of coal based power stations through establishment of 15-20 Mtoe of more efficient natural gas versions, whereas no significant changes were made in other forms (Nuclear, Renewables, etc). In addition the report did not provide information on the *end-use* of energy; for example an average 10% carbon reduction was observe in the residential sector, this most notably being attributed to the use of natural gas for space heating and cooking, however no information on electrical energy used for the same purposes (or any other task).

In March of 2014 this issue was resolved through the release by DECC of the *2013 UK Greenhouse Gas Emissions, Provisional Figures and 2012 UK Greenhouse Gas Emissions, Final Figures by Fuel Type and End-User* report in which GHG emissions were given as attributed to *end user* use within each sector ((DECC) 2014). *Figure 1.1 – 1.2* show the main findings in relation to the emission data from both mentioned reports for the sectors included in the UK. The largest savings having been achieved in the *Business* (70-

75 MtCO$_2$e) and *Industry Process* (44-46 MtCO$_2$e) sectors, all others having average savings below 25 MtCO$_2$e (*Figure 1.2*). The three sectors that contributed the largest proportion of pollution (*Transport, Residential*, and *Business*) accounted for *71.6%* of emissions in 1990 and *79.4%* in 2012. Governmental policies to reduce UK emissions would therefore be most effective targeted at these sectors; however as of 2014 progress has only been made in *Business*:

- *Transport* emissions were 133.6 MtCO$_2$e, reduced 4.2% from 139.6 MtCO$_2$e in 1990; this sector accounts for 23.2% of 2012 UK emissions
- *Residential* emissions were 145.3 MtCO$_2$e, reduced 14.4% from 169.7 MtCO$_2$e in 1990; this sector accounts for 25.3% of 2012 UK emissions.
- *Business* emissions were 178.2 MtCO$_2$e, reduced 28.3% from 248.5 MtCO$_2$e in 1990; this sector accounts for 31% of 2012 UK emissions
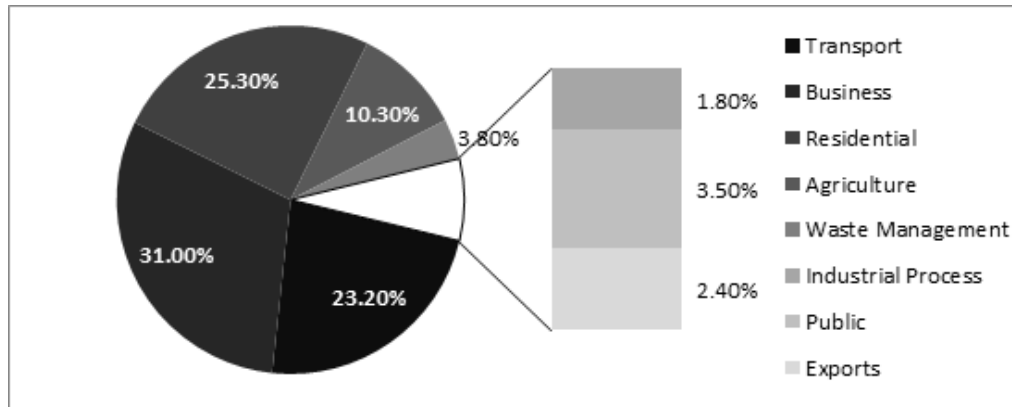
Figure 1.2 – 2012 percentage of UK emissions per sector attributed to the end user (575 MtCO$_2$e) ((DECC) 2014)
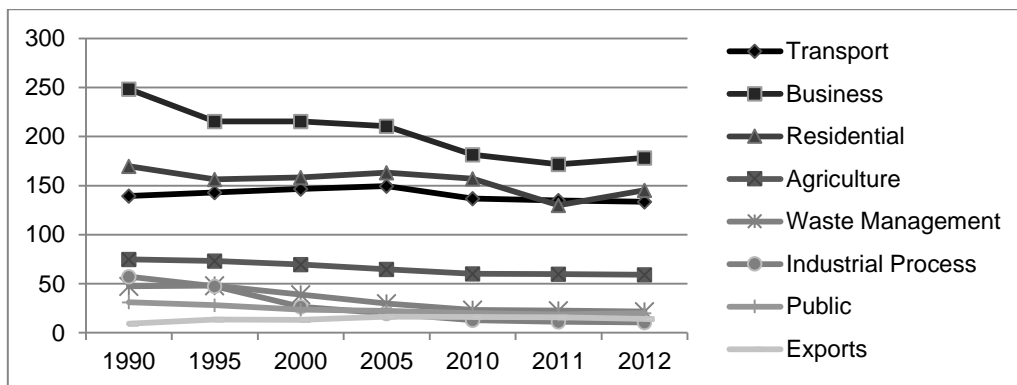
Figure 1.3 – UK GHG emission figures across all sectors, including end user data in MtCO2e from 1990 to 2012 ((DECC) 2014)

Other areas proportionate savings were made (>25 MtCO$_2$e) were in *Waste Management* and *Industry;* however, post 2014 no significant further progress can be made in either as emission levels are below or equal to 20 MtCO$_2$e. The UK's challenge remains in reducing emissions in the three sectors listed above and Agriculture (albeit this having emissions a third that of the former - 59.1 MtCO$_2$e as of 2012). According to the report figures 26% of the 80% reduction has already been achieved for the 2050 target ((DECC) 2014). Considering it is 13 years since the UK ratified Kyoto and 35 remain until the target date, relative progress has been made to date. However, it should be noted that all *Business, Industry* and *Waste Management* are subject to direct authoritative influence of imposed regulations in the UK economy. Based on the data shown it could be argued savings to date in the sectors mentioned were relatively easier in comparison to those in others; these being the *low-hanging fruit* of the 1990 emission content. This is most relevant when we compare the ease of making carbon reductions in the aforementioned sectors, to those that are to be made in *Transport* and *Residential*.

2.2. Strategies to reduce emissions of the UK residential sector

Emissions from the *Residential* sector were reported to arise from the use of energy in peoples' homes for central heating, cooking, lighting, etc. ((DECC) 2014). Unlike *Business* and *Transport* sectors, this element of UK emissions is likely to incorporate a higher scope with respect to the *voting public*; therefore any governmental action to reduce emissions could compromise political popularity if too stringent. An example would be the increase of climate change taxation on energy bills, as these directly affect public standard of living. As of 2014, this levy currently stands between 9-10% (~£110) of an average annual energy bill (~£1200) (Ofgem 2013). The 15% reduction observed in the 2012 figures is likely to have been achieved through increasing stringency of the building regulations (G. 2005; OPDM 2010; OPDM 2010), and a number of government financial mechanisms including: the *Carbon Emissions Reduction Target (CERT)*, the *Community Energy Savings Programme (CESP)*, the *Decent Homes* standard, and the *Warm Front* scheme (Dowson, Poole et al. 2012; Hamilton, Shipworth et al. 2014). Albeit the general intension of energy taxation is towards improvement of public health and mitigation of climate change, studies have shown there is a lack of trust about use of the revenues generated, and difficulty in public understanding the tax purpose (Dresner, Jackson et al. 2006). Additionally the changing of energy consumption habits is difficulty in the housing sector, especially as low-income households often face problematic housing conditions and utilise inefficient appliances, but lack the resources to make energy-saving investments (Schaffrin and Reibling 2015).

Of the approximate 27.5 million dwellings in the UK, 21 million are in England (Government 2012; David Beckett 2014) and Figures 1.4 shows the distribution of UK house types. This figure were presented in an extensive review of the UK housing stock and the barriers to performance written by Dowson et al (Dowson, Poole et al. 2012). Within this study it was stated there is a strong correlation between age and tenure characteristics of dwellings and their thermal efficiency, with around nine million houses being classified as *Hard to Treat*. Dowson reported in order for the UK to meet its 2050 target for residential energy efficiency the national average SAP rating would need to be 80, this standing at 52.1 in 2006 (these figures referenced from Roberts (Roberts 2008)). Additionally, the most effective measure identified to achieve this target is the installation of solid wall insulation, this providing double the savings of all alternatives (Shorrock L. 2008). Albeit this the case, the level of market penetration of this technology will be limited prior 2050 based on forecasts using existing data where the number of installations taking place per year stands at 15-20,000 (Figure 1.4) (Shorrock L. 2008; Dowson, Poole et al. 2012)
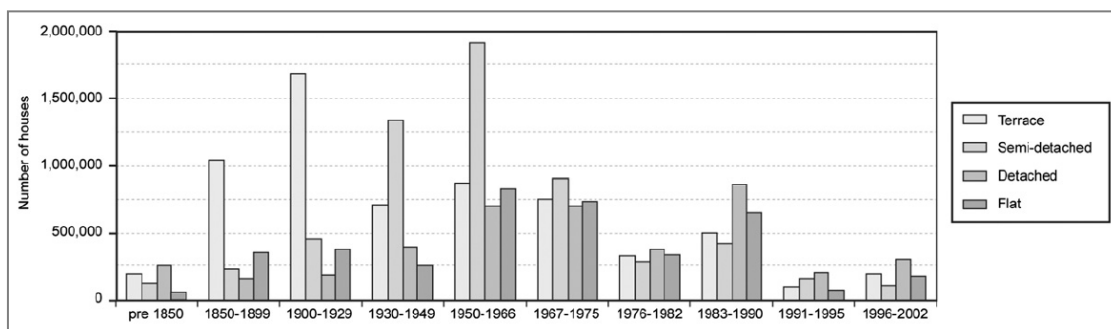
Figure 1.4 - Profile of the UK Housing stock by age and type (Dowson, Poole et al. 2012; Government 2012)
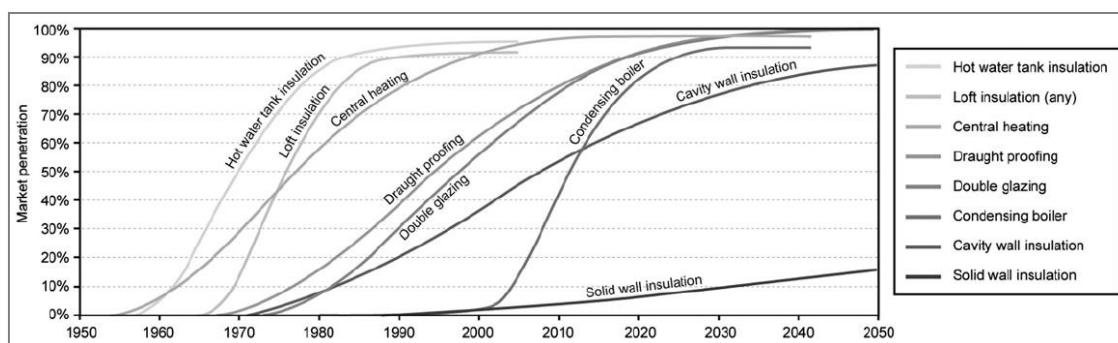

Figure 1.4 - Market penetration of conventional energy efficiency measures (Dowson, Poole et al. 2012; Government 2012)

In an attempt to catalyse the uptake of retrofit measures and the rate at which solid wall insulation was installed nationally, the UK government launched its *Green Deal* Scheme in 2012. Where previous funds

had been grant based, the new scheme was aimed at the introduction of loans that were placed against the building and recuperated over a 25-30 year period via savings in the energy bills. The foundation of scheme was based on the concept of the *Golden Rule* that stipulated in order for the loan to be given, the size of the monthly repayments had to be below the saving provided by the installed retrofit measures (Change 2010).

Unfortunately, post its soft launch the scheme came under severe criticism due to lack of transparency in its definitions (most notably in financial details), and after over 30,000 surveys in its first month only four loans were taken. The acute failure of the initial version of this scheme has been led to its re-launching in 2014, with the grant system replacing the loan concept. In the past three years the subject of the *Green Deal* and its shortcomings has been the focus of many academic studies (2012; James 2012; Booth and Choudhary 2013; Hope and Booth 2014; Marchand, Koh et al. 2015), however it is the general consensus that the main barriers to its success are based in three areas: (1) the lack of occupant awareness and understanding of its mechanisms; (2) its costs being too high with respect to loan interest repayments; and, (3) lack of a technically viable solution for a large proportion of the buildings to be retrofitted. The remainder of this article will be focussed on addressing the 3rd statement for external or internal wall insulation installation.

The building regulations currently stipulate that if a retrofit to a wall element is to be done, the U-Value should be improved to a maximum 0.3 $W/m^2.K$ threshold (OPDM 2010). In relation to the existing commercially available retrofit systems (i.e. those based on either: polystyrene, mineral fibre, polyurethane, etc.), this creates a problem in relation to certain house types where space is a limited commodity; most notably in terrace and semi-detached houses which account for two thirds of the housing stock (see Figure 1.4) (Government 2012). To reduce a typical solid wall U-Value from 2.1 to the 0.3 requirement, between 90 -120mm of insulation is required (thickness dependant on insulation) ((CIBSE) 2006). The most convenient place to attach the insulation measures is externally; however, in many cases this cannot occur. For example, the wall where the intervention is to be positioned could stand at a property boundary, and the remaining internal option would then have to be utilised. With the average internal floor areas for UK terrace and semi-detached houses standing at 70m^2 and 85m^2 respectively (Government 2012), many building owners are choosing not to insulate as the current technology is not fit for purpose in relation to their expectations. This is most notably relevant in wealthy city centre locations of the UK where house purchase prices are often double the national average for equivalent types (Statistics 2015).

A high proportion of homes in the UK are rented either: privately, through housing associations, or via local authorities, the figure currently standing at 37% (David Beckett 2014). With energy prices being relatively low (UKGOV 2015) compared to the national average income (Statistics 2015) there is little incentive for landlords to upgrade their buildings as the figures indicate the average building tenant in the UK can afford to pollute in addition to rent and other life costs. Albeit this the case, it was reported in 2011 that around 11% of home rented in the private sector had *Energy Performance Certificate (EPC)* ratings of F (7%) or G (3%); with houses in this condition being known to cause a variety of physical and mental health problems as well as forcing low income families into fuel poverty (Change 2014). With the mediocre impact of schemes such as the Green Deal, aimed at provision of subsidies for building retrofit to improve the mentioned issues, the UK government has turned to regulatory strategies to enforce owners to upgrade he buildings they rent to tenants (Change 2014; Government 2015). From April 2016, any UK tenant living in a grade F or G rated rental house will be permitted to request it be upgraded to a grade E, with the landlord being legally bound to carry out the required measures; by April 2018 it will not be permitted to rent out a house with a rating below E. The overall government aim of this legislator strategy is to make all rental homes a grade C standard by 2030 via law.

Achieving the 2018 target would be relatively straight forward for landlords, as to achieve an E-rating the number of SAP points must be between 39-54 (Change 2012). For example, in an average size building the installation of a condensing boiler the SAP rating could be improved between 44-47 points (the value depending on the existing circumstances). Considering this, it could be argued that landlords are being given a grace period to make easier improvements, although two scenarios are set to occur. Firstly, the methodology of SAP is regularly being updated and the quantities of points certain measures are scored are likely to be reduced in favour for those with higher energy reducing impact. Secondly, in order to achieve a D-Rating (55-68 points) or C-Rating (69-80 points) the list of available inexpensive measures that could be installed reduces. Additionally, considering the previous point that the national SAP-rating average would need to be 80 by 2050 (i.e. the border between SAP C and B-Ratings), it would be logical to predict that further legislation will be imposed post 2030.

Accounting all points discussed, by the end of the current decade through to 2030, it is feasible to expect that UK landlords will be in a position to decide what measures are most effective to achieve the SAP ratings so their solid wall hard to treat properties can remain legally rented. As identified the best option available to achieve this is solid wall insulation, however current commercial technology renders this impractical due to the inherent loss of space, most notably with internal applications. A market opportunity is thus available for any insulation manufacturer that can address this issue, as the resistivity of the insulation inevitably affects the main thickness of the solid wall system. Understanding this point, certain manufacturers have invested in the development of super-insulation based systems, these being based on either Aerogel or Vacuum Insulated Panels (VIPS). Both aerogel and VIP systems have been market available for many years from American and German manufacturers, however these have been marginalised to niche applications as the inherent insulation cost is seven to ten times that of commercial equivalents. This paper will assess the financial feasibility of the installation of VIPs on a Nottingham terrace house that is being retrofitted with VIPs via the Holistic Energy-efficient Retrofit of Buildings (HERB) project. Cases will be identified where the financial feasibility will be acceptable and the potential impacts of this in the future.

3. THE NOTTINGHAM CASE STUDY
3.1. The existing conditions

The house is based on a terrace design that was popular in the UK in the later part of the 19th century, with numerous buildings of this type located across the centre of the city of Nottingham. This design is ubiquitous in many other UK cities, due to the large manufacturing activities that took place towards the end of the industrial revolution (R 2003; B 2007). The house is based on a *two up / two down* design and is an end-terrace with one side façade being an external wall used as an access route to its backyard; the house would normally be inhabited by a couple or a small family. Figure 3.1 shows photographs of the front and rear of the property, and the occupied internal floor area of this house is 59m^2.

Figure 3.1 – Front, side and rear images of the Nottingham End-terrace house

The images in figure 3.1 highlights two areas on the property that create a significant challenge in retrofitting the house; the first of these is that the front of the property is directly on its outer boundary, with the external façade being directly on a public pathway; the second issue is that the side façade boundary is in direct contact with a shared access route to the rear of the property, this being used by seven other of the neighbouring buildings. The surveyed wall thickness of these facades was 240mm, this incorporating both brick and internal plaster layers.

3.2. Solid wall retrofit options

Assuming a condensing boiler is installed, all windows have been upgraded to double-glazing, and the loft space has been insulated to the regulatory standard of 0.16 W/m.K, the building would currently achieve a high D-rating in RdSAP (between 64-68 points); the inclusion of external wall insulation would provide enough additional points to increase the score to a C-Rating (80+ points). On the assumption that the thickness of the brick layer matches that referenced in CIBSE Guide A, each façade would have a U-Value of 2.1 W/m^2.K; using this value the minimum thicknesses of insulation were calculated for a range of typical commercial insulations, aerogel and vacuum insulated panels, to enable the U-Value to be reduced to the 0.3 benchmark (Table 3.1).

Table 3.1 – Required thickness values to reduce external façade U-Values to retrofit regulation requirement

Insulation	EPS (superior)	Mineral Fibre (superior)	Polyurethane	Phenolic	Aerogel	VIPs
λ-value (W/m.K)	0.035	0.035	0.028	0.021	0.014	0.007
Required thickness (mm)	100	100	80	60	40	20

The thickness requirements of current commercial insulations in Table 3.1 cause a problem in retrofitting this end-terrace externally. Both front and side façades are directly on access routes, and the addition of a 60-100mm layer of insulation would encroach over this space. This most notably causes a problem with the side access with the width of this area being only one meter. For example, this route is regularly utilised to transfer domestic waste from the back of the building (and neighbouring houses) via large 60mm wide wheel based bins, and if 100mm of insulation were to theoretically be applied to the side facades of both houses on the access the amount of space to manoeuvre would be limited. Only portions of the rear façade could be externally insulated with current products without any disruption. In the internal wall area of the external façades, a further set of challenges occur, these can be observed via the highlighted sections of figures 3.2 and 3.3. On both ground and first floor levels 800mm wide access routes are inset into a mid-house load-bearing partition wall and are directly connected to the external wall. If an internal insulation solution were to be applied, the access route would have to be either relocated or have its width reduced below 700mm. The first option of these would be highly expensive as it would encroach onto the stairwell space (which would have to be repositioned), and the second option would cause issues in reduction of access space; for example, a wheel chair based disabled person could have difficulties. In the kitchen and bathroom spaces, a significant proportion of inset furniture (bath, kitchen cupboards, worktops, etc) and building services (electrical, water, and mains gas) are located on or close to (<100mm) the external walls to be retrofitted. The inclusion of internal insulation would require the removal and repositioning of these objects during the installation process, incurring further added cost. Mitigating the financial impacts of the mentioned points would therefore be paramount in ensuring cost efficiency of the retrofit process.
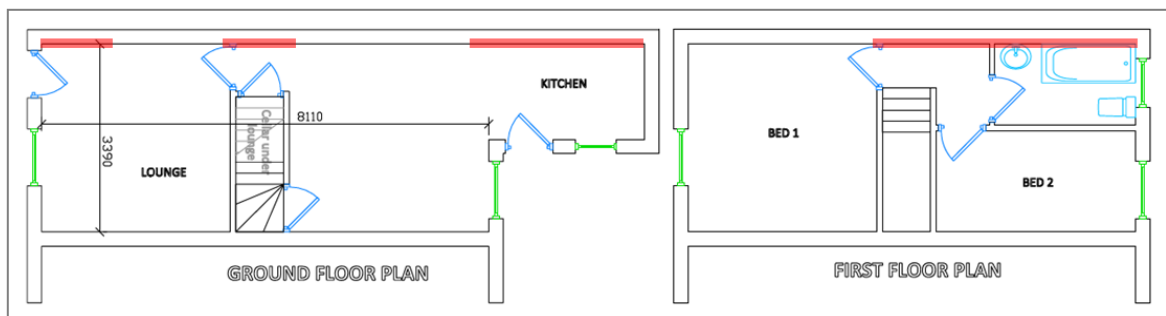

Figure 3.2 – Ground and first floor plans with highlighted problem areas

Figure 3.3 – Images showing problem areas: (far-left) ground floor access way; (mid-left) ground floor kitchen; (mid-right) first floor access way; and, (far-right) first floor bathroom

Table 3.2 – Typical costs of UK insulation systems [ref]

System Insulation	EPS (superior)		Mineral Fibre (superior)		Polyurethane		Phenolic		VIPs	
Methodology	EWI	IWI	EWI	IWI	EWI	IWI	EWI	IWI	EWI	IWI
Typical cost range (£/m²)	65-70	55-60	65-70	55-60	75-80	65-70	80-85	70-75	125-130	195-200
Cost for end-terrace retrofit(£)	7350	6300	7350	6300	8400	7350	8925	7875	13,650	21,000
Payback* (years)	16.5	14	16.5	14	18.75	16.5	20	17.5	30	46
(with £3k subsidy)	(9.75)	(7.5)	(9.75)	(7.5)	(12)	(9.75)	(13.25)	(11)	(23.75)	(40)

based upon a 75% saving on annual gas bill of £600 [UK national average ref]. This is assuming the maximum installation cost per square meter shown is used in the calculation for the retrofit install. All payback rounded up to the nearest quarter, with the final assumption that £3000 would be provided for a Green Deal subsidy.

Based on the observations made, it would be unlikely that a solid wall insulation solution could be specified by a typical UK based installation company for this building, as it is likely only existing commercial systems would be available. This case study would therefore be an ideal example where a superinsulation system, based on aerogel or VIPs, could be used as an application as the magnitude of space requirement to achieve the regulations would be considerably less. The problem with the use of super insulation systems is the additional premium that must be paid via their substitution for commercial insulations. The terrace house surveyed areas of each external facade to be insulated are approximately 20m² (Front), 25m² (Rear), and 60m² (side); a total of 105m². Table 3.2 shows the range of typical install costs for commercial systems, these being compared against potential internal VIP solutions.

3.3. Quality of investment

The table 3.2 costs incorporate all additional material and labour based expenses for a typical installation company, and for the purpose of this paper these have been set to the same for each technology (£50-60/m²). The only exception is the internal application the VIP product, this being more expensive than its external version; the additional costs are attributed to the complete repositioning of the internal building services. Normally, in IWI system applications the insulation is cut or holes in the panels are made onsite to make room for services, however this would compromise the thermal efficiency of VIP panels due to loss of vacuum via film penetration, the mentioned alternative measures have to be made with an additional impact to labour and material costs; conservatively estimated to a maximum value of £60-65/m². In the recent loan based Green Deal scheme the cost of the retrofit would be repaid via a 25 year loan, with an element of this finance incorporating an interest payment; this indicating the inherent finance would have been raised via financial investment mechanisms (pension funds, etc.). The timescales in Table 3.2 show all commercial products fall under the 25 year period, therefore in concept making considerations for the assumptions used, room for the additional interest payments could fall within these spaces; the timescales for both VIP systems would not be acceptable for the Green Deal loan. This mechanism has now been abandoned by the UK government and has been replaced with a subsidy based system where one third to a half of the install cost for a typical UK commercial retrofit product is covered by the scheme, the remainder being covered by the building owner.

For the owner occupier the return on investment of the retrofit would be both financial via bill savings and better living conditions in the form of a warmer house. However, in the case where the building is let, all main benefits mentioned would be passed to the tenant. If the former loan based system had been successful, the circumstances may have been acceptable to many landlords as the retrofit costs would eventually be paid off via remuneration through energy bills. Therefore, with respect to the subsidy option, the question posed is *'Where is the selling point?'* It could be argued that as the building is energy efficient and has better comfort post retrofit, a larger amount of rent could be charged for its tenancy or would be more valuable in a sale; unfortunately, this investment condition would have to be considered over a long term period, could be open to fluctuations in economic conditions depending on location, and as a result many landlords would likely not be comfortable making the investment. In this case, now that the carrot has been provided via subsidy, the stick of legislation would have to be considered; this being *'How much income is there to lose, through a non-compliant in-efficient building?'* It is likely the answer to this would depend on a range of factors, however with the cost of retrofit being relatively set through the industry; the

most import consideration would therefore be location. The building in Nottingham is located in a relatively low-income based area, and the rental costs for a house of this type are £350-£400 per chartered month. If the building were to be sold on the current 2015 market, the price would range at £60-70,000 (both rental and sale prices are dependent on the building's condition). The surveyed internal floor area of the building was measured at 59.5m^2, which would give a specific rental value of £6-9 per square meter per chartered month (pcm).

Table 3.3 – Matrix of potential income loss in comparable UK cities

Region (related City)	East Midlands (Nottingham)	North West (Manchester)	South West (Bristol)	London
Related City population	285,000	420,000	380,000	7,200,000
Potential rental loss (£/m^2)*	368 - 450	375 - 475	450 - 575	875 – 1,387

*****These numbers reflect all house types in UK cities**

It is likely as regulation becomes imposed the demand for insulation systems including those with VIPs will increase. The case study used in this paper is relatively small in relation to UK terrace houses, using the national average of 65-70m^2 (Government 2012). Using the UK national statistics for rental values (GOV 2014), loss if income in other regions of the country are shown in Table 3.3; the number of pre-1920 terrace houses in these locations is given which indicates the size of the potential markets for VIP based solid wall systems.

4. FINAL DISCUSSION AND SUMMARY

The purpose of this paper was to highlight a specific area of the UK retrofit market that is still in its infancy in industrial capacity terms and the drivers that will lead to its potential maturity. Albeit many assumptions have been made, the impact of rental market legislation has potential to cause large demand in super insulation based solid wall systems due to the inherent loss of income that will be imposed on landlords that do not comply. Taking this into account it is through the assumptions made in this study that further research questions can be made prior any clarity in the potential market being achieved; these being: (1) Of the energy savings that are required in the housing sector, what proportion are accounted for in buildings under similar restrictions to that used in this study?; (2) If the SAP method is to be revised, when is this likely to occur and will the changes made have significant impacts to the number of points that are awarded to the retrofit measures, including solid wall systems, and what implications will that have to the houses similar to the one used in this study?; (3) To get an account of the potential market, what number of houses with circumstances similar to that in this study exist in the UK?; (4) with respect to the thickness of the available insulation systems, what amount of saving in £/m^2 is saved via the use of super insulation systems and would this be more applicable in more expensive areas? Pursuit into the investigation of these questions is recommended for future research as this paper has highlighted a potential demand in future retrofit markets for super insulation based systems within the next 10-15 years, most notably in areas where building owners have a lot to lose financially in rent.

5. REFERENCES

(2012). "UK 'Green Deal' under threat?" Renewable Energy Focus 13(2): 8.

(CIBSE), C. I. o. B. S. E. (2006). Guide A: Environmental Design. CIBSE.

(DECC), D. o. E. C. C. (2014). 2012 UK Greenhouse Gas Emissions, Final Figures Statistical release 4th February 2014. D. o. E. C. Change. 3 Whitehall Place, London SW1A 2AW: 45.

(DECC), D. o. E. C. C. (2014). 2013 UK Greenhouse Gas Emissions, Provisional Figures and 2012 UK Greenhouse Gas Emissions, Final Figures by Fuel Type and End-User. N. Statistics. 3 Whitehall Place, London SW1A 2AW: 44.

B, B. (2007). Home Truths: A low carbon strategy to reduce UK housing emissions by 80%. F. o. t. E. University of Oxford. London, UK.

BOOTH, A. T. and R. Choudhary (2013). "Decision making under uncertainty in the retrofit analysis of the UK housing stock: Implications for the Green Deal." Energy and Buildings 64: 292-308.

Change, D.-D. o. E. a. C. (2010). The Green Deal - A summary of the Governments proposals, Crown Copyright, Ref 10D/996.

Change, D.-D. o. E. a. C. (2012). The Government's Standard Assessment Procedure for Energy Rating of Dwellings. DECC, BRE.

Change, D.-D. o. E. a. C. (2014). Private Rented Sector Energy Efficiency Regulations (Domestic) (England and Wales). DECC.

BECKETT, D, O.-O. f. N. S. (2014). Trends in the United Kingdom Housing - Market.

DEFRA (2006). The UK's Initial Report under the Kyoto Protocol C. E. S. A. Division. London: 40.

DOWSON, M., A. Poole, et al. (2012). "Domestic UK retrofit challenge: Barriers, incentives and current performance leading into the Green Deal." Energy Policy 50: 294-305.

DRESNER, S., T. Jackson, et al. (2006). "History and social responses to environmental tax reform in the United Kingdom." Energy Policy 34(8): 930-939.

G., K. (2005). Built Fabric & Building Regulations. 40% House Project. E. C. Institute. Oxford, UK, University of Oxford.

GOV, U. (2014). "Private rental market statistics (England only)." from https://www.gov.uk/government/statistics/private-rental-market-statistics-england-only.

Government, C.-C. a. L. (2012). English house condition survey, Headline Report 2010-2011. London, UK, CLG Publications.

Government, H. (2008). The Climate Change Act 2008 (c. 27). United Kingdom.

Government, U.-U. (2015). ENERGY CONSERVATION, ENGLAND AND WALES - The Energy Efficiency (Private Rented Property) (England and Wales) Regulations 2015 2015 No. 0000 UK.

HAMILTON, I. G., D. Shipworth, et al. (2014). "Uptake of energy efficiency interventions in English dwellings." Building Research & Information 42(3): 255-275.

HOPE, A. J. and A. Booth (2014). "Attitudes and behaviours of private sector landlords towards the energy efficiency of tenanted homes." Energy Policy 75(0): 369-378.

IPCC (2013). Climate Change 2013: The Physical Science Basis. Contribution of Working Group I to the Fifth Assessment Report of the Intergovernmental Panel on Climate Change T. F. Stocker, D. Qin, G.-K. Plattner, M. Tignor, S.K. Allen, J. Boschung, A. Nauels, Y. Xia, V. Bex and P.M. Midgley. Cambridge, United Kingdom and New York, NY, USA, , Cambridge University Press: 1552.

JAMES, P. (2012). "Overcoming barriers to low carbon dwellings: The need for innovative models of finance and service-provision." Environmental Development 2(0): 6-17.

MARCHAND, R. D., S. C. L. Koh, et al. (2015). "Delivering energy efficiency and carbon reduction schemes in England: Lessons from Green Deal Pioneer Places." Energy Policy 84(0): 96-106.

Ofgem (2013). Update dhousehold energy bills explained - Factsheet. O. o. G. a. E. Markets. London, UK: 1-4.

OPDM (2010). Building Regulations Part L1A - Conservation of Fuel & Power in new dwellings. P. Portal. Available at: <http://www.planningportal.gov.uk/uploads/br/BR_PDF_AD_L1A_2011.pdf>.

OPDM (2010). Building Regulations Part L1B - Conservation of Fuel & Power in existing dwellings. P. Portal. Available at: <http://www.planningportal.gov.uk/uploads/br/BR_PDF_AD_L1B_2011.pdf>.

R, O. (2003). The survey and repair of traditional buildings. Shaftesbury, Donhead Publishing.

ROBERTS, S. (2008). "Effects of climate change on the built environment." Energy Policy 36(12): 4552-4557.

SCHAFFRIN, A. and N. Reibling (2015). "Household energy and climate mitigation policies: Investigating energy practices in the housing sector." Energy Policy 77: 1-10.

SHORROCK L., H. J., Utley J. (2008). Reducing Carbon Emissions from the UK housing stock. BRE Press, Watford, UK.

Statistics, O.-O. f. N. (2015). Statistical Bulletin - House Price Index, March 2015, OfNS.

Statistics, O.-O. f. N. (2015). Understanding Average Earnings for the Continuously Employed - Using the Annual Survey of Hours and Earnings 2014. OfNS.

UKGOV (2015). Special Feature Variation in Tariff types and Energy bills. OfNS.

UNFCC (1997). Kyoto Protocol to the United Nations Framework Convention on Climate Change. IPCC. Kyoto, Japan.

UNFCC (2008). Kyoto Protocol Reference Manual on Accounting of Emissions and Assigned Amounts. Martin-Luther-King-Strasse 8, 53175 Bonn, Germany, Climate Change Secretariat (UNFCCC): 130.

UNFCC (2012). Doha amendment to the Kyoto Protocol IPCC. Doha, Qatar.

SESSION 35: ENERGY EFFICIENCY IN BUILDINGS

181: Calibration of the simulation model of the HERB building in bologna in its present state

Enzo Zanchini[1], Claudia Naldi[2], Stefano Lazzari[3],
Stefania Falcioni[4], Gian Luca Morini[5]

1 University of Bologna, Department of Industrial Engineering, Viale Risorgimento 2, 40136 Bologna, Italy, enzo.zanchini@unibo.it
2 University of Bologna, Department of Industrial Engineering, Viale Risorgimento 2, 40136 Bologna, Italy, claudia.naldi2@unibo.it
3University of Genova, Department of Sciences for Architecture, Stradone S. Agostino, 37, 16123 Genova, Italy, stefano.lazzari@unige.it
4University of Bologna, Department of Industrial Engineering, Viale Risorgimento 2, 40136 Bologna, Italy, stefania.falcioni@unibo.it
5University of Bologna, Department of Industrial Engineering, Viale Risorgimento 2, 40136 Bologna, Italy, gianluca.morini3@unibo.it

In the framework of the EU-funded Project HERB (Holistic Energy-efficient Retrofitting of residential Buildings), the University of Bologna and the Municipality of Bologna are performing the energy retrofitting of a detached house with 6 apartments in Bologna. The annual saving of primary energy obtained by the retrofitting will be assessed through dynamic simulations of the building before and after retrofitting, performed through a model implemented in TRNSYS 17 and calibrated by comparison with monitoring results. In this paper, the calibration of the building model in its present state is described.

The 3-D hourly simulation model of the building was obtained starting from 3-D drawings performed through Google SketchUp. Four thermal zones were considered for each small apartment (bedroom, bathroom, kitchen-living room, entrance) and five thermal zones for a larger apartment. The characteristics of the building enclosure were determined by accurate inspections and tests, which included infrared thermography, blower door tests and direct measurements of the transmittance of the external vertical wall.

The building was monitored during the heating season 2013-2014. The use of natural gas for heating was determined by periodic readings of the gas meter placed in the distribution duct to the central boiler, hourly values of the internal air temperature and relative humidity in each room were recorded, while hourly weather data were taken from the Bologna Urbana Weather Station, close to the building. The internal heat gains were evaluated through measurements of the use of electricity and of natural gas in single apartments.

A comparison between the measured values of the primary energy use for heating during 16 time intervals and those determined by dynamic simulation revealed that the simulation model widely fulfils the accuracy requirements stated by ASHRAE Guide 14 and yields the measured total energy use for heating during the season considered with an accuracy better than 0.4%.

Keywords: building dynamic simulation – building monitoring – model calibration

1. INTRODUCTION

The economic growth of the 20th century has been based on a progressive increase of the world annual use of fossil fuels. Even now, the world annual use of fossil fuels is increasing and, as is well known (see, for instance IPCC Fifth Assessment Report – AR5, https://www.ipcc.ch/report/ar5/wg1/), the emission of carbon dioxide and of other greenhouse gases is causing an important climate change. Therefore, all the industrialized and developing countries and, most of all, the European Union, are struggling to shift the economic growth towards a sustainable development, based on the increase of energy efficiency and on the use of renewable energy sources. An important reduction of the use of fossil fuels in Europe could be obtained by enhancing the energy efficiency of buildings. Since the replacement rate of the existing stock is very small (1-2 % per year), the energy retrofitting of existing buildings is of primary importance; thus, a wide research activity in this field has been carried out in recent years. Some studies have concerned the optimization of thermal insulation, others the improvement of the plant efficiency, others again the energy-saving potential.

Ucar and Balo [Ucar, Balo 2009] determined the optimum insulation thickness of external walls for four cities with different climatic conditions in Turkey, with reference to Foamboard, extruded polystyrene and fiberglass as insulation materials. Yu et al. [Yu, Yang, Tian, Liao 2009] studied the optimization of the insulation thicknesses of expanded polystyrene, extruded polystyrene, foamed polyurethane, perlite, and foamed polyvinyl chloride, for a typical residential wall in China. Cuce et al. [Cuce, Cuce, Wood, Riffat 2014] analyzed the optimum thermal insulation thickness of aerogel and its environmental impacts for the climatic conditions of Nottingham, UK. In these studies, the yearly use of primary energy for heating per unit wall area was evaluated by considering the degree-days of the locations considered, the heat loss coefficient of the wall and the plant efficiency. Daouas [DAOUAS 2011] evaluated, by an analytical method based on Complex Finite Fourier Transform, the optimum insulation thickness, the energy saving and the payback period for a typical wall structure in Tunisia, in the presence of both cooling and heating loads.

Zhao et al. [ZHAO, YANG, DUAN, RIFFAT 2009] investigated the feasibility of a novel dew point air conditioning system in several China regions. Terlizzese and Zanchini [TERLIZZESE, ZANCHINI 2011] studied, through an economic and an exergy analysis, the feasibility of alternative plants for a zero carbon building complex in Italy. Brignoli et al. [BRIGNOLI, CECCHINATO, ZILIO 2013] performed an experimental investigation on air-to-water heat pumps, and compared a multiport aluminum flat-tube heat exchanger to a round-tube finned one. Liu et al. [LIU, NI, LAU, LI, 2013] studied a new kind of heat pump system, which utilizes gray water as heat source and sink for heating and cooling of residential buildings. Naldi et al. [NALDI, MORINI, ZANCHINI 2014] developed a MATLAB code for the dynamic simulation of air-to-water heat pumps for heating.

Amstalden et al. [AMSTALDEN, KOST, NATHANI, IMBODEN 2007] investigated the profitability of energy-efficient retrofit investments in the Swiss residential building sector from the house owner's perspective. Dall'O and Sarto [DALL'O', SARTO 2013] investigated the technical end economic potential for increasing energy efficiency of 49 school building complexes in Lombardia (Northern Italy). Shahrokni et al. [SHAHROKNI, LEVIHNC, BRANDT 2014] evaluated the energy efficiency potential in Stockholm, and showed that the retrofitting of the building stock to current building codes would reduce heating energy use in the city by one third.

A reliable method to assess the potential for energy saving in building energy retrofitting is to employ simulation codes which are calibrated by comparison with experimental data obtained by building monitoring. Few studies on the calibration of simulation models by comparison with measured data are available in the literature.

Ascione et al. [ASCIONE, DE ROSSI, VANOLI 2011] analyzed the effectiveness of several energy retrofit solutions for a historical building in Italy through a dynamic simulation model implemented in EnergyPlus. The model was calibrated through endoscopy, core sampling, in situ measurements of transmittance and analysis of energy use data. Royapoor and Roskilly [ROYAPOOR, ROSKILLY, 2015] calibrated the simulation model of a 5-storey office building in United Kingdom, implemented in EnergyPlus, through hourly monitoring data collected during the year 2012. The model was calibrated to achieve, according to ASHRAE Guide 14, Mean Bias Error (MBE) within ±5% and Coefficient of Variation of Root Mean Square Error (CVRMSE) below 10%. Terés-Zubiaga et al. [TERÉS-ZUBIAGA, CAMPOS-CELADOR, GONZALES-PINO, ESCUDERO-REVILLA, 2015] analyzed, by dynamic simulations performed through TRNSYS, the energy saving obtainable by enhancing building envelope performance in residential buildings in Northern

Spain. The simulation model was calibrated by comparison with monitoring data collected on a selected dwelling during three months.

In the framework of the EU-funded Project HERB (Holistic Energy-efficient Retrofitting of residential Buildings), the University of Bologna and the Municipality of Bologna are performing the energy retrofitting of a detached house with 6 apartments in Bologna. The annual saving of primary energy will be assessed by dynamic simulations of the building before and after retrofitting, performed through a model implemented in TRNSYS 17 and calibrated by comparison with monitoring results. In this paper, the calibration of the simulation model of the building in its present state is presented.

2. DESCRIPTION OF THE BUILDING AND CLIMATIC DATA

The house to be retrofitted is located in an area very close to the center of Bologna, main city of the region Emilia-Romagna, North-Center Italy. It is composed of three floors, with 2 apartments each, an unheated attic, and an unheated basement which contains the boiler room. The roof has 4 pitches, with orientations Southeast, Southwest, Northeast and Northwest. The first floor is larger than the second and the third, which are identical. The house has a small garden, with high trees. Street views of the Northeast and of the Southwest side of the house are reported in Figure 1; 3-D models of the house, which illustrate the Northeast and Northwest sides and the Southwest and Southeast sides, are reported in Figure 2. In the 3-D models, most trees have been hidden.

Figure 1: Street views of the house: Northeast side (left) and Southwest side (right)

Figure 2: 3-D models of the house: Northeast and Northwest sides (left); Southwest and Southeast sides (right)

Apartments have been numbered as follows: apartments 1a and 1b at the first floor; apartments 2a and 2b at the second floor; apartments 3a and 3b at the third floor. Apartments with letter a are facing Northwest; those with letter b are facing Southeast. The first floor is larger than the second and the third. One of the apartments at the first floor (apartment 1b) has, as a part of the roof, an inaccessible plane terrace. The second and the third floor are identical. Plans of the apartments are reported in Figure 3: the first floor is represented on the left, the second and the third floor (which are identical) are represented on the right. The rectangle which appears in the lower part of the figure at right represents the inaccessible terrace which forms a plane roof for a part of apartment 1b. The heated floor areas of the apartments are as follows:

apartment 1a: 44.7 m²; apartment 1b: 80.2 m²; apartments 2a and 3a: 39.2 m²; apartments 2b and 3b: 39.3 m². The total heated floor area is 281.9 m².

The external wall, made of solid brick masonry, is 31 cm thick and uninsulated. Most windows are single glazed, with wood frame, except those of apartments 2b and 3b, which are double glazed with aluminum frame. The internal height of each floor is 3.36 m, and the floor thickness is 0.27 m. The unheated basement is placed under apartment 1a and under about one third of apartment 1b. The rest of apartment 1b is on the ground. No thermal insulation is placed between the first floor and the basement, or the ground, as well as between apartment 1b and the terrace. The unheated loft is non ventilated and uninsulated; its lowest height is 0.20 m (at the sides), and its highest height is 1.60 m (at the center). It has a very small window, which is closed.

Space heating is supplied by means of a gas boiler, placed in the basement, and radiators in the rooms, under windows. The gas boiler is a modulating one, installed in 2007; it has a nominal power of 62 kW, a certified efficiency equal to 0.93 at nominal power and slightly higher at reduced power. A constant efficiency equal to 0.93 has been considered. The distribution, emission and control efficiencies of the heating system, according to the national standard UNI TS 11300-2, are equal to 0.90, 0.95 and 0.97 respectively, Thus, the overall efficiency of the heating system according, to UNI TS 11300-2, is 0.771. DHW is supplied by single apartment boilers: electric boilers in apartments 1a, 2a, 2b, 3a, 3b; a gas boiler in apartment 1b. No summer air conditioning is present. All rooms, including bathrooms, have windows.
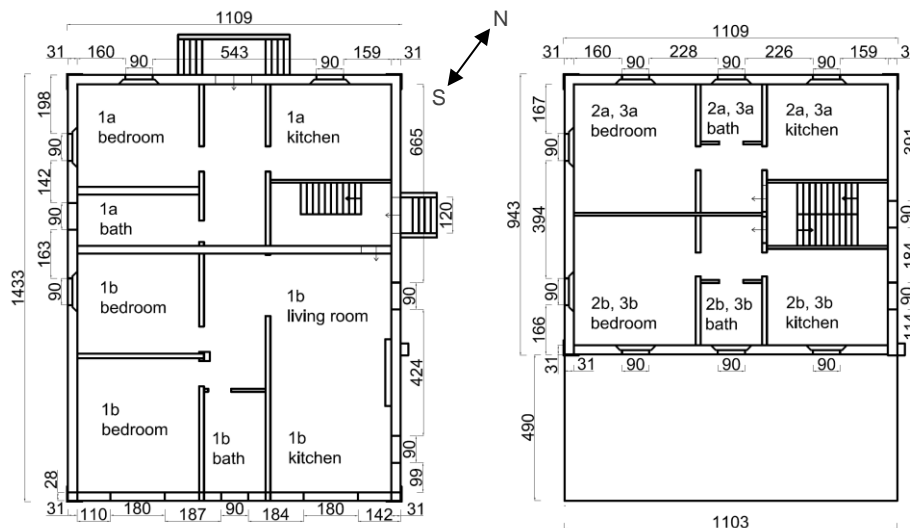

Figure 3: Plans of the apartments: first floor on the left; second and third floor on the right

Accurate inspections allowed to determine the stratigraphy of the opaque enclosure elements. The main properties of these elements (description, thickness s, transmittance U), are summarized in Table 1; for each element, the description starts from the internal (heated) space. The heat transfer coefficients reported in Table 1 have been determined by considering standard thermal conductivities of the enclosure materials. The transmittance of the external vertical wall has been then corrected by employing the results of in situ measurements, as is shown in Section 3. The transmittance of single-glazed windows has been assumed equal to 5.0 W/(m²K), and that of double-glazed windows equal to 2.72 W/(m²K).

Table 58: Main properties of the opaque enclosure elements

ELEMENT	DESCRIPTION	s [m]	U [W/(m²K)]
Vertical wall	Internal plaster, solid brick masonry, external plaster	0.31	1.797
Floor on basement	Tiles, subfloor, floor brick and concrete, plaster	0.26	1.476
Floor on ground	Tiles, subfloor, floor brick and concrete	0.25	1.845
Terrace floor	Plaster, floor brick and concrete, subfloor, tiles	0.26	1.476
Loft floor	Internal plaster, floor brick and concrete	0.09	2.903
Roof	Internal plaster, floor brick and concrete	0.21	2.279

Bologna is located in the center of the region Emilia Romagna, at the border between the Padana flat and the foot of the mountains Appennino Tosco-Emiliano. The mean altitude is 54 m above sea level, the

latitude is 44° 29' North, the longitude is 11° 20' East. The mean monthly values of the temperature T_e and of the relative humidity φ_e of the external air, according to the TRNSYS Typical Meteorological Year (TMY) for Bologna, are listed in Table 2.

Table 2: Monthly mean temperature and relative humidity of the external air, according to TRNSYS TMY

Month	Jan	Feb	March	April	May	June	July	Aug	Sept	Oct	Nov	Dec
T_e [°C]	1.7	4.3	9.4	13.8	20.2	21.5	24.4	24.1	20.9	14.4	8.4	3.9
φ_e	0.82	0.78	0.71	0.73	0.71	0.70	0.66	0.68	0.71	0.75	0.83	0.82

3. EXPERIMENTAL TESTS

Some building characteristics relevant for analyzing the energy use for heating were investigated experimentally by performing an infrared thermography, blower door tests and in situ measurements of the transmittance of the external vertical wall.

The thermographic examination of the house was made on 10th February 2014, in agreement with UNI EN 13187: 2000. The test started at 11:45 a.m.; in that morning the external air temperature was 8.3°C and the relative humidity was 87%. Inside the building there was an average temperature of about 20°C. The temperature difference across the envelope was sufficiently large to allow the detection of thermal irregularities. The day of the examination was cloudy, so that the walls were never exposed to direct solar radiation. The wind was weak and constant. The test was made by a NEC Avio IR camera, model TVS-200EX, with the infrared radiation sensor that operates at a wavelength between 8 μm and 14 μm. The temperature resolution is better than 0.08°C (with averaging) and the accuracy is ±2°C or ±2% of the measurement. The IR detector is an uncooled Vox microbolometer of 320 (H) x 240 (V) pixel with frame time of 60 Hz. A surface emissivity 0.93 was considered for the building façade. The infrared thermography evidenced the high transmittance of windows and of the thin wall below windows (due to recessed radiators), the lack of thermal insulation in the risers of the hot water distribution system, and the bad performance of window frames. These features are illustrated in Figure 4.
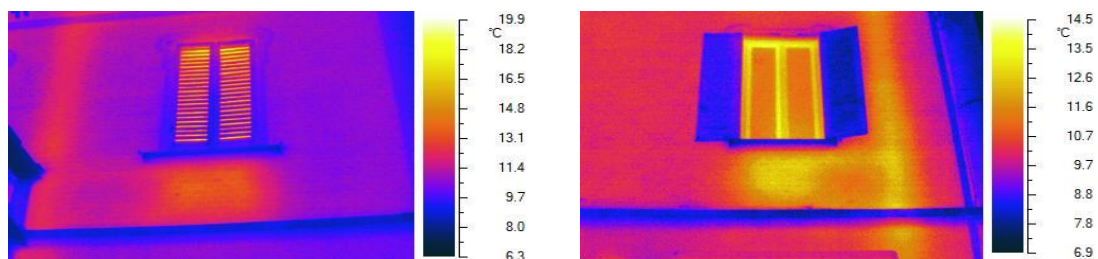

Figure 4: Some results of the infrared thermography

The determination of the air permeability of the building envelope through blower door tests was made by the fan pressurization method, according to UNI EN 13829:2002. The tests were carried out in two different apartments, one on the second floor (apartment 2b) and one on the first floor (apartment 1a), in two different days, 24th and 25th September 2014. For each apartment, two sets of measurements were made, for pressurization and depressurization. For each test, ten equally spaced data points between the highest and the lowest pressure difference were considered. The tests evidenced a high air exchange rate for both apartments at a pressure difference of 50 Pa, namely 7.93 h^{-1} for apartment 1a and 7.06 h^{-1} for apartment 2b.

Three in situ measurements of transmittance of the external vertical wall were performed, by measuring the heat flow rate through an element and the temperatures on both sides of the element, under quasi-steady conditions, according to ISO 9869-1:2014. The tests were performed by a ThermoZig Wireless Standard with datalogger DL02, four RTD Pt1000 as temperature sensors, and a Heat Flux Meter characterized by a thermal resistance lower than 0.006 m^{2}K/W and an accuracy of ±5%. The building has two different kinds of external vertical wall, with the same thickness (31 cm) and the same stratigraphy, but slightly different materials because constructed in different periods. They will be called "old wall" and "new wall". The old wall was constructed in the period 1930-1940, while the new wall was constructed in the period 1960-1970.The new wall is present only in a part of apartment 1b, at the first floor.

Two measurements of the transmittance of the old wall were performed: the first in apartment 1b, from January 13th to January 16th 2015; the second in apartment 2b, from January 29th to February 2nd 2015. One measurement of the transmittance of the new wall was performed, from January 9th to January 13th 2015. The main results of the measurements of transmittance are reported in Table 3.

Table 3: Results of the measurements of transmittance

	Old wall – 1b	Old wall – 2b	New wall
Mean temperature difference °C	8.46	5.5	9.3
Mean heat flux W/m^2	18.92	11.47	24.06
Solid thermal resistance m^2K/W	0.44715	0.47951	0.38653
Internal thermal resistance m^2K/W	0.13	0.13	0.13
External thermal resistance m^2K/W	0.04	0.04	0.04
Total thermal resistance m^2K/W	0.61715	0.64951	0.55653
Transmittance W/m^2K	1.62	1.54	1.80

As is shown in Table 3, the first measurement of transmittance of the old wall took place with a higher difference between the temperature of the internal surface and that of the external surface, and is more reliable. Therefore, a weight 2 was assumed for this measurement and a weight 1 was assumed for the second measurement: this assumption yielded a measured transmittance equal to 1.60 $W/(m^2K)$ for the old wall. The measurement of transmittance of the new wall took place with a good temperature difference, so that it was not necessary to repeat the test: the result is 1.80 W/m^2K, in agreement with the transmittance estimated through standard values of thermal conductivity of the constituent materials.

4. BUILDING MONITORING

The use of primary energy for heating during the heating season 2013-2014 was determined by periodic readings of the gas meter installed by the gas provider in the gas distribution duct to the central boiler of the building. The use of natural gas for space heating started on October 15th 2013 and ended on April 15th 2014. It was not possible to install a new gas meter during the heating season 2013-2014. However, to check the accuracy of the readings of the existing gas meter, a TERZ 94 DN 25 electronic turbine meter was installed at the beginning of March 2015. The installed electronic turbine meter has a flow-rate range between 2.5 and 25 m^3/h; the accuracy is ±3% at flow rates between 2.5 and 5 m^3/h, ±2% at flow rates between 5 and 25 m^3/h. The comparison of the readings of the first and of the second gas meter was carried out from March 9th 2015 to April 15th 2015, and is illustrated in Table 4. The results show that a 5.38% higher gas use is recorded by the second gas meter. Since the accuracy of the second gas meter is higher, the readings of the existing gas meter during the heating season 2013-2014 were corrected by a multiplying factor 1.0538.

The lower heating value of the natural gas supplied to the building was certified by the gas distribution company as 9.7 kWh/m^3. Values of the gas volume used in each time interval considered for the heating season 2013-2014, of the time-interval duration in hours, of the primary energy of the gas used, and of the corresponding mean power are reported in Table 5. The total volume of gas used during the heating season 2013-2014 is 5877 m^3 and corresponds to the use of 57007 kWh of primary energy, i.e., 202.2 kWh/m^2.

Table 4: Comparison of the readings of the gas meters, from March 9th to April 15th 2015

Period	Meter 1, m^3	Meter 2, m^3	% difference
Mar. 9 - Mar. 16	192.8	202.8	5.19
Mar. 16 - Mar. 23	169.3	178.2	5.26
Mar. 23 - Mar. 29	132.2	139.6	5.60
Mar. 29 - Apr 1	30.8	32.4	5.19
Apr.1 - Apr 7	138.0	145.6	5.51
Apr.7 - Apr 13	88.3	93.2	5.55
Apr.13 - Apr 15	7.6	8.0	5.26
Total	759.0	799.8	5.38

Table 5: Use of primary energy for heating from October 15th 2013 to April 15th 2014: measured values

Period	Hours	Volume m³	Energy kWh	Mean power kW
Oct. 15 - Oct. 30	360	115.92	1124.4	3.12
Oct. 30 - Nov. 30	744	912.59	8852.1	11.90
Nov. 30 - Dec. 12	288	615.42	5969.6	20.73
Dec. 12 - Jan. 20	936	1670.27	16201.6	17.31
Jan. 20 - Jan. 27	168	287.69	2790.6	16.61
Jan. 27 - Feb. 03	168	344.59	3342.5	19.90
Feb. 03 - Feb. 10	167.5	277.15	2688.3	16.05
Feb. 10 - Feb. 17	167.5	255.02	2473.7	14.77
Feb. 17 - Feb. 24	167	236.05	2289.7	13.71
Feb. 24 - March 03	169	248.70	2412.4	14.27
March 03 - March 10	170.5	225.51	2187.5	12.83
March 10 - March 17	167	173.88	1686.6	10.10
March 17 - March 24	168.5	142.26	1380.0	8.19
March 24 - March 31	166.5	180.20	1747.9	10.50
March 31 - April 07	170	113.81	1104.0	6.49
April 07 - April 15	190.5	77.98	756.4	3.97

In order to evaluate the internal heat gains, the use of natural gas and of electricity in single apartments was also monitored. The use of natural gas was determined through periodic readings of the gas meters, the use of electricity was monitored by 6 OWL+USB CM160 Electricity Monitors. Natural gas was used only for cooking in apatments 2a, 2b, 3a and 3b, and also for Domestic Hot Water (DHW) production in apartment 1b. Electricity was used only for lighting and appliances in apartment 1b, and also for DHW production through electric boilers in apartments 2a, 2b, 3a and 3b. Apartment 1a was empty and had no use of natural gas and electricity.

The electricity meters were installed in December 2013 and were all correctly working starting from January 1st 2014. Since measurements revealed no sharp difference in the use of electricity between different months, a 6-month period from January 1st 2014 to June 30th 2014 was considered for the use of electricity, slightly displaced with respect to the 6-month period of the other monitoring data considered here. Acquisitions of electricity use were performed every minute, then the data were transformed into hourly averages, thus obtaining the mean power absorbed during each hour. Plots of the mean electric power absorbed by apartments 3a and 3b are reported, as examples, in Figure 6. For all the apartments, values of the electric energy used from January 1st 2014 to June 30th 2014 and of the gas primary energy used from October 15th 2013 to April 14th 2014 are reported in Table 6. In the same table, also the values of the mean power absorbed, for both electricity and gas, are reported. The hours considered are 4344 for both electricity and gas, except for the electricity used by apartment 2b, where the period is shorter (3379 hours) because the tenants left the apartment on May 21st.

A precise measurement of the internal heat gains is not possible for the building considered, because electricity was used also for DHW production in apartments 2a, 2b, 3a and 3b, while gas was used also for DHW production in apartment 2b. The heat gain values reported in the penultimate column of Table 6 have been calculated by assuming that the heat gain is equal to 60% of the electric energy absorbed plus the thermal energy absorbed for apartments 2a, 2b, 3a and 3b, while it is equal to 60% of the thermal energy absorbed plus the electric energy absorbed for apartment 1b. The second and the last column in Table 6 report the number of persons present in the apartments and the values of the standard internal heat gains evaluated according to the National Standard UNI/TS 11300-1, through the expression

Equation 1: Standard internal heat gains, UNI/TS 11300-1

$$Q_{int} = 5.294 \, A_f - 0.01557 \, A_f^2$$

where the power is in watt and A_f is the heated floor area in square meters. While the values for single apartments determined experimentally are very different from each other and from the standard values, the sum is rather close to the standard value.
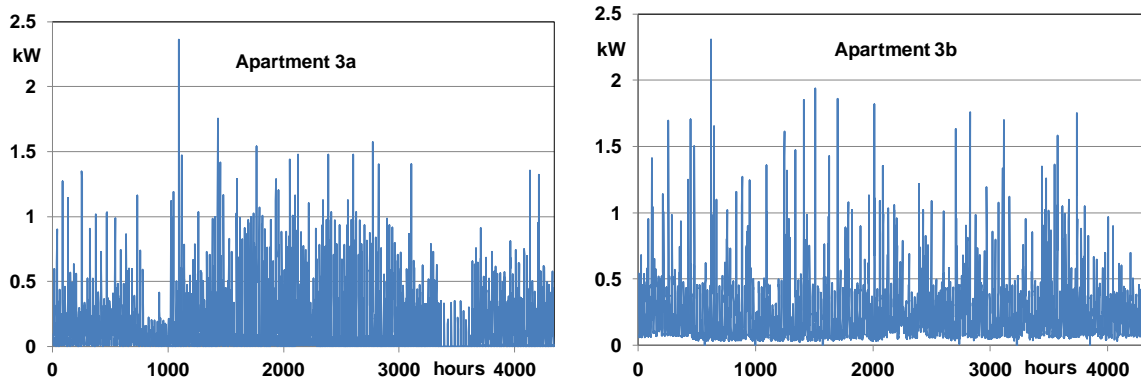
Figure 6: Electric power absorbed by apartments 3a (left) and 3b (right), from January 1st to June 30th 2014

Table 6: Use of electricity and gas and estimated internal heat gain in each apartment

Apartment	Persons	Electricity kWh	Gas kWh	Electricity W	Gas W	Gain W	Standard gain W
1a	0	0	0	0	0	0	206
1b	1	588.8	281	136	65	174	324
2a	1	639.8	39	147	9	97	184
2b	4	2326.8	805	689	185	598	184
3a	1	552.0	0	127	0	76	184
3b	2	944.1	1950	217	449	579	184
Total	9	5051.5	3075	1316	708	1526	1265

The temperature and the relative humidity of the internal air were monitored in two rooms for each apartment, namely bedroom and kitchen-living room, from July 1st 2013 to June 30th 2014. The sensors employed are 12 Temperature, Humidity and Dew Point Data Loggers Omega OM-EL-USB-2-PLUS, with temperature accuracy ± 0.3 °C. The relevant period for the present study is from October 15th 2013 to April 15th 2014. The mean value of the internal air temperature for each room during this period is reported in Table 7. The mean value for the whole building is 20.4 °C, close to the set point temperature 20 °C.

Table 7: Mean value of the internal air temperature for each room, from October 15th 2013 to April 15th 2014

	Apartment 1a	Apartment 1b	Apartment 2a	Apartment 2b	Apartment 3a	Apartment 3b
Bedroom	20.14	21.46	19.99	20.49	20.34	20.29
Kitchen	19.88	20.45	20.02	20.65	20.88	20.41

Hourly values of the external air temperature and relative humidity were taken from the Bologna Urbana Weather Station, which is rather close to the building. Also the hourly values of the total radiation on a horizontal surface were taken from the same Weather Station. The monthly mean values of the external air temperature and relative humidity during the heating season 2013-2014 are reported in Table 8. A comparison with Table 2 reveals that the autumn-winter season 2013-2014 was much milder than usual. The mean value of the external air temperature from October 15th to April 15th was 10.15 °C, while the corresponding value of the TRNSYS TMY is 6.99 °C. A similar anomaly happened again in the heating season 2014-2015.

Table 8: Monthly mean temperature and relative humidity of the external air from October 2103 to April 2014

Month	Oct	Nov	Dec	Jan	Feb	March	April
T_e [°C]	16.0	10.4	6.3	6.8	9.0	11.8	15.4
φ_e	0.81	0.77	0.76	0.87	0.79	0.62	0.63

5. BUILDING SIMULATION

A 3-D hourly simulation model of the building was implemented in TRNSYS 17, starting from 3-D drawings performed through Google SketchUp. Four thermal zones were considered for each small apartment (bedroom, bathroom, kitchen-living room, entrance), and five thermal zones for apartment 1b, which has two bedrooms. Standard values of the thermal conductivity and of the specific heat capacity of the building materials were considered for all walls and floors, except for the thermal conductivity of the solid brick masonry of the external vertical wall. The latter was corrected to yield the transmittances measured experimentally, namely 1.60 W/(m^{2}K) for the old wall and 1.80 W/(m^{2}K) for the new wall. The linear transmittances of thermal bridges were calculated by finite element simulations performed through COMSOL Multiphysics. The result for the total heat loss coefficient due to thermal bridges is 171.2 W/K.

Since in nearly all rooms the mean value of the internal air temperature during the heating season was very close to the set point temperature, the internal air temperature was set equal to the set point temperature, 20 °C, and the small deviations from this value were taken into account through the control efficiency. The certified efficiency 0.93 was considered for the gas boiler. The distribution and emission efficiencies were considered as equal to those recommended by UNI TS 11300-2, namely 0.90 and 0.95 respectively. The control efficiency was assumed as equal to 0.98. Thus, the overall plant efficiency was assumed as equal to 0.779. The internal heat gains determined through the monitoring (penultimate column of Table 6) were considered, together with an air exchange rate equal to 0.3 h^{-1}. The standard meteorological data available in TRNSYS 17 for Bologna were modified by inserting real measured data of external air temperature and relative humidity, as well as of direct and diffuse radiation on a horizontal surface, taken from the Bologna Urbana Weather Station.

The main results of the simulation are reported in Table 9. For each period considered, the values of the primary energy use determined through simulation, of the corresponding mean power and of the external air temperature are reported. Plots of the mean power versus the external air temperature, usually called building energy signatures, determined experimentally and through dynamic simulation, are reported in Figure 7. The figure shows an excellent agreement between the energy signature determined experimentally and that determined by dynamic simulation. The equations of the energy signatures, evaluated through linear interpolation, are

Equation 2: Energy signatures
$$Q_{exp} = 27.615 - 1.4267\, T_e \;;\quad Q_{sim} = 27.636 - 1.4351\, T_e$$

Where Q_{exp} is the power determined experimentally, in kW, Q_{sim} is that determined through simulation and T_e is the temperature of the external air in °C.

A comparison between the use of primary energy during each period determined experimentally and that determined through simulation allowed to calculate the accuracy parameters Normalized Mean Bias Error *NMBE* and Coefficient of Variation of the Root Mean Square Error *CVRMSE* defined in ASHRAE Guide 14. If one denotes by y_i^{sim} the simulation outcomes, by y_i^{meas} the measurement outcomes, by $\overline{y}^{meas}$ the mean value of the measurement outcomes and by n the number of measured data (16 in our case), these parameters are given by

Equation 3: Accuracy parameters
$$NMBE = \frac{\sum_{i=1}^{n}\left(y_i^{sim} - y_i^{meas}\right)}{(n-1)\,\overline{y}^{meas}} \;;\quad CVRMSE = \frac{1}{\overline{y}^{meas}}\left(\frac{\sum_{i=1}^{n}\left(y_i^{sim} - y_i^{meas}\right)^2}{n-1}\right)^{1/2}$$

The results in the present case are *NMBE* = 0.004 and *CVRMSE* = 0.088; both values are considerably lower than the limits recommended ASHRAE Guide 14, namely *NMBE* < 0.05 and *CVRMSE* < 0.15. The total use of primary energy for space heating during the season 2013-2014 is 57007 kWh according to the monitoring results and 57232 kWh according to the dynamic simulation, with a discrepancy lower than 0.4%.

Table 9: Use of primary energy for heating from October 15th 2013 to April 15th 2014: simulation results

Period	hours	Energy kWh	Mean power kW	External air temp °C
Oct. 15 - Oct. 30	360	1281.5	3.56	17.23
Oct. 30 - Nov. 30	744	8409.0	11.30	10.68
Nov. 30 - Dec. 12	288	5627.5	19.54	5.10
Dec. 12 - Jan. 20	936	17192.2	18.37	7.00
Jan. 20 - Jan. 27	168	2787.6	16.59	7.91
Jan. 27 - Feb. 03	168	3314.1	19.73	5.18
Feb. 03 - Feb. 10	167.5	2544.9	15.19	8.64
Feb. 10 - Feb. 17	167.5	2522.1	15.06	9.13
Feb. 17 - Feb. 24	167	2352.1	14.08	9.24
Feb. 24 - March 03	169	2449.8	14.50	9.34
March 03 - March 10	170.5	2350.8	13.79	10.43
March 10 - March 17	167	1747.4	10.46	12.34
March 17 - March 24	168.5	1163.0	6.90	13.66
March 24 - March 31	166.5	1841.8	11.06	11.88
March 31 - April 07	170	895.3	5.27	15.35
April 07 - April 15	190.5	753.5	3.96	16.10
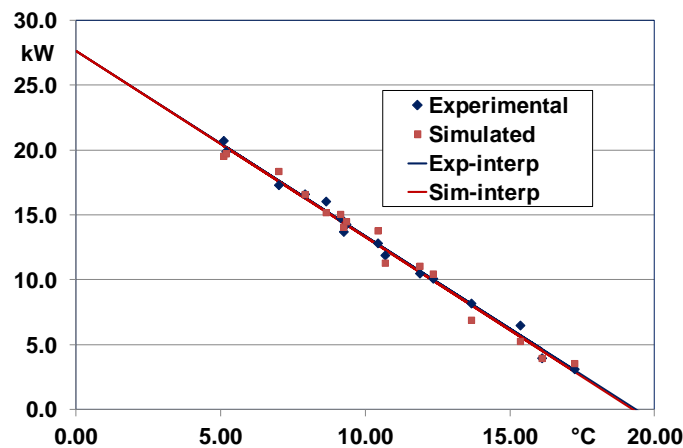
Figure 7: Experimental energy signature and simulated energy signature

6. CONCLUSIONS

An accurate 3-D simulation model of a residential building in Bologna, which will undergo an energy retrofitting in the framework of the EU funded Project HERB, has been implemented in TRNSYS 17. The model has been prepared by accurate inspections of the building characteristics, finite-element simulations of thermal bridges, in situ measurements of transmittance of the external vertical wall, and evaluations of the internal heat gains through records of the use of natural gas and of electricity in the apartments. The model has been validated by comparison with monitored values of the primary energy used for heating by the central gas boiler during the autumn-winter season 2013-2014. The results have revealed that the model widely fulfils the accuracy requirements stated by ASHRAE Guide 14 and yields the measured total energy use for heating during the season considered with an accuracy better than 0.4%.

7. ACKNOWLEDGMENT

8. REFERENCES

AMSTALDEN Roger W., Kost Michael, Nathani Carsten, Imboden Dieter M., 2007. Economic potential of energy-efficient retrofitting in the Swiss residential building sector: The effects of policy instruments and energy price expectations. Energy Policy, 35, 1819–1829.

ASCIONE Fabrizio, De Rossi Filippo, Vanoli Giuseppe Peter, 2011. Energy retrofit of historical buildings: theoretical and experimental investigations for the modelling of reliable performance scenarios. Energy and Buildings, 43, 1925–1936.

BRIGNOLI Riccardo, Cecchinato Luca, Zilio Claudio, 2013. Experimental analysis of an air–water heat pump with micro-channel heat exchanger, Applied Thermal Engineering, 50, 1119–1130.

CUCE Erdem, Cuce Pinar Mert, Wood Christopher J., Riffat Saffa B., 2014. Optimizing insulation thickness and analysing environmental impacts of aerogel-based thermal superinsulation in buildings. Energy and Buildings, 77, 28–39.

DALL'O' Giuliano, Sarto Luca, 2013. Potential and limits to improve energy efficiency in space heating in existing school buildings in northern Italy. Energy and Buildings, 67, 298–308.

DAOUAS Naouel, 2011. A study on optimum insulation thickness in walls and energy savings in Tunisian buildings based on analytical calculation of cooling and heating transmission loads. Applied Energy, 88, 156–164.

LIU Xiaoyu, Ni Long, Lau Siu-Kit, Li Haorong, 2013. Performance analysis of a multi-functional heat pump system in heating mode. Applied Thermal Engineering, 51, 698–710.

NALDI Claudia, Morini Gian Luca, Zanchini Enzo, 2014. A method for the choice of the optimal balance-point temperature of air-to-water heat pumps for heating. Sustainable Cities and Society, 12, 85–91.

ROYAPOOR Mohammad, Roskilly Tony, 2015. Building model calibration using energy and environmental data. Energy and Buildings, 94, 109–120.

SHAHROKNI Hossein, Levihn Fabian, Brandt Nils, 2014. Big meter data analysis of the energy efficiency potential in Stockholm's building stock. Energy and Buildings, 78, 153–164.

TERÉS-ZUBIAGA Jon, Campos-Celador Álvaro, Gonzáles-Pino Iker, Escudero-Revilla César, 2015. Energy and economic assessment of the envelope retrofitting in residential buildings in Northern Spain. Energy and Buildings, 86, 194–202.

TERLIZZESE Tiziano, Zanchini Enzo, 2011. Economic and exergy analysis of alternative plants for a zero carbon building complex. Energy and Buildings, 43, 787–795.

UCAR Aynur, Balo Figen, 2009. Effect of fuel type on the optimum thickness of selected insulation materials for the four different climatic regions of Turkey. Applied Energy, 86, 730–736.

YU Jinghua, Yang Changzhi, Tian Liwei, Liao Dan, 2009. A study on optimum insulation thicknesses of external walls in hot summer and cold winter zone of China. Applied Energy, 86, 2520–2529.

ZHAO Xudong, Yang Shuang, Duan Zhiyin, Riffat Saffa B., 2009. Feasibility study of a novel dew point air conditioning system for China building application. Building and Environment, 44, 1990–1999.

149: Passive and active solutions to improve the energetic efficiency of buildings

CLITO AFONSO[1], RICARDO PEREIRA[2]

1 Porto University, FEUP, R. Dr. Roberto Frias, 4200-465 Porto, clito@fe.up.pt
2 Porto University, FEUP, R. Dr. Roberto Frias, 4200-465 Porto,ricardo@fe.up.pt

Today the building sector has a significant weight in energy consumption and a high potential for increasing its energy efficiency. With the enforcement of the energetic certification, it has been tried to find and select different solutions that presents less energy consumption and waste, which translates into an effective reduction of CO2 emissions. It is in this perspective that this work fits, since its main aim is to evaluate the contribution of passive and active solutions of a hotel for the improvement of the energetic efficiency, as well as to evaluate the contribution of some renewable energy sources. Within them, the contribution of solar systems for hot water heating and electric energy production has been approached. Despite the importance assumed by using renewable energies in the buildings sector, cogeneration remains as the most effective technology on the conversion of primary energy into electricity and heat. The application of cogeneration technologies in the buildings sector gains notability facing the rise of fuel prices and the need to ensure adequacy and comfort of spaces. Relatively to the practical case in study, the building is a hotel located in Portugal. Multizone dynamic codes for simulations were used. To improve the building performance, there were made several changes on the model with the goal of evaluating the contribution of different solutions, either at passive and active level, in order to increase the energetic efficiency of the hotel. It was concluded that they contribute to a reduction of thermal needs of 25.2% and avoided emissions of equivalent tons of CO_2 of 30.4%.The analysis of the technical/economic viability of the implementation of the CHCP becomes executable, using a system based on an internal combustion engine that runs with natural gas, with an absorption chiller to produce cooling. The payback period of this solution is less than 8 years which proves that there is an economic viability of this technology.

Keywords: Energy analysis, Avoided CO2 emissions, Economic analysis.

1. INTRODUCTION

Hotels are buildings which have high energy demands and water consumption that decisively reflects in operating costs. It is in the tertiary sector where there are great potentials for improving energy efficiency.

It is thus essential to develop a sustainable strategy to keep in account the environmental, social and economic impact of all and each one the parts that make up the building. In this sense, energy optimization and resources plays a major role in driving the operation of buildings. These concerns must be present and reflect up from the design phase, that is, in the early stages of development of their project. The energy optimization is to select the solutions that promote the reduction of energy consumption, waste and a reduction of emissions of greenhouse gases (CO_2). It should be noted that the energy optimization of a building does not pass only by mandatory large measures with high energy impacts and operating costs. It is many sometimes the result of the adoption of small actions that represent small impacts, the sum which are of importance for the intended purpose - to reduce energy consumption and associated operating costs.

Despite the importance assumed by using renewable energies in the third sector, cogeneration remains as the most effective technology on the conversion of primary energy (fossil or renewable sources) into electricity and heat, (Çengel, 2002; Afonso, 2012)]. The application of cogeneration technologies on the third sector gains notability facing the rise of fuel prices and the need to ensure adequacy and comfort of spaces, (Commission of the European Communities, 1997; Cogeneration, 2010; Cogenportugal,com, 2010; Afonso, 2014).

The micro-power generation, (Polimeros, 2013), as an activity for low tension electricity production with the possibility of energy delivery to the public grid, was regulated by several Decree-Laws, (Decree-Law, 99 and 2001). The actual ordinance stipulates that the electricity produced is destined predominantly for their own consumption, and the surplus that can be delivered to third parties or to the public, with 150 kW limit in the case of power delivery to be made public. For the production of electricity on a large scale, using photovoltaics systems, the remuneration given to national electric system network is regulated by Decree-Law No 225/2007 of 31 May. Thus, the use of photovoltaic panels is becoming increasingly common practice more visible in several countries. So along with energy efficiency measures, the increasing integration of renewable energy in buildings, fits to aims to reach the 2020 targets stipulated. The energy consumption of the building is directly related to passive and active the solutions that will be analyzed.

In this work a hotel located in Portugal was studied. The dynamic codes TRACE700 v. 6.2.5 and TSOL were used respectively for the evaluation of energy needs in HVAC system and for sanitary hot water demand. It was verified that the higher consumptions were on the electric ones, specifically the one of lightning (32.4%) and the equipment's (25.8%), followed by the HVAC, ventilation (11.6%) and cooling (10.8%). To analyze the contribution of different solutions, in order to increase the energetic efficiency of the hotel, there were made several changes on the transient computer model. The analysis of the technical/economic viability of the implementation of a cogeneration/trigeneration becomes at two levels, where the technologies tested were analyzed to adapt them to the thermal needs of the building. Among several solutions, namely micro turbines and fuel cells, it was chosen a system based on an internal combustion engine running on natural gas, with the help of an absorption chiller to produce cold. The payback period of this solution is less than 8 years.

2. PARAMETERS TO BE EVALUATED

- Payback time: is the project's operating time necessary to obtain the sum of revenue and expenditure flows that equalize the value of the investment:

Equation 1: Payback period
$$Payback = \frac{Initial\ Investment}{Annual\ Revenues}$$

- Energy Efficiency Index (EEI) [kgep.m-².year-¹]. According to Decree-Laws already specified, there are several formulas to evaluate the EEI (not shown here) and deals with specific consumption for heating, cooling and lighting, for each typology. This parameter is important in order to define in which energy classes the building belongs.
- EEE (Equivalent Electrical Efficiency). By the Decree Laws in force, this parameter is given by:

Equation 2: EEE

$$EEE = \frac{E}{C - \dfrac{T}{0.9 - 0.2\dfrac{CR}{C}}} \geq 0.55$$

Where:

- E [kWh]: electricity generated annually by the cogeneration system, excluding the consumption in internal auxiliary power generation systems
- T [kWh]: useful thermal energy consumed annually from the thermal energy produced by cogeneration, excluding the consumption in the internal auxiliary power generation systems;
- C [kWh]: the primary energy consumed annually in the cogeneration system, evaluated from the lower heating value of fuel and other resources used;
- CR [kWh]: equivalent energy of renewable resources or industrial waste, agricultural or urban consumed annually in cogeneration facility.

EEE can assume the following values, according to the same Decrees-Laws:

- EEE ≥ 0.55 for installations using natural gas as fuel, gas petroleum or liquid fuels with the exception of fuel;
- EEE ≥ 0.50 for installations using fuel oil as fuel, alone or together with waste fuels;
- EEE ≥ 0.45 for installations using biomass as fuel or residual fuels, alone or in conjunction with a fuel support, a percentage not exceeding 20% annual average.

In the case study, it will not be analysed the contribution of renewable resources. Thus the formula of the EEE is reduced to the following expression:

Equation 3: New formula for the EEE

$$EEE = \frac{E}{C - \dfrac{T}{0.9}} \geq 0.55$$

For the CHP and CHCP the following parameter must also be evaluated.

- Electrical efficiency, ηelectrical = Egrosselctricity/Total fuel consumed
- Thermal efficiency, ηthermal = Egross thermal/Total fuel consumed
- E_{er}: Maximum quantity of electricity to provide annually to the Electric System of Public Service not higher than the value given by the following equation:

Equation 4: E_{er}

$$E_{er} = \left(4.5\frac{E + T}{E + 0.5T} - 4.5\right)E$$

- Saving Energy Index (ESI): ratio of the fuel economy obtained in the cogeneration engine when compared to the amount of fuel consumed in a conventional installation, i.e. an electrical plant with an efficiency η_c, a boiler with an efficiency η_b and an electric chiller with a COP$_{comp}$. It is given by the following expression:

Equation 5: ESI

SUSTAINABLE CITIES & ENVIRONMENT

$$ESI = 1 - \cfrac{1}{\cfrac{\eta_{e,C}}{\eta_c} + \cfrac{\eta_{e,C}\,xRCE}{\eta_b} + \cfrac{\eta_{e,C}\,xRFE}{COP_{comp}}}$$

Where:

- RCE and RFE are respectively the ratios between heat and electricity and the ratio between cooling and electricity in the CHCP.

3. ANNUAL THERMAL ANALYSIS OF THE HOTEL

In the base case, it was followed the RCCTE (Council Regulation of the Characteristics of the Thermal Behavior of Buildings). The U values of the internal and external envelope were calculated and are shown in Table 1.

Table 59: U values [Wm^{-2}°C^{-1}] for the base case.

		U values [Wm^{-2}°C^{-1}]
External envelope	Walls	1.8
	Roof and floor	1.25
Internalenvelope	Walls	2
	Roof and floor	1.65

As already mentioned, the energy needs of the hotel were simulated with the dynamics codes TRACE700 v. 6.2.5 and TSOL, the results being displayed in Table 2. It is also shown the values of EEI as well as the emitted CO_2 associated with the energy consumption. It must be noticed that the electric heating corresponds to the consumption of operation of heating systems, including pumps condensate, burner and control panel of the boilers. The gas heating corresponds to the consumption of boilers, with an efficiency of 83.3%, and cooling corresponds to the electrical consumption of chillers with a COP of 3.2. The ventilation represents the consumption of the air handling equipment, while the pumps corresponds to the consumption associated with all fluid pumping equipment.

The maximum thermal power loads for heating and cooling are respectively equal 1775.8 kW and 1920.1 kW. The values given above were obtained with a reference system composed of an electric air-to-air chiller (COP of 3.2) and a conventional boiler with an efficiency of 83.3%. It should be noted that the electric heating, represents the consumption of operation of heating systems, including pumps condensate, the burner and control panel of the boilers. The gas heating represents consumption of boilers and the cooling corresponds to the electrical consumption of chillers.

Is important to highlight that the "parameters" which most contribute to the nominal consumption of primary energy are the lighting consumption and electrical equipment. Also, it is noted that the building presents an elevated energy consumption, due to the fact it is a large service building. However, even in the base case on predefined conditions, the building is already within the minimum required by RSECE, (Decree-Law, 2006).

The annual energy bill and associated costs are shown in Table 3.

Table 2: Annual thermal needs of the hotel (base case).

			Useful thermal needs [kWh.year^{-1}]	Nominal primary thermal energy [kgep.year^{-1}]	EEI [kgep.m^{-2}.year^{-1}]	CO$_2$ emissions [tons CO$_2$]
H&C	Heating	Electric	19724	5720	0.27	6.9
		Gas	246731	21219	1.0	25.3
	Cooling		521389	151203	5.19	181.4
Others	Lighting		1141168	330939	15.61	397.1
	Electric equipment		909071	263631	12.43	316.4
	Gas equipment		439081	37761	1.78	45.3
	Ventilation		498000	144420	5.56	173.73
	Pumps		238800	69252	2.67	83.1
	Hydraulic equipment		4729	1371	0.06	1.6
	SWH	Gas	636318	54723	2.58	65.7
		Electric	10143	2941	0.14	3.5
	SPH	Electric	4840	1404	0.07	1.7
		Gas	161678	13904	0.66	16.7
	Mechanical equipment		6572	1906	0.09	2.3
	Total		4.84 [GWh .year^{-1}]	1100 [tep.year^{-1}]	48.1	1320.5

Table 3: The annual energy billing and associated costs.

	Total thermal load [MWh/year]	Fuel Bill [€/year]
Electricity	3354.43	275890
Gas	1483.81	46148
Total	4838	322038

4. IMPROVED PASSIVE SOLUTIONS
4.1. Opaque envelope

The interior space of the building is physically separated from the outside by an envelope that is composed of opaque (walls, roof, and floor) and a transparent part (glazing). Note that for this first analysis, to the glazed envelope have been given the maximum permissible values of solar factor and heat transfer, set out in RCCTE, (Decree-Law, 2006). In order to improve the efficiency of the building, regarding the opaque envelope, four alternatives were proposed. These ones are only due to changes of the U value of the internal and external opaque envelope due to the changes in thermal insulation. The alternatives are (always according to RCCTE):

Alternative 1 (ALT 1): the U values are the reference ones;
Alternative 2 (ALT 2): 25% improvement on the reference values;
Alternative 3 (ALT 3): 50% improvement on the reference values;
Alternative 4 (ALT 4): 75% improvement on the reference values;

The alternatives are shown in Table 4.

Table 4: U values [Wm-2ºC^{-1}] for the base case and for four different alternatives.

		Base case	Alt 1	Alt 2	Alt 3	Alt 4
External envelope	Walls	1.8	0.7 (61%)	0.525 (25%)	0.35 (33%)	0.175 (50%)
	Roof and floor	1.25	0.5 (60%)	0.375 (25%)	0.25 (33%)	0.125 (50%)
Internal envelope	Walls	2	1.4 (30%)	1.05 (25%)	0.7 (33%)	0.35 (50%)
	Roof and floor	1.65	1 (39%)	0.75 (25%)	0.5 (33%)	0.25 (50%)

The values in parenthesis correspond to the reduction of heat transfer coefficients between the alternatives. From this analysis it is emphasized that the greatest reduction occurs between the base case and alternative one.

The optimization process of the opaque envelope, goes through the analysis of its contribution to the energy consumption of the building. Table 5 shows the annual energy consumption of the hotel regarding the alternatives for the opaque envelope as well as the values of EEI and the emitted CO_2 associated with the energy consumption. There are also shown the total costs and the payback time of all alternatives.

The baseline for this analysis is the opaque envelope, the base case, from which follows that it is not relevant to improve the U value of the opaque envelope beyond the reference values stipulated by RCCTE, since the decrease of the U values of the opaque envelope, beyond the benchmarks, do not translates into a significant improvement of the final value of the primary energy consumption (table 5, consumption: between Alt 1 and Alt 4 the difference is 0.73%). As can also be observed in the same table, it is apparent that the transition of the U values of the opaque envelope when compared with the alternative one (ALT 1), presents a decrease in the consumption, both for heating (4.27%) and cooling (14.3%) and consequent reduction of ventilation and pumping systems. As can be seen, alternative 1 is the best one when compared to the base case, even due to the payback time. Besides these benefits there is no improvement in the energetic classification of the hotel (to reach class B the EEI should be less than 44.1 Kgep.m^{-2}.year).

4.2. Glazed envelope

As the best solution for the opaque envelope is alternative 1, its values were fixed in order to evaluate the alternatives for different types of glazing and frames. With the code Calumen of Saint-Gobain there were analyzed four different alternatives of double glazing regarding the Solar Factor (SF):

Table 5: Annual thermal needs of the hotel: base case simulation and alternatives for the opaque envelope.

		Base case	Alt 1	Alt 2	Alt 3	Alt 4	
Heating	Electric	0.27	0.25	0.24	0.22	0.22	Kgep.m^{-2} year^{-1}
	Gas	1	0.36	0.27	0.2	0.15	
Cooling		5.19	4.59	4.53	4.48	4.45	
Ventilation		5.56	4.99	4.97	4.87	4.91	
Pumps		2.67	1.41	1.38	1.37	1.37	
EEI$_{nominal}$		48.1	44.99	44.77	44.53	44.49	
Consumption		1100.4	1029.5	1026	1021.6	1022	tep.year^{-1}
Total Energy		228	211	210	209	208	kWh.m^{-2}.year^{-1}
CO_2 emissions		1320.5	1235.4	1231.2	1225.9	1223.4	tons CO_2 equiv.year^{-1}
Costs		-	104.5	189.4	316.4	845.5	[€.10^3]
Payback time			5.6	9.6	15.1	40.4	Years

Alternative 1 (ALT 1): SF = 0.45
Alternative 1 (ALT 2): SF = 0.4
Alternative 1 (ALT 3): SF = 0.35
Alternative 1 (ALT 4): SF   = 0.3

For each alternative, there were analyzed different frames being them metallic with or without thermal cut or of wood or plastic. The energetic and economic analyses are displayed respectively in Table 6 and Table 7.

From the results of the analysis it is concluded that a window with a low solar factor there is a reduction in thermal cooling requirements. However, it causes increased heating requirements, leading the need to find an optimal point associated with the improvement of the glazed envelope. It was chosen a glass with a solar factor 0.40, since this solution becomes attractive in terms of payback time.

Table 6: Cost savings using glazed envelope with different frames.

Double glazing		Type of consumption	Annual energetic consumption [MWh.year^{-1}]	Annual energetic costs [€.10^3.year^{-1}]	Total [€.10^3.year^{-1}]	Cost savings [€.10^{3}year^{-1}]
Frame	SF					
Base case (0.56)		Electricity	3157	262	303.4	-
		Gas	1327	41.6		
Metal without thermal cutting	0.45	Electricity	3105	258	300	3.6
		Gas	1329	42		
	0.4	Electricity	3068	255	297	6.2
		Gas	1332	42		
	0.35	Electricity	3036	253	295	8.3
		Gas	1336	42		
	0.3	Electricity	3005	251	293	10.4
		Gas	1338	42		
Metal with thermal cutting	0.45	Electricity	3118	259	300	2.9
		Gas	1321	41		
	0.4	Electricity	3084	257	298	5.2
		Gas	1322	41		
	0.35	Electricity	3118	259	300	7.6
		Gas	1323	41		
	0.3	Electricity	3020	252	294	9.7
		Gas	1325	42		
Wood	0.45	Electricity	3131	260	301	2
		Gas	1318	41		
	0.4	Electricity	3097	258	299	4.5
		Gas	1318	41		
	0.35	Electricity	3064	255	297	6.8
		Gas	1318	42		
	0.3	Electricity	3031	253	294	9.1
		Gas	1319	41		
Plastic	0.45	Electricity	3139	261	302	1.5
		Gas	1317	41		
	0.4	Electricity	3100	258	299	4.3
		Gas	1317	41		
	0.35	Electricity	3066	255	297	6.7
		Gas	1317	42		
	0.3	Electricity	3033	253	294	9
		Gas	1318	41		

Table 7: Payback time of different kinds of windows.

	Total costs[€.10^3]	Increase in investment [€.10^3]	Payback time [years]
SF			
Base case (0.56)	332	-	-
0.45	362	30.2	8.4 - 19.7
0.4	377	45.3	7.3 - 10.6
0.35	407	75.4	9.1 - 11.3
0.3	422	91	8.7 - 10.0

5. ACTIVE SOLUTIONS

5.1. Solar thermal panels for sanitary hot water and swimming pool and PV´s for electricity production.

Decree-Law No. 79/2006 turns out the compulsory installation of solar panels for hot water in new buildings or major rehabilitation of buildings. In this hotel they will be used for sanitary hot water and swimming pool. The main characteristics of the solar thermal panels are: optical yield of 0.74, a solar capture area of 2m^2 and a thermal loss coefficient $a_1 = 3.9$ W/m^2/K and $k_2 = 0.013$ W / m ^{2} / k^2.

An economic study was also done, similar to the previous cases. For the building under consideration, if using a solar capture area higher to 200m^2, the system is no longer economically viable because the payback time is greater than the lifetime of the equipment. It should be noted that the selection criteria of this type of equipment cannot be only based on an economic assessment. It should also be taken into account the energy contribution that this type of equipment has to each situation under review. The lower payback time is around 8 years which corresponds to an area of 25 m2. For this situation, the EEI is 41.5 Kgep.m^{-2}.year^{-1} and becomes less than the reference value, 44.1 Kgep.m^{-2}.year^{-1}. So the hotel can be included in class B.

The PV panels, in despite of the high initial investment, is ecologically clean, with long life and do not require great care in terms of maintenance. For the contribution of this technology in the building, the analysis was done according to the maximum power peak of the photovoltaic system to be used, where it was tested the contribution of three different types of panels, such as amorphous silicon ones, the polycrystalline silicon and their integration in the facades (BiPV). The results of the comparison between them are shown in Table 8. The BiPV was discard from the analysis because the modules are arranged vertically which harms much the production of these panels.

Table 8: Comparison between solar thermal panels: amorphous silicon, and polycrystalline silicon.

Amorphous silicon panels							
Power peak [kW$_p$]	-	3.68	10	20	30	100	150
Solar capture area [m^2]	-	62.92	171.6	343.2	500.5	1716	2516.8
Nº of modules	-	44	120	240	350	1200	1760
Produced energy [MWh.year^{-1}]	-	6.6	18.3	36	53	186	268
EEI$_{nominal}$ [Kgep.m-^{2}year^{-1}]	44.25	44.16	44	43.8	45.6	42	41
Polycrystalline silicon panels							
Power peak [kW$_p$]	-	3.68	10	20	30	100	150
Solar capture area [m^2]	-	28.9	76.9	147	368	736	1088
Nº of modules	-	18	48	92	230	460	680
Produced energy [MWh.year^{-1}]	-	6.9	19	35	89	182	270
EEI$_{nominal}$ [Kgep.m-^{2}year^{-1}]	44.25	44.16	44	43.8	41	42	41

From the obtained results for the two types of photovoltaic panels, it was concluded that for the same peak power, the annual energy produced by amorphous silicon panels and the poly-crystalline silicon is quite similar between them, which is reflected in a decrease the overall consumption of the building in a very similar manner. Although these two different types of panels has for the same peak power a very similar annual energy production, the amorphous silicon panels are penalized because they require more than twice the solar capture area. So it was chosen for the following analyses the polycrystalline silicon panels – 92 modules with a power pick of 20 kW$_p$. The EEI is 42 Kgep.m-^{2}·year^{-1} which maintains the hotel in class B, beside the benefits shown in table 8.

5.2.   Other improvements

Several other improvements were taken into account. In order to not repeat the same kind of tables, only the final results of each one will be shown in this subsection.

– Ventilation devices - In order to improve the efficiency of ventilation equipment, consideration will be given to influence of HVAC systems with and without heat recovery, as well as the influence of consumption of the equipment associated with them. Between several options, the final one was that the air velocity in the batteries (heating and cooling), did not exceed 2.5m.s-1 whit the respective reduction of the total pressure drop in ducts and with heat recovery. Comparing with the base case, the percentage of the total energy saved is 2.9%, and the avoided CO_2 emissions represents 4.1%. The EEI value is 42.79 Kgep.m-2.year, less than the reference value.

– Lighting control equipment – Dimmers. The control of artificial lighting in a building aims to maximize the use of natural lighting, requiring only lighting and occupancy sensors in the spaces. These detect the presence of space lighting power, comparing it with the preset. If it is not achieved by natural lighting is driven artificial lighting. The TRACE 700 software has an algorithm that allows the inclusion of the concept of natural light into the building, creating in each space a variable named daylight factor, defined by the ratio between indoor luminance and the horizontal exterior luminance. The implementation of such control systems, reverts in a reduction of the annual energy bill of around 7%. The contribution to this decrease comes from the electricity consumption that is reduced considerably due to lower power consumption in the building using this technology. The payback time is 1.3 years.

– Chillers using heat recovery of hot water from the condensers to heat the sanitary hot water (SHW). After an energetic and economic analysis it was found out that using this technique, there is an expected increase in power consumption by the latter, by the reason of its contribution to the SHW (there is a significant reduction in nominal power to SHW). The greatest contribution of this equipment to satisfy the SWH takes place in the cooling season (summer), since in this period the chillers are running permanently (feeding the cooling batteries).

- Condensing boilers. They take advantage of the flue gas from the combustion. The use of condensing gas boilers lead to a decrease in overall building consumption due to better performance they have when compared to conventional boilers.

5.3 Further improvements

Taking into account the better solutions for each active solutions shown before, it's possible to compare them with the initial conditions. Table 9 displays the overall results of the best choices in order to reduce the energy consumption of the building.

As can be seen, with the features inherent in the initial solution (base case) when compared to the optimal solution set, the differences in all consumption levels decrease in a meaningful way. The reduced overall consumption of the building is approximately 25%. For the base case an according to the Portuguese legislation, the energy rating of the hotel was B- category. Therefore, after the changes carried out the building was rated to class A.

5.4 Overall solutions

Taking into account the better solutions for each active solutions shown before, it's possible to compare them with the initial conditions. Table 9 displays the overall results of the best choices in order to reduce the energy consumption of the building. As can be seen, with the features inherent in the initial solution (base case) when compared to the optimal solution set, the differences in all consumption levels decrease in a meaningful way. The reduced overall consumption of the building is approximately 25%. For the base case an according to the Portuguese legislation, the energy rating of the hotel was B- category. Therefore, after the changes carried out the building was rated to class A.

5.5 Cogeneration (CHP) and Trigeneration (CHCP)

Depending on the electrical power of the engine to be used and of the annual operating hours of the system, it's possible to evaluate the electricity produced annually by the equipment. In turn, the useful thermal energy depends on the thermal requirements of the building, because such a system only produces heat (besides the electricity). To be able to produce cooling it is necessary to have an absorption chiller that runs with the heat generate by the CHP. In this case such systems are designated as trigeneration systems – Combined production of Heat, Cooling and Power (CHCP). In the case study, due to the involved thermal needs, is interesting to couple an absorption chiller for the cooling needs.

Table 9: Results of the final solution.

		Final solution		Initial solution		Reduction of energy consumption	Avoided emissions of CO_2
		[kgep .m^{-2}.year^{-1}]	tons CO_2	[kgep.m^{-2}.year^{-1}]	tons CO_2	% [-]	% [-]
Heating	Electric	0.27	6.8	0.27	6.9	1.6	
	Gas	0.36	9.1	1.0	25.3	64.2	
Electric Cooling		4.49	157	5.19	181.4	13.5	
Lighting		12.95	329	15.61	397.1	17.1	
Electric equipment		12.43	316.4	12.43	316.4	-	
Gas equipment		1.78	45.3	1.78	45.3	-	
Ventilation		2.62	85.8	5.56	173.73	52.9	
Pumps		0.52	16.9	2.67	83.1	80.7	
Hydraulic equipment		0.03	0.08	0.06	1.6	46.5	
SWH	Gas	0.54	13.7	2.58	65.7	79.1	
	Electric	0.14	2941	0.14	3.5	0.9	
SPH	Electric	0.07	1.7	0.07	1.7	5.4	
	Gas	0.52	13.1	0.66	16.7	21.9	
Mechanical equipment		0.09	2.3	0.09	2.3	0.1	
Solar thermal		-0.32	-8.1	-	-	-	
PV		-0.48	-12.1	-	-	-	
Total		36	918.8	48.1	1320.5	25.2	30.4

There were analyzed several types of cogenerations systems, namely four strokes engines running with natural gas, micro turbines and fuel cells. Among them, the one that better fits to the thermal needs of hotel is a specific one with the following characteristic as shown in Table 10:

Table 10: Results of the final solution.

Electric power [kW]	Thermal power [kW]	Gas consumption [kW]	Electric efficiency [%]	Thermal efficiency [%]	Global efficiency [%]
330	363	851	38.78	42.66	81.43

It should be noted that the operating system defined for the system CHCP is that the heat produced by the system first meets the heating needs, and only supplies heat to the absorption chillers to satisfy the cooling demands with the surplus heat not used in heating.

In order to verify the feasibility of this type of system, it is necessary to define its annual operating hours, which for the case study, will be analyzed three different possibilities. It runs 24 hours a day (8760h / year), or from 7 am to 24 hours (6205h / year) because this schedule eliminates much of the super-peak and standard empty electricity (uninteresting of the remuneration level), or from 10 am to 21h (4380h / year). Table 11 shows the contribution of the CHCP when compared to the base case.

Table 11: Contribution of the CHCP for the energetic needs as a function of the running hours per year.

Thermal needs	CHCP	Conventional system	CHCP	Conventional system	CHCP	Conventional system
	%		%		%	
Heating	94.28	5.72	70.97	29.03	41.75	58.25
Cooling	39.32	60.68	39.22	60.78	41.12	58.88
Annual operating hours	8760h year^{-1}		6205h year^{-1}		4380h year^{-1}	

For the chosen engine, the EEE value is checked (EEE≥0.55) using just one or two engines. It is also be concluded that the use of this engine and its hours operation, there is the economic viability of this technology as well as the obligation to use it (payback time <8 years.)

6. CONCLUSION

In this work it was carried out an energetic and economic analysis of the contribution of passive and active solutions for buildings in order to reduce its energy consumption as well as the avoided CO_2 emissions. The contribution of renewable energy sources and the assessment of the contribution of a CHCP system was also studied. For that, dynamic codes were used to obtain all the thermal needs of a hotel located in Portugal. The simulations with nominal conditions (base case) showed that the total energy consumed in the building is 4.84 GWh / year, where under the conditions set for this model, it achieved a EEI nominal of 48.1 kgep.m-2.year-1, indicating that the building features an energy rating of B- [EEI nominal (48.10) < EEI reference (49.02) kgep.m-2.year-1. Regarding the emission level of CO_2, this building would emit 1320.5 equivalent tons of CO_2 per year. The consumption of HVAC (heating, cooling, ventilation and pumps), represents 35.7% of primary energy consumption, lighting 30.1%, consumption on the equipment is 27.6% and 6.6% referred to sanitary hot water and swimming pool water.

At a passive level, a sensitivity analysis to the base case was also done. Regarding the changes in the opaque envelope, the best solution was ALT1 shows a decrease in the consumption, both for heating (4.27%) and cooling (14.3%) and a consequent reduction of ventilation and pumping systems. The avoided CO_2 emissions are 6.4% and the payback time is 5.6 years. Regarding the glazing envelope and from the results of the analysis it is concluded that a glass with a solar factor of 0.40 is the best one, since this solution becomes attractive in terms of payback time in the range of 7.3 - 10.6 years as a function of the different types of frames that can be used.

At an active level it was analysed the use of solar thermal panels for hot water heating. The lower payback time is around 8 years. For this situation, the EEI is 41.5 Kgep.m-2.year-1 and becomes lower than the reference value, 44.1 Kgep.m-2.year-1. Also two types of photovoltaic panels were analysed: amorphous silicon and poly-crystalline silicon. It was concluded that the amorphous silicon panels are penalized because they require more than twice the solar capture area. So it was chosen the polycrystalline silicon panels whit 92 modules. The power pick is 20 kWp and the EEI is 42 Kgep.m-2.year-1. With this solutions, it was concluded that they contribute to a reduction of thermal needs of 25.2% and avoided emissions of equivalent tons of CO_2 of 30.4%. Regarding the use of CHCP the best solution chosen was a four stroke internal combustion engine running with natural gas, and coupled to an absorption chiller. The contribution of this type of engine to fulfil the heating requirements of the building lies in the range of 44 to 94% and for cooling the range is 39-61% (depending upon the working system profiles). It is also concluded that, the use of this engine and its operating hours, there is the economic viability of this technology as well as the obligation to use it (payback time <8 years).Check list - please ensure that you:

7. REFERENCES

ÇENGEL, 2002,. Thermodynamics. Mc Graw Hill.

AFONSO, C., 2012. Thermodynamics for Engineers, FEUP ed., Porto, Portugal. (In Portuguese).

AFONSO, C., Moutinho, T., 2014 Energetic, Economical Analysis and Avoided CO2 Emissions in a Cogeneration System Regarding the Legislation. International Journal of Mechanical Engineering and Automation. Vol. 1, nº2,

A Review of Cogeneration Equipment and Selected Installations in Europe, 1997. Directorate-General XVII for Energy, OPET, Commission of the European Communities.

Cogeneration - Fact sheet No. 1, 2010.

Decree-Law nº 538/99, December (CHP) and Decree-Law nº 313/2001 (CHP).

Decree-Law n.º 225/2007 (photovoltaics systems).

Decree-Law nº 79/2006 (RSECE - Regulamento dos Sistemas Energéticos de Climatização em Edifícios. In English: Regulation of Energy Systems for HCVAC of buildings).

Decree-Law nº 80/2006, (RCCTE - Regulamento das Características de Comportamento Térmico dos Edifícios. In English: Regulation Characteristics of the Thermal Performance of Buildings).

POLIMEROS, George. Energy Cogeneration Handbook, Industrial Press Inc.

The European Association for the Promotion of Cogeneration. www.cogen.org/ . Accessed on 2013.

http://www.cogenportugal.com/ficheirosupload/Fact%20Sheets.pdf.. Accessed on 2013.

236: Investigating the effect of tightening residential envelopes in the Mediterranean region

GEORGIOS GEORGIOU[1], MAHROO EFTEKHARI[2], TOM LUPTON[3]

1 Loughborough University, Loughborough-UK, g.georgiou@lboro.ac.uk
2 Loughborough University, Loughborough-UK, m.m.eftekhari@lboro.ac.uk
3 Loughborough University, Loughborough-UK, t.l.lupton@lboro.ac.uk

Nowadays, buildings are responsible for the 40% of energy consumption (36% of greenhouse gas emissions) in the European Union. The European Council pointed out the need to refurbish a large amount of the existing building inventory, as new buildings are related to the 1-2% of the total energy consumption. Air-infiltration and tightness of buildings are usually neglected parameters during retrofitting or building design, especially in the Southern European counterparts, where air-tightness standards are absent from the national building regulations. To this effect, this study investigates the impact of tightening existing residential envelopes, focusing on the impact to the default construction and synergies arisen between air-tightness and other interventions (i.e. thermal insulation). The study was undertaken in the Mediterranean climate conditions, examining detached houses located in Cyprus. This is the first study in national level, presenting the air-tightness characteristics of buildings as these were collected by a blower door test. In general, the outcome shows that the improvement of air-tightness primarily reduces the energy associated with winter thermal loads. Apart from that the tightness of building envelopes beneficially contributes on the performance of other energy saving measures. In particular, the reduction by thermal insulation can be enhanced up to 12%, while the synergy with a glazing system may reduce heating demand up to 7%.

Keywords: Air-tightness, Infiltration, Residential envelopes, Mediterranean region, Cyprus

1. INTRODUCTION

In the European Union, buildings are responsible for nearly 40% (22% dwellings and 18% commercial buildings) of energy consumption (and 36% of GHG emissions) (EUC, 2012). The Europe-wide initiatives on transforming the energy system for a decarbonized future recognize the importance of buildings in reducing carbon emissions (EUC, 2011). Due to the evolution of technology and industrialization, houses relied on artificial systems, ignoring the adaptive ability of the human body (Clements-Croome, 2000; Roaf et al., 2010). Evidently, householders consume most of their energy to maintain comfortable conditions, due to a poor building design and operation. Lapillone and Wolfgang (2009) presented a breakdown of the residential energy use, claiming that space conditioning contributes heavily up to 68%.

There seems to be two lines of thought with regards to the strategies on existing buildings; demolition or retrofitting. Undoubtedly, demolition and new buildings may be defined as better solutions. Though, an enormous amount of the European housing inventory will need refurbishment that will substantially result in energy reduction and its associated CO_2 emissions (Burton, 2012). Borgeson and Brager (2011) pointed that the achievement of energy targets must not lead to scarification of thermal comfort and indoor air-quality.

Dokka and Rodsjo (2005) developed the Kyoto pyramid, categorizing the actions that must be considered during the "passive" design of commercial or private buildings (see Figure 98). The Kyoto pyramid classifies the reduction of heat losses as the primary measure towards passive design, followed by the reduction of electricity use, utilization of solar energy, regulation of energy and selection of local energy source (Dokka and Rodsjo, 2005).
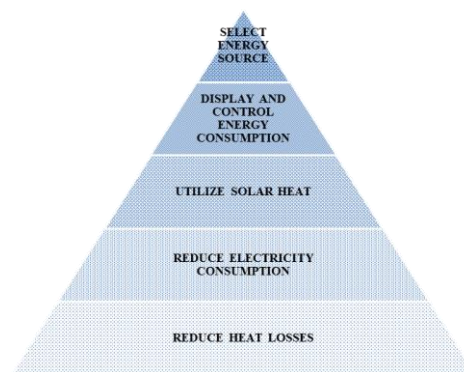

Figure 98 The Kyoto pyramid (Dokka and Rodsjo, 2005)

The tier referring to heat losses is coherent with the external envelope which determines the physical boundaries between the indoor and outdoor environments. Regulating the impact of heat transfer mechanisms, results on a stable indoor environment and lower energy consumption for maintaining thermal comfortable environment.

A neglected parameter, especially in southern European counterparts, is the air-tightness of the building. In spite the implementation of EPBD, only Spain is regulated by partially requirements, concentrating on the windows' performance (Erhorn-Kluttig et al., 2009). The air-tightness of the building determines the resistance on the unintended flow of air through the building envelope (CIBSE, 2000).The excess air infiltration is usually inherent with the irrational energy consumption and indoor thermal comfort. For instance, the warm air is leaking through the gaps and cracks, enhancing the heat losses of the envelope. As a result, an amount of energy is wasted to condition air which escapes from the building (EST, 2005). In a study by Chen et al. (2012), it was concluded that a reduction of 12.6% was achieved when the permeability was reduced from 0.98-0.5 ACH. Additionally, in an investigation of different air-tightness scenarios, Logue et al. (2013) observed a reduction of residential energy demand when the houses' leakage was decreased.

Another common notion, referring to infiltration impacts, is the negative effect on the efficiency of thermal insulation due to deterioration of the insulation. Due to excessive leakage, the air may penetrate the structure and thus, the effectiveness of insulation is reduced (CIBSE, 2000). Moreover, USDOE (2010) exemplary states that infiltration is like an open window for 24 hours, annually. In essence, the addition of thermal insulation may reduce the transmission loses, however a convective link will still encounter between indoor environment and outdoors ("short-circuiting", (CIBSE, 2000)). Furthermore, in the context of thermal

comfort, draughts arise, due to the unintended flow of air, causing discomfort and complaints to the occupants (EST, 2005).

The improvement of building permeability and thereby, the reduction of the unintended flow of air will enhance the indoor environment while the residential energy demands will be reduced. However, it is mandatory to mention and point out the cases where the ventilation of the whole building is reliant on infiltration. Due to the leakage areas on the existing envelope, the ventilation requirements may be occasionally satisfied, but the target rates are unreliable in the context of time and location (EST, 2006). By tightening the envelope, there is an indoor air quality risk because of the possible increased concentration of hazardous pollutants (VOCs, CO, CO_2, dust, moisture) generated by residential actions such as smoking, combustion, cooking or furniture. Thereby, it is indispensable to provide an alternative ventilation solution such as a mechanical ventilation system or a well-versed natural ventilation system.

This study investigates the impact of tightening existing residential envelopes, focusing on the impact to the default construction and synergies arisen between air-tightness and other interventions (i.e. thermal insulation). The study was undertaken in the Mediterranean climate conditions, examining detached houses located in Cyprus. This is the first study in national level, presenting the air-tightness characteristics of buildings as these were collected by a blower door test.

6   METHODOLOGY

As aforementioned, the study seeks to investigate the impact of reducing air infiltration by tightening building envelope of the default structure and also, to examine the synergies arisen by other energy saving measures (i.e. thermal insulation, glazing). In order to accomplish this study, a procedure was adopted, comprising a blower door test and a building simulation, utilizing data collected from actual residential buildings. Essentially, 3 air-tightness scenarios will be contacted, listed in Table 60.

Table 60: Air-tightness scenarios

Scenario	Air Permeability (m^3/h.m^2 @ 50Pa)	Details
Infiltration (1)	-	*Default building's air permeability*
Infiltration (2)	≈3	*This requirement is based on Energy Saving Trust best practise and Germany average of 2.8~3.0 m^3/(h.m^2)) @ 50 Pa*
Infiltration (3)	≈1	*Passivhaus Standard*

2.1 Case studies

Initially, 9 detached houses were selected for investigation. The dwellings are located at the south-west coast of Cyprus, in the urban area of Paphos town. In particular, 7 buildings were constructed prior 2007 (implementation of EPBD), which will be used during the building simulation. The remaining case studies were constructed in 2011, and their tightness will only be measured during blower door test, in order to examine the trend in the construction industry. Table 61 and Figure 99 present the selected houses for investigation and a short description of the construction year and floor area.

2.1 Blower Door Test

A blower door test has been carried out, measuring the default air permeability of the building enclosure. The procedure was aligned with the EN 13829:2001 (CEN, 2001), with additional enhancements by (ATTMA, 2010). The guidelines were strictly followed, initially to avoid any damage on the envelope of the private properties during the depressurization of the building and also, to ensure the quality of the results. The results from the blower door test will be used on the generation of building models, in order to examine in depth the impact of reducing air infiltration.

Figure 99 Exterior view of case studies

Table 61: Sample Characteristics

Index	Construction Year	Floor Area (m^2)
SD1	1995	290
SD2	1987	188
SD3	1996	384
SD4	1994	176
SD5	1987	117
SD6	2007	120
SD7	2006	208
SD A	2011	500
SD B	2011	450

2.2 Building Simulation

In order to examine the air tightness scenarios, mentioned earlier in this section, the building simulation will be applied. Through EPlus software, the models were generated, following the concept of model calibration. Data collected from actual buildings were used to build realistic simulation models. The whole procedure is extensively described in a previous study (Georgiou et al., 2014).

Following the successful validation of the models, a normalization was applied in order to globalize the outcome of the study. In particular, the models were normalized with regards to the weather conditions, occupancy patterns and HVAC operation. Referring to the outdoor climate, the simulation is based on two TMYs databases; coastal (Paphos Station) and low lands (Athalassa Station). The interventions will be examined during the heating and cooling periods, at any time of occupation, setting the HVAC set-point temperature according to EN 15251 (CEN, 2007), assuming a metabolic rate≈1.2 met and clothing value 1.0 and 0.5, for winter and summer, respectively. Table 62 presents the parameters related with the occupancy pattern and set-point temperatures of HVAC.

Table 62: Normalized occupancy pattern and set-point temperatures for HVAC systems

Space	Occupied Hours		Set-point temperature (°C)	
	Weekdays	Weekends	Winter	Summer
Living Room	17:00-22:00	08:00-13:00 & 14:00-22:00		
Kitchen	13:00-14:00 & 20:00-21:00	13:00-14:00 & 20:00-21:00	20	25
Bed Room	22:00-07:00	22:00-07:00		

3   RESULTS

This section presents the results by the analysis of the findings of blower door test and building simulation. The study focuses on the performance of the houses constructed prior 2007. In general, a graphical approach was adopted for the presentation of results, applying box-whisker plots (mainly in the case of building simulation results).

3.1 Blower Door Test

The results from the blower door test are automatically produced by the TECTITE software. The Figure 100 presents the relation between air-tightness and construction year.
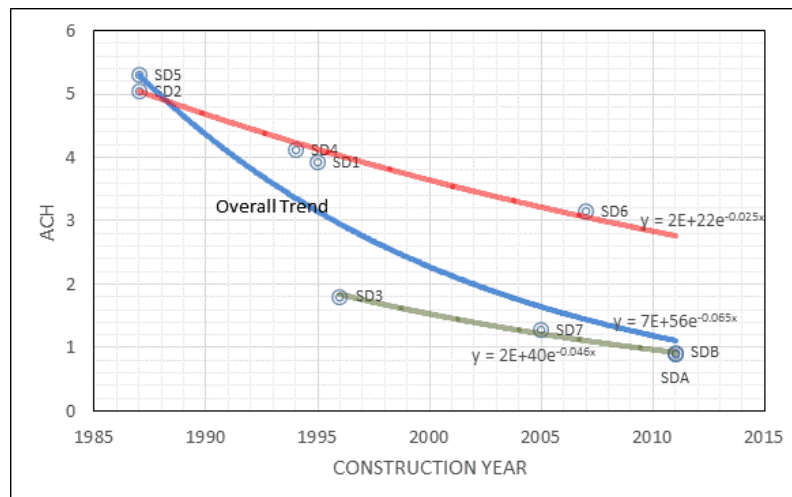

Figure 100 ACH against construction year

Overall, the trend declined dramatically through the years, due to tightened envelopes. As it can be noticed, two sub categories are presented in the Figure 100, with both having slight decrement. In spite the fact that local constructors are not obligated to any building regulations in terms of building air-tightness, air-tightness was improved since 1985. Possible facts for this trend are the high quality materials, the construction techniques or even the bearing structure of the buildings. The latter may be explained by the fact that the bearing structure of national stock is founded on concrete and bricks, eliminating the paths of air. In essence, the major infiltration sources of infiltration are the external openings. This is the main reason of the resultant sub categories, presented in the findings of blower door test. In particular, the houses comprising the lower region, have tighter door and window frames, as this was observed during the walk-trough visits. Consequently, in such buildings constructions, high levels of air-tightness can be achieved by sealing the frames of the openings, taking the exemplary performance of the newly constructed buildings (SDA and SDB).

3.2 Building Simulation

Effect on default construction

Tightening envelope seems to be more effective during the winter season, as lower impact was observed during summer period. Figure 101 presents the impact on annual heating and cooling load of the base construction, by tightening the building under two scenarios (intermediate-Infiltration 2 and strict-Infiltration 3).
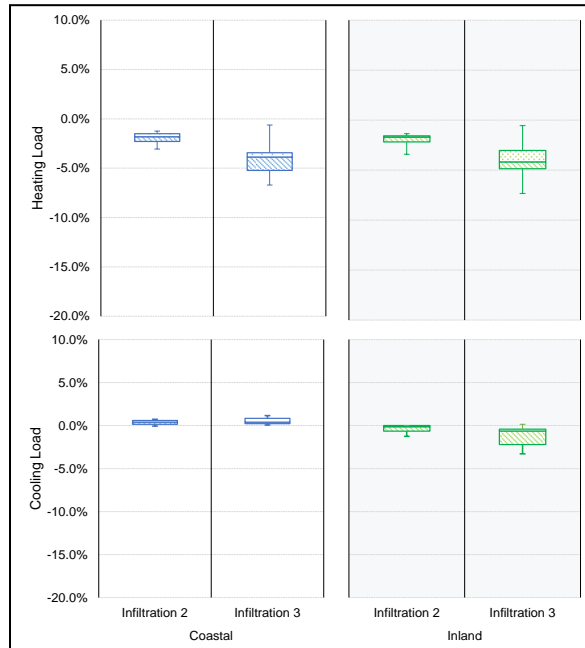
Figure 101 Impact on base loads by tightening building envelope

In particular, for both climates the median value of reduction during the winter season is 2% and 4% for Scenario (2) and Scenario (3), respectively. In some cases, the energy consumption may be reduced by up to 7%, with 75% of the samples found between 4-5% for coastal areas and 3-4% for inland areas.

 Observing the impact on heating load, it can be noticed that the impact is lower during the summer season. During the cooling period, a converse relation is noticed between the two weather files. A negligible increment occurs at the coastal conditions, with the median equals to +0.4% (both Scenarios). On the contrary, at the inland conditions the houses presented an average reduction on thermal load by -0.4% and -1.2%, Scenario (2) and Scenario (3), respectively. In order to realize the difference between the weather conditions, Figure 102 illustrates the indoor conditions during summer.
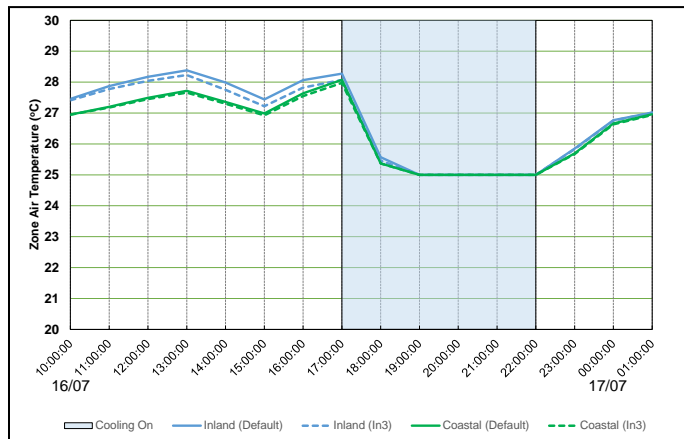

Figure 102 Difference of air temperature for coastal and inland-SD1

Due to the higher indoor temperature of the default state (case of inland weather), the Scenario (3) causes higher reduction of indoor temperature. As a result, the mechanical system operates in lower temperature difference, corresponding to higher energy reduction.

Now, in the perspective of thermal comfort, Figure 103 shows the effect of tightening on the seasonal thermal comfort score.
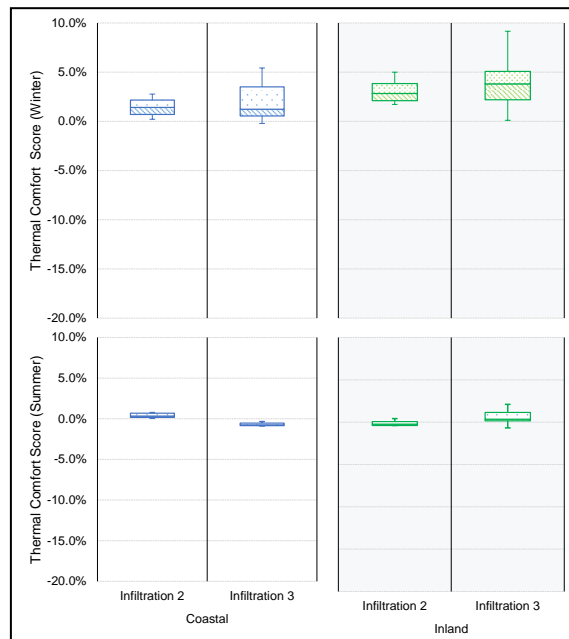
Figure 103 Impact on seasonal thermal comfort

As it can be noticed by Figure 103, the reduction of the air infiltration improves the indoor thermal conditions, especially during the heating period. In general, the indoor thermal conditions during winter can be improved up to 5% (coastal) and 9% (inland). Moreover, during the winter period, the results of the application of Passivhaus show a substantial variation. This is primarily based on the default properties of the building. Leaky houses (i.e. SD1, S2, and SD5) are associated with higher effect by tightening. For instance (see Figure 103, inland section), the 9% is presented in the case of SD1 dwelling, while for the SD4 (tighter building), the impact was estimated at ≈0.2%. Now, in the context of the cooling season, as in the case of energy performance the effect is not substantial, with median values close to 0%.

Effect on the performance of thermal insulation and glazing

The importance of air tightness is also revealed when comparing the performance of interventions with the permeability of base case. Figure 104 shows the comparison of the performance for the categories of thermal insulation and glazing systems, when tightening the building enclosure.
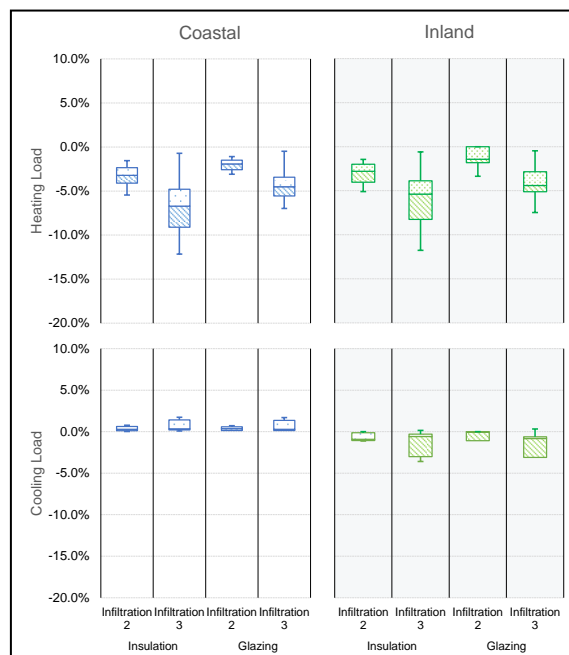

Figure 104 Impact on energy saving measures by tightening the envelope

During the winter season, the performance of thermal insulation (roof, external walls or floor) was dramatically improved when the Passivhaus standard was applied. In particular, 50% of the samples lie within the range of 5-9% (coastal) and 4-8% (inland) of heating reduction and can reach up to 12%, while Scenario (2) may reduce heating demand by 2-6% (coastal) and 2-5% (inland). In the same line, the impact of glazing performance ranges between -0.5% to -7% (both climates).

As in the case of base load performance, the impact of air tightness on the cooling performance is negative for the coastal areas and positive for inland weather conditions. Again, the effectiveness of tightening the building is lower for coastal areas with an increment for both thermal insulation and glazing that can reach up to 2%, while in the inland areas an improvement of approximately 4% is possible for both categories of interventions.

The same scene is also presented within the context of thermal comfort. Figure 105 shows the results on alternation of thermal environment by the synergies of air-tightness, thermal insulation and glazing system.
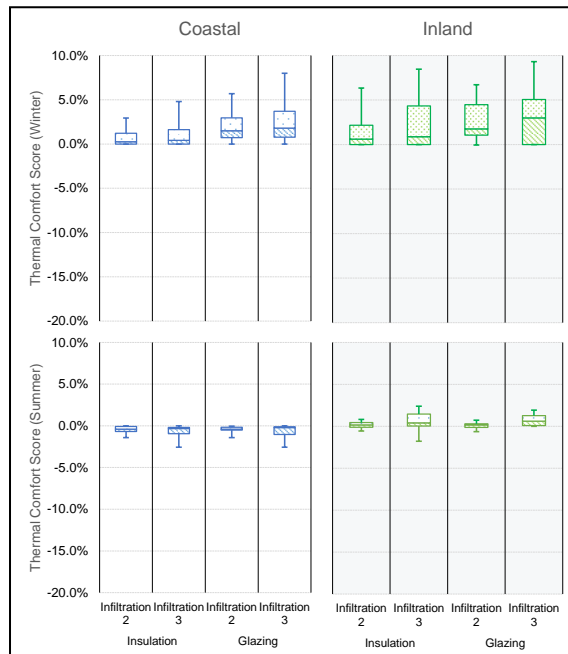

Figure 105 Impact of envelope tightening on the thermal comfort of thermal insulation and glazing measures

Again, the effect on winter season is higher for both climates. Comparing with thermal loads, the air-tightness shows greater impact on the glazing system, especially during the winter period. The median values, for glazing systems, are slightly higher than those of thermal insulation. The thermal comfort score is compromised (not substantially) during cooling season, as at the case of energy performance.

Air-tightening and Indoor Air Quality (IAQ)

Evidently, tightening building envelope may reduce the air infiltration, however this has an impact on the indoor pollutant's concentration. In general, leaky dwellings rely on the mechanism of the uncontrolled ventilation (infiltration) to provide occupants with fresh air and dilute pollutants. This effect is outside the context of this study, but it was considered critical to present the impact of tightening the envelope on the concentration of indoor pollutants. Due to the amount of data, only an example is depicted in the Figure 106, for the case of living room of a leaky house (SD4). In particular, the CO_2 concentration (left y-axis) of the space is plotted with the air temperature (right y-axis) for a day period, under the 3 scenarios of air tightness. The blue region on the graph indicates the period when the heating system is switched on.
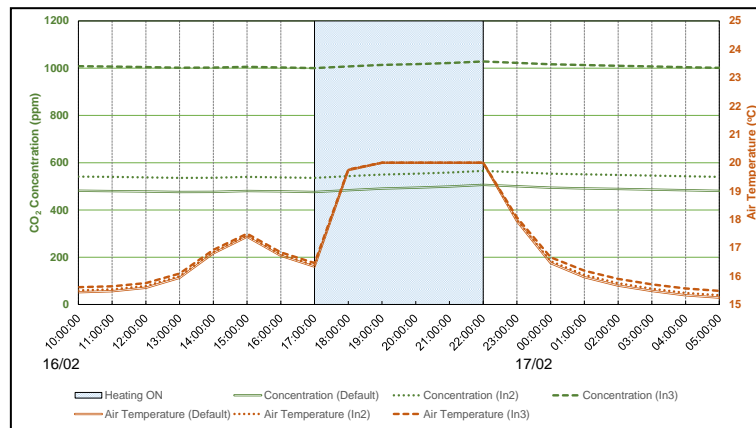
Figure 106 Living room CO$_2$ concentration-SD4

It can be clearly noticed that the CO$_2$ concentration is dramatically increased under the Scenario (3), while an increment is presented on the air temperature. The CO$_2$ levels are daily accumulated within the space, resulting on high levels of concentration.

4   CONCLUSIONS

The study presented the investigation of air infiltration in residential envelopes at the Mediterranean region. The results comprises by the findings of a blower door test and the analysis of building simulation. The study examined 9 single detached houses, located in Cyprus.

The blower door test results revealed a decreasing trend on envelope air-tightness in the last decades. Newly constructed buildings showed exemplary levels of air-tightness (Passivhaus Standard), under no obligation on energy efficiency building regulations. Due to the concrete structure and the location of air paths, these examples may motivate the tightening of building envelopes during retrofitting, as the majority of national housing inventory is founded on the particular building structure.

The building simulation results showed that air penetration seems to affect positively the winter performance of the envelope, with the Scenario 3 (Passivhaus Standard) having higher impact. Meanwhile, during the winter season the thermal comfort is enhanced, on the contrary with the summer season, where tightness may slightly compromise the overall scene. In addition, it can be concluded that tightening can beneficially contribute on the performance of the other measures, especially during heating period. Particularly, the improvement of air-tightness under the scenario of Passivhaus standard can improve the winter performance of thermal insulation up to 12%, while the synergy with a glazing system may reduce the heating demand up to 7%.

5   REFERENCES

ATTMA, 2010. Technical Standard L1. Measuring Air permeability of Building Envelopes (Dwellings).

BORGESON, S., Brager, G., 2011. Comfort standards and variations in exceedance for mixed-mode buildings. Build. Res. Inf. 39, 118–133. doi:10.1080/09613218.2011.556345

BURTON, S., 2012. Handbook of Sustainable Refurbishment-Housing, 1st ed. Taylor & Francis.

CEN, 2007. CEN Standard EN 15251: Indoor environmental input parameters for design and assessment of energy performance of buildings-addressing indoor air quality, thermal environment, lighting and acoustics. Comité Européen de Normalisation.

CEN, 2001. CEN Standard EN 13829: Thermal performance of buildings-Determination of air permeability of buildings-Fan pressurization method. Comité Européen de Normalisation.

CHEN, S., Levine, M.D., Li, H., Yowargana, P., Xie, L., 2012. Measured air tightness performance of residential buildings in North China and its influence on district space heating energy use. Energy Build. 51, 157–164. doi:10.1016/j.enbuild.2012.05.004

CIBSE, 2005. Heating, ventilating, air conditioning and refrigeration (Guide B). CIBSE, London, UK.

CIBSE, 2000. Testing Buildings for Air Leakage (Technical Memoranda No. TM 23). CIBSE, London, UK.

CLEMENTS-CROOME, D., 2000. Creating the productive workplace. E & FN Spon, London,UK.

DOKKA, T.K., Rodsjo, A., 2005. Kyoto Pyramid [WWW Document]. Hvordan Planlegge En Lavenergibolig. URL www.lavenergiboliger.no (accessed 6.10.12).

ERHORN-KLUTTIG, H., Erhorn, H., Lahmidi, H., 2009. Airtightness requirements for high performance building envelopes (ASIEPI Information paper No. P157).

EST, 2006. Energy efficient ventilation in dwellings-a guide for specifiers (No. GPG268). Energy Saving Trust, London, UK.

EST, 2005. Improving airtightness in dwellings (No. GPG224). Energy Saving Trust, London, UK.

EUC, 2012. Financial support for energy efficiency buildings. European Commission, Brussels, Belgium.

EUC, 2011. Energy Roadmap 2050. European Commission, Brussels, Belgium.

GEORGIOU, G., Eftekhari, M., Eames, P., 2014. Calibration and validation of residential buildings: 8 case studies of detached houses. Presented at the Building Simulation and Optimization, IBPSA, London, UK.

LAPILLONE, B., Wolfgang, E., 2009. Overall Energy Efficiency Trends and Policies in the EU 27 (Brochure). ODYSSEE-MURE project.

LOGUE, J.M., Sherman, M.H., Walker, I.S., Singer, B.C., 2013. Energy impacts of envelope tightening and mechanical ventilation for the U.S. residential sector. Energy Build. 65, 281–291. doi:10.1016/j.enbuild.2013.06.008

ROAF, S., Nicol, J.F., Humphreys, M.A., Tuohy, P., Atze, B., 2010. Twentieth century standards for thermal comfort: promoting high energy buildings. Archit. Sci. Rev. 53, 65–77.

USDOE, 2010. Retrofit Techniques & Technologies: Air Sealing-A Guide for Contractors to Share with Homeowners. U.S. Department of Energy.

POSTER SESSION A

426: Energy management systems for microgrids

VICTOR MARYAMA[1], VITOR S. ZENI[1], FREDERICO V. JORDAN[1],
CESARE Q. PICA[1], GABRIEL A. OLIVEIRA[2]

1 CERTI Foundation, Federal University of Santa Catarina Campus - Sector C - Brazil, vma@certi.org.br
2 Tractebel Energy, Pachoal Apóstolo St. 5064 - Florianópolis - Brazil, goliveira@tractebelenergia.com.br

This work presents a pilot hybrid (AC and DC) microgrid, comprised of a gas microturbine emulator, a small wind turbine emulator, photovoltaic panels, an energy storage system, controllable AC and DC loads and static converters. This is a project sponsored by Tractebel Energy Brazil, aimed at studying microgrids in order to evaluate its use in creating value for customers. This allows them to use their energy in the most efficient way, taking advantage of intelligent distributed energy resources.

The focus of this paper is mainly on the microgrid energy management system, which plays the role of the economic dispatcher. The cost of operation is minimized by taking into consideration grid energy costs, fuel costs, O&M and equipment wear as well as diverse operation restrictions of the system, such as grid exchange limits, power limits of the sources, battery dynamics, among others. The resulting optimum power set points for the sources are calculated based on demand and renewable generation forecasts, in order to guarantee the most economic operation.

A simulation platform was developed to evaluate the behaviour and costs of similar microgrids, in which the specification of the sources can be arbitrarily defined. The static operation can be viewed and the resulting electrical transient dynamics can be analysed for user-defined moments within the simulated results. Study scenarios will be presented using this tool, showing the effectiveness of a microgrid management system in real-life representative situations.

Keywords: microgrids, energy management systems, distributed energy resources, economic dispatch

1. INTRODUCTION

In the context of Smart Grids, the concept of microgrids is becoming an increasingly attractive approach to distributed generation and efficient energy consumption. It can provide improvements on technical issues of availability and power quality in different applications, as well as new business models and operation of electrical systems. A microgrid can be defined as a group of distributed generation, energy storage systems and local loads operating in an integrated way by means of electrical networks, communication and control. In general, a microgrid has a well-defined boundary and a single point of connection to the external power grid. It can work in connected or in islanded mode and has a control and energy management system that causes a microgrid to be presented to the electrical system as a single, well-controlled energy unit, that consumes energy and can provide services to the grid as well. Figure 107 illustrates a topology of a smart microgrid.
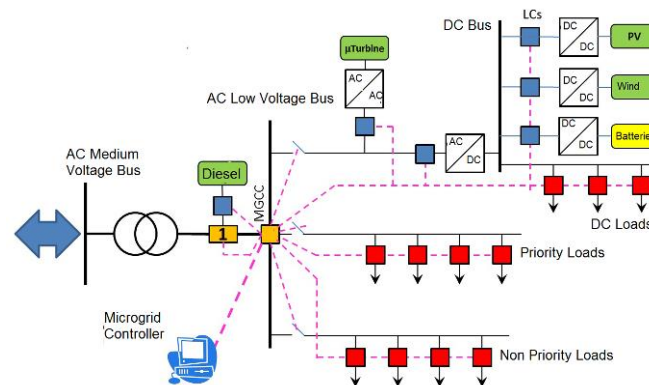

Figure 107 - Typical microgrid

Microgrids can meet different applications, such as industrial plants and commercial establishments (in which case the microgrid elements can be installed on a single customer system); in buildings and residential condominiums; and parts of the distribution network (in this case the microgrid elements may be located in different consumers). During operation of microgrids in connected mode, there may be exchange of energy between the microgrid and the external grid, depending on the energy surplus availability and / or any order from the microgrid operating agent. During islanded operation, there may be several other situations, for example, in the case of renewable generation surplus, this energy can be used to recharge the battery system; in the event of greater demand than the renewable energy generation, load-shedding actions may occur (according to priority), or the batteries and other dispatchable machines may be used to meet the microgrid energy balance. In both operation modes, but also in times of transition between modes, a key element is the microgrid central controller, which plays also the role of the microgrid's Energy Manager (EM).

The goal of this work is the development of energy management strategies for an experimental smart microgrid, with focus on the intelligence of the network, seeking an efficient, reliable and economic system, which may be characterized as an attractive solution to the electricity sector.

This paper is organized as follows: Section II presents an overview of energy management and specifications of models and strategies used in the project. A developed simulator with static and dynamic simulations is presented in Section III. Section IV presents simulation results of the energy management. Finally, Section VI presents the conclusions.

2. ENERGY MANAGEMENT

In general, the microgrid energy manager aims to define an operating strategy for the generation sources and demand, for instance, the operating status (on / off) and the power output set-point for a source, over a given time horizon, which meets some predefined criterion (in some cases multiple criteria are used). The operation strategy should take into consideration a series of individual operating constraints of the sources, loads and other components of the microgrid as well as so-called systemic constraints such as meeting the demand, reserve requirements and exchanges with the utility, for example. This management is defined as an optimization problem. Figure 2 illustrates the concept of an energy manager (represented as MGCC) showing inputs and outputs of the system.
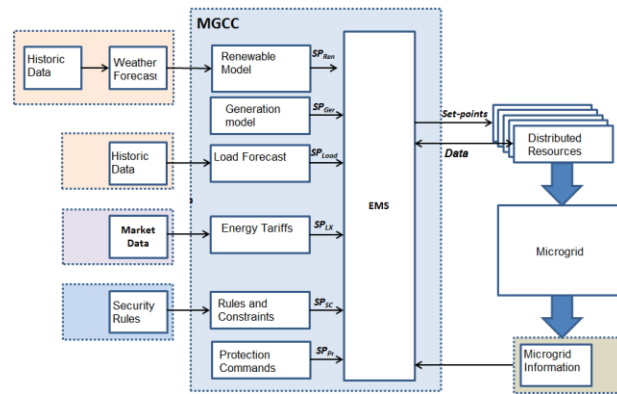
Figure 108 - Conceptual operation of a microgrid Energy Management System (EMS)

As said before, mathematically the energy management problem is solved based on the solution of an optimization model. The size of this problem depends primarily on the following factors: number of generating units, transmission elements, length and granularity of the planning horizon. For the most part, it is assumed that the problem is deterministic in nature – that means that demanded power, solar and photovoltaic generation and power purchase prices forecasts are considered acceptable enough.

Data such as demanded power and renewable generation should be provided during this horizon and are, consequently, subject to forecasting errors. For this reason, the algorithm is rerun periodically, in order to incorporate different information about the operating status of the network and new information regarding predictions.

Modelled cost and operation aspects of the microgrid and its components are shown below.

Cost Function

The cost function is the function to be minimized concerning the optimization model of the microgrid, given that the restrictions are valid. This seeks to represent the financial cost of the microgrid operation for every instant of time during the prediction horizon. It is also possible to assign arbitrary costs for unwanted behavior of the system sources such as, for example, exaggerated variations of the storage system power output. The definition of the individual costs for the sources will be detailed below.

Operating Constraints

The constraints correspond to situations that must necessarily be met by solutions. It includes the power balance of the microgrid (so that there is no power surplus or shortage), limitations of maximum power transfer of inverters and generating units, minimum levels of the spinning reserve (in order to ensure a power reserve for possible estimation errors on the load demanded power and renewable generations without the need to perform any additional energy source start-up), among others.

Dispatchable Generating Units

Costs modeled for components such as gas microturbines, diesel generators and fuel cells correspond to the fuel consumption curve, maintenance costs and costs related to start-up and shutdown. Furthermore, the effect of temperature on the efficiency of the sources is modeled as well as maximum power variation constraints and limitations on the maximum number of start-ups in a given time interval.

Utility Grid

The grid is modeled according to energy tariffs and limits on the exchanged power.

Battery Bank

For the battery system, power variation constraints and wearing costs were modelled.

Sheddable Loads

In fault situations, the energy manager can come to dismiss electrical loads if the available energy in the microgrid is not sufficient to meet all consumer units. In this case, costs for the shutdown of these loads are considered. These values are arbitrary - higher priority loads should have a higher cost and will be discarded less frequently.

To avoid the constant switching of loads in the microgrid, a minimum run time for each load after the restart was defined. Thus, the load can only be turned off after being in operation for a certain amount of time.

Misc

Other modelled aspects include costs related to deficit or excess energy in the system.

3. SIMULATION PLATFORM

To evaluate the efficacy and view the operation of the system under various conditions, a simulation platform has been conceived in the context of this project. This platform consists of two different instances: A static and a dynamic simulator.

Static Simulator

The static simulation corresponds only to the operation of sources on a steady-state basis, not considering the transient dynamics in the system between the operating points, which are calculated from demand and renewable resources (wind speed and solar radiation) data. The levels of renewable generation are computed based on conversion ratios of renewable resources to electric power: as a function of generation curves from wind speed for wind generators and relation of photovoltaic generation according to the instantaneous solar radiation.

The system is simulated comparing the generated and consumed power at each instant of time. The energy balance is checked, considering the energy management algorithms chosen (which defines generating set points) and the droop characteristic of the generators – a primary control within the energy sources to share load variations -, as shown in Figure 109 and Figure 110.
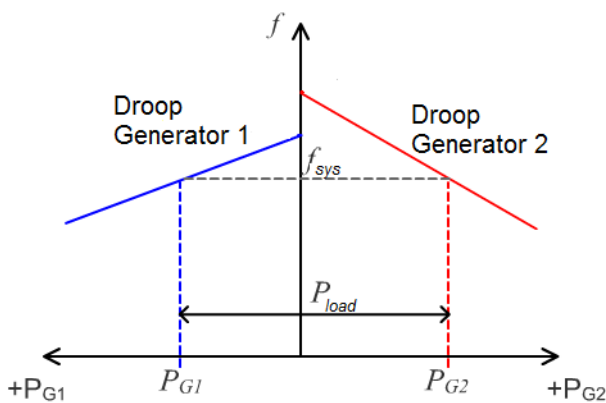

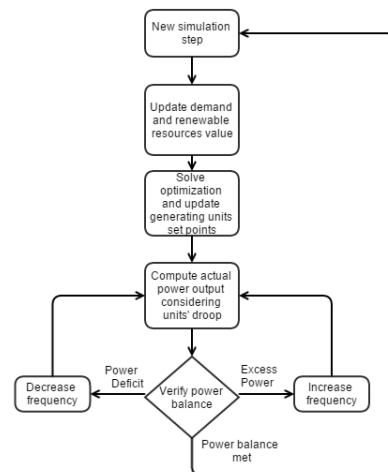Figure 109 - Generator droop example

Figure 110 - Static simulation diagram

This scheme allows for load-sharing among generating units. The demanded power may be greater or lower than the set points sent to the sources and the droop is necessary due to variations in the interval between the set point calculations and due to prediction errors within the algorithm itself.

Dynamic Simulator

The dynamic simulation, on the other hand, contains detailed continuous models of the dynamics of the components and the electrical network and its control systems. It is ran from the selection of different steady-state operating points of the static simulation and allows you to view different data, such as frequency and amplitude of voltage, as well as current and power variations of the system components.

These models were developed as controlled voltage and current sources according to the component being modelled. These include converters, generators and loads, incorporating different characteristics such as droop (for converters and generators) and other power controllers.
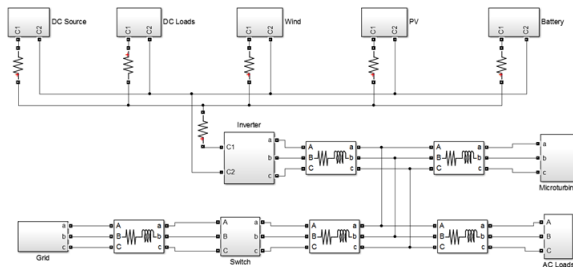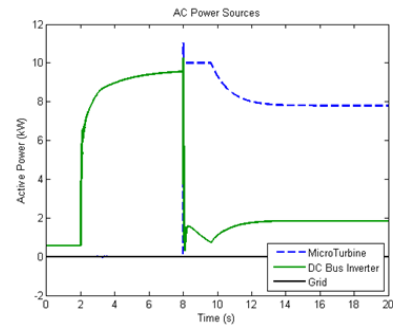

Figure 111 - Dynamic simulation diagram

Figure 112 - Dynamic simulation result example

Simulation Parameters

Regarding the dispatch methods, two different strategies can be applied: The first, called cyclic-charging, causes the sources to be dispatched when the battery charge drops below a threshold, and to be switched off when it reaches an upper threshold. The second strategy is to minimize the total cost of the operation using the optimization algorithm described above, which calculates the minimum cost of operation.

Using the platform, the user can also define certain parameters that guide the behavior of the optimizer. The prediction horizon refers to the number of hours in the future that the optimizer will try to predict to calculate the optimal dispatch. A higher number of hours will increase the performance optimizer, but in return increases exponentially the time required to find the optimal solution, lowering the simulation speed. It is also possible to define the number of points in the prediction horizon. The greater the granularity of this horizon, the smaller the optimizer forecast errors, but with a higher computational cost.

Furthermore, one can choose the quality of prediction for each of the microgrid components. When using the forecast called "Perfect", the consumption curves and planned generation coincide exactly with the actual values. For this prediction model, the optimizer ensures that its solution is in fact optimum, and is the minimum cost to operate the microgrid. In the forecasting model called "Persistence", the manager considers that the levels of consumption and instantaneous generation will be maintained throughout the prediction horizon. For the forecasting called "Random Error " ensures that the predicted values are within a normal distribution around the real value. Finally, the "Average Value" prediction considers that the generation level will be constant throughout the period, maintaining the average of the past values.

Some of the simulator input parameters are defined as a time series of values. This is the case of real curves of renewable resources and consumption, kWh price over time or availability of the network.

4. SIMULATION RESULTS

To evaluate the different dispatch strategies, a microgrid was simulated using different approaches over a period of 30 days, considering only the static simulation. The simulated microgrid had the same components in all cases, varying only the dispatch strategy used for the energy manager and the forecast methods for demand and renewable generation.

The scenario modeled in the tests consisted of the following electrical components: a gas microturbine, a set of photovoltaic panels, a wind farm, a battery system and a load profile representing the demand to be met. The model does not consider a connection to an external power grid, so that the microgrid operates

"islanded". The load to be met is represented by a commercial load profile, designed to consume about 20 kW at peak times.
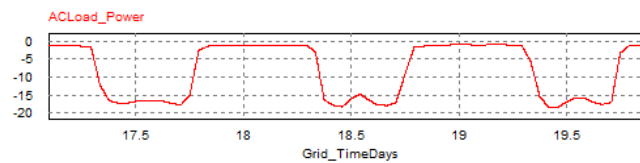

Figure 113 - Demand power profile

Solar panels were chosen such that they could provide the load when in peak power generation. For this, it was considered a set of 80 240Wp-rated panels, totaling an installed potential of 19.2 kW.
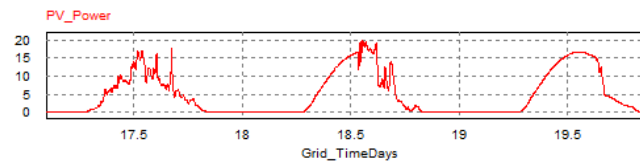

Figure 114 - Photovoltaic power profile

The wind farm has been designed in a similar way to the panels, equating its maximum generation with maximum demand consumption. Thus, it was considered a set of 9 2400W wind turbines, a total of 21.6 kW installed. The wind profile was obtained from nearby locations to the site of the pilot microgrid of this project.
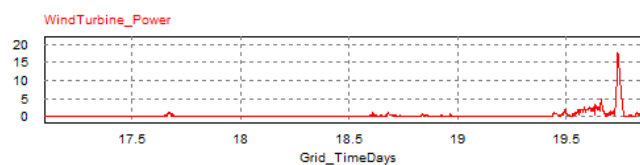

Figure 115 - Wind turbine power profile

The microturbine was included in order to meet demand when there is not enough renewable generation. A maximum power of 10 kW, about half the consumption in peak demand, was defined for the microturbine. Therefore, it had not enough power to keep the load at peak consumption and had to be used together with renewable generation and energy stored in the battery to ensure the balance between generation and demand. To account for the costs of microturbine, fuel consumption curves and start-up/shutdown profiles were considered from commercial models, with fuel prices from local suppliers.

The battery storage system exerts a strong influence over the operation. In the case of a very large battery bank, any fluctuation in renewable generation is absorbed by the battery and the operation of the microgrid becomes trivial. On the other hand, If the capacity is too low, there is little slack to operate and its influence is greatly undermined. The selected capacity was 80 kWh, sufficient to maintain the load at maximum power for about 4 hours. Its initial capacity was defined as 50% of total capacity.

Table 3: Final set of indicators suggested for measuring the urban infrastructure systems sustainability of the Middle Eastern cities

Water Systems Indicators	Wastewater Indicators	Transportation indicators	Energy Indicators
Water intake by municipal services	Population served by Sewage system	Expenditure on roads, parking, public transit, ports, etc.	Service/commercial energy strengths
Borne diseases through the water	Municipal revenues, from wastewater management	Per capita congestion	Domestic energy intensities
Connections of water and sewer	Municipal costs of wastewater management	Proportion of portion of trips by non-motorized modes	Agricultural energy strengths
The possibility of affected of Groundwater	Population served by wastewater treatment plants	Crash deaths and injuries	End-use energy costs by fuel and by sector
Population served by water supply systems	Expenditure per 1000 inhabitants on wastewater management	Quality of walking, cycling, public transit, driving, taxi, etc./	External prices of energy use

Total water intake	Rate of Wastewater produced	Quality of accessibility for people with disabilities	Efficiency of energy transformation and supply
Total water treated	Rate of wastewater treatment	Land devoted to transport facilities	Domestic energy use for each income group and equivalent fuel mix
Total public water consumption	Wastewater treatment in wastewater treatment plant	Total vehicle emissions	Joined heat and power generation
Water losses		Proportion of emissions from facility construction	Annual energy consumption, total and by main user group
Leakage of water		Economic costs of traffic collisions	Reserves-to-manufacture ratio
		Proportion of people exposed to traffic noise	Industrialized energy intensities
		Affordable housing accessibility	Transport energy strengths
		Using a method of investment in transport infrastructure	Fuel shares in energy and power
		Modal divided of passenger transport	Renewable energy share in energy and power
			Net energy import need
			Pollutant discharges in liquid effluents from energy systems
			Ratio of solid waste generation of units of energy produced
			Air pollutant emissions from energy systems
			Reserves-to-manufacture ratio

resumes the components used for the simulation.

Table 63: Sizing of the simulated energy resources

Component	Capacity
Demand	20 kW
Gas Microturbine	10 kW
Photovoltaic Modules	19,2 kW
Wind Turbines	21,6 kW
Battery storage system	80 kWh

This scenario was used to compare the optimum cost strategy against cyclic-charging strategy.

The optimum cost strategy uses a power generation and consumption forecast for each non-dispatchable component over a period of time, called the prediction horizon. This data is then fed into the optimizer that calculates the power set point for the dispatchable components operating in the microgrid at the lowest possible cost, ensuring the follow-up of the technical restrictions of the components and the desired behavior constraints. This technique assures us a minimal cost of operation over the entire horizon prediction considering that the forecast for non-dispatchable components is correct.

Considering the difficulty of having an accurate prediction, especially for the components that depend on the availability of natural resources, the same strategy was tested using a more realistic forecast. Three different prediction methods were used. For the load, random errors were defined over the actual profile with a standard deviation of 5% of the demand. For the wind profile, each point on the horizon is considered constant throughout the forecast period, assuming the average value of wind speed over the last 60 minutes. Finally, the solar power generation is provided according to a profile based on the maximum solar irradiation. This profile is rescaled according to the level of solar irradiation on the calculated moment, so it is considered that the percentage reduction relative to the maximum level of irradiation will remain constant over the horizon of prediction.

As the scenario involved a strong contribution of renewable generation sources and the battery was not large enough, there was excess energy at various times throughout the month. It is important that the

dispatch strategy is able to manage the battery to absorb the greatest amount of energy possible, avoiding having to operate dispatchable sources at times of high demand.

Using the cyclic-charging strategy, the microgrid experienced two moments where there was a power shortage during the month. As the microturbine did not have enough power to meet demand, a good battery charge management was necessary to avoid such contingency scenarios. One of the moments where the battery was fully discharged and there was not enough energy for the loads is depicted in Figure 116.
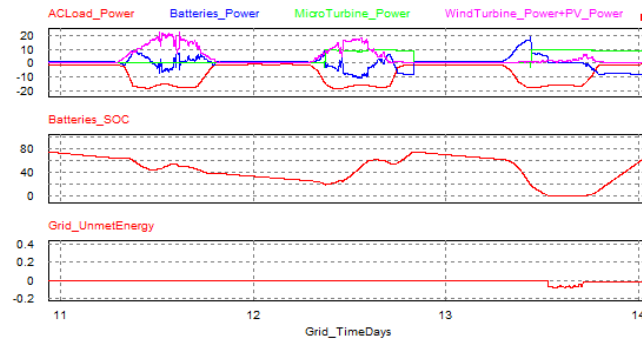

Figure 116 - Operation with cyclic-charging strategy

In the case of optimized dispatch, as the prediction horizon was 24 hours, the manager was able to predict power outages well in advance and the microturbine was started before to charge the battery. Thus, the battery was able to operate in conjunction with the microturbine during the peak period and there was no lack of energy, as shown in Figure 117.
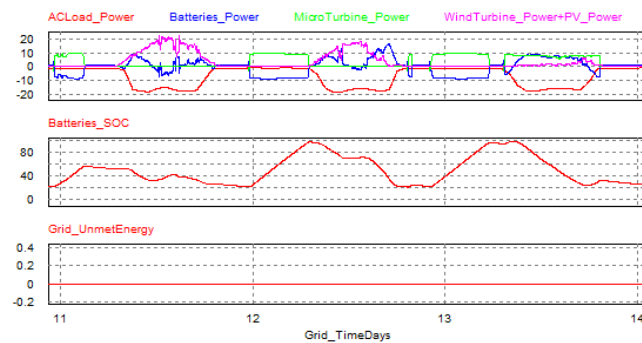
Figure 117 - Operating with optimizer using perfect forecast
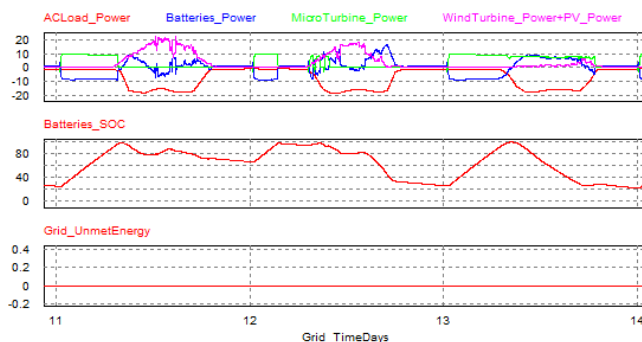
Figure 118 - Operation with optimizer considering forecast errors

Figure 118 shows the operation of the microgrid during the same period, including the prediction errors on the horizon optimizer.

At the end of operation, the cyclic-charging strategy had an energy shortage of about 34 kWh. The strategy of optimum cost, even with forecast errors, avoided these moments of contingency. In the case of perfect forecast, there was a noticeable reduction in the surplus power, which was better used by the battery.

As the energy shortage cost was not included, there was an increase in operating costs of the microgrid with the optimal dispatch strategy because the microturbine was used more often and for longer periods of time to avoid running out of energy. Still, the better usage of energy provided from renewable sources could reduce costs in such way that the optimizer with perfect forecast was able to meet demand continuously and still cost less than the cyclic-charging strategy. In contrast, in the case without perfect forecast, the errors led to additional spending so that the total cost was above that of the cyclic-charging strategy.

Figure 119 shows the aforementioned results. The total amount of excess energy (when the power generation is higher than the load demands) and the total amount of energy deficit (when there is not enough energy to supply the demand) can be observed from the entire simulation period.
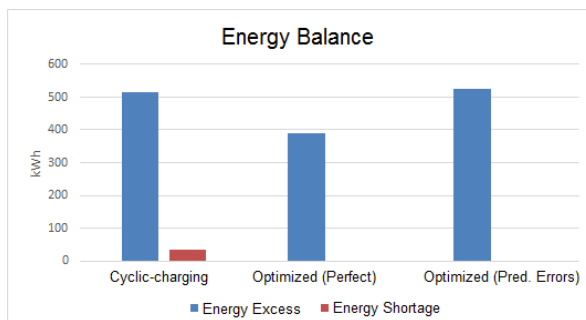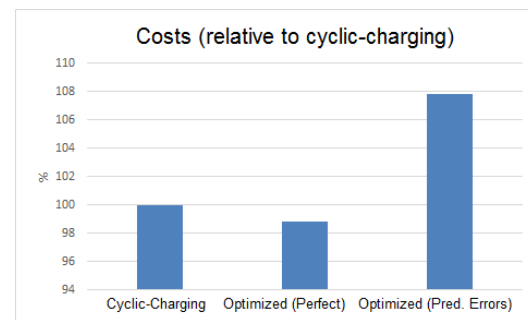

Figure 119 - Energy balance comparison

Figure 120 - Costs comparison

5. CONCLUSIONS

In this paper, it was presented the development of an energy manager for smart microgrids, applied to a pilot microgrid which is currently being implemented in Brazil. The document presented the problem of energy management in its fundamental aspects, a description of adopted mathematical models and optimization strategies made and implemented in the project.

It was also presented a simulation platform for microgrids, which is actually the implementation of GE's design, ready to be integrated into the physical system once it is installed.

With the results of static and dynamic simulations from the developed tools, the benefits of an intelligent optimization system for the management of the microgrid energy resources were demonstrated. The strategy adopted makes the operation of a microgrid with energy management more advantageous from an economic point of view and from an energy availability standpoint. Based on the models considered in the project, the results show that the energy manager really stands out when the microgrid is operating in islanded mode. However, even when in connected mode, the implementation of an energy management allows microgrid to be designed with a more convenient initial cost, because the power sources can be used to their full extent.

6. REFERENCES

R. H. LASSETER, 2002, "MicroGrids," in *Power Engineering Society Winter Meeting, 2002. IEEE*, pp. 305-308 vol.1.

J. A. PEÇAS LOPES, C. L. Moreira, and A. G. Madureira, 2006, "Defining control strategies for MicroGrids islanded operation," *Power Systems, IEEE Transactions on,* vol. 21, pp. 916-924.

N. HATZIARGYRIOU, H. Asano, R. Iravani, and C. Marnay, 2007, "Microgrids," *Power and Energy Magazine, IEEE,* vol. 5, pp. 78-94.

DoE, 2012, " Summary Report: 2012 DOE Microgrid Workshop DOE EERE, ," Department of Energy - Office of Electricity Delivery and Energy Reliability Smart Grid R&D Program, Chicago, EUA.

H. MORAIS, P. Kádár, P. Faria, Z. A. Vale, e H. M. Khodr, 2010, "Optimal scheduling of a renewable micro-grid in an isolated load area using mixed-integer linear programming", Renewable Energy, vol. 35, no. 1, p. 151-156, jan.

X. LIU, 2010, "Economic Load Dispatch Constrained by Wind Power Availability: A Wait-and-See Approach", IEEE Transactions on Smart Grid, vol. 1, no. 3, p. 347 -355, dez.

M. D. HOPKINS, A. Pahwa, e T. Easton, 2012, "Intelligent Dispatch for Distributed Renewable Resources", IEEE Transactions on Smart Grid, vol. 3, no. 2, p. 1047 -1054, jun.

H. M. KHODR, N. El Halabi, e M. García-Gracia, 2012, "Intelligent renewable microgrid scheduling controlled by a virtual power producer: A laboratory experience", Renewable Energy, vol. 48, no. 0, p. 269-275, dez.

F. A. MOHAMED e H. N. Koivo, 2012, "Multiobjective optimization using Mesh Adaptive Direct Search for power dispatch problem of microgrid", International Journal of Electrical Power & Energy Systems, vol. 42, no. 1, p. 728-735, nov.

C. X. GUO, Y. H. Bai, X. Zheng, J. P. Zhan, e Q. H. Wu, 2012, "Optimal generation dispatch with renewable energy embedded using multiple objectives", International Journal of Electrical Power & Energy Systems, vol. 42, no. 1, p. 440-447, nov.

T. GOYA, T. Senjyu, A. Yona, N. Urasaki, e T. Funabashi, 2012, "Optimal operation of thermal unit in smart grid considering transmission constraint", International Journal of Electrical Power & Energy Systems, vol. 40, no. 1, p. 21-28, set.

A. TAKEUCHI, T. Hayashi, Y. Nozaki, e T. Shimakage, 2012, "Optimal Scheduling Using Metaheuristics for Energy Networks", IEEE Transactions on Smart Grid, vol. 3, no. 2, p. 968 -974, jun.

S. X. CHEN, H. B. Gooi, e M. Q. Wang, 2012, "Sizing of Energy Storage for Microgrids", Smart Grid, IEEE Transactions on, vol. 3, no. 1, p. 142-151.

118: Role of electric vehicles in PV self-consumption optimisation

Dainius ALONDERIS[1], Mark GILLOTT, Rabah BOUKHANOUF

Department of Architecture and Built Environment, Faculty of Engineering, University of Nottingham,
1Corresponding author - ezxda3@nottingham.ac.uk

One of the problems with increasing photovoltaic (PV) penetration is related to the fact that the actual generation profiles usually do not match the energy demand of a typical domestic house. There are a number of different ways which can be used to bridge this energy gap including demand side management (DSM) and energy storage techniques, allowing manipulation of energy consumption and distribution within households. This paper analyses an alternative way for increasing self-consumption of distributed energy in a zero carbon house serving as an office for research staff at the University of Nottingham. The initial focus of the work looks at electric vehicle (EV) as alternative energy storage or consumption solution for excess electricity generated from an onsite PV system.

The energy distribution within the office as well as EV charging profiles were obtained and evaluated using a state-of-the art wireless control and monitoring platform. One year data of PV exported electricity was compared to the average diurnal office energy demand. Any excess PV export then was evaluated against different EV charging approaches in order to find and relate, if any, self-consumption benefits of localised PV generation. Thus, the actual observed PV generation and EV charging profiles with controlled and uncontrolled EV charging strategies were analysed to find any possible reduction in exported electricity, increasing PV power utilisation onsite. The results show that the smart EV charging methods can increase self-consumption of electricity generated from PVs as well as may moderate the likely rise in peak energy demand associated with increasing EV penetration in the domestic built environment. In addition, results were shown that the energy demand and costs associated with charging EV batteries could be reduced when utilising PV export output.

Keywords: Building control and monitoring system; Distributed generation; Load matching ; Electric vehicles

1. INTRODUCTION

Photovoltaic, PV cumulative capacity is increasing at roughly 25% annually in the UK, according to the statistics provided by Department of Energy & Climate Change (DECC, 2014). The deployment of PV systems is partially supported by the financial incentives such as Feed-in Tariffs (FITs) introduced in 2010 in the UK. The main purpose of this scheme is to support financial returns and, thus encourage uptake of investments in a renewable energy technologies. This is achieved by being paid for each kWh that is generated and exported back to the grid, depending on the installation size and renewable energy technology. Currently, the tariffs stand at approximately 12p/kWh and 4.85p/kWh for domestic scale PV generation and export respectively (OFGEM, 2015). However, the electricity FITs for PV export is currently lower than the actual electricity price in the UK (14p/kWh) which is projected to reach 20p/kWh by 2020 according to the most recent statistics provided by the UK government (DECC, 2014). Exporting any excess energy hence means losing the highest potential economic benefits of a PV system. In addition, since FITs were first introduced as an incentive to promote distribution of renewable energy technologies, it is likely to be omitted in future due to substantially increased PV penetration levels (WARREN, 2014: pp.941-951). Maximising utilisation of onsite PV power output generated, thus may increase financial returns and reduce/offset future financial uncertainties.

The total generated electricity is not always consumed on-site and may be exported to the grid. This is mainly related to the fact that the peak PV output occurs during midday whereas domestic building energy demand is highest during early morning and late evening hours as illustrated in Figure 1. If a substantial amount of PV generation output is not utilised onsite and is rather exported to the gird, it can cause grid stability and management problems requiring additional investments in upgrading the power grid infrastructure (ALI et al. 2012). Recently the self-consumption levy of onsite PV generation has been introduced in Germany for systems of up to 10 kWe capacity to tackle rising concerns of high PV deployment in residential sector (EEG, 2014). Thus, financial incentives are also being introduced nationally to encourage utilisation of distributed generation at the point of production.
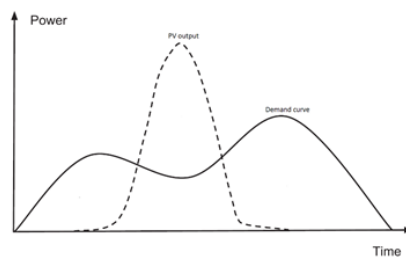

Figure 121: Typical domestic energy demand and PV generation profiles

Deviation between peak energy generation and demand can be minimised by applying energy storage as a solution to shift any excess PV generation for later use (CASTILLO-CAGIGAL et al. 2011: pp.2338-2348). However, the batteries are not always installed together with a PV system due to the high extra expenditures involved. In such case energy demand side management strategies could be employed to better manage energy distribution within the building and were found to be effective in certain research cases (SHARMA and GALIPEAU, 2012),(MATALLANAS et al. 2012: pp.90-97). This can be achieved by means of using smart control and monitoring system that can utilise onsite distributed generation by redirecting electricity output from PV to specific areas where it can be used locally. One of such example would be turning high energy demand appliances such as washing machine, dishwasher or tumbler drier on when there is excess energy being generated on-site. The alternative and still less popular way could be achieved by employing electric vehicles, EVs as the energy storage solution where there is any excess PV generation available on site (ESA, 2015), (SCHULLER and HOEFFER, 2014: pp.32-39). Although a number researches have been done in order to evaluate impact of EVs on the power and localised power grids, not much research were found involving actual EVa in testing various energy charging and storage strategies next to the system/charging point comprising of distributed generation.

The popularity of EVs has been rising recently with increasing number of ultra-low emission vehicles being registered each year according to the statistics provided by the Office for Low Emission Vehicles (OLEV) in the UK (OLEV, 2015). For instance, between year 2013 and 2015 approximately 30000 new EVs had been bought in the UK, while only around 5000 were driven on roads back in 2013 (LANE, 2015). Let alone in the first quarter of 2015 more than 9 thousand electric cars were registered in the UK. Thus, the increasing penetration of EVs is to continue according to the recent statistics and is being supported by the

national incentives such as grants that can reach up to 35% off the cost of a car (limited up to 5000£) when purchasing your first EV (OLEV, 2015). However, in recent research, a possible high deployment of EVs in the UK was estimated to increase the stress on the power grid (MUNKHAMMAR et al. 2015: pp.439-448). The key findings were mainly constructed on assumption that most of EVs are going to be charged at household when people come back from work and plug-in vehicles, adding up to the total energy supply requirements. It is argued that the main problems associated with high penetration of EVs can be reduced with an introduction of smart-optimised charging methods that exploit locally generated electricity from PVs (FATTORI et al. 2014: pp.438-451). Since EV charging and PV generation cycles may not overlap, the associated problems could be minimised by charging EVs at work next to the office building with excess PV generation where available (RICHARDSON, 2013: pp.247-254). This would reduce the peak energy demand associated with charging EVs at home before and/or after the work as well as increase self-consumption rate of distributed generation.

Therefore, the purpose of this research is to analyse EV as an alternative energy storage solution which can be used to increase self-consumption of distributed generation and reduce the grid stress from increasing energy demand when charging EVs. A fully instrumented office facility with on-site PV generation and an actual EV was used to test various smart control strategies in order to analyse merits and any disadvantages of utilising and managing excess renewable energy for EV charging purposes.

6 METHODOLIGY

The research has been performed on the data obtained from the tests involving an actual EV and fully instrumented office house with onsite PV generation. Various controlled and uncontrolled EV charging strategies were introduced and analysed to find any advantages and disadvantages on PV self-consumption and building energy performance in general. The detailed descriptions of the research facilities and approach are given below.

2.1 Electric vehicle

This study is focused on using EV provided by CENEX (the Low Carbon and Fuel Cells Centre of Excellence) for 3 months duration. EV tested is a small two seated car (Smart) supplied with a 16.5 kWh lithium-ion battery storage. The average typical range was found and suggested to be around 110 km (CARROLL, 2012: pp.113-122). According to the charging data, EV takes a constant 2.95 kW power supply and requires approximately 8 hours charging to reach its maximum state of charge, SOC from 0% SOC. A picture of an EV at its charging station installed next to the office building can be seen in Figure 2.
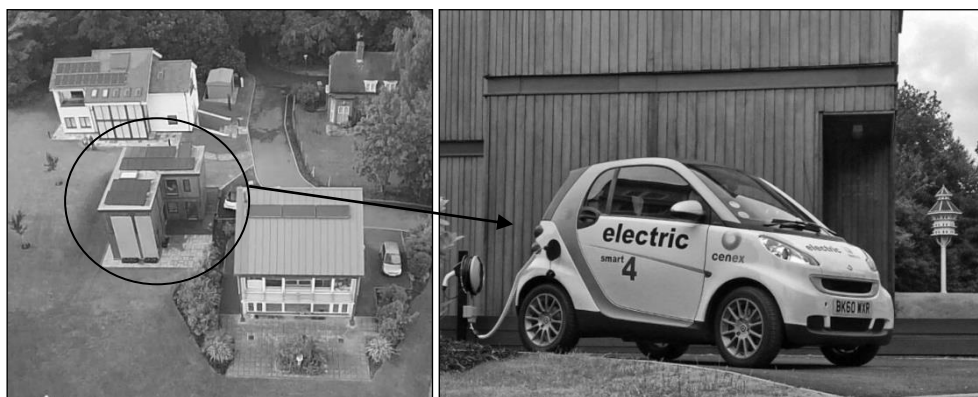
Figure 122: EV parked next to the office and its charging station

2.2 Nottingham H.O.U.S.E

EV and associated specialised charging strategies were tested in the Saint Gobain Nottingham H.O.U.S.E – House Optimising Use of Solar Energy - located at the University of Nottingham. A low energy house has been built as part of Creative Energy Homes (CEH) smart community project. It is equipped with PV system rated at 3.24 kWp. There was no static battery storage system available at the time of research. Most of energy demand in the house is associated with using office equipment during typical working hours between 9am and 6pm. These mainly include: lighting circuits and 3 individual PCs. The building is not supplied with

any active or power intensive heating nor cooling system and only during cold winter days immersion heaters were turned on to heat the office. There is also a kitchen with fridge, kettle and other necessities, since the house was first designed and built as a domestic house. However, the house currently serves as an office for 3 research staff members at the university. The occupancy, total and individual energy demand profiles of the office were defined and taken into the account when analysing various scenarios of using EV as part for optimising energy distribution within the building as well as looking at potential of charging EV on-site with any excess solar energy output from the PV system.

2.3 H.O.U.S.E Control and monitoring platform

The office building is instrumented with state-of-the-art wireless and low energy control and monitoring system that uses Enocean communication protocol (868.3 MHz) to communicate between the different devices. The monitoring side is focused on measuring the total, individual power and energy consumption, temperatures, generated and exported electricity from the PV system. The office is also equipped with controllers for individual loads and circuits to facilitate full control of electricity distribution. Majority of the sensors were provided by Eltako GmbH, a German company that specialises in low energy wireless Enocean monitoring and control equipment manufacturing and distribution (ELTAKO, 2015). The Eltako equipment installed in the building provided inaccuracy in range of 10% or less for monitoring purposes. A universal controller from CAN2GO™, currently known as Multi-Purpose Manager (MPN-UN) and sold by Schneider Electric SE, was used as the main information gateway for communication between control and monitoring devices (SCHNEIDER-ELECTRIC, 2015). The power measuring device with integrated relay functionality (FSR70W-16A) was installed to measure and control the power supply of the EV charging station. During the research only the control over charging EV was assumed to take place.

2.4 Energy balance and control strategies / research approach

Since the house was used as an office, the energy demand patterns were produced using the data obtained from the individual power sensors and import, export and generation energy meters. One year historic data, spanning from April 2014 to April 2015, were obtained for PV generation. The energy demands within the office was evaluated and averaged based on the actual observed historical data variations. Based on the generation and energy demand profiles, any potential PV output was evaluated on daily and hourly basis for hours between 9 am and 6 pm. This information was selected as an input to the self-consumption optimisation models in order to find the benefits, if any, of using EV as energy storage solution for any excess PV generation output. In addition, overall energy performance of an office building was investigated for various controlled and uncontrolled EV charging scenarios.

EV charging profiles were observed by control and monitoring platform installed in the office with dedicated charging station. The rate of change in state-of-charge, SOC (%) against time and energy input was derived as a function to simplify the analysis when evaluating EV role in PV self-consumption optimisation and its overall effects on energy demand and distribution within the building.

The analysis has been performed in two parts. These were defined as controller and uncontrolled EV charging scenarios. Uncontrolled charging meaning that EV is plugged in and charged during office working hours without any prior control scheduling done to optimise charging and self-consumption of PV electricity generated onsite. Controversially, controlled charging strategies were implemented to test scenarios when charging is managed according to the amount of available excess energy from PV generation.

I.   *Uncontrolled charging*

Uncontrolled charging was applied to evaluate building energy performance when EV is plugged-in and charged continuously at its power rating throughout the working day (9am to 6pm). Yearly, monthly and daily charging performance, in terms of the imported electricity both from the grid and PV system, was analysed respectively to find any potential of utilising PV export onsite.

II.   *Controlled charging*

Controlled charging strategies were selected thus that they enabled dynamic charging approaches to be modelled. The data fed into the calculations mainly consisted of historical PV generation, energy demand and EV charging profiles. Controller charging strategies were divided into two parts: (1) EV charging with total daily PV export under net metering consideration (2) real time EV charging with PV export. The initial

controlled charging approach was introduced to work under the net metering case. Net metering means that any PV export can be imported back from the grid at any time and with no extra costs. In this particular situation the charging was only allowed to be performed using the total energy that is available from the PV system on a daily basis. Charging time in hours was then found and suggested using the derived SOC function that takes into account the total energy that could be fed into the batteries and outputs time for which charging can be carried out. Lastly, an ideal case controlled charging situation was analysed, where EV charging was assumed to be dynamic and to follow the real time PV electricity export. Since, PV export data were shown to vary, the potential EV charging outcomes, such as changes in SOC and total annual and daily energy utilisation factors were evaluated. The results were then used to judge if charging EV at the office by PV export can sufficiently provide battery recharging for daily commuting compared to the statistic of average daily mileage driven in the UK.

Finally, an economic analysis was performed for both controlled and uncontrolled scenarios to evaluate any financial benefits and returns of charging EV at office with PV system rather than directly from the grid. The calculations were performed using the total PV export energy that could supplied for charging EV batteries. Current average electricity tariffs and export FITs were taken into account when evaluating and comparing costs and saving for charging EV from the grid and PV system respectively. In addition, percentage cost reduction was calculated to compare the total costs when charging EV with and without PV contribution.

7   RESULTS

3.1 H.O.U.S.E energy profiles

The office was found to consume 2.1 kWh of energy daily when unoccupied. During working hours, the additional load consumption from the equipment and lighting was observed to bring the total daily energy demand to around 4.1 kWh and 7.5 kWh respectively. The power consumption from individual loads can be seen in Figure 3. Figure 3 (a) shows actual observed power changes whereas Figure 4 (b) represents cumulative averaged power consumption of a typical working day in the office. Power consumption for immersion heaters were not considered here, since the heating was required during cold months with no usable PV export (more details to follow below).
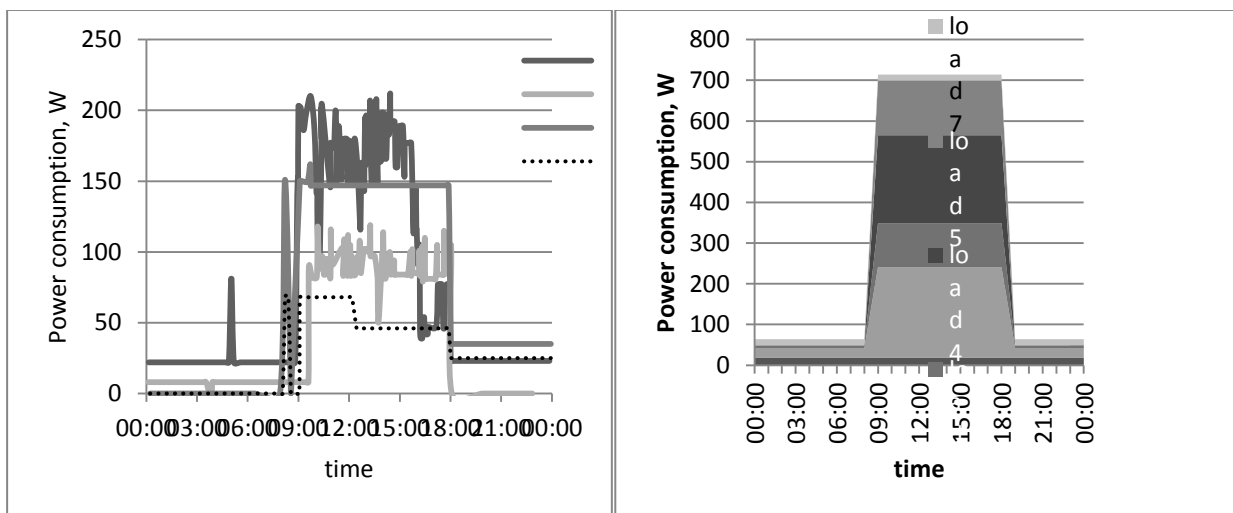
Figure 123 : Power consumption profiles a) real time b) cumulative. Where, load1 - entrance sockets; load2 – first floor sockets; load3 – ground floor sockets; load4 – ground floor lighting; load5 – first floor lighting; load7 – kitchen sockets

The daily PV energy generation from 9am to 6pm and for period between April 10th, 2014 and April 10th, 2015 can be seen in Figure 4. Two cases were considered for energy consumption for hours between 9 am and 6 pm: (a) worst case scenario with lighting on (E1), averaging to 6638Wh, (b) base case scenario – energy consumption without lighting on (E2), averaging to 3238Wh. The daily PV export potential after deducing energy demand in the office can be seen in Figure 5.
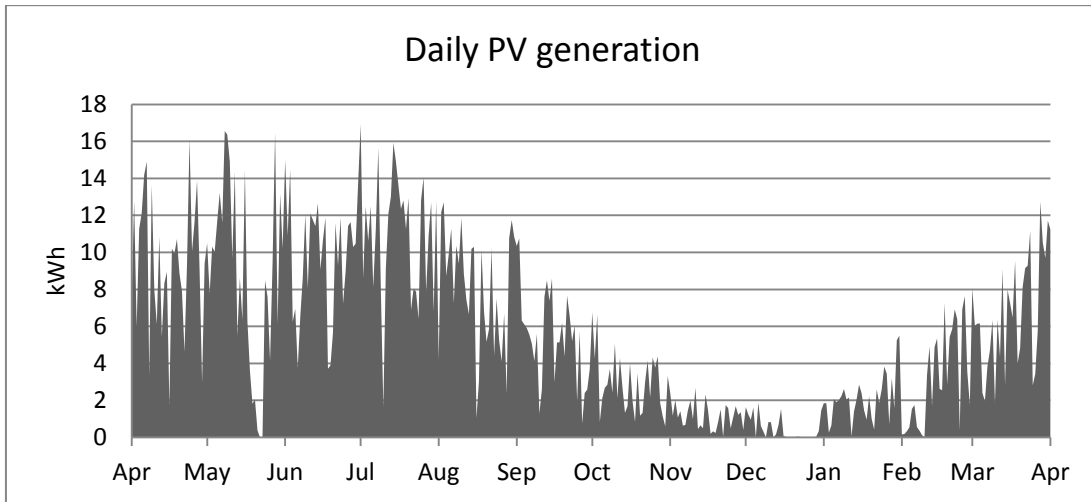
Figure 124: Historical daily PV generation data
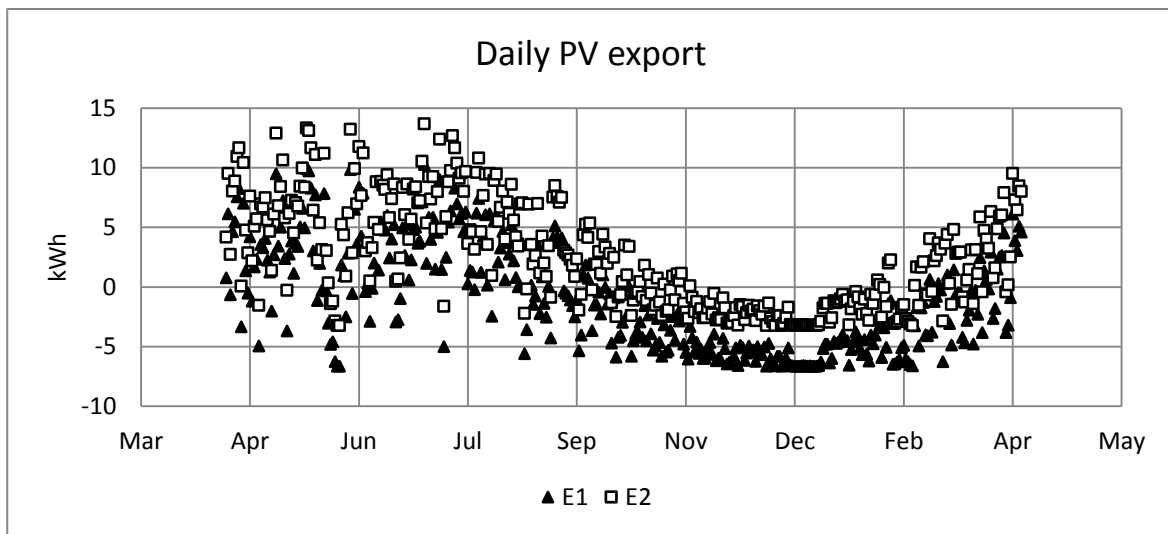
Figure 125: Daily PV export potential

From the graphs above, it can be seen that the PV export is highest and focused between months spanning from April to September. Therefore, the highest suitability for charging EV was assumed to be around these months when evaluating any benefits of utilising PV export that is available onsite.

3.2 EV charging profile, SOC(t) & SOC(E$_t$)

Based on the complete EV charging profile obtained through charging EV batteries from 0% to 100% SOC, change in state of charge, ΔSOC was derived as a function of time, ΔSOC(t) and total energy input, ΔSOC(E) as shown in Equation 1 and Equation 2 respectively.

Equation 21: ΔSOC as a function of time.

$$\Delta SOC(t) = 12.11 \times t - 0.1166$$

Equation 2: ΔSOC as function of energy input.

$$\Delta SOC(E_t) = 4.105 \times E_t - 0.1166$$

Where:

- t = time in hours (hr)
- E$_t$ = total energy input (kWh)
- ΔSOC(t) = change in state of charge over time, t (%)
- ΔSOC(E$_t$) = change in state of charge for energy input, E$_t$ (%)

3.3 Uncontrolled charging results

The results from uncontrolled charging approach are presented in Table1. A distribution of total percentage contributions from daily PV export towards EV charging needs (%PV) were found for each day 9 am to 6 pm as presented in Figure 6. Both worst case (E_1) and best case (E_2) energy consumption profiles were evaluated towards self-consumptions of PV export. Evaluations were performed against the total energy required to charge EV (E_{EV}) for duration of car parked next to the office building. Thus, daily $E_{EV} = 2.95W * 9hrs = 26.55$ kWh.

Table 64: Results from uncontrolled charging analysis

	E_1 at 6638 Wh demand	E_2 at 3238 Wh demand
Max %PV	39 %	52 %
Min %PV	0 %	0 %
Mean %PV	7 %	14 %
Max E_{im}	26550 Wh	26550 Wh
Min E_{im}	16273 Wh	12873Wh
Mean E_{im}	24738 Wh	22860 Wh
Total EV import	10118 kWh	9350 kWh
Average EV grid import	24738 Wh	22860 Wh
Total PV export	746 kWh	1372 kWh

Where:

- E_{im} – imported electricity from the grid, Wh
- %PV – PV percentage share in charging EV baterries, %
- E_1 and E_2 – average daily office biulding energy demand, Wh
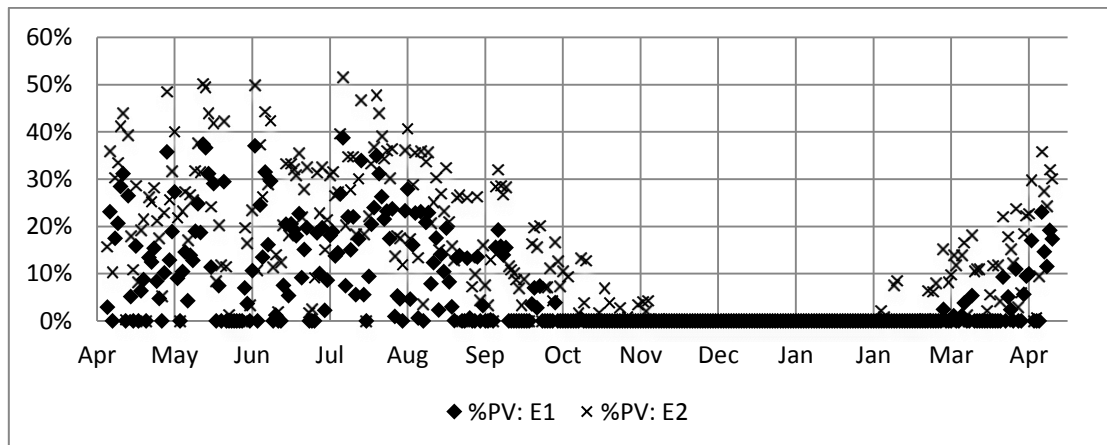
Figure 126: PV percentage contribution towards charging of EV

3.4 Controlled charging results

Differently to uncontrolled charging, controlled charging was evaluated focusing on the direct PV export potential in charging EV. Only days with any PV export were considered and included in the calculations. Daily PV export data were fed into the Equation 2 to find ΔSOC or how much EV batteries can be charged when utilizing PV export from the PV system. The results for daily achievable ΔSOC are shown in Figure 7. Two different cases were presented and evaluated for energy demand that could be present in the office building namely E1 and E2. E1 and E2 representing 6638Wh and 3238Wh office building energy demand respectively.
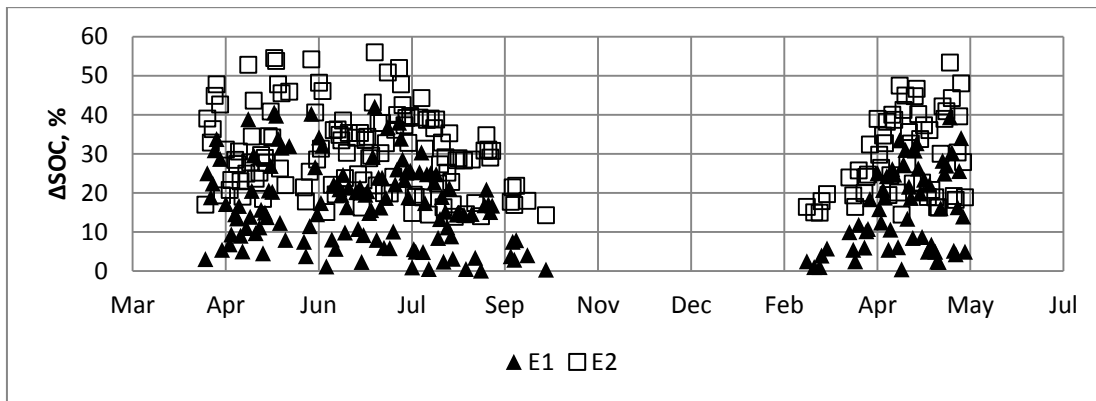
Figure 127: PV export contribution towards ΔSOC

Tabulated results from controlled charging investigation can be seen in Table 2. Maximum, minimum and average ΔSOC were calculated and included in the findings. In addition, Table 2 consists of the distance results (km) that were calculated using ΔSOC data, based on the assumption that the range of EV could be linked to its battery SOC linearly. I.e. 110km can be driven with fully charged batteries at 100% SOC.

Table 65: Results from controller charging analysis

|	E$_1$ at 6638 Wh demand	E$_2$ at 3238 Wh demand
Max ΔSOC	42 %	56 %
Min ΔSOC	0 %	14 %
Mean ΔSOC	17 %	30 %
Max range	46 km	62 km
Min range	0 km	15 km
Mean range	18 km	34 km
Annual accumualtive SOC	3063 %	5631 %
Annual drivable range	3370 km	6195 km

3.5 Economical comparison between controlled and uncontrolled charging scenarios

Finally, an economic analysis was done to find any potential in gaining financial returns when charging EV partially or entirely by PV export that is available on-site. Majority of the results were evaluated for the uncontrolled charging situation, since it involved additional cost considerations associated with total or supplementary import requirements from the grid. The financial benefits for controlled charging are presented in terms of savings made when charging EV entirely with electricity supplied from the PV system. The economic results are presented in Table 3 below.

Table 66: Results obtained from the economic analysis

	E$_1$ at 6638 Wh demand	E$_2$ at 3238 Wh demand
Total required EV import, kWh	6850 *(March to September)*	
Energy supplied from PV, kWh	746	1372
Total initial costs for charging EV via grid import*, £	923	892
Savings from PV export utilisation, £	104	192
Savings, %	11.3	22.5
Savings from PV export utilisation*, £	68	126
Savings*, %	7.4	14.1

Taking into account (1) money that is received for any PV export at 0.0485£ FIT, (2) electricity import tariff of 0.14£

8 DISCUSSION AND CONCLUSION

From the PV export data it can be seen that the potential of charging EV with excess solar generation is only valid during month from April to early September. The maximum potential in self-consuming PV generation thus can only be achieved within this period. Evaluation of uncontrolled charging strategy has shown that, even though the worst case scenario was applied to charge EV canorously from 9am to 6pm, on average 10% reduction could be achieved in total electricity import required. When there are enough solar gains available, this value can peak at 52% which is a substantial reduction in energy needed to fully charge EV. As seen in Figure 6, the highest PV contribution towards charging EV was achieved in summer and thus should be prioritised when focusing on EV charging optimisation through renewable energy sources. However, since uncontrolled charging scenario assumed all working day charging that could bring EV batteries from 0% to 100% SOC, a more realistic situation would be where charging is only done for a limited time depending on initial on-come-to-work EV SOC. In such case, limited duration charging would occur and could be prioritised or scheduled to be turned on around mid-day where there is highs PV generation potential.

The main problem with uncontrolled charging arises due to the fact that the charging takes a constant 2.95 kW power inputs requiring additional electricity import form the grid. Only small amount of PV generation was available compared to the total energy requirements of 26.6 kWh of charging between 9am to 6pm. In order to evaluate the direct benefits of charging EV by PV export, controlled charging scenarios were introduced and analysed assuming that only the output from the PV system contributed to the EV charging. In this way, a potential in achievable ΔSOC and drivable range could be evaluated to check if PV output is enough to support minimum daily charging needs.

According to the net metering situation, or case when EV is only charged with energy generated daily, it can be seen that the batteries could be charged on average to17% and 30% of its capacity depending on the energy demand within the office building. The maximum achievable ΔSOC was shown to reach around 42% or 56% and nearly to or half of the battery capacity could be charged directly from the PV system. ΔSOC results were then applied to calculate average drivable distance. It has been found that the mean achievable EV range could spans from 18km to 34km depending on the building energy demand. These measures were found competitive, since according to the UK transport statistics, average UK daily commuting distance stands at 14.1 km (DfT, 2014). In addition, annual EV range that could be driven using the energy supplied from PV export was found comparable to the average annual distance driven of 5200 km (2050 km for commuting trips) within the UK (DfT, 2014). However, since the PV output is low and not sufficient during winter or when there is low solar irradiance, the EV batteries would need to be charged from the grid, and driving EV on PV energy entirely would not be achievable even though the suggested average achievable range from PV export is close to the national transport statistics.

From the results obtained after economic analysis, it can be seen that the costs associated with charging EV from the national grid could be reduced from 7.4% to 14.1% or approximately 80£ annually when charged partially by the PV system. This is not significant cost reduction since the uncontrolled charging required additional import from the grid whereas the PV generation contribution towards EV charging is only considerably higher during summer months. Nevertheless, charging EV at the office rather than at home on peak energy demand times could reduce the power grid stress and generate some of the financial returns, while increasing self-consumption of distributed generation.

In conclusion, the uncontrolled and controlled EV charging strategies were investigated and analysed using the energy data obtained from the office building with onsite renewable electricity generation and observed EV charging profiles. It has been shown that charging EV at work can maximise PV self-consumption while reducing the total energy needs as well as can be used to achieve a sustainable batteries recharging during months with PV export available. Further analysis should focus on the actual algorithms implementation for smart charging in order to test EV charging strategies under actual and controlled charging scenarios. This could be achieved by employing dynamic control and monitoring platform able to define and perform optimised charging schedules. In addition, since the analysis focused on historically observed or approximated data, an approach involving real time data and PV predictions could be tested to verify autonomy of smart EV charging controller systems.

9 REFERENCES

Ali, S., Pearsall, N. and Putrus, G. (2012). Impact of High Penetration Level of Grid-Connected Photovoltaic Systems on the UK Low Voltage Distribution Network. In: *International Conference on Renewable Energies and Power Quality (ICREPQ'12)*. [online] ICREPQ. Available at: http://www.icrepq.com/icrepq%2712/368-ali.pdf [Accessed 5 Jun. 2015].

Carroll, S. et al. (2012). Electric vehicle efficiency mapping. *Sustainable Vehicle Technologies*, pp.113-122.

Castillo-Cagigal, M. et al. (2011). PV self-consumption optimization with storage and Active DSM for the residential sector. Solar Energy, [online] 85(9), pp.2338-2348. Available at: http://dx.doi.org/10.1016/j.solener.2011.06.028

Department for Transport (DfT), (2014). *National Travel Survey: 2013 - Publications - GOV.UK*. [online] Available at: https://www.gov.uk/government/statistics/national-travel-survey-2013 [Accessed 5 Jun. 2015].

Department of Energy & Climate Change (DECC), (2014). *Solar photovoltaics deployment - Publications - GOV.UK*. [online] Available at: https://www.gov.uk/government/statistics/solar-photovoltaics-deployment [Accessed 5 Jun. 2015].

Department of Energy & Climate Change (DECC), (2014). *Updated energy and emissions projections: 2014 - Publications - GOV.UK*. [online] Available at: https://www.gov.uk/government/publications/updated-energy-and-emissions-projections-2014 [Accessed 5 Jun. 2015].

Eltako (2015). *The Wireless Building - eltako electronics - switch components, power supply units, energy meters for installations in buildings and use in control technology*. [online] Available at: http://www.eltako.com/en/the-wireless-building.html [Accessed 5 Jun. 2015].

Energy Storage Association (ESA), (2015). *Electricity Storage and Plug-In Vehicles | Energy Storage Association*. [online] Energystorage.org. Available at: http://energystorage.org/energy-storage/technology-applications/electricity-storage-and-plug-vehicles [Accessed 7 Jun. 2015].

Fattori, F., Anglani, N. and Muliere, G. (2014). Combining photovoltaic energy with electric vehicles, smart charging and vehicle-to-grid. *Solar Energy*, 110, pp.438-451.

Federal Ministry for Economic Affairs and Energy, D. (2015). *BMWi - Federal Ministry for Economic Affairs and Energy - 2014 Renewable Energy Sources Act*. [online] Bmwi.de. Available at: http://www.bmwi.de/EN/Topics/Energy/Renewable-Energy/2014-renewable-energy-sources-act.html [Accessed 5 Jun. 2015].

Lane, B. (2015). *Electric vehicle market statistics*. [online] Nextgreencar.com. Available at: http://www.nextgreencar.com/electric-cars/statistics/ [Accessed 7 Jun. 2015].

Matallanas, E. et al. (2012). Neural network controller for Active Demand-Side Management with PV energy in the residential sector. Applied Energy, [online] 91(1), pp.90-97. Available at: http://dx.doi.org/10.1016/j.apenergy.2011.09.004

Munkhammar, J. et al. (2015). Household electricity use, electric vehicle home-charging and distributed photovoltaic power production in the city of Westminster. *Energy and Buildings*, 86, pp.439-448.

Office for Low Emission Vehicles (OLEV), (2015). *Number of newly registered ultra low emissions vehicles - Publications - GOV.UK*. [online] Gov.uk. Available at: https://www.gov.uk/government/publications/number-of-newly-registered-ultra-low-emissions-vehicles [Accessed 5 Jun. 2015].

Office for Low Emission Vehicles (OLEV), (2015). *Plug-in car grant - Publications - GOV.UK*. [online] Gov.uk. Available at: https://www.gov.uk/government/publications/plug-in-car-grant [Accessed 7 Jun. 2015].

Ofgem.gov.uk, (2015). *Feed-in Tariff Scheme: Tariff Table 1 July 2015 PV Only | Ofgem*. [online] Available at: https://www.ofgem.gov.uk/publications-and-updates/feed-tariff-scheme-tariff-table-1-july-2015-pv-only [Accessed 5 Jun. 2015].

Richardson, D. (2013). Electric vehicles and the electric grid: A review of modeling approaches, Impacts, and renewable energy integration. *Renewable and Sustainable Energy Reviews*, 19, pp.247-254.

Schneider-electric.com, (2015). *SmartStruxure Lite solution - Schneider Electric Corporate*. [online] Available at: http://www.schneider-electric.com/products/ww/en/1200-building-management-system/1210-building-management-systems/62191-smartstruxure-lite-solution/?BUSINESS=2 [Accessed 5 Jun. 2015].

Schuller, A. and Hoeffer, J. (2014). Assessing the Impact of EV Mobility Patterns on Renewable Energy Oriented Charging Strategies. *Energy Procedia*, 46, pp.32-39.

Sharma, S. and Galipeau, D. (n.d.). Optimization of residential grid-tied PV systems without net-metering using load management. 2012 IEEE Third International Conference on Sustainable Energy Technologies (ICSET). [online] Available at: http://dx.doi.org/10.1109/icset.2012.6357367

Warren, P. (2014). A review of demand-side management policy in the UK. Renewable and Sustainable Energy Reviews, [online] 29, pp.941-951. Available at: http://dx.doi.org/10.1016/j.rser.2013.09.009

487: Development of energy monitoring centre for demonstrative research of energy network of KIER

Ho-Sang Ra, Gilbong Lee, Sun Ik Na, Junhyun Cho And Young-Soo Lee

Thermal Energy Conversion Laboratory, Korea Institute of Energy Research, 152, Gajeong-ro, Yuseong-gu, Daejeon, Korea

The energy network technology is needed to maximize energy efficiency through optimal matching of demand with supply and utilization of unused energy. It is expected to maximize the energy availability and minimize the exergy loss. Demonstrative researches have been considered for the headquarters of KIER (Korea Institute of Energy Research). As the first stage of energy network research, an integrated energy monitoring centre is developed. KIER uses various types of energies and it also has its own coal-fired power plant. Most of the energy-related facilities and devices are made without consideration of information exchange. Common protocol is selected and devices are connected on the internal network. A web-based monitoring system is developed and data base structure is composed to make web-based EMS possible. This information infra will be beneficial for further demonstrative researches.

Keywords: Energy centre, protocol, network, web-based EMS

1. INTRODUCTION

Thermal energy network is a technology which tries to optimize the use of thermal energy by matching the generation and demand, and through utilizing unused low temperature energies. By maximizing total energy efficiency and minimizing exergy loss, it can also contribute to the reduction of energy cost, greenhouse gases emission and so on. Therefore many researches have been conducted on this topic. Figure 1 is the concept diagram of thermal energy network suggested by KIER. On the research topic of thermal energy network, KIER has focused on the development of new devices which utilize low temperature energies such as air, sea water, sewage water and geothermal energy. KIER also developed several network models for the Daejeon headquarter of KIER since it has many energy facilities like coal-fired power plant for electricity generation, absorption chiller-heater for cooling and heating, solar water heater, and geothermal heat pumps. One of them is an energy network model that analyses the feasibility of type 1 absorption heat pump in saving heating energy when it is connected with the condensing part of coal-fired power plant. Energy network model using heat pump and power plant is suggested and energy consumption analysis is performed for conventional network and new energy network case. Before getting into the next research stage of demonstration, development of integrated data monitoring system is required. This is because most of the energy-related facilities and devices are made without the consideration of information exchange. Furthermore individual manufactures prefer to use their own communication protocol. Therefore addition and unification of communication protocol is required. This paper is about the activities of building integrated web-based monitoring system of KIER.
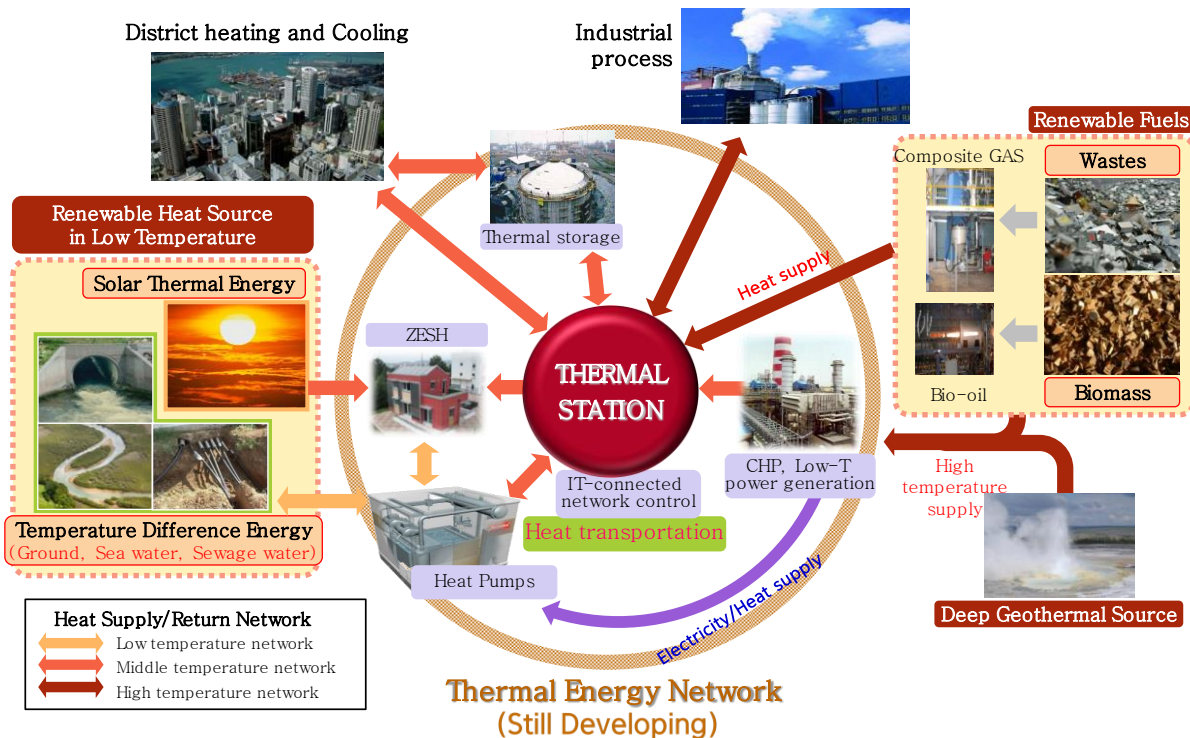
Figure 1. Concept diagram of thermal energy network

7 TARGET OF KIER ENERGY CENTRE

There are two main targets for building energy monitoring centre as a intermediate stage of demonstrative researches. The first is constructing central infra for monitoring current status of energy usage. Each building has different thermal load and electricity load patterns. The type and capacity of installed devices also vary among buildings. For examples, one building is for office purpose while other's main purpose is experiment. Direct exchange of operation data is difficult between different products of different manufacturers. Central monitoring infra which can gather real time operation data from different devices is needed. The second is building data base of energy production and energy consumption. The accumulated energy data will be used to analyse past trends and to predict future demands. With this information, optimum operation of facilities and maximization of energy usage will be possible.

8   CONSTRUCTION OF ENERGY MONITORING CENTRE

Integration of monitoring protocol on the Ethernet TCP/IP was performed. Since manufactures adopt their own protocol, OPC and MODBUS protocol were selected as communication protocols and transformation tasks were performed. As integration is conducted on the existing Ethernet network, there will be cost benefit. Other researchers will easily access to the data base. RTDB (real time data base) using InSQL was adopted. Data saved in RTDB is to be used for energy pattern analysis.
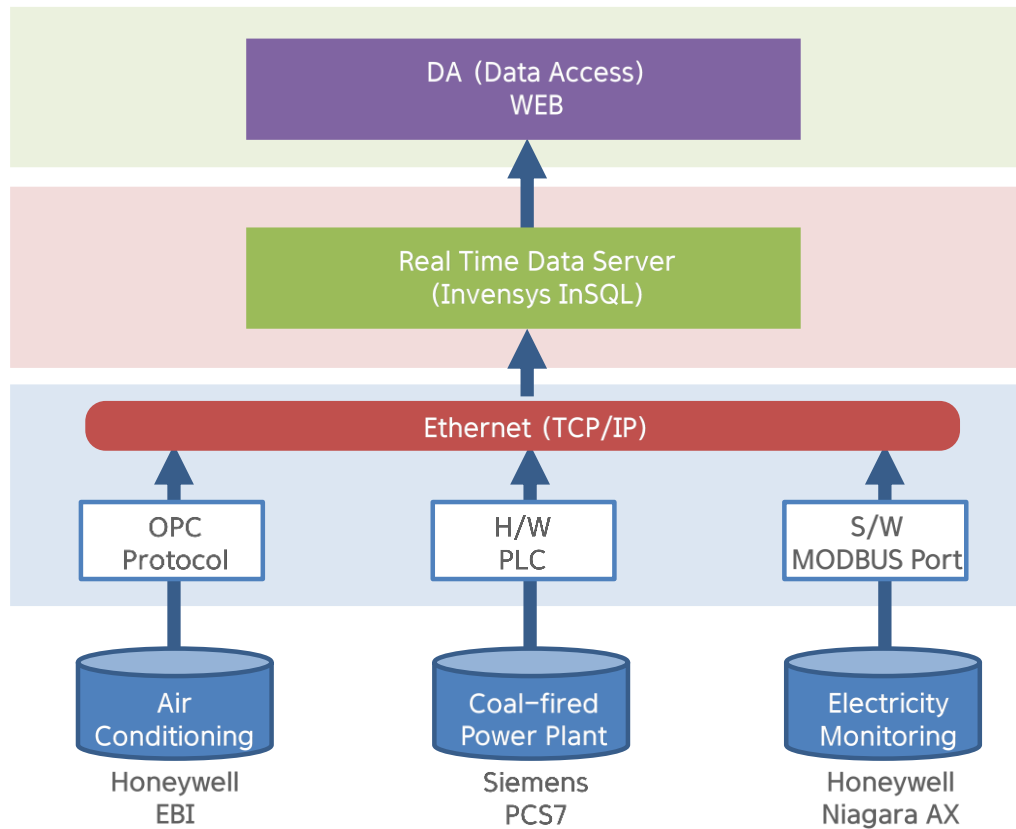

Figure 2. Architecture of data transfer

3.1 Monitoring Air Conditioning Devices

Honeywell EBI system is used to monitoring indoor temperatures, controlling air conditioning devices and detecting gas leakage. The monitoring system of EBI system displays information of operation status, current/target values and devices errors. Honeywell EBI provide data analysis tools. However the information is limited. Therefore constructing additional mirroring server is required in this point. Through OPC protocols, all of the EBI data are transferred to the main monitoring server.

3.2 Coal-fired Power Plant

To deal with the peak electricity demand of the institute, a 2 MW grade coal-fired plant is installed in the main headquarter. The operation system is PCS7 of Siemens. Since the version of operation system is outdated, adding OPC or MODBUS protocol required almost the same amount of work as installing new operation system. Therefore indirect method was adopted. The approach is to bypass the electric signals to the monitoring mosaic panel. The bypassed signals are converted to MODBUS protocol and transferred to main server through the Ethernet TCP/IP.

Figure 3. Mosaic panel of coal-fired power plant and signal bypassing device

3.3 Electricity Monitoring System

The electricity of KIER headquarter is monitored by Honeywell Niagara system. However the monitored data are not saved in a separate server. MODBUS protocol was added to the monitoring system of Honeywell Niagara. Therefore electricity data can be saved in newly constructed RTDB system.

3.4 Web-based Monitoring System

Infra to transfer data to RTDB system was constructed in KIER. Since RTDB system is not user friendly one, web-based monitoring system was developed. The purpose of web-based system is to provide basic energy information of thermal and electric energy usage, primary energy usage, CO2 emission, peak demand, etc. Since functions provided by inSQL are not enough for this purpose, relational database was added. Figure 4 shows the whole data flow of KIER energy monitoring centre.

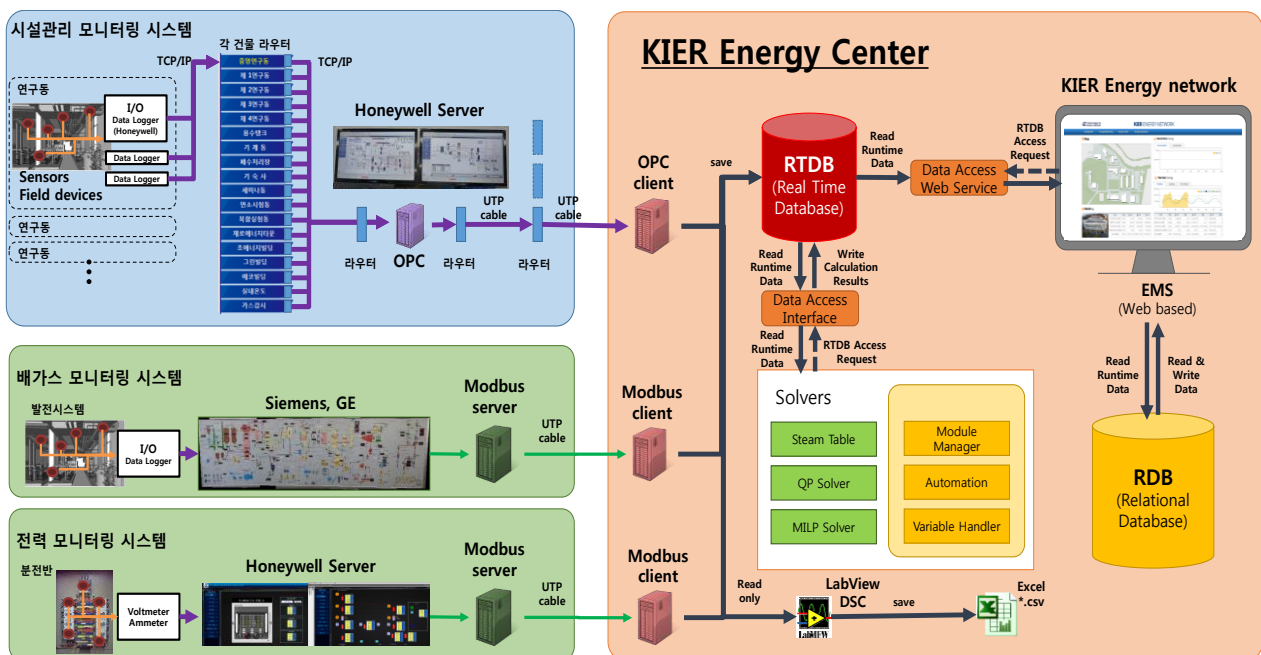Figure 4. Data communication flow of KIER energy center

4   CONCLUDING REMARKS

The KIER energy monitoring centre started operation in last January. It just experienced winter operation. After collecting the whole year data, one can extract unique characteristics of energy usage in KIER. The characteristics later will give basic direction for more refined energy network model.

5   ACKNOWLEDGMENT

392: Environmental effects of ground source heat pump system with vegetation on the ground surface

XUANYU CHANG, YONG LI, RUZHU WANG, HONGYUN ZHOU

Institute of Refrigeration and Cryogenics, Shanghai Jiao Tong University, Shanghai 200240, China, liyo@sjtu.edu.cn

Research on the interactions among Ground Source Heat Pump (GSHP) system, vegetation and microclimate is needed due to exhausted heat from the GSHP system to surrounding environment and ambient temperature reduction by vegetation transpiration. Models in previous study are intended to research the heat transfer underground and to improve the heat transfer efficiency of ground heat exchangers. In addition to these heat transfer models, previous research shows that the performance of a ground heat pump system was found to depend strongly on the moisture content and the soil type, and a number of studies have been conducted to investigate the cooling effect of urban green space using analytical modeling approaches and empirical analysis. The aim of this study is to compare the heat exhausted from GSHP system to the microclimate and the influences of transpiration of vegetation on the surrounding environment in the summer season. In this article, energy balance models of soil and vegetation has been set up to analyze the heat flow among the vertical tubes of a GSHP system, soil, vegetation and the ambient environment. Heat released from GSHP system after long-term operation is predicted on the basis on simulation results. Furthermore, transpiration experiments are conducted to evaluate its cooling effects. The energy influence of the vegetation and GSHP on the environmental atmosphere has been compared. Based on the calculated results and measurement data in Shanghai city (southeast in China), suggestions are given to the application of GSHP system combined with vegetation to balance microclimate.

Keywords: GSHP, vegetation, energy use, transpiration, microclimate

1. INTRODUCTION

Over recent decades, ground source heat pump (GSHP) systems have been shown to be a promising technology due to higher energy efficiencies than conventional heating and cooling systems. The GSHP systems operate with open or closed ground heat exchangers (GHEs). In closed loop systems, GHEs comprise pipes embedded in specifically drilled boreholes or trenches or even built into foundations, all within a few tens of metres from the surface. After years' operation, heat is accumulated underground. During summer operation season, heat extraction from GSHP system to ambient environment can contribute to minor increase of ambient temperature. To describe the heat transfer process in the surrounding soil of the GHEs, classical analytical solutions are the infinite line source (ILS) model, the infinite cylindrical source (ICS) model, and the finite line source (FLS) model(Shao, Schelenz et al.,2014). When considering the influence of groundwater flow, then the Moving Finite Line Source (MFLS) model can also be adopted (Giraldo N., Blum P.,2011).These analytical solutions are then integrated together with numerical optimization algorithm, so that the best geometric arrangement and operation mode can be found for maximum energy extraction(Hecht-Méndez J., de Paly M.2012).All these models are intended to research the heat transfer underground and to improve the heat transfer efficiency of GHEs. In addition to these heat transfer models, previous research shows that the performance of a ground heat pump system was found to depend strongly on the moisture content and the soil type (mineralogical composition) by W.H Leong et al. through computer simulations in three different soils (sand, silty loam and silty clay) with five different degrees of saturation (0, 12.5, 25, 50 and 100%)(Leonga,Tarnawskib1998).However, it's far from sufficient for evaluating long-term environmental effects of GSHP system. Research on the performance of GSHP system after long-term operation should include the influence on the surrounding environment.

At the same time, various kinds of vegetation are planted on the ground surface where GHEs are buried, the landscaping design is for environmental purpose and to increase land use efficiency. A number of studies have been conducted to investigate the cooling effect of urban green space using analytical modelling approaches and empirical analysis(Skelhorna, Lindleya, Levermoreb.2014). In order to investigate changes in air and surface temperatures, wind, and shading due to different types and configurations of green space, a suitable energy balance model is required. Numerical models based on the physical processes integrated with environmental factors, including radiative exchanges, turbulence, and evapotranspiration have established. Baklanov et al. had an excellent comparison of recent models(Baklanov,A.,Grimmond,C.S.B.2009).

While previous studies have considered much about how the heat from GSHP system influence soil temperature filed and cooling effects of vegetation, little is yet known about the interactions among GSHP system, vegetation and microclimate and that's the main purpose of this study. In this article, an energy balance model above the ground where GSHP system is installed and with vegetation on it has been developed. Meanwhile, heat released from GSHP system to the ambient environment and heat absorbed by transpiration of vegetation are calculated respectively and compared. All results provide reference for further discussion regarding the environmental effect of thermal balance surrounding a GSHP system. They are essential and valuable for the development of GSHP systems in downtown area.

2. ENERGY BALANCE MODEL

In the common ecosystem, evapotranspiration, which is comprised by evaporation from soil surface, transpiration and evaporation from the vegetation and the soil, plays an important role in maintaining global energy balance and regulating climate. As a crucial process in the terrestrial ecosystem connecting atmosphere, vegetation, and soil, evapotranspiration is an important component of the water and energy cycles, Global evapotranspiration consumes more than 50% of absorbed solar energy (Trenberth, K. E. 2009), and returns about 60% of annual land precipitation to the atmosphere (Oki, T., & Kanae, S. 2006).

In this article, the system is the comprehensive ecosystem which is combined with common ground atmosphere ecosystem and GSHP underground heat exchanger system. To study the heat flow in the entire system and interactions among all the energy balance contributors, analytical method of thermodynamics is adopted. The schematic diagram of the heat flow in the microclimate system is shown in Figure 1.
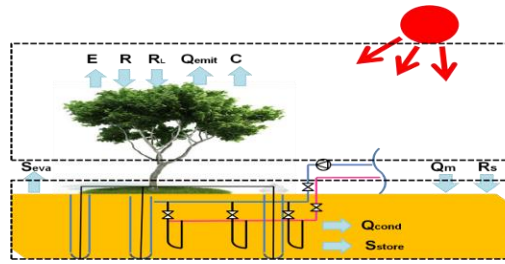
Figure 128: Schematic diagram of the heat flow in the microclimate system

The general equation for the whole system can be described as Equation1.

Equation 1： General equation for the whole system

$$Q_{in} - Q_{out} = Q_{storage}$$

Where:

- Q_{in} = energy into the whole system, W/m²
- Q_{out} = energy out of the whole system, W/m²
- $Q_{storage}$ = energy stored by the whole system, W/m²

This principle was applied to analyze the entire integrated system which is constituted by GSHP system, vegetation and microclimate. Energy balance equation for soil is Equation 2.

Equation 2： Energy balance equation for the soil

$$R_s + Q_m + Q_{cond} - S_{eva} = S_s$$

Where:

- R_s = solar radiation to the soil, W/m²
- Q_{cond} = heat conduction between buried pipes and soil, W/m²
- Q_m = energy of water into the soil W/m²
- S_{eva} = water evaporation from the soil, W/m²
- S_s = energy stored in the soil, W/m²

Solar radiation into the soil can be measured by solar irradiation meter, the value of water into the soil and water evaporation from the soil can be measured by remote sensing or site measuring. Heat conduction between buried pipes and soil is calculated as Equation 3.Heat stored in the soil can be calculated in Equation 4.

Equation 3： Heat conduction between buried pipes and soil

$$\lambda(\frac{\partial^2 t}{\partial^2 x} + \frac{\partial^2 t}{\partial^2 y} + \frac{\partial^2 t}{\partial^2 z}) + Q_t = c\frac{\partial t}{\partial \tau} \quad \tau \geq 0 (x, y, z) \in \Omega$$

$$t(x, y, z, 0) = t_0(x, y, z)(\tau = 0, (x, y, z) \in \Omega)$$

$$t(x, y, z, \tau) = t_1(x, y, z)(\tau \geq 0, (x, y, z) \in \Gamma)$$

Where:

- λ = thermal conductivity, W/(m·K)
- Q_t = heat source or heat sink of heat transfer between GSHP system and soil, W/m²
- c = heat capacity of per unit volume soil, J/(m³/K)
- $t(x,y,z,\tau)$ = soil temperature, ℃
- $t_0(x,y,z,0)$ = initial soil temperature, ℃

- t₁(x,y,z,**τ**)=known buried pipe temperature as the first boundary condition, °C
- **τ**=time

Equation 4：Heat stored in the soil

$$S_s = \sum cm_s \Delta t$$

Where:

- m_s= mass of the soil, kg
- Δt= temperature increase in the soil, °C. It's different in the different space of the soil.

It is well known that leaf is the main organ of vegetation for heat and mass transfer with ambient environment. The energy exchange of an individual leaf can be defined by the balance Equation 5 (K. R. Knoerr 1965). Where energy flow toward the leaf is considered positive, and away from the leaf is negative. Solar radiation, *S*. and long-wave radiation, S_L, provide the major energy supply to the leaf. The efficiency of the leaf for absorbing this radiation is determined by its absorptivity for solar and long-wave radiation, α_S and α_L. Major losses of heat from the leaf are through emission, *R*, convection, *C*, and latent heat exchange through transpiration, *E*. Under conditions of low incident radiation, the leaf can gain heat through convection if leaf temperature is lower than air temperature, or through latent heat in condensation if leaf temperature falls below the dew point. Changes in leaf energy storage, *Q*, and leaf metabolic balance, *M*, are minor components in the leaf energy balance. Since they usually represent less than 5% of the combined convective and latent heat losses, the metabolic and heat storage terms can be neglected in most energy balance calculations (Park S. Noble, 2010).

According to the Stefan-Boltzmann law Equation 6,reradiation from the leaf is a function of its absolute temperature, t_l, and the Stefan-Boltzmann constant, σ. The efficiency of the leaf in reradiation is determined by its emissivity, ε, which is essentially the same as its absorptivity for long-wave radiation, α_L. For most leaves ε and α_L are about 0.97 or almost unity. Because upper and lower surfaces of thin leaves area essentially the same temperature, radiation losses from these surfaces can be considered equal.

Equation 5：Energy balance equation for leaf

$$\alpha_S S + \alpha_L L - R \pm C \pm E \pm Q \pm M = 0$$

Where:

- S= solar radiation to the vegetation, W/m²
- L= long wave radiation to the vegetation leaf , W/m²
- α_S, α_L = leaf absorptivity for solar and long-wave radiation
- R=emission, W/m²
- C= heat conduction between leaf and air, W/m²
- E=latent heat exchange through transpiration, W/m²
- Q=changes in leaf energy storage, Wm²
- M= leaf metabolic balance, W/m²

Solar radiation and long wave radiation into the leaves can be measured by infrared radiometer. Heat convection between vegetation and ambient air can be calculated as Equation 7. Heat loss of vegetation transpiration can be calculated as Equation 8.

Equation 6：Reradiation from the leaf

$$R = \varepsilon\sigma(t_l)^4$$

Where:

- ε = emissivity of leaf
- σ = the Stefan-Boltzmann constant, 5.67×10^{-8} W/(m²·K⁴)
- t_l = leaf temperature, ºC

Equation 7：Heat convection between vegetation and ambient air

$$C = h_c A(t_l - t_a)$$

Where:

- h_c = heat convection coefficient, W/(m² · ºC)
- A = leaf area, m²
- t_a = ambient air temperature, ºC

To estimate the heat convective transfer coefficient, it is necessary to distinguish between two convection situations. Forced convection is produced by mechanical mixing of air through the inertial forces of wind flow. Free convection results from temperature differences, and thus mixing caused by density or buoyancy differences between leaves and air. Because of these fundamental differences in the two convection processes, the convective heat transfer coefficients, for forced convection are different from those for free convection. With free convection the coefficient for the upper surface of a horizontal leaf is also different from that for the lower surface. The detailed discussion of the heat convection coefficient can refer to Heat Transfer and will not be introduced in this article.

Equation 8：Heat loss of vegetation transpiration

$$E = M \times L$$

Where:

- E = heat of vegetation transpiration ,J/m²/d
- M = water loss of vegetation, g/m²/d
- L = latent heat of evaporation, J/g, it means heat absorbed by water of one gram during transpiration, its value is negative linear correlation with the temperature of evaporation surface, in this article, $L = 2495 - 2.38^x t_l$.

For ground with vegetation, heat convection and evapotranspiration play an important role in heat transfer, temperature of the system is usually lower than the area without vegetation. However, for the comprehensive system which constitute of GSHP system after long-term operation, heat released from the GSHP system will not only transfer into the soil but also penetrate into the ambient air, thus, temperature of ground surface will increase significantly and surrounding microclimate will be influenced.

Based on the energy balance model of the soil and vegetation, heat absorbed by vegetation transpiration is determined by ambient environment to some degree. However, heat released from GSHP system to ambient environment is continuous and stable during operation season. Supposing that the previous ecosystem is in energy balance, from the Equation 2 to Equation 8, the newly increased heat flow from GSHP system may be offset by the heat-absorbing of vegetation transpiration. The following part will quantify the heat flow.

3. HEAT RELEASED FROM GSHP SYSTEM TO AMBIENT ENVIRONMENT

Due to large amount of heat released from GSHP system is accumulated in the soil and by yet there is no available result of monitoring how much heat from GSHP system to the ambient environment as well as increase of outside air temperature caused by heat from GSHP system. In this article, a steady state heat transfer model indicated in Figure 2 has been proposed to analyze and calculate the heat released from the GSHP system to the ground surface environment.
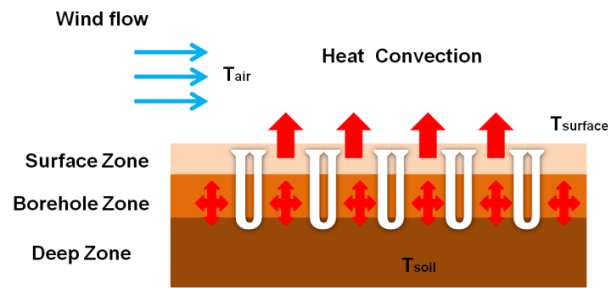
Figure 2: Steady State Heat Transfer Model

In summer operation season, water is circulated through the heat exchanger to transfer heat with ambient soil. Thermal conduction and moisture migration characteristics of Shanghai mucky clay indicate it is a geo-material with good heat storage but poor heat release(Tang, Zhou, Zhang, Liu, 2015),hence, after long-term operation, there will be large amount of heat stored in the soil and lead to significant temperature increase in the soil. Naturally, through heat conduction and heat convection, heat will penetrate into ambient air and affect the surrounding microclimate.

Because of experimental data of long-term operation GSHP system is not available, in this article, we refer to the simulation results of a model which simulate a hotel building in Shanghai in long-term operation condition to calculate the heat released from GSHP system to ground surface environment. Simulation results in the reference is based on thermo physical properties of soil and buried pipes and other systematic parameter settings which are respectively presented in Table 1 and Table 2.

Table 1: Thermo physical properties of soil and buried pipes

	Density(kg/m^3)	Heat conductivity(W/(m·^{o}C))	Specific heat(J/(kg·^{o}C))	Porosity
Buried pipes	950	0.44	2300	
Soil	1600	1.8	1645	0.2

Table 2: Parameter settings in the referred simulation

Parameter settings in the simulation		
Initial temperature of soil	16.9	^{o}C
Amount of buried pipes	60	--
Inner diameter of pipes	46	mm
External diameter	56	mm
Space between pipes	4	m
Velocity of fluid in the pipes	0.2	m/s

4. MEASUREMENTS OF VEGETATION TRANSPIRATION

It is well known that one of the most important functions of vegetation is its ability in reducing the temperature and increase the humidity of the surrounding air in hot summer. In terms of thermodynamics, vegetation transpiration is a process of heat-absorbing accompanied by water loss. To calculate the heat absorbing during the transpiration and to conduct research on how environmental factors affect vegetation transpiration, portable photosynthesis system CIRAS-2 was used to measure the vegetation transpiration rate as well as other parameters of ambient environment and leaves, its parameters are summarized in Table 3. Measurement work was done in Shanghai Jiao Tong University. In this article, each measured vegetation is typical in Shanghai and usually planted on the ground surface where GSHP systems are installed.

Table 3: Parameters of CIRAS-2

Instrument	Parameter	Range	Accuracy(μmol/mol)
Mainframe	Temperature	0~50ºC	
	Concentration of CO_2	0~9999μmol/mol	concentration:300,accuracy:0.2 concentration:1750,accuracy:0.5 concentration:9999,accuracy:3
	Concentration of H_2O	0~75mb	concentration:0,accuracy:0.015 concentration:10,accuracy:0.02 concentration:50,accuracy:0.03
Leaf chamber	Light intensity	0~2000μmol/m²/s	
	Temperature	8ºC lower the ambient air to 40ºC	
	Humidity	0 to saturation	

Due to vegetation transpiration depends on solar radiation to a great extent, and is weak at night, rarely on rainy days, all the measurement was done at daytime on sunny and cloudy days. Measurement work was done every 2 hours a day which began at 8:00 am and ended in 16:00 pm. Table 3: Final set of indicators suggested for measuring the urban infrastructure systems sustainability of the Middle Eastern cities

Water Systems Indicators	Wastewater Indicators	Transportation indicators	Energy Indicators
Water intake by municipal services	Population served by Sewage system	Expenditure on roads, parking, public transit, ports, etc.	Service/commercial energy strengths
Borne diseases through the water	Municipal revenues, from wastewater management	Per capita congestion	Domestic energy intensities
Connections of water and sewer	Municipal costs of wastewater management	Proportion of portion of trips by non-motorized modes	Agricultural energy strengths
The possibility of affected of Groundwater	Population served by wastewater treatment plants	Crash deaths and injuries	End-use energy costs by fuel and by sector
Population served by water supply systems	Expenditure per 1000 inhabitants on wastewater management	Quality of walking, cycling, public transit, driving, taxi, etc./	External prices of energy use
Total water intake	Rate of Wastewater produced	Quality of accessibility for people with disabilities	Efficiency of energy transformation and supply
Total water treated	Rate of wastewater treatment	Land devoted to transport facilities	Domestic energy use for each income group and equivalent fuel mix
Total public water consumption	Wastewater treatment in wastewater treatment plant	Total vehicle emissions	Joined heat and power generation
Water losses		Proportion of emissions from facility construction	Annual energy consumption, total and by main user group
Leakage of water		Economic costs of traffic collisions	Reserves-to-manufacture ratio
		Proportion of people exposed to traffic noise	Industrialized energy intensities
		Affordable housing accessibility	Transport energy strengths
		Using a method of investment in transport infrastructure	Fuel shares in energy and power
		Modal divided of passenger transport	Renewable energy share in energy and power
			Net energy import need
			Pollutant discharges in liquid effluents from energy systems
			Ratio of solid waste generation of units of energy produced
			Air pollutant emissions from energy systems
			Reserves-to-manufacture ratio

lists all the measured vegetation.

Table 4: Measured vegetation

Vegetation kind	Measured vegetation name(abbreviation)
Shrub	Photinia serrulata(PS)
	Berberisthunbergiicv atropurpurea(BA)
	Chinese littleleaf box(CLB)
Arbor	Cinnamomum camphora(CC)
	Weeping willow(WW)
Herbal	Alfalfa (AL)

We choose leaves which are well-grown in the different parts of vegetation and measure solar radiation(μmol/m²/s),ambient temperature(°C),ambient relative humidity, leaf temperature(°C),stomatal conductance(μmol/m²/s),vapour pressure deficit(kPa) and transpiration rate(mmol/m²/s) three times each time. Fig 3 shows the measurement instrument and some of the measured vegetation.

Figure 3: Measurement instrument and some of the measured vegetation.

To calculate the daily total transpiration of per unit area leaf, which is equal to the integration value of each measured transpiration rate and transpiration time can be described as Equation 9.

Equation 9：Daily total transpiration

$$E = \sum_{i=1}^{m}\left[(\frac{e_m + e_{m+1}}{2}) \times (t_{i+1} - t_i) \times 3600/1000 \right]$$

Where:

- E= daily total transpiration, mol/m²/d
- e_m, e_{m+1} = transpiration rate of initial measure time point, transpiration rate of next measure time point
- t_{i+1} , t_i= he next measurement time, the initial measurement time
- m= the measurement times a day

5. RESULTS AND DISCUSSION

5.1. Heat Released from GSHP System to Ambient Air

Assuming a rectangular soil region which area is 32m×48m, and depth is 100m.Without groundwater seepage condition, heat storage capacity of soil increases year by year. After successive ten year operation, heat stored in the soil has reached 809.7MWh, the average temperature of soil has rose 7.2°C (Xu.2013). Assuming that coefficient of convective heat transfer between soil surface and coming air h_c is 12W/(m² • °C), the wind velocity is 3m/s, and average temperature of the air closet to the ground surface in Shanghai is 21.1°C. According to Newton's law of cooling, heat convection between ambient air and soil can be calculated.

Thus, heat convection rate between ambient air and soil is 36W/m², that is to say, heat released from GSHP system to surrounding microclimate may be 3110.4kJ/m²/d supposing that the air closet to the ground surface is stable all day long. Heat transfer in the soil is influenced by many factors such as soil property

and ground water seepage velocity, with the increase of water seepage velocity, heat transfer rate in the soil will go up, thus, less heat will be stored in the soil and lower temperature increase of the soil after long-term operation of GSHP system. What should be mentioned here is that, in the referred simulation model, the velocity of the fluid in the pipes is only 0.2m/s, which is less than the usual actual value 0.4~0.5m/s, so, theoretically, heat stored in the soil is more than the simulation results and further aggravate the increase of temperature in the soil and in the ambient air.

5.2. Heat Absorbed by Transpiration of Vegetation

The measurement results of one typical day in summer in Shanghai area (May 22, 2015) has been analysed. The weather conditions of the experimental day is shown in Figure 4. Average temperature of 8:00~18:00 that day was 22.8°C, average relative humidity was 59.9%.At noon time, temperature is the highest 24.7°C and solar radiation has reached 988W/m^2,to the contrary, the relative humidity at that time was 46.3%.The average wind velocity during the measurement time varied from 0.1m/s to 3.5m/s, with an average value of 1.5m/s.
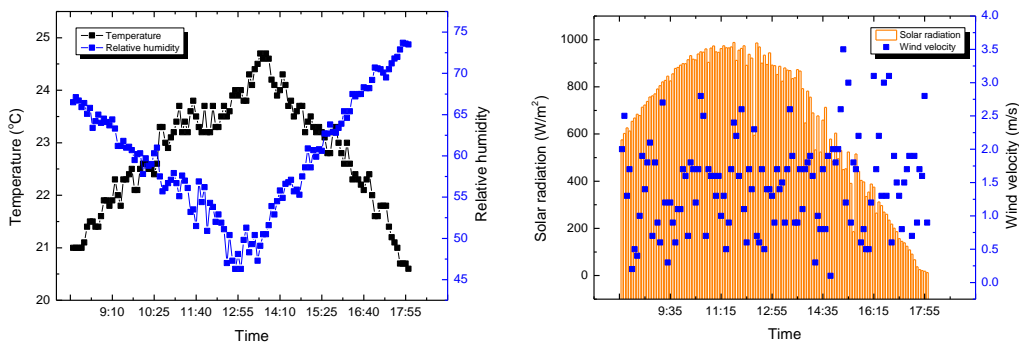

Figure 4 :Environmental conditions of May,22 (Left: Temperature and relative humidity Right:Solar radiation and wind velocity)

The water loss and absorbed heat during transpiration in a day of each measured vegetation are shown in Figure 5. Herbal AL has the largest water loss 4315.8g/m^2/d and absorbing-heat 10473.9kJ/m^2/d, it's different from the traditional grass due to its high photosynthetic rate. Among shrub, BA has the highest transpiration rate, the daily water loss has reached 3045.6 g/m^2/d and absorbing-heat is 7930.8kJ/m^2/d. Among arbor, WW has the best cooling effect, its water loss during transpiration a day is 2903.1kJ/m^2/d and absorbing-heat is 7031.1kJ/m^2/d.
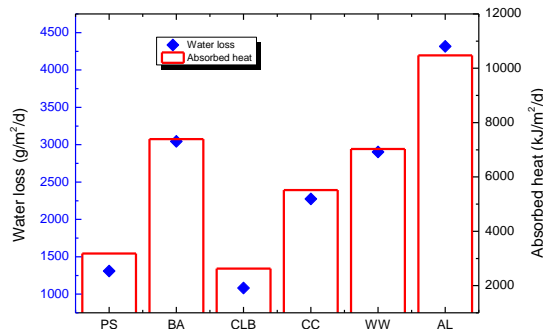
Figure 5: Water loss and absorbed heat during transpiration in a day of each measured vegetation.

However, vegetation transpiration amount above a ground surface during a day is usually determined by the vegetation coverage ratio and the leaf area index. Naturally, more heat will be absorbed by higher vegetation coverage ratio, due to all the leaves measured in the experiment are exposed to the sun which has higher photosynthetic rate, so calculated absorbing heat of per unit area in this article is comparatively higher.

5.3. Cooling Effects of Vegetation

Usually, vegetation in green space can mitigate the Urban Heat Island (UHI) effect due to its fine cooling effects during transpiration. Cooling effects of each kind of measured vegetation in this article is calculated as Equation 10 and revealed in Figure 6.Therotically, in an hour, an AL tree can reduce the temperature of $1000m^3$ air bar by 0.8^oC, and the average temperature reduction ability of measured vegetation on the typical day can be 0.5^oC.

Equation 220: Cooling effects of vegetation
$$\Delta t_c = \frac{Q_h}{\rho c V}$$

Where:

- Δt_c= temperature decrease due to vegetation transpiration, ^oC
- Q_h= heat absorbed in an hour during transpiration, $J/m^2/h$
- ρc= volumetric heat capacity of air, $J/m^3/^oC$
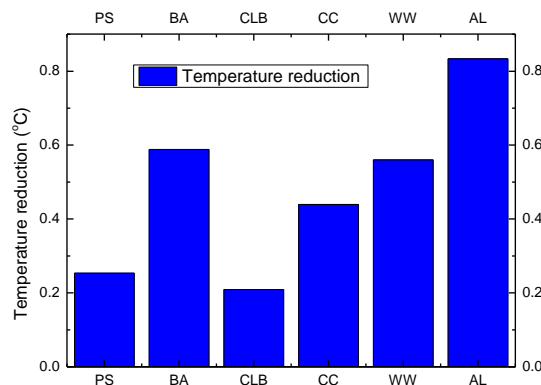- V=volume of air bar,m^3

Figure 6: Cooling effects of each measured vegetation

5.4. Factors Influence on Vegetation Transpiration

Vegetation transpiration rate is significantly influenced by many environmental factors such as solar radiation, ambient temperature, ambient air relative humidity and vapour pressure deficit (VPD) as well as its own speciality such as stomatal conductance(Gs)(Soonja Oh, Kyung Hwan Moon et al. 2015).

The relationship between main environmental factors and transpiration rate changing with time is shown as Figure 7, it is observed that transpiration rate is obviously influenced by solar radiation and ambient temperature. Along with enhanced solar radiation, temperature of ambient air increases, and transpiration rate goes up. At noon time, solar radiation and ambient temperature reaches the highest level in a day, and that's when the transpiration is strongest. In the afternoon, solar radiation and ambient temperature decrease, hence, transpiration rate drop. For AL and BA, transpiration rate drop sharply with the solar radiation decreases, for BA, CC, PS and CLB drop smoothly.

Transpiration rate of each kind of vegetation vary with solar radiation and ambient temperature is shown in Figure 8, transpiration rate varies with solar radiation present two peak values during the measurement time, respectively when the solar radiation is 1458μmol/m²/s and 2145.5μmol/m²/s. While, transpiration rates increase with the temperature
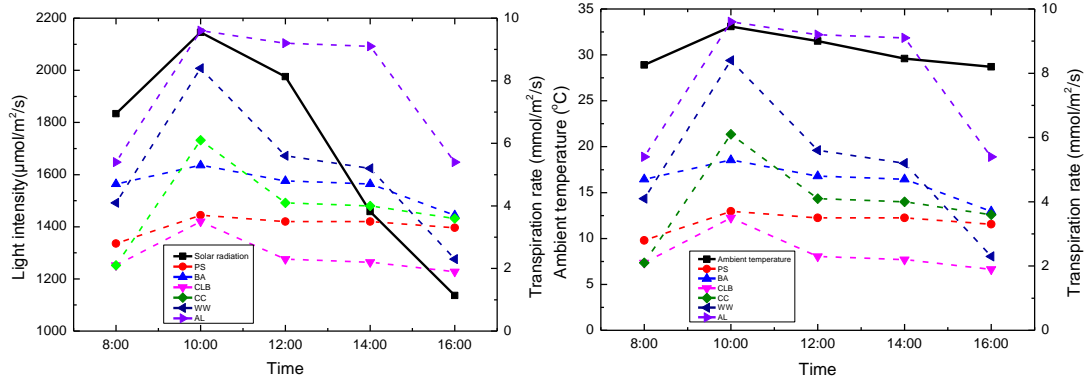
Figure 7: Environmental factors (left: light intensity right: ambient temperature) and transpiration vary with time
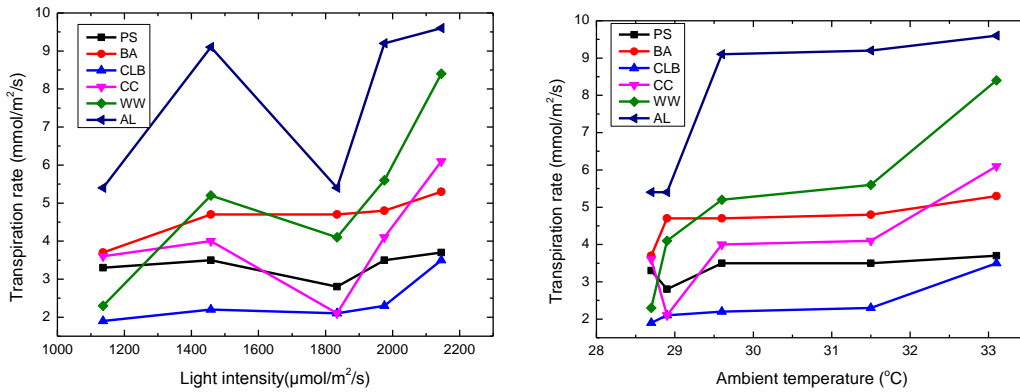

Figure 8: Transpiration rate of each kind of vegetation vary with light intensity (left) and ambient temperature (right)

5.5. Proportion of Energy Release and Energy Absorb in the Whole System

In the overall system，GSHP system is releasing heat to the ambient environment, on the other hand, vegetation is absorbing heat from soil and surrounding environment by transpiration. Assumption is made that, each kind of measured vegetation is planted on the ground surface and the amount of each kind of vegetation is only one. From the comparison of the energy share in one day, conclusions can be made that heat released to the ambient air from GSHP system after long-term operation to the total energy absorbed by the vegetation transpiration is nearly 1:9.

6. CONCLUSION

This study proposed the energy balance model for the system combined with GSHP system and vegetation on the ground surface, what's more, quantified heat fluxes on the ground surface where GSHP systems are installed and vegetation are planted.

According to above results, we make a comparison of the heat released from GSHP system to ambient air and heat absorbed from transpiration of vegetation, **heat released from GSHP system to surrounding microclimate may be 3110.4kJ/m²/d,** absorbing-heat of one plant of a typical kind of vegetation in Shanghai area varies from 2903.1 kJ/m²/d to 10473.9kJ/m²/d. So, in the whole microclimate system, heat from GSHP system can be used in vegetation transpiration to avoid the temperature increase and balance the surrounding microclimate.

Heat stored in the soil depends on the soil property, the fluid velocity and the heating/cooling load of the GSHP system, vegetation transpiration rate is mainly determined by solar radiation and ambient air temperature. Integrated analysis of heat flow in the whole system indicates that long-term environmental effects of GSHP system with vegetation on the ground surface should be deeply studied in the future through in site measurement and modelling analysis.

With large-scale application of GSHP system, heat will be released and stored in the soil. At the same time, heat released from GSHP system has apparent influence on the surrounding microclimate, one of the negative one for stable ecological is temperature increase. Since vegetation have favourable cooling effects, by planting suitable vegetation on the ground surface where heating exchangers are buried underground the energy in and out of the system can be offset and the Urban Heat Island Effect can be mitigated.

7. REFERENCES

HAIBING Shao, Sophie Schelenz, Norman Kist, Byoung Ohan Shim, Anke Boockmeyer, and Olaf Kolditz, 2014. Numerical Modeling of Borehole Heat Exchangers (BHEs) and its interactions with the surrounding soil. Karlsure,Germany.

MOLINA-GIRALDO N., Blum P., Zhu K., Bayer P., Fang Z. 2011A moving finite line source model to simulate borehole heat exchangers with groundwater advection, International Journal of Thermal Sciences 50(12): 2506-2513, DOI: 10.1016/j.ijthermalsci.2011.06.012.

HECHT-MÉNDEZ J., de Paly M., Beck M., Bayer P. 2012Optimization of energy extraction for vertical closed-loop geothermal systems considering groundwater flow, Energy Conversion and Management 66: 1-10, DOI: 10.1016/j.enconman.2012.09.019.

W.H LEONGA, V.R Tarnawskib, A Aittomäkic. 1998 Effect of soil type and moisture content on ground heat pump performance[J]. Int. J.Refig . 1998,21(8): 595~609.

Cynthia SKELHORNA, Sarah Lindleya, Geoff Levermoreb. 2014 The impact of vegetation types on air and surface temperatures in a temperate city: A fine scale assessment in Manchester, UK. Landscape and Urban Planning 121 (2014) 129–140.

BAKLANOV,A.,Grimmond, C.S.B.,Mahura,A.,&Athanassiadou,M.(Eds.). 2009.Meteorological and air quality models for urban areas. Berlin,Heidelberg: Springer-Verlag.

TRENBERTH, K. E., Fasullo, J. T., & Kiehl, J. 2009.Earth's Global Energy Budget. Bulletin of the American Meteorological Society, 90, 311–323.

OKI, T., & Kanae, S. 2006. Global hydrological cycles and world water resources. Science,313, 1068–1072.

K. R. KNOERR and L. W. Gay. 1965.Tree leaf energy balance. Ecological society of America, Vol. 46, No. 1/2 (Jan.,), pp. 17-24

Park S. NOBLE, 2010 Physicochemical and Environmental Plant Physiology[M], Science Press, 2010,319~350.

Yiqun TANG, Jie Zhou, Modan Zhang,Yuting Liu, 2015. Research on the thermal conductivity and moisture migration characteristics of Shanghai mucky clay. I: Experimental modeling Bull Eng Geol Environ :74:577–593.

Lei XU. 2013 Application research of GSHP system in hot summer and cold winter area in china[M], Nanjing University of Science & Technology, 2013.

Soonja OH, Kyung Hwan Moon, Eun Young Song, In-Chang Son, Seok Chan Koh. 2015 Photosynthesis of Chinese cabbage and radish in response to rising leaf temperature during spring. Horticulture, Environment, and Biotechnology(2015), Volume 56, Issue 2, pp 159-166.

SUSTAINABLE CITIES & ENVIRONMENT

POSTER SESSION D

99: Embodied energy of fired bricks: the case of Uganda and Tanzania

ARMAN HASHEMI[1], HEATHER CRUICKSHANK[2]

1 Centre for Sustainable Development, Department of Engineering, University of Cambridge, UK.
a.hashemi@eng.cam.ac.uk
2 Centre for Sustainable Development, Department of Engineering, University of Cambridge, UK.
hjc34@cam.ac.uk

This paper evaluates the embodied energy of fired/burned bricks as one of the major construction materials in East African countries. Production processes of bricks by artisans, and small- and medium-scale manufacturers are explained. Embodied energy of brick walls is also calculated and the key factors in the energy efficiency of brick kilns are discussed in detail. Low quality, high material waste and excessive energy waste during production and handling are highlighted as the major issues associate with traditional manufacturing processes of burned bricks in Uganda and Tanzania. The results reveal that small clamp kilns lose up to 3.5 times more energy through their cooling surfaces compared to large kilns. The results also indicate that clamp fired bricks are up to 60% more energy intensive than generic bricks and the embodied energy of artisan brick walls is 35% more than standard brick walls with comparable thicknesses. Improving kiln construction and production methods, educating artisan producers, replanting tress, providing alternative renewable energy sources, and design improvements to control fire intensity and air circulation in brick kilns are some of the recommendations to improve the energy efficiency and mitigate the environmental impacts of fired bricks in East African countries.

Keywords: Embodied Energy, Life Cycle Assessment, Fired Brick, Burned Brick, East Africa, Uganda, Tanzania

1. INTRODUCTION

Traditional construction methods and materials have historically been a sustainable response to housing demands in developing countries. The production methods of locally manufactured materials in Uganda and Tanzania have more or less remained unchanged during the last few decades. Brick walling is a major construction method in both rural and urban areas of East African countries including Uganda (UBOS, 2010). Fired/burned brick, however has negatively affected the local environment contributing to issues such as deforestation, desertification, air pollution, excessive soil extraction and fuel crisis (Perez, 2009; CRAterre, 2005; World Bank, 1989). This is mainly due to the excessive energy and material waste and inefficient production processes of burned bricks which are mainly delivered by artisan producers (World Bank, 1989). Increased use of energy intensive materials such as concrete and burned bricks has raised concerns over the long-term environmental impacts of such trends in East Africa. The forestry cover in Uganda, for example, has reduced by 25% from 45% coverage in 1990 to around 20% in 2005. This means an annual deforestation rate of 1.7% which is increasing year by year. Considering the current situation, Uganda's forests could be vanished during the next few decades (ILO, 2010).

Environmental impacts of buildings and products are evaluated using Life Cycle Assessment (LCA) method (Figure 129). The total carbon footprint of buildings consists of the embodied carbon of building products plus the operational carbon which is the energy consumption during building lifetime. The majority of the embodied carbon of building products is linked to CO_2 emissions from fossil fuels during extraction and manufacturing processes of construction materials (Anderson & Thornback, 2012). The embodied carbon of building fabrics is becoming more important due to increasing energy efficiency requirements which reduce the operational carbon of buildings during their lifetime.
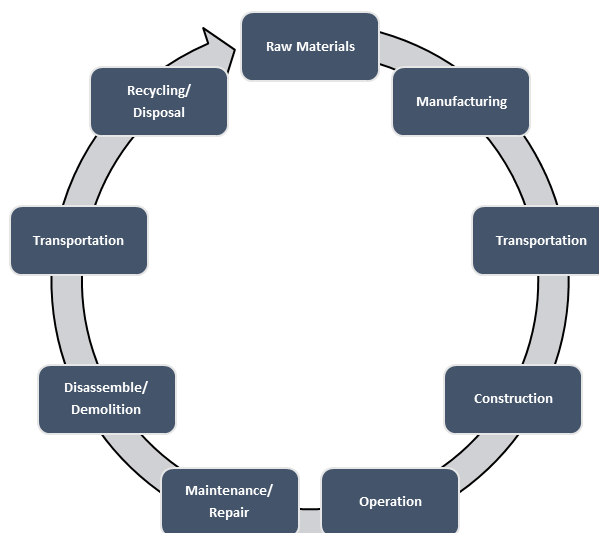

Figure 129: Building Life Cycle

Yet, considering the negligible operational energy for space heating and cooling in East African low-income housing, the embodied energy of construction materials is the main factor in evaluating the environmental impacts of the low-income housing sector. The embodied energy of construction materials such as burned brick in contrast is a major concern. Improving energy efficiency and reducing material wastes during production processes could therefore reduce the overall greenhouse gas emission rates and mitigate the environmental impacts of the construction industry. To this end, this study intends to evaluate the production processes of fired/burned bricks produced by artisan, small- and medium-scale manufacturers in order to identify the key areas for improvement.

2 METHODOLOGY

Literature review, and primary data gathered from site visits and photographic surveys in two East African countries (Uganda and Tanzania) are the main methods of data collection for this paper. Available literature is reviewed to assess the actual fuelwood consumption and brick sizes as well as production rates by artisans and small- and medium-scale manufacturers in Uganda. Energy consumption and potential saving rates during production processes are then calculated using the outcomes of the literature review. The embodied energy rates of burned bricks and brick walling are also calculated and compared with other

generic bricks/ brick walls using the available data in the "Embodied Carbon: The Inventory of Carbon and Energy" developed by the University of Bath (Hammond & Jones, 2011).

3   WALLING METHODS AND MATERIALS

Figure 130 shows the main walling methods and materials during 2009/2010 in Uganda. Brick walling (either adobe or fired) is the most common construction method in Uganda. More than 80% of houses in urban areas have brick walls compared to around 50% in rural areas. Mud and poles walling is also very common particularly in rural areas where more than 40% of homes are built with mud and poles. Overall, around 84% of all houses in Uganda have brick walls compared to around 12% which are built with mud and poles (UBOS, 2010).
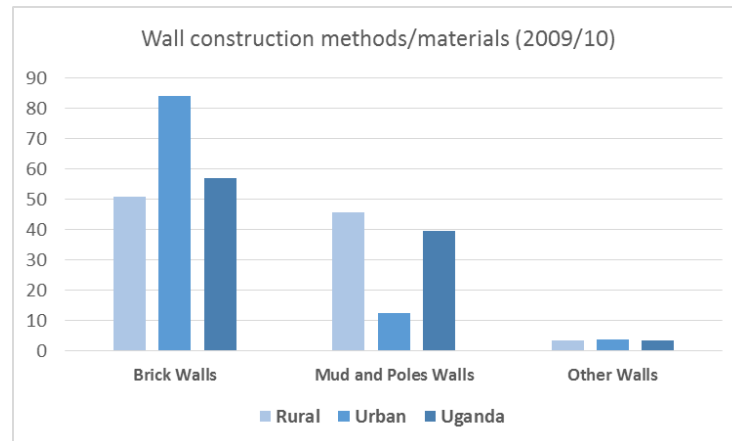
Figure 130: Main walling types during 2009-2010 (%).

Source of table: (UBOS, 2010)

Although burned brick is considered as a durable material, its high embodied energy makes it an environmentally harmful material compared to other prevailing construction materials in East African countries. The very inefficient production methods of kiln fired bricks, which mainly use local wood as their fuel, contribute to issues such as deforestation and air pollution (Perez, 2009; CRAterre, 2005; World Bank, 1989). In fact wood is the main source of energy particularly in rural Uganda. Two major reasons of deforestation in Uganda are cutting trees for firewood, and charcoal, and for creating agricultural land (ILO, 2010). Fuelwood (firewood and charcoal) and agricultural waste account for 93% of energy consumption in Uganda (The Government of the Republic of Uganda, 2001). Around 95% of supplied wood in Uganda is used for energy generation (The Government of the Republic of Uganda, 2001) including in the brick manufacturing industry (Figure 131). Around 91% of the required energy for brick production is from firewood and the rest is from agricultural waste (World Bank, 1989).

Figure 131: Inefficient production processes and use of fuelwood contribute to deforestation, air pollution and fuel crisis (Uganda).

Source: The authors

4   PRODUCTION PROCESSES OF BRICK

Low quality, energy intensive traditional methods of brick production by artisans is a major concern which has negatively affected the local environment in both Uganda and Tanzania. In the traditional production method (Figure 131), unfired moulded bricks are prepared using local clay and water and are then left to dry out before being fired in field kilns for 4-6 days using gradually intensified wood fire (Nyakairu et al., 2002; Batchelder et al., 1985; Practical Action). Energy and material wastes are the two major issues associated with traditional production methods of fired brick. One of the major issues is the lack of control over burning and fuel consumption (Batchelder et al., 1985). Considerable energy is also wasted through hot exhaust gases during production processes (World Bank, 1989).

Larger rectangular kilns and clamps can achieve better fuel efficiency thanks to lower heat losses due to the lower volume to surface ratio. Cubic kilns are assumed to have four cooling faces (on the sides) and the heat losses through the top and ground facing surfaces are considered separately (Practical Action). Table 67 shows the common brick and kiln sizes in Uganda along with the cooling ratios and average wastes of different kilns. The results of calculations reveal that a 1.5x2x2m brick kiln loses 3.5 times more energy through cooling surfaces compared with a 6x6x4.3m kiln due to much higher cooling area/volume ratio. There is also a direct relationship between the kiln sizes and the portion of under fired/ low quality bricks. According to World Bank (1989), around 46% of clamp fired bricks in a 3x3x3.1m kiln have low quality compared to 24% for a 6x6x4.3m clamp kiln. This is while, according to Batchelder et al. (1985), smaller kilns provide a more uniform distribution of fire improving the quality of final products. The latter requires more investigation to evaluate the relationships between kiln sizes and overall waste and quality of bricks.

The average size of field kilns in Uganda is 2.4-3 metres (Batchelder et al., 1985). Despite higher fuel efficiency of larger kilns, the width/length of country kilns should not be more than 4.5-6 metres mainly due to increases in total fuel consumption, labour and costs. The overall process of production from clay moulding to finished product takes around three weeks for 4,000 to 10,000 bricks. It takes an average of 5 weeks for 5 people to excavate, mould and fire up to 9,000 bricks (Emerton et al., 1998). Around 60-75 metres of 4" to 8" dry wood (in addition to woodchip and coffee/rice husks) is required to produce 20,000 bricks (Batchelder et al., 1985) and nearly 80% of the required timber for fuel is provided from locally grown trees (Naughton-Treves et al., 2007).

Table 67: Brick kiln sizes and cooling ratios

Clamp Kiln Size (W x L x H) (m)*	Brick/Block Size (mm)*	Total Surface Area (m²)	Cooling Surface Area (m²)	Volume (m³)	No. of bricks	Mass of Bricks (tonne)	Ratio: Cooling Area/Volume	Relative Cooling Area/Volume energy waste	Low quality/ under fired portion*
1.5x2x2	228x111x76	20	14	6	~2100	~6.6	2.33	348%	-
3x3x3.1	290x140x90	55.2	37.2	27.9	5300	31	1.33	199%	46%
4.5x4.5x4.3	290x140x90	117.9	77.4	87.1	16860	98.6	0.89	133%	31%
6x6x4.3	290x140x90	175.2	103.2	154.8	30840	180.4	0.67	100%	24%

* Source of information: (Batchelder et al., 1985; World Bank, 1989)

Firing the bricks creates a ceramic bond in a specific temperature (900-1200° C) which increases the strength of the brick making it water resistant. Using the right amount of fuel is very important not only for fuel and cost efficiency but also to provide the right temperature for bonding. Low temperature results in poor quality/bonding while high temperature would either slump or melt the bricks. Controlling cold air flow thought the brick kiln is also a key factor to make the kiln more energy efficient. Too much air circulation will cool down the bricks and wastes the energy while too little air flow will stop the fuel from burning properly. Providing dampers and wind breaks to control/protect the fire could greatly improve the fuel efficiency of kilns (Practical Action).

5   BRICK SUPPLIERS

Artisans, small- and medium-scale manufactures are the three major types of suppliers of bricks in Uganda (Table 68). Bricks produced by artisans take a larger share of the market compared to small- and medium-scale manufactured bricks. The handmade bricks and blocks produced by artisans are suitable for single storey buildings. The length of the bricks/blocks may vary between 220-295mm; the width between 100-

150mm; and the thickness between 60-130mm. The weight may also vary between 2.5 and 7.6 kg per brick/block. The final sizes/dimensions of produced bricks and blocks in a lot may also vary greatly (World Bank, 1989). This, in fact has been regarded as the major reason for extensive use of mortar (up to 30mm) in the construction of brick walls (Perez, 2009).

Table 68: Brick production scales (World Bank, 1989)

Production scale	No. of bricks (per day)	Production process	Area
Artisans	1,000	Handmade, clamp fired	Rural areas
Small-scale	10,000	Semi-mechanised	Towns
Medium-scale	40,000	Mechanised	Industrialised areas with high demand

Firewood is mainly used by artisans for brick production. The firing period and temperature are kept low to save as much wood as possible. This results in a rather poor quality bricks and blocks with compressive strengths of usually lower than 8 N/mm^2. Moreover the bricks which are within 300 mm from the external surfaces of the field kilns have a very low quality and are not completely waterproof (Figure 132). The portion of the low quality bricks produced using traditional methods varies between 25% and 45% of the entire production (World Bank, 1989).

Figure 132: Bricks within 300mm of the clamp kiln's surfaces have a very low quality (Tanzania).

Source: The authors

Moreover, around 10-17% of materials is wasted during transportation, handling and construction processes on site (Anderson & Thornback, 2012; World Bank, 1989) which has considerable impacts on the construction sites (Figure 133). Material waste is in fact one of the major concerns which has negatively affected the overall performance of the Ugandan construction industry. Improving the brick quality could, to some extent, address the abovementioned issues.

Figure 133: High material waste during production and handeling (Tanzania).

Source: The authors

6   EMBODIED ENERGY OF FIRED BRICKS

Firewood along with coffee/rice husks are the main fuels used to produce burned bricks in Uganda and Tanzania. The effective calorific value of wood is highly dependent on the water content of the wood and therefore seasonality factors are significant. On average, 0.5 m^3 of wood is required to produce a tonne of clamp fired brick (World Bank, 1989). Assuming a density of 0.56 g/cm^3 (Kumar et al., 2011) and a lower heating value of around 17 MJ/kg (Musinguzi et al., 2012) for Eucalyptus wood, as the major fuel for artisan brick production (World Bank, 1989), an average of 4760 MJ is required to produce one tonne of burned brick. According to the Inventory of Carbon and Energy ICEV2.0, the embodied energy value for "General simple backed clay products" and "General Clay Bricks" is 3.0 MJ/Kg (Hammond & Jones, 2011). This means that the energy consumptions by artisans is 1.6 times more than the required energy for the production of generic fired bricks. Table 69 summarises the fuel consumption and embodied energy of artisan bricks.

Table 69: Embodied energy of burned bricks

Product	Required equivalent fuelwood per tonne of product (m^3)	Energy consumption per tonne of product (MJ)	Energy consumption compared to "General Clay Bricks"
General Clay Bricks	Est. 0.315	3000	100%
Artisan/ Clamp Fired Bricks	0.5	4760	159%

The embodied energy values of artisan clamp fired brick walling and general clay brick walling are also calculated in Table 70. According to the information provided by the World Bank (1989), artisan-produced brick and block dimensions could vary greatly from 220 to 295 mm (length), 110 to 150 mm (width), and 65 to 130 mm (height). An average of 20mm, 1:4 cement mortar with an embodied energy of 1.1 MJ/Kg (Hammond & Jones, 2011) are assumed to calculate the embodied energy of artisan brick walling. It should be noted that mortar thicknesses of up to 30mm (Figure 133) is normally considered to compensate for uneven sizes of bricks in Uganda (Perez, 2009). According to the results, the embodied energy of 300 mm and 220 mm artisan brick walls are 1619 and 1067 MJ/m^2, respectively. Assuming the same brick density and mortar thickness of 10 mm for a "General Clay Bricks" with a dimension of 215x102.5x65 mm (UK standard brick dimensions), the embodied energy of a 215 mm solid brick wall would be 791 MJ/m^2 which is around 26% lower than the embodied of energy of a 220 mm artisan brick wall. The per square metre embodied energy of the 300 mm artisan brick wall is around 100% and 50% higher than the embodied energy of 215 mm General Clay Brick and 220 mm artisan brick walls, respectively.

The results also indicate that walls built with smaller bricks (e.g. 220x110x65 mm) have a lower embodied energy compared to walls constructed with larger bricks (e.g. 300x150x130 mm). This is mainly due to the considerably lower embodied energy of cement mortar compared to fired bricks. In other words, increased mortar to brick ratio for smaller bricks reduces the total embodied energy per square metre of walls due to the much higher embodied energy of fired bricks compared to mortar.

Figure 5: Mortar thicknesses of up to 30mm is normal for brick walling (Uganda)

Source: The authors

Table 70: Embodied energy of brick walls

Product	Brick size, (mm)	Wall thickness (mm)	Embodied energy of material (MJ/Kg)	Mass per item/littre (Kg)	Embodied energy of wall per m²	Embodied energy of (MJ/m³)	Relative embodied energy of walls per m²
Artisan Clamp Fired Brick/Block	300x150x130	300	4.76	7.6	1619	5398	205%
	20mm Mortar		1.11	1.65			
	220x110x65	220	4.76	2	1067	4849	135%
	20mm Mortar		1.11	1.65			
General Clay Brick	215x102.5x65	215	3	2	791	3677	100%
	10mm Mortar		1.11	1.65			

7 CONCLUSIONS

This paper discussed the production processes of fired bricks produced by artisans and small- and medium-scale manufactures in Uganda and Tanzania. Low quality of bricks, high material wastes and excessive energy consumption were identified as the major issues associated with traditional manufacturing processes of burned bricks. The results indicate that the embodied energy of artisan clamp fired brick walling per square metre of the wall is 35% more than generic brick walls with comparable thicknesses. The embodied energy of artisan bricks is also around 60% more than the embodied energy of generic bricks. Yet, considering the high wastes and low quality (and therefore lower durability and shorter lifespan of clamp fired bricks) it could be argued that the overall environmental impacts of artisan bricks is much higher than generic bricks.

The results of this paper also reveal that small kilns can lose between 1.33 and 3.48 times more energy through their cooling surfaces compared with large clamp kilns. Up to 46% of the entire production of small kilns is also under fired, low quality bricks which increases the wastes and breakage rate during handling, transportation and construction on site. It should be noted that burned bricks are one of the major consumers of firewood in East African countries contributing to issues such as deforestation, air pollution, excessive soil extraction and other negative environmental impacts. Improving brick quality and reducing material wastes help to mitigate the negative environmental impacts of fired bricks. Improving the production methods and energy efficiency of brick kilns could also reduce the embodied energy of burned bricks. In this respect, following are recommended to mitigate the environmental impacts of bricks:

a) Encourage the use of unfired bricks/ adobe instead of burned bricks;
b) Encourage replanting trees used for fuel;
c) Provide alternative renewable energy sources as a replacement of fuelwood;
d) Educate artisans to use larger rectangular clamp kilns which are more energy efficient;
e) Provide means to control fire intensity and improve air circulation in kilns to reduce energy consumption and achieve higher quality bricks;
f) Improve the design of kilns and develop affordable heat recovery systems for field kilns to reduce heat losses through radiation and hot exhaust gases.

8 ACKNOWLEDGMENTS

9 REFERENCES

ANDERSON, J., Thornback, J., 2012. A guide to understanding the embodied impacts of construction products, Construction Products Association, London.

BATCHELDER, D., Caiola, R., Davenport, S., 1985. Construction Reference Manual, A source book For the Use of Local materials In Construction, The Experiment in International Living, Brattleboro, USA.

CRAterre, 2005. Earth Architecture in Uganda, Pilot project in Bushennyi 2002-2004; CRATerre Editions.

EMERTON, L., Iyango, L., Luwum, P., Malinga, A., 1998. The Present Economic Value of Nakivubo Urban Wetland, Uganda. IUCN — The World Conservation Union, Eastern Africa Regional Office, Nairobi, Kenya and National Wetlands Programme, Wetlands Inspectorate Division, Ministry of Water, Land and Environment, Kampala, Uganda.

HAMMOND G., Jones C., 2011. Embodied Carbon: The Inventory of Carbon and Energy (ICE). BSRIA, Bracknell, UK.

ILO, 2010. Skills for green jobs in Uganda: unedited background country study, International Labour Office, Skills and Employability Department, Geneva.

KUMAR, R., Pandey, K.K., Chandrashekar, N., Mohan, S., 2011. Study of age and height wise variability on calorific value and other fuel properties of Eucalyptus hybrid, Acacia auriculaeformis and Casuarina equisetifolia, Biomass and Bioenergy, 35 (3): 1339–1344. doi:10.1016/j.biombioe.2010.12.031

MUSINGUZI, W. B., Okure, M. A.E., Wang, L., Sebbit, A., Løvås, T., 2012. Thermal characterization of Uganda's Acacia hockii, Combretum molle, Eucalyptus grandis and Terminalia glaucescens for gasification, Biomass and Bioenergy, 46: 402–408. doi:10.1016/j.biombioe.2012.08.001

NAUGHTON-TREVES, L., Kammen, D. M., Chapman, C., 2007. Burning biodiversity: Woody biomass use by commercial and subsistence groups in western Uganda's forests, Biological Conservation, 134: 232-241. doi:10.1016/j.biocon.2006.08.020

NYAKAIRU, G. W.A., Kurzweil, H., Koeberl,C., 2002. Mineralogical, geochemical, and sedimentlogical characteristics of clay deposits from central Uganda and their applications, Journal of African Earth Sciences 35:123–134.

PEREZ, A., 2009. Interlocking Stabilised Soil Blocks, Appropriate earth technologies in Uganda; HS/1184/09E, United Nations Human Settlements Programme: Nairobi, Kenya.

Practical Action, Ten rules for energy efficient, cost effective brick firing, a guide for brickmakers and field-workers, Practical Action, The Schumacher Centre, Rugby, UK. http://cdn1.practicalaction.org/t/e/541ae1a5-d2f4-4255-928e-54760a000047.pdf (Accessed 20/05/2015)

The Government of the Republic of Uganda, 2001, National Biomass Energy Demand Strategy 2001-2010, The Government of the Republic of Uganda, Ministry of Energy and Mineral Development, Kampala, Uganda.

UBOS, 2010. Uganda National Household Survey 2009/10; Uganda Bureau of Statistics: Kampala, Uganda.

World Bank, 1989. Uganda - Energy efficiency improvement in the brick and tile industry. Activity completion report; no. ESM 97 89. Energy Sector Management Assistance Programme. Washington, DC: World Bank.

111: A design study of an amphitheatre in Delphi: nuances of form, fabric and soundscape

Sat Ghosh[1,2], Rahul Harimohan Pillai[3], Anand Murali[4], Amitesh Roy[5], Saif ul Haque[6]

1VIT University, Vellore, Tamil Nadu, India
2 School of Earth and Environment, University of Leeds, United Kingdom, satyajitg@vit.ac.in
3 VIT University, Vellore, Tamil Nadu, India, rahul.pillai93@gmail.com
4 VIT University, Vellore, Tamil Nadu, India, anandVITA411@gmail.com
VIT University, Vellore, Tamil Nadu, India, amiteshroy94@yahoo.in
6 VIT University, Vellore, Tamil Nadu, India, saif.haque9@gmail.com

The open air amphitheatre at Delphi in Greece is a structure of sublime architectural sanctity that has been the subject of study for ancient theatrical performances. This study explores through architectural and fluid mechanical modelling, the connection between layout, natural topography and the amphitheatre's orientation. A SolidWorks rendition of the centre stage along with the stepped gallery is embedded into sophisticated environmental fluid mechanical software ENVImet, for the very first time. A historical retelling is effected through the inclusion of Delphi's tree-scape around the amphitheatre. In addition, effects of dappled lighting of the mellow Mediterranean sunshine as the shadows lengthened for an evening spectacle is all replicated. Study of the ingress of winds and levels of coolth and warmth in the amphitheatre is also studied. Thereafter, the quality of the direct, reflected and the echoed notes are re-enacted through Autodesk Ecotect modelling. Theatrical grandeur is a subject of utmost importance in the plan of the Delphi Theatre. Exemplary transmission of sound has been achieved by creating a balance between the still surroundings of the slope overlooking the temple of Apollo, which prevents reverberations from external sources, whilst evenly distributing the sound by reflection from the orchestral area – all this is vividly recreated through the combination of architecture and fluid mechanics.

Keywords: Delphi, soundscape, day-lighting, form, orientation.

1. INTRODUCTION

The glory of Greek mythology has deep roots. The congruence in the architectural styles of the Archaic and Hellenic periods, 500 years apart proliferated the start of a rich culture the world had yet to see.

The open air amphitheatre at Delphi is an exemplary structure. Built in the Late Archaic Period (800-400 BC), it was considered the seat of the Oracle at the Temple of Apollo [1]. Geographically located at the foot of Mount Parnassus, the site overlooks the mountain valley with a plethora of vegetation scattered along the slopes, adding to its natural aestheticism. A stage for culture, art and philosophy, the theatre of Delphi has captivated the attention of historians and philosophers for its art and tradition. The Delphi theatre came alive every four years, when it hosted the *Pythian* Games, a forerunner of the modern Olympic Games, commemorating the victory of *Apollo* over the Dragon Python [2].

Although, the 21st century has ushered in an enhanced level of awareness among engineers to design smarter buildings, they often lack the elegance and sublimity of their ancient counterparts. The current emphasis is to build functional buildings – only recently are architects focusing on energy efficiency. This paper has explored idioms that resonate even today in the realms of stage architecture – combining the Delphic marvels with hi-tech fluid mechanical designs.

With the clear sound quality in the Delphi Amphitheatre (without artificial amplifiers), one wonders how modern stage architects can liaise with acoustic engineers to achieve this Delphic wonder. Sound levels of 60-65 decibels, propagated to the most distant row of spectators without any artificial amplifiers [3]. Further, one needs to address the question of optimum spacing between each row for an Amphitheatre and finally, the building fabric properties, not only modulates the sound transmission, but also the stage comfort level. These are some of the over-arching issues the paper has addressed.

The scheme of the paper is as follows: First, a brief discourse has been presented on the tools used for modeling and various analyses on the theatre. Thence, the importance of the embedded landscape around Delphi is highlighted. Following this is a section discussing the properties of the limestone fabric. Quantitative analyses of solar exposure, wind patterns around the theatre, and predicted mean vote, an index of comfort, in and around the theatre, follows. The acoustic measurement of the theatre concludes the paper.

The requirement of software for suitable rendering of the design and its analysis was fulfilled primarily with the help of **DSS Solidworks** [4]. This design package by *Dassault Systemes* has been used for the reconstruction of the Delphi theatre. It provides a very user friendly Graphical User Interface. With strong modeling tools, this package was employed for the reconstruction of the theatre under study. The analysis of the temperature profile as well as sun path measurements were carried out on **Autodesk Ecotect** [5], the primary use of which, is for the study of energy, light and solar heat gains and savings. Wind flow patterns of the surrounding area were computed with respect to the wind velocity vectors with the help of **WinAIR 4.0** and then embedded into Autodesk Ecotect. The rendition of sound analysis was also carried out in **Autodesk Ecotect**. Post modeling of the theatre embedded into a landscape setting was designed in **Google SketchUp** which included visual surface patterns [6]. Finally, an analysis on the comfort levels of the theatre was carried out on **ENVI-met** [7].

This is perhaps the first study that combines the air flow around the Delphi theatre based on accurate microclimatic prescription. Moreover, the paper also showcases a systematic use of modeling tools to discern telling facets of Delphi's unique orientation, form, light and soundscape vis-à-vis, its fabric properties. The study also seamlessly combines the rigors of CFD with the romances of Greek Amphitheatre.

2. LANDSCAPE

The landscape has a considerable significance on the theatre's appeal to the crowd. The appropriately chosen location for the site, over the mountainous slopes, sets a cool ambience with the right temperature for the theatrics and visitors. The theatre was located outside the city, ridding the plays off any adulterated sounds which was necessary for the theatrics [8].The gentle mountain slope added to the stillness around the theatre while the valley created a beautiful backdrop. As most of the events were held at either dusk or dawn, it was in regular practice that the sky had a beautiful tinge of orange, which added to the surreal surrounding. All of these elements were seamlessly incorporated with the theatre, through a harmony

between the structure and the landscape. Moreover, the theatre could have been built from the limestones locally quarried from the adjacent Mount Parnassus.

The paper now discusses how the structure performed with the embedded landscape qualitatively.

3. STRUCTURAL REMODELING

A structural remodeling of the Delphi Theatre was carried out in order to perform the acoustic analysis. This was done in DSS SolidWorks and then imported to Google SketchUp where visual enhancement was carried out by adding the landscape features along with the trees and surface materials. Figure 1(b) & 1(a) respectively, show the comparative view of the remodeled structure of the theatre in Google SketchUp along with the top view image on Google Earth.

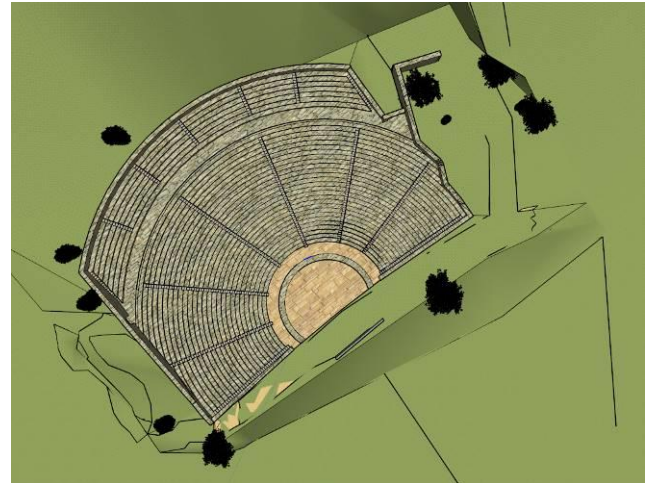*Figure 1(a): Plan view of the Delphi theatre landscape from Google Earth*

Figure 1(b): Plan view of the Delphi theatre landscape rendered in Google SketchUp

The main features of the theatre have been shown in figure 2. Figure 2(a) shows the top view. The semi-circular centre is the *Orchestra,* which held all the performances by actors, singers and dancers. The crowds were let into the theatre through the entries on either side of the *koilon.* The *koilon* includes the entire semi-circular structure of the amphitheatre. The entries from either side lead to the *cavea* which divides the upper and lower *koilon*, further parted almost equally into six on the lower and seven on the upper *cunei,* respectively [9]. The *cunei* were separated by staircases, which allowed people to move along the column to reach their allotted rows. The bottom rows were mostly reserved for distinct dignitaries, while the subsequent ones were kept open for the common folk.

A recent renewal has revealed that the Delphi theatre has been through significantly rough external pressure from climatic agents, for centuries. The absence of the *skene* is a possible indication of the influence of time on the qualitative features of the theatre. In its current state, the existence of this important feature, which is assumed to have transmitted some of the direct sound rays through reflection, can only be vaguely established.

In this paper, the remodeled version of the theatre has omitted the presence of the *skene*, owing to the dubiousness arising from the factor of geographical forces, having completely marred the structure from its original form, since ancient times.
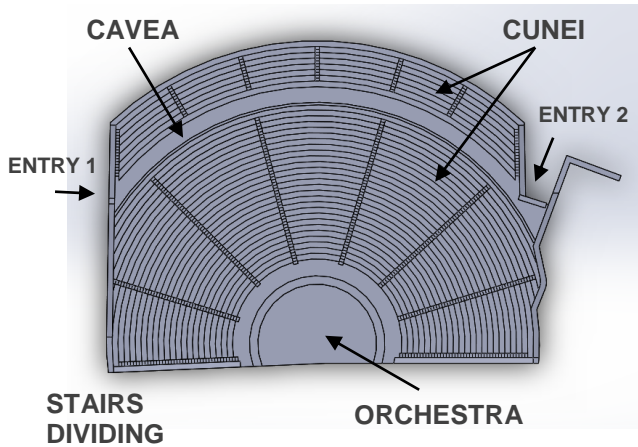
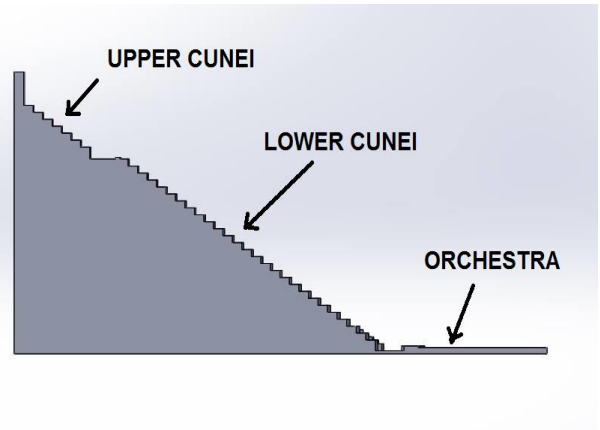Figure 2(a) – Rendered top view of the theatre

Figure 2(b) – Sectional view of the theatre

The specifications of various features of the theatre are shown in Table 1. An important parameter to be taken into account is the number of rows. A possible conclusion of the considerable number of rows reserved for the art loving folk is the perception of the importance given to theatre among other forms of Grecian Art. The capacity of the theatre is roughly established to be between 3000-5000 [10].

Table 88 - Geometrical specifications of the Delphi Theatre

Component	Number / Dimension
Orchestra Diameter	18.4 m
Theatre Height	15.5m
Slope angle	34.29°
Cavea Width	52 m
Number of *Cunei* (Upper)	6
Number of *Cunei* (Lower)	7
Cunei Angle (mean)	31°

With respect to the overall height of the amphitheatre, a simple observation can be derived from its effect on the transmission of sound. A greater overall height would result in a higher probability of transmission of direct sound to the audience, but another noteworthy observation is the increase in sound attenuation [11]. In order to minimise such a loss, an optimum height was perhaps deduced by the architects of the theatre.

4. AMPHITHEATRE FABRIC

A thorough scrutiny of the fabric of the Delphi Theatre in its current state revealed that the architects of the period used white limestone as the material for the seats of the *cavea* as well as the orchestra. The pristine limestone was perhaps locally quarried from the nearby Mount Parnassus [12]. This limestone, while still in its original form, is capable of reflecting sound waves as it was built for, thus establishing its durable nature as a fabric. Most of the incoming sound waves are reflected off the surface of limestone while a very small portion is absorbed (See Figure 7). Only some of the exclusive parts may have been made of marble, however, most of these have perished by centuries of erosion. Nevertheless, the limestone fabric has time and again through modern analyses, proved to be a contributing factor to the enhancement of sound within the theatre.

SUSTAINABLE CITIES & ENVIRONMENT

Table 2: Fabric Property Specification

Property	Value
Density	2500 kg/m^3
U-Value	2.6 W/m^{2}K
Porosity	0.31 % vol.
Water Absorption	0.14 Dry Mass.
Specific Heat	0.91 KJ/Kg-K
Heat absorbed per Volume	2.193 MJ/m^{3}K

Besides rendering a smooth acoustic scape, the limestone plays another important role – improving levels of thermal comfort within the theatre. The moderately high thermal mass of the limestone is responsible for absorbing heat during the day, whilst dissipating it at the onset of dusk. The thermal mass depends upon the specific heat and the heat absorbed per unit volume of the limestone – these values are shown in table 2 [13].

5. ANALYSIS OF SOLAR EXPOSURE, WINDS AND TEMPERATURE BASED ON ORIENTATION

The orientation of the theatre was embedded into Autodesk Ecotect, facing south-east. A discourse on the solar exposure, winds and temperature is mentioned below.

Solar Exposure

Solar exposure, an important parameter, affects the comfort level of the theatre. On a hot day in summer, the discomfort within the theatre due to solar heat was observed to be an inconvenience. A sun path diagram at dawn and dusk with shadows is shown in figure 3(a) and figure 3(b) respectively. Average time for dusk and dawn has been taken into consideration in order to trace the sun path diagram.

As can be seen from figure 3(b), the time before dusk may have been the most favorable for theatrical performances owing to the stage being covered by the shadows which would have been appropriate for holding any theatrical performances.

From a perspective of economic prudence, by the assumption that if plays were held in the earlier hours of the day, the tax collectors could have levied more fee for the cuenies on the right as they were in the shadows, which can further imply where the aristrocrats, wealthy merchants and other notable digniteries may have had their seats.
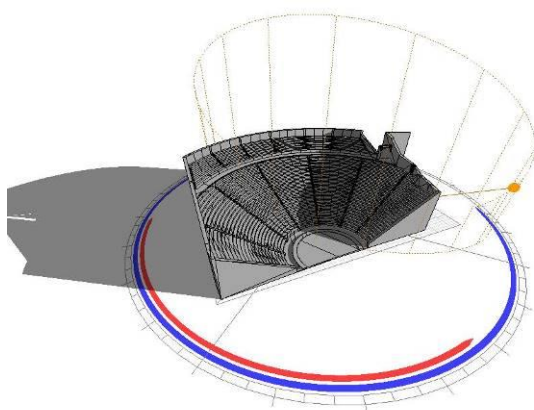

Figure 3(a) – Sun path diagram at 6.30 AM, illustrating areas of shade and light, adding to the dramatic allure of the theatrical performance. Also, note extended shades where the spectators can be comfortably seated.
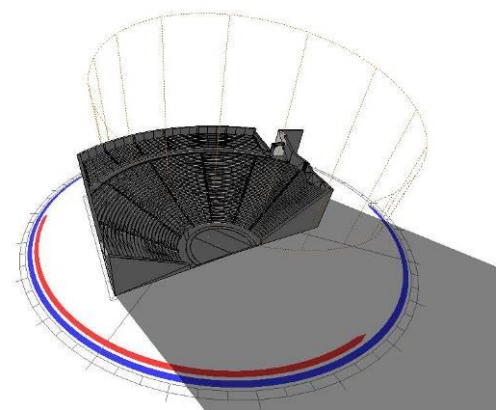
Figure 3(b) – Sun path diagram for 7.00PM. Simulation during dusk of June 21st

Temperature Distribution inside the Amphitheatre

A complete understanding of the temperature contour given in figure 4 below reveals that even with the solar insolation at its highest, the temperature at the steps should be moderate. Note that the temperature throughout the cavea is below 19^0 C, with temperatures at certain points in the theatre as low as 15^oC. This is desirable, because it implies that the seats are not over-heated due to prolonged exposure to the sun during the day and it directly links to the thermal mass of the limestone as discussed in section 4.
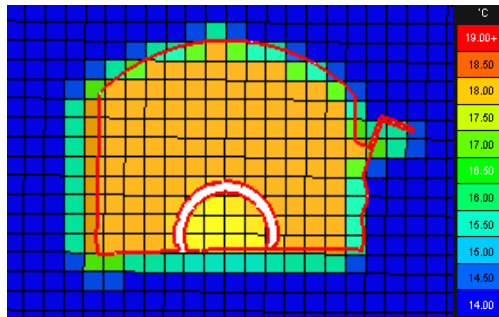

Figure 5 – Temperature contours in the Delphi Amphitheatre, note the yellow band with the temperature ranging in the high teens, even for the hottest months of

Thermal Comfort Indices in the Delphi Theatre

Since the solar insolation heats up the Delphi Theatre diurnally as discussed in the previous section, the boundary layer in contact with the surface warms up and sets up localized wind currents. The evening spectacle is typically assumed to be around 6 p.m. and it is essential that we show case the meanders, twists and turns of the wind flow in and around the Delphi Theatre.

Salubrious Wind Flow Pattern

Much of the Delphi Theatre's sound quality is a reflection of the influence of the ingress of the south eastern winds directed towards the koilon. The calm fervour of the voices of the actors is a result of the soft breeze from the south west. These winds were analysed in WINAir 4.0 and then simulated in Autodesk Ecotect. The Figure below shows the vectors of these winds at two different levels from the ground. Figure 6(a) is a plotting of velocity vectors within the orchestra and around the theatre at the ground level. Figure 6(b) is a similar plotting, midway up the lower cunei. The plot legend shows 0.6 m/s of wind speed emanating from the centre of the orchestra, travelling in the direction of the audience. This is an optimum level of ingress for the path of melodious sound to reach the ears of the anticipating crowd in the early hours of dusk.

It is clear that during the months of May - June when the Solar Insolation are at their highest and when the evenings are the longest, the performances are at their prime. The spectators are also amply aerated – one can see the presence of vortical structures (see figures below with vectors turning at the corner) where the wind speeds are a comfortable 0.2 m/s.
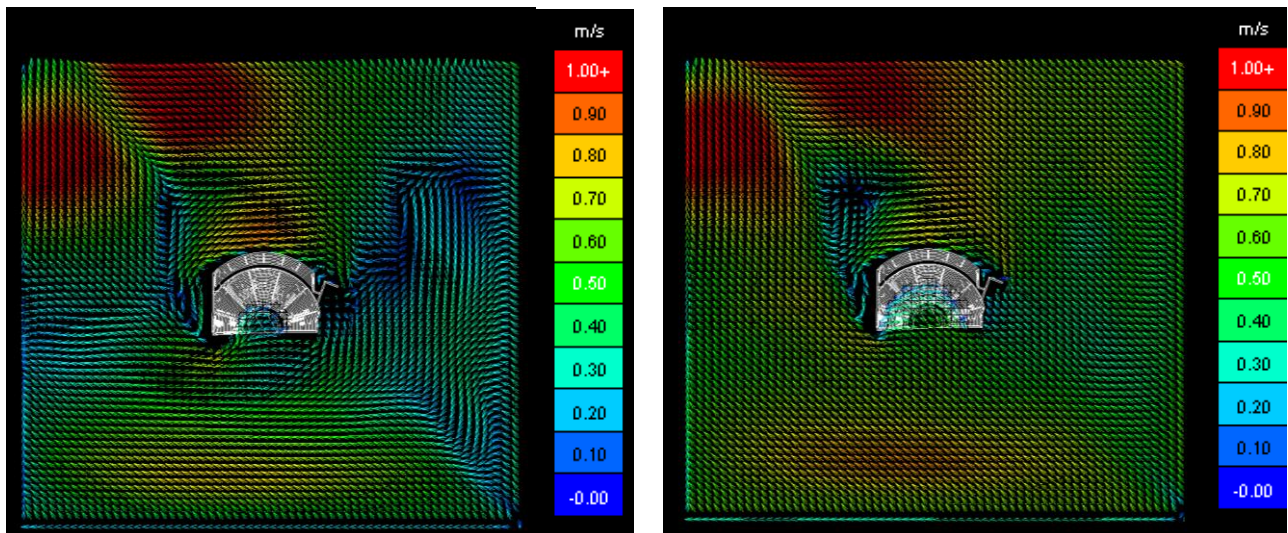
Figure 6(a) – Wind flow patterns at the ground level contrasted with flow pattern at a higher level shown in the neighboring figure.

Figure 6(b) – Flow of wind around the Delphi at the level of the cavea.

Comfort Index

Another closely associated index is the *Predicted Mean Vote (PMV).* The comfort index is given by the Predicted Mean Vote. It defines the thermal satisfaction through a subjective analysis of the environment. The method is based on the principles of heat balances in a controlled climate chamber under steady state conditions [14]. The range of PMV is shown in table 3. From the table it can be said that a range of -1 to 1 is desirable.

Table 89 - Predicted Mean Vote value and the corresponding sensation

Value	Sensation
-3	Cold
-2	Cool
-1	Slightly Cool
0	Neutral
1	Slightly Warm
2	Warm
3	Hot

The PMV analysis of the theatre was carried out in ENVI-met, with an area of 300 m x 240 m resulting in 100 x 80 x 30 cells with a resolution of 3 m x 3 m x 2m. The trees are assumed to have heights less than 15 m and are dense with a distinct crown layer, as can be seen from figure 5. The simulations were carried out for 23rd May 2013 with the initial temperature being 25°C.

Figure 5 – The plan view of the Delphi Theatre and surrounding landscape in ENVI-met. Note: the green areas signify tall trees and the

A wind speed of 2.8 m/s at 10 m above the ground level is assumed in the north-west direction. The relative humidity is set at 60% at the start of the simulation. The height has been set to 10 m above the ground level, by assuming a mean height for the entire theatre, where the entire 3D structure has been sandwiched to create a plane on which the PMV analysis was required to be carried out. The Predicted Mean Vote is shown in figure 6 below at 6 PM on 23.05.2013.

As can be seen from the figure, the region around Delphi is somewhere in between 0.56 to 1.59, with 0.56 in the area near the orchestra. The observations were deduced at neutral to slightly warm conditions even during the hottest months of May-June, predicting that the spectators and performers had been comfortable

even during the climates spanning over this time period. Thus, this paper demonstrates, through high end computational fluid dynamics, that the stepped amphitheatre modulates wind patterns and adjusts the temperature profile therein, to an extent that both the performers and the spectators are ensured of a pleasant spectacle.
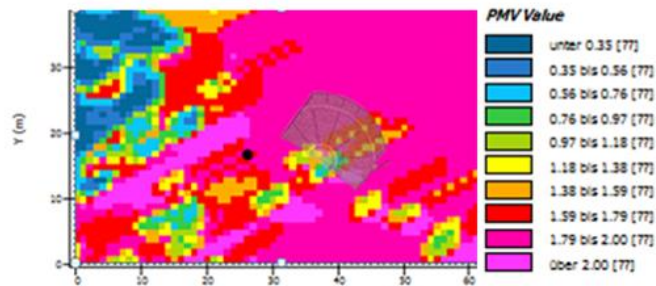
Figure 6 – PMV values in and around Delphi.

The next focus of attention is how the established wind flow patterns carry speech and musical notes across.

6. ACOUSTICS OF DELPHI THEATRE

The use of spatial freedom, form and fabric to enhance sound quality, having been established, requires a deeper understanding through the analysis carried out on Autodesk Ecotect. The basic idea was to compute the sound levels of optimum speech volume over various steps of the amphitheatre. An acoustically well qualified room or system, irrespective of whether the setting is an open or closed environment, is judged on the basis of the clarity of speech. This clarity is inversely related to the time taken for sound from a direct source to decay completely after reflections from surrounding surfaces, called as the reverberation time. This masking or overlapping quality of sound is an implication of higher reverberation time. Suffice to say, whether the architects of the Greek amphitheatres were scientifically equipped to work with such sophistication is unknown to us, nevertheless their sense of orientation is exemplary in its compatibility with the natural surroundings.

Figure 7 – The distribution of direct, reflected and echoed rays

A profile of direct, reverberated, and echoed rays were rendered using Autodesk Ecotect (as shown in figure 7). Among the rays generated, it was observed that the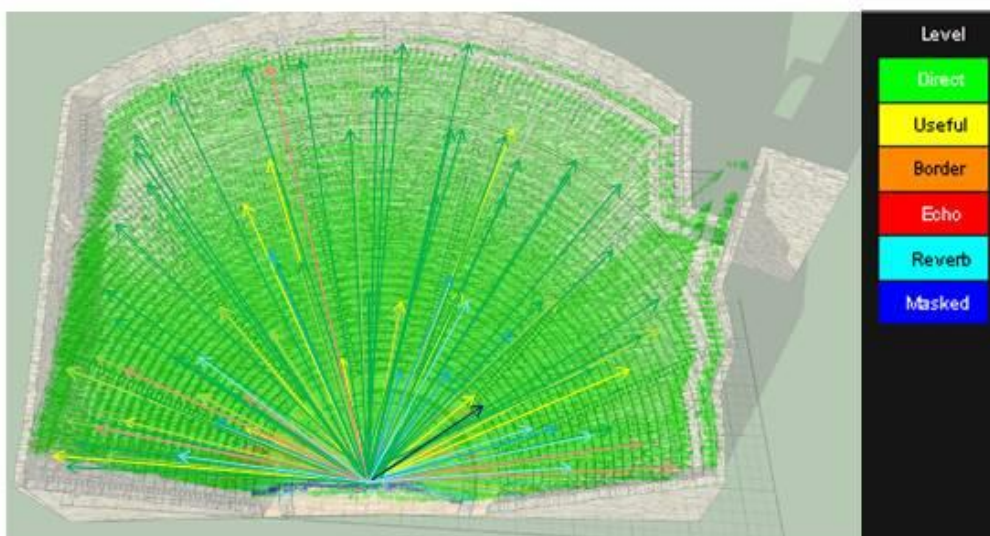 green (direct rays) were the most pervasive, constituting more than 80% of all the generated rays, and the yellow (reflected) were confined to the periphery, constituting about 10% of all the generated rays. The red lines, showed the presence of echoes, were limited to less than 2.5% (10 in 413) of the generated rays, while the masked rays (represented by dark blue lines) were confined to less than 1.5% (5 in 413) of the total rays. The reverberated rays (light blue lines) constituted around 12% of the generated rays. Moreover, the effect of reverberation was more profound only in the lower *cunei,* as none of the reverberated rays reached the last row of the upper *cunei.* This can be attributed to the open conical structure of the theatre.

The attenuation loss in the theatre is shown by figure 8. The legend can be interpreted as decrease in decibels at a particular point in the theatre as a demarcation from its original decibel level. The decibel levels throughout the theatre more or less remained without any loss, except for the extreme *cuneis,* two on each side of the theatre*,* which suffered a maximum loss of 1.4 dB. This is perhaps a result of the absence of upper cunei on the sides of the theatre, resulting in early reflection of sound rays travelling in this direction, in contrast to those propagating to the upper cunei, subsequently causing a pronounced loss of decibels.
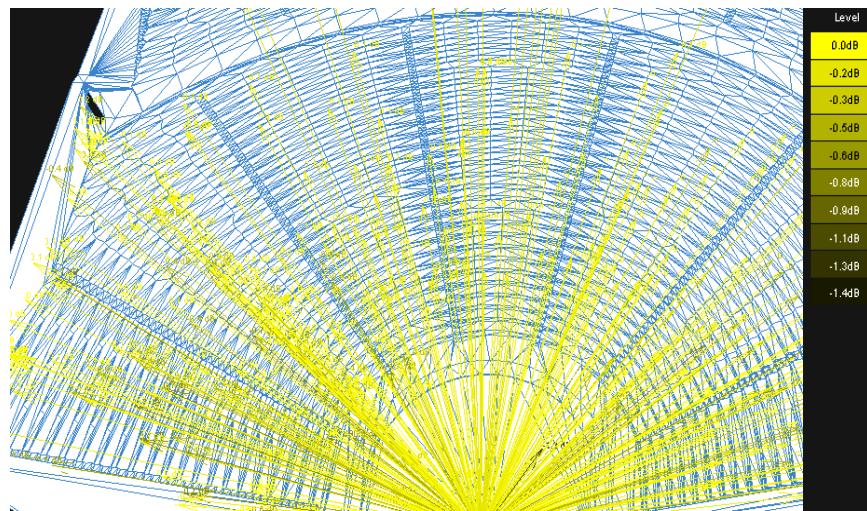
Figure 8 – The attenuation loss in decibels at various parts in the theatre.

7. CONCLUSION

This paper showcases the prowess of modern architectural modelling coupled with computational fluid dynamical analysis. The primary focus was to ascertain the levels of spectator comfort within Delphi's famed Amphitheatre, followed by a discourse on its acoustic profiling. Simulations done for the hottest day of the year show that the unique stage form and fabric complemented its orientation and positioning so perfectly that the spectators and the performers were always comfortable. A detailed day-lighting analysis, again for the month of May, yielded large swathes of shaded areas. Finally and quiet remarkably this piece by piece reconstruction, showed in telling details, that even a sound level of 60-65 decibels reached the farthest nooks and crannies of the theatre, with the least of acoustic interference and echoing effects. It is anticipated that this analysis will be an aid to architectural modellers worldwide, to vividly recreate many such sites scattered across all the continents, most notably in Asia, Europe and ancient Egypt.

8. REFERENCES

[1] KONSTANINOU, Ioanna, Delphi: the Oracle and its Role in the Political and Social Life of the Ancient Greeks, Hannibal Publishing House, Athens.

[2] CHAPPELL, Mike, Dec., 2006, Delphi and the Homeric Hymn to Apollo, the Classical Quarterly New Series, Vol. 56, No. 2, pp. 331-348, Published by: Cambridge University Press on behalf of The Classical Association.

[3] KREITH, Frank, The CRC Handbook of Mechanical Engineering, Second Edition, Section 20, p 79-83.

[4] SOLIDWORKS, 2014, registered to VIT University, Vellore, by Dassault Systemes, 2014.

[5] Autodesk Inc., Autodesk Ecotect Analysis, 2011, http://usa.autodesk.com/ecotect-analysis/

[6] SKETCHUP 2014, Google, Google SketchUp Workshop: Modeling, Visualizing and Illustrating, Focal Press, 2010.

[7] ENVI-MET v3.1, December 2009, Michael Bruse, http://envi-met.software.informer.com/3.1/

[8] BERVE, H., Gottfried, G., 1963, Greek Temples, Theatres and Shrines, New York: Harry N. Abrams(1962), ID-3089, Archaeologia Books and Prints.

[9] RUZZA, Lucca, Tancredi, Maurizio, 1987, Storie degli spazi teatrali (History in the theatre spaces), Vol.1, Published by Euroma Goliardica, Roma.

[10] ANANIADES, D., 2010, Ancient Greece: Temples & Sanctuaries, Toubis, Athens.

[11] MOH'D Basem K., June 2009, Compressive Strength of Vuggy Oolitic Limestones as a Function of Their Porosity and Sound Propagation, Jordan Journal of Earth and Environmental Sciences, Volume 2, Pages - 18-25.

[12] PAPAGEORAKIS, J., Kolaiti, E., 1992, The Ancient Limestone Quarries of Profitis Elias near Delfi (Greece), Ancient Stones: Quarrying, Trade and Provenance: Interdisciplinary studies on Stones and Stone Technology in Europe and Near East from the Prehistoric to Early Christian Period, Part 1, Pages – 37 – 39, Leuven University Press.

[13] DERNIE, David, 2003, New Stone Architecture, Laurence King Publishing.

[14] LINDEN, Willemijne van der, Loomans, Marcel and Hensen, Jan, 2008, Adaptive Thermal Comfort Explained by PMV, Proceedings of the 11th International Conference on Indoor Air Quality and Climate, p.8, Copenhagen: International Centre for Indoor Environment and Energy, Technical university of Denmark.

121: Investigating the role of façade design in improving energy efficiency for residential tall buildings in Saudi Arabia

Noura Ghabra [1], Philip Oldfield[2], Lucelia Rodrigues[3]

1 University of Nottingham, Department of Architecture and Built Environment, University Park, Nottingham, NG7 2RD, United Kingdom, laxng5@nottingham.ac.uk
2 University of Nottingham, Department of Architecture and Built Environment, University Park, Nottingham, NG7 2RD, United Kingdom, philip.oldfield@nottingham.ac.uk
3 University of Nottingham, Department of Architecture and Built Environment, University Park, Nottingham, NG7 2RD, United Kingdom, lucelia.rodrigues@nottingham.ac.uk

In Saudi Arabia, 53% of the primary energy is consumed in the residential sector due to the significant use of air conditioning to cool the indoor spaces. Moreover, actively conditioned tall building poses many environmental challenges as major contributors to CO2 emissions arising from the combustion of fossil based fuels. Despite the efforts reflecting the government's growing concern about domestic energy consumption, the scattered conservation efforts have been largely ineffective. As for the local building codes, the typical approach deals only with the minimum requirements of the 'engineering parameters' of building envelope (e.g. adjusting glazing and wall properties, thermal transmittance values), without addressing the façade's 'architectural design parameters' such as shading devices and intelligent use of transparency and opacity, that interact with the building design and have an impact on performance of the building.

In this paper, the authors explored the hypothesis that the current approach focussing on the façade's engineering parameters is not sufficient to achieve the necessary energy efficiency in residential tall buildings in the hot climate of Saudi Arabia, and architectural design parameters, which are less common in their application in the region, could be explored to reduce cooling loads. In order to investigate this hypothesis, the current architectural characteristics of residential tall buildings in the region were identified to establish a representative hypothetical base case in the city of Jeddah, and then 27 sets of dynamic thermal simulations were compared. The best and worst combinations of glazing ratio, wall and glazing type were identified in order to understand the most influential parameter impacting the cooling energy loads in the building. The findings suggest that the difference between the best case and worst case build up ranges between 92 and 128%, outlining the huge role even simple facade design changes can make in terms of energy performance.

The work aims to contribute to the effectiveness and potential enhancement of building codes and regulations for residential tall buildings in Saudi Arabia, especially in terms of energy efficiency measures and benchmarks, and the quality of indoor environment for this building type.

Keywords: Energy Efficiency, Tall buildings, Residential, Façade Design

1. INTRODUCTION

The energy demand in the Gulf Cooperation Council (GCC), consisting of Saudi Arabia, the United Arab Emirates, Qatar, Bahrain, Kuwait and Oman has been increasing sharply in the last decades as a result of the rapidly growing population and the expansion in industrialisation and mega-scale projects. Power generation plants in Gulf countries are conventional fossil fuel thermal plants, using natural gas, heavy fuel oil, crude oil and diesel oil (Obaid and Mufti, 2008). Consequently, this dependence on hydrocarbons made the six GCC countries some of the top contributors to pollution in the world (Reiche, 2010), which emphasises the need for ecological modernisation and environmental improvements in the region. In Saudi Arabia, 40% of the total energy is used by utilities (electricity and water), and 53% of this primary energy is consumed in the residential sector due to the significant use of air conditioning to cool indoor spaces (Lahn and Stevens, 2011). This means that residential buildings account for more than half of all delivered energy consumption across the country, and can be regarded as major contributors to carbon dioxide emissions arising from the combustion of fossil based fuels.

Rapid development in the region is strongly associated with tall building construction, that led to the ascending race to build the world's tallest building – currently the Kingdom Tower in Jeddah, which will rise over 1km in height upon completion in 2018. In the city of Jeddah, on the west coast of Saudi Arabia, 56% of tall buildings are residential or includes residential floors. Despite the fact that most of the tall buildings in the region are residential, very few studies have been conducted regarding the environmental performance of this building type. The increased prevalence of residential tall buildings and the high residential energy and air-conditioning requirements in the hot climate of the region led to a major research question: how can we increase energy efficiency and reduce energy consumption in residential tall buildings in the region?

According to Brown and DeKay (2001), three factors have a major influence on a building's energy use; (1) climate, (2) program (function and occupancy) and (3) form (envelope, building shape and construction). Also, the building systems and their efficiency significantly impact the energy use. The buildings' envelope is responsible for a significant portion of the total energy consumption in the built environment; Lam and Li (1990, cited in Haase and Amato, 2006) have analysed the energy consumption for office buildings in Hong Kong, and found that the building envelope design accounted for 36% of the peak cooling loads. Elkadi et al. (1990, cited in Al-Hosany, 2002, p.33) has simulated office buildings in Abu Dhabi, and found that the building envelope was responsible for 30% of the building's total cooling loads (solar, glass and fabric). However, the rapid urbanisation in the region in addition to the availability of cheap heating and cooling energy has created tall buildings with semi-transparent to fully glazed facades, which relied completely on extensive mechanical air conditioning dependant on low cost, fossil fuel derived electricity. Therefore, the work presented in this paper focused on the building envelope factor in reducing energy consumption in residential tall buildings.

1.2. Building codes and regulations in the region

The development and implementation of building codes and standards should be one of the highest priorities to help reduce energy use and increase energy efficiency in buildings. Reflecting on the current energy regulations and the local green building codes and rating systems, it is apparent that the GCC countries have adopted a more pro-active approach toward environmental issues which started to set a trend amongst decision makers and developers in the region. In the United Arab Emirates, the government of Abu Dhabi launched the Estidama Program and the Pearl Rating System (PRS), which are expected to be integrated into the building code. Further to that, the Green Building Code (GBC) in Dubai has been established and The Electricity and Water Authority in Dubai issued the second phase of its Green Building Regulation in April 2010 that aimed at reducing energy demand in new buildings by up to 40% (Meir et al., 2012). In Qatar, there is an emerging GBC which is also promoting the Qatar Sustainability Assessment System (QSAS), an assessment tool for green buildings. Interestingly, QSAS is now being evolved into a regional code for the Gulf region in the name of Global Sustainability Assessment System (GSAS) soon to be adopted by other GCC countries as a regional green building code (Construct, 2012). In Saudi Arabia, The Saudi Building Code (SBC) was set up based on the International Code Council (ICC) and published in 2007. It included The Saudi Building Code Energy Conservation Requirements (SBC 601) that is based on the International Energy Conservation Code (IECC). These requirements establish minimum perspective and performance- related regulations for the design of energy-efficient buildings and structures (SBCNC, 2007).

In general, there are two approaches for compliance with building codes: the 'prescriptive approach', which sets minimum requirements for energy efficiency in buildings for building envelopes and systems, and the 'performance approach' (also mentioned as the 'simulation method' or the 'building performance rating method'), which is to obtain a building efficiency level by comparing the performance of the real building (proposed design) with a similar building (standard design) whose enclosure elements and energy consuming systems are designed according to a reference requirement. The Saudi Building Code Energy Conservation Requirements (SBC601) and Dubai Green Building Regulations and Specifications (GBRS) outline both approaches for compliance, while the Estidama Pearl Building Rating System (PBRS), used in Abu Dhabi, specifies a Performance Approach. The Global Sustainability Assessment System (GSAS) from Qatar introduces a new approach of setting minimum target for energy performance at a building level.

However, in terms of façade design, current energy codes, regulations and environmental guidance only consider the minimum thermal requirements of building envelopes, such as adjusting glazing and wall thermal transmittance values (Meir et al., 2012), with little consideration for architectural design parameters such as shading devices, the balance between transparency and opacity, or diversity of building form and organisation, all of which can have a significant impact on energy performance.

Consequently, the aim of this study was to compare common high-rise facade design strategies of tall buildings in the Middle East, in order to identify the most promising and least promising arrangements. In doing so, two objectives were pursued:

1) The identification of the limitations of current façade design approaches and building regulations for residential tall buildings in the Gulf Region.

2) The comparison of energy performance of current facade design approaches with local building codes and green buildings regulation in the Gulf Region.

2   RESEARCH METHODOLOGY

The city of Jeddah, located on the western coast of Saudi Arabia, was the primary location for this work as it is growing into a future tall building hub in the region. In order to achieve the work's objectives, a parametric study through dynamic building simulation, using Tas software by EDSL, was used to evaluate the thermal performance of the building envelope and determine the energy demand for cooling, in a hypothetical base case representing typical residential tall buildings in the region.

Tas is a building modelling and simulation tool capable of performing dynamic thermal simulation for buildings. It allows for an accurate prediction of energy consumption, CO_2 emissions, operating costs and occupant comfort. The dynamic building simulations in Tas are conducted through an hourly analysis of the thermal state of the building throughout a typical year based on weather data selected by the user, which result in 8760 data outputs for each simulated variable (EDSL, 2012). The weather file for Jeddah, containing the hourly data for one year (2005) from EnergyPlus, was used in the simulation. The analysis of Jeddah's climate concludes that the climate is predominantly hot with high relative humidity levels. Due to Jeddah's latitude, nearly half of the year, from April till September, the sun could appear in northern part of the sky dome. In addition to the high solar altitude all year around, the clear and cloudless sky allows the abundant solar radiation to cause surface heating and raise the air temperature. Therefore, minimising heat gains and maximising heat loss are key considerations especially in the warmer seasons.

2.1 Base Case Model Formation

According to Hamza (2004) there are two methodologies underpinning the construction of a base case morphology: the existing base case and the conceptual base case. In the context of this research, a conceptual base case was constructed as a hypothetical building compiled from statistical data based on the findings of a qualitative and quantitative analysis of 12 residential buildings in Jeddah, Dubai and Abu Dhabi. For over a year, data was collected on residential tall buildings numbers and architectural characteristics. Several sources of information were identified and consulted, including: literature review of previously published work, local building codes and regulations, the Skyscraper Centre data base of the Council on Tall Buildings and Urban Habitat (CTBUH, 2014), the Municipality for the city of Jeddah, and interviews and contacts with building architects, engineers, developers and managers. The literature review and dimensional audit in the buildings surveyed were undertaken to develop a benchmark building that is representative of a residential tall building located in the city of Jeddah in Saudi Arabia.

The base model was then created considering several building design aspects such as building storey count and height, floor-to-floor height, core location, building plan geometry, and lease span. The overall architectural and engineering specifications that have been assumed for the base case model are outlined in Table 1, with a typical floor plan in Figure 1.

The simulation model consisted of five mid floors with the middle floor considered for data analysis. The results were plotted for eight perimeter zones only since they will reflect the thermal performance of the building envelope; these are marked in Figure 1. Each analysed zone was 6 x 6 and faced a different orientation: North, South, East, West, Northwest, Northeast, Southwest, and Southeast. The internal conditions for the simulated zones were set for a 24hrs air-conditioned space, with an infiltration rate of 0.57 ach for 24 hours –set according to the required value in the Saudi Building Code Energy Conservation Requirements (SBC601). The temperature set-point was set according to the thermal comfort range for Dubai GBRS, which is 22.5 to 25.5 °C.

Table 73 Base case building specification (Source: Author)

Parameter	Base Case Building Assumptions
Total Building	
Location	Jeddah, Saudi Arabia
Height	223.2m
Storeys	62
Core location	Central
Building plan form	Square
Residential Floor Plan	
Typical floor GFA (m²)	1296
Typical floor NFA (m²)	1040
Floor Plate Efficiency	80.2%
Typical floor lease span (m)	10
Floor-to-floor height (m)	3.6
Envelope to floor ratio	0.5
Number of apartments per floor	8
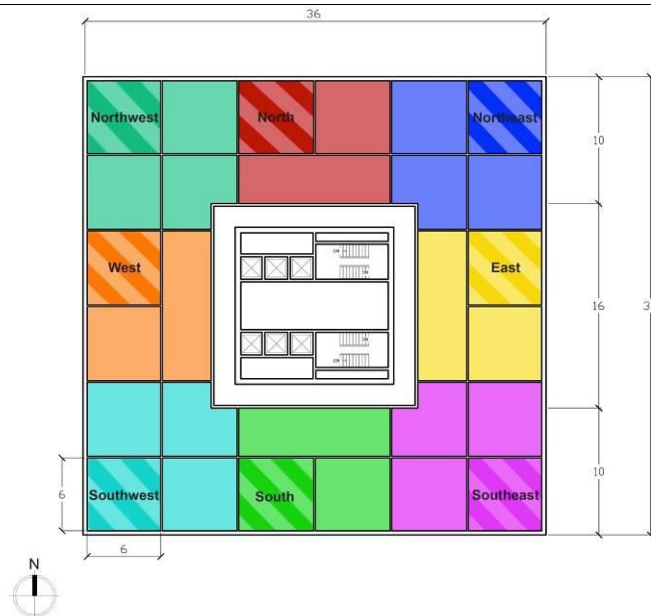
Figure 134 Base case building typical residential floor plan consisting of eight flats per floor. Each flat is represented by a colour in different orientation, and in each flat, one 6x6 space is tested and analysed for the results

2.2 The Simulation input Parameters and Assumptions

The focus of the simulation was to investigate the impact of different building façade parameters on the thermal and energy performances of a residential tall building in Jeddah. The selection of façade

parameters was based on the most common characteristics specified in the local building codes (SBC601 and Dubai GBRS). These consisted of wall U-value and glazing U-value (W/m²k), and glazing shading coefficient (SC), which is based on the façade glazing ratio (%). The output metric to express the results is the annual cooling loads per metre square of the floor area (kWh/m2) for the perimeter zones. Three types o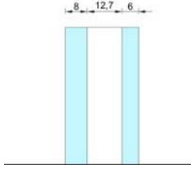f wall construction and glazing compositions with different thermal transmittance values (Table 2 and 3) were selected based on the findings of the building survey mentioned earlier. Also, three glazing ratios were chosen: 20%, 40% and 60%. Each parameter was changed one-at-a-time with the aim of identifying the most influential parameter in terms of perimeter cooling loads. Table 4 illustrates the matrix for 28 sets of simulations: the base case representing the case study as built is labelled (20-UCW-32) meaning a 20% façade glazing ratio, unventilated cavity wall type and a 32mm thickness double insulated glazing make-up.

Table 74: Wall Construction Types for the simulation (Source: Author)

Wall Construction Types	U-value	Section
a. Unventilated Cavity Wall (UCW) Total thickness 204mm Layers from outside to inside: 1. Aluminium Cladding (4mm) 2. Unventilated Air Cavity (100mm) 3. Gypsum Blocks (60x60x10cm)	1.13 W/m²K	
b. Thermal Blocks Wall (TBW) (as per Estidama specifications) Total thickness 300mm Layers from outside to inside: 1. Concrete block (70mm) 2. Expanded polystyrene (160mm) 3. Concrete block (70mm)	0.21 W/m²K	
c. Shadow Box Spandrel Glass (SSG) (The Gate District Tower in Abu Dhabi) Total thickness 137mm Layers from outside to inside: 1. Monolithic heat strengthened glass (6mm) 2. Rigid powder coated aluminium (1mm) 3. Air cavity (80mm) 4. Rigid Rockwool Insulation (50mm)	0.3 W/m²K	

Table 75 Glazing compositions for the simulation (Source: Author)

Glazing composition	U -value	Shading coefficient	Visible light Transmittance	Section
a. 32mm Double Insulating Glass (32 DIG) - 6mm K-LITE -14 ON tempered - 20mm air space - 6mm EFG tempered Clear colour (Cornish Dreams, Jeddah)	2.7 W/m²K	0.23	13	
b. 28mm Double glazing insulated unit (28 DIG) - 6mm heat strengthened glass with solar/thermal protective coating - 16mm air space - 6mm laminated glass with PVB interlayer (Landmark Tower, Abu Dhabi)	1.4	0.3	50	

| c. 26mm Double glazing insulating unit (26 DIG)
 - 8mm Fully tempered
 - 12.7mm air space
 - 6mm Fully tempered
 Light and Dark Grey colours
 (Lamar Towers, Jeddah) | 2.8 | 0.51 | 39 | |

3   ENERGY PERFORMANCE RESULTS

A total of 27 sets of simulations were conducted representing different façade build-ups (Table 4). The results for the dynamic thermal simulation were evaluated in terms of annual cooling loads. The best and worst combinations of glazing ratio, wall and glazing type were identified in order to understand the most influential parameter impacting the cooling energy loads in the building.

Table 4 shows that an insulated thermal blocks wall following Estidama Standards represented in the combination (20-TBW-32) performed best in all the different orientations. Factors that contributed to this include the low glazing ratio (20%) and lower shading coefficient (0.32) in the glazing type. The uninsulated air cavity wall type (UCW) with 60% glazing ratio and higher shading coefficient (0.51) in glazing type, performed worst, followed by the shadow box spandrel glass (SSG) build-ups, this could be due to the high solar gain through large glazing area with poor shading properties.

Comparing the results for the different orientations in Figure 2, it is clear that there are a similar pattern in the simulation results, with the thermal blocks wall type build-ups (TBW) performing best and the cooling loads increasing gradually with larger glazing ratio. Overall, the difference between the best case and worst case build up ranges between 92 and 128%, outlining the huge role even simple facade design changes can make in terms of energy performance.

Further analysis for the result compared the heat gain coefficient for the building fabric to the cooling degree hours (Figure 3), the analysis shows a correlation between the heat gain coefficient and the glazing ratio of the building fabric, indicating the string impact of glazing ratio and heat gain.
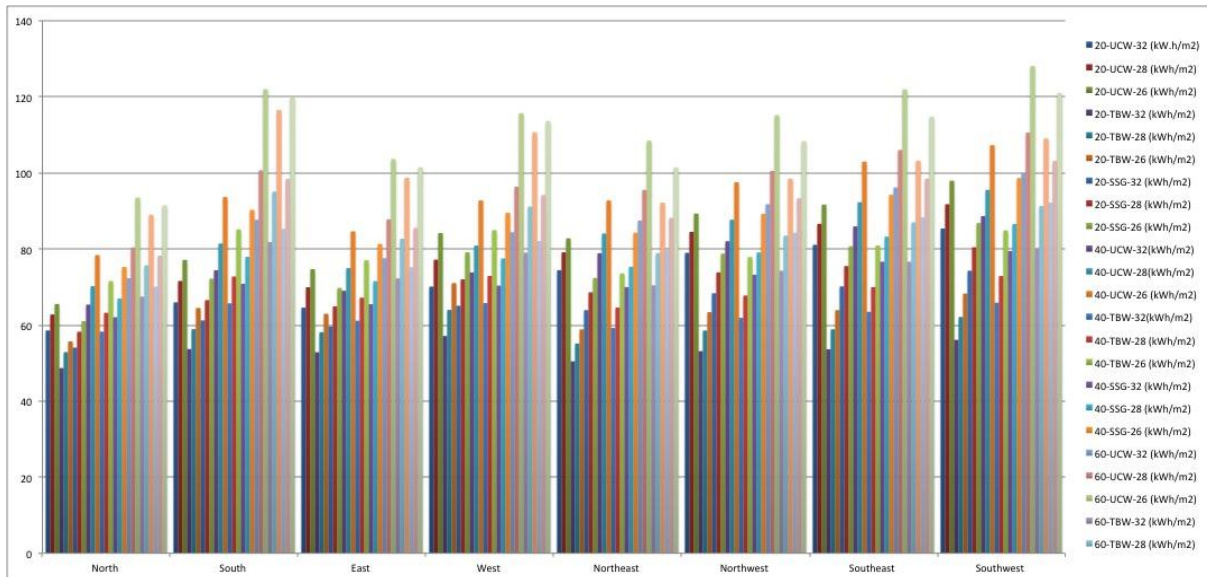

Figure 135 The results for the energy performance simulation for each orientation (Source: Author)

The results of this parametric study indicated the following:

-        Due to the high air temperature and solar radiation characterising the climate in the region, the insulation in the wall construction type is the dominant factor in reducing cooling energy loads, following this, the glazing ration and the thermal characteristics of the glazing type such as shading coefficient, especially for skin-loaded buildings such as residential high-rise, have a major impact as well.

-        The use of spandrel glass, commonly used to achieve an aesthetically unified slick façade has a significant negative impact on tall buildings in the hot climate of the region, increasing their cooling loads.

-        The reliance on a prescriptive approach for building envelope specifications outlined in the local building codes and green buildings regulations does not achieve the required energy efficiency in tall buildings, and development of more stringent building codes then could have a significant impact on energy use.

Table 76 The results for the energy performance simulation, the green row illustrates the best case scenario while the orange row shows the worst case scenario

| Simulation Combination	North	South	East	West	Northeast	Northwest	Southeast	Southwest
20-UCW-32	58.58	65.98	64.58	70.12	74.43	78.99	81.10	85.38
20-UCW-28	62.78	71.59	69.94	77.19	79.13	84.51	86.62	91.78
20-UCW-26	65.54	77.14	74.71	84.21	82.80	89.31	91.67	97.96
20-TBW-32	48.68	53.68	52.85	57.12	50.45	53.14	53.64	56.11
20-TBW-28	52.88	58.93	58.14	63.98	55.15	58.56	58.88	62.12
20-TBW-26	55.69	64.49	62.96	71.03	58.87	63.39	63.93	68.29
20-SSG-32	54.07	61.21	59.62	65.07	63.92	68.37	70.17	74.29
20-SSG-28	58.25	66.56	64.92	72.03	68.61	73.86	75.53	80.47
20-SSG-26	61.05	72.20	69.75	79.11	72.38	78.78	80.74	86.82
40-UCW-32	65.38	74.43	69.02	73.84	78.88	82.04	85.94	88.67
40-UCW-28	70.23	81.43	74.98	80.89	84.07	87.69	92.30	95.55
40-UCW-26	78.41	93.65	84.65	92.77	92.76	97.55	102.96	107.29
40-TBW-32	58.27	65.71	61.14	65.78	59.22	61.89	63.49	65.87
40-TBW-28	63.22	72.78	67.20	72.93	64.60	67.76	69.98	72.90
40-TBW-26	71.56	85.16	77.04	84.97	73.58	77.89	80.92	84.91
40-SSG-32	62.05	70.85	65.49	70.36	69.97	73.24	76.65	79.46
40-SSG-28	66.98	77.94	71.54	77.51	75.33	79.10	83.25	86.58
40-SSG-26	75.27	90.30	81.33	89.52	84.29	89.25	94.25	98.66
60-UCW-32	72.32	87.68	77.57	84.42	87.50	91.77	96.17	99.97
60-UCW-28	80.40	100.67	87.81	96.38	95.54	100.52	106.03	110.61
60-UCW-26	93.51	121.99	103.65	115.73	108.48	115.20	121.97	128.10
60-TBW-32	67.47	81.85	72.27	79.00	70.45	74.28	76.64	80.13
60-TBW-28	75.72	95.08	82.71	91.17	78.92	83.52	86.98	91.27
60-TBW-26	89.01	116.55	98.72	110.68	92.20	98.47	103.22	109.07
60-SSG-32	70.07	85.29	75.19	82.09	79.89	84.29	88.31	92.18
60-SSG-28	78.25	98.42	85.56	94.18	88.21	93.36	98.51	103.15
60-SSG-26	91.47	119.86	101.51	113.65	101.48	108.38	114.83	121.05
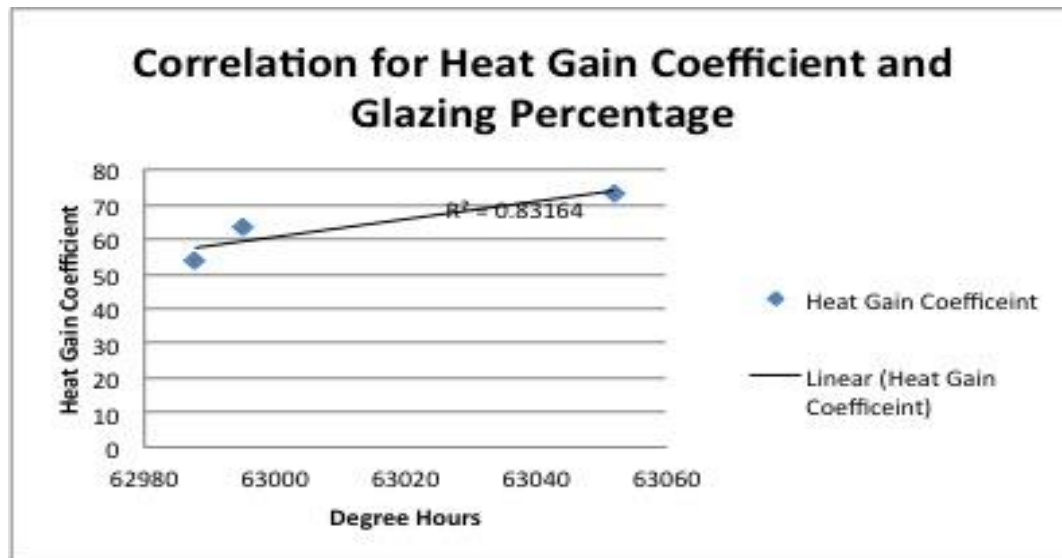
Figure 136 The Correlation between the heat gain coefficient and glazing percentage (Source: Author)

4   CONCLUSION

This paper highlights the limitations of the local building codes and the common practice in the region, especially in Saudi Arabia. The reliance on a prescriptive approach for building envelope specifications outlined in the local building codes and green buildings regulations is not sufficient to achieve energy efficiency in residential tall buildings in the hot climate of the region. And development of more stringent building codes then could have a significant impact on energy use. Moreover, further design consideration should be implemented such as shading for the facades. Examples in the region such as Doha Tower in Qatar demonstrate the potential in encouraging architects to go beyond relying on simple building envelope parameters.

The analysis of the results for the dynamic thermal simulations in terms of annual cooling loads showed that the difference between the best case and worst case build up ranges between 92 and 128%. The main factors contributing to this he difference are the glazing ratio and shading coefficient in the glazing type. Comparing the results for the different orientations, it is clear that the thermal blocks wall type build-ups (TBW) performed best, which highlights that the insulation in the wall construction type is the dominant factor in reducing cooling energy loads, following this, the glazing ration and the thermal characteristics of the glazing type such as shading coefficient, especially for skin-loaded buildings such as residential high-rise, have a major impact as well.

This work forms a part of the process of an ongoing PhD methodology. The aim of the paper to define the limitations with current design approaches and building regulations in order to identify avenues for potential enhancement of building regulations and existing tall building guideline documents in the Gulf Region. Further work consisting of parametric studies and data measurements will define the most promising solution using the current approach in relation to cooling loads, thermal and visual comfort. Also, further studies aim to identify to what extent can an alternative approach –focusing on design parameters such as building form and orientation, plan arrangement and core placement and shading approach, can improve the environmental performance of the residential tall building type.

5   ACKNOWLEDGMENTS

6   REFERENCES

AL-HOSANY, N. 2002. Sustainable facade design and virtue in incarceration architecture :the case of prison buildings in Abu Dhabi.

BROWN, G. & DEKAY, M. 2001. Sun, Wind & Light: Architectural Design Strategies, USA, John Wiley & Sons, Inc.

CONSTRUCT, A. 2012. Updated Building Regulations in the GCC. Venture Middel East.

CTBUH. 2014. The Skyscraper Center [Online]. Council on Tall Buildings and Urban Habitat.

ESTIDAMA. 2010a. Pearl Building Rating System [Online].

GBRS 2010. Green Building Regulations & Specifications. In: AUTHORITY, D. E. A. W. (ed.). Dubai: Government of Dubai.

GSAS 2013. Commercial and Residential GSAS Training Manual. Qatar: Gulf Organisation for Research and Development.

HAASE, M. & AMATO, A. 2006. Sustainable Dacade Design for Zero Energy Buildings in the Tropics. The 23th Conference on Passive and Low Energy Architecture. Geneva, Switzerland: PLEA.

LAHN, G. & STEVENS, P. 2011. Burning Oil to Keep Cool: The Hidden Energy Crisis in Saudi Arabia. London: The Royal Institute of International Affairs.

MEIR, I., PEETERS, A., PEARLMUTTER, D., HALASAH, S., GARB, Y. & DAVIS, J. 2012. Green buildings standards in MENA: An assessment of regional constraints, needs and trends. Advances in Building Energy Research, 6.

OBAID, R. & MUFTI, A. Present State, Challenges, and Future of Power Generation in Saudi Arabia. IEEE Energy 2030, 2008 Atlanta, GA USA.

REICHE, D. 2010. Energy Policies of Gulf Cooperation Council (GCC) countries—possibilities and limitations of ecological modernization in rentier states. Energy Policy, 38, 2395-2403.

SBC601 2007. The Saudi Building Code Energy Conservation Requirements. Saudi Arabia: The Saudi Building Code National Committee.

159: Methodology of energy monitoring and assessment of the energy saving due to the building retrofit

B. MEMPOUO[*], S. B. RIFFAT,

Architecture, Climate & Environment (ACE) Research Group, Institute of Sustainable Energy Technology, Department of Architecture & Built Environment, University of Nottingham; University Park, NG7 2RD Nottingham, United Kingdom, Tel: +44(0) 1158467132, Fax: +44(0) 1159513159

Buildings account for more than 40% of Europe's Energy consumption, where about 64% is accounted for by existing buildings. Retrofitting of these existing buildings offers significant opportunities for achieving the EU objective of reducing energy consumption and greenhouse gas emissions by 20% by 2020.The methods to identify the most cost-effective retrofit measures for particular buildings are still a major technical challenge, which is leading to a "progressive widening of the gap between theory and practice". Drawing on the lack of real life data for whole buildings and technologies energy use patterns, a baseline of existing whole buildings and technologies energy usage (pre-retrofitting) must be established from which improvement and efficiencies can be measured. Since, one can't simply compare the total amount of energy the building used in the year before and the year after, due to weather difference conditions from year to year, so an abnormally warm winter the year before followed by a really cold winter might cause the house to use even more energy than before. This paper recommends a systematic approach to proper selection of energy monitoring and explores a weather-normalisation method for estimating the energy savings due to building retrofit. The energy signature and the so-called Normalised-Annual-Consumption were developed from the utilities (gas and electrical) meter readings/bills. The paper also describes the propose methodology for an on-going longitudinal energy monitoring (post-retrofitting) to determine actual energy saving brought about by a wide range of retrofitting technologies.

Keywords: Utilities (gas and electricity) bills, Monitoring, Energy Saving, Existing Dwellings, Building Retrofitt

1. INTRODUCTION

The EU is committed to reducing CO2 emissions relative to the base year of 1990 by 20 per cent by 2020. Buildings account for more than 40% of Europe's Energy consumption. Developments in sustainable energy technologies and building management systems have enabled new buildings to meet the European Directive on Energy Performance of Buildings. However, at least 75% of the building stock that will be present in the next 20 to 30 years is already in existence and of this 70-80% is residential. As is pointed out in the EU Green Papers [1, 2], rational use of energy and integration of renewable energy technologies could substantially improve the energy performance of buildings, reducing the conventional energy demand in new and existing buildings by at least 20% and substantially contributing to reducing energy intensity. As residential buildings dominate building stock with respect to living space, and have an unfavorable ratio of building envelope compared to the floor area, this type of building has a high specific heating/cooling energy demand, and a significant contribution to greenhouse gas emissions. The energy consumption for heating/cooling are greatly influenced by the type of the building envelop and by the weather conditions. Hence, the comparison between the energy consumption of pre- and post-retrofit of existing buildings must take into consideration the weather variations.

Several weather-normalized techniques have been suggested [3, 5], but there is no single method, which has unanimously accepted to correct the effects of the weather conditions on the energy consumption. On envelope load dominated building, by assuming steady state heat transfers between the building and the environment, the relationship between the energy consumption and the outdoor temperature can only be provided at approximate building balance point temperature. Using a range of balance point temperatures, the energy consumption can be calculated using energy signature method or the performance line method to take into consideration the differences in weather conditions. In the energy signature method, a plot is created mapping electric energy consumption against mean outdoor temperature. The point on the chart at which weather independent and weather dependent electricity demand intersect is the balance point temperature. This method only works if large quantities of data on the building energy use are available, preferably on a daily resolution [6]. In the performance line method multiple plots of electric energy consumption against heating degree days (HDD) and cooling degree days (CDD) are created, using a range of balance point temperatures to calculate the degree days. This method may be applied to buildings in which the availability of energy use data is less granular, perhaps only available on a weekly or monthly basis [7].

In this paper is presented the so-called "Normalized Monthly Consumption – NMC", which has been used as a holistic approach to eliminate the effect of weather severity in the analysis of energy savings due to the holistic buildings retrofit in Nottingham, UK. The NMC method uses the pre-retrofit and post -retrofit monthly average energy consumption (M_i) and the average monthly heating degree-days (H_{mi}) computed to the balance point temperature ($t_{balance}$) or to reference monthly temperatures ($T_{ref.}$).

2 METHODOLOGY

2.1 Normalized Monthly/Annual Consumption – NMC/NAC

The so-called "Normalized Monthly Consumption – NMC" has been developed from the utility meter readings or bills, M_i (Monthly energy consumption) expressed in kWh, before and after the building retrofit. A linear model (Equation 1) between the average monthly consumption (M_i) and the average monthly heating degree-days (H_{mi}) computed to the balance point temperature ($t_{balance}$) or to reference monthly temperatures ($T_{ref.}$).

$$M_i = a + bH_{mi}(T_{ref})$$
(1)

Where: a is the intercept so a base level or non-weather-dependent energy use in kWh (non-weather dependent monthly consumption such as the amounts of energy used for appliances or purposed other than heating, cooling, ventilation, hot water, or lighting); b is the.heating or cooling slope ($(b = \dfrac{L}{\eta})$ the ratio

between the heat losses rate (L) in W/°C/m2 and the efficiency (η) of heating/cooling system. T_{ref} (or $T_{Thermostat}$ the building indoor thermostat set-point temperature).

2.2 Internal and external heat gains and losses in a building

The drawback of analyzing energy savings due to buildings retrofit is comparing the energy consumption of buildings with different internal and external heat gains and losses (see Figure 1) is that the comparison is more a comparison of these gains and losses than comparison of the performance of the buildings and energy savings. In this context, T_{ref} (or $T_{Thermostat}$ the building indoor thermostat set-point temperature) is assumed constant about 26°C over the heating season, and the following factor are also assumed to be constant:

- Indoor temperature T$_{in}$, ($T_{in} = T_{ref} + \dfrac{Q_g}{L}$), where Q_g represents the internal heat gains (lighting, people, appliances)
- Internal heat gains and solar heat gain, Q_g
- Heat losses of building,

<center>a)</center>
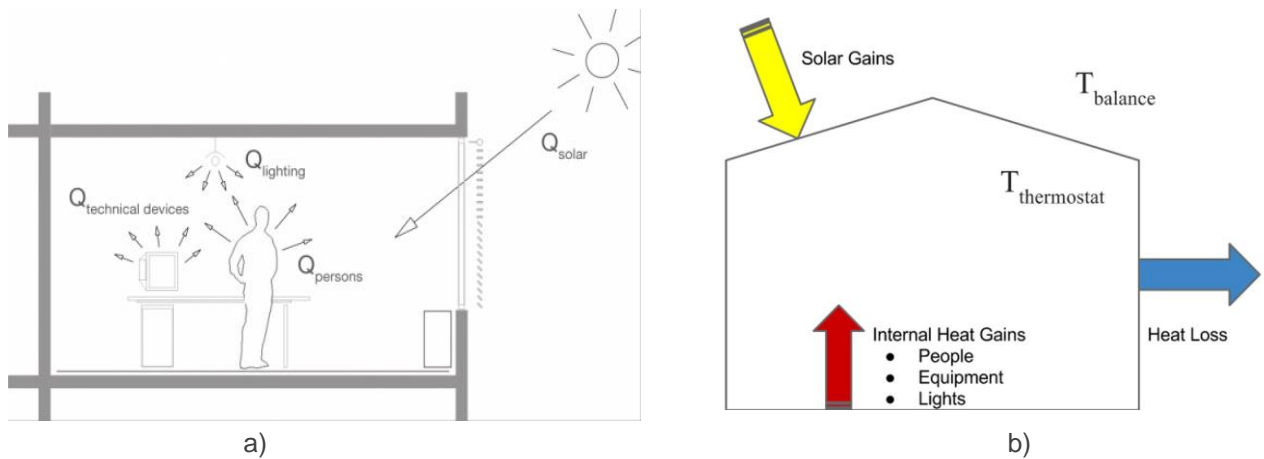

<center>b)</center>

Figure 1: a) Internal Heat Gains, b) Internal and external heat gains and losses in a building

The balance point temperature is mathematically defined as:

$$T_{balance} = T_{thermostat} - (Q_{IHG} + Q_{SOL}) / U_{bldg}$$

Where:

- $T_{balance}$ is the balance point outdoor air temperature, given in °C.
- $T_{Thermostat}$ is the building thermostat set-point temperature, given in °C.
- Q_{IHG} is the internal heat generation rate per unit floor area due to occupancy, electric lighting and mechanical equipment, given in W/m². This internal heat generation is not constant due to variability in occupancy, lighting, and equipment operation schedule but is largely considered constant to a first order approximation.
- Q_{SOL} is the building heat gain per unit floor area due to solar radiation, given in W/m². This heat gain is not constant due to solar variability with time of day and year but is largely considered constant to a first order approximation. In winter, it is reasonable to assume $Q_{SOL}=0$.
- U_{bldg} is the rate of heat transfer across the building envelope per degree temperature difference between outdoor and indoor temperature and per unit floor area, given in W/°C/m². This heat transfer

can vary due to variations of fresh air ventilation rate but is largely considered constant to a first order approximation.

First the values of the parameters a (the non-weather-dependent energy use in kWh) and b (the heating slope) are calculated by the least squares linear-regression, for a given value of the average monthly balance point outdoor air temperature ($T_{balance}$, given in °C). Then, optimum value of the outdoor air temperature yields linear relationship between the average monthly consumption (M_i) and the average monthly heating degree-days (H_{mi})($T_{balance}$), for which the correlation coefficient R^2 is highest. The so-called "Normalized Annual Consumption – NAC" is, then, obtained by applying the parameters a and b to equation (1) to a long term annual average of heating degree-days (H_a)(T_{ref}):

$$NAC = 12a + bH_a(T_{ref})$$

(2)

In this paper, the Normalized Annual Consumption method is proposed to be used for analysis of energy savings, eliminating the differences in weather conditions before and after holistic retrofit. The method consists of the following steps (**Figure 2**).

i) The available data (monthly energy consumption, average monthly indoor temperature average and average monthly heating-degree day) are used to develop the Normalized Annual Consumption of the building before retrofit $NAC_1=12a_1-b_1H_{a1}(T_{ref})$ and after retrofit $NAC_2=12a_2-b_2H_{a2}(T_{ref})$, The method is based on assumption that, the building indoor thermostat set-point temperature is constant over the heating season, and the internal and external heat gains and losses in a building do not vary for the pre-retrofit and post-retrofit period, consequently the *NAC1* and *NAC2*, become a linear relationship between them and the heating degree-days.

ii) The annual heating degree-days are used together with the average outdoor temperature and indoor thermostat set-point temperature to obtain the Normalized Annual Consumption of the building before and after retrofit, and then to calculate the energy savings.

PRE-RETROFIT (SIX MONTHS OR TWELVE MONTHS PERIOD)
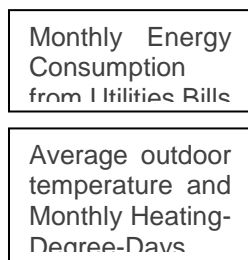
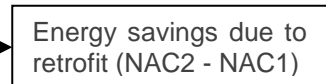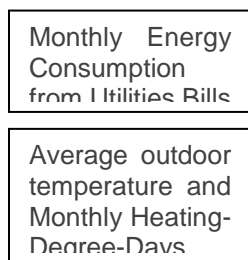**POST-RETROFIT** (SIX MONTHS OR TWELVE MONTHS PERIOD)

Figure 2: Flowchart of the proposed method.

In the equation (2), the slope b is a useful parameter, since it helps to determine efficiency of the building envelop and different heating system components. It also gives factors such as conductive heat loss rate

(U_{bldg}) across the building envelope per degree temperature difference between outdoor and indoor temperature and per unit floor area, given in W/°C/m².

3   DWELLING TYPOLOGY AND ENERGY CONSUMPTION

The dwelling under consideration is occupied single family residential semi-detached house, built circa 1920, and contains families of three people. The house is based in the sub-urban districts of Nottinghamshire, Bilsthorpe. The average floor area is about 80m².

3.1 Dwelling Typology

The house (Figure 3) has external cavity walls and naturally ventilated. Ground floor is slab-on-grade with suspended timber first floor. The attic space is of typical cold roof construction with insulation between ceiling and joists. The main characteristics are presented in the **table a** - **table d** in the Appendix.

Figure 3: Semi-detached house in the sub-urban districts of Nottinghamshire, Bilsthorpe.

In 2013, the house was retrofitted, all windows and doors have been upgraded with efficient double glazing windows and doors (see appendix, table b); and from previous refurbishment schemes the house association replaced the boiler heating systems with natural gas central heating. The boiler has simple on/off timer controls with temperature controlled by the boiler, no room thermostats.

Dwelling annual gas and electrical consumption

The house the annual gas and electrical consumption, as from the utilities companies are presented in the Table 1 below. A short discussion on this table shows the need for comparing the energy consumption before (2013) and after (2014) widows retrofit for reference year, to eliminate the severity of climate.

Table 1: the annual gas and electrical consumption				
	Pre-retrofit		**Post-retrofit**	
Year	Gas Bills (kWh)	Electricity (kWh)	Gas Bills (kWh)	Electricity (kWh)
2011-2012	13334.77	7300.18	-	-
2012-2013	14076.10	7276.06	-	-
2013-2014	-	-	10852.06	7604.49

3.2 Heating Degree-Days (HDD)

As a general rule of thumb, the range of 19∘–25∘C is proposed for human comfort. The average indoor thermostat set-point of 18 °C, 20 °C and 21°C has been used to estimate the HDD. The annual heating needed in an N-day definite period i, equation (3) and (4) were used, where k is the day number in the

month. In this equation, HDD is the need for heating on the basis of degree-day; T_i is the daily mean temperature.

$$HDD_i = (T_{thermostat} - T_{daily\ balance}) \quad (3)$$

The average monthly heating degree-days (H_{mi}) computed to the balance point temperature ($t_{balance}$) or to reference monthly temperatures (Tref.).

$$H_{mi} = \sum_{k=1}^{n} HDD_i \quad (4)$$

The average monthly Heating Degree Days have been calculated for Nottingham (Bilsthorpe) and summarised the figure 4:
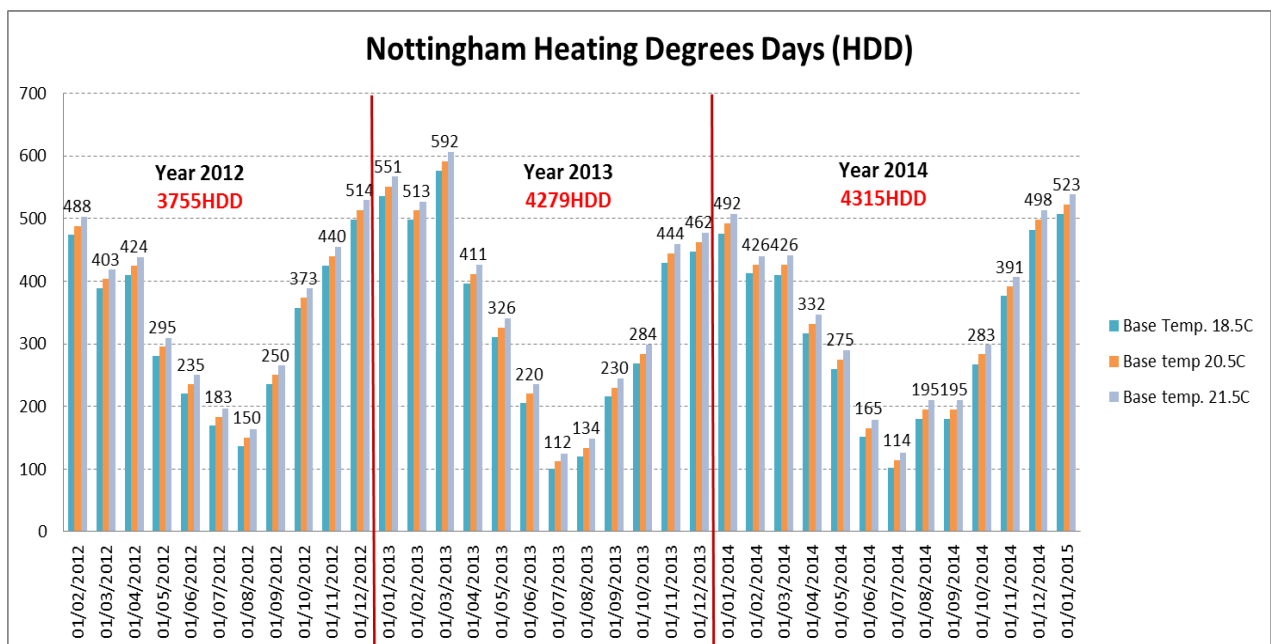
Figure 4: *The average monthly Heating Degree Day (HDD), districts of Nottinghamshire, Bilsthorpe.*

4   ANALYSIS OF RESULTS

The whole-building approach was applied via utility meters (gas and electric) and bills from energy/utility companies. The electricity and the gas consumption were monitored by recording the readings every month using the monthly consumption readings from the energy company provider bills.

The monthly gas and electricity consumptions have been monitored and recorded for sufficient period of time of one year 2014 to cover weather variations of all year semesters. In order to better understand the energy consumption and energy savings due to windows retrofit. The electricity and gas consumption monthly bar graphs were drawn.

4.1 Gas consumption

Figure 5 shows the annual monthly consumption of gas. For gas consumption: from Figure 5, It can be seen that the highest use of gas was during winter. This difference is most likely due to higher heating demand on central heating compared to summer heating demand. Total annual monthly gas consumption ranged from 50-1900 kWh/ month with total annual consumption of 10852.06kwh.
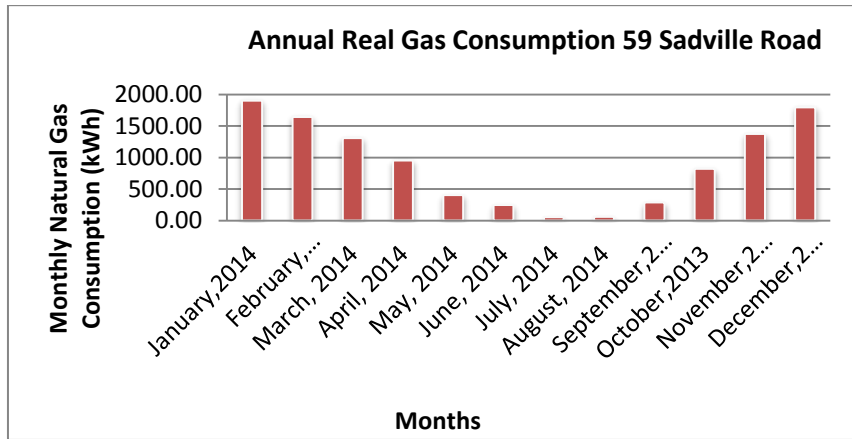
Figure 5*: The Monthly Gas consumption for year 2014 at 59 Sadville Road , districts of Nottinghamshire, Bilsthorpe*

The house (Figure 3) has external cavity walls and naturally ventilated. Ground floor is slab-on-grade with suspended timber first floor. The attic space is of typical cold roof construction with insulation between ceiling and joists. The main characteristics are presented in the **table a** - **table d** in the Appendix.

4.2 Analysis of Energy Savings - Gas consumption

Using equation (2), the annual Normalisation Annual Consumption, NAC have been calculated as show in the table 2 and figure 6 below, one can clearly see that there was reduction in gas consumption in 2013 of 7.32% instead of the increase of 5.60%, directly from the gas bills.

Table 2*: Normalisation Annual Gas Consumption*

Year	Gas Bills (kWh)	% Change	H_{mi}	KWh/ H_{mi}	% Change	NAC kWh
2011-2012	13334.77	--	3755	3.55	--	14612.97
2012-2013	14076.10	+5.60%	4279	3.29	-7.32**%**	13542.72
2013-2014	10852.06	-23.00%	4315	2.51	-24.00**%**	10332.00

Figure 6*: The Normalized Annual Gas Consumption*

4.3 Electrical consumption

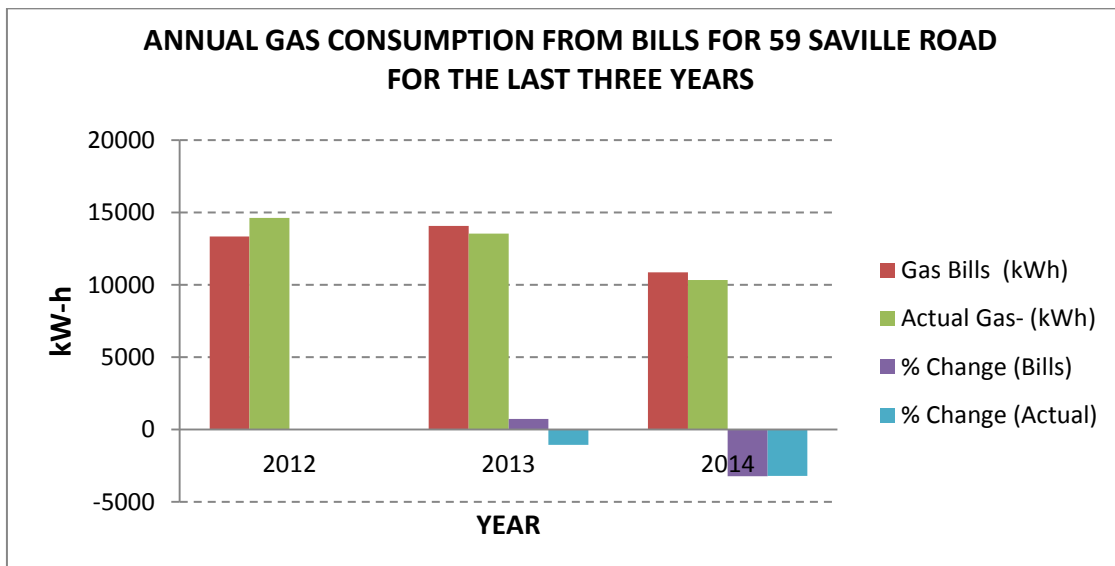Figure 7 shows the annual monthly consumption of electricity as it can be seen that the electrical consumption is a proximately constant over the year of average 620 kWh. In contrast December and January were recorded 800 and 1050 kWh/ month respectively and this can be explained due to the fact that the external temperatures for January and December are the lowest and the occupants might use electrical assisting heaters to balance the comfort temperature in addition to the use of more lighting due to the short period of day lighting.
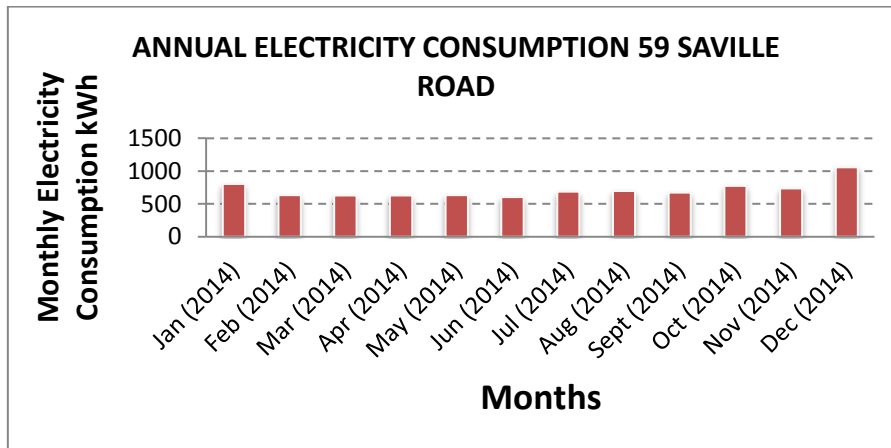
Figure 7: Monthly Electricity consumption for year 2014

4.4 Analysis of Energy Savings - Electrical consumption

Using equation (2), the annual Normalisation Annual Consumption, NAC have been calculated as show in the table 3 and figure 8 below, one can clearly see that the electricity bills for instance reduction in kilowatt-hours, it looks like a 0.33% reduction. When they are normalized for the colder winter, though, one can see that in 2013 the house really reduced the consumption by 12.53%.

Table 3: Normalisation Annual Electrical Consumption

Year	Bills Electricity (kWh)	% Change	H_{mi}	KWh/ H_{mi}	% Change	NAC kWh
2011-2012	7300.18	--	3755	13334.77	--	8026.85
2012-2013	7276.06	-0.33%	4279	14076.10	-12.53%	6997.76
2013-2014	7604.49	4.51%	4315	10852.06	3.64%	7244.74

Figure 8: The Normalized Annual Electrical Consumption

The effect of different weather conditions on the gas and electrical consumption of the pre- and post -retrofit building can respectively be observed in the Table 2 and Table 3 columns 8. For instance the gas consumption from the utility bills in 2013 is greater by about 3.64% than 2012. The difference, between the gas energy consumption in 2013 (pre-retrofit), and the gas energy consumption in 2014 (post-retrofit) shows saving of about 24%, which is due to the building retrofit and the different weather conditions.

5   CONCLUSION

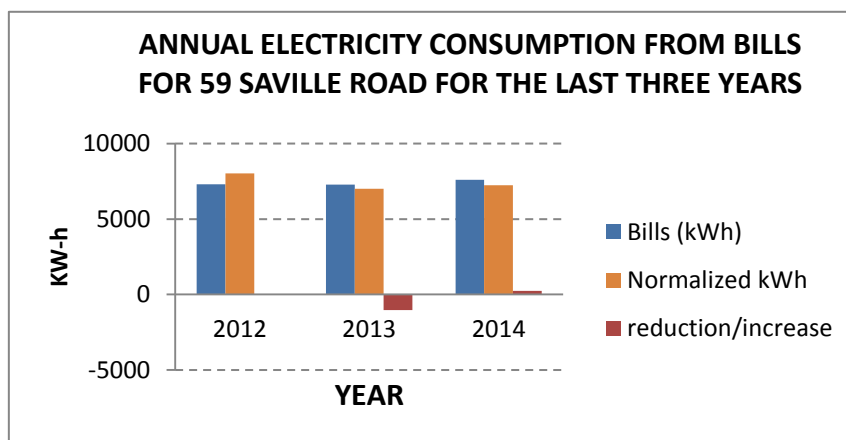The Normalized Annual Consumption method has been proposed, it can developed for one year, using the monthly energy consumption and monthly heating degree-day and the average outdoor temperature, and then remains constant for all year, provided that no modifications of the building envelope or HVAC system are been performed. The NACs of the pre- and post –retrofit building can be used to calculate the energy savings due to the building retrofit as the difference between these two NACs.

This weather-normalisation technique provides fast results. In this particular case, the linear relationship between the electrical and gas consumption and the heating degree-days provides better estimates of energy savings. From the electricity bills, after the weather-normalisation technique, the house reduced the consumption by 12.53%, and Gas consumption by 24%.

The propose methodology can also be implemented in an on-going longitudinal energy monitoring (post-retrofitting) to determine actual energy saving brought about by a wide range of retrofitting technologies. It can provide to the building manager fast and useful information about the net effect of different retrofit strategies on the energy consumption.

6   ACKNOWLEDGEMENTS

7   REFERENCES

European Commission, 2005, Green Paper on energy efficiency or doing more with less, Brussels

European Commission, 2001, Green Paper - Towards a European strategy for the security of energy supply, Luxembourg.

ETO, J.H.., A comparison of weather normalisation techniques for commercial building energy use. Proceedings of the ashrae/doe/BTECC Conference Thermal Performance of the Exterior Envelopes of Buildings III, American Society of Heating, Refrigerating and Air-Conditioning Engineers, Atlanta, GA, pp. 109 – 121 (1985)

FELS, M.F, PRISM: an introduction. Energy Buildings 9, 5-18 (1986).

JACOBSEN, F.R., Energy signature and energy monitoring in building energy management systems. Proceedings of the Clima 200 World Congres on Heating, Ventilating and Air-Conditioning, Vol. 3: Energy Management, Copenhagen, pp. 25 – 31 (1985).

LEE, Kyoungmi; Baek, Hee-Jeong; Cho, ChunHo (2014). "The Estimation of Base Temperature for Heating and Cooling Degree-Days for South Korea". Journal of Applied Meteorology and Climatology 53 (2): 300–309. doi:10.1175/jamc-d-13-0220.1.

DAY, A. R.; Knight, I.; Dunn, G.; Gaddas, R. (2003). "Improved methods for evaluating base temperature for use in building energy performance lines". Building Services Engineering Research and Technology 24 (4): 221–228.

8   APPENDIX

Main characteristic of the house under consideration:

Table 1: Thermal characteristics of the building envelope

Construction	U value (W/m². K)	Thickness (mm)	Materials (outer to inner)
External wall	1.969	238	Brick (225 mm)-outer, plaster (13 mm)-inner
Ceiling	1.942	115	Oak beams (100 mm)-outer, plaster (15 mm)-inner
Roof unoccupied	2.811	105	State tiles (5 mm)-outer, oak beams (150 mm)-inner
Ground floor	1.375	170	Carpeted concrete slab on grade floor
First floor	1.505	185	Oak (20 mm)-outer, Oak beams (150 mm) and plaster (15 mm)-inner
Loft insulation	0.119	300mm	Mineral wool (300 mm)-outer, oak beam (100 mm) and Plasterboard (15 mm)-inner

Table 2: Thermal characteristics of the building openings pre and post retrofit.

Opening	Pre-retrofit	Post-retrofit
Glazing type	Single	Double (K Glass in the back pane; and Optiwhite front pane)
Thickness	6 mm	6 mm/ (6/13mm)
Gas	None	Air / gas filled and special warm edge spacer
Glazing U - value	5.778 (W/m^2.K)	1.6 (W/m^2.K)
Frame type	Wood	UPVC
Frame U - value	3.633 (W/m^2.K)	1.6 (W/m^2.K)
Shading	None	None
Doors		
Material	Oak wood	UPVC
Thickness	50 mm	50 mm
U - value	2.911 (W/m^2.K)	1.911 (W/m^2.K)

Table 3 Characteristics of the building lightings

Lighting	As Built	As Reality
Lighting type	Low standard	Low standard
General lighting	5 (W/m²) - 100 (Lux)	5 (W/m²) - 100 (Lux)
Visible Fraction	0.18	0.18
Radiant Fraction	0.42	0.42
Convective Fraction	0.40	0.40
Lighting control	None	None

Table 4: *Characteristics of the building HVAC systems*

Boiler	As Built	As Reality
Boiler type	Old style high temperature boiler	Condensing Boiler
Fuel	Natural gas	Natural gas
Boiler efficiency (%)	65%	69% – 89 %
Humidity Control	None	
DHW delivery temperature	70 ºC	70 ºC
DHW supply temperature	10 ºC	10 ºC
Ventilation rate	3 (ac/h)	3 (ac/h)

167: Development of energy simulation software for high-tech frication plants (1)

Theoretical model and verification

TI LIN, SHIH-CHENG HU, YI-YUN CHUENG

Department of Energy and Refrigerating Air-Conditioning Engineering, National Taipei University of Technology, 1, Sec. 3, Chung-Hsiao E. Rd., Taipei City 106, Taiwan (R.O.C.), schu.ntut@gmail.com

High-tech manufacturing consumes huge of energy. For example, a 12 in DRAM (Dynamic Random Access Memory) semiconductor wafer fabrication plant (hereafter referred "fab") consumes about 400,000 MWh annually [1] in electricity (as much as 25,000 homes use, each consumes about 4,000 kWh/year [2]). The potential for energy savings in fabs is commensurate with the magnitude of their energy consumption. For air-conditioning, fabs are different from those commercial buildings. Fabs need a lot of outside air to keep a positive pressure, while outside air and circulating air often treated separately. The general building energy analysis software handles the air-conditioning system for the outside air mixed with return air through the centralized system, which is different from that of a fab. Plus, the general building energy analysis software does not include electricity consumption items, such as process cooling water system (PCW), compressed dry air (CDA) system, nitrogen system, vacuum system and exhaust system. Process equipment cooling system is not included in the general building energy analysis software modules either. In this study, a Fab Energy Simulation (FES) software was developed. FES with features such as: open source code, multi-language interface, capable of handling different arrangements of components in the make-up air unit (MAU). In this paper, mathematical model is presented in detail. The results are verified by the power consumption data of an operating semiconductor wafer fab, with less than 4% in each output category.

Keywords: Energy Simulation, Cleanrooms, Annual Energy Consumption

1. INTRODUCTION

High-tech manufacturing consumes huge of energy. For example, a 12 in DRAM (Dynamic Random Access Memory) semiconductor wafer fabrication plant (hereafter referred "fab") consumes about 400,000 MWh annually [HU, 2010: page 3788-3792] in electricity (as much as 25,000 homes use, each consumes about 4,000 kWh/year [BUREAU OF ENERGY, 2009]). The potential for energy savings in fabs is commensurate with the magnitude of their energy consumption. In a fab, factory facility shares about a half of the total plant power consumption, while process equipment accounts for about 45%, general buildings such as office, parking lot etc. account for another 4% [HU, 2003: PAGE 895-907][HU, 2008: PAGE 1765-1770]. In the facility sector, air conditioning, and exhaust system etc. accounted for more than 70% of the electricity consumption. In addition to annual maintenance, most fabs run a 24-hour operation mode. Thus, to save the power consumption of the facility system, air conditioning can be classified as the first priority. The HVAC system for a fab requires stability, which is different than the one in commercial buildings, which adopt variable air volume (VAV) and/or variable water volume (VWV) systems for saving energy. Furthermore, in order to achieve designed cleanliness, the air change rate for cleanroom is normally much higher than the one for commercial buildings. (Figure 1) shows the recirculation cooing unit (RCU) type air circulation system for a cleanroom, the air conditioning processes are:

1. Outdoor air (OA) mixed with return air (RA) from cleanroom.
2. The mixed air properly treated to design fresh air (FA) condition.
3. The fresh air pass thought the supply air duct and final filter (such as HEPA or ULPA filter), which is installed on the ceiling of cleanroom, into the cleanroom.

As the entire air conditioning system is united and the air change rate is 10 times larger than commercial buildings, which causes the huge air pressure loss due to the long air duct distance from RCU, cleanroom and back to RCU.
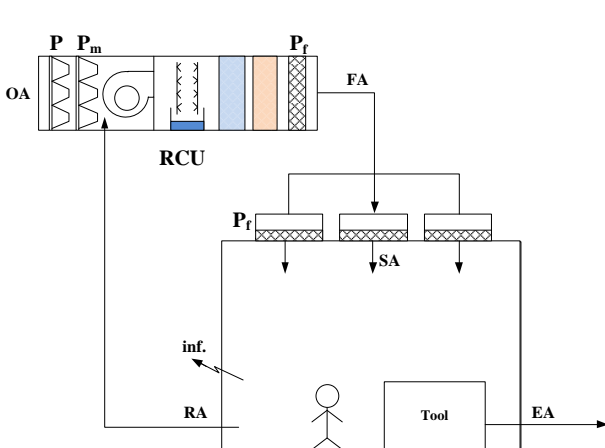
Figure 137: Centralized HVAC system for a cleanroom.
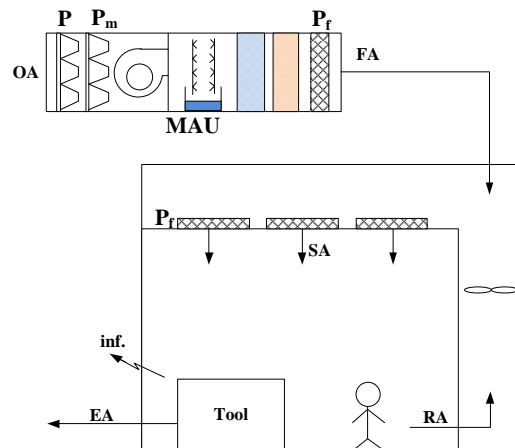
Figure 138: Segregate HVAC system (MAU+FFU) for a cleanroom.

Due to the huge air pressure loss in the air duct of RCU type cleanroom, the so-called segregate HVAC system (as shown in Figure 2) which combines the make-up air unit (MAU) and fan filter unit (FFU) was introduced. The air conditioning processes are:

1. The outdoor air was treated to designed fresh air condition.
2. The return air pass thought the dry cooling coil removes sensible heat then mixed with fresh air which is supplied from make-up air unit.
3. The mixed air was drag into the suction of fan filter unit, filtrated and supplied to cleanroom.

In this type of cleanroom, required air flow for air circulation and cleanroom pressurization were separated, therefore the required static pressure for both fan can be reduced.

High-tech fabs are different from those commercial buildings. A fab needs a lot of outside air, while outside air and circulating air often treated separately. In such arrangement, a great energy on transporting air and ductworks can be saved. The general building energy analysis software are designed to handle the air-conditioning system for the outside air mixed with return air through the so-called centralized system, which is totally different from that of air-conditioning system. Plus, the general building energy analysis software does not include electricity consumption items, such as process cooling water system, compressed dry air system, nitrogen system, vacuum system and exhaust system. Process equipment cooling system is not included either. For the implementation of green building labeling system on fabs, it should not focus only the energy consumption on building envelops or offices.

The power consumption of fabs influence the production cost, and cause environmental pollution indirectly. WSC (World Semiconductor Council) and SEMI announce the energy white paper, which suggest the normalization of semi-conductor fabs' energy saving [JOINT STATEMENT, 2005]. In order to achieve the measurable result for energy saving, the energy consumption base line is required for both fab owners and tool/equipment suppliers to specify the goal of energy saving. Thus, a tool for energy saving potential assessment is necessary. Energy consumption in facility and utility was ignored in the past mostly because energy consumption takes only a small part of total wafer production cost. Moreover research paper for fab energy consumption is also rare.

Several assessment works of HVAC energy savings potential in in cleanroom were conducted in 1990s [BROWN 1990, page: 609-615] [NAUGHTON 1990, page 620-625, 626-633]. Brown [BROWN, 1990: page 609-615] presented the energy saving opportunities in makeup air system based on the five weather zones in US. Naughton [NAUGHTON, 1990: page 609-615, 620-625] review the system components and dynamics of HVAC Systems for Semiconductor Cleanrooms. Busch [BUSCH, 1998] indicated that the modelling of energy baseline and efficiency in cleanrooms with DOE-2 was not a straightforward exercise. The main reason is that the typical HVAC systems for cleanrooms are not typical for most buildings. DOE-2 users cannot specify more than one HVAC system serving a single zone. Basically, the above literatures were focused on HVAC in cleanroom, not a fab that including facility system and process tools. By energy benchmarking of cleanrooms in California [TSCHUDI, 2003: page 733-739], Tschudi et al. proposed best practices and outlined means [TSCHUDI, 2004: page 770-775] for cleanroom design and operation [TSCHUDI, 2005: page 29-35]. A benchmarking report on the cleanroom in New York state was performed by Mathew et al. in 2008 [MATHEW, 2009]. Kircher et al. [KIRCHER, 2010: page 282-289] carried out an energy simulation study of a lab-scale fab facility (6600 m2) using general building energy simulation software TRNSYS [SOLAR ENERGY LABORATORY, 1996], which with sophistication in dealing with complex HVAC systems, as well as the available libraries for modeling nontraditional HVAC such as industrial cleanroom. At the new fab design stage, often based on past experience and includes inbuilt flexibility margins, an over-sized facilities system is adopted and inherently resulted in wasteful of energy. The software, FRS (Fab Resource Simulation) was introduced aiming to fit facility capacity and actual operating requirements [MASUDA, 2005: page 17-20]. Results of FRS show a planned nitrogen plant for the fab was halved in size. The concept of linking energy/utility requirements with lot flow simulation could potentially be a very valuable prediction tool. However if accurate utility usage rates are unavailable, significant measurement data will be required for the input of simulation. Cohen **Error! Reference source not found.** developed an energy consumption software dedicated to fab called Cleancalc II. The program is robust but the HVAC devices and system control can't be customized to fit the practice application. Naughton **Error! Reference source not found.** propose a concept to evaluate utility energy consumption based on process tool requirement by using Energy Conversion Factors (ECF) which is recommended in SEMI S23 standard [SEMI S23-0813, 2008]. By using ECF values, reasonable acceptance criteria can be formed by fab owner and process engineer [NAUGHTON, 2006: page 428-432]. In view of the above literature, we try to develop an energy simulation software dedicated to fabs (we call this software FES). The software features with some characteristics other than current simulation tools such as: best fit for typical HVAC systems in cleanrooms, automatic coil control and various arrangements of components in MAU, which can improve the energy consumption simulation quality making it closer to real application. Moreover, all utility energy consumptions are included by S23 ECF approaches [SEMI S23-0813, 2008]. In this article, mathematical model is presented in detail. The results are verified by the data of an operating semiconductor wafer fab. In next article, application of the FES focusing on the energy conservation approaches for a semiconductor fab is reported.

4   MODEL DESCRIPTION

2.1   Calculating strategy

The type of HVAC system in FES software is based on the typical cleanroom design with MAU, Fan Filter Unit (FFU) and Dry Cooling Coil (DCC). Design parameters such as room temperature, relative humidity, and chiller water supply/return temperature can be imported by excel file. The simulation results can be exported as graphical data or texture data for further case comparison. The energy consumption simulation was divided into several parts including: HVAC system, process tool, fan, water pump and lighting. First, the MAU, DCC, and other cooling loads are calculated as energy consumption of HVAC system. Second, the process tool, exhaust system, process cooling water (PCW) system (transport only), nitrogen system, vacuum system, compress dry air (CDA) system and ultra-pure water (UPW) system are calculated as energy consumption on facility with process tool. Third, the fan of MAU, fan of RCU and fan of FFU are calculated as energy consumption of fans. Forth, the hot water pump, chilled water pump and other pumps were calculated as energy consumption of pumps. (Figure 3) shows the calculating processes in the FES software.
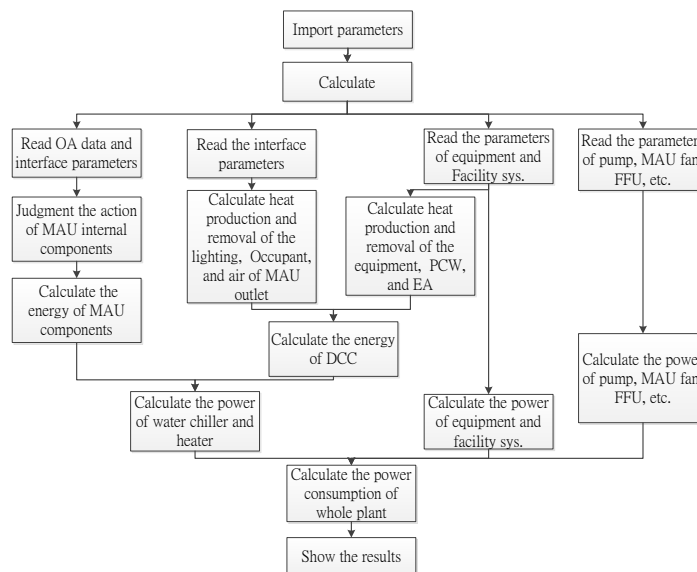
Figure 139: Calculating processes in the FES software

2.2   Power consumption calculating and introduction

Structure introduction of cleanroom

The segregate type HVAC system was adopted as the air circulation system in our simulated cleanroom. The main components of air circulation system are make-up air unit, fan filter unit and dry cooling coil. The HVAC system was divided into three major parts: outdoor air conditioning, indoor sensible heat removal and air circulation. The outdoor air was treated to design air condition in the MAU system, which adjusts the temperature and humidity by using cooling/heating coils and humidifier respectively, and then introduced into return air plenum. The circulation air adsorb the cooling inside cleanroom and return to the sub-fab which is also called return air plenum. After the return air pass through the dry cooling coil which removes the sensible heat in the air and mixed with the conditioned outdoor air, FFU on the ceiling will pull the air from supply air plenum to the cleanroom.

The indoor air conditioning loading can be divided into three major parts: 1.heat gain, 2. cooling load and 3. heat extraction rate. Heat gain is the rate at which energy is transferred to or generated within a space. The heat gain can be divided into sensible heat and latent heat which should be calculated separately. The sources of heat gain are:

1. Solar radiation through openings.
2. Heat conduction through boundaries with convection and radiation from the inner surface into the space.
3. Sensible heat convection and radiation from internal process tools, occupants, lightings, and fans
4. Ventilation (outside air) and infiltration air.
5. Latent heat gains generated within the space.

The cooling load is the rate at which energy must be removed from a space to maintain the temperature and humidity at the design value. The cooling load will generally differ from the heat gain because the radiation from the inside surface of walls and interior objects as well as the solar radiation coming directly into the space through openings does not heat the air within the space directly. This radiation energy is mostly absorbed by floors, interior walls and furniture, which are then cooled primarily by convection as they attain temperatures higher than that of the room air. Only when the room air receives the energy by convection does this energy become part of cooling load. The heat storage and heat transfer characteristics of the structure and interior objects determine the thermal lag and therefore the relationship between heat gain and cooling load. For this reason the thermal mass (product of mass and specific heat) of the structure and its contents must be considered in such case **Error! Reference source not found.**.

However, the partition material used in cleanroom construction is well insulated. As the surface of cleanroom external wall does not direct contact with the surface of building internal wall, the energy is difficult to transfer through cleanroom walls. Therefore, the cooling load through partitions into cleanroom is usually neglected. As the external cooling load is negligible, the heat sources inside cleanroom are mainly from the lighting, operator and process tool.

In FES, the annual electric energy consumption is divided into six parts: 1. HVAC system, 2. Facilities, 3. Process tool, 4. Air circulating fans, 5. Lightings and 6. Water pumps.

The energy consumption of HVAC system can be simply divided into water chiller, humidification and heating. Water chiller adsorb the heat from cooling coil of MAU, process cooling water and dry cooling coil. The humidifier in MAU system can be chosen as steam type, vapor type or air washer type. In order to simplify the heater energy consumption calculation, only the electric heating source is considered in this research.

The energy conversion factors (ECF) of nitrogen system, vacuum system, compressed dry air system and ultrapure water system are used in facilities energy consumption estimation.

The process tool energy consumption is the summary of electricity each process tool consumes. This summary is usually 30% ~ 50% of annual energy consumption of an operating cleanroom. The fan power of MAU, FFU, RCU and exhausts are considered as electric energy consumption of circulation fans. The lighting energy consumption is the summary of electricity which lighting consumes in the cleanroom. The chilled water pumps, hot water pumps and other pumps are calculated in the pump energy consumption.

HVAC system

In this system, the energy consumption of the MAU, DCC and PCW are calculated. The electricity consumption of water chiller and heater are calculated as the electric energy consumption. The following descripts the calculation method of air conditioning energy consumption and power consumption. FES is able to handle the case of different arrangements of MAU internal component and specific control mode of each arrangement, which is a more realistic condition. In FES, the psychrometric property is based on the ASHRAE Handbook of Fundamentals.**Error! Reference source not found.**

Equations for components in MAU system
Heat removal rate for cooling coils

The air mass flow rate in MAU system can be calculated from air flow rate and specific volume of air. The coil heat removal rate can be calculated from the air mass flow rate and enthalpy difference between coil inlet and outlet (Equation 1)

Equation 23: Heat removal rate for cooling coils.

$$q_{cooling} = \frac{\dot{Q}_{MAU}}{v_{air}} \times (h_{out} - h_{in})$$

Heating rate for heating coil

The air mass flow rate in MAU system can be calculated from air flow rate and specific volume of air. The coil heating rate can be calculated from the air mass flow rate and enthalpy difference between coil inlet and outlet (Equation 2).

Equation 24: Heating rate for heating coil

$$q_{heating} = \frac{\dot{Q}_{MAU}}{v_{air}} \times (h_{out} - h_{in})$$

Water flow rate for humidification process

The air mass flow rate in MAU system can be calculated from air flow rate and specific volume of air. The water flow rate can be calculated from the air mass flow rate and humidity ratio difference between humidifier inlet and outlet (Equation 3).

Equation 25: Required humidification water flow rate.

$$\dot{m}_{humidification} = \frac{\dot{Q}_{MAU}}{v_{air}} \times (w_{out} - w_{in})$$

Where:

- $q_{cooling}$:Heat exchange rate of cooling coil [kW]
- $q_{heating}$:Heat exchange rate of heating coil [kW]
- $\dot{m}_{humidification}$:Water flow rate of humidifier [kg/s]
- $\dot{Q}_{MAU}$:Air flow rate of MAU [m³/s]
- V_{air} :Specific volume of air [m³/kg]
- h_{in} 、 h_{out} :Enthalpy of coil inlet and coil outlet [kJ/kg]
- w_{in} 、 w_{out} :Humidity ratio of humidifier inlet and humidifier outlet [kg/kg]

Dry cooling coil

In order to achieve constant dry bulb temperature inside a cleanroom, the heat gain and heat removal must be balanced. The heat gain source consist process tool, lighting and operators. The heat removal component consist process cooling water, process exhausts, dry cooling coil and the cool fresh air from MAU. Therefore, the required heat exchange rate for dry cooling coil can be found by balancing the heat gain and heat source in a cleanroom.

Cooling load balance equations

By combining the equations mentioned in the introduction section, the cooling load can be derivative in to (Equation 4) and (Equation 5).

Equation 26: Energy balance.

$$\sum q_{heat\ gain} = \sum q_{heat\ removal}$$

Equation 27: Energy balance in cleanroom.

$$q_{light} + q_{FFU} + q_{people} + q_{tool} = q_{EA} + q_{pcw} + q_{MAU} + q_{DCC}$$

The heat emission from lighting, fan of FFU, operators and process tool are considered as the heat gain of cleanroom. The heat removed by exhaust air, process cooling water, cooled fresh air from MAU and dry cooling coil are considered as the heat removal of cleanroom.

Required heat exchange rate of the dry cooling coil

The required heat exchange rate," q_{DCC}", which is derivative from (Equation 6).

Equation 28: Cooling load of DCC
$$q_{DCC} = q_{light} + q_{FFU} + q_{people} + q_{tool} - q_{EA} - q_{pcw} - q_{MAU}$$

Where:

- $q_{heat\ gain}$: Heat gain of cleanroom [kW]
- $q_{heat\ removal}$: Heat removal of cleanroom [kW]
- q_{light}: Heat emission from lighting [kW]
- q_{FFU}: Heat emission from FFU [kW]
- q_{people}: Heat emission from operator [kW]
- q_{tool}: Heat emission from process tool [kW]
- q_{EA}: Heat removal by exhaust air [kW]
- q_{pcw}: Heat removal by process cooling water [kW]
- q_{DCC}: Heat removal by dry cooling coil [kW]
- q_{MAU}: Cold energy recovery by cool fresh air from MAU [kW]

Water chiller

Total cooling load of water chiller can be calculated by summery the coils (i.e. pre-cooling coil, cooling coil, dry cooling coil), PCW and other cooling loads. The electric energy consumption of water chiller can be calculated by dividing the total cooling load of chiller by COP of water chiller.

Equation 29: Water chiller power consumption.
$$W_{chiller} = \frac{\sum q_{cooling\ load}}{COP}$$

Equation 30: Cooling loads for water chiller power consumption calculation.
$$W_{chiller} = \frac{q_{pre-cooling} + q_{cooling} + q_{DCC} + q_{pcw} + q_{other\ cooling\ load}}{COP}$$

Where:

- $W_{chiller}$: The electric energy consumption of water chiller [kW]
- $q_{cooling\ load}$: Total cooling load of water chiller [kW]
- *COP*: Coefficient of Performance
- $q_{pre-cooling}$: Cooling load of pre-cooling coil [kW]
- $q_{cooling}$: Cooling load of cooling coil [kW]
- q_{DCC}: Cooling load of dry cooling coil [kW]
- q_{pcw}: Heat exchange rate of process cooling water [kW]
- $q_{other\ cooling\ load}$: Cooling load of other items [kW]

Heater

Most of the heat source of heater used in MAU system is electric heater or boiler. The required quantity of heat of electric heater can be calculated as the summation of total heat requirement (coils for preheating and reheating) divided by efficiency of heater (η_{heater} =1). For boiler, the required quantity of heat of boiler can be calculated as the summation of total heat requirement (coils for preheating and reheating) divided by efficiency of heater (η_{boiler}). Second, the required quantity of fuel can be calculated as required quantity of heat of boiler (W_{boiler}) divided by fuel heat value.

Process tool, exhaust system and utility system

As the manufacturing tool in cleanroom does not operating 24hr per day which will cause the loading of the utility system floating, therefore the uptime of tools and utilities should be considerate in the calculation. (

Table 77) shows the suggested ECF values for a specific utility system in SEMI S23 guideline [SEMI S23-0813, 2008].

Table 77 Suggested ECF values in SEMI S23 [SEMI S23-0813, 2008]

Utility or Material	ECF	Basis of Conversion Factor (other units)
Exhaust	0.004 kWh/m^3	Exhaust pressure:19.6E+2 Pa (200 mm H$_2$O; 7.9 in H$_2$O)
Vacuum	0.075 kWh/m^3	Vacuum pressure:58.8E+2 Pa (600mmAq)
Dry Air	0.147 kWh/m^3	Supply pressure:4.9E+5 Pa (71 psi; 5 kg/cm^2)
Cooling Water (20-25°C)	1.78 kWh/m^3	Water cooled by refrigeration process Supply pressure:4.9E+5 Pa(71 psi; 5 kg/cm^2)
Cooling Water (32-37°C)	0.250 kWh/m^3	Water cooled by open cooling tower Supply pressure:4.9E+5 Pa (71 psi; 5 kg/cm^2)
UPW / DIW (under pressure)	10.2 kWh/m^3	Supply pressure: 19.6E+4Pa (28.4 psi; 2 kg/cm^2)
UPW / DIW (ambient pressure)	10.0 kWh/m^3	Power for distilling
N$_2$*	0.250 kWh/m^3	Supply pressure: 7.93E+5 Pa (115 psi; 8.1 kg/cm^2)
Electricity	$1 \times (V_{RMS} \times I_{RMS}) \times$ measurement period = kWh	This is electrical energy supplied. This is not the same as energy used to generate the electricity

* Volume calculated at one atmosphere pressure and 20 °C

3 MODEL VERIFICATION
3.1 Measured data vs. FES simulated data

The operating parameters of a fab (named fab A) in Hsinchu Taiwan were used as a base data for model validation. (Tables 2, 3, and 4) show the indoor air conditions, make-up air unit properties, and properties of various utilities of the fab, respectively.

Table 78: cleanroom indoor air conditions.

Item	Value
Cleanroom dry bulb temperature	23°C
Cleanroom relative humidity	45%
Cleanroom total floor area	13,812 m2
Cleanroom height	3.5 m
Intensity of lighting	0.01186 kW/m2
Lighting coverage	100%
Cooling load of occupant	0.6 kW/person
Population	150

Table 79: Make-up Air Unit (MAU) design properties

Item	Value
OA condition	Weather data of Hsinchu, Taiwan
Relative humidity of cooling coil exit	100 %
MAU supply air dry bulb temperature	14 °C
Air washer pump head	93.8 m
Efficiency of air washer pump	65 %
Water flow rate of air washer pump	200 l/min

Table 80: Properties of various utilities

	Processing	Standby	Δt(°C)	ECF(kWh/m^3)
Utilization rate (%)	100	0	-	-
Process tool power consumption (kW)	9,300	0	-	-
General Ex. (CMH)	205,800	0	7.2	0.000723
Acid Ex. (CMH)	238,000	0	0.3	0.000723
Base Ex. (CMH)	49,000	0	0.3	0.000723
VOC Ex. (CMH)	61,200	0	5	0.000723
PCW(17-22°C)	810	0	5	0.383
PCW(20-25°C)	390	0	5	0.383
N$_2$(CMH)	3,600	0	-	0
Vacuum(CMH)	2,000	0	-	0.04
CDA(CMH)	5,700	0	-	0.1713
HCDA(CMH)	830	0	-	0.1713
UPW(CMH)	120.563	0	-	8

(Table 5) shows the difference between the measured data of the fab and the calculated data based on FES. Note that the differences are less than 4%. As the heating source of fab A is from heat recovery chiller, the energy consumption of electric heater was neglected and assumed to be zero. The nitrogen was purchased from external supplier; therefore the energy consumption of nitrogen system was to be zero too. Moreover, as the humidification was combined with MAU and RCU, we combine these two items into one in the comparison. In this sector, the percentage difference of total energy consumption between measured data and the simulated result is only 0.73%.

Table 81: Annual energy usage: measured data of the fab vs. simulated data of FES.

Item	measured data	simulated data	Error (%)
Water chiller (kWh)	35,136,151	33,880,442	-3.57
Heater (kWh)	-	-	-
Humidification (kWh)	1,917,398	248,703	-3.51
MAU、RCU Fan (kWh)		1,601,343	
FFU (kWh)	2,914,014	2,925,496	0.39
Exhaust Fan (kWh)	3,506,546	3,518,361	0.34
Lighting (kWh)	1,435,084	1,438,910	0.27
Process tool (kWh)	81,533,340	81,691,200	0.19
PCW system (kWh)	4,026,875	4,037,126	0.25
N2 system (kWh)	-	-	-
Vacuum system (kWh)	712,154	702,720	-1.32
CDA/HCDA system (kWh)	9,803,277	9,825,686	0.23
UPW system (kWh)	8,449,073	8,472,203	0.27
HW PUMP (kWh)	72,907	72,907	0.00
Total	149,506,819	148,415,097	-0.73

*Heat recovery chiller is applied, which provides hot water. Therefore, no electric heater is required.
**N$_2$ is purchased from supplier, therefore, no energy consumption in this item.
***Energy consumption data of DI system is merged to the UPW system.

Based on the result of verification in the above, the reliability of FES is confirmed.

3.2 Simulated data of CleanCalc II vs. simulated data of FES

The CleanCalc II was developed by Cohen and released in 2009 by ISMI [COHEN, 2009]. Using the data of fab A, the differences of simulated data between the two programs are discussed here. **Error! Reference source not found.** shows the energy consumption in utility by CleanCalc II and FES. As shown in the table, differences for all items are below 3%. Table 7 shows the annual total energy usage simulated by CleanCalc II and by FES. The difference in total annual cooling electric energy is notable (1.8%). This may be due to that the weather data adopted in CleanCalc II does not consist with weather data used in FES. The default averaged 1982-1999 weather data in various locations (Taipei city in this case) in the world was used in CleanCalc II and the weather data used in FES was the hourly weather data in Hsinchu Taiwan in 2012 [CENTRAL WEATHER BUREAU, 2012]. In using CleanCalc II, we find the following differences in calculation schemes of both programs. In Cleancalc II, fan power of MAU is considered to be completely converted to heating load. In the FES, that heating load is the portion of fan power of MAU subtracted by mechanical work (the work to move air over the fan). The cooling load of PCW is not included in the loading of chiller in Cleancalc II, but FES is. These may also result some differences in simulated annual cooling electric energy by the two programs. Overall, in annual total energy consumption from both programs, the difference is only 0.09%.

Table 82: Annual energy usage in various utilities: measuring data of Avs. simulated data of FES

Item	CleanCalc II	FES software	Error (%)
PCW - Chiller Cooled Annual Load (kWh)	2,717,948.56	4,026,096.00	-0.01
PCW - Evaporative Cooled Annual Load(kWh)	1,308,636.25		
Nitrogen Annual Load(kWh)	-	-	0.00
OFA Annual Load(kWh)	8,552,431.80	8,553,351.60	0.01
HP OFA Annual Load(kWh)	1,246,539.24	1,245,488.04	-0.08
Process Vacuum Annual Load(kWh)	701,115.36	700,800.00	-0.04
UPW Annual Load(kWh)	8,448,701.14	8,449,055.04	0.00
Exhaust-1 (Scrubbed) Annual Load(kWh)	1,273,308.05	3,508,747.92	2.37
Exhaust-2 (Heat) Load(kWh)	1,472,541.98		
Exhaust-3 (Solvent) Annual Load(kWh)	681,818.83		
TOTAL Utility Annual Load(kWh)	26,385,120.00	26,483,538.60	0.37

Table 83: Annual total energy usage: simulated data by CleanCalc II vs. simulated data by FES.

Item	CleanCalc II	FES software	Error (%)
Total Annual Cooling Electric energy(kWh)	12,611,549	12,842,920	1.83
Total Annual HVAC Electric energy(kWh)	19,860,945	19,841,408	-0.10
Total Annual Process Tool Electric energy(kWh)	81,468,000	81,468,000	0.00
Total Annual Internal Electric energy(kWh)	85,779,133	85,820,481	0.05
Annual utility total energy(kWh)	26,385,120	26,483,539	0.37
Total Annual Electric energy(kWh)	132,025,198	132,145,428	0.09
Total Annual Electric energy per unit area(kWh/m2)	9,558	9,567	0.10

4   CONCLUSIONS

A dedicated energy simulation program entitled FES for fabs was developed. Detailed calculation processes and equations are discussed. The features of the software were highlighted. The result of this program was verified with a fab's measured data and with a similar program Cleancalc II. Promising results are reached. Based on the results, it is believed that the FES program can be a reliable software to simulate power consumption of a fab, which can produce the baseline data for advancing energy conservation approaches, and for benchmarking the energy performance of fabs that produce similar products

5   REFERENCES

ASHRAE, 2005. ASHRAE Handbook of Fundamentals, American Society of Heating, Refrigerating and Air Conditioning Engineering Inc., Atlanta, P6.1-6.17

BROWN, WK., 1990. Makeup Air Systems Energy Saving Opportunities, ASHRAE Transactions, 96, 609-615.

BUREAU OF ENERGY, the Ministry of Economic Affairs. Taiwan, 2009. Handbook of home energy conservation. 2nd edition.

BUSCH, J., 1998, Cleanroom of the Future: An Assessment of HVAC Energy Savings Potential In a Semiconductor Industry Facility, Lawrence Berkeley National Laboratory, Berkeley, CA 94720.

CENTRAL WEATHER BUREAU, 2012, Hourly weather data in Hsinchu Taiwan.

COHEN, Ralph M., 2009. ISMI CleanCalc Ⅱ User Help Manual,International SEMATECH Manufacturing Initiative.

HU, S. C., XU, T., Chuang, T., Chan, Y.L., 2010. Characterization of Energy Use in Typical 300 mm Dynamic Random Access Memory Wafer Fabrication Plants in Taiwan, Energy 35, 3788-3792.

HU, S.C., Wu, J.S., Chan, Y.L., Hsu, T.C., Lee, C.C., 2008. Power consumption of a semiconductor cleanroom facility system", Energy and Buildings, 40, 1765-1770.

HU, S.C., Chuah, Y.K., 2003, Power consumption of semiconductor s in Taiwan", Energy, 28, 895-907.

JOINT STATEMENT ON THE NINTH MEETING OF THE WORLD SEMICONDUCTOR COUNCIL, May 19, 2005, Kyoto, Japan.

KIRCHER, K., Shi, X., Patil, S., Zhang, K. Max, 2010. Cleanroom energy efficiency strategies: Modeling and simulation. Energy and Buildings 42 282–289

MASUDA, T., Samata, S., Mikata, Y., 2005. Virtual fab technology utility simulation and its application to 300 mm CR facility design and energy reduction", Proc. ISSM, 17-20, San Jose.

MATHEW, P., Foley, S., Hebert, A., 2009. Cornell University Cleanroom Energy Benchmarking Summary Report, Technical report prepared for NYSERDA.

MCQUISTON, F.C., Parker, J.D., Spitler, J.D., 2005. Heating, Ventilating, and Air Conditioning: Analysis and Design, 6th Ed., John Wiley & Sons, Inc., U.S.A.

NAUGHTON, P., 1990. HVAC Systems for Semiconductor Cleanrooms, ASHRAE Transactions 96 (1), 620-625.

NAUGHTON, P., 1990. HVAC Systems for Semiconductor Cleanrooms, ASHRAE Transactions 96 (2), 626-633.

NAUGHTON, P., 2005. Measurement of Conservation of Energy by Semiconductor Manufacturing Equipment and setting of targets for improvements, IEEE International Symposium on Semiconductor Manufacturing (ISSM 2005), 7-16, San Jose.

NAUGHTON, P., 2006. New tool for targeting energy improvements in semiconductor manufacturing equipment, Proc. ASMC, 428 – 432, Boston.

SEMI S23-0813, 2008. Guide for Conservation of Energy, Utilities, and Materials Used by Semiconductor Manufacturing Equipment.

SOLAR ENERGY LABORATORY, 1996. TRNSYS User Manual, University of Wisconsin-Madison.

TSCHUDI, W., Mills, E., Xu, T., Rumsey, P., 2005. Measuring and managing cleanroom energy use, Heating/Piping/Air Conditioning Engineering: HPAC, 77 (12), 29–35.

TSCHUDI, W., Rumsey, P., 2004. Using benchmarking to identify energy efficiency opportunities in cleanrooms: the labs 21 approach, ASHRAE Transactions, 110 (1), 770–775.

TSCHUDI, W., Xu, T., 2003. Cleanroom energy benchmarking results, ASHRAE Transactions, 109 (2), 733–739.

198: A Study on the development of measuring equipment of the solar heat gain performance by using a natural sunlight

SEOK-HYUN KIM[1], SANG-HOON LIM[2], SOO CHO[3]

1 Korea Institute of Energy Research (KIER), 152, Gajeong-ro, Yuseong-gu, Daejeon, Korea, ksh7000@kier.re.kr

2 Korea Institute of Energy Research (KIER), 152, Gajeong-ro, Yuseong-gu, Daejeon, Korea, shlim@kier.kr

3 Korea Institute of Energy Research (KIER), 152, Gajeong-ro, Yuseong-gu, Daejeon, Korea, scho@kier.re.kr

In the middle of the effort of the energy consumption reduction in buildings, the area of window at building was increasing according to the view of exterior and the method of construction. The insulation performance of window is low than the building envelope and the solar heat gain performance affects the building energy consumption of heating and cooling. Many efforts to improve the window performance have been made. The method how to verify the window performance was also proposed. This method helped designer to choose of type of window and performance of window. The solar heat gain performance test method by the use of solar simulator was developed. But the measuring equipment about solar heat gain performance of window by use of natural sunlight was not utilized. This study proposed the measuring equipment about solar heat gain performance of window by use of natural sunlight.

1. INTRODUCTION

Along with the increase of the overall area of the window on the envelop of building, it is required to improve the efficiency of the window. As a window has lower performance of thermal insulation comparing to the envelop of building, various ways to enhance the performance of thermal insulation is currently studying to strengthen the performance of the thermal insulation. Especially the government of KOREA is given a level of 'Certification for Energy Labeling' that is required the performance of thermal insulation and airtightness. Heat transfer coefficient was lowered to ameliorate the performance of thermal insulation of the window; however, unlike envelope of building, windows have the characteristic of transmission body. In other words, when natural sunlight approaches to the building, the solar heat gain occurs through the window toward the interior of the building. Because of this, during the summer seasons, in the case of buildings that have high window to wall ratio, it can provoke serious heating load. Efforts to decrease the cooling load through controlling the performance of solar heat gain of the window are underway in many researches. Unlike the performance of thermal insulation, if the solar heat gain performance is deliberately set to attenuate the solar heat gain, it can rather cause the increase of heating load by decreasing the solar heat gain that penetrates into the building. According to Kim's research (2014), when performance of thermal insulation of the window meliorates, Indoor heating and cooling energy consumption declines; and, under the same condition, when solar heat gain coefficient increases, indoor heating and cooling energy consumption rather increases [1]. Kim(2014) also identified that, in the case of installing the horizontal shading, indoor cooling and heating energy consumption inverses according to the solar heat gain coefficient [2]. Because of this reason, designers are careful in choosing the solar heat gain performance of windows. Along with the importance of the solar heat gain performance comes to the fore, it is underway to develop the way to measure the performance of solar heat gain in Korea. Ordinarily the performance of solar heat gain of windows or blind shades has predicted using the method of optical analysis of glazing (i.e., analyzing, calculating, or simulating the transmissivity of wavelength range), but recently solar simulator appears as a new way to measure the solar heat gain performance. However, as it is using artificial light sources, it is impracticable to create the same solar heat gain phenomenon of natural sunlight; and also, it is difficult to verify the effect of solar radiation that penetrates to the building from various angles, just like the actual building on the street.

Therefore, this study aims to develop measurement methods or devices of solar heat gain performance from natural sunlight , contemplating the solar heat gain coefficient from artificial light sources and natural light.

2 SOLAR HEAT GAIN COEFFICIENT (SHGC)

Among the indexes that indicate the solar heat gain performance of windows, solar heat gain coefficient (SHGC) currently receives more attention while shading coefficient (SC) that describes the level of solar shading based on the 3 mm glass was widely used in the past. Solar heat gain coefficient is a ratio that describes amount of solar energy that enters a building through the windows. ASHRAE Fundamentals(2009) suggest solar heat gain coefficient, like following equation 1 [3].

Equation 31: Solar heat gain coefficient $$SHGC = q_b / E_D$$

Where:

- SHGC = Solar Heat Gain Coefficient
- q_b = Total solar gain (W/m²)
- E_D = Direct solar irradiance to window (W/m²)

Solar heat gain coefficient (SHGC) refers to the ratio of solar radiation amount, before and after admitted through windows. As not only it is applicable to the shading that sets up on the exterior of the windows but also it describes solar heat gain performance of glazing material like windows, SHGC replaces shading coefficient (SC). Also, if penetration ratio of windows is identifiable, considering the solar radiation influence that is absorbed into the windows, it contemplates the effect of indoor re-radiation. Equation 2 is a method of calculation of solar heat gain coefficient which takes both solar transmittance of fenestration system and inward-flowing of absorbed radiation into account.

Equation 2: Solar heat gain coefficient by
transmittance

$$SHGC = \tau_s + N_i \bullet \alpha_S$$

Where:

- τ_S = Solar transmittance of fenestration system
- N_i= inward-flowing fraction of absorbed radiation
- α_S= solar absorptance of a single-pane fenestration system

Although glass transmissivity is easy to gauge with the method of optical analysis, calculating transmissivity of window is obscure because, depend on the shape and quality of the material of windows, each part of the window shows various value. Therefore, if installing the windows, it is required to develop the experimental equipment that allows ascertaining the quantity of radiated outdoor solar radiation for the received indoor solar insolation.

3   METHOD OF MEASURING OF SOLAR HEAT GAIN COEFFICIENT

There is a way to calculate solar heat gain coefficient (SHGC) through the simulation using transmissivity of the components, however it has a shortcoming that it is difficult to measure SHGC about various non-uniform types of windows. In the following section, it will discuss about existing methods that assess solar heat gain coefficient of windows.

3.1 KS L 9107

KS L 9107: Testing method for the determination of solar heat gain coefficient of fenestration product using solar simulator, which was enacted by Korea Industrial Standards, is using the SHGC measuring equipment of windows [4]. The equipment that Korea Industrial Standards suggested consists of solar simulator that enables to control the amount of solar radiation and climatic chamber and metering box that create indoor and outdoor environment. The solar radiation which was irradiated from solar simulator penetrates the climatic chamber that portrayed outdoor environmental condition. Solar radiation that penetrated the specimen flows into the metering box that copied indoor environmental conditions, and measuring and removing of solar heat gain coefficient is proceeding at the same time. Figure 1 describes the scheme of measuring equipment and equation 3 is the calculation of SHGC by KS L 9107.

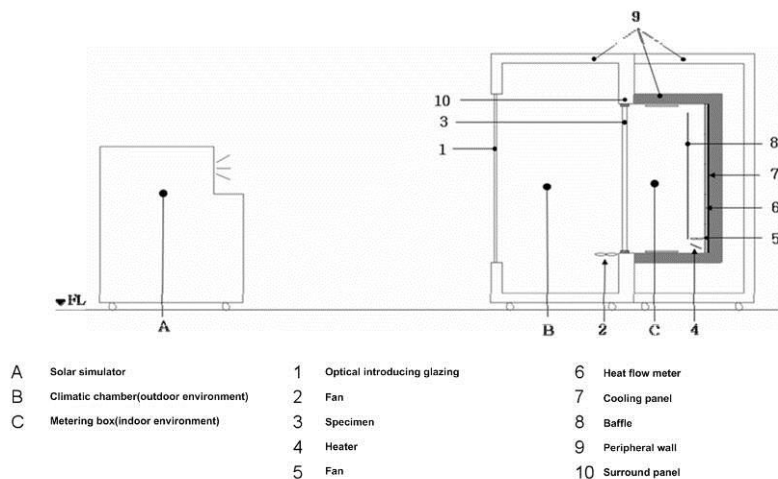| A | Solar simulator | 1 | Optical introducing glazing | 6 | Heat flow meter |
B	Climatic chamber(outdoor environment)	2	Fan	7	Cooling panel
C	Metering box(indoor environment)	3	Specimen	8	Baffle
		4	Heater	9	Peripheral wall
		5	Fan	10	Surround panel

Figure 140: Scheme of measuring equipment

Equation 3: Calculation of SHGC by KS L 9107 $$SHGC = \frac{Q_{gain}}{Q_{solar}} = \frac{(Q_C - Q_f - Q_h \pm Q_p) - Q_{sp}}{Q_{solar}}$$

Where:

- Q_{gain} = Heat flux through specimen (W)

- Q_{solar}= Intensity of solar radiation at surface of specimen (W)

- Q_c= Removed heat flux of cooling panel (W)

- Q_f= Calorific value of fan (W)

- Q_h= Input calorie of heater (W)

- Q_p= Heat flux at surround panel (W)

- Q_{sp}= Heat flux through thermal transmittance of specimen (W)

To confirm heat flux through specimen (Q_{gain}), KS L 9107 calculates the removed heat flux of cooling panel (Q_c), calorific value of fan (Q_f), input calorie of heater (Q_h), and heat flux at peripheral wall (Q_p). Also, heat flux through thermal transmittance of specimen (Q_{sp}) is calculated using heat transmittance coefficient that was identified through the measurement of thermal transmittance of specimens under no solar radiation conditions. In this standard, as it uses solar simulator, it is ambiguous to confirm the solar heat gain of windows of the actual buildings. As cooling panel is checking heat flux with heat flux meter, maintenance can be also problematic because of the frequent corrections of systematic errors of heat flux meter.

3.2 NFRC 201

To measure the solar heat gain coefficient of windows, NFRC 201 (i.e., Procedure for interim standard test method for measuring the Solar Heat Gain Coefficient of Fenestration Systems using calorimetry hot box methods) suggests a measurement device that applies calorimeter from natural sunlight exposed external environment [5]. In NFRC, the calculation of SHGC mentions solar irradiation incident on the test specimen and the difference between heat flux through test specimen (Q_S) and heat flux due to air temperature difference of test specimen ($Q_{U\text{-}factor}$). Following equation 4 refers to the calculation of SHGC that penetrated the test specimen.

Equation 4: Calculation of SHGC by NFRC 201

$$SHGC = \frac{Q_S - Q_{U-factor}}{A_S E_S}$$

Where:

- Q_S = Heat flux through test specimen (W)

- $Q_{U\text{-}factor}$= Heat flux due to air temperature difference of test specimen (W)

- A_S= Projected area of test specimen (m²)

- E_S= Solar irradiation incident on the test specimen (W/m²)

To confirm Heat flux through test specimen (Q_S), it is necessary to check heat flux through solar calorimeter walls (Q_{Walls}), heat flux through surround panel (Q_{SP}), heat flux by flanking loss (Q_{fl}), heat removed by fluid heat extraction system (Q_{fluid}), and Heat input into solar calorimeter by pumps and fans (Q_{AUX}). Equation 5 indicates the calculation of heat flux through text specimen (Q_S), and Figure 2 illustrates the scheme of the measuring device.

Equation 5: Calculation of Heat flux through test specimen

$$Q_S = Q_{Walls} + Q_{SP} + Q_{fl} + Q_{fluid} + Q_{AUX}$$

Where:

- Q_{Walls} = Heat flux through solar calorimeter walls (W)

- Q_{SP} = Heat flux through surround panel (W)

- Q_{fl} = Heat flux by flanking loss (W)
- Q_{fluid} = Heat removed by fluid heat extraction system (W)
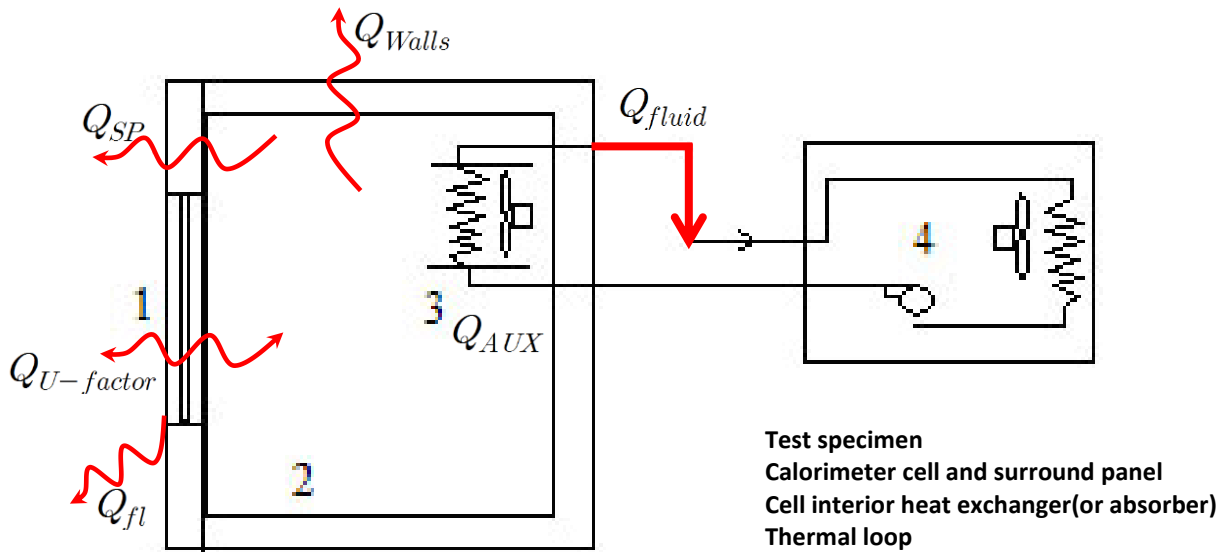- Q_{AUX} = Heat input into solar calorimeter by pumps and fans (W)

Figure 141 Typical components used in a calorimeter apparatus by NFRC 201

As calorimeter apparatus by NFRC 201 should consider heat flux through surround panel (Q_{SP}), it is essential to confirm the performance of thermal insulation of the surround panel of specimen. Since it is exposed to the external environment and easily influenced by the external condition, the wall of calorimeter heavily affects the measuring of solar heat gain coefficient. Also, as natural sunlight is used as a light source, solar incidence angle is changing with installation location and experiment time; therefore, it is necessary to come up with an effective solution for coping with the variation of angle.

Through considering the existing measurement methods of solar heat gain coefficient of windows, in this study, the author proved the necessity of development of the SHGC calculating equipment that not only uses natural sunlight but also strengthens the limit of current measurement techniques. Table 1 compares KSL 9107 and NFRC 201 according to the light source and measuring method.

Table 1 Comparison of measuring method

	KS L 9107	NFRC 201
Light Source	Solar simulator	Actual sun
Measuring method	Heat flow meter	Calorimeter(cooling water)

4   DEVELOPEMENT OF THE SHGC MEASURING EQUIPMENT

In this study, the authors intend to develop the SHGC measuring equipment that assesses the SHGC of windows after eliminating the heat flux through the windows and computing the eliminated heat flux. The device is created based on NFRC 201 method that uses natural sunlight. NFRC 201 SHGC measuring method can be affected by the external environment through the wall of calorimeter and surround panel. After assessing the factor of outdoor environment, it applies to the component of property of material that constitutes the measuring equipment; therefore, this method is difficult to calculate the SHGC by outdoor temperature, wind velocity and the convection heat transfer coefficient. Thus, to minimize the flow of heat flux that is created from the parts except for the specimen, through installing the thermal guard that surrounds the calorimeter, it was constructed to equally operate the internal temperature of calorimeter and thermal guard temperature. Additionally, specimen surround panel and calorimeter was unitized, and a part of the calorimeter was designed to be filled with the specimen. Then, it does not consider the heat flux through surround panel (Q_{SP}), and it is to avoid heat loss and heat gain of another specimen surround wall. Measuring equipment also enables to move and change the direction depends on the solar altitude and direction of the sun to control the incidence angle. For counting the Q_S, Q_{SP} was excluded. Equation 6 is the calculation of heat flux through test specimen (Q_S), and figure 3 indicates the scheme of developed measuring equipment.

*Equation 6: Calculation of Heat flux through test specimen by developed measuring equipment of SHGC*

$$Q_S = Q_{Walls} + Q_{fl} + Q_{fluid} + Q_{AUX}$$
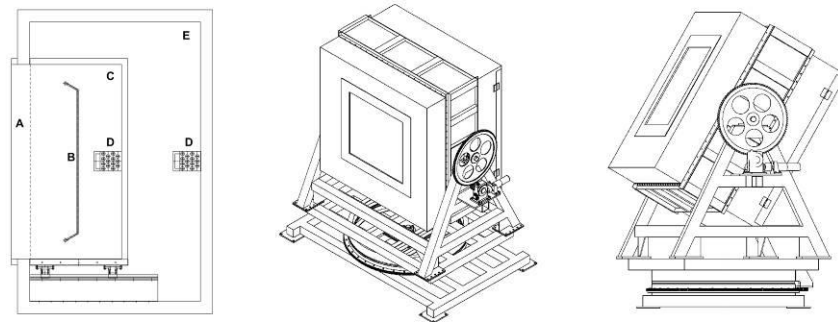
A : Specimen Frame position   B : Absorber plate   C : Calorimeter box   D : Fan and Heat exchanger   E : Thermal guard

Figure 142 Scheme of developed measuring equipment

To verify the maintain set point of internal temperature of the developed SHGC measuring device, 6mm clear glass was installed and it was confirmed whether maintained or not. Experiment was proceeded from 7 p.m. to 5 a.m. when there is no solar heat gain, and set point of internal temperature was 20℃; and, heating and freezing machine was operated. After checking the air temperature at B(between specimen to absorber plate) and air temperature at C(between absorber plate to calorimeter box's back), mean air temperature in calorimeter box was calculated; and, outdoor air temperature was also confirmed. Figure 4 shows sensor position scheme and exterior of measuring equipment.
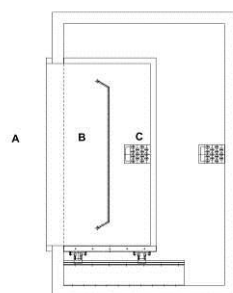
A : Outdoor Air Temp.
B : Between specimen to absorber plate
C : Between absorber to calorimeter box´s back

(a) Sensor position of air temperature   *(b) Exterior of measuring equipment*

Figure 143 Sensor position scheme and exterior of measuring equipment

Developed measuring equipment was operated to maintain the set point of the indoor temperature, and the average indoor air temperature was 20℃±1℃ even when lowest outdoor temperature was dropped to -8℃. Air temperature between specimen and absorber plate dropped by the influence of the outdoor temperature, and this is because 6 mm clear glass, which was used on the experiment, has lower performance of thermal insulation; and, this characteristic makes the glass easy to be affected by the outdoor temperature change. Figure 5 describes the variation of air temperature by result of pretest.
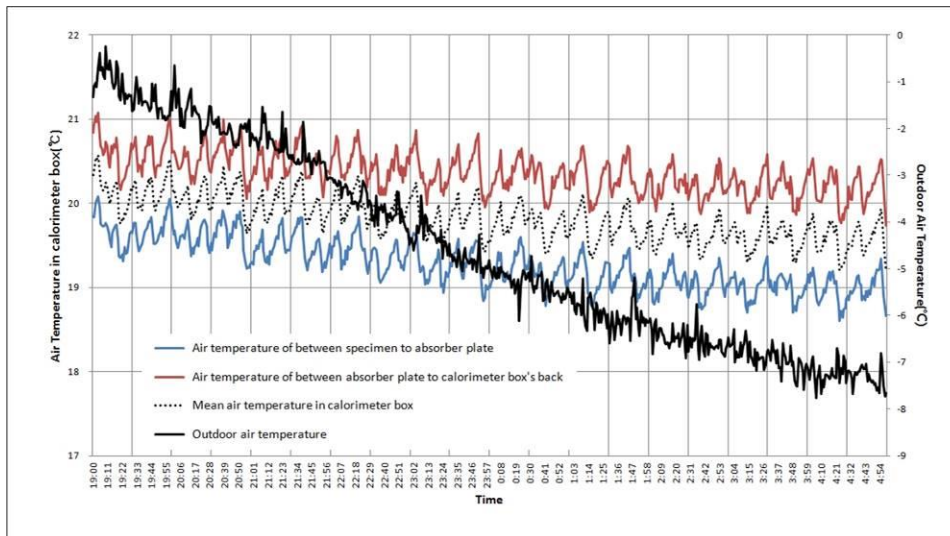

Figure 144 Variation of air temperature by result of pre-test

5   CONCLUSION

In this research, newly developed SHGC measuring equipment essentially aims to use calorimeter and natural sunlight as a light source, and it was constructed by comparing the types of light sources and measuring methods. After the pre-test, It also proved the stability of the internal temperature of the metering box when it sets up the set point of indoor temperature of the calorimeter even during the nighttime when there is no solar radiation effect.

6   REFERENCES

KIM, Seok-Hyun, Kim, Sun-Sook, Kim, Kwang-Woo, Cho, Young-Hum, 2014, A study on the proposes of energy analysis indicator by window elements of office buildings in Korea, Energy and buildings, Vol. 73, 153-165.

KIM, Seok-Hyun, Shin, Kyung-Ju, Choi, Bo-Eun, Jo, Jae-Hun, Cho, Soo, Cho, Young-Hum, 2015, A Study on the Variation of Heating and Cooling Load According to the Use of Horizontal Shading and Venetian Blinds in Office Buildings in Korea, Energies, Vol. 8, 1487-1504.

ASHRAE, 2009, ASHRAE Handbook-Fundamentals, http://www.ashrae.org.

Korean agency for technology and standards, 2014, KS L 9107:Testing method for the determination of solar heat gain coefficient of fenestration product using solar simulator, www.kats.go.kr.

National Fenestration Rating Council, 2010, NFRC 201 :Procedure for interim standard test method for measuring the solar heat gain coefficient of fenestration systems using calorimetry hot box methods, www.nfrc.org.

KIM, Seok-Hyun, Park, Jeong-Hwan, Cho, Soo, 2014, A Study on the development of measuring equipment about the solar heat gain performance of window by use natural sunlight, Korea J. Archit. Instit. Spring Conf. 2014, Vol. 33(1), 239-240.

210: Optimising housing design to improve energy efficiency in Jordan

HEBA NAZER[1], LUCELIA RODRIGUES[2]

1 Middle East University, Jordan, Nazerheba @gmail.com
2 University of Nottingham, UK, Lucelia.Rodrigues @nottingham.ac.uk

Jordan faces an energy crisis aggravated by the limitation of energy resources and coupled with the high dependency on neighbouring countries. In addition, the raise in the country's population has resulted in excessive pressure on the residential sector to hasten housing construction projects resulting in a reduction of quality in favour of speed. A viscous cycle was created in which new buildings with poor thermal performance further exacerbate the energy crisis. Adding to the problem, a significant rise in summer temperatures is anticipated in the near future as a result of climate change, which would result in even more demand for active means of space conditioning.

The objective of this research was to assess the thermal performance of a typical residential apartment in Amman, and propose interventions that would help reduce its reliance on mechanical methods of space conditioning during cooling periods. Through dynamic simulation modelling, a parametric analysis was developed involving a number of iterations exploring different fenestration designs and thermal transmittance values for walls. In order to improve the models' accuracy, the results of a longitudinal survey of residents in 145 similar apartments were utilized to inform the simulation assumptions. The survey gathered data on the occupants' thermal perception and behaviour, their socio-economical attributes and the building physical characteristic and use.

The authors concluded that small amendments in the design, such as the incorporation of natural ventilation for parts of the year, could enhance the thermal performance up to 45%. The optimum glazing to wall ratio for more energy efficient residential buildings within the context of Jordan was defined as 15% to 20% in all orientations, whereas the thermal transmittance for walls and roofs as 0.13W/m2K. The conclusions were proposed as a set of recommendations to help designers to choose optimal building element characteristics and orientation for each function in early design stages.

Keywords: Thermal comfort, Energy efficiency, Design codes

1. INTRODUCTION

Jordan is facing an energy crisis due to the limited availability of fossil fuels, the excessive reliance on imported resources from neighbouring countries, combined with a high demand for energy (Mohsen and Akash, 2001). The main contributor of the energy crisis is the remarkable growth in population during the past several years. This phenomenal expansion in population is causing pressure on the construction sector to provide 55 thousand housing units annually (Al-Momani, 2013). Consequently, the real estate agencies and developers are responding by providing a large range of market oriented buildings to satisfy these prerequisites. Such buildings are constructed with speed dissenting environmental and contextual attributes and transforming the look and feel of the city. As a result, this elevates the urge for essential transcribes to support and evaluate these buildings' performance in order to prevent further exacerbating the crisis.

The residential sector has the highest energy consumption amongst all sectors, accounting for 61% of the electricity demand; this is anticipated to increase by 5.5% between 2008-2020 (Iwaro and Mwasha, 2010). Consequently, addressing energy efficiency in housing by providing comfortable environments that reduce the need for mechanical cooling and heating is essential. Multiple guidelines have been proposed by the government as starting steps to ensure the compliance with climate-conscious design (Awadallah, Adas et al., 2009), however, the pressure on the construction industry to build faster and cheaply leads the developers to often sacrifice adhering to these guidelines. In this work, the authors assessed a typical residential building in Amman in the context of these guidelines in order to identify simple yet effective strategies to enhance the building's performance, and support the argument towards the need for a more robust implementation of energy efficiency focused regulations.

2 JORDAN'S CONTEXT

The Hashemite Kingdom of Jordan extends between the latitudes of 29º and 33º N in the centre of the Middle East and the Arab world. Its climate presents contrast from the subtropical climate in the west to semi-arid deserts in the east. During summer, this climate is moderate to hot and dry, whereas the winters are cold and rainy (Alzoubi and Malkawi, 2015). The coldest month in the year is January with temperatures as low as 0ºC, whereas the hottest month is July with extreme temperatures reaching around 35ºC. The summer season starts in May and extends four months, whereas winter ranges from November until February. Spring and autumn occupy two months each, however, temperatures in both seasons are still considered moderate to hot. In contrast to these hot weather conditions that occupy a significant duration of the year, residential buildings fall short of comfort conditions in cooling seasons which is resulting with extreme energy consumption from mechanical cooling, therefore, this will present the focus of the study.

Thermal comfort depends on a series of factors such as temperature, humidity and air movement, which are reliant on a number of interrelated parameters of physical building attributes such as orientation, fenestration design and building envelope (Darby and White, 2002). Modifications on these characteristics will directly affect the level of comfort in the interior environment and consequently impact on energy efficiency; hence it is essential to achieve the required values of thermal comfort in buildings.
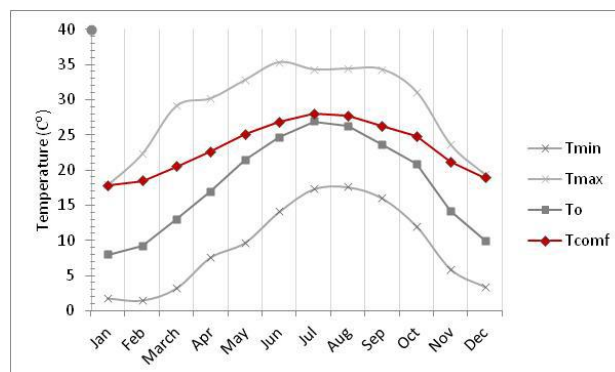
Figure 1: Thermal comfort ranges in Amman

Various studies explored the effect of building design on the energy consumption and total reduction in heating and cooling loads; Hassouneh and Alshboul et al. (2010) explored the effect of window design on the energy balance in residential apartments in Amman. They concluded that some types of glazing could decrease heating costs in winter when placed in a specific orientation. It recommended increasing the

glazing ratio in the south, east and west facades to promote energy saving during winter. Al Zyood and Harahsheh et al. (2010) highlighted the importance of passive strategies in reducing annual heating loads in typical apartments in Jordan. Through computer simulations, they concluded that 82% of annual reduction can be achieved by orienting the house properly with the addition of optimum insulation and the trombe wall system. On the other hand, Ouahrani (2010) had a wider scope of work on apartments in Amman, involving amendments on glazing and thermal properties of roofs and walls. The study came up with requirements on thermal transmittance (U-values) for both roofs and walls to be between 0.5 and 0.7 W/m²K. The optimum window to wall ratio for a south oriented façade was found to be between 12% and 20%. If implemented, these would allow total savings in energy up to 70%. Unlike similar studies that mostly considered calculating heating loads and energy consumption during winter, this paper will link the effect of design element characteristics to the required level of thermal comfort during cooling seasons which occupy most of the year. Additionally, it will result with optimum glazing ratios for all orientations depending on the occupancy patterns in various functions of the house.

3   METHODOLOGY

The research objectives were achieved through dynamic simulation modelling of a typical apartment using TAS software by EDSL. The parametric analysis was developed involving a number of iterations on opaque and transparent elements of the building as displayed in Figure 2. Additionally, due to the importance of occupants' behaviour in the simulation of the thermal performance of buildings, a survey was designed to inform the model assumptions.
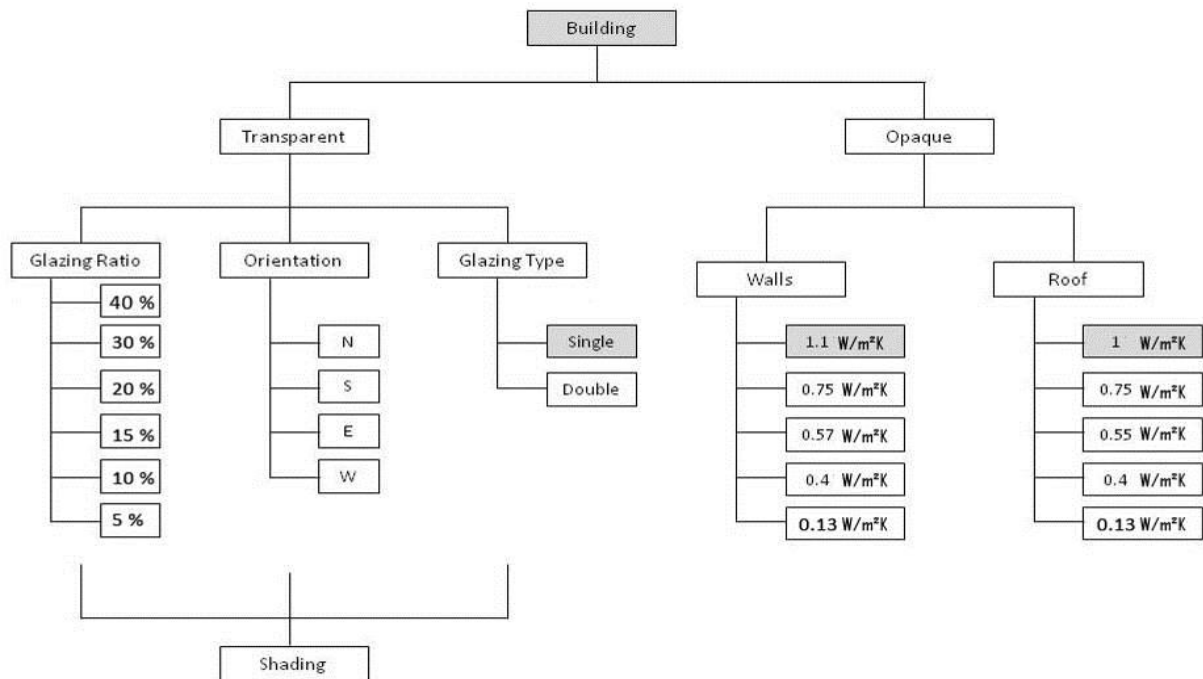

Figure 2: The building optimisation process developed by the authors through dynamic modelling

3.1 Occupants' Behaviour

Field surveys are key to understanding people's interaction with their environment (Nicol and Humphreys, 2012). From occupants' perception and thermal sensation in their buildings we can understand the problems faced by the occupants. Furthermore, their thermal attitudes and behaviour in response to their culture and context reveals the adaptation opportunities the building may offer.

Consequently, a longitudinal thermal comfort survey was designed by the authors on Qualtrix website. It followed the classic type of thermal comfort field surveys (level 2) defined by Nicol and Humphreys in their book "Adaptive Thermal Comfort" (2002). It was chosen because the survey involved measurements of the thermal environment along with subjective responses from occupants. Invitations were distributed via email to the targeted sample of residents in apartment buildings in Amman. The internet was a valued tool to obtain information from respondents living in remote with simple, quick and low cost methods (Evans and Mathur, 2005). The total respondents were 145 with an achieved response rate of 88.5%. The questionnaire

was structured in two pages of four main sections. The coherence and design of the questions affected reliability and varied according to the type of investigation. The 7-point scale, which is the most used in thermal environmental studies (Haddad, King et al., 2012), was adopted to measure the subjective response of occupants. It merged between thermal sensation and comfort following the Bedford scale from "too cool" to "too warm" (Zhang and Zhao, 2008).

The first set aimed to collect information about the socio-economic characteristics of the respondents in relation to their apartment. This included the respondents' age and gender, followed by the total number of occupants and the time they spent at home. Consequential to that were questions that identified the building's overview containing location, area, and number of floors. The second section explored the users' satisfaction of lighting and minor environmental issues. Additionally, the main part was structured to appraise the thermal sensation and behaviour of occupants in winter and summer. Due to the important relation between thermal comfort and temperature, a section was devoted to assess the residents' perception of air temperature during both seasons. The results of the survey were used to informed behavioural aspects that were incorporated in the thermal performance simulations.

3.2 Model Assumptions

The input parameters in the dynamic simulation model regarding occupancy were based on the survey and set as follow:

– Calendar: The year was divided to heating periods from November to March, and free running period from March to October, which represents the main scope of this study.
– Equipment: The kitchen was equipped with an oven, a fridge, a microwave and a water kettle, while the living room only had a television.
– Schedule of occupancy: According to the survey results, the house was occupied by the average household in Amman of 5 family members. The schedule was suggested based on personal experience to suit the culture and context of Amman. All heat outputs of the average body were taken as 100W (Szokolay 2008. p.16), where 35W was sensible heat and 65W was latent heat.
– Infiltration rate: According to the Jordan's Insulation code, infiltration in Jordan could range between 1 to 1.5 ach. However, in order to evaluate the effect of other parameters, the value was set to 0.5 ach referring to the assumptions by (Ouahrani, 2010) in their assessment of apartments in Amman.
– Ventilation: Natural ventilation was enabled in Cases B and C. It was controlled by the building simulator to begin to open when the resultant temperature in the zones exceeded 19ºC and fully open when it reached 29ºC. However, if the external temperature surpassed the internal values, the windows will close to reduce heat gain. The openable proportion of the aperture types was set to 0.5 in sliding windows, and 0.35 in the bathroom casement windows.
– Comfort temperature range: According to the climatic analysis, the coldest month in Amman is January and the warmest is July with average temperatures of 8ºC and 26.9ºC respectively. The acceptable operative temperature for 90% of the people ranges from 19ºC to 29ºC according to the ASHRAE 55 standard (ASHRAE, 2004). However the range designated in the research, was narrowed between 19ºC to 26ºC following the equation (Tcomft=17.8+0.31To) to maintain higher levels of comfort. The simulation results were illustrated by means of the percentage of hours in the year (excluding winter).
– Dwelling's context and typology: The apartment selected for simulation followed the typical design in Amman with a total area of 150m^2. The three main zones designated for investigation, as displayed in Figure 3 and 4, were: the living room, the kitchen and the bedroom modelled with similar areas of 20m^2.
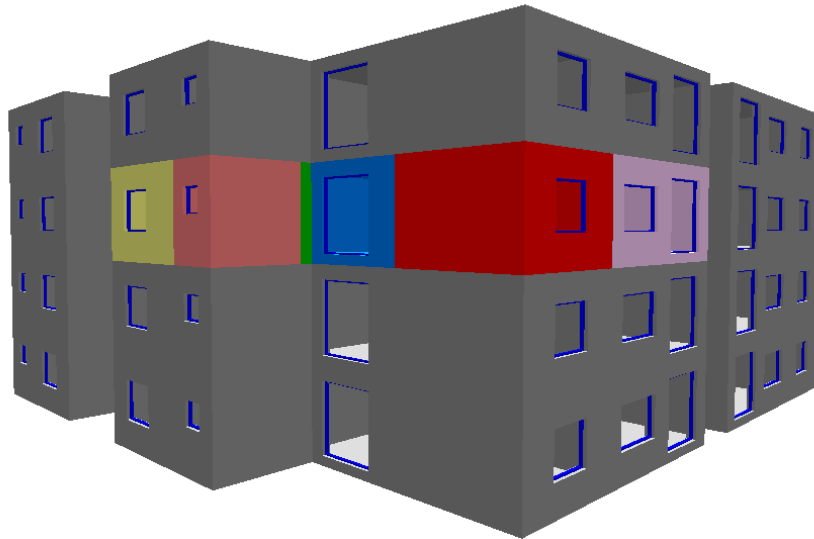
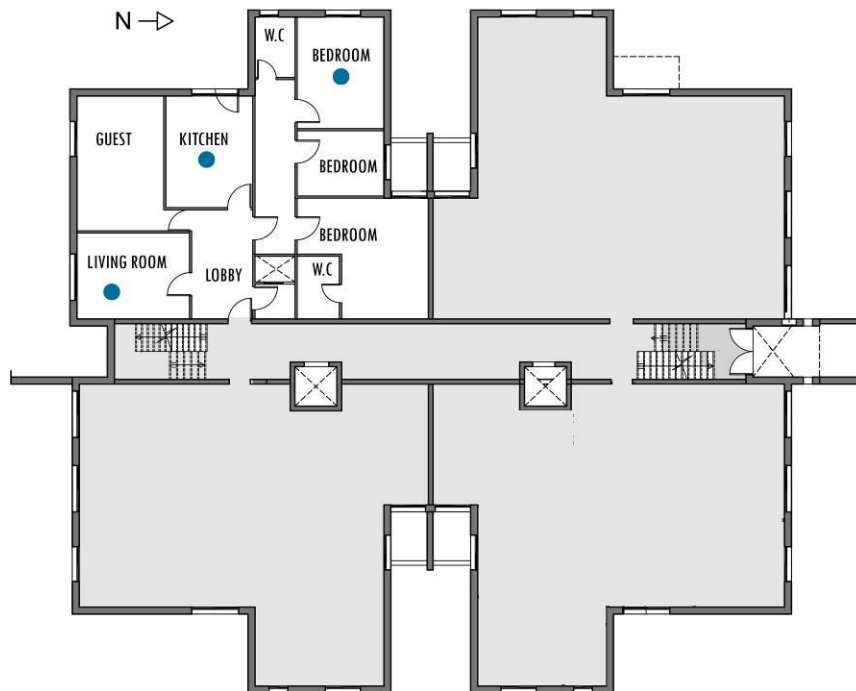*Figure 3: The apartment building simulated on TAS software*

Figure 4: Typical plan of simulated building

3.3 Scenarios

The simulations were conducted in three scenarios marked as A, B, C. Case A was a simplified model without heat gains and ventilation, Case B had the addition of natural ventilation, whereas Case C included the actual occupancy, internal heat gains, and ventilation.

Fenestration Design: The first set of parametric study tested the effect of window to wall ratios on the interior comfort level in reference to natural ventilation and orientation. The glazing ratios tested were 40%, 30%, 20%, 15%, 10% and 5%.

Building Envelope: The base case represented the typical method of construction with U-values equal to 1.1 W/m²K. Furthermore, the insulation layer was increased to comply and surpass the Jordanian Insulation Code with U-values equal to 0.75 W/m²K, 0.57 W/m²K, 0.4 and 0.13 W/m²K. The selected material properties are presented in Figure 5.

	width	conductivity	Density	Specific Heat
	(mm)	W/m.C	(kg.m)	J/Kg.C
Uvalue=0.13 (W/m2)				
Enhanced Cement Plaster	25	0.042	2000	1000
Hollow block	150	0.04	1380	1080
Extruded Polystrene	100	0.04	20	1500
Concrete	100	0.4	2400	840
Lime Stone	70	0.1	2500	860
Uvalue=0.57 (W/m2)				
Cement plaster	25	1.7	2000	1000
Hollow block	100	0.7	1380	1080
Extruded Polyestrene	50	0.04	20	1500
Concrete	150	1.85	2400	840
Limestone	70	2.2	2500	860
Uvalue=0.75 (W/m2)				
Cement Plaster	25	1.7	2000	1000
Hollow block	100	0.7	1380	1080
Extruded Polystrene	30	0.04	20	1500
Concrete	150	1.85	2400	840
Limestone	70	2.2	2500	860

Figure 5: Sample of building fabric characteristics

4 RESULTS

The results were organised in two parts according to the elements of the optimisation process.

4.1 Fenestration optimizations

When natural ventilation was disabled, thermal comfort increased 20% in south and west orientations, and 10% in the north and east as glazing ratios were minimised to 5%. West facing rooms achieved the least thermal comfort in all cases. South orientations performed better than north only when glazing ratios were 15% or less (Figure 6). In Case B, displayed in Figure 6, when natural ventilation was enabled, thermal comfort improved by around 30%. The optimum glazing ratios varied between 15% to 20% in all orientations. The highest values of comfort, equal to 75%, were achieved in rooms located in south facades.
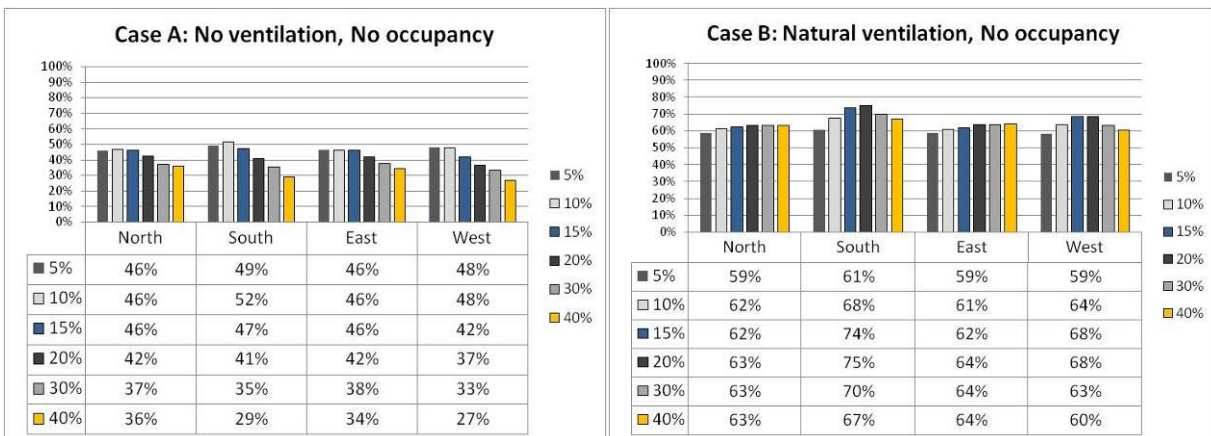

Case A: No ventilation, No occupancy

	North	South	East	West
5%	46%	49%	46%	48%
10%	46%	52%	46%	48%
15%	46%	47%	46%	42%
20%	42%	41%	42%	37%
30%	37%	35%	38%	33%
40%	36%	29%	34%	27%

Case B: Natural ventilation, No occupancy

	North	South	East	West
5%	59%	61%	59%	59%
10%	62%	68%	61%	64%
15%	62%	74%	62%	68%
20%	63%	75%	64%	68%
30%	63%	70%	64%	63%
40%	63%	67%	64%	60%

Figure 6: Case A and B testing glazing ratios and orientation

4.2 Fabric optimizations

All rooms performed better with U-values equal to 1.1 W/m²K when considered without natural ventilation. North oriented rooms achieved the highest values as oppose to west oriented rooms. Increasing thermal transmittance values resulted with a reduction in thermal performance around 6% in all orientations due to the compactness of the envelope.

The effect of material thermal properties was more obvious with the incorporation of natural ventilation as tested in Case B. Thermal comfort improved by 10% in north and east orientations when U-values were

equal to 0.13 W/m²K. However, south facing rooms achieved equal percentages of comfort when u-values were 0.57, 0.4, and 0.13 W/m²K. This represented the optimum comfort values equal to 78% which was around 10% better than other orientations.
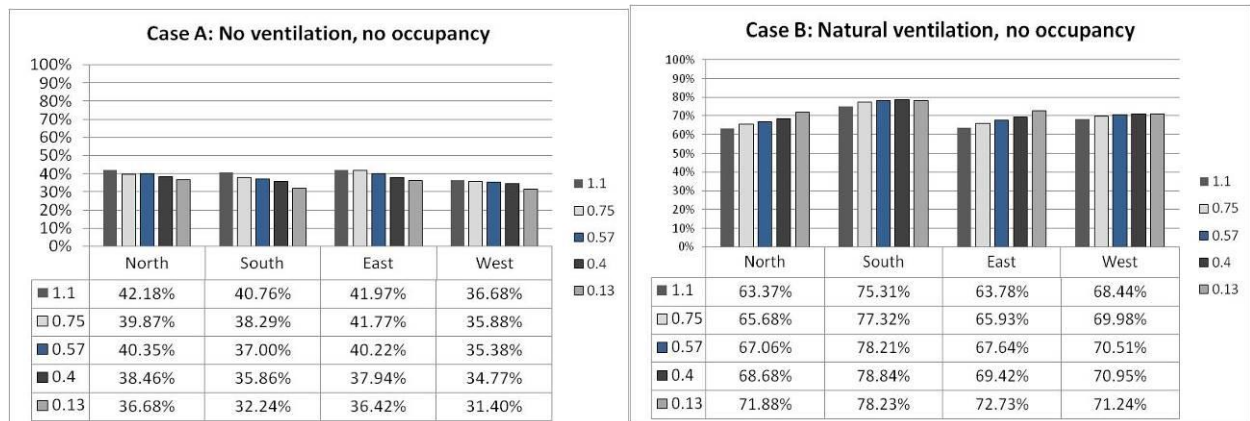

Case A: No ventilation, no occupancy

	North	South	East	West
1.1	42.18%	40.76%	41.97%	36.68%
0.75	39.87%	38.29%	41.77%	35.88%
0.57	40.35%	37.00%	40.22%	35.38%
0.4	38.46%	35.86%	37.94%	34.77%
0.13	36.68%	32.24%	36.42%	31.40%

Case B: Natural ventilation, no occupancy

	North	South	East	West
1.1	63.37%	75.31%	63.78%	68.44%
0.75	65.68%	77.32%	65.93%	69.98%
0.57	67.06%	78.21%	67.64%	70.51%
0.4	68.68%	78.84%	69.42%	70.95%
0.13	71.88%	78.23%	72.73%	71.24%

Figure 7: Case A and B representing building fabric optimisation

The pattern of occupancy was modelled with optimum glazing ratios equal to 20% according to the previous simulations. Results varied according to the function and orientation of the space. Kitchens performed 8% better if placed on north or east facades; however, living spaces were best located on east orientations due to the time of occupancy. Similarly, bedrooms performed best on south facades with 79% of time within comfort.

Shading is considered an essential factor in passive design and should be considered in the early stages. Therefore, vertical and horizontal shading were modelled for all apartment windows and displayed in Figure 8. This resulted with an additional 10% improvement in the overall thermal performance.
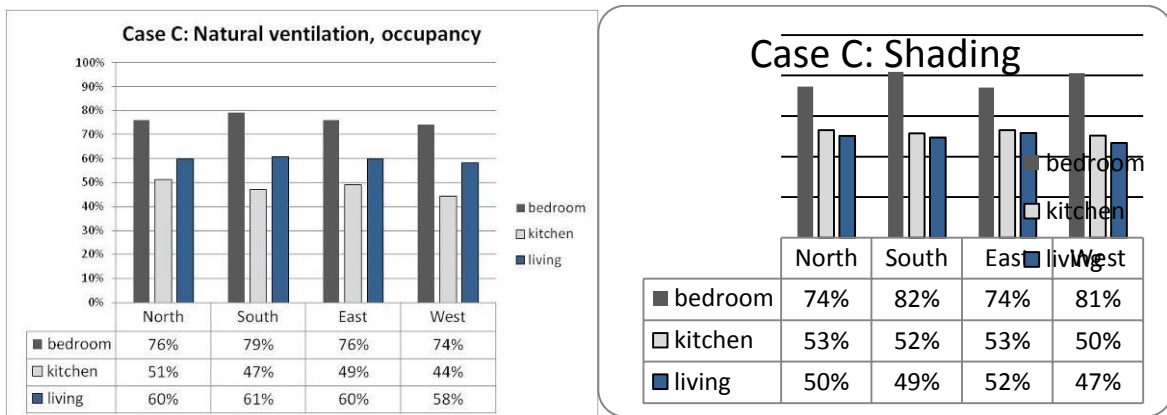

Case C: Natural ventilation, occupancy

	North	South	East	West
bedroom	76%	79%	76%	74%
kitchen	51%	47%	49%	44%
living	60%	61%	60%	58%

Case C: Shading

	North	South	East	West
bedroom	74%	82%	74%	81%
kitchen	53%	52%	53%	50%
living	50%	49%	52%	47%

Figure 8: Case C (left): occupancy, (right): occupancy and shading

5 DESIGN RECOMMENDATIONS

In typical apartment design where each floor consists of two or more apartments, it is not applicable to specify a favourable orientation for each function. Therefore, the authors proposed a draft design guide that helps designers decide on the optimal glazing ratios depending on their design attributes.

The guide is displayed in three tables according to the occupancy and incorporation of cross ventilation (Figure 9,10,11). The designers select from the table, the orientation of their space and the glazing type which is used, and then apply the optimum glazing ratio proposed in the table. This enables them to predict the maximum resultant temperatures and the percentage of hours when their space will be within thermal comfort during the cooling season according to their decision.

		3. CHOOSE GLAZING TYPE					
		SINGLE GLAZING		DOUBLE GLAZING		SHADING	
ORIENTATION		T(Max)	WWR	T(Max)	WWR	T(Max)	WWR
N		30.2C / 46.00%	5%	30°C / 46.00%	5%	29.7°C / 47.00%	5%
S		30.2°C / 49.00%	5%	29.9°C / 52.00%	10%	31.5°C / 50.00%	20%
E		30.1°C / 46.00%	5%	29.9°C / 46.00%	5%	29.5°C / 50.00%	5%
W		30.7°C / 48.00%	5%	30.5°C / 48.00%	5%	29.8°C / 49.00%	5%

Figure 9: Design guide example for apartments without cross ventilation

		3. CHOOSE GLAZING TYPE					
		SINGLE GLAZING		DOUBLE GLAZING		SHADING	
ORIENTATION		T(Max)	WWR	T(Max)	WWR	T(Max)	WWR
N		30.3° / 60.00%	15%	30° / 63.00%	20%	29.5° / 65.00%	15-20%
S		30.4° / 70.00%	15%	30° / 75.00%	20%	29.7° / 73.00%	10%
E		31° / 62.00%	20%	30.5° / 64.00%	20%	28° / 75.00%	20%
W		32.1° / 66.00%	15%	32° / 68.00%	15%	29.5° / 59%	15%

Figure 10: Design guide example for apartments with natural ventilation

1. CHOOSE ORIENTATION		3. CHOOSE FUNCTION						
	ORIENTATION	LIVING ROOM		BED ROOM		KITCHEN		
		T(Max)	WWR	T(Max)	WWR	T(Max)	WWR	
	▲	32°	5%	32°	10%	29.7°	15%	
		59.80%		64%		62.90%		
	▼	32°	5%	32°	5%	29.4°	5%	
		64.70%		69.20%		70.00%		
	►	29°	20%	32°	20%	29.7°	20%	
		61.00%		69.30%		71.90%		
	◄	30°	20%	30°C	20%	31°	20%	
		55.70%		64.00%		63.70%		

Figure 11: Design guide example for apartment with ventilation and actual occupancy

6 CONCLUSIONS

This research involved the study of physical building characteristics along with the social behavior of occupants to demonstrate improvements in the thermal comfort of typical apartments in Amman. The pattern of occupancy was traced from a survey conducted on 145 apartments and used in the thermal simulation model.

Through a series of building optimizations, the study revealed that small amendments in the design could enhance the thermal performance up to 45% with the incorporation of shading and natural ventilation. The optimum glazing ratio for more energy efficient buildings within the context of Jordan was defined as 15% to 20%, whereas the thermal transmittance for walls as 0.13W/m^{2}K.

The results were displayed as a set of recommendations that helps designers to choose optimal building characteristics according to their design situation to achieve suitable thermal performance and temperatures. Although initial guidance was drawn from this study, it is essential to further develop such a guide to cover more design strategies that are based on actual evaluated cases. This will help improve the thermal performance of housing in Jordan and help alleviate the energy crisis.

7 REFERENCES

AL MOMANI, H. M., & Ali, H. H. (2008).Sick building syndrome in apartment buildings in Jordan. Jordan Journal of Civil Engineering, Vol.2, No.4.

ASHRAE, A. N. S. I. (2004). Standard 55-2004, Thermal environmental conditions for human occupancy. American Society of Heating, Refrigerating and Air-Conditioning Engineering, Atlanta, GA.

ALZOUBI, H. H., & Malkawi, A. T. (2015). The optimal utilization of solar energy in residential buildings in light of the Jordanian building regulations. Sustainable Cities and Society, 14, 441-448.

ALZYOOD, M., Harahsheh, H., & Hammad, M. A. (2010). THERMAL ECONOMICAL ANALYSIS OF RENEWABLE ENERGY BUILDINGS, TOWARDS LOW ENERGY HOUSE IN JORDAN. In International Renewable Energy congress, Sousse, Tunisia.

ATTIA, S.,& Zawaydeh, S. (2014).Strategic decision making for zero energy buildings in Jordan. In the 1st International Conference on Energy & Indoor Environment for Hot Climates. Doha.

AWADALLAH, T., Adas, H., Obaidat, Y., & Jarrar, I. (2009). Energy efficient building code for Jordan. Energy, 1.

BATAINEH, A., & Ali, H. Study of Thermal Performance Analysis of Low-Income Housing in Jordan: Case of SOS Buildings. jeaconf.org

DARBY, S., & White, R. (2002). Thermal Comfort. Energy and Buildings, 4, 6.

EVANS, J. R., & Mathur, A. (2005). The value of online surveys.Internet research,15(2),195-219.

HADDAD, S., King, S., Osmond, P., & Heidari, S. (2012). Questionnaire Design to Determine Children's Thermal Sensation, Preference and Acceptability in the Classroom. PLEA.

HASSOUNEH, K.,Alshboul,A., & Al-Salaymeh,A. (2010).Influence of windows on the energy balance of apartment buildings in Amman. Energy Conversion & Management,51(8),1583-1591.

IWARO, J., & Mwasha, A. (2010). A review of building energy regulation and policy for energy conservation in developing countries. Energy Policy, 38(12), 7744-7755.

MOHSEN, M. S., & Akash, B. A. (2001). Some prospects of energy savings in buildings. Energy conversion and management,42(11),1307-1315

OUAHRANI, D. (2010). Towards energy efficient buildings in Amman, Jordan: Defining thermal requirements by mean of thermal simulations. 44th Annual Conference of the Architectural Science Association, Unitec Institute of Technology,New Zealand.

NICOL, J. F., & Humphreys, M. A. (2002). Adaptive thermal comfort and sustainable thermal standards for buildings. Energy and buildings, 34(6), 563-572.

NICOL, F., Humphreys, M., & Roaf, S. (2012). Adaptive thermal comfort: Principles and practice. Taylor & Francis.

SZOKOLAY, S. (2008). Introduction to Architectural Science: The Basis of Sustainable Design. EL SEVIER. Second edition

ZHANG, Y., & Zhao, R. (2008). Overall thermal sensation, acceptability and comfort. Building and environment, 43(1), 44-50.

281: Occupant behaviour and thermal comfort in naturally ventilated office buildings in China

Field Studies in Zhejiang

JINDONG WU[1], LUCELIA RODRIGUES[2], BRIAN FORD[3]

1 The University of Nottingham, University Park, Nottingham, UK, NG7 2RD, Laxjdw1@nottingham.ac.uk
2 The University of Nottingham, University Park, Nottingham, UK, NG7 2RD, Lucelia.rodrigues@nottingham.ac.uk
3 Natural Cooling, UK, DE4 5AR, brian@naturalcooling.co.uk

In China, heating, ventilation and air conditioning systems account for 40% to 60% of the energy consumed in office buildings. Despite the widely known benefits of using natural ventilation as a passive cooling method and the potential reduction in energy demand the implementation of this strategy may bring, most office buildings in China are not designed to be naturally ventilated and little work has been developed in this area. In particular, there is a significant gap in knowledge with regard to how occupants adjust their indoor environmental conditions to achieve thermal comfort by controlling the opening and closing of windows. Understanding the patterns of this behaviour, and the relationship between this and other indoor environmental factors, is of great significance to the study of thermal comfort and energy efficiency.

In this study, the authors attempted to demonstrate the relationship between the occupant behaviour with regard to window control and various indoor environmental factors, mainly through empirical data collected during field studies in Zhejiang province (a typical area with the climate of hot summer and cold winter in China). Field measurements and the results of questionnaires were correlated to establish the patterns of window openings in a naturally ventilated office building. It was found that window state changes mainly happen at the moment of occupant arrival and leaving, and a clear relationship between occupant window control behaviour, indoor temperature and indoor air speed was identified.

Keywords: Window Control Behaviour, Thermal Comfort, Natural Ventilation

1. INTRODUCTION

Evidence shows that the increase in greenhouse gas emissions from burning fossil fuels such as coal, gas and oil has resulted in a rise in global temperatures (Hansen et al., 1989; Kukla and Karl, 1993; IPCC, 2007). Coal is the main energy source in China, which produces large quantities of carbon dioxide and is the main greenhouse gas. According to government records in China, carbon dioxide emissions were 5.07 billion tons in 2004 and this number has been increasing steadily (NDRC, 2007, p.6). In China, approximately 35% of the total produced energy is used in the construction industry each year, responsible for nearly 20% of the total carbon dioxide emissions in the country (Wu, 2003, p.14).

In office buildings in China, heating, ventilation and air conditioning systems account for 40% to 60% of the energy consumption (Zhou and Lin, 2007, p.1069). Reducing the usage of active conditioning systems can result in a decrease in energy consumption. Natural ventilation is a passive cooling method which may help to reduce buildings' energy consumption and improve the indoor thermal comfort condition (Allard, 1998; Gratia and De Herde, 2003). Well-designed natural ventilation strategies in buildings can replace the air conditioning system to a certain extent (McCartney and Nicol, 2002, p.623). Haase and Amato (2009) used dynamic computer simulations to analyse the natural ventilation potential for improving thermal comfort in buildings. They found that the thermal comfort improvement potential by well-designed natural ventilation was between 36% and 50% in a tropical climate and between 18% and 29% in a subtropical climate.

Air movement can raise the heat convection rate between the human body and the surrounding environment; it moves the heat away by evaporating perspiration. Humphreys (1970) defined a relationship between the air velocity and the change of equivalent comfort temperature. Many other studies proved increasing air movement is conducive for occupants to achieve comfort (Givoni,1998; Nicol et al., 1999; Zain et al., 2007; Hwang et al., 2009).

Natural ventilation can improve occupants' thermal comfort condition in the buildings, but this is dependent on the way occupants use their buildings. The lack of understanding of occupants' behaviour and thermal comfort may result in energy waste in buildings. Baker and Steemers (2000) indicated that the actual energy used in an office building was much more than the amount predicted by energy simulation tools, mainly because of occupants' behaviour, lights and appliances in actual use.

Many other studies have proved that the lack of understanding of occupant behaviour in offices could lead to discomfort, which would also result in energy waste (Norford et al., 1994; Branco et al., 2004; Lindelof and Morel, 2006; Masoso and Grobler, 2010). Thus, a good understanding of occupant behaviour can help designers to achieve design aims, reduce the energy consumption and promote comfort.

In spite of the benefits of using natural ventilation listed above and its potential impact on energy demand, most office buildings in China are not designed to be naturally ventilated and little work has been developed in this area. In particular, there is a significant gap in knowledge with regard to how occupants adjust their indoor environmental conditions to achieve thermal comfort by controlling the opening and closing of windows. In this context, the authors present the results of a correlation between occupants' thermal comfort and behaviour in office buildings in a subtropical monsoon climate zone characterised by hot and humid climate in Zhejiang province, South-east China.

2. METHOD

The study included indoor and outdoor environmental condition measurements, thermal comfort survey applications, and occupant window control behaviour monitoring. The field studies were taken in four naturally ventilated office buildings in Yuhuan, Zhejiang (Figure 145, Figure 146 and Figure 147) which are located in a hot and humid climate zone in China. Measurements were taken between 24th September and 18th October 2013, lasting three weeks, and the outdoor temperature varied between 19°C and 31°C.

Twelve cellular offices were monitored (Table 84). Office building A was built in the 1980s with an open-air corridor on the north side. Two offices named as A1 and A2 on the third floor were used for measurement. Office building B was built in the 1970s. The office rooms in it were on both sides of a corridor. Four office rooms named as B1, B2, B3 and B4 were selected on the second floor. There is a window on a side corridor in each office that can be used to encourage cross ventilating in the offices. Office building C was built in the 1990s, and the offices were on both sides of a corridor. Three offices named C1, C2 and C3 were

chosen for measurement on the third floor. Office building D was a tall building with 14 floors which was built in 2009. Three offices named D1, D2 and D3 on the third floor were used for measurement.

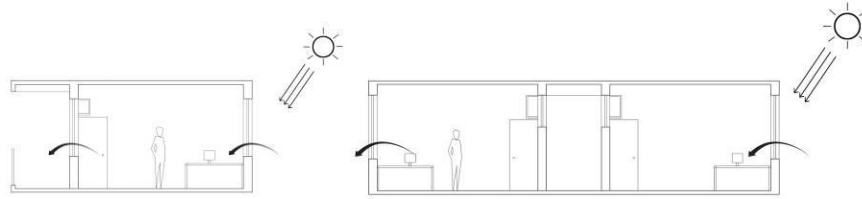*Figure 145: Office buildings A, B, C, D (from left to right)*

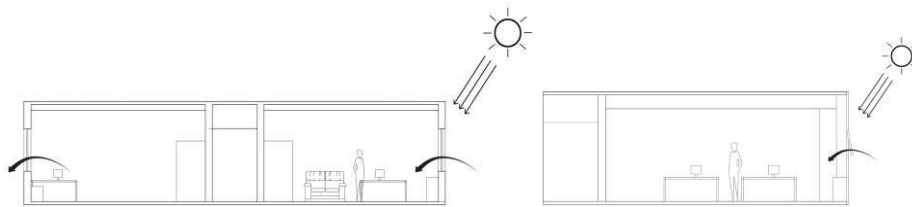*Figure 146: Draft section of office buildings A and B*

Figure 147: Draft section of office buildings C and D

Table 84: Typical offices and windows in the four buildings monitored

		Office A1	Office B1	Office C1	Office D1
Dimensions	Width (m)	3.6	3.6	3.9	4.3
	Depth (m)	4.8	4.8	6.3	6.5
	Height (m)	3.0	3.1	3.0	2.7
Glazing area	Size (m2)	2.9	3.5	3.3	7.2
	Glazing Ratio (%)	28	35	30	58
Window type		Casement	Casement/ Top hung	Sliding	Top hung
Maximum openable area (m²)		2.50	3.12	1.60	0.25
Other windows in the office Type Size(m²) Openable area(m²)		Casement 2.40 2.00	Pivot 1.10 0.95	N/A	N/A

The indoor and outdoor air temperature and relative humidity were measured using Tinytag (TGP-4500) data loggers. The outdoor air temperature and relative humidity were measured on the top of office building A. The data logger was well sheltered from direct sunlight and rainfall. The data were recorded in two-minute intervals. The indoor air temperature and relative humidity were measured in each office with a data logger set up on the desk near an occupant. The data loggers were carefully located to avoid both the heat source in the office and direct sunlight. The data were plotted into psychrometric chart for analysis. In addition, Givoni's (1998) comfort standard was used to identify the comfort zone.

The size of the window and the extent of the opening area were measured first. Window state changing was recorded by state loggers (NOMAD, OM-51). The state loggers were set on the window frame to record window state changes. The window state was recorded as close to open or from open to close. Questionnaires were used to gather evidence on occupant thermal comfort. The aim was to identify the occupants' perceptions on indoor environmental conditions, including comfort, indoor temperature, indoor relative humidity and indoor air quality. A seven-point evaluation scale was used, with a range of -3 to +3. For instance, the comfort perception was from very uncomfortable (-3) to very comfortable (+3), 0 was the neutral point. The questionnaires were given to occupants four times a day during the working hours (8:30 to 17:30), at 8:50, 11:00, 14:50 and 17:00. These records were related to indoor air temperature and relative humidity to establish occupant comfort threshold.

3. THERMAL COMFORT RESULT

In these office buildings, the occupants were mainly doing office working during the monitored period. Their metabolic rate was assumed to be steady and considered as light activity. The met rate was assumed as 1.2met. Clothing level for the occupants was assumed according to the check list in ASHRAE standard 92 (1992). In the monitored period, the occupants' clothing level was considered to be 0.39clo and 0.55clo when outdoor temperature rapidly dropped to 15.5OC. According to Givoni's (1998) comfort zone, the comfort temperature was between 20OC and 29OC. It was used to identify the comfort temperature range in the study. Figure 148 shows the indoor air temperature proportion during working hours in twelve offices.

3.1. Office building A

The air temperature variations in offices A1 and A2 during the working hours were within the comfort temperature range (Figure 148). However, the indoor temperature range in office A2 was wider than the indoor temperature in the office A1, which may be because office A2 was cross ventilated. The thermal perception results in offices A1 and A2 (Figure 149 and Figure 150) are similar to those in Figure 148, showing that the occupants were comfortable. The thermal perception vote results in office A1 shows that all votes were between -1(Cool) and 1(Warm), and most of the votes were on 0(Neutral). It means the indoor environment in office A1 was acceptable. The result in office A2 was similar to office A1, that all votes were located between -1(Cool) and 1(Warm).

3.2. Office building B

The indoor air temperatures in offices B1 and B3 were within the comfort temperature range as well (Figure 148). In offices B2 and B4 the indoor air temperature was over 29OC in 3% and 6% of working hours. Thus, there was more variation of comfort perception in offices B2 and B4 when compared with offices B1 and B3. This may be because offices B2 and B4 were single-side ventilated. According to the observation record, in office B2, the natural ventilation type was changing related to occupants' behaviour of controlling the door in the office. When they opened the door, the office was cross ventilated and when they closed the door the room was single-side ventilated. The proportion of time of the indoor temperature being higher than 29OC in office B2 was lower than in office B4. Therefore, if cross-ventilation was applied in these two offices, the indoor comfort temperature range could potentially have been extended.

According to survey results, the comfort results in office B1 were similar to the results presented in Figure 148, that the indoor environmental condition can be accepted by occupants during the working hours (Figure 151). Although when the indoor temperature rose over 27OC some occupants felt hot (vote on +2) in office B2 (Figure 152), compared with occupants' comfort sensation vote the results showed that the occupants felt slightly uncomfortable (vote on -1) when the indoor temperature was over 28.5OC. This result indicated that the indoor environmental condition was still acceptable by occupants.

In office B3, the indoor temperature was within the comfort temperature range, but when the indoor temperature was over 27OC occupants felt hot in the office. Comparing the thermal sensation results with the comfort perception results shows that, when the indoor air temperature rose over 27OC, the uncomfortable perception vote appeared (Figure 153). Most of the uncomfortable vote was on slightly uncomfortable (-1). In a few hours, occupants felt uncomfortable (-2). In office B4, the time that the indoor temperature was higher than 29OC was more than the other three offices in the building. Compared with the comfort perception vote result, the occupants felt slightly uncomfortable (-1) for only a little time, even when the indoor temperature was over 29OC (Figure 154). It seems that, when the indoor air temperature was between 29OC and 30OC, occupants still could accept the indoor environmental condition.

3.3. Office building C

Office C1, was single-side ventilated, and presented more than 20% of working hours when the indoor air temperature was higher than 29OC (Figure 148). In office C2, which was cross ventilated, this percentage was 6%. Office C3, which was cross ventilated, presented comfortable temperatures throughout the working hours.

Office C1 had the highest proportion of hours that indoor air temperature was higher than 29OC (Figure 148). This number was much higher than other offices. When the occupant thermal sensation vote and the occupant comfort perception vote were compared, the results show that, when the indoor air temperature rose over 27OC, the occupants started to vote on -1 (Slightly uncomfortable) (Figure 155). Most of the uncomfortable votes (-2) were started when the indoor air temperature was over 29OC. Although occupants felt hot in office C1 none of them voted very uncomfortable (-3). So, it seems occupants still could tolerate the indoor environment when the temperature was around 29OC.
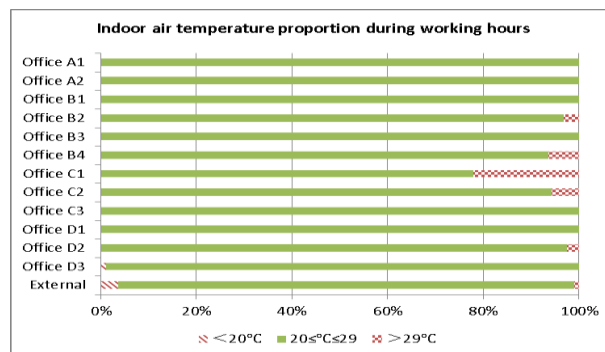

Figure 148: The indoor air temperature variation in twelve offices and outdoor in the monitored period
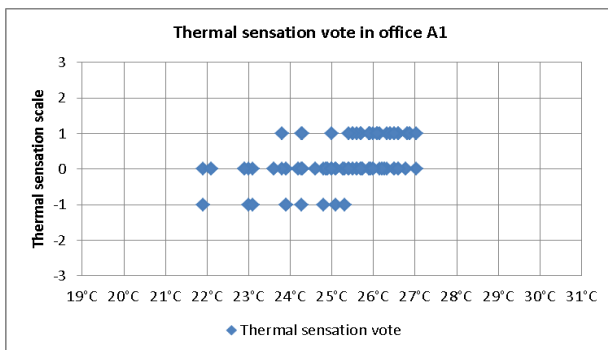

Figure 149: Thermal sensation vote in office A1 during the working hours in the monitored hours
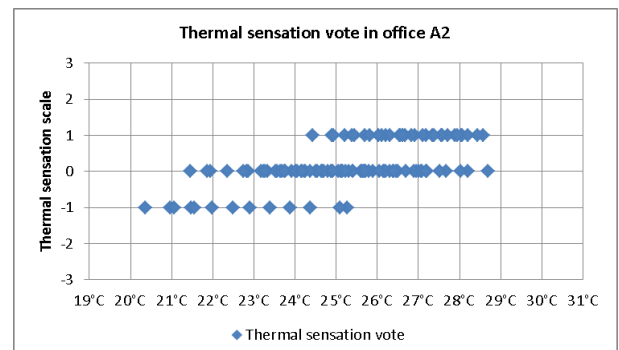

Figure 150: Thermal sensation vote in office A2 during the working hours in the monitored hours
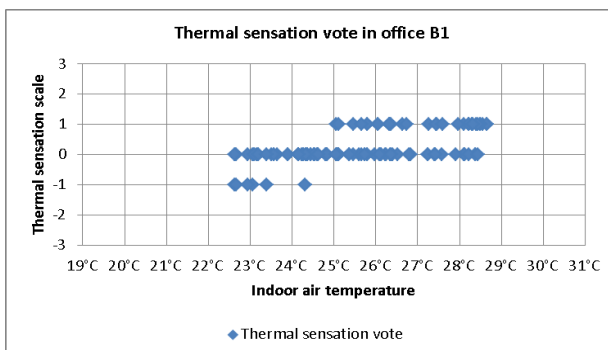

Figure 151: Thermal sensation vote in office A1 during the working hours in the monitored hours
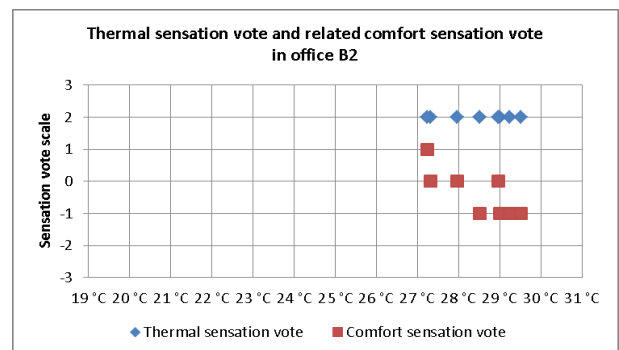

Figure 152: Thermal sensation vote and related comfort sensation vote when occupants felt hot and uncomfortable in office B2
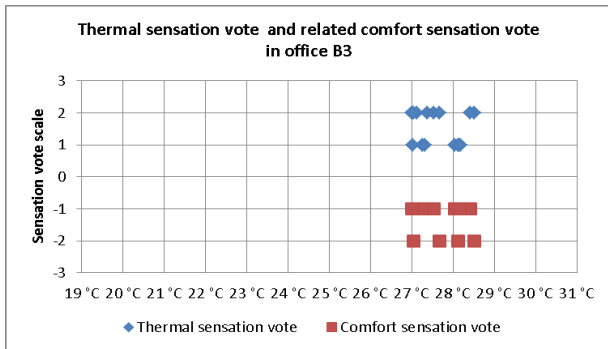
Figure 153: Thermal sensation vote and related comfort sensation vote when occupants felt hot and uncomfortable in office B3
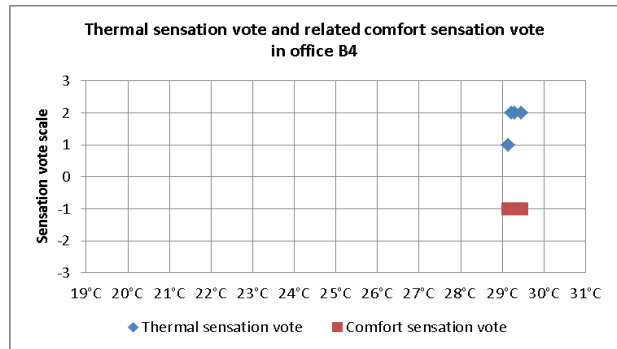

Figure 154: Thermal sensation vote and related comfort sensation vote when occupants felt hot and uncomfortable in office B4
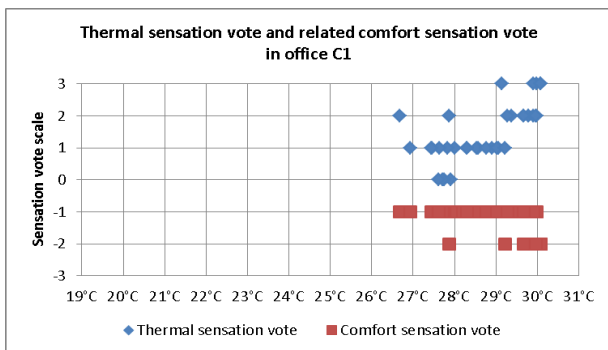

Figure 155: Thermal sensation vote and related comfort sensation vote when occupants felt hot and uncomfortable in office C1
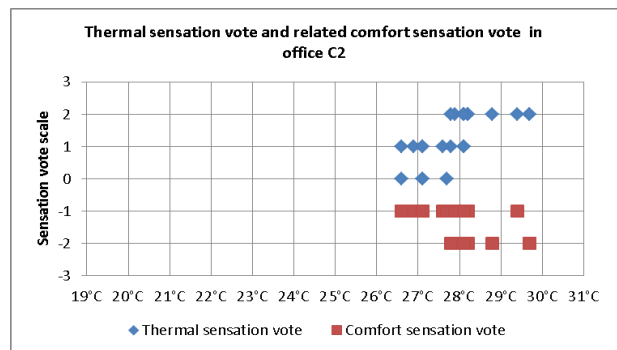

Figure 156: Thermal sensation vote and related comfort sensation vote when occupants felt hot and uncomfortable in office C2

Compared to office C1, occupants would vote on hot (+2) or very hot (+3) when the indoor air temperature was over 29OC; however, in office C2 some occupants still felt warm (+1) and none of them felt very hot (+3) (Figure 156). So, it seems occupants in office C2 can still accept the indoor environment during the working hours. When correlating the thermal sensation vote with the comfort perception vote, it shows that the occupants felt slightly uncomfortable (-1) when the indoor air temperature was over 26.6OC and even when the temperature was over 29OC. But some occupants felt hot when the indoor air temperature was over 28OC. In 5% of working hours occupants felt uncomfortable (-2) in the office, and in 20% of working hours occupants voted on hot (+2). Some occupants voted on hot (+2), but they did not feel uncomfortable in the office. Thus, the environmental conditions were still acceptable. In office C3, the result was similar to that in Figure 148, by which the indoor environmental condition was acceptable.

3.4. Office building D

In office building D, three offices were facing different orientations. The indoor air temperature in office D1 (facing north-east) was in the comfort temperature range. Office D2 (facing south-west) had 3% of working hours when the indoor air temperature was higher than 29OC, which may have caused occupants to feel uncomfortable. In office D3 (facing north-west), there was 1% of working hours that the indoor air temperatures were below 20OC. In most of the working hours, the occupants in office D3 should feel comfortable.

In office D1, the result was the same as Figure 148; occupants felt comfortable during the working hours. Although, in office D3, there was 1% of working hours that the indoor air temperatures were below 20°C, but it did not affect occupants' thermal comfort.

In office D2, according to Figure 148, it seems occupants may feel hot and cause discomfort in the office, when the indoor air temperature was higher than 29°C. However, the comfort perception vote results (Figure 157) show that the uncomfortable votes were located on -1 (Slightly uncomfortable), which would not cause significant impact on occupant comfort perception. Thus, the indoor environment was acceptable by occupants as well.
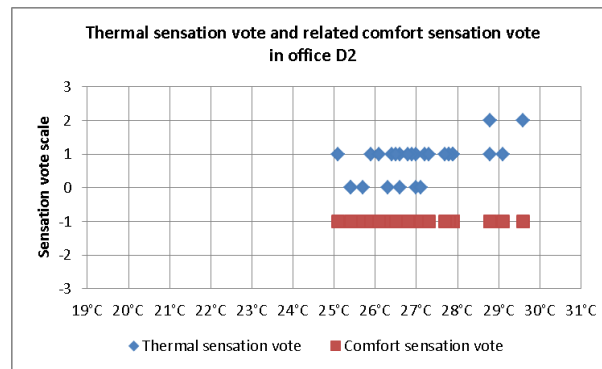
Figure 157: Thermal sensation vote and related comfort sensation vote when occupants felt hot and uncomfortable in office D2.

4. WINDOW CONTROL BEHAVIOUR RESULTS

The aim of monitoring window control behaviour was to establish the occupant window control pattern in naturally ventilated offices. The relationship between occupant window control behaviour and indoor air temperature and air flow speed has also been investigated. The window control was monitored by three stages during the recorded period: arrival, working and leaving. And in each stage four window states were included, which were from close to opened, from open to closed, no change and opening area change. The limitation in this stage was that the exact free opening area was difficult to measure, so the general measured opening area was used for analysis.

4.1. Window control patterns in building A

The window control patterns in building A are shown in Figure 158. In office building A, the main window state change occurred when occupants arrived in the office and when they left the office. During the working hours, the free opening area changes were the main part of the window state change. In these two offices, the major window state change at the arrival time was from close to open, and none of the windows were closed. In office A2, in more than 90% of the working hours occupants would change the opening area. This percentage was higher than the number in office A1. In office A1, there was 10% of time that the window stayed open, which was because occupants did not fully close the window. In office A2, the occupants always closed the window when they left the office.
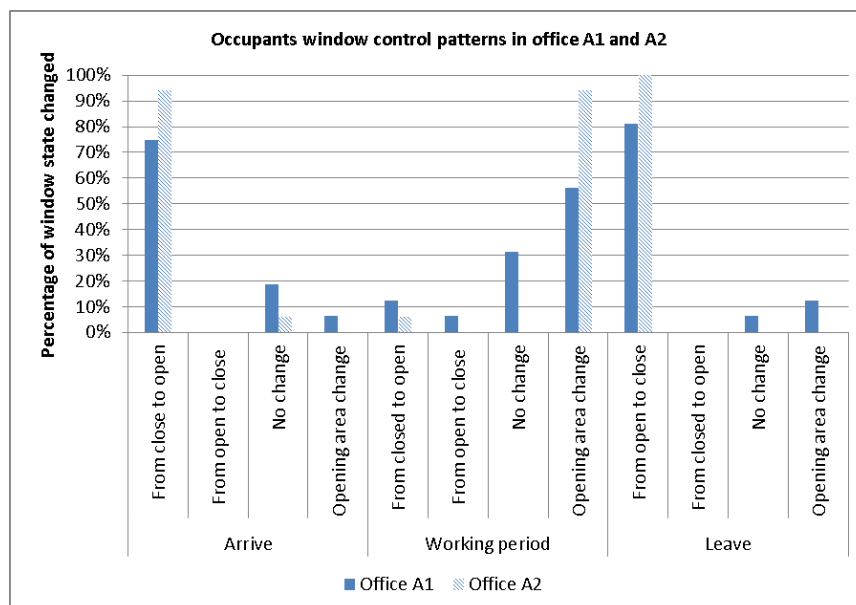

Figure 158: The percentage of occupants' window state control in building A.

4.2. Window control patterns in building B

In office building B (Figure 159), at arrival time the window opening area change mainly happened in offices B1 and B3. In offices B2 and B4, the main window state change was from closed to open. Windows in offices B1 and B3 were not closed when occupants left the office the day before. The percentage was 55% in office B1 and 80% in office B3. However, according to the observation record, the window was closed when occupants left the office. The reason was as same as office A1, that the window was not fully closed, so the window state logger considered the window as open. During the working hours, the opening area changing was also the highest in building B. In addition, in offices B1 and B3 the opening area change percentages were higher than those in offices B2 and B4. It may because offices B1 and B3 were cross ventilated and offices B2 and B4 were single-side ventilated.

4.3. Window control patterns in building C

In building C, the results were similar to other buildings (Figure 160). Most of the window state changes from closed to open when occupants arrived and most of the window states would change from open to close when occupants left the office. During the working hours, the window open area changed quite often except in office C1 which was much lower than other offices. As in offices B2 and B4, office C1 was single-side ventilated.

4.4. Window control patterns in building D

In building D, no windows were used by occupants, so the results were not presented.
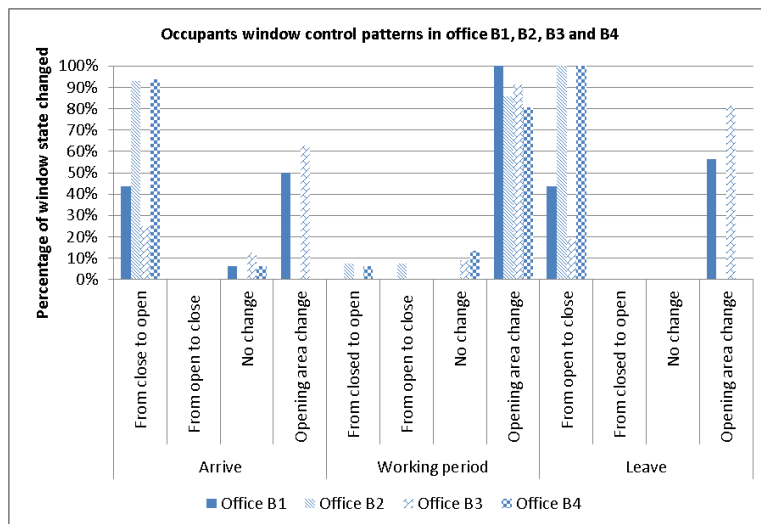

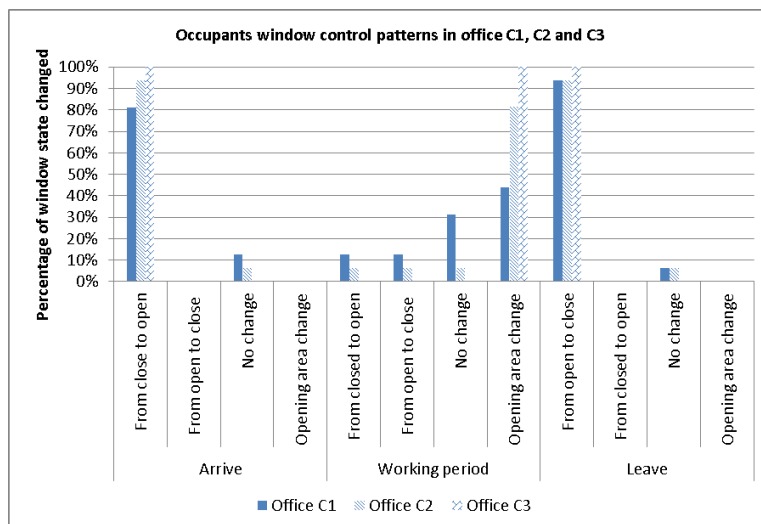*Figure 159: The percentage of occupants' window state control in building B.*

Figure 160: The percentage of occupants' window state control in building C.

4.5. Effective opening area as a function of indoor air temperature

Windows in these offices were frequently used during the working hours and the effective opening area change was the main state changing. The windows were important for occupants to control their indoor environment condition and adjusting occupants' comfort. Figure 161 shows the recorded window state and related indoor air temperature in office A2 in the first week. The geometrical figure on the top of the chart presents the time when occupants changed the window state. The result was found that there was an indoor temperature drop when occupants arrived in the office and opened the windows. This may be because, at the arrival time, the indoor air temperature was higher than the outdoor air temperature; once a window was opened the indoor air temperature would gradually decrease. However, during the working hours, the indoor air temperature and outdoor air temperature was much closer than at the occupant arrival time. Changing the opening area would not result in a large indoor temperature variation. The results were the same in the other offices. Thus, it was clear that increasing or decreasing the opening area would not result in significant indoor air temperature variations during the working period.
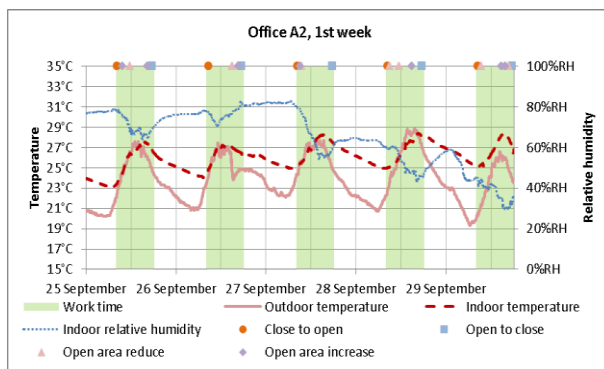

Figure 161: Indoor environmental condition and window state record in office A2 in the first week.
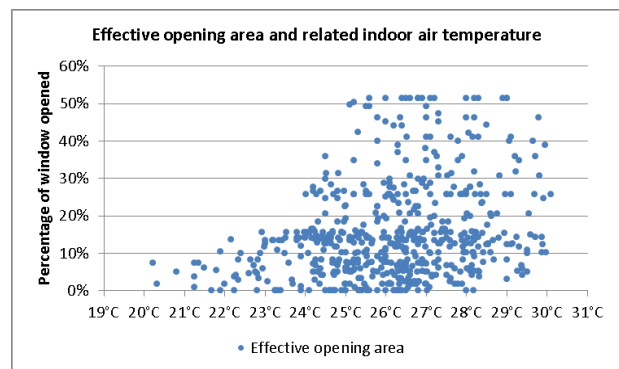

Figure 162: The relationship between the window open percentage and indoor air temperature.

Figure 162 shows the relationship between window opening percentage and indoor air temperature. The window opening area was not increased when the indoor air temperature rose. But when the indoor air temperature increased from 20°C to 25°C, the largest opening percentage was gradually increased when the indoor air temperature rose. And the largest opening area was about 50% of the window area. This was because not all the window panels were opened: occupants only controlled a few window panels in a window. When the indoor air temperature rose over 25°C, the window opening area was randomly distributed. No windows were closed when the indoor temperature was over 28°C because occupants may have felt hot in the office and maintained the window state at opened which can keep the office naturally ventilated.

5. CONCLUSIONS

The window state was mainly changed from closed to opened at occupant arrival time and closed when they left the office. During the working hours, the opening area changing was the main activity, although in office building B the window was not fully closed when occupants left the office. But, based on the observation record the occupants' behaviour tended towards closing the windows when they left the office; this was because the occupants wanted to reduce the effect on offices of rainfall or gusty wind during the night time.

The effective opening area change accounted for the highest proportion during the working period. In a cross ventilated office this proportion was higher than in a single-side ventilated office. Occupants in cross ventilated offices were more frequently adjusting the window than in single-side ventilated offices. This behaviour can help occupants to adjust indoor air flow and achieve personal comfort. This was the reason that occupants in cross ventilated offices felt more comfortable than in a single-side ventilated office, even when they felt slightly hot in the office.

The opening area would reduce with an indoor air temperature drop when the temperature was lower than 25°C. This may be related to occupant thermal sensation. Occupants would start to feel cool when the

indoor air temperature dropped below 26°C. Decreasing the opening area can reduce the indoor air flow rate which can reduce the heat loss from the offices and the heat loss from occupants themselves. This behaviour can help occupants to adapt to the indoor air temperature drop. When the indoor air temperature was higher than 28°C, no windows were closed. Occupants kept the window opened which can maximum the indoor air flow and keep the office naturally ventilated.

Although all the windows could be fully opened in these buildings, such as buildings A and B, in fact the occupants only controlled the window panel which was closest to them, because it was easier to reach. The distance between the occupant and the window affected the opening area; the occupant would have to stand up to have a large opening area if the window was not near the occupant. This was also a reason for only the window near the occupant being used. The accessibility of a window was important to occupants' window control behaviour.

6. REFERENCES

ALLARD, F. (Ed.) (1998), Natural ventilation in buildings: A design handbook. James & James Ltd, London.

ASHRAE (1992), ASHRAE Standard 55–92: Thermal environment conditions for human occupancy. American Society of Heating, Refrigerating and Air-conditioning Engineers, Atlanta.

BAKER, N. and Steemers, K. (2000), Energy and Environment in Architecture: A Technical Design Guide. Taylor & Francis Group, Oxon.

BRANCO, G., Lachal, B., Gallinelli, P. and Weber, W. (2004), Predicted versus observed heat consumption of a low energy multifamily complex in Switzerland based on long-term experimental data. Energy and Buildings, 36, pp.543–555.

GIVONI, B. (1998), Climate Considerations in Building and Urban Design. Van Nostrand Reinhold, New York.

GRATIA, E. and DE Herde, A. (2003), Design of low energy office buildings. Energy and Buildings, 35, pp.473-491.

HAASE, M. and Amato, A. (2009), An investigation of the potential for natural ventilation and building orientation to achieve thermal comfort in warm and humid climates. Solar Energy, 83, pp.389–399.

HANSEN, J., Lacis, A. and Prather, M. (1989), Greenhouse effect of chlorofluorocarbons and other trace gases. Journal of Geophysical Research, 94, pp.16417-16421.

HUMPHREYS, M.A. (1970), A simple theoretical derivation of thermal comfort condition. Journal of the Institute of Heating and Ventilating Engineers, 33, pp.95–98.

Hwang, R.L., Cheng, M.J., Lin, T.P., Ho, M.C. (2009), Thermal perceptions, general adaptation methods and occupant's idea about the trade-off between thermal comfort and energy saving in hot-humid regions. Building and Environment, 44, pp.1128–1134.

IPCC (2007), Climate change 2007. The Physical Science Basis Cambridge, Cambridge University Press.

KUKLA, G. and Karl, T.R. (1993), Nighttime warming and the greenhouse effect. Environ. Sci. Technol., 27(8), pp.1468-1474.

LINDELOF, D. and Morel, N. (2006), A field investigation of the intermediate light switching by users. Energy and Buildings, 38, pp.790-801.

MASOSO, O.T. and Grobler, L.J. (2010), The dark side of occupants' behaviour on building energy use. Energy and Buildings, 42(2), pp.173-177.

MCCARTNEY, K.J. and Nicol, J.F. (2002), Developing an adaptive control algorithm for Europe. Energy and Buildings, 34, pp.623-635.

NDRC (2007), China National Plan for Coping with Climate Change. National Development and Reform Commission People's Republic of China, 2007 [viewed 12 June 2010]. Available from http://www.ndrc.gov.cn/xwfb/t20070604_139486.htm

NICOL, J.F., Raja, I.A., Alauddin, N.G and Jamy, N.G. (1999), Climate variations on comfortable temperature: the Pakistan projects. Energy and Buildings, 30, pp.261-279.

NORFORD, L.K., Socolow, R.H., Hsieh, E.S. and Spadaro, G.V. (1994), Two-to-one discrepancy between measured and predicted performance of a 'low-energy' office building: insights from a reconciliation based on the DOE-2 model. Energy and Buildings, 21(2), pp.121-131.

WU, Y. (2003), China building energy efficiency: Current status, issues and policy recommendations. China Ministry of Construction.

ZAIN, Zainazlan Md., Taib, Mohd Nasir., Baki, Shahrizam Mohd Shah. (2007), Hot and humid climate: prospect for thermal comfort in residential building. Desalination, 209, pp.261-268.

ZHOU, N. and Lin, J. (2007), Energy use in commercial building in China: Current situation and future scenarios, 8th ECEEE Summer Study, Lawrence Berkeley National Laboratory.

285: Impact of weather dependent variables on minimizing dehumidifying load on air conditioned office

EUNICE AKYEREKO ADJEI[1], SAFFA RIFFAT[2], SIDDIG OMER[3]

1 Department of Architecture and Built Environment, University of Nottingham, laxeaa@nottingham.ac.uk
2 Department of Architecture and Built Environment, University of Nottingham, Lazsbr@exmail.nottingham.ac.uk
3 Department of Architecture and Built Environment, University of Nottingham, Siddig.Omer@nottingham.ac.uk

Dehumidifying load remains the largest contributing load to total cooling load in hot humid tropical climate. Minimizing dehumidifying load at a low cost in a new building design and existing building in developing country comes with design challenges. This paper uses ESDL TAS building simulation software to perform dynamic simulation of whole office building envelope using weather sensitive variables for parametric study. Significant findings are: a. The total dehumidifying load of the base case was reduced by 55% with a corresponding reduction of 45 % of the total cooling load by the following significant strategies: i. Changing the thermostat temperature and relative humidity setting to 26oC and 60% respectively. ii. Reducing infiltration arising from all leakages to a practically feasible minimum of 0.20 ACH as well as ventilation gain of 1 ACH. b Vapour diffusion property of building materials had insignificant effect on minimizing the dehumidifying load. The following were concluded: 1. There is no single approach in minimizing dehumidifying load and maintaining indoor environmental building performance. 2. ESDL Tas, is inadequate software package for predicting vapour diffusion. Finally, dehumidifying load of air-conditioned buildings in hot humid climate in developing country can be minimized at cost effective approach by changing the weather dependent variables (ventilation gain, thermostat setting and infiltration gain).

Keywords: dehumidification load, air-conditioning, electricity consumption, hot-humid climate and Ghana

1. INTRODUCTION

Vapour-compression air conditioning unit, is the dominant air conditioning unit use in hot-humid climate mainly for ventilation and regulation of indoor environmental quality to acceptable comfort stated in CIBSE Guide, ASHRAE 55-2004 and ASHRAE standard 62. Vapour-compression air conditioning is the dominant energy end-use service equipment in hot-humid climate representing about 50% of the total energy consumed in building, (N and K, 2011; I et al, 2011; Chua et al, 2013,and Vakiloroaya et. al ,2014) The astonishing percentage of energy consumption by vapour-compression air conditioning is not the only concern by researchers but the environmental impact of emissions arising from the refrigerants as well, (N and K, 2011; Enteria and Mizutani, 2011; Chua et al, 2013; and Vakiloroaya et. al, 2014). This significant percentage is predominantly due to removal of both sensible and latent heat loads arising from the external hot-humid climate. It is well known fact that, dehumidification in buildings remain dominant contributor to the latent heat load in hot-humid climate irrespective of the cooling technology being use; hence high energy consumption.

Cooling load is dependent on the following six main factors: Architectural, External Climate, Technologies, Building service equipment, Building regulation/codes and Occupants, (Eicker et al, 2008; Yu et al, 2011; Zhao and Magoulès, 2012 and Evins, 2013). However, the dehumidifying load is dependent on the latent gain as stated above. The latent gain mainly arises from the internal moisture generation by the metabolic rate of the occupants; ventilation, infiltration gain and vapour diffusion through the building envelope and are external climate condition dependent factors, (Mardiana-Idayu and Riffat, 2012 and Buker and Riffat, 2015).

Several significant researches have been conducted on solving dehumidifying load issues using technology, efficient equipment, phase change materials for building fabric, building demand management systems, moisture permeability retarders and many more, (Eicker and Vorschulze, 2009; Fauchoux et. al, 2010; Aynur, 2010; Enteria and Mizutani, 2011; Chen et al, 2013; Ronghui et al, 2014; Buker and Riffat, 2015 and Sultan et. al, 2015). Among the outputs of the typical solutions resulting from the above researches are desiccant air-conditioning; air handling unit (AHU); ejector refrigeration technologies; heat recovery technology; variable refrigerant flow (VRF) system; heat exchangers, desiccant materials; desiccant dehumidifiers; cooling towers; rotary desiccant wheel and many more. All the researchers concluded that, dehumidifying load in vapour compression air-condition system in building can be reduced by about 5-30% by the integration of the above approaches, (Eicker and Vorschulze ,2009; Fauchoux et. al, 2010; Aynur, 2010; Enteria and Mizutani, 2011; Chen et al, 2013; Ronghui et al, 2014; Buker and Riffat, 2015 and Sultan et. al, 2015). Contrary, Qin et al, 2009 considers that the dehumidification load can be reduced by using alternative cooling load calculations; heat and moisture transfer in building envelopes as well as the hygrothermal interactions between the envelopes and its environment.

From the field study 2014 conducted in a selected hot-humid country case -Ghana; shows that although the above approaches have proven as an effective means of minimizing dehumidifying load in the vapour compression air-conditioning unit; they are expensive. Hence designing building envelope, selecting and sizing service equipment to minimizing dehumidifying load in hot-humid climate in developing country at an effective cost remains a challenge to building professionals

Substantial research have been conducted on impact of external climate condition dependent factors on energy consumption and concluded there is strong correlation between climate and energy consumption arising from cooling, (Lam et al, 2010; Wang et al, 2011; Lu et al, 2012 and Kolokotroni et al, 2012). However, the researchers did not significantly demonstrate how climate dependent variables can be used to minimize the dehumidification load. The present challenges confronting building professionals in Ghana has led to high percentage increase in electricity consumption in commercial and institutional building sector above other sectors, Ghana Electricity outlook, 2012.

In view of this, the research aims at minimizing dehumidification load arising from climatic dependent design variables at a cost effective approach and acceptable indoor environmental conditions. The specific objectives are:

1. To critically review climatic dependent design variables that impacts on dehumidification load. This would be achieved by reviewing scientific and technical publications.
2. To select, model and simulate a typical whole office building using ESDL Tas to identify the percentage constituent of the dehumidifying load to the overall cooling load. This would be accomplished by survey questionnaire for design variables and ESDL TAS.

3. To conduct parametric dynamic numerical simulation of potential cost effective approaches in minimizing dehumidification load on the selected building.

One of the fundamental requirement of building is the protection and comfort it offers to occupants who live and work within them from the weather. The objective of environmental building design is the creation of a comfortable yet energy efficient indoor environment. The successful design of buildings relies on an appropriate understanding of the climate. That is, to analyse the interaction between the energy supply and energy demand of a building, which results from different climate influences. Hence depending on the climate and season, positive climatic elements can be used. For example in temperate climate, during winter, solar radiation can be used for heating and lighting. Whiles in tropical climate, wind and solar radiation can be used for ventilation, cooling and lighting respectively. However, the negative effects of climatic elements needs to be controlled; for an example, heat losses due to low ambient temperature in winter; heat gain from ambient temperature and air moisture transfer in the tropical climate.

According to Oxford dictionary, climate can be defined as the weather conditions prevailing in an area in general or over a long period of time. Weather data forms an integral part of building envelope design and simulation for performance assessment, hence there is the need to know how accurate the weather data was generated. Since most of building simulation programs require hourly meteorological input data for their thermal comfort and energy evaluation, the provision of suitable weather data becomes critical, Qin et al, 2009 and Chua et al, 2013.

From Zhao and Magoulès, 2012, the weather conditions have elements as: Solar radiation, ambient temperature, air humidity, precipitation, wind and sky condition

Examples of weather condition elements for Accra is as shown in Figure 1.
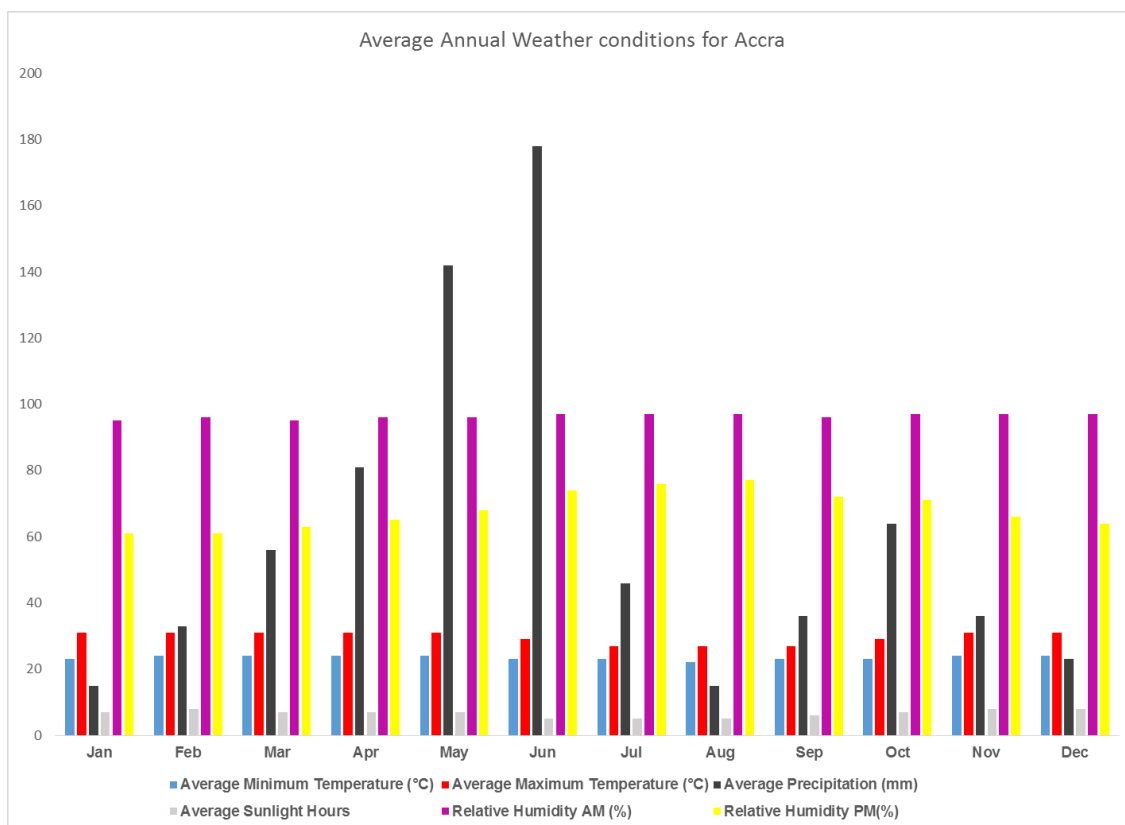
Figure 1: Some Weather condition elements

Source: BBC Weather

The weather data for Accra was obtained from EnergyPlus weather data. The geographical coordinates of Accra, Ghana is at latitude 5.56° N and longitude 0.2° E at an altitude of 298ft above sea level. It is a tropical climate mainly hot and humid with temperature range from 22 to 34 °C. The average wind speed is 3.5 ms^{-1} with an average irradiation of 1402 Wm^{-2}. The relative humidity goes up to 97%.

2   METHODOLOGY

2.1 Dynamic Numerical Modelling and Simulation software

Computer simulation has been proven as an effective approach to assessing the performance of building envelopes. Building performance simulation takes into account the integration, interaction of building components and systems. Simulation of building thermal performance is vital in estimating environmental comfort of occupants in buildings , to identify alternative cooling control system for achieving improved energy efficiency and indoor environmental comfort. There are several building simulation software's in practice; among them are Transys, Esdl Tas, EnergyPlus, Esp-r, ECOTECT among others. The building simulations software were evaluated based on the cooling load calculation method used, building type, accreditation of software, compliance of software with building regulation, integration of user input variables, output results and accuracy of the calculations. From the above evaluation factors, Esdl Tas was selected as the appropriate and adequate software for the research. Environmental Design Solutions Limited Thermal Analysis Software (ESDL Tas) was selected for calculating the thermal loads and analysing the effects of varying parameters. ESDL Tas building simulation software is a dynamic building simulation package with 3D modeller, building simulator and result viewer. ESDL Tas uses steady-cyclic or cyclic model which is a dynamic model. In cyclic modelling, the analysis is based on the assumption of using a sequence of identical days for the external weather conditions which vary on a 24-hour repeated period. A typical example is CIBSE admittance method. Cyclic models are only suitable for applications that require an assessment of conditions after a long period of identical periods. For example, the calculation of design sensible cooling load, hence best suited for space cooling. Cyclic models can also be used for assessment of: Peak summertime temperatures and Preheat requirement

Assumptions:
1. All parameters associated with thermal storage can be represented by the response of sine wave with a period of 24-hours
2. Heat interchange between room surfaces follows the heat transfer assumption for simple steady state model.
3. A uniform distribution of transmitted shortwave solar radiation over room surfaces.

The parameters used by the model to characterise the model performance of space are as follows: thermal response, admittance, decrement factor, surface factor and solar gain factor.

Limitations of Cyclic model
1. Cyclic model is simple model hence its application must be treated with caution
2.   Cyclic model analysis predicts a limit state, which under some circumstances may never be reached. For example, for unoccupied weekends and holidays, the predicted peak may not occur since the model cannot predict this type of event hence the actual benefit of mass cannot be assessed.
3. The cooling load may be overestimated as a result of high proportions of convective gain.

Equation used for calculating heat transfer through surfaces

Conduction in the fabric of the building is treated dynamically, using two methods for the analysis of wall heat flows. State-representation and finite difference methods are applied whereas conductive heat flows at the surfaces of walls and other building elements are calculated with a response factor method.
Equation used for calculating heat transfer through surfaces:

$$q_{i,\theta} = \left[h_{ci}\left(t_{a,\theta} - t_{i,\theta}\right) + \sum_{j=1, j \neq i}^{m} g_{ij}\left(t_{j,\theta} - t_{i,\theta}\right) \right] A_i + RS_{i,\theta} + RL_{i,\theta} + RE_{i,\theta} \quad \text{eqn 1}$$

For i=1,2,3,4,5,
Where

m = number of surfaces in room
qi,θ = rate of heat conducted into surface i at inside surface at time θ
Ai = area of surface i
hci = convective heat transfer coefficient at interior surface i

gij = radiation heat transfer factor between interior surface i and interior surface j

ta,θ = inside air temperature at time θ

ti,θ = average temperature of interior surface i at time θ

tj,θ = average temperature of interior surface j at time θ

RSi,θ = rate of solar energy coming through windows and absorbed by surface i at time θ

RLi,θ = rate of heat radiated from lights and absorbed by surface i at time θ

REi,θ = rate of heat radiated from equipment, occupants and absorbed by surface i at time θ

The admittance procedure for cooling load calculation recognises that a person's feeling of thermal comfort depends on the heat exchanges between the body of a person to the indoor environment by convective heat loss to the indoor air and by radiant heat loss to the indoor environment.

The application creates the sensible heat balance for a zone by setting up equations representing the individual energy balances for the air and each of the surrounding surfaces. These equations are then combined with further equations representing the energy balances at the external surfaces, and the whole equation set is calculated simultaneously to generate air temperatures, surface temperatures and room loads. Convection is treated using a combination of empirical and theoretical relationships. Long-wave radiation exchange is modelled using the Stefan-Boltzmann law. Long-wave radiation from the sky and the ground is treated using empirical relationships (EDSL 2007).

Typical building energy simulation models have several design variables (building characteristics, indoor design conditions, outdoor design conditions, building envelope configurations, weather data, operational schedules, geographical site, among others). The methodologies of (Chowdhury et al. 2008 and Rysanek and Choudhary 2012) for simulation were adopted and modified.

Critical scientific and technical literature review was carried out to ascertain the gaps in existing research in minimizing dehumidifying load, appropriate whole building numerical simulation software, appropriate simulation design variables and acceptable building electricity consumption. Due to lack of significant typical design input variables for building envelope design, building fabric, service equipment and occupant's operational schedule, survey questionnaire was administered followed by experimental study of building materials in Ghana.

2.2 Selection of Design Variables

The parameters and data required to design the building were selected in accordance of BS EN ISO 9000, literature review on tropical designs and typical parameters obtained from survey questionnaire in Ghana. The rationale for the selection of the design parameters were:

1. Most of CIBSE Guides A on environmental design parameters were based on temperate weather conditions.

2. Validity of literature review on tropical designs parameters cannot be ascertain

3. The actual parameters obtained from survey questionnaire as typical practice of building professional practices could not be verified due to the prescriptive and non-performance nature of the Ghana building regulation. Hence the selection of the design variables which is the core of this research required knowledge and creative thinking.

Among the parameters are: Location of site; Internal conditions; Infiltration and ventilation requirements; Internal gains and patterns of use; Building Fabric properties; Building geometry and External design conditions

Due to lack of reliable and sufficient literature on input variables for the simulation; survey questionnaire were administered. However, insignificant percentage of building materials manufacturers undertake thermo-physical analysis of products hence the thermo-physical experimental study were undertaken. The remaining input variables were acquired from CIBSE Guide and ASHRAE standards.

From the survey questionnaire; the following data were acquired for typical office building variables: Office schedules, Annual cooling calendar, Typical thermostat setting for temperature and relative humidity,

Typical Infiltration and ventilation gain, Building service equipment types, Building description including details of measurements of building and Building performance variables (floor-to-window ratio and floor-to-ceiling height) are summarised in Table1.

According to CIBSE Guide A, CIBSE Guides B and lighting code 2002,the internal gain include the gains from lighting, occupant and equipment. For office building with general use for occupancy density of 12/person/m^2 at an internal gain of 24^{0}C and 50% relative humidity is summarised in Table 2. The summary of all the input variables are shown in Tables 1 and 2..

Table 1: Building envelope Fabric Properties

Envelope Fabric	Description	U-values (W/m^2·°C)
Wall (internal and external)	Single mortar wall layer with light weight plaster in the internal and external as well as paint finish	2.92
Roof and ceiling	Reinforced concrete	0.902
Window pane	6mm eclipse 43/54 clear *1	5.68
Window frame	Smooth Planed timber	1.44
Foundation/Ground floor	Sand, dark clay, concrete and finished with floor tiles	0.43
Door	Smooth Planed timber	0.573
Door frame	Smooth Planed timber	1.44
Inter floor Ceiling	Reinforced concrete	2.13

Table 2: Internal Condition Variables

Internal Gain Variables	Value
Occupant sensible heat gain(W/m^2)	6-7
Lighting sensible heat gain(W/m^2)	8-12
Equipment sensible heat gain(W/m^2)	15
Occupant Latent heat gain (W/m^2)	5
Lighting Latent heat gain (W/m^2)	-
Equipment Latent heat gain (W/m^2)	-
Infiltration (ACH)	0.5
Ventilation(ACH)	2
Upper dry bulb temperature for comfort cooling	24°C
Lower dry bulb temperature for heating	-50 °C
Upper relative humidity	50%
Lower relative humidity	40%
Compact Fluorescent task illuminance (lux)	500

3   MODELLING OF REFERENCE BUILDING

The base building is a standard medium-sized single use rectangular four story office building commissioned in 1951 before the building regulation of Ghana was enacted into law in 1996. Rectangular building form is the shape of typical office buildings in Ghana; as seen in Figure 2a.The base building has a total floor area of about 1848m^2, each floor has north-south window facing position representing 30% wall-to-window ratio and increasing floor-to-ceiling height as a result of the conversion from the natural room ventilation to air conditioned building. The building was constructed with single layer concrete blocks wall as well as internal mortar wall plaster with aluminium window frame, clear louvers blades, reinforced concrete inter floor ceiling and reinforced mono-pitched roof. There are about 200 sedentary occupants with occasional movements of people in-out of the offices; operating on 8 hours schedule on weekdays through the year and closed on Ghana public holiday calendar. The occupant's electricity dependent equipment are computer, printer, artificial lighting and photocopier. Summary of the base building is represented in Figure 2a to 2d been selected office building, layout of the air-conditioned floors, detailed dimension of floors and ESDL Tas model of the office building respectively.
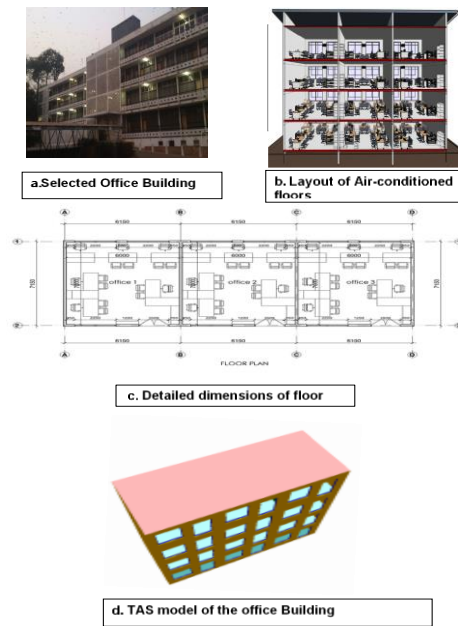
Figure 2: Base Case building description

4   RESULTS AND GRAPHS

Base Case

The summary of the ESDL Tas simulation results for the base case on annual loads, monthly loads, predicted mean votes and predicted percentage of dissatisfaction are as shown in figures 3, 4, 5 and 6 respectively.
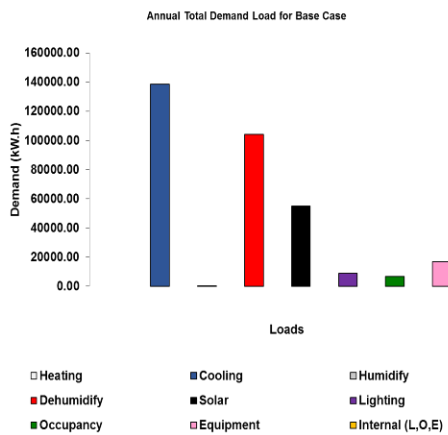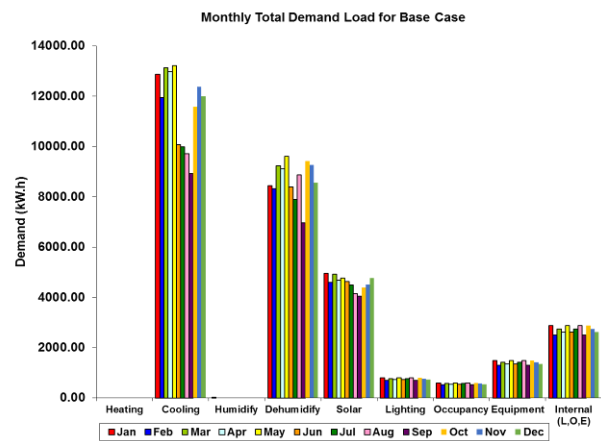

Figure 3: Annual Loads for Base Case Ghana

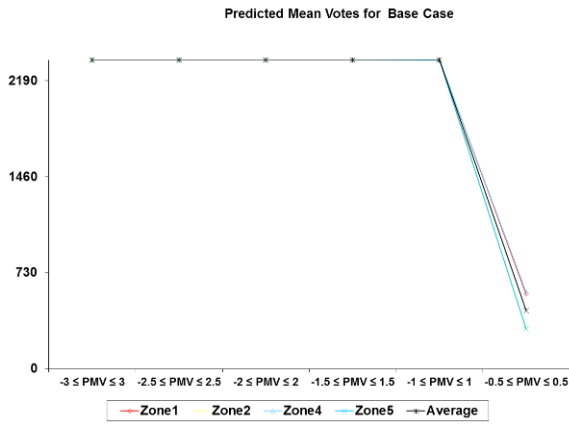*Figure 4: Monthly Loads for Base Case Ghana*
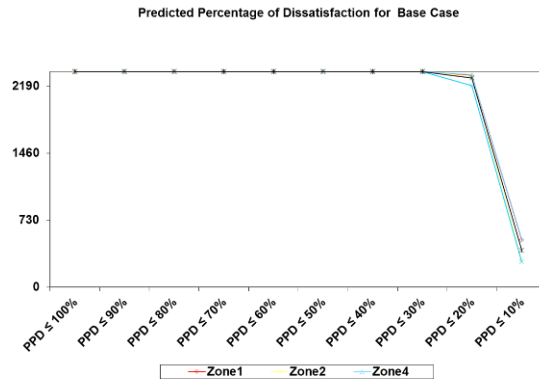
Figure 5: Predicted Mean vote for the Base Case

Figure 6: Predicted Percentage of Dissatisfaction of Base

From the base case, the current single wall and roof design for typical office building in Ghana, cannot attain the u-values of 0.3 and 0.25 respectively for wall and roof design as stated in Ghana building regulation. Hence the building envelope elements (roof and wall system) of the base case was unacceptable. The simulated cooling load is highly dominated by 56.3% and 26.8 for dehumidifying load and solar gains load respectively. The obtained cooling load of the base case results is inconsistent with a similar hot-humid weather climate assessment by Qin et al 2009. However, the cooling load obtained was about 9 times more than the recommended CIBSE Guide for good practice. According to ASHRAE 55 standard, for comfortable indoor condition, at least 80% of occupants should be satisfied. Thermal comfort was achieved, since the PMV is within -0.5 and +0.5 with less than 10% Predicted Percentage Dissatisfaction (PPD). Hence the indoor environmental comfort of the base case is acceptable within the ASRAE 55 standard. From these deductions, the parametric simulation focused on weather dependent variables to minimize the dehumidification load with an attempt to achieving the u-values of the single wall layer and the roof design using minimum thermal conductivity of building fabric.

5   PARAMETRIC SIMULATION

The parametric simulation was structured into the following subgroups: 1. Varying Thermostat Setting: temperature setting and relative humidity setting 2. Varying Ventilation Gain 3. Varying Infiltration Gain and 4 Varying vapour diffusion factor of cement based building fabric. Five different values of each sub groups were selected and simulated keeping all other variables constant. The results of each simulation at given values were plotted for all the subgroups. The summary of all the parametric simulations are as shown figures 7 to 10 and figure 11 is the combination of all practical minimum values for the parametric simulations.
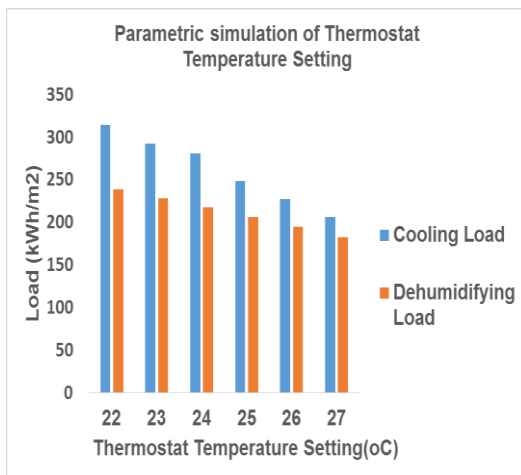

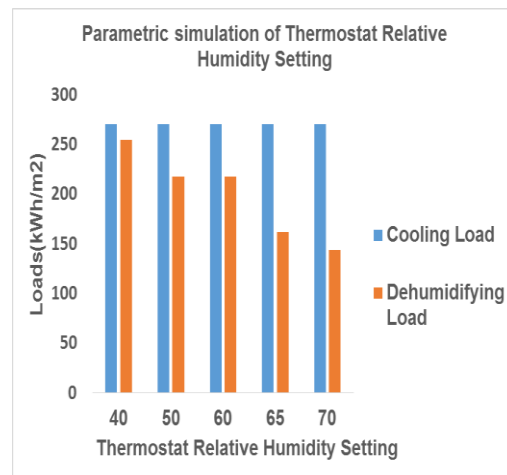Figure 7: Thermostat temperature setting

Figure 8: Relative humidity setting

From the CIBSE Guide A & B, the required temperature setting for comfortable indoor environment is 24°C; hence the parametric simulations for temperature variations from the standard temperature with its equivalent loads is shown in figure 7. From the graph it can be seen that both dehumidifying and cooling loads decreases with increasing temperature. However, since the research seeks to achieving the minimization of cooling load arising from dehumidification load at an acceptable indoor comfort the temperature cannot be increased beyond 26°C. The percentage mean vote and the predicted percentage of dissatisfaction shows that the new recommended thermostat temperature setting of 26°C is thermally comfortable for hot-humid climate. By setting thermostat temperature setting to 26°C will lead to reduction of cooling and dehumidifying load by 19% and 11% respectively.

From figure 8, .it can be seen that, dehumidifying loads decreases with increasing relative humidity setting; whiles cooling load remains constant. However, since the research seeks to achieve the minimization of cooling load arising from dehumidification load at an acceptable indoor comfort stated CIBSE Guide A & B; the relative humidity cannot be increased beyond 60%. The percentage mean vote and the predicted percentage of dissatisfaction shows that the new recommended thermostat relative setting of 60% is thermally comfortable for hot-humid climate. By setting thermostat relative humidity setting to 60% will lead to reduction of dehumidifying load by 17%; however the cooling load remained unchanged.
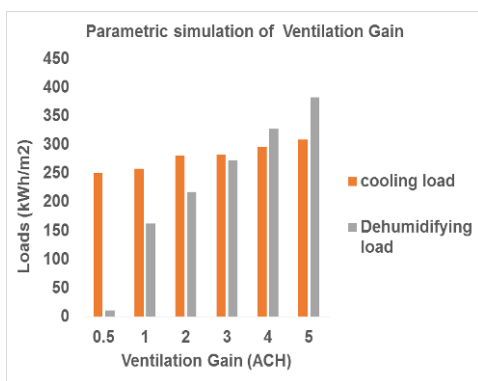

Figure 8: Varying Ventilation Gain
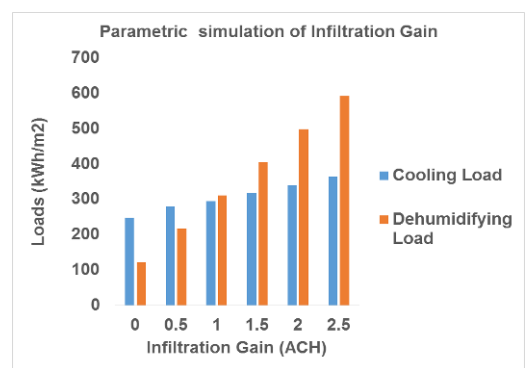
Figure 9: Varying Infiltration Gain

From the graph in Figure 8, .it can be inferred that dehumidifying loads and cooling load increases with increasing ventilation gain. However, the variation of cooling loads with increasing ventilation gain is not significant as compared to dehumidifying load. Due to the inability of this research to access the indoor air quality, caution was taken as to how low the ventilation gain can be set.

From Figure 9, it can be inferred that dehumidifying loads and cooling loads increases with increasing infiltration gain. However, the variation of dehumidifying loads with increasing infiltration gain is really substantial as compared to cooling load. The cooling load gradually increases with increasing infiltration gain. From the graph; there is a strong correlation between infiltration gain and dehumidifying load. Hence, designing a tighter building in hot-humid climate remains vital in minimizing the infiltration gain leading to a lower dehumidifying load.

Figure 10: Varying Vapour Diffusion Factor.

Figure 11: Combination of all minimum Parametric Simulations

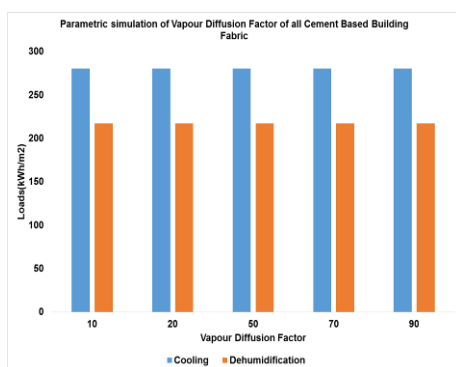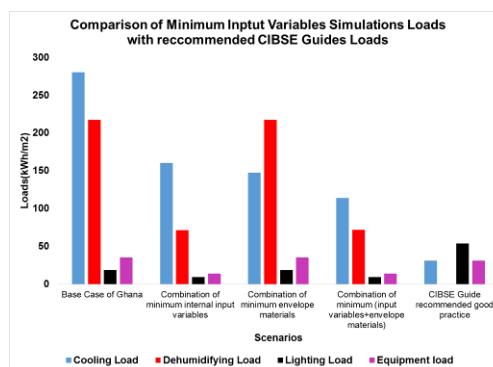From Figure 10, it was observed that the vapour diffusion factor of all the cement based building fabric did not have any impact on both the cooling and dehumidifying load as was expected. The only reason to this is that; the ESDL Tas admittance cooling load calculation method do not account for the vapour diffusion factor accurately.

As can be seen in figure 11, the various scenarios show significant reduction in the dehumidification load with the exception of the vapour diffusion factor. The combined parametric simulation (input variables and minimum envelope materials) showed the most significant reduction of 67.2% and 39.8% in both dehumidification and cooling load respectively, but the commended CIBSE Guide for good practice for cooling energy consumption was not attained. From the combinations of minimum sensitive variables scenarios simulations; it can be affirmed that, the dehumidifying load remains the dominant contributing load to the overall cooling load in hot-humid climate and no single approach can be used to address the problem.

5.1 Parametric Simulation Findings

1. The vapour diffusion property of materials had no effect on minimizing the dehumidify load.
2. Increasing the thermostat temperature setting beyond 26oC reduces the cooling load; however this leads to thermal discomfort for occupants. The variation of the relative humidity setting on the thermostat has no influence on the cooling load.
3. The total dehumidifying load of the base case was reduced by 67.2% with a corresponding reduction of 39.8 % of the total cooling load by the following significant approaches: i. Changing the thermostat temperature and relative humidity setting to 26°C and 60% respectively. ii. Reducing infiltration arising from all leakages to a practically feasible minimum of 0 ACH as well as ventilation gain of 1 ACH.

6   CONCLUSION

ESDL Tas, is inadequate software package for predicting the total moisture transfer (vapour diffusion, ventilation and infiltration) through the entire building fabric and service equipment. Minimization of infiltration gain has as shown a key approach in minimizing dehumidifying load compared to thermostat setting, ventilation gain and vapour diffusion of cement based fabric. The calculation of space cooling load by CIBSE admittance method has been shown to be comparable with CIBSE Guide A &B. However, the cooling load annual calendar used in predicting the commended CIBSE Guide for good practice for cooling energy consumption was just about 3 months annually for summer conditions in temperate climate. Hence there is the need for commended standard for good practice for cooling energy consumption in hot-humid climate with the incorporation of 12 months schedule as applied to practical typical office schedule. Reducing electricity consumption arising from building service dehumidifying and cooling load at a cost effective approach; can be achieved with the parameter building performance of climate dependent design variables.

7   REFERENCES

MARDIANA-IDAYU, A. and Riffat, S.B. 2012. Review on heat recovery technologies for building applications. Renewable and Sustainable Energy Reviews 16 (2012) 1241– 1255

ENTERIA N, Mizutani K, 2011.The role of the thermally activated desiccant cooling technologies in the issue of energy and environment. Renew Sustain Energy Rev 2011:15:2095–122.

ZHAO Hai-xiang and Magoulès Frédéric, 2012. A review on the prediction of building energy consumption. Renewable and Sustainable Energy Reviews 16 (2012) 3586– 3592

WANG, J., Zhai, Z., Jing, Y,. Zhang X., and Zhang, C., 2011, Sensitivity analysis of optimal model on building cooling heating and power system, Applied Energy 88 (2011) 5143–5152

KOROLIJA I, Marjanovic-Halburd L, Zhang Y, Hanby VI, 2011. Influence of building parameters and HVAC systems coupling on building energy performance. Energy Build 2011; 43:1247–53.

CHUA, K.J., Chou, S.K., Yang W.M., andYan, J.,2013. Achieving better energy-efficient air conditioning – A review of technologies and strategies. Applied Energy 104 (2013) 87–104.

FAUCHOUX, Melanie, Bansal Mohit, Talukdar Prabal, Simonson Carey J. and Torvi David, 2010. Testing and modelling of a novel ceiling panel for maintaining space relative humidity by moisture transfer. International Journal of Heat and Mass Transfer 53 (2010) 3961–3968

BUKER, Mahmut Sami and Riffat, Saffa B., 2015. Recent developments in solar assisted liquid desiccant evaporative cooling technology—A review. Energy and Buildings 96 (2015) 95–108

KOLOKOTRONI M., Ren X., Davies M. and Mavrogianni A., 2012. London's urban heat island: Impact on current and future energy consumption in office buildings. Energy and Buildings 47 (2012) 302–311

SULTAN, Muhammad, El-Sharkawy Ibrahim I., Miyazaki Takahiko, Saha Bidyut Baran and Koyama Shigeru, 2015. An overview of solid desiccant dehumidification and air conditioning systems. Renewable and Sustainable Energy Reviews 46(2015)16–29

QIN, Menghao., Belarbi, Rafik,. Aït-Mokhtar Abdelkarim.,nd Allard. Francis Simulation of coupled heat and moisture transfer in air-conditioned buildings. Automation in Construction 18 (2009) 624–631

QI Ronghui, Lu Lina and Huang Yu, 2014.Energy performance of solar-assisted liquid desiccant air-conditioning system for commercial building in main climate zones. Energy Conversion and Management 88 (2014) 749–757

EVINS, Ralph, 2013. A review of computational optimisation methods applied to sustainable building design. Renewable and Sustainable Energy Reviews 22 (2013) 230–245

LAM, T.N.T., Wan K.W., Wong S.L. and Lam J.C., 2010. Impact of climate change on commercial sector air conditioning energy consumption in subtropical Hong Kong, Applied Energy 87 (2010) 2321–2327

EICKER, Ursula and Vorschulze, Christoph, 2009. Potential of geothermal heat exchangers for office building climatisation. Renewable Energy 34 (2009) 1126–1133

VAKILOROAYA, Vahid., Samali Bijan., Fakhar Ahmad and Pishghadam Kambiz., 2014.A review of different strategies for HVAC energy saving. Energy Conversion and Management 77 (2014) 738–754

CHEN, Xiangjie, Omer, Siddig., Worall, Mark and Riffat, Saffa, 2013. Recent developments in ejector refrigeration technologies. Renewable and Sustainable Energy Reviews 19(2013)629–651

PEREZ, Yael Valerie and Capeluto, Isaac Guedi ,.2009. Climatic considerations in school building design in the hot–humid climate for reducing energy consumption. Applied Energy 86 (2009) 340–348

YU, Zhun, Fung, Benjamin C.M., Haghighat, Fariborz., Yoshino, Hiroshi and Morofsky, Edward, 2011. Systematic procedure to study the influence of occupant behavior on building energy consumption. Energy and Buildings 43 (2011) 1409–1417

306: A Review on resource potential in africa and energy consumption in some buildings of Cameroon

MODESTE KAMENI NEMATCHOUA[1*], BLAISE MEMPOUO[2*], TCHINDA RENE[3] ,
CHRYSOSTÔME R.R. RAMINOSOA[4] ,ANDRIANAHARINJAKA ARO-ZO[4].

*1Environmental Energy Technologies Laboratory, University of Yaounde I, Cameroon,
2Institute of Sustainable Energy Technology, University of Nottingham, Nottingham NG7 2RD, UK,
3LISIE, University Institute of Technology Fotso Victor University of Dschang, Cameroon,
4Fluid and Energy Laboratory, University of Antsiranana , Madagascar.
*Correspondingauthors:Email:kameni.modeste@yahoo.fr(K.Modeste),blaise.mempouo@arpedac.org(M.
Blaise)*

Presently the human energy requirements are enormous and still growing. All the countries of the world need energy, which is the main source of development. The shift to renewable source is not only environmental friendly but it is almost available in every country. The development of African continent is still very slow; it is mainly due to the limited policy interest and investment levels. The aim of this paper is to review the status and current trends of potential of the resources in some African countries and energy consumption in the residential sector of Cameroon. It was found that the Africa's energy needs are constantly growing and should exceed 50% of current levels in next century .Moreover Africa has substantial new renewable energy resources, most of which are under-exploited. We found that 83% of the rural population in Africa has no access to electricity. This rate reached 92% in some countries in sub-Saharan Africa. Nigeria is known as an oil producing state; Cameroon has the second largest forestry potential in the Congo Basin, while South Africa is among the 20 highest contributors to CO_2 emissions in the world.

Keywords: Energy consumption, Resource potential , buildings, Africa.

1. INTRODUCTION

The energy used by nations which are developing will exceed the advanced countries by 2020 (Lombard,2008:395) Energy is essential for the economic and social development and improved quality of life. Much of the world's energy is currently produced and consumed in ways that could not be sustained and significantly higher than the environmentally friendly renewable energy source. According to The International Energy Agency, during the last two decades (1984–2004) primary energy has grown by 49% and CO_2emission by 43% with an average annual increase of 2% and 1.8%, respectively (Payam, 2015:855). The rapid economic growth in the developing countries has led to an increase in energy consumption and supply difficulties. In Africa, for example, the renewable energy resource potential has not been fully exploited, mainly due to the limited policy interest and investment levels. In addition, technical and financial barriers have contributed to the low levels of uptake in technologies of renewable energy (RET) the region (Karekezi,1997:3). There are, however, prospects for the wide-scale development and dissemination of RETs in the region. There is growing realization that Africa is likely to be disproportionately affected by the impacts of climate change. The access to shapes of modern energy brings advantages for the human well-being and the economic development. These modern energies include electricity, LPG, natural gas, and solar energy. They are more efficient and cleaner and facilitate better conditions of life (Ruijven,2012:389) . Housing and industry remain two sectors where energy consumption has increased rapidly during recent decades in many countries. More than 70% of the population depending on the traditional energy type stays in Africa. Africa has many potential resources in renewable energy and fossil not-exploited. The most important objective of a building is to provide its inhabitants with a comfortable indoor climate in the respect of energy efficiency (Nematchoua,2014:690). Energy in residence of Cameroon is in great part used for cooking and cooling. This paper is to review the status and current trends of potential of the resources in some African countries but also the cooling and heating energy consumption in the residential sector of Cameroon.

2 RESOURCE POTENTIALS IN AFRICA

Africa is one of the richest continents in terms of natural resources but has remained the poorest due to unsustainable utilization of her natural resources, conflicts and lack of innovation to create wealth such resources. Globally , Africa owns 95% of the world's platinum group metals (PGM) reserves, 90% of chromite ore reserves, 85% of phosphate rock reserves and more than half of the world's cobalt. Meanwhile, Africa's potential is equally alluring in a range of commodities for which future production prospects are elevated: Africa possesses roughly one-third of global bauxite reserves, but accounts for only 8% of global bauxite mine production. Between 2006 and 2010, copper production in Africa increased by 75%(kameni,2015:837) .All these following countries are the highest producer and sometime also the highest consumer of energy in their sub-region.

2.1 Case of West-Africa :Nigeria

Nigeria, was a population of more than 150 million (2013) and a growth rate of 3.5 % , has a total land area of 923, 768 km². The energy resources in Nigeria include: Natural gas, coal, tar sand Crude oil and renewable (biomass, hydro, solar, wind et.c). The Nigeria Energy Policy Report estimated that less than 40 per cent of the population is connected to the national grid. Nigeria is known as an oil producing state. Thank to the economic crisis, Nigeria occupy yet second place as a producer of oil in Africa . Current estimated oil reserve in Nigeria is 35.9 billion barrels with daily production capacity of 2.4 million barrels of crude oil. The 35.9 billion barrels of oil reserve will be depleted by 30-35 years period(Obioh,2009:20; Edirin,2012:150). The oil boom came at a point where the country was unstable politically and the resulting oil wealth was grossly mismanaged. The primary commercial energy sources remain crude oil and natural gas and are the most developed source of fossil energy nationally (Nnamdi,2011:17). Solar Radiation varied between 3 to 7 Kwh/m²/day and Wind energy is available at annual average speeds of about 2.0m/s at the coastal regions of the South and 4.0m/s at the far Northern region of the country. Moreover ,in all the country, Hydropower's capacity was 10,000MW(large scale) and 734 MW (small scale)(Omokaro,2008:55). Nowadays, the reserves of non- Renewable Energy resources are estimated to 36 billion barrels for rude oil; 185 trillion cubic feet for natural gas and 2.75 billion metric tons for Coal(Nnamdi,2011:17) . Globally, In Nigeria, the distribution of the energy consumption is 50.45% as fuel wood; 41.28% as petroleum products and hydro electricity (8%). Fuel wood is used by over 60% of people living in the rural areas and 80% of Nigerians as energy source. Nigeria consumes over 50 million metric tonnes of fuel wood annually (Karekezi ,2002:15) .Africa can be divided to six regions.

2.2 Case of East Africa :Kenya

Kenya has the largest economy in the East African Community and one of the largest in Africa. It also has one of the most diverse economies on the continent. Kenya has registered significant progress in exploring geothermal energy for power generation. It has an installed capacity of 3,000 MW, equivalent to more than 20% of the country's installed electricity generation capacity(Luke,2014:3) .The   Ministry of Energy indicated that the country received on average 4.5kWh per square meter per day of solar radiation .On the other hand, Wood fuel is however the major source of energy for most domestic activities in the rural areas. Today, Kenya's oil resources are estimated around 600 million barrels. The country is counted as a small African producer .

2.3 Case of North-Africa :Libya

Libya is the second biggest North African country.It is located between Algeria and Tunisia in the west and Egypt in the east, bordering the Mediterranean Sea in the north and (from west to east) Niger, Chad and the Sudan in the south. Libya has virtually no accessible water resources on the earth's surface, which consists to more than 90% of desert or semi-desert. It is a nation that suffers from water scarcity. Libyan climate ranges from Mediterranean along the coast line to extremely dry in the interior when going south. Most prominent natural resources are petroleum, natural gas and gypsum. Especially the first two natural resources are the main driving factor for the Libyan economy. Hydrocarbons contribute about 95% of export earning, 65% of the GDP and about 80% of government revenue. In 2011, Libya has produced about 30,962 ktoe of energy. Libya has a great potential for solar energy. In the coastal regions, the daily average of solar radiation on a horizontal plane accounts to 7.1 $kWh/m^2/day$ whilst the radiation is 8.1 kWh/m2/day in the southern region. The average sun duration is of more than 3,500 hours per year. This is equivalent to a layer of 25 cm of crude oil per year on the land surface. Moreover, we can easily produce electricity thank to wind speed because the average is always between 5 and 8m/s. Biomass energy sources are small and can only be used on an individual level as an energy source.

2.4 Case of South-Africa

South Africa has an energy-intensive economy that is very reliant on fossil fuels. Its emissions are amongst the highest in the world, and the country ranks among the 20 highest contributors to CO2 emissions overall (Conference,2004:10). Meanwhile, In South Africa renewable energy accounts for approximately 10% of total energy consumption (2000). Most of this energy is generated from fuel-wood and dung and not modern renewable energy technologies. Less than 1% of the total electrical energy used in South Africa originates from renewable energy sources (National E. M. 2008:15) .South africa has one of the highest levels of solar radiation in the World. The total potential concentrating solar power plants generation capacity for South Africa was estimated   around to 547.6GW, (Thomas,2009:5075). The average daily solar radiation in South Africa varies between 4.5 and 6.5 kWh/m2 , compared to about 2.5 kWh/m^2 for Europe and about 3.6 kWh/m^2 for parts of the United States(DME,1999:16) . Moreover, Wave Energy potential is very important. A mean annual power level of about 40 kW/m wave crest is typical offshore at the Cape Peninsula. An estimated total average power of 56 800 MW is available along the entire coast (Douglas,2006:110) . The wind power potential is generally good along the entire coast with localised areas. The mean annual speeds are above 6 m/s and power exceeds 200 W/m^2during all the year(DME, 1998:25) .Moreover, in South Africa, In 2000, biomass was reported to be 8.7 percent of final energy consumption. The main sources of biomass varied according to area . The fuelwood is the most used   in the rural domestic sector, bagasse in the sugar industry, and pulp and paper waste in the commercial forestry industry for in-house heat and electricity generation (Shell, 1997:10) . The potential energy from grass reached 84 GJ/ha/year in the most favourable areas(Fecher,2003: 21) . On the other hand, The conditions can be suitable for the extraction of geothermal energy from the earth. In regions of volcanic activity. Approximately 8 000 MW of geothermal power is generated in the Worldwide (Abiodun ,2007:5). According to the estimations economic reserves of geothermal energy in 10 to 20 years time could be equivalent to current global primary energy use in South Africa . The Council conservatively estimated that, globally, 30 EJ could be extracted sustainably by 2100. This is equivalent to seven times South Africa's current total primary energy demand.

2.5 Case of India-Ocean : Madagascar

In Madagascar, the energy sources and more specifically, electricity sources differ from one region to another. Since 2011, electrical energy production has continued to increase in Madagascar. The total net production of electricity in Madagascar was 832.741 MWh in 2001, to reach 1,267,647 MWh in 2011. Since

2001, the power energy production has increased to 50%. The share produces by power plants was from 268.796 MWh in 2001, representing 32% of total production 577.302 in 2011, representing 45.5% of total production (Electrification,2006:13). Compared to this, production of hydropower plants reached 563.945 MWh in 2001 representing 68% of the total production to 690.337 MWh in 2011, representing 54% of the total production. The potential hydro electricity of Madagascar was estimated to 7.800MW, at the present time, only 2.5% of this resource is used. Madagascar has huge potential in biomass which stays again inexhaustible.

2.6 Case of Central Africa :Cameroon

In 2008, the oil resources of Cameroon were estimated to be 30 million ton and natural gas reserves to be 186 billion m^3 (MINEE,2004:10). Cameroon has 20 GW fair hydroelectric potential, which is exploited at less than 5% [11]. Furthermore, Cameroon has the second largest forestry potential in the Congo Basin, unevenly distributed between the North and South of the country. The necessity to develop the energy infrastructure is a priority of the government's energy policy and to hire an ambitious program which intends to triple the energy capacity by 2020, which is about 3.000 MW as against 1.022 MW in 2009 in the public facility (MINFOF,2005). In 2009, energy production was estimated to be 9.016 ktoe in which more than 51% was coming from biomass, 45% from oil, and only 4% from electricity (MINEE ,2011). Electricity generation is dominated by hydro (69%), followed by self-production (22%). The total installed electric power increased from 932 MW in 2000 to 1,558 MW in 2009, with a production potential of 103 terawatt-hours (TWh) per year. The biomass production in 2009 is estimated to be thirteen 118 KTM consisting almost entirely of firewood [9]. Utilization of palm oil for biodiesel is also a viable prospect for the country. At present, around 108.000 hectares (ha) of land are affected by palm oil crop. However, between 2001 and 2006, a total of 30.000 ha of forest were cleared to allow for the expansion of palm oil crop (MINEE,2006). Cameroon is a small oil producer with a decline in production (84.000 barrels per day in 2008) after reaching a peak of about 168.000 barrels per day in 1985. Cameroon has the second largest African hydropower potential (294 TWh) after the Democratic Republic of Congo, less than 4% shall be recovered to date (MINEE,2006;SIE,2008). The exploitable potential is nevertheless considerable: 19.7 GW for an average energy production of 115 TWh per year. Its potential for renewable energy (firewood, agro-industrial and forestry waste, and solar and wind energy) is also considerable (SIE,2010). In the northern part, facing the advancing desert, wood energy deficit is noticeable. The average insolation in the northern part of the country is 5.8 kilowatt-hour (kWh)/m²/day and in the southern part, the average insolation is 4 kWh/m²/day. Thus, there is an average insolation of 4.9 kWh/m²/day for the whole country (Nkue,2009: 103).This solar potential is sufficient for the development of energy uses. The national average is estimated at a theoretical 2.327.5 TWh, about 20 times the hydroelectric potential. The wind potential is rather low for the energy production. Wind speeds on the entire territory hardly reach 5 m/s. Most of the country has wind speed average of 2–4 m/s at the height of 100 m. Wind energy potential exists in the north of Cameroon and the littoral region. Northern areas have average wind speed of 5–7 m/s. With regard to the geothermal energy, up to now, its potential is unknown, but hot springs are found in many cities of the country. Deposits of natural gas were estimated to be 186 billion per m^3 (Agenda 21,2001).

3 METHODOLOGY
3.1 Analysed cities

The study area is constituted of five climatic zones. This study was carried out in a warm zone in sub-Saharan Africa (Cameroon). Cameroon stretches in length from 2 to 13 degree of North latitude, and spreads in large from 9 to 16 degree of East longitude. It covers 475,442 km2 of area and presents various climatic nuances summarizing all bioclimates of African continent. This diversity is simplified by the distribution of different climatic nuances: in north of 6th parallel, the dry tropical climate dominates; while in the south, equatorial climate becomes more and more humid towards the coastline and Mount Cameroon. Cameroon is divided into three climatic zones, namely, the Sudanese, the Sudano−Sahelian, and the equatorial regions. Cameroon is characterized by an equatorial climate with two main seasons of equal amplitudes: a long rainy season from mid-March to mid-November (8 months) and a short dry season from mid-November to mid-March (4 months). The study was conducted in the equatorial city of Douala. Douala is the economic capital of Cameroon, the main business centre, and one of the largest cities in the country. It is the most industrialized city in central Africa. It is proven that the industries, the cars, and the buildings emit more than 60% of the total CO2 in the atmosphere. Douala's port is the main place of entry of cars not only in Cameroon, but also in Chad, and in Republic of central Africa (RCA). This city is located on the Atlantic Ocean coast, from 4∘ to 4∘4N of latitude and from 9∘40 to 9∘48E of longitude, with an area of nearly 210 km2. Climate in Douala is tropical wet and hot, characterised by temperatures between 18∘ and 34∘C, accompanied by heavy precipitation, especially during the rainy season from June to October. The air

almost always records 99% relative humidity during the rainy season, and about 80% during the dry season from October to May.

3.2 Climatic data

Outdoor daily data of the last 40 years of temperature (minimum and maximum), precipitation and sunshine was taken in five meteorological stations within the study area. The various data are measured from 3 to 10 m in height from the ground and with a frequency of 10–15 min. In selected weather stations, data like the relative and absolute humidity, wind speed, and evaporation are also available. The mentioned stations are selected because their administrative staff was qualified, measuring devices were reliable and also installed in a place far from any type of hindrance. Measurement errors on the temperature and relative humidity are estimated to be $\pm 0.1 \circ$C and 1%, respectively.

3.3 Climate change models

In the present research, 14 GCM models and three scenarios have been used (B1, A2, A1B). The most significant input of these models is the rate of emission of greenhouse gases in the future eras. However, a precise final determination is not possible. Accordingly, different emission scenarios with a variety of gas qualities in future have been offered. On the other hand,to define the effect of global warming by means of the rise in global temperature, it was necessary to employ a LARS-WG model. LARS-WG is one of the most well-known meteorological stochastic data-generating models used for generation of the quantities of rainfall, solar radiation, and daily maximum and minimum temperatures in both present and future climates of a meteorological station . The first version of the above-mentioned model was invented as a tool for statistical exponential microscaling in Budapest in 1990. In a LARS-WG model, some complex statistical distributions are used for modelling of meteorological variables. Fourier's series estimates the temperature. Daily maximum and minimum temperatures are simulated as stochastic processes with daily standard deviations and means, depending on dry or wet conditions of the relevant day(Orosa,2014:1890). In this assessment, Douala's temperature data in the time intervals of 1970–2000, were chosen as the basic data and temperature changes for the years 1985–2005 were studied based on the proposed scenario, so that the proper model accords with the experimental data of temperature in the proposed years. After testing the best model with Pearson correlation coefficient, the changes in Douala's temperature components were predicted in the worldwide heating bed for the periods 2013–2043 and 2045–2075. Based upon these changes, the degree day index values were calculated and compared with those in the past and present periods.

3.4 Calculation of heating and cooling degree-days

Degree-day methods are simple, yet efficient and fairly reliable for quantifying the heating and cooling energy demands in a building. Estimations are accurate if the internal temperature, thermal gains, and building properties are relatively constant. The severity of a climate can be characterized concisely in terms of degree-days. According to a recent survey carried out in Douala by Kameni et al.(Nematchoua,2014:381), it has been found that the temperature of human comfort varies following the seasons. The threshold temperatures vary for different conditions and as a general rule, the range of $19 \circ$– $25 \circ$C is proposed for human comfort. In order to estimate the amount of cooling needed in an N-day definite period, equation (1) was used

$$CDD = (T - \theta_2) \, , \, \theta_2 = 25. \tag{1}$$

In equation (1), the CDD is the required amount of cooling and T, the daily mean temperature. The temperature threshold θ_2 considered for Douala is $25 \circ$C. In order to calculate the need of θ_2 to heating, equation (2) must be employed

$$HDD = (\theta_1 - T) \, , \, \theta_1 = 19. \tag{2}$$

In this equation, HDD is the need for heating on the basis of degree-day; T and θ_1 have the same concept as in the previous equation and regarding Douala's condition s *19°C* has been chosen as the temperature threshold. The heating degree-days (HDD) and cooling degree-days (CDD) can be defined in accordance with [35] the equations (3) and (5):

$$HDD (\theta i, \theta th) = mk \sum_{k=1}^{n} 1(\theta i - \theta e, k) \tag{3}$$

where θi is the internal temperature, $\theta e,k$ the daily mean external temperature, θth the threshold temperature for heating, and k is the day number in the year. In this sense, the annual heating demand of a building Qh may be written as equation (4):

$$Q_h = K\text{totHDD} - \eta Qs \qquad (4)$$

$\sum_{k}^{n} 1(\theta e, k - \theta\text{tc})$where Ktot is the total thermal loss due to transmission and infiltration, Qs is the internal heat
source and solar gain and η is an efficiency to factor in the share of Qs that serves to reduce heating demand. In equation (5), θ_{tc} is the threshold temperature for cooling:

$$\text{CDD } (\theta\text{tc}) = mk. \qquad (5)$$

Finally, it is interesting to note that, if building properties are assumed to be constant, the cooling energy demand is proportional to the number of CDD.

4   RESULTS AND DISCUSSION

The energy used for heating is almost null, because we are in warm region. The total maximum cooling energy is obtained in February with an amount of 1745 degree days (see figure 1). In August and September, energy used for cooling is very weak . In October, a total of 384 degree days is used for cooling. The increase in outdoor heat rate requires a strong demand of cooling energy, it explains why in December, cooling energy increases up to 1370 degree days during the same period. In the present period (2013–2033), maximum cooling energy is obtained in March (2453 degree days). This cooling energy decreases linearly between May and July and a minimum value is obtained in August (673 degree days). From this month, an increasing demand for the cooling energy is observed until December (2033 degree days). In the future (2045–2065), a maximum of total cooling energy is obtained in February (2317 degree days) then, a minimum is obtained in August (755 degree days). An analysis of general averages of total cooling energy in all three periods indicates that the demand in energy is stronger in dry seasons (January, February, March, April, May, November, and December).
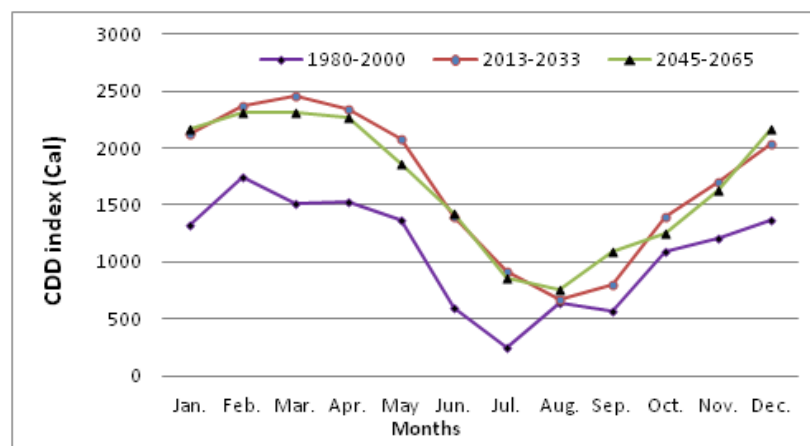

Figure 1. Calculation of the monthly average CDD index during the three studied periods.

 Figure2, shows the total cooling energy during the three periods. It is observed that in the period 1980–2000, cooling energy was 13580 degree days. From 2013 to 2033, cooling energy shall be 20276 degree days . Between 2045 and 2065, cooling energy will be 20090.
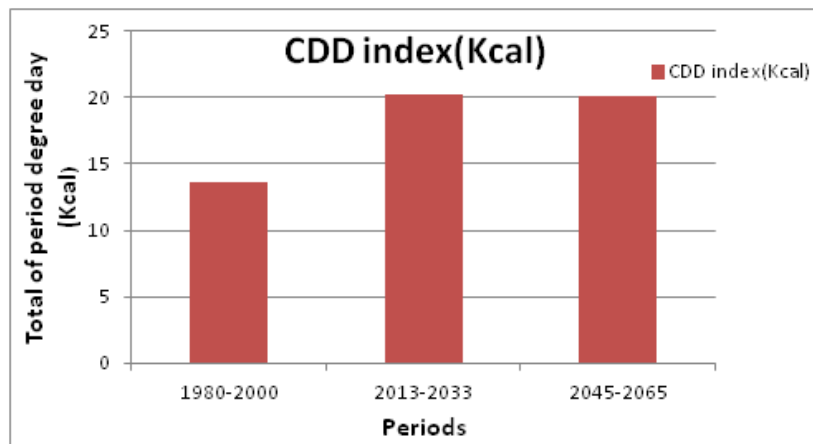
Figure2. Calculation of the monthly average CDD indices during the three studied periods.

An analysis of these data shows that cooling energy demand will be very high in the future between 2013 and 2033, and less elevated from 1970 to 2000. Such a result is not surprising, because the more warm it is, the more cooling energy demand is developed.

5   CONCLUSION

In this research, a review on the potential of the resources in some Africa countries and a survey has been carried to value cooling and heating energy demand in Douala city buildings. The increasing demand of air conditioning and artificial lighting for the improvement of human comfort in the tropics also greatly contributes to the increase in energy usage. Energy consumption in the sector increased by 14% during the last decade, which was mostly due to rapid urbanization, population growth and economic development in developing countries. The increase in outdoor heat rate requires a strong demand of cooling energy. The cooling energy demand is more in the future between 2013 and 2033 and less elevated from 1970 to 2000.

6   REFERENCES

ABIODUN O. (2007). Biofuel Opportunities and Development of renewable energies Markets in Africa: A paper presented during the biofuel market Africa 2007 conference, Cape Town, South Africa

ASHRAE Fundamentals Hand book (2009) Energy Estimating and Modeling Methods; SI edn, American Society of Heating, Refrigerating, and Air-conditioning Engineers, Atlanta, GA, Chapter 19.

BAS J, Ruijven van, Schers J, Detlef P,Vuuren V (2012) Model-based scenarios for rural electrification in developing countries; Energy 38, 386–397.

DIAB,(1995) Generalised map of wind power potential in South Africa.

DME,(1998) White Paper on the Energy Policy of the Republic of South Africa, Department of Minerals and Energy, Pretoria, December 1998.

DME (1999) Digest of South African Energy Statistics, compiled by CJ Cooper, Department of Minerals and Energy, Pretoria.

DOUGLAS B., Schäffler J.(2006) The potential contribution of renewable energy in South Africa. February -1(115).

EDIRIN B., Agbro , Nosa. A. Ogie. A comprehensive review of biomass resources and biofuel production potential in Nigeria. Research Journal in Engineering and Applied Sciences 1(3) 1 49-1 55.

FECHER(2003)Residential solar water heating as a potential Clean Development Mechanism project: a South African case study. Mitigation and adaptation strategies for global change Spalding-Fecher, R, Thorne, S & Wamukonya, N forthcoming 2003.

International Geothermal Association. (2004). Available Internet: http://iga.igg.cnr.it/ geoworld/geoworld.php?sub=elgen

J'aime Madagascar. Electrification rurale en Marche . Septembre-Octobre 2006, N°13, 8 pages .

KAREKEZI, S., and Ranja, T. (1997). Renewable Energy Technologies in Africa. ZED Books and AFREPREN. Oxford, U.K. 1-10.

KAREKEZI S., et al, (Eds.) 2002. "Africa: Improving modern energy services for the poor" in Energy Policy Journal – Special Issue, Vol 30, No. 11-12, Elsevier Science Limited, Oxford.

LOMBARD L, Ortiz J, Pout C.(2008) A review on buildings energy consumption information. Journal of Energy and Buildings 40 (2008) 394–8.

PATEY. Luke, Kenya: An African oil upstart in transition,Octobre2014,1-26.

MINFOF et FAO,(2005) Evaluation, des resources forestiéres du Cameroun.

MINEE(2004)Etude du marché de GPL, Cameroun.

MINEE(2011) Systéme d'information énergétique du Cameroun.

Ministère de l'Energie et de l'Eau (2006)-Plan de Développement à long terme du Secteur de l'Électricité Horizon 2030 (PDSE 2030). Rapport Final Volume 3 – ETUDE DE L'OFFRE DE PRODUCTION.

Mise en œuvre de l'agenda 21 par le cameroun. Rapport national du cameroun sur l'environnement et le developpement durable (rio +10). Septembre 2001.

NEMATCHOUA M.K., Tchinda R., Orosa J. A.,(2014)Thermal comfort and energy consumption in modernversus traditional buildings in Cameroon: A questionnaire-based statistical study. Applied Energy,114 ,687-699.

NEMATCHOUA M. K., Tchinda R., Ricciardi P., Djongyang N.(2014) "A field study on thermal comfort in naturallyventilated buildings located in the equatorial climatic region of Cameroon," Renewable and Sustainable Energy Reviews, vol. 39, pp. 381–393.

NEMATCHOUA M.K., Tchinda R., Orosa J. A.(2014) "Adaptation and comparative study of thermal comfort in classrooms and buildings naturally ventilated in wet tropical zones," Energy and Buildings, vol. 85, pp. 321–328.

NEMATCHOUA M. K., Roshan Gh. R., Tchinda R,. Ricciardi P.(2015)Climate change and its role on forecasting energy demand in building:A case   study of Douala city, Cameroon. J. Earth Syst. Sci. 124, 269–281.

NKUE et Njomo (2009), Analyse du système énergétique camerounais dans une perspective de développement soutenable. Revue de l'Energie, n° 588, mars-avril 2009, pp 102–116.

NNAMDI I. Nwulu, O. Phillips Agboola(2011). Utilizing Renewable Energy Resources to Solve Nigeria's Electricity Generation Problem, Int. J. of Thermal & Environmental Engineering Volume 3, 15-20.

National Environmental Management Act. 1998. Government ofSouth Africa.

OBIOH I. and Fagbenle R.O. (2009). Energy Systems: Vulnerability Adaptation Resilience (VAR). Hello International

OMOKARO O. (2008). Energy Development in a Fossil Fuel Economy: The Nigerian Experience. The report of a National Dialogue to Promote Renewable Energy and Energy Efficiency in Nigeria. 55p.

OROSA A, Roshan G R and Negahban S.(2014) Climate change effect on outdoor ambiences in Iranian cities; Environ. Monit. Assess. **186** 1889–1898.

PAYAM N.,Fatemeh J., Mohammad M.T., Mohammad G.,Muhd Z.(2015). A global review of energy consumption, CO_2 emissions and policy in the residential sector (with an overview of the top ten CO_2 emitting countries). Renewable and Sustainable Energy Reviews 43, 843–862.

Système d'Information Energétique (2008). Rapport annuel.

Système d'Information Energétique (2010). Rapport annuel

FREEMANTLE Simon The five trends powering Africa's enduring allure, Africa Macro Insight & Strategy, Standard bank, (2011)1-15.

Shell,   (1997). Shell International Renewables – Bringing Together the Group's Activities in Solar Power, Biomass and Forestry, **www.shell.com**.

THOMAS P. . The potential of concentrating solar power in South Africa. Energy Policy 37 (2009) 5075–5080

402: A case study of energy efficiency retrofit and renewable technology utilisation in a UK schools group

LI ZHANG1, MENG TIAN[1], HANBING FAN[1], NHUNG THANH TRAN[1], RICHARD SMEETON[2], SARAH IQBAL[2], YUEHONG SU[1]*

1 Department of Architecture and Built Environment, The University of Nottingham, Nottingham, UK, NG7 2RD
2 3 Burton Walks, Loughborough Endowed Schools, Loughborough, UK, LE11 2DU
* Corresponding Author: yuehong.su @nottingham.ac.uk

This paper presents a study on assessment for energy efficiency by utilizing a series of renewable technologies in Loughborough Endowed Schools (LES) refurbishments. In the assessment, economic evaluation of energy saving measures was also considered. In light of inefficient energy usage issues identified in the LES project, five measures including internal wall insulation, double glazing, combined heat and power, heat recovery ventilation and PV were chosen and investigated in the simulation by using software packages EnergyPlus and PVSyst. Three representing buildings, which are historic brick building (Boarding House), modern education building (LHS Science Building) and special functional building (Swimming Pool) were simulated as examples to investigate every measure and technology adopted. The results were compared with the original energy consumption. In terms of traditional brick wall building, it has been found in this research that internal wall insulation and double glazing played significant improvement on energy performance. Changing traditional ventilation to heat recovery ventilation in swimming pool and using high performance unit CHP were strong suggested. However, PV presented less saving compared with others. The economic evaluation involved simple payback period, net present value, internal rate of return, levelised cost of energy and benefit-to-cost ratio. The results showed that over the 15-year analysis, combined heat and power, Heat recovery ventilation and photovoltaics were financially feasible, while internal wall insulation was only viable over a longer period.

Keywords: energy efficiency; retrofit; renewable technology; EnergyPlus; PVSyst; economic evaluation

1. INTRODUCTION

In the UK, Energy consumption in domestic and non-domestic buildings is responsible for approximately 43% of the carbon emissions (UKGBC, 2011). It was estimated that non-domestic buildings emitted 20.1 MtCO$_2$e annually and schools were responsible for 3.0 MtCO$_2$e of this total (Gill Bryan et al., 2011). Under the Act of Kyoto Protocol which was signed in 1998, the UK government sat an ambition of reducing 80% of carbon emission by 2050 compared with 1990 level (Government, H., 2009). In terms of UK schools, the government targeted to cut down 53% of current carbon emission by 2020 (DCSF, 2009). In Loughborough, a Sustainable Energy Project has been undertaken for Loughborough Endowed Schools (LES). A number of renewable technologies are considered to be utilised to retrofit the exciting inefficiency buildings.

Managing schools' energy use effectively, a balanced action plan should be considered by bring the widest of retrofit measures together (DES, 2002). Xing et al. (2011) established a hierarchical process as shown in Figure 1. Three phases retrofitting approaches were identified. The first step is retrofitting fabrics of the exciting building to higher standards in order to reduce the energy demand. The second step is to install more efficient equipment. Micro generation, which is to establish on-site low carbon energy supply technologies, combined smart grid connections and control is the last step of this process. The characteristics of every measure and technology in each step have been briefly introduced as following.

Figure 163: A hierarchical process towards zero carbon refurbishment (Xing et al., 2011)
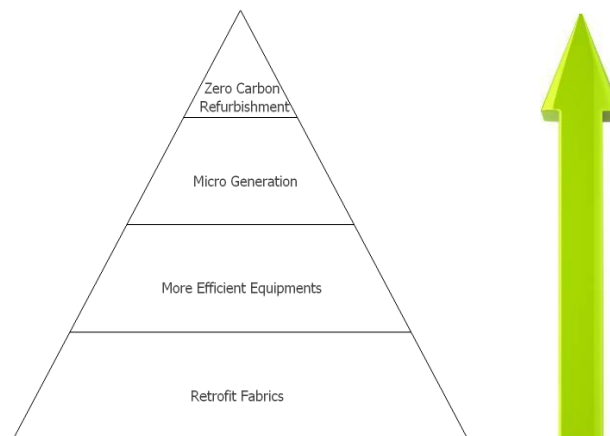
1.1 Retrofit Fabrics

Retrofit Fabrics normally includes wall insulation and double glazing. Construction of the exciting wall should be surveyed before applying insulation. According to the different develop stages of building, traditional wall constructions vary from single thin skin brick, stone walls to much thicker rubble filled walls (English, Heritage, 2010). The 100mm single skin brick wall is a common traditional solid wall, which often contains multiple material including soft porous chalk, hard impervious flint etc. Kolaitis reveals 12% to 47% of energy consumption for HVAC (heating, ventilating, and air conditioning) can be reduced in UK by utilizing wall insulation. Both external wall insulation and internal wall insulation improve the thermal performance in buildings and reduce the energy demand. Generally speaking, the effectiveness of external wall insulation is 8% higher than internal wall insulation. However, in terms of historic and traditional buildings, internal wall insulation is always preferred as it would maintain the appearance of the building, as well as significant lower installation cost compared with external wall insulation (Kolaitis et al., 2013). Attention should be paid on moisture condensation by applying internal wall insulation.

A well-insulated building with optimized windows brings low energy demand as it has a small amount of heating loss in winter and cooling loss in summer (Jaber et al., 2011). The heat loses through windows always contributes a larger proportion than other elements in a building (Freire et al., 2011). Single glazing window owns approximately twice of heat transfer coefficient of double glazing window with the same material (Yang et al., 2004). Replacing single glazing to double glazing can significantly enhance the thermal performance of a building and greatly improve the thermal and acoustic comfortable. Mortimer evaluated 39% to 53% energy can be saved by installing double glazing window instead of single glazing window (Mortimer et al., 1998). UK schools often occupy historic and traditional buildings. Replacement of single glazing to double glazing windows need the balance of building conservation and building retrofit.

Most historic windows are timber-framed. These windows are suggested applying drought-proofing, secondary glazing and shutters (CIBSE, 2002). Secondary glazing needs to be emphasized that improving the insulation by adding a glazing layer near the original window, which is different from the traditional double glazing.

1.2 More Efficient Equipment

Combined heat and power (CHP) system generates both thermal energy, both heating and cooling as well as electricity in a single process (ASHRAE, 2000). Electricity generates from waste heat which always released to the surrounding environment in the processing and heat generates on site or closed to the site. As shown in Figure 2, compared with conventional heat and electricity generation separately, the overall energy efficiency is usually higher than 80%. The system can only be economic and reduce CO_2 emission when it is running. The high demand of heat, the more saving can achieve. Generally, a building which demands heating more than 4,500 hours a year, CHP enough for installed and benefit can be observed obviously.
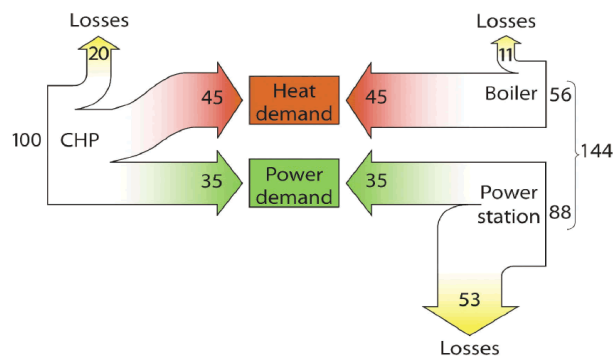

Figure 2: CHP versus conventional generation (Carbon Trust, 2004).

Indoor swimming pool as a special function building always need constant warm water, high internal temperatures (usually around 29 °C and substantial ventilation to maintenance the indoor comfort. BRE reported that energy required by swimming pool per unit is approximately five times than office building (BRE, 1997). Figure 3 shows a typical UK swimming pool energy consumption proportion. According, energy using in space heating and water heating contribute more than half of the energy consumption. Energy recovery need well organized both in heating water and ventilation.
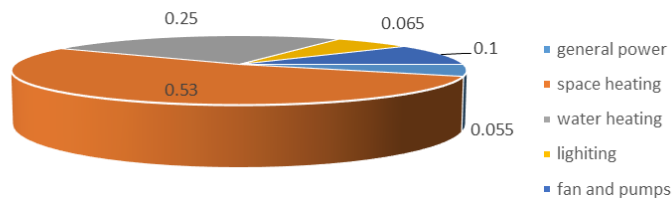

Figure 3: Proportion of energy used in a typical indoor swimming pool (BRE, 1997).

A study carried out by Kampel et al. (2014), revealed that heat exchangers and heat pump recovery energy is beat saving measures. HAVC system with heat recovery from air and distributed to air, water of pool and tap was proved the main factor for energy saving. Two wide used technologies are mechanical heat pumps and open absorption system. The energy consumption of swimming pool under these technologies compared with congenital ventilation technique, although the electricity required for two new systems increase 63 MWh and 57 MWh per year, the overall energy consumption reduce 611 MWh and 484 MWh, which correspond 14% and 20% respectively (Johansson et al., 2001).

1.3 Micro Generation

Photovoltaics (PV) panels system presents four significant advantages in built environment. It is good design element for the appearance of buildings, which can be applied on roofs, façades, shading devices and windows. For the operation of PV, it is easily and silently and low maintenance required. Most PV panels in market can use more than 20 years. Financially, support mechanisms can help to encourage the utilization of PV as the investment is financially viable the household can receive revenue from FiT and exporting. Compared with other energy source, it shows low influence on environment for manufacturing, installation and maintenance (Pester and Crick, 2013). Annual yield and performance ratio (PR) are the two main factors reflect the performance of the system. For an average benchmark in the UK, annual yield is 850 kWh/kWp and a well-designed PV system has a PR, which is a ratio 75% to 85% of the actual energy output over a given period.

Location and building factors including shading, mounting types, array orientation and tilt angels are the most import factors required analysis when considering the PV system. UK schools usually operate in daytime and have large available for roof installation, which makes PV a more appealing alternative (DECC, 2014). In order to optimise overall annual output, it is pivotal to avoid shading from surrounding obstacles as well as fit the panel with an approximately 30° tilt angle and facing south.

It is clearly that a variety of opportunities can be suitable for UK school retrofit to achieve the zero carbon emission. According to the situation of LES buildings, retrofit measures and technologies should be carefully chased to achieve the desired reduction in energy consumption, costs and carbon emission.

2 LOUGHBOROUGH ENDOWED SCHOOLS SITUATION

The case study is conducted on the Loughborough Endowed Schools (LES), which was date back to 1495. It is located in the south of the town centre of Loughborough, Leicestershire, UK. It comprises three individual schools – Loughborough Grammar School (LGS), Loughborough High School (LHS), Fairfield Preparatory School (FPS). There are fifty-four buildings in total in this campus. Figure 4 shows a view of building and distribution in LES. Collating living energy bills of this campus has been finished already. It comes from 2012 to 2015 three yeas electricity and gas bills. Table 1 shows energy consumption situation in chosen analysed building in LES. It helps to identify the most efficiency building to most inefficiency building, which help the school to decide which building is needed to retrofit emergency and which can be concerned later.

Figure 4: Typical historic Victorian brick building and building distribution in LES

Table 1: LES energy consumption per year per m² of each building

Energy consumption per year per square meter (kWh)		
Grammar	Pullinger building	3.074
Grammar	5 Burton walks	3.670
High	Chesterton building	4.151
Foundation	4 Burton walks	4.366
Grammar	Cope&Barrow	4.395
Grammar	Physics	5.035
Grammar	Denton house	6.057
Foundation	1 Burton walks	6.201
High	Charles & English & Drama	6.304
Fairfield	Music school	6.330
High	Main buidling& Cloister	6.900
High	Science building	6.997
High	Rokeby & 28 Burton street	7.480
Grammar	English & Drama	7.500
Foundation	Quorn	7.821
Grammar	School house	8.197
Grammar	Tower building	8.200
Grammar	6 Burton walks	8.443
Fairfield	Fairfield school	9.390
Foundation	2 Burton walks	9.522
Grammar	Library&ICT&Pavilion	9.909
Grammar	Year6&scourt&sport hall	10.190
Foundation	3 Burton walks	10.206
Grammar	Hodson hall&Geography	11.017
Grammar	Art&design	11.320
Foundation	Estates workshops	11.320
Grammar	Biology	11.588
High	Gym	14.189
Grammar	Burton hall&CDT	14.368
Foundation	Lodge	14.668
Grammar	Swimming pool	15.784

In addition to the electricity and gas bills collating, visual inspection of the buildings is conducted, i.e., plant rooms and associated systems, the building fabric and glazing. The purpose is to review all systems, understand the details of their operation and design, and identify opportunities for improvement and modification that will improve operational efficiency and reduce energy consumption.

First of all, most buildings are poorly insulated including wall and roof. Single glazing window can be found in many buildings. This can be more evidently seen in LGS and LHS. Although several refurbishments have been done for the old Victorian and Edwardian period buildings, wall/roof insulations and window has been improved less. The annual energy required for these building all presents considerable amount of gas. Internal wall insulation and double glazing is considered to utilise in those buildings in order to reduce the energy demand of the buildings and improve the internal thermal environment as well. In order to easier for installing and unnecessary to alter the appearance of the building, internal wall insulation needed to be applied. Secondly, the condition of heating systems varies greatly. Some boilers have been use more than 10 years. Since the efficiency of regular natural gas boiler has been developed a lot and the efficiency drops with the serving age, old boilers usually present an evidently lower efficiency. An estimating done by Sedbuk (Sedbuk, 2013) that the efficiency of 15 years old conventional natural gas boiler ranges from 55% to 65%. However, combine heat and power (CHP) can reach an overall efficiency higher than 90% by using the dissipated waste heat for power generation simultaneously (Hwang J, 2012).Therefore, replace the old conventional boilers with condensing boilers or CHP would largely reduce the gas demand. Thirdly, the ventilation system for the swimming pool at LES is badly designed and the water supply pipe is poorly insulated. The swimming pool has one vent located in the southwest of the building for heated fresh air supply and one extract fan place on the other side on top of the building. Poor air distribution, insufficient airflow and over humidity are appeared in the building with varying degrees. These problems not only affect the indoor thermal comfort but also reduce the energy efficiency and damage the building fabric. As to the water pipe of the pool, the circulating pipe for hot water supplying to the pool is not insulated and exposed outside of the building, which has a length longer than 30m. As a result a large proportion of heat is lost due to inefficiently delivering. Therefore, heat recovery ventilation has been considered in simulation. Finally, considering the scale and the energy demand of the buildings, PV panels can be considered. With the utilisation of renewable energy technologies building can cut the greenhouse gas emission and also saving the cost on energy.

3 SIMULATION AND ANALYSIS

As discussed, three representative buildings are chosen to carry out the simulation and five measures and technologies are investigated on those buildings. EnergyPlus and PVSyst have been used to conduct the simulation. PV analysis is based on PVSyst and other results are from EnergyPlus.

3.1 Wall Insulation for Boarding House

The wall of the Boarding House is brick. In order to maintain the appearance of the historic façade of the building, a thickness of 50mm quilt mineral wool insulation has been chosen as the internal wall insulation. Table 2 presents the properties of the insulation. As calculated from the real measurement, the total area of the internal wall insulation is approximate 770m2. The U-value for the original 230mm wall is 2.57W/m²K and the one with 50mm quilt mineral wool insulated wall is 0.68W/m²K, which comes from the Dynamic Thermal Properties Calculation (Version 10.1). The U-value can achieve as low as 0.38W/m²K when the thickness of the insulation is 100mm. However, it would take too much indoor space.

Table2: Properties of the chosen internal wall insulation

Properties	
Thermal conductivity	0.039 W/Mk
Density	18 kg/m³
Water absorption (100% RH)	20% w/w
Specific heat capacity	1800 J/jgK
Ignition point	> 500 °C

Table 3 shows the monthly energy demand both in heating and cooling in the case of original and insulated. The sensible heating energy requires is 241,782.9kWh annually. Assume the boiler efficiency is 0.8, the gas required should be 302,228kWh. Plus the gas required for hot water which is 100,587.1kWh according to the simulation, the total energy consumption is 402,815kWh while the actual energy in bills is 417.027kWh. It is only 3.4% difference between the actual number from bills and simulation result. According to result, 37,113kWh, which 15.3% heating energy can be reduced annually. Considering the boiler efficiency approximately 46,391kWh gas can be saved every year. Cooling takes a small amount of energy as shown. However, the building uses natural ventilation for summer cooling so it does not affect energy consumption increasing.

Table3: Monthly heating and cooling energy demand (kWh) for base and wall insulated of Boarding

Time	Base (kWh)		wall insulated (kWh)	
	Heating	Cooling	Heating	Cooling
Jan	43333.33	0	3.79E + 04	0
Feb	43611.11	0	3.76E + 04	0
Mar	33611.11	0	2.86E + 04	0
Apr	18114.71	0	1.52E + 04	0
May	12181.39	53.79792	9.35E + 03	104.981
Jun	2389.809	1444.042	1.65E + 03	2032.892
Jul	72.47142	4132.619	3.99E + 01	4935.33
Aug	0	0	0.00E + 00	0
Sep	4009.261	0	3.11E + 03	0.698497
Oct	19737.47	0	1.61E + 04	0
Nov	34166.67	0	2.90E + 04	0
Dec	30555.56	0	2.62E + 04	0
Total	241782.9	5630.459	2.05E + 05	7073.901

House

3.2 Double Glazing for Boarding House

Although double glazing is not suitable for historic building, it has still been assumed to be applied in this study to obtain a scope about how much energy could be saved by using double glazing. It is assumed 3mm double glazing with 13mm air gap window was applied in this simulation. Similar with the trend of the internal wall insulation retrofit measure, Table 4 presents annual heating energy consumption of the building can be reduced 22.7% which is 54,831kWh. Although cooling in summer increases 2,181kWh every year, it still not affect the energy require much as the nature ventilation applied in Boarding House.

Table4: Monthly heating and cooling energy demand (kWh) for base

Time	Base (kWh)		Double glazing (kWh)	
	Heating	Cooling	Heating	Cooling
Jan	43333.33	0	34953.42	0
Feb	43611.11	0	34810.57	0
Mar	33611.11	0	26226.9	0
Apr	18114.71	0	13697.85	0
May	12181.39	53.79792	8071.341	133.8605
Jun	2389.809	1444.042	1373.158	2342.793
Jul	72.47142	4132.619	27.21665	5317.57
Aug	0	0	0	0
Sep	4009.261	0	2689.651	18.0165
Oct	19737.47	0	14374.57	0
Nov	34166.67	0	26504.64	0
Dec	30555.56	0	24192.55	0
Total	241782.9	5630.459	186921.9	5630.459

3.3   Combines Heat and Power for Boarding House

Optimal Combined Heat and Power (CHP) size should be identified through understanding the site's heat and electricity consumption before staring simulation. A 24-hour energy operating model in a typical day monthly had been gained. Figure 5 Energy consumption proportion for heating in each month in Boarding House. As can be seen, from that November to February takes 63% of the total heating amount. The 24-hour model shows four this situation heat load varies from 40kW to 90kW is suitable. To avoid the peak heat load case which is high cost with low return on capital and the base heat load case which low energy saving and low return on capital, the intermediate CHP, the product from ENER-G with 61kWth heat output and 35 kWe electricity output was selected in this site. And the maximum efficiency can reach up to 86.5%.
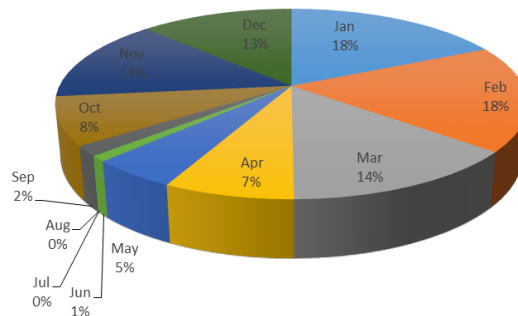

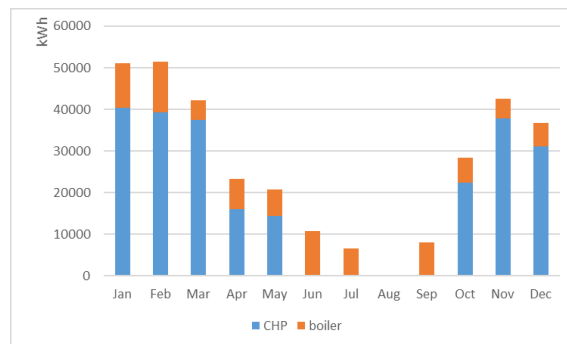Figure 5: Energy consumption proportion for heating in each month in Boarding House

Figure 6: Monthly heat output from spare boiler and CHP

Figure 6 shows the monthly heat output from spare boiler and CHP. Because of winter holidays, the building is out of operating, total heating demand in December is lower than November. In summer (Jun-Sep), only spare boiler is used as operating CHP at low-load cause energy loosing and maintenance cost increasing.

Consequently, setting CHP as part-load or use spare boiler is the optimum operating. Table 5 shows CHP offers 74% of total energy consumption in space heating and hot water heating.

The electricity output from CHP and required from the grid is shown in Figure 7 and Table 5. A considerable amount of electricity can be produced from October to March. In the meantime, the electricity can be supplied to other buildings on site or sold to grid. In this period, CHP is high-load and only very limited electricity needed from the grid to offer the CHP system. The annual electricity required by the building reduces 60.6%, which equals 72,160kWh. Total annual electricity amount required from grid is 46,962.22kWh and the total annual exported electricity is 51,072.6kWh which means the net electricity energy required from grid by the building is negative for a period of one year.

Table 5: Monthly heat produced by spare boiler and CHP

| Time	HW(kWh)	heating(kWh)	total(kWh)	CHP(kWh)	boiler(kWh)	CHP/total %
Jan	7805.22	43333.33	51138.56	40295.85	10842.71	0.79
Feb	7825.25	43611.11	51436.36	39332.48	12103.88	0.76
Mar	8663.67	33611.11	42274.78	37387.39	4887.39	0.88
Apr	5112.60	18114.71	23227.30	16016.06	7211.24	0.69
May	8663.67	12181.39	20845.06	14349.32	6495.74	0.69
Jun	8384.20	2389.81	10774.01	0.00	10774.01	0.00
Jul	6523.15	72.47	6595.62	0.00	6595.62	0.00
Aug	212.04	0.00	212.04	0.00	212.04	0.00
Sep	3981.52	4009.26	7990.78	0.00	7990.78	0.00
Oct	8663.67	19737.47	28401.14	22323.29	6077.84	0.79
Nov	8384.20	34166.67	42550.87	37850.35	4700.51	0.89
Dec	6250.52	30555.56	36806.07	31086.91	5719.17	0.84
Total	80469.71	241782.88	322252.60	238641.65	83610.94	0.74
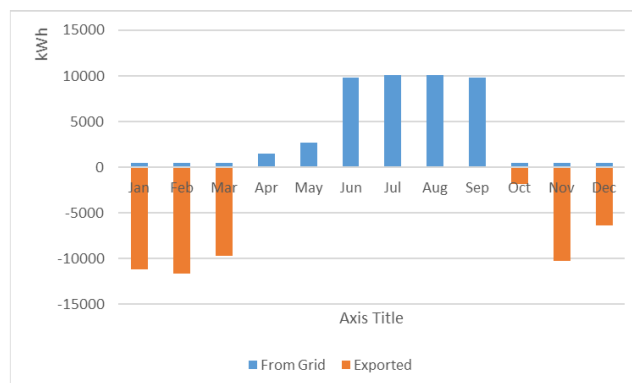
Figure 7: Monthly electricity inport/output from grid (kWh

Table 6: Monthly heat produced by spare boiler and CHP

Time	Electricity kWh	CHP power kWH	From Grid kWh	Exported kWh
Jan	10119.68	20808.51	492.00	11180.83
Feb	9142.68	20311.03	492.00	11660.35
Mar	10128.10	19306.60	492.00	9670.50
Apr	9779.60	8270.59	1509.01	0.00
May	10128.10	7409.90	2718.21	0.00
Jun	9799.63	0.00	9799.63	0.00
Jul	10105.65	0.00	10105.65	0.00
Aug	10095.70	0.00	10095.70	0.00
Sep	9782.02	0.00	9782.02	0.00
Oct	10125.30	11527.60	492.00	1894.31
Nov	9799.63	19545.67	492.00	10238.04
Dec	10116.49	16053.07	492.00	6428.58
Total	119122.60	123232.99	46962.22	51072.61

Table 7: Monthly gas using (kWh) by conventional and CHP system

Time	Convntional system gas boiler	CHP system gas for boiler	Gas for CHP
Jan	61971.89	13553.39	91656.54
Feb	62339.14	15129.85	89465.27
Mar	50677.56	6109.24	85040.99
Apr	27755.98	9014.05	36429.98
May	23890.41	8119.67	32638.83
Jun	11371.46	13467.51	0.00
Jul	6613.74	8244.53	0.00
Aug	212.04	265.05	0.00
Sep	8993.09	9988.47	0.00
Oct	33335.51	7597.30	50776.35
Nov	51092.53	5875.64	86094.04
Dec	44444.96	7148.96	70709.97
Total	382698.32	104513.68	542811.96
Total	382698.32	647325.64	

3.4 Heat Recovery Ventilation for Swimming Pool

The recommend condition of the indoor swimming pool in the UK is listed in Table 8. The air changes per hour should range from 4/hour to 6/hour depending on the height of the pool hall. The volume of the pool hall is 2,780 m^3 and the floor area including the pool is 505 m^2. Two air – volume of 2.5m^3/s heat recovery air handling units offered by ECOVENT are utilized to meet the performance. Assuming the boiler efficiency is 75%, the annual energy demand for the pool hall heating could decrease 165,257.63kWh which is 20.23% energy for heating. Because the energy required for swimming pool air heating is significant, this measure is considerable. However, the electricity spend on maintenance is 40,955kWh and 30,660kWh electricity is required every year on the old system 33.6% (10,295 kWh) electricity consumption on HVAC system increases.

Table 8: Indoor swimming pool ventilation recommended in UK

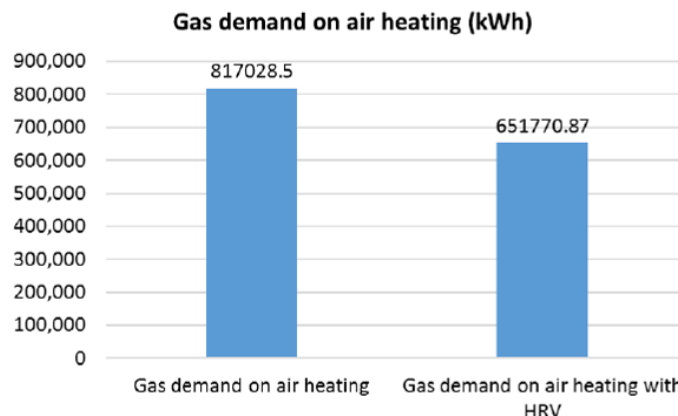| Recommended conditions	
Air temperature	Typical 30 °C
Relative humidity	50%-70%
Ventilation	10 litres per second per square metre of total
	4-6 air changes per hour standard use 8-10 air
	Minimum 12 litres per person second

Figure 8: Monthly electricity import/output from grid (kWh).

3.5 Photovoltaic for Science Building

PVSyst and EnergyPlus were applied to evaluate the electricity production from photovoltaic. Science building has approximately 540m² flat roof area and 25m² polycrystalline PV collector with 15 modules was applied in this simulation. The PV is set at 30° tilt facing south and the azimuth angle is 0°. The arrangement of the layout is decide to set as either 3 strings of 5 modules in series or one string of 15 modules in series. As different arrangement concerns the inverter chooses which may affect the final output of the system. A comparison of these two arrangements is presented in Table 9. In the table the output data is based on the simulation from PVSyst. The electricity generated by the system is 3356 kWh and 3479 kWh annually respectively. One string of 15 modules is applied in modelling finally.

Table 9: Comparison of electricity output of two different module arrangements

Module area	Number of modules	Modules in series	Number of strings	Number of inverters	Nominal PV power	Max PV power	Nominal AC power	Inv. unit power	Prod/ year	%
25 sqm	15	5	3	3	3.8	3.4	2.5	0.85kW	3356	0.245591
25 sqm	15	15	1	1	3.8	3.4	3	3kW	3479	0.254592

PV system with the same characters is also simulated in EnergyPlus and the output results are also the similar. Results from EnergyPlus are 172.61kWh/ year, which is more than the one from PVSyst. The electricity production difference is 5% which can be neglected. Figure 9 shows the PV system reaches its peak around the noon time of a day and does have output during night time which product meets the building operating time. It can be regards as an advantage for applying PV to cut the electricity demand in peak time.
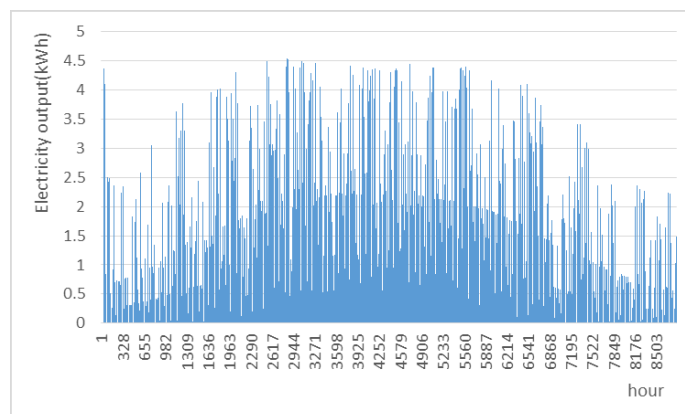

Figure 9: Hourly electricity production of the PV system (kWh)

3.6. Summary and Comparison

Table 10: Summary and comparison of each measure

Measures	Gas (kWh)				Electricity (kWh)			
	original	new	saving	%	original	new	saving	%
Wall insulation	241782.9	204669.9	37113.04	0.153497				
Double glazing	241782.9	186921.9	54861.02	0.226902				
CHP	382698.3	647325.6	-264627	-0.69148	119122.6	46962.22 -51072.6		
HRV	817209	651770.9	165438.1	0.202443	30660	40955	-10295	-0.33578
PV					13665	10186	3479	0.254592

The summary and comparison were listed in Table 10. Internal wall insulation and double glazing were both applied in Boarding House. Compared to Internal wall insulation, the double glazing can reduce 7.34% annual energy spending. However, these two measures are both suggested in retrofitting historic brick buildings on campus which not only saving the energy but also increase the comfort of the occupants.

Combined heat and power is perfectly applied in building which required high and constant demand for heating. In cold days, the system under high-load save energy is considerable, but in warm days, the system is not suggested use under part-load condition, because the energy saving is not obviously and the maintenance is significant high. By using CHP, the gas consumption is 69% higher than the original ones but the electricity is less than half. The most saving in achieved by heat recovery ventilation in Swimming Pool among five measures. 20.24% energy which is 165,438kWh gas saving and only a small amount of electricity consumption increase because setting the new system. PV saves 3,479kWh annually which 25% to cut down the electricity consumption.

4   ECONOMIC EVALUATION

The economic evaluation considered the Simple Payback Period (SPP), the Net Present Value (NPV), the Internal Rate of Return (IRR), the Levelised Cost of Energy (LCOE), and the Benefit-to-Cost (B/C) ratio. With the assumptions in Table 11, the internal wall insulation, CHP, HRV and PV has been taken economic evaluated. The result shows that CHP, HRV, and PV are financially viable over the 15 years analysis period, whilst wall insulation has unfavourable results for the same analysis period as summarised in Table 12. Before rejecting the wall insulation project, assessments were conducted for different time horizons that are equal to the lifespans of the four solutions.

Table 11: Key assumptions in economic evaluation

Input factors	Starting key assumptions	Variations for sensitivity analysis
Time period	15 years	5, 10, 20, 25, 30 years
Energy unit price	Gas: 3.02 pence per kWh	
	Electricity: 10.06 p/ Kwh	
CCL	Gas: 0.193 p/ Kwh	0 % and 5 %
	Electricity: 10.06 p/ Kwh	
	Annual increase: 3.3 %	
GHG emissions conversion	Gas: 0.184 kgCO$_2$e[11] per kWh	
	Electricity: 0.445 kgCO$_2$e per kWh	
Discount rate	4.22	0 % and 7.5 %
Standing charges	Gas: 294.6 p/ day	0 % and 5 %
	Electricity: 18.64 p/	
	Annual increase: 2.5 %	
Inflation		
Decrease in efficiency	10 % over 15 years, approximately 0.75 % annually	
Tax		

Table 12: Results of 15-year analysis in economic evaluation

	Wall insulation	CHP	HRV	PV
NPV	-£ 7,169	£ 8,180	£ 36,388	£ 3,430
IRR	0.27 %	9.08 %	27.87 %	7.62 %
LCOE	5.29 p/ kWh	3.09 p/ kWh	4.81 p/ kWh	8.97 p/ kWh
SPP	17.59 years	6.52 years	3.68 years	9.62 years
B/C ratio	0.73	1.04	2.20	1.21

It has been found that a longer analysis periods allows the assessment to consider more yields, hence it resulted in beneficial outcomes from both wall insulation investments economically feasible as shown in Table 12.

Table 13: Results of expected lifespan analysis in economic evaluation

	Wall insulation	CHP	HRV	PV
Analysis period	30 years	15 years	20 years	25 years
NPV	£ 8,242	£ 8,180	£ 49,785	£ 9,914
IRR	6.30 %	9.08 %	28.49 %	10.45 %
LCOE	3.44 p/kWh	3.09 p/kWh	5.02 p/ kWh	2.66 p/ kWh
SPP	17.59 years	6.52 years	3.68 years	9.62 years
B/C ratio	1.31	1.04	2.45	1.64

5   CONCLUSION

With the UK government ambitions of the 2008 Climate Change Act to reduce its greenhouse emission by 80% at 2050 and the clock click in 5th December, 2015, according to potential of reduce the energy cost approximately 44 million pounds and the CO_2 emission 625,000 tonnes annually by UK school buildings, The Sustainable Energy Project is undertaking in Loughborough Endowed Schools (LES). This paper is based on the case study of the project. Actually, all the fifty-four buildings have been simulating in progress, only three buildings with five energy efficiency measures were presented in this paper. This article briefly introduced the site situation and the exciting issues in energy using firstly. Then five measures and technologies including internal wall insulation, double glazing, combined heat and power, heat recovery ventilation and PV were applied according to three buildings, which are Boarding House, LGS Science Building and Swimming Pool optimum opportunities.

Boarding House was chose for internal wall and double glazing retrofit measures. A wool quilt internal insulation is analysed and it obviously observed that 15.3% gas (27,113kWh) can be saved annually. For double glazing, up to 22.7% gas emission can be saved. These two measures reveals that improve the envelope of traditional buildings are significant effective CHP, another measures using in Boarding House, which operates very frequently and a number of electricity can be exported to other buildings in winter times. As the results presented, CHP is strongly suggested to apply on Boarding House and other building requires high and constant heating. Heat recovery ventilation in swimming pool shows big saving in gas. A total of 165,438kWh gas consumption can be reduced. Issues of poor air distribution, insufficient airflow and over humidity all can be improved. As to 25m² polycrystalline PV is applied on the flat roof in LHS Science Building. Approximately 25.5% (3,479 kWh) annually electricity required by the building can be generated by the system.

The economic evaluation considered the economic evaluation considered the Simple Payback Period (SPP), the Net Present Value (NPV), the Internal Rate of Return (IRR), the Levelised Cost of Energy (LCOE), and the Benefit-to-Cost (B/C) ratio. At the assumptions as mentioned above, the results showed CHP, HRV and PV are financially viable over the 15-year analysis period, whist wall insulation have unideal for the same period. However, conducted for different time which equal to the lifespans of them, it has been found that longer period allows the assessment to consider more yields, hence it resulted in beneficial in wall insulation.

6   REFERENCES

UK GREEN BUILDING COUNCIL, 2011. Carbon reductions in existing non-domestic buildings. UK Green Building Council

BRYAN Gill, Cohen R, Stepan P, 2011. Wider public sector emissions reduction potential research. London

GOVERNMENT, H, 2009. The UK low carbon transition plan: national strategy for climate and energy. Department of Energy and Climate Charge: London

DCSF, 2009. Climate change and schools, a carbon management strategy for the school sector. London

DEPARTMENT FOR EDUCATION AND SKILLS, 2002. Energy and water management: A guide for schools. Nottingham

ENGLISH HERITAGE, 2010. Energy efficiency and historic buildings: Insulating solid walls.

DI, Kolaitis, E, Malliotakis, DA, Kontogeorgos, I Mandilaras, DI Katsourinis, MA Founti, 2013. Comparative assessment of internal and external thermal insulation systems for energy efficient retrofitting of residential buildings. Energy and Buildings, 64, 123-131.

CARBON TRUST, 2012. Schools: learning to improve energy efficiency.

AL-HOMOUD, M.S., 2005. Performance characteristics and practical applications of common building thermal insulation materials. Building and Environment, 40 (3), 353-366.

JABER S, Ajibs, 2011, Thermal and economic windows design for different climate zones. Energy and Buildings. 43, 3208-3215.

FREIRE, R.Z., Mazuroski, W, Abadie, M.O., Mendes, N, 2011. Capacitive effect on the heat transfer through building glazing systems. Applied Energy. 88, 4310-4319.

YANG Z, Liu B, Zhao H, 2004, Energy saving in building construction in china: a review. International Journal of Green Energy. 1, 209–225.

MORTIMER ND, Ashley A, Moody CAC, Rix JHR, Moss SA, 1998. Carbon dioxide savings in the commercial building sector. Energy Policy, 26, 615–624.

CIBSE, 2002. Guide to Building Services in Historic Buildings. London: Chartered Institution of Building. Services Engineers

ASHRAE, 2000. ASHRAE Handbook HVAC Systems and Equipment, ASHRAE Inc., USA.

BRE, 1997. Energy efficiency in swimming pools-for centre managers and operators. Good Practice Guide. 219.

KAMPEL W, Aas B, Bruland A, 2014. Characteristics of energy-efficient swimming facilities-A case study. Energy, In Press.

JOHANSSON L, Westerlund L, 2001. Energy savings in indoor swimming-pools: comparison between different heat-recovery systems. Applied Energy, 70(4), 281-303.

PESTER S, Crick F. Performance of photovoltaic systems on non-domestic buildings. BRE Trust

DECC, 2014. Power to pupils. Solar PV for schools – the benefits.

Low Carbon Living, 2011. Solar PV: The school project.

HWANG JJ, 2013. Transient efficiency measurement of a combined heat and power fuel cell generator. Journal of Power Sources, 223, 325-335.

296: Thermal environment of an atrium enclosed with an ETFE foil cushion envelope

SABRINA AFRIN[1], JOHN CHILTON[2], BENSON LAU[3]

1, 2, 3 University of Nottingham, University Park, NG7 2RD
Sabrina.Afrin@nottingham.ac.uk, 2John.Chiton@nottingham.ac.uk, 3Benson.Lau@nottingham.ac.uk

Ethylene-tetrafluoroethylene (ETFE) foil is most commonly employed in buildings as a replacement for glazing to enclose transitional spaces, for example atria and circulation areas, although, increasingly, it is used as a secondary or primary façade for more intensively occupied architectural spaces where thermal comfort needs to be more precisely controlled. Despite the different thermal/optical properties, thickness and form in use of this material when compared to glass, there has been only limited investigation of the influence of these characteristics on the dynamic thermal responsiveness of the envelope and its impact on the thermal environment of the enclosure.

This paper presents results of an ongoing investigation into the thermal environment of an approximately 625m2 atrium enclosed by a two-layer ETFE-foil cushion roof recorded by onsite monitoring conducted from April 2014 to April 2015. In order to examine the thermal environment of the atrium during different seasonal conditions, continuous field measurements of indoor thermal environmental parameters were recorded under varying external climatic conditions at different vertical levels and horizontal positions in the atrium with and without operation of the HVAC system and with variable occupancy. The effects of solar transmission, outdoor air temperatures, surface temperatures of the ETFE cushion on internal air temperatures and mean radiant temperatures at different levels of the atrium are compared and discussed

Keywords: ETFE foil cushion, thermal environment, thermal performance, temperature stratification, cushion envelope.

1. INTRODUCTION

Ethylene-tetra-fluoro-ethylene (ETFE) is a synthetic fluoropolymer. Although patented by DuPont in 1940, it was not used commercially until the 1970s. ETFE foil is very resistant to environmental influence where the material is exposed to a diverse range of aggressive actions e.g. UV radiation, acids, alkalis etc. and it exhibits excellent long-term resistance to soiling [5]. Its application reduces embodied energy of the construction, increases transparency of the building envelope, reduces overall weight of the building; it is also 100% recyclable [1, 2]. These attributes have increased ETFE foil's use in architectural applications [4] such that the material is now employed most frequently in building for enclosing components where high translucency, low structural weight and complex shape is desirable.

The impact of façade materials on the built environment is currently one of the major considerations for designers. This awareness is due to the effect of energy consumption/CO_2 production on global climate change. Therefore, as with other building materials, ETFE foils have become a subject of critical consideration, as they are increasingly installed across different continents [6]. By exploiting the high transparency of ETFE foil it is possible to save energy use in buildings but at the same time it can adversely impact the building's internal environment by affecting thermal comfort. It is evident that the thermal environment of ETFE foil enclosures is, as yet, relatively unexplored. Thus, it is valid to examine its thermal performance so that it can compete with other transparent building materials available for building application. A discussion of the earlier results can be found in [3] and [7]. Mainly thermal data collected in the critical summer 2014 and winter 2014 situations is highlighted and analysed here.

2 FIELD MEASUREMENT

The Nottingham High School was built in 1860. The school building is three storeys high. It had a central courtyard used as parking space. This courtyard was modified and renovated during 2009 to form a three storey atrium. This atrium contains dining hall, cafeteria and study space at ground floor, first floor and second floor respectively. The renovated atrium roof consists of 25 double layer ETFE foil cushions covered with a rain suppression mesh, Figure 1. Each cushion consists of a top fritted layer and bottom clear layer both of 200μm complete with aluminium framing, inflation unit and air handling pipe work. All of these systems are supported by steel trusses and columns.

When required, the atrium central heating system operates from 08.00 to 18.00, Monday to Friday, and consists of fan coil units, fan convectors and underfloor heating system. Natural ventilation operates through high windows located on the west side only along with dampers located on top of the entrance doors at the ground floor (located on north and south).

To understand thermal behaviour of ETFE foil cushions and its impact on the internal thermal environment continuous field monitoring of this double-layer ETFE foil cushion covered 625m^2 atrium has been carried out since December 2013. Results obtained under two different sky conditions and its impact on the internal thermal environment during the months of May to July 2014 and November 2014 to January 2015 are presented here.

Table 85: Measurement sensors

Measurement type	Sensor type
Air temperature and foil surface temperature	ϕ0.1 mm K-type thermocouple connected to dataTaker DT 85 or dataTaker DT 80 data logger
Total horizontal solar radiation (internal & external)	Kipp & Zonen CMP3 Pyranometer (spectral range: 0.3-2.8μm)

Table 2: Location of temperature and solar radiation sensors

Sensor ID	Location
TSi 1_NH_Month	Ground floor (occupied level)
TSi 2_NH_ Month	First floor (occupied level)
TSi 3_NH_ Month	Second floor (occupied level)
TSi 4(a)_NH_ Month	Internal Temperature adjacent to ETFE cushion 1
TSi 4(b)_NH_ Month	Internal Temperature adjacent to ETFE cushion 1
OPTSi_NH	Operative temperature of second floor
Ts Loc 1	External foil surface temperature of cushion 1
Ts Loc 4	Internal foil surface temperature of cushion 1
Ts Loc 7	Internal foil surface temperature of cushion 2
OAT_NH_Month	External ambient temperature
ExIR	Incident solar radiation
InIR	Transmitted solar radiation

Weather data was collected from a station located on an adjacent roof. External and internal monitoring was performed using a set of temperature and solar radiation sensors, as listed in Table1, connected to dataTaker DT85 and dataTaker DT80 data loggers. The screened thermocouples continuously recorded diurnal variations of cushion surface temperature and air temperature at various levels in the atrium, at 1 minute intervals, from November 2013 onwards. For analysis, data recorded at 5 minute intervals were extracted. Mean Radiant temperature was measured by a thermocouple placed inside a black globe. Despite the low adherence characteristics of ETFE foil, it was found possible to tape thermocouples to the ETFE cushion surface for the duration of the monitoring. To validate the accuracy of the surface temperature measurements thermal imaging was also used.

The in situ method was used to monitor indoor and outdoor thermal environmental parameters. It includes outdoor ambient temperature, mean radiant temperature and air temperatures at different vertical and horizontal levels in the atrium, internal and external humidity, internal and external incident solar radiation, external surface temperature of an ETFE cushion and internal surface temperature of two different cushions. The recorded data represents the thermal behaviour of an ETFE foil cushion and space enclosed by it under different sky conditions e.g. overcast and sunny conditions, day and night, with and without operation of the HVAC system.
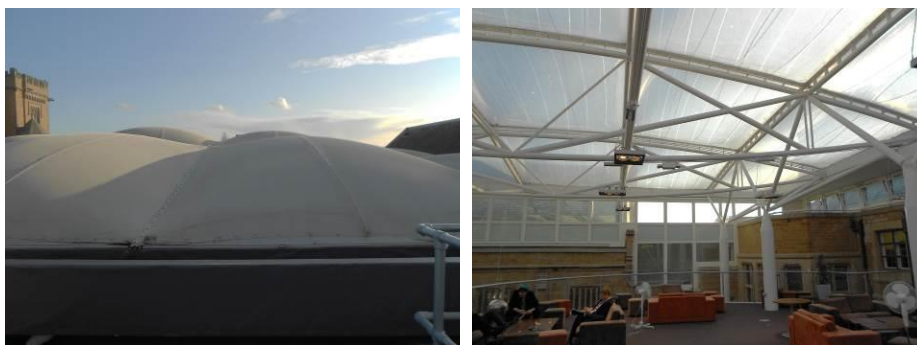

Figure 1: ETFE foil cushion roof External (left), Internal (right)

3   RESULTS AND DISCUSSION

Results obtained from May 2014 to July 2014 and November 2014 to January 2015 are assessed to evaluate thermal behaviour of the school atrium and ETFE foil cushion roof. Analysis of the thermal behaviour of the atrium during summer and winter was carried through the analysis of indoor air temperature and incident solar radiation whereas thermal behaviour of the ETFE-foil cushion envelope is evaluated through the analysis of its surface temperature.

3.1 Variation of internal air temperature

Figure 2 presents internal and external air temperatures and transmitted total solar radiation on 24th July 2014 and 19th December 2014. Indoor temperatures of each occupied floor are measured along the same

vertical line. Hourly and daily profiles of the measured thermal parameters were assessed to quantify their variability. The fourth week of July 2014 was the hottest of the year recorded. The highest air temperature was observed on 24th July 2014. Table 2 presents maximum, minimum and average air temperature and standard deviation of temperature at each occupied level for the selected dates in July and December. Standard deviation of each occupied level showed that air temperature of occupied level 3 (TSi3_NH) varies significantly in summer whereas in winter temperature of each occupied level is stable.

Table 2: Maximum, minimum, average and standard deviation (SD) air temperatures recorded in school atrium, 24th July 2014, 19th December 2014

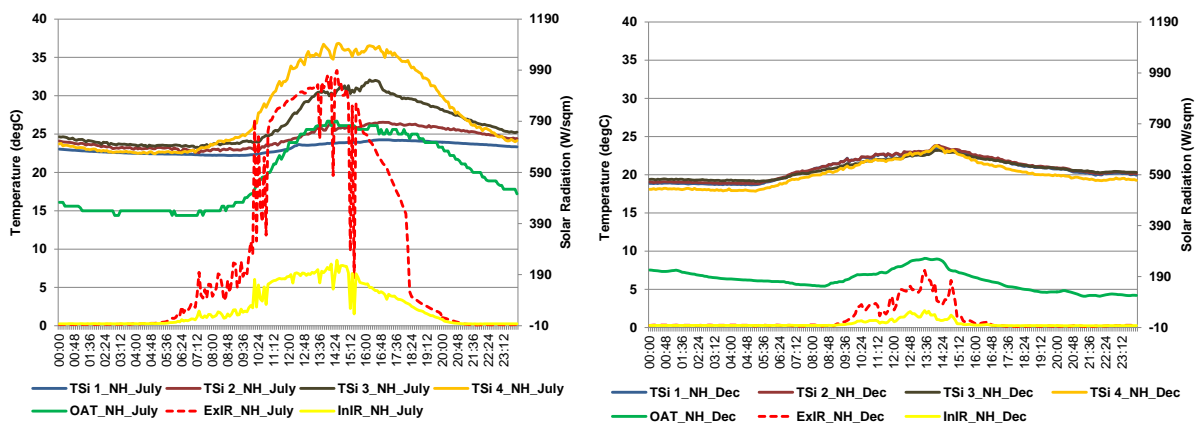| Location	TSi 1_NH_July	TSi 2_NH_July	TSi 3_NH_July	TSi 1_NH_Dec	TSi 2_NH_ Dec	TSi 3_NH_ Dec
Maximum	24.3 °C	26.7 °C	32.1	23.6	23.8	23.2
Minimum	22.2 °C	22.56	23.2	18.7	18.8	19.12
Average	23.2 °C	24.4	26.4	20.8	20.9	20.8
SD	0.71	1.3	2.83	1.5	1.5	1.2

Figure 2: Thermal stratification demonstrated by air temperatures at different levels averaged over 24th July 2014 (left) and 19th December 2014 (right) respectively. Cushion surface temperatures are also shown.
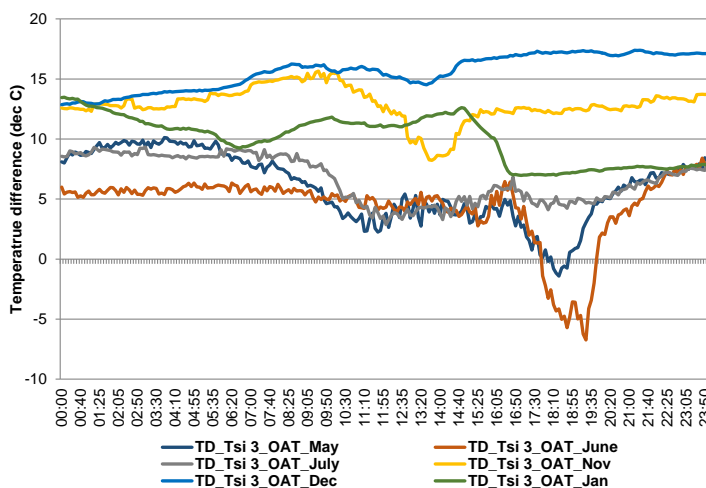

Figure 3: Difference between second floor air temperature (peak temperature recorded) and external ambient temperature on 19th May, 18th June, 24th July, 4th November and 15th December 2014 and 9th January 2015.

Figure 2 illustrates the vertical stratification recorded on two selected dates during the months of July and December 2014. During July incident radiation transmitted through the translucent ETFE foil cushion affects significantly the air temperature of the atrium, predominantly in the space immediately adjacent to the ETFE foil cushion roof. Maximum air temperature recorded was 32.1°C at the second floor occupied level (TSi 3_NH) which was 6 °C higher than external ambient temperature and 8 °C higher than that at the ground

floor (TSi 1_NH). Maximum deviation of external ambient temperature from that measured at ground floor and first floor was 3 °C and 1.3 °C respectively during the afternoon. At the second floor the air temperature stayed between 28°C and 32 °C from noon till evening. On average, air temperature at this level was 6.7°C higher than the external ambient temperature which compares with the equivalent 4.7°C at first floor and 3.5°C at ground floor. It is also noticeable from Figure 4 that during July for around 10% of the time temperature at this level was between 26°C to 28°C and for approximately 2% it was above 30°C. For 50% of the time the air temperature at ground floor level was between 22°C to 23°C while air temperature at first floor varied between 22°C and 26°C for 86% of the time. In December the maximum temperature recorded was 23.8°C at the first floor which was 15.9°C warmer than the external ambient temperature. Temperature difference between the occupied levels stayed between +/-0.6 °C clearly demonstrating that the temperature stratification is not as strong as that observed during July. Due to operation of the HVAC system in winter, air temperature of occupied levels was mostly stable during occupied hours. This is also noticeable from Figure 4 that where for the month of was predominantly between 18°C to 22°C.. Whereas air temperature adjacent to ETFE foil cushion remained lower in the absence of solar radiation than that of occupied levels during winter, also in summer but the extent of increase of air temperature of that level is significant in summer especially during the presence of high solar radiation and external ambient air temperature

Figure 3 illustrates the difference between second floor air temperature (peak temperature recorded) and external ambient temperature on 19th May, 18th June, 24th July, 4th November and 15th December 2014, and 9th January 2015. The difference between the second floor indoor air temperature and outdoor ambient temperatures showed more variability during summer months than in winter. This diurnal variability reflected largely the fluctuation of external ambient temperature. The internal air temperature was relatively constant during winter. Significant variation of temperature was observed during the months of May and June in the evening, when external ambient temperature went up 6.5°C (in June) compared to that of second floor air temperature. The impact of this variation was found on measured surface temperature of the ETFE foil cushion which is discussed in section 3.2.
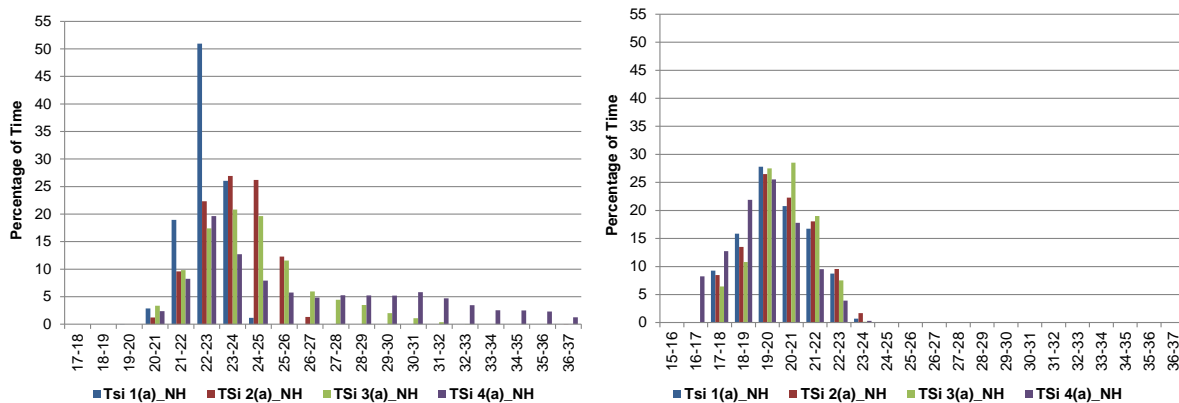

Figure 4: Percentage time spent within each 1°C temperature band for each occupied level in July 2014 (left), December 2014 (right)

It can also be seen from Figure 4 that the air temperature adjacent to the internal cushion surface at occupied level 3 was between 28°C and 37°C for approximately 30% of the time in July, mainly during occupied hours. This range of air temperature has an adverse impact on thermal comfort of the occupants. To assess this impact, operative temperature of level 3 was calculated using measured mean radiant temperature. Operative temperature combines air and mean radiant temperatures in a single index.

$$T_{op} \approx (T_r + T_a)/2$$

– Where, T_{op} = Operative temperature
– T_a = Air temperature
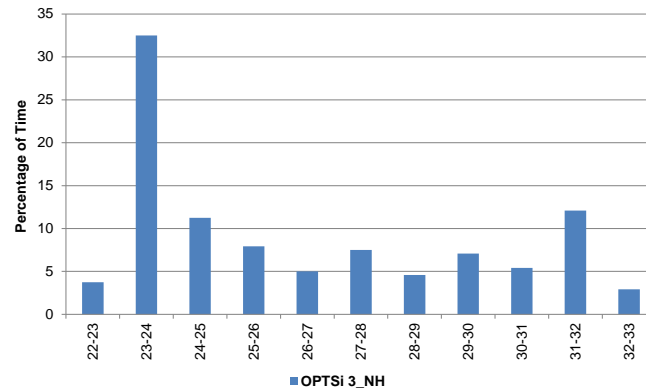– T_r = Mean radiant temperature

Figure 5: Percentage duration for different operative temperatures at second floor occupied level on 24th July 2014

Figure 5 presents the percentage of time of different operative temperature range at the second floor occupied level. From this it can be stated that, although for above 30% of the day operative temperature was within 23-24°C, for 12% of the time operative temperature was between 31-32 °C. , which coincided with the time the space was mainly occupied. Therefore 44.6% time operative temperature was outside the comfort zone (18°C-26°C).

3.2 Thermal behaviour of ETFE foil cushion

The dynamic thermal responsiveness of ETFE foil cushions under variation of external weather conditions was assessed from the variation of internal and external surface temperature. Figure 6 presents the internal air temperature adjacent to the bottom of the cushion (TSi 4(a)_NH, TSi 4(b)_NH), external (Ts Loc 1) and internal (Ts Loc 4 (cushion 1), Ts Loc 7 (cushion 2)) foil surface temperature, external ambient temperature (OAT), incident and transmitted total solar radiation during the 18th June 2014. Figure 7 shows external and internal foil temperatures relative to external ambient temperature (TD_Ts Loc 1_OAT and TD_Ts Loc 4_OAT respectively), temperature difference between internal surface and external foil surface (TD_ Ts Loc 4_ Ts Loc 1), internal foil surface temperature relative to the adjacent air temperature (TD_Ts Loc 4_TSi 4(a)_NH) and temperature difference of internal foil surface and average of external temperature and air temperature adjacent to the cushion (TD_Ts Loc 4_Avg Tsi 4(a)_NH).

During the night the external foil surface temperature stayed below external ambient air temperature due to longwave radiation exchange to the cold sky while the internal foil surface stayed on average 2°C higher than external ambient temperature due to the impact of the higher internal air temperature adjacent to the cushion (TSi 4 (a)_NH) and the insulation provided by the air layer in between foil surfaces. During that time the minimum temperature of external and internal foil surfaces was observed to be 14.5°C and 17.6°C respectively, when the external ambient temperature was 16.5°C.

Significant temperature difference between external and internal foil surface was found to be 5.22°C in the early evening, with the external surface temperature hotter than the internal, due to the influence of the high external ambient temperature (33.5°C) and diffuse solar radiation. During the night the external foil cooled, due to the drop in external ambient temperature and the exchange of long wave radiation at the surface, while the internal surface temperature remained up to 4°C warmer than the external surface. The maximum recorded external surface temperature was 45.3°C when the internal surface temperature was 39.2°C (at noon) and the maximum internal surface temperature was 42.7°C when external surface temperature was 40.83°C (in the afternoon).

Rapid change in internal and external foil surface temperature was observed as an impact of fluctuations in incident solar radiation and the minimal thickness of the foil. This phenomenon was very evident when a sudden decrease of incident radiation from 1090.17 W/m^2 to 236.06 W/m^2 caused a decrease of external surface temperature from 42.31°C to 28.34°C. Subsequently, the surface temperature rose rapidly over the next five minutes to 43.35°C as the incident solar radiation increased to 1098.54 W/m^2. Nevertheless, variations in incident solar radiation cause the cushion external surface temperature to vary more rapidly than that of the internal surface. For instance, a rise of 6 to 14°C was observed within one 5-minute interval whereas for the internal surface the temperature fluctuation was 1 to 4 °C. Because of radiation exchange

towards the clear sky at night external surface temperature remained 1 to 2°C below external ambient temperature whilst the internal surface, was 1.5 to 5°C cooler than the adjacent atrium air. Also, the position of sun with respect to the cushion was found to affect cushion surface temperature. The temperature difference between the internal surface of cushion 1 and cushion 2 was not significant during the night. However, from late morning till late afternoon, the internal surface of cushion 2 was on average 1.56°C warmer than that of cushion 1, with a maximum recorded temperature difference of 3.7°C.
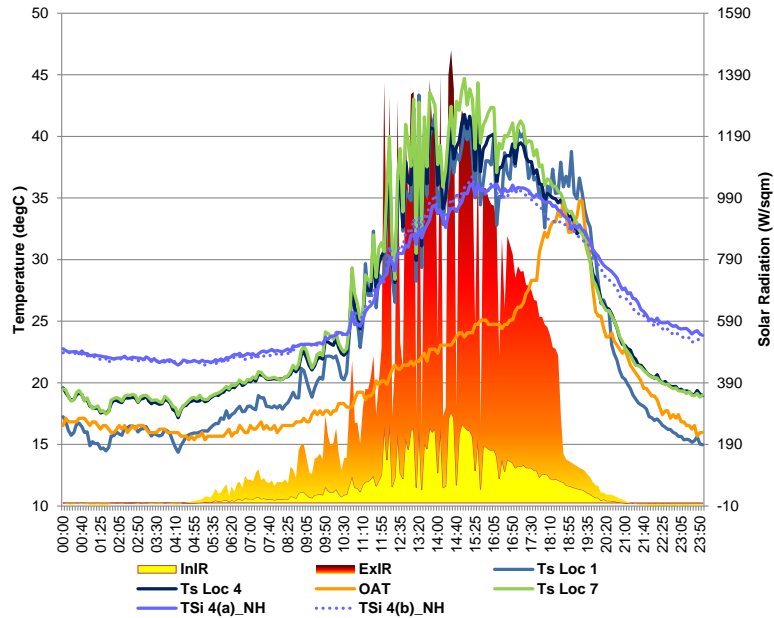

Figure 6: Variation of ETFE foil cushion internal and external surface condition on 18th June 2014
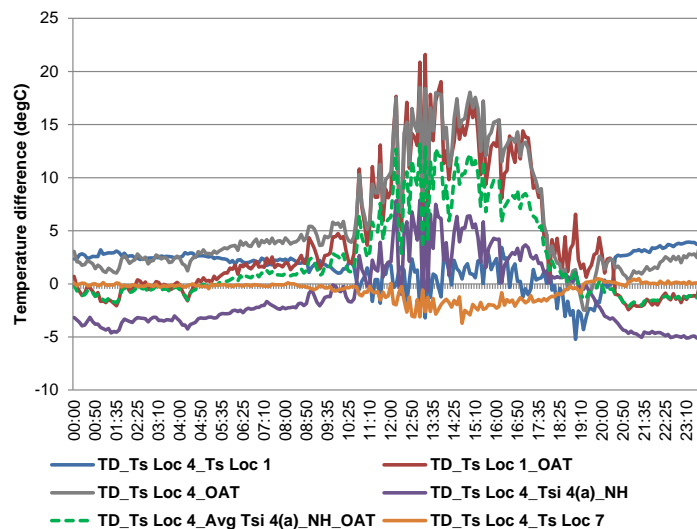

Figure 7: Surface temperatures with respect to external ambient (OAT) and TSi 4(a)_NH on 18th June 2014

4   CONCLUSIONS

The extent of vertical stratification recorded during the summer months seemed directly related to ETFE foil surface temperature, itself governed by the clearness of the sky and correspondingly by the amount of solar radiation incident on and transmitted through the surface. During the winter months, as a result of low solar gain into the enclosures the vertical temperature stratification was rather weak throughout the day and night with an almost uniform air temperature within the occupied spaces this is due to the effect of HVAC system.

During the summer the air temperature and mean radiant temperature went up higher, thus 12% of time of the day (24th July) operative temperature stayed between 31-32 °C which is occupied hour for the school, adversely impacting thermal comfort of the user. The atrium ventilation system includes blower and automatic windows (west part operable only), but high temperature range during occupied hour suggests that these systems are not sufficient to keep the internal thermal environment comfortable for the occupants. Therefore without sufficient ventilation, this type of innovative envelope system may cause thermal discomfort during the summer time.

It is evident from the study that solar radiation (direct and diffuse), external ambient temperature and longwave radiation are the main three environmental parameter that effect continuously surface temperature of ETFE foil cushion by the process of radiative and convective heat transfer. In summer external and internal foil surface temperatures ranged from 14°C to 45°C and 18°C to 43°C respectively. Due to insulation properties of air layer between the foil surfaces, the internal foil surface temperature was generally different from that of the external surface; the maximum temperature difference observed was 5.22°C (18th June) when external surface temperature was higher than internal surface but later on the same day at night internal surface temperature increase and raised up to 4.04°C higher than that of external surface. On 24th July maximum internal surface temperature (40.6°C) was observed at about 16.00, which along with the transmitted radiation induced a rise in air temperature in the occupied level below ETFE foil cushion. As a consequence, the maximum temperature (32.1°C) of the occupied level occurred at about 16.15, which was 5.96°C warmer than external ambient temperature and 7.96°C warmer than air temperature at ground floor occupied level. On the same day temperature range of ground floor, first floor and second floor occupied level was 22.2°C to 24.3°C, 22.6°C to 26.7°C and 23.2°C to 32.1°C respectively.

5   REFERENCES

[1] MONTICELLI C, Campioli A and Zanelli A. (2009). Environmental load of ETFE cushions and future ways for their self-sufficient performances, In Evolution and Trends in Design, Analysis and Construction of Shell and Spatial Structures, Proceedings of the International Association for Shell and Spatial Structures (IASS) Symposium 2009 (Domingo A and Lazaro C (eds)). Universidad Politécnica de Valencia, Spain, pp. 754–766.

[2] CHILTON J, Pezeshkzadeh SA and Afrin S. (2013). Embodied energy in ETFE foil construction, In [RE]THINKING lightweight structures. Proceedings of TensiNet Symposium 2013, Istanbul, Turkey (Bögner-Balz H, Mollaert M and Pusat E (eds)). TensiNet, Brussels, Belgium, pp. 457–466.

[3] AFRIN S, Chilton J and Lau B. (2014). Thermal Environment of an atrium enclosed by an ethylene-tetrafluoro-ethylene (ETFE) foil roof, In Shells, Membranes and Spatial Structures Footprints, Proceedings of the International Association for Shell and Spatial Structures (IASS)-SLTE Symposium 2014 (Reyolando M.L.R.F. and Ruy M.O. (eds.)). Brasilia, Brazil.

[4] CHILTON J. 2013. Lightweight envelopes: ethylene tetra-fluoro-ethylene foil in architecture. Proceedings of the ICE - Construction Materials. 2013;166(6):343 –357.

[5] LECUYER A., ETFE Technology and Design, Germany: Birkhauser, 2008.

[6] GÓMEZ-GONZÁLEZ A., Neila J., and Monjo J. (2011). Pneumatic Skins in Architecture. Sustainable Trends In Low Positive Pressure Inflatable Systems, Procedia Engineering, vol. 21, pp. 125-132.

[7] AFRIN S, Chilton J and Lau B. (forthcoming 2015). Evaluation and Comparison of Thermal Environment of Atria Enclosed with ETFE Foil Cushion Envelope, In 6th International Building Physics Conference, IBPC 2015, Energy Procedia.

476: Integrated smart indoor – outdoor web based energy management system for university campuses

Kostas Gombakis[1], Christina Georgatou[1], Dionysia Kolokotsa[1], Sotiris Papantoniou[1], Nikolaos Kampelis[1], Kostantinos Kalaitzakis[2] Mattheos Santamouris[3], Konstantina Vasilakopoulou[3]

1 Technical University of Crete, School of Environmental Engineering, Crete, Greece
2 Technical University of Crete, School of Electronic and computer engineering, Crete, Greece
3 National Kapodistrian University of Athens, Physics Department, Athens, Greece

University campuses can be considered as small towns due to their size, number of users and mixed and complex activities, including numerous actions usually met in urban environments. In the framework of Camp IT project, existing Information & Communication Technology (ICT) is exploited in order to create a micro-grid by integrating sensors, actuators, control algorithms etc, aiming at minimizing energy consumption of buildings and activities within Campuses. The single building is considered part of a "district" approach, where real time interaction of indoor and outdoor spaces is monitored and controlled. The overall aim of the project is to contribute to a future smart grid community by the deploying and testing of a decision support tool and optimization method for a web based energy management system in real time conditions, taking into account indoor / outdoor environmental parameters and user preferences.

The aim of the present paper is to analyze the methodology that has been followed, including techniques of building modelling incorporating outdoor spaces, the use of neural networks for the prediction of environmental parameters and energy load as well as the development of control algorithms, in order to create new frontiers for research and development in energy management of university campuses.

Keywords: University campus, energy management, energy savings, control algorithms, user comfort

1. INTRODUCTION

University campuses can be considered as small towns due to their size, number of users and mixed and complex activities, including numerous actions, usually met in urban environments. Energy wastage in various space types, such as teaching auditoriums, working areas (offices, laboratories, computer rooms, etc) or residential buildings (dormitories) can be encountered. Furthermore, overheating phenomena, by human energy release and solar radiation absorption from dark surfaces and buildings, are possible, thus creating an urban – kind climate in campuses. The energy and environmental impact of universities could be considerably reduced by applying organizational, technological and energy optimization measures. To design and operate a sustainable campus, it is necessary to holistically and strategically integrate the indoor – outdoor environment parameters and information into the planning and operational process.

Since the post-modern era, when scientists and designers realized the disadvantages of the continuously growing artificial environment, the improvement of the outdoor environment has gained a substantial attention. Open urban spaces can contribute to the quality of life within cities, or contrarily, enhance isolation and social exclusion. The major factor that determines the quality of the open urban spaces is the climate conditions that occur in the micro scale environment. The strategies to improve urban environment include the use of smart materials, the increase of vegetation, ventilation, shading and evaporation.

On the other hand, Information & Communication Technology (ICT) for energy management has evolved considerably during the last decades. Advances in the design, operation optimization, and control of energy-influencing building elements and systems (e.g., HVAC, solar, fuel cells, CHP, shading, natural ventilation, etc) unleashed the potential for achieving significant energy savings and efficiencies in the operation of both new and existing building sites worldwide.

Last but not least, nowadays, it is vital that Europe's electricity networks are able to integrate all low carbon generation technologies as well as to encourage the demand side to play an active part in the supply chain. In this part, ICT technology plays a vital role. Currently the issue of Energy Management for large sites, such as University Campuses, is addressed by the Energy Information Systems (EIS) which have evolved out of the electric utility industry in order to manage time-series electric consumption data. However, other energy management technologies have also expanded their functionalities, and have partly come to merge with EIS technology. Since EIS products are relatively new technologies, they are changing quickly as the market unfolds (Motegi et al, 2003).

Based on the above analysis, there is considerable room for improvement and research potential in energy management, when leaving from a single building and moving towards a "district" approach where different buildings and outdoor spaces are considered. Towards this "district approach" the use of University Campuses, as a field of application, is considerably advantageous compared to a community or city district as the overall area belongs to a single owner.

CAMP-IT project's aim was to develop, test and validate an integrated and holistic indoor - outdoor Web based Energy management System for University campuses. This major objective is pursued within CAMP-IT via a number of multifaceted actions and S&T Objectives: (a) Advance the state of the art in modelling of buildings and outdoor spaces by creating a modelling procedure and a holistic methodology. In addition a simplification process was developed to provide "district models" as accurate as possible. (b) Advance the state of the art in expert systems and control algorithms for energy load prediction and shaping in small communities by developing an efficient, robust and rapidly-adapting real-time expert system capable of providing optimal – or nearly optimal – demand balance, while maintaining users' safety and health and, most importantly, complying with end-users comfort-related commands and requests. (c) Advance the state-of-the-art in user-interaction, sensing and interfacing by either employing wireless technologies or using the existing IP infrastructure and connectivity of campuses to ensure interoperability, expandability, flexibility and easiness of installation. (d) Integrate the above-mentioned systems and designs in order to come up with a fully functional system capable of providing efficient, robust, safe and user-acceptable conditions on Campus level. (e) Application and validation of the developed system in TUC Campus during its ordinary operation.

This paper includes a short description of all the above processes. The buildings selected from the campus of the technical University of Crete and their exterior space was modelled, neural networks were developed for the prediction of the environmental parameters affecting the energy consumption and the control algorithms have been developed and assessed. Currently, the real energy savings due to the use of these control algorithms are measured, with the help of advanced sensing and recording equipment, installed in the buildings under study.

2   DEVELOPMENT AND VALIDATION OF INDOOR AND OUTDOOR THERMAL MODELS

In order to implement the Camp IT power management system, two buildings in the campus of the University of Crete in Chania were selected and modelled.

2.1 Description of the Buildings and Exterior Space under Study

Chania is a city on the eastern part of the island of Crete, the southernmost region of Greece. The climate in Chania is primarily Mediterranean, with mild winters and hot summers. The University Campus is located approximately 6 km northeast of the city centre of Chania, 137 m above sea level. The campus area, where five University departments, administrative buildings and student dormitories are located, has a total area of 2,900 m^2. The buildings (K1 & K2) selected for the CAMP-IT project, house the Environmental Engineering Department facilities and services and comprise both of the same type of materials and systems.

Table 86 summarizes the main characteristics of the selected buildings.

Table 86: Characteristics of the modelled spaces

Characteristics of building K1	
General Dimensions (m)	(Length/ Width/ Height): 86.40 / 15.20 / 12.00
Number of Floors	3
Facilities on Ground floor	14 laboratories, 3 offices, 2 mechanical rooms, elevators, stairs, WC
Facilities on 1st floor	17 offices, 1 meeting room, 2 mechanical rooms, elevators, stairs, WC
Facilities on 2nd floor	Laboratories & mechanical rooms
Characteristics of building K2	
General Dimensions (m)	(Length/ Width/ Height): 48.00 / 15.20 / 11.00
Number of Floors	3
Facilities on Ground floor	5 computer rooms, 1 printer room, 1 office, 1 mechanical room, elevators, stairs, WC
Facilities on 1st floor	3 laboratories, 14 offices, elevators, stairs, WC
Facilities on 2nd floor	Mechanical rooms
Characteristics of exterior spaces	
Exterior spaces	Soil, marble, stone, tiles (cotto), plants, trees

Building K1 is located at the northern end of the campus with its main façade facing north-west. The distance between K1 and K2 is approximately 16.20 m, with building K2 being to the south of K1. Each floor of K1 is separated in two wings, connected with an atrium. The structural materials of K1 and K2 are described in Table 87.

Table 87: Structural materials of buildings K1 and K2

Structural materials of K1 & K2	
Exterior walls a) Double plasterboard (width:18mm each) b) Insulation: 5 cm rockwool, d= 80kg/m^3 c) Cement board: 12 mm	**Ground and first floors ceilings** a) Uncoated concrete: 2 cm b) Insulation: 5 cm rockwool, d=80kg/m^3 c) Ceramic tiles: 10 mm
Second floor ceilings a) Uncoated concrete: 2 cm b) Insulation: 10 cm c) Asphalt membrane: 10 mm	**Windows (104 windows in K1 & 68 windows in K2)** a) Double pane windows b) Aluminium frames c) Exterior lamellas
Floor top coating a) Ceramic tiles: 10 mm (in all spaces) b) Industrial flooring: 20 mm (Chemistry lab)	

Picture 1**Error! Reference source not found.** shows the buildings under study and the exterior spaces around them.

Picture 1: North-west façade of building K1. Building K2 is seen on the left, behind K1.

2.2 Modelling of Exterior Spaces

The expansion of the towns and cities borders, as well as the development of new constructions and residential or commercial areas, cause significant changes on the distribution and nature of the materials that cover the ground. Artificial surfaces of urbanized areas tend to generate large amounts of heat and modify the microclimate and air quality (Rassia & Pardalos, 2014). The simulation of outdoor environmental conditions enables the design of urban areas that have the minimum environmental and energy impact on the surrounding constructions. Moreover, this type of simulations may have effect on the energy management of the neighbouring buildings. Exterior environmental conditions can be predicted by complex microscale or mesoscale computer models (CFD, OpenFoam, MIST, ENVIMET, WW5, etc.). For the simulations of the conditions in the exterior area between the buildings of the Technical University of Crete, the three-dimensional microclimate model ENVI-met was used (Bruse 2004). The materials and the sizes of the buildings, the exterior surfaces and the trees/plants were as accurately reproduced as possible. The weather parameters that were used as input (air temperature and relative humidity) were acquired by the University's weather station and the parameters that were simulated, are:

- Surface temperature (^{o}C),
- Air temperature at a height of 1.80m above ground level (^{o}C),
- Wind velocity (m/s).

The outdoor model has been linked with the indoor energy model described below, in order to improve the accuracy of the indoor energy management system.

2.3 Building Modelling

The ESP-r energy modelling tool was selected for simulating the conditions inside the University buildings. Esp-r can simulate complicated elements of the building envelope and any electrical/ mechanical equipment available (Hand, 2011). The various computational subroutines of the particular software exchange information (interaction between the parameters of the various thermal zones) in order to accurately calculate the interactions between the systems of the building. One of the most important characteristics of ESP-r is that it co-operates with other simulation tools to provide a wider range of very accurate results. Moreover, ESP-r was selected for the specific study as it can model all the electric devices and the systems producing and storing energy from renewable energy sources, it has a very wide range of control algorithms for the various systems, including fuzzy logic algorithms, it uses airflow networks which enable the calculation of the movement of air masses inside or outside buildings, etc.

The parameters that were simulated and validated, based on the respective measurements, were the air temperature and the internal gains due to the use of lighting and other appliances.

The developed model was validated by comparing the simulation results with the respective thermal and energy measurements. The model was adapted to provide results of adequate accuracy.

3 DEVELOPMENT OF PREDICTION MODELS FOR THE ENERGY LOAD AND EXTERIOR CONDITIONS

Neural networks were used for the prediction of the energy loads of buildings K1 and K2 and for the prediction of the exterior environmental parameters affecting the energy consumption and user comfort.

The input parameters for the neural network predicting the energy load of the buildings were the exterior temperature, measured by a weather station positioned opposite to the studied buildings, the day of the week and minutes of the day. Also, the energy demand, recorded every five minutes, by smart meters was used. The training of the neural network was repeated every day, after receiving the weather data and using it as new input. The comparison of the predicted energy load with the load measured by the smart meters, shows that the neural networks predict the load with acceptable accuracy (Figure 164).

Accordingly, the parameters used as inputs for the network predicting the exterior temperature for the 24 hours following a specific moment were the exterior temperature, the total horizontal radiation, relative humidity, wind speed and direction and the time of day. The weather data also come from the weather station positioned opposite to the studied buildings.

The values predicted by the developed neural networks have been compared to the actual recordings of a local weather station. The results of this comparison were satisfactory, even though the networks are continuously being trained with new input parameters (
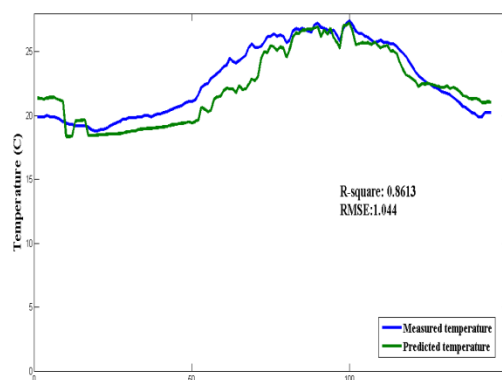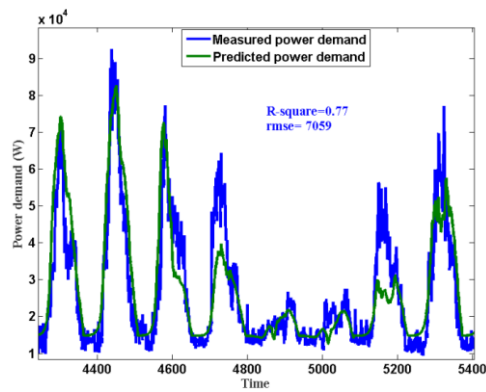

Figure 165).

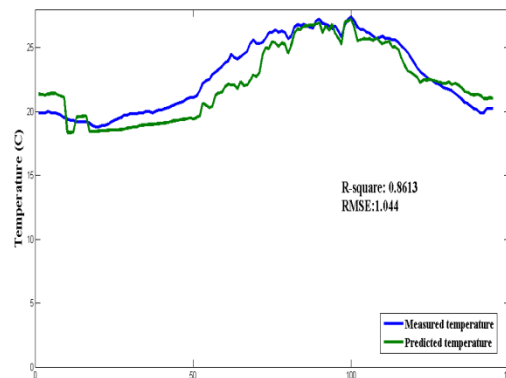*Figure 164. (left) Comparison of the Measured (blue line) and the Predicted power demand (green line).*

Figure 165. (right) Comparison of the Measured (blue line) and the Predicted exterior temperature (green line).

4   DEVELOPMENT OF CONTROL ALGORITHMS

After the development of the indoor and outdoor thermal models and their validation, control algorithms for the indoor air quality, thermal comfort and lighting levels were developed. The development of these algorithms was made in Matlab, since it provides the appropriate libraries and graphical representation of the controls behaviour. Also the control algorithms can be exported in various different programming languages, so that they can be incorporated in systems incompatible to Matlab's programming environment (Kolokotsa et al. 2009; Papantoniou et al. 2014).

The developed control algorithms were based on fuzzy logic. The algorithm for the control of the lighting can dim or turn on/off the luminaires, depending on the available daylight and the desired lighting levels. The algorithm for the indoor air quality controls the mechanical ventilation system. The algorithm for the thermal comfort uses the PMV index parameters (temperature, humidity, radiation, air velocity, metabolic rate, clothing), in order to change the thermostat regulation or increase/decrease the flow of fresh air through the ventilation system. The control algorithms run online on field controllers which continuously monitor the indoor conditions using the installed sensors.

The performance of the control algorithms in reducing the energy consumption and in providing comfortable indoor conditions has been theoretically assessed, by linking the control algorithms with the simulation models for the interior and exterior environment, then by specifying the input and output variables and finally, by running the algorithms and the simulation models at the same time. This process leads to the conclusion whether the algorithms work properly and how much energy is saved.

The control algorithms in Matlab environment exchange data in real-time with the thermal model, through the Building Control Virtual Test Bed (BCVTB) software.

The algorithm controlling the illuminance levels in the interior spaces, should keep the lighting levels stable at 500 lux from 8:00 until 18:00, regardless the exterior illuminance, while the lighting levels should be 0 during the rest of the day. The following graphs show that the algorithm can keep the desired illuminance level stable, by choosing which luminaires will be turned on. The energy saved by the use of the control algorithm was calculated by comparing the initial energy consumption and the energy consumption after the regulation of the artificial lighting with the use of the control algorithm. The initial energy consumption for lighting was 31.5 kWh/m², while the energy saved is 6.9 kW/m² per year, which is translated into 22% reduction.
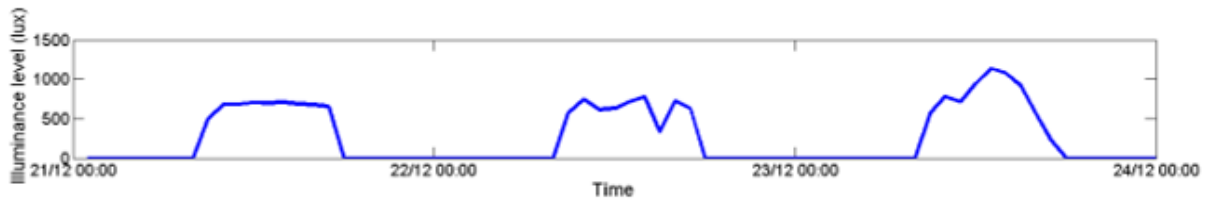

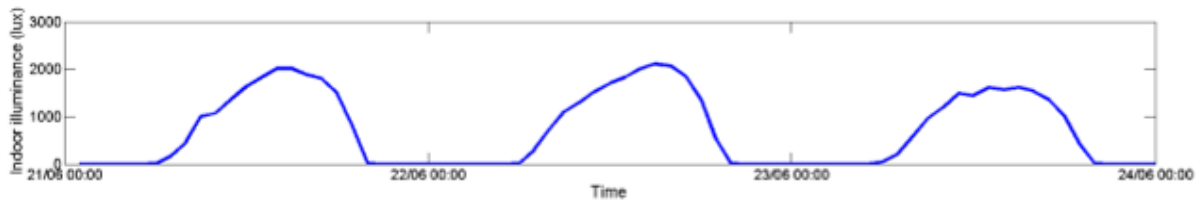*Figure 166: Interior illuminance levels from the 21st until the 23rd of December*

Figure 167: Interior illuminance levels from the 21st until the 23rd of June

Concerning the system for the control of thermal comfort and air quality, the minimum requirements have to be met even in extreme cases. During winter, the thermostat is set at 20°C, from 8:00 until 16:00, while during the rest of the day the heating is off. During summer, the thermostat is set at 26°C from 8:00 until 16:00, and the heating system is turned off for the rest of the day. The desired air quality is 800ppm of CO_2 at maximum, during the whole year.

The results from monitoring the control algorithm's behaviour show that the PMV index is improved both during summer and during winter and has an average value close to 0. However, during the winter, in order for the PMV index to be 0, the consumption has to be significantly increased, by 2.63MWh (43.32%) (Figure 168, Figure 169). During the summer period, the control algorithm leads to a reduction of the cooling load by 12.52 MWh (46.96%) (Figure 170, Figure 171).
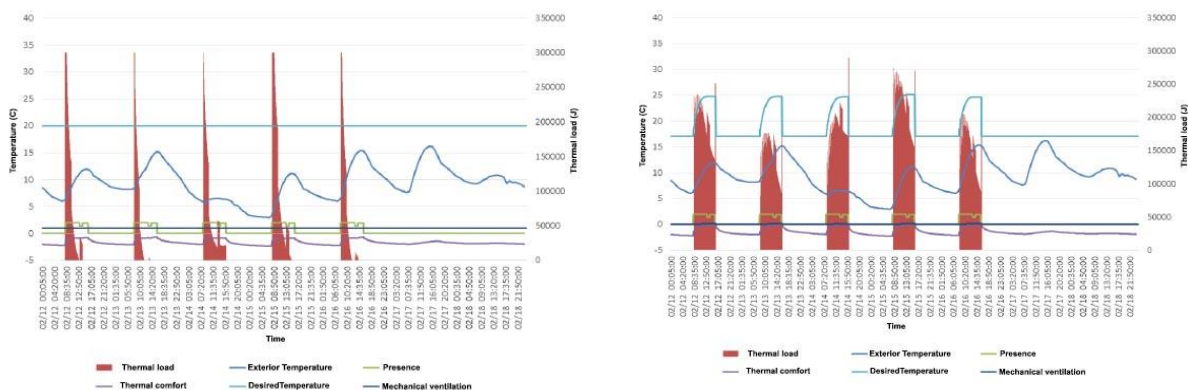
Figure 168. (left) Heating load and thermal comfort levels during the coolest week of the year, with the existing heating/control system.

Figure 169. (right) Heating load and thermal comfort levels during the coolest week of the year, with the use of the developed control algorithm.
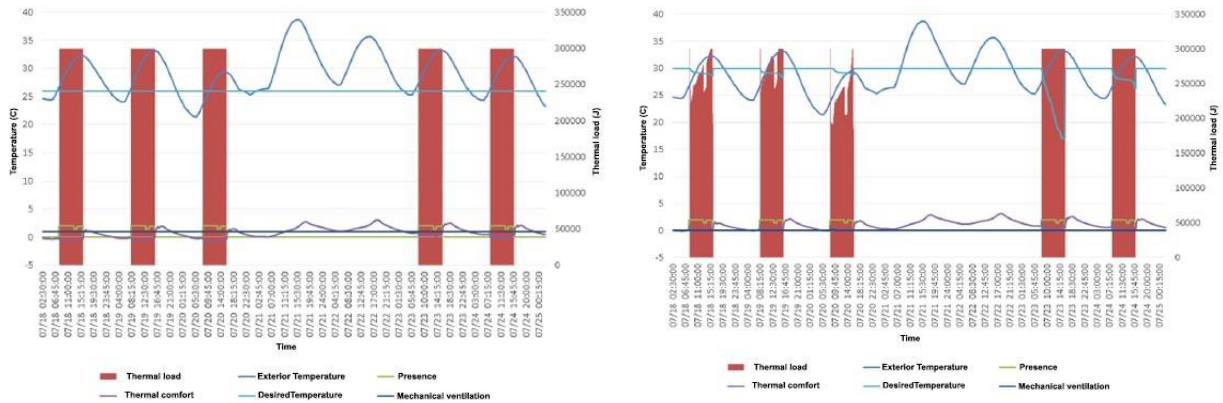

Figure 170. (left) Cooling load and thermal comfort levels during the warmest week of the year, with the existing cooling/control system.

Figure 171. (right) Cooling load and thermal comfort levels during the warmest week of the year, with the use of the developed control algorithm.

By comparing the initial energy demand for heating and cooling and the energy demand after the application of the developed algorithm, the annual energy savings were calculated. The comparison is performed for the same exterior conditions and for the same set points. The energy consumption is considerably decreased and the total energy savings are approximately 9.88 MWh (30.22%) for the heating and cooling of the entire building under study for one year. The following figures (Figure 172, Figure 173) show the relation between the power demand (W) and the exterior temperature (°C) before and after the application of the control algorithm. The energy efficiency achieved is verified by the decrease of the power demand gradient versus exterior temperature after the application of the control algorithm (Belussi, Danza, 2012).
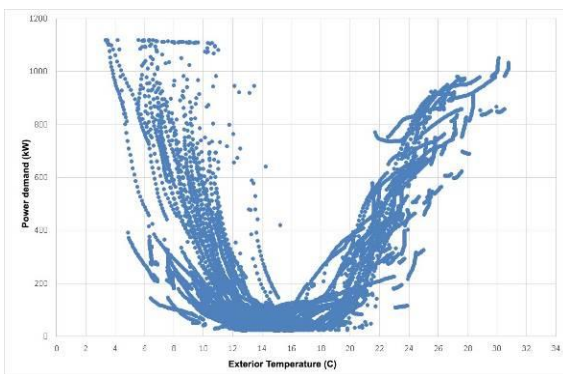

Figure 172: Left: Power demand related to the exterior temperature, before the application of the control algorithm.
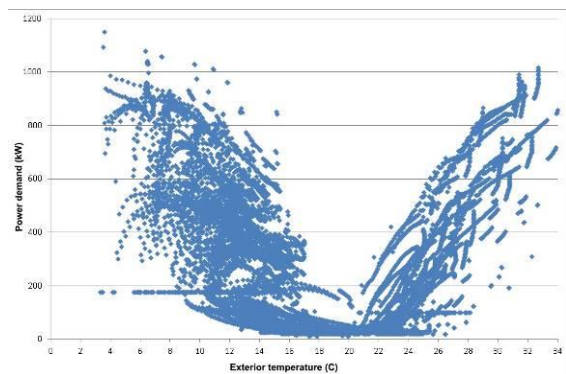
Figure 173. Right: Power demand related to the exterior temperature, after the application of the control algorithm.

5   FUTURE ACTIONS

After developing the control algorithms, a variety of sensors and meters have been installed in selected rooms of the University buildings that were selected for this study. The equipment includes temperature and humidity sensors, indoor CO_2 sensors, indoor CLC sensors, (for illuminance control), relays, motion detection sensors, multipurpose management appliances- local controllers (MPM), opening/closing window and door detectors and energy meters. All equipment provides the input data for the control algorithms. A StruxureWare platform is used for the support of the data exchange between MPM and the control algorithms. The detailed recording of the energy and environmental data of the selected rooms will make the comparison of the real and the predicted energy savings possible. Finally, a user friendly dashboard was created for the CAM-IT website (www.campit.gr), for the visualisation of the measurements and the energy consumption. The temperature (^{o}C) the air quality (ppm CO2) the relative humidity (%), the power demand (kW) and the presence and windows situation (0-1) are illustrated real time, so that the users of the University can have overview of the conditions in each room.

6   CONCLUSION

After the completion of the installation, the verification in order to ensure the proper functionality of the system in the campus site will be performed, i.e. the data collection and processing software, the Sensors, Actuators & User-Interfaces, as well as the interconnection with smart metering and with the power substations will be checked. The necessary off-line testing will also take place mainly for the public spaces. The energy savings that are calculated to be achieved by the use of the control algorithm is significant, reaching 30% of the initial consumption, for achieving the same comfort conditions. The actual energy savings will be recorded and compared to the theoretical percentage. Nevertheless, this project constituted a part of TUC's Strategic Sustainable Development Plan aiming at measurable results and promoting the University's goal to become an "open lab" for research and technology in sustainable development.

7.   ACKNOWLEDGEMENTS

8.   REFERENCES

BELUSSI, L. & Danza, L., 2012. Method for the prediction of malfunctions of buildings through real energy consumption analysis: Holistic and multidisciplinary approach of Energy Signature. Energy and Buildings, 55, pp.715–720.

BRUSE, M., 2004. ENVI-met website. Available at: http://www.envimet.com.

KOLOKOTSA, D. Pouliezoa, A., Stavrakakis, V., Lazos, C. 2009. Predictive control techniques for energy and indoor environmental quality management in buildings. Building and Environment, 44(9), pp.1850–1863.

PAPANTONIOU, S., Kolokotsa, D. & Kalaitzakis, K., 2015. Building optimization and control algorithms implemented in existing BEMS using a web based energy management and control system. Energy and Buildings. Volume 98, pp. 45–55

HAND, J.W., 2011. The ESP-r Cookbook: Strategies for Deploying Virtual Representations of the Built Environment. Energy Systems Research Unit. Department of Mechanical Engineering. University of Strathclyde, Glasgow, UK. (Available at: http://www.esru.strath.ac.uk/Documents/ESP-r_cookbook_july_2011.pdf)

RASSIA, S., Pardalos, P. 2014. Cities for Smart Environmental and Energy Futures: Impacts on Architecture and Technology. Chapter: Cities for Smart Environmental and Energy Futures: Urban Heat Island Mitigation Techniques for Sustainable Cities. pp. 215-233. Springer Berlin Heidelberg

MOTEGI, N. Piette, M.A. Kinney, S., Herter, K. 2003. Web-based energy information systems for energy management and demand response in commercial buildings. Lawrence Berkeley National Laboratory Report. (Available at: https://cbs.lbl.gov/publications/web-based-energy-information-system-0)

POSTER SESSION E

98: A study on use of three-dimensional miniature dielectric compound parabolic concentrator (3D dCPC) for daylighting control application

MENG TIAN, YUEHONG SU

Institute of Sustainable Energy Technology, Department of Architecture and Built Environment, University of Nottingham, University Park, Nottingham NG7 2RD, UK, yuehong.su @nottingham.ac.uk

Low-concentration solid dielectric parabolic concentrator (dCPC) is regarded as a high-potential design in daylighting control and energy saving in lighting system. The incident light could penetrate the lateral surfaces of dCPC as its incident angle is beyond the acceptance angle of dCPC, by which dCPC will control the amount of daylighting coming into the room according to the sun position. The light within the incident angle will be concentrate to the bottom of dCPC. This study is a further research based on the evaluation of two-dimensional (2D) dCPC, which aims to investigate the advantages of three-dimensional (3D) miniature solid dCPC comparing with 2D dCPC based on their daylight transmittance values under sunny sky. An optical analysis software Photopia is used to simulate the daylighting control performance of different types of concentrators. The performances of concentrators in Nottingham, UK (53° N, 1.2° W) are put forward as a case study. It is demonstrated that 3D dCPC has great advantages than 2D dCPC in control daylight, which performs higher transmittance in the morning and afternoon and lower transmittance at noon. Then, two types of 3D dCPC are compared for its tolerance on horizontal rotation angle. One has polygonal apertures with 4 sides (3D s-dCPC), and the other is revolved 3D dCPC (3D r-dCPC). Each dCPC has two different structures, which are with non-reflective material affixing on base and without base coating. Results show that the 3D non-coated r-dCPC may be the best choice in application with the advantages of installation, more stable illuminance level it provides and lower cost in manufacture.

Keywords: daylighting control, dielectric compound parabolic concentrator, transmittance, illuminance, Photopia

1. INTRODUCTION

1.1 Background

The utilization of daylighting has been developed through human history, which was used as dominant source and became to be dependent on artificial lighting. In recent years, daylight is proposed again to be used on energy saving in a natural way as the issue of energy shortage arises. The dependence on artificial lighting leads to many problems in respect of environmental pollution, light quality and human health. The artificial lighting is increasing by around 6% annually (Hölker et al. 2010a) in worldwide. Artificial lighting systems become the major contributors to CO2 emissions and global warming at the same time. Different types of light also affect human psychology and physiology. The constant variations of pattern, intensity and color composition afforded by daylight are more pleasant to be accepted by human being comparing with other light (Holmes 1975, CIBSE 1999).

As the significance of daylight was recognized, it was begun to be integrated in lighting technologies and building design. Dielectric compound parabolic concentrator (dCPC) is a new material used to control daylight for building. Because the high concentration efficiency of dCPC, it was applied to the photovoltaic generation of electricity initially put forward by Cole et. al. (1977) in 1977. It is an improvement of the well known solar collecting concentrator - compound parabolic concentrator (CPC), the curved reflective surfaces of which allow the capture of diffuse UV sunlight without solar tracking and produce illumination over base surface. The dielectric concentrator arrays are made of acrylic plastic and the absorbers are photovoltaic arrays. A series of research is conducted to develop its efficiency in collecting solar energy. During this period, the potential of integrating with building design of dCPC is discovered. Nabin Sarmah et. al. (2014) proposed a dCPC design for building facades integration in northern latitudes. Another application of dCPC for receiving daylight is also put forward. Thomas Cooper et. al. (2013) discussed the performance on receiving daylight of compound parabolic concentrators with different polygonal apertures. It was found that the dCPCs with polygonal apertures having different number of sides perform different efficiencies and flux distributions. In the study conducted by Xu Yu et. al. (2014:74), the performances of dCPC under different sky conditions are evaluated, which provides an idea on daylight control of dCPC except for solar energy collection. This study is a further research of the work by Xu Yu et. al. (2014:74), the improvement on dCPC structures are put forward and their performances under sunny sky condition will be explored.

1.2 Dielectric-Filled Compound parabolic concentrator (dCPC)

Compound parabolic concentrator (CPC) is a wide known collector in collecting solar energy. The first time of CPC being described as a collector for light from Cerenkov counters by Hinterberger and Winston (1966a, b). In 1974, Winston (1974) described the CPC in 2D geometry and did further elaborations with Hinterberger (Winston and Hinterberger 1975) and Rabl (Rabl and Winston 1976), which become the general principles of CPC design in 2D geometry then. CPC consists of two sections of a parabola of second degree, symmetrically located about the mid-plane of a collector. Winston (1976a) also put forward an improvement of 2D and 3D CPCs which are filled with dielectric and using total internal reflection. Compared to CPC, dCPC can accept more lights with larger incident angle as a result of the refractive index of dielectric. The refraction index also makes the parabolic surfaces reflect light to the bottom surface and constrain the light to go out through the curved surfaces. When light travels from one material with higher refraction index n_1 to another material with lower refraction index n_2, the light can go through the interface only if the incident angle is smaller than the critical incident angle.
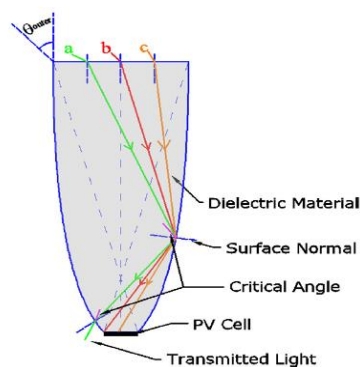

Figure 1.1 Representative ray paths of dCPC (Yu et. al. 2014:74)

The working principle of critical incident angle is shown in Figure 1.1. The dCPC made of acrylic is set as an example. Therefore the interface is acrylic-air with n_1=1.5 and n_2=1. The critical incident angle is around 41.8°. Ray a represents the diffused skylight and sunlight in low elevation angle which incident angle is larger than the acceptance angle of dCPC. It escapes from the curved surface to the air after reflections in dCPC. The incident angle of ray b is equal to the acceptance angle which stands for the edge condition. Ray c with small incident angle refers to the sunlight in high elevation angle and it is concentrated to the bottom of dCPC.

2 METHODOLOGY
2.1 Photopia

Photopia is a fast and accurate photometric analysis program which is for producing comprehensive performance evaluations for non-imaging optical designs. It provides a large selection of sun and sky dome models to analogue real sky conditions. In terms of material selection, numerous material data sorted by refractive, transmissive and refractive could be chosen in database. By the cooperation with AutoCAD software, the optical properties of designed dCPCs could be simulated. In simulation, Photopia uses probabilistic method to obtain results (Photopia 2015). Therefore, the simulated results may not be demonstrated in perfect and smooth curves. The source models provided in Photopia are based on the ISENA RP-21 daylight equations which include variable luminance values across the hemisphere. In the research produced by Wittkopf S. K. (2007), the difference between experimental values and simulated results from Photopia ranges from 1% to 2%, which shows the high accuracy of Photopia in optical efficiency simulation. The dCPC used for simulation is made of acrylic. In material input data of Photopia, refraction index of outside material (air), refraction index of inside material (acrylic) and extinction coefficient are required. As it is known that the refraction index for air is 1.0 and 1.5 for standard acrylic. The extinction coefficient is a measurement of the extent by which the intensity of a beam of any transmitted light is reduced by passing through a distance x. The acrylic used in this research is same as it in work conducted by Yu. X (2014:74) in which the extinction coefficient is 0.0641 inch^{-1}.

2.2 Summary of previous work

This research continues the dCPC study put forward by Yu. X (2014:74) in which daylighting control performance of dCPC rods in Nottingham, UK (53° N, 1.2° W) were discussed. The structures of them are shown in Figure 2.1 below. The dCPC with two parabolic surfaces and symmetrically to its mid plane is named as two-dimensional dCPC (2D dCPC). All of them are made of acrylic with refraction index 1.5. The length of dCPCs rod are 96mm, and the two parabolic surfaces are symmetrically located about the mid-plane of a collector along the long edge. One of the dCPC rod is without coating on its bottom surface, which is considered for daylight application only. This dCPC is represented by non-coated dCPC. The base of another dCPC rod referred as base-coated dCPC is affixed with non-reflective material. Because the outer half acceptance angle of dCPC is about 22.05°, and the solar zenith angle at noon various from 30° to 54° in Nottingham during March to September, simulation was processed when dCPC is tilted to 37° and facing to south. According to the sun path in whole year, four specific day, which are spring equinox, summer solstice, autumn equinox and winter solstice are chosen to obtain the change of transmittance and transmitted daylight illuminance in each day. The results demonstrate the dCPC rod preforms adequate control of sunlight in daytime under sunny sky conditions in four specific day, which presents great potential of daylight control of dCPC. However, the transmitted illuminance is expected to be higher in the morning and afternoon, and under overcast sky condition to guarantee the indoor illuminance level.
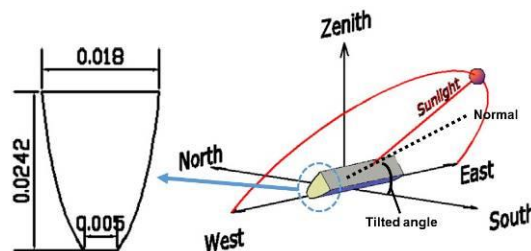

Figure 2.1 Schematic diagram of dCPC structure in previous research

2.3 Improvement of dCPC in current research

dCPC controls the light mainly by its curved surfaces. 2D dCPC performs huge differences on transmittance in summer solstice, spring equinox (autumn equinox) and winter solstice. This is caused by the different solar zenith angle at noon. However, it does not provide strong control in one day because there is no curved surfaces in east-west direction. An improvement on structure of 2D non-dCPC is expected to achieve better control of sunlight. Therefore, two kinds of three-dimensional dCPCs (3D dCPC) are proposed. One has polygonal apertures with 4 sides, which is named as 3D s-dCPC. The four curved surfaces whose dimensions are same as 2D dCPC on east-west and north-south direction, which can not only controls the sunlight from south, also acts on the east-west sunlight. The entry aperture of one 3D dCPC element is a 0.018m*0.018m square, and the 2D dCPC rod could be assumed as a composition of small 2D dCPC elements as well. Another 3D dCPC is cylindrical symmetry whose reflecting surface is obtained by rotating the parabola about the concentrator axis (not about the axis of the parabola), and it is referred to as 3D r-dCPC (3D revolved dCPC). The input and output apertures of this dCPC are circular. A research put forward by Thomas Cooper et. al. (2013) demonstrates that the performance of this revolved CPC is slightly better than polygonal CPCs and revolved CPCs performs more uniform flux distribution. The parabolas applied on the 2D dCPC, 3D r-dCPC and 3D s-dCPC are the same so that the section views of them are the same. The dimensions of them are shown in Figure 2.2 below.
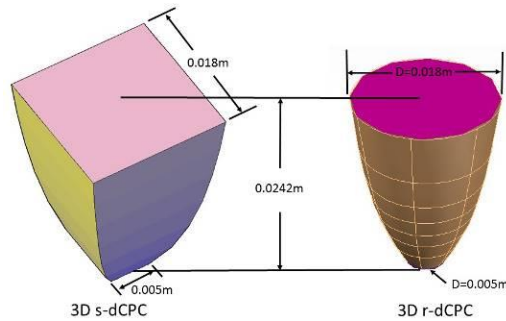

Figure 2.2 Dimension of 3D dCPC

Similar to 2D dCPC, the difference between 3D base-coated and non-coated dCPC is whether the non-reflective material is affixed on the base. Firstly, the performance of daylight control between 2D dCPC and 3D dCPC will be explored under sunny sky conditions. The 3D s-dCPC has four curved surfaces which are used to reflect incident light to bottom surface or out of dCPC. It is easy to have deviation of angles in practical installation. Hence the tolerance of horizontal rotation angle of 3D s-dCPC will be investigated then. Because 3D s-dCPC is symmetry about mid-plane, four angles, which are 0°, 15°, 30°and 45°(Figure 2.3), are chosen to compare their transmittances under 37° tilted angle and sunny sky conditions. The 3D r-dCPC is compared together. Because the sun paths are almost same in spring equinox and autumn equinox, this research will focus on three specific days, which are summer solstice, spring equinox and winter equinox. The results demonstrate the optical properties of dCPC for every 30mininutes at daytime by Photopia. For the purpose of investigating optical properties of dCPCs, transmittance and transmitted daylight illuminance are the two aspects for comparison in this paper.
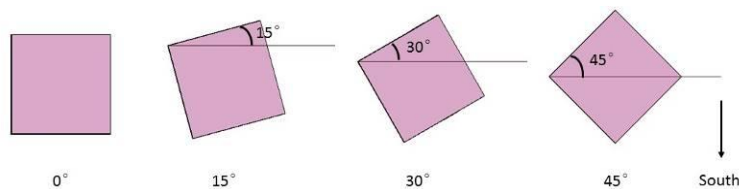

Figure 2.3 Top view of 3D s-dCPC with different horizontal rotation angle

3   RESULTS AND DISCUSSION

3.1 Transmittance of 2D dCPC and 3D s-dCPC under clear sky

In order to compare the optic properties between 2D and 3D dCPC, the transmittances of them under sunny sky conditions in the three specific days are shown in Figure 3.1 which are simulated by Photopia. It is observed that 3D dCPC has great advantages than 2D dCPC in controlling sunlight in three specific day. For 2D base-coated dCPC, sunlight is prevented from 8:00 to 16:00, during which its transmittance is lower than 0.2 in spring equinox, and it is similar to summer solstice. In winter solstice, 2D base-coated dCPC does not provide control to sunlight. Comparing with this, 3D base-coated dCPC provides remarkable control of sunlight in these three days. It lets light come in before 10:00 and after 13:30, and prevents light during 10:00 to 13:30 in spring equinox and summer solstice. In winter solstice, it controls the light from 9:00 to 15:00, and the lowest transmittance is 0.4, which could provide adequate illuminance for indoor environment. Similarly, 3D non-coated dCPC also has great advantages than 2D non-coated dCPC. It has same control strategy with 3D base-coated dCPC, while the lowest transmittance is 0.2 higher than 3D base-coated dCPC. 2D non-coated dCPC hardly provides control on sunlight. The reason is that dCPC controls the incident lights by reflecting them to the bottom surface or out of dCPC by the curved surfaces. 2D dCPC has only two curved surface so that it can only control the sunlight with different solar zenith angle. Therefore the transmittances of 2D dCPC have large difference in different season during the whole year. However, it is difficult to control the sunlight at different time in the same day. 3D dCPC has four curved surfaces facing four different directions which could control the sunlight not only for different seasons, but also for different times in one day. It is obviously demonstrated that 3D dCPCs have strong control not only in different seasons during whole year, but also at different time in one day. Therefore, 3D base-coated and non-coated dCPC provides better control on daylight than 2D dCPC. 3D dCPC will be investigated in the following sections in different criteria.

(a)

Spring Equinox

(b)

Summer Solstice
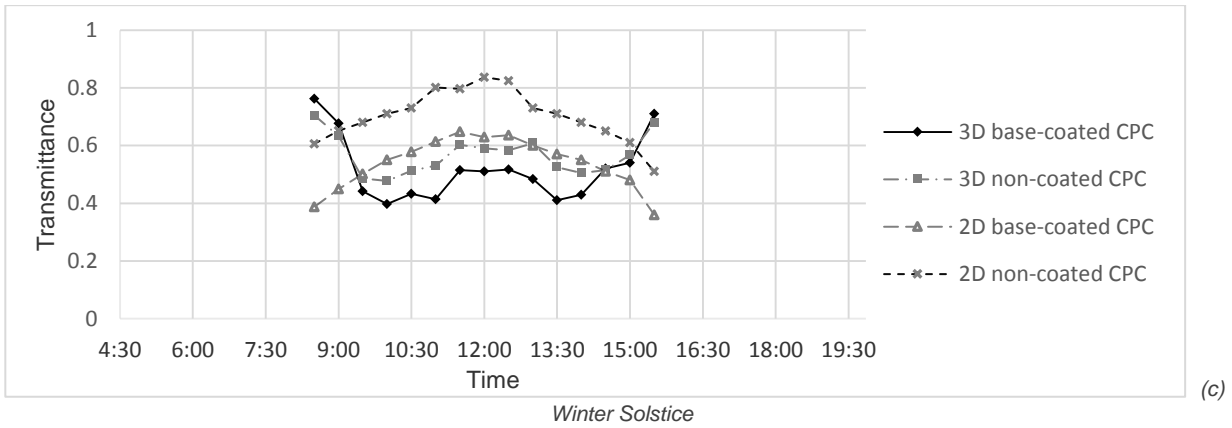
(c)
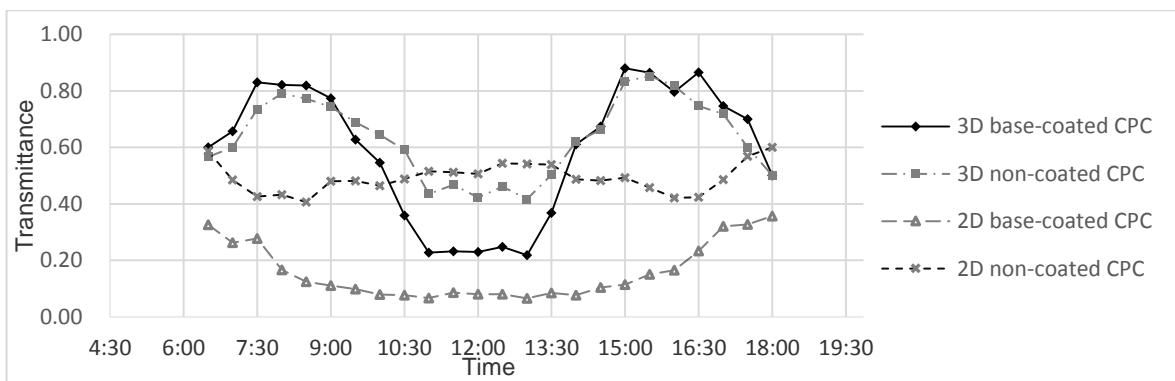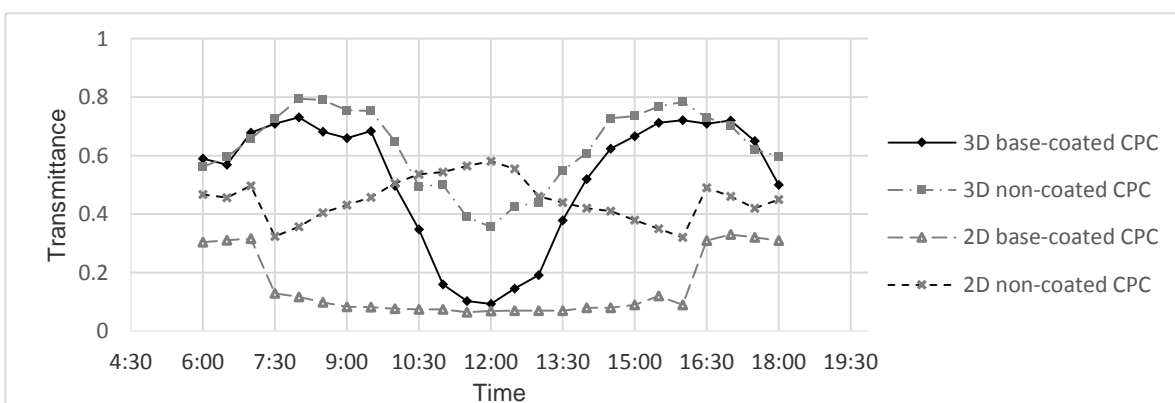
Winter Solstice

Figure 3.1 Transmittance of 2D and 3D s-dCPC in Spring Equinox, Summer Solstice and Winter Solstice under sunny sky (Nottingham, south-facing, 37°tilted)
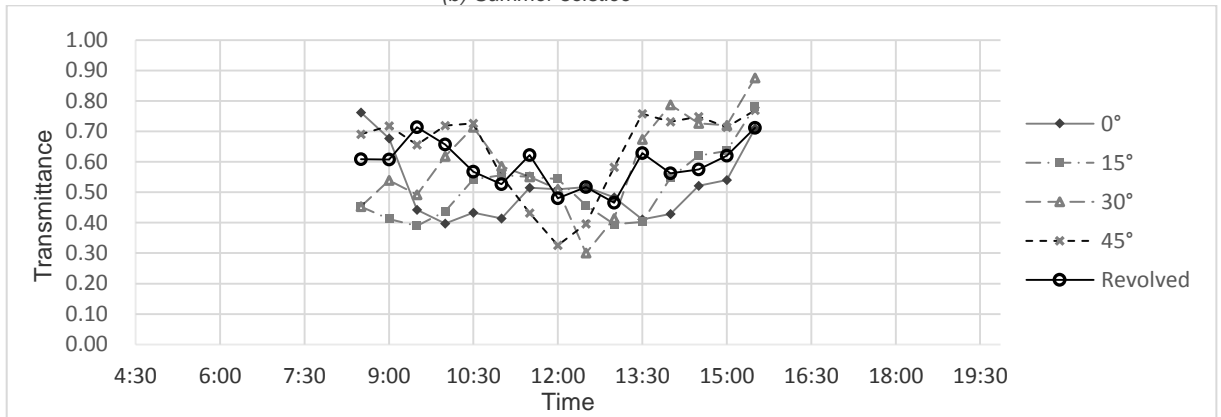
3.2 Effects of horizontal rotation angle of 3D base-coated s-dCPC

According to Figure 3.2, it can be seen that the horizontal rotation angle does affect the transmittance of 3D s-dCPC according to Figure 4.4. For the dCPC without horizontal rotation (0°), the curve of transmittance is almost symmetric about the Y axis at 12:00. However, the transmittances of dCPCs with 15°and 30°are not symmetric. Both of them perform lower transmittances in the morning than that in the afternoon in spring equinox, and lower transmittances in the afternoon than that in the morning in summer equinox. In spring equinox, the dCPC without rotation provides longer control to daylight which is between 10:30 to 13:30, for the other three dCPCs, the period of controlling light at noon is around 11:30 to 1:00. The transmittance of dCPC with 45°horizontal rotation angle is almost symmetric about the Y axis at noon as well, while it has lower transmittance in the morning and afternoon than the dCPC with 0°rotation angle in summer solstice. It is worth to point out that this dCPC also provide daylight control at noon in winter solstice which is different from all the other three dCPCs. However, the r-dCPC demonstrates the similar transmittance with non-rotational s-dCPC.in spring equinox; the transmittances in summer and winter solstices seems to be close to the average of s-dCPCs with different rotation angles. In order to compare the practical performance, the transmitted daylight illuminance through dCPCs are shown in Figure 3.3.
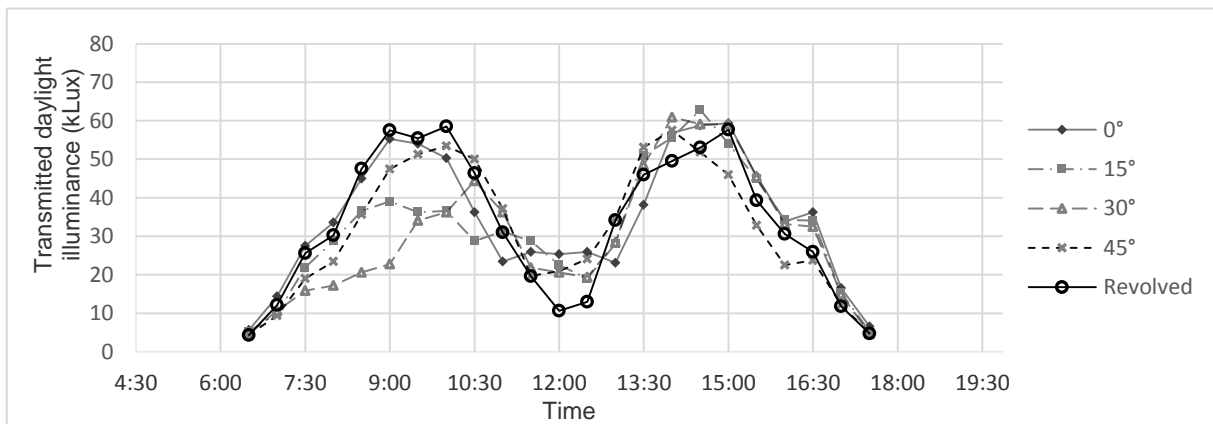

(a)
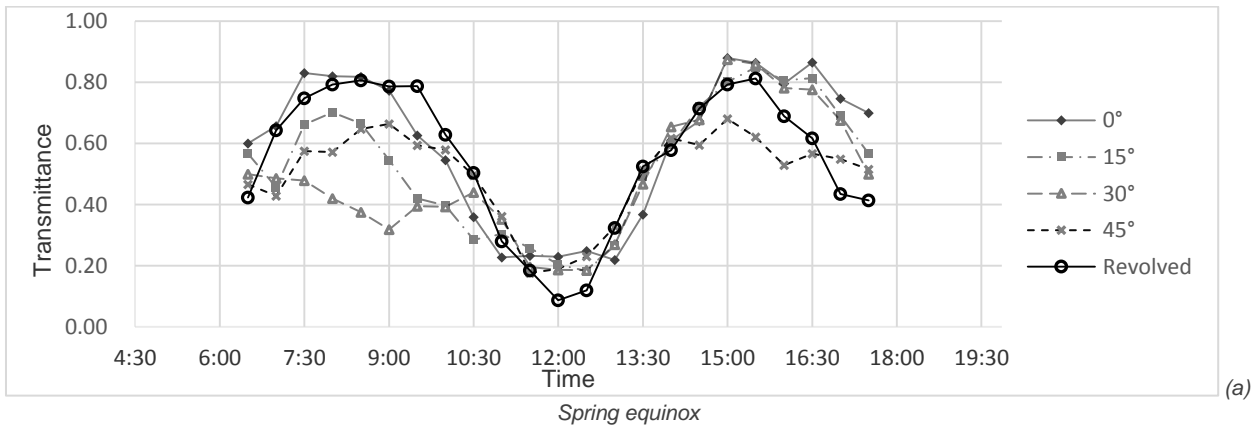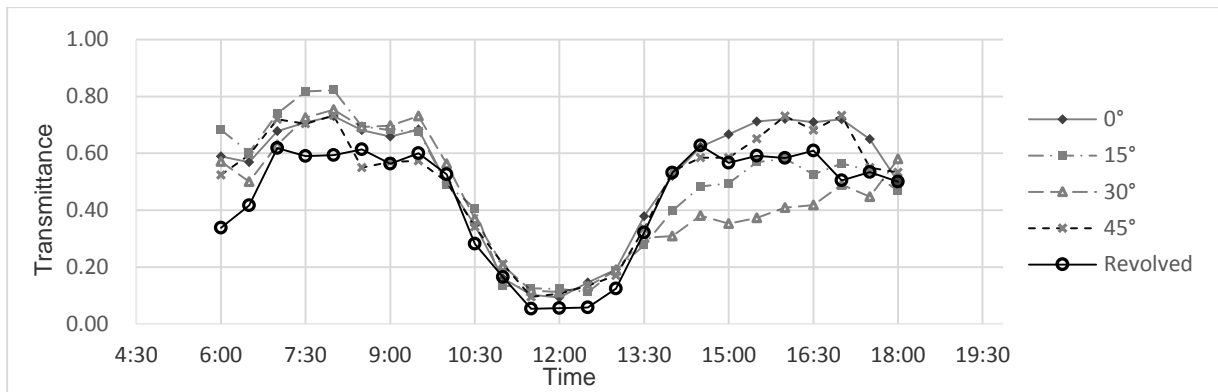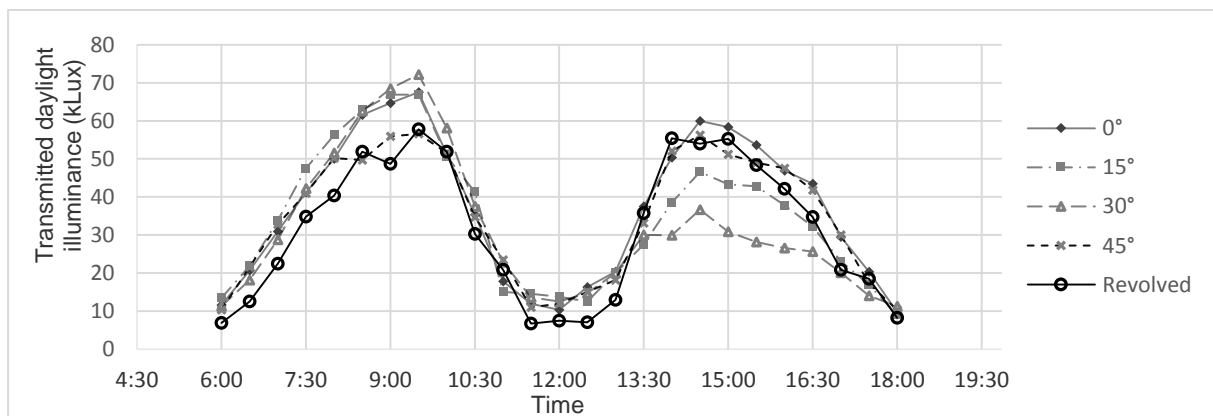
Spring equinox

(b) Summer solstice

(c) Winter solstice

Figure 3.2 Transmittance of 3d base-coated dCPC with 0°, 15°, 30°and 45°horizontal rotation angle under sunny sky (Nottingham, south facing, tilted 37°)

(a)

Spring equinox
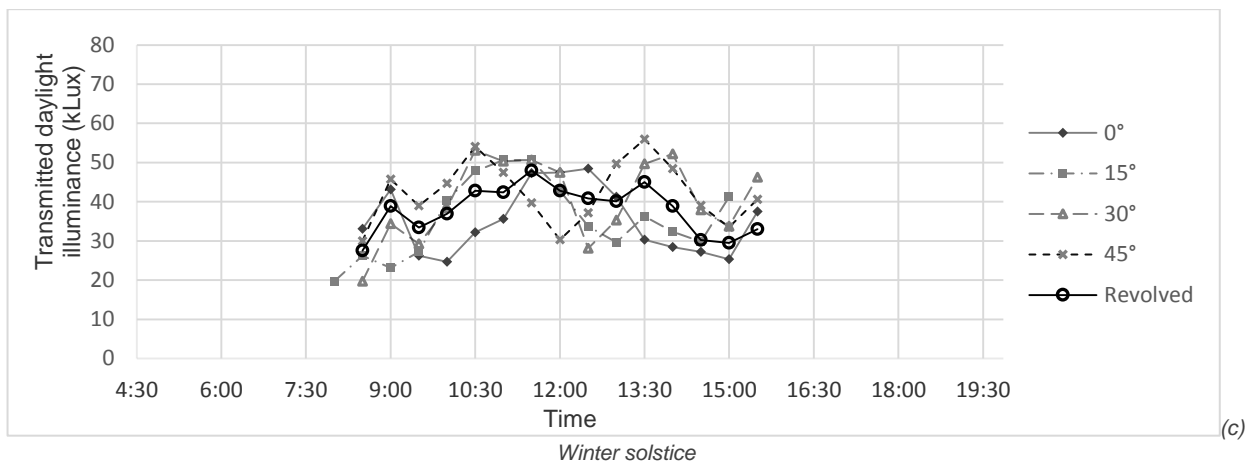

(b)

Summer solstice

Winter solstice

(c)

Figure 3.3 Transmitted daylight illuminance of 3d base-coated dCPC with 0°, 15°, 30°and 45°horizontal rotation angle under sunny sky (Nottingham, south facing, tilted 29°)

With the influences of transmittance, the transmitted illuminance shows similar properties. Comparing with the symmetric changing trend of the dCPC without rotation, the transmitted illuminance of dCPCs with 15°and 30°rotation angle in the morning are lower than that in the afternoon in spring equinox, and this is reversed in summer solstice. The dCPC without rotation controls the illuminance level under 50kLux from 10:00 to 15:00 in spring equinox, while the other three dCPCs have same results between 11:30 and 13:00. The dCPC with 45°horizontal angle has better control of daylight during the whole day of summer solstice: the transmitted illuminance is 45kLux which is much smaller than the peak illuminance, 60-70kLux, provided by other three dCPCs. In winter solstice, it reduces the illuminance to 30kLux at noon. For other three dCPCs, the transmitted illuminance is around 50-60kLux. Both s-dCPC and r-dCPC perform excellent daylight control in spring equinox and summer solstice, which achieve the objective to provide high illuminance level in the morning/afternoon and reduce solar gain at noon. In winter, the relatively stable transmitted illuminance could reduce the heating load. However, in practical installation, it is difficult to control the angular deviations, which may affect the solar distribution in room. The advantages of revolved dCPC (r-dCPC) is stand out. It has similar control ability compared to s-dCPC and does not need to concern the angular deviation in practical installation.

3.3 Effects of horizontal rotation angle of 3D non-coated s-dCPC

The properties of transmittances for the 3D non-coated s-dCPCs in different horizontal rotation angle are same with the properties for 3D base-coated dCPC referred in Section 3.2. According to Figure 3.4 and 3.5, the transmittances of dCPCs with 15°and 30°in the morning are lower than them in the afternoon in spring equinox, and reversed in summer solstice. The dCPC with 45°rotation angle still has better control on the peak illuminance for the summer solstice day and the lowest transmittance is 30kLux which is enough for indoor environment. The transmitted illuminance for winter solstice day are close for the four different types of dCPCs. The transmittance and transmitted illuminance of 3D r-dCPC take the average value of 3D s-dCPCs with different rotation angles approximately.

The properties of transmittances for the 3D non-coated s-dCPCs in different horizontal rotation angle are same with the properties for 3D base-coated dCPC referred in Section 3.2. According to Figure 3.4 and 3.5, the transmittances of dCPCs with 15°and 30°in the morning are lower than them in the afternoon in spring equinox, and reversed in summer solstice. The dCPC with 45°rotation angle still has better control on the peak illuminance for the summer solstice day and the lowest transmittance is 30kLux which is enough for indoor environment. The transmitted illuminance for winter solstice day are close for the four different types of dCPCs. The transmittance and transmitted illuminance of 3D r-dCPC take the average value of 3D s-dCPCs with different rotation angles approximately.

Figure 3.4 Transmittance of 3D non-coated s-dCPC with 0°, 15°, 30°, 45°horizontal rotation angle and 3D non-coated r-dCPC under sunny sky (Nottingham, south facing, tilted 37°)

ecause base-coated dCPC have an affixed non-reflective material on base, base-coated dCPC has stronger control abilities in controlling daylight at noon. The reason is that most of incident lights are reflected to the base and they are emitted out for non-coated dCPC; for base-coated dCPC, they are absorbed by non-reflective material on base. The main differences occur from 10:30 to 13:30 in spring equinox and summer solstice. During this time, the transmittance of base-coated dCPC ranges around 0.1-0.2 and the corresponding transmitted daylight illuminance ranges from 10-30kLux. For non-coated dCPC, the transmittance is around 0.4 and daylight illuminance is within 40-60kLux. It is important to point out that the optical performance of base-coated and non-coated dCPCs are almost same in winter. Both of them almost do not provide control on daylighting. Base-coated dCPC is more difficult on manufacture due to base coating. If the real weather is taken into account, which includes sunny sky and overcast sky conditions, the base-coated dCPC may not provide enough indoor illuminance level under overcast sky. Non-coated dCPC provides more stable illuminance level from 9:00 to 15:00. The less control of daylight at noon would also guarantee a sufficient illuminance level under overcast sky condition. Therefore, the 3D

non-coated r-dCPC may be the best choice in application with the advantages of installation, the more stable illuminance level it provides and lower cost in manufacture.

(a) Spring equinox

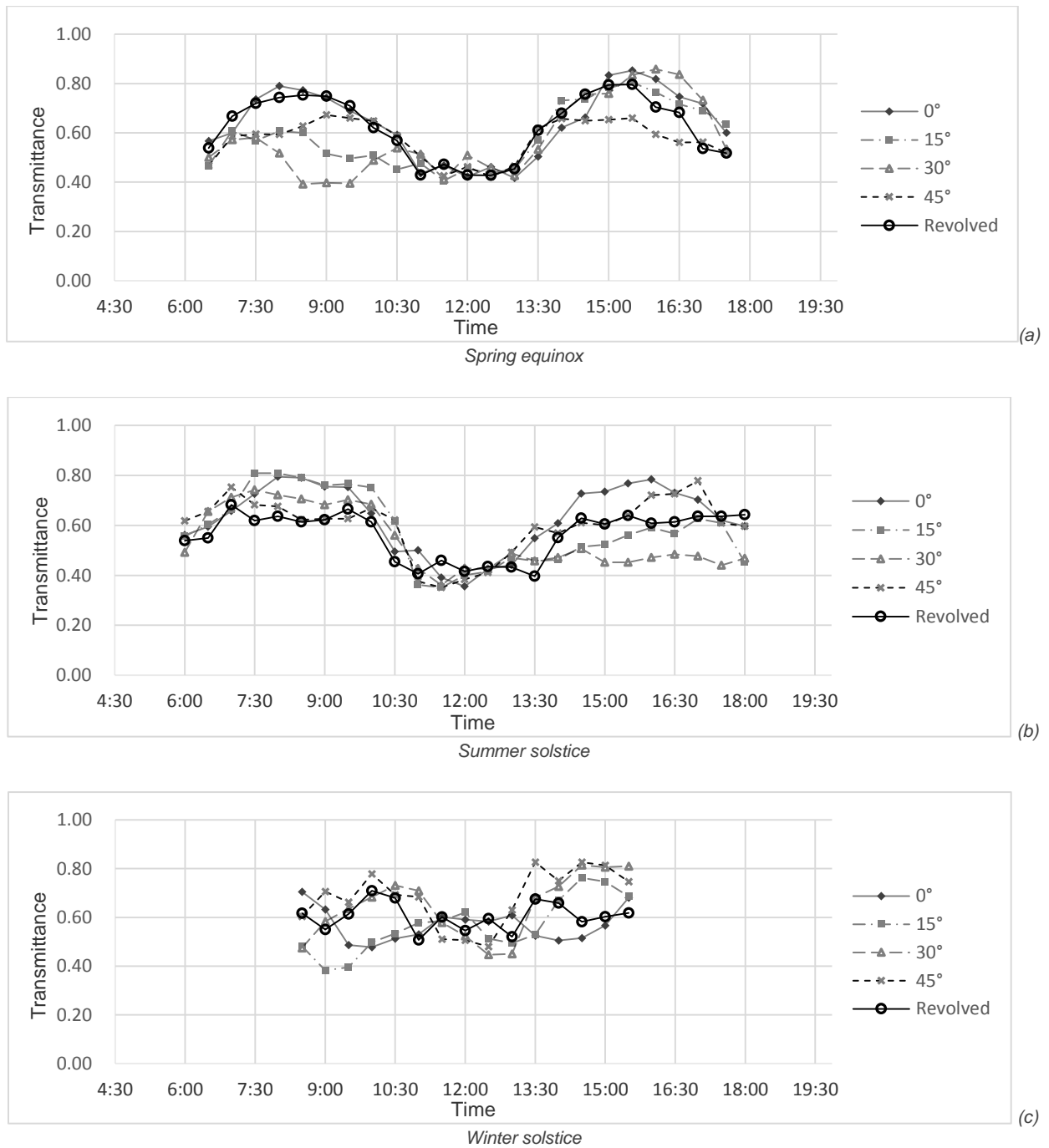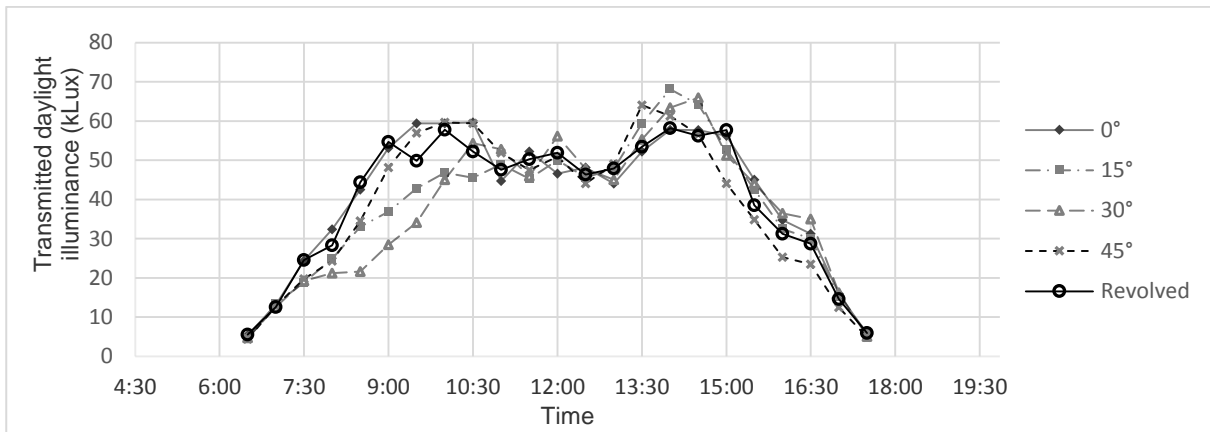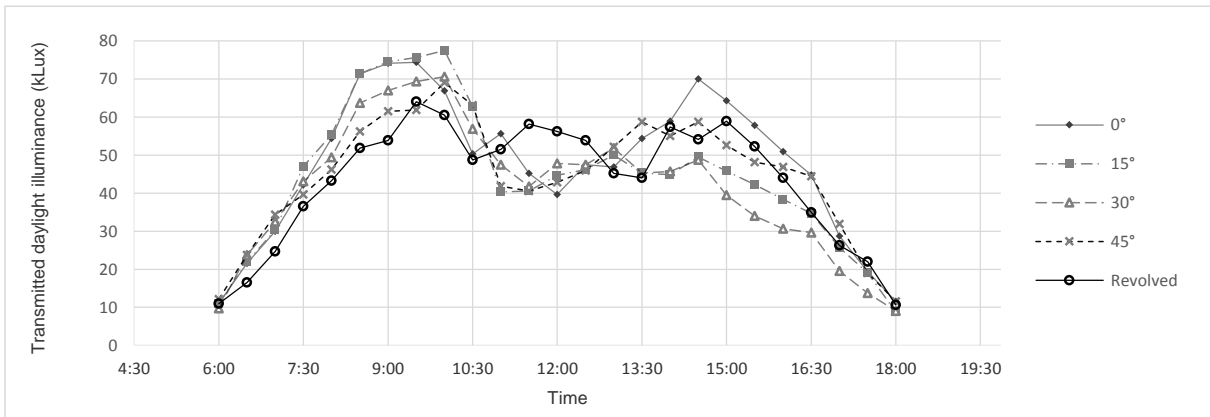*(b) Summer solstice*
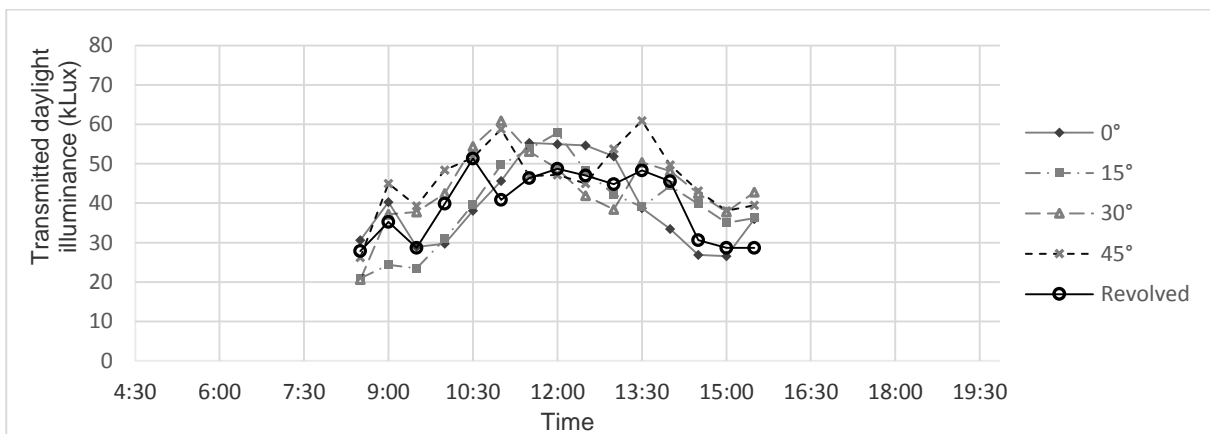
(c) Winter solstice

Figure 3.5 Transmitted daylight illuminance of 3d base-coated dCPC with 0°, 15°, 30°, 45°horizontal rotation angle and 3D non-coated r-dCPC under sunny sky (Nottingham, south facing, tilted 37°)

4   CONCLUSION

This paper is the further research of the daylight control ability of two-dimensional dCPC (2D dCPC). Two different three-dimensional dCPCs (3D dCPC) are put forward. One is s-dCPC with four parabolic surfaces and square apertures, the other is r-dCPC with the curved surface by revolving the parabola and cubic

apertures. In addition, each type of dCPC is separated into base-coated and non-coated. The optical properties of 3D dCPCs are compared with 2D dCPC, which demonstrates that both base-coated and non-coated 3D dCPCs have strong advantages in control daylight not only in different seasons during the whole year but also at different time during a day. 3D base-coated dCPC provides remarkable control of sunlight in these three days. It lets light come in before 10:00 and after 13:30, and prevents light during 10:00 to 13:30 in spring equinox and summer solstice. In winter solstice, it controls the light from 9:00 to 15:00, and the lowest transmittance is 0.4, which could provide adequate illuminance for indoor environment. Then the tolerance of horizontal rotation angle for 3D s-dCPC is put forward and compared with 3D r-dCPC. Results show that 3D s-dCPC without horizontal rotation and 45° has symmetric optical performances in the morning and afternoon about 12:00 while the 3D s-dCPCs rotated to 15° and 30° demonstrate non-symmetric optical properties. 3D r-dCPC has similar optical performances with 3D s-dCPC and do not need to concern the effects by horizontal angular deviations due to installation, which is a better choice in practical installation. The principles are also applicable for base-coated and non-coated 3D s-dCPC and r-dCPC. With the comparison of 3D base-coated and non-coated dCPC, it is illustrated that the base-coated dCPC provides stronger control on daylight at noon, between 10:30 to 13:30, in spring equinox and summer solstices. During this time, the transmittance of base-coated dCPC ranges around 0.1-0.2 and the corresponding transmitted daylight illuminance ranges from 10-30kLux. For non-coated dCPC, the transmittance is around 0.4 and daylight illuminance is within 40-60kLux. The optical performances of non-coated and base-coated in winter are almost same. Considering the real sky conditions, non-coated dCPC could provide sufficient indoor illuminance level under overcast sky conditions and more stable illuminance level from 9:00 to 15:00. To conclude, the 3D non-coated r-dCPC may be the best choice in application with the advantages of installation, the more stable illuminance level it provides and lower cost in manufacture.

5   REFERENCES

CIBSE. Lighting Guide LG10: 1999 --- Daylighting and window design. 1999.

COLE, R.L., A.J. Gorski, R.M. Graven, W.R. McIntire, W.W. Schertz, R.Winston, and S. Zwerdling. 1977. Applications of compound parabolic concentrators to solar energy conversion. Report AMLw42. Argonne National Laboratory, Chicago.

HINTERBERGER, H., and Winston, R. (1966a) Efficient light coupler for threshold Cerenkov counters. *Rev. Sci. Instr*. 37, 1094-1095.

HINTERBERGER, H. and Winston, R. (1966b). Gas Cerenkov counter with optimized light-collecting efficiency. *Proc. Int. Conf. Instrumentation High Energy Phys*. 205-206.

HÖLKER et al., (2010a). The dark side of light: a transdisciplinary research agenda for light pollution policy. *Ecol. Soc.*, 15 (4) (2010) http://resolver.sub.uni-goettingen.de/purl?gs-1/7268

HOLMES, G. J. *Essays on lighting*. London: Rank Precision Industries, 1975.

NABIN SARMAH, et. al. (2014) Design, development and indoor performance analysis of a low concentrating dielectric photovoltaic module. *Solar Energy*. Vol 103, 390-401.

PHOTOPIA (2015) Photopia User's Guide. http://www.ltioptics.com/en/photopia-standalone-base.html

Rabl, A., and Winston, R. (1976) Ideal concentrators for finite sources and restricted exit angles. *Appl. Opt*. 15, 2880-2883.

THOMAS COOPER, et. al. (2013) Performance of compound parabolic concentrators with polygonal apertures. *Solar Energy*. Vol 95, 308-318.

WINSTON, R. (1974) Principle of solar concentrators of a novel design. *Sol. Energy* 16, 89-95.

WINSTON, R. (1976a) Dielectric compound parabolic concentrators. *Appl. Opt 15*, 291-292.

WINSTON, R., and Hinterberger, H. (1975) Principles of cylindrical concentrators for solar energy. *Sol. Energy* 17, 255-258.

WITTKOPF. S. K. (2007) Daylight performance of anidolic ceiling under different sky conditions. *Solar Energy*. Volume 81, issue 2, 151-161.

YU Xu, Yuehong Su, Hongfei Zheng, Saffa Riffat. 2014. A study on use of miniature dielectric compound parabolic concentrator (dCPC) for daylighting control application. *Building and Environment*. 74, 75-85.

124: The application of vernacular australian environmental design principles on contemporary housing

Lessons Learnt from the Marie-Short House by Glenn Murcutt

MAURICIO LECARO[1], LUCELIA RODRIGUES[2], BENSON LAU[3]

1The University of Nottingham, Department of Architecture and Built Environment,
mauricio.lecaro @alumni.nottingham.ac.uk
2The University of Nottingham, Department of Architecture and Built Environment,
lucelia.rodrigues @nottingham.ac.uk
3The University of Nottingham, Department of Architecture and Built Environment,
Benson.Lau @nottingham.ac.uk

Glenn Murcutt's deep knowledge of the Australian landscape and understanding of the climate challenges resulted in buildings designed to respond, rather than impose on the local context. The unintended greatness of his work lies on his mastery ability to adopt, reinterpret and reinvent the elements found in vernacular Australian architecture. Murcutt's buildings are narrow in plan, light, airy and in tune with seasonal climatic variations; above all, they are designed to minimise their environmental impact, guided by an unwavering belief that we have to touch this Earth lightly.

In this paper, the authors investigated and assessed the impact and implications, which the reinterpreted elements of Australia's vernacular architecture, (e.g. verandahs, overhangs, roofing shape and narrow spaces) had on the performance and spatial delight of the Marie-Short House. Through computer aided modelling, both daylight and thermal environments were assessed and analysed in correlation with Murcutt's environmental design strategies, (i.e. enhancing shading and natural ventilation) in order to achieve comfortable spaces, which enrich and enhance the inhabitants' spatial experience and comfort conditions.

The findings revealed that when Murcutt's simple environmental design strategies, (i.e. natural ventilation, shading and buildings on stilts) were combined with the reinterpreted vernacular elements, they were not sufficient for the house to perform as expected; the results showed that while Murcutt's natural ventilation strategy, when combined with the shading provided by the verandahs, is fundamental to improve thermal comfort within the house, the blinds and overhangs as designed, are not sufficient to prevent visual discomfort.

In spite of this, Murcutt's work is intuitive yet well-informed and more significantly, it is born from the uniqueness of each place. The combination of Murcutt's environmental design principles with the reinterpreted vernacular elements, reflected the skilfulness and significance that lies in his work, he envisioned a low energy consuming building that through a permanent connection with nature like an orchestra, adapted and silently merged into the landscape.

Keywords: Spatial delight, environmental comfort, vernacular inspirations, climate responsive architecture

1. INTRODUCTION

During his first years in practice, Mies van der Rohe's influence in Murcutt's work was undeniable, as was the case with the Laurie-Short house, whose design, as described by Fromonot (2003, p. 92) was a Meisian styled transparent glass and steel box; a foreign language which didn't respond to the Australian context. As Fromonot (2003) clarified, once Murcutt realized the importance of carefully studying Australia's climate and landscape, he then analysed and reinterpreted elements of Australian vernacular architecture and indigenous life, as a method to achieve designs that responded to the specific Australian context.

This process of proficiently understanding the Australian climate and landscape, has yielded several basic design principles, which he skilfully applies and readapts consequently in each project. Among his basic design principles orientation (facing north) can be considered essential, as it defines two fundamental design aspects: access to sunlight and prevailing winds. Additionally, Murcutt closely studies the site's geomorphology and views, (Figure 174) in order to make a confident decision on the building's setting.
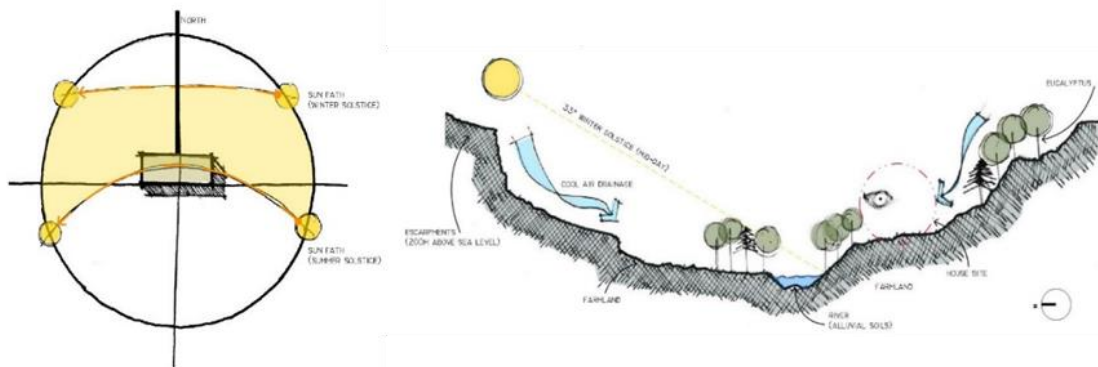
Figure 174. Left: Orientation as a basic design principle, allows the project to benefit from sunlight and prevailing winds. Right: Site analysis based on Glenn Murcutt's sketches. Heath, K (2009).

Once these key aspects were considered, Murcutt studied the rainfall and solar angles to define the roofing and overhangs shape and dimensions. Subsequently, he favours to design slim spaces with a standard height (commonly 2,10 m.) and permeable, light skins based on vernacular architecture and aboriginal traditional shelters, as shown in Figure 175; these spaces are then complemented by reinterpreted elements, (i.e. verandahs, clerestory windows, glazing louvres and blinds) whose form, function and materiality are intended to act as the catalysts for Murcutt's responsive architecture.

Figure 175. Left and middle: Australian aboriginal bark shelters on stilts (off the ground). From Lee, D (2010). Right: Australian verandah. From, West End Cottage (2012).

Murcutt was commissioned in 1975 the design of the Marie-Short house, set in a farmland near the coast of Kempsey, (NSW); considering the site's location and building materials available locally, Murcutt opted to reinterpret the simple design of traditional Australian woolsheds, (Figure 176) while providing a design whose form and materiality, responded accurately to the project's site and climatic conditions.

Figure 176. Left: Traditional Australian woolshed. Murray Johnson. Right: Marie-Short House (1980). Richard Powers

With the Marie-Short House, Murcutt discovered his own architectural language, thus representing a landmark in his career. In order to provide further evidence and assess the overall performance and spatial delight delivered by the Marie-Short House, further analysis and simulations were necessary.

In order to holistically identify the effect that natural ventilation, shading strategies and the reinterpreted vernacular elements had on the performance and spatial delight of the house, both luminous and thermal environments were analysed through detailed computer aided models, in order to have reliable data. It is important to acknowledge that Brisbane's (Queensland) weather file was used for all simulations, (as the closest weather file available) during midday on the 1st of January (as the worst case scenario), to determine the influence that Murcutt's environmental design principles, had on the comfort levels of the house during the warmest day of the year, according to weather data.

2   SPATIAL DELIGHT IN THE MARIE-SHORT HOUSE

Murcutt's profound understanding of the site, (its landscape, views and climate conditions), led him to outline a house whose main function was to provide shelter, while allowing its spaces to adjust according to their inhabitants needs. During summer, he considered the heavy rains and high temperatures, which consequently would convey in significant levels of humidity; Murcutt also recognised that winter was mild and solar access would be his main concern. Murcutt's in-depth knowledge of the site's climate, seemed to have led him instinctively to overlay the traditional elongated woolshed, with the lean aboriginal bark shelter on stilts, as a new, reinterpreted building typology (Figure 177); one which once raised off the ground '…also enhances airflow and ventilation' as Murcutt explained (Beck and Copper, 2002).
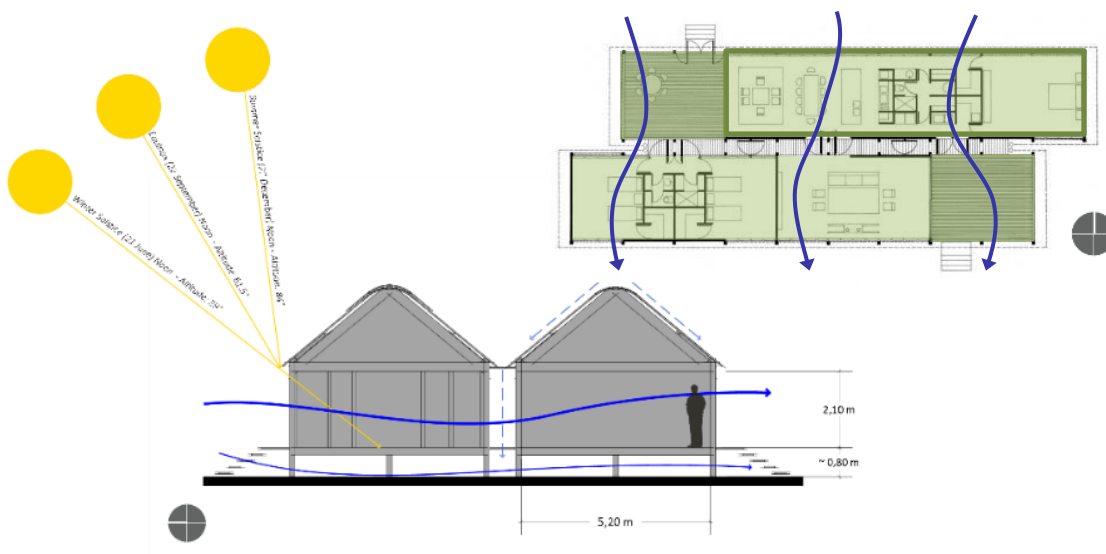

Figure 177. Top: Current layout of the house, by Oz.e.tecture (2013). Bottom: Sun, wind and rainfall analysis in the MSH. From authors.

As Figure 177 illustrates, the final design is composed by two symmetrical modular wings, (one north oriented, the other facing south) connected through a central corridor that acts as a rain gutter; both

modules are staggered and raised from the ground with wooden stilts; the roofing shape and overhang's responds to the solar altitude (84.8°) in summer solstice at noon, in order to prevent any direct sunlight and heat gains from accessing the interior. According to Murcutt, designing separate wings decreased the project's scale and if relocation is needed, disassembly will be effortless; nevertheless he 'wanted the quality of living to be close to the edge, and to enjoy the landscape views.' (Beck and Copper, 2002). This link between the interior and exterior is maintained throughout the building, by openings on both main facades composed by glazed louvres with blinds, providing the inhabitant the control on the amount of daylight and fresh air inflowing.

The northern wing (facing the sun), contains the house's main living spaces (i.e. main bedroom, dining room and kitchen) whereas, the southern wing contains the secondary bedrooms and a more secluded living room. The central corridor is vital, as the pivot-hinged doors alongside connect the main social spaces, while improving the conditions for cross ventilation. At the end of the corridor, both wings are buffered by verandahs, which act as shading devices.

When analysing the house's current layout, it seems contradictory that Murcutt positioned the main bedroom to the east, exposing the space to morning heat gains; nonetheless, as Figure 178 demonstrates, the original layout was conceived differently, as two wings with distinct uses, (i.e. north wing contained social spaces, while the southern wing, the bedrooms) and therefore, with different needs and expected performances.
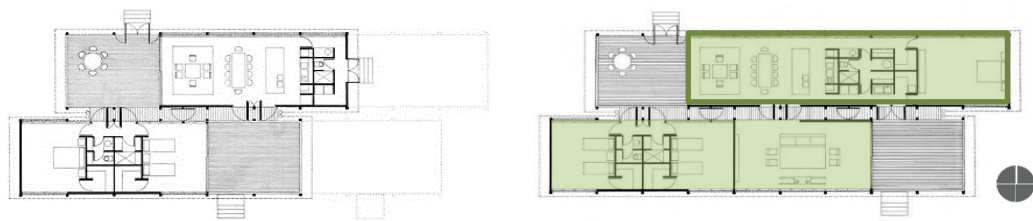
Figure 178. Original layout (1975) and current layout after renovation (1980). Layouts by Oz.e.tecture (2014)

The northern wing, was designed to be exposed to northern sunlight and prevailing winds, whereas the southern wing was intended as a relaxing area thus, sheltered from direct exposure to daylight and heat gains. After the expansion and their variation in activities, Murcutt was seemingly conscious of the environmental consequences of this alteration; when examining the luminous environment of each wing, (while overlapping the sunpath diagram) as

Figure 179 illustrates, Murcutt intentionally arranged the spaces, so that the northern (and
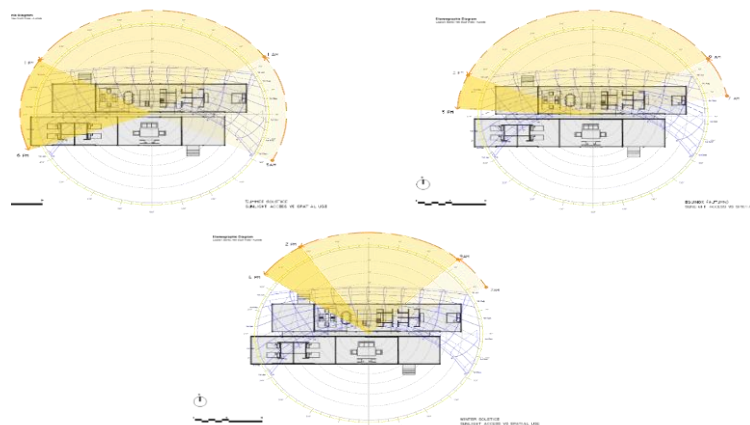
public) wing, received daylighting throughout the year

Figure 179. Time and spatial arrangement. Sunpath analysis during summer solstice, equinox and winter solstice.
From: Authors

3   DAYLIGHT ASSESSMENT OF THE MARIE-SHORT HOUSE

In order to assess the interior daylight conditions during summer, the house's main spaces, (i.e. living rooms and bedrooms) were analysed under an overcast sky condition at noon, on the 1st of March (warmest day), with all the blinds fully opened. In favour of attaining meaningful results between the daylight performances of the spaces in both wings, both the daylight factor and the illuminance outcomes were compared in two categories, each one corresponding with the activity held in each zone.

Table 88. Daylight performance comparison between living rooms. Daylight Factor (%) and Illuminance assessment in ECOTECT and Radiance. From: Authors

As the measurements in Table 88 show, the northern living room (NLR) has an average DF of 5% and an illuminance level greater than 650 lux towards the exterior and lower than 150 lux towards the back wall; while the average daylight factor implies that there is no need for artificial lightning, the illuminance levels surpass CIBSE's Code for Interior Lighting recommendations, suggesting that the strong contrast existing between the exterior and the back wall, can create visual discomfort (i.e. glare), providing evidence that once the blinds are shut, they will ease this visual discomfort, nevertheless in order to improve the visual comfort levels, the window sizing should comprise approximately 20% of the wall area as Heywood (2012) advises.

Given the different orientation of the southern living room (SLR), different results were expected compared to the NLR; as shown in Table 88, surprising results were drawn for the daylight simulations; while the average DF was of 9%, the lux levels incident on the interior surfaces, ranged between 250 and 750 lux. Despite daylight is more uniformly distributed when compared to NLR, (as it receives both indirect daylight from the exterior, and direct daylight from the skylight Murcutt designed for this space), the illuminance levels indicate the risk of experiencing visual discomfort too.

The bedroom areas, (given their use and arrangement) were expected to perform differently from the living rooms previously assessed. As Table 89 demonstrates, the average daylight factor for the northern bedroom (NB) is 4.5%, whereas the illuminance levels rapidly increase from 150 lux in the centre, to 750 lux towards the openings. Although no artificial lighting is needed, again the risk of visual discomfort is present but not significant because of the use of these spaces.

Table 89. Daylight performance comparison between bedrooms. Daylight Factor (%) and Illuminance assessment in ECOTECT and Radiance. From: Authors

The more sheltered southern bedroom (SB), was strategically positioned by Murcutt to receive less direct sunlight (and heat gains) throughout the year as Table 89 revealed. Nevertheless, as showed, the average DF was 9% (reassuring no artificial lighting is needed), while the illuminance levels ranged similarly to the NB, (i.e. between 150 - 750 lux) pointing the blinds as an essential, yet not sufficient element, in order to achieve greater visual comfort toward the edges of the building.

4   THERMAL ASSESSMENT OF THE MARIE-SHORT HOUSE

To assess the thermal conditions in the selected spaces (during summer), a model of the house was built in EDSL TAS, distributing each space as a separate thermal zone (Figure 180), and analysing the connection between their resultant temperatures in relation to their openings, building materials and adjacent buffer zones (i.e. verandahs). These thermal simulations were performed from day 355 until day 80, corresponding to the Australian summer time.
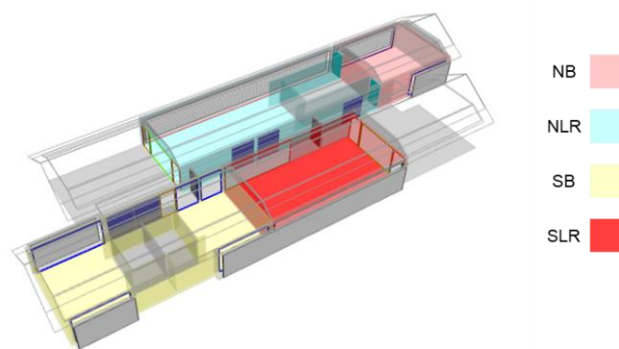

Figure 180. Thermal zoning of key spaces for simulation in the Marie-Short house. Thermal assessment in EDSL Tas. From: Authors

The assessment considered four possible cases (Table 90), all having a constant natural infiltration rate of 0,25 ACH and shading as designed, but varying in the levels of internal heat gains and natural ventilation rates. Case 1 was set up as a base example, case 2 as the worst possible scenario without natural ventilation; cases 3 and 4 represented the best possible scenarios, were natural ventilation was introduced initially by a 50% of aperture to the openings, and a 95% of aperture correspondingly, in order to have a clear perspective on the impact natural ventilation had on thermal comfort.

Table 90. Summary of thermal cases examined

	Presence (Yes / No)	Presence (Yes / No)	Presence (Yes / No)	Presence (Yes / No)
Internal heat gains	NO	YES	YES	YES
Natural ventilation	NO	NO	YES (50%)	YES (95%)
Case	1	2	3	4

The following assumptions were considered for the simulations:

- Weather: Energy Plus weather data for Brisbane, Queensland.
- Comfort range: during summer it was assumed to be between 25°C to 28°C.
- Calendar: summer period was assumed to be from the 21st of December until the 22nd of March.
- Internal Gains: the following values were assumed:
  - Three people occupying the house, whose heat gains were assumed to be 120W per person, 75W sensible and 45W latent.
  - The occupancy schedule was set assuming a weekly work schedule, were occupancy is highest during sleep time and falls during daytime, experiencing peaks during early morning (6-9am), lunch (12-2pm) and evenings (5pm onwards).
- Lighting: compact low-energy florescent bulbs with a 25W thermal load per light bulb, with a total load of 9 W/m^2
- Equipment and appliance gains: equipment's considered were a hob, a washing machine, a dishwasher and a fridge, all with a total load of 27 W/m^2.
- Infiltration rate: was considered to be 0.25 ACH in all zones.
- Ventilation: all openings have the same opening pattern during the periods when the house was occupied and set to start opening when the temperature reached 25°C and to be fully opened at 28°C.
- All the cases included shading from the blinds and verandahs.

Thermal Assessment Results

Similarly to the daylighting performance results, thermal analysis outcomes were compared in each thermal zone with similar activities, examining any correlations amongst them. The results were shown as a percentage of time when the resultant interior temperature ranged between 25°C and 30°C.

As Table 91 shows, both living rooms present different thermal performances. It is important to emphasize, that while both zones have a similar area, the heat gains vary greatly, as the northern room includes the kitchen's appliances heat gains

- Case 1: in both zones the probability of achieving comfort levels was 46:54, as in practically 45% of the hours, both spaces are above the comfort range.
- Case 2: the addition of internal heat gains while the envelope remains closed, (without any ventilation) led to an outstanding increase in the frequency of hours out of the comfort range in both zones; representing for the NLR over 48% of the hours out of the comfort range, while for the SLR, over 84%, showing that the envelope and shading strategies designed alone are not enough.
- Case 3: 50% of aperture in doors and windows significantly increased the frequency of hours within the comfort range for both zones, proving that natural ventilation work as intended. For over 60% of the time the resultant temperatures are within the comfort range.
- Case 4: 95% aperture in openings did not significantly improve what was achieved in the previous case and comfort is achieved for over 60% of the hours, proving that a partial aperture of the openings is enough to cool down the interior temperatures.

Table 91. Thermal performance comparison in living rooms. Thermal assessment in EDSL TAS. From: Authors

THERMAL ZONE	FREQUENCY OF HOURS (%) OF RESULTANT TEMPERATURE DURING AUSTRALIAN SUMMERTIME (DAY 355 – 80)
North Living room (NLR)	

Band (°C)	< 25°C	25°C >=	26°C >=	27°C >=	28°C >=	29°C >=	30°C >=
Case 1	19,6%	14,6%	17,9%	13,8%	9,0%	6,9%	18,1%
Case 2	8,8%	6,5%	13,3%	17,0%	15,6%	13,5%	25,3%
Case 3	22,5%	17,7%	21,1%	12,4%	9,9%	6,8%	9,6%
Case 4	26,4%	19,8%	18,7%	11,5%	9,7%	5,9%	8,0%

THERMAL ZONE	
South Living room (SLR)	

Band (°C)	< 25°C	25°C >=	26°C >=	27°C >=	28°C >=	29°C >=	30°C >=
Case 1	1,1%	4,0%	11,1%	17,7%	17,9%	15,1%	33,2%
Case 2	0,1%	0,2%	1,4%	3,7%	10,5%	17,5%	66,5%
Case 3	11,9%	16,9%	20,3%	16,9%	11,3%	9,5%	13,2%
Case 4	16,0%	18,1%	19,9%	16,0%	9,9%	8,5%	11,5%

Thermal performance in both bedrooms had a comparable behaviour as Table 92 shows.

- Case 1: in both zones, the probability of achieving comfort levels without any ventilation present is over 65% of the hours; the exposed facades, plus the screening provided by the verandahs influenced, nevertheless for 35% of the hours, the rooms exceed the comfort range.
- Case 2: the results indicated that the addition of internal heat gains (while the envelope is closed), do not affect substantially the frequency of hours the bedrooms are within the comfort range (over 50%). The spatial arrangement of these spaces within the house is key to attain thermal comfort levels.
- Case 3: 50% of aperture in doors and windows increased the frequency of hours (above 70%) when resultant temperatures are within the comfort range in the bedrooms, demonstrating that both natural ventilation improves the thermal comfort.

- Case 4: A 95% of aperture in openings, slightly increased the frequency (above 75%) of hours that resultant temperatures were within the comfort range, showing that openings are essential to improve the thermal comfort of these spaces.

Table 92. Thermal performance comparison in bedrooms. Thermal assessment in EDSL TAS. From: Authors

THERMAL ZONE	FREQUENCY OF HOURS (%) OF RESULTANT TEMPERATURE DURING AUSTRALIAN SUMMERTIME (DAY 355 – 80)
North Bedroom (NB)	**North Bedroom - Case comparison** Frequency (hours) of resultant temperatures during Australian summertime (day 355 to 80)

Band (°C)	< 25°C	25°C >=	26°C >=	27°C >=	28°C >=	29°C >=	30°C >=
Case 1	19,3%	14,5%	17,7%	13,5%	9,8%	6,0%	19,1%
Case 2	10,5%	8,6%	14,7%	18,1%	13,8%	12,3%	21,9%
Case 3	26,4%	17,9%	18,0%	12,0%	9,7%	6,2%	9,9%
Case 4	29,6%	16,9%	18,6%	11,0%	9,0%	6,4%	8,6%

South Bedroom (SB)

South Bedroom - Case comparison
Frequency (hours) of resultant temperatures during Australian summertime (day 355 to 80)

Band (°C)	< 25°C	25°C >=	26°C >=	27°C >=	28°C >=	29°C >=	30°C >=
Case 1	23,6%	15,5%	17,7%	13,4%	8,5%	8,0%	13,3%
Case 2	18,4%	16,6%	17,5%	15,9%	11,3%	9,6%	10,8%
Case 3	26,8%	18,4%	17,5%	13,1%	10,5%	5,5%	8,2%
Case 4	29,8%	18,6%	17,5%	11,3%	9,9%	5,3%	7,7%

5   CONCLUSION

The greatness of the Marie-Short house at first glance might be disguised as a modest woolshed. It stands lightly, quiet and unpretentious surrounded only by the Australian landscape.

Through this humble design, Murcutt transformed a seemingly artless woolshed, into a fascinating almost-like machine, allowing its inhabitants to adjust the spaces accordingly to their needs. Just as Heath (2009) described Murcutt's work as a choreography, 'designed so it can literally be tuned like an instrument to respond to seasonal cycles', the Marie-Short house performed as it was designed to, as a free-running building.

Murcutt's environmental design principles, (i.e. orientation, natural ventilation, shading and designing a light weighted building, raised off the ground on stilts) yielded in a low energy consuming building, whose constant interaction with the outside, makes it reliant on the inhabitants', whose needs will dictate how to operate and adapt their spaces. Undoubtedly as the results demonstrated, in order increase thermal comfort, the key living spaces are dependent on natural ventilation, as the shading alone will not significantly decrease resultant temperatures. On the other hand, and even though Murcutt provided the main facades with integrated blinds, the results have proven that when left opened, the inhabitants will experience visual discomfort, indicating that even when Murcutt wanted to have a constant connection with the exterior, reconsidering the opening sizes might improve the visual comfort and spatial delight of the house.

Even when the Marie-Short house is fully disassembled and its performance verified, Murcutt's design brilliance and skilfulness overlaps his apparent deficiencies. The Marie-Short house has to be analysed as a free-running building, one which constantly changes and adapts to the climate and therefore its inhabitants needs.

It is important to consider that in spite of the findings, Murcutt designed this building with unpretentious local materials and construction techniques, whose sole aim was to provide shelter, while constantly connecting his man-made space with the sacred natural realm; his ingenious application of reinterpreted vernacular elements such as: verandahs, overhangs and narrow spaces with permeable skins, have demonstrated that once combined with Murcutt's environmental design principles, yield in a self-reliant, low energy consuming building.

Murcutt's spatial quality transcends from mere aesthetics into comfortable and delightful spaces; through his designs, he has revitalized the importance of vernacular architecture as a method of responding to the environmental conditions, rather than imposing; through humble, yet innovative architectural solutions lies the significance of Murcutt's work; through a modest design, he has provided the inhabitants with a priceless self-sufficiency to manoeuvre and adapt their spaces accordingly to their needs, while always praising the Australian landscape.

6 REFERENCES

ATKINS, J, 2011. Glenn Murcutt – Internationally Recognized Australian Architect. Greater Port Macquarie Focus. Available at: http://focusmag.com.au/pmq/interviews/glenn-murcutt-internationally-recognised-australian-architect. [Accessed 16 May 2014].

BECK, H., Cooper, J., 2002. Glenn Murcutt: A Singular Architectural Practice. Edition. Images Pub.T

CIBSE, 2002. Code for Lighting. 1 Edition. Butterworth-Heinemann.

DREW, P, 2000. Touch This Earth Lightly: Glenn Murcutt in His Own Words. First Edition. Duffy & Snellgrove.

FROMONOT, F, 2003. Glenn Murcutt: Buildings and Projects 1962-2003, Second Edition. Rev Sub Edition. Thames & Hudson.

HEATH, K, 2009. Vernacular Architecture and Regional Design. Edition. Routledge.

HEYWOOD, H, 2012. 101 rules of thumb for low energy architecture. RIBA Publishing.

LEVENE, R. C., & Márquez, C. (2012) Glenn Murcutt 1980-2012: Plumas de Metal - Feathers of Metal. Madrid. El Croquis.

LEWIS, J, 2007. The Native Builder. New York Times. Available at: http://www.nytimes.com/2007/05/20/magazine/20murcutt-t.html?pagewanted=all&_r=0. [Accessed 16 May 2014].

MURCUTT, G, The Marie Short House (2014) OZETECTURE. Available at: http://www.ozetecture.org/2012/marie-short-glenn-murcutt-house/. [Accessed 17 May 2014].

West End Cottage (2012). Verandahs and Sleep outs. Available at: http://westendcottage.blogspot.co.uk/2012/07/verandahs-and-sleepouts_20.html [Accessed 16 May 2014].

163: Development of timber structure and green building in China

XIAOYANG LI[1],SHANGQUN XIE[2]，1, QINGQIN WANG[1], ZHIJUN CHENG[1]

1 China Academy of Building Research, China
Beijing Jiaotong University, China.

This paper introduces the development, current situation and insufficiency of timber structure in China，and offers a proposal. After analysing technical standards of timber structure, the paper supplies the ideas and development proposals of timber structure in China.

Keywords: timber structure, green building, technical standard, Chinese standard.

1. INTRODUCTION

With the continual growth of globe economy, we have to face the problems like resource shortage and environment pollution. In 2014, over 28% of the total energy consumption had been consumed by the building in China. The building energy consumption accounts for the total energy consumption of 35%, by the prediction of international experience and the current technical level of the building, in 2020. Building energy consumption will be the main use of the social energy consumption. In recent years, almost 2 billion square meters of the buildings have been built per year. No matter the construction land and materials, or the level of the economic development, couldn't afford the construction requirements. The development of green building has become a strategic choice to reduce the energy consumption and pollution emissions, enhance resource conservation and environmental protection, and realize the coordinated development, such as economy, population, resources and environment. Timber constructions have lots of advantages, such as easy to construct, eco-friendly, energy saving, lower-carbon, close to natural, etc. In the whole life cycle, the timber construction can make the most of the resource saving, environmental protection, and reduce the pollution emissions, harmonious coexistence, which is one of an important forms of green building. Due to widespread misunderstanding on the timber structures, such as safety, this kind of structure stay on a low proportion.

2 HISTORY OF TIMBER STRUCTURE DEVELOPMENT IN CHINA

With a long history, the timber structures in ancient China has get an excellent achievement, and occupies a unique position in the ancient building development. The technology of timber structures has important influence on Japan, Korea and other countries, in the period of ancient China. The research on the Zhejiang Yu'yao He'mu'du ruins and Xi 'an Ban'po site, which represent the two reveler civilization, shows that the technology of timber structures had reached a quite high level as early as 7000 to 5000 years ago. The ancient timber structures is the connection of beam and column by use of mortise and tenon, which had basically formed in West Han Dynasty. Rules of Architecture, written by Zhang Jie, unified the construction practices in Late Tang Dynasty. Through the effort of thousands of years, architects made a great innovation in practice and theory. Books like Yuan ye and Engineering Practice Cases of ministry of Works in Qing Dynasty, appeared yin Ming and Qing dynasty, had promoted the technology of timber structures to make brilliant achievements. The Sakyamuni pagoda of the fogong temple in Shanxi Yingxian and Hanging Temple in Shanxi Yingxian, Chinese oldest and highest timber structures building, is still well preserved for more than1000 years.

By the mid of 1970s, the timber structures is always an important member of Chinese buildings. Since 1980s, in order to protect forest resources, the government advocate of using the steel or plastic to replace the wood. The research on timber structures has been slow in the last 20 years. The timber structures enjoyed new opportunities for development, because of light wood frame construction come from North America had been introduced in China, by the 1990s. Some high-grade houses (and also high price) had been built for foreigners, because of the most component of the structure had been imported from North America. Since China's accession to the World Trade Organization in 2001, wood imports to zero tariff, the number of timber for structures imported increases year by year. To get the useful experience through study the technologies of timber structures from USA and Canada, the teaching, researches, and the standard setting for timber structures engineer and application, are facing with t a new period of development.

3 THE DEVELOPING STATUS ,PROBLEMS AND SUGGESTION OF TIMBER STRUCTURE IN CHINA

3.1 The Status of Timber Structure in China

In recent decades, timber structures is facing with rapidly development. First, amount of the light wood frame construction have been used in large industry constructions and civil buildings. In estimated, since 2000, more than 10 thousand of light wood frame construction have been built in Beijing, Shanghai, Nanjing, Hangzhou, Xi'an, Wuhan, and some cites in Hainan province. Secondly, glued timber structures appeared and developed at a great speed. Hangzhou Xiangji Temple, Jiangsu Xujiang Wooden Arch Bridge and Liuzhou Kai'yuan Temple, are best practices for the glued timber structures. Thirdly, application research on bamboo and bamboo-wood composite materials, with Chinese characteristics, has made remarkable progress. Light bamboo structure system has basically taken shape and got the patents. Fourth, a series of standards for timber structure has made or is underway, including design, construction, and quality acceptance. Last, courses and research on timber structures have been restarted in some colleges and

institutes. By providing funds from the government, researcher began to pay more attention on timber structure and carried out international cooperation and exchanges.

According to estimation, more than 1000 companies engaged in timber structure constructions or materials supply in China. The companies are main located in Shanghai, Beijing, Tianjin and other cities, Guangdong, Sichuan, Fujian, Heilongjiang, Jilin, Jiangsu, Shandong, Guizhou, Hu'nan, Xinjiang and other provinces.

The existing buildings of timber structure, in China, less than one over one thousands of foreign countries. But the enormous market demanding give the timber structures a bright future. According to China Modern Wood Structure Construction Technology Industry Alliance projections, market volume of the whole timber structure is expected to reach 3.5 million square meters per year in China, in the coming 3 years. Including: 34% of villas, 17% of welfare houses, 14% of buildings in vacation areas, 9% buildings for education & culture, 9% buildings for community service, 6% of the landscape architecture, and so on. Timber combined with concrete structures market is expected to reach 0.5 million square meters per year. The concrete structure for foundation and lower structures, and timber structure for top structure (less than 3 layers, the whole structures less than 7 layers). This kind of structure has more potential application, is expected to 30% of the timber structures.

3.2 Problems and Suggestions of Timber Structure

With the rapid development of timber structures in China, there are many problems and challenges in the developments and applications. The analysis and proposals are as follows.

Land Utilization

Limited land, large population and growing prices lead to high construction costs. Ministry of Land and Resources of PRC claim that control the construction of villas and high-end residential, stop the approval of land use for villas, in 2003. The limit of villa construction limits the development of Chinese timber structure.

As the reasons above, we should put timber structure development emphasis on the new village construction, earthquake-prone area, rural-urban fringe and temporary structure in the tourist area. The villagers have their own bungalows and reconstructions will increase the land utilization efficiency. The earthquake-prone areas are mainly distributed in the extensive rural or mountainous areas. Chinese timber structure can be used for earthquake prevention and disaster reduction in those areas. Multi-story timber structure can be built in the rural-urban fringe to meet the demand of the new development of urbanization. Timber landscape structures built in the tourist area not only protect cultivated land but also beatify the environment.

Forest Resources

The shortage of forest resources makes the lack of timber in China. We can import timber and learn timber structure technology from international market in the globalization era, such as low cost dimension lumber (SPF) from North America, larch and Pinus sylvestris from Russia. We can make full use of planted fast-growing forests instead of nature forests which are protected and forbidden to cut in China. There are more than 4000 hectares planted fast-growing forests in China, the largest quantity of the world. Multiply plywood and laminated veneer lumber (LVL) can be made from poplar to import.

Ideological Understanding

The structure safety, endurance, flammable, and damaged by insect or humid situation, is the common misunderstanding about timber structure. Even the modern timber structure hasn't been accepted by consumers too. So engineers have the duty to tell the consumers about the advantages of modern timber structure, by project demonstration, can change the people's ideological understanding. Its green essence will be recognized gradually.

Construction Cost

The cost for construction is always a top question, concerned by developers, builders and consumers. Most of the timber materials used is imported. Due to lack of technology, parts of the main units for timber structures have to take abroad for produce. So the construction cost for timber structures reaches RMB 4,000-6,000 per square meters (does not include the cost of land). Higher than concrete block buildings, combined with the cost for maintained, the cost for timber structure couldn't be afforded by common people. How to reduce the construction cost of timber structure is important for large scale application. Material is the main cost, and it's easy to be replaced by using different origin or grade materials. So it's possible to control the construction cost in an affordable range. First of all, using the local material, especially using the numbers of fast-growth trees, instead of imported material, also could reduce the cost for transportation. Secondly, improving the technology level for timber processing, reducing production cost. Thirdly, optimization the structure design, timber frame combined with concrete frame, wood wall combined with block wall, light timber structure combined with light bamboo structure, etc.

The Technology of Design and Construction

In recent decades, building in China base more on concrete structure and masonry structure so design professionals on timber structure building relatively scarce. At the same time, domestic professional construction qualification is not set, different from foreign timber construction. Especially some small construction units construct by experience and do not ensure quality, which severely restricted the development of timber construction.

This phenomenon is gradually improving. Tongji University, Harbin Industrial of University, Southeast University and other colleges and universities are actively involved in the research and development of timber construction and churn out generations of undergraduate talent. Exploration on design with the Chinese model of the Chinese culture and unique structure and design software suitable for the development of the Chinese timber structure helps timber construction occupies an important position in the construction field in 5 ~ 10 years in the world. On the production technology, domestic enterprise create own industry and manufacturers through the introduction of foreign advanced manufacturing technology and product, digestion and innovation. They research on building materials, structure, indoor and outdoor decoration, focus on the structure of materials, components production and construction technology to speed up the localization of timber construction.

Function and Protection

Being reliable and having functions are the basic requirements to the timber structure. Timber is susceptible to be damaged by pests. Especially, the strength stability and durability of timber structure will be weakened when eroded by termites, which may lead to serious accidents. In addition, that whether the timber structure can ensure the functions of sound insulation, heat preservation and insulation, vibration isolation, seismic and fire safety are widely worried and concerned. However, we can completely be cleared away the barriers of development of timber structures by several ways in China. On one hand, there are plenty of mature experiences on the protection of timber structure can be used for reference, especially absorb the experience of timber structures in ancient China. On the other hand, we can take preventive measures according to the requirements of the national standard "Standard for Design of Timber Structures" to avoid the damages of fire, pests, and corrosion.

4 ANALYSES ON CHINESE STANDARDS OF TIMBER STRUCTURE
4.1 Introduction to Chinese Standards of Timber structure

Technical code for maintenance and strengthening of ancient timber structures had been issued by the Ministry of Construction of the People's Republic of China as a national standard with a serial number of GB50165-1992, in 1992. This standard specified technical requirements for maintenance and reinforcement of ancient timber structures. With acceleration of industrialization, the activities of standardization for wood structure in China are carried out constantly.

Standards Currently in Effect

- National standard GB 50005-2003:code for design of timber structures
- National standard GB/T50772-2012:code for construction of timber structures

- National standard GB50206-2012:code for acceptance of construction quality of timber structures
- National standard GB 50016-2014:code for fire protection design of buildings
- National standard GB/T50708-2012:technical code of glue laminated timber structures
- Professional standard JGJ/T265-2012:technical code for light wood trusses
- National standard : technical code for partitions with timber frame wore
- Professional standard JG/T 303-2011:wood compound door
- National standard GB/T 27654-2011: wood preservatives
- National standard GB/T 27651-2011:use category and specification for preservative-treated wood
- National standard GB/T 22102-2008:preservative-treated wood
- National standard GB/T 50329-2002:standard for test methods of timber structures
- National standard GB/T 26899-2011:structurl glued laminated timber
- Shanghai local standard DG/TJ08-2059-2009:technical specification for wood frame construction
- Handbook of design of timber structures

Standard Drafting

- National standard: timber classified machine
- National standard: Standard methods for development of characteristic mechanical values for structural lumber

. Other Important Standards

- National standard GB 50009-2001:load code for the design of building structures
- National standard GB50011-2010: code for seismic design of buildings
- National standard GB 50176-93:thermal design code for civil buildings
- National standard GB50189-2015:design standard for energy efficiency of public buildings
- Professional standard JGJ 26-2010:design standard for energy efficiency of residential buildings in severe cold and cold zones
- Professional standard JGJ 75-2012:design standard for energy efficiency of residential buildings in hot summer and warm winter zone
- Professional standard:JGJ134-2010:design standard for energy efficiency of residential buildings in hot summer and cold winter zone
- National standard GB/T 50824-2013:design standard for energy efficiency of rural residential buildings
- National standard GB50118-2010:code for design of sound insulation of civil buildings
- National standard GB50300-2013:unified standard for constructional quality acceptance of building engineering

Abstract of Important Standards Issued in Recent Years

Technical code for light wood trusses governs requirements for material, construction, quality of light wood trusses. Thereof the goal is to enable the achievement of higher quality, durability and structural safety. National standard GB50206 amended in 2012 not only governs higher requirements for acceptance of materials, but also improves quality control of construction and standards for acceptance of construction quality of timber structures.

Especially, the chapter named as "timber structures" was first inserted in GB 50016-2014, which contains the requirements of fire protection design of buildings as follows:

- Enlarges the scope which is this code is applicable, not only civil buildings, also commercial buildings and some industrial building.
- Reduces the requirements of fire protection design of single-family or multifamily light wood trusses.
- Allows timber frame applied in existing concrete buildings.
- Increase the maximum allowable stories of building, up to 7 layers
- Allows glue laminated timber structures applied in some civil or Industrial buildings.

4.2 Problems of Chinese Standards of Timber structure

The development of timber structure has to be restrained by the Technical Standards for sustainable. Series of standards for timber structure in China have been established, although there are many problems. The analysis and proposals are as follows.

First of all, existing theory of design for timber structure in China come from the former Soviet Union, which is only applicable to timber structures made of cast-in-situ component.

Secondly, the division and boundaries between the existing standards should be clear-cut, each one being charged with specific responsibilities. For example, it is suggested that production requirements of glue laminated timber in GB50206-2012 should be moved into standards of wooden product.

Thirdly, when code for design of timber structure GB 50005-2003 is revised, significant improvements will be made in the following areas:

1) Strength grade of timber in GB 50005-2003 was based on the type of wood, so reliability cannot be guaranteed. Strength grade of timber should be classified by standard stress, which is widely used in the field.

2) Degrees of reliability of timber structure and strength design values optimization should be amended. Wooden components shall meet the requirements of reliability governed by GB 50068. So, considering the influence on strength of timber by sustained load in all phases of the usage cycle GB 50005-2003 Specifies reliability of the tension member, compression member, bending member, and shearing member as 4.3, 3.8, 3.8 and 3.9, respectively. But the requirements of reliability met by wood components other than log and square timber can't be affirmed. Further work is needed to be done. From another point of view. The question whether wooden components need to meet the requirements of reliability governed by GB 50005 is worth consideration, because wooden component is replaceable and its service life can properly be shortened。

3) The design calculation method of resistance and bearing capacity of structural members is not yet ripe. A key characteristic of code for design of timber structures in advanced countries is that his design calculation method normally is applicable to all kinds of wooden structural members. However, GB50005-2003 requires timber classified machine randomly use some formulate of log and square timber. Whether it is scientific and reasonable is needed to test and verify.

Consequently, Chinese code for design of timber structures should be amended to focus on prefabricated, standardized, industrialized timber instead of log. At the same time, standards of wooden product will take charge of production of wood products, classification and identification of products. The division of labour is clear-cut, each one being charged with specific responsibilities.

5   CONCLUSION AND SUGGESTION

Suggestions on the Implementation of Promotion to the Development of Green Building in China were issued jointly by the Ministry of Finance and the Ministry of Housing and Urban-Rural Development on April 27, 2012. Action Plan for Green Building was announced by the General Office of the State Council on January 1, 2013. "Twelfth Five-year" Green Building and Eco-City Development Program was issued by the Ministry of Housing and Urban-Rural Development on April 3, 2013. The government strongly promotes the developments and applications of green buildings, green materials, green manufacture technology by industry policy, the revenue policy and so on.

Timber constructions have lots of advantages, such as lower-carbon, energy saving, easy to construct, eco-friendly, etc. so, the development of timber constructions meets the requirements of state energy saving, pollution reducing and Sustainable Development Strategy. China shall not only draw lesson from the successful practice in Japan, North America and northern Europe, but also according to characteristic of our own architecture culture, material, technology, with the concept of science and technology, innovation and development, establish its own policy system, regulations and standards system of timber structure. Furthermore, the proposals are as follows.

Firstly, it is to formulate the development plan and perfect industry policy that is very significant for sustainable development of timber structure.

Secondly, it is necessary to establish wood structure technology alliance composed of enterprises, academies, colleges, and so on. Through research collaboration, the technical problems of timber structures in China will be solved, and its competitiveness will be strengthened. To carry out demonstration projects, to draw on experiences, to popularize and apply gradually is a good solution.

Thirdly, it is a good idea to perfect standards series of timber structures with Chinese characteristics learnt from foreign standards, which focuses on prefabricated, standardized, industrialized timber. At same time, product accreditation system can contributed to better quality of timber.

Finally, international communications and cooperation for timber structure are necessary. By making the standards and codes of timber structure, execute its strictly quality control and improve the quality of the buildings, the timber structure will be acceptable by common people. As a result, the application of timber structure in China will be widely used in the coming soon.

213: Architectural design principles for passive cooling in Cyprus climate

PERVIN ABOHORLU[1], SAFFA RIFFAT [2]

1 Department of the Built Environment, University of Nottingham, University Park, Nottingham NG7 2RD, UK, pervinabohorlu@hotmail.com
2 Department of the Built Environment, University of Nottingham, University Park, Nottingham NG7 2RD, UK, saffa.riffat@nottingham.ac.uk

Energy consumption in houses in Cyprus is mostly for cooling, with buildings responsible for 30,84% of total energy consumption. The electricity is mainly produced and consumed during the summer as demand for cooling is increased.

The aim of this study is to analyse and emphasise passive cooling strategies in traditional building of Cyprus, in order to maximize comfort level, while reducing energy consumption and the level of CO_2 emissions to the environment. Architectural design principles are analysed in terms of passive cooling to focus on the importance of climate. These passive cooling methods are reviewed in order to prevent energy consumption through the use of mechanical air conditioners.

Cyprus is hot and dry in summer, mild and rainy in winter. It is formed by two dominant mountains: the slopes facing to the north of the mountains are humid, whereas the south facing slope is drier. Different design parameters for the two different climatic regions are evaluated to show the relationship between space and passive cooling energy use.

The climatic analysis techniques such as sun path diagram and wind rose diagrams are used to evaluate the design principles of buildings. Then, Autocad is used as a drawing software to show the buildings and the cooling methods for each climatic regions, hot-dry and hot-humid. These are evaluated according to the following design principles: building shape and orientation, shading, vegetation, building layout, wall openings, topography and thermal mass material. These design principles and passive cooling methods are clearly illustrated as tables and figures to make comparison of different climatic conditions.

Keywords: Passive Cooling, Cyprus, Architectural Design Principles, Orientation

1. INTRODUCTION

The earth is usually warmed according to the natural behaviour of the sun, such as the radiation difference between summer and winter. However, human activities today are increasingly responsible for the warming of the earth. This started particularly after the Industrial Revolution in the 18th century. As Cyprus has a subtropical climate, the energy consumption in the houses is caused by the usage of heating, daylighting, and mostly, for cooling. Electricity is mainly produced and consumed during summer. Due to the extreme weather conditions, a mechanical way of cooling, i.e. air-conditioning is used. The high use of fossil fuels, as non-renewable resources can lead to environmental pollution, the need to import energy and an effect on climate change. In order to prevent these effects, passive solar architectural design principles should be considered. By formulating these building design principles, it is possible to maximize human comfort and minimize the use of energy for cooling.

2. GEOGRAPHY AND CLIMATE OF CYPRUS

The island of Cyprus is located in the north-eastern part of the Mediterranean sea, on latitude 35° N and longitude 33° E. It has an intense Mediterranean climate which is hot and dry in summer, mild and rainy in winter. It is formed by two dominant mountains, Troodos range, rising to 1,952 m, covers the south and west part, and Five Fingers (FFM) in the northern part of the island at 1,024 m, the Mesaoria Plain and the narrow coastal areas. These different topographical characteristics play an important role on the climate of Cyprus and make the island as "multi-climate" region, particularly in the distribution of wind speeds, directions, rainfalls, humidity and solar radiation (ABOHORLU, 2010, p. 65).

Due to the topographical location of the mountains, the southern slopes are exposed to the sun, creating hot and sunny weather conditions. On the other hand, the northern slopes of the mountains are cool and shaded, since it gets less radiation and the length of shadow is too long (ERLEY, 1979, pp.18-19). This area is also more humid than the southern slope as it is nearer to the sea.

3. METHODOLOGY

In this paper, architectural design principles are analysed for different climatic region of Five Finger Mountains in terms of wind and sun control by using sun path diagram and wind rose. Kozan village which is in the southern slope and Bellapais village in the northern slope of the FFM are selected as case study. The design principles are evaluated based on passive solar cooling methods such as ventilative, comfort and earth cooling. The methodology of the study is structured in order to explain clearly (Figure 1).
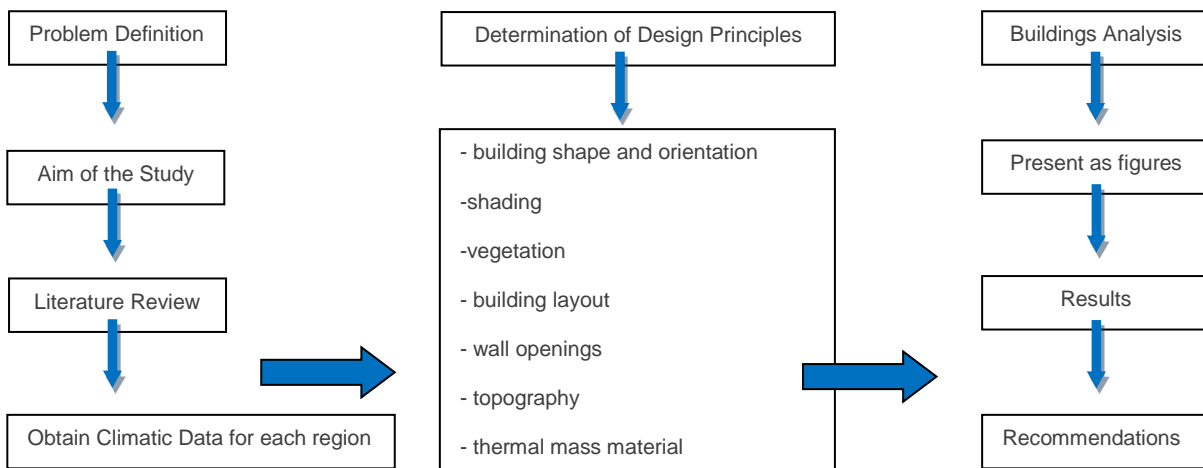

Figure 1: Methodology of the Study

4. EVALUATION OF ARCHITECTURAL DESIGN PRINCIPLES

The architectural design principles are depend on many parameters such as: *building shape and orientation, shading, vegetation, building layout, wall openings, topography and thermal mass material.* These differ according to the specific location of the buildings. Therefore, it is crucial to know the climatic conditions of the surroundings.

The **building shape and orientation** influence the effect of cooling in terms of heat gain and loss. Buildings in Kozan village are rectangle or square shaped. They have a compact-shaped design, which minimizes the surface area exposed to the sun and prevents heat gain. Since it has less surface area, the wind exposure is also reduced, particularly in winter. Orientation of the buildings is mostly elongated in the east and west direction towards the inner part of the island. Therefore, the surface area exposed to the sun for shorter east and west facade is minimized in summer. In winter, buildings receive more radiation than east and west facades. It is reversed on summer that south facade gets less radiation when comparing roof, south and west facade (MAZRIA, 1979, pp. 82-83). There are some buildings which are located in the north-south axis due to the landform. In Bellapais village, buildings are mostly rectangular in shape and elongated along the east-west axis facing to the Mediterranean sea. They are also faced to the prevailing wind direction to introduce air movement in their spaces and prevent excessive humidity. Thus, the building shape and orientation play a vital role in enhancing the effect of ventilative cooling (Figure 2).

Figure 2: building shape and orientation in Kozan and Bellapais Village

Shading devices such as canopies, louvres, screens…etc. are used to eliminate the effect of solar insolation in particularly hot regions. In Kozan and Esentepe villages, wooden shutters are mostly used to limit sunlight penetration to the living space through the window (Figure 3). As direct sunlight disturb comfort conditions for people in summer, these devices are used to prevent the effect of brightness and heat gain during the day. Additionally, the velocity of air movement can be increased by changing the positioning of casements, serving as wing walls. Narrowing the distance of two casements to the inward direction creates a venturi effect that increases the wind speed through the building. It is essential to enhance the air movement in Bellapais village due to the high level of humidity.

Figure 3: shading devices in Kozan and Bellapais Village

Vegetation can be used to shades any facades and guide wind into the building. Deciduous trees, hedges, shrubs, tree canopies, trellises...etc. are interwoven with the buildings to control air ventilation and shading. In both villages, vine-covered trellises are used to create a shaded area in summer; the dropping leaves

mean the situation is reversed on winter. In Kozan, hot-dry breeze disturbs the occupants. Therefore, shrubs are used to shade the ground and cool the air that penetrates to the building through the walls or windows. The dense planting of shrubs also acts as a wind break around the outside wall. As the roof is made from soil, plants and flowers can be grown naturally, which creates a green roof. In Bellapais village, trees are located to channel a cool breeze to lower the humidity effect within the buildings (Figure 4).
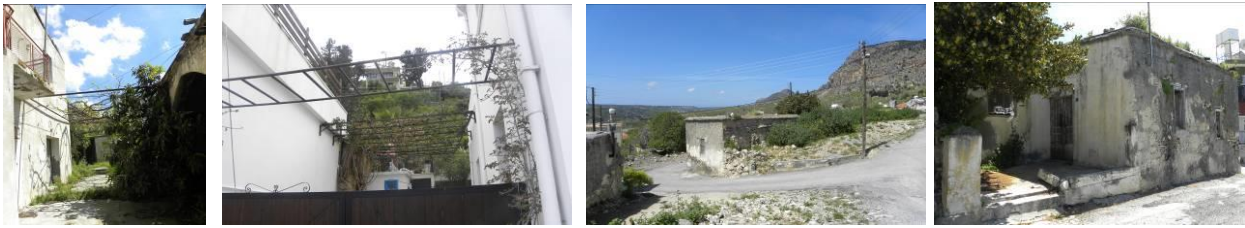
Figure 4: Vine-covered trellis, shrubs, green roof and wind control in site

Building layout plays a vital role for natural ventilation. The mostly used spaces tend to face to the south, whereas non-inhabitable areas such as storage, toilet or kitchen are placed along the north face to create a thermal buffer zone between the exterior environment and interior in Kozan village. As the sun is at a high angle in summer (13.00 with 77° altitude) and low angle in winter (12.00 with 32° altitude), living spaces are not exposed to excess sunlight in summer, but get benefit from it in winter. Additionally, better ventilation is improved in these spaces. In Bellapais, the difference is that the buildings are faced towards the north (to the sea view) according to the topography of the villages.

Building layout in mountainous areas is responsible for earth cooling as some rooms have contact with ground (Figure 5). As soil has a high specific heat capacity, it can store and conduct heat. Earth temperature changes slowly due to the large time lag of earth (BROWN and DEKAY, 2001, p. 56). It is meant that the ground is cooler in summer and warmer in winter. It takes time to loss and gain heat. Rooms facing to the ground become cooler in summer due to the properties of soil.

Figure 5: Facing to the south, west and Building layout in Kozan

Wall openings such as doors and windows enhance the level of ventilation inside the buildings. Windows placed above the door create cross ventilation and a hot air beneath the ceiling of the space is also allowed to escape to the outside in both villages, which is most useful for ventilative cooling. Sunlight causes glare discomfort in hot-dry region (GIVONI, 1994, P. 26). Thus, facades with small windows or without windows are observed in Kozan in order to reduce glare and strong wind from the prevailing wind direction. However, the number of window is more and sizes are large in Bellapais to provide better ventilation because of the excess humidity ratio (Figure 6).

Figure 6: Doors and Windows

Topography can be used to increase suitable microclimates for different kinds of location in terms of passive cooling. The streets are organized according to the topography in both villages. Since earth has high density, the heat loss in buildings in contact with earth is minimized due to conduction through the walls, providing energy saving. Earth is significantly crucial for cooling strategies. Topography can also control wind by placing some parts of the building in hollows to create short or tall facades (RAPOPORT, 1969, p. 100). In Kozan, as buildings are oriented to the south and semi-buried, low north facades are exposed to the strong wind and shading is maximized. In Bellapais, the semi-buried buildings are faced to the north which means shading is provided and great amount of wind is exposed to the tall south face of the buildings. It is observed that both villages are located at nearly the same elevation above sea level. Kozan is located on the lower part of the slope, which is in a favourable microclimate location for hot regions and exposed to cold air flow. However, Bellapais can be localized at the top of the slope for wind exposure. They can be both oriented to the east for mitigating solar exposure in the afternoons (Figure 7).

Figure 7: Control of wind

Thermal mass is used as a heat sink while absorbing and releasing heat for passive cooling. Adobe is used in Kozan where there is high temperature gradient between day and night. In Bellapais, stone are used as wall material and the temperature fluctuation is low between day and night (Figure 8). They are exposed to the sun during the day and keep the heat for extended time, because external walls delay the heat transfer from exterior to interior. At summer night, the indoor temperature can be reduced if night ventilation is created. Cool air contacts with the wall thus, cooling it naturally. However as Bellapais is a humid region, nocturnal (ventilative) cooling is not recommended because of not having large daily temperature ranges. The comfort ventilation (ventilative cooling) can be suggested by creating physiological cooling effect by evaporation of perspiration from the skin (LECHNER, 2009, p. 281). However, it is observed that in some summer nights, Bellapais is cooler than the lower part of the mountain.

Figure 8: Adobe and Stone

5. RESULTS AND DISCUSSIONS

These architectural design principles create the fundamental idea of this study in terms of enhancing the passive cooling within the indoor environment. From this point of view, these principles are analyzed and some criteria are identified as an illustrated table (Table 1).

Table 1: Evaluation of design principles

Summary of the results:

- Square shaped of building in hot-dry and rectangularly shaped in hot-humid region. In both regions, the buildings are oriented to the south. Ventilative cooling is improved.

- Shutters are mostly used for shading device creating venturi effect which is good for ventilative cooling.

- Vine-covered trellises and shrubs are used for ventilative cooling.

- The mostly used area are faced to the south in hot-dry region and to the sea view in hot-humid region. Rooms facing to the ground are naturally cooler due to the passive earth cooling methods in summer.

- Small windows are used in hot-dry region and large windows in hot-humid region. Window above the door is created in both regions that creates cross ventilation based on ventilative cooling.

- In hot-dry region, short facade is faced to the prevailing wind due to the topography. Conversely, tall facade is faced to the wind in hot-humid region. In both regions, earth cooling is provided.

- Adobe is used in hot-dry and stone is used in hot-humid region as a thermal mass material. In hot-dry region, ventilative cooling is created as the temperature fluctuation is high. It is achived by cooling the building for the following day. The comfort ventilation is enhanced in hot-humid region by increasing evaporation from the skin and increasing thermal comfort level.

6. CONCLUSION AND RECOMMENDATIONS

Renewable energy sources such as wind and sun should be used to reduce energy consumption of buildings. The design principles based on building shape and orientation, shading, vegetation, building layout, wall openings, topography and thermal mass material should be considered at the beginning of the design stage of any building to meet all the thermal requirements of the occupants. These can be achieved by considering the advantages of passive cooling methods and increase the rate of ventilation within the indoor environment. In this study, it is concluded that only ventilative and earth cooling is considered as a passive cooling method in in both settlement in Cyprus climate.

The main strategy for Cyprus is to reduce heat gain. The buildings on the lower part of the south-facing slope mountain are better in a better comfort condition for dry regions, whereas, the buildings in the humid region can best be localized in the higher part of the south or north-facing slope of mountain in order to improve ventilation. From this point of view, passive cooling strategies can be maximized by integrating design principles at the design stage. Table 2 shows architectural design principles in different climatic zones.

	Hot-Dry Region	Hot-Humid Region
Building shape and orientation	Square/rectangular shape and south facing building	rectangular shape and north facing building
Shading	Wooden shutter to control sun and wind	
Vegetation	Vine-covered trellises to control sun and wind	
	Green roof for insulation	Trees on site for effective ventilation
Building layout	Mostly used area faces to the south	Mostly used area faces to the north
Wall openings	Small window for controlling wind	Large window to the prevailing wind
Topography	Low north facade towards the wind	High north facade towards the wind
Thermal mass material	Adobe	Stone

Table 2: Design Principles for hot-dry and hot-humid region

The villages in Five Fingers Mountains are unique due to their location on the slope and having different climates in different part of it. They can respond to where they are in a way that is respectful of nature. However, they are not in good conditions now as they are mostly abandoned. Design principles in terms of passive cooling can be learned from these buildings.

The effect of climate is very important factor in building design. The climatic features of the specific location and the architectural design principles should be integrated together for human comfort conditions, energy consumption and less harm to the environment.

The main strategy for Cyprus is to reduce heat gain. The buildings on the lower part of the south-facing slope mountain are in a better comfort condition for dry regions, whereas the buildings in the humid region can best be localized in the higher part of the south or north-facing slope of mountain in order to improve ventilation. From this point of view, passive cooling strategies can be maximized by integrating passive solar architectural design principles at the early design stage according to the climatic conditions of the surroundings. It is very clear that these buildings are adapted to the climatic conditions of Cyprus. In this study, the benefits of passive solar design principles are reviewed again to be used by any building designers. They should combine these principles as a fundamental part of the design. This is not only to be achieved by designers, but policy makers, politicians, environmentalists should also establish passive solar building regulations. Finally, public demand should be created to integrate this type of approach for energy saving future.

7. REFERENCES

ABOHORLU, Pervin, 2010. Investigation Of Traditional Cypriot Houses In The Areas Around The "Five Fingers" Mountain Range Of North Cyprus Regarding The Climatic Parameters, unpublished master thesis, Near East University, Cyprus.

BROWN, G. Z., Dekay, Mark, 2001. Sun, Wind and Light: Architectural Design Strategies, New York: John Wiley & Sons.

ERLEY, Duncan, Martin S. Jaffe, and Dava, Lurie, 1979. Site Planning for Solar Access: A Guidebook for Residential Developers and Site Planners. Washington: U.S. Dept. of Housing and Urban Development, Office of Policy Development and Research.

GIVONI, Baruch, 1994. Passive and low energy cooling of buildings. New York: Van Nostrand Reinhold.

LECHNER, Norbert, 2009. Heating, Cooling, Lighting: Sustainable Design Methods for Architects, Third Edition, Hoboken, NJ: John Wiley & Sons.

MAZRIA, Edward, 1979. The passive solar energy book: A complete guide to passive solar home, greenhouse, and building design. Emmaus, PA: Rodale Press.

RAPOPORT, Amos, 1969. House form and culture. Englewood Cliffs, N. J.: Prentice-Hall.

221: An experimental study of the thermoelectric properties of oriental hornet silks and their application in buildings

Mark Worall[1], Bianca Laura Latini[2], Theo Elmer[3], Rabah Boukhanouf[4]

1 University of Nottingham, University Park, Nottingham, NG7 2RD, Email. mark.worall@nottingham.ac.uk
2 University of Nottingham, University Park, Nottingham, NG7 2RD, Email: bllatini@libero.it.
3University of Nottingham, University Park, Nottingham, NG7 2RD, Email theo.elmer@nottingham.ac.uk
4University of Nottingham, University Park, Nottingham, NG7 2RD, Email rabah.boukhanouf@nottingham.ac.uk

This paper investigates the thermoelectric and thermoregulatory properties of Oriental hornet silk. The larvae of the Oriental hornet produce silks, which it uses to create a silken cap at the end of a vertically orientated comb. It has been found that the silk caps also play a part in hornet nest thermoregulation. The nest of the Oriental hornet is maintained at a constant temperature of 28°C whilst the ambient temperature outside ranges from 20 to 40°C. Silk caps possess thermoelectric and thermophotovoltaic properties that help to regulate the temperatures in the nest by storing excess heat as an electric charge in the caps as temperatures rise and releases the energy as heat as temperatures fall.

Controlled experiments have been carried out on silk cap samples in which we measured resistance, voltage and current during variations in temperature and relative humidity (RH). We have showed that in dry conditions, silk caps act as high resistance materials. The material therefore acted as a dielectric. We measured the charge and discharge characteristics and found that it behaved as a high performance capacitor. In humid conditions, silk caps acted as low resistance materials. The material therefore acted as a thermoelectric energy generator. Doping of the silk caps with LiCl reduced the resistance and increased thermoelectric generation in comparison to results found during high RH conditions. It was shown that resistance was temperature dependent and reached a peak between 25 and 32°C, which is thought to correspond with the glass transition temperature.

We discuss how the principles could be applied to buildings and other applications. Energy harvesting is a growing field of study and by using variations in ambient conditions, such as temperature, RH, and solar irradiation, we could develop multifunctional structures for buildings integrated with high efficiency buildings, and so reduce reliance on distributed energy and conventional supply infrastructure.

Keywords: thermoregulation, homeostasis, biomimetics, silk, thermoelectric

1. INTRODUCTION

Thermoregulation and homeostasis are vital processes in nature and most animals, including human beings, have evolved strategies to enable them to survive in highly variable and hostile environments. Here, thermoregulation is defined as "the maintenance of body temperature or temperature range independent of passive processes and the body's metabolism during different activities", according to Heinrich (1993) and homeostasis is defines as "a regulated dynamic disequilibrium, sustained by the active management of fluxes of matter and energy" (Turner (2008)). Mankind has been able to exist in nearly all regions of the earth and beyond because of our ability to adapt to the local environment through our engineering skills and technical innovation. However, almost a half of all energy consumed world-wide is used to provide thermoregulation and homeostasis. As the vast majority the primary energy supplied is from fossil fuels such as coal, oil and gas, carbon dioxide emissions attributable to thermal comfort in buildings are almost 40% of the total world-wide.

If we wish to maintain our current living conditions and enable people in developing countries to improve theirs, whilst reducing overall energy consumption and minimising carbon dioxide emissions, then we need to develop innovative solutions. Most buildings require ancillary heating and cooling devices, such as boilers, heat pumps, chillers, etc, to maintain conditions within set parameters, and it is these machines that consume most of the energy. The main reason that we need machinery is to compensate for losses through building envelopes. If we could develop building envelopes such as walls, roofs, windows, floors, etc, as active components in the homeostasis process then we could reduce significantly the need for ancillary heating and cooling, and so minimise the impact on the environment.

Most animals have evolved strategies to enable them to regulate the out of balance fluxes that are part of the diurnal and annual cycles. The Oriental hornet (*Vespa orientalis*) can maintain a nest temperature of 28-32°C in tropical, sub-tropical and temperate areas according to Ishay and Ruttner (1971). This is achieved using many techniques, including building nests below ground to provide insulation from ambient temperature swings, the beating of wings to provide air flow and enhance heat and mass transfer, and the distribution of water droplets from the adult to hydroscopic materials in the nest that can be evaporated to produce a cooling effect. However, it has been found that other cooling mechanisms are also in play.

2 BACKGROUND

It has been found that when the adult population are removed from the nest, a temperature of 28-32°C is maintained for a number of days afterwards, according to Ishay and Beranholz-Paniry (1995). It was concluded that materials in the nest were contributing to a thermoregulatory effect. The oriental hornet nest houses both the adult population and combs that contain the brood. The combs are hexagonal in structure and are formed vertically downwards as in the paper nests found in temperate climates. The combs are formed from organic building material gathered locally and masticated by saliva of the adult hornets, which quickly polymerises to form a robust structure. Eggs are placed in the walls of the comb and when they hatch the pupa spin a silk weave and form a silk cap at the open entrance, sealing it from the outside. The pupa continues to spin silk and form a layer on the comb wall, thus fully enclosing itself in a protective cocoon.

In studying the thermoregulatory properties of hornet nests, it has been shown in experiments by Kirshboim and Ishay (2000) and Ishay *et al* (2002a, 2002b) that the silk cap and walls of the comb have thermoelectric properties that could help regulate the temperature in the comb. It was shown that as ambient temperature increases, the current intensity increases. It was conjectured that a thermoelectric effect was charging the silk cap with electrical energy as the ambient temperature increased. Any excess heat was assumed to be released by the evaporation of water from the silk cap. When the ambient temperature falls, the energy stored was discharged with a flow of electric current from high to low potential, transferring heat by Joule heating and the Peltier effect. The Peltier effect is the release or absorption of a finite heat transfer rate at the junction between two constant temperature electrical conductors made of different materials.

Figure 1. Photograph of silk fibre (b) with its envelope (a) Kirshhoim, Ishay (2000).

But how can the nest provide a thermoelectric effect? The hornet nest silk cocoon consists of two types of material, a silk fibre that consists of an elastic protein called fibroin, and a surrounding protein called sericin. The fibroin core is double stranded. Kirshboim and Ishay (2000) presented scanning electron micrographs of the structure of the silk, which can be seen in Figures 1 and 2. Figure 1 shows the construction of a silk fibre, where (a) is the surrounding sericin and (b) is the double stranded fibre made of fibroin. Each silk fibre is elliptical in shape, and varies between 1 and 5μm on the minor diameter with an aspect ratio of approximately 2 to 1. The silk cap is made of a tangle of silk fibres and sheets. Figure 2 shows a photograph of the structure of the silk. A material with good thermoelectric properties is difficult to find because on the one hand, it should have a high electrical conductivity to minimise Ohmic losses and on the other hand, it should have a low thermal conductivity to minimise conduction heat losses. The materials possessing the most desirable thermoelectric properties in engineering have been found to be semiconductors, for example Bismuth Telluride (Bi_2Te_3).
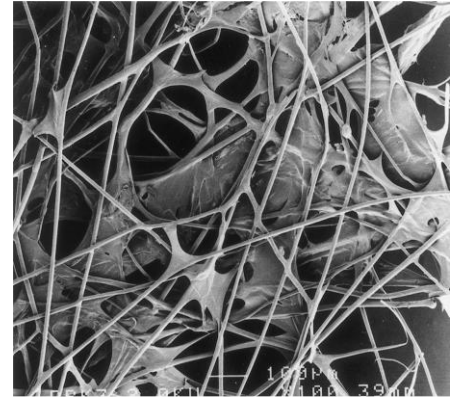
Figure 2. Micrograph of silk weave, showing fibres and sheets. Kirshhoim, Ishay (2000).

Kirshboim and Ishay (2000) proposed that the double stranded fibre was comparable with a semiconductor, where the inner fibroin strand performed the function of the *p* junction and the outer sericin envelope performed the function of the *n* junction. Thermoelectric properties are not limited to hornet silk and are known to be present in the silk spun by the silkworm *Bombyx mori* (Ishay and Barenholz-Paniry, 1995). However, comparisons of *Vespa orientalis* and *Bombyx mori* show that the hornet silk is an order of magnitude better in terms of thermoelectric properties. On the face of it, the structure of the silk does not seem to provide a good candidate for a thermoelectric device. The nearest engineering materials comparable with hornet silk are the electrically conductive polymers, such as polyaniliyne and polythiophane doped with Iodine.
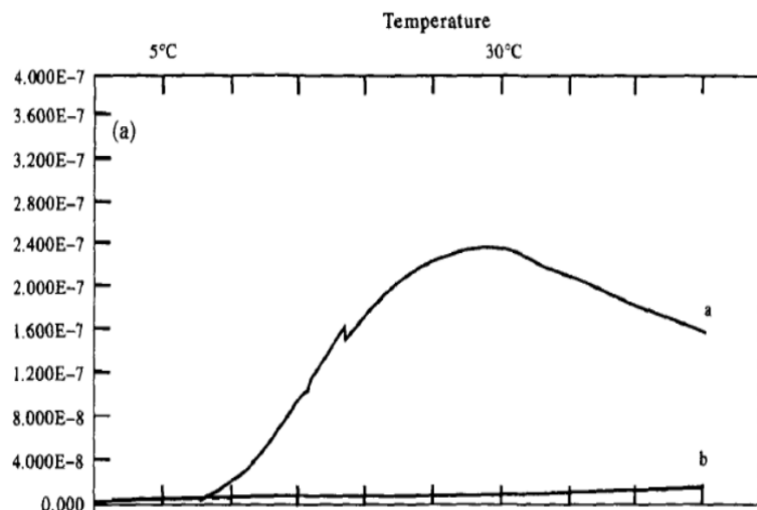

Figure 3. Influence of temperature of current levels where curve b is the control measurement (Barenholz-Paniry, Ishay, 1995)

These materials were studied by Shiohari, et al (2003) where it was shown that the Seebeck coefficient was 10,000 times less than the inorganic semiconductor Bi_2Te_3. The Seebeck effect is the creation of a potential difference due to the temperature difference maintained at junctions between two different materials and is the principle behind the thermocouple. The Seebeck coefficient is a non-linear relationship between temperature and potential difference. The papers published on the thermoelectric properties of the oriental hornet do not describe thermoelectric properties such as the Seebeck coefficient, so it is difficult to compare them with semiconductor devices or conductive polymers. However, conductive polymers are the engineering material most likely to be of use if the phenomenon of thermoregulation in hornet nests is to be developed as a technology in buildings. Although the Seebeck coefficient is much lower in a conductive polymer than an inorganic semiconductor, it can be manufactured using organic materials, at low cost, at ambient conditions, with increase in safety in manufacture and use and can be separated, recovered and recycled easily. As a thermoelectric generator or refrigerator it may impractical because it may be much larger than an equivalent device manufactured from inorganic materials and may not be able to attain the output needed, but as a heat storage device it may be applicable to air handling units in ventilation systems and coatings on the envelope of buildings, where a large surface area could be available and the low Seebeck coefficient is less relevant.

Barenholz-Paniry and Ishay (1995) showed how current varied with temperature over a range 0-45°C.Figure 3 shows that current increased from 0°C at low temperature and increases with increasing temperature until it reaches a maximum at about 28°C. Current then decreases beyond 28°C. The maximum current measured was 25nA.

Ishay and Krishboim (2000) compared voltage and current in light and in darkness. Figure 4 shows that voltage was approximately 0.2V in light conditions and decayed slowly over time. When the sample was exposed to

Figure 4. Measurement of voltage and current in light, then in the dark. (Ishay and Krishboim, 2000)

darkness at 1400minutes, there was sharp increase in current generated to about 1.7 µA. At the same time voltage decreased sharply. Voltage and current declined to zero at about 2100minutes.

Figure 5 shows the change in resistance with temperature, as described by Ishay and Krishboim (2000). It can be seen that there is very high resistance at low temperatures and resistance decreases with increasing temperature until it reaches a peak at around 28°C. There is plateauing off between 21°C and 32°C and then resistance increases again beyond 32°C.

Tulachan, et al (2014) followed up previous work and described work on developing silks that could generate electrical power. Tulachan, et al (2014) used *Bombyx Mori* (silkworm) silk to test silks in a dry state in humid air and doped with NaCl. A cell was constructed to test the electrical properties and constructed from a sample silk, an electrode constructed from aluminium and an electrode constructed of copper wire would around the silk sample. Figure 6 shows a photograph of the cell.
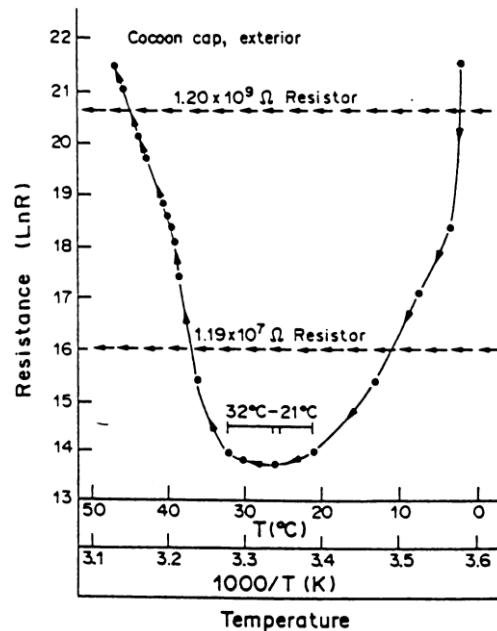
 The silk caps tested by Ishay and colleagues were set up by attaching thin copper wire to the surface of the caps by conductive silver ink. Tulachan and his colleagues devised the method to ensure good connections to the silks and external circuits and without the need for conductive inks.

Figure 5. Temperature dependence of the electrical resistance (Ishay, Krishboim. 2000)

Tulachan, et al (2014) observed that "there is a lowering of the current values in demineralised cocoons exposed to water vapour and increase in current value by doping the coon with NaCl" and hence confirmed results from earlier publications. They also assessed the influence of humidity in more detail and found that water droplets promoted water-mediated proton hopping, and enhanced the ability of silks to generate electrical power. They observed that around 60°C there was a spike in voltage and current due to the increased mobility of the water molecules and hence the rearrangement of hydrogen bonds in the silk. Their final aim will be for their research to contribute to a sustainable solution in the power generation sector, by building a system that would "utilize the humidified waste of heat for energy
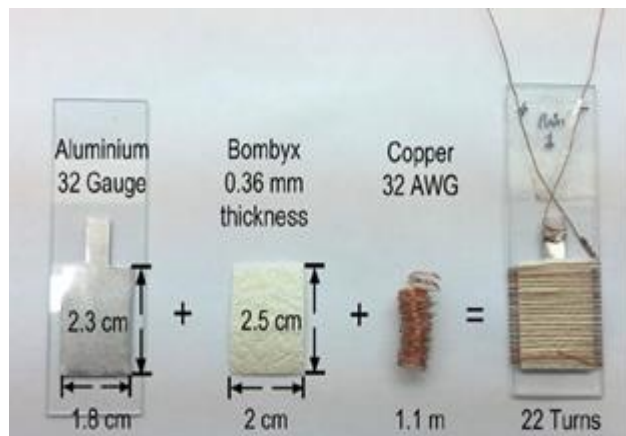

Figure 6. Cell constructed to test electrical properties of silk. (Tulachan, 2014)

harvesting" (Tulachan et al, 2014). Since "Film formation and structural characterization of silk in the hornet Vespa simillima xanthoptera Cameron" (Fujiwara, et al 2005) mentions that vespa silk would be more stable as a thermoregulatory material, Tulachan's experiments' results could be even more successful if applied to *Vespa Orientalis* silk.

In order to develop an electrical cell capable of generating electricity, storing electrical energy and storing and releasing heat this paper describes the design and testing of single cell silk

3   METHODOLOGY

The main aim of the project was to gain an understanding of the electrical and thermal properties of Oriental Hornet silk and investigate its application to energy storage, harvesting and management in buildings.

Oriental Hornet silk caps were obtained from the Professor Jacob Ishay and Dr Marian Plotkin of Sackler Institute of Medicine at the University of Tel Aviv, Israel. The silk caps were originally obtained from nests in the field. The samples used in our experiments were from the queen of the Oriental Hornet at a nominal diameter of approximately 12mm. The caps were kept in a refrigerated condition until testing.

An experimental rig was designed and built to test the silk samples over a range of environmental conditions including variations in temperature and relative humidity, as well as enabling samples to be exposed to daylight and darkness

3.1. EXPERIMENTAL RIG DESCRIPTION

Figure 7 shows a schematic diagram of the experimental rig designed and built to carry out experiments on the Oriental Hornet silk samples.
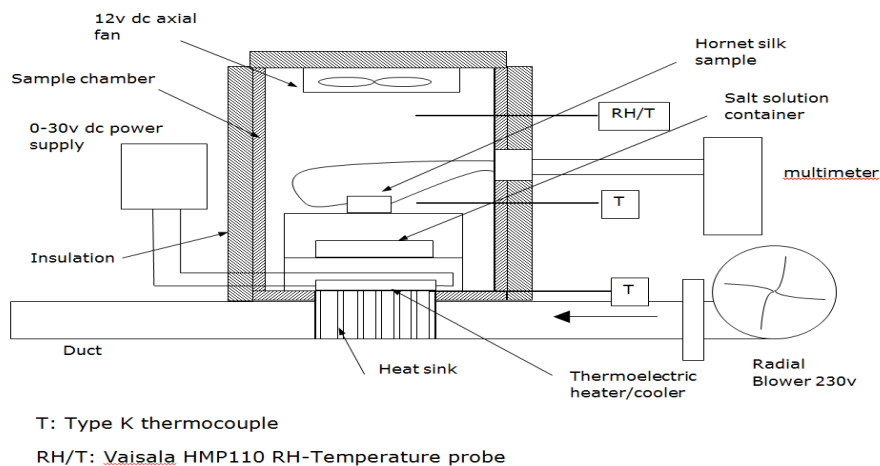

T: Type K thermocouple

RH/T: Vaisala HMP110 RH-Temperature probe

Figure 7. Schematic diagram of thermoelectric silk cap test rig.

A cylindrical sample chamber is provided to create a controllable environment (temperature, relative humidity, light and darkness). The cylinder is constructed from aluminium, 64 mm in diameter, 3 mm thick and 148 mm in height. A cap was provided at the top of the cylinder and was secured by two M3 studs. A 12v dc axial fan was fitted to the bottom of the cap to provide air circulation in the chamber. The sample cylinder fitted into a base plate manufactured from aluminium. A 67W thermoelectric module 40mm x 40mm x 3.4mm was provided in the base plate to provide close control heating and cooling to the sample cylinder. A heat sink connected the thermoelectric module to a ducted air stream to dissipate the heat from the cold side of the thermoelectric module. A 55W 230v ac radial blower/fan was fitted to provide ventilation air flow and dissipate the heat from the thermoelectric module. A raised sample platform was provided inside the sample cylinder to enable the silk sample to be mounted and secured. A salt solution container was provided and located above the silk sample. The container enabled a salt solution to be installed inside the cylinder so that relative humidity could be controlled. It works on the principle that for a given volume of air, the relative humidity of the air will reach equilibrium with the salt/water solution, and its value will depend

on the composition of the solution. For instance, air above a potassium chloride (ClK)/water solution at equilibrium will have a relative humidity of approximately 90%.
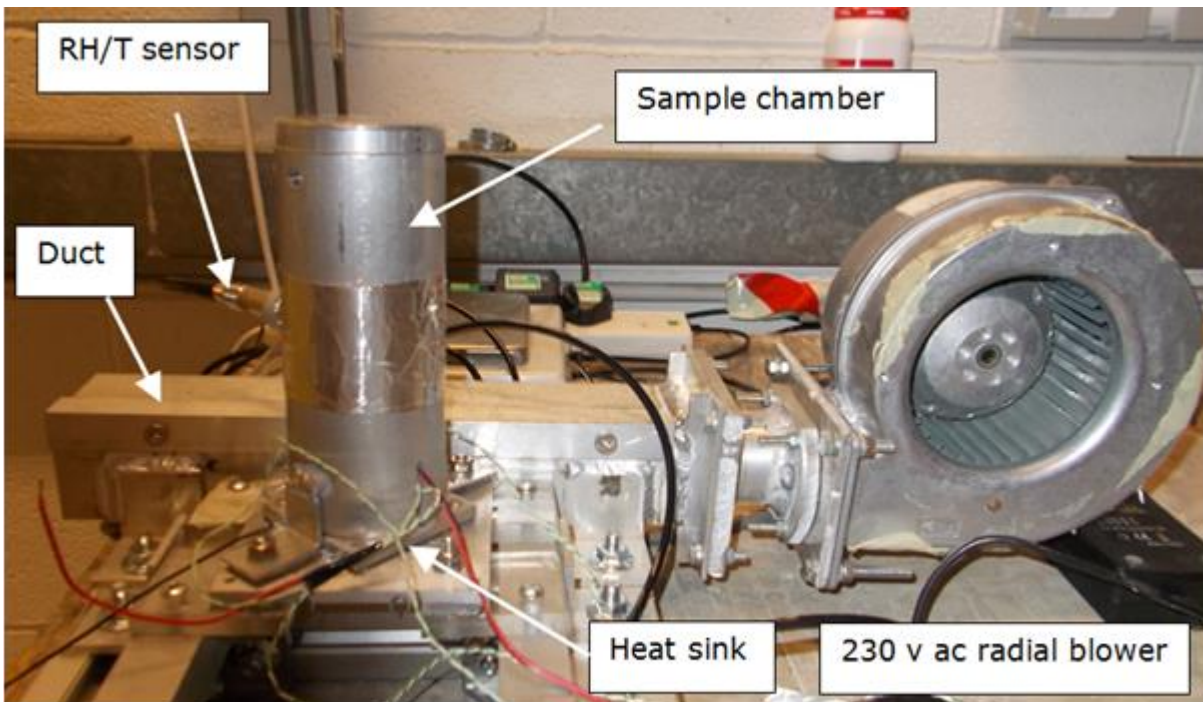

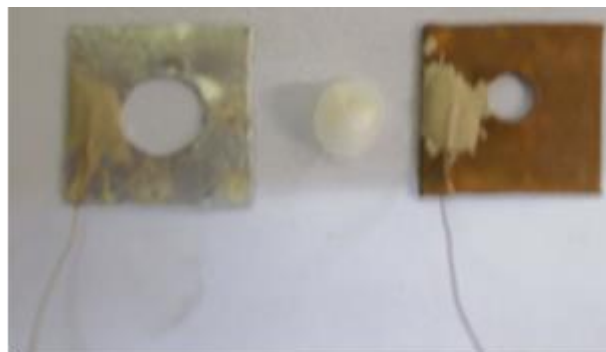*Figure 8. Photograph silk cap test rig.*

Figure 9. Silk cap sample holder assembly.

Type K thermocouples were located at the bottom of the sample cylinder, mid-way of the cylinder, on the hot and cold sides of the thermoelectric module, and on the sample platform. A relative humidity probe was provided to measure relative humidity in the cylinder. A 0-30V dc power supply was used to provide a controllable power to the thermoelectric module. A digital multimeter was used to measure the current, voltage and resistance of the silk samples.

Figure 9 shows a photograph of the silk cap sample holder. It consists of two 30mm x 30mm plates, 1mm in thickness, one constructed from aluminium and one constructed from copper. The aluminium plate was drilled with a 12mm hole and the copper plate was drilled with a 9mm hole. The holes were provided to enable air and light to come into contact with both sides of the silk cap and provide a good electrical contact around the perimeter of the holes. Copper wire, 0.25mm in diameter was connected to each of the plates by silver conductive ink.

4   RESULTS

Figure 10 shows the discharge curve of the silk sample when exposed to light. The silk cap was exposed to a voltage of 20v for 5 seconds. As soon as the voltage source was switched off, the current discharged. The charge is defined in Equation 1 below:

$$C = Q / V$$
(1)
Where:
Q – charge (C)
V - voltage applied to the silk (V)
C – capacitance (F)

Using the Trapezoidal Rule, the area under the curve can be found, which is equivalent to the charge. The charge, Q, was found to be approximately 0.433 C. From Equation 1, the capacitance was found to be 21.7 mF. This value lies within the results found by Ishay et al (1993) for five silk caps arranged in parallel, which is comparable to a good commercial battery (Ishay et.al, 1993).

Figure 11 shows the variation in resistance and voltage with temperature, with the resistance ranging from 15.8 MΩ to a minimum of 2.6 MΩ. The trend in resistance increases from 35°C onwards. Resistance remains relatively constant between 28 and 35°C. Voltage shows a gradual decrease as temperature increases, ranging from a maximum of 60 mV at the starting point (22°C) to 23 mV at 40°C. The trend in resistance below approximately 25°C increases as temperature decreases. Figure 11 also shows two distinct spikes in resistance around 36-38°C, This effect has also been reported by Liu et al (2013), where the parameters such as resistivity and thermal conductivity showed spikes in a semiconductor material at temperatures consistent with a phase transition. The trend in resistance below approximately 25°C increases as temperature decreases.

In comparison, Plotkin's results (Plotkin et al 2007) showed that the resistance above approximately 35°C would increase, and decrease below approximately 25°C. It is suggested that the increase in resistance above 35°C is due to a phase change of the first order, which would utilise any excess heat to cool the environment around it.
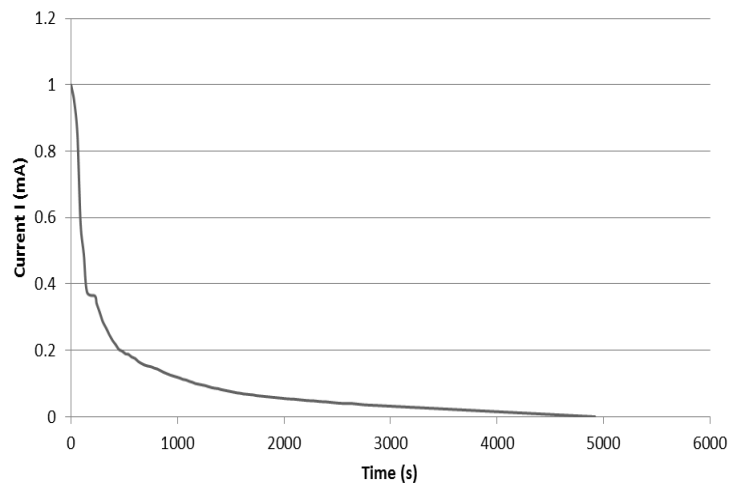

Figure 10. Discharge curve of silk cap after being charged at 20v for 5 seconds.
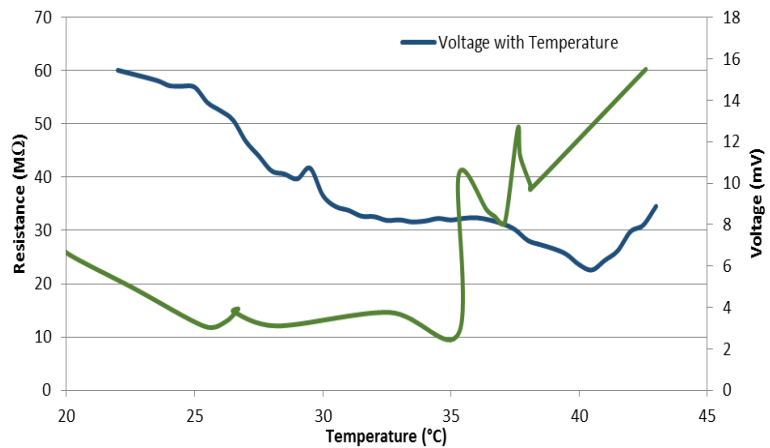

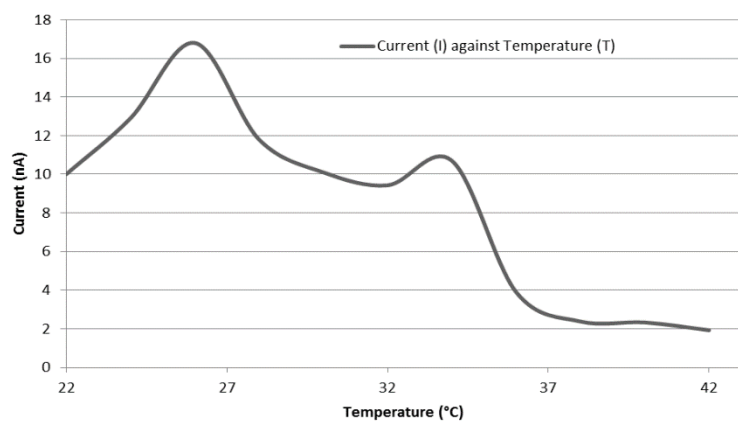*Figure 11. Variation in resistance and voltage with temperature.*

Figure 12. Variation in current with temperature.

A high resistance shows the potential to be a good insulator, whereas a low resistance would make it a good conductor. Therefore, at higher temperatures a hypothetical material would behave as an insulator, and at lower temperatures the material would behave as an RH sensitive semiconductor, which would allow for better thermoregulation.

Figure 12 shows the current generated over a temperature ranging from 20°C to 40°C. A double peak is observed at 27°C and 33°C. The first peak is a maxima and represents a phase transition and which corresponds to the optimum temperature in the nest of the oriental hornet. The second peak represents a phase transition in the composite material of the hornet silk.
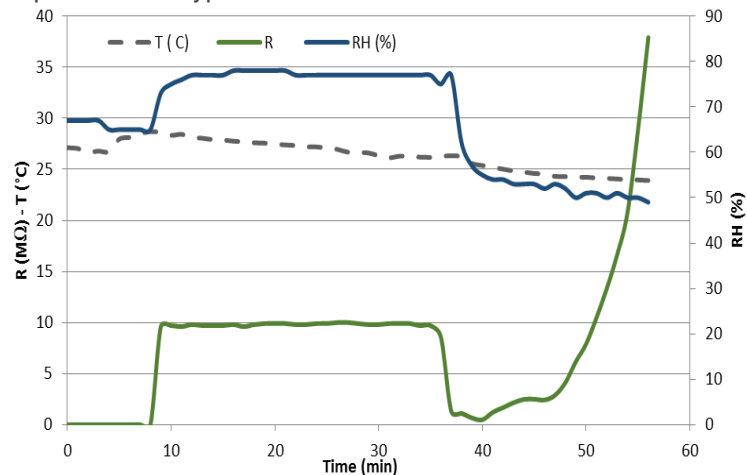

Figure 13. A comparison with resistance and relative humidity (RH) with time.

Figure 13 shows how the resistance was affected by the relative humidity change. The resistance follows the same trend as that of the relative humidity, which as expected, increases when the transparent film prevents the exchange of air with the outside environment. However, the resistance of the silk increases exponentially after 40 minutes. This increasing trend in resistance is thought to be mainly due to drying of the silk cap. Since the test chamber maintains approximately constant RH conditions using a salt solution, moisture is continually evaporating from the solution and hence the concentration (mass of salt/mass of solution) increases. There exists a partial pressure difference between the moisture in the air, the moisture contained within the silk cap, and liquid water in the solution. As the RH decreases, the partial pressure decreases, driving evaporation from the silk cap and drying out the sample. Hence as the silk cap dries out, its resistance increases.

5   CONCLUSIONS

The results obtained were able to show electrical power generation, electrical storage, heat storage and temperature dependent resistance. This is consistent with a material acting as an organic semiconductor. Performance and functionality are dependent both on temperature and relative humidity. In a dry state the silk caps act as insulators and so have the potential to be used as capacitors. The silks form a composite material constructed from two types of material, a fibrous protein and a gummy, resin type protein. The two materials create junctions in which current can be generated on the application of heat, however, moisture plays a major role in electrical transport, and converts it from an insulator to a conductor.

The discharge curve was successful in providing data to calculate the capacitance, which was found to be 21.7 mF. This value, being within the range found by Ishay (2000), supported the aim of this experiment. Similarly, the results given by voltage and resistance data provided the means to calculate current generation, and hence assess whether enough would be generated to provide the expected thermoregulatory effect. The data for resistance in itself not only behaved similarly to that described by Plotkin et al, (2007), but also indicated a trend that is associated with a phase-change of the first order, as described by Liu et al (2013).

Doping, both with distilled water and with a ClK solution, was found to be an efficient method of increasing current generation.

A robust and easily fabricated thermoelectric cell was constructed and can be easily scaled-up for large scale testing and product development.

The results presented here and disseminated elsewhere in the public domain reveal a fascinating natural phenomenon that has evolved over millions of years and probably created thermoregulatory and homoestatic properties as a by-product of other functions. Our engineered world has created materials with similar functions but from inorganic and unsustainable feedstocks, but the properties and functions of natural silks give is an insight into other ways of approaching problems. By developing thermoelectric fibres

based on our understanding of natural silks we have opportunities to create highly functional materials, but at low economic and environmental cost.

Fibres and composite materials possessing thermoelectric, thermoregulatory and energy storage properties are easily integrated into building elements to give added functionality and adaptive and responsive capabilities. The range of applications is wide and diverse, from building elements such as composite walls that could act as electricity generators or capacitors, dynamic thermal insulation systems, membrane heat and mass transfer devices and air filtration systems.

6   ACKNOWLEDGEMENTS

7   REFERENCES

FUJIWARA, S., Kameda, T., Kojima, K., Miyazawa, M., (2005), Film formation and structural characterization of silk in the hornet Vespa simillima xanthoptera Cameron. Z. Naturforsch C., 60 (11-12), 906-914.

HEINRICH, J, (1993). The hot blooded insects: Strategies and mechanisms of thermoregulation, Harvard: Harvard University Press, p600.

ISHAY, J.S., Benshalom-Shimony, T., Dabah, B., Shurz, I. S., Shevach, Y., Ben-Shalom, A., Barenholz-Paniry, V., 1993. Electrical properties of the cuticle, silk caps, and comb of oriental hornet Vespa Orientalis (Hymenoptera: Vespidae). Great Britain: Pergamon Press.

ISHAY, J, Barenholz-paniry, V, (1995). Thermoelectric effect in hornet (Vespa orientalis) silk and thermoregulation in a hornet's nest, J. Insect Physics 4, Vol. 41, No. 9, 753-759.

ISHAYA. J.S, Litinetsky, L, Pertsis, V, Linsky, D, Lusternik, V, Voronel, A, (2002a). Thermoelectric conversion and specific heat of hornet combs, Journal of Optoelectronics and Advanced Materials, V. 4, No. 1, 135-145.

ISHAYA. J.S, Litinetsky, L, Pertsis, V, Linsky, D, Lusternik, V, Voronel, A, (2002b). Hornet silk: thermophysical properties, Journal of Thermal Biology. V 27, 7–15.

LIU, H, Yuan, X, Lu, P, Shi , X, Xu, F, He, Y, Tang, Y, Bai , S, Zhang, W, Chen, L, Lin, Y, Shi, Y, Lin, H, Gao, X, Zhang, X, Chi, H, Uher, C, (2013), Ultra-high Thermoelectric Performance by Electron and Phonon Critical Scattering in Cu2Se1-xIx, Advanced Materials, 25, 6607–6612.

PLOTKIN, M., Ermakov, N. Y., Volynchik, S., Bergman, D. J., Ishay, J. S., 2007. Prevention of Hyperthermia With Silk of the Oriental Hornet, Vespa Orientalis: A Hypothesis. Microscopy Research and Technique, 70, pp.69–75.

Shiohari, Y, Ohara, K, Imai, Y, Isoda, Y, Nagashi, H, (2003). Problems of conductive polymers as thermoelectric materials. 22nd Conference on thermoelectrics. La Grande Motte, France.

TULACHAN, Brindan, Meena, S. K., Rai, R K., Mallick, C., Kusurkar, T. S., Teotia, A. K., Sety, N. K. Bhargava, K., Bhattacharya, S., Kumar, A., Sharma, R. K., Sinha, N., Singh, S. K., Das, M., (2014), Electricity from the Silk Cocoon Membrane, Scientific Reports, 4, pp.5434.

TURNER, J, S, (2008). Homeostasis, Complexity, and the problem of biological design, Emergence: Complexity and Organization, V 10 No2, pp. 76–89.

225: A review of polymer heat exchanger

XIANGJIE CHEN[1], YUEHONG SU[2], DAVID REAY[3], SAFFA RIFFAT[4]

1Department of Architecture and Built Environment, University of Nottingham
2Department of Architecture and Built Environment, University of Nottingham
3David Reay & Associates
4Department of Architecture and Built Environment, University of Nottingham
Contact: Xiangjie Chen email:xiangjie.chen@nottingham.ac.uk

Due to its low cost, light weight and corrosive resistant features, polymer heat exchangers have been intensively studied by researchers with the aim to replace metallic heat exchangers in a wide range of applications. This paper reviews development of polymer heat exchanger in recent decade, including cutting edge materials characteristics, heat transfer enhancement methods of polymer materials and a wide range of polymer heat exchanger applications. Theoretical modelling and experimental testing results have been reviewed and compared with literatures. It is shown that polymer materials do hold promise for use in the construction of heat exchangers in many applications, but that a considerable amount of research is still required into material properties, thermal performance and life-time behaviour

1. INTRODUCTION

Since the first polymer heat exchanger was introduced by DuPont(Githens, Minor et al. 1965), many attempts have been made for promoting the commercial utilization of polymer heat exchanger. The conventional heat exchanger manufactured by metal (such as stainless steel, copper and aluminium) has the disadvantages in terms of weight and cost. In addition, specially treated metal heat exchanger is needed if the working fluids are corrosive. Given these considerations, it is desirable to find an alternative material for heat exchanger apparatus that can overcome these disadvantages and also acquire comparable heat exchange efficiency and be easily fabricated. This is where the use of polymer heat exchanger comes into place. With the advantages of greater fouling and corrosion resistance, greater geometric flexibility and ease of manufacturing, reduced energy of formation and fabrication, and the ability to handle liquids and gases (i.e, single and two-phase duties), polymer heat exchangers have been widely studied and applied in the field of mico-electronic cooling device, water desalination system, solar water heating system, liquid desiccant cooling system, etc. Most importantly, the use of polymer materials offers substantial weight, space, and volume savings, which makes it more competitive compared with exchangers manufactured from other alloys. Moreover, the energy required to produce a unit mas of polymers is about two times lower than common metals, making them environmentally attractive(El-Dessouky and Ettouney 1999). In this paper, recent developments of polymer heat exchangers have been presented. Materials selection and properties, innovative simulation models and various experimental and theoretical applications for polymer heat exchangers have been summarized and reported.

2. APPLICATIONS OF POLYMER HEAT EXCHANGERS

The following section will emphasis on the applications of polymer heat exchanger in various areas such as heat recovery system, evaporative cooling system, desiccant cooling system, electronic device cooling and water desalination system.

2.1 Heat recovery application

Rousse et al.(Rousse, Martin et al. 2000) presented the theoretical and experimental analysis for using plastic heat exchanger as a dehumidifier in greenhouse for agriculture industry. With the aim to recover some of the lost heat from ventilation system, the heat exchanger was designed as corrugated and flexible thermoplastic drainage tubing with four thermoplastic tubes wrapped around a central tube (as shown in Figure 1). The numerical simulation was based on Brundrett's model(E. Brundrett, T.J. Jewett et al. 1984) for dehumidifiers in greenhouses. Experimental tests were then preformed in a greenhouse of 576m^3. The testing results indicated average efficiency of 84% and 78% for air volumetric change rates of 0.5 and 0.9 change/h.
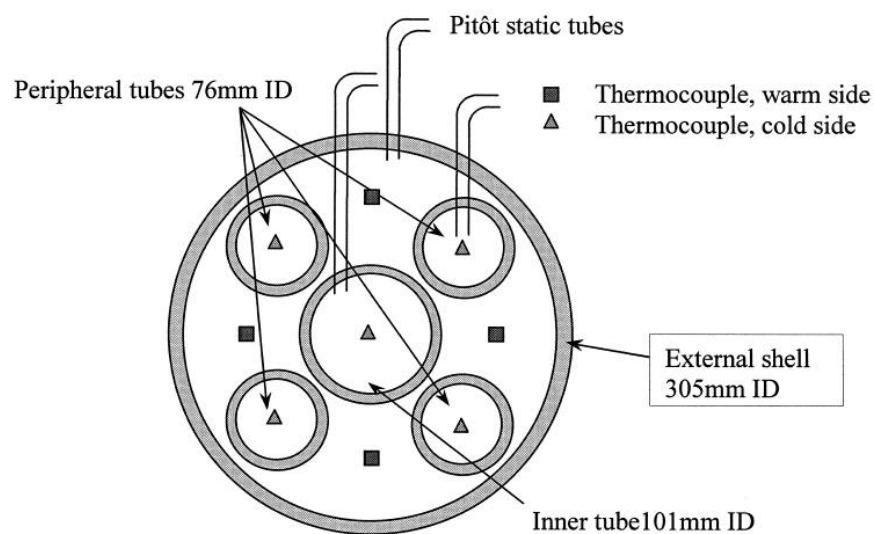

Figure 1 Plastic heat exchanger cross-section(Rousse, Martin et al. 2000)

Because of the corrosive resistant feature, polymer heat exchangers are also applied for flue gas recovery in power generation process. An experimental study on the heat transfer performance of wet flue gas heat recovery system using a plastic longitudinal spiral plate heat exchanger was presented by Jia et al.(Jia, Peng et al. 2001). The plastic heat exchanger was used as air preheater which avoided acid corrosion in the low temperature field for boiler using fuel containing sulphur and recover latent heat of the water vapour from the wet flue gas. The experimental results showed that of the water vapour condensation significantly improved the heat transfer performance, with the heat transfer coefficients increased about twice compared with single-phase convection transfer. Chen et al. (Chen, Sun et al. 2014) compared experimentally on the heat transfer performance between PTFE tube bundle heat exchanger and fin-tube heat exchanger made of thermally conductive plastic for the heat recovery in a 1000MW power plant with heat recovery temperature of 80◦C. In order to improve heat transfer, the plastic exchanger was designed with fin-tube as shown in Figure 2. The simulation results indicated that the PTFE bundle heat exchanger had a higher heat transfer coefficient and consumed less raw materials for manufacturing, while the fin-tube heat exchanger had smaller volume and fewer fins.
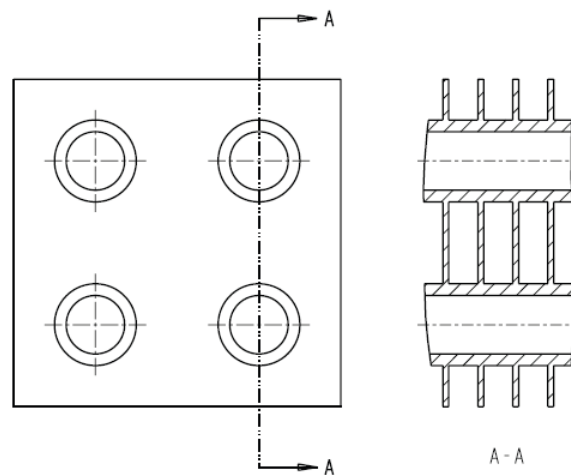

Figure 2 Structural parameters of thermally conductive plastic fin-tube heat exchanger(Chen, Sun et al. 2014)

2.2 Evaporative cooling application

Pescod(Pescod 1979) proposed a simply design method for indirect evaporative cooler using parallel plastic plates with small protrusions. Although the thermal conductivity of plastic is very low, the heat transfer resistance across a thin plastic plate would be less than that of the thermal resistance between the air and plate in dry side. Predictions of the efficiencies of Pesod's wet surface plate heat exchanger were found to be higher than experimental data. Thus incomplete wetting of plate surfaces was suspected.

An indirect evaporative cooling system using a plastic plate heat exchanger (PPHE) was proposed by Dartnall and Giotis(Dartnall, Revel et al. 2009). The heat exchanger (as shown in Figure 8) is made of multi-layered clear polymer plastic sheets, which were bound together by using a patented thermo-forming process. The outside air passed horizontally through the primary side of PPHE, where it was cooled before being supplied to conditioned space. A surprisingly high COP of 4.7 was reported from the preliminary experimental results(Giotis and Revel 2008) where ambient dry bulb temperature was at 27.7◦C and relative humidity was 66%. The authors concluded that when coupled with conventional air conditioning system, this indirect evaporative cooling system can operate efficiently in climates with high humidity.

Kachhwaha and Preahhakar(Kachhwaha and Prabhakar 2010) analysed heat and mass transfer performance for a direct evaporative cooler using a thin plastic plate. The evaporative cooler was fabricated using a galvanized iron sheet and a rigid media cellulose (RMC) pad is attached in upstream side of the fan. The prototype was tested with inlet dry bulb temperature in the range of 24.8-28.4◦C, the air humidity ratio of 2.3-5.8g/kg and mass flow rate of 0.13, 0.2, 0.3 and 0.4g/s. The experimental testing results indicated that the outlet air temperatures were obtained between 16◦C and 21◦C, which was within the range of 15% of the temperature predications of the simulation results.

2.3 Liquid desiccant cooling application

Saman and Alizadeh (Saman and Alizadeh 2001) conducted theoretical analysis on the performance of a cross-flow type plate polymer heat exchanger as an absorber in a liquid desiccant cooling system. The polymer heat exchanger (as shown in Figure 10) was designed with the dimension of 600*600*600mm^3, and a thickness of 0.2mm. The liquid desiccant (calcium chloride solution) was injected into one air stream in order to dehumidify, while water is injected into secondary stream to provide evaporative cooling. The heat exchanger effectiveness was found to be 0.7 for mass flow rate of 0.1kg/s. The authors (Saman and Alizadeh 2002) later conducted experimental tests on the same system configuration. The testing results demonstrated that at heat exchanger angle of 45∘, there was an optimum value of air mass flow rate at which the effectiveness and dehumidification efficiency of the plate heat exchanger were maximized.

Another low-flow liquid desiccant conditioner using plastic-plate heat exchanger (as shown in Figure) was presented by Lowenstein et al.(Lowenstein, Slayzak et al. 2006). The cross section of the plate (as shown in Figure 3) was 2.5mm by 305mm, with 110 cooling passages running the length of the extrusion. The experimental testing results indicated that this liquid desiccant conditioner offered very low droplet carryover, without the use of separate droplet filters. The COP of the regenerator was found to be 0.93 when concentrating a solution of lithium chloride from 36% to 40% and supplied with hot fluid at 93.3∘C.

Figure 3 A 6,000 cfm low-flow liquid-desiccant conditioner(Lowenstein, Slayzak et al. 2006)

When using CFC or HCFC as refrigerants in liquid desiccant cooling system, the generator temperature has to be above 150∘C. If solar energy is used as main driving force for the system, the solar collector has to been evacuated tube solar collectors instead of simple flat plate collectors, this will definitely lead to higher costs. Alizadeh(Alizadeh 2008) carried out feasibility study of a solar driven liquid desiccant cooling system (as shown in Figure 4) with a cross-flow polymer plate heat exchanger for dehumidification and cooling. A 20kW cooling air conditioner with solar collector area of 120 m^2 was developed and tested in Australia. The testing results indicated good agreement with theoretical models and the system efficiency of 82% could be achieved.
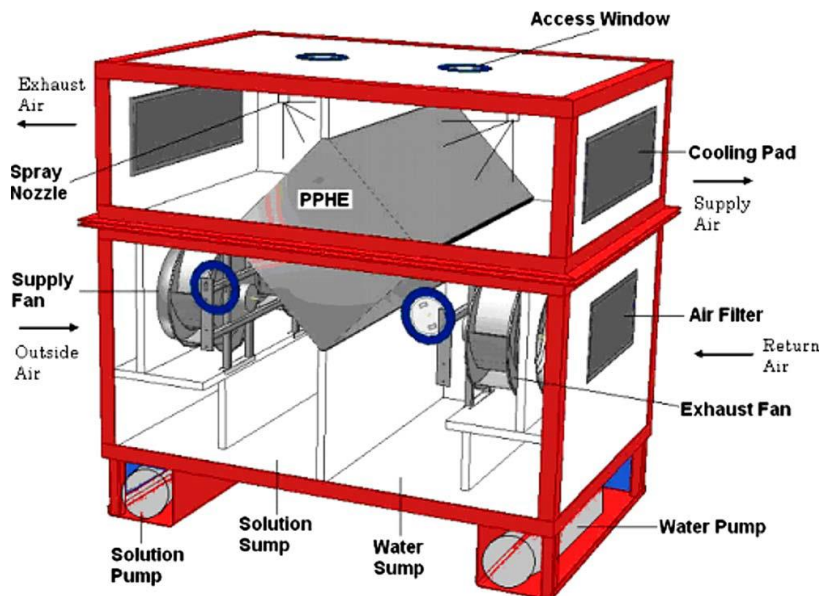
Figure 4 Three dimensional view of the liquid desiccant cooling system- absorber unit(Alizadeh 2008)

A finned tube heat exchanger (as shown in Figure 5) was presented by Chen et al.(Chen, Li et al. 2009) for a liquid desiccant cooling system. The heat exchanger is manufactured by two modified types of PP with high thermal conductivity up to 2.3W/mK and 16.5W/mK. For fabrication technologies, injection molding is used for manufacturing the finned-tube heat exchanger manufacture. The experimental testing results found that the plastic finned tube heat exchanger could achieve thermal conductivity of 16.5W/mK with overall heat transfer coefficient of 34W/mK^2, which offered more than 95% of the titanium heat exchanger performance and 84% of the aluminium or copper performance at the same dimension.
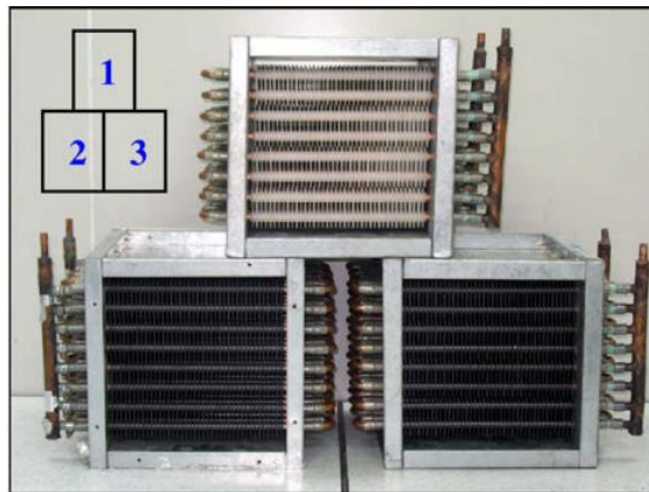

Figure 5 Plastic heat exchangers made from different PP (1 ordinary PP; 2 modified PP-a; 3 modified PP-b) (Chen, Li et al. 2009)

Tather and Senatalar (Tatlıer and Erdem-Şenatalar 2004) investigated the system performance of a polymeric (PTFE) heat exchanger tubes in adsorption heat pumps employing zeolite coating. The polymeric heat exchanger was chosen to replace metal heat exchangers with the aim to improve the thermodynamic efficiency. The simulation results showed that compared with the metal heat exchanger coated with zeolite, the power of the adsorption heat pumps with polymer heat exchanger remained to be unchanged, but the system COP increased about 1.5 to 2.5 folds for easily employing relatively thinner zeolite coatings (5-100μm).

A numerical simulation of a hybrid absorber-heat exchanger using hollow fibre membrane (HFMAE) for water-ammonia absorption cycle was conducted by Chen et al.(Chen, Chang et al. 2006). The hollow fibre membrane heat exchanger was manufactured with outer, inner fibre diameter and wall thickness of 300μm,

240μm and 60μm respectively. The performance of HFMAE as an absorber on ammonia-water absorption system were analysed and compared with a plate heat exchanger falling film type absorber (PHEFFA). The simulation results indicated that the application of HFMAE in such absorption system allowed the increase of COP by 14.8% and the reduction of the overall system exergy loss by 26.7%.

2.4 Solar water heating application

With the attempt to replace traditional metal heat exchanger with low-cost polymer heat exchanger in solar water heating system, a group of researchers from University of Minnesota (Liu et al.(Liu, Davidson et al. 2000)) presented two types of heat exchanger: tube-in-shell and immersed tube (as shown in Figure 6). The heat exchanger was tube-in-shell type, with shell ID of 7.5cm, tube OD of 0.381cm. The heat exchangers were manufactured either from high temperature nylon (HTN) and cross-linked polyethylene (PEX). The thermal performance analysis showed that the polymer heat exchangers can provide thermal output equivalent to conventional copper heat exchangers at lower cost. The design challenge remained is how to overcome the added conduction resistance across the poor conducting polymer wall and at the same time provide sufficient strength to withstand the pressure requirement.

Another aspect when considering the polymer heat exchanger for solar water heating system is its stability over the life cycle at a constant pressure. According to Wu et al.(Wu, Mantell et al. 2004), the polymer tubes must be able to withstand a continuous working pressure of 0.55MPa while immersed in potable water at 82 ∘C for at least 10 years. In order to analyse this long term stability, the mechanical performances of two types polymer heat exchangers made from polybutylene and nylon 6,6 were tested. Two possible failure modes (burst failure and strain failure) were analysed. The results showed that if the tubing is designed to meet the burst failure criteria, the maximum ratio of outer diameter to thickness is 13.5 for polybutylene and 16.7 for nylon.
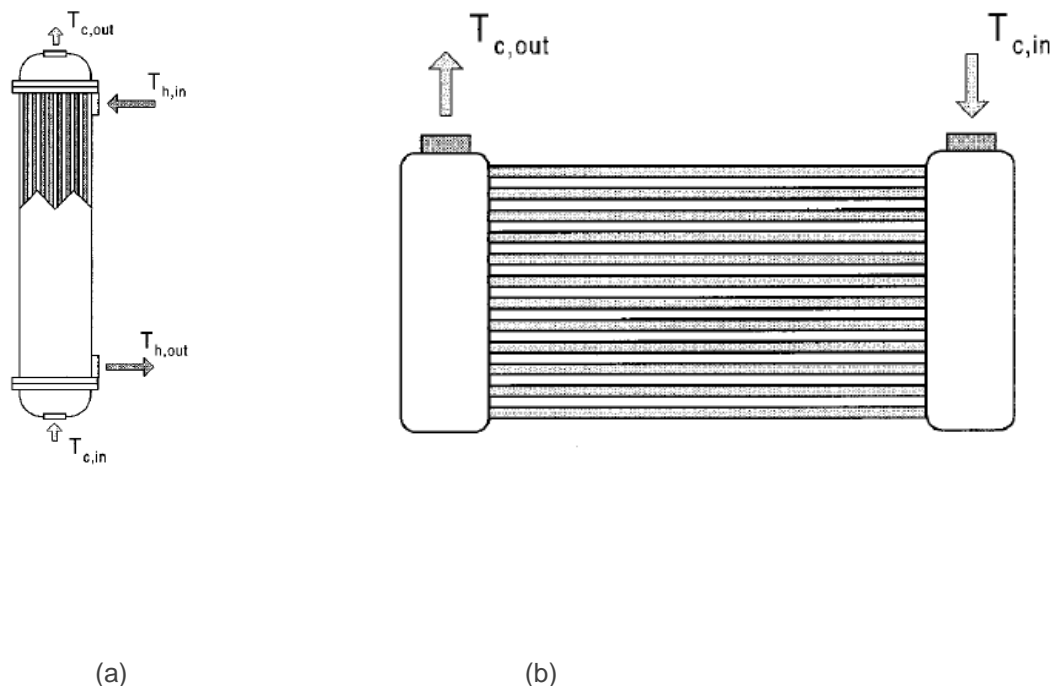

(a)   (b)

Figure 6 Two types of heat exchangers (a) tube in shell and (b) immersed tube presented in(Liu, Davidson et al. 2000)

Scaling can be another issue for solar water heat system using polymer heat exchangers. In the solar water heat systems, particularly in absorber rise tubes and heat exchangers, long term scaling can dramatically reduce the heat transfer due to the additional conductive resistance across the calcium carbonate layer. Wang et al.(Wang, Davidson et al. 2005) conducted experimental study of the growth scale of heat exchangers made from copper, nylon 6,6, semiaromatic high performance nylon, polypropylene, polybutylene, and Teflon tube. Due to the hydrophilic nature of polymers, nylon 6,6 showed the higher scaling rates than other materials. Copper did not demonstrate any major enhanced tendency to scale compared with other materials.

Antar et al.(Antar, Feller et al. 2013) proposed to use a conductive polymer nanocomposites (CPC) for solar absorbers design. Polylactic acid (PLA) and poly (amide 12) (PA12) filled with carbon nanotube were selected used to replace the traditional copper absorbers. Several parameters including thermal performance, electrical resistivity, light absorption and thermal conductivity were analysed. The thermal conductivity of PLA and PA12 were reported to be 0.28W/mK and 0.26W/mK, with 5 wt% of carbon nanotube. However, these values were still too lower to be used in solar absorber application (normally between 1W/mK and 1.5W/mK).

2.5 Water desalination/distillation application

Because of the limited and poor availability of fresh water source around the world, the industrial process of desalination the sea water and brackish water remains to be a hot topic. Most of the water desalination process use mainly on expensive construction material (such as high steel alloys, copper-nickel alloys and titanium) for manufacturing various metallic heat exchangers. The attempts to replace the metal heat exchangers with polymers have been made by many researchers during past decades.

Bourouni et al.(Bourouni, Martin et al. 1997) presented experimental data on a falling film evaporator and condenser made of 2.5 cm diameter circular PP tubes (wall thickness of 5 mm) used in an 'aero-evapo-condensation process' for desalination. The results were compared to a model which examined the impact of the water mass flow rate and inlet temperature. Good agreement was observed, but economic analysis indicated that the unit would only be viable if cheap heat was available, such as a geothermal power source.

Plastic and compact heat exchangers made from PTFE for single-effect desalination system was proposed by El-Dessouky et al.(El-Dessouky and Ettouney 1999). In the model, thin walled polymer tubes and plates were studied (40–150 mm), indicating a need for spacers to prevent the structure from collapsing and for very fine filtering, should this unit ever be constructed. The heat transfer areas with respect to hot brine boiling temperature for heat exchanger made from PTFE were studied and compared to these made from metals (titanium, high alloy steel, and Cu–Ni alloys). The results indicated that heat transfer area of the PTFE preheaters and evaporator was 2–4 times larger than that of the metal heat exchangers with varying boiling brine temperature. However, the polymer heat exchanger had the lowest cost.

Christmann et al.(Christmann, Krätz et al. 2010, Christmann, Krätz et al. 2013) studied a falling film plate evaporator (as shown in Figure 7) made from high performance PEEK for multi-effect distillation (MED) plants. The experimental testing results showed the mean overall heat transfer coefficients for evaporation in the range of 3182 to 3765W/m^{2}K, which were comparable to literature values of metallic falling film heat exchangers. The heat transfer simulations were also presented in this paper, and a good agreement between theoretical and experimental testing results was achieved.
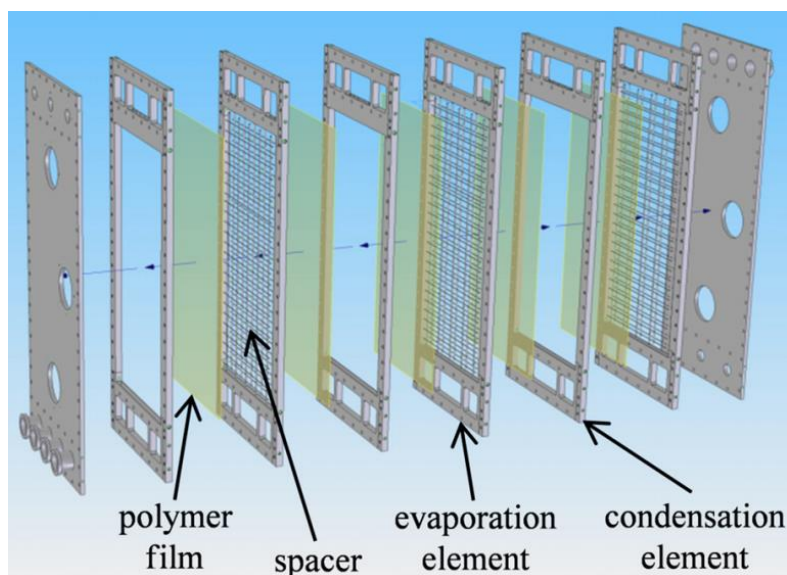

Figure 7 Exploded assembly drawing of the falling film plate heat exchanger with PEEK film heat transfer surfaces and spacers(Christmann, Krätz et al. 2013)

A similar multi-effect distillation system was designed and fabricated by Scheffler and Leao(Scheffler and Leao 2008). Polyolefins such as high density polyethylene (HDPE) and PP were chosen because of their high heat transfer performance and low cost. The U values of HDPE and PP were about 71-105% to cupro-nickel tubes. The authors presented into details about the material selection criteria and manufacturing process of this system, however, the experimental testing results were not well disclosed.

Olefin/paraffin distillation system using hollow fibre structured packings (HFSP) (as shown in Figure 19) was proposed by Yang et al.(Yang, Barbero et al. 2006). Several commercially available hollow fibres, such as PP, polysulfone and PVDF were conceptually demonstrated. The model showed that, with small inner diameter, thin wall and small pore size, celgard PP hollow fibres was the best candidate for HFSPs application. This group of researchers recently scaled up the experiment and long-term operational testing results were obtained and reported (Yang et al.(Yang, Le et al. 2013)). The results demonstrated that the HFSPs technology could provide high sepration efficiency and column capacity in iso-/n-butane distillation for 18 months. After long-term exposure to light hydrocarbon environments (≤70◦C), the mechanical properties of the PP polymer did not degrade significantly. However, the commercially available Teflon and PVDF fibres are not applicable for this system, as they have larger pore size and thicker walls. Therefore, some R&D effort should be dedicated to fabricate the fibres with smaller dimensions and pore sizes to extend this technology to broader chemical stream.

2.6 Polymer micro-hollow fibre heat exchanger

The relatively low overall heat transfer coefficients achieved in plastic heat exchangers can be improved and reach values comparable to metal heat exchangers, if the polymer tube thickness is kept below 100μm(Bandelier, Deronzier et al. 1992). Several researches have been focused on the heat transfer mechanism of polymer micro-hollow fibre heat exchanger. Such kind of polymer micro hollow fibre normally has a relatively smaller inside and outside diameter (ID and OD < 0.1mm).

Zarkadas and Sirkar(Zarkadas and Sirkar 2004, Zarkadas, Li et al. 2005) reported polymeric hollow fibre heat exchangers (PHFHE) for low temperature (up to 150-200◦C) and low pressure application (testing rig as shown in Figure 20). Polypropylene (PP), polyethereth-erketone (PEEK) and asymmetric polyethersulfone (PES) hollow fibres have been used to manufacture heat exchangers. The overall heat transfer coefficients for the water-water, ethanol-water, and stream-water systems reached 647-1314, 414-642, and 2000 W/(m^{2}K), respectively. The experimental testing results of PHFEH presented in this paper indicated that PHFHE can achieve high thermal effectiveness (up to 95%), large number of transfer units (NTU), and very small height of a transfer unit (HTU=6cm, 20 times less than the lower limit for shell-tube heat exchangers) if prospered designed. If PHFHE is designed like commercial membrane contractors, they can achieve up to 12 transfer units in a single device with length less than 70cm. The authors concluded that PHFHE could offer comparable heat transfer performance with reduced weight and cost compared with metal heat exchangers.

Astrouski I. et al.(Astrouski I., Raudensky M. et al. 2013) studied the fouling effect of polymeric heat exchanger made from PP (inner and out fibre diameter of 0.461mm and 0.523mm respectively) for the purposed to cool TiO2 suspension. The experimental testing results showed a very high overall heat transfer coefficient, with up to 2100W/m2K for clean conditions and 1750W/m2K for dirty conditions at the flow velocities of 0.05m/s. The experimental results were used by second-order polynomials and the fouling coefficient was correlated into one function. However, this correlation was not enough to characterize the fouling coefficient, as it was only validate for Re number in the range of 800-1600.

Zhao et al.(Zhao, Li et al. 2013) presented numerical analysis of novel PP hollow fibre heat exchanger for low temperature applications. A 3D model of tube-and-shell application of hollow fibre heat exchangers were simulated using CFD modelling tool FLUENT. The impacts of velocities and packing factors in tube-side and shell-side on total heat transfer coefficients were studied parametrically. The heat transfer coefficient of PP fibres was achieved at 1109w/m2K with inside and outside fibre diameters of 0.6mm and 1mm respectively. An optimal packing faction of 13-19% was concluded by the authors.

Song et al.(Song, Li et al. 2010) proposed experiments and numerical simulation on solid polymeric hollow fibres heat exchangers (PHFHE) for thermal desalination process. Three types of polymeric hollow fibres (as shown in Figure 21) including solid PP, solid PEEK and asymmetric polyethersulfone (PES) with nonporous coatings were used to produce the heat exchangers. The heat transfer performances of these devices were studied for a hot brine (4%NaCl, 80-98◦C)-cold water (8-25◦C) system and a steam –cold water (8-25◦C) system. Compared to metallic heat exchangers, these polymer heat exchangers have an

order of magnitude larger surface area per unit volume. The results indicated that the overall heat transfer coefficient of the hollow fibre heat exchanger made from solid PP (wall thickness of 75μm and outside diameter of 575μm) was 2000W/m2K for brine-water system and 1600-1800 W/m2K for steam-water system.

3. CONCLUSIONS

In the present work, the merits and drawbacks of various polymer materials and filler enhanced polymer composite materials are reviewed in detail. Based on the review, recent successful applications of polymer heat exchangers in a wide range of applications have been summarized, which includes heat recovery system, evaporative/desiccant cooling system, and solar water heating system, water desalination system and electronic cooling device. Recent years, special research interests have been placed on the thermal performance and application of polymer hollow fibre heat exchangers. Despite of polymer materials' low thermal conductivities (0.1-0.4W/mK, which is 100-300 times lower than metals), by using hollow polymer fibres with the diameters less than 10^3μm, the surface area/volume ratio of polymer hollow fibre heat exchangers are significantly high. This makes them extremely efficient with superior thermal performance. Taken into considerations of the lost cost, light weight, low fouling coefficients and corrosive resistant features, polymer heat exchangers should seriously considered as substitutes for metal heat exchangers.

Current research works for the heat transfer performance analysis of polymer heat exchanger are mainly concentrated on shell and tube polymer heat exchangers, with very few experimental and theoretical results published for other types of heat exchangers (such as plate heat exchanger, finned tube exchangers). Moreover, the applications of heat exchangers in various fields are mostly presented by theoretical simulation. For the very few experimental applications of polymer heat exchanger applied in various heat recovery and cooling system, the emphasis have been laid on the overall system performance, while the actual thermal performance of polymer heat exchangers are hardly revealed. Therefore, a considerable amount of research is still required to fully analysis the thermal performance of various types of polymer heat exchangers, as well as the manufacturing cost in comparisons with metal counterparts. Further research is needed to experimentally tailor the structure configurations and obtain the thermal performance of polymer heat exchangers in wide range of industrial and mechanical applications. Since the thermal conductivity and wall resistance of polymer heat exchangers are quite different from metallic heat exchangers, the procedures/parameters applied for polymer heat exchanger design could be unique as well. Besides, a disinclination of the industry to depart from well established metal heat exchanger practices remains a big barrier to the commercialization of polymer heat exchangers. In order to overcome this and ensure a good penetration of polymer heat exchanger in the commercial market in the future, research cooperation with industrial partners is strongly recommended.

4. ACKNOWLEDGEMENT:

5. REFERENCES

Alizadeh, S. (2008). "A feasibility study of using solar liquid-desiccant air conditioner in Queensland, Australia." Journal of Solar Energy Engineering **130**(2): 021005.

Antar, Z., J.-F. Feller and G. Vignaud (2013). "Eco-friendly conductive polymer nanocomposites (CPC) for solar absorbers design." Polymers for Advanced Technologies **24**(7): 638-645.

Astrouski I., Raudensky M. and D. M. (2013). "Particulate fouling of polymeric hollow fiber heat exchanger." Proceedings of international conference on heat exchanger fouling and cleaning, June 09-14, 2013, Budapest, Hungary.

Bandelier, P., J. C. Deronzier and F. Lauro (1992). "Plastic heat exchangers." Matériaux & Techniques **9-10**: 67-70.

Bourouni, K., R. Martin, L. Tadrist and H. Tadrist (1997). "Experimental investigation of evaporation performances of a desalination prototype using the aero-evapo-condensation process." Desalination **114**(2): 111-128.

Chen, J., H. Chang and S.-R. Chen (2006). "Simulation study of a hybrid absorber–heat exchanger using hollow fiber membrane module for the ammonia–water absorption cycle." International Journal of Refrigeration **29**(6): 1043-1052.

Chen, L., Z. Li and Z.-Y. Guo (2009). "Experimental investigation of plastic finned-tube heat exchangers, with emphasis on material thermal conductivity." Experimental Thermal and Fluid Science **33**(5): 922-928.

Chen, L., Y. Sun, X. Du, G. Wei and L. Yang (2014). "Performance Analysis of Anti-corrosion Heat Exchangers Made of Special Plastics for Flue Gas Heat Recovery." Proceedings of the CSEE **34**(17): 2778-2783.

Christmann, J. B., L. J. Krätz and H.-J. Bart (2010). "Novel polymer film heat exchangers for seawater desalination." Desalination and Water Treatment **21**(1-3): 162-174.

Christmann, J. B., L. J. Krätz and H.-J. Bart (2013). "Falling film evaporation with polymeric heat transfer surfaces." Desalination **308**: 56-62.

Dartnall, W. J., A. Revel and V. Giotis (2009). "Air-Conditioning Employing Indirect Evaporative Cooling Can Be Shown to Derive Its Energy From the Solar Source." ASME Proceedings | Energy Systems: Analysis, Thermodynamics and Sustainability, November 2009, Florida, USA.

E. Brundrett, T.J. Jewett and R. Quist (1984). "Evaluation of polytube heat exchangers for greenhouse ventilation." Acta-horticultarae **148**: 49-55.

El-Dessouky, H. T. and H. M. Ettouney (1999). "Plastic/compact heat exchangers for single-effect desalination systems." Desalination **122**(2–3): 271-289.

Giotis, V. and A. Revel (2008). "Performance assessment of indirect evaportive cooling air-conditioning system, installed at University of Technology Sydney." Master of Engineering Project, UTS, NSW, Australia.

Githens, R. E., R. W. Minor and V. J. Tomsic (1965). "Flexible tube heat exchangers." Chemical Engineering Progress **61**(7): 55-62.

Jia, L., X. Peng, J. Sun and T. Chen (2001). "An experimental study on vapor condensation of wet flue gas in a plastic heat exchanger." Heat Transfer—Asian Research **30**(7): 571-580.

Kachhwaha, S. S. and S. Prabhakar (2010). "Heat and mass transfer study in a direct evaporative cooler." Journal of Scientific & Industrial Research **69**: 705-710.

Liu, W., J. Davidson and S. Mantell (2000). "Thermal analysis of polymer heat exchangers for solar water heating: A case study." Journal of Solar Energy Engineering, Transactions of the ASME **122**(2): 84-91.

Lowenstein, A., S. Slayzak and E. Kozubal (2006). A zero carryover liquid-desiccant air conditioner for solar applications. ASME 2006 International Solar Energy Conference, American Society of Mechanical Engineers.

Pescod, D. (1979). "A heat exchanger for energy saving in an air-conditioning plant." AsHRAE Transaction **85**: 238-251.

Rousse, D. R., D. Y. Martin, R. Thériault, F. Léveillée and R. Boily (2000). "Heat recovery in greenhouses: a practical solution." Applied Thermal Engineering **20**(8): 687-706.

Saman, W. and S. Alizadeh (2002). "An experimental study of a cross-flow type plate heat exchanger for dehumidification/cooling." Solar Energy **73**(1): 59-71.

Saman, W. Y. and S. Alizadeh (2001). "Modelling and performance analysis of a cross-flow type plate heat exchanger for dehumidification/cooling." Solar Energy **70**(4): 361-372.

Scheffler, T. B. and A. J. Leao (2008). "Fabrication of polymer film heat transfer elements for energy efficient multi-effect distillation." Desalination **222**(1–3): 696-710.

Song, L., B. Li, D. Zarkadas, S. Christian and K. K. Sirkar (2010). "Polymeric hollow-fiber heat exchangers for thermal desalination processes." Industrial and Engineering Chemistry Research **49**(23): 11961-11977.

Tatlıer, M. and A. Erdem-Şenatalar (2004). "Polymeric heat exchangers to increase the COP values of adsorption heat pumps utilizing zeolite coatings." Applied Thermal Engineering **24**(1): 69-78.

Wang, Y., J. Davidson and L. Francis (2005). "Scaling in polymer tubes and interpretation for use in solar water heating systems." Journal of solar energy engineering **127**(1): 3-14.

Wu, C., S. C. Mantell and J. Davidson (2004). "Polymers for solar domestic hot water: Long-term performance of PB and nylon 6, 6 tubing in hot water." Journal of solar energy engineering **126**(1): 581-586.

Yang, D., R. S. Barbero, D. J. Devlin, E. Cussler, C. W. Colling and M. E. Carrera (2006). "Hollow fibers as structured packing for olefin/paraffin separations." Journal of membrane science **279**(1): 61-69.

Yang, D., L. Le, R. Martinez and M. Morrison (2013). "Hollow fibers structured packings in olefin/paraffin distillation: apparatus scale-up and long-term stability." Industrial & Engineering Chemistry Research **52**(26): 9165-9179.

Zarkadas, D. M., B. Li and K. K. Sirkar (2005). Polymeric hollow fiber heat exchangers (PHFHEs): A new type of compact heat exchanger for lower temperature applications. Proceedings of the ASME Summer Heat Transfer Conference.

Zarkadas, D. M. and K. K. Sirkar (2004). "Polymeric Hollow Fiber Heat Exchangers: An Alternative for Lower Temperature Applications." Industrial & Engineering Chemistry Research **43**(25): 8093-8106.

Zhao, J., B. Li, X. Li, Y. Qin, C. Li and S. Wang (2013). "Numerical simulation of novel polypropylene hollow fiber heat exchanger and analysis of its characteristics." Applied Thermal Engineering **59**(1–2): 134-141.

417: Sustainable and renewable energy architectural initiatives for COMSATS Institute of Information Technology Islamabad Campus- Pakistan

ADNAN AMIN

COMSATS Institute of Information Technology, Park Road, Chak Shehzad, Islamabad
adnan_amin@comsats.edu.pk, architectadnan@hotmail.com

Application of sustainable and renewable energy generation initiatives and architectural design solutions can help in making any educational campus energy-efficient and sustainable. These initiatives and solutions are helpful to conserve energy in the built structures and at the same time generate additional energy at the master plan level. The scope of research encompasses the COMSATS campus in Islamabad. In-depth study and research is done, to highlight the significance of application of green design solutions like green roof on an existing building to make it energy efficient and thermally comfortable. The project focuses on different modes of renewable energy generation and conservation of energy by applying appropriate green and sustainable techniques. A comparative study for different architectural design solutions with minimum cost and maximum advantages to reduce heat gain through building envelope that is the walls, the roof and windows of the buildings has been provided. At the same time suggestions have been made to generate additional energy through renewable sources and by application of latest technology.

Keywords: Sustainable Renewable Initiatives, Green Solutions, Educational Campus, Building Envelope, Thermal comfort

1. INTRODUCTION

In the prevalent energy crises and highly increasing energy fuel costs it is the need of hour to adopt the renewable and sustainable means of energy. Especially in Pakistan the energy-crisis is much more severe than the rest of world. *Pakistan is facing this severe energy crisis since last decade (Ahmed et.al, 2013).* "*The power sector crisis has been engaging attention of the public and the media over the last 5 years due to continuing long power outages, ranging from 12 to 16 hours in urban areas and up to 20 hours in rural areas. Nearly one third of demand for electricity, during the last year, could not be met due to supply constraints. On average, a supply deficit of around 5,000 Megawatt (MW) was experienced, while it touched the peak of over 7,000MW last July 2013*" (Saeed, 2013). *In order to meet the increased energy demand and ensure its sustainable supply, different energy options are being considered.* Due to lack of interest by the relevant institutions and organizations made by the government across Pakistan the total contribution of renewable energy in the total energy generation for the country is 1% only. If a proper attention is given, this can be increased up to 30% which will result in saving more than 60% of foreign exchange which is being spent to purchase oil etc. to generate electricity and other energy modes (Sheikh et.al, 2010).

In the backdrop of energy conservation and efficiency the energy-efficient or smart buildings have relatively reduced energy demand and better efficiency that can significantly contribute to the conservation of energy. These buildings provide the human comfort level temperatures to the people living inside and reduce energy usage in different forms i.e. electricity, natural gas, etc. for heating, cooling and lighting purposes. Janssen (2004) claims that any action taken up by producer or user of energy products is assumed to be improving energy efficiency, as it decreases energy use per unit of output, without affecting the level of service provided (Zainordin et. al, 2012).

The data on energy saving potential of energy smart buildings in terms of building envelope, lighting and air conditioning gives an overview of the cumulated potential of these three areas. This cumulated potential is used for calibration and extrapolation of energy conservation potential. And for this purpose sensitivity analysis approach is used to assess the monetary saving from energy conservation. Overall saving of aforementioned three potential energy conservation areas is 29% that means roughly 29% of the energy consumption can be reduced and saved. Consequently, same percentage of the energy cost or price paid in terms of electricity bills can be saved (Ahmed et. al, 2013).

Climate responsive design has been in traditional cultures since the beginning of recorded history. Its energy-free architectural design principles seek to maintain a building and interior environment within a balanced comfort range without additional inputs of non-renewable energy. With global interest in low-energy high-performance buildings, energy-free design principles are increasingly promoted for a range of climates and for many parts of the world. The Passivehaus movement and interest in double skin facades are two contemporary examples of high adaptable building envelope-based strategies which successfully integrate the benefits of energy-free design (Trubiano, 2013).

1.1 Renewable Energy Sources

Different Renewable sources of energy in the world are adopted to generate electricity and other modes of energy in different sectors including the education sector. In order to compensate the energy requirements, it is possible to produce energy by renewable energy sources like solar, hydraulic, geothermal, wind, wave and biomass etc (Midilli et.al, 2006). Renewable energy sources made 18% of the world's total primary supply in the year 2007. Major contributor was Biomass but there are other sources as well namely hydro power, geothermal energy, biomass energy, solar energy and wind power. (Yuksel et.al, 2011)

1.2 Educational Campuses and Energy Conservation in Pakistan

Educational sector in Pakistan is one of the biggest consumers of energy as most of the campuses constructed are energy intensive. Energy can be conserved and generated at educational campuses to make them self-sufficient for their energy requirements. University of Minnesota Morris U.S.A, Masdar Institute of Science and Technology Abu Dhabi U.A.E and Universitite International de Rabat (UIR) are examples. With the changing climatic scenario and different environmental issues, universities must be designed to be green and energy-efficient. In this regard there are a lot of activities and tasks which can be done. For category of energy one must use renewable energy sources like solar and other energy saving appliances and smart energy management systems. So this is extremely seriously needed to carryout research and find sustainable and renewable energy initiatives/solutions best suitable for energy conservation and generation in Pakistan especially in the academic buildings. It is also needed to re-

evaluate the thermal performance of existing buildings and if found, rectify the errors and deficiencies in architectural design of these buildings to make them climate friendly and energy-efficient.

1.3 Research Gaps

Researches already done in the study areas related to this proposed project have mainly focused different sources and provisions for energy generation only. There has been a lesser or no emphasis on the architectural design of buildings to reduce energy consumption and become thermally comfortable as well. So with other provisions of energy generation, this project will fulfill the major deficiencies in the area of improvement of thermal efficiency of building envelope and architectural design specially in case of existing buildings along with other renewable and sustainable initiatives for energy generation at COMSATS Islamabad campus. Also there is a need to raise awareness among the university people about the significance of the applications of renewable energy architectural initiatives.

1.4 Objectives

Following are the main objectives to be achieved through the implementation of proposed project:

• To critically evaluate the thermal efficiency and Architectural design of an existing building at CIIT Islamabad for recommendation of cost efficient Architectural Design solutions to reduce the heat transfer through building envelope.

• To Identify and recommend the most suitable sustainable and renewable energy initiatives for application at CIIT Islamabad campus to increase the self-sufficiency of CIIT Islamabad for energy generation through renewable means.

• To recommend cost effective application of recommended sustainable and renewable energy initiatives.

2 LITERATURE REVIEW

2.1 Background

Schools designed with an understanding how the brain and mind of children respond to the attributes of spaces and places can lead to enhanced learning. Such research is adding to our architectural knowledge base an understanding of how daylight, acoustics and views of nature are deeply influential on the cognitive processes of children (Ford, 2007). There are methods of passive conditioning of outdoor air which are categorized as wind breaks, natural air-conditioning, cooling ponds, sun traps, basement coolers and the wind catchers. In parallel to design with good natural ventilation, one needs to incorporate the sun at its best to increase the perfection of a passive solar design of buildings (Roaf, 2013).

2.2 Building Envelope

Major ingredients to be studied to design a perfect building envelope are: Heat transfer through the building walls and roof; Roof design; Walls design; and Windows design (ENERCON, 1990).

2.3 Green Roof and Walls

Green roof installation saves energy while cooling the buildings. An example is installation of green roofs on 50% of existing roof surfaces in urbanized Southern California. The result came in the form of direct energy saving from reduction of building cooling energy use which got reduced up to 1.6 million megawatt-hours per year. This brought a saving for residents around 211 million US Dollars in electricity cost. It also reduced the greenhouse emission by up to 465 thousands metric tons of CO_2 equivalent per year (Garrison and Horowitz, 2012). Older buildings with poor existing insulation are deemed to benefit the most from a green roof. Green roofs can be helpful for energy saving for different degrees of insulations for different roofs.

Green walls or living walls benefit in a number of ways. They improve the air quality at one hand and reduce the surface temperature in built structures. Evaporative cooling through leaves makes the temperature of

building surface and surrounding spaces. Similarly direct shading of the external wall surfaces is also helpful for thermal comfort inside buildings (Sheweka and Magdy, 2011).

2.4 What is our contribution?

Following are the main contributions that have been made through this research to contribute to the benefit of all.

- First time in Pakistan a whole educational institution has been evaluated in terms of energy used in different forms.
- First time in Pakistan solutions have been worked out to convert an energy-intensive educational campus / Institution into an energy-efficient campus through the application of sustainable and renewable initiatives including wind, solar and biomass.
- Impact of architectural design of existing building in an educational campus has been evaluated for its contribution towards thermal performance of the building.
- Cost efficient architectural design solutions have been suggested to convert the existing buildings at COMSATS Islamabad campus in to energy-efficient ones and thus these suggestions will be put in to the practical form.
- The sustainable and renewable initiatives will be evaluated for their feasibility in context of climate of Islamabad and the context / surroundings of CIIT Islamabad campus and the most suitable ones will be recommended.

3 METHODOLOGY AND DATA COLLECTION

Research methodology comprising of literature review, Physical inspection and documentation of whole campus area, Case studies and computer based simulations was adopted to collect data for all the campus area and the Academic Block-1 building situated at CIIT Islamabad campus to be provided with renewable and sustainable solutions for energy conservation, energy generation and thermal comfort as follows:

3.1 Study of climate of Islamabad

Normal composites climate of Islamabad comprises of:

Hot dry period	Hot humid period	Cold period	Transitional period
Summer (April-June)	Monsoon (Jul-Sep)	Winter (Dec-Mar)	(Oct- Nov)

Research is done for identification of time durations in each climatic period in Islamabad which are very much uncomfortable and finding the reasons of discomfort. Objectives were set to attain comfort in each climatic period after the identification of reasons of discomfort.

3.2 In Depth study and critical analysis of architectural design of Academic Block-1 building

The study has been carried out to critically analyze the Architectural design of existing building of Academic Block-1 at the campus for its energy efficiency and performance and will be extended to cover all the existing buildings in context of the following important factors

1. Climate of Islamabad.
2. Human comfort level.
3. Site Planning.
4. Building Orientation and Form.
5. Building Envelope.
6. Lighting both natural and artificial.
7. Ventilation and indoor air quality.

The building of Academic Block-1 is situated in the North-Eastern area of the campus. It is facing North-West. The building due to its location and orientation carries a lot of diversity and challenges in terms of its behavior towards solar axis and wind direction etc. which ultimately affect the thermal performance of this building. Here is a critical evaluation to understand the thermal performance of this building.

Ventilation and air circulation

Class room's area is ventilated as the lobbies & corridors are well oriented for cross ventilation. Whereas the Faculty area and Labs have poor ventilation.
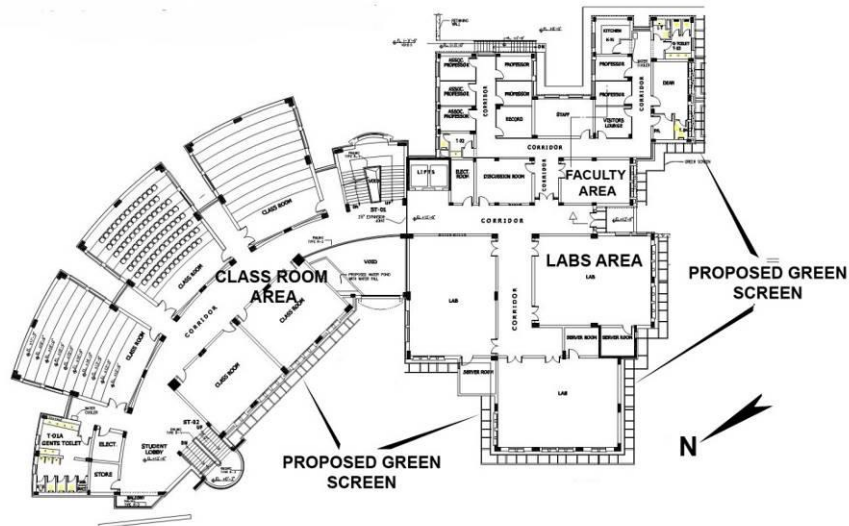

Figure 1: Ground Floor Plan of Academic Block - 1

Natural / day lighting vs. artificial lighting
Labs have insufficient glazing (less than 30% wall area). There is an unequal distribution of natural light in the building. Class rooms have insufficient light and almost half of the circulation areas are poorly lit up.

West facing wall
This wall is most challenging in terms of heat gain and incident angle of solar radiations. There is an inappropriate protection for the building against the sun/ solar radiations.

North-west facing wall
Through this wall there is a heat gain for more than 3 hours.

South-West facing Wall
This is the most critical wall surface. It gets almost 5-6 hours of direct solar radiation and heat gain in one day. The intensity of solar radiations is maximum on this side of the building.

Roof Surface
Roof surface of this building has an area of 19500 sqft which is throughout the day time exposed to the direct solar radiations. The heat insulation of the roof is not sufficiently done and it gets extremely hot inside the building because of heat gain through roof.

3.3. Solar Study of an Existing Building at CIIT, Islamabad

Detailed Solar study is done for academic block – 1 demonstrating the patterns of incident solar radiations and shadows cast as a result. This study highlights the critical timings in a day when the sun is required to be avoided and desired by the building envelope. This study also verifies the conclusions drawn by the analysis of climatic data about identification of time period of discomfort for building occupants throughout the year.

Shadow study and analysis have been conducted at following times

- 8 am   ● 12 pm   ● 5 pm

On Following Days

- Jan 1st   ● March 1st   ● May 1st   ● July 1st   ● Sept 1st   ● Nov 1st
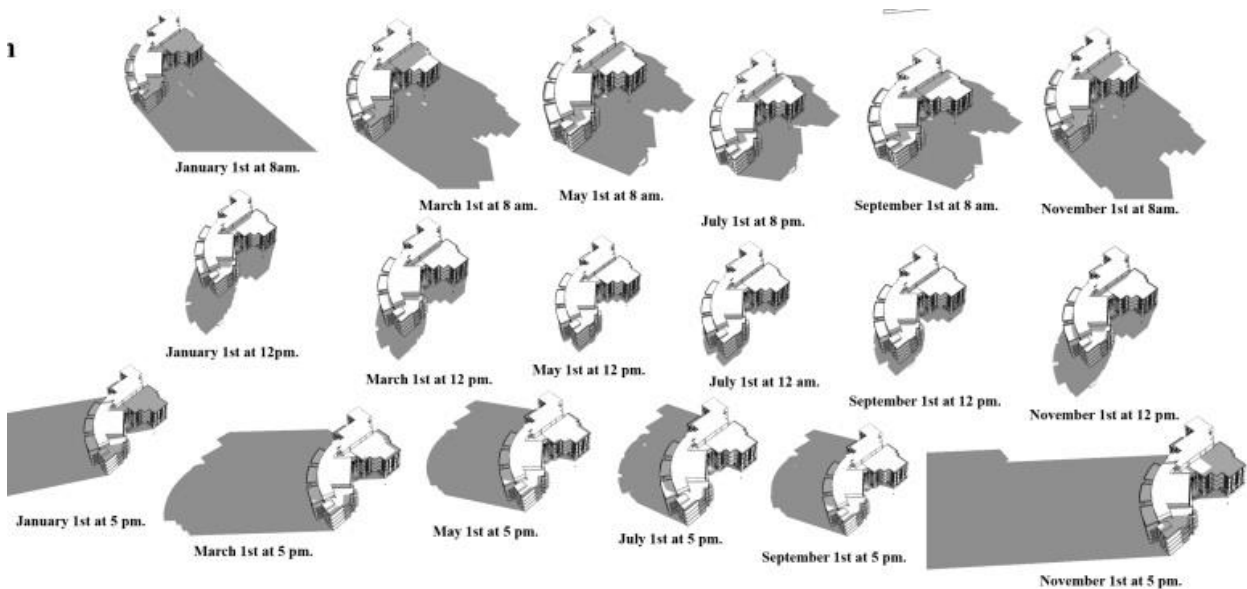

Figure 2: Solar study is done for academic block – 1

3.3 Study of Sustainable and Renewable Energy Sources and Their Application

a) Application of renewable and sustainable energy techniques in terms of Solar, Wind and Biomass etc.
b) Cost evaluation of the renewable and sustainable energy techniques for their installation and maintenance

3.4 Study and Recommendation of Passive and Active Solar Systems and Techniques Most Suitable in the Climate of Islamabad

Techniques have been divided into 4 categories according to their functions. The 4 categories are Techniques for Air movement, solar heat reflection, landscaping, humidification (in hot dry period) & dehumidification (in warm humid period).

3.5 Case Studies

a) Case studies have been done through literature review to evaluate the efficiency of techniques for thermal comfort and energy-efficiency.
b) To study the building envelope.
c) To evaluate the efficiency of renewable energy and sustainable energy techniques for thermal comfort and energy-efficiency incorporated in those buildings.

3.6 Analysis of Climatic Data

The analysis of the climatic data of Islamabad suggests that this is a city with diversified weathers including winter, summer, spring and Monsoon with their extremes. The temperature climbs up to 47°C in summer

and falls to -4°C in winters. Similar is with the Precipitations. It rains extremely high at the Monsoon. Overall it's almost seven to eight months with heat and humidity including the summer and the monsoon in total. The cold weather provides a challenge only in the winters which are almost three months long.

It is concluded that the handling of weather extremes during the longer span i.e. of heat needs to be settled on priority basis to gain thermal comfort inside the built structures and to improve thermal efficiency of built structure. For the application of renewable energy generation sources, the climatic data also suggests that Islamabad has a very long period from 8-9 months with good sunshine overall during the year so application of Solar panels for water heating and energy generation can be very effective. It is further concluded that due to a very low wind velocity there is not a good potential to generate electricity through wind mills.

4. RESULTS AND SOLUTIONS:

After an in depth study and research following are renewable energy initiatives / techniques and Architectural design solutions recommended to be implemented at COMSATS Islamabad campus through the implementation of this research project.

4.1 Solar energy:

Application of Solar energy is encouraged to generate additional amount of energy in the form of electricity, solar water heating and other applications because

a)   There is abundance of sunlight available throughout the year as shown in the graph below.

Table 1: Cloud Cover Types

Source http//weatherspark.com/averages/32869/Islamabad-Punjab-Pakistan
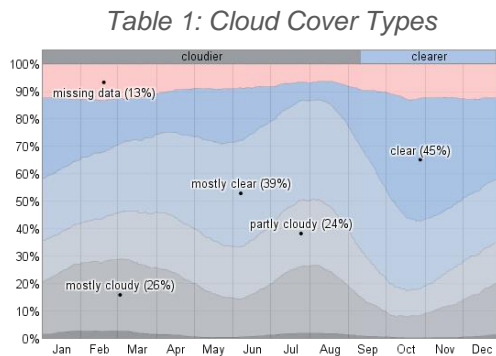
b)   There is already an existing example of a Solar Tube well at CIIT Islamabad campus which is functional and is generating electricity to operate the electric pump to water the whole sports arena.
c)   There is already an existing example of solar water heaters installed on the roof top of academic block 2 and they are functional.
d)   There is a huge diversity and variation in sizes of photovoltaic panels which are available locally.

Present day advancement in renewable energy and technology related has made it possible for everyone to get benefit (Omer, 2008) has discussed in his paper about people of far off areas of poor country like Sudan who are generating energy using solar panels to illuminate their village houses.

4.2 Bio Gas Plants:

The CIIT Islamabad has no supplies of natural gas at the moment. This is a big handicap for CIIT. Small scale bio gas plants are suggested to be made so that they could generate gas which can be used as fuel

1)   For heaters of security guards on different entrance gates who are surviving the extreme cold of Islamabad at the cost of electric heaters.
2)   To keep academic buildings warm partially as these buildings are big and a bio gas plant produces a very calculated amount of gas produced.

There are a few good reasons which support the idea of making bio gas plants. These are

    a) Animal dung, the major raw material for a biogas plant to produce gas is available very easily because CIIT Islamabad is situated in an agricultural suburban area.
    b) The cost of construction of a biogas plant is very low.
    c) The skilled labor to construct small and big scale plants is easily available.
    d) The maintenance and smooth running of the plant is very easy and skilled labor is available for this from local sources.

4.3 Techniques and Architectural Design Solutions Recommended for Energy Conservation In The Building

Folowing are the details of Architectural Design solutions and techniques to improve the thermal efficiency of building envelope to conserve energy.

Roof Heat Insulation Specifications

Specially designed treatment for heat insulation is recommended for roof tops. In this regard details have been worked out with the mathematical data gained through computer based simulations indicating the efficiency and performance of the roof against heat gain. The image below is a graphical representation of roof insulation details suggested.

Figure 3: Roof heat insulation specifications

Mathematical Calculations through Computer Based Simulations for suggested roof heat insulation specifications

As per BECP (Building energy code for Pakistan)

Allowable maximum OTTV (overall thermal transmittance value for roof = 26.8W/m²

Calculated OTTV for roof with recommended insulation details = 46.63 W/m²

Modified OTTV for roof with recommended insulation details = 25.73 W/m².

Suggestions

Change the brick orientation from horizontal to vertical for creating bigger cavity.

Improved Output

It reduces the heat gain or loss up to **59.93 %** through the roof surface.

The improved output indicates that due to change in placement of bricks from horizontal to the brick on edge formation the heat transmitted through the roof top into interiors is lesser than what is acceptable for human comfort range.

4.4 Green Roof

Green roof is recommended with vegetation for the roof top of Academic block-1. Impact of green roofs is amazing in contributions to conserve energy. In summers the roof passive cooling effect can be three times more efficient. In winters it can reduce the roof heat losses during cold days. Also the green roof helps making the building energy efficient by reducing heat transmission through the roof top. If done with more precision it can bring down the indoor temperature up to 6°C (Lie et.al, 2003)

4.5 Green Facades

Green facades are facades systems in which climbing plants or hanging port shrubs are developed using special support structures, mainly in a directed way, to cover the desired area. A microclimate between the wall of the building and the green curtain is created, and it is characterized by slightly lower temperatures and higher relative humidity. This means that green screens can act as wind barriers and confirms the evapotranspiration effect of the plants (Perez et.al, 2010). Green walls are helpful in lower greenhouse gas emissions; they have a positive effect on hydrology, improve the indoor air quality and also reduce the noise pollution. These benefits of green walls are the need of hour as they help improving the health of the people inside the buildings (Loh, 2008).
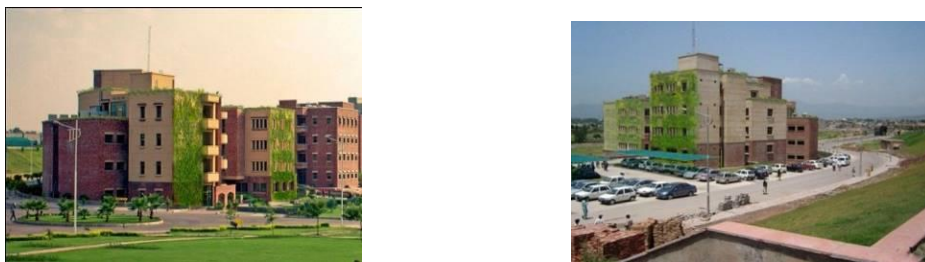

Figure 5: View of North Western Green Façades of Academic Block -1 (on left) and South Western Green Façade (on right) at CIIT Islamabad with application of proposed Green Vertical System.

4.6 Proposed Sustainable and Renewable Energy Architectural Initiatives at Master Plan level.

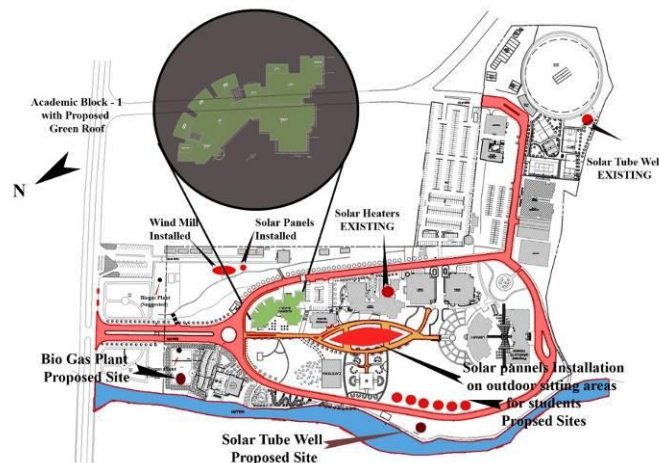*Figure 6: Master Plan of CIIT Islamabad with existing and proposed Locations of Renewable Energy Generation*

5.   FINDINGS AND IMPLEMENTATIONS:

5.1 Findings

The findings of research work highlight the need of energy conservation and generation for the COMSATS Institute of information technology Islamabad both at individual building and Master plan level. Most of buildings are exposed to direct solar radiations and need some kind of protection from the incident radiations. Computer based Solar study of the academic block -1 reveals that more than half of this

building's envelope is exposed to direct solar radiations at the time of the day when the solar radiations are not easy to manage and they heat up the building resulting in additional load on the air conditioning systems that increases the amount of electricity bills. Roof top of this building is with just the conventional heat insulation layers which do not sufficiently protect the interior of building from solar heat gain through the roof.

The critical evaluation of rest of the campus in terms of energy consumption and utilization suggests there is possibility for energy conservation and energy generation inside the campus. Due to availability of solar radiations in abundance for whole year it is possible adapt the solar energy for multipurpose uses. As the buildings are located at a closer distance there is a potential to use this to shadow the walkways in between using some landscaping to provide comfort for the pedestrians.

Roof tops of the buildings can be used for effective solar energy generation and solar water heating purposes as the neighboring structures are at a distance and there is one high rise structure on the North-East of the campus. Also there is availability of animal dung in abundance as the campus is situated with a village neighborhood. This can help in energy generation through biogas plants etc. that can help in reducing some load for heating during the winters in the form of gas heater. At the moment the campus has no heating system on gas heaters and there are only electric heaters used.

5.2 Implementations

The solutions recommended by this research at both renewable energy generation and for the existing building to save energy and become energy-efficient are practical as these solutions are implementable and executable with help from local skilled labor which makes it extremely economical. For the existing buildings the roof heat insulation technique developed indigenously has been recommended after proven to reduce heat gain through roof surface up to 59%. So as the heat intake is reduced by 59% that means there is a reduction of cooling load which results in reduction of total amount of electricity bills reduced. Similarly Green Roof and Green Vertical system have been recommended to cover the building envelope and protect it from the direct heat gain. Protection of the building envelope's surfaces critically exposed to solar radiations helps in both provision of thermal comfort and the reduction in the amount of electricity bills paid by CIIT. With an in depth study of availability and suitability the renewable energy generation is recommended through solar panels and Biogas plants. The walkways and central lawns can be covered with roofs made of solar panels providing shaded circulation and sitting outdoor areas with additional electricity generation.

The excessive water available in the Natural Storm water drain can become a sustainable source of water supplies for irrigation of plants along with the rainwater harvesting resulting in saving a lot of money as the present systems of irrigation and watering the fields and plants is based on the water supply system operated by electric pumps.

6 REFERENCES

AMJID, S.S., Bilal, M.Q.,Nazir, M.S & Hussain, A.(2011). Biogas, renewable energy resource for Pakistan, Renewable and Sustainable Energy Reviews, 15, 2833-2837.

AHMED A, Energy smart buildings potential for conservation and efficiency of energy, PIID AGM, 2013.

CARTER,T & Keeler, A.(2008). Life cycle cost-benefit analysis of extensive vegetated roof systems, Journal of Environmental Management, 87, 350-363.

CASTLETONA, H.F., Stovin, V., Beck, S.B.M & Davison J.B.(2010). Green roofs; building energy savings and the potential for retrofit, 42, 1582-1591.

EVANS, A., Strezov, V & Evans, T.J.(2009). Assessment of sustainability indicators for renewable energy technologies, Renewable and Sustainable Energy Reviews, 13, 1082-1088.

GARRISON, N & Horowitz, C.(2012). Looking up, how Green Roof and Cool Roof can reduce Energy use, Address Climate Change and Protect Water Resources in Southern California, NRDC Report.

HOSEINI, A.H.G., Dahlan, N.D., Berardi,U., Hoseini, A.G., Makaremi, N & Hoseini, M.G.(2013). Sustainable energy performances of green buildingsa review of current theories, implementations and challenges, Renewable and Sustainable Energy Reviews, 25, 1-17.

KOKOGIANAKIS, G., Tietje A & Darkma, J.(2011). The role of Green Roofs on Reducing Heating and Cooling Loads: A Database across Chinese Climates, Sci Verse Science Direct, 11, 604-610.

LIE, K., & Bskaren, B.(2003). Thermal performance of green roofs through field evaluation. NRCC, 1-10.

LOH, Susan.(2008). Living walls-a way to green the built environment. TEC, 26.

MIDILLI, A., Dincer, I., & Ay, M.(2006). Green energy strategies for sustainable development, 34, 3623-3633.

OMER, A.M. (2008). Green energies and the environment, Renewable and Sustainable Energy Reviews, 12, 1789-1821.

PEREZ, G., Rincon, L., Vila, A., Gonzalez, J.M & Cabeza, L.F.(2011). Green vertical systems for buildings as passive systems for energy savings, Applied Energy, 88, 4854-4859.

SAEED, Khalid.(2013). Pakistan's power crises: Challenges and the Way forward, Criterion Quarterly, Vol 8 no 4.

SHEIKH, M.A.(2010). Energy and renewable energy scenario of Pakistan, Renewable and Sustainable Energy Reviews, 14, 354-363.

SHAH, A.A., Qureshi, S.M., Bhutto, A & Shah, A.(2011). Sustainable development through renewable energy the fundamental policy dilemmas of Pakistan, Renewable and Sustainable Energy Reviews, 15, 861-865.

SHEWEKA, S., & Magdy, N.(2011)The living walls as an Approach for a Healthy Urban Environment, 6, 592-599.

YUKSEL, I & Kaygusuz K.(2011). Renewable energy sources and sustainable energy policies in Turkey, Renewable and Sustainable energy Review, 15, 4132-4144.

ZHAI, X.Q., Wang , R.Z., Dai,Y.J., Wu, J.Y., Xu, Y.X., and Ma, Q.(2007). Solar integrated energy system for a green building, Energy and buildings, 39, 985-993.

ZAINORDINA B. N., Abdullah B. M. S. and Ahmad B. Z. (2012), 'Light and Space: Users Perception towards Energy Efficient Buildings', Procedia - Social and Behavioral Sciences 36, 51 – 60.

377: Lighting performance investigation of heat insulation solar glass (HISG) for potential utilization in greenhouses as facade material

ERDEM CUCE, SAFFA RIFFAT, CHIN-HUAI YOUNG

*Department of Architecture and Built Environment, Faculty of Engineering,
University of Nottingham, University Park, NG7 2RD Nottingham, UK*

In this short communication, a novel thin-film photovoltaic glazing material called heat insulation solar glass (HISG), which has recently been developed at the University of Nottingham, is introduced and its lighting efficiency for the potential utilization in greenhouses as a unique facade material is theoretically and experimentally investigated. Within the scope of the research, lighting performance assessment of HISG is presented in a comparable way with the conventional facade technologies such as ordinary single or double glazed building elements. Two test houses consisting of HISG and ordinary glass are constructed, and the lighting efficiency is evaluated for each glass house for different climatic conditions. Visual quality is also investigated through several retrofitting cases. The results indicate that HISG curtain walls provide 24.9% better lighting performance than ordinary glass curtain walls in terms of average values. This result can be attributed to the superior sandwich structure of HISG containing photovoltaic module and highly reflective film, leading to notable increase in light reflection into the house and thus sensible enhancements in lighting levels.

Keywords: Heat insulation solar glass, conventional glazing technologies, lighting performance, greenhouses

1. INTRODUCTION

In this short communication, a novel building facade material called heat insulation solar glass (HISG) is introduced and its potential utilization in greenhouses is discussed [1-4]. Currently, heating and cooling demand of greenhouses are significantly high as a consequence of poor thermal insulation characteristics of conventional facade technologies. Therefore in this paper, this dramatic scenario is aimed to enhance via HISG owing to its extraordinary physical properties.

2. EXPERIMENTAL WORK

Within the scope of this experimental research, two separate experimental test houses are constructed as shown in Figure 1. The first house is integrated with ordinary glass curtain walls while the second one with HISG as illustrated. External dimensions of the test houses are given in Table 1. Each house is supported by aluminium frames for a lightweight construction. Detailed optical and thermal properties of the glazing materials utilized in the curtain wall systems are presented in Table 2. For a reliable testing procedure, each curtain wall system is investigated simultaneously under the identical climatic conditions. The duration of the experimental research covers the summer time. The tests basically aim at comparing the performances of ordinary glass and HISG curtain walls in terms of illuminative penetration, UV penetration, solar radiation and indoor lighting ability. For the thermal and optical performance measurements, JIS3106 JIS3107 and JIS A5759 are adopted as test standards. The accuracy of the measurements is also considered within the scope of this research, and the evaluation is performed through a simple uncertainty analysis. The total uncertainty for the worst case is found to be less than 2 %, which is satisfactory.

Table 1. Dimensional parameters of the test houses.

	Ordinary glass	HISG
Thickness (mm)	12.00	28.00
Length of the house (m)	3.04	3.04
Width of the house (m)	2.51	2.51
Height of the house (m)	3.17	3.17
Vertical glazing area (m^2)	24.64	24.64
Roof glazing area (m^2)	6.16	6.16

Figure 1. Photograph of the ordinary glass (left) and HISG (right) curtain walls.

Table 2. Optical and thermal properties of ordinary glass and HISG curtain walls.

	Ordinary glass	HISG
Visible light transmittance (%)	87.00	7.15
Solar thermal transmittance (%)	60.00	2.60
Absorption rate (%)	5.75	79.35
Thermal conductivity (W/mK)	1.05	0.032
Overall heat transfer coefficient (W/m^{2}K)	5.97	1.10
Shading coefficient	0.87	0.144

3. RESULTS FOR LIGHTING PERFORMANCE OF HISG

In the first part of the experimental research, illuminative penetration performances of ordinary glass and HISG curtain walls are investigated. In this respect, indoor light intensity measurements are done through nine different locations, and the results are compared with the outdoor illumination intensity as shown in Table 3. The average indoor light intensity values of ordinary glass and HISG curtain walls are determined to be 40087 and 2960 Lux whereas it is 58965 Lux for the outdoor environment. It is clearly seen from the results that the curtain walls equipped with ordinary glass cause excessive illuminative penetration to the indoor environment which is inappropriate for thermal comfort conditions of the occupants. It is reported in literature that the occupants usually complain about headaches, indigestion, nausea, blurred or double vision, flickering sensations, itching and burning eyes, tension, and vision fatigue when they are exposed to excessive illumination. On the contrary to the ordinary glass house, HISG curtain walls provide a comfortable indoor illumination as a consequence of its remarkably low visible light transmittance.
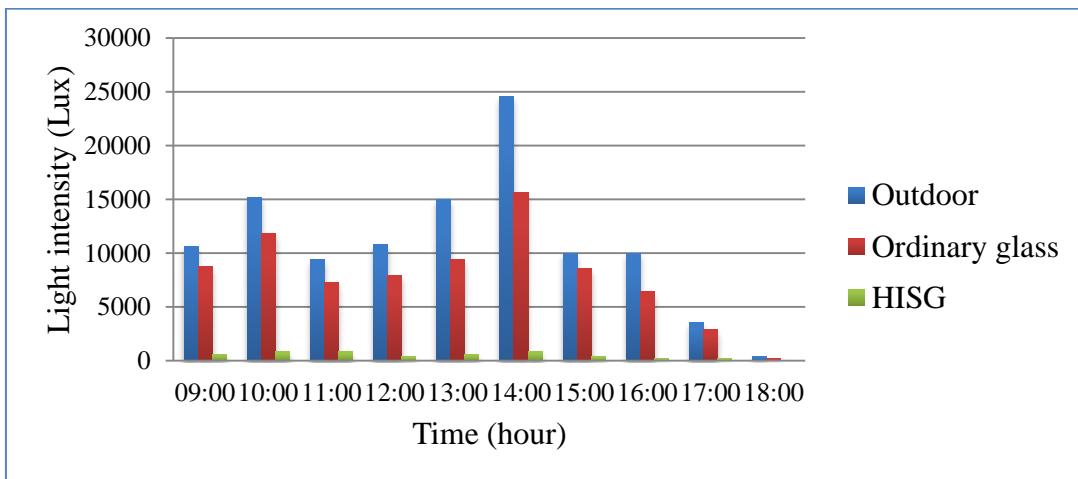
Table 3. Illuminative penetration test results for ordinary glass and HISG curtain walls.

| Light intensity for different locations (Lux)		Ordinary glass	HISG
Location 1		39059	2862
Location 2		34755	2916
Location 3		37445	2991
Location 4		41211	2927
Location 5		42825	3067
Location 6		44116	3077
Location 7		38736	2894
Location 8		40458	2905
Location 9		42179	3002
	Average	40087	2960
	Outdoor	58965	58965

In addition to the indoor and outdoor illumination measurements, illuminative penetration performances of ordinary glass and HISG curtain walls are also investigated as a function of direction. In this respect, light penetration through north, south, east and west facing facades as well as the roof glazing is measured for

various sky conditions from 9:00 to 18:00, and the results are compared for each curtain wall system as shown in Figure 2. The indoor illumination intensity through the top facade is found to be maximum with 1500-3100 Lux in the test house constructed with HISG curtain walls. It is well-documented in literature that the comfortable illumination values in office buildings are in the range of 750-1500 Lux. Although the light penetration through the other facades is somewhat lower than the required illumination, this is compensated by the top glazing resulting to a comfortable environment with adequate lighting. On the other hand, ordinary glass curtain walls allow excessive light to penetrate into the living space resulting to totally uncomfortable indoor environments. Overall, it is concluded from the illuminative penetration performance tests that HISG curtain walls provide incomparably more appropriate indoor conditions to the occupants owing to its ability to maintain the illumination in a comfortable range.

In the second part of the experimental research, UV penetration from ordinary glass and HISG curtain walls are analysed. Similar to the previous approach utilized in illumination performance tests, indoor UV values are measured through nine different locations, and the results are compared with outdoor data as illustrated in Table 4. The average rate of UV is measured to be 5080 mW/cm^2 at the front of ordinary glass curtain walls whereas it is 1231 mW/cm^2 at the back. In light of this, it is understood that around 76 % of UV in incoming solar radiation is absorbed which is notable. However, the results for HISG curtain walls clearly indicate that a 100 % UV-blocking rate is achieved through this novel technology, which is of vital importance for the health of the occupants. UV penetration tests are also applied to each facade separately as shown in Figure 3. The results reveal that the average UV absorption efficiency of ordinary glass curtain walls is about 68.9, 72.5, 70.0, 69.0 and 73.5 % through north, south, east, west facing facades and top glazing, respectively. On the other hand, HISG curtain walls demonstrate an excellent UV absorption as a consequence of superior structural details.
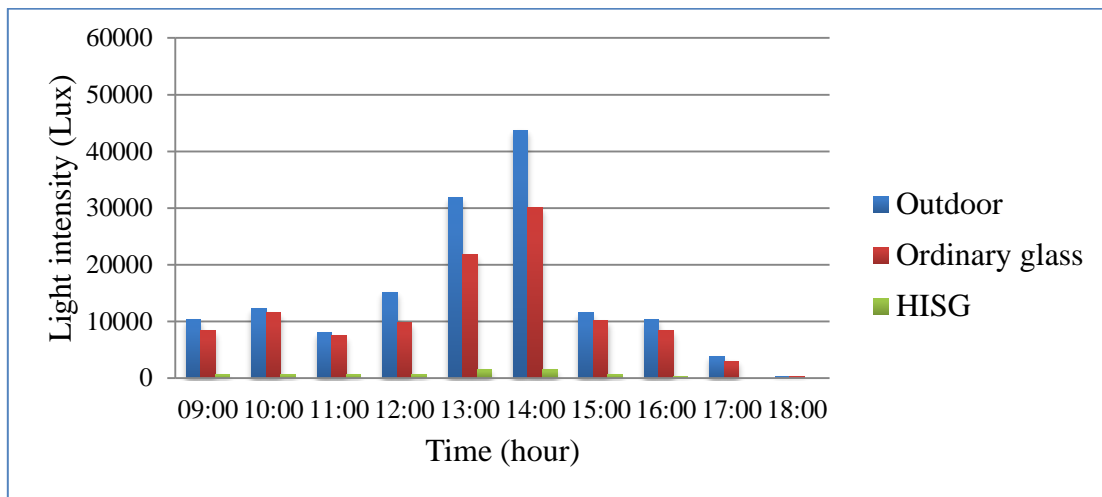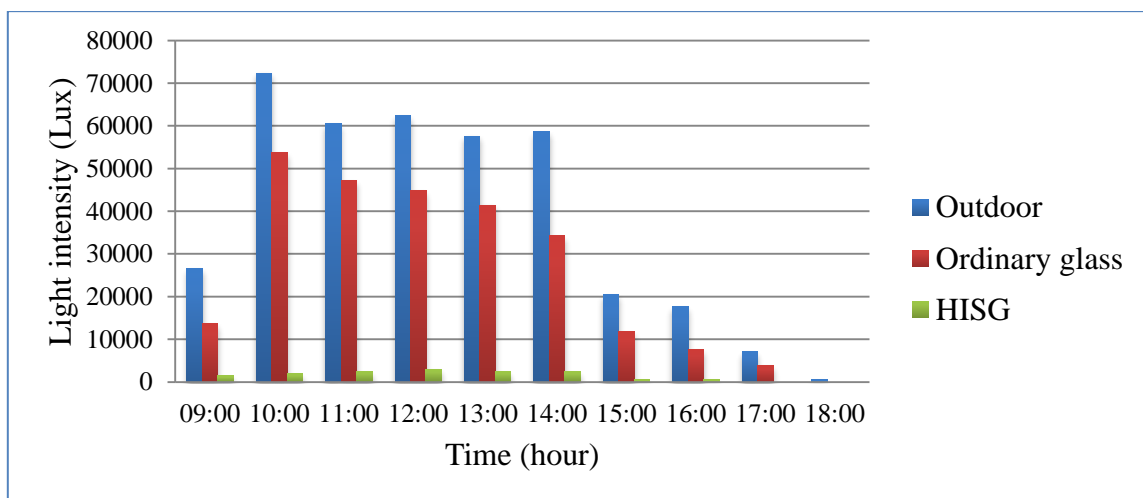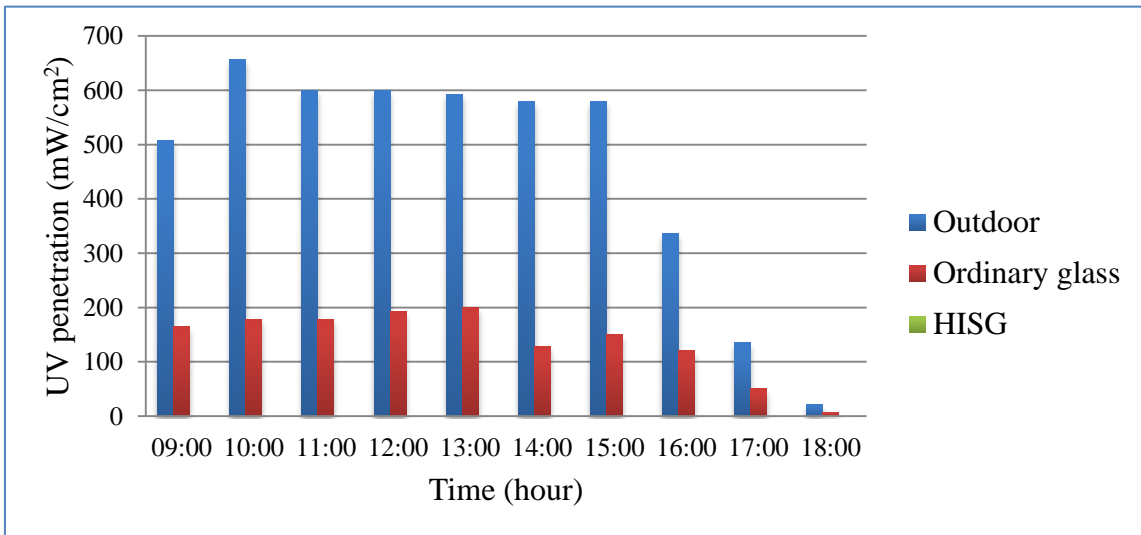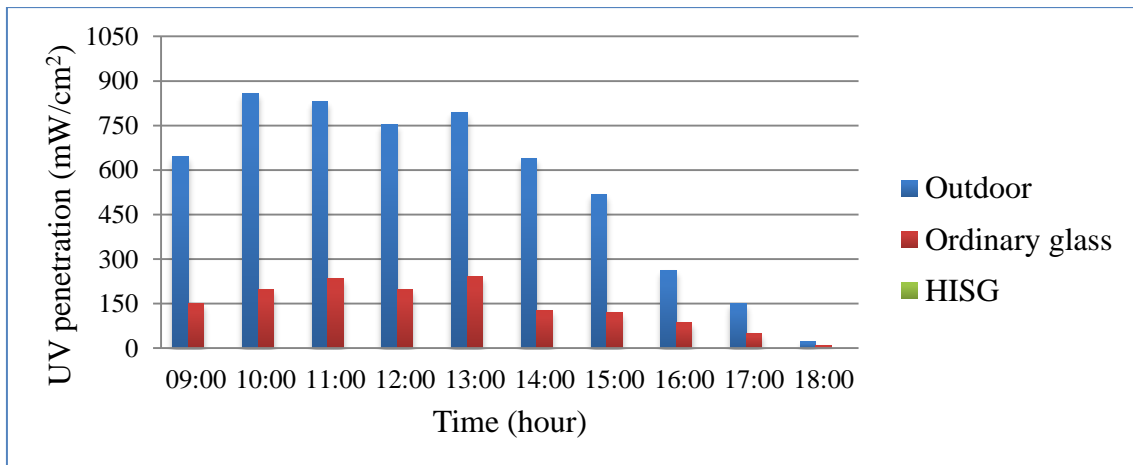

a)
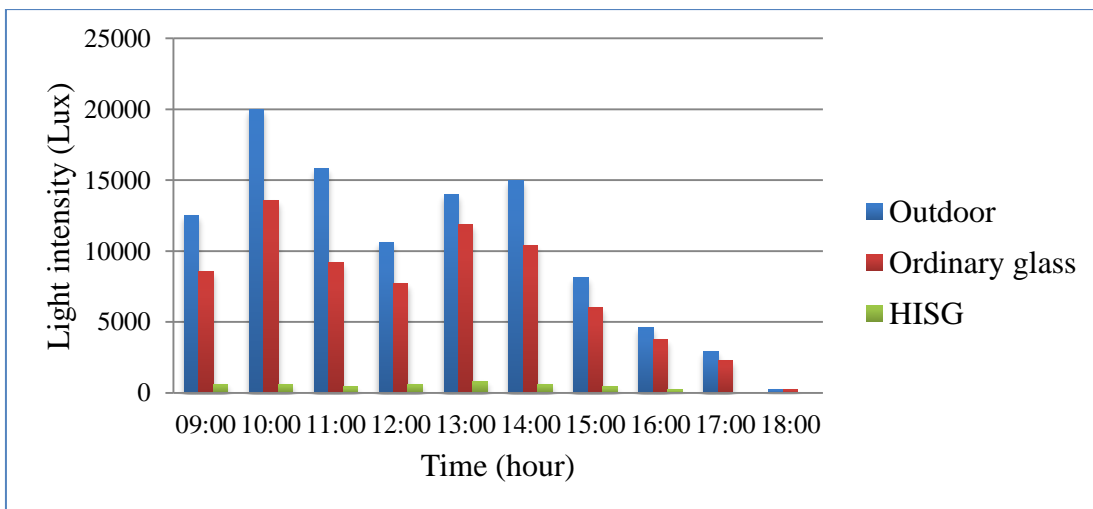
b)
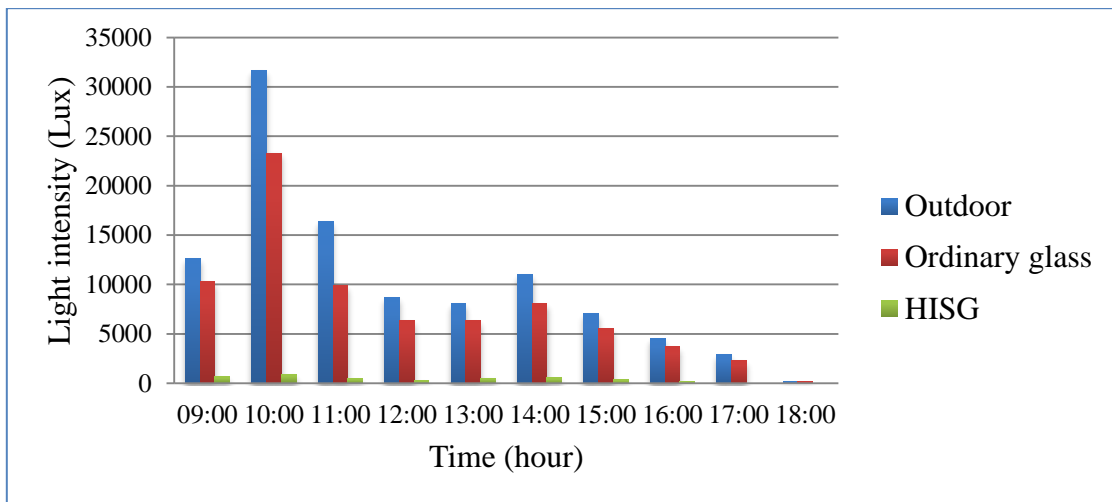
c)

d)

e)

Figure 2. Illuminative penetration through a) north, b) south, c) east, d) west and e) top facades.

Table 4. UV penetration test results for ordinary glass and HISG curtain walls.
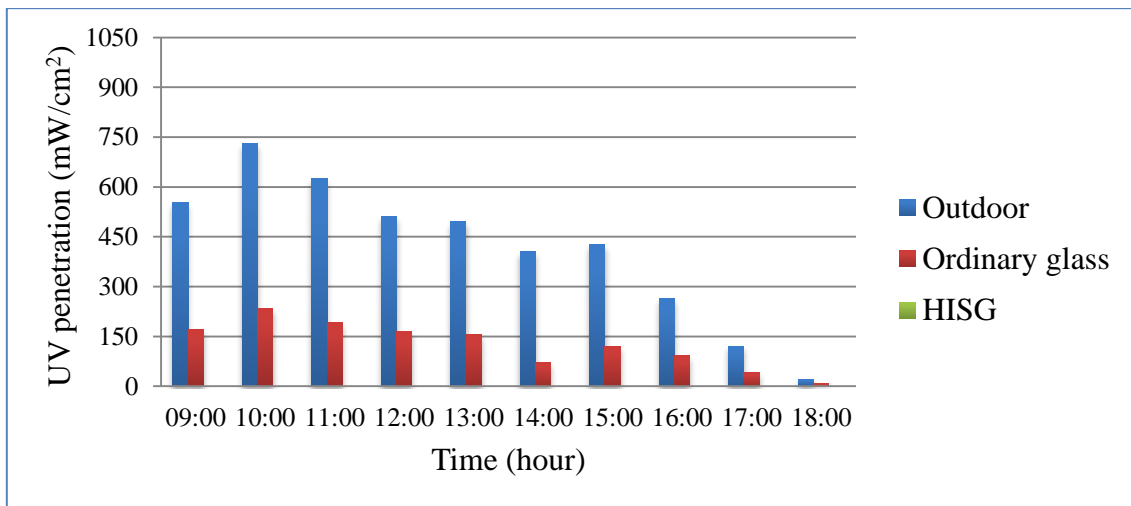
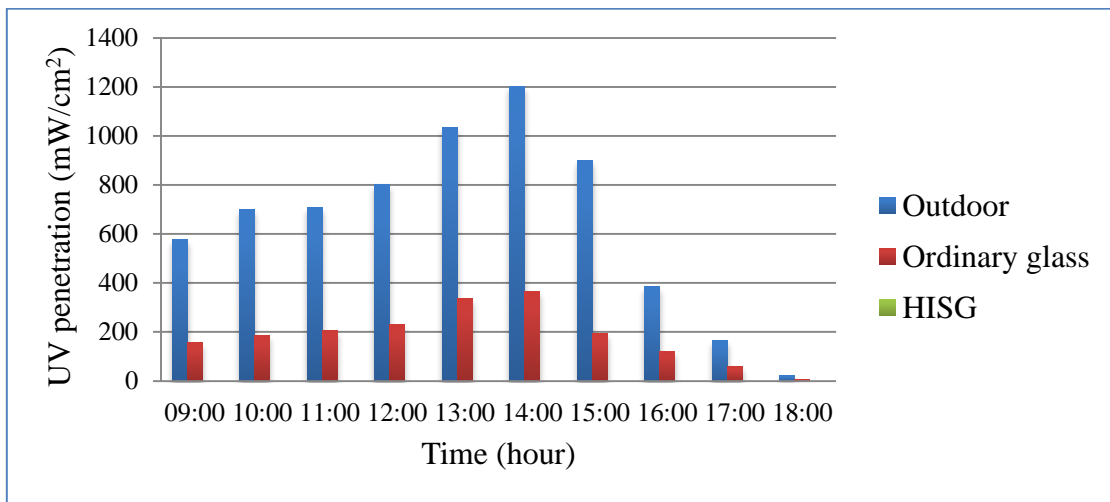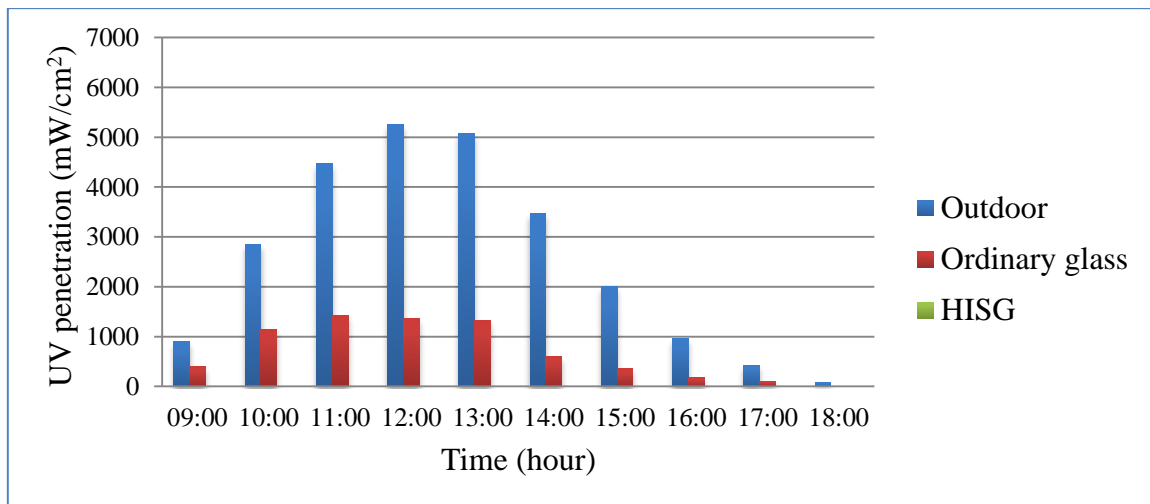| UV values for different locations (mW/cm^2)	Ordinary glass	HISG
Location 1	1139	0
Location 2	1219	0
Location 3	1149	0
Location 4	1216	0
Location 5	1255	0
Location 6	1265	0
Location 7	1279	0
Location 8	1261	0
Location 9	1300	0
Average	1231	0
Outdoor	5080	

a)

b)

c)

d)

e)

Figure 3. UV penetration through a) north, b) south, c) east, d) west and e) top facades.

In the fourth part of the research, lighting performances of ordinary glass and HISG curtain walls are investigated. In this respect, each test house is powered by a 40W light bulb fixed on the ceiling, and lighting performance is measured through nine different locations for curtain wall system as depicted in Table 5. HISG curtain walls provide 24.9 % better lighting performance than ordinary glass curtain walls in terms of average values, and this can be easily observed through comparative visual data given in Figure 4. This result can be attributed to the superior sandwich structure of HISG containing PV module and highly reflective film, leading to notable increase in light reflection into the house and thus sensible enhancements in lighting levels. Lighting performances of the curtain wall systems are also analysed for each facade, and it is observed that HISG curtain walls provide better indoor lighting efficiency for each direction as shown in Figure 5. As a consequence of light penetration from indoor to outdoor during the night time, the test house integrated with ordinary glass curtain walls is found be less efficient.
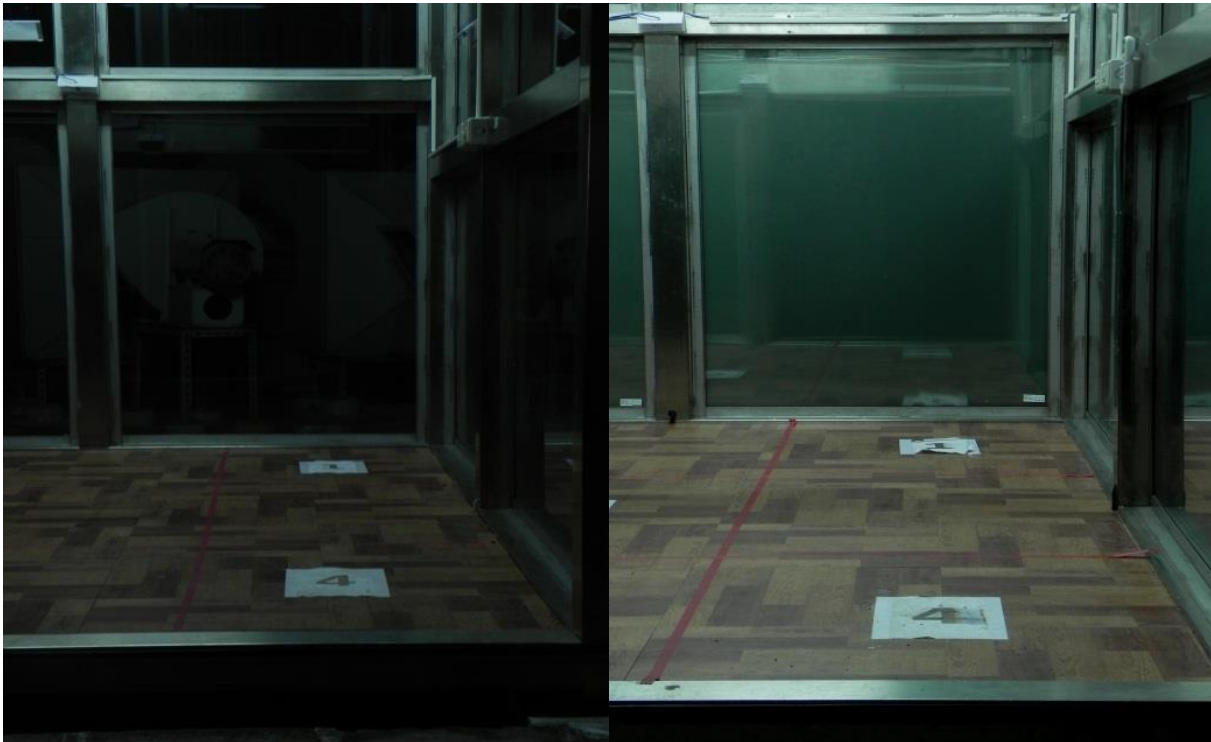

Figure 4. Lighting performance of ordinary glass (left) and HISG curtain walls (right).
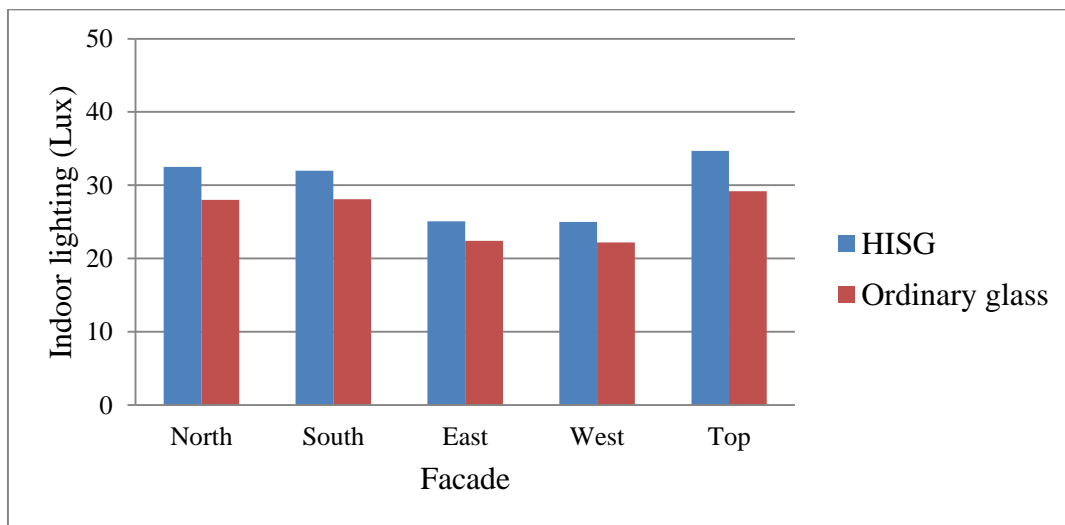

Figure 5. Lighting performance of ordinary glass and HISG curtain walls for each facade.

Table 5. Indoor lighting performances of ordinary glass and HISG curtain walls.

Light intensity (Lux)	Ordinary glass	HISG
Location 1	15.2	20.9
Location 2	17.9	22.2
Location 3	15.6	20.7
Location 4	16.6	19.4
Location 5	18.0	20.5
Location 6	16.6	19.3
Location 7	15.9	20.1
Location 8	17.4	21.8
Location 9	15.3	20.6
Average	16.5	20.6
Incoming light (W)	40.0	40.0

4. CONCLUSIONS

In this work, a novel thin-film photovoltaic glazing material called heat insulation solar glass (HISG) is introduced and its lighting efficiency for the potential utilization in greenhouses as a unique facade material is theoretically and experimentally investigated. Lighting performance assessment of HISG is presented in a comparable way with the conventional facade technologies such as ordinary single or double glazed building elements. The results indicate that HISG curtain walls provide 24.9% better lighting performance than ordinary glass curtain walls in terms of average values. This result can be attributed to the superior sandwich structure of HISG containing photovoltaic module and highly reflective film, leading to notable increase in light reflection into the house and thus sensible enhancements in lighting levels.

5. REFERENCES

1.   CUCE E, Young CH, Riffat SB. Thermal insulation, power generation, lighting and energy saving performance of heat insulation solar glass as a curtain wall application in Taiwan: A comparative experimental study. Energy Conversion and Management 2015; 96: 31–38.

2.   CUCE E, Young CH, Riffat SB. Thermal performance investigation of heat insulation solar glass: A comparative experimental study. Energy and Buildings 2015; 86: 595–600.

3.   CUCE E, Riffat SB. A state-of-the-art review on innovative glazing technologies. Renewable and Sustainable Energy Reviews 2015; 41: 695–714.

4.   CUCE E, Young CH, Riffat SB. Performance investigation of heat insulation solar glass for low-carbon buildings. Energy Conversion and Management 2014; 88: 834-841.

147: Case study on Korean style ecological architecture

SANG-HOON LIM[1], JEONG-HWAN PARK[2,] SOO CHO[3]

1 Korea Institute of Energy Research(KIER), 152, Gajeong-ro, Yuseong-gu, Daejeon, Korea, shlim@kier.re.kr
2 Kyungpook National University, E2-302, 1370 Sangyeok-dong, Buk-gu, Daegu, Republic of Korea, parkkim0716@gmail.com
3 Korea Institute of Energy Research(KIER), 152, Gajeong-ro, Yuseong-gu, Daejeon, Korea, scho@kier.re.kr

Ecological architecture is the understanding of elements internal to architecture that can be inferred using ecological concepts, and the establishment of consistently complementary relations with human lifestyles, creating a kind of ecosystem. Dealing with the architectural environment involves recognizing the effect of human elements on the design and structural aspects of architecture, as well as the roles of environmental factors, such as real estate development, scientific research, and education, which affect building construction. Also, architectural environment considers how decision making regarding materials and institutional resources is conducted by government agencies, economic agents, and families. Thus, ecological architecture can be described as being derived from knowledge of the environments, resources, and energy that affect human life. People responsible for designing the future society are obligated more than ever to reflect the ecological demands and direction of the architectural environment into their designs. Such designers need to pursue ideal designs based on ecological knowledge where the architectural environment can become a part of the circulation pattern of the ecosystem. In this study, from among domestic ecological architecture construction cases, the Geumsan ecological architecture was analysed as a case study of ecological architecture planning and system.

Keywords: The Geumsan ecological architecture, Eco-friendly plan, Natural elements, Direct gain system, Attached sun space system

1. INTRODUCTION

1.1 Research Background and Objective

Ecological architecture is the understanding of elements internal to architecture that can be inferred using ecological concepts, and the establishment of consistently complementary relations with human lifestyles, creating a kind of ecosystem. Dealing with the architectural environment involves recognizing the effect of human elements on the design and structural aspects of architecture, as well as the roles of environmental factors, such as real estate development, scientific research, and education, which affect building construction. Also, architectural environment considers how decision making regarding materials and institutional resources is conducted by government agencies, economic agents, and families. Thus, ecological architecture can be described as being derived from knowledge of the environments, resources, and energy that affect human life. People responsible for designing the future society are obligated more than ever to reflect the ecological demands and direction of the architectural environment into their designs. Such designers need to pursue ideal designs based on ecological knowledge where the architectural environment can become a part of the circulation pattern of the ecosystem. In this study, from among domestic ecological architecture construction cases, the Geumsan ecological architecture was analysed as a case study of ecological architecture planning and system.

3 ENERGY RESOURCES APPLICABLE TO ECOLOGICAL ARCHITECTURE

2.1 Solar Energy

Solar energy is a clean renewable energy source of infinite supply. There are three ways to utilize solar energy: direct conversion of the light from the sun to electrical energy through solar cells, thermal power generation, using collected solar energy to turn a turbine by creating high temperature vapour, and using a solar heat collector to create hot water for residential and building heating or for thermal processing in factories. However, due to the fact that solar energy has a low density and is dependent on the climate and time, solar energy is highly unstable in comparison to conventional fossil fuels such as petroleum, coal, and natural gas. In order to overcome such problems, a cost reduction solution for advanced technological development and distribution expansion is necessary.

2.2 Wind Power

Wind energy has a low energy density and is of smaller scale compared to traditional large scale power plants, and because the output varies according to the wind direction and velocity, it has the disadvantage that stable energy provision is difficult. However, wind power is a promising, clean, and renewable energy source, where its economic feasibility can be increased by selecting sites of suitable wind conditions to enhance the operation rate of the facilities. The rate of growth in wind power generation capacity is on the rise. Presently, wind energy development is based on two approaches: the top down approach, where government becomes the main supporter of development, and the bottom up approach where development is pursued by private entities with a focus on field experience. The bottom up approach adopted by Denmark is commonly evaluated as successful while the top down approach experimentally adopted by the U.S., U.K., and Germany is experiencing difficulties due to excessive costs.

2.3 Biomass and Waste Energy

Biomass energy is the utilization of solar energy accumulated in plant life through direct combustion; gasification through pyrolysis and partial oxidation; and methanation, ethanolysis, and direct liquefaction through fermentation of microorganisms. This clean, renewable energy, being used globally in various forms including the traditional energy source of firewood and renewable bio energy sources such as methane gas, carbonated rice-hull, and bio-ethanol, is responsible for 14% of the global energy source supply. Waste energy is the extraction of energy from wastes generated by agriculture, forestry, and livestock production processes and fixed garbage from cities. Methods for utilizing waste energy include waste power generation, methane gas production using waste products, and oil recovery or gasification of wastes. Also, because waste power generation operates a steam turbine generator using high temperature combustion gas by incinerating waste products, such waste products have to be somehow collected and processed. Research and development is being pursued all over the world with an emphasis on improving the generation efficiency in terms of integrated processing of wastes.

2.4 Geothermal Energy

Geothermal energy has great potential due to the recent development of geothermal reservoirs deep underground, and active progress in the development of hydrothermal technology. Also, geothermal energy is considered to be an alternative energy source to fossil fuels and is a clean energy source with an insignificant carbon dioxide emission footprint, which is a cause of global warming. For that reason, geothermal energy is a promising energy source that is expected to contribute to the global environment protection efforts after the adoption of the convention on climate change (94.3).

2.5 Small Hydraulic Power and Marine Energy

Small hydraulic power generation produces electrical energy by utilizing water resources with small head drop like an agricultural watershed. Such electrical energy refers to less than 3,000 kW for Korea, and small hydraulic power is an energy source that is increasingly gaining more international attention due to economic and environmental advantages, especially in cases where the construction of large scale hydroelectric power plants is technologically difficult or requires excessive investment costs. Next, marine energy includes a wide range of methods including temperature difference, wave power, and tidal power generation. Marine energy is an infinite potential energy source since approximately 70% of the Earth surface is covered by ocean waters. Ocean thermal energy conversion uses the temperature difference between the hot water of the ocean surface and the deep sea cold water, and approaches are differentiated into the closed cycle and open cycle methods. The closed cycle method is more commonly used. Wave power uses the up-and-down motion of seawater produced by waves to compress air and turn a turbine for generation using the compressed air. Tidal power generation employs the head drop of the seawater which occurs due to tides.

2.6 Fuel Energy, Hydrogen Energy, and Coal Reformation

Fuel cells employ direct power generation through the electrochemical reaction of the air in the atmosphere and hydrogen, which can be obtained by improving the quality of fuels including natural gas and methanol.

Fuel cells have high generating efficiencies of $40 \sim 60\%$ and their overall energy efficiency when using exhaust heat reaches 80%. This energy source is able to contribute to global warming prevention as various fuels such as natural gas, methanol, LNG, naphtha, and kerosene can be used and there is very little nitrogen oxides emission. Hydrogen energy can be produced with water as the raw material and since water is the most abundant resource available, hydrogen energy boasts high heat per unit mass and electrical energy conversion efficiency. Hydrogen energy is a clean energy source as no pollutants are produced from combustion when hydrogen energy is used as a fuel other than small amounts of nitrogen dioxide (NO_2). Also, hydrogen can be conveniently transported in gaseous and liquid states and can be conveniently stored in various forms including high-pressure gas, liquid hydrogen, and metal hydride. Coal reformation is a method of resolving the inconveniences and environmental problems (dust, sulphur oxides (SOx), nitrogen oxides (NOx)) of directly using coal. Research and development of gasification, liquefaction, and slurry fuel technologies is underway, and Japan is pursuing development of technologies regarding bituminous coal liquefaction, coal gasification integrated generation, and hydrogen production using coal, as well as development of technologies for the extraction and utilization of coalbed methane (CBM) which is available in the coal bed. In the U.S., Texaco has invested around 3 billion U.S. dollars beginning in 1953 to develop a slurry-fed coal gasification technology and EHDN has been pushing forward a wide range of research and development activities since 1975 including coal slurry fuel technology. Other countries including China, Canada, and Russia are all focusing their efforts on the development of coal slurry fuel technologies based on the fact that these countries have rich coal resources within their borders.

3 ECOLOGICAL ARCHITECTURE OF GEUMSAN

The Geumsan ecological architecture is an architecture experience centre where ecological architecture as an alternative for future architecture can be taught and promoted to regular people and students. The following table shows an overview of the details of the Geumsan ecological architecture.

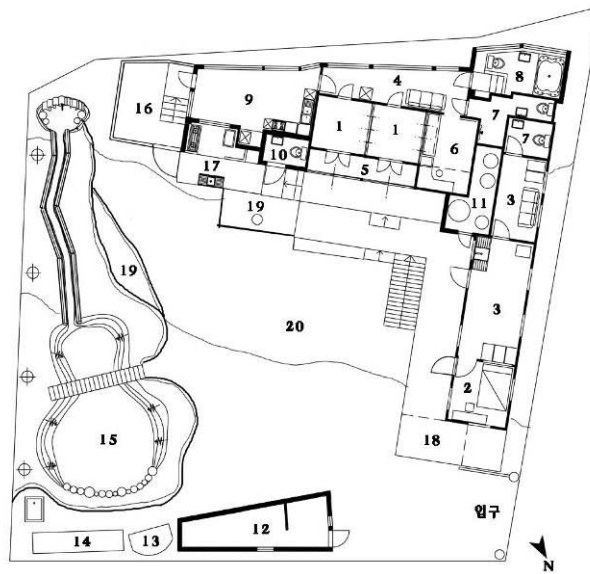| Item	Content
Location	505-5, Baegam-ri, Boksu-myeon, Geumsan-gun, Chungcheongnam-do, Korea
Completion date	2002 November 9
Lot area	583.2㎡
Building area	130㎡
Applied methods	Solar energy collector(vacuum tube, flat plate) Solar power generation facility Wind turbine, biotope, attached sun space structure

Figure 1: The Geumsan ecological architecture ground plan

1.Han-ok bedroom
2.Director's office and education preparation room
3.Office and education center
4.Hallway of light and heat
5.Han-ok toenmaru
6.Playroom
7.Shower room(natural lighting)
8.Bathroom(whirlpool,outdoor landscape view)
9.Kitchen and living room
10.Outdoor toilet
11.Machine room
12.Storage/flat plate collector
13.Solar cell and wind turbine
14.Vacuum tube collector
15.Biotope
16.Terrace and outdoor meeting room
17.Outdoor kitchen
18.Solar energy exhibition
19.Green farm
20.Recreation ground

The Geumsan ecological architecture adopted natural energy technologies and planning elements to provide a place for people to experience, and to expand the base of eco-friendly architecture. The Geumsan ecological architecture is always open so that everyone can be educated when they wish. The experience program at the Geumsan ecological architecture teaches about ecological architecture and alternative energy to regular people and teenagers as well as providing demonstrations, and board and lodging is possible for all guests. In particular, teenagers can participate in the solar cooker making, wind turbine model making, and solar energy car making activities. Such activities were prepared to teach about ecological architecture and the value of alternative energy sources.

Planning Direction

Characteristics

This experience centre has a building area of 139㎡ on a lot of 595 ㎡. The centre has the following characteristics.

·Remodelling of existing Han-ok buildings
·Natural solar energy system
·Skylight installation and lighting system implemented for the bathroom and machine room
·Hot water supply from solar energy using a flat plate collector
·Biotope (small ecosystem) created
·Installation of pump for the biotope water circulation. This pump is operated using a solar cell (150W) and wind turbine (400W)
·Hanji and soybean oil finish for the bedroom floor for maximum protection of nature

Efforts were made to utilize nature as much as possible while also protecting it.

Surrounding Environment

The site of the Geumsan ecological architecture is surrounded by mountains with a stream flowing right in front of the site, which is reminiscent of a remote mountain village. This area is located inland, south on the Korean peninsula, so the climate is of inland southern-type, and because the surrounding area is more mountainous than other regions, the area experiences a significant contrast between hot and cold weathers along with relatively heavy rainfall. The annual average temperature of the area is 11.8℃ and since the northern and southern areas are divided along the geographical line with an annual average temperature of 10℃, the area belongs to the southern region and climate. Moreover, as temperate and warm temperate climates are categorized based on the line of average 12℃, the area is closer to a temperate climate. The average temperature is highest for August at 25.8℃ while January is the lowest at –2.7℃, so the difference in temperature extremes of the year is 28.5℃. The hottest day of the year was recorded to have a temperature of 35.2℃ while the coldest day was –20.4℃ so the temperature difference is severe, and the summer season tends to be hot and humid. Also, compared to Daejeon City located nearby, the area is 0.5℃ lower in January and 1.2℃ higher in August. The annual average precipitation amount is approximately 1,300 mm which is more than the average amount of precipitation for the entire country, which is 1,159 mm, while being about 100 mm greater than the precipitation amount of Daejeon City. This is because the summer season of this area as explained before has an oceanic climate, hot and humid, and has heavy rainfall due to its location in a mountainous basin. The rock forming the country rock of the area is mostly composed of Okcheon sedimentary rock and granite. Therefore, the area has a lot of sedentary deposits from the continuous erosion due to the heavy downpours during summer, severe temperature differences, and a significant mountain slope. This area is a well-known locale for its Korean native cattle and numerous persimmon trees.

Eco-Friendly Plan

In the case of ecological architecture no.0, the entire process from planning to construction was focused on preventing the existing natural environment from being damaged and harmed. In this regard, the existing linear Han-ok and container house were not removed but renovated. A glass gate entrance and hallway were created about the linear Han-ok and in the direction of the eaves, the kitchen of the existing Han-ok was modified to a room, and a 16.5 ㎡ sized kitchen was created on the side through masonry (1.0B) stacking. These decisions allowed the minimization of waste production that can occur when removing an existing building, and by utilizing wastes that are created during construction, the damage that can be done to the environment due to such construction waste was minimized and the construction cost (0.33 million Korean won/㎡) could be conserved.

Compatibility with the External Environment

With regard to compatibility with the external environment, ①natural light enters the building. An outside view is available. With this openness it's possible to check on the outside weather condition from inside the

building, and ②the woods and garden are visible as well. Two aspects of grounding, where the garden or the ground outside is directly connected, can be considered. In the case of the Geumsan ecological architecture, both openness and grounding coexist from the perspective of eco-friendliness. The southern side of the kitchen is made open using a window, the southern side of the Han-ok building is made open by using the space below the eaves as a hallway through masonry stacking, and the bathroom side in contact with the outside air is made open using a window. These features satisfy grounding, as people inside can exit at ground level at any point in time from the hallway, kitchen, or rooms. However, connecting the inner spaces causes problems with regard to privacy due to excessive openness. Thus, there is a need to satisfy both openness and privacy simultaneously. Hence, the following plan was made for the Geumsan ecological architecture.
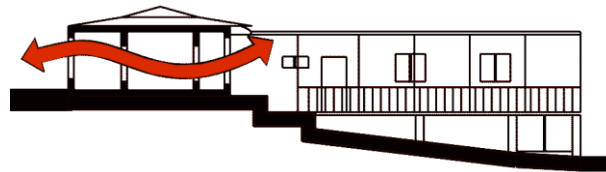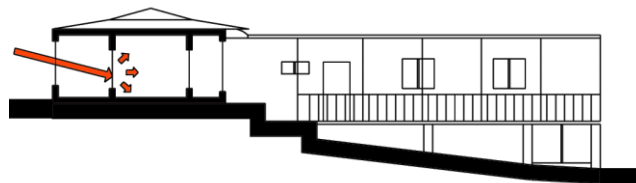

Figure 2: Grounding and openness

Figure 3: Indoor lighting

Bricks were stacked in the space below the eaves of the existing Han-ok building and windows were used to create openness, while the privacy of the master room was protected by creating a semi-outdoor space. However, since openness can also be applied to the master room, the existing door was used so openness can be felt when the doors are open and privacy was protected when the doors are closed. Also, to secure sufficient lighting when the master room doors are closed during the day, window paper was adhered to the door so that light can seep in. In the case of the bathroom, special glass was installed so that the inside cannot be seen from the outside but the outside can be seen from the inside. A lamp was installed outside the bathroom for the night-time so that the inside cannot be seen from the outside due to the brightness of the lighting from both in and outside the bathroom at night. Moreover, a skylight was installed to let in natural lighting.

3.1 Solar Energy

Eco-Friendly Plan
Direct gain
This system adopted for the kitchen space of the Geumsan ecological architecture was planned to utilize the abundant amount of sunlight entering through the south-facing collector window during winter, and store it as heat energy in the floor and wall, allowing for heating during the night and cloudy days. The planning and implementation of this system is convenient enough for regular people to easily apply and the system is not costly as well. Also, the collector window achieves various functions including lighting, ventilation, and view.

Attached sun space
This hallway style space with a sandwich solar panel attached to the Han-ok roof eaves and walls made of glass is an attached sun space system that acts independently from the heating space of the building, where the collector window and heat-storage object is separated from the living spaces. This system takes on the role of a sun space and simultaneously controls the temperature of the living spaces. In addition, the system has the advantage of being easy to apply to buildings, so it was selected to be installed here. This space can be utilized as a resting space or garden where various plants can be grown and it has a small temperature variation range.

Solar Thermal System
Flat plate collector

·Characteristics
  -The absorption area increases thermal conductivity by connecting the copper tube and copper plate through Roll Forming
  -Selective Coating of the absorption area
  -Low iron tempered glass is used for the glazing device
  -Circulation method involving Rise and Header for the thermal fluid

 ·Subject of application
  -Hot water heating system for residential and commercial buildings
  -Greenhouse ground heating and cattle heating
  -Swimming pool hot water and heating systems

Vacuum tube collector
·Characteristics
  - Durability and stability enhancements using Pyrex heat resistance glass tubing
  - Heat collection is done through the Condensation Particular Counter (CPC) method, so there is little influence on the installation angle
  - Vacuum-insulation between the double glass tubing to minimize heat loss to the outside
  - Special coating was applied to obtain excellent solar energy heat collection performance of above 95%
  - Exceptional performance for the winter season and environments lacking insolation
  - Elegant exterior design, high efficiency of over 20%, and ability to reach high temperatures of above 90℃

Table 2: Solar thermal system specifications

Item	Etsen vacuum tube collector CPC-1800
No. of vacuum tubes	18
Vacuum tube dimensions	Ø47㎜×L1,500㎜×Th1.6㎜
Collection area	3㎡
Collection efficiency	60%(standard of plat plate, 45%, ΔT=50℃)
Max. allowable pressure	10bar
Mass	54kg
Daily collection capacity	Appr. 150ℓ
Collection method	Double vacuum tube and CPC

3.2 Wind Energy

Wind power generation utilizes the wind to turn a power generator from a windmill. This wind energy does not cause atmospheric pollution and fuel consumption but the surrounding areas nearby the wind turbines can experience noise and radio interference. Wind power generation is categorized according to the capacity: below 100㎾ is small, 100㎾ ~ 1,000㎾ is middle, and above 1,000㎾ is large.

The wind turbine installed in the Geumsan ecological architecture is a small capacity generator with a generation performance of 400w.

Table 3: Wind power specifications

Item	Content
Rotor diameter	: 46″(1.14m)
Weight	: 13lbs (6kg)
Start-up wind speed	: 7mph(3㎧)
Voltage	: 12, 24, 48 volts
Output	: 400watts at 28mph(12.5㎧)

3.3 Photovoltaic System

A solar cell is a semiconductor device that converts solar energy to electrical energy, and they are widely employed in various fields. Solar cells are used as the power source for artificial satellites in space, remote islands, and isolated villages as well as streetlamps, ships, and automobiles. Commercialization cases include application of solar cells in calculators and clocks. With regard to buildings, solar cells are used to obtain the electrical energy needed for use in the building. Although the total amount of solar energy is generally great, the density is low, thus, solar energy is difficult to use as an energy source. Therefore, the technological development of heat collectors and accumulators is necessary to resolve such issues, and the current technological level is still lacking. Solar cells are used at the Geumsan ecological architecture and the electrical energy obtained through the solar cell is used to circulate the water of the ecological pond.

Table 4: Solar cell specifications

Item		Solar tech STM50
Solar cell		Polycrystalline
Rated capacity(WP)		50
Open circuit voltage(V)		21.0
Short circuit current(A)		3.23
Rated voltage(V)		16.8
Rated current(A)		2.97
Dimensions	A(㎜)	934
	B(㎜)	502
	C(㎜)	50
	Weight(kg)	6.3
	Terminal box	1 terminal
hole	D(㎜)	900
	E(㎜)	610
	F(㎜)	467

3.4 Ecological Pond

An ecological pond is a type of marsh, an artificial wetland created in place of natural marshes which have disappeared or have been harmed by urbanization and industrialization, in an effort to create an environment which various species can inhabit. Such areas are necessary for modern man suffering from environmental pollution and today's industrialization.
This system established at the Geumsan ecological architecture implemented a separate plumbing system using rainwater or recycled water to provide an opportunity for guests to witness the renewability of water and alternative energy, through water foundation tests using solar cells.
The function and expected effect of the ecological pond are as follows.

·Physical environment improvement
  -Groundwater cultivation and flood prevention
  -Microclimate control effect

·City landscape improvement
 -Waterfront and scenery presentation
 -Establishment of varied scenery within the city

·Chemical environment improvement
  -Harmful gas absorption and oxygen creation due to increase of plant productivity
  -Organic matter decomposition by microorganisms

·Biological environment improvement
  -Adoption of aquatic life and wetland plants
  -Opportunity for hideout, proliferation, and travel route for animals
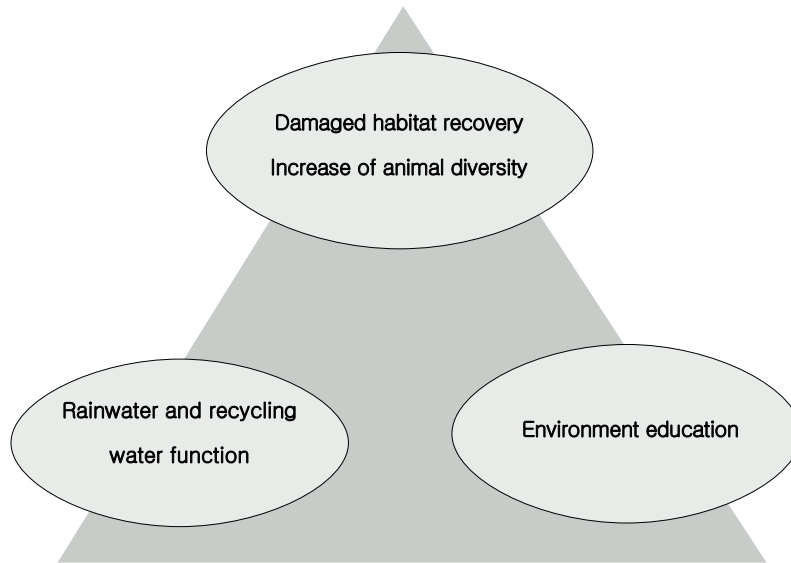 -Increase in variety of animal and plant life

Figure 4: Necessity of an ecological pond

The most critical element in establishing an environment having the above roles is the securing of sufficient sunlight, and interaction between habitats, by having nearby forests close by.

3.6 RAINWATER USAGE

At this point in time where the eco-friendly securement of water resources is urgently needed worldwide, the expansion of rainwater use is important. In particular, according to Population Action International (PAI) under the UN, Korea is already categorized as a country lacking water like Morocco and South Africa. Ecological architecture uses rainwater for residential and various types of buildings.
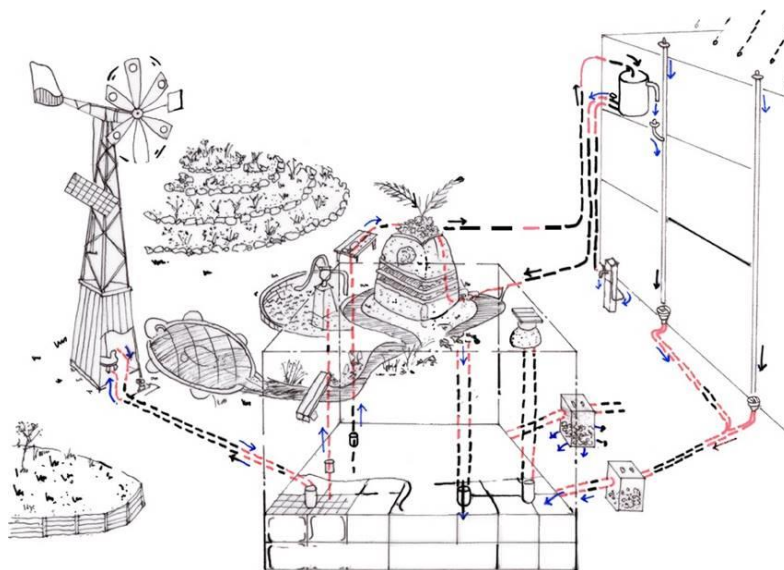

Figure 5: Rainwater system of the Geumsan ecological architecture

Rainwater on the roof is filtered then stored in a water tank to be used as cleaning water, for watering, and car washes. Rainwater usage can conserve water resources and rainwater can be used as drinking water during emergencies. Also, a water tank for rainwater collection on the roof can create a community centred around the tank and a prosperous residential environment can be established by using the rainwater for a foundation or streamlet. In the Geumsan ecological architecture, rainwater is used to supply water to the ecological pond. This water is circulated using the pump operated using the wind turbine and solar cell so that the water does not become stagnant.

3.5 Eco-Friendly Materials for Construction

At The production of polluting substances during production, transportation, and construction need to be considered for the selection of construction materials, to create a sustainable building. Even technically high quality materials could have a negative impact on indoor conditions and resident health.
The following aspects can be considered for construction material selection.

·Impact on the health and comfort of the resident
·Material with minimal energy consumption during the production process and no harmful material production
·Recyclability and renewability
·Suitability of the material for its usage
·Production and usage of regional resources

By remodelling the existing old Han-ok building, the Geumsan ecological architecture minimized the creation of waste materials produced by tearing down a building, and the materials used in the remodelling process were eco-friendly and energy conserving.
Non-toxic paint was used for the wood columns so that insects may live and soybean oil was used rather than varnish after spreading conventional floor paper. Also, recycled products were used for the table and doors.
Transparent polycarbonate was used for the ceiling and walls of the storage and bathroom for maximum natural lighting. Recycled bricks and glass were used for the stairs and ramp for the disabled which connect the building with the front yard, and most of the waste materials from the building were recycled.

4 CONCLUSION

Ecological architecture is based on a reasonable philosophy and design theory, with the goal of establishing an ideal and quality relationship between people and the environment. Ecological architecture is an economic architecture method when considering the overall costs from the construction to demolition of a building.

The Geumsan ecological architecture was experimentally constructed to promote ecological architecture and was established with the following objectives. First, protection and utilization of nature was maximized. Most of the energy used by the Geumsan ecological architecture is derived from natural energy. By using natural energy in this manner, the energy consumption of the building was minimized as much as possible. Also, the finishing materials of the building were materials like floor paper, which do not harm the environment, and minimize waste products from the building construction process. The construction waste material that can result from the construction was re-used as much as possible to protect the environment, to minimize the construction waste product. The second objective was the issue of how to improve the rural housing. The traditional trend in rural housing was to demolish the existing building and build a new one on top of that land. The Geumsan ecological architecture has a clear objective in utilizing the existing structure as much as possible even though it may be difficult. Third, numerous special purpose architectures have been adopted in Korea like green buildings, however, the significance of the Geumsan ecological architecture lies in its attempt to recreate a regular residential building through ecological architecture, although it may be at a basic level at this point. Lastly, the project has contributed to the basic expansion of ecological architecture. By promoting and educating regular people and students about ecological architecture, the concept has become more approachable to regular people. Also, by leaving a precedent case where ecological architecture has been accomplished with a regular construction budget, the establishment can be considered one of the starting points to bring about a fundamental expansion of ecological architecture. In this way, by presenting an architectural environment which can provide comfort to people while harmonizing with the environment, the Geumsan ecological architecture can be considered the starting point of the base expansion of ecological architecture.

5 ACKNOWLEDGEMENT

6 REFERENCES

地球環境住居研究會 環境共生住宅 計劃· 建築編　ケイブン出版(株) 1994年

都市綠化技術開發機具, NEO - GREEN SPACE DESIGN 東京：誠文堂新光社 1995.11

Judy CORBETT, Micheal Corbett, 'Designing sustainable communities learning from village homes', Island press.

Timothy BEATLEY, 'Green urbanism - Learning from European cities', Island press

Laura C, ZEIBER, 'The Ecology of Architecture', Whitney Library of Design, 1996.

Beyond The Petroleum Age-Designing The Solar Economy, World Watch Report, 1991.

CROSIBIE, Michael. Green Architecture : A Guide to Sustainable Design. Washington, DC : AIA Press, 1994

DODGE, Sue E. "Green by Design," National Parks Magazine. September/ October 1994